SHOUT
SHARE
IT

MBL

THE
BIOLOGICAL BULLETIN
FEBRUARY 1999

FEB 23 1999

Editor	MICHAEL J. GREENBERG	The Whitney Laboratory, University of Florida
Associate Editors	LOUIS E. BURNETT	Grice Marine Biological Laboratory, College of Charleston
	CHARLES D. DERBY	Georgia State University
	MICHAEL LABARBARA	University of Chicago
	RUDOLF A. RAFF	Indiana University
Section Editor	SHINYA INOUÉ, *Imaging and Microscopy*	Marine Biological Laboratory
Online Editors	JAMES A. BLAKE, *Keys to Marine Invertebrates of the Woods Hole Region*	ENSR Marine & Coastal Center, Woods Hole
	WILLIAM D. COHEN, *Marine Models Electronic Record and Compendia*	Hunter College, City University of New York
Editorial Board	PETER B. ARMSTRONG	University of California, Davis
	ANDREW R. CAMERON	California Institute of Technology
	ERNEST S. CHANG	University of California, Davis
	THOMAS H. DIETZ	Louisiana State University
	RICHARD B. EMLET	Oregon Institute of Marine Biology, Univ. of Oregon
	DAVID EPEL	Hopkins Marine Station, Stanford University
	GREGORY HINKLE	Cereon Genomics, Cambridge, Massachusetts
	MAKOTO KOBAYASHI	Hiroshima University of Economics, Japan
	DONAL T. MANAHAN	University of Southern California
	MARGARET MCFALL-NGAI	Kewalo Marine Laboratory, University of Hawaii
	MARK W. MILLER	Institute of Neurobiology, University of Puerto Rico
	TATSUO MOTOKAWA	Tokyo Institute of Technology, Japan
	YOSHITAKA NAGAHAMA	National Institute for Basic Biology, Japan
	SHERRY D. PAINTER	Marine Biomed. Inst., Univ. of Texas Medical Branch
	J. HERBERT WAITE	University of California, Santa Barbara
	RICHARD K. ZIMMER-FAUST	University of California, Los Angeles
Editorial Office	PAMELA CLAPP HINKLE	Managing Editor
	VICTORIA R. GIBSON	Staff Editor
	CAROL SCHACHINGER	Editorial Assistant
	PATRICIA BURNS	Subscription & Advertising Secretary

Published by
MARINE BIOLOGICAL LABORATORY
WOODS HOLE, MASSACHUSETTS

Cover

The hydrozoan *Podocoryne carnea* (Phylum Cnidaria), consists—in its colonial benthic phase—of two principal elements: polyps and stolons. The polyps are the feeding members of the colony and grow to a length of about 1 mm. The stolons are branched, vascular tissues that connect the gastric cavities of polyps; these gastrovascular vessels are about 60–70 μm in external diameter. Polyps are propagated asexually through the differentiation of cells in the stolon. Typically, hydractiniid colonies, like those of *Podocoryne,* comprise several hundred polyps, all interconnected by a network of branched stolons that covers the gastropod shells occupied by hermit crabs (diagram, top; reproduced from G. J. Allman, 1872. A monograph of the gymnoblastic or tubularian hydroids. Part II. Ray Society, London. 155–450). Individual polyps with a bit of attached stolon can be transplanted onto microscope slides where they generate clonal replicates of colonies for experimental use. Such a cloned colony, growing on the edge of a slide, is shown on the left (photograph by Neil Blackstone). A vegetative polyp in the center of the picture is flanked by polyps that are budding off medusae (containing orange structures).

The relatively small size and transparency of these hydractiniid hydroids, as well as the ease with which replicate colonies can be produced, make them excellent systems with which to study the physiology of vascular fluid transport. The colony-wide distribution of nutrients and dissolved gases is now thought to play a critical role in the morphogenesis and life history of the colony.

In this issue, Dudgeon *et al.* use videomicroscopy and automated image analysis to characterize the feeding-related dynamics of the gastrovascular system, particularly the oscillations of polyps and stolons that occur during and after feeding. The photomicrograph at right (differential interference contrast, 100×; photograph by Neil Blackstone) shows a branching stolon of *Podocoryne carnea* in its open state; that is, the lumen of the stolon is expanded, permitting the export of fluid from the polyps into the colonial gastrovascular system. In contrast, the lumen of the nearby stolon tip is closed. This investigation is the first quantitative treatment of cnidarian feeding behavior at high temporal resolution. It suggests that a cnidarian colony can be reasonably and readily treated as a system of coupled nonlinear oscillators distributed in space.

CONTENTS

VOLUME 196, NO. 1: FEBRUARY 1999

PHYSIOLOGY

Dudgeon, Steve, Andreas Wagner, J. Rimas Vaišnys, and Leo W. Buss
Dynamics of gastrovascular circulation in the hydrozoan *Podocoryne carnea:* the one-polyp case 1

Kelly, Robert H., and Paul H. Yancey
High contents of trimethylamine oxide correlating with depth in deep-sea teleost fishes, skates, and decapod crustaceans 18

Beaven, Amy E., and Kennedy T. Paynter
Acidification of the phagosome in *Crassostrea virginica* hemocytes following engulfment of zymosan 26

Smith, Andrew M., Tonya J. Quick, and Rachel L. St. Peter
Differences in the composition of adhesive and nonadhesive mucus from the limpet *Lottia limatula* 34

Kawaii, Satoru, Keiji Yamashita, Mitsuyo Nakai, Miyuki Takahashi, and Nobuhiro Fusetani
Calcium-dependence of settlement and nematocyst discharge in actinulae of the hydroid *Tubularia mesembryanthemum* 45

RESEARCH NOTE

Tapley, David W., Garry R. Buettner, and J. Malcolm Shick
Free radicals and chemiluminescence as products of the spontaneous oxidation of sulfide in seawater, and their biological implications 52

DEVELOPMENT AND REPRODUCTION

Froggett, Stephan J., and Esther M. Leise
Metamorphosis in the marine snail *Ilyanassa obsoleta*, yes or NO? 57

Stewart-Savage, J., Bradley J. Wagstaff, and Philip O. Yund
Developmental basis of phenotypic variation in egg production in a colonial ascidian: primary oocyte production versus oocyte development 63

Schwarz, Jodi A., David A. Krupp, and Virginia M. Weis
Late larval development and onset of symbiosis in the scleractinian coral *Fungia scutaria* 70

ECOLOGY AND EVOLUTION

Lopez, Jose V., Ralf Kersanach, Stephen A. Rehner, and Nancy Knowlton
Molecular determination of species boundaries in corals: genetic analysis of the *Montastraea annularis* complex using amplified fragment length polymorphisms and a microsatellite marker 80

Bingham, Brian L., and Nathalie Reyns
Ultraviolet radiation and distribution of the solitary ascidian *Corella inflata* (Huntsman) 94

NEUROBIOLOGY AND BEHAVIOR

Cromarty, S.I., J. Mello, and G. Kass-Simon
Time in residence affects escape and agonistic behavior in adult male American lobsters 105

ULTRASTRUCTURE

Hirose, Euichi, Satoshi Kimura, Takao Itoh, and Jun Nishikawa
Tunic morphology and cellulosic components of pyrosomas, doliolids, and salps (Thaliacea, Urochordata) 113

THE BIOLOGICAL BULLETIN

THE BIOLOGICAL BULLETIN is published six times a year by the Marine Biological Laboratory, 7 MBL Street, Woods Hole, Massachusetts 02543.

Subscriptions and similar matter should be addressed to Subscription Manager, THE BIOLOGICAL BULLETIN, Marine Biological Laboratory, 7 MBL Street, Woods Hole, Massachusetts 02543. Subscription per year (six issues, two volumes): $205 for libraries; $95 for individuals. Subscription per volume (three issues): $102.50 for libraries; $47.50 for individuals. Back and single issues (subject to availability): $40 for libraries; $20 for individuals.

Communications relative to manuscripts should be sent to Michael J. Greenberg, Editor-in-Chief, or Pamela Clapp Hinkle, Managing Editor, at the Marine Biological Laboratory, 7 MBL Street, Woods Hole, Massachusetts 02543. Telephone: (508) 289-7428. FAX: 508-457-1924. E-mail: pclapp@mbl.edu.

http://www.mbl.edu/BiologicalBulletin/

The home page for the electronic companion to THE BIOLOGICAL BULLETIN—*the Marine Models Electronic Record*—and other BIOLOGICAL BULLETIN publications is available on the World Wide Web at the address shown above.

THE BIOLOGICAL BULLETIN is indexed in bibliographic services including *Index Medicus* and MEDLINE, *Chemical Abstracts, Current Contents, Elsevier BIOBASE/Current Awareness in Biological Sciences,* and *Geo Abstracts.*

Printed on acid free paper,
effective with Volume 180, Issue 1, 1991.

POSTMASTER: Send address changes to THE BIOLOGICAL BULLETIN, Marine Biological Laboratory,
7 MBL Street, Woods Hole, MA 02543.

Copyright © 1999, by the Marine Biological Laboratory

Periodicals postage paid at Woods Hole, MA, and additional mailing offices.
ISSN 0006-3185

INSTRUCTIONS TO AUTHORS

The Biological Bulletin accepts outstanding original research reports of general interest to biologists throughout the world. Papers are usually of intermediate length (10–40 manuscript pages). A limited number of solicited review papers may be accepted after formal review. A paper will usually appear within four months after its acceptance.

Very short, especially topical papers (less than 9 manuscript pages including tables, figures, and bibliography) will be published in a separate section entitled "Research Notes." A Research Note in *The Biological Bulletin* follows the format of similar notes in *Nature.* It should open with a summary paragraph of 150 to 200 words comprising the introduction and the conclusions. The rest of the text should continue on without subheadings, and there should be no more than 30 references. References should be referred to in the text by number, and listed in the Literature Cited section in the order that they appear in the text. Unlike references in *Nature,* references in the Research Notes section should conform in punctuation and arrangement to the style of recent issues of *The Biological Bulletin.* Materials and Methods should be incorporated into appropriate figure legends. See the article by Lohmann *et al.* (October 1990, Vol. **179:** 214–218) for sample style. A Research Note will usually appear within two months after its acceptance.

The Editorial Board requests that regular manuscripts conform to the requirements set below; those manuscripts that do not conform will be returned to authors for correction before review.

1. ***Manuscripts.*** Manuscripts, including figures, should be submitted in quadruplicate, with the originals clearly marked. (Xerox copies of photographs are not acceptable for review purposes.) The submission letter accompanying the manuscript should include a telephone number, a FAX number, and (if possible) an E-mail address for the corresponding author. The original manuscript must be typed in no smaller than 12 pitch or 10 point, using double spacing (*including* figure legends, footnotes, bibliography, etc.) on one side of 16- or 20-lb. bond paper, 8 by 11 inches. Please, no right justification. Manuscripts should be proofread carefully and errors corrected legibly in black ink. Pages should be numbered consecutively. Margins on all sides should be at least 1 inch (2.5 cm). Manuscripts should conform to the *Council of Biology Editors Style Manual,* 5th Edition (Council of Biology Editors, 1983) and to American spelling. Unusual abbreviations should be kept to a minimum and should be spelled out on first reference as well as defined in a footnote on the title page. Manuscripts should be divided into the following components: Title page, Abstract (of no more than 200 words), Introduction, Materials and Methods, Results, Discussion, Acknowledgments, Literature Cited, Tables, and Figure Legends. In addition, authors should supply a list of words and phrases under which the article should be indexed.

2. ***Title page.*** The title page consists of a condensed title or running head of no more than 35 letters and spaces, the manuscript title, authors' names and appropriate addresses, and footnotes listing present addresses, acknowledgments or contribution numbers, and explanation of unusual abbreviations.

3. ***Figures.*** The dimensions of the printed page, 7 by 9 inches, should be kept in mind in preparing figures for publication. We recommend that figures be about 1 times the linear dimensions of the final printing desired, and that the ratio of the largest to the smallest letter or number and of the thickest to the thinnest line not exceed 1:1.5. Explanatory matter generally should be included in legends, although axes should always be identified on the illustration itself. Figures should be prepared for reproduction as either line cuts or halftones. Figures to be reproduced as line cuts should be unmounted glossy photographic reproductions or drawn in black ink on white paper, good-quality tracing cloth or plastic, or blue-lined coordinate paper. Those to be reproduced as halftones should be mounted on board, with both designating numbers or letters and scale bars affixed directly to the figures. All figures should be numbered in consecutive order, with no distinction between text and plate figures and cited, in order, in the text. The author's name and an arrow indicating orientation should appear on the reverse side of all figures.

Color: The Biological Bulletin will publish color figures and plates, but must bill authors for the actual additional cost of printing in color. The process is expensive, so authors with more than one color image should—consistent with editorial concerns, especially citation of figures in order—combine them into a single plate to reduce the expense. On request, when supplied with a copy of a color illustration, the editorial staff will provide a pre-publication estimate of the printing cost.

4. ***Tables, footnotes, figure legends, etc.*** Authors should follow the style in a recent issue of *The Biological Bulletin* in preparing table headings, figure legends, and the like. Because of the high cost of setting tabular material in type, authors are asked to limit such material as much as possible. Tables, with their headings and footnotes, should be typed on separate sheets, numbered with consecutive Roman numerals, and placed after the Literature Cited. Figure legends should contain enough information to make the figure intelligible separate from the text. Legends should be typed double spaced, with consecutive Arabic numbers, on a separate sheet at the end of the paper. Footnotes should be limited to authors' current addresses, acknowledgments or contribution numbers, and explanation of unusual abbreviations. All such footnotes should appear on the title page. Footnotes are not normally permitted in the body of the text.

5. ***Literature cited.*** In the text, literature should be cited by the Harvard system, with papers by more than two authors cited as Jones *et al.*, 1980. Personal communications and material in preparation or in press should be cited in the text only, with author's initials and institutions, unless the material has been formally accepted and a volume number can be supplied. The list of references following the text should be headed Literature Cited, and must be typed double spaced on separate pages, conforming in punctuation and arrangement to the style of recent issues of *The Biological Bulletin*. Citations should include complete titles and inclusive pagination. Journal abbreviations should normally follow those of the U. S. A. Standards Institute (USASI), as adopted by BIOLOGICAL ABSTRACTS and CHEMICAL ABSTRACTS, with the minor differences set out below. The most generally useful list of biological journal titles is that published each year by BIOLOGICAL ABSTRACTS (BIOSIS List of Serials; the most recent issue). Foreign authors, and others who are accustomed to using THE WORLD LIST OF SCIENTIFIC PERIODICALS, may find a booklet published by the Biological Council of the U.K. (obtainable from the Institute of Biology, 41 Queen's Gate, London, S.W.7, England, U.K.) useful, since it sets out the WORLD LIST abbreviations for most biological journals with notes of the USASI abbreviations where these differ. CHEMICAL ABSTRACTS publishes quarterly supplements of additional abbreviations. The following points of reference style for THE BIOLOGICAL BULLETIN differ from USASI (or modified WORLD LIST) usage:

A. Journal abbreviations, and book titles, all underlined (for *italics*)

B. All components of abbreviations with initial capitals (not as European usage in WORLD LIST *e.g., J. Cell. Comp. Physiol.* NOT *J. cell. comp. Physiol.*)

C. *All* abbreviated components must be followed by a period, whole word components *must not* (*i.e., J. Cancer Res.*)

D. Space between all components (*e.g., J. Cell. Comp. Physiol.*, not *J.Cell.Comp.Physiol.*)

E. Unusual words in journal titles should be spelled out in full, rather than employing new abbreviations invented by the author. For example, use *Rit Vísindafjélags Islendinga* without abbreviation.

F. All single word journal titles in full (*e.g., Veliger, Ecology, Brain*).

G. The order of abbreviated components should be the same as the word order of the complete title (*i.e., Proc.* and *Trans.* placed where they appear, not transposed as in some BIOLOGICAL ABSTRACTS listings).

H. A few well-known international journals in their preferred forms rather than WORLD LIST or USASI usage (*e.g., Nature, Science, Evolution* NOT *Nature, Lond., Science, N.Y.; Evolution, Lancaster, Pa.*)

6. ***Reprints, page proofs, and charges.*** Authors of articles in black and white (no color figures) receive their first 50 reprints (without covers) free of charge. Color reprints and additional black-and-white reprints may be purchased; authors will receive order forms. Reprints normally will be delivered about 2 to 3 months after the issue date. Authors (or delegates for foreign authors) will receive page proofs of articles shortly before publication. They will be charged the current cost of printers' time for corrections to these (other than corrections of printers' or editors' errors). Other than these charges for authors' alterations, *The Biological Bulletin* does not have page charges.

Reference: *Biol. Bull.* **196:** 1–17. (February, 1999)

Dynamics of Gastrovascular Circulation in the Hydrozoan *Podocoryne carnea:* the One-Polyp Case

STEVE DUDGEON[1,*], ANDREAS WAGNER[2], J. RIMAS VAIŠNYS[3,4], AND LEO W. BUSS[3,5]

[1]*Department of Biology, California State University, Northridge, California 91330-8303;* [2]*Department of Biology, The University of New Mexico, 167A Castetter Hall, Albuquerque, New Mexico 87131-1091;* [3]*Departments of Ecology and Evolutionary Biology,* [4]*Electrical Engineering,* [5]*Geology & Geophysics, Yale University, New Haven, Connecticut 06520*

Abstract. Time-lapse video microscopy and image analysis algorithms were used to generate high-resolution time series of the length and volume of a single hydrozoan polyp before and after feeding. A polyp of *Podocoryne carnea* prior to feeding is effectively static in length and volume. At 20°C, feeding elicits 8-millihertz (mHz) oscillations in polyp length and volume. A polyp connected to a colony by a single stolon displayed an abrupt transition from low-amplitude, 8-mHz oscillations to large-amplitude, 6-mHz oscillations at 1.5–2 h after feeding. The transition was preceded by a substantial decrease in polyp volume and increase in length which coincided with the export of food items from the digestive cavity of the polyp into the colonial gastrovascular system. In contrast, 8-mHz oscillations of a polyp isolated from a colony continued for 12.7 h after feeding, at which time particulates from the digestive cavity were exported into the hydrorhiza and a 4-mHz subharmonic became briefly dominant. Regular oscillatory behavior was terminated by regurgitation at comparable intervals post-feeding in coupled and isolated polyps. These observations are compatible with the hypothesis that the presence of nutrients in the digestive cavity induces polyp oscillations and that release of nutrients into the gastrovascular system similarly induces unfed polyps to oscillate, thereby distributing the contents of the fed polyp throughout the colony.

Introduction

The gastrovascular system is the only physiological system of hydrozoans whose behavior is known to be manifested colonywide. The system transports fluid between the digestive cavities of polyps through the lumens of the endodermal canals between polyps, resulting in the colonywide exchange of nutrients and dissolved gases. Recent studies have shown that perturbation of gastrovascular transport has marked effects upon colony ontogeny and life history. Specifically, the production of polyps and the frequency of stolon branching and anastomosis are accelerated, and the age at which medusae are produced is altered, in *Podocoryne carnea* (Sars, 1846), by perturbations of energetic metabolism that reduce the volumetric flow rate through stolons (Blackstone and Buss, 1992, 1993; Blackstone, 1997, 1998). Moreover, surgically manipulating the relative sizes of stolons within a colony of *Hydractinia symbiolongicarpus* (Buss and Yund, 1989) is sufficient to stably convert a runner-like colony into a sheet-like colony and *vice versa* (Dudgeon and Buss, 1996).

Control of vascular morphology by response to internal hydromechanical signals is increasingly well-known in vertebrate systems (Bevan *et al.*, 1995). Murray (1926) proposed that tree-like vascular designs minimize the total energy expended in propelling the fluid and maintaining the tissues. The predicted optimum is one in which the wall shear stress is constant throughout (Zamir, 1977; Sherman, 1981; LaBarbera, 1990). Several genes are known to be differentially expressed upon perturbation of wall shear stress in a fashion that adjusts vessel radii to values that restore a systemwide constant shear stress (Bevan *et al.*, 1995). Similar design optimizations and flow-dependent gene expression may underlie the response of hydrozoan colonies to altered patterns of gastrovascular transport. However, the task of identifying the relevant hydromechanical features and the patterning elements that respond to

Received 20 February 1998; accepted 25 November 1998.

* E-mail: steve.dudgeon@csun.edu

such features requires an understanding of how fluid circulates within a colony.

Unlike the vertebrates, which have a vascular system with a single pump that propels a unidirectional flow of fluid within a dichotomously branching tree, a hydrozoan colony can be composed of thousands of individual polyps connected to one another by a complex array of anastomosing stolons within which fluid may flow alternately in any direction. Understanding how an array of pumps and vessels generate a time- and space-varying distribution of metabolites and hydrodynamic signals is a considerable challenge. Our approach has been to characterize the dynamics of a single polyp, in the hope that the behavior of an isolated unit will prove simple enough to allow us to develop a mathematical model. Polyp models, when coupled by suitably developed models of the stolon, may eventually permit systematic analysis of the consequences of the arrangement of polyps in various geometries. To this end, we have documented the feeding behavior of single polyps of the colonial hydroid *Podocoryne carnea*. We present time series of the length and volume of a single isolated polyp and contrast this behavior with that of a single polyp coupled to a colony, both before and after feeding.

Materials and Methods

Animals and their maintenance

The hydrozoan *Podocoryne carnea* produces encrusting colonies of a typical filiform form. Our observations are restricted to young colonies bearing only gastrozooids (hereafter called polyps). Polyps extend upright atop the stolons, which adhere to the substratum. The polyp is the sole component of the system that can exchange fluid with both the external medium (*via* the mouth) and the rest of the gastrovascular system (*via* a contractible opening between its gastric cavity and the stolon or stolons coextensive with it). Exclusive of epithelial conductance, the gastrovascular system is the only known colonywide conducting system in this species (*i.e.*, neither a nerve net nor muscle fibers occur in the stolons; Stokes, 1974; Schierwater *et al.*, 1992).

All colonies of *P. carnea* were asexually propagated from a single clone (P34) collected at the Peabody Museum Field Station, Guilford, Connecticut, in September 1989. Colonies were grown on the surface of either glass slides (25 × 20 × 1 mm) or coverslips (484 mm^2) in 40-l aquaria containing artificial seawater (REEF CRYSTALS, Aquarium Systems, Mentor, Ohio) at 18 ± 1°C. Animals were fed to repletion twice per week on a diet of 3- to 5-day-old brine shrimp (*Artemia salina* (Linnaeus, 1758)) nauplii. Colonies were propagated asexually by surgically explanting single polyps onto the surface of a glass slide or coverslip. Explanted polyps were held in place by a loop of thread until the growth of stolons attached them to the surface.

Observational protocol

Colonies were not fed for 2 days prior to treatment and subsequent observation. Polyps growing on the edge of a glass slide were standardized to lengths of ± 100 μm, and stolons were severed as necessary to establish two treatments. For observation of isolated polyps, all stolons connecting the chosen polyp to the colony were severed so as to retain a segment of stolon roughly 800 μm long with two blind ends and the polyp positioned near the center. Severed stolons heal and become occluded instantly (Berrill, 1953). For observations of coupled polyps, all but one stolonal connection to the colony was severed. In this case, the polyp was situated about 300–400 μm from the blind end of the stolon. The size of the colony varied between replicates, but was in all cases vastly larger than the internal volume of the chosen polyp.

Following surgery, the colony was maintained under standard conditions for 12 h prior to the start of observations. The colony to be observed was then placed within a temperature-controlled chamber in 10 ml of 0.45-μm filtered seawater at 20 ± 0.1°C and viewed at 100× using a Zeiss Axiovert 35 inverted microscope. The polyp was positioned so as to provide a longitudinal profile extending from the mouth to the base of the polyp. Illumination was arranged to optically filter the tentacles, leaving only the body column visible (*i.e.*, the field was flooded with light sufficient to render the polyp outline black and the remainder of the field uniformly white). Polyp behavior was videotaped, typically for 1.5–2 h prior to feeding, using a Dage MTI camera connected to the microscope and a videocassette recorder. The polyp was then removed from the chamber, hand-fed a single newly hatched brine shrimp nauplius, returned to the chamber immediately after ingesting the food item, and videotaped for the following 24 h.

Image analysis

Images were recovered from the videotaped record of polyp behavior using a PCVISION frame grabber and OPTIMAS image analysis software. A series of programs, written in the OPTIMAS macro language, were used to extract polyp length and diameter at multiple points along the longitudinal axes from each binary image of a polyp's outline. Figure 1 and its legend illustrate the steps by which length and width measurements are generated from an image. Polyp volume was estimated from these measurements of polyp length and diameters, using the extended Simpson's rule (Press *et al.*, 1992). The macros used and an extensive discussion of the reasoning which led to their development are available at http://www.csun.edu/~sd51881.

There are three sources of error in the procedures we employ: (1) errors associated with sampling the coordinates that compose the outline of the polyp, (2) errors associated with the assumption that the polyp is rotationally symmetric

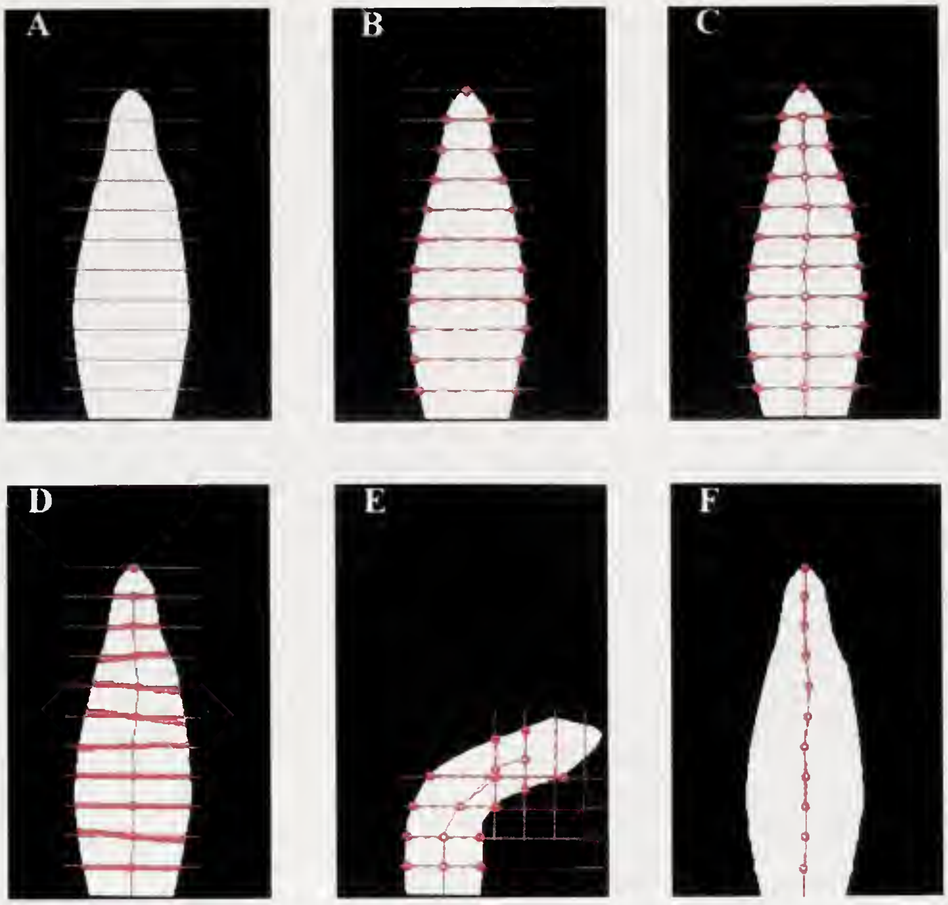

Figure 1. Steps used by image-processing algorithm following inversion of the binary image (black pixels to white and *vice versa*). (A) Establishing 11 evenly spaced transects along the longitudinal polyp axis; (B) detecting and marking the edge of the polyp at both ends of each transect line; (C) determining the midpoint of each transect line along the body column with respect to the marked edges of the polyp and connecting the midpoint segments along the longitudinal polyp axis; and (D) establishing the line normal to the midpoint-to-midpoint line segment at each transect—the length of these normal lines constitute the diameter measurements. (E) Example illustrating the switch between horizontal and vertical scans by the algorithm when a bend of the polyp exceeding 53° is detected. (F) Fitting a 4th order polynomial function to the set of midpoint coordinates for determining polyp length.

about the axis of the focal plane, and (3) errors associated with bending of the polyp outside the focal plane. The first two sources of error were estimated from an analysis of sampling efficiency and by extensive experimentation on volume fluxes observed in colonies of known stolonal volume; they constitute an error of $< 5\%$, which corresponds to an error in estimates of volume amplitude of ± 0.7 nl. The relevant experiments and data upon which this error estimate is based are available at http://www.csun.edu/~sd51881. With respect to the remaining source of error, our algorithms cannot detect the bending of polyps outside the focal plane. Such bends, however, constituted only a small fraction of the overall record (5.9% and 2.6% in the coupled and isolated records, respectively). These data points are spurious and are denoted as such by tickmarks along the abcissa in plots of the time series we present below.

Time-series analysis

Using the algorithms described above, one of the four replicates in each treatment was analyzed to generate a high-resolution time series of polyp length and estimated volume. Measurements were made at 8-s intervals from the onset of feeding to 436:09 and 1474:12 min:s post-feeding for coupled and isolated treatments, respectively.

Time-series data were analyzed using Mathematica (Version 2.2, Wolfram Research, Inc.) on a Hewlett-Packard Apollo 9000 workstation. From each raw time series of length and volume, we calculated a low- and high-pass-filtered version (Priestley, 1981). A low-pass-filtered time series is one from which short-term fluctuations have been removed. The low-pass-filtered time series was computed as a sliding running average, using a uniform window spanning 201 points and centered about the point in question. The (complementary) high-pass-filtered time series was obtained by subtracting the low-pass-filtered series from the original series, giving a series with a mean of zero from which long-term drifts had been removed.

To detect trends within the time series, the high-pass-filtered series was further analyzed by examining a succession of windowed Fourier transformations. The entire high-pass-filtered time series was divided into segments ("windows") comprising 20 min of observational data, with two consecutive windows overlapped by 15 min. Fourier coefficients were estimated for each of the windows separately using a Fast Fourier transformation, and the power spectrum was calculated.

Efficient techniques for analyzing time-series data depend on having a complete time series that has been sampled at equal time intervals. If data points are missing, an error proportional to the number of missing points is introduced into the estimation of the series spectrum. In the series analyzed here, missing observations are rare; they contribute 1.90% and 0.39% to the variability in the spectrum in the coupled and isolated treatments, respectively.

"Aliasing," a frequent problem in the spectral analysis of discretely sampled time series (Priestley, 1981), does not appear to bias the spectra we present below. This conclusion was reached on the basis of an exploratory analysis in which data sampled at a higher temporal resolution did not display any qualitative changes in the spectral composition. The observation that none of the spectra derived at the chosen sampling density have any peaks in the high-frequency range support this conclusion.

Repeatability

In addition to the high-resolution time series, data were collected from the remaining three replicate video records for each treatment at the same 8-s resolution for 20-min intervals to determine whether patterns observed in the high-resolution analysis were repeatable. These 20-min intervals were chosen haphazardly, with the added criterion that the images of the polyp were of good quality with respect to contrast, brightness, and definition of the outline against the background. In both treatments, power spectra and amplitudes of length and volume oscillations were calculated for at least 1 (and up to 5) 20-min intervals in both the pre- and post-export phases of digestion for each replicate polyp.

From each power spectrum, we identified the frequency of each peak and calculated its signal-to-noise ratio as the ratio of peak height to the maximum height of noise in the plot (*i.e.*, the highest point remaining on the landscape after excluding the set of peaks). We report the frequency and the signal-to-noise ratio for only those frequencies > 3.3 and ≤ 10 mHz (millihertz). The lower frequency limit is set by the duration of the record, and the higher limit is set to avoid reporting bends and contractions as frequency signals. The upper limit of a 10-mHz frequency also excludes harmonics (if present) at twice and three times the principal frequency.

To estimate amplitude, length or volume measurements from the same 20-min window were subdivided into four segments of 5 min each (*i.e.*, approximately 2 oscillation cycles). Each of these shorter segments was viewed as an unordered sample of length or volume measurements. The difference between length (volume) at the 97.5 percent quantile and length (volume) at the 2.5 percent quantile in a segment was used as an estimate of amplitude. The mean amplitude of the four 5-min segments was used as the amplitude of length (volume) for the 20-min interval. This measure not only reflects short-term polyp oscillations, it also effectively excludes trends in length (volume) within the window and the effect of short polyp contractions.

Shape variation

We do not present extended time series of the width of each polyp cross-section. Rather, to characterize changes in polyp shape, 25 widths along the body column of the polyp were measured every 8 s for two 15-min intervals for each treatment. The first interval was taken at 90 min post-feeding in both treatments and the second at about 180 and 700 min post-feeding in the coupled and isolated treatments, respectively. The coefficient of variation of each of the widths was calculated and plotted against the position of that width along the longitudinal polyp axis.

Stolon observations

A series of observations were made on stolon behavior in an attempt to correlate features of the polyp time series with events observed within the stolons. The rationale for doing so is that the mouth of the polyp remains closed over the time periods analyzed here, hence any changes in polyp volume (exclusive of experimental error) must represent exchange with the stolon. Three replicate records were made of both isolated and coupled treatments, established as described above, but with the focal plane established adjacent to the polyp-stolon junction at 400×. We do not present detailed time series for stolonal oscillations here (see Buss and Vaišnys, 1993); rather, we use these videotapes to describe events observed in stolons at times corresponding to principal features in the polyp record.

These descriptions are supplemented with limited measurements. From the videotapes, we measured the onset of oscillations in stolon diameter after feeding and the time at which the polyp initiated export of particulates from its digestive cavity into the stolon. In addition, from frame-grabbed images we measured lumen diameters, amplitudes and frequency of stolon oscillations for three consecutive cycles preceding and following export. Measures were obtained before and after feeding, but prior to export, at 30 min post-feeding in the stolons of coupled polyps and at 30 and 150 min post-feeding in the stolons of isolated polyps. Post-export measures were obtained at 150 min post-feeding in the coupled treatment and at 1 h after export in the isolated treatment. To facilitate comparisons between stolons with different diameters (Blackstone and Buss, 1992), stolon measurements were standardized to measures of the periderm-to-periderm width.

Results

Pre-feeding behavior and return to pre-feeding conditions

Prior to feeding, polyps behaved similarly in both isolated and coupled treatments. A representative record appears in Figure 2A, showing that polyp length and volume remained constant prior to feeding, exclusive of occasional volume-conserving contractions in length (*e.g.*, at $t = -22$ min). Feeding was terminated by regurgitation of undigested materials, which occurred at 18–22.5 h post-feeding in both treatments. After regurgitation, the polyp regained near-original values of length and volume (Fig. 2B; see also min 1350 in Fig. 6B). Contraction pulses and asymmetric polyp bends occurred frequently before and after regurgitation.

Polyps connected to a colony

The raw time series for both polyp length and volume is shown in Figure 3. The presentation of the time series is simplified by treatment of three different intervals:

0–15 minutes post-feeding. After ingesting the brine shrimp, the polyp contracted from about 950 to 400 μm in length, and its volume increased from about 7 to 18 nl (*cf.* Figs. 2A and 3). In the first 15 min following feeding, the polyp displayed a trend of increasing length and decreasing volume, but otherwise lacked regular behavior. At 8 min post-feeding, volume decreased sharply, from about 18 to 14 nl, coinciding with the repositioning of the brine shrimp nauplius within the digestive cavity. Coincident with the rapid decrease in volume was an apparent stabilization of volume (at *ca.* 12–14 nl) and length (at *ca.* 550 μm). Regular oscillations in both polyp length and volume began shortly after this repositioning.

15–125 minutes post feeding. The oscillatory behavior, as well as the plateau in length and volume established by 15 min post-feeding, was retained until about 100 min post-feeding. Throughout this period of oscillation, changes in polyp shape were largely restricted to variation in the width of the hypostomal region of the polyp (Fig. 4A). At 100 min, regular oscillations were interrupted as volume underwent another substantial decrease, dropping from about 14 nl to a minimum of about 5 nl at 110–120 min, only to increase to 8 nl at 125 min.

Prior to the volume decrease at 100 min, the polyp was opaque. In the interval between 95 and 105 min, the polyp became increasingly transparent, indicating an export of contents of the digestive cavity. Since no material was seen leaving the mouth, the exchange must have occurred between the polyp and the colony gastrovascular system.

125–436 minutes post-feeding. The rapid decline in volume immediately preceding this interval was followed by a change in length dynamics and a return to regular oscillatory dynamics in volume. Length, which had reached a plateau at 550 μm, began to increase to a new plateau at 750 μm. The volume oscillations commencing at 125 min were of substantially greater amplitude than those which preceded it, with changes in volume often exceeding 100% with each cycle. These pronounced oscillations were accompanied by a change in the regions of the polyp showing the greatest variation in width. In contrast to the preceding interval, during which most shape change was restricted to the hypostome, the large-amplitude oscillations characterizing this time interval displayed the largest coefficient of variation in the mid-gastric region of the body column (Fig. 4B).

Large-amplitude volume oscillations continued until about 225 min, after which they gradually declined in amplitude from up to 8 nl at the beginning of the interval to less than 2 nl at the end of the record. Polyp length over the interval spanning 170–200 min showed a gradual lengthening trend from 750 to 900 μm, after which the plateau at 900 μm in length persisted for several hours. Both contraction pulses and polyp bending became increasingly common as the amplitude of volume contractions attenuated.

Oscillations in both length and volume of the polyp throughout the feeding cycle were characterized by a single dominant frequency component (Fig. 5). The dominant component, however, shifted from an initial dominant frequency of about 8 mHz (corresponding to 1 cycle every 2 min) to 6 mHz at 125 min. This shift to the lower frequency between 125 and about 200 min coincided with the large-volume oscillations of the polyp (*cf.* Fig. 3). Weak harmonics of two and three times the dominant frequency were also present in the length spectrum during the first 100 min. Subharmonics were not evident. Because most of the volume spectrum was dominated by the massive oscillations between 125 and 200 min, oscillations before and after this period, although present, left only faint traces in the spectrum of Figure 5. No appreciable contributions to either length or volume oscillations came from frequencies greater than 24 mHz.

The frequency and amplitude of oscillations over the course of a feeding cycle were repeatable with respect to both length and volume among replicates of the coupled polyp treatment (Table 1). For all replicates, a single frequency predominated both before and after the export of the contents of the gastric cavity. Moreover, the predominant

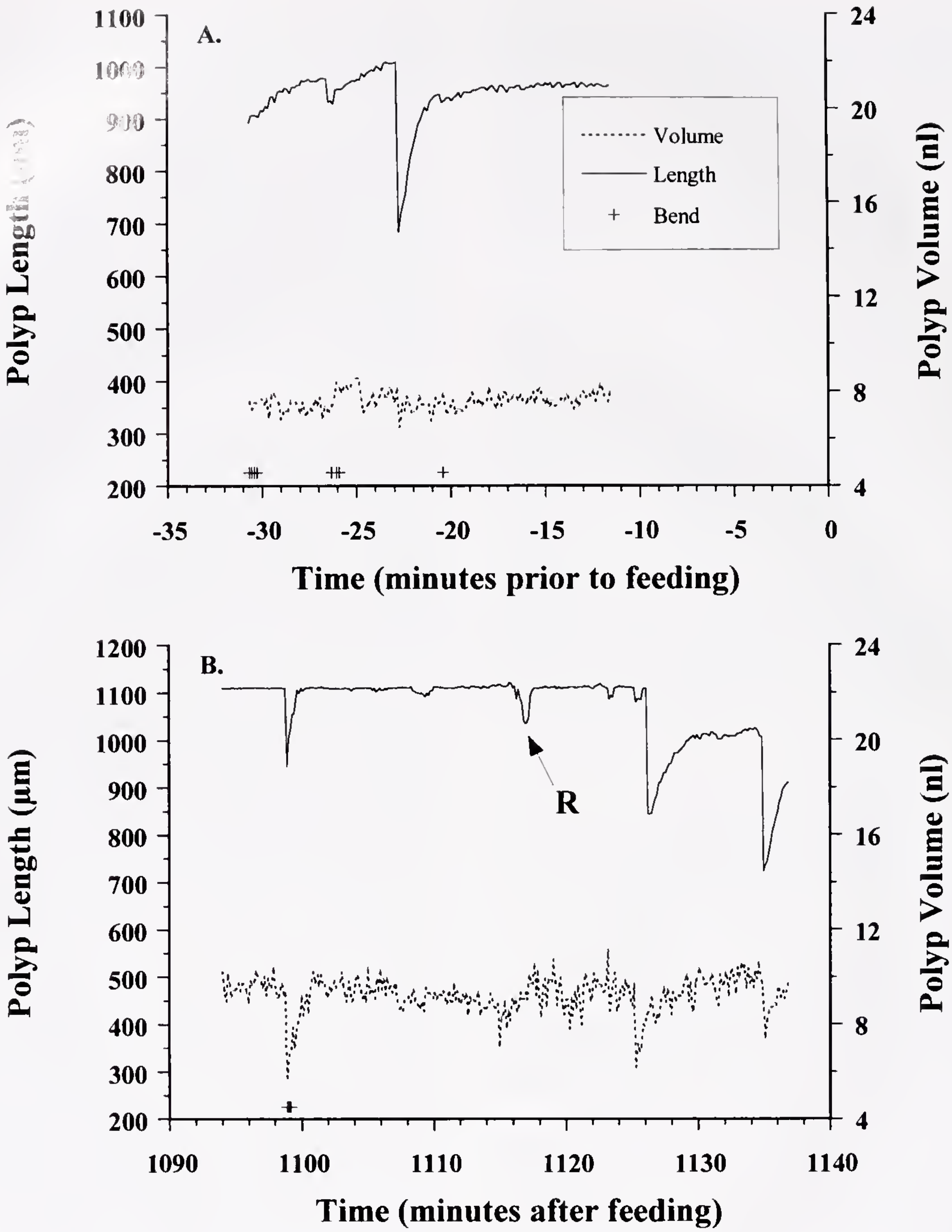

Figure 2. Time series of length (solid line) and volume (dashed line) dynamics of a polyp coupled to a colony by one stolon (A) prior to feeding and (B) at the end of digestion showing the return to initial conditions. R denotes regurgitation. Tickmarks along the abcissa represent spurious data points (see text for further discussion) corresponding to rapid bends drawing the polyp outside the focal plane. Large-amplitude variations in length that are not accompanied by a tickmark represent contraction pulses and are not spurious.

frequency shifted from the pre-export level (range of means among replicate polyps: for length, 8.3–9.1 mHz; for volume, 7.9–9.1 mHz) to a lower post-export level (range of means: length, 7.1–7.5 mHz; volume, 6.6–7.5 mHz) in all replicate polyps.

Polyps isolated from a colony

The raw time series for both polyp length and volume (Fig. 6) is conveniently summarized in three intervals:

0–15 minutes post-feeding. As in the case of the coupled

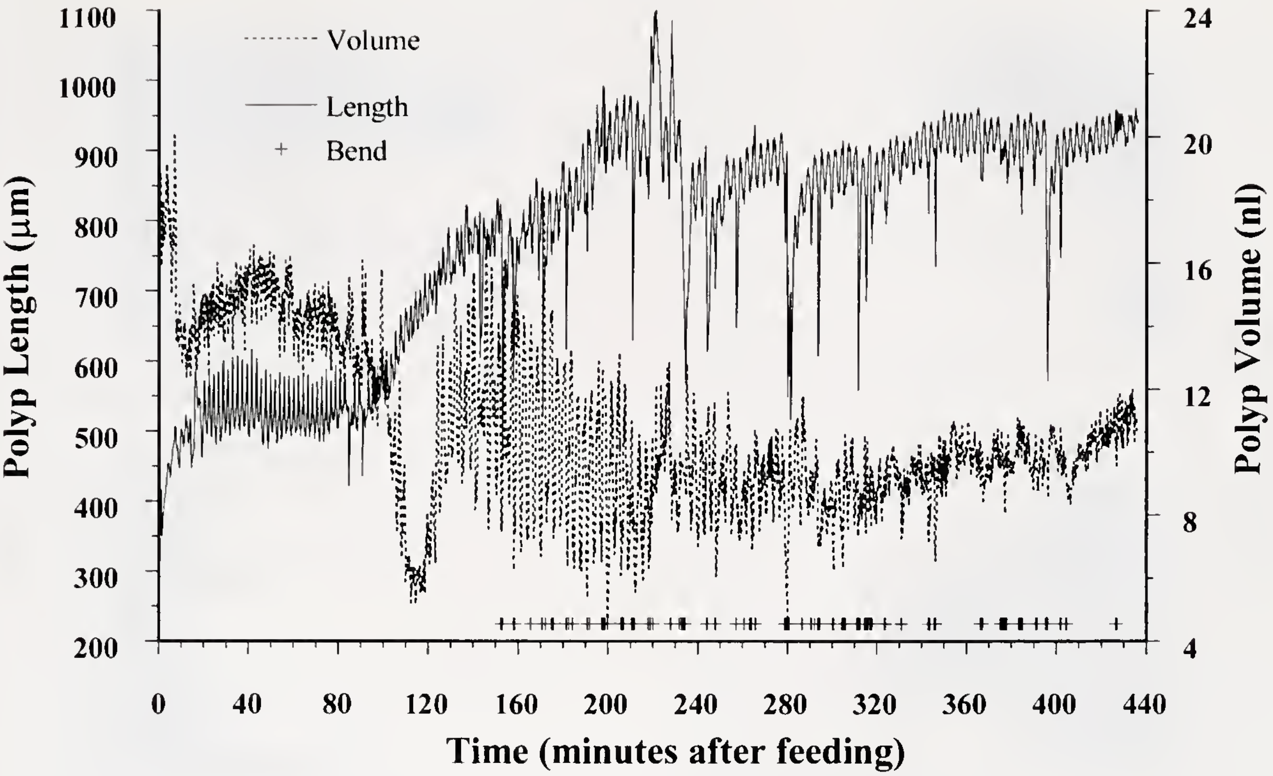

Figure 3. Time series of length (solid line) and volume (dashed line) dynamics of a polyp coupled to a colony by one stolon from 0 to 436.15 min after ingestion of a single brine shrimp nauplius. Tickmarks along the abcissa represent spurious data points (see text for further discussion) corresponding to rapid bends drawing the polyp outside the focal plane. Large-amplitude variations in length that are not accompanied by a tickmark represent contraction pulses and are not spurious.

polyp, feeding resulted in a contraction in polyp length and an increase in volume (not shown). A detailed record of the onset of oscillations immediately after ingestion from a replicate isolated polyp record is shown in Figure 7. As in the coupled treatment (Fig. 3, min 0–20), behavior was irregular for a short time after feeding, and regular oscillations began about 10–15 min post-feeding.

15–763 minutes post-feeding. Like the coupled treatment, the isolated polyp increased in length and volume after feeding (Fig. 6A). As in the coupled case, volume reached a plateau about 40 min. after feeding, whereas the plateau in length was not attained until roughly 150 min post-feeding. The variation in polyp shape 90 min after feeding mirrors that characterizing the early post-feeding period in the coupled treatment, with the greatest variation in polyp width occurring in the hypostome (Fig. 4C). In the isolated case, however, shape also varied substantially at the base of the polyp. Figure 8 compares widths at the polyp base during the period of polyp lengthening (Fig. 8A) with that occurring after the plateau in length has been reached at 150 minutes post-feeding (Fig. 8B). The latter record reveals that the polyp base alternated every other length cycle in maximal and minimal width, which made every other length cycle of greater amplitude (Fig. 8B).

Next, for about 9 h the polyp displayed a trend of gradually increasing length and gradually decreasing volume (Fig. 6A). Regular oscillations in length and volume continued for the entire period. This record is in marked contrast to the coupled treatment, where similar behavior terminated abruptly at about 110 min post-feeding with a large decrease in volume and the onset of large-amplitude volume oscillations. Neither rapid declines in volume nor large-amplitude volume oscillations comparable to those in the coupled case were observed in the isolated case.

763–1474 minutes post-feeding. 763 minutes after feeding, the polyp underwent a 7-min interval of rapid, repeated length contractions, accompanied by variation in volume dynamics (Fig. 6B). From 770 to 790 minutes post-feeding, both length and volume regained values comparable to those that preceded the event at 763 min. The digestive cavity of the polyp had previously been largely opaque; after the event, regions of the cavity became increasingly transparent. This change coincided with a marked alteration in the shape of the polyp as it oscillated. In Figure 9 these

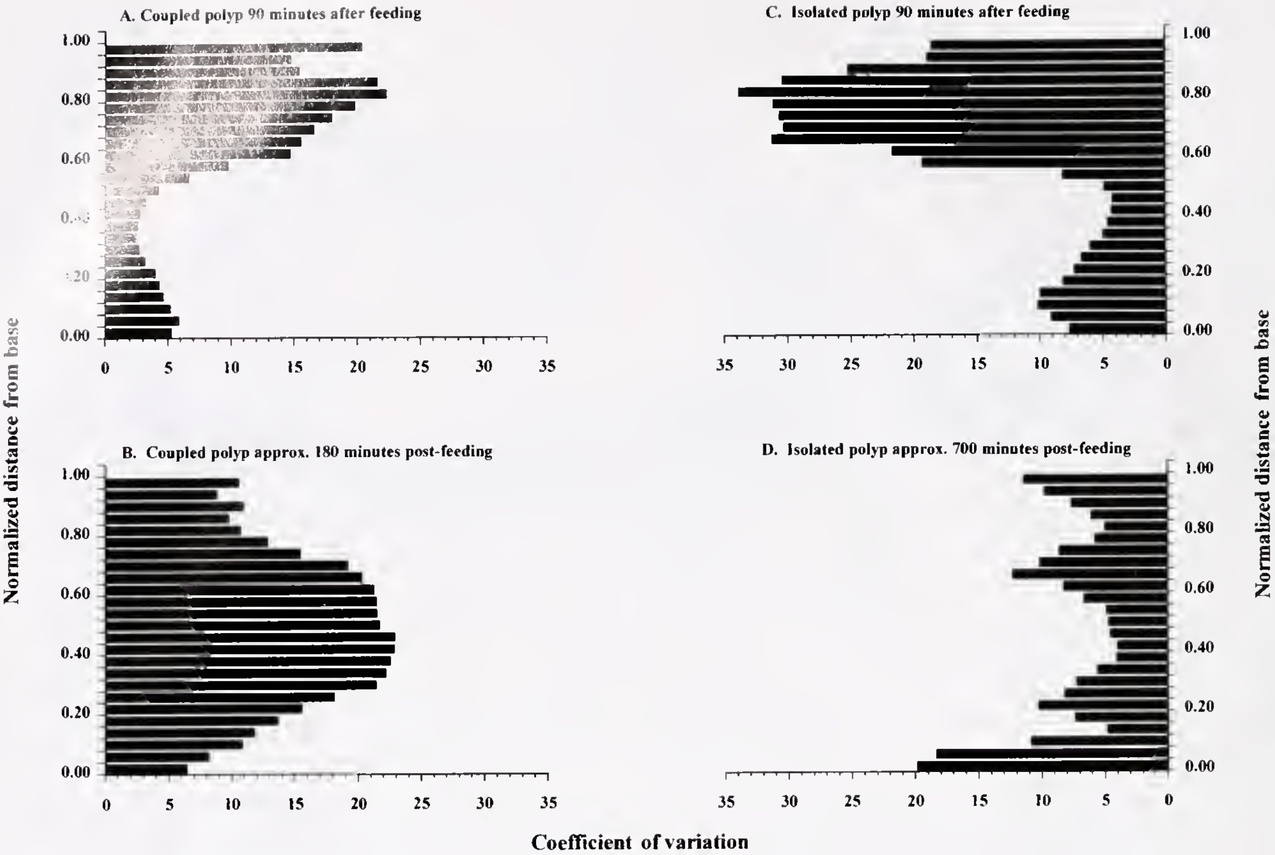

Figure 4. Coefficients of variation from samples of width measures taken every 8 s over a 15-min timecourse at each of 25 loci along the longitudinal axis of a polyp (polyp-stolon junction at 0.00, mouth of polyp at 1.00) for (A) a coupled polyp 90 min after feeding, (B) a coupled polyp 180 min after feeding, (C) an isolated polyp 90 min after feeding, and (D) an isolated polyp 700 min after feeding.

polyp shapes are superimposed on the corresponding record of length and basal width. With every other length maxima the polyp alternated between maintaining a bolus of fluid in the center of the digestive cavity and maintaining two such boli—one in the subtentacular region and one in the basal body column—separated by a constriction in the polyp's center. The same pattern of oscillation is evident in Figure 4D. Variation was maximal in the basal and subtentacular regions of the body column during this interval.

The polyp continued to display regular oscillations in length and volume for an additional 10 h after the event at 763 min (Fig. 6B). Just as in the coupled polyp, contraction pulses and polyp bending became increasingly common in later stages of the record. At 1338–1343 min the polyp regurgitated undigested materials through the mouth and regained a length and volume comparable to those observed prior to feeding (Fig. 6B). Regurgitation in the isolated treatment differed from that in the coupled case (Fig. 2B). In the isolated case, the return to initial conditions was far more abrupt.

The isolated polyp showed a dominant, and remarkably stable, 8-mHz oscillation frequency and a weaker harmonic at 16 mHz that persisted throughout the feeding cycle (Fig. 10). A subharmonic of ~ 4 mHz (*i.e.*, corresponding to events that occurred every other cycle) emerged nearly 150 min after feeding, at the point when basal widths began alternating every other cycle. This subharmonic coexisted with the dominant frequency for the duration of the record. In the period following the event at 763 min (while the polyp displayed movement of fluids between the subtentacular and basal regions of the body column with every other cycle; Fig. 9), the 4-mHz frequency became dominant for 200 min. No appreciable contributions to either length and volume spectra came from frequencies greater than 24 mHz.

The principal features of behavior in isolated polyps were repeatable among replicates (Table I). The principal oscillation frequency varied among replicates (range: 6.7 to 9.0 mHz) but, unlike the frequency in the coupled-polyp treatment, did not shift consistently downward during the post-feeding period. Also, subharmonic frequencies were detected only in the isolated polyps. Finally, the amplitude of

a) Sliding Window Spectrum (Length)

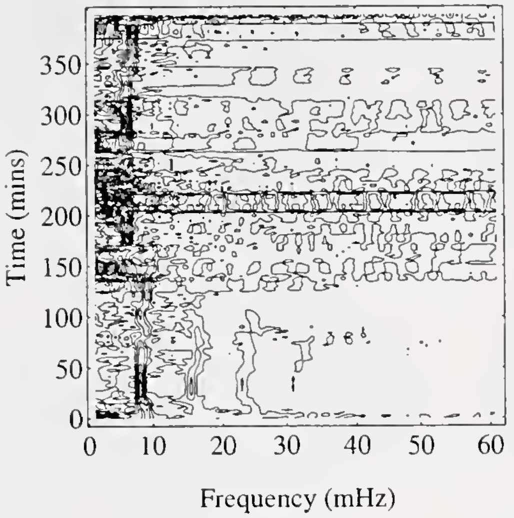

b) Sliding Window Spectrum (Volume)

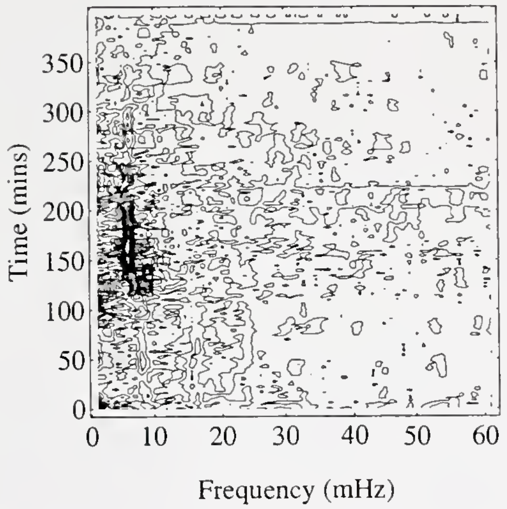

Figure 5. Contour plot, based on the time-series data in Figure 3, of sliding window spectral analysis of (a) length and (b) volume of the coupled polyp. Abcissa represents frequency of oscillation, ordinate represents the sliding window of time (in minutes), and contour lines represent the height of peaks (coming out of the page) that signify the relative importance of a given frequency underlying the cyclic behavior.

volume oscillations was consistently much lower than the larger amplitude volume oscillations characteristic of post-export coupled treatments. (Fig. 3; Table 1).

Stolon observations

Feeding was associated with a closing of the polyp-stolonal junction and a momentary cessation of gastrovascular flow in colonies that had been experiencing fluid movement prior to feeding. As the polyp lengthened after the initial contraction, the polyp-stolon junction reopened. The stolon lumen began to oscillate in diameter at 13 and 8 min (on average) in the coupled and isolated treatments respectively: export into the stolon accompanied polyp contraction and import into the polyp accompanied polyp lengthening. The interval between feeding and the onset of stolonal oscillations did not significantly differ from the interval between feeding and the onset of regular oscillations in polyp length and volume (Student's t test; $t = 0.27$, df = 8, $P = 0.80$).

Stolon observations made after this initial period are most conveniently treated separately for the two experimental treatments.

Polyp connected to colony. The frequency of stolon contractions in the first hour after feeding did not differ significantly from the frequency of polyp oscillations (Table II, $t = 0.23$, df = 5, $P = 0.83$). Neither was a significant difference detected in the average lumen diameter of stolons before feeding and in the first hour after feeding (Table II; Student's t test; lumen diameter, $t = 1.19$, df = 4, $P = 0.30$). However, after feeding, stolons contracted significantly more frequently and with greater amplitude than they did before feeding (amplitude, $t = 3.13$, df = 4, $P = 0.03$; frequency, $t = 17.43$, df = 4, $P < 0.01$). Despite the observed export of fluid from the polyp into the stolon, export of particulate matter was only rarely observed in the stolon at this time; on the few occasions when particles were evident, they were few and did not exceed 2 μm in diameter.

The period of interruption in polyp oscillations and decrease in volume, seen at 100 min in the coupled-polyp record, was correlated with events observed on average at 79 min in replicate stolon records. In each stolon replicate, the stolon became greatly expanded with fluid imported from the colony, and the contents of the fed polyp were observed leaving the polyp in a dense stream of large particles (up to 100 μm in length and 15 μm in diameter). Stolonal oscillations changed markedly in the period after export: they were smaller in amplitude and lower in frequency than before export, and the average lumen diameter of the stolens was larger (Table II; lumen diameter $t = 2.88$, df = 4, $P = 0.04$; amplitude, $t = 11.46$, df = 4, $P < 0.01$; frequency, $t = 6.11$, df = 4, $P < 0.01$). Notably, the frequency of stolon oscillations following export mirrored the shift in the frequency of polyp oscillations. Before export, both polyps and stolons oscillated at a frequency of ~8 mHz, whereas after export both oscillated at a frequency of ~6 mHz—the same frequency as in stolons prior to feeding.

Polyp isolated from colony. As in the coupled case, stolon oscillations did not significantly differ in frequency from those observed in polyps ($t = 0.44$, df = 5, $P = 0.68$). Similarly, stolon oscillations prior to export were more frequent and of greater amplitude than stolon oscillations

Table I

Repeatability of length and volume dynamics for coupled and isolated polyps based on observing three replicate polyps in each treatment; values represent means ± standard errors (in parentheses)

	Polyp Length					Polyp Volume				
Pre- or Post- Export	Amplitude (μm)	Principal Frequency (mHz)	Signal : Noise ratio	Subharmonic (mHz)	Signal : Noise ratio	Amplitude (nl)	Principal Frequency (mHz)	Signal : Noise ratio	Subharmonic (mHz)	Signal : Noise ratio
Coupled polyps										
Pre	84.42 (3.71)	8.57 (0.27)	3.69 (1.13)	—	—	4.36 (1.98)	8.30 (0.41)	2.80 (0.69)	—	—
Post	92.43 (18.33)	7.27 (0.13)	2.66 (0.70)	—	—	6.19 (1.59)	7.06 (0.25)	3.31 (0.55)	—	—
Isolated polyps										
Pre	93.56 (3.95)	7.89 (0.67)	5.36 (1.04)	4.14*	2.60*	1.54 (0.08)	7.84 (0.51)	2.08 (0.12)	3.95† (0.16)	2.28 (0.12)
Post	65.11 (8.43)	7.50 (0.42)	2.11 (0.31)	5.14 (0.77)	2.30 (0.13)	1.84 (0.24)	7.93 (0.64)	2.40 (0.86)	3.32 (0.01)	2.08 (0.33)

Pre- and post-export phases of coupled polyps were distinguished visually on the basis of shape variation of the polyp body column while it was oscillating (see Fig. 4a,b); those of isolated polyps were inferred from the coexistence of strong subharmonic frequencies in length or volume and time of occurrence (see text and Fig. 9). Signal-to-noise ratio represents a ratio of a peak height of a frequency to the maximum height of noise in the spectrum.

* Values lacking standard errors indicate that only one replicate displayed a subharmonic.

† Value was based on two replicates instead of three.

prior to feeding, but no difference in average lumen diameter was detected (Table II; lumen diameter $t = 0.42$, df = 4, $P = 0.69$; amplitude, $t = 3.26$, df = 4, $P = 0.03$; frequency, $t = 5.10$, df = 4, $P < 0.01$). Unlike the coupled treatment, however, these oscillations displayed similar average lumen diameters and similar amplitudes and frequencies for 10+ hours post-feeding (Table II). Continuous observation of stolons showed that the isolated polyp, despite the continued fluid exchange with the stolon, exported little particulate matter into the stolon over this extended interval. Three replicate isolated stolon films showed export of a dense stream of large particulates at an average time of 807 min (13.5 h) after feeding, an interval comparable to the event observed in the high-resolution isolated polyp record at 763 min (12.7 h). The average lumen diameter of the stolon after export was not significantly different from that before export, but the oscillations were of smaller amplitude (*i.e.*, stolons remained expanded and filled with particulates throughout oscillation cycles; lumen diameter $t = 1.14$, df = 4, $P = 0.32$; amplitude, $t = 8.40$, df = 4, $P < 0.01$). After export, the frequency of oscillation of the stolon was comparable to that prior to feeding, as well as to that of the stolon in the coupled polyp case after export; but it was distinct from the isolated polyp signal pre- and post-export (Table II).

Discussion

Although it has long been known from anecdotal accounts that hydrozoan polyps undergo periodic changes in shape after ingesting a food item, the results presented above represent, to our knowledge, the first quantitative treatment of this behavior. These data reveal three distinct phases of post-feeding behavior. Phase 1 corresponds to the onset of oscillatory behavior immediately following ingestion, phase 2 to the subsequent period during which the polyp oscillates with limited exchange of particulates with the gastrovascular system, and phase 3 to the interval initiated by the export of particulates from the polyp into the gastrovascular system and terminated by regurgitation. In what follows, we elaborate details of each phase, contrast differences among coupled and isolated polyps, and hypothesize physiological mechanisms for the transitions between behaviors.

Phase 1. In both isolated and coupled treatments, ingestion does not immediately elicit oscillations by the polyp (Figs. 3, 7). Rather, oscillations begin 5–15 min after ingestion and are characterized by a gradual increase in amplitude up to a value which thereafter (phase 2) remains constant. These findings bear on the mechanism that triggers the oscillatory behavior. One obvious candidate for such a trigger is the change in the internal dimensions of the polyp, as might be sensed by stress or strain receptors. Alternatively, the polyp might sense the presence of nutrients or their correlates (*e.g.*, the titer of digestive enzymes). If the former were the case, one would expect polyps to oscillate immediately following ingestion, whereas the latter would imply that oscillation would be delayed by the length of time required for digestion to release nutrients and digestive enzymes. Moreover, if the polyp does respond to some product of digestion, one might expect the titer of such a product to increase gradually as digestion proceeds and, as seen in Figures 3 and 6A for length, the oscillations to increase in amplitude as the titer increases, up to some threshold set by the size of the polyp.

Phase 2. At the end of phase 1, oscillations are constant in amplitude and their frequency does not differ between isolated and coupled treatments (Table I). During phase 2, polyps of both treatments display comparable patterns of shape variation (Fig. 4A, C) and similar frequencies and relative amplitudes of stolon oscillations (Table II). Although the polyp exchanges fluid with the stolon throughout this interval, particulate exchange is only rarely observed in either treatment. The similarity of the coupled and isolated polyp records during this period suggests that coupled polyps are behaving as autonomous elements.

The treatments, however, differ markedly in the duration of phase 2. Isolated polyps retain this behavior for ~13 h (Fig. 6, Table II), whereas coupled polyps undergo an abrupt transition to phase 3 at 1.5–2 h (Fig. 3, Table II). The difference in duration between the two treatments may reflect a simple mechanical limit: a minimum pressure differential between the polyp and the hydrorhiza may be required to move large particulates through the polyp-stolon junction. If so, the long duration of phase 2 in the isolated polyp may reflect the time required to solubilize food items to the extent that pressure differentials generated by a single polyp are sufficient to drive particulates through the junction. Conversely, the short duration of phase 2 in the coupled case may reflect the far greater pressure differentials associated with colonywide behavior (see below).

Beginning in phase 2, isolated polyps display a trend of gradually decreasing volume (*e.g.*, Fig. 6, *ca.* 0.3 nl/h) that continues until regurgitation. This gradual decrease in volume likely reflects the transfer to endodermal cells that is associated with digestion (Schierwater *et al.*, 1992); the increase in length of the stolon lumen that is associated with tip growth; and perhaps, leakage. Estimating the extent of the latter will require monitoring of endodermal cell volume and stolon length, which we have not attempted here.

Phase 3. Phase 3 is initiated by the export of dense streams of particulate material from the polyp into the stolon. Phase 3 differs between the isolated and coupled cases, as might be expected from the differences between the gastrovascular systems to which the polyps are exporting. In the coupled case, fluid is exchanged with an entire colony. The volume of the colonial gastrovascular system is very large relative to that of the fed polyp, and the colony possesses many other polyps which themselves oscillate to drive large fluid volumes to effect exchanges with the fed polyp. In contrast, the isolated polyp is exporting to a gastrovascular system that lacks other polyps and whose total volume is but a fraction of its own. These differences are interpreted to underlie both the differences and the commonalities in phase 3 between the isolated and coupled treatments.

In the coupled case, phase 3 is marked by an abrupt decline in polyp volume (Fig. 3). In the stolon records this decline is correlated with a large import of fluid from the colony and subsequent export of the contents of the fed polyp into the colonial gastrovascular system (Table II). Export is followed by the onset of regular high-amplitude oscillations in volume that have a frequency distinct from that displayed in phase 2 (Fig. 5) and identical to that of the stolon oscillations in phase 3 (Table II). The repeated appearance of these features in all coupled records (Table I), their absence in all isolated records (Table I), and the temporal correlation of these events with distinctive signatures in stolon records (Table II) lead us to interpret phase 3 in the coupled case as a colonywide exchange distinct from the autonomous behavior displayed during phase 2. Phase 3 is also accompanied by changes in the way that polyp shape varies when oscillating (Fig. 4), and this transition is likewise attributable to the large-volume fluxes associated with exchange of particulates with the colony. Prior to export, the prey fills the gastric cavity; hence, most of the variation in volume is attributable to changes in the dimensions of the hypostome. The gastric cavity is emptied during export to the stolon; thereafter, its shape is presumably limited only by its own extensibility. Finally, with multiple polyps contributing to volume exchange with the fed polyp, the frequency of oscillation may be expected to be determined not by the polyp's autonomous rhythm, but by a frequency characteristic of fluxes through the stolon (Table II).

In the isolated case, phase 3 is similarly marked by the export of particulate matter from the polyp into the stolon, but without the large volume fluxes observed in the coupled case. Since the volume of the gastrovascular system in the isolated case is only a fraction of that of the polyp, the absence of large-volume fluxes and associated variations in polyp shape to accommodate such fluxes is expected. Another notable difference between isolated and coupled cases is that the oscillation frequency of isolated polyps does not change during phase 3 to the frequency characteristic of the stolon (Fig. 10), as it does in the coupled case (Fig. 5). Phase 3 in the isolated case retains the same two frequencies, ~4 and ~8 mHz, that were established at the end of phase 1 and retained throughout phase 2, although the predominant frequency shifts to the subharmonic in phase 3 (Fig. 10, Table I). These differences are likewise interpreted as a consequence of the differences in volume fluxes between the two cases. In the coupled case, the principal force driving fluid movement is the activity of the colony communicating with the fed polyp through the stolon. In the isolated case, the fed polyp remains the principal driving force in exchange with the stolon. The shift between the subharmonic and principal frequencies likely derives from similar considerations. Prior to export, the gastric cavity is rich in particulates, which constrains variation in shape; following export this constraint is released and shape variation associated with the 4-mHz phase 3 signal predominates (Figs. 4D, 9; Table I). Finally, the fact that the stolon in the isolated case oscillates at a frequency different from that of the isolated polyp and identical to that of the post-

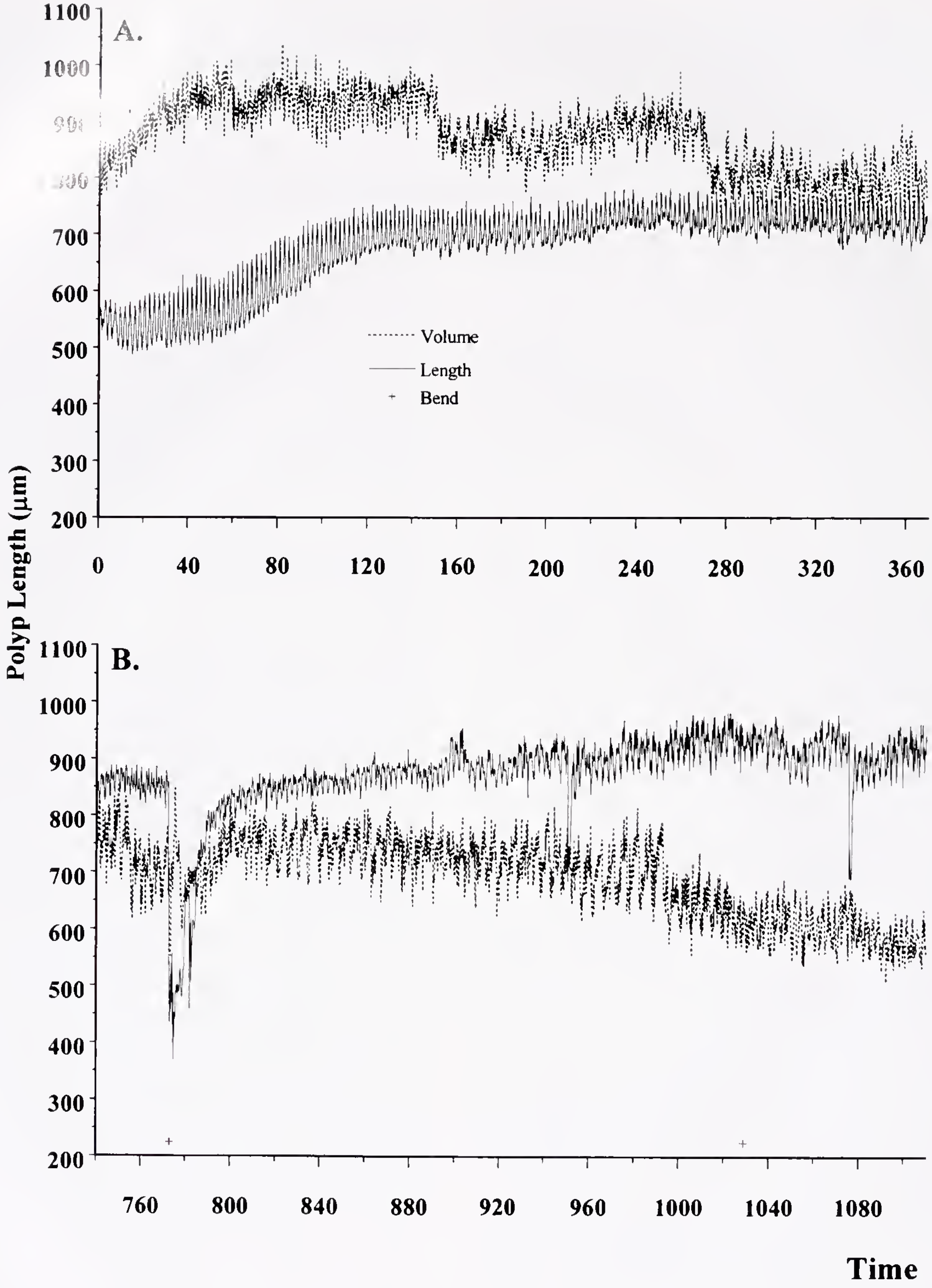

Figure 6. Time series of length (solid line) and volume (dashed line) dynamics of an isolated polyp after ingestion of a single brine shrimp nauplius from (A) 0 to 740 min and (B) 740 to 1474.2 min. R denotes regurgitation. Tickmarks along the abcissa represent spurious data points (see text for further discussion) corresponding to rapid bends drawing the polyp outside the focal plane. Large-amplitude variations in length that are not accompanied by a tickmark represent contraction pulses and are not spurious.

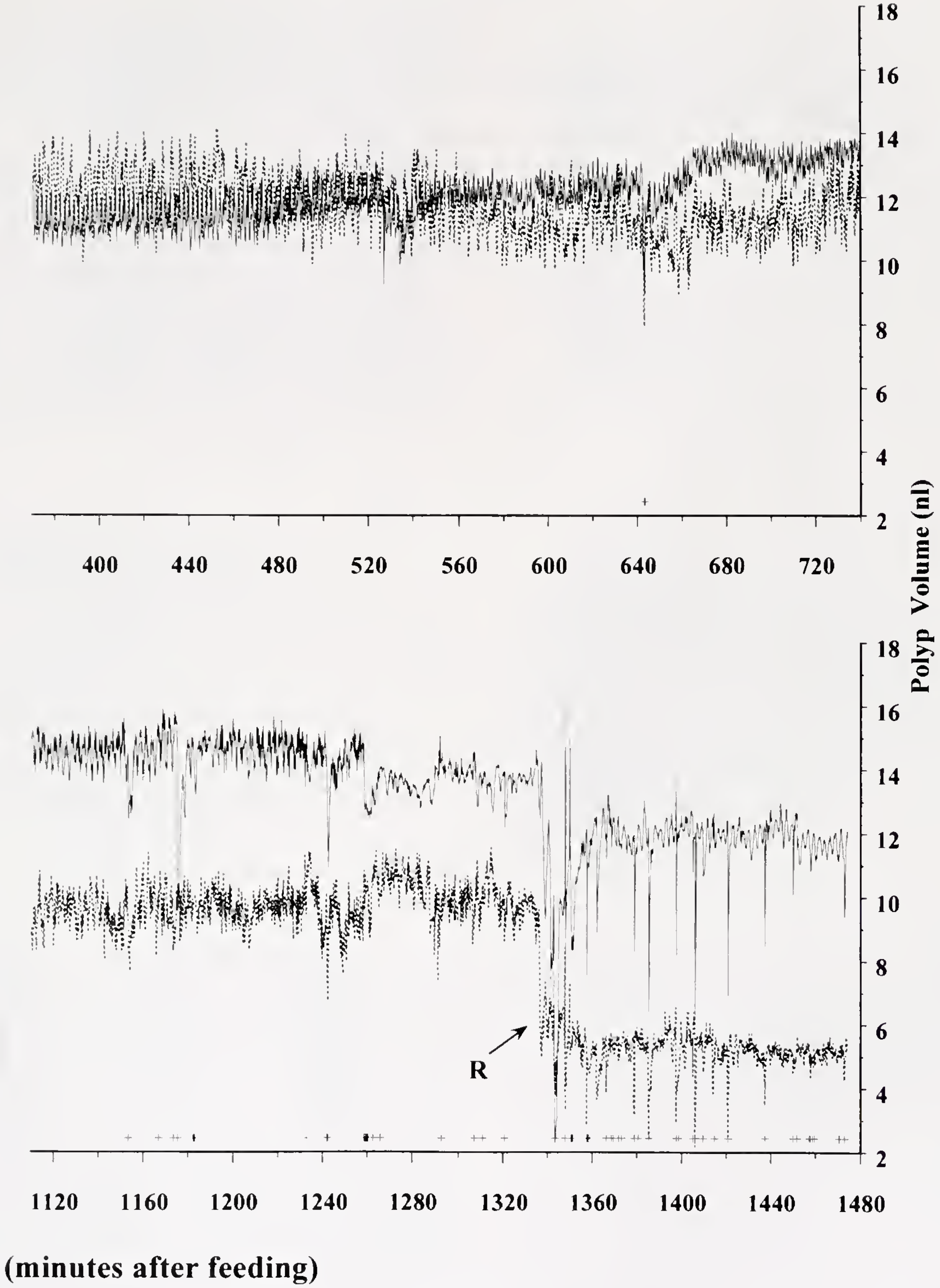

Figure 6. *(Continued)*

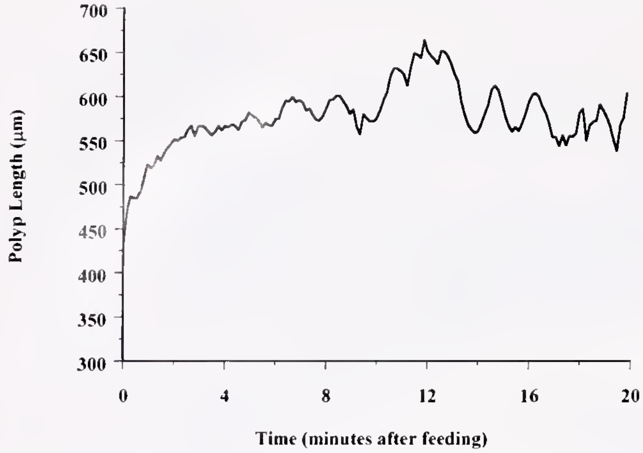

Figure 7. Time series, in minutes after ingestion, of polyp length showing the commencement of regular osciltations of an isolated polyp.

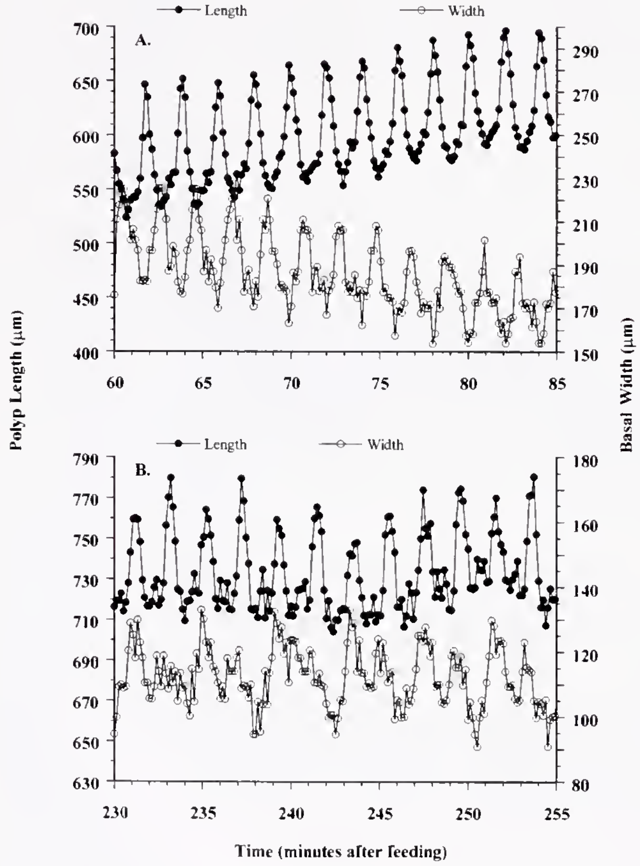

Figure 8. Development of the subharmonic associated with basal width alternating every other length cycle in the isolated polyp record. (A) Polyp length (filled circles) and width (open circles) at the basal-most section for 12 cycles from a representative period (60 to 86 min) when the polyp is lengthening from 0 to 150 min post-feeding. (B) Polyp length (filled circles) and width (open circles) at the basal-most section for 12 cycles from a representative period (230 to 255 min) > 150 min following the development of the 4-mHz subharmonic.

export coupled case strongly suggests the existence of hydrorhizal-specific dynamics (Table II). Indeed, previous observations have established that isolated stolons (*i.e.*, stolons without polyps) in *Hydractinia symbiolongicarpus* exhibit endogenous oscillatory dynamics (Buss and Vaišnys, 1993).

In both treatments, the contraction pulses and rapid polyp bends become increasingly frequent during phase 3 (Figs. 3, 6), consistent with known suppression of contraction pulses during digestion (Passano and McCullough, 1962, 1964; Josephson and Mackie, 1965; Shibley, 1969; Stokes, 1974). The interaction between the contraction pulse system and the digestive oscillations we characterize here bears further attention. Winfree (1970) has shown that a key feature of certain nonlinear oscillators is the capacity for the oscillation to be terminated by perturbations occurring at specific

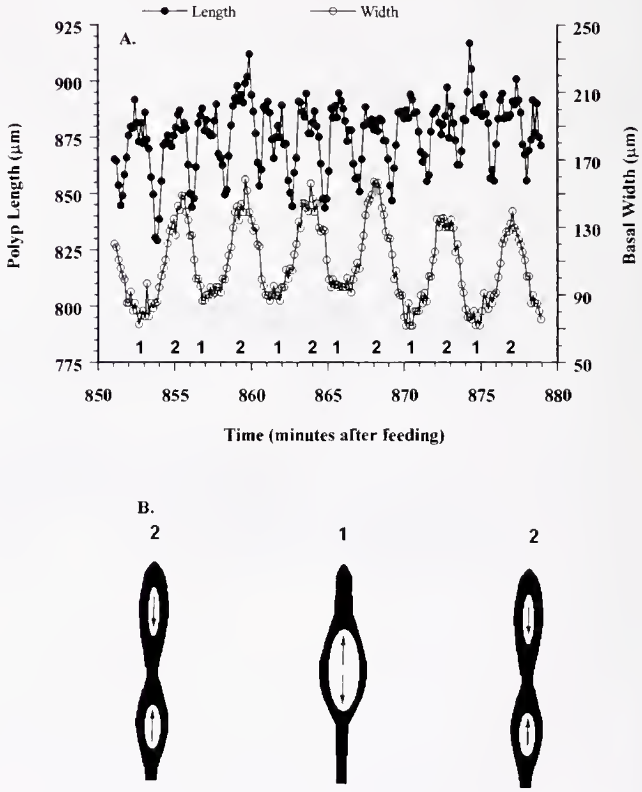

Figure 9. Polyp oscillations during the dominant period by the 4-mHz subharmonic following the 763-min event in the isolated polyp. (A) The length (filled circles) and basal-most width (open circles) of the isolated polyp for 12 cycles from 851 to 878 min after feeding that is representative of the period when the subharmonic dominates the power spectrum. (B) Schematic illustrations of the pattern of shape change of the bolus of transparent fluid in the digestive cavity during three consecutive length maxima of the polyp. Numbers above the polyp correspond to those along the abcissa in (A) that indicate the appearance of the polyp at the maximal polyp length of each cycle. Schematics redrawn from frame-grabbed images during this interval. Arrows within boli inside polyp gastric cavity in (B) indicate the direction of movement of the bolus during the subsequent oscillation cycle.

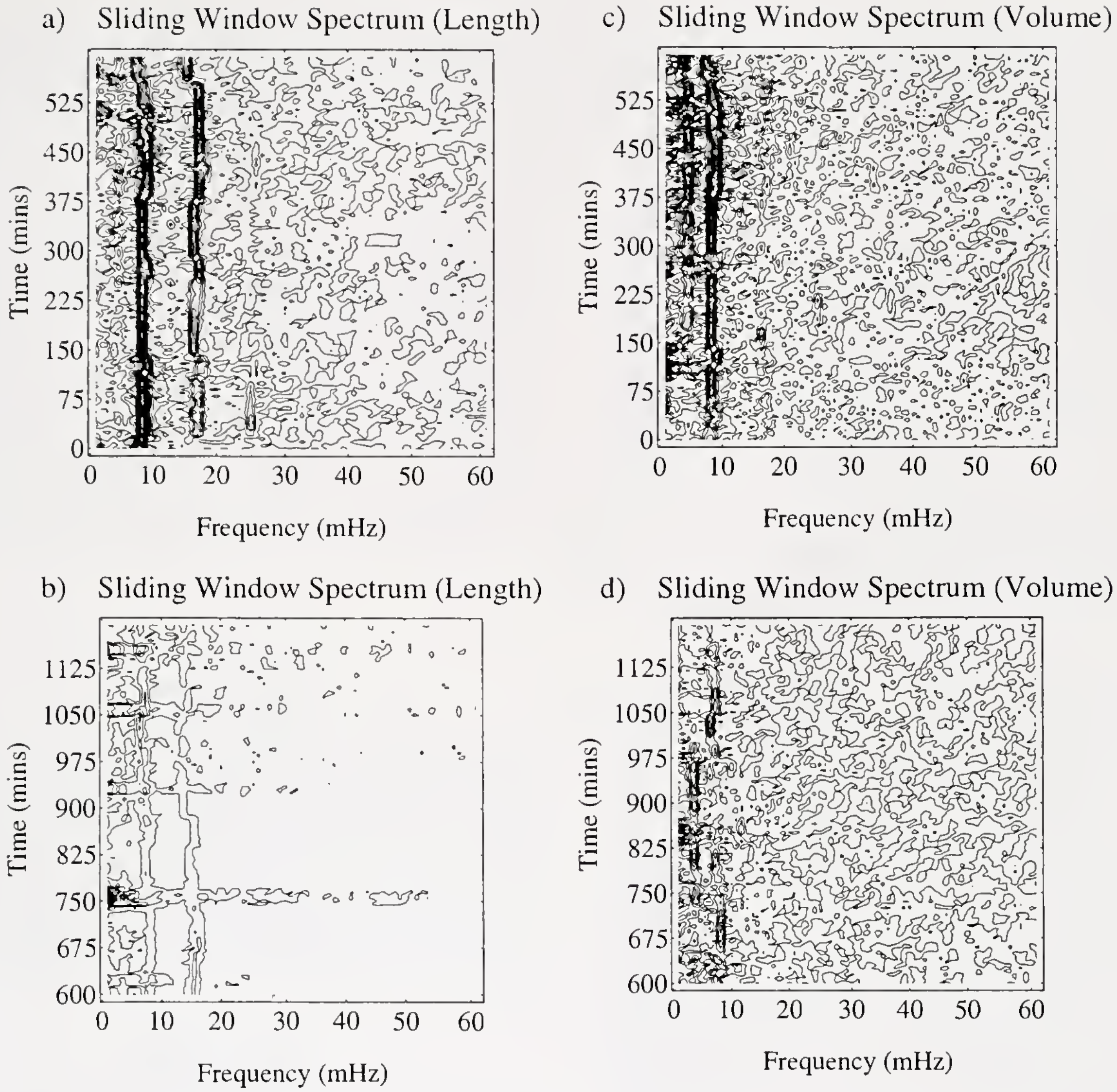

Figure 10. Contour plot, based on the time-series data presented in Figure 6, of sliding window spectral analysis of the isolated polyp for length from (a) 1 to 600 min, and (b) 601 to 1200 min, and for volume from (c) 1 to 600 min, and (d) 601 to 1200 min after ingestion. Abcissa represents frequency of oscillation, ordinate represents the sliding window of time (in minutes), and contour lines represent the height of peaks (coming out of the page) that signify the relative importance of a given frequency underlying the cyclic behavior.

phase relationships. Taddei-Ferretti and Cordella (1976) have shown that contraction pulses can be experimentally annihilated in the predicted fashion. It is conceivable that feeding annihilates contraction pulses and, similarly, that the contraction pulses which reappear in phase 3 annihilate digestive oscillations by this mechanism.

Phase 3 is terminated at comparable times in both the isolated and coupled treatments by regurgitation through the mouth, followed by a return of length and volume to values characteristic of pre-feeding conditions. The dynamics of regurgitation differ between isolated and coupled polyps (*cf.* Figs. 2B and 6B). Whereas regurgitation in the coupled case is not a conspicuous feature of either the length or volume record, regurgitation in isolated polyps is abrupt. The isolated polyp exhibits several rapid, large contractions in length and an associated decline to half of its previous volume. Coupled polyps regurgitate less material that appears more finely particulate, whereas the contractions of isolated polyps are associated with the export of larger pieces of undigested debris. We attribute the differences between treatments in the behavior of polyps and the nature of the material regurgitated to the vastly larger colonial gastrovascular system with its many additional polyps from which undigested particles could be regurgitated.

Table II

Characteristics of oscillations of stolons in the isolated and coupled polyp treatments; values represent the mean and standard errors (in parentheses) of three replicates in each treatment

	Isolated Polyp			Coupled Polyp		
Onset of Oscillations (min)		8.34 (4.99)			13.19 (11.87)	
Export to Hydrorhiza (min)		807.33 (203.95)			78.67 (12.50)	
Stolon Oscillations	Lumen Diameter	Amplitude	Frequency (mHz)	Lumen Diameter	Amplitude	Frequency (mHz)
Pre-feeding	0.29 (0.03)	0.07 (0.03)	5.69 (0.29)	0.24 (0.02)	0.11 (0.03)	5.63 (0.13)
Pre-export						
(30 min post-ingestion)	0.32 (0.06)	0.23 (0.04)	8.48 (0.46)	0.20 (0.03)	0.19 (0.02)	8.40 (0.10)
(150 min post-ingestion)	0.37 (0.05)	0.25 (0.02)	8.64 (0.43)			
Post-export	(Time of export + 60 minutes)			(150 minutes post-ingestion)		
	0.45 (0.05)	0.05 (0.01)	6.00 (0.21)	0.32 (0.03)	0.07 (0.01)	6.07 (0.37)

Data for onset of oscillations and export to hydrorhiza are presented in minutes after ingestion. Means and standard errors for lumen diameter, amplitude, and frequency estimated from the sample of means of each replicate determined from measures taken over three consecutive cycles. Lumen diameter and amplitude are dimensionless indices calculated using the following formulas:

Lumen diameter = (max + min lumen diameter)/(2 × periderm diameter)
Amplitude = max − min lumen diameter/periderm diameter

A theoretical model. These findings suggest a simple conceptualization of the feeding response of an isolated hydrozoan polyp. The principal phases of behavior reflect differing input-output relationships between the polyp and either the external (*via* the mouth) or internal (*via* the polyp-stolon junction) environment. Inputs in the form of food items elicit oscillatory behavior (phase 1), which leads to the output of fluid, but few particulates, to the stolonal system (phase 2). The final phase begins with the export into the stolon of particulates (phase 3) and is terminated by export of undigested material (regurgitation) from the mouth and subsequent return to initial conditions. These data lead us to suggest that an input of food releases elicitors (*e.g.*, nutrients or digestive enzymes) whose action triggers an underlying biochemical system (*e.g.*, ion potentials at neuromuscular junctions), and that the oscillation of that system is reflected in corresponding oscillations in length and width. An ordinary differential equation model of a nonlinear oscillator that can undergo a supercritical Hopf bifurcation as the concentration of an elicitor is increased has been shown to be capable of reproducing principal features of the isolated polyp data presented here (Wagner *et al.*, 1998). Elaboration of such a single-polyp model is easily imagined based on the hypothesis that elicitors are circulated in gastrovascular fluids during phase 2 and that when these elicitors reach a threshold value they trigger oscillations of adjacent polyps, thereby generating the behavior described above for a coupled polyp. These considerations suggest that a spatially distributed system of coupled nonlinear oscillators is a reasonable abstraction of the gastrovascular system of a hydrozoan colony.

Acknowledgments

We thank Dr. Arvydas Matiukas for his development of early versions of the algorithms for this project, Dr. Harald Freund for advice in developing the volume analysis algorithm, and Jim Bonacum for technical assistance. We thank Neil Blackstone and an anonymous reviewer for improving the quality of this manuscript. This research was supported by the National Research Council Twinning Program and the National Science Foundation (OCE-93-15082) to Leo Buss.

Literature Cited

Berrill, N. J. 1953. Growth and form in gymnoblastic hydroids. VI. Polymorphism within the Hydractiniidae. *J. Morphology* **92:** 241–272.

Bevan, J. A., G. Kaley, and G. M. Rubanyi (eds.) 1995. *Flow-Dependent Regulation of Vascular Function.* Oxford Univ. Press, Oxford, UK.

Blackstone, N. W. 1997. A dose-response relationship for experimental heterochrony in a colonial hydroid. *Biol. Bull.* **193:** 47–61.

Blackstone, N. W. 1998. Physiological and metabolic aspects of experimental heterochrony in colonial hydroids. *J. Evol. Biol.* **11** (in press).

Blackstone, N. W., and L. W. Buss. 1992. Treatment with 2,4-dinitrophenol mimics ontogenetic and phylogenetic changes in a hydractiniid hydroid. *Proc. Natl. Acad. Sci. USA* **89:** 4057–4061.

Blackstone, N. W., and L. W. Buss. 1993. Experimental heterochrony in hydractiniid hydroids: why mechanisms matter. *J. Evol. Biol.* **6:** 307–327.

Buss, L. W., and J. R. Vaišnys. 1993. Temperature stress induces dynamical chaos in a cnidarian gastrovascular system. *Proc. Roy. Soc. Lond.* **B 252:** 39–41.

Buss, L. W., and P. O. Yund. 1989. A sibling species group of *Hydractinia* in the northeastern United States. *J. Mar. Biol. Assoc. UK* **69:** 857–875.

Dudgeon, S. R., and L. W. Buss. 1996. Growing with the flow: on the maintenance and malleability of colony form in the hydroid *Hydractinia. Am. Nat.* **147:** 667–691.

Josephson, R. K., and G. O. Mackie. 1965. Multiple pacemakers and the behavior of the hydroid *Tubularia. J. Exp. Biol.* **43:** 293–332.

LaBarbera, M. 1990. Principles of design of fluid transport systems in Zoology. *Science* **249:** 992–1000.

Murray, C. D. 1926. The physiological principle of minimum work applied to the angle of branching of arteries. *Proc. Natl. Acad. Sci. USA* **12:** 835–841.

Passano, L. M., and C. B. McCullough. 1962. The light response and the rhythmic potential of *Hydra. Proc. Natl. Acad. Sci. USA* **48:** 1376–1382.

Passano, L. M., and C. B. McCullough, 1964. Coordinating systems and behavior in *Hydra.* II. The rhythm potential system. *J. Exp. Biol.* **42:** 205–231.

Press, W. H., S. A. Teukolsky, W. T. Vetterling, and B. P. Flannery. 1992. *Numerical Recipes in C.* Cambridge University Press, New York.

Priestley, M. B. 1981. *Spectral Analysis and Time Series.* Academic Press, New York.

Schierwater, B., B. Piekos, and L. W. Buss. 1992. Hydroid stolonal contractions mediated by contractile vacuoles. *J. Exp. Biol.* **162:** 1–21.

Sherman, T. F. 1981. On connecting large vessels to small. *J. Gen. Physiol.* **78:** 431–453.

Shibley, G. A. 1969. Gastrodermal contractions correlated with rhythmic potentials and pre-locomotor burst in *Hydra. Am. Zool.* **9:** 586.

Stokes, D. R. 1974. Physiological studies of conducting systems in the colonial hydroid *Hydractinia echinata* I. Polyp specialization. *J. Exp. Zool.* **190:** 1–18.

Taddei-Ferretti, C., and L. Cordella. 1976. Modulation of the *Hydra attenuata* rhythmic activity: phase response curve. *J. Exp. Biol.* **65:** 737–751.

Wagner, A., S. R. Dudgeon, J. R. Vaišnys, and L. W. Buss. 1998. Non-linear oscillations in polyps of the colonial hydroid *Podocoryne carnea. Naturwissenschaften* **85:** 117–120.

Winfree, A. T. 1970. An integrated view of the resetting of a circadian clock. *J. Theor. Biol.* **28:** 327–374.

Zamir, M. 1977. Shear forces and blood vessel radii in the cardiovascular system. *J. Gen. Physiol.* **69:** 449–461.

Reference: *Biol. Bull.* **196:** 18–25. (February, 1999)

High Contents of Trimethylamine Oxide Correlating With Depth in Deep-Sea Teleost Fishes, Skates, and Decapod Crustaceans

ROBERT H. KELLY AND PAUL H. YANCEY*

Biology Department, Whitman College, Walla Walla, Washington 99362

Abstract. In muscles of shallow-living marine animals, the osmolyte trimethylamine *N*-oxide (TMAO) is reportedly found (in millimoles of TMAO per kilogram of tissue wet weight) at 30–90 in shrimp, 5–50 in crabs, 61–181 in skates, and 10–70 in most teleost fish. Recently our laboratory reported higher levels (83–211 mmol/kg), correlating with habitat depth, in deep-sea gadiform teleosts. We now report the same trend in muscles of other animals, collected off the coast of Oregon from bathyal (1800–2000 m) and abyssal plain (2850 m) sites. TMAO contents (mmol/kg ± SD) were as follows: zoarcid teleosts, 103 ± 9 (bathyal) and 197 ± 2 (abyssal); scorpaenid teleosts, 32 ± 0 (shallow) and 141 ± 16 (bathyal); rajid skates, 215 ± 13 (bathyal) and 244 ± 23 (abyssal); caridean shrimp, 76 ± 16 (shallow), 203 ± 35 (bathyal), and 299 ± 28 (abyssal); *Chionoecetes* crabs, 22 ± 2 (shallow) and 164 ± 15 (bathyal). Deep squid, clams, and anemones also had higher contents than shallow species. Osmoconformers showed compensation between TMAO and other osmolytes. Urea contents (typically 300 mmol/kg in shallow elasmobranchs) in skates were 214 ± 5 (bathyal) and 136 ± 9 (abyssal). Glycine contents in shrimp were 188 ± 17 (shallow) and 52 ± 20 (abyssal). High TMAO contents may reflect diet, reduce osmoregulatory costs, increase buoyancy, or counteract destabilization of proteins by pressure.

Introduction

There are two different adaptive strategies that allow marine organisms to regulate cell volume in the face of the high osmotic pressure of seawater (about 1000 mosm). First, most marine organisms are osmoconformers, maintaining cellular water balance with certain organic osmolytes, especially polyols, neutral amino acids, and methylamines. Unlike most inorganic ions, organic osmolytes are mostly "compatible" because they raise cellular osmotic pressure without adversely affecting macromolecules (Yancey *et al.*, 1982). Recently, Carr *et al.*, (1996) showed that the types of osmolytes used by fishes, crustaceans, and molluscs correlate highly with taxa; *e.g.*, bivalve molluscs use predominantly taurine and betaine (*N*-trimethylglycine), whereas decapod crustaceans use mainly glycine and betaine. This suggests that many osmolytes are interchangeable in their compatibility properties, and whether there are selective forces for different specific combinations of osmolytes in different animals is uncertain in many cases. One possible selective pressure involves trimethylamine *N*-oxide (TMAO) and related osmolytes, which are termed "counteracting" (Yancey *et al.*, 1982) or "compensatory" (Gilles, 1997) because they can enhance the binding activity and stability of proteins and offset the adverse effects of salt ions, high temperature, and the osmolyte urea in cartilaginous fish (Yancey, 1994). In the literature, TMAO is reported to be low or absent in many taxa and found at the highest amounts in the muscles of crustaceans (up to 90 mmol/kg wet wt. in decapod shrimp), squids (up to 140 mmol/kg), and cartilaginous fishes (up to 180 mmol/kg in skates) (Dyer, 1952; Hebard *et al.*, 1982).

The second osmotic strategy is hypo-osmotic regulation, exemplified by marine teleost fishes (except for some polar fishes with high glycerol; Raymond, 1994). With internal fluids at 300–400 mosm (Lange and Fugelli, 1965), most teleosts should have no need to accumulate large amounts of organic osmolytes. They generally contain TMAO, but until recently the levels reported were only 10–70 mmol/kg

---

Received 1 September 1998; accepted 24 November 1998.

* To whom correspondence should be addressed. E-mail: yancey@whitman.edu

Abbreviations: TMAO, trimethylamine *N*-oxide; TMA, trimethylamine muscle, with gadiform fishes (cods and relatives) having the highest amounts (Hebard *et al.*, 1982). Recently, however, exceptions have been found: some polar fishes have TMAO contents up to 154 mmol/kg muscle (Raymond and DeVries, 1998); and our laboratory has found high levels (83–211 mmol/kg muscle) in deep-sea gadiform teleosts, with abyssal species having more than bathyal species (Gillett *et al.*, 1997).

Why should deep-sea osmoregulators need to retain such large amounts of TMAO? We hypothesized that high levels of TMAO might lower the energetic costs of hypo-osmoregulation in the energy-poor deep sea or stabilize proteins under high hydrostatic pressure, which is known to affect protein activity and structure adversely (Siebenaller, 1987; Balny *et al.*, 1997). Although some enzymes in deep-sea organisms function normally under high pressures, presumably because of structural adaptations in the proteins, others exhibit significant pressure sensitivities (Siebenaller, 1987). The previous study in our laboratory found that, for macrourid lactate dehydrogenase, the Michaelis constant for cofactor was increased by high pressure, but decreased with the addition of TMAO (Gillett *et al.*, 1997). A third hypothesis is based on calculations that TMAO solutions are more buoyant than solutions of other osmolytes (Withers *et al.*, 1994), though not more buoyant than pure water. Thus TMAO might increase buoyancy in an osmoconformer, but not in a hypo-osmoregulator.

To elucidate further the possible roles of TMAO in the deep sea, in this study we analyzed TMAO contents in other families of teleosts and in osmoconforming animals, which presumably would not save osmoregulatory energy by using TMAO in place of other osmolytes.

Materials and Methods

Species analyzed

A complete list of species used in this study is given in Table 1. Deep-sea animals were caught by otter trawl off the Oregon coast in April 1996 and 1997. Two sites were trawled from the R/V *Wecoma:* one was on the abyssal plain at 2850 m (44°46′N, 125°39′W) and the other was a bathyal site on the continental slope at 1800–2000 m (44°28′N, 125°08′W). Samples were taken from the dorsal white muscle of teleost fish, wing muscle of skates, abdominal muscle of shrimp, leg muscle of crab, mantle of squid, and internal septal tissue of anemones.

Similar tissue samples were taken from a variety of shallow-living animals, most of which were collected north of Lopez Island, Washington State, in March 1998. These animals were caught by otter trawl at 40–80 m from the R/V *Nugget.* Fresh specimens of a few species (see Table 1) were purchased at the Pike Street Fishmarket in Seattle, Washington, in June 1998. In addition, G. Somero from Hopkins Marine Station, Pacific Grove, California, kindly provided fresh specimens of *Pachygrapsus crassipes* (a brachyuran crab) and *Squalus acanthias* (the dogfish shark). These two species (not listed in Table 1) were used to provide additional data for comparison (see Results).

Table 1

Species, with depth range (if known), used to compare content of trimethylamine N-oxide (TMAO) in tissue of marine animals from three depth habitats*

Shallow	Bathyal (1800–2000 m)	Abyssal (2850 m)
Teleost fishes—gadiform families Gadidae, Macrouridae (cods, grenadiers)		
Gadus macrocephalus (12–549 m)	*Coryphaenoides cinereus* (225 –2830 m)	*Coryphaenoides armatus* (2000–5200 m)
Teleost fishes—gadiform family Moridae (morid cod)		
	Antimora microlepis (530–2940? m)	*Antimora microlepis* (530–2940? m)
Teleost fishes—scorpaeniform family Scorpaenidae (rockfish etc.)		
Sebastes melanops† (0–366 m)	*Sebastolobus altivelis* (305 to >1500 m)	
Teleost fishes—ophidiiform family Zoarcidae (zoarcid eels)		
	Lycenchelys sp.	*Pachycara* sp.
Elasmobranch fishes—rajiform family Rajidae (skates)		
	Bathyraja spinosissima (1280–1829 m)	*Bathyraja* unnamed‡ (>2500 m)
Decapod crustaceans—suborder Caridea (shrimp)		
Pandalus danae	*Pandalopsis ampla*	*Neocrangon abyssorum*
Decapod crustaceans—decapod suborder Brachyura (crabs)		
Chionoecetes bairdi	*Chionoecetes angulatus*	
Cephalopod molluscs—families Loliginidae, Gonatidae, Onychoteuthidae (squid)		
Loligo opalescens† (inner shelf to surface)	*Berryteuthis magister* (30–1500 m near bottom)	*Gonatus borealis* (epipelagic-abyssal) *Moroteuthis robusta* (subtidal-bathyal?)
Pelecypod molluscs—eulamellibranch family Veneridae, septibranchia family Cuspidaridae		
Saxidomus giganteus†	*Cuspidaria glacialis*	*Cuspidaria glacialis*
Anthozoan cnidaria—order Actiniaria		
Urticina lofotensis	*Actinauge abyssorum*	*Actinauge abyssorum*

* From Eschmeyer *et al.* (1983); Pearcy *et al.* (1982); Allen and Smith (1988); Nesis (1987).

† Specimens obtained from Pike's Fishmarket, Seattle.

‡ Close relative of *Bathyraja trachura* (Eschmeyer *et al.*, 1983).

Analytical procedures

Samples were frozen at −80°C on the ships, transported to Whitman College on dry ice, and stored at −70°C. Muscle was processed with perchloric acid, then neutralized and filtered as previously described (Wolff *et al.*, 1989). The TMAO content was determined according to the procedure of Wekell and Barnett (1991), by reducing TMAO to trimethylamine (TMA) with an iron-EDTA reagent. TMA was extracted in toluene and reacted with 0.02% picric acid; the colored product was measured spectrophotometrically. Standards were treated similarly with each run. The TMA content of tissues, which was <3 m*M* in all cases, was also measured by omitting the reduction step; the results were subtracted from the TMAO values. Sugars, neutral amino acids, and urea were analyzed in extracts by high performance liquid chromatography using a Waters Sugarpak column as previously described (Wolff *et al.*, 1989).

Statistical analysis of the osmolyte contents was performed with analysis of variance (ANOVA) followed by the Student-Newmann-Keuls post-test.

Results

We analyzed the TMAO content of muscles of deep-living fishes, crustaceans, squids, and clams and compared the results with published data for shallow-living species. Published values have been generally consistent over many decades, but they have been obtained by different techniques (Hebard *et al.*, 1982); therefore, whenever possible, we also analyzed fresh tissue from related shallow-living species for comparison.

In general, the TMAO content of tissue increased significantly with the depth at which the animal was caught—in the order of shallow < bathyal < abyssal (Table II). The results for fishes and crustaceans are shown in Figure 1. We initially confirmed our previous finding of this trend in gadiform teleosts (shallow Gadidae and deep Macrouridae and Moridae). For the gadid and macrourids, the trend was found among different species at each depth. However, the morid *Antimora microlepis* was caught at both depths, and the single animal from the abyssal site had much higher amounts of TMAO than did the same species from the bathyal site (288 mmol/kg wet wt. compared to 211; Table II, Fig. 1).

Similar patterns occurred in two other, not closely related teleost families. Values in the literature for the TMAO contents of shallow Scorpaenidae are relatively low (Hebard *et al.*, 1982). The value of 32 mmol/kg we found in shallow *Sebastes melanops* was well within this range, and was much less than the 141 mmol/kg we measured for the bathyal *Sebastolobus altivelis* (Table II, Fig. 1). No shallow species of Zoarcidae were available to us; however, a published value of 51 mmol/kg for one species (Dyer, 1952) was much less than the value of 103 for the bathyal species, which in turn was less than the 197 for the abyssal species (Table II, Fig. 1).

Among cartilaginous fishes, only deep Rajidae (skates) in the genus *Bathyraja* were caught. In the literature, many species in the closely related genus *Raja* have been found to contain TMAO in muscle over a wide range, from 61–181 mmol/kg (Hebard *et al.*, 1982). The TMAO content was higher in the deep-living *Bathyraja* species, although the values for bathyal and abyssal specimens (215 and 244 mmol/kg, respectively) were not quite significantly different from each other (Table II, Fig. 1).

Table II

Comparison of trimethylamine N-oxide (TMAO) content (mmol TMAO/kg tissue wet weight) of tissues of marine animals from three depth habitats

	Habitat			
Data Source	Shallow	Bathyal (1800–2000 m)	Abyssal (2850 m)	*P* value
Teleost fishes—cods and grenadiers (muscle)				
This study	46 ± 2 (2)	133 ± 19 (5)	179 ± 12 (8)	<0.001
Published	66 ± 4 (6)*			
Teleost fishes—morid cods (muscle)				
This study		211 ± 18 (4)	288 (1)	
Teleost fishes—scorpaenids (muscle)				
This study	32.2 ± 0 (2)	141 ± 16 (5)		<0.001
Published	6–64†			
Teleost fishes—zoarcids (muscle)				
This study	—	103 ± 9 (3)	197 ± 2 (2)	<0.001
Published	51 ± 5 (2)§			
Elasmobranch fishes—skates (muscle)				
This study		215 ± 13 (4)	244 ± 23 (4)	0.075
Published	61–181†			
Decapod crustaceans—caridean shrimp (muscle)				
This study	76 ± 19 (5)	203 ± 35 (7)	299 ± 28 (5)	<0.001
Published	30–90†			
Decapod crustaceans—brachyuran crabs (muscle)				
This study	22 ± 2 (2)	164 ± 15 (3)		<0.001
Published	5–50†			
Cephalopod molluscs—squids (mantle)				
This study	48 ± 7 (3)	219 (1)	333, 377	
Published	30–140†			
Pelecypod molluscs—venerid and cuspidarid (siphons)				
This study	3 ± 5 (3)	46 (1)	134 ± 20 (2)	
Published	0–50†			
Anthozoan cnidaria (internal septa)				
This study	0 (3)	10.6 ± 0.6 (3)	31.6 ± 3.3 (3)	<0.001

Note: TMAO values are means (*n* value in parentheses) ± SD. See Table I for species used in this study.

* *Theragra chalcogramma* (Alaskan pollock) analyzed by Wekell and Barnett (1991).

† Numerous species reviewed by Hebard *et al.* (1982).

§ *Macrozoarces americanus* (depth 10–180 m) analyzed by Dyer (1952).

The depth trend in decapod crustaceans is also shown in Figure 1 for caridean shrimp and brachyuran crabs. For the shallow shrimp *Pandalus danae*, the average TMAO of 76 mmol/kg fell in the published range for many caridean species, while averages were significantly higher in bathyal and abyssal species (203 and 299 mmol/kg, respectively; Table II, Fig. 1). The value of 22 mmol/kg for the shallow subtidal snow crab *Chionoecetes bairdi* fell in the published range for several brachyuran species (Table II, Fig. 1). Similarly, the intertidal crab *Pachygrapsus crassipes* gave a value of 20 ± 5 mmol/kg ($n = 3$) (not shown in tables or figures). Again, a bathyal species, the congener snow crab

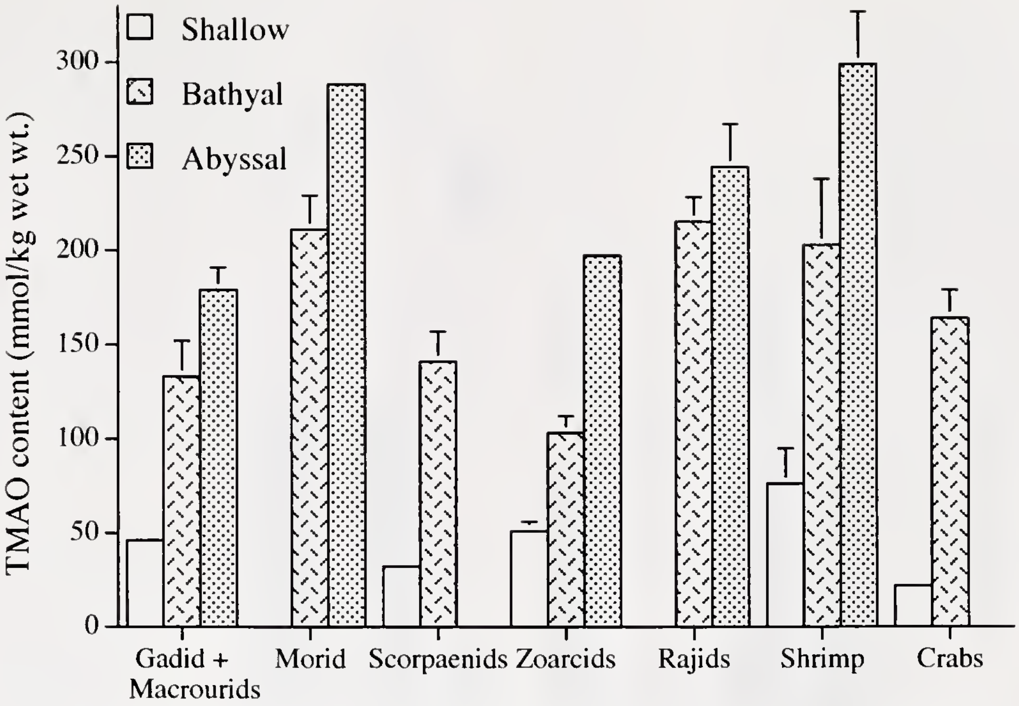

Figure 1. Trimethylamine *N*-oxide (TMAO) content (from Table II) in muscles of marine animals from shallow habitats and bathyal (1800–2000 m) and abyssal (2850 m) trawl sites (see Table I for species). Error bars indicate SD. All differences between depths within each animal type were significant except for the morid (n = 1 for abyssal) and the rajids (see Table II).

C. angulatus, had much higher levels at 164 mmol/kg (Table II, Fig. 1).

For deep-living squid, only one specimen each of three species was caught. The TMAO contents were highest (333, 377 mmol/kg) in the two species caught in the abyssal trawls, moderate (219) in the species from a bathyal trawl, and low (48) in the shallow-living *Loligo* squid (Table II), within the published range of 35–55 mmol/kg for other Loliginidae (Carr *et al.*, 1996). However, the actual depth of capture could not be determined for the deep squid, which have been found from the deep-sea bottom to the epipelagic zone (Nesis, 1987).

Only two specimens of abyssal and one of bathyal clams (Cuspidaridae) were obtained; for this group and the anemones, no closely related shallow species are known. The abyssal (though not the bathyal) clams had much higher TMAO contents (134 mmol/kg) than reported in the literature for shallow-living pelecypods: negligible in oysters, mussels, clams, and cockles, and up to 50 mmol/kg in scallop muscles (Table II; Hebard *et al.*, 1982). Similarly, a shallow anthozoan anemone had no detectable TMAO, whereas the deeper species had significant amounts correlating with depth (Table II); of note is that the tissue used was muscle, epithelia, and very watery, gelatinous mesoglea with presumably low intracellular space, suggesting that the actual cellular TMAO levels were much higher.

For the osmoconforming animals (skates, decapods), the higher amounts of TMAO should be compensated for by lower amounts of other osmolytes. In the literature, the dominant osmolyte in cartilaginous fishes is urea at about 300 mmol/kg average, with TMAO generally the second most concentrated. Most studies show urea in a content ratio of 3:1 or 2:1 (about 2:1 intracellular) to TMAO and other methylamines such as betaine and sarcosine (Yancey, 1985). As another check on our methodology, we measured TMAO in a shallow elasmobranch, the Pacific dogfish *Squalus acanthias*, finding TMAO at 158 and urea at 301 mmol/kg (n = 1). This agreed well with published data for the North Sea *S. acanthias* (144 and 315 mmol/kg, respectively; Vyncke, 1970). In the deep *Bathyraja* species, we found a significant depth trend ($P < 0.001$) of decreasing urea content: 214 ± 5 mmol/kg (bathyal) and 136 ± 8.6 mmol/kg (abyssal), with urea:TMAO ratios of approximately 1:1 and 1:2, respectively (Fig. 2).

In shallow decapods, glycine is the dominant osmolyte (Carr *et al.*, 1996). We confirmed this in shallow caridean shrimp (188 ± 17 mmol/kg glycine), but found considerably less glycine (52 ± 20; $P < 0.001$), along with the much higher levels of TMAO (299), in the abyssal species (Fig.

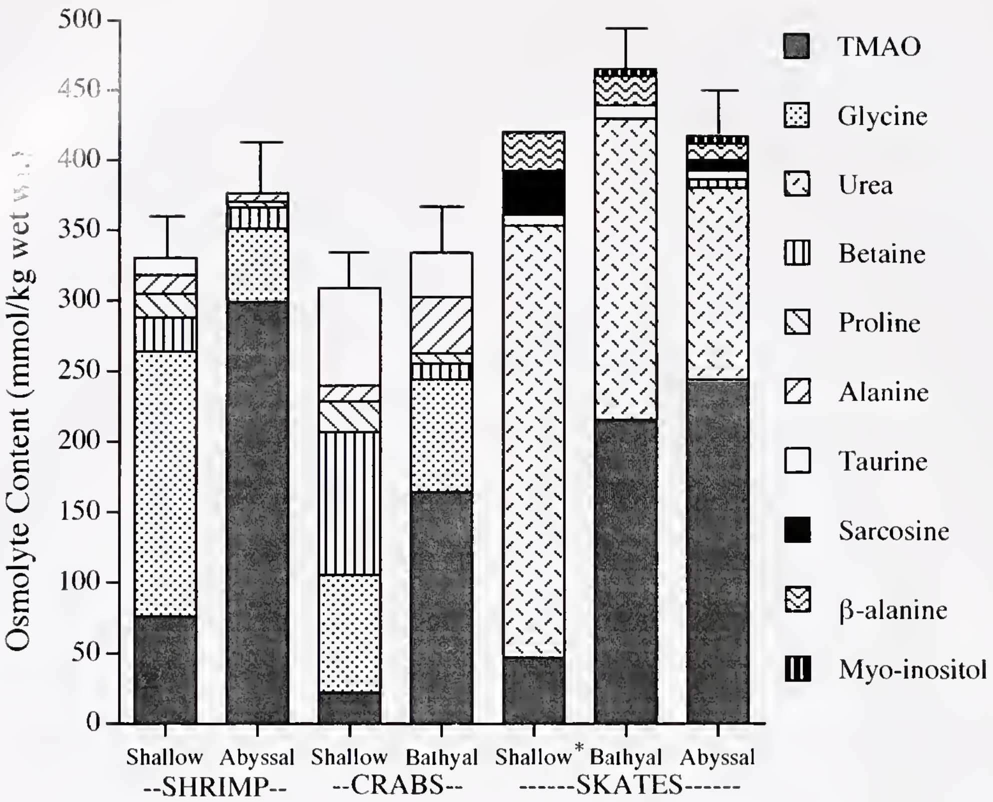

Figure 2. Osmolyte content in muscles of marine animals from shallow habitats and bathyal (1800–2000 m) and abyssal (2850 m) trawl sites (see Table I). Trace amounts of other amino acids are not shown. Error bars indicate SD for summed osmolytes; totals were not significantly different between animals of the same type. **Raja erinacea* data calculated from Forster and Goldstein (1976) and King *et al.* (1980).

2). Other minor osmolytes were also lower in the abyssal specimens; the overall sum of the major osmolytes detected are shown in Figure 2. Similarly, shallow crabs were dominated by glycine, betaine, and taurine, the latter two of which were considerably less ($P < 0.001$) in the bathyal species (Fig. 2).

Discussion

This study greatly extends our previous finding (Gillett *et al.*, 1997) that there is a significant trend of increasing contents of TMAO in muscles with habitat depth. The pattern has now been found among three teleost families of the order Gadiformes (a gadid, a morid, and a macrourid *Coryphaenoides* congener); possibly within the morid species *Antimora microlepis;* within two other teleost families—the Zoarcidae (order Ophidiiformes) and the Scorpaenidae (order Scorpaeniformes); and in the crustacean order Decapoda within the suborders Caridae and Brachyura, including congeners in the latter. In the elasmobranch Rajidae, although the average TMAO content in the abyssal species was not quite significantly greater than in the bathyal one, both were well above that previously reported for rajiform skates (Table II). The data for clams and anemones were also consistent with the trend, though interpretation is limited by the lack of close shallow relatives. Squids caught in deep trawls also had much higher TMAO levels than shallow species (Table II), but limited specimen numbers, distant relationships, uncertain capture depths, and poorly known habitat ranges make significant conclusions impossible.

We have previously shown that TMAO concentrations are quite low in plasma in the macrourid teleosts; thus a whole-tissue content of 170 mmol/kg should be equivalent to an intracellular concentration of perhaps 250 m*M* TMAO. However the morid cod (*A microlepis*) had very high plasma TMAO (159 m*M*); thus its muscle content of 211 mmol/kg (bathyal) would correspond to 250–300 m*M* intracellular also (Gillett *et al.*, 1997). Interestingly, the one *A. microlepis* caught at the abyssal site contained much higher amounts of TMAO than individuals of the same species caught from the bathyal site (Table II, Fig. 1). This species is thought to migrate between continental slopes and abyssal depths (Allen and Smith, 1988). The possibility that individuals within a species could be regulating TMAO levels at different depths requires further study.

These patterns suggest that a high TMAO content is an adaptive response in animals to living at great depths. We are examining several hypotheses.

Diet

For many species, high concentrations of TMAO could simply reflect diet; if, for example, shrimp or smaller animals low in the food chain have high TMAO and are eaten by the other animals in this study. However, that would leave open the questions of why TMAO is high in lower trophic levels, and why hypo-osmoregulators retain it.

Hypo-osmoregulation costs

Because hypo-osmoregulation is energetically costly (Griffith and Pang, 1979), a greater amount of TMAO may be an adaptation to conserve energy in the low-energy environment of the deep sea. Higher concentrations of solute in tissue might decrease the amount of energy needed to actively transport ions in deep-sea osmoregulators. TMAO could also be used to detoxify ammonia if water is limiting (Dyer, 1952). However, recent calculations by Kirschner (1993) suggest that hypo-osmoregulating is no more metabolically expensive than osmoconforming. Also, if a higher osmotic content saves energy, it is not clear why most shallow-living teleosts have not evolved such a strategy. The issue remains unresolved. In any case, hypo-osmoregulation costs would not apply to osmoconforming skates and invertebrates in our study.

Buoyancy

A third hypothesis is based on calculations that dissolved TMAO is more buoyant (1000 g/ml for 1 *M* solution) than common physiological solutes (Withers *et al.*, 1994). TMAO may save energy in shrimp, for example, by replacing less buoyant osmolytes (Fig. 2), especially glycine (1.029 g/ml for 1 *M* solution). High levels of similarly buoyant TMA (128 m*M*) have been reported in the carapace fluid of a deep-sea oplophorid shrimp (*Notostomus gibbosus*) and calculated to increase buoyancy over other ions (Sanders and Childress, 1988). Because TMA is toxic, one might predict it to be low in cells, but *N. gibbosus* has not been tested for tissue TMA (or TMAO) content. However, we did find TMA concentrations to be less than 3 mmol/kg in muscle extracts (which include intra- and extracellular fluids) for all of our specimens.

Interestingly, some pelagic squid (such as cranchiids) reportedly have high amounts of ammonium ions in their fluids for buoyancy (Nesis, 1987). However, Sanders and Childress (1988) note that the tests used did not discriminate between ammonium and TMA. High fluid TMA would correspond with our finding of high muscle TMAO in oceanic squid (Table II). The squids in this study are vertical migrators and could readily benefit from TMAO buoyancy. But if this is the case, the question remains why epipelagic animals (*e.g.*, shallow shrimp, Fig. 2) do not have higher amounts. Finally, the deep-sea skates, crabs, clams, and anemones with higher TMAO levels are primarily or fully benthic, so they do not require enhanced buoyancy.

Regardless of its function in shrimp, TMAO should not elevate buoyancy in hypo-osmotic fishes: TMAO solutions have the same buoyancy as pure water, which is effectively what TMAO replaces in these fish compared to shallow-water relatives (with their lower osmotic pressures; Gillett *et al.*, 1997). One possibility is that the density of TMAO solutions might decrease relative to pure water at high hydrostatic pressure, but that has not been measured. Finally, grenadiers are demersal, but scorpaenids are primarily benthic and thus probably do not require enhanced buoyancy.

Temperature

Another characteristic of deep habitats is cold temperatures. The depth trend in TMAO content may reflect some property of the osmolyte that is of more selective value in the cold. For example, another methylamine osmolyte, β-dimethylsulfonioproprionate, is a better stabilizer in the cold (Nishiguichi and Somero, 1992), but TMAO has not been tested extensively for this property. Raymond and DeVries (1998) have shown that some Antarctic teleosts have high levels (74–154 mmol/kg muscle) of TMAO as well, and they hypothesize that it either acts as an antifreeze or counteracts salt effects on proteins (see below). However, the temperatures at our deep sampling sites were about 2° (abyssal) to 3°C (bathyal) (Kennish, 1989). Since these are above freezing, and since TMAO levels are not particularly high in many shallow, cold-adapted fish (*e.g.*, the gadid Alaskan pollock [Table II; Wekell and Barnett, 1991]), an antifreeze function can be ruled out for our species. Moreover, TMAO contents were roughly linearly correlated with depth but temperatures are not, so the temperature hypothesis is further weakened.

Macromolecular stabilization

The final hypotheses are based on the well-documented protein-stabilizing capabilities of TMAO: for example, TMAO in elasmobranchs (up to 200 mmol/kg) can counteract the destabilizing effects of urea, their main and noncompatible osmolyte (Yancey, 1985, 1994). Recently, it has also been shown that TMAO can rescue misfolded proteins of medical importance such as the cystic fibrosis transmembrane conductance regulator (Welch and Brown, 1996). We have hypothesized that high TMAO levels may counteract the adverse affects of hydrostatic pressure on proteins in deep-sea teleosts (Gillett *et al.*, 1997), and Raymond and DeVries (1998) have proposed counteraction of the effects of elevated NaCl in Antarctic teleosts. Testing of these hypotheses has just begun; we did find that at 300 atm, the inhibition of cofactor binding by lactate dehydrogenase from a macrourid teleost was fully offset with 250 m*M* TMAO (Gillett *et al.*, 1997). We are currently studying the effects of TMAO on other proteins at high pressure.

The stabilization hypothesis is further supported by the finding of reduced glycine in deep-sea shrimp and urea in skates, along with higher TMAO (Fig. 2). Glycine does not generally have as great a protein-stabilizing capability as TMAO (Yancey, 1994). Similarly, urea is a protein destabilizer, and its ratio to TMAO is reversed in abyssal skates compared to most shallow species (Fig. 2). Indeed, to our knowledge the urea values for the abyssal skate are the lowest yet reported for a marine cartilaginous fish. Of course, it is possible that substantial urea was lost from deep skates during their 90- to 120-min trips to the surface. As evidence against this urea loss, skates ranged in size from 10–90 cm, but the standard deviations were quite low (6% in abyssal, 2% in bathyal).

The stabilization hypothesis could be valid for all species examined here. Wang and Bolen (1997) have shown that unfavorable interactions between TMAO and peptide backbones stabilize protein structure, supporting earlier hypotheses that such osmolyte effects are universal (Yancey *et al.*, 1982). The effect on proteins under pressure remains speculative, but we know that destabilizing inorganic ions alter water structure in a manner essentially identical to pressure effects (Leberman and Soper, 1995). Perhaps compensatory osmolytes do the opposite (Gillett *et al.*, 1997).

It is possible that all of these hypotheses are correct but only one or two apply to each group of animals. In conclusion, this study suggests that osmolyte properties may play a far more important role in adaptation to specific marine habitats than previously known.

Acknowledgments

This work was supported by the M. J. Murdock Charitable Trust and a Stanley Rall-Whitman College Research Grant. We thank J. Siebenaller of Louisiana State University for providing ship time and animals on his NSF grant IBN-9407205, G. Somero for additional specimens, and J. Orr and M. Wicksten for help with species identifications.

Literature Cited

Allen, M. J., and G. B. Smith. 1988. Atlas and zoogeography of common fishes in the Bering Sea and northeastern Pacific. *NOAA Technical Report NMFS*, 66. U.S. Dept. Commerce, Springfield, VA.

Balny, C., V. V. Mozhaev, and R. Lange. 1997. Hydrostatic pressure and proteins: basic concepts and new data. *Comp. Biochem. Physiol.* **116A:** 299–304.

Carr, W. E. S., J. C. Netherton III, R. A. Gleeson, and C. D. Derby. 1996. Stimulants of feeding behavior in fish: analyses of tissues of diverse marine organisms. *Biol Bull.* **190:** 149–160.

Dyer, W. J. 1952. Amines in fish muscle. VI. Trimethylamine oxide content of fish and marine invertebrates. *J. Fish. Res. Board. Can.* **8:** 314–324.

Eschmeyer, W. N., E. S. Herald, and H. Hammann. 1983. *A Field Guide to Pacific Coast Fishes of North America.* Houghton Mifflin, Boston.

Forster, R. P., and L. Goldstein. 1976. Intracellular osmoregulatory role of amino acids and urea in marine elasmobranchs. *Am. J. Physiol.* **230:** 925–931.

Gilles, R. 1997. "Compensatory" organic osmolytes in high osmolarity and dehydration stresses: history and perspectives. *Comp. Biochem. Physiol.* **117A:** 279–290.

Gillett, M. B., J. R. Suko, F. O. Santoso, and P. H. Yancey. 1997. Elevated levels of trimethylamine oxide in muscles of deep-sea gadiform teleosts: a high-pressure adaptation? *J. Exp. Zool.* **279:** 386–391.

Griffith, R. W., and P. K. T. Pang. 1979. Mechanisms of osmoregulation of the coelacanth: evolutionary implications. *Occas. Pap. Calif. Acad. Sci.* **134:** 79–92.

Hebard, C. E., G. J. Flick, and R. E. Martin. 1982. Occurrence and significance of trimethylamine oxide and its derivatives in fish and shellfish. Pp. 149–175 in *Chemistry and Biochemistry of Marine Food Products*, R. E. Martin, ed. AVI Publishing, Westport, CT.

Kennish, M. J. 1989. *Practical Handbook of Marine Science.* CRC Press, Boca Raton, FL.

King, P. A., C-J. Cha, and L. Goldstein. 1980. Amino acid metabolism and cell volume regulation in the little skate, *Raja erinacea*. *J. Exp. Zool.* **212:** 79–86.

Kirschner, L. B. 1993. The energetics of osmotic regulation in ureotelic and hypoosmotic fishes. *J. Exp. Zool.* **267:** 19–26.

Lange, R., and K. Fugelli. 1965. The osmotic adjustment in the euryhaline teleosts, the flounder, *Pleuronectes flesus* L., and the three-spined stickleback, *Gastrosteus aculaetus* L. *Comp. Biochem. Physiol.* **15:** 283–292.

Leberman, R., and A. K. Soper. 1995. Effect of high salt concentrations on water structure. *Nature* **378:** 364–367.

Nesis, K. N. 1987. *Cephalopods of the World.* T. F. H. Publications, Neptune City, NJ.

Nishiguichi, M. K., and G. N. Somero. 1992. Temperature- and concentration-dependence of compatibility of the organic osmolyte β-dimethylsulfonioproprionate. *Cryobiology* **29:** 118–123.

Pearcy, W. G., D. L. Stein, and R. S. Carney. 1982. The deep-sea benthic fish fauna of the northeastern Pacific Ocean on Cascadia and Tufts abyssal plains and adjoining continental slopes. *Biol. Oceanogr.* **1:** 375–428.

Raymond, J. A. 1994. Seasonal variations of trimethylamine oxide and urea in the blood of a cold-adapted marine teleost, the rainbow smelt. *Fish Physiol. Biochem.* **13:** 13–22.

Raymond, J. A., and A. L. DeVries. 1998. Elevated concentrations and synthetic pathways of trimethylamine oxide and urea in some teleost fishes of McMurdo Sound, Antartica. *Fish Physiol. Biochem.* **18:** 387–398.

Sanders, N. K., and J. J. Childress. 1988. Ion replacement as a buoyancy mechanism in a pelagic deep-sea crustacean. *J. Exp. Biol.* **138:** 333–343.

Siebenaller, J. F. 1987. Pressure adaptation in deep-sea animals. Pp.

33–48 in *Current Perspectives in High Pressure Biology.* H. W. Jannasch, R. E. Marquis, and A. M. Zimmerman, eds. Academic Press, London.

Vyncke, W. 1970. Influence of biological and environmental factors on nitrogenous extractives of the spurdog *Squalus acanthias. Mar. Biol.* **6:** 248–255.

Wang, A., and D. W. Bolen. 1997. A naturally occurring protective system in urea-rich cells: mechanism of osmolyte protection of proteins against urea denaturation. *Biochemistry* **36:** 9101–9108.

Wekell, J. C., and H. Barnett. 1991. New method for analysis of trimethylamine oxide using ferrous sulfate and EDTA. *J. Food Sci.* **56:** 132–138.

Welch, W. J., and C. R. Brown. 1996. Influence of molecular and chemical chaperones on protein folding. *Cell Stress Chaperones* **1:** 109–115.

Withers, P. C., G. Morrison, G. T. Hefter, and T.-S. Pang. 1994. Role of urea and methylamines in buoyancy of elasmobranchs. *J. Exp. Biol.* **188:** 175–189.

Wolff, S., P. H. Yancey, T. S. Stanton, and R. Balaban. 1989. A simple HPLC method for quantitating the major organic solutes of the renal medulla. *Am. J. Physiol.* **256:** F954–956.

Yancey, P. H. 1985. Organic osmotic effectors in cartilaginous fishes. Pp. 424–436 in *Transport Processes, Iono- and Osmoregulation,* R. Gilles and M. Gilles-Ballien, eds. Springer-Verlag, New York.

Yancey, P. H. 1994. Compatible and counteracting solutes. Pp. 81–109 in *Cellular and Molecular Physiology of Cell Volume Regulation,* K. Strange, ed. CRC Press, London.

Yancey, P. H., M. E. Clark, S. C. Hand, R. D. Bowlus, and G. N. Somero. 1982. Living with water stress: Evolution of osmolyte systems. *Science* **217:** 1214–1222.

Reference: *Biol. Bull.* **196:** 26–33. (February, 1999)

Acidification of the Phagosome in *Crassostrea virginica* Hemocytes Following Engulfment of Zymosan

AMY E. BEAVEN[1] AND KENNEDY T. PAYNTER*

[1] *Department of Biology and Chesapeake Biological Laboratory, University of Maryland, College Park, Maryland 20742*

Abstract. Phagocytic hemocytes are responsible for engulfing and internally degrading foreign organisms within the hemolymph and tissue of the eastern oyster, *Crassostrea virginica*. Since rapid acidification of the phagosome lumen is typically essential for activation of hydrolytic and reactive oxygen intermediate (ROI) producing enzymes in vertebrate cells, we measured phagosomal pH in oyster hemocytes by using the emission fluorescence of two fluorescent probes, rhodamine and Oregon Green 488 (OG 488), conjugated to zymosan to determine whether oyster hemocyte phagosomes become acidified after phagocytosis of zymosan. The average pH of 1079 phagosomes within 277 hemocytes 1 h after phagocytosis of zymosan was 3.9 ± 0.03. Observations of 141 hemocytes with internalized zymosan by light microscopy revealed that, over a 60-min time period, 51% of highly granular hemocytes became partially granular, and 29% became agranular. In addition, 83% of partially granular hemocytes containing zymosan at time = 0 became agranular within 60 min. A comparison revealed that the phagosomes of agranular hemocytes were much more acidic (pH 3.1 ± 0.02) than those of highly granular hemocytes (4.9 ± 0.02; $P < 0.05$). These values are significantly lower than most reported in the literature for blood cells from metazoan organisms.

Introduction

Phagocytic hemocytes are the primary cells involved in the oyster's internal defense response against invading organisms (Alvarez *et al.*, 1989; McCormick-Ray and Howard, 1991). Oyster hemocytes morphologically resemble vertebrate monocytes and macrophages (Anderson, 1981; Adema *et al.*, 1991) and, like these immune cells, have the ability to recognize, engulf, and internally degrade a variety of particles within the hemolymph and tissue (Foley and Cheng, 1975). The phagocytic process begins with recognition of a foreign particle and its engulfment into a phagosome. Once sequestered within the phagosome, the particle is subjected to various hydrolytic enzymes and reactive oxygen intermediates (ROIs), which aid in destroying the particle (Adema *et al.*, 1991; Anderson *et al.*, 1995). Many of the enzymes contained within the hemocytes of bivalves, including lysozyme (Rodrick and Cheng, 1974), β-glucuronidase (Cheng and Rodrick, 1975), and myeloperoxidase (MPO) (Wojcik and Paynter, 1995), have acidic pH optima ranging from pH 4.5–5.5. In addition, phagocytosis of foreign organisms by vertebrate macrophages and polymorphonuclear leukocytes (PMNs), as well as by hemocytes of *Mytilus edulis*, is accompanied by rapid acidification of the phagosome lumen (Jensen and Bainton, 1973; Rathman *et al.*, 1996; Kroschinski and Renwrantz, 1988). This suggests that, as in vertebrate phagocytes, phagosomal acidification may be required for activation of hydrolytic and ROI-producing enzymes in bivalve hemocytes, and may therefore be essential for the hemocyte antimicrobial defense response in molluscs.

Over the past few decades, the protozoan parasite *Perkinsus marinus* has caused widespread oyster mortalities in the Atlantic coast region. Although oyster hemocytes readily engulf *P. marinus*, it appears that the parasite may be able to survive within the hemocyte (Chu and La Peyre, 1993). In fact, many microorganisms can escape intracellular destruction by blocking phagosome-lysosome fusion (Jones and Hirsch, 1972; Horwitz, 1983; Mauel, 1984) or phagosomal acidification (Horwitz and Maxfield, 1984; Black *et al.*, 1986; Sibley *et al.*, 1985; Crowle *et al.*, 1991), or by adapting to the acidic environment of the phagosome

---

Received 9 July 1998; accepted 25 November 1998.

* To whom correspondence should be addressed. E-mail: paynter@mees.umd.edu

(Antoine *et al.*, 1990; Maurin *et al.*, 1992; Rathman *et al.*, 1996). Characterization of the oyster's normal defense response to foreign organisms is essential to understanding how oyster hemocytes respond to parasites such as *P. marinus*. Therefore, we measured phagosomal pH from hemocytes of *C. virginica* following phagocytosis of a noninfectious particle, zymosan, to characterize hemocyte phagosomal acidification in response to a nonpathogenic particle.

Measurement of pH with internalized zymosan labeled with pH-sensitive fluorescent dyes indicates that hemocyte phagosomes become highly acidified after phagocytosis of zymosan. Individual hemocytes containing zymosan that were continuously monitored over time underwent a morphological transition from highly granular to partially granular or agranular in appearance. A comparison of the two distinct morphologies showed that the phagosomes of the agranular hemocytes were much more acidic than those of the highly granular hemocytes.

Materials and Methods

Animals

Specimens of *Crassostrea virginica* were obtained from Horn Point Laboratory (Cambridge, Maryland). Oysters were maintained in aerated aquaria containing artificial seawater (Instant Ocean) at room temperature and at the salinity of the site from which they were collected, typically 12–16 ppt. Oysters were not fed during their captivity and were kept in the aquaria for at least 5 days before being used in any experiment.

Isolation of hemocytes

Hemolymph was collected from oysters by notching the valve, draining the mantle fluid, and withdrawing hemolymph from the adductor muscle sinus using a 10-ml syringe equipped with a 22-gauge, 1.5-in. needle. Hemolymph from two or three oysters was expelled slowly into a glass test tube and kept on ice to prevent cell clumping. Pooled hemolymph (1–2 ml) was layered on the cover slip of a glass-bottomed microwell (MatTek Corporation, Ashland, Massachusetts) for 15 min, during which time the hemocytes adhered to the cover slip. The monolayer was rinsed and covered with 0.2-μm filtered artificial seawater (FAS 30 ppt; Instant Ocean) buffered to pH 7.0 with 40 m*M* Hepes (Buffer 1).

Quantification of morphological transitions in granular hemocytes

Oyster hemocytes include two types of cells, granulocytes and hyalinocytes, which were classified on the basis of electron microscope studies (Cheng, 1996). Granulocytes are the most phagocytic hemocytes and contain many acidophilic or basophilic granules, whereas hyalinocytes contain few or no granules (Foley and Cheng, 1972; Cheng, 1996; Fisher, 1985). Because our study was conducted at the light microscope level, hemocytes were classified according to the overall granularity of the cytoplasm, as identified by their unstained appearance by light microscopy (600×). Hemocytes in which 90% or more of the cytoplasm was filled with highly refractile granules were termed "highly granular," and those that were 30%–89% granular were considered "partially granular." Hemocytes with 30% or less granular material were termed "agranular."

Zymosan, a preparation of *Saccharomyces cerevisiae* cell wall that is readily engulfed by oyster hemocytes (Austin and Paynter, 1995; Anderson *et al.*, 1995), was prepared by boiling (10 mg/100 ml distilled water) for 30 min. The solution was centrifuged (400 × *g*) for 5 min, washed with Buffer 1 (pH 7.0) three times, and resuspended in Buffer 1 (pH 7.0) at a final concentration of 10 mg/ml. Ten microliters of the zymosan solution was then layered over the hemocytes and incubated for 20 min to allow maximal uptake of zymosan (Anderson *et al.*, 1995). Hemocyte monolayers were washed after the 20-min incubation, covered with Buffer 1 (pH 7.0), and incubated an additional 10 min to allow time for any adhering zymosan to be fully engulfed. A total of 30 min after the addition of zymosan (time = 0), a central field of 4–8 hemocytes and 3–4 adjacent fields of cells per dish were visually selected by light microscopy (Nikon 60×, N.A. 1.4 objective) and monitored for an additional hour. All incubations and monitoring of hemocytes were performed at 25°C to promote rapid spreading and initial phagocytosis of zymosan (Fisher, 1985) and to allow comparison of data to other studies (Anderson *et al.*, 1992, 1995; Austin and Paynter, 1995). At the beginning of the time course, the central and adjacent fields of cells were noted and hemocytes with and without engulfed zymosan were identified and numbered. Numbered hemocytes were then scored as highly granular, partially granular, or agranular on the basis of their morphology. Because hemocytes are mobile, the cells were continuously monitored by noting the specific morphology of each cell and frequently returning to adjacent fields of cells to ensure that each hemocyte being monitored was correctly identified throughout the time course. Although many of these hemocytes became progressively agranular, the cells could still be easily identified according to their overall size and shape. The hemocytes were rescored at 30 and 60 min after time 0.

Three replicate experiments were performed. During experiment one, four monolayers containing a total of 65 hemocytes within selected fields were monitored. In experiment 2, two monolayers were prepared and 39 hemocytes monitored. Experiment 3 consisted of 4 monolayers and 37 hemocytes. The total number of hemocytes monitored was 141.

Preliminary phagosomal pH experiments

Preliminary experiments using the ratiometric fluorescence method of pH quantification, which uses the ratio of the emission intensities of a pH-sensitive dye (fluorescein) and a pH-insensitive dye (rhodamine) to quantify pH (Dunn *et al.*, 1994) indicated that agranular hemocyte phagosomes became acidified beyond the sensitivity range of fluorescein, which is strongly quenched below pH 5.0 (Haugland, 1996). This ratiometric method was modified by substituting Oregon Green 488 (OG 488), a fluorophore that is sensitive between pH 6.0 and 2.0, for fluorescein. Dual labeling of zymosan with rhodamine and OG 488 has been used to measure phagosomal pH in macrophages (Vergne *et al.*, 1998).

Fluorescent labeling of zymosan

Zymosan was prepared for conjugation with fluorescent probes by boiling (10 mg/100 ml distilled water) for 30 min. The solution was centrifuged (400 × *g*) for 5 min, washed with fresh 0.1 *M* $NaHCO_3$ buffer (Buffer 2), pH 8.3, three times, and resuspended in Buffer 2 at a final concentration of 10 mg/ml.

The active succinimidyl ester forms of carboxytetramethylrhodamine (TMR) and OG 488 were dissolved in anhydrous *N,N*-dimethylformamide (DMF) (3 mg/ml) and added to the zymosan suspension. The final reaction mixture (9.09 mg/ml zymosan, 0.27 mg/ml TMR, 0.27 mg/ml OG 488) was stirred at room temperature for 2 h. Labeled zymosan was removed from the mixture by centrifugation (15,000 × *g*). The pellet was resuspended in Buffer 2, centrifuged for 30 s (15,000 × *g*) and washed (Buffer 2) three times. The labeled zymosan was resuspended in Buffer 2 (10 mg/ml) and stored in 1-ml aliquots in the dark (−4°C) until use.

Calibration images

Quantification of pH was obtained using a ratio of the emission intensities of rhodamine, which is pH insensitive, and OG 488, which is pH sensitive. Images of fluorescent zymosan were collected with a microscope (Nikon 60×, N.A. 1.4 objective) equipped with a krypton-argon laser scanning confocal attachment (BioRadMRC 1024). Fluorescent zymosan was excited (488 nm) and OG 488 emission (green light) was collected using a 522/32 nm band pass filter. Rhodamine emission (red light) was collected using a 598/40 nm band pass filter. Laser power, photomultiplier gain, confocal aperture, and background levels were adjusted manually.

Extracellular calibrations. Calibration images were obtained by centrifuging labeled zymosan (15,000 × *g*) for 30 s, and resuspending zymosan (10 mg/ml) in Buffer 1 titrated to pHs of 6.0, 5.0, 4.0, 3.0, and 2.0. Aliquots of labeled zymosan at each pH were layered on the coverslip of a microwell and three fields of zymosan at each pH were selected, scanned with a krypton-argon laser (488 nm), and images collected digitally.

Intracellular calibrations. To determine if internalization of zymosan within hemocytes had any effect on the ratio of emission intensities of the two fluorescent dyes, intracellular calibrations were performed. Hemocyte monolayers were prepared as described previously. The microwells were filled with Buffer 1 (pH 7.0) so that the bottom of each microwell was fully covered. Labeled zymosan was centrifuged (15,000 × *g*) for 30 s and resuspended (10 mg/ml) in Buffer 1. Ten microliters of this solution was layered just above the hemocyte monolayer. The monolayers were placed in the dark and incubated for 30 min. After incubation, the monolayers were washed thoroughly with Buffer 1 (pH 7.0) and then covered with Buffer 1 (pH 7.0) containing 4% formaldehyde for 15 min. The monolayers were washed three times with Buffer 1 (pH 7.0) and placed in the dark. Monensin, a Na^+ ionophore used to neutralize pH gradients (Horwitz and Maxfield, 1984), was dissolved in 95% ethanol (1 m*M*) and added to Buffer 1 titrated to pH 6.0, 5.0, 4.0, 3.0, and 2.0 for a final concentration of 50 μM. Hemocyte monolayers were washed three times in the appropriate pH buffer and then immersed in Buffer 1 (pH 6.0, 5.0, 4.0, 3.0, or 2.0) containing 50 μM monensin. For each pH, 10 hemocytes with internalized zymosan were selected visually (600×) and scanned with the confocal laser as described above.

Measurement of phagosomal pH

Hemocyte monolayers were prepared and incubated with zymosan as described for the intracellular calibrations. However, after the 30-min incubation period, the monolayers were washed to remove any extracellular zymosan, covered again with Buffer 1 (pH 7.0), and incubated for another 30 min to ensure that any zymosan adhering to the hemocyte cell surface was fully engulfed. After the 60-min incubation period, hemocytes with internalized zymosan that appeared highly granular, partially granular, or agranular were visually selected and scanned with the confocal laser as described previously. Within a 15-min time period, about 25 hemocytes containing internalized zymosan were imaged per microwell. Four separate experiments (experiment 1–4) were performed on different days. In experiment 1, 3 monolayers were prepared and 69 hemocytes containing a total of 300 zymosan particles were selected and scanned. In experiment 2, 120 hemocytes with 430 zymosan particles were scanned from four monolayers. In experiments 3 and 4, two monolayers were prepared and 44 hemocytes with 202 zymosan particles (experiment 3) and 44 hemocytes with 147 zymosan particles (experiment 4) were scanned. Overall, 277 hemocytes containing 1079 engulfed particles of zymosan were scanned. Of these hemocytes, 83 were agranular (containing a total of 364 zymosan) and 83 were highly granular (containing 297 zymosan). Hemocytes containing unlabeled zymosan were also scanned to ensure that the fluorescent emission detected was not due to the autofluorescence of hemocytes or zymosan.

Image analysis

All images were processed and analyzed using the NIH-Image v. 1.61 software package (Wayne Rasband, National Institutes of Health). Rhodamine and OG 488 emissions were analyzed separately. First, the background fluorescence was subtracted from each image. The image was then duplicated and a threshold was applied to include zymosan with intensities of at least 2 on a scale of 256 grays (where 255 is the most intense, and 0 corresponds with no emission intensity). Each image was binarized, and the two resulting images were multiplied to create a mask image of pixels shared by both rhodamine and OG 488 emissions. The mask image was multiplied by each original background-corrected image to eliminate any unshared pixels. The final rhodamine image was divided by the final OG 488 image to obtain an image that was a ratio of the rhodamine to OG 488 emission intensities. Each zymosan particle was then analyzed manually by selecting an area and measuring the mean rhodamine/OG 488 fluorescence intensity for that set of pixels.

Data analysis

All data were analyzed using a statistical software package (StatView, Abacus Concepts, Berkeley, California). The ratio of rhodamine to OG 488 fluorescence for measurements of intracellular phagosomal pH were converted to pH values using a second- or third-order polynomial regression equation obtained from the calibration images collected for each experiment. Differences in mean phagosomal pH over time and between agranular and granular hemocytes were analyzed with a one factor factorial ANOVA. The percentages of granular and agranular hemocytes at times 0, 30, and 60 min were analyzed with a one factor ANOVA to determine whether the percentages of hemocytes types were statistically different between time points. Data groups were considered significantly different if $P < 0.05$.

Materials

Zymosan, DMF, and monensin were obtained from Sigma (St. Louis, Missouri). OG 488, Cl-Nerf, fluorescein, and TMR were purchased from Molecular Probes (Eugene, Oregon).

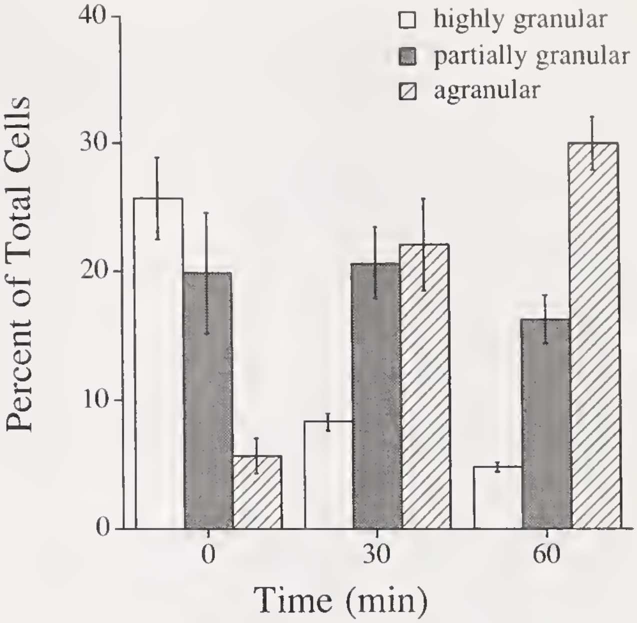

Figure 1. Percentage of 72 highly granular, partially granular, and agranular hemocytes containing zymosan at each time interval following a 30-min incubation period with zymosan (see text for specific conditions). The 69 hemocytes that did not contain zymosan are not shown because no change in morphology occurred. Error bars represent the standard error of the means.

Results

Morphological transition of hemocytes over time

The results of three experiments in which a total of 141 hemocytes were monitored continuously for 1 h indicate that granular hemocytes containing internalized zymosan undergo a morphological transition over time. A comparison of the total population of highly granular, partially granular, and agranular cells containing zymosan at times 0, 30, and 60 min indicated that the percentage of highly granular cells decreased over time, while the percentage of agranular cells increased (Fig. 1). In addition, because individual hemocytes were monitored continuously, the total number of zymosan-containing hemocytes that changed in morphology between each time point could be quantified (Table I). Most of the highly granular hemocytes with internalized zymosan identified at time = 0 became partially granular over a 30-min period, and less frequently they changed directly from highly granular to agranular within this time (Table I). Of those hemocytes at time = 0 that were partially granular, 83% became agranular within 1 h (Table I). Zymosan-containing hemocytes that remained granular throughout the time course (Table I) typically had only one or two engulfed zymosan particles, whereas those that became increasingly agranular over time typically had three or more internalized particles. In addition, 83% of the cells whose morphology remained the same throughout the

Table I

Number of cells of specific hemocyte types—with (z+) and without (z−) engulfed particles of zymosan—that exhibited a change in morphology over a 60-minute time course, compared with hemocytes (z+ and z−) that did not change in morphology

	Change in morphology							
	Highly granular to partially granular		Partially granular to agranular		Highly granular to agranular		No Change in morphology	
Time period (minutes)	z+	z−	z+	z−	z+	z−	z+	z−
0 to 30	17	0	17	0	6	0	7	57
30 to 60	5	0	7	0	0	0	5	0
Total	22	0	24	0	6	0	20	69

Hemocytes were identified as highly granular, partially granular or agranular after a 30-min incubation with zymosan (time 0; see text for specific conditions) and were continually observed for an additional 60 minutes. Morphologies of a total of 141 hemocytes at 0, 30 and 60 minutes were recorded.

time course contained no zymosan, and the hemocytes—with and without zymosan—that were agranular at time = 0 remained agranular throughout the time course (Table I).

pH calibration curves

Extracellular and intracellular calibration data collected before each experiment fit a second- or third-order polynomial regression equation with an adjusted R^2 of at least 0.94 ($P < 0.0001$; Fig. 2). Intracellular calibrations in which hemocytes with internalized zymosan were treated with monensin and equalized with buffer resulted in rhodamine/OG 488 emission ratios that were not statistically different from fluorescent emission ratios of extracellular zymosan at each pH. Because fluorescence emission of OG 488 was recoverable after addition of monensin to hemocyte monolayers, the emission intensities of the dyes were not altered by factors other than pH.

Phagosomal pH of random hemocytes

After the 30-min exposure to zymosan, hemocytes typically contained from 1 to 10 internalized zymosan particles. The results of four experiments indicate that the average pH of a total of 1079 phagosomes within 277 hemocytes at 60 min was 3.9 ± 0.03, with the distribution of pH values ranging from 5.9 to 2.4.

Phagosomal pH of granular and agranular hemocytes

The pH values of 297 phagosomes within 83 granular hemocytes from four experiments ranged from pH 3.8 to 5.9, with a mean pH of 4.9 ± 0.02 (Fig. 3). In contrast, the mean pH of 364 phagosomes within 83 agranular hemocytes was much lower (pH 3.1 ± 0.02; $P < 0.05$). The pH of phagosomes in agranular hemocytes ranged from 2.4 to 4.0 (Fig. 3).

Discussion

The average pH of eastern oyster hemocyte phagosomes after engulfment of zymosan falls below the ranges reported in the literature for most phagocytic cells (Table II). Phagosomal acidification, which is probably necessary for activation of digestive enzymes, varies depending on the or-

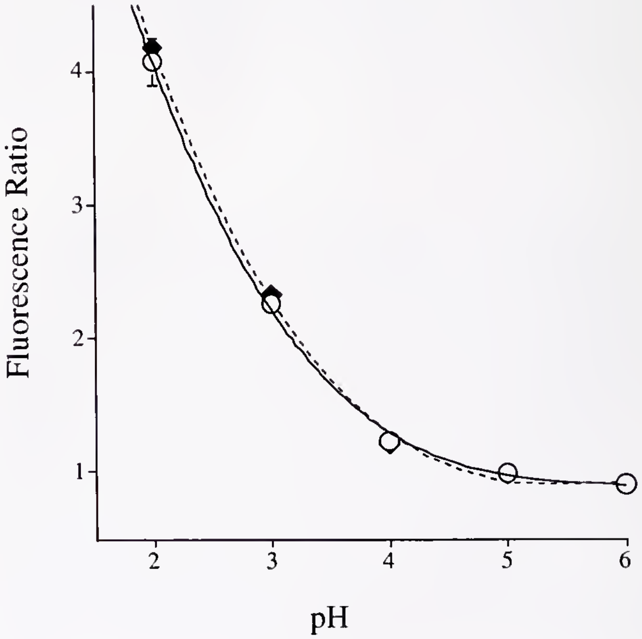

Figure 2. Example of a calibration curve for determination of pH values from the ratio of rhodamine to OG 488 emission intensities. Calibration curves were generated from extracellular zymosan placed in buffers of different pH values (- ○ -) or from zymosan engulfed within hemocytes that were fixed with 4% formaldehyde and incubated in buffers of different pH values containing 50 μM monensin to dissipate the pH gradient (- - ◆ - -). Ratio data were fitted to a second- or third-order polynomial regression equation that was then used to determine the pH of the zymosan engulfed within the hemocytes. Error bars indicate one standard deviation of the mean.

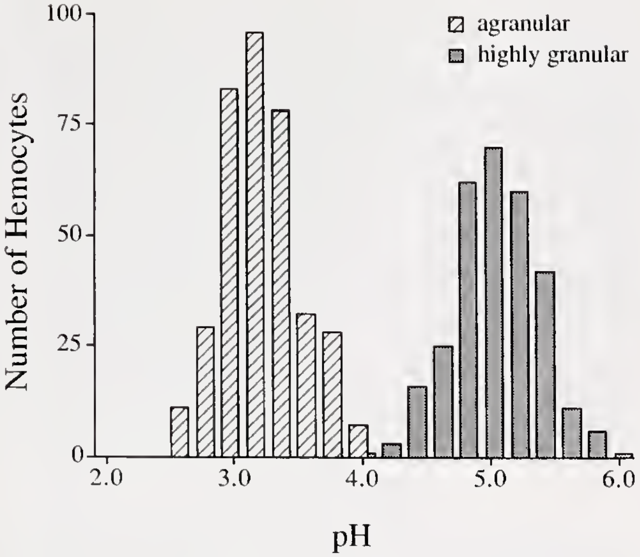

Figure 3. Distribution of pH associated with zymosan engulfed by granular and agranular hemocytes after a 30-min exposure to zymosan and an additional 30-min incubation. Hemocytes were classified as granular or agranular on the basis of the overall granularity of the cytoplasm as observed by light microscopy, and the pH of engulfed fluorescent zymosan was calculated from the ratio of the emission intensities of rhodamine and OG 488. The mean pH was 4.9 ± 0.02 for 297 phagosomes within 83 granular hemocytes, but much lower (mean pH 3.1 ± 0.02; $P < 0.05$) for 364 phagosomes within 83 agranular hemocytes.

ganism and cell type. For instance, the lowest phagosomal pH value reported in mouse macrophages after phagocytosis of yeast was 5.0 (Geisow *et al.*, 1981), and hemocyte phagosomes of *Mytilus edulis* reached a low pH of 4.5 ± 0.5 (Kroschinski and Renwrantz, 1988). In contrast, digestive vacuoles of *Paramecium* become acidified to pH 3.0 after acidosomes bind with the digestive vacuole (Fok and Allen, 1990). In most cells, acidification of the phagosome lumen may occur in as little as 7–15 min after engulfment of foreign material (Jensen and Bainton, 1973; Geisow *et al.*, 1981; Bassoe and Bjerknes, 1985), and the phagosome in some cell types can remain acidified for 5 h or more after phagocytosis (Horwitz and Maxfield, 1984; Rathman *et al.*, 1996).

Like the digestive vacuoles of *Paramecium*, the hemocyte phagosomes of *C. virginica* become highly acidified. However, the degree of acidification varies, and this variation appears to be related to the final morphology of the hemocyte. Most of the individual hemocytes monitored over time underwent a morphological transition from highly granular to increasingly agranular in appearance after engulfment of zymosan, and measurements of phagosomal pH revealed that hemocytes remaining highly granular were not as acidic as those of the agranular form. In fact, preliminary experiments that used fluorescein as the pH-sensitive dye were unsuccessful due to the very low pH of the agranular hemocyte phagosome.

The granular hemocytes of bivalves contain many cytoplasmic granules and morphologically resemble vertebrate immune cells such as macrophages and PMNs (Cheng, 1996; Adema *et al.*, 1991). Like their vertebrate counterparts, hemocytes may degranulate after engulfing foreign particles (Cheng, 1996). In vertebrate PMNs, degranulation of the cytoplasm only takes place after engulfment of a foreign particle (Hirsch, 1962), and typically occurs within 30 min after phagocytosis (Hirsch and Cohn, 1960). Similarly, the transition in oyster hemocyte morphology typically occurred within 0–30 min after engulfment of zymosan, and granular hemocytes without engulfed particles remained granular throughout the time course. This suggests that granular hemocytes containing zymosan became more agranular in appearance over time as the result of increasing phagosome-lysosome fusion and subsequent degranulation of the hemocyte cytoplasm. This also suggests that the highly acidic pH of the agranular hemocyte phagosome may be the result of increased lysosomal fusion. Although *Paramecium* phagosomes subsequently become alkaline after lysosomal fusion (Fok and Allen, 1990), degranulation of mouse macrophages is associated with a gradual reduction in phagosomal pH (Geisow *et al.*, 1981). *Amoeba proteus* phagosomes also become further acidified as lysosomal fusion occurs (McNeil *et al.*, 1983).

The corresponding decrease in pH from the granular to agranular morphological state suggests the hemocyte is attempting to digest the engulfed zymosan. A similar rapid

Table II

Typical phagosomal pH values and method of measurement for a variety of phagocytic cells

Organism	Cell type	Target particle	Minimum pH of phagosome	Method	Source
rat	PMN*	yeast	3.5–4.5	indicator dyes	Jensen & Bainton, 1973
mouse	macrophage	yeast	5.0	fluorescein	Geisow *et al.*, 1981
mouse	macrophage	latex beads	4.0–5.0	DM-Nerf	Rathman *et al.*, 1996
Mytilus edulis	hemocyte	yeast	4.5 ± 0.5	indicator dyes	Kroschinski & Renwrantz, 1988
Paramecium		yeast	3.0	fluorescein	Fok & Allen, 1990

* PMN—polymorphonuclear leukocyte.

decrease in pH occurs in *Paramecium,* in which the phagosomal pH decreases from 7.0 to 3.0 after the digestive vacuole containing the phagocytized material binds with acidosomes, initiating the process of prey killing and protein denaturation (Fok and Allen, 1990). Electron micrographs of degranulated bivalve hemocytes show that digestive lamellae form around partially degraded foreign material engulfed within the phagosome, and numerous glycogen granules appear in the cytoplasm (Cheng and Foley, 1975). On the basis of these observations, Cheng and Foley (1975) proposed that degranulated hemocytes were in the process of intracellular digestion of engulfed materials.

The lowest measured pH of oyster hemocyte phagosomes (pH 2.4) is much more acidic than the lowest pH value estimated from hemocyte food vacuoles of *Mytilus edulis* (Table II). However, it is important to note that these researchers did not report any change in the granularity of the hemocytes (Kroschinski and Renwrantz, 1988). In addition, the average pH of the agranular form of hemocytes was much lower than the pH optima of digestive enzymes contained within molluscan hemocytes (4.5–5.5). This suggests that these enzymes may be inactivated or that perhaps other enzymes with more acidic pH optima become active. Alternatively, it is possible that a subsequent alkalinization of the phagosome occurs, as in *Paramecium* and *Chaos carolinensis* (Fok and Allen, 1990; Heiple and Taylor, 1982). However, we have observed that agranular hemocyte phagosomes remained acidified for up to 4 h after phagocytosis (data not shown).

As in vertebrate immune defense cells, phagocytosis of foreign organisms by oyster hemocytes causes a biochemical cascade resulting in the production of ROIs such as superoxide anion and hypochlorous acid (HOCL) which contribute to oxidative killing of phagocytized foreign microorganisms (Adema *et al.,* 1991; Anderson *et al.,* 1992). The production of ROIs by oyster hemocytes reaches a peak 10 to 15 min after introduction of zymosan to hemocytes, and then gradually declines over a period of 120 min (Austin and Paynter, 1995). Myeloperoxidase (MPO), the enzyme responsible for the production of HOCL, was partially purified from oyster hemocytes and shown to have a pH optimum of 5.5 (Wojcik and Paynter, 1995). The phagosomal pH of granular hemocytes (mean pH 4.9 ± 0.02) is very close to the pH optimum of MPO. Thus, the production of ROIs by hemocytes just after stimulation may be the hemocyte's first line of defense against invading organisms. Over time, granular hemocytes become increasingly agranular in appearance as lysosomes fuse with the phagosome, resulting in a concomitant decrease in pH. The production of ROIs may also decline as the pH decreases below the optimal pH of the ROI-producing enzymes such as MPO. In fact, at pH values less than 4, only 40% of MPO would be active (Wojcik and Paynter, 1995).

In conclusion, highly and partially granular hemocytes are most often associated with internalized zymosan at the beginning of the time course. Corresponding with this early time point and morphological state is a mean pH similar to optimal pH values of hydrolytic and ROI-producing enzymes. Over a period of 60 minutes, however, the hemocyte becomes increasingly agranular as lysosomes apparently fuse with the phagosome, further reducing the pH within the phagosome. Although the pH within the phagosome of the highly granular hemocyte is comparable to that of most other phagocytic cells, the phagosomal pH of the agranular hemocyte is more typical of the digestive vacuole in *Paramecium,* which reaches a low pH of 3.0 (Fok and Allen, 1990), suggesting that phagosomal acidification is a vital component of the oyster hemocyte's defense response.

Acknowledgments

The authors thank Dr. Kenneth Dunn, Indiana University Medical Center, for his help in learning the confocal technique and for his patience in answering all of our questions.

Literature Cited

Adema, C. M., M. P. W. van der Knapp, and T. Sminia. 1991. Molluscan hemocyte-mediated cytotoxicity: the role of reactive oxygen intermediates. *Rev. Aquat. Sci.* **4:** 201–223.

Alvarez, M. R., F. E. Friedl, J. S. Johnson, and G. W. Hinsch. 1989. Factors affecting *in vitro* phagocytosis by oyster hemocytes. *J. Invertebr. Pathol.* **54:** 233–241.

Anderson, R. S. 1981. Comparative aspects of the structure and function of invertebrate and vertebrate leucocytes. Pp. 629–641 in *Invertebrate Blood Cells 2,* N. A. Ratcliffe and A. F. Rowley, eds. Academic Press, New York.

Anderson, R. S., K. T. Paynter, and E. M. Burreson. 1992. Increased reactive oxygen intermediate production by hemocytes withdrawn from *Crassostrea virginica* infected with *Perkinsus marinus. Biol. Bull.* **183:** 476–481.

Anderson, R. S., E. M. Burreson, and K. T. Paynter. 1995. Defense responses of hemocytes withdrawn from *Crassostrea virginica* infected with *Perkinsus marinus. J. Invertebr. Pathol.* **66:** 82–89.

Antoine, J., E. Prina, C. Jouanne, and P. Bongrand. 1990. Parasitophorous vacuoles of *Leishmania amazonenesis*-infected macrophages maintain an acidic pH. *Infect. Immun.* **58:** 779–787.

Austin, K. A., and K. T. Paynter. 1995. Characterization of the chemiluminescence measured in hemocytes of the Eastern oyster, *Crassostrea virginica. J. Exp. Zool.* **273:** 461–471.

Bassoe, C. F., and R. Bjerknes. 1985. Phagocytosis by human leukocytes, phagosomal pH and degradation of seven species of bacteria measured by flow cytometry. *J. Med. Microbiol.* **19:** 115–125.

Black, C. M., M. Paliescheskey, B. L. Beaman, R. M. Donovan, and E. Goldstein. 1986. Acidification of phagosomes in murine macrophages: Blockage by *Nocardia asteroides. J. Inf. Dis.* **154:** 952–958.

Cheng, T. C. 1996. Hemocytes: Forms and functions. Pp. 299–326 in *The Eastern Oyster, Crassostrea virginica,* V. S. Kennedy and A. F. Newell, eds. Maryland Sea Grant College, College Park.

Cheng, T. C., and D. A. Foley. 1975. Hemolymph cells of the bivalve mollusc *Mercenaria mercenaria:* an electron microscopical study. *J. Invertebr. Pathol.* **26:** 341–351.

Cheng, T. C., and G. E. Rodrick. 1975. Lysosomal and other enzymes in the hemolymph of *Crassostrea virginica* and *Mercenaria mercenaria. Comp. Biochem. Physiol.* **52B:** 443–447.

Chu, F. E., and J. F. La Peyre. 1993. *Perkinsus marinus* susceptibility and defense-related activities in eastern oysters *Crassostrea virginica:* temperature effects. *Dis. Aquat. Org.* **16:** 223–234.

Crowle, A. J., R. Dahl, E. Ross, and M. H. May. 1991. Evidence that vesicles containing living, virulent *Mycobacterium tuberculosis* or *Mycobacterium avium* in cultured human macrophages are not acidic. *Infect. Immun.* **59:** 1823–1831.

Dunn, K. W., S. Mayor, J. N. Myers, and F. R. Maxfield. 1994. Applications of ratio fluorescence microscopy in the study of cell physiology. *FASEB J.* **8:** 573–582.

Fisher, W. S. 1985. Structure and functions of oyster hemocytes. Pp. 25–35 in *Immunity in Invertebrates: Cells, Molecules and Defense Reactions,* M. Brehelin, ed. Springer-Verlag, New York.

Fok, A. K., and R. D. Allen. 1990. The phagosome-lysosome membrane system and its regulation in *Paramecium. Int. Rev. Cytol.* **123:** 61–95.

Foley, D. A., and T. C. Cheng. 1972. Interaction of molluscs and foreign substances: the morphology and behavior of hemolymph cells of the American oyster, *Crassostrea virginica, in vitro. J. Invertebr. Pathol.* **19:** 383–394.

Foley, D. A., and T. C. Cheng. 1975. A quantitative study of phagocytosis by hemolymph cells of the pelecypods *Crassostrea virginica* and *Mercenaria mercenaria. J. Invertebr. Pathol.* **25:** 189–197.

Geisow, M. J., P. D. Hart, and M. R. Young. 1981. Temporal changes of lysosome and phagosome pH during phagolysosome formation in macrophages: studies by fluorescence spectroscopy. *J. Cell. Biol.* **89:** 645–652.

Haugland, R. P. 1996. *Handbook of Fluorescent Probes and Research Chemicals,* 6th ed. Molecular Probes, Inc., Eugene, Oregon.

Heiple, J. M., and D. L. Taylor. 1982. pH changes in pinosomes and phagosomes in the ameba. *Chaos carolinensis. J. Cell Biol.* **94:** 143–149.

Hirsch, J. G. 1962. Cinemicrophotographic observations on granule lysis in polymorphonuclear leucocytes during phagocytosis. *J. Exp. Med.* **116:** 827–833.

Hirsch, J. G., and Z. A. Cohn. 1960. Degranulation of polymorphonuclear leucocytes following phagocytosis of microorganisms. *J. Exp. Med.* **112:** 1005–1014.

Horwitz, M. 1983. The Legionaires' disease bacterium (*Legionella pneumophila*) inhibits phagosome-lysosome fusion in human monocytes. *J. Exp. Med.* **158:** 2108–2126.

Horwitz, M. A., and F. R. Maxfield. 1984. *Legionella pneumophila* inhibits acidification of its phagosome in human monocytes. *J. Cell Biol.* **99:** 1936–1943.

Jensen, M. S., and D. F. Bainton. 1973. Temporal changes in pH within the phagocytic vacuole of the polymorphonuclear neutrophilic leukocyte. *J. Cell Biol.* **56:** 379–388.

Jones, T. C., and J. G. Hirsch. 1972. The interaction between *Toxoplasma gondii* and mammalian cells. II. The absence of lysosomal fusion with phagocytic vacuoles containing living parasites. *J. Exp. Med.* **136:** 1173–1194.

Kroschinski, J., and L. Renwrantz. 1988. Determination of pH values inside the digestive vacuoles of hemocytes from *Mytilus edulis. J. Invertebr. Pathol.* **51:** 73–79.

Mauel, J. 1984. Mechanisms of survival of protozoan parasites in mononuclear phagocytes. *Parasitology* **88:** 579–592.

Maurin, M., A. M. Benoliel, P. Bongrand, and D. Raoult. 1992. Phagolysosomes of *Coxiella burnetti*-infected cell lines maintain an acidic pH during persistent infection. *Infect. Immun.* **60:** 5013–5016.

McCormick-Ray, M. G., and T. Howard. 1991. Morphology and mobility of oyster hemocytes: evidence for seasonal variations. *J. Invertebr. Pathol.* **58:** 219–230.

McNeil, P. L., L. Tanasugarn, J. B. Meigs, and D. L. Taylor. 1983. Acidification of phagosomes is initiated before lysosomal enzyme activity is detected. *J. Cell Biol.* **97:** 692–702.

Rathman, M., M. D. Sjaastad, and S. Falkow. 1996. Acidification of phagosomes containing *Salmonella typhimurium* in murine macrophages. *Infect. Immun.* **64:** 2765–2773.

Rodrick, G. E., and T. C. Cheng. 1974. Kinetic properties of lysozyme from the hemolymph of *Crassostrea virginica. J. Invertebr. Pathol.* **24:** 41–48.

Sibley, L. D., E. Weidner, and J. L. Krahenbuhl. 1985. Phagosome acidification blocked by intracellular *Toxoplasma gondii. Nature* (London) **315:** 416–419.

Vergne, I., P. Constant, and G. Laneelle. 1998. Phagosomal pH determination by dual fluorescence flow cytometry. *Anal. Biochem.* **255:** 127–132.

Wojcik, J., and K. T. Paynter. 1995. Putative myeloperoxidase activity from hemocytes of the Eastern oyster, *Crassostrea virginica. Am. Zool.* **35:** 33A.

Reference: *Biol. Bull.* **196:** 34–44. (February, 1999)

Differences in the Composition of Adhesive and Non-Adhesive Mucus From the Limpet *Lottia limatula*

ANDREW M. SMITH*, TONYA J. QUICK, AND RACHEL L. ST. PETER

Department of Biological Sciences, Butler University, Indianapolis, Indiana 46208

Abstract. The mucus used by the limpet *Lottia limatula* to form glue-like attachments was compared biochemically to the slippery mucus produced during other activities, such as suction adhesion. Colorimetric assays revealed the protein content of the adhesive mucus to be 2.1 times greater than that of the non-adhesive form, and the carbohydrate content to be 1.9 times greater. Both forms of mucus contained roughly six times as much protein as carbohydrate, and there was no difference in their inorganic elemental compositions. Quantitative analysis of the protein content by SDS-PAGE and a scanning densitometer revealed a similar protein composition in both forms of mucus; but three notable differences emerged. First, the overall difference in protein concentration was confirmed. In addition, there was a 118 kD protein that was common only in the adhesive mucus, and a 68 kD protein that occurred only in the non-adhesive mucus.

Introduction

Limpets are known for their ability to attach firmly to rocks in the wave-swept intertidal zone. Recently, Smith (1992) showed that many limpets alternate between two attachment mechanisms. At high tide on the California coast, most limpets use suction adhesion; when the tide goes out, most switch to a glue-like adhesion. Suction adhesion has been studied in limpets and cephalopod molluscs (Smith, 1991a,b; Smith *et al.*, 1993), but the glue-like adhesion of limpets has not been well studied. This adhesive forms a powerful, durable attachment, yet it is based on mucus rather than a solid cement.

This glue-like adhesive can be so strong that when one tries to remove limpets from a hard surface, the shell sometimes tears off before the adhesive fails. Smith (1992) estimated that the average tenacity, defined as force per unit area of attachment, of the adhesive secreted by four species of limpets from California is 230 kPa. Tenacities up to 518 kPa have been reported in other species (Branch and Marsh, 1978). Whether the forces reported by Branch and Marsh (1978) were due to suction or gluing was not made clear, but it is likely that the mechanism was gluing. This is because cavitation normally causes failure of suction adhesives at tenacities between 100 and 200 kPa at sea level (Smith, 1996).

The strength of this adhesive is surprising, because it is composed of mucus. Mucus is typically a dilute network of proteins and polysaccharides. These molecules take on an extended configuration that causes them to become entangled, thus forming a weak gel (Wainwright *et al.*, 1976). The viscoelasticity of such a gel can provide some mechanical strength (Denny, 1980, 1989; Grenon and Walker, 1980), but its stiffness is normally much lower than necessary for the tenacities limpets achieve (Smith, 1991b). Also, although high-viscosity materials can function as Stefan adhesives (Grenon and Walker, 1981), this mechanism has limitations that make it unlikely to be effective for invertebrates (see Discussion).

Mucous secretions are widely used as lubricants, not adhesives. For example, lubricating mucous gels line and protect the mammalian digestive, reproductive, and respiratory tracts (Silberberg and Meyer, 1982). In marine invertebrates, mucus typically forms a slippery coating that prevents bacteria and debris from accumulating on the body surface (Baier *et al.*, 1985), and keeps other organisms from adhering to it (Harrold, 1982). Thus, we would not expect typical mucous secretions to be good adhesives. Nevertheless, limpets do modify mucus so that it functions in this way.

The mechanical properties of mucus can be modified in

Received 3 September 1997; accepted 1 December 1998.

* To whom correspondence should be addressed. E-mail: ansmith@thomas.butler.edu

various ways (Chantler and deBruyne, 1977). For example, changing the pH or ion content of the water in the gel could cause the gel to shrink and thus stiffen. Alternatively, specific proteins or carbohydrates could be added to cross-link the gel-forming polymers. Finally, a different type of gel-forming polymer could be synthesized and secreted. Of course, some combination of these changes could occur. Moreover, all seem equally plausible: limpets can probably move specific ions across their pedal epithelia (Hermans, 1983), and there are a wide variety of glands secreting onto their pedal sole (Grenon and Walker, 1978). We propose that limpets secrete a specific form of mucus for lubrication while moving or using suction adhesion; then, when a stronger attachment is needed, the mucus is modified in one of the ways suggested above. To test this hypothesis, we compared the compositions of adhesive mucus and non-adhesive mucus, aiming to identify biochemical differences that might be correlated with the change in function.

Materials and Methods

Sample collection

Specimens of *Lottia limatula* (Carpenter) were purchased from Pacific Bio-Marine Labs, Inc. (Venice, CA, United States) and maintained in a recirculating marine aquarium at 18°C. Samples of mucus were collected primarily during the first 2 or 3 weeks after the arrival of the limpets, although the animals survived and continued to produce mucus for several months.

Adhesive mucus was collected from limpets that had been left undisturbed on a clean, glass aquarium wall for at least 24 h. In this situation, roughly one-third of the limpets would be attached using the glue-like mechanism (Smith, 1991b). These limpets were easily distinguished from those using suction; the limpets using glue stuck much more firmly, but their tenacity decreased dramatically once dislodged from their initial spot. After each limpet was dislodged, a thin film of mucus remained tightly adhered at the point of attachment. One could easily feel this patch of adhesive mucus, even underwater, where most of the samples were collected. This mucus was scraped off with a clean razor blade, forming distinct, irregular clumps that clung to the blade. The blade was gently shaken and tilted to remove excess water from the surface of the sample, which was then scraped into a microcentrifuge tube. Each tube contained between 10 and 50 mg of mucus collected from at least five limpets. The samples were pooled and stored at −70°C.

Non-adhesive mucus was collected as follows. Groups of 6 to 10 limpets were placed in a small plastic bag (roughly 1 liter) filled with seawater. The limpets rarely adhered to the bag and instead stayed active, often climbing on one another's shells, using suction. When removed from the bag after 4 to 8 h, many of the limpets had thin sheets and aggregations of mucus on the shell and across the sole of the foot. This mucus, which could be collected by gently rubbing it off of the shell or foot, was quite different from the adhesive mucus, which resisted fairly vigorous rubbing. Also, when compared side by side, the non-adhesive mucus seemed less elastic and dense than the adhesive mucus. After collection, excess water was removed in the same way as with the adhesive samples. The samples were then pooled and stored as above. Note that this collection method could not ensure that all the mucus was from the sole of the foot; some of it might have come from the hypobranchial glands, the mantle, or the sides of the foot. Nevertheless, this procedure provided a good sample of non-adhesive mucus.

Comparison of total protein and carbohydrate content, and inorganic content

The wet weights of three samples each of adhesive and non-adhesive mucus were measured on an analytical balance. They were then dehydrated in a SpeedVac, and their dry weight was measured.

The protein concentration of the mucus was measured using the Bradford assay (Bradford, 1976; Bio-Rad protein assay kit). Eleven samples of adhesive mucus and ten of non-adhesive mucus were assayed. Each sample of 10–40 mg of mucus was thawed, weighed, and placed in 200 μl of distilled, de-ionized water with 1% sodium dodecyl sulfate (SDS) and 1% dithiothreitol (DTT). The samples were dissolved by sonication for roughly 10 mins, then diluted so that the final SDS concentration was less than 0.1% to avoid interference with the Bradford assay. Several dilutions of bovine serum albumin with the same concentration of SDS and DTT were used as standards. In addition to the Bradford assay, many of the samples were also assayed at 230 and 280 nm (correcting for absorption at 260 nm as described by Boyer, 1993). Several samples were also dissolved in 1 *M* NaOH and assayed at 230 and 280 nm.

The carbohydrate concentration of the mucus was assayed using the orcinol-sulfuric acid method described by Kennedy and Pagliuca (1994). Seven samples of adhesive mucus and six samples of non-adhesive mucus were tested. The only differences from the published method were that orcinol was not recrystallized before use, and the assays were made at 510 nm, as suggested in the original method, rather than 420 nm, which Kennedy and Pagliuca suggest. Data were also collected at 420 nm, but the 510 absorbance gave more consistent results for the samples and the glucose standard.

The inorganic composition of five samples each of adhesive and non-adhesive mucus was also determined. Samples were dried in a SpeedVac and analyzed with a JEOL JSM-U3 scanning electron microscope outfitted with a Tracor Northern 5500 EDS (Energy Dispersive X-ray System). Samples were mounted on graphite backing and scanned at

20 kV. Of these 10 samples, 2 of each type were sonicated before drying to improve sample homogeneity. Sonication did not noticeably affect the results.

Comparison of protein composition using SDS-PAGE

The protein compositions of adhesive and non-adhesive mucus were compared by sodium dodecyl sulfate polyacrylamide gel electrophoresis (SDS-PAGE). Eleven samples of each type were compared, and they were trimmed with a razor blade so that similar wet weights were used. Nevertheless, on average, there was 1.13 ± 0.15 times (mean ± SD) as much of the non-adhesive form. Samples were dissolved as in the protein assays. They were run on discontinuous gels, based on the method of Laemmli (1970) and the detailed protocols of Hames (1990). The gel dimensions were 8 × 9 cm by 0.75 mm thick, and the total acrylamide concentration was 10%. Gels were stained with Coomassie blue R-250.

The SDS-PAGE results were averaged to eliminate variation due to proteins unrelated to adhesion. Each lane was scanned with a densitometer, measuring the absorbance at 580 nm. The results were recorded on a Macintosh computer using a MacADIOS II digitizer and Superscope II software (GW Instruments, Somerville, MA). The data for each lane were transferred to a spreadsheet and converted to a molecular weight scale. This conversion was based on calibration curves specific to each gel that were generated with a set of standard proteins (high molecular weight range, Sigma Scientific). The molecular weight values appear to be accurate to within 1 or 2 kD, except for the protein identified at 203 kD. This protein may be 10 to 20 kD larger. Once the data were converted, the staining intensity at each molecular weight was averaged for all 11 samples of each type of mucus.

In addition to the detailed comparison described above, other samples were tested under a variety of conditions. Different buffers were tested for their ability to solubilize the mucus. Factors that were varied included pH, salt content, and the presence and concentration of reagents such as urea, SDS, and 2-mercaptoethanol. Varying degrees of shear were also tested, ranging from sonication to mild rocking overnight. Gels with total acrylamide concentrations of 5% and 20% were also run. In a number of samples, the stacking gel was also scanned with the densitometer to quantify any material that was too large to enter the running gel.

Characterization of proteins

Several samples each of adhesive and non-adhesive mucus were stained for the presence of glycoproteins. The samples were dissolved in 0.125 *M* Tris-Cl (pH 6.8), 2% SDS, 5% 2-mercaptoethanol, and 10% glycerol and run on a 10% gel as described previously. The proteins were then transferred to a nitrocellulose membrane in a Mighty Small Transphor tank transfer unit (Hoefer Scientific Instruments), using the buffer of Towbin *et al.* (1979). Transfer conditions were 400 mA for 1 h. The membrane was stained transiently with Ponceau-S to ensure that all the proteins transferred. Glycoproteins were detected using a DIG Glycan Detection Kit (Boehringer Mannheim) following the instructions in the manual. Briefly, this protocol involved periodic acid oxidation followed by binding of digoxigenin to the oxidized sugars. These were marked by anti-digoxigenin antibodies conjugated to alkaline phosphatase.

Amino acid analysis was performed on some of the major proteins identified through SDS-PAGE. Samples of adhesive and non-adhesive mucus were solubilized as described in the previous paragraph and run on a 10% gel. Proteins were transferred to an immobilon-P membrane (Millipore), using 22.5 m*M* Tris-borate, 0.1 m*M* EDTA, 0.1% SDS and 25% methanol as a tank buffer. Running conditions were 400 mA for 3 h. The membrane was stained with Coomassie blue G-250 and destained with 40% methanol. Selected bands and a blank from outside the lanes were excised from the membrane and hydrolyzed in 6 *M* HCl with 10% phenol and 10% trifluoroacetic acid under vacuum at 150°C for 40 min. Amino acid compositions were then determined on a Beckman System 6300 Auto Analyzer. The amino acid composition of two whole, dried samples of adhesive mucus was also analyzed. The samples were dissolved in either ammonium hydroxide or trifluoroacetic acid, hydrolyzed for 22 h at 110°C with 6 *M* HCl and phenol, then run on a Beckman analyzer.

Samples were also analyzed by two-dimensional electrophoresis. Iso-electric focusing was used as the first dimension, followed by SDS-PAGE. Proteins were focused for 3 h in the presence of 9 *M* urea and 2% CHAPS. Iso-electric focusing was carried out using pH gradients from 3 to 10 and from 4 to 6. Two-dimensional gels were silver stained (Silver stain plus kit, Bio-Rad).

Results

Comparison of total protein and carbohydrate content

The overall polymer concentration of the adhesive secretion was roughly two times greater than that of the non-adhesive secretion (Fig. 1). On average, there was 2.1 times as much protein in the adhesive form as the non-adhesive form (Student's *t* test, $P < 0.001$). There was also 1.8 times as much carbohydrate in the adhesive form ($P < 0.001$). In both forms of mucus, protein made up a greater part of the secretion than carbohydrate. Assuming that protein and carbohydrates were the primary organic molecules present, protein made up 86% of the organic material in adhesive mucus and 85% in non-adhesive mucus.

The values for protein and carbohydrate concentration were slightly lower than what has been reported in other

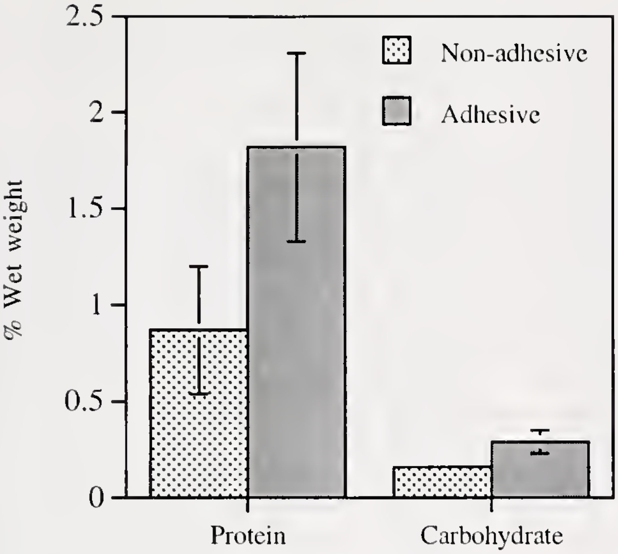

Figure 1. Comparison of the protein and carbohydrate contents of non-adhesive and adhesive mucus.

limpet species (typically about 3% protein and 1% carbohydrate; Davies *et al.,* 1990). This may be due partly to the resistance of limpet mucus to solubilization. Even under the conditions used in our experiments, some of the material failed to go into solution. Further tests were carried out using 4% SDS or 1 *M* NaOH to improve solubility. Since these reagents interfered with the Bradford assay, samples were assayed at 230 and 280 nm. The results of these tests support the finding that the adhesive form contains twice as much protein. The protein contents determined by these assays varied much more widely, but were typically somewhat higher than the values in Figure 1.

The water content of limpet pedal mucus was similar to values reported by Davies *et al.* (1990). The adhesive form of mucus contained 92.5% ± 3.3 water and the non-adhesive form contained 92.9% ± 1.3 water. Presumably, an additional 4% to 5% of the wet weight was composed of salts.

Comparison of inorganic content

There was no difference between the inorganic elemental compositions of adhesive and non-adhesive mucus (Fig. 2). The inorganic composition of both forms of mucus is similar to that of seawater, since mucus is typically more than 90% water. There was relatively more sulfur and phosphorus than in seawater, as expected for a solution containing organic molecules. Note that 3 of the 10 samples were omitted from the analysis because they appeared to be contaminated; more than 39% of the inorganic content was calcium in one non-adhesive sample and roughly 30% of the inorganic content was iron in the other two (one adhesive and one non-adhesive). In all but one of the other samples, calcium and iron each made up just 1% to 3% of the inorganic content. One of the adhesive samples in the analysis had 11% iron. This one sample accounted for the appearance of a slight difference in iron content between the two types of mucus. The presence of some heavy metals is probably also attributable to contamination. Mercury was found only in one sample, as was zinc.

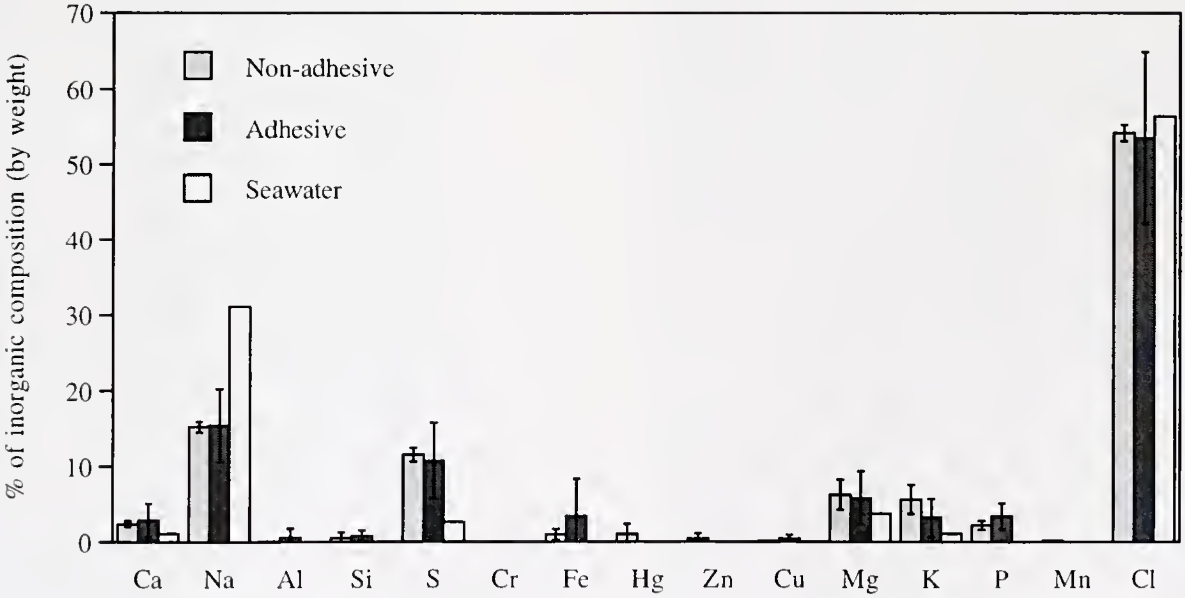

Figure 2. Scanning electron microscope elemental analysis of non-adhesive and adhesive mucus. Data for seawater are adapted from Schmidt-Nielsen (1990) and are included for comparison. The relative contribution of each element to the total weight of inorganic matter is shown.

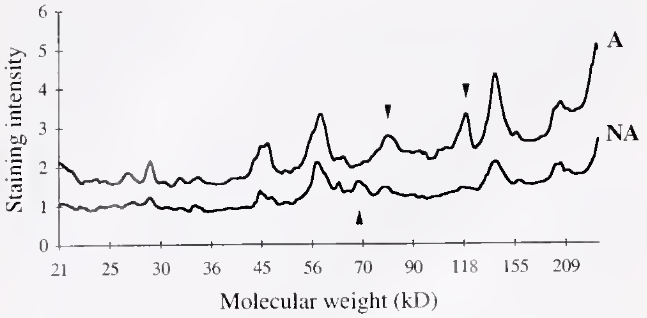

Figure 3. Average staining intensity of the bands resulting from SDS-PAGE performed on adhesive (A) and non-adhesive (NA) mucus. The relative staining intensity is measured by the absorbance at 580 nm. The 118 kD, 80 kD, and 68 kD proteins are marked by arrowheads.

Comparison of protein composition

SDS-PAGE showed that, with a few significant exceptions, the same proteins were present in the adhesive and non-adhesive forms of mucus (Figs. 3, 4). The most striking difference was a 118 kD protein that was common in the adhesive form, but rare in the non-adhesive form. In addition, an 80 kD protein was more common in the adhesive form; but it was not consistently present. Conversely, a 68 kD protein was usually found in the non-adhesive mucus, though in relatively smaller quantities, and it was not found in the adhesive mucus.

There was some variability in the amount of many of the proteins. In Figure 4, for example, the 57 kD protein appeared to be more common in the non-adhesive mucus, but this was not a consistent difference. In some samples, this protein was more common in the adhesive mucus instead. In addition, the 80 kD protein was sometimes quite a bit darker than shown in Figure 4. Thus, it was important to average a number of samples to identify consistent differences.

In addition to the consistent difference in a few specific proteins, the SDS-PAGE results also supported the overall difference in protein concentration. On average, the intensity of staining of lanes containing adhesive mucus was 1.8 times greater than that of lanes containing non-adhesive mucus. Adjusting for the slight difference in the amount of mucus loaded gave a figure of 2.0 times as much protein in the adhesive mucus.

Analysis of samples run on gels with different pore sizes showed that the proteins shown in Figures 3 and 4 make up the bulk of the secretion. Lower and higher percentage gels showed no significant proteins above 220 kD or below 20 kD. There was, however, often material that failed to enter the stacking gel, forming a band at the top. Using the densitometer, it was calculated that this amounted to roughly 10% of the total protein. Several lines of evidence suggested that this band was due to aggregation of the other proteins (see Discussion). In any case, there was no difference in the staining intensity of this band between the two forms of mucus.

Solubility

The mucus was difficult to solubilize, but certain conditions improved its solubility. Solubility was improved in basic rather than acidic conditions. Urea, SDS, and reducing agents improved the solubility, but each of these on their own extracted only one-quarter to one-half of the protein extractable by all three together. Moreover, buffers that increased extraction did so by extracting more of the same proteins; *i.e.*, the banding pattern in SDS-PAGE did not change. The effect of reducing agents, however, was exceptional: gels run without reducing agents were more prone to defects and had bands that were less distinct, so these gels were harder to read. Some proteins appeared to be poorly extracted in the absence of reducing agents, but this difference was not clear cut.

The effect of shear during extraction was similar to the effect of stronger buffers. Stronger shear gave greater ex-

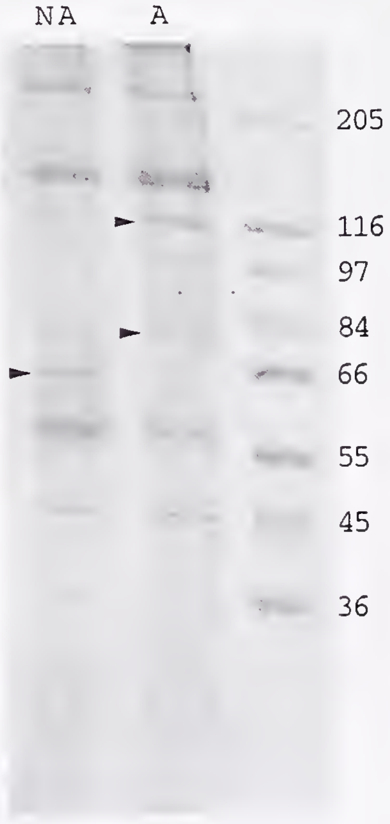

Figure 4. Example of an SDS-PAGE comparison of a non-adhesive (NA) and an adhesive (A) mucus sample (7 and 10 μg protein loaded respectively). The gel was stained with Coomassie blue R-250. Molecular weight markers are in the right lane and have the following molecular weights: 205, 116, 97, 84, 66, 55, 45 and 36 kD. The 118 kD, 80 kD, and 68 kD proteins are marked by arrowheads.

Table I

Amino acid compositions of selected proteins found in the pedal mucus of the limpet Lottia limatula *(values in residues per thousand)*

	45 kD	57 kD	68 kD	118 kD	140 kD	Whole mucus (adhesive)
ASX	96 (95)	117 (102)	138 (104)	142 (118)	154 (129)	127
THR	52 (51)	63 (54)	57 (47)	72 (60)	76 (63)	116
SER	66 (71)	74 (88)	120 (114)	97 (105)	49 (69)	90
GLX	125 (124)	134 (122)	98 (101)	144 (130)	140 (128)	115
PRO	46 (45)	37 (38)	42 (41)	48 (46)	113 (89)	79
GLY	133 (141)	89 (121)	108 (144)	79 (122)	80 (110)	80
ALA	72 (71)	77 (75)	97 (83)	55 (64)	55 (61)	52
VAL	53 (49)	40 (59)	0 (42)	22 (52)	32 (51)	72
MET	27 (25)	44 (27)	39 (18)	21 (13)	25 (17)	11
ILEU	55 (53)	42 (45)	34 (44)	51 (37)	45 (47)	52
LEU	73 (72)	65 (67)	76 (73)	51 (61)	49 (57)	51
TYR	31 (35)	39 (35)	34 (32)	26 (18)	30 (30)	18
PHE	39 (35)	55 (41)	56 (35)	39 (31)	38 (32)	26
HIS	22 (23)	32 (32)	17 (26)	28 (31)	26 (28)	10
LYS	57 (57)	51 (47)	66 (51)	90 (70)	58 (52)	59
ARG	52 (52)	46 (46)	41 (44)	30 (38)	32 (37)	33
CYS/2	—	—	—	4 (2)	—	20

For each amino acid, the first value is corrected for the blank; values in parentheses are unblanked. Note that cysteine was not quantified, only the acid-stable, disulfide-bonded form CYS/2. These bonds were reduced in the individual proteins, but not the whole mucus sample.

traction, but SDS-PAGE showed that exactly the same proteins were present in the same proportions as in samples dissolved with mild shear. This is significant because Sajdera and Hascall (1969) showed that sonication can fracture the large molecules that make up mammalian mucous gels. This did not appear to be the case with limpet mucus.

The adhesive mucus was typically more difficult to dissolve than the non-adhesive mucus. It often took twice as long to break up visibly during any extraction. In addition, it was much less soluble in neutral salt buffers than the non-adhesive form.

Characterization of proteins

Most of the major proteins were acidic. The 118 kD protein had an isoelectric point between 5 and 5.3. The 203, 140, 57, and 45 kD proteins had isoelectric points ranging from 4.7 to 5.3. The 80 and 68 kD proteins appeared to fall within a similar range of isoelectric points, but they did not show up clearly enough to be identified unequivocally. The only significant proteins that were not so acidic were a 29 kD protein at a pI of 6.5, and a 53 kD protein at a pI of about 8.6.

Of the proteins identified by electrophoresis, only the 140 kD protein was a glycoprotein. This finding was based on glycan staining of adhesive and non-adhesive mucus samples that were run on SDS-PAGE and transferred to nitrocellulose. Transient staining with Ponceau-S showed that all the proteins transferred successfully. The glycan detection kit stained the 140 kD protein darkly in the adhesive and non-adhesive samples. No other protein was marked by this stain. The blot showed a fair amount of background staining at the top of both samples, at about 100 kD and above.

The proteins that were analyzed had similar amino acid compositions (Table I). The method of Marchalonis and Weltman (1971) gave relatedness values (SΔQ) ranging from 54 to 101 for the comparison between the 118 kD protein and the other proteins in Table I; any value lower than 100 suggests relatedness. All of the proteins had many polar or charged amino acids, especially acidic ones. The 118 kD protein had the largest proportion of these, with 65% of its amino acids either electrically charged at physiological pH, or polar. Finally, the amino acid compositions of the identified proteins were similar to the composition of whole adhesive mucus. This supports the finding that they make up the bulk of the secretion. Note that our hydrolysis conditions did not allow us to quantify cysteine. In addition, due to high backgrounds, slow transfer of some of the proteins, and small initial quantities, the correction based on the blank was significant and may have led to some errors, especially for the 68 kD protein.

Though most of the proteins transferred easily, the 118, 80, and 53 kD proteins transferred several times more slowly in the Tris-borate buffer, despite the presence of SDS. This finding was based on quantitative comparison of stained pre-transfer and post-transfer lanes and blots, adjusting for the effect of molecular weight. The slow transfer of the 80 kD protein, combined with its small initial quantities and position near several minor bands that transferred well, made it difficult to identify unequivocally on the membrane. Thus, its amino acid composition was not analyzed.

Discussion

Adhesive limpet mucus differs from non-adhesive limpet mucus in three clear ways: first, an overall twofold increase in protein and carbohydrate concentration; second, the addition of a 118 kD protein; third, the absence of a 68 kD protein. Another difference is the presence of an 80 kD protein in adhesive mucus, though this was not consistently present. There may be similar differences in specific carbohydrates, but this study did not analyze carbohydrate composition in detail. Therefore, although we have identified clear biochemical differences, these may not be the only differences between the two forms of mucus. Nevertheless, the identified changes could account for much of the difference in function.

To understand the possible effects of these changes, we will first review what is known of the structure of mucous gels, and how limpet pedal mucus compares to other mucous gels. Then we can consider the factors that affect mucous gel mechanics. This will give insight into the significance of the biochemical changes identified in this paper. With this understanding, we can consider limpet adhesion in the context of other invertebrate adhesives.

Structure of mucous gels

Mucous gels are typically made of poly-anionic polymers that take up an expanded configuration due to electrostatic repulsion (Wainwright *et al.*, 1976). Mammalian mucus, the best studied mucous gel, is based on the mucin glycoprotein. Mucin is enormous; gastric mucin is composed of four disulfide-linked subunits of over 500 kD each, resulting in a molecule of about 2000 kD (Allen, 1977; Allen *et al.*, 1984). Other mucins may be much larger (Silberberg, 1989). These molecules are heavily glycosylated (Jentoft, 1990), typically consisting of 70%–80% carbohydrate (Hafez, 1977). Hundreds of short carbohydrate chains are attached to serine and threonine residues in the glycosylated region (Silberberg and Meyer, 1982). Thus, serine and threonine typically make up 30% of the amino acids in mucin (Pearson *et al.*, 1982; Allen *et al.*, 1984; Smith and Lamont, 1984). The carbohydrates carry a substantial negative charge, which causes the molecule to take on an extended configuration and fill a large volume. When the mucin concentration reaches 2% to 4%, the molecules interact and become entangled, forming a viscoelastic gel (Allen, 1977).

Limpet pedal mucus also forms gels from a protein-polysaccharide mixture at similar concentrations. Nevertheless, it appears to be based on a different type of molecule. Carbohydrates make up only about 15% of the organic material, and only one of the proteins is glycosylated. The amino acid compositions of the proteins in limpet mucus are also different from mucin; for example, in the identified proteins, serine and threonine make up 12% to 18% of the total residues, rather than 30%. A comparison of the amino acid composition of vertebrate mucin (Smith and Lamont, 1984) with that of the 140 kD glycoprotein of limpet pedal mucus gives an SΔQ value of 342. This strongly suggests that the proteins are not related.

Limpet mucus appears to be made of smaller subunits than vertebrate mucus. The bulk of the material was composed of proteins ranging from 20 to 220 kD. There was a component that was too big to enter the stacking gel, but it represented only about 10% of the protein, and may have been due to aggregation of the other proteins. The gels showed characteristics typical of aggregation at the top, such as streaking and high background staining in the lanes (Hames, 1990). Also, other experiments have suggested that the proteins in limpet mucus have a strong tendency to aggregate; in gel filtration columns using gel media that should achieve some separation of these proteins, the proteins tended to elute together, even when urea or guanidine hydrochloride was added to the buffer (personal communication).

Limpet pedal mucus also appears to be stronger than mammalian mucus. Mammalian tracheal mucin typically has a dynamic viscosity of 1 to 1000 poise. Its storage and loss moduli, which are measures of elasticity and viscosity, are typically 1 to 10 Pa, depending on the strain rate (Litt *et al.*, 1977). Other mammalian mucous secretions have similar values. In contrast, Grenon and Walker (1980) found the viscosity of pedal mucus from the limpet *Patella vulgata* to be on the order of 10^6 to 10^7 poise, and the elastic modulus to be between 300 and 7000 Pa. These were preliminary measurements derived from a creep test rather than a dynamic tester, so they are not strictly comparable; moreover, the four samples tested by Grenon and Walker varied considerably. Nevertheless, these data indicate a substantial difference in mechanical properties from vertebrate mucus. Such a difference was also apparent when solubilizing the mucus. Mammalian mucin dissolves easily in 6 *M* GuCl (Allen, 1977) or 0.2 *M* 2-mercaptoethanol (Allen *et al.*, 1984). Limpet mucus does not dissolve well, especially without strong shearing. This is not surprising, since a glue must be insoluble to function effectively.

Though limpet mucus differs from mammalian mucus in biochemistry and strength, it probably forms gels in the same way. Presumably, the proteins and polysaccharides are linked together into a larger network. They may form large complexes that entangle, or they may form a fully cross-linked network. The effect of SDS, urea, and reducing agents on the solubility of limpet mucus suggests that disulfide bonds and a variety of non-covalent bonds are important for linking these subunits together.

Factors that affect the mechanics of polymer gels and their relation to adhesion

Polymer gels are dominated by the effects of entanglement between large macromolecules. To deform such a gel, the polymers must be pulled apart. At short time intervals, the "knots" between polymers cannot be undone, and the gel behaves elastically. Over longer time periods, though, the polymers can creep and work out of their local entanglements, effectively slipping through the boundaries imposed by their neighboring molecules. This process is called reptation (deGennes and Leger, 1982).

A variety of factors affect the mechanics of polymer gels (Doi and Edwards, 1988). Clearly the polymer concentration will be critical. As the concentration increases, each polymer interacts with a larger number of others, further impeding its ability to creep. Characteristics of the polymers also affect the mechanics of the gel. Longer polymers entangle more easily and have a harder time pulling out of these entanglements. Any branching of the polymers dramatically slows their ability to pull free of one another, as does any other interaction between polymers.

Given these considerations, what is the significance of the identified changes in limpet pedal mucus? The twofold increase in concentration certainly would increase the stiffness and viscosity of the gel. Silberberg and Meyer (1982) argue that, in practice, the polymer concentration may be the most important factor regulating the mechanics of mucous gels. This has been demonstrated for mammalian cervical mucus (Tam and Verdugo, 1981).

Though the effect of increased concentration is clear, the cause of the increase is unknown. It is probably not as simple as secreting a higher concentration of protein, since a gel will swell or shrink to reach an equilibrium volume determined by a variety of factors. These include the rubbery elasticity of the polymers, the osmotic pressure of ions trapped in the polyanionic network, and the interactions between polymer and solvent (Tanaka, 1981). Change in any of these factors can cause shrinkage or swelling of the gel, thus effectively changing the polymer concentration. For example, salt concentration and pH both affect the swelling pressure of the gel. These factors could be controlled by the secreting epithelium (Tam and Verdugo, 1981, 1982). A large change in conditions may not even be necessary; if the conditions are right, a small change in one factor may trigger a phase change in the gel from swollen to collapsed (Tanaka, 1981), which could easily produce a twofold increase in concentration. The addition of a protein containing large numbers of basic residues could trigger such a collapse. For this reason, it is suggestive that the 118 kD protein contains significantly more basic amino acids than the other proteins in the secretion.

Though the concentration of the gel clearly affects its mechanics, the significance of the 118 kD protein in adhesion is less certain. It probably plays a central role, however, since the total polymer concentration of adhesive limpet mucus is similar to that of mammalian mucus, yet the former is dramatically more effective as an adhesive. It seems that there must be a change in addition to the concentration increase to account for the adhesiveness of limpet mucus. Perhaps the 118 kD protein links gel-forming polymers into larger functional molecules, possibly introducing branching. If so, it would strengthen the entangling interactions, and might even lead to the formation of a fully cross-linked network. Otani *et al.* (1996) show that hydrogels composed of gelatin and poly(L-glutamic acid) can increase in adhesiveness roughly a hundred-fold with the addition of a cross-linking agent. Incidentally, gelatin units of 20 to 60 kD form gels at a concentration just above 4.4% (Otani *et al.*, 1996), thus a molecule need not be enormous to form effective gels.

The 68 kD and 80 kD proteins were not as consistently linked to the change in adhesiveness as the 118 kD protein, but it is likely that they also have roles. The 80 kD protein may have a function similar to that of the 118 kD protein. The 68 kD protein, on the other hand, may release the adhesion by breaking some of the connections between gel-forming molecules; it could also be a breakdown product of one of these proteins. Alternatively, it could be a different type of gel-forming molecule that forms weaker links.

The inorganic composition does not appear to be related to the adhesiveness of limpet mucus. It has been suggested that divalent ions stiffen mucus by forming electrovalent cross-links (Hermans, 1983; Thomas and Hermans, 1985). Marriott *et al.* (1982) showed that increasing the calcium concentration from 0 to 30 m*M* can roughly triple the viscosity of mucus. Multivalent ions in general have a prominent effect on polyanionic gels (Tanaka, 1981). Nevertheless, there were no differences in the relative proportions of ions such as calcium and magnesium between adhesive and non-adhesive mucus.

Significance for invertebrate adhesion

In contrast to mucus-based adhesives, solid adhesives have been studied more thoroughly. Barnacles adhere using a proteinaceous cement that includes relatively little water (see Walker, 1972; Barnes and Blackstock, 1974; Walker and Youngson, 1975; Yule and Walker, 1987; Naldrett, 1993; Kamino *et al.*, 1996). As with limpets, disulfide bonds and non-covalent linkages appear important for linking the barnacle's adhesive proteins (Naldrett, 1993; Kamino *et al.*, 1996). Mussels adhere using proteinaceous byssal threads and adhesive plaques (see Waite and Tanzer, 1981; Waite, 1983, 1985; Waite *et al.*, 1989; Rzepecki *et al.*, 1992; Papov *et al.*, 1995). These are typically cross-linked using a quinone-tanning process that relies on the presence of the amino acid DOPA (Waite and Tanzer, 1981). Also, certain tube-dwelling worms secrete a proteinaceous cement containing DOPA (Jensen and Morse, 1988). A fundamental difference between these adhesives and limpet pedal mucus is that mucus is 90% to 95% water and therefore has much lower tensile stiffness. Thus, the mechanism by which it forms strong attachments has been poorly understood.

Some studies have suggested that mucus is inherently adhesive due to its viscoelasticity (Grenon and Walker, 1981). This is unlikely to be true; as pointed out in the Introduction, mucus is more often used as a lubricant. Despite their viscoelasticity, typical mucus secretions are not sticky.

It has also been suggested that mucus forms bonds through Stefan adhesion, which occurs when a high-viscosity secretion is trapped between two closely apposed, rigid plates. Because of its viscosity, the secretion resists the flow that must accompany the separation of the plates (Grenon and Walker, 1981). However, Stefan adhesion produces much weaker bonds than the Stefan equation predicts for two reasons. First, it depends on having rigid adherends. Any flexibility in the adherends dramatically reduces the adhesive force. Thus, the Stefan equation is not relevant to soft-bodied invertebrates. Second, even if the adherends were rigid enough, Stefan adhesion is limited because cavitation of water in the mucus would typically cause failure at tenacities of roughly 50 kPa (Banks and Mill, 1953). This is considerably weaker than the tenacities of most limpets using glue-like adhesion. Furthermore, Stefan adhesion provides little shear resistance, yet greatly increased shear resistance is one of the defining characteristics of the change from suction to glue-like adhesion (Smith, 1992). Smith (1991b) provides further evidence that limpets, in particular, do not use Stefan adhesion.

Although many mucous secretions are not normally adhesive, the present study shows that they can be modified to become adhesive. This is particularly interesting given the wide variety of animals that use mucus-based secretions for adhesion. Echinoderm tube feet adhere using a viscous secretion typically identified as mucus (Chaet and Philpott, 1964; Harrison, 1966; Souza Santos, 1966; Thomas and Hermans, 1985; Ball and Jangoux, 1990; Flammang *et al.*, 1991; Flammang and Jangoux, 1992, 1993). Various holothurians capture food on their tentacles with a viscous mucus or proteinaceous secretion (Cameron and Fankboner, 1984; McKenzie, 1987). In many of these studies, mucus is defined as a viscous secretion containing protein and mucopolysaccharides. Brown algae also adhere with a mucopolysaccharide or glycoprotein (Oliveira *et al.*, 1980). Many turbellarians and gastrotrichs also produce viscid adhesive secretions, and possibly releasing secretions, some of which may involve mucus (Tyler, 1976; Tyler and Rieger, 1980). Barnacle larvae apparently produce a viscous, proteinaceous adhesive secretion (Walker and Yule, 1984).

What makes these secretions adhesive instead of slippery? Many of the studies cited demonstrate the presence of more than one type of secretory cell on the adhesive epithelium, each capable of adding a different component to the secretion. The difficulty is the relative lack of direct evidence that identifies which components are responsible for adhesion. Most of the evidence is based on the locations and arrangements of the different cells. In some cases, mucopolysaccharides are believed to be adhesive, and in others the protein components are believed to be adhesive. Hermans (1983) suggested that many adhesive organs produce two separate secretions: an adhesive secretion that may be proteinaceous and a releasing or de-adhesive secretion based on mucopolysaccharides. The present study provides a related possibility—one fundamental secretion that can be modified to be either adhesive or non-adhesive. The type of changes identified in limpet pedal mucus may provide a paradigm that will be useful in understanding the adhesion of other mucus-secreting animals.

Acknowledgments

We thank J. H. Waite for performing amino acid analyses and R. Walson for his assistance with the scanning electron microscopy. We thank two anonymous reviewers for their thoughtful comments. This research was supported by a grant from the Holcomb Research Institute to A.M.S., and student research awards to T.J.Q and R.L.S. from the Holcomb Research Institute.

Literature Cited

Allen, A. 1977. Structure and function in gastric mucus. In *Mucus in Health and Disease*, M. Elstein and D. Parke, eds. *Adv. Exp. Med. Biol.* **89:** 283–299. Plenum Press, New York.

Allen, A., D. A. Hutton, J. P. Pearson, and L. A. Sellers. 1984. Mucus glycoprotein structure, gel formation and gastrointestinal mucus function. In *Mucus and Mucosa*, J. Nugent and M. O'Connor, eds. *Ciba Found. Symp.* **109:** 137–156. Pitman, London.

Baier, R. E., H. Gucinski, M. A. Meenaghan, J. Wirth, and P. O. Glantz. 1985. Biophysical studies of mucosal surfaces. Pp. 83–95 in *Oral Interfacial Reactions of Bone, Soft Tissue and Saliva*, P. O. Glantz, S. A. Leach, and T. Ericson, eds. IRL Press, Oxford.

Ball, B., and M. Jangoux. 1990. Ultrastructure of the tube foot sensory-secretory complex in *Ophiocomina nigra* (Echinodermata, Ophiuridae). *Zoomorphology* **109:** 201–209.

Banks, W. H., and C. C. Mill. 1953. Tacky adhesion—a preliminary study. *J. Colloid Sci.* **8:** 137–147.

Barnes, H., and J. Blackstock. 1974. The biochemical composition of the cement of a pedunculate cirripede. *J. Exp. Mar. Biol. Ecol.* **16:** 87–91.

Boyer, R. F. 1993. *Modern Experimental Biochemistry.* Benjamin/Cummings, Redwood City, CA. 555 pp.

Bradford, M. M. 1976. A rapid and sensitive method for the quantitation of microgram quantities of protein utilizing the principle of protein-dye binding. *Anal. Biochem.* **72:** 248–254.

Branch, G. M., and A. C. Marsh. 1978. Tenacity and shell shape in six

Patella species: adaptive features. *J. Exp. Mar. Biol. Ecol.* **34:** 111–130.

Cameron, J. L., and P. V. Fankboner. 1984. Tentacle structure and feeding processes in life stages of the commercial sea cucumber *Parastichopus californicus* (Stimpson). *J. Exp. Mar. Biol. Ecol.* **81:** 193–209.

Chaet, A. B., and D. E. Philpott. 1964. A new subcellular particle secreted by the starfish. *J. Ultrastruct. Res.* **11:** 354–362.

Chantler, E., and E. Debruyne. 1977. Factors regulating the changes in cervical mucus in different hormonal states. In *Mucus in Health and Disease,* M. Elstein and D. Parke, eds. *Adv. Exp. Med. Biol.* **89:** 131–141. Plenum Press, New York.

Davies, M. S., H. D. Jones, and S. J. Hawkins. 1990. Seasonal variation in the composition of pedal mucus from *Patella vulgata* L. *J. Exp. Mar. Biol. Ecol.* **144:** 101–112.

deGennes, P. G., and L. Leger. 1982. Dynamics of entangled polymer gels. *Annu. Rev. Phys. Chem.* **33:** 49–61.

Denny, M. W. 1980. The role of gastropod pedal mucus in locomotion. *Nature* **285:** 160–161.

Denny, M. W. 1989. Invertebrate mucous secretions: functional alternatives to vertebrate paradigms. In *Mucus and Related Topics,* E. Chantler and N. A. Ratcliffe, eds. *Symp. Soc. Exp. Biol.* **43:** 337–366. Society for Experimental Biology, Cambridge.

Doi, M., and S. F. Edwards. 1988. *The Theory of Polymer Dynamics.* Clarendon Press, Oxford. 391 pp.

Flammang, P., and M. Jangoux. 1992. Functional morphology of the locomotory podia of *Holothuria forskali* (Echinodermata, Holothuroida). *Zoomorphology* **111:** 167–178.

Flammang, P., and M. Jangoux. 1993. Functional morphology of coronal and peristomeal podia in *Sphaerechinus granularis* (Echinodermata, Echinoida). *Zoomorphology* **113:** 47–60.

Flammang, P., C. DeRidder, and M. Jangoux. 1991. Ultrastructure of the penicillate podia of the spatangoid echinoid *Echinocardium cordatum* (Echinodermata) with special emphasis on the epidermal sensory-secretory complexes. *Acta Zool. (Stockh.)* **72:** 151–158.

Grenon, J. F., and G. Walker. 1978. The histology and histochemistry of the pedal glandular system of two limpets, *Patella vulgata* and *Acmaea tessulata* (Gastropoda: Prosobranchia). *J. Mar. Biol. Ass. UK* **58:** 803–816.

Grenon, J. F., and G. Walker. 1980. Biomechanical and rheological properties of the pedal mucus of the limpet, *Patella vulgata* L. *Comp. Biochem. Physiol. B.* **66:** 451–458.

Grenon, J. F., and G. Walker. 1981. The tenacity of the limpet, *Patella vulgata* L.: an experimental approach. *J. Exp. Mar. Biol. Ecol.* **54:** 277–308.

Hafez, E. S. E. 1977. Functional anatomy of mucus-secreting cells. In *Mucus in Health and Disease,* M. Elstein and D. Parke, eds. *Adv. Exp. Med. Biol.* **89:** 19–38. Plenum Press, New York.

Hames, B. D. 1990. One-dimensional polyacrylamide gel electrophoresis. Pp. 1–147 in *Gel Electrophoresis of Proteins: A Practical Approach,* B. D. Hames and D. Rickwood, eds. IRL Press, Oxford.

Harrison, G. A. 1966. Subcellular particles in echinoderm tube feet. I. Class Asteroidea. *J. Ultrastruct. Res.* **16:** 537–547.

Harrold, C. 1982. Escape responses and prey availability in a kelp forest predator-prey system. *Am. Nat.* **119:** 132–135.

Hermans, C. O. 1983. The duo-gland adhesive system. *Oceanogr. Mar. Biol. Annu. Rev.* **21:** 283–339.

Jensen, R. A., and D. E. Morse. 1988. The bioadhesive of *Phragmatopoma californica* tubes—a silk-like cement containing L-Dopa. *J. Comp. Phy. B.* **158:** 317–324.

Jentoft, N. 1990. Why are proteins O-glycosylated? *Trends Biochem. Sci.* **15:** 291–294.

Kamino, K., S. Odo, and T. Maruyama. 1996. Cement proteins of the acorn barnacle, *Megabalanus rosa. Biol. Bull.* **190:** 403–409.

Kennedy, J. F., and G. Pagliuca. 1994. Oligosaccharides. Pp. 43–72 in *Carbohydrate Analysis: A Practical Approach,* M. F. Chaplin and J. F. Kennedy, eds. IRL Press, Oxford.

Laemmli, U. K. 1970. Cleavage of structural proteins during the assembly of the head of bacteriophage T4. *Nature* **227:** 680–685.

Litt, M., D. P. Wolf, and M. A. Khan. 1977. Functional aspects of mucus rheology. In *Mucus in Health and Disease,* M. Elstein and D. Parke, eds. *Adv. Exp. Med. Biol.* **89:** 191–201. Plenum Press, New York.

Marchalonis, J. J., and J. K. Weltman. 1971. Relatedness among proteins: a new method of estimation and its application to immunoglobins. *Comp. Biochem. Physiol.* **38B:** 609–625.

Marriott, C., M. F. Beeson, and D. T. Brown. 1982. Biopolymer induced changes in mucus viscoelasticity. In *Mucus in Health and Disease II,* E. N. Chantler, J. B. Elder, and M. Elstein, eds. *Adv. Exp. Med. Biol.* **144:** 89–92. Plenum Press, New York.

McKenzie, J. D. 1987. The ultrastructure of the tentacles of 11 species of dendrochirote holothurians studied with special reference to the surface coats and papillae. *Cell Tissue Res.* **248:** 187–199.

Naldrett, M. J. 1993. The importance of sulphur cross-links and hydrophobic interactions in the polymerization of barnacle cement. *J. Mar. Biol. Ass. UK* **73:** 689–702.

Oliveira, L., D. C. Walker, and T. Bisapultra. 1980. Ultrastructural, cytochemical and enzymatic studies on the adhesive plaques of brown algae *Laminaria saccharina* (L.) and *Nereocystis luckeana* (Nert.). *Protoplasma* **104:** 1–15.

Otani, Y., Y. Tabata, and Y. Ikada. 1996. Rapidly curable biological glue composed of gelatin and poly(L-glutamic acid). *Biomaterials* **17:** 1387–1391.

Papov, V. V., T. V. Diamond, K. Biemann, and J. H. Waite. 1995. Hydroxyarginine-containing polyphenolic proteins in the adhesive plaques of the marine mussel *Mytilus edulis. J. Biol. Chem.* **270:** 20183–20192.

Pearson, J. P., R. Kaura, W. Taylor, and A. Allen. 1982. The composition and polymeric structure of mucus glycoprotein from human gallbladder bile. *Biochim. Biophys. Acta* **706:** 221–228.

Rzepecki, L. M., K. M. Hansen, and J. H. Waite. 1992. Characterization of a cystine-rich polyphenolic protein family from the blue mussel *Mytilus edulis* L. *Biol. Bull.* **183:** 123–137.

Sajdera, S. W., and V. C. Hascall. 1969. Proteinpolysaccharide complex from bovine nasal cartilage. *J. Biol. Chem.* **244:** 77–87.

Schmidt-Nielsen, K. 1990. *Animal Physiology: Adaptation and Environment.* Cambridge University Press, Cambridge. 607 pp.

Silberberg, A. 1989. Mucus glycoprotein, its biophysical and gel-forming properties. In *Mucus and Related Topics,* E. Chantler and N. A. Ratcliffe, eds. *Symp. Soc. Exp. Biol.* **43:** 43–63. Society for Experimental Biology, Cambridge.

Silberberg, A., and F. A. Meyer. 1982. Structure and function of mucus. In *Mucus in Health and Disease II,* E. N. Chantler, J. B. Elder, and M. Elstein, eds. *Adv. Exp. Med. Biol.* **144:** 53–74. Plenum Press, New York.

Smith, A. M. 1991a. Negative pressure generated by octopus suckers: a study of the tensile strength of water in nature. *J. Exp. Biol.* **157:** 257–271.

Smith, A. M. 1991b. The role of suction in the adhesion of limpets. *J. Exp. Biol.* **161:** 151–169.

Smith, A. M. 1992. Alternation between attachment mechanisms by limpets in the field. *J. Exp. Mar. Biol. Ecol.* **160:** 205–220.

Smith, A. M. 1996. Cephalopod sucker design and the physical limits to negative pressure. *J. Exp. Biol.* **199:** 949–958.

Smith, A. M., W. M. Kier, and S. Johnsen. 1993. The effect of depth on the attachment force of limpets. *Biol. Bull.* **184:** 338–341.

Smith, B. F., and J. T. LaMont. 1984. Hydrophobic binding properties of bovine gallbladder mucin. *J. Biol. Chem.* **259:** 12170–12177.

Souza Santos, H. D. 1966. The ultrastructure of the mucous granules from starfish tube feet. *J. Ultrastruct. Res.* **16:** 259–268.

Tam, P. Y., and P. Verdugo. 1981. Control of mucus hydration as a Donnan equilibrium process. *Nature* **292:** 340–342.

Tam, P. Y., and P. Verdugo. 1982. Mucus hydration: a Donnan equilibrium controlled process. In *Mucus in Health and Disease II,* E. N. Chantler, J. B. Elder, and M. Elstein, eds. *Adv. Exp. Med. Biol.* **144:** 101–103. Plenum Press, New York.

Tanaka, T. 1981. Gels. *Sci. Am.* **244** (January): 124–138.

Thomas, L. A., and C. O. Hermans. 1985. Adhesive interactions between the tube feet of a starfish, *Leptasterias hexactis,* and substrata. *Biol. Bull.* **169:** 675–688.

Towbin, H., T. Staehelin, and J. Gordon. 1979. Electrophoretic transfer of proteins from polyacrylamide gels to nitrocellulose sheets: procedure and some applications. *Proc. Natl. Acad. Sci. USA* **76:** 4350–4354.

Tyler, S. 1976. Comparative ultrastructure of adhesive systems in the Turbellaria. *Zoomorphologie* **84:** 1–76.

Tyler, S., and G. E. Rieger. 1980. Adhesive organs of the Gastrotricha I. Duo-gland organs. *Zoomorphologie* **95:** 1–15.

Wainwright, S. A., W. D. Biggs, J. D. Currey, and J. M. Gosline. 1976. *Mechanical Design in Organisms.* Princeton University Press, Princeton. 423 pp.

Waite, J. H. 1983. Adhesion in bysally attached bivalves. *Biol. Rev. Camb. Philos. Soc.* **58:** 209–231.

Waite, J. H. 1985. Peptide repeats in a mussel glue protein: theme and variations. *Biochemistry* **24:** 5010–5014.

Waite, J. H., and M. L. Tanzer. 1981. Polyphenolic substance of *Mytilus edulis:* novel adhesive containing L-Dopa and hydroxyproline. *Science* **212:** 1038–1040.

Waite, J. H., D. C. Hansen, and K. T. Little. 1989. The glue protein of ribbed mussels (*Geukensia demissa*): a natural adhesive with some features of collagen. *J. Comp. Physiol. B.* **159:** 517–525.

Walker, G. 1972. The biochemical composition of the cement of two barnacle species, *Balanus hameri* and *Balanus crenatus. J. Mar. Biol. Ass. UK* **52:** 429–435.

Walker, G., and A. Youngson. 1975. The biochemical composition of *Lepas anatifera* (L.) cement (Crustacea: cirripedia). *J. Mar. Biol. Ass. UK* **55:** 703–707.

Walker, G., and A. B. Yule. 1984. Temporary adhesion of the barnacle cyprid: the existence of an antennular adhesive secretion. *J. Mar. Biol. Ass. UK* **64:** 679–686.

Yule, A. B., and G. Walker. 1987. Adhesion in barnacles. Pp. 389–402 in *Crustacean Issues: Barnacle Biology,* Vol. 5, A. J. Southward, ed. Balkema, Rotterdam.

Reference: *Biol. Bull.* **196:** 45–51. (February, 1999)

Calcium Dependence of Settlement and Nematocyst Discharge in Actinulae of the Hydroid *Tubularia mesembryanthemum*

SATORU KAWAII[1], KEIJI YAMASHITA[2], MITSUYO NAKAI, MIYUKI TAKAHASHI, AND NOBUHIRO FUSETANI[3,*]

Biofouling Project, ERATO, Research Development Corporation of Japan, c/o Yokohama R&D center, Niigata Engineering Co. Ltd., 27 Shin-isogo-cho, Isogo-ku, Yokohama, 235, Japan

Abstract. The influence of Ca^{2+} and Mg^{2+} ions on both *atrichous isorhiza* (AI) discharge and settlement of actinular larvae of the hydroid *Tubularia mesembryanthemum* was investigated. Mg^{2+}-supplemented artificial seawater (ASW) completely inhibited both events at a concentration of 206 m*M*, whereas lowered Mg^{2+} concentrations enhanced them. Ca^{2+} ions in the bathing solution highly regulated AI discharge and settlement, and Mg^{2+} ions may down-regulate these events. The effect of inorganic Ca^{2+}-channel blockers, including Gd^{3+} and La^{3+}, was also examined. Larval settlement was inhibited by Co^{2+}, Ni^{2+}, Cd^{2+}, La^{3+}, and Gd^{3+}, with half inhibitory concentrations (IC_{50}) of 5800, 260, 53, 45, and 7 μM, respectively; AI discharge was also inhibited by these ions, with IC_{50} values of 6600, 500, 78, 41, and 5 μM, respectively. These results suggest possible involvement of stretch-activated Ca^{2+} channels in the signal transmission of both AI discharge and larval settlement.

Introduction

The colonial marine hydroid *Tubularia mesembryanthemum* Allman, 1871 (Hydrozoa: Tubulariidae) is a prolific marine fouling organism that frequently dominates artificial substrata used in aquaculture. Actinula larvae, produced as a means of dispersal, are composed of a conical manubrium, oral- and aboral tentacles, and a basal protrusion that later becomes the settlement organ. Settlement-competent actinulae initiate settlement behavior by contact of the aboral tentacle tip (ATT) with the substratum surface, which triggers discharge of *atrichous isorhiza* (AI), the agglutinant nematocysts located at the ATT.

Upon reception of appropriate stimuli, nematocysts can eject adhesive tubules (Tardent, 1988). Nematocyte excitation requires both mechanical and chemical stimuli (Pantin, 1942). Two classes of chemoreceptors were identified in the tentacle of the sea anemone *Aiptasia pallida:* one sensitive to low molecular weight amino/imino compounds, and the other specific for N-acetylated sugars (Thorington and Hessinger, 1988a). In addition, two types of mechanoreceptors are involved in triggering nematocyst discharge; one is contact-sensitive (Thorington and Hessinger, 1988b) and the other is tunable, vibration- and frequency-sensitive (Watson and Hessinger, 1989, 1991).

The necessity of external Ca^{2+} ions for nematocyst discharge has been demonstrated in *Aiptasia mutabilis* (Santoro and Salleo, 1991b), *Pelagia noctiluca* (Salleo *et al.*, 1994a), *Calliactis parasitica* (Salleo *et al.*, 1994b), *Charybdea rastonii* (Yanagita, 1973), and *Anthopleura elegantissima* (McKay and Anderson, 1988). In *Hydra vulgaris*, discharge of *stenotele* is regulated by a voltage- and Ca^{2+}-dependent mechanism, allowing Ca^{2+} influx from the bathing solution (Gitter *et al.*, 1994). The involvement of intracellular Ca^{2+} ions in the metamorphosis of hydrozoan larvae has also been suggested on the basis of studies monitoring the emission of bioluminescence from photoproteins, thereby visualizing changes in $[Ca^{2+}]_i$ during

---

Received 3 February 1998; accepted 19 October 1998.

[1] Present address: Natl. Inst. Fruit Sci., Min. Agric. Forest. Fish., Okitsu, Shimizu, Shizuoka 424-0204, Japan. E-mail: kw4682@okt.affrc.go.jp

[2] Present address: Himeji Kisho Co. Ltd., 1417-1 Kiba, Himeji-shi, Hyogo 672, Japan.

[3] Present address: Laboratory of Aquatic Natural Products Chemistry, Graduate School of Agricultural and Life Sciences, The University of Tokyo, Bunkyo-ku, Tokyo 113, Japan.

* Author to whom correspondence should be addressed.

Abbreviations: AI, *atrichous isorhiza;* ATT, aboral tentacle tip.

planular metamorphosis (Freeman and Ridgway, 1987, 1990).

Previous work has shown that Ca^{2+} release from intracellular stores triggered AI discharge in *Tubularia mesembryanthemum* actinulae, followed by the inflow of Ca^{2+} ions from the bathing solution into the nematocysts (Kawaii *et al.*, 1997). Furthermore, AI discharge was usually accompanied by sinuous movement of the aboral tentacle. The involvement of Ca^{2+}-mediated signal transduction in actinular settlement and metamorphosis was suspected. To clarify the role of Ca^{2+} ions in actinular settlement, we examined AI discharge and larval settlement using intact larvae that were bathed in artificial seawater (ASW) containing various concentrations of Ca^{2+} and Mg^{2+} ions. The influence of di- and trivalent cations and Ca^{2+}-channel blockers (Yang and Sachs, 1989; Santoro and Salleo, 1991; Salleo *et al.*, 1994a, b; Gitter *et al.*, 1994) was also examined.

Materials and Methods

Reagents

Reagent grade artificial seawater (ASW) consisting of NaCl (460 m*M*), KCl (10.1 m*M*), $CaCl_2$ (9.2 m*M*), and $MgCl_2$ (42.6 m*M*) at pH 7.6 was adjusted by addition of 5 m*M* imidazole. The concentration of Ca^{2+} was reduced, without altering the osmolarity of the ASW, by adjusting Mg^{2+} accordingly. Mg^{2+}-supplemented ASW with 59, 75, 125, and 206 m*M* of Mg^{2+} was prepared by mixing the regular ASW with 370 m*M* $MgCl_2$ aqueous solution (which is isotonic to ASW) in the ratios of 1:19, 1:9, 1:3, and 1:1, respectively, to compensate for the osmolarity. In the case of Ca^{2+}-channel blockers, the osmolarity was adjusted by Na^+. All Ca^{2+}-channel blockers were purchased from Wako Pure Chemical Industries (Osaka, Japan).

Biological materials

Mature *Tubularia mesembryanthemum* colonies were collected mainly from submerged fisheries nets and ropes in the vicinity of Nagai Port in Sagami Bay (eastern Japan, 139°30′E, 31°70′N). Colonies were divided into male and female, and were maintained separately with sand-filtered running seawater at 16° ± 2°C as described by Yamashita *et al.* (1997). After fertilization, branches of female colonies with polyps bearing many actinulae were placed in filtered seawater (FSW; pore size, 0.45 μm), and sinking actinulae were collected. A single polyp could produce up to 300 actinulae, which were maintained at 4°C prior to use in an experiment. The actinulae were transferred to an ASW-containing beaker and maintained at 21 ± 2°C for several hours to recover normal responsiveness. Larval age was defined as time following release from the maternal gonophore, and 24-h-old actinulae were used in the following experiments unless otherwise stated.

Settlement assay

Actinular settlement was assayed using six-well polystyrene plates (Corning Cell Wells, Corning, NY), each well containing 6 ml of ASW and 5 actinulae. The plates were placed on an orbital shaker at 21 ± 2°C. The number of settled actinulae was counted under a binocular dissection microscope after 30 h. Each experiment was performed in triplicate.

To determine the reversibility of actinular settlement upon replacement of the test ASW with regular ASW, larvae that were largely sinking or attaching to the bottom of the well were washed by several replacements of the surface of the test ASW with regular ASW (roughly half the volume of the test ASW was exchanged with each replacement).

Larval behavior and atrichous isorhiza *discharge*

Each actinula was independently examined for the effect of Ca^{2+}, Mg^{2+}, or Ca^{2+}-channel blockers on its behavior when an ATT was contacted with a clean micropipette or on AI discharge. Actinulae in regular ASW were washed and suspended in test ASWs containing various concentrations of Ca^{2+}, Mg^{2+}, or Ca^{2+}-channel blockers. Each actinula was held by suction applied through a micropipette attached to the side of the adhesive protrusion. Behavioral responses to ATT contact with a clean micropipette were examined on suction-held actinula whose ATTs did not contact any substrata.

For monitoring AI discharge, an ATT of a suction-held actinula was immobilized and attached to the bottom of a petri dish by applying gentle suction through a second micropipette attached to the "wrist," which is the part between an ATT and an aboral tentacle. AI discharge of the immobilized ATT was then triggered by the addition of 100 μl of ASW that contained 200 m*M* K^+ ions (K^+-ASW) and had been adjusted to the osmolarity of regular ASW by reducing the Na^+ concentration. AI discharge was observed through the 40 × objective of a microscope, and the number of AI discharged before the K^+-ASW application (usually 0–1) was subtracted from the final total.

To avoid larval disintegration in Ca^{2+}-free ASW, a micropipette-held actinula in regular ASW was quickly and thoroughly washed and suspended in Ca^{2+}-free ASW. Immediately afterward, an ATT of the actinula was immobilized as described above and AI discharge was triggered.

$[Ca^{2+}]_i$ measurement

$[Ca^{2+}]_i$ was measured in whole mounts of living actinulae ATT in which AI discharge was induced. The actinulae had been treated with the Ca^{2+}-chelating fluorescent indicator fura-2 (Kawaii *et al.,* 1997). The fluorescence intensities of ATTs from fura-2-loaded actinulae were approximately 100 times stronger than those from non-labeled actinulae, and were strong enough for $[Ca^{2+}]_i$ measurement. The value of the fluorescence ratio between excitation at 340 nm and 380 nm ($R_{340/380}$) was used to indicate $[Ca^{2+}]_i$. The minimum interval was 1.9 s for ratiometric imaging.

Results

Ca^{2+} dependence of actinular settlement

Reducing the external Ca^{2+} concentration had a significant effect on actinular settlement, and the effect was competitively antagonized by Mg^{2+} (Fig. 1A). Settlement was comparable to normal in 4.6–9.2 m*M* Ca^{2+}, but it was inhibited at lower concentrations (70% ± 31% at 2.3 m*M* Ca^{2+}, 8% ± 10% at 1.1 m*M* Ca^{2+}).

Raising the Mg^{2+} concentration inhibited actinular settlement; 100% settlement was obtained at 75 m*M* Mg^{2+}, 50% at 125 m*M* Mg^{2+}, and 6.7% ± 11.6% at 206 m*M*.

The relative inhibitory effect of Mg^{2+} on actinular settlement was magnified at lower Ca^{2+}. In ASW containing 2.3 m*M* Ca^{2+}, settlement was reduced to 53% ± 12% at 59 m*M* Mg^{2+} and completely inhibited at 206 m*M* Mg^{2+}. The effects of Ca^{2+} and Mg^{2+} concentration on settlement were statistically significant as assessed by two-way ANOVA (Table 1). Furthermore, there was a significant interaction between Ca^{2+} and Mg^{2+}. In each case the dose-dependent reduction of actinular settlement was reversed by rinsing the larvae with regular ASW 9 h after the experiment.

Antagonistic effect of Mg^{2+}

Raising the Mg^{2+} concentration in an otherwise regular ASW had an inhibitory effect on AI discharge (Fig. 1B); the number of discharged AI was 4.0 ± 4.2 at 125 m*M* Mg^{2+}, and AI discharge was completely arrested at 206 m*M* Mg^{2+}. The inhibitory effect of Mg^{2+} increased when the external Ca^{2+} ion concentration was lowered. In ASW containing 4.6 m*M* Ca^{2+}, AI discharge was reduced to 5.7 ± 3.8 at 59 m*M* Mg^{2+} and 4.4 ± 3.1 at 75 m*M* Mg^{2+}. In ASW containing 2.3 m*M* Ca^{2+}, discharge was lowered to 4.3 ± 1.4 at 59 m*M* Mg^{2+}, and was completely inhibited at 125 m*M* Mg^{2+}. Two-way ANOVA revealed that the effects of Ca^{2+} and Mg^{2+} concentration on AI discharge were statistically significant, and that there was a significant interaction between Ca^{2+} and Mg^{2+} (Table 1). Again, this dose-dependent reduction of AI discharge was reversed by rinsing the larvae with regular ASW 3 h after the experiment.

Figure 2 indicates significant enhancement of AI discharge in Mg^{2+}-reduced ASW (one-way ANOVA; $F = 11.9759$, $P < 0.0001$). In this experiment, AI discharge was triggered by K$^+$-ASW (100 m*M*). The number of discharged AI was 2.1 ± 0.6 at 50 m*M* Mg^{2+} (regular ASW) and increased to 7.6 ± 1.6 and 9.2 ± 1.9 at 25 and 10 m*M*, respectively. Addition of Mg^{2+}-reduced ASW (5 m*M*) also induced sinuous movement of the aboral tentacles.

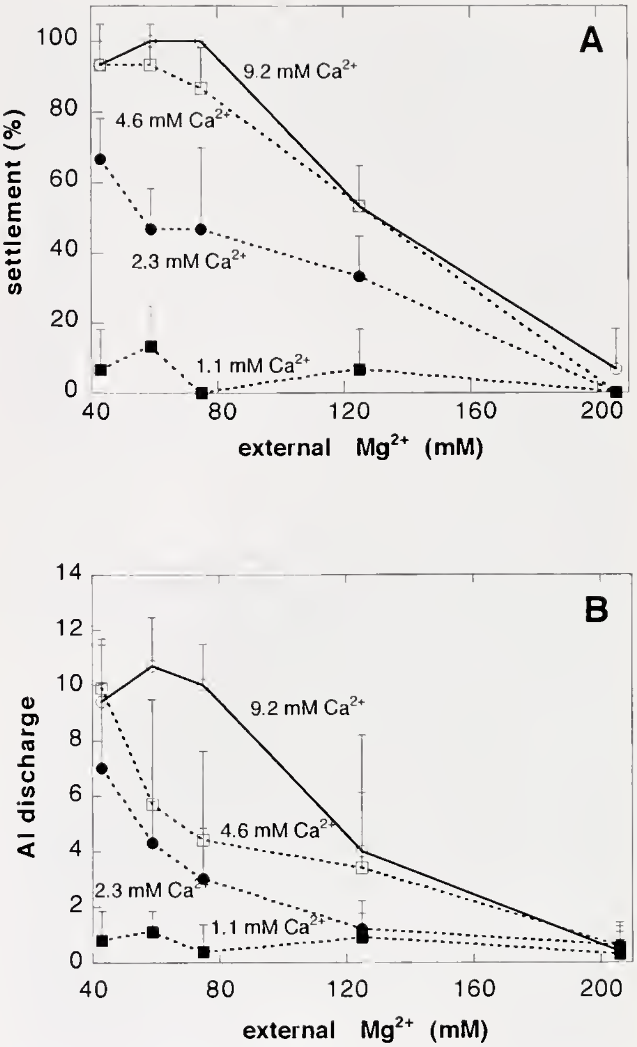

Figure 1. (A) Actinula settlement in artificial seawater with different concentrations of calcium and magnesium. Five larvae were incubated at specified concentrations of external Ca^{2+}. Vertical bars indicate standard deviations ($n = 5$). (B) K$^+$-ASW triggered *atrichous isorhiza* (AI) discharge in artificial seawater containing different concentrations of Ca^{2+} and Mg^{2+} ions. Means were obtained by averaging the number of discharged AI in each aboral tentacle tip ($n = 10$). Vertical bars indicate standard deviations.

Effects of Ca^{2+}-channel blockers on actinular settlement

The effects of inorganic Ca^{2+}-channel blockers on actinular settlement were examined in various concentrations of chloride salt cations added to regular ASW. In each case, a dose-dependent reduction of actinular settlement was observed (Fig. 3A). The following ions are listed in order of increasing inhibition efficiency: Co^{2+} < Ni^{2+} < Cd^{2+} < La^{3+} < Gd^{3+}.

Table I

Results of two-way ANOVA to assess the effects of Ca^{2+} and Mg^{2+} concentrations on (A) actinular settlement and (B) atrichous isorhiza *(AI) discharge*

Source*	*df*	*F*-ratio	*P*
(A) settlement			
Ca^{3+}	3	118.4902	<0.0001
Mg^{2+}	4	75.7353	<0.0001
Ca^{2+}-Mg^{2+}	12	9.2255	<0.0001
(B) AI discharge			
Ca^{2+}	3	1022.1822	<0.0001
Mg^{3+}	4	1012.5841	<0.0001
Ca^{2+}-Mg^{2+}	12	534.8241	<0.0001

* Ca^{2+}-Mg^{2+} represents the interaction between Ca^{2+} and Mg^{2+} concentrations.

The 50% inhibition concentrations (IC_{50}) were approximately 5800, 260, 53, 45, and 7 *μM*, respectively. Observed settlement percentages were similar to controls when the blocker was removed 5 h after the experiment.

K^+-induced AI discharge was also inhibited by these inorganic Ca^{2+}-channel blockers (Fig. 3B). IC_{50} values for Gd^{3+}, La^{3+}, Cd^{2+}, Ni^{2+}, and Co^{2+}, were approximately 5, 41, 78, 500, and 6600 *μM*, respectively. When 10^4 *μM* Co^{2+}, 10^3 *μM* Ni^{2+}, and 10^2 *μM* Cd^{2+} were added to ASW, AI discharges were lowered to 1.0 ± 0.9, 0.8 ± 1.2, and 0.6 ± 1.1, respectively. AI discharges were similar to controls when the blocker was removed prior to K^+-ASW stimulation 1 h after onset of the experiment. ASW containing 25 *μM* Gd^{3+} or 100 *μM* La^{3+} decreased the AI discharge to 1.2 ± 0.8 and 0.8 ± 1.1, respectively, but the discharge was not restored completely when the blockers were removed.

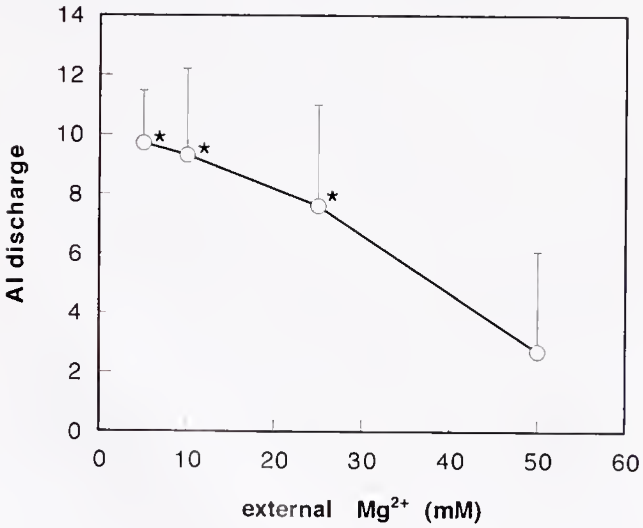

Figure 2. Enhancement of *atrichous isorhiza* (AI) discharge and settlement by low Mg^{2+} artificial seawater (ASW). Actinulae were bathed in ASW containing various concentrations of Mg^{2+} (regular ASW = 42.6 m*M* Mg^{2+}) for 1 h, and AI discharge was triggered by K^+-ASW (50, 100, or 200 m*M*) treatment. Means were obtained by averaging the number of discharged AI in each ATT ($n = 10$). Vertical bars indicate standard deviations. Asterisks (*) indicate significant differences relative to the untreated controls at $P < 0.05$ by the Tukey-Kramer honestly significant difference test.

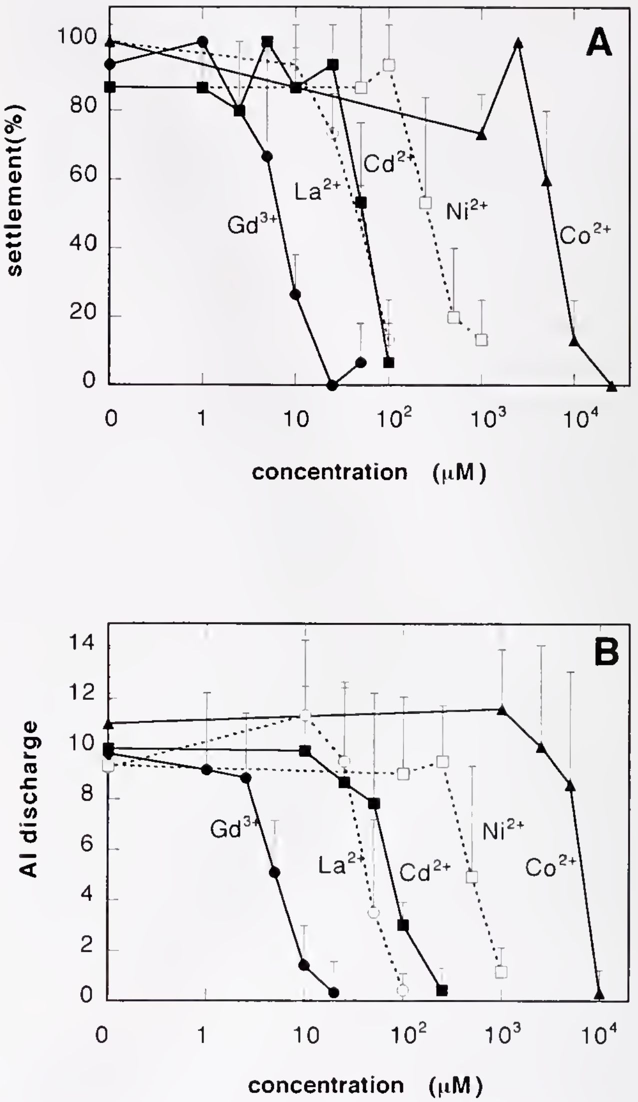

Figure 3. Effects of Ca^{2+}-channel blockers on actinular settlement (A) and *atrichous isorhiza* (AI) discharge (B). All experiments were performed using sulfate-free artificial seawater (ASW) at normal pH. Five larvae were incubated for 30 h in ASW containing various concentrations of Ca^{2+}-channel blockers.

Squashing an ATT with a micropipette caused AI discharge even in the presence of 20 *μM* Gd^{3+}, but sinuous tentacle movement, which was usually observed in regular ASW, was inhibited.

$[Ca^{2+}]_i$ transients during atrichous isorhiza *discharge*

Figure 4 compares representative changes of $R_{340/380}$ of ATT during AI discharge in Ca^{2+}-free ASW, Mg^{2+}-supple-

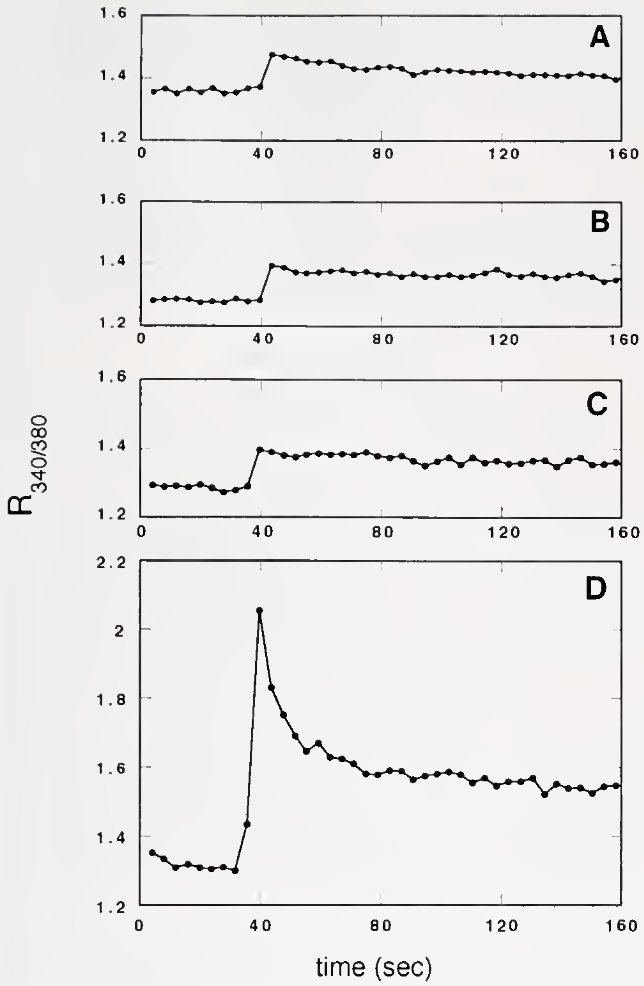

Figure 4. $[Ca^{2+}]_i$ transients during *atrichous isorhiza* discharge in (A) Ca^{2+}-free artificial seawater (ASW), (B) Mg^{2+}-supplemented ASW (200 m*M* Mg^{2+}), (C) 20 μM Gd^{3+}-ASW, and (D) regular ASW.

mented ASW (200 m*M* Mg^{2+}), 20 μM Gd^{3+}-ASW, and regular ASW. Despite the discharge inhibition by Gd^{3+} ions, $R_{340/380}$ transients were induced by the addition of K^+-ASW (200 m*M*). The rise of $R_{340/380}$ measured in the presence of Gd^{3+} ions was similar to that observed in Ca^{2+}-free ASW and considerably lower than that observed in regular ASW [$\Delta R_{340/380} = 0.23 \pm 0.11$, 0.18 ± 0.17, and 0.62 ± 0.24, respectively]. No significant difference was observed between Ca^{2+}-free ASW ($\Delta[Ca^{2+}]_i = 0.31 \pm 0.09$, $n = 6$) and Mg^{2+}-supplemented ASW (0.28 ± 0.11, $n = 6$).

Discussion

Ca^{2+}-dependence of settlement and atrichous isorhiza *discharge*

Although external Ca^{2+} ions have been reported as being required for nematocyst discharge in several species of cnidaria (Salleo *et al.*, 1993; Santoro and Salleo, 1991a, b), this is the first demonstration of Ca^{2+}-dependent nematocyst discharge in larvae. We also confirmed and quantified the Ca^{2+}-dependence of actinular settlement in *Tubularia mesembryanthemum*. Reduced-Ca^{2+} seawater also inhibits metamorphosis of *Hydractinia echinata* planula larvae (Berking, 1988; Müller, 1985). The EC_{50} of external Ca^{2+} was 3 m*M* for *T. mesembryanthemum* actinular settlement, comparable to that of both *H. echinata* settlement and actinular AI discharge (Kawaii *et al.*, 1997). Since actinulae immersed in Ca^{2+}-free ASW tended to disintegrate, settlement assays were not performed in Ca^{2+}-free ASW.

The action of K^+-ASW was strongly inhibited by increasing the Mg^{2+} concentration of the bathing solution, and the inhibitory effects of the Mg^{2+} ion increased when the external Ca^{2+} concentrations were lowered. Similarly, Müller (1985) found that TPA-induced metamorphosis of *H. echinata* was promoted in Mg^{2+}-reduced seawater. Mg^{2+} and Ca^{2+} ions compete with each other in many biological processes; consequently, we expected that an increase of Mg^{2+} concentration in the bathing solution would reduce the Ca^{2+} influx, thus inhibiting actinular settlement and AI discharge. However, the rise of $R_{340/380}$ values measured in Mg^{2+}-supplemented ASW was equivalent to that observed in Ca^{2+}-free ASW, and there was no influx of Ca^{2+} ions from the Mg^{2+}-supplemented ASW to nematocytes. These observations indicate that inhibition of AI discharge by Mg^{2+} did not result from the lowering of nematocyte $[Ca^{2+}]_i$ level by competitive influx of Mg^{2+} and Ca^{2+} ions. The enhancement of AI discharge and larval settlement by Mg^{2+} reduction may be a result of cation-mediated alteration of membrane-associated cell function in signal transduction, and Mg^{2+} ions would therefore regulate AI discharge and settlement of the hydroid as an inhibitory element.

Involvement of stretch-activated (SA) channels

It is natural for us to speculate about involvement of stretch-activated (SA) channels in actinular settlement, because the inhibitory effect of gadolinium ions at low concentrations in our study is comparable to that of opening SA channels in patch-clamped *Xenopus* oocytes (Yang and Sachs, 1989). Gd^{3+} is the most effective blocker of SA channels found to date, although it also has some effect on Ca^{2+} channels (Sadoshima *et al.*, 1992).

We previously demonstrated that both ATT contact with substrata and chemical stimuli are necessary to induce AI discharge (Kawaii *et al.*, 1997). By itself, a mechanical stimulus, such as immobilization of ATT by suction and vibration applied through a clean micropipette, did not trigger AI discharge. However, contact with a bacterial-film-coated micropipette did trigger discharge and also induced sinuous movement of the tentacles. Moreover, K^+-ASW treatment did not result in AI discharge from ATTs that were not in contact with any substrata. These results suggest that K^+-ASW treatment replaced sensory input of chemical stimuli, but did not mimic physical stimuli from ATT contact. Therefore, the observation that the stretching caused by immobilization of ATT did not trigger AI discharge does not rule out the involvement of SA channels in the discharge mechanism.

Effect of Ca^{2+}-channel blockers

All the Ca^{2+}-channel blockers tested for inhibitory effects on K^+-ASW triggered AI discharge and larval settlement demonstrated similar dose-response curves and similar IC_{50} values. This consistency suggests that similar Ca^{2+}-channel types were involved in these events. Previously, we showed close relationships between discharge of AIs and sinuous movement of aboral tentacles (Kawaii *et al.*, 1997). Aboral tentacles that had discharged AIs usually initiated sinuous movements, resulting in settlement behavior. Thus AI discharge can be considered as the first step in the settlement process, and inhibition of AI discharge by Ca^{2+}-channel blockers interrupts the subsequent processes. Squashing of ATTs caused AI discharge, but no sinuous movement was observed when ASW was treated with a Ca^{2+}-channel blocker. These results suggest that these cations inhibited not only the AI discharge but also the signal transmission system that follows discharge and leads to the induction of sinuous movement or the aboral tentacle sinuous movement itself.

Direct monitoring of intracellular Ca^{2+} ions also indicated that AI discharge required both Ca^{2+}-release from intracellular stores and Ca^{2+}-influx from bathing solution, and that Ca^{2+}-channel blockers inhibited the large Ca^{2+} influx. Taking into consideration that K^+-ASW treatment triggered limited AI discharge in Ca^{2+}-free ASW (Kawaii *et al.*, 1997) or in ASW containing Ca^{2+}-channel blocker, a Ca^{2+} release from intracellular stores functioned as the signal transmission system in AI discharge. In the sea anemone *Haliplanella luciae,* a precise pharmacological study demonstrated that Ca^{2+} acts as a second messenger, and intracellular Ca^{2+} stores play an important role in the regulation of nematocyst discharge (Russell and Watson, 1995), via a mechanism of "calcium-induced calcium release" (Endo, 1977). It is conceivable that similar mechanisms for regulating nematocyst discharge are present in different types of nematocytes. In Ca^{2+}-free ASW or ASW containing 10 μM Gd^{3+}, K^+-ASW treatment triggered limited AI discharge and caused slight elevation of $R_{340/380}$. These small $[Ca^{2+}]_i$ transients could be interpreted as a Ca^{2+} release from intracellular stores to nematocyte cytosol.

In conclusion, AI discharge was the primary action in actinular settlement, and signals from this discharge were spread throughout the larva, initiating actinular metamorphosis. The inhibitory effect of the Ca^{2+}-channel blockers demonstrated that AI discharge and subsequent signal transmission require involvement of Ca^{2+} channels.

Acknowledgments

The authors thank Dr. E. Hunter (The Centre for Environment, Fisheries & Aquaculture Science, Suffolk, U. K.) and Dr. C. G. Satuito (JAPAN NUS Co., Ltd., Tokyo, Japan) for their valuable suggestions.

Literature Cited

Berking, S. 1988. Ammonia, tetraethylammonium, barium, and amiloride induce metamorphosis in the marine hydroid *Hydractinia. Roux's Arch. Dev. Biol.* **197:** 1–9.

Endo, M. 1977. Calcium release from the sarcoplasmic reticulum. *Physiol. Rev.* **57:** 71–108.

Freeman, G., and E. B. Ridgway. 1987. Endogenous photoprotein, calcium channels and calcium transients during metamorphosis in hydrozoans. *Roux's Arch. Dev. Biol.* **196:** 30–50.

Freeman, G., and E. B. Ridgway. 1990. Cellular and intracellular pathways mediating the metamorphic stimulus in hydrozoan planulae. *Roux's Arch. Dev. Biol.* **199:** 63–79.

Gitter, A. H., D. Oliver, and U. Thurm. 1994. Calcium- and voltage-dependence of nematocyst discharge in *Hydra vulgaris. J. Comp. Physiol.* A **175:** 115–122.

Kawaii, S., K. Yamashita, M. Nakai, and N. Fusetani. 1997. Intracellular calcium transients during nematocyst discharge in actinulae of the hydroid, *Tubularia mesembryanthemum. J. Exp. Zool.* **278:** 299–307.

McKay, M. C., and P. A. V. Anderson. 1988. Preparation and properties of cnidocytes from the sea anemone *Anthopleura elegantissima. Biol. Bull.* **174:** 47–53.

Müller, W. A. 1985. Tumor-promoting phorbol esters induce metamorphosis and multiple head formation in the hydroid *Hydractinia. Differentiation* **29:** 216–222.

Pantin, C. F. A. 1942. The excitation of nematocysts. *J. Exp. Biol.* **19:** 294–310.

Russell, T. J., and G. M. Watson. 1995. Evidence for intracellular stores of calcium ions involved in regulating nematocyst discharge. *J. Exp. Zool.* **273:** 175–185.

Sadoshima, J., T. Takahashi, L. Jahan, and S. Izumo. 1992. Roles of mechanosensitive ion channels, cytoskeleton, and contractile activity in stretch-induced immediate-early gene expression and hypertrophy of cardiac myocytes. *Proc. Natl. Acad. Sci. USA* **89:** 9905–9909.

Salleo, A., G. Santoro, and P. Barra. 1993. Spread of experimentally induced discharge of the nematocytes in acontia of *Calliactis parasitica. Comp. Biochem. Physiol.* **104A:** 565–574.

Salleo, A., G. La Spada, and R. Barbera. 1994a. Gadolinium is a powerful blocker of the activation of nematocytes of *Pelagia nocticuca. J. Exp. Biol.* **187:** 201–206.

Salleo, A., G. La Spada, M. Drago, and G. Curcio. 1994b. Hyposmotic shock-induced discharge in acontia of *Calliactis parasitica* is blocked by gadolinium. *Experientia* **50:** 148–152.

Santoro, G., and A. Salleo. 1991a. Cell-to-cell transmission in the activation of *in situ* nematocytes in acontia of *Calliactis parasitica. Experientia* **47:** 701–703.

Santoro, G., and A. Salleo. 1991b. The discharge of *in situ* nematocysts of the acontia of *Aiptasia mutabilis* is a Ca^{2+}-induced response. *J. Exp. Biol.* **156:** 173–185.

Tardent, P. 1988. History and current state of knowledge concerning the discharge of cnidae. Pp. 309–332 in *The Biology of Nematocysts,* D. A. Hessinger and H. M. Lenhoff eds. Academic Press, San Diego.

Thorington, G. U., and D. A. Hessinger. 1988a. Control of cnida discharge. I. Evidence for two classes of chemoreceptors. *Biol. Bull.* **174:** 163–171.

Thorington, G. U., and D. A. Hessinger. 1988b. Control of discharge: factors affecting discharge of cnidae. Pp. 233–253 in *The Biology of Nematocysts,* D. A. Hessinger and H. M. Lenhoff, eds. Academic Press, San Diego.

Watson, G. M., and D. A. Hessinger. 1989. Cnidocyte mechanoreceptors are tuned to the movements of swimming prey by chemoreceptors. *Science* **243:** 1589–1591.

Watson, G. M., and D. A. Hessinger. 1991. Chemoreceptor-mediated elongation of stereocilium bundles tunes vibration-sensitive mechanoreceptors on cnidocyte-supporting cell complexes to lower frequencies. *J. Cell Sci.* **99:** 307–316.

Yamashita, K., S. Kawaii, M. Nakai, and N. Fusetani. 1997. Behaviour and settlement of actinula larvae of *Tubularia mesembryanthemum* Allman, 1871 (Hydrozoa: Tubulariidae). Pp. 512–516 in *The Proceedings of the 6th ICCB,* J. C. den Hartog, ed. National Museum of Natural History, Leiden.

Yanagita, T. M. 1973. The 'cnidoblast' as an excitable system. *Publ. Seto Mar. Biol. Lab.* **20:** 675–693.

Yang, X. -C., and F. Sachs. 1989. Block of stretch-activated ion channels in *Xenopus* oocytes by gadolinium and calcium ions. *Science* **243:** 1068–1071.

Reference: *Biol. Bull.* **196:** 52–56. (February, 1999)

Free Radicals and Chemiluminescence as Products of the Spontaneous Oxidation of Sulfide in Seawater, and Their Biological Implications

DAVID W. TAPLEY[1,*], GARRY R. BUETTNER[2], AND J. MALCOLM SHICK[1]

[1] *Department of Zoology and Center for Marine Studies, University of Maine, Orono, Maine 04469-5751; and* [2] *ESR Facility/EMRB 68, College of Medicine, The University of Iowa, Iowa City, Iowa 52242-1101*

The discovery of symbioses between marine invertebrates and sulfide-oxidizing bacteria at deep-sea hydrothermal vents and in other high-sulfide marine environments has stimulated research into the adaptations of metazoans to potentially toxic concentrations of sulfide. Most of these studies have focused on a particular action of sulfide—its disruption of aerobic metabolism by the inhibition of mitochondrial respiration—and on the adaptations of sulfide-tolerant animals to avoid this toxic effect (1). We propose that sulfidic environments impose another, hitherto overlooked type of toxicity: exposure to free radicals of oxygen, which may be produced during the spontaneous oxidation of sulfide, thus imposing an oxidative stress. Here we present evidence that oxygen- and sulfur-centered free radicals are produced during the oxidation of sulfide in seawater, and we propose a reaction pathway for sulfide oxidation that is consistent with our observations. We also show that chemiluminescence at visible wavelengths occurs during sulfide oxidation, providing a possible mechanism for the unexplained light emission from hydrothermal vents (2, 3).

In the presence of molecular oxygen and trace metal catalysts, hydrogen sulfide spontaneously oxidizes. Oxidation-reduction reactions frequently involve free-radical intermediates, and a metal-catalyzed pathway in which the initial reactions of sulfide oxidation form superoxide and sulfide radicals has been proposed (4). The proposed reaction begins with four steps:

$$HS^- + O_2 \rightarrow HS^\bullet + O_2^\bullet \qquad (1)$$

$$HS^\bullet + O_2 \rightarrow HO_2^\bullet + S \qquad (2)$$

$$HS^\bullet + O_2^{\bullet -} \rightarrow S + HO_2^- \qquad (3)$$

At near-neutral pH, HO_2^- will immediately protonate:

$$HO_2^- + H^+ \rightarrow H_2O_2 \qquad (4)$$

The proposed metal-catalyzed mechanism underlying reaction 1 is (4):

$$M^{n+} + O_2 \rightarrow M^{(n+1)+} + O_2^{\bullet -} \qquad (5)$$

$$M^{(n+1)+} + HS^- \rightarrow M^{n+} + HS^\bullet \qquad (6)$$

Notice that, once either radical is formed, a chain reaction ensues. The superoxide that is formed can undergo a subsequent reduction or dismutation to form hydrogen peroxide (H_2O_2), a known product of sulfide oxidation (5, 6), which is also produced in reactions 3 and 4. In the presence of transition-metal catalysts, superoxide and H_2O_2 will react to form the hydroxyl radical, $HO^\bullet$, perhaps the most oxidizing radical that can arise in a biological setting.

A similar pathway, in which reaction 2 yields an addition product, was proposed later (7):

$$HS^\bullet + O_2 \rightarrow HSO_2^\bullet \qquad (7)$$

According to this mechanism, the addition product then reacts with molecular oxygen:

$$HSO_2^\bullet + O_2 \rightarrow HSO_4^\bullet \qquad (8)$$

A subsequent series of reactions produces a variety of reactive intermediates, including superoxide, hydrogen peroxide, and the sulfide radical (7).

Although these free-radical mechanisms for sulfide oxi-

Received 18 May 1998; accepted 4 December 1998.

[*] Present address: Department of Biology, Salem State College, 352 Lafayette St., Salem, MA 01970-5353.

dation have been proposed (4, 7), no direct experimental support for such a mechanism has been provided to date. We have therefore employed electron paramagnetic resonance (EPR) spin trapping to gather direct evidence that free-radical intermediates are produced during sulfide oxidation. EPR spectrometry is similar to nuclear magnetic resonance (NMR) spectrometry, but relies on magnetic moments resulting from unpaired electrons instead of those from the atomic nucleus. Samples are exposed to microwave radiation at a fixed wavelength and amplitude while a magnetic field is swept through an appropriate range of field densities. At appropriate combinations of wavelength and magnetic field strength, the unpaired electrons will resonate, thereby absorbing microwave energy. This absorbance is recorded as the first derivative. In an EPR spectrum, the relative positions of peaks (lines) are more important than their absolute positions, so spectra typically are plotted with no abscissa, only a scale bar indicating the change in magnetic field strength over a given distance. The ordinate is in arbitrary absorbance units. Spin trapping is a technique for detecting ephemeral radicals by providing a molecule that preferentially reacts with them, forming more stable radical adducts with characteristic spectra. These spectra typically result from a primary peak, due to the radical that was trapped, being split one or more times by adjacent paramagnetic nuclei, typically hydrogen and nitrogen. The splitting of peaks is the result of the magnetic moments of the adduct being oriented either parallel or antiparallel to the magnetic moments of adjacent nuclei, with either orientation being equally likely. The magnetic field of half of the population of adducts will be incrementally increased, while that of the other half will be equally decreased. The values of these splittings (a^N and a^H) for various adducts of spin-trapping agents are well known and have been tabulated.

When sulfide was introduced into artificial seawater (ASW) containing the spin-trapping agent dimethylpyrroline-N-oxide (DMPO), a prominent EPR spectrum was obtained (Fig. 1A, B). The greater intensity of the high-field line compared to the low-field line is consistent with ongoing free radical formation by oxidizing sulfide, since the high-field line is detected by the EPR spectrometer several seconds after the low-field line. The appearance of a four-line spectrum with a total width of approximately 45 G suggests that the DMPO-hydroxyl radical adduct (DMPO/HO$^\bullet$; $a^N = a^H = 14.9G$) is present (8). But the asymmetry suggests that there are at least two radical species. The second radical should have hyperfine splittings that would produce asymmetries in the two middle lines, yet have a total spectral width near that of DMPO/HO$^\bullet$. Appropriate candidates are the sulfide radical adduct, DMPO/S$^\bullet$ ($a^N = 16.09G$, $a^H = 16.19G$) and the sulfite radical adduct, DMPO/$^\bullet SO_3^-$ ($a^N = 14.5G$, $a^H = 16.0G$) (8, 9). The splittings for DMPO/S$^\bullet$ are inconsistent with the spectra we obtained; but a computer simulation of the composite of DMPO/HO$^\bullet$ and DMPO/$^\bullet SO_3^-$ (Fig. 1C) reproduces the experimental spectrum well.

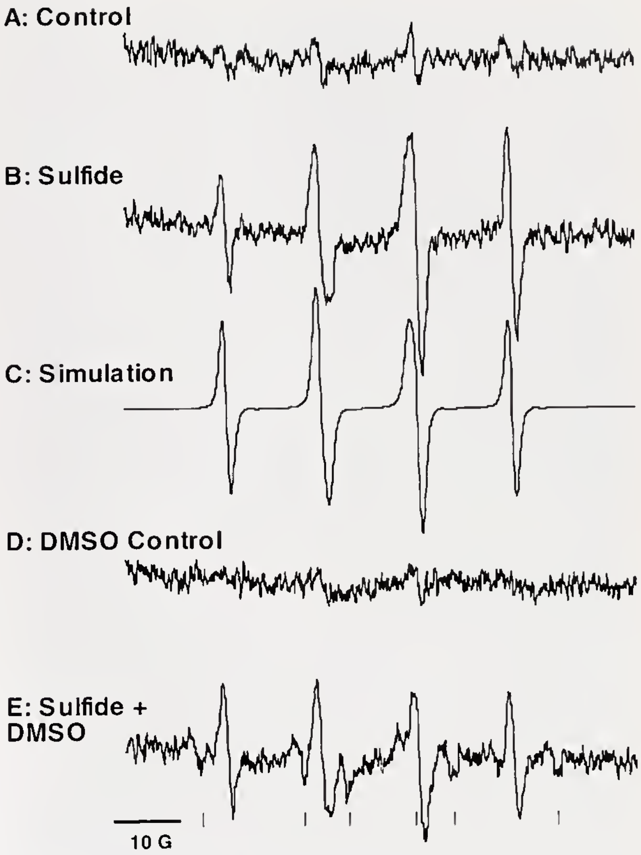

Figure 1. Electron paramagnetic resonance (EPR) spectra of DMPO adducts formed during sulfide oxidation in air-saturated artificial seawater (ASW) (27) at pH 7.4 and room temperature (≈20°C). (A) Control spectrum of DMPO in ASW with no sulfide added. (B) Spectrum obtained when sulfide (1 m*M*) is added. (C) Computer simulation of the spectrum in B, a composite of DMPO/HO$^\bullet$ (30%) and DMPO/$^\bullet SO_3^-$ (70%). (D) Control spectrum of DMPO and dimethyl sulfoxide (DMSO) in ASW with no sulfide added. (E) Spectrum obtained when 1 m*M* sulfide is added to DMPO and DMSO in ASW. Computer simulation of this spectrum indicates these relative abundances: DMPO/HO$^\bullet$ (20%), DMPO/$^\bullet SO_3^-$ (60%), and DMPO/$^\bullet CH_3$ (20%). Horizontal scale = 10 gauss; since in this type of spectrometry the relative positions of the lines are more important than their absolute positions, spectra do not usually include an absolute scale. The vertical axis is in arbitrary units. The vertical ticks in (E) mark the positions of DMPO/$^\bullet CH_3$ peaks. Reaction components, when present, were in the following final concentrations: DMPO, 50 m*M*; sulfide, 1 m*M*; DMSO, 0.7 *M*. Sulfide was added after all the other reactants, and immediately before transferring the sample to the EPR cell. Spectra were obtained with a Bruker ESP 300 EPR spectrometer equipped with a TM_{110} cavity and an aqueous flat cell. Computer simulations of spectra were carried out using SIMEPR software (28).

Chen and Morris (4) postulated superoxide production in their reaction mechanism, but the experiment shown in Figure 1 does not directly support this proposal. However, trapping superoxide is difficult, first because the k_{obs} for its reaction with DMPO is low ($\approx 30\ M^{-1} \cdot s^{-1}$ at pH 7.4; *cf.* k_{obs} for DMPO/HO$^\bullet$ formation is approximately 3.4×10^9

$M^{-1} \cdot s^{-1}$) (10, 11), and also because the superoxide adduct (DMPO/$^{\bullet}$OOH) can undergo further reactions, including reductions (12), to form DMPO/HO$^{\bullet}$ or EPR-silent products (10, 12). We included DMSO in the reaction mixture to distinguish between these potential routes by which DMPO/HO$^{\bullet}$ can form (Fig. 1D, E). The rate constants for the reactions of HO$^{\bullet}$ with DMPO and DMSO are 3.4×10^9 $M^{-1} \cdot s^{-1}$ and 7×10^9 $M^{-1} \cdot s^{-1}$, respectively (11, 13). Under our reaction conditions DMSO should have scavenged about 96% of the HO$^{\bullet}$ formed; however, the relative abundance of DMPO/HO$^{\bullet}$ in the composite spectrum decreased by only 33%, from 30% to 20% of the composite area (Fig. 1E). This implies that some DMPO/HO$^{\bullet}$ is formed artifactually (10, 14). The DMPO/HO$^{\bullet}$ adduct can also arise from nucleophilic substitution reactions of spin adducts (14 and references therein). For example, DMPO/$^{\bullet}$OSO$_3^-$ will hydrolyze to DMPO/HO$^{\bullet}$ in aqueous solution. Although formation of $SO_4^{\bullet -}$ is possible in our experiments, no evidence for DMPO/$^{\bullet}$OSO$_3^-$ ($t_{1/2} = 95s$) was seen in the spectra collected. But our data do not rule out the possibility that hydrolysis gave rise to a portion of the DMPO/HO$^{\bullet}$ observed. The presence of sulfide, a strong reductant, suggests that direct reduction of DMPO/$^{\bullet}$OOH to DMPO/HO$^{\bullet}$ (12) may have occurred in these experiments.

The conjecture—that superoxide is produced during sulfide oxidation, but is not detected by spin trapping—is supported by investigations into the mechanisms of thiol oxidation. Superoxide can be produced during the oxidation of thiols (15–17), but it is difficult to spin trap. In most experiments, superoxide production is demonstrated indirectly by including a molecular probe that is indicative of it. We were unable to find a probe for superoxide that would not react with sulfide, and were thus unable by this method to demonstrate superoxide production; but the results when DMSO is included in the reaction mixture, as well as the analogy with thiol oxidation, strongly suggest that superoxide is produced but not detected in our experiments.

The reaction mechanism proposed by Chen and Morris postulates the production of the sulfide radical (reaction 1), but no direct evidence for its formation is yet available. The sulfide radical has been spin trapped in anoxic conditions (9), but in our oxic experiments, conversion of the sulfide radical to oxygenated products appears to be efficient.

Since the reaction pathways discussed above (reactions 1–8) were first proposed, some of the postulated reactions, as well as other reactions relevant to the mechanism, have been demonstrated and their kinetics quantified. We suggest that reaction 2 is not likely to predominate; we propose instead that the addition reaction (reaction 7) predominates ($k_6 = 7.5 \times 10^9$ $M^{-1} \cdot s^{-1}$ at pH 7) (18, 19) and its product is then immediately deprotonated at near-neutral pH:

$$HSO_2^{\bullet} \leftrightarrow H^+ + SO_2^{\bullet} \qquad (9)$$

Kinetic data for reaction 2 are not available (18), but the rate is not likely to exceed that of reaction 7.

Once $SO_2^{\bullet -}$ is formed, it can oxidize to yield SO_2 and $O_2^{\bullet -}$ ($k_{10} = 1 \times 10^8$ $M^{-1} \cdot s^{-1}$ at pH 6.5) (20), which will subsequently hydrate to form HSO_3^-:

$$SO_2^{\bullet} + O_2 \rightarrow SO_2 + O_2^{\bullet -} \qquad (10)$$

$$SO_2 + H_2O \rightarrow H^+ + HSO_3^- \qquad (11)$$

If a strongly oxidizing radical is present, HSO_3^- will be oxidized to $SO_3^{\bullet -}$. For example, it will react with HO$^{\bullet}$ ($k = 5.1 \times 10^9$ $M^{-1} \cdot s^{-1}$ at pH 11.2) (21):

$$HSO_3^- + HO^{\bullet} \rightarrow SO_3^{\bullet -} + H_2O \qquad (12)$$

Our results (Fig. 1) strongly suggest the presence of such an oxidizing radical. Therefore, we propose that the reaction sequence 1, 7, and 9–12 occurs during the oxidation of sulfide. This sequence produces both oxygen- and sulfur-centered radicals, and is consistent with the results of our EPR spin-trapping study (Fig. 1). The oxidation of sulfide is catalyzed by trace metals (4) (see below). Therefore we believe that first-chain initiation is accomplished by reaction 6.

Sulfide-generated free radicals could impose an oxidative challenge to tissues exposed to them, and could represent a previously unrecognized type of sulfide toxicity: oxidative stress resulting from chronic, subacute exposure to sulfide. Marine animals living in environments where sulfide and molecular oxygen coexist are at risk from exogenously formed free radicals, as well as from radicals resulting from sulfide oxidation within their own tissues. This is true in spite of generally hypoxic conditions in sulfidic environments, since the presence of a strong reductant (sulfide) will enhance the production of free radicals (Fig. 1). We have evidence from studies on protobranch bivalves that sulfide exposure does impose an oxidative stress on these animals, and that they possess thermolabile defenses against this (22). Spectra similar to that in Figure 1B are obtained when sulfide is added to heat-denatured homogenates of tissues from the protobranch bivalves *Solemya velum* and *Yoldia limatula*, but are reduced or absent if undenatured homogenates are used (22).

A free-radical mechanism of sulfide toxicity might explain the symptoms associated with subacute sulfide poisoning in humans and laboratory animals. The primary symptom of subacute hydrogen sulfide poisoning is local inflammation of moist tissues exposed to the gas (6, 23, 24), especially the conjunctivae of the eye and the respiratory epithelia. In particular, sulfide-induced pulmonary edema is similar to that which appears under pulmonary oxidative stress (6, 25). Since these symptoms are restricted to moist tissues, the mechanism of irritation probably involves the aqueous reactions of hydrogen sulfide, including those producing radicals.

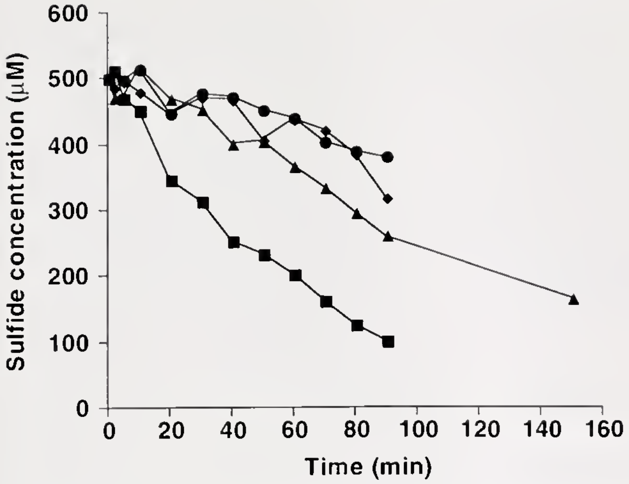

Figure 2. Time course of the disappearance of sulfide from ASW (pH 7.4) continuously sparged with air or nitrogen gas. Sulfide rapidly disappeared from solution in the aerated treatment (■). When DTPA was present, the loss of sulfide from aerated solution (▲) was reduced to control rates (●: nitrogen-sparged; ◆: nitrogen-sparged, DTPA present). In the anoxic control experiments, as well as those with DTPA, the loss of sulfide was owing to the degassing of H_2S by the nitrogen or air stream, not to the chemical oxidation of sulfide. In experiments where the pH was more acidic (and the proportion of sulfide as H_2S was therefore greater), the loss of sulfide under otherwise identical conditions was greatly increased (data not shown). ASW (50 ml) was placed in a glass Erlenmeyer flask and sparged with air or nitrogen for 1 h before the experiments were begun and continuously thereafter. The experiments were started by addition of sufficient sulfide stock, pH 7.4, to result in an initial sulfide concentration of 500 *μM*. Sulfide concentration was determined at 10-min intervals using the diamine method (29).

Evidence for metal catalysis of sulfide oxidation is provided by sulfide-depletion studies (Fig. 2) and chemiluminescence studies (Fig. 3). The rate at which sulfide disappears from solution (Fig. 2) decreases to control levels when the transition metal chelator diethylenetriaminepentaacetic acid (DTPA) is included in the system. This is consistent with previous studies demonstrating catalysis of sulfide oxidation by trace metals (4). The chemiluminescence plots for 200 and 500 *μM* sulfide (Fig. 3) show little or no induction period. When ethylenediaminetetraacetic acid (EDTA), which leaves one of the d-orbitals of iron available for reaction, is included in the system, a distinct induction period is seen. When DTPA, which coordinates all the d-orbital electrons of ferric iron, is included, light emission is reduced to blank rates. This suggests that trace iron is the primary transition metal catalyst under the conditions of this study (10).

The weak chemiluminescence at visible wavelengths observed during sulfide oxidation (Fig. 3) provides a potential mechanism for light production at the deep-sea hydrothermal vents (2, 3), as suggested by Hastings (in ref. 2). Pelli and Chamberlain (26) have proposed that thermal blackbody radiation is a source of visible light. However, since the vent plumes contain millimolar concentrations of sulfide and are mixing with the ambient oxygenated seawater, the conditions necessary for sulfide-dependent chemiluminescence to occur are present. To determine whether chemiluminescence is a source of light at the vents, spectra from the vent plumes must be compared with those from sulfide oxidation. Sulfide oxidation spectra should preferably be determined at the temperature and pressure found at the vents, and the measurement should be made with a low-resolution, high-sensitivity spectrograph of the type under consideration for future vent work (2).

The results presented here have established that both oxygen- and sulfur-centered free radicals are produced during the oxidation of sulfide, and that this is accompanied by measurable chemiluminescence at visible wavelengths. Production of free radicals during sulfide oxidation has the

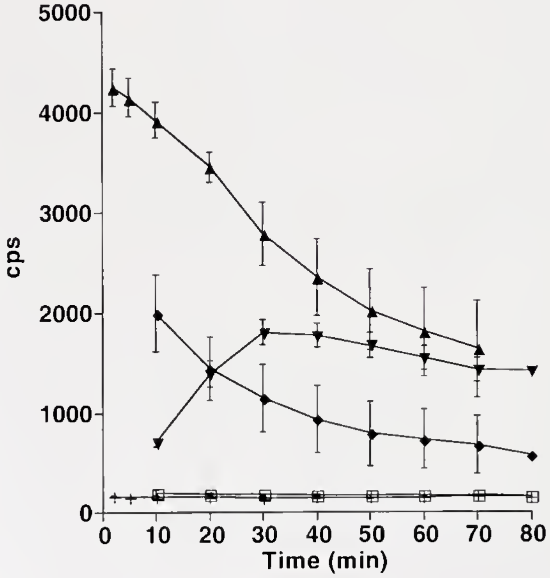

Figure 3. Time course of chemiluminescence, measured as counts per second (cps), during sulfide oxidation at various initial sulfide concentrations, with and without chelators. Each point is the average of three determinations; error bars are ± one standard deviation. The amount of light emitted was positively correlated with initial sulfide concentration (□: 0 *μM*; ◆: 200 *μM*; ▲: 500 *μM*). Luminescence was reduced substantially, and there was a 30 min induction period, when the chelator EDTA was included in 500 *μM* sulfide (▼). No chemiluminescence was observed in the presence of DTPA and 500 *μM* sulfide (+) or with 500 *μM* sulfide under anoxic conditions (data not shown). Reaction mixtures were prepared in ASW adjusted to pH 7.4 after the addition of chelators, when they were used. Chemiluminescence was measured in a Packard Tri-Carb model 3255 liquid scintillation counter set on the tritium channel in the out-of-coincidence mode (30). The photomultiplier in this counter is sensitive to wavelengths between 380 and 620 nm. Background counts from the empty chamber were 172 ± 4 cps (mean ± SD) and of an empty vial were 186 ± 11 cps. For each determination 20 ml of aerated ASW were placed into a vial, and a sufficient amount of sulfide stock was added to obtain the desired concentration. Counts were accumulated over 10-min intervals; for the experiments employing 500 *μM* sulfide, counts were accumulated over 1-min intervals for the first 10 min.

potential for imposing an oxidative stress on organisms living in sulfidic environments, with ramifications in toxicology, physiology, and clinical medicine.

Acknowledgments

We thank Dr. James North for help with the SIMEPR software. Funding was provided by grants from the Association of Graduate Students and a research assistantship from the Center for Marine Studies at the University of Maine.

Literature Cited

1. **Childress, J. J., and C. R. Fisher. 1992.** The biology of hydrothermal vent animals: physiology, biochemistry, and autotrophic symbioses. *Oceanogr. Mar. Biol. Annu. Rev.* **30:** 337–441.
2. **LITE Workshop Participants. 1993.** *Light in Thermal Environments (LITE).* National Science Foundation and National Aeronautics and Space Administration, Woods Hole, MA.
3. **Van Dover, C. L., J. Delaney, M. Smith, and J. R. Cann. 1988.** Light emission at deep-sea hydrothermal vents. *EOS* **69:** 1498.
4. **Chen, K. Y., and J. C. Morris. 1972.** Oxidation of sulfide by O_2: catalysis and inhibition. *J. Sanit. Eng. Div. Proc. Am. Soc. Civ. Eng.* **98:** 215–227.
5. **Bittersohl, G. 1971.** Beitrag zum toxischen Wirkungsmechanismus von Schwefelwasserstoff. *Z. Gesamte Hyg. Grenz.* **17:** 305–308.
6. **National Research Council. 1979.** *Hydrogen Sulfide.* University Park Press, Baltimore.
7. **Kotronarou, A., and M. R. Hoffmann. 1991.** Catalytic autoxidation of hydrogen sulfide in wastewater. *Environ. Sci. Technol.* **25:** 1153–1160.
8. **Buettner, G. R. 1987.** Spin trapping: ESR parameters of spin adducts. *Free Radical Biol. Med.* **3:** 259–303.
9. **Bilski, P., C. F. Chignell, J. Szychlinski, A. Borkowski, E. Oleksy, and K. Reszka. 1992.** The photo-oxidation of organic and inorganic substrates during UV-photolysis of nitrite anion in aqueous solution. *J. Am. Chem. Soc.* **114:** 549–556.
10. **Buettner, G. R., and R. P. Mason. 1990.** Spin-trapping methods for detecting superoxide and hydroxyl free radicals *in vitro* and *in vivo. Methods Enzymol.* **186:** 127–133.
11. **Finkelstein, E., G. M. Rosen, and E. J. Rauckman. 1980.** Spin trapping. Kinetics of the reaction of superoxide and hydroxyl radicals with nitrones. *J. Am. Chem. Soc.* **102:** 4994–4999.
12. **Rosen, G. M., and B. A. Freeman. 1984.** Detection of superoxide generated by endothelial cells. *Proc. Natl. Acad. Sci. USA* **81:** 7269–7273.
13. **Dorfman, L. M., and G. E. Adams. 1973.** *Reactivity of the Hydroxyl Radical in Aqueous Solutions.* U.S. Government Printing Office, U.S. National Bureau of Standards, Washington, DC.
14. **Davies, M. J., B. C. Gilbert, J. K. Stell, and A. C. Witwood. 1992.** Nucleophilic substitution reactions of spin adducts. Implications for the correct identification of reactions intermediates by EPR/spin trapping. *J. Chem. Soc. Perkin Trans.* **2:** 333–335.
15. **Misra, H. P. 1974.** Generation of superoxide free radical during the autoxidation of thiols. *J. Biol. Chem.* **249:** 2151–2155.
16. **Saez, G., P. J. Thornalley, H. A. O. Hill, R. Hems, and J. V. Bannister. 1982.** The production of free radicals during the autoxidation of cysteine and their effect on isolated rat hepatocytes. *Biochim. Biophys. Acta* **719:** 24–31.
17. **Buettner, G. R., and R. D. Hall. 1987.** Superoxide, hydrogen peroxide, and singlet oxygen in hematoporphyrin derivative, -cysteine, -NADH and light systems. *Biochim. Biophys. Acta* **823:** 501–507.
18. **Ross, A. B., W. G. Mallard, W. P. Helman, G. V. Buxton, R. E. Huie, and P. Neta. 1994.** *NDRL-NIST Solution Kinetics Database: Ver. 2.0.* National Institute of Standards and Technology, Gaithersburg, Maryland.
19. **Mills, G., K. H. Schmidt, M. S. Matheson, and D. Meisel. 1987.** Thermal and photochemical reactions of sulfhydryl radicals. Implications for colloid photocorrosion. *J. Phys. Chem.* **91:** 1590–1596.
20. **Creutz, C., and N. Sutin. 1974.** Kinetics of the reactions of sodium dithionite with dioxygen and hydrogen peroxide. *Inorg. Chem.* **13:** 2041–2043.
21. **Huie, R. E., and P. Neta. 1987.** Rate constants for some oxidations of S(IV) by radicals in aqueous solution. *Atmos. Environ.* **21:** 1743–1747.
22. **Tapley, D. W. 1993.** *Sulfide-dependent oxidative stress in marine invertebrates, especially thiotrophic symbioses.* Ph.D. thesis, University of Maine, Orono.
23. **Yant, W. P. 1930.** Hydrogen sulphide in industry. Occurrence, effects, and treatment. *Am. J. Public Health* **20:** 598–608.
24. **Lopez, A., M. G. Prior, R. J. Reiffenstein, and I. R. Goodwin. 1989.** Peracute toxic effects of inhaled hydrogen sulfide and injected sodium hydrosulfide on the lungs of rats. *Fundam. Appl. Toxicol.* **12:** 367–373.
25. **Halliwell, B., and J. M. C. Gutteridge. 1989.** *Free Radicals in Biology and Medicine.* Clarendon Press, Oxford, England.
26. **Pelli, D. G., and S. C. Chamberlain. 1989.** The visibility of 350°C black-body radiation by the shrimp *Rimicaris exoculata* and man. *Nature* **337:** 460–461.
27. **Cavanaugh, G. M. 1975.** *Formulae and Methods VI of the Marine Biological Laboratory Chemical Room.* Marine Biological Laboratory, Woods Hole, Massachusetts.
28. **Duling, D. R. 1994.** Simulation of multiple isotropic spin-trap EPR spectra. *J. Magn. Reson.* **104:** 105–110.
29. **Cline, J. D. 1969.** Spectrophotometric determination of hydrogen sulfide in natural waters. *Limnol. Oceanogr.* **14:** 454–458.
30. **Gonzalez Flecha, B., S. Llesuy, and A. Boveris. 1991.** Hydroperoxide-initiated chemiluminescence: an assay for oxidative stress in biopsies of heart, liver, and muscle. *Free Radical Biol. Med.* **10:** 93–100.

Reference: *Biol. Bull.* **196:** 57–62. (February, 1999)

Metamorphosis in the Marine Snail *Ilyanassa obsoleta*, Yes or NO?

STEPHAN J. FROGGETT* AND ESTHER M. LEISE†

Department of Biology, University of North Carolina Greensboro, Greensboro,
North Carolina 27402-6174

Abstract. Metamorphosis is a crucial life-history event that can change an organism's form, function, behavior, and ecological interactions. In the Mollusca, several neurotransmitters and neuromodulators play inductive or inhibitory roles in the pathways that govern larval metamorphosis. Nitric oxide (NO) has been implicated in developmental processes in vertebrates and arthropods, but not previously in molluscs. We determined that NO donors block pharmacologically induced metamorphosis in the mud snail *Ilyanassa obsoleta,* whereas injections of inhibitors of nitric oxide synthase (NOS) allow competent larvae to become juveniles. We describe a new developmental role for NO, as an endogenous inhibitor of molluscan metamorphosis.

Introduction

Marine molluscs are an ecologically and economically significant group of organisms, yet the regulatory mechanisms underlying their metamorphosis, a key developmental process, are still poorly understood. Environmental factors that influence or directly induce metamorphosis in physiologically competent larvae are known for a handful of species, but often not in specific molecular detail (Hadfield and Pennington, 1990; Pawlik, 1992; Morse, 1994; Zimmer-Faust and Tamburri, 1994). The downstream neuroendocrine actions that control the events of larval metamorphosis have been studied in some of these same organisms, but in no instance are the molecular mechanisms that subserve an entire pathway understood. The actions of several neurotransmitters in this process have been investigated, but no previous report implicates NO as playing a role in molluscan development. Early reports of this work have been published only in abstract format (Froggett and Leise, 1996; 1997).

Several neuroactive compounds are known to be involved in the induction of metamorphosis in marine molluscs. For example, catecholamines, such as norepinephrine and dopamine, regulate metamorphosis in oysters of the genus *Crassostrea* (Coon and Bonar, 1986; Bonar *et al.*, 1990) and in the nudibranch *Phestilla sibogae* (Pires *et al.*, 1996, 1997). Elevated levels of endogenous serotonin (5-HT) also activate metamorphosis in the prosobranch gastropod *Ilyanassa obsoleta* (Couper and Leise, 1996). Immunocytochemical and high performance liquid chromatographic studies have demonstrated that these neurotransmitters and others, such as FMRFamide and the small cardioactive peptides, are present in the central nervous systems (CNSs) of several marine gastropods during larval development (Coon and Bonar, 1986; Bonar *et al.*, 1990; Barlow and Truman, 1992; Kempf *et al.*, 1992, 1997; Marois and Carew, 1997).

Lin and Leise (1996b) used NADPH diaphorase (NADPHd) histochemistry to describe a gradual increase in the occurrence of NOS (Dawson *et al.*, 1991) in the CNS of *Ilyanassa* during larval development. During metamorphosis, NADPHd staining in all ganglia drops dramatically, particularly in the apical ganglion. This ganglion, also described as the apical or cephalic sensory organ (Bonar, 1978; Lin and Leise, 1996a; Marois and Carew, 1997), innervates the velum, the larval swimming and feeding organ. During post-metamorphic development, juvenile

---

Received 10 June 1998; accepted 21 October 1998.

* Present address: Department of Biology, Morrill Science Center, University of Massachusetts, Amherst, MA 01003.

† Author to whom correspondence should be addressed. E-mail: esther_leise@uncg.edu

Abbreviations: Carboxy-PTIO, 1*H*-imidazol-yloxy,2-(4-carboxyphenyl) -4,5-dihydro-4,4,5,5-tetramethyl-3-oxide; cGMP, cyclic guanosine 3′,5′ monophosphate; CNS, central nervous system; FIO, 0.2μm filtered Instant Ocean; 5-HT, 5-hydroxytryptamine (also serotonin); L-NAME, *N*-nitro-L-arginine methyl ester; L-NMMA, *N*-methyl-L-arginine acetate; NADPHd, nicotinamide adenine dinucleotide phosphate diaphorase; NO, nitric oxide; NOS, nitric oxide synthase; SIN-1, 3-morpholino-sydnonimine; SNAP, *S*-nitroso-*N*-acetyl-D,L-penicillamine.

NADPHd levels increase to produce a different staining pattern in all ganglia but the apical one. This ganglion is lost by the fourth day after metamorphic induction (Lin and Leise, 1996a). The distinct changes in NADPHd staining patterns observed by Lin and Leise suggested that NO might play an important role in the regulation of metamorphosis in *Ilyanassa* and are consistent with three hypotheses: (a) that NO promotes metamorphosis, (b) that NO is necessary for the maintenance of the larval state, or (c) that NO is uninvolved in metamorphosis, having other larval and juvenile actions. To distinguish between these possibilities, we employed nitrergic reagents that allowed us to manipulate the function of the NOS enzyme and larval exposure to NO.

Materials and Methods

Detailed experimental protocols have previously been published (Couper and Leise, 1996). Briefly, in bath application experiments, competent larvae were placed in 2 ml of solution in wells of 24-well plastic Falcon tissue culture plates, at 10 larvae/well. In all experiments, Instant Ocean, filtered to 0.2 μm (FIO), and 10^{-4} M 5-HT served as negative and positive controls, respectively. In most cases, experimental and control conditions were simultaneously replicated three times, yielding a typical sample size of 30 larvae for each treatment. Graphs with more than 30 animals per treatment indicate additional experimental replications. Larvae in experimental treatments and control groups were usually obtained from one culture. If more than one culture was used, animals from both cultures were distributed among all conditions, but in separate wells so that any significant differences resulting from culture conditions could be detected. The number of larvae and metamorphosed individuals were counted at 24 and 48 h in all experiments. In all treatments in which metamorphosis was induced, some animals became juveniles by the end of the experiment (2 days after induction). However, even in a natural inducer (Leise *et al.*, 1996) or 10^{-4} M 5-HT, all larvae do not begin metamorphosis simultaneously. As a result, specific criteria that indicated the initiation of this irreversible process were used to evaluate larval response to each treatment. Metamorphosis was determined by an examination of the morphology of each larva. Animals that had partially or totally lost velar cilia or the velar lobes were scored as having metamorphosed.

Nitrergic reagents were obtained from Cayman Chemical Co., Tocris Cookson, Inc., or Sigma Chemical Co. and prepared just before use. During the bath experiments, mortality in control solutions was insignificant, but it was near 10% in the higher concentrations of SNAP.

Direct injection of compounds into the larval hemocoel allowed us to avoid confounding factors, such as metabolism of reagents in the seawater bath or variable uptake across the larval epidermis, that can occur in bath application experiments (Couper and Leise, 1996). To prepare competent larvae for injection experiments, they were rinsed with FIO four times, then decalcified in Ca^{2+}-free seawater for 12 h (Pires and Hadfield, 1993). Decalcified larvae were then embedded in 1% low melting point agarose (Type VII, Sigma Chemical Co.) in FIO to impede movement. Larvae were freed from the agarose and pressure injected with approximately 6 nl of experimental solution delivered subepidermally through a glass micropipette connected to a Picospritzer II (General Valve Corp). Larvae were then placed in FIO at a density of 10 larvae/2 ml. Controls always included bath applications and injections of FIO and 10^{-4} M 5-HT.

Animals that died during experiments were not scored. Numbers of animals (n = X) on the graphs indicate numbers at the beginning of an experiment for all concentrations unless otherwise indicated in the legend. Injection experiments had variable rates of mortality, from 2.5% to 30%, but occasionally higher (40% in L-NAME experiments). Mortality rates in Carboxy-PTIO solutions were relatively low (0%–7%). In all instances of higher mortality, rates were similar in experimental and control groups, suggesting that larval death occurred because the nervous system was inadvertently damaged during the injection procedure.

Results from each experiment were pooled and tested for statistical significance ($P = 0.05$) in 2-way chi-square contingency tables (Zar, 1974; Sokal and Rolf, 1981). We used the Bonferroni method to correct for multiple comparisons (Bland, 1995). If the corrected α level fell between published values, we rounded down to the nearest α value. Raw percentage data were normalized by an arcsine transform, and standard deviations were calculated on the transformed data. Data were transformed back to percentages for graphing. Graphs were produced with Deltagraph 4.0 software.

Results

Initial bath experiments utilized either *S*-nitroso-*N*-acetyl-D,L-penicillamine (SNAP) or 3-morpholino-sydnonimine (SIN-1), both NO donors, alone or in combination with the metamorphic inducer 5-HT, to determine whether metamorphosis was affected by exogenously generated NO. SIN-1 or SNAP alone in bath solutions did not significantly affect the percentage of larvae undergoing metamorphosis (Fig. 1).

Bath application of the NO-donors SIN-1 and SNAP at high concentrations reduced the ability of 5-HT to induce metamorphosis (Fig. 2). Because of these results, NOS inhibitors were injected into competent larvae to determine whether experimentally manipulated levels of endogenous NO would promote metamorphosis in the absence of any known inducer.

Injections of the NOS inhibitors *N*-nitro-L-arginine methyl ester (L-NAME) and *N*-methyl-L-arginine acetate (L-NMMA), or the NO scavenger 1*H*-imidazol-yloxy,2-(4-carboxyphenyl)-4,5-dihydro-4,4,5,5-tetramethyl-3-oxide

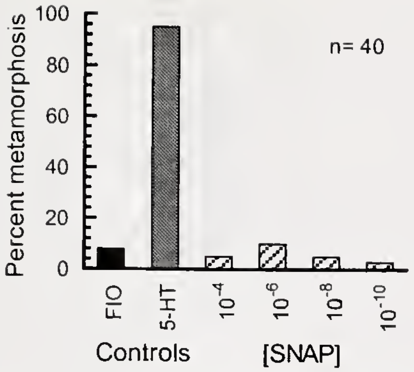

Figure 1. SNAP alone induces no metamorphosis in competent larvae by 48 h. Bath application of SNAP without 5-HT induced rates of metamorphosis similar to those induced by filtered Instant Ocean (FIO). The positive control (10^{-4} *M* 5-HT) induced 95% of the larvae to metamorphose by 48 h, a typical result. Concentrations of SNAP greater than 10^{-4} *M* were toxic to larvae, causing abnormal behavior and decalcification but no loss of velar tissue or any indication of metamorphosis (data not shown). Data from SIN-1 experiments (also not shown) were similar to those obtained with SNAP.

(Carboxy-PTIO) directly into the larval hemocoel allowed us to determine how a decrease in endogenous levels of NO affects metamorphosis. Both L-NAME and L-NMMA induced significant levels of metamorphosis by 24 h when injected in the absence of 5-HT (Figs. 3, 4). Injections of the inactive isomer D-NAME did not significantly affect the percentage of larvae undergoing metamorphosis (Fig. 3B). In a final set of experiments, we attempted to induce metamorphosis by injecting Carboxy-PTIO into competent larvae (Fig. 5). These results were insignificant after application of Bonferroni's method.

Discussion

All of our pharmacological data support the idea that NO acts to inhibit metamorphosis in *Ilyanassa.* Injections of NOS inhibitors into competent larvae allowed metamorphosis to proceed. Active concentrations of the NO reagents that we used were similar to or lower than those found to be active on other molluscan neural preparations (Gelperin, 1994a, b; Jacklet and Gruhn, 1994; Elphick *et al.*, 1995; Huang *et al.*, 1998). Unlike the NOS inhibitors, Carboxy-PTIO was not effective (Fig. 5). The levels of metamorphosis detected after injections of Carboxy-PTIO were significantly different from those obtained with 5-HT but not from those in the FIO controls, suggesting that the concentrations we used may have incompletely scavenged the available NO. Results with injections of the NOS inhibitors L-NAME and L-NMMA were more robust; a range of concentrations of both reagents was effective by 24 h (Figs. 3, 4). Interestingly, the FIO controls in the L-NMMA injection experiments (Fig. 4) showed unusually high levels of metamorphosis, especially by 48 h. Larvae in cultures older than 3 weeks will normally begin to metamorphose spontaneously (Leise *et al.*, 1996; unpubl. data), and the high levels of metamorphosis seen in the FIO controls at 48 h in the L-NMMA experiments (Fig. 4) suggested that spontaneous metamorphosis was occurring. In these experiments, bath application of 5-HT elicited nearly 100% metamorphosis by 24 h, suggesting that the 48-h results were irrelevant; most metamorphosis that would occur had done so within 24 h. In the field, *Ilyanassa* larvae are probably induced to metamor-

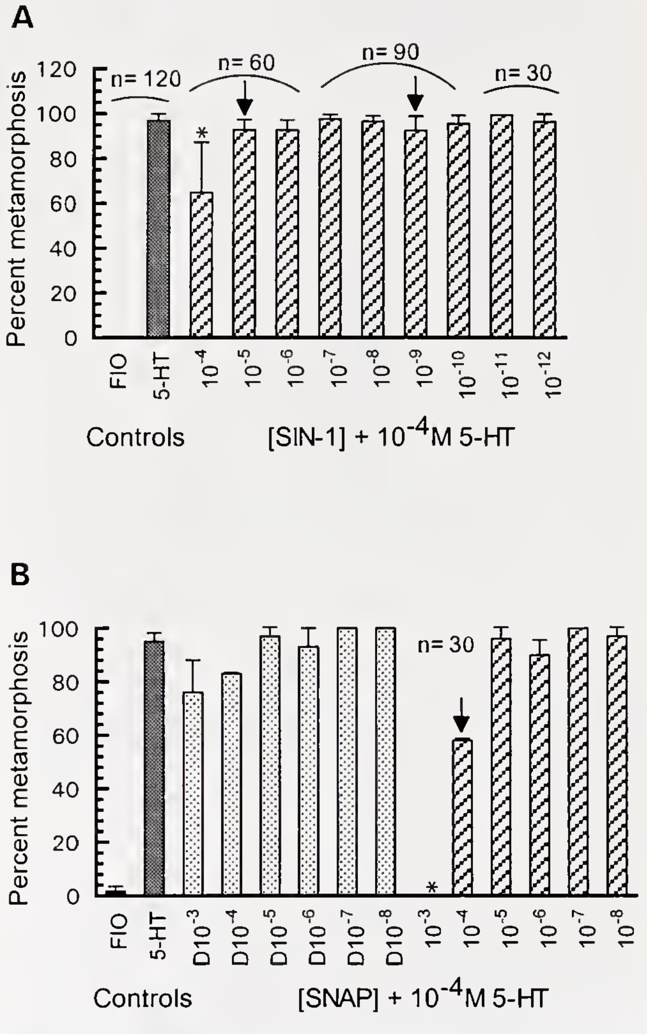

Figure 2. Inhibition of 5-HT-induced metamorphosis by SIN-1 (A) and SNAP (B) at 48 h. (A) Asterisk indicates concentration of unreplaced SIN-1 that significantly inhibited 5-HT-induced metamorphosis at 24 h (41% metamorphosis in 10^{-4} *M*, $\chi^2_{0.005(1)} = 15.5$) and 48 h (65% metamorphosis, $\chi^2_{0.005(1)} = 30.77$) compared to the 5-HT control. Arrows indicate concentrations that showed significant inhibition compared to 5-HT only at 24 h (*e.g.*, 59% metamorphosis in 10^{-9} *M* at 24 h, $\chi^2_{0.005(1)} = 13.9$), but not at 48 h. All SIN-1 solutions contained 10^{-4} *M* 5-HT. (B). Asterisk indicates concentration of SNAP that significantly inhibited 5-HT-induced metamorphosis at 24 and 48 h. Arrow indicates concentration that was inhibitory only at 24 h (40% metamorphosis in 10^{-4} *M*, $\chi^2_{0.005(1)} = 11.3$), but not at 48 h. Solutions of SNAP have a half-life of about 1 h and were changed every 6 h to maintain relatively steady concentrations of NO. $D10^{-X}$ = degassed solution of 10^{-X} *M* SNAP plus 10^{-4} *M* 5-HT; 10^{-X} = active solution of 10^{-X} *M* SNAP plus 10^{-4} *M* 5-HT.

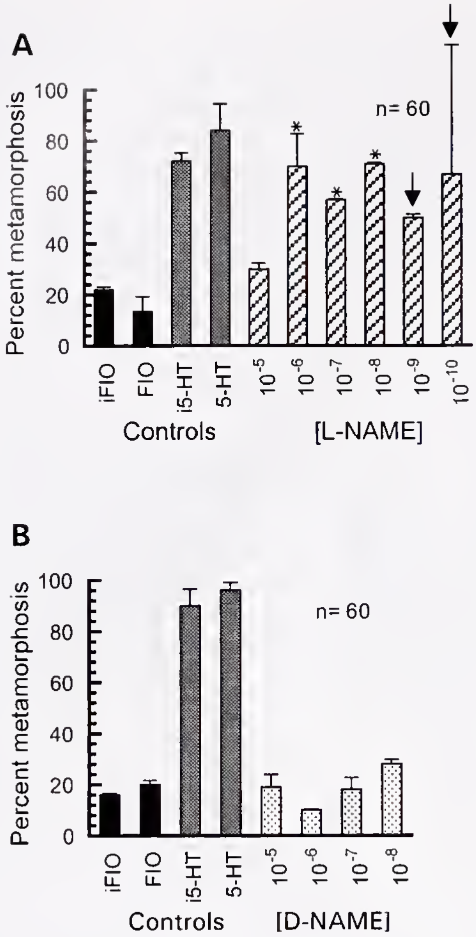

Figure 3. (A) Injections of L-NAME induced metamorphosis in competent larvae by 48 h in the absence of any inducer. Asterisks indicate levels of metamorphosis significantly different from those induced by injected FIO (iFIO) (*e.g.*, 10^{-7} *M*, $\chi^2_{0.005(1)} = 14.5$). Arrows indicate concentrations that were significantly effective by 24 h but not at 48 h. $n = 30$ for 10^{-9} and 10^{-10} *M* L-NAME. (B) Injections of the inactive isomer D-NAME induced no significant rates of metamorphosis by 48 h. (i5-HT = injected 5-HT).

phose by diatoms or associated organisms that occur naturally in their littoral habitats (Leise *et al.*, 1996), but we have no understanding of the time course for metamorphosis in that situation. Our results have led us to hypothesize that NO production is necessary for the maintenance of the larval state until an appropriate metamorphic cue is detected. Preliminary data from experiments on *Phestilla sibogae* suggest that NO may be active in the metamorphic pathway in this species as well (Meleshkevitch *et al.*, 1997). The ubiquity of NO in molluscan metamorphosis and its specific actions in this process remain to be determined.

Although the tranformations that invertebrate larvae undergo in reaction to metamorphic cues are among their most well known activities (Pawlik, 1992), unsuitable habitats can also elicit distinctly negative responses from some larvae, such as those of the polychaetes *Nereis vexillosa* and *Capitella sp.* (Woodin, 1991). We recently found a similar effect on *Ilyanassa* larvae from one species of benthic diatom. Extracts of cultures of a sheathed pennate diatom species that were isolated from sediments obtained at Myrtle Grove, North Carolina, inhibit spontaneous metamorphosis in older (>3 weeks in culture) *Ilyanassa* larvae (Leise *et al.*, 1996; unpubl. data). Such negative metamorphic actions and the uncertainty of larval encounters with appropriate juvenile habitats suggest that the maintenance of the larval life-history phase is an integral component of the metamorphically competent state. For *Ilyanassa*, the production of NO by competent larvae appears to be necessary for this purpose. However, maintenance of the larval state is likely to depend upon more than one inhibitory compound. For example, Pires *et al.* (1996) suggested that norepinephrine might inhibit the circuits controlling metamorphosis in the slipper limpet *Crepidula fornicata*. We do not yet know how *Ilyanassa* larvae utilize dopamine or other catecholamines.

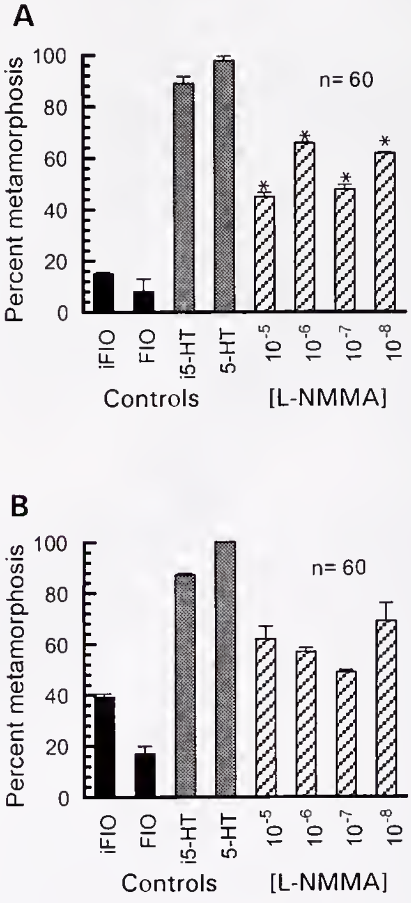

Figure 4. (A) Injections of all concentrations of L-NMMA induced significant rates of metamorphosis by 24 h in the absence of any inducer. Asterisks indicate concentrations that triggered rates of metamorphosis significantly different from those induced by iFIO (*e.g.*, at 10^{-5} *M*, $\chi^2_{0.01(1)} = 11.5$). Note unusually high levels of metamorphosis in both 5-HT controls. (B) Levels of metamorphosis detected at 48 h. No concentrations remained significantly different from iFIO ($\chi^2_{0.05(1)} = 6.2$). Note the unusually high levels of metamorphosis in both iFIO and FIO.

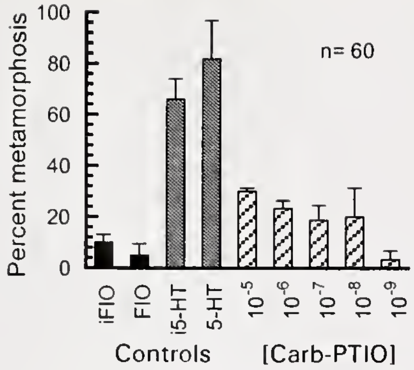

Figure 5. No concentrations of injected Carboxy-PTIO (Carb-PTIO), an NO scavenger, induced significant rates of metamorphosis by 48 h when compared to iFIO (10^{-5} *M* $\chi^2_{0.01(1)} = 5.76$, 10^{-6} *M* $\chi^2_{0.01(1)} = 3.84$). n = 30 for 10^{-5} and 10^{-9} *M* Carboxy-PTIO. Significance levels for 24 and 48 h data were the same.

Developing nervous systems in vertebrates and arthropods express NO transiently in a variety of areas (Bredt and Snyder, 1994; Truman *et al.*, 1996; Gibbs and Truman, 1998; Scholz *et al.*, 1998). NO has been reported to cause growth cone collapse (Rentería and Constantine-Paton, 1996) and may act in the regulation of neuronal proliferation (Peunova and Enikolopov, 1995; Kuzin *et al.*, 1996), affecting the ability of axons to reach appropriate targets and initiate synaptogenesis (Bredt and Snyder, 1994; Wu *et al.*, 1994; Truman *et al.*, 1996; Gibbs and Truman, 1998; Scholz *et al.*, 1998). Comparable roles for this molecule in molluscs are just beginning to come under investigation.

How NO exerts its effects in larval *Ilyanassa* is still unknown. Typically, NO binds to guanylyl cyclase, stimulating the formation of cyclic guanosine 3′,5′ monophosphate (cGMP) (Murad *et al.*, 1978); the biochemistry of the nitrergic signaling pathway appears to remain applicable to both vertebrate and invertebrate systems (Dawson *et al.*, 1991; Elphick *et al.*, 1993; Elofsson *et al.*, 1993; Huang *et al.*, 1998). Recent work on the growth and survival of cultured neurons suggests that NO may also affect cGMP-independent intracellular signaling pathways (Gonzalez-Zulueta *et al.*, 1997). We cannot yet distinguish between these two mechanisms in our experimental animal. At present, we suggest that NO is produced within the developing molluscan nervous system and diffuses to its target cells to activate guanylyl cyclase, thereby increasing intracellular levels of cGMP. We hypothesize that high levels of cGMP are necessary for the maintenance of larval tissues. We anticipate that neuronal somata in the apical ganglion—the brain region that governs key larval functions—will express high levels of NOS. In the presence of a natural metamorphic inducer, nitrergic neurons are probably inhibited, either directly by serotonergic neurons or by feedback from activated NO targets. Activation of serotonergic neurons and the resultant inhibition of NOS activity would decrease levels of cGMP, allowing metamorphosis to proceed. Investigations into the downstream actions of NO are just beginning.

Given its widespread occurrence in behaviorally significant neural circuits throughout the animal kingdom, NO would appear to be a relatively ancient neurotransmitter. In adult molluscs, NO functions as an intercellular messenger in behaviorally important circuits. NO appears to be necessary for learning in cephalopods (Chichery and Chichery, 1994; Robertson *et al.*, 1994, 1995, 1996), olfaction in pulmonates (Gelperin, 1994a, b; Gelperin *et al.*, 1996), and feeding in several gastropods (Moroz *et al.*, 1993; Elphick *et al.*, 1995; Teyke, 1996). Our understanding of the importance of this molecule in developing organisms is still relatively immature, but the growing literature indicates that this molecule can be differentially activated to coordinate specific developmental events occurring throughout a field of maturing neural tissue (Edelman and Gally, 1992; Bredt and Snyder, 1994; Wu *et al.*, 1994; Peunova and Enikolopov, 1995; Kuzin *et al.*, 1996; Rentería and Constantine-Paton, 1996; Truman *et al.*, 1996; Gibbs and Truman, 1998; Scholz *et al.*, 1998). In larvae of marine molluscs, nitrergic pathways may have been exploited to regulate diverse target tissues, much as the ecdysteroids coordinate activity during insect metamorphosis (Riddiford and Truman, 1993). Ecdysteroid synthesis is inhibited in crustaceans by molt-inhibiting hormone (reviewed in Fingerman, 1997), which may have a molluscan analog in NO. Our comprehension of the mechanisms that drive molluscan metamorphosis will be aided by further explorations of this pathway.

Acknowledgments

This work was supported in part by NSF grant IBN-9604516.

Literature Cited

Barlow, L. A., and J. W. Truman. 1992. Patterns of serotonin and SCP immunoreactivity during metamorphosis of the nervous system of the red abalone, *Haliotis rufescens*. *J. Neurobiol.* **23:** 829–844.

Bland, M. 1995. *An Introduction to Medical Statistics.* Oxford University Press, Oxford.

Bonar, D. B. 1978. Ultrastructure of a cephalic sensory organ in larvae of the gastropod *Phestilla sibogae* (Aeolidacea, Nudibranchea). *Tissue Cell* **10:** 153–165.

Bonar, D. B., S. L. Coon, M. Walch, R. M. Weiner, and W. Fitt. 1990. Control of oyster settlement and metamorphosis by endogenous and exogenous chemical cues. *Bull. Mar. Sci.* **46:** 484–498.

Bredt, D. J., and S. H. Snyder. 1994. Transient nitric oxide synthase neurons in embryonic cerebral cortical plate, sensory ganglia, and olfactory epithelium. *Neuron* **13:** 301–313.

Chichery, R., and M.-P. Chichery. 1994. NADPH-diaphorase in a cephalopod brain (*Sepia*): presence in an analogue of the cerebellum. *NeuroReport* **5:** 1273–1276.

Coon, S. L., and D. B. Bonar. 1986. Norepinephrine and dopamine content of larvae and spat of the Pacific oyster, *Crassostrea gigas*. *Biol. Bull.* **171:** 632–639.

Couper, J. M., and E. M. Leise. 1996. Serotonin injections induce metamorphosis in larvae of the gastropod mollusc *Ilyanassa obsoleta*. *Biol. Bull.* **191:** 178–186.

Dawson, T. M., D. S. Bredt, M. Fotuhi, P. M. Hwang, and S. H. Snyder. 1991. Nitric oxide synthase and neuronal NADPH diaphorase are identical in brain and peripheral tissues. *Proc. Natl. Acad. Sci. USA* **88:** 7797–7801.

Edelman, G. M., and J. A. Gally. 1992. Nitric oxide: linking space and time in the brain. *Proc. Natl. Acad. Sci. USA* **89:** 11651–11652.

Elofsson, R., M. Carlberg, L. Moroz, L. Nezlin, and D. Sakharov. 1993. Is nitric oxide (NO) produced by invertebrate neurones? *NeuroReport* **4:** 279–282.

Elphick, M. R., I. C. Green, and M. O'Shea. 1993. Nitric oxide synthesis and action in an invertebrate brain. *Brain Res.* **619:** 344–346.

Elphick, M. R., G. Kemenes, K. Staras, and M. O'Shea. 1995. Behavioral role for nitric oxide in chemosensory activation of feeding in a mollusc. *J. Neurosci.* **15:** 7643–7664.

Fingerman, M. 1997. Crustacean endocrinology: a retrospective, prospective, and introspective analysis. *Physiol. Zool.* **70:** 257–269.

Froggett, S., and E. M. Leise. 1996. Does nitric oxide inhibit metamorphosis in a larval mollusc? *Soc. Neurosci. Abstr.* **22:** 364.

Froggett, S., and E. M. Leise. 1997. Endogenous nitric oxide inhibits metamorphosis in a larval mollusc. *Soc. Neurosci. Abstr.* **23:** 1234.

Gelperin, A. 1994a. Nitric oxide mediates network oscillations of olfactory interneurons in a terrestrial mollusc. *Nature* **369:** 61–63.

Gelperin, A. 1994b. Nitric oxide, odour processing and plasticity. *Neth. J. Zool.* **44:** 159–169.

Gelperin, A., D. Kleinfeld, W. Denk, and I. R. C. Cooke. 1996. Oscillations and gaseous oxides in invertebrate olfaction. *J. Neurobiol.* **30:** 110–122.

Gibbs, S. M., and J. W. Truman. 1998. Nitric oxide and cyclic GMP regulate retinal patterning in the optic lobe of *Drosophila*. *Neuron* **20:** 83–93.

Gonzalez-Zulueta, M., H. -Y. Yun, V. L. Dawson, and T. M. Dawson. 1997. Nitric oxide mediates activity-dependent neuronal survival. *Soc. Neurosci. Abstr.* **23:** 630.

Hadfield, M. G., and J. T. Pennington. 1990. Nature of the metamorphic signal and its internal transduction in larvae of the nudibranch *Phestilla sibogae*. *Bull. Mar. Sci.* **46:** 455–464.

Huang, S., H. H. Kerschbaum, and A. Hermann. 1998. Nitric oxide-mediated cGMP synthesis in *Helix* neural ganglia. *Brain Res.* **780:** 329–336.

Jacklet, J. W., and M. Gruhn. 1994. Nitric oxide as a putative transmitter in *Aplysia:* neural circuits and membrane effects. *Neth. J. Zool.* **44:** 524–534.

Kempf, S. C., G. V. Chun, and M. G. Hadfield. 1992. An immunocytochemical search for potential neurotransmitters in larvae of *Phestilla sibogae* (Gastropoda, Opisthobranchia). *Comp. Biochem. Physiol. C* **101:** 299–305.

Kempf, S. C., L. R. Page, and A. Pires. 1997. Development of serotonin-like immunoreactivity in the embryos and larvae of nudibranch mollusks with emphasis on the structure and possible function of the apical sensory organ. *J. Comp. Neurol.* **386:** 507–528.

Kuzin, B., I. Roberts, N. Peunova, and G. Enikolopov. 1996. Nitric oxide regulates cell proliferation during *Drosophila* development. *Cell* **87:** 639–649.

Leise, E. M., J. E. Nearhoof, S. J. Froggett, and L. B. Cahoon. 1996. Benthic diatoms induce metamorphosis in larvae of the caenogastropod mollusc *Ilyanassa obsoleta*. *Am. Zool.* **36:** 107A.

Lin, M. -F., and E. M. Leise. 1996a. Gangliogenesis in the prosobranch gastropod *Ilyanassa obsoleta*. *J. Comp. Neurol.* **374:** 180–193.

Lin, M. -F., and E. M. Leise. 1996b. NADPH-Diaphorase activity changes during gangliogenesis and metamorphosis in the gastropod mollusc *Ilyanassa obsoleta*. *J. Comp. Neurol.* **374:** 194–203.

Marois, R., and T. J. Carew. 1997. Ontogeny of serotonergic neurons in *Aplysia californica*. *J. Comp. Neurol.* **386:** 477–490.

Meleshkevitch, E. A., D. Y. Budko, S. W. Norby, L. L. Moroz, and M. G. Hadfield. 1997. Nitric oxide-dependent modulation of the metamorphosis in mollusc *Phestilla sibogae* (Gastropoda, Nudibranchia). *Soc. Neurosci. Abstr.* **23:** 1233.

Moroz, L. L., J. H Park, and W. Winlow. 1993. Nitric oxide activates buccal motor patterns in *Lymnaea stagnalis*. *NeuroReport* **4:** 643–646.

Morse, D. E. 1994. Molecular mechanisms controlling metamorphosis and recruitment in abalone larvae. Pp. 107–119 in *Abalone of the World*, S. A. Shepherd, M. J. Tegner, and S. A. Guzman del Proo, eds. Blackwell, Oxford.

Murad, F., C. Mittal, W. Arnold, S. Katsuki, and H. Kimura. 1978. Guanylate cyclase: activation by azide, nitro compounds, nitric oxide and hydroxyl radical and inhibition by hemoglobin and myoglobin. *Adv. Cyclic Nucleotide Res.* **9:** 145–158.

Pawlik, J. R. 1992. Chemical ecology of the settlement of benthic marine invertebrates. *Oceanogr. Mar. Biol. Annu. Rev.* **30:** 273–335.

Peunova, N., and G. Enikolopov. 1995. Nitric oxide triggers a switch to growth arrest during differentiation of neuronal cells. *Nature* **375:** 68–73.

Pires, A., and M. G. Hadfield. 1993. Responses of isolated vela of nudibranch larvae to inducers of metamorphosis. *J. Exp. Zool.* **266:** 234–239.

Pires, A., J. A Skiendzielewski, and J. V. Mitten. 1996. Depletion of norepinephrine and metamorphosis in a gastropod. *Am. Zool.* **36:** 13A.

Pires, A., S. L. Coon, and M. G. Hadfield. 1997. Catecholamines and dihydroxyphenylalanine in metamorphosing larvae of the nudibranch *Phestilla sibogae* (Gastropoda: Opisthobranchia). *J. Comp. Physiol. A* **181:** 187–194.

Rentería, R. C., and M. Constantine-Paton. 1996. Exogenous nitric oxide causes collapse of retinal ganglion cell axonal growth cones *in vitro*. *J. Neurobiol.* **29:** 415–428.

Riddiford, L. M., and J. W. Truman. 1993. Hormone receptors and the regulation of insect metamorphosis. *Am. Zool.* **33:** 340.

Robertson, J. D., J. Bonaventura, and A. Kohm. 1994. Nitric oxide is required for tactile learning in *Octopus vulgaris*. *Proc. R. Soc. Lond. B.* **256:** 269–273.

Robertson, J. D., J. Bonaventura, and A. Kohm. 1995. Nitric oxide synthase inhibition blocks octopus touch learning without producing sensory or motor dysfunction. *Proc. R. Soc. Lond. B.* **261:** 167–172.

Robertson, J. D., J. Bonaventura, A. Kohm, and M. Hiscat. 1996. Nitric oxide is necessary for visual learning in *Octopus vulgaris*. *Proc. R. Soc. Lond. B* **263:** 1739–1743.

Scholz, N. L., E. S. Chang, K. Graubard, and J. W. Truman. 1998. The NO/cGMP pathway and the development of neural networks in postembryonic lobsters. *J. Neurobiol.* **34:** 208–226.

Sokal, R. R., and F. J. Rolf. 1981. *Biometry.* W. H. Freeman, New York.

Teyke, T. 1996. Nitric oxide, but not serotonin, is involved in acquisition of food-attraction conditioning in the snail *Helix pomatia*. *Neurosci. Lettr.* **206:** 29–32.

Truman, J. W., J. De Vente, and E. E. Ball. 1996. Nitric oxide-sensitive guanylate cyclase activity is associated with the maturational phase of neuronal development in insects. *Development* **122:** 3949–3958.

Woodin, S. A. 1991. Recruitment of infauna: positive or negative cues? *Am. Zool.* **31:** 797–807.

Wu, H. H., C. V. Williams, and S. C. McLoon. 1994. Involvement of nitric oxide in the elimination of a transient retinotectal projection in development. *Science* **265:** 1593–1596.

Zar, J. H. 1974. *Biostatistical Analysis.* Prentice-Hall, Englewood Cliffs, NJ.

Zimmer-Faust, R. K., and M. N. Tamburri. 1994. Chemical identity and ecological implications of a waterborne, larval settlement cue. *Limnol. Oceanogr.* **39:** 1075–1087.

Reference: *Biol. Bull.* **196:** 63–69. (February, 1999)

Developmental Basis of Phenotypic Variation in Egg Production in a Colonial Ascidian: Primary Oocyte Production *Versus* Oocyte Development

J. STEWART-SAVAGE*, BRADLEY J. WAGSTAFF[1], AND PHILIP O. YUND[2]

Department of Biological Sciences, University of New Orleans, New Orleans, Louisiana 70148

Abstract. Colonies of the ascidian *Botryllus schlosseri* (a cyclical hermaphrodite) exhibit extreme variability in egg production, and there is a large genetic component to this phenotypic variation. Therefore, the developmental bases of variation among different genotypes was investigated. Colonies differing in egg production (assayed as number of eggs per asexual bud) were cultured in a common garden experiment, and buds were collected and fixed early in the reproductive cycle. The buds were serially sectioned, and the number and size of the oocytes in the developing ovaries were determined for the different genotypes. Because the buds were collected prior to the onset of vitellogenesis, they contained oocytes at the three previtellogenic stages. In reproductive colonies (>0.7 eggs per bud), there were negative relationships between the final number of eggs per bud and (1) the total number of oocytes present, (2) the number of stage 1 oocytes present, and (3) the number of stage 2 oocytes present. There was no relationship between these parameters in nonreproductive colonies (<0.3 eggs per bud). In contrast, the number of stage 3 oocytes per bud was positively correlated with the final number of eggs per bud in both reproductive and nonreproductive colonies. In reproductive animals there was a negative relationship between the total number of oocytes per bud and the percentage of oocytes at stage 3 in oogenesis. A principal component analysis revealed that a single vector equally weighted for the number of eggs per bud, the total number of oocytes per bud, and the percentage of oocytes at stage 3 accounted for 84% of the observed variation in reproductive colonies. These data indicate that the phenotypic variation in egg production among the *B. schlosseri* colonies in the Damariscotta River, Maine, is controlled by genetic variation in both the number of oocytes that populate developing ovaries, and the percentage of oocytes that reach stage 3 in oogenesis.

Introduction

The production of ova is an exceedingly important aspect of the life-history strategy of any female or hermaphroditic organism. Because egg production is a primary determinant of evolutionary fitness, the mechanisms by which genetic and environmental factors may produce variation in fecundity among individuals must be assessed. Nutritional studies in teleosts and lizards have demonstrated that suboptimal diet reduces the number of ovulated eggs, either by reducing the number of oocytes that enter vitellogenesis, or by increasing oocyte atresia (Mendez-de la Cruz *et al.*, 1993; Tyler and Sumpter, 1996). Although a genetic basis for the variation in female fecundity has been demonstrated in many taxa, analysis of the genetic and developmental mechanisms that produce phenotypic variation in egg production has largely lagged behind (but see Land and Robinson, 1985, for studies in sheep). The genetic and developmental mechanisms controlling egg production in marine invertebrates are unknown and unstudied.

The colonial marine ascidian *Botryllus schlosseri* has characteristics that make it a desirable candidate for an investigation of the developmental mechanisms controlling intraspecific variation in egg production. First, both ovarian development and oocyte maturation occur in a number of repeated cycles, once an animal attains sexual maturity (Milkman, 1967; Sabbadin and Zaniolo, 1979; Manni *et al.*,

---

Received 28 May 1998; accepted 9 November 1998.

* To whom correspondence should be addressed. E-mail: jssavage@uno.edu.

[1] Current Address: Department of Zoology, University of Texas, Austin, TX 78712.

[2] Current Address: School of Marine Science, c/o Darling Marine Center, Walpole, ME 04573.

1994; Yund *et al.*, 1997). Colonies grow by asexual budding, and each developing bud within the colony has the capacity to form a pair of ovaries and testes (though the oogenic potential of buds varies within a colony; Sabbadin and Zaniolo, 1979). Consequently, the number of eggs produced per bud, rather than total colony-wide egg production, is generally used to assay relative female fecundity. Secondly, phenotypic variation in egg production occurs both within and among populations. The population in the Damariscotta River, Maine, exhibits a continuous range of variation, from 0 to 6 eggs per bud (Yund *et al.*, 1997). In contrast, the population in the Eel Pond at Woods Hole, Massachusetts, has a bimodal distribution in egg production, with the low mode at 2 eggs per bud and the high mode at 10 eggs per bud (Grosberg, 1988). Finally, in both populations, phenotypic variation in egg production is known to have both genetic and environmental components (Grosberg, 1988; Yund *et al.*, 1997).

In this report, we examine both ovarian development and oocyte maturation in the population of *B. schlosseri* living in the Damariscotta River. We evaluate three mutually compatible hypotheses for the production of a continuous range of phenotypes in the number of eggs produced per bud: (1) the number of oocytes that populate the developing ovaries within a bud varies by genotype, and a fixed percentage of these oocytes mature; (2) a fixed number of oocytes populate a developing bud, but different percentages of the oocytes mature in different genotypes; (3) a fixed number of oocytes populate a developing bud, and a fixed percentage of them mature, but the number of maturing oocytes that become atretic varies by genotype.

Materials and Methods

Study organism

Colonies of *Botryllus schlosseri* are composed of asexually produced zooids arranged in clusters, or systems, with all zooids in a system sharing a common exhalant siphon. Throughout the life of a colony, all of the zooids undergo a series of synchronous, overlapping sexual and asexual cycles. The asexual zooid replacement cycle starts when a new generation of zooids, called buds, form on the side of existing zooids (Berrill, 1941). After about 14 days of development and growth at 16°C, these buds swell and their inhalant siphons open. As the new zooids take over the function of the previous generation of zooids, which are quickly resorbed, they enter into their sexual cycle. The reproductive cycle includes the internal fertilization of the mature eggs soon after the inhalant siphons open (Milkman, 1967); the continuous release of sperm starting 16 h later (Stewart-Savage and Yund, 1997); and the brooding of the developing embryos, which are released just before the zooids degenerate (Milkman, 1967). *B. schlosseri* colonies can be staged according to their 14-day bud development cycle (Berrill, 1941; Izzard, 1973), or according to their 7-day reproductive cycle (Milkman, 1967). Because the next generation of buds is formed halfway through the bud development cycle, there are always three generations of zooids in a colony. During most of the reproductive cycle these three generations are adult zooid, primary bud, and a younger secondary bud. When the zooids of a new generation open their siphons (stage 0 according to Milkman, 1967), the colony contains degenerating zooids, newly opened zooids (which were primary buds), and primary buds (which were secondary buds).

Colony staging and bud collection

The *B. schlosseri* colonies used in this study were collected from the Damariscotta River, Maine. Animals were grown on glass microscope slides in the flowing seawater system at the University of Maine's Darling Marine Center in a common garden experiment, and thus experienced identical environmental conditions. Colonies were staged according to Milkman's (1967) six-stage reproductive cycle: colonies are at stage 0–1 during the first 24 h after a new generation of zooids open their siphons and at stage 3–4 when the expanding primary buds contain oocytes at the end of vitellogenesis. Over the experimental period, colonies at stage 3–4 were assayed for the number of zooids, the number of primary buds per zooid, and the average number of mature eggs per bud. To assay overall genotypic egg production, the average number of mature eggs per bud was determined by recording the number of eggs per bud in 10 randomly chosen primary buds (Yund *et al.*, 1997). This subsampling technique should minimize the effect of intracolony variation in oogenic potential (Sabbadin and Zaniolo, 1979). When the colonies reached stage 0–1, the area containing the primary buds was collected by making midline cuts through two adjacent zooids and removing the entire tunic between them. For each colony, 10 pieces of tunic from at least two areas of the colony were collected and fixed (see below). The colonies were reassayed when they reached stage 3–4.

The excised buds were fixed in 2% glutaraldehyde in 20 m*M* TRIS-buffered seawater, pH 8.0. After being fixed for at least 24 h, the buds were rinsed in seawater and then in distilled water, and then stained with Harris hematoxylin (Sigma, St. Louis, MO) for 15 min. After a distilled water rinse, the buds were dehydrated and embedded in methacrylate plastic (JB-4, Polysciences, Warrington, PA). Blocks, which contained 3–5 buds from a colony, were serially sectioned at 6 μm. A calibrated reticle at 160× magnification was used to measure the largest diameter of the oocytes within a bud; the size of elliptical oocytes was determined by averaging the two dimensions. For each animal, the total number of oocytes and the number of oocytes at each stage of oogenesis were determined by averaging the data from 6.4 ± 1.9 (X ± SD; range: 4–11) buds.

Because of the tradeoff between sexual reproduction and asexual growth (Yund *et al.*, 1997), the 20 colonies used in this study were all of medium size (110 ± 44 zooids, X ± SD) and had equal rates of asexual growth (1.6 ± 0.2 buds per zooid, X ± SD). To limit the effect of food supply on the number of eggs per bud (Grosberg, 1988; Yund *et al.*, 1997), all samples were collected over an 11-day period (27 June–8 July 1995). Six of the 20 colonies were producing few, if any, eggs. Because colony age and the environment can both affect egg production (Grosberg, 1988; Yund *et al.*, 1997) and we do not know if the lack of egg production in these colonies is the result of genetic factors, environmental factors, or a combination of both, we separated the colonies into "reproductive" (>0.7 eggs per bud) and "nonreproductive" (<0.3 eggs per bud) groups.

Results

Oocyte morphology and staging

The primary buds collected from *B. schlosseri* colonies between stages 0 and 1 in the reproductive cycle described by Milkman (1967) were, based on their histological appearance, at stage 7 according to Izzard's classification (1973). As expected, the ovaries of these developing buds contained only previtellogenic oocytes at three stages (Manni *et al.*, 1994) of oogenesis (Fig. 1). The small stage 1 oocytes (Fig. 1C) can be easily distinguished from the other cells in the developing ovary and from the testes rudiment by their larger size (10–15 μm *versus* 6–8 μm, respectively) and their large and prominent nucleolus. Stage 2 oocytes are characterized by an increase in both cell and nuclear size, and by an increase in the basophilia of the cytoplasm (Fig. 1A, B). Although Manni *et al.* (1994) described stage 2 oocytes as being 40–60 μm, we found definitive stage 2 oocytes that were only 20 μm. Stage 3 oocytes are distinguished from stage 2 oocytes by a further increase in oocyte and nuclear size, by a decrease in cytoplasmic basophilia, and by the presence of a cuboidal follicular layer (Fig. 1A). On the basis of these morphological criteria, stage 3 oocytes ranged in size from 60 to 100 μm. In the 126 buds sectioned, we observed only four atretic stage 3 oocytes (not shown). These oocytes were classified as atretic because test cells had migrated into oocyte cytoplasm, and the oocyte had no germinal vesicle. These four stage 3 oocytes were excluded from the data set.

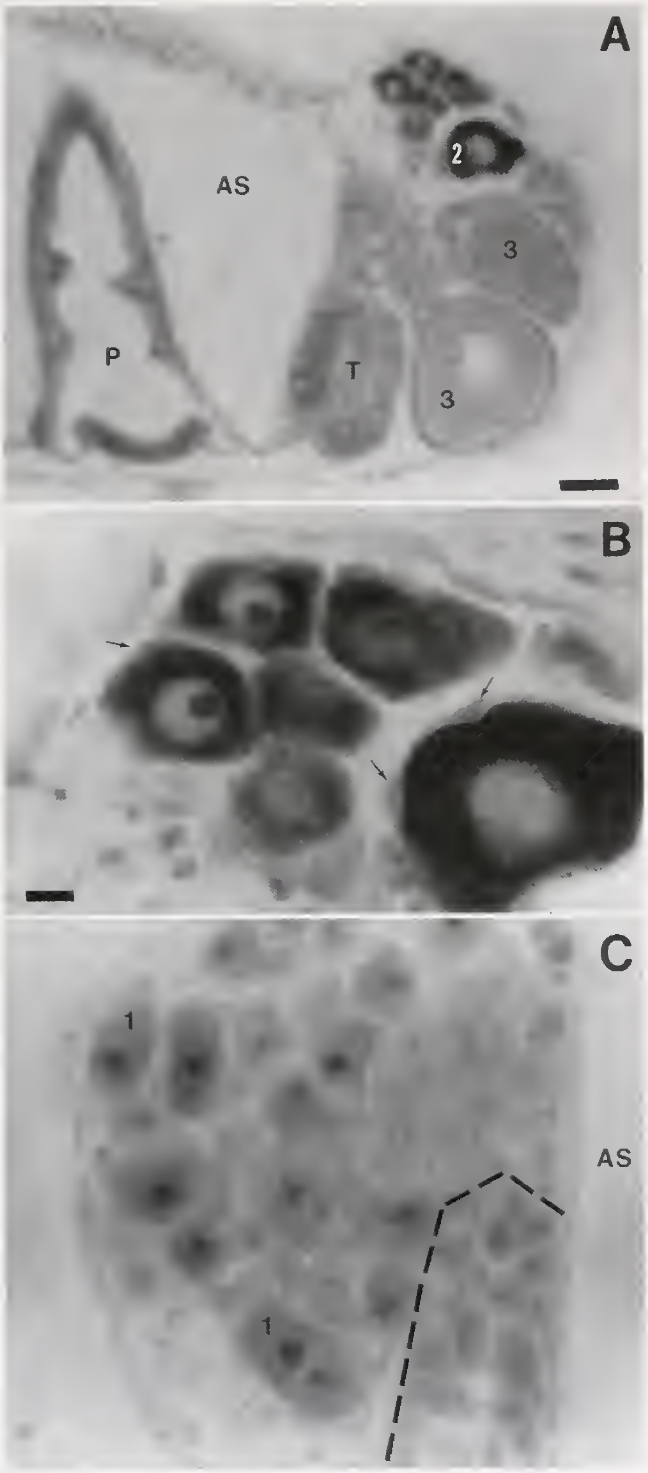

Figure 1. Micrographs of the different stages of oocyte development seen in developing buds of *Botryllus schlosseri* (stage 7 according to Izzard, 1973). See Results for details of oocyte staging. 1–3, stage 1–3 oocytes; AS, antral sac; P, developing pharynx; T, testis rudiment. (A) Cross section of a bud with a developing testes and stage 2 and 3 oocytes. The lightly stained stage 3 oocytes are surrounded by a darker, cuboidal follicular layer. 165×, bar = 50 μm. (B) Higher magnification of stage 2 oocytes shown in A. Small primary follicle cells (arrows) can be seen around each of the six stage 2 oocytes. 650×, bar = 10 μm. (C) Cross section of a bud containing only stage 1 oocytes. Notice the difference in cell size and nucleolar morphology between the stage 1 oocytes and the cells in the developing testes (area within broken line). 650×.

Relationship between oocyte number and stage, and final egg number

As discussed in the Introduction, the average number of eggs produced in each bud (the colony's eggs-per-bud phenotype) may be controlled by the total number of oocytes within each developing bud. In reproductive colonies (>0.7 eggs per bud), the final eggs-per-bud phenotype is negatively related to the total number of oocytes within each bud, whereas in nonreproductive colonies (<0.3 eggs per bud) there is no relationship (Fig. 2A). This relationship indicates that the final number of eggs produced within each bud may be negatively regulated by the number of oocytes that populate the bud, but that the final determination of a colony's eggs-per-bud phenotype must occur during oogenesis.

To determine the stage or stages of oogenesis at which the final eggs-per-bud phenotype is determined, we examined the relationship between the number of oocytes at each stage of oogenesis and the final eggs-per-bud phenotype. In reproductive colonies, there is a negative relationship between the final eggs-per-bud phenotype and both the number of stage 1 and stage 2 oocytes per bud (Fig. 2B and C). In nonreproductive colonies, there is no relationship between the final eggs-per-bud phenotype and the number of stage 1 and 2 oocytes. The number of stage 3 oocytes per bud is positively correlated with the final eggs-per-bud phenotype in both reproductive and nonreproductive colonies (Fig. 2D).

The correlation of a colony's final eggs-per-bud phenotype with both the total number of oocytes in each bud (Fig. 2A) and the number of oocytes at stage 3 in oogenesis (Fig. 2D) indicates that the processes determining these two conditions may be coordinated. To determine the relationship between these processes, we converted the number of stage 3 oocytes per bud to a percentage to remove the negative relationship between the final eggs-per-bud phenotype and the total number of oocytes per bud. The number and percentage of oocytes in a bud at stage 3 in oogenesis are equivalent measures of oocyte maturation ($R = 0.797$). As seen in Figure 3, there is a negative relationship in reproductive colonies between the total number of oocytes per bud and the percentage of those oocytes that have reached stage 3 in oogenesis, whereas there is no relationship in nonreproductive colonies. When both variables are plotted against the final eggs-per-bud phenotype, the data points fall in the vicinity of a line (data not shown). A

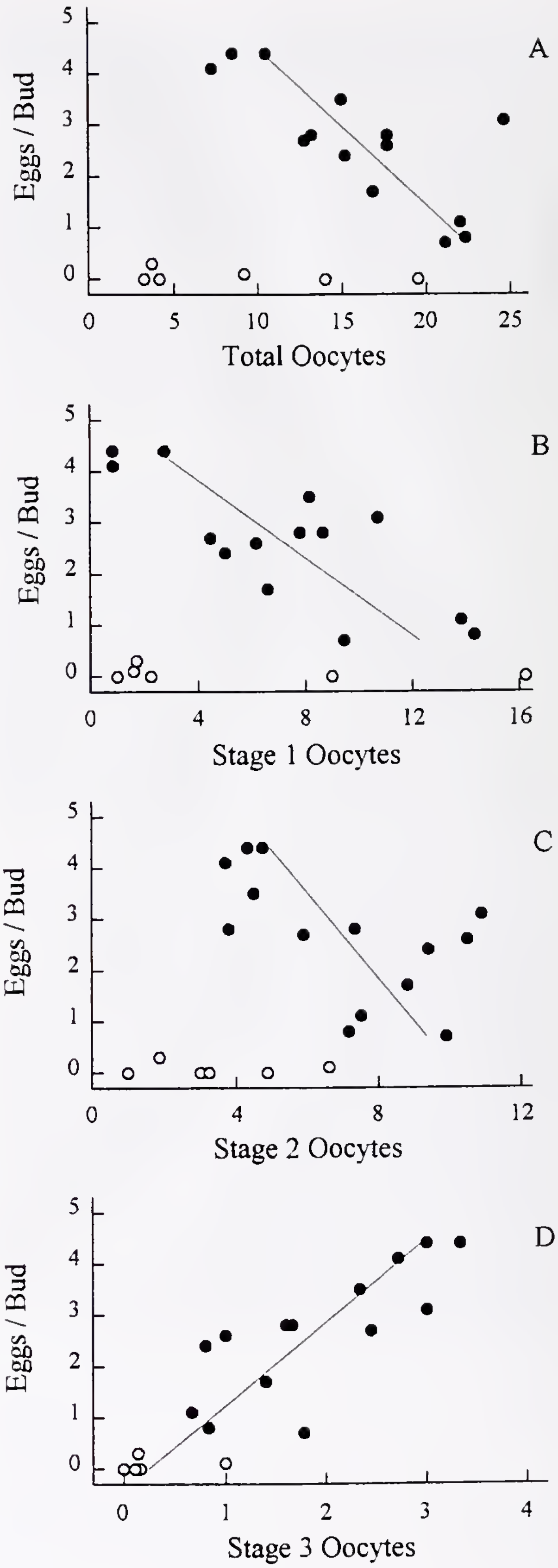

Figure 2. Relationship between the eggs-per-bud phenotype at Milkman stage 3 and the number of oocytes per bud at Milkman stage 0. See Results for details of oocyte staging. ○, nonreproductive colonies (<0.3 eggs per bud); ●, reproductive colonies (>0.7 eggs per bud). Lines are least squares linear regression of reproductive colonies in A–C and all colonies in D; A: $R = 0.756$, B: $R = 0.774$, C: $R = 0.568$, D: $R = 0.780$.

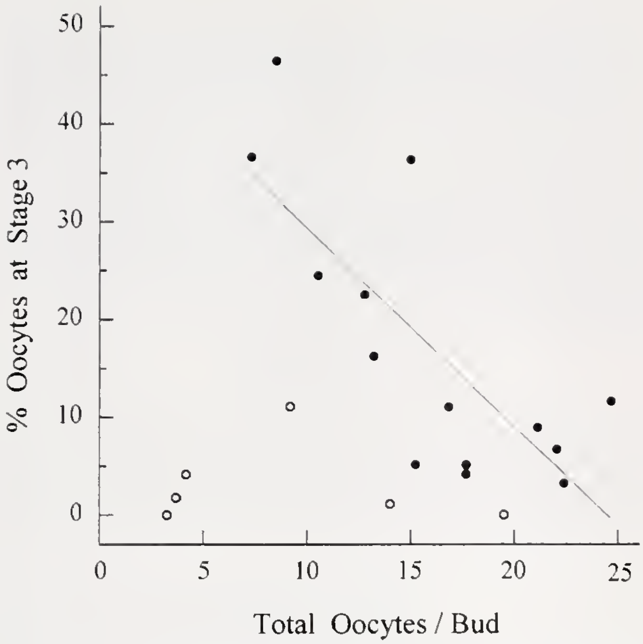

Figure 3. Relationship, at Milkman stage 0, between the total number of oocytes per bud and the percentage of oocytes at stage 3 in oogenesis. Line is least squares linear regression of reproductive colonies ($R = 0.763$). ○, nonreproductive colonies (<0.3 eggs per bud); ●, reproductive colonies (>0.7 eggs per bud).

principal component analysis (Table 1) reveals that a single vector equally weighted for the three variables accounts for 84% of the variation.

Discussion

The strong relationship between a *B. schlosseri* colony's final eggs-per-bud phenotype and both the total number of oocytes that are in the developing ovary and the number of oocytes at stage 3 of oogenesis indicates that two separate mechanisms operate to determine the final number of eggs that a colony produces. In reproductive colonies, a variable number of oocytes populate a developing ovary, a variable percentage of those oocytes reach stage 3 in oogenesis, and the final eggs-per-bud phenotype is determined by the negative relationship between the two. Although the strong relationship between these two variables in reproductive colonies suggests that they may be genetically linked, the data from nonreproductive colonies demonstrate that the control of oogenesis can be uncoupled from the number of oocytes that populate a developing ovary.

Control of the number of oocytes within a developing bud

The development of the ovaries in *B. schlosseri* is not a one-time event, but occurs during each asexual cycle. Studies on the development of buds in *Botryllus* have demonstrated that germ cells are not seen in the developing bud until after it is vascularized (Izzard, 1973; Mukai and Watanabe, 1976; Sabbadin and Zaniolo, 1979; Manni *et al.*, 1995). Histological and genetic data indicate that germ cells do not arise from the bud epithelium but enter the developing bud from the blood. First, cells similar in morphology to stage 1 and stage 2 oocytes have been seen in the peripheral circulation during the time when germ cells start appearing in the developing buds (Izzard, 1968; Mukai and Watanabe, 1976; Sabbadin and Zaniolo, 1979; pers. obs.). Second, the migration of germ cells *via* the vascular system has been demonstrated by genetic assays. When two colonies that were genetically different for either pigment genes (Sabbadin and Zaniolo, 1979) or microsatellites (Pancer *et al.*, 1995) were allowed to become vascularly fused and were then separated, about 50% of the separated colonies produced gonads or offspring containing the same genetic component as the previously fused partner. It may be that the number of migrating germ cells that take up residence within a developing bud is genetically controlled.

In addition to the possibility that germ cell migration is genetically controlled, *B. schlosseri*'s reproductive life-history parameters indicate that mitosis of the germ cells must occur sometime during each bud cycle. As we have shown in this report, colonies that produce about 4 eggs per bud have only about 5–8 oocytes at stage 1 or 2 in each bud. Since *B. schlosseri* colonies produce about the same number of eggs per bud in each cycle (Yund *et al.*, 1997) and reproduce for up to 10 cycles (Grosberg, 1988), mitosis must be occurring within the germ cell population. If the total number of germ cells in a colony were fixed, either egg production would decline with age or the number of reproductive cycles would be low. The above observations indicate that the genetic mechanism that determines the total number of oocytes in each bud may operate by controlling the migration of germ cells into the developing buds, the number of mitotic divisions in the germ cells during each bud cycle, or both.

Table 1

Principal component analysis of the three-way relationship between eggs-per-bud phenotype, total number of oocytes per bud, and percentage of oocytes at stage 3 in oogenesis

	Principal Components		
	PC1	PC2	PC3
Eigenvalue	2.52	0.24	0.24
Percent of variance	84.02	8.14	7.84
Cumulative percent of variance	84.02	92.16	100.00
Eigenvector loadings			
No. Eggs per bud	0.58	0.80	−0.18
No. Oocytes per bud	−0.58	0.56	0.60
% Oocytes at oogenesis stage 3	0.58	−0.24	0.78

Control of oogenesis

Oogenesis in *B. schlosseri* has been divided into five stages by Manni *et al.* (1994), with stages 1–3 being previtellogenic and stages 4–5 being vitellogenic. The nearly 1:1 relationship between the final eggs-per-bud phenotype and the number of stage 3 oocytes (Fig. 2D) indicates that all oocytes that reach stage 3 will continue on to stage 4 and undergo vitellogenesis. This 1:1 relationship also indicates that oocyte atresia after the initiation of vitellogenesis is not a genetic mechanism used to regulate oocyte number in *B. schlosseri.* The number of oocytes that complete oogenesis in *B. schlosseri* is apparently regulated at the transition between stages 2 and 3 of oogenesis, because the ovaries of nonreproductive colonies contain variable numbers of stage 1 and stage 2 oocytes, but few stage 3 oocytes (Fig. 2). Thus, germ cell migration and the early stages of oogenesis are occurring in these nonreproductive colonies, but the oocytes are prevented from entering stage 3 of oogenesis.

Modes of genetic inheritance of fecundity

The genetic control of the number of eggs per bud in *B. schlosseri* colonies shares striking similarities with the genetic control of the number of eggs ovulated by sheep. Populations of both animals exhibit a continuous range of phenotypes, and this phenotypic variation has a large genetic component. In the sheep, increased fecundity is a polygenetic trait in some breeds and the result of a single gene mutation in others. In the two sheep breeds where litter size is polygenetically controlled, the heritability of increased fecundity is about 0.50 (Hanrahan and Quirke, 1985; Mavrogenis, 1985). The heritability of litter size in sheep breeds not selected for increased fecundity has been estimated to be around 0.07 (Bradford, 1985). The heritability of these polygenetically based increases in sheep fecundity is similar to the broad-sense heritability calculated for the eggs-per-bud phenotypes of *B. schlosseri* in the Damariscotta River, Maine (Yund *et al.*, 1997).

Of the two populations of *B. schlosseri* in which the genetic basis of the eggs-per-bud phenotypes has been examined, only the population in Eel Pond at Woods Hole, Massachusetts, has both iteroparous (1–5 eggs per bud, reproduce multiple times) and semelparous (9–14 eggs per bud, die at end of first reproductive cycle) life-history morphs (Grosberg, 1988; pers. obs.). The inheritance of the two life-history morphs may be controlled by a single gene because the number of eggs produced per bud of F_1 progeny from iteroparous and semelparous crosses does not deviate significantly from 1:1 (Grosberg, 1988). The heritability of the iteroparous and semelparous morphs may be related to the single-gene mutations responsible for increased fecundity in two breeds of sheep. Both the X-linked Inverdale gene (Smith *et al.*, 1997) and the Booroola gene (Davis *et al.*, 1982) cause a dose-dependent increase in ovulation rate. The Booroola gene appears to increase ovulation rate by increasing the number of oogonia and primordial follicles in the developing ovary (Smith *et al.*, 1994) and not by elevating hormone levels in the adult (Wheaton *et al.*, 1996). Further work is needed to determine if a homolog of the Booroola or the Inverdale gene is responsible for the iteroparous and semelparous life-history morphs seen in *B. schlosseri.*

Acknowledgments

We thank T. Miller and the staff at the Darling Marine Center for facilitating our work in Maine. Financial support was provided by the National Science Foundation (OCE-94-15548 and OCE-98-96153).

Literature Cited

Berrill, N. J. 1941. The development of the bud in *Botryllus. Biol. Bull.* **80:** 169–184.

Bradford, G. E. 1985. Selection for litter size. Pp. 3–18 in *Genetics of Reproduction in Sheep,* R. B. Land and D. W. Robinson, eds. Garden City Press, Letchworth, England.

Davis, G. H., G. W. Montgomery, A. J. Allison, R. W. Kelly, and A. R. Bray. 1982. Segregation of a major gene influencing fecundity in progeny of Booroola sheep. *N. Z. J. Agric. Res.* **25:** 525–529.

Grosberg, R. K. 1988. Life-history variation within a population of the colonial ascidian *Botryllus schlosseri.* I. The genetic and environmental control of seasonal variation. *Evolution* **42:** 900–920.

Hanrahan, J. P., and J. F. Quirke. 1985. Contribution of variation in ovulation rate and embryo survival to within breed variation in litter size. Pp. 193–201 in *Genetics of Reproduction in Sheep,* R. B. Land and D. W. Robinson, eds. Garden City Press, Letchworth, England.

Izzard, C. S. 1968. Migration of germ cells through successive generations of pallial buds in *Botryllus schlosseri* [abstract]. *Biol. Bull.* **135:** 424.

Izzard, C. S. 1973. Development of polarity and bilateral asymmetry in the pallial bud of *Botryllus schlosseri* (Pallas). *J. Morphol.* **139:** 1–26.

Land, R. B., and D. W. Robinson. 1985. *Genetics of Reproduction in Sheep.* Garden City Press, Letchworth, England.

Manni, L., G. Zaniolo, and P. Burighel. 1994. Ultrastructural study of oogenesis in the compound ascidian *Botryllus schlosseri* (Tunicata). *Acta Zool.* **75:** 101–113.

Manni, L., G. Zaniolo, and P. Burighel. 1995. Oogenesis and oocyte envelope differentiation in the viviparous ascidian *Botrylloides violaceus. Invertebr. Reprod. Dev.* **27:** 167–180.

Mavrogenis, A. P. 1985. The fecundity of the chios sheep. Pp. 63–67 in *Genetics of Reproduction in Sheep,* R. B. Land and D. W. Robinson, eds. Garden City Press, Letchworth, England.

Mendez-de la Cruz, F. R., L. J. Guillette, Jr., and M. Villagran-Santa Cruz. 1993. Differential atresia of ovarian follicles and its effect on the clutch size of two populations of the viviparous lizard *Sceloporus mucronatus. Funct. Ecol.* **7:** 535–540.

Milkman, R. 1967. Genetic and developmental studies on *Botryllus schlosseri. Biol. Bull.* **132:** 229–243.

Mukai, H., and H. Watanabe. 1976. Studies on the formation of germ cells in a compound ascidian, *Botryllus primigenus* Oka. *J. Morphol.* **148:** 337–362.

Pancer, Z., H. Gershon, and B. Rinkevich. 1995. Coexistence and possible parasitism of somatic and germ cell lines in chimeras of the colonial urochordate *Botryllus schlosseri*. *Biol. Bull.* **189:** 106–112.

Sabbadin, A., and G. Zaniolo. 1979. Sexual differentiation and germ cell transfer in the colonial ascidian *Botryllus schlosseri*. *J. Exp. Zool.* **207:** 289–304.

Smith, P., R. Braw-Tal, K. A. Corrigan, N. L. Hudson, D. A. Heath, and K. P. McNatty. 1994. Ontogeny of ovarian follicle development in Booroola sheep features that are homozygous carriers or non-carriers of the FecB gene. *J. Reprod. Fertil.* **100:** 485–490.

Smith, P., W-S. O, K. A. Corrigan, T. Smith, T. Lundy, G. H. Davis, and K. P. McNatty. 1997. Ovarian morphology and endocrine characteristics of female sheep fetuses that are heterozygous or homozygous for the Inverdale prolificacy gene (fecX^I). *Biol. Reprod.* **57:** 1183–1192.

Stewart-Savage, J., and P. O. Yund. 1997. Temporal pattern of sperm release from the colonial ascidian, *Botryllus schlosseri*. *J. Exp. Zool.* **279:** 620–625.

Tyler, C. R., and J. P. Sumpter. 1996. Oocyte growth and development in teleosts. *Rev. Fish Biol. Fish.* **6:** 287–318.

Wheaton, J. E., D. L. Thomas, N. T. Kusina, R. G. Gottfredson, and R. L. Meyer. 1996. Effects of passive immunization against inhibin-peptide on secretion of follicle-stimulating hormone and ovulation rate in ewes carrying the Booroola fecundity gene. *Biol. Reprod.* **55:** 1351–1355.

Yund, P. O., Y. Marcum, and J. Stewart-Savage. 1997. Life-history variation in a colonial ascidian: broad-sense heritabilities and tradeoffs between growth and allocation to male and female reproduction. *Biol. Bull.* **192:** 290–299.

Reference: *Biol. Bull.* **196:** 70–79. (February, 1999)

Late Larval Development and Onset of Symbiosis in the Scleractinian Coral *Fungia scutaria*

JODI A. SCHWARZ[1], DAVE A. KRUPP[2], AND VIRGINIA M. WEIS[1,*]

[1] *Department of Zoology, Oregon State University, Corvallis, Oregon 97331, and*
[2] *Department of Natural Sciences, Windward Community College, Kaneohe, Hawaii 96744*

Abstract. Many corals that harbor symbiotic algae (zooxanthellae) produce offspring that initially lack zooxanthellae. This study examined late larval development and the acquisition of zooxanthellae in the scleractinian coral *Fungia scutaria,* which produces planula larvae that lack zooxanthellae. Larvae reared under laboratory conditions developed the ability to feed 3 days after fertilization; feeding behavior was stimulated by homogenized *Artemia.* Larvae began to settle and metamorphose 5 days after fertilization. In laboratory experiments, larvae acquired experimentally added zooxanthellae by ingesting them while feeding. Zooxanthellae entered the gastric cavity and were phagocytosed by endodermal cells. As early as 1 h after feeding, zooxanthellae were observed in both endodermal and ectodermal cells. Larvae were able to form an association with three genetically distinct strains of zooxanthellae. Both zooxanthellate and azooxanthellate larvae underwent metamorphosis, and azooxanthellate polyps were able to acquire zooxanthellae from the environment. Preliminary evidence suggests that the onset of symbiosis may influence larval development; in one study symbiotic larvae settled earlier than aposymbiotic larvae. Protein profiles of eggs and larvae throughout development revealed a putative yolk protein doublet that was abundant in eggs and 1-day-old larvae and was absent by day 6. This study is the first to examine the onset of symbiosis between a motile cnidarian host and its algal symbiont.

Introduction

The life history of symbiotic associations between organisms necessarily includes a stage during which a new generation of hosts first acquires its symbionts (Douglas, 1994). Symbionts may be acquired either vertically, whereby the symbiont is transmitted directly from parent to offspring, or horizontally, whereby the offspring must acquire symbionts from the environment (Trench, 1987). Vertical transmission ensures that offspring are provided with a complement of symbionts, whereas horizontal transmission is more uncertain; environmental variability may prevent contact between symbiont and host, resulting in the failure of the host to become infected by its symbiont.

Many members of the phylum Cnidaria (such as corals, sea anemones, and jellyfish) harbor intracellular photosynthetic dinoflagellates (*Symbiodinium* spp.) in a mutually beneficial symbiotic association. The dinoflagellates, also known as zooxanthellae, contribute to host nutrition by translocating photosynthetically fixed carbon, while the hosts provide the zooxanthellae with nutrients and a protected, high-light environment. Many cnidarian host species are obligately symbiotic with zooxanthellae, thus vertical transmission might be predicted to be the dominant mode of symbiont transmission. However, this is not the case, at least in scleractinian corals. Most scleractinian coral species spawn gametes that are azooxanthellate (*i.e.,* lack zooxanthellae) (Fadlallah, 1983; Babcock and Heyward, 1986; Harrison and Wallace, 1990; Richmond and Hunter, 1990; Richmond, 1997). The gametes are fertilized within the water column and develop into azooxanthellate planula larvae that must acquire zooxanthellae at some stage of their development (Trench, 1987).

Offsetting the uncertainty of infection *via* horizontal transmission is the benefit that acquisition of symbionts from the environment might allow the host to form an association with genetically distinct symbionts that are adapted to local conditions. Rowan and Knowlton (1995) found that the corals *Montastraea faveolata* and *M. annu-*

Received 30 April 1998; accepted 25 September 1998.

* To whom correspondence should be addressed. E-mail: weisv@bcc.orst.edu

laris naturally associate with several species of *Symbiodinium* that occur along an environmental gradient, and that hosts can contain two species at one time. Many studies have compared the uptake and influence of heterologous and homologous zooxanthellae on experimentally infected cnidarian host polyps (literature summarized most recently in Davy *et al.*, 1997). Thus although vertical transmission ensures that offspring are provided with zooxanthellae, horizontal transmission may allow for the acquisition of symbionts that are adapted to the specific environment in which the offspring ultimately settle.

There are several mechanisms by which initially azooxanthellate cnidarian hosts may acquire their algal symbionts from the environment and incorporate them into endodermal cells, where they ultimately reside. First, zooxanthellae may be incorporated into the embryo. Second, zooxanthellae may be incorporated into the host's ectoderm and then migrate into the endoderm. Both these mechanisms occur in the scyphozoan *Linuche unguiculata*; both embryos and young, nonfeeding planulae are capable of becoming infected by experimentally added zooxanthellae (Montgomery and Kremer, 1995). Third, zooxanthellae may be incorporated directly into endodermal cells, as was first described in scyphistomae (post-planula polyps) of *Cassiopeia xamachana* (Trench, 1980; Fitt and Trench, 1983a, b). In this third mode of infection, symbionts enter through the mouth of the host and are phagocytosed by endodermal cells lining the gastric cavity (Colley and Trench, 1983; Fitt and Trench, 1983a, b).

Although many studies have either documented in detail or anecdotally noted zooxanthella acquisition by naturally azooxanthellate polyps (scyphozoans: Sugiura, 1964; Trench, 1980; Colley and Trench, 1983; Fitt and Trench, 1983a, b; anthozoans: Kinzie, 1974; Babcock and Heyward, 1986; Benayahu *et al.*, 1989), little information exists about either the life-history events or the mechanisms of infection associated with the onset of symbiosis in initially azooxanthellate planulae. Montgomery and Kremer (1995) found that young planulae of the scyphozoan *Linuche unguiculata* became infected (by an unknown mechanism) by experimentally added zooxanthellae. Schwarz (1996) found that planulae of the temperate sea anemone *Anthopleura elegantissima* acquired zooxanthellae *via* phagocytosis after feeding on animal tissue that contained zooxanthellae recently isolated from a previous host.

Given that most scleractinian corals produce azooxanthellate planulae, it is likely that at least some acquire zooxanthellae during the planula stage. Planulae are motile and represent the dispersal stage of corals; the acquisition of symbionts during this stage might therefore be advantageous because it presents an opportunity for the planulae to acquire symbionts adapted to the environment in which the larval hosts will settle live.

In this study we examined the process of symbiont acquisition in the scleractinian coral *Fungia scutaria*. This solitary coral is gonochoric, and the females spawn azooxanthellate eggs that are fertilized within the water column and develop into azooxanthellate larvae (Krupp, 1983). Krupp reported on the early development of this species and observed that larvae reared in aquaria with adult corals acquired zooxanthellae 4 to 5 days after spawning. He observed a "mouth opening" response to the addition of zooxanthellae obtained from homogenized tissues of adult *F. scutaria*, but did not observe zooxanthellae entering the mouths of the larvae. In this paper we describe late larval development and the process of symbiont acquisition (infection) in *F. scutaria*, including the developmental stages at which the host is competent to become infected by zooxanthellae, the mechanisms by which the zooxanthella are acquired and incorporated into host tissue, the effect of feeding behavior on the infection rate, the specificity of the host-symbiont relationship, and the protein profiles of azooxanthellate and zooxanthellate larvae through development.

Materials and Methods

Gamete collection and larval cultures

About 75 adult specimens of *Fungia scutaria* are maintained year-round in running seawater tables at the Hawaii Institute of Marine Biology on Coconut Island, Kaneohe Bay, Hawaii. For our experiments, the corals were rinsed with seawater and placed in standing seawater in individual glass finger bowls. Filtered (0.45 μm) seawater was used for all cultures. This species generally spawns between 1700 and 1900 h, 2–4 days after the full moon during June through August. In August 1995, August 1996, and June and July 1997, eggs were collected by removing the adults from the finger bowls and leaving the eggs in the bowl into which they were spawned. If the egg density was greater than a single layer of eggs at the bottom of the dish, some of the eggs were collected with a turkey baster and transferred to a new finger bowl. Within 30 min after spawning, water from the dishes of all spawning males was combined and a small volume was gently pipetted into the dishes containing eggs. The dishes were left in a seawater table overnight for fertilization and early larval development. The following day, the water was changed. Larvae from all parental crosses were combined, and the larvae were maintained in large glass finger bowls in filtered seawater, which was changed every day.

Preparation of zooxanthella isolates

Zooxanthellae were isolated from adult specimens of *F. scutaria* by using the spray from an oral hygiene device (Water Pik) to remove and homogenize coral tissue; they were then concentrated using a tabletop centrifuge at

2000 × *g*. The zooxanthella pellet was rinsed twice in filtered seawater to partially clean it of animal tissue and was again concentrated by centrifugation. Zooxanthella isolates were used within 2 h of preparation. The same methods were used to isolate zooxanthellae from the sea anemone *Aiptasia pallida*, except that whole animals were homogenized in a ground-glass tissue grinder.

Preparation of homogenized Artemia *sp.*

To stimulate feeding behavior in larvae, homogenized *Artemia* sp. (brine shrimp) was added to larval cultures. A small pinch of frozen *Artemia* was homogenized in a ground-glass tissue grinder in about 1 ml of seawater and filtered through a 60-μm mesh to remove large particulate matter. The resulting slurry was used within 15 min of preparation.

Acquisition of zooxanthellae

To identify (a) the developmental stages at which *F. scutaria* is competent to become infected and (b) the mechanisms of zooxanthella acquisition, larvae from four stages of development (Table 1) were exposed to zooxanthellae from different sources, with or without homogenized *Artemia* (a feeding stimulant). Homologous algae were freshly isolated from adult *F. scutaria*, and heterologous algae were either freshly isolated from the sea anemone *Aiptasia pallida* or taken from algal cultures originating from the jellyfish *Cassiopeia xamachana*. Three replicates were established for all treatments. Larvae were concentrated in glass finger bowls ($>10^4$ larvae per bowl), and an even layer of zooxanthellae was pipetted along the bottom of the bowls. Several drops of homogenized *Artemia* were added to the appropriate treatments. Zooxanthellae and *Artemia* slurry were removed either 4 or 24 h later (Table 1) by concentrating larvae on a filter and placing them into clean filtered seawater. Some larvae from each treatment were observed under a compound microscope, either immediately after zooxanthellae were removed or 24 h later, to determine if they had become infected with zooxanthellae.

For treatments C1 and C2 (Table 1), we used the following method to determine the fraction of larvae that became infected. Twenty-four h after the larvae were exposed to zooxanthellae, the water in the larval cultures was swirled and one aliquot was removed from each replicate. Between 25 and 56 larvae per aliquot were examined under a compound microscope to count how many contained zooxanthellae.

Larval development

To observe and quantify the developmental progression of both azooxanthellate and zooxanthellate larvae, six replicate cultures of each were maintained in plastic 6-well culture dishes (300–500 larvae per well in 5 ml of filtered seawater). Water was changed roughly once a day. Larval development was monitored for about 2 weeks. Each replicate well was placed haphazardly under a dissecting microscope, and within the field of view, the number of larvae at each developmental stage was counted.

Electron microscopy

To follow the process of zooxanthella incorporation into host tissue, larvae from treatment C2 were sampled and fixed for electron microscopy 1 and 24 h after zooxanthellae were added to larval cultures. The larvae were placed in sampling cups, which were prepared by cutting off the bottoms of microfuge tubes and affixing 50-μm mesh across the bottom. The cups were placed in 1% glutaraldehyde in phosphate-buffered saline (PBS, 0.1 *M* sodium phosphate, 0.45 *M* sodium chloride, pH 7.2) for 1 h; rinsed 3 × 10 min in PBS; postfixed for 1 h in 1% osmium tetroxide in PBS; rinsed 3 × 10 min in PBS; and dehydrated for 15 min each in 30%, 50%, and 70% ethanol, and then 1 h each in 80%, 95%, and 3 × 100% ethanol. Samples for scanning electron microscopy were dried for 15 min in hexamethyldisilane,

Table 1

Experimental treatments of Fungia scutaria *larvae*

Treatment: Developmental stage	Source of Algae	*Artemia* added?	Exposure duration	Infection determined
A: embryo-early planula (0–12 h old)	*F. scutaria*	no	overnight	immediately
B: early planula (1–2 days old)	*F. scutaria*	no	overnight	immediately
C1: fully developed planula (3 days old)*	*F. scutaria*	no	4 h	after 24 h
C2: fully developed planula (3 days old)*		yes	4 h	after 24 h
D1: fully developed planula (3 days old)*	*A. pallida*	no	4 h	after 24 h
D2: fully developed planula (3 days old)*		yes	4 h	after 24 h
E1: fully developed planula (3 days old)*	*C. xamachana*	no	4 h	after 24 h
E2: fully developed planula (3 days old)*		yes	4 h	after 24 h
F: polyp (after metamorphosis)	*F. scutaria*	no	overnight	after 24 h

* Planulae were considered fully developed once they had acquired the ability to feed.

mounted on stubs, coated with 60:40 Au:Pd, and viewed on an Amray 3300FE scanning electron microscope. Samples for transmission electron microscopy were infiltrated with Spurr's resin in 1:1 ethanol:resin for 2.5 h, 1:3 mix for 2.5 h, 2 × 100% resin for 1 h, and 100% resin overnight at 60°C. Thin sections were prepared on an ultramicrotome, stained with uranyl acetate and lead citrate, and viewed on a Philips CM12 transmission electron microscope.

Polyacrylamide gel electrophoresis

We prepared one-dimensional SDS-PAGE protein profiles of both azooxanthellate and zooxanthellate larvae through development (eggs through 6-day-old larvae). For each sample, about 1000 larvae were counted, collected by centrifugation, and frozen at −80°C. Protein extracts were prepared by homogenizing frozen larvae over ice in a ground-glass grinder in 100 μl of homogenization buffer (40 m*M* Tris-HCl, 10 m*M* EDTA, protease inhibitor cocktail (Sigma), pH 7.4). Homogenates were centrifuged for 10 min at 14,000 × *g* to pellet zooxanthellae and animal debris. The protein concentration of the supernatant was determined spectrophotometrically (Bradford, 1976): larvae contained approximately 50–100 ng protein/larva. Larval proteins were resolved on 12.5% SDS-PAGE gels under reducing conditions (methods modified from Laemmli, 1970). Gels were silver stained (methods modified from Heukeshoven and Dernick, 1986) and scanned on an Imagemaster desktop scanner (Pharmacia) and analyzed using Imagemaster software (Pharmacia).

Results

Larval development

Larval development was observed over three summers (1994, 1996, 1997). Larvae from all years followed the same progression of developmental stages, as illustrated in Figure 1A and detailed below in Figure 2, progressing from swimming to creeping to settled. The duration of each developmental stage, however, was variable; for the later stages it differed by up to several days both within and among replicates. Figure 1B shows the time course of developmental events for zooxanthellate larvae from 1996.

All larvae progressed through the following series of stages. Within 12 h after fertilization, slowly moving, ciliated spherical planulae developed; within 24 h, barrel-shaped planulae, roughly 100 μm in length (shown in Fig. 2A), had developed and were actively swimming at all depths in the culture dishes. By day 3, larvae had fully formed mouths and functional gastric cavities, and were capable of feeding. Upon addition of food (homogenized *Artemia*), larvae ceased swimming and dropped to the bottom of the dish. They extruded mucus, their oral ends expanded, and they ingested whatever they landed on, including experimentally added zooxanthellae. As they fed, their gastric cavities became filled with particulate matter (Fig. 2B). Some larvae resumed swimming while trailing a strand of mucus; the mucus trapped particulate matter that slowly entered the mouth. Larvae continued to feed for several hours and then resumed swimming. Except for

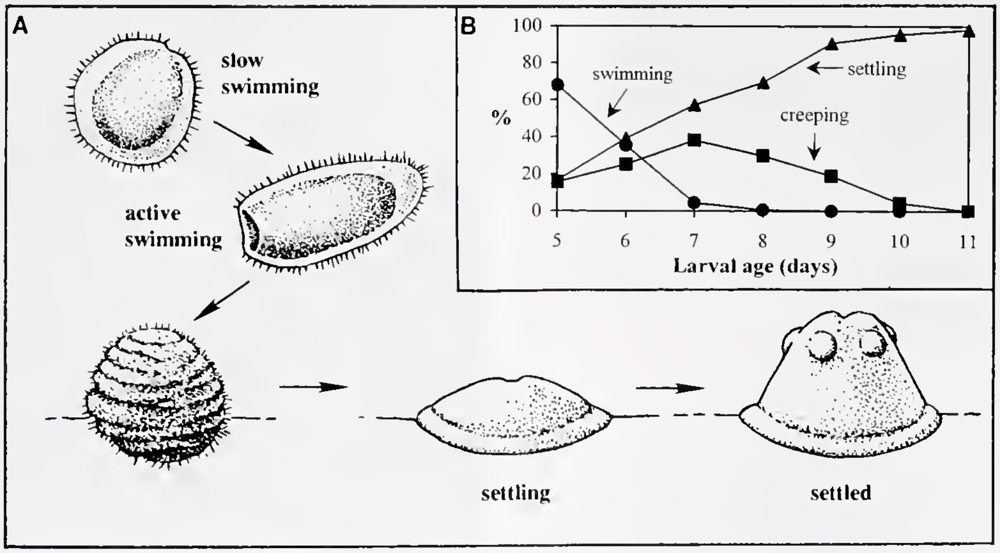

Figure 1. Progression of developmental events in *Fungia scutaria* larvae. (A) Schematic representation of developmental stages from the early planula through metamorphosed polyp. (B) Example of the time course of developmental events. Data shown are from zooxanthellate larvae in 1996. Larvae were infected with zooxanthellae on day 3 and then divided into six replicate dishes, which were monitored daily. Each point represents data pooled from the six replicates. Larvae progressed from swimming to creeping to settling.

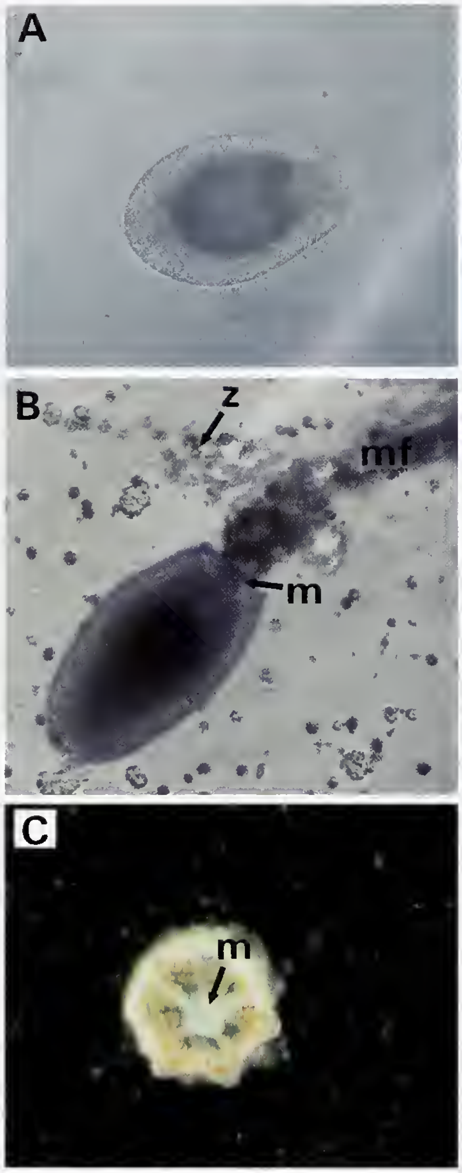

Figure 2. Light micrographs of stages in the development of *Fungia scutaria* larvae. (A) Two-day-old planula larva, prior to development of a mouth. (B) Three-day-old feeding planula (m = mouth, mf = mucous strand with food particles attached, z = zooxanthella). (C) Polyp with tentacles, 6 days after settling. Zooxanthellae are visible as golden spheres. Planula length and polyp diameter, approximately 100 μm.

zooxanthellae, all ingested particulate matter was digested or expelled by the following day. When larvae were about 4 days old, they assumed a ball shape, ceased active swimming, and began creeping slowly over the substrate. Starting on day 5, the ball-shaped larvae began to settle. They spread out over the substrate and metamorphosed into volcano-shaped polyps, which began to develop tentacle buds several days after metamorphosis (Fig. 2C).

Acquisition of zooxanthellae and onset of symbiosis

Prior to the development of a functional mouth on day 3, planulae of *F. scutaria* did not become infected by experimentally added zooxanthellae. Once the mouth was functional, however, the planulae were able to acquire zooxanthellae. When stimulated to feed, larvae indiscriminately ingested any particulate matter, including experimentally added zooxanthellae. Zooxanthellae either were ingested as part of a larger mass that was fully engulfed by the mouth, or they adhered to mucous strands that were ingested by the larvae. Figure 3A shows a zooxanthella adhered to a larval mucous strand, and Figure 3B shows several zooxanthellae surrounding and contained within the oral cavity of a larva. One hour after zooxanthellae were added, larvae were sampled and fixed for transmission electron microscopy. Figure 4 shows a representative planula 1 h postfeeding, in longitudinal section, with several algae resident in endodermal

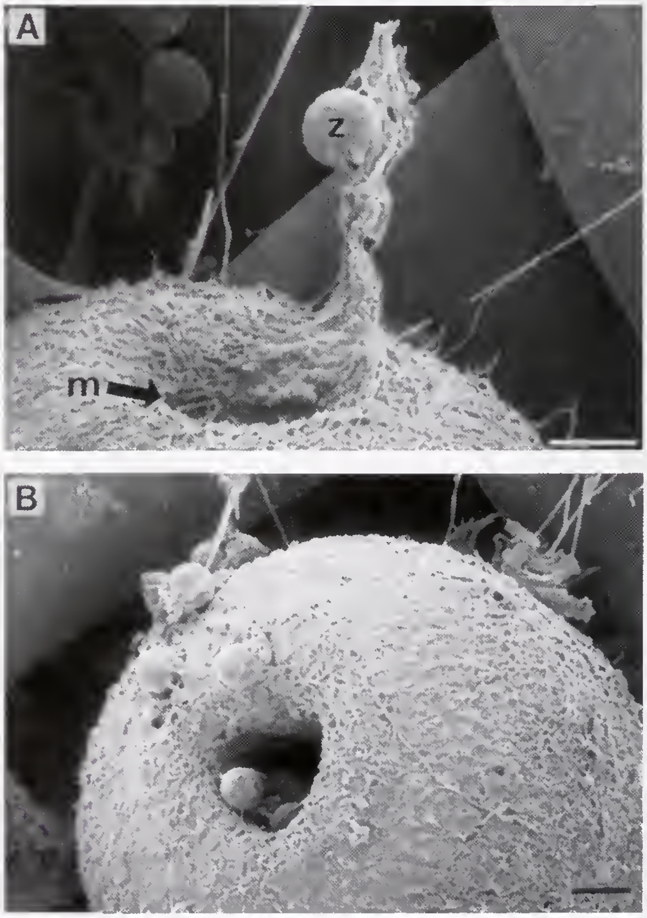

Figure 3. Scanning electron micrographs detailing zooxanthella acquisition by 3-day-old *Fungia scutaria* planulae. (A) Feeding planula with zooxanthella adhered to mucous strand (m = mouth, z = zooxanthella). (B) Feeding planula, with multiple zooxanthellae entering the mouth. Larvae were fixed for electron microscopy 1 h after exposure to zooxanthella isolates and homogenized *Artemia* (see Methods). Bars = 10 μm.

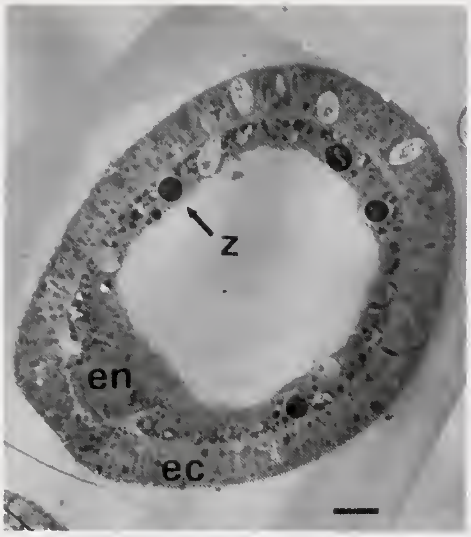

Figure 4. Transmission electron micrograph of a longitudinal section through a *Fungia scutaria* larva infected with zooxanthellae. Thickened oral end at lower left. Zooxanthellae appear in the endoderm as dark spheres. Light ellipses, mostly in the ectoderm, are poorly preserved nematocysts. ec = ectoderm, en = endoderm, z = zooxanthella. Bar = 20 μm.

cells. Micrographs suggest that zooxanthellae are phagocytosed by endodermal cells lining the coelenteron (Fig. 5A, B) and appear in both endodermal (Fig. 5C) and ectodermal tissue (Fig. 5D). Although zooxanthellae were still present in ectoderm 24 h later, we did not determine how long zooxanthellae remained within the ectoderm or whether they eventually migrated into the endoderm or were digested or expelled from the host.

Larvae were not limited to forming an association with a specific strain of zooxanthellae; planulae were capable of becoming infected by zooxanthellae isolated from *F. scutaria* (Treatment C2) and *Aiptasia pallida* (Treatment D2), as well as by cultured zooxanthellae from *Cassiopeia xamachana* (Treatment E2) (see Table 1). To determine whether the host had retained zooxanthellae, larvae from Treatments C2 and D2 were observed over a period of 10 to 14 days. Larvae that had acquired zooxanthellae on day 3 remained infected as they progressed through development and metamorphosis into polyps.

Infection by zooxanthellae was not required for metamorphosis: both zooxanthellate and azooxanthellate larvae successfully settled and metamorphosed into polyps (Fig. 6). Larvae infected with zooxanthellae from *F. scutaria* (Treatment C2) and *A. pallida* (Treatment D2) both underwent metamorphosis (we did not monitor settlement for larvae infected with zooxanthellae cultured from *C. xamachana*). Aposymbiotic polyps were able to ingest experimentally added zooxanthellae *via* ciliary currents produced by the polyps that swept particulate matter, including zooxanthellae, over and into their mouths. Observations over the 6 days following showed that the zooxanthellae were retained within the polyps throughout this period.

The proportion of larvae that became infected by zooxanthellae isolated from adult *F. scutaria* (Treatment C) depended on the strength of the feeding response. Feeding was observed to be strongly stimulated (*i.e.*, virtually all larvae began to feed) by the addition of homogenized *Artemia*, but was also stimulated to a lesser extent (*i.e.*, some larvae began to feed) simply by the addition of zooxanthella-isolates, which contained residual animal host tissue. We quantified the effect of larval feeding strength on zooxanthella acquisition for treatments C1 (zooxanthellae alone) and C2 (zooxanthellae and *Artemia*). In the zooxanthellae alone treatment, 25.0% ± 0.02% ($n = 2$) of larvae acquired zooxanthellae, whereas 96.8% ± 0.01% ($n = 2$) became infected when exposed to both zooxanthellae and *Artemia*. It was clear that larvae in Treatments D and E also became infected at a higher rate when exposed to both zooxanthellae and homogenized *Artemia* than to zooxanthellae alone, although the results were not quantified.

An experiment in 1996 provided preliminary evidence that symbiotic state may influence developmental events in *F. scutaria*. Zooxanthellate larvae settled and metamorphosed earlier than azooxanthellate larvae, most of which became arrested in the "ball stage" and then eventually died (Fig. 7). However, the same experiment repeated in 1997 showed low rates of metamorphosis for both zooxanthellate and azooxanthellate larvae and no difference in the timing of metamorphosis.

Larval protein profiles

Protein profiles of larvae through development showed changes with the age of the larvae. Two bands, at 84 and 79 kilodaltons (kDa), were abundant in eggs and 1-day-old larvae (Fig. 8A). As shown in Figure 8B, this protein doublet comprised a significant proportion (36%) of total protein in 1-day-old larvae, but was almost absent by day 6. The apparent depletion of this protein corresponds to the onset of settlement and metamorphosis. The abundance of the putative yolk protein did not differ between 6-day-old azooxanthellate and zooxanthellate larvae.

Discussion

Larval development and acquisition of zooxanthellae

Development in *Fungia scutaria* was similar to that reported in other broadcast-spawning species of coral (Babcock and Heyward, 1986; review in Harrison and Wallace, 1990). Planula larvae had fully developed within 24 h after fertilization, which is within the range of one to several days reported for other species. Larvae of *F. scutaria* were about 100 μm long, ciliated, and barrel-shaped; they exhibited active swimming behavior until they settled at an age of 5

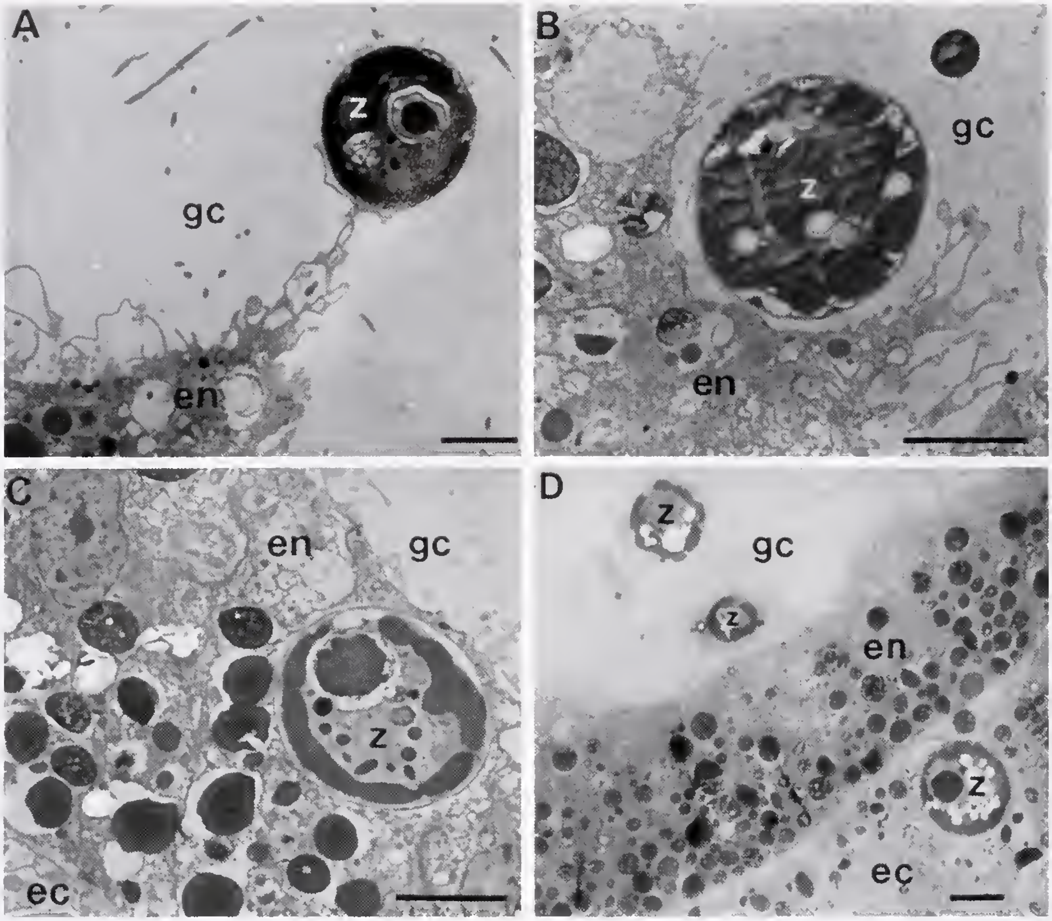

Figure 5. Transmission electron micrographs of onset of symbiosis between *Fungia scutaria* planulae and zooxanthellae. (A) Section through endoderm and gastric cavity of a planula showing initial contact between an endodermal cell and a zooxanthella. Host endodermal membranes are very closely associated with the alga. (B) Endodermal cell partially surrounding a zooxanthella, suggesting that the alga is being ingested by the host cell. (C) Zooxanthella resident within a vacuole in an endodermal cell. (D) Two zooxanthellae in gastric cavity (one is being phagocytosed) and one resident within a vacuole in an ectodermal cell. gc = gastric cavity ec = ectoderm, en = endoderm, z = zooxanthella. Bars = 5 μm.

days to approximately 2 weeks. This appearance and behavior is typical for externally developed planula larvae.

Very little is known about the feeding ability or behavior of coral planulae. Although it appears that many species, particularly brooding species, produce a nonfeeding larva, the ability to feed has probably gone unrecognized in some species because rearing techniques generally do not expose larvae to a source of particulate food. We found that the feeding behavior of *F. scutaria* was very similar to that reported for the temperate coral *Caryophyllia smithi* (Tranter *et al.*, 1982) and for the temperate sea anemones *Anthopleura elegantissima* and *A. xanthogrammica* (Siebert, 1974; Schwarz, 1996). Feeding consisted of a mouth-opening response to the addition of ground animal tissue, as well as secretion of mucous strands that trapped particulate matter for ingestion.

Although most scleractinian coral species spawn azooxanthellate gametes that develop into azooxanthellate planulae (review in Richmond, 1997), little is known about how planulae might acquire zooxanthellae from the environment. The results of this study support the idea that for corals, competency for infection by zooxanthellae may generally depend on the development of a functional mouth. We found that *F. scutaria* did not become infected by experimentally added zooxanthellae until after a mouth developed. Once the mouth was functional, all developmental stages were competent to become infected. Reports of infection events in other species support this hypothesis—species that are infected at the polyp stage appear to have a nonfeeding planula that does not develop a mouth until the polyp stage (Kinzie, 1974; Babcock and Heyward, 1986; Benayahu *et al.*, 1989). Studies of the feeding behavior of planulae also support this hypothesis: planulae of both *F. scutaria* (this study) and *A. elegantissima* (Schwarz, 1996)

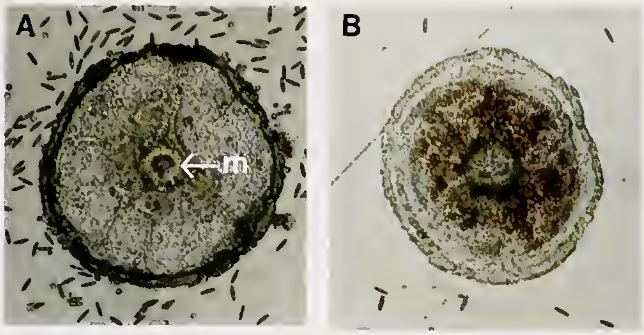

Figure 6. Light micrographs of newly settled polyps of *Fungia scutaria*. (A) Azooxanthellate polyp (m = mouth). (B) Zooxanthellate polyp. Zooxanthellae appear as brown spheres in the polyp. The two polyps shown in this figure were settled in the same dish, adjacent to one another. Contaminating diatoms appear as small ellipses around the polyps. Polyp diameter = 100 μm.

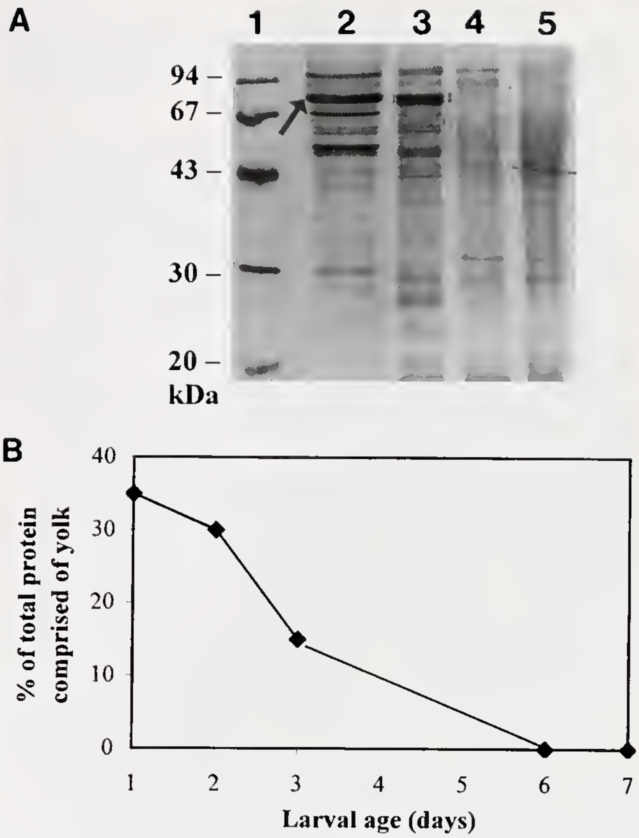

Figure 8. Protein profiles and abundance of putative yolk protein in *Fungia scutaria* larvae. (A) Silver-stained 1D SDS-polyacrylamide gel of total protein extracted from eggs (lane 2), 1-day-old larvae (lane 3), 6-day-old azooxanthellate larvae (lane 4), and 6-day-old zooxanthellate larvae (lane 5). Each lane contained 1.2 μg protein. Molecular weight standards in lane 1. Arrow highlights a putative yolk protein doublet (84 and 79 kDa) that is abundant in eggs and 1-day larvae but absent by day 6. (B) Decline in abundance of putative yolk protein through larval development. The depletion of putative yolk protein corresponded with the onset of settlement on day 7. There was no difference in putative yolk protein abundance in azooxanthellate and zooxanthellate larvae (days 5 and 6); data shown represent the average of the two treatments.

exhibit feeding behavior that leads to the ingestion of zooxanthellae. It will be interesting to determine whether other species that produce a feeding planula larva acquire zooxanthellae in the same manner as shown for *F. scutaria* and *A. elegantissima*.

Both endodermal and ectodermal cells incorporated zooxanthellae within 1 h after larvae were exposed to zooxanthellae. The appearance of zooxanthellae in ectodermal tissue was surprising because zooxanthellae phagocytosed by endodermal cells would not be expected to be transported into tissues where they do not ultimately reside. We did not determine how the zooxanthellae entered the ectoderm. Future work will include long-term sampling of newly infected larvae to investigate the fate of the ectodermal zooxanthellae.

Horizontal transmission of symbionts would appear to be disadvantageous for obligately symbiotic species because of the possibility that infection may not occur. However, for planulae dispersed to areas with different environmental conditions, the ability to acquire zooxanthellae from the environment might confer a greater advantage to the host than directly inheriting maternal zooxanthellae. This study found that planulae of *F. scutaria* were capable of forming an association with members from three clades of zooxanthellae classified by Rowan and Powers (1991a, b): zooxanthellae from *C. xamachana* are in group A, those from *A. pallida* are in group B, and those from *F. scutaria* are in group C. The degree to which zooxanthellae from different clades persist in *F. scutaria* remains to be investigated, but our results suggest considerable flexibility in host-symbiont specificity in this species. In contrast, planulae of *A. elegantissima*, although able to form an association with zooxan-

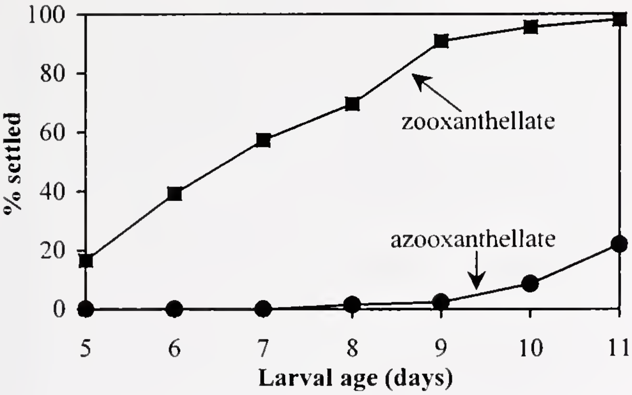

Figure 7. Effect of symbiotic state on larval settlement. Results from 1996 experiment. Nearly 100% of zooxanthellate planulae underwent settlement and metamorphosis by day 10, whereas most azooxanthellate planulae failed to settle. Each point represents data pooled from six replicate dishes for each treatment.

thellae recently isolated from a conspecific adult, were unable to do so with cultured *S. californium*, which is the species reported to occur in *A. elegantissima* (Banaszak *et al.*, 1993; Schwarz, 1996).

The finding that a stronger larval feeding response resulted in higher rates of infection indicates that larval feeding behavior may play an important role in acquiring zooxanthellae from the ambient environment. Because so little is known about the distribution and abundance of zooxanthellae in the natural environment, it is difficult to speculate on potential sources of these symbionts. However, one source that is likely to occur in abundance is mucus expelled by corals. Cnidarian hosts regularly expel mucus containing high concentrations of zooxanthellae (Steele, 1975; McCloskey *et al.*, 1996; Schwarz, pers. obs.), and increased rates of expulsion have been reported to accompany spawning (Montgomery and Kremer, 1995; D. Krupp, pers. obs.). Although this study did not examine whether planulae of *F. scutaria* will feed on coral mucus, planulae of the sea anemone *Anthopleura elegantissima* did feed on mucus expelled by adults and became infected by the zooxanthellae within it (Schwarz, 1996). These results suggest that ingestion of zooxanthellae could occur either at the spawning site or at the sites in which the larvae ultimately settle, allowing them to acquire symbionts adapted to different environments.

Effect of symbiont acquisition on larval development

Zooxanthellae are known to affect the physiology of their adult hosts, and the acquisition of zooxanthellae by larval hosts probably influences larval development. For example, the acquisition of symbionts may act as a settlement cue. An experiment in 1996 demonstrated that zooxanthellate larvae settled earlier than azooxanthellate larvae (Fig. 6)—indeed, most azooxanthellate larvae failed to settle. However, the same experiment repeated the following year showed no differences in settlement (data not shown). It is possible that symbiotic state does influence developmental events but either acts in concert with, or is overridden by, environmental variables such as temperature. The 1996 experiment was conducted during a period of anomalously warm water temperatures that induced a bleaching event on the reef flat in Kaneohe Bay, whereas the 1997 experiment was characterized by normal temperatures. Thus larval development may have been influenced more strongly by water temperature than by symbiotic state. Experimental manipulation of environmental parameters will allow us to examine this question in more detail.

Potential effect of symbiont acquisition on larval energetic strategies and dispersal

The larval stage serves as a means for dispersal in the life histories of sessile marine invertebrates. The length of the larval stage depends in part on the amount of energy available for metabolism (Boidron-Métairon, 1995; Levin and Bridges, 1995). Larvae of *F. scutaria* have several potential sources of energy that may allow them to extend the larval stage sufficiently to explain their widespread occurrence throughout the Pacific. First, larvae may initially obtain nutrition from yolk protein supplied through the egg. The presence and the pattern of decline of two abundant 84 kDa and 79 kDa proteins and the correlation between their depletion and the onset of settlement suggest that larvae may metabolize this protein over the course of their development. Second, once the mouth has developed, larvae may obtain energy through feeding. Third, larvae that have acquired zooxanthellae may receive nutrition in the form of organic carbon translocated by zooxanthellae. Richmond (1981, 1987) demonstrated that symbiotic planulae of the coral *Pocillopora damicornis* received about 13%–27% of the carbon fixed by zooxanthellae. Each of these modes of nutrition may operate at different times in development, and each may function to extend the length of the dispersal stage.

Acknowledgments

This work was supported by grants from the Office of Naval Research (N000149710101) to V. M. W., and from Sigma Xi and Oregon State University Zoology Department to J. A. S. We thank P. Jokiel, B. Kinzie, F. Cox, and the staff of the Hawaii Institute of Marine Biology for facilities, zooxanthella cultures (B. Kinzie), and support. We thank the OSU Department of Botany and Plant Pathology Electron Microscope facility staff for their assistance. Rick Jones prepared the illustration for Figure 1. This is Contribution #1043 from the Hawaii Institute of Marine Biology.

Literature Cited

Babcock, R. C., and A. J. Heyward. 1986. Larval development of certain gamete-spawning scleractinian corals. *Coral Reefs* **5:** 111–116.

Banaszak, A. T., R. Iglesias-Prieto, and R. K. Trench. 1993. *Scrippsiella velellae* sp. nov. (Peridiniales) and *Gloeodinium viscum* sp. nov. (Phytodiniales), dinoflagellate symbionts of two hydrozoans (Cnidaria). *J. Phycol.* **29:** 517–528.

Benayahu, Y., Y. Achituv, and T. Berner. 1989. Metamorphosis of an octocoral primary polyp and its infection by algal symbiosis. *Symbiosis* **7:** 159–169.

Boidron-Métairon, I. F. 1995. Larval nutrition, Pp. 223–238 in *Ecology of Marine Invertebrate Larvae*. Larry R. McEdward, ed. CRC Press, Boca Raton, FL.

Bradford, M. B. 1976. A rapid and sensitive method for the quantitation of microgram quantities of protein utilizing the principle of protein-dye binding. *Anal. Biochem.* **72:** 248–254.

Colley, N. J., and R. K. Trench. 1983. Selectivity in phagocytosis and persistence of symbiotic algae by the scyphistoma stage of the jellyfish *Cassiopeia xamachana. Proc. R. Soc. Lond. B* **219:** 61–82.

Davy, S. K., I. A. N. Lucas, and J. R. Turner. 1997. Uptake and persistence of homologous and heterologous zooxantheltae in the temperate sea anemone *Cereus pedunculatus* (Pennant). *Biol. Bull.* **192:** 208–216.

Douglas, A. E. 1994. *Symbiotic Interactions.* Oxford University Press, Oxford. 148 pp.

Fadlallah, Y. H. 1983. Sexual reproduction, development and larval biology in scleractinian corals. *Coral Reefs* **2:** 129–150.

Fitt, W. K., and R. K. Trench. 1983a. Infection of invertebrate hosts with the symbiotic dinoflagellate *Symbiodinium microadriaticum. Endocytobio.* **2:** 675–681.

Fitt, W. K., and R. K. Trench. 1983b. Endocytosis of the symbiotic dinoflagellate *Symbiodinium microadriaticum* Freudenthal by endodermal cells of the scyphistomae of *Cassiopeia xamachana* and resistance of the algae to host digestion. *J. Cell Sci.* **64:** 195–212.

Harrison, P. L., and C. C. Wallace. 1990. Reproduction, dispersal and recruitment of scleractinian corals. Pp. 133–207 in *Ecosystems of the World: Coral Reefs,* Vol. 25, Z. Dubinsky, ed. Elsevier. New York.

Heukeshoven, J., and R. Dernick. 1986. Neue Ergebnisse zum Mechanismus der Silberfarbung. *Electrophores Forum* **86:** 22–27.

Kinzie, R. A. 1974. Experimental infection of aposymbiotic gorgonian polyps with zooxanthellae. *J. Exp. Mar. Biol. Ecol.* **15:** 335–345.

Krupp, D. A. 1983. Sexual reproduction and early development of the solitary coral *Fungia scutaria* (Anthozoa: Scleractinia). *Coral Reefs* **2:** 159–164.

Laemmli, U. K. 1970. Cleavage of structural proteins during the assembly of the head of bacteriophage T4. *Nature* **227:** 680–685.

Levin, L. A., and T. S. Bridges. 1995. Pattern and diversity in reproduction and development. Pp. 1–48 in *Ecology of Marine Invertebrate Larvae.* Larry R. McEdward, ed. CRC Press, Boca Raton, FL.

McCloskey, L. R., T. G. Cove, and E. A. Verde. 1996. Symbiont expulsion from the anemone *Anthopleura elegantissima* (Brandt) (Cnidaria: Anthozoa). *J. Exp. Mar. Biol. Ecol.* **195:** 173–186.

Montgomery, M. K., and P. M. Kremer. 1995. Transmission of symbiotic dinoflagellates through the sexual cycle of the host scyphozoan *Linuche unguiculata. Mar. Biol.* **124:** 147–155.

Richmond, R. H. 1981. Energetic considerations in the dispersal of *Pocillopora damicornis* (Linnaeus) planulae. *Proc. 4th Int. Coral Reef Symp., Manila* **2:** 153–156.

Richmond, R. H. 1987. Energetics, competency, and long-distance dispersal of planula larvae of the coral *Pocillopora damicornis. Mar. Biol.* **93:** 527–533.

Richmond, R. H. 1997. Reproduction and recruitment in corals: critical links in the persistence of reefs. Pp. 175–197 in *Life and Death of Coral Reefs.* C. Birkeland, ed. Chapman and Hall, New York.

Richmond, R. H., and C. L. Hunter. 1990. Reproduction and recruitment of corals: comparisons among the Caribbean, the tropical Pacific, and the Red Sea. *Mar. Ecol. Prog. Ser.* **60:** 185–203.

Rowan, R., and N. Knowlton. 1995. Intraspecific diversity and ecological zonation in coral-algal symbiosis. *Proc. Natl. Acad. Sci. USA* **92:** 2850–2853.

Rowan, R., and D. A. Powers. 1991a. Molecular genetic identification of symbiotic dinoflagellates (zooxanthellae). *Mar. Ecol. Prog. Ser.* **71:** 65–73.

Rowan, R., and D. A. Powers. 1991b. A molecular genetic classification of zooxanthellae and the evolution of animal-algal symbioses. *Science* **251:** 1348–1351.

Schwarz, J. A. 1996. Feeding behavior and acquisition of zooxanthellae by the planula larvae of the temperate sea anemone *Anthopleura elegantissima.* Masters Thesis, University of California Santa Cruz.

Seibert, A. E. 1974. A description of the embryology, larval development, and feeding of the sea anemones *Anthopleura elegantissima* and *A. xanthogrammica. Can. J. Zool.* **52:** 1383–1388.

Steele, R. D. 1975. Stages in the life history of symbiotic zooxanthellae in pellets extruded by its host *Aiptasia tagetes* (Duch. and Mich.) (Coelenterata, Anthozoa). *Biol. Bull.* **149:** 590–600.

Sugiura, Y. 1964. On the life history of rhizostome medusae. II. Indispensability of zooxanthellae. *Embryologia* **8:** 223–233.

Tranter, P. R. G., D. N. Nicholson, and D. Kinchington. 1982. A description of spawning and post-gastrula development of the cool temperate coral, *Caryophyllia smithi. J. Mar. Biol. Assoc. UK.* **62:** 845–854.

Trench, R. K. 1980. Integrative mechanisms in mutualistic symbioses. Pp. 275–279 in *Cellular Interactions in Symbiosis and Parasitism,* C. B. Cook, P. W. Pappas, and E. D. Rudolph, eds. Ohio State University Press, Columbus, OH.

Trench, R. K. 1987. Dinoflagellates in non-parasitic symbioses. Pp. 530–570 in *The Biology of Dinoflagellates,* F. J. R. Taylor, ed. Blackwell Scientific, Oxford.

Reference: *Biol. Bull.* **196:** 80–93. (February, 1999)

Molecular Determination of Species Boundaries in Corals: Genetic Analysis of the *Montastraea annularis* Complex Using Amplified Fragment Length Polymorphisms and a Microsatellite Marker

JOSE V. LOPEZ[1], RALF KERSANACH, STEPHEN A. REHNER[2], AND NANCY KNOWLTON[3]

Smithsonian Tropical Research Institute, Apartado 2072, Balboa, Republic of Panama

Abstract. Analyses of DNA have not been widely used to distinguish coral sibling species. The three members of the *Montastraea annularis* complex represent an important test case: they are widely studied and dominate Caribbean reefs, yet their taxonomic status remains unclear. Analysis of amplified fragment length polymorphisms (AFLPs) and a microsatellite locus, using DNA from sperm, showed that *Montastraea faveolata* is genetically distinct. One AFLP primer yielded a diagnostic product (880 bp in *M. faveolata*, 920 bp in *M. franksi* and *M. annularis*) whose homology was established by DNA sequencing. A second primer revealed a 630 bp band that was fixed in *M. faveolata*, and rare in *M. franksi* and *M. annularis;* in this case homologies were confirmed by Southern hybridizations. A tetranucleotide microsatellite locus with several alleles exhibited strong frequency differences between *M. faveolata* and the other two taxa. We did not detect comparable differences between *M. annularis* and *M. franksi* with either AFLPs (12 primers screened) or the microsatellite locus. Comparisons of AFLP patterns obtained from DNA from sperm, somatic tissues, and zooxanthellae suggest that the technique routinely amplifies coral (animal) DNA. Thus analyses based on somatic tissues may be feasible, particularly after diagnostic differences have been established using sperm DNA.

Introduction

The recognition of species boundaries in sympatry is straightforward in principle, because the absence of interbreeding implies the existence of at least some fixed genetic differences between taxa (Avise and Ball, 1990). However, the number of such differences may be very small if the isolation of taxa is recent or the rate of evolution is slow. If in addition sporadic hybridization occurs, the problem of defining species becomes particularly difficult (*e.g.*, Howard *et al.*, 1997).

Closely related coral species appear to be especially challenging in this regard (Veron, 1995; Knowlton and Weigt, 1997). Species boundaries are in flux for a number of well-studied groups (*e.g.*, Miller and Babcock, 1997; Miller and Benzie, 1997; Odorico and Miller, 1997; Willis *et al.*, 1997; Knowlton and Budd, unpubl.), and it is unclear whether these controversies are due to the technical challenge of finding diagnostic characters between generally similar but reproductively isolated taxa, or alternatively, to the blurring of species boundaries by hybridization (Veron, 1995; Knowlton and Weigt, 1997; Willis *et al.*, 1997). Molecular methods have great potential to resolve the nature of species boundaries because of the large number of unambiguous characters they provide (Avise, 1994).

A clear example of these issues is presented by the proposed members of the *Montastraea annularis* species complex: *M. annularis* (formerly morphotype I or columnar morph), *M. faveolata* (formerly morphotype II or massive morph), and *M. franksi* (formerly morphotype III or bumpy morph) (Knowlton *et al.*, 1992; Van Veghel and Bak, 1993;

Received 5 June 1998; accepted 1 December 1998.

[1] Current address: Division of Biomedical Research, Harbor Branch Oceanographic Institution, 5600 U.S. 1 North, Ft. Pierce, FL 34946; E-mail: Lopez@hboi.edu

[2] Current address: Department of Biology, P.O. Box 23360, University of Puerto Rico, Rio Piedras, San Juan, Puerto Rico, 00931.

[3] Also at Marine Biology Research Division 0202, Scripps Institution of Oceanography, University of California San Diego, La Jolla, CA 92093-0202; E-mail: nknowlton@ucsd.edu

Abbreviations: AFLP - amplified fragment length polymorphism, a registered trademark of Keygene.

Weil and Knowlton, 1994). In sympatry, these taxa differ in colony morphology, growth rate, stable isotope chemistry, aggressive behavior, allozymes, corallite structure, and life history (Tomascik, 1990; Van Veghel and Bak, 1993, 1994; Van Veghel, 1994; Van Veghel and Kahmann, 1994; Weil and Knowlton, 1994; Van Veghel and Bosscher, 1995; Van Veghel *et al.*, 1996; Szmant *et al.*, 1997; Knowlton and Budd, unpubl.). Such concordance of suites of independent characters in sympatric taxa strongly suggests reproductive isolation (Avise and Ball, 1990), and differences in the timing of spawning and apparent barriers to interspecific fertilization (Knowlton *et al.*, 1997) also support this interpretation (but see Szmant *et al.*, 1997). Overall, these data support separate species status regardless of the species concept used (Templeton, 1989; Cracraft, 1989; Mallet, 1995; Knowlton and Weigt, 1997).

Nevertheless, a preliminary molecular survey revealed no fixed DNA sequence differences among these taxa in two regions that might, *a priori*, be expected to have them: the ITS regions of rDNA and an intron in a β-tubulin gene (Lopez and Knowlton, 1997). Sequence-based methods can only be used to examine a limited stretch of DNA, however, and methods that screen a larger proportion of the genome appear to offer greater promise (Lopez and Knowlton, 1997). One such approach is analysis of amplified fragment length polymorphisms (AFLPs), which screens for polymorphisms at, or adjacent to, restriction endonuclease sites (Zabeau and Vos, 1995). In a preliminary survey, we found evidence for potentially diagnostic differences between *M. faveolata* and *M. franksi* using two AFLP primers (Lopez and Knowlton, 1997).

In the present study we wished to (1) determine whether these apparently diagnostic AFLP differences hold up when sample sizes are increased, (2) screen additional AFLP primers to see if any show promise for distinguishing *M. annularis* and *M. franksi*, (3) determine, using Southern hybridization and DNA sequencing, whether apparently similar AFLP bands are indeed homologous, and (4) assess whether diagnostic polymorphisms detected using high-quality DNA derived from sperm could also be seen in more readily collected, but potentially less pure, somatic tissue samples.

During earlier work on tubulin introns (Lopez and Knowlton, 1997), we also uncovered a tetranucleotide microsatellite locus (here called Mfra-gttt1) in a genomic clone derived from *M. franksi*. Microsatellite or simple repeat loci have become increasingly important tools in evolutionary and population studies because of their high levels of polymorphism and codominant inheritance (Jarne and Lagoda, 1996). Here we report on evidence for allelic frequency differences at this locus among the *Montastraea* taxa.

Materials and Methods

Sample acquisition and DNA preparation

All corals were collected from the San Blas Islands, Panama. Colonies were identified to species in the field, based on colony morphology, and brought to waters near the laboratory shortly before the anticipated date of spawning (Knowlton *et al.*, 1997). At dusk, each colony was placed in a separate container; spawning generally occurred 2–4 h after sunset, and the gamete bundles were collected immediately after release. The gamete bundles from each container were washed separately over plankton netting. The eggs were retained on the netting, while the sperm passed through with the wash water, which was collected and centrifuged. The pelleted sperm were quick frozen (details in Lopez and Knowlton, 1997). Abundant DNA (hundreds of micrograms) was extracted from 1–2 ml of highly concentrated sperm solution using standard techniques (Sambrooks *et al.*, 1989), as previously described (Lopez and Knowlton, 1997).

Sperm provide an ideal source of coral DNA (McMillan *et al.*, 1988), but they cannot be collected routinely. However, high molecular weight DNA is difficult to extract from somatic tissues (McMillan *et al.*, 1988) and may be contaminated by DNA from symbiotic dinoflagellates (zooxanthellae), which the gametes of *Montastraea* lack (Szmant, 1991). To determine whether DNA extracted from somatic tissues is of sufficient quality for AFLP analyses, we compared the analyses of DNA from sperm with those of DNA from somatic tissues from the same colonies. DNA from somatic samples was extracted according to the protocol of Rowan and Powers (1991), except that tissue was removed from 25–50 cm^2 of coral with an airbrush at 75–100 psi and suspended in 5–20 ml of L buffer (100 m*M* EDTA, 10 m*M* Tris-Cl, pH 7.6). To enrich for coral (animal) DNA within somatic tissues, frozen samples were ground in a glass homogenizer 5–10 times and centrifuged in an RT6000B Sorvall centrifuge at 50–100 $\times$ *g* for 10 min at room temperature. This spin was repeated one or two times for samples especially rich in zooxanthellae. The animal-enriched DNA was then incubated for 3 h in 20–50 μg/ml proteinase K with 1% SDS (final concentration), followed by successive phenol:chloroform extractions (Sambrook *et al.*, 1989). DNA that remained resistant to restriction digestions was further purified by the GeneClean (Bio 101) protocol. To clarify further the potentially confounding contribution of zooxanthellae in coral somatic samples, we also analyzed zooxanthella DNA provided by Rob Rowan. This DNA came from other colonies of *Montastraea* (primarily *M. faveolata*) from the same region, and was not necessarily entirely free of coral (animal) DNA.

AFLP-PCR

The AFLP method and preparation of templates using the Pst I adapter system have been described in detail (Mueller *et al.*, 1996). Genomic DNA was cut at specific 6-base recognition sequences by the Pst I restriction enzyme, and then a synthetic, 21 bp adapter was ligated to the ends of the fragments. The polymerase chain reaction (PCR) was then used to amplify these restriction fragments, using primers matching the adapter sequence. To limit the number of different fragments that are amplified (and hence improve the clarity of the resulting products), several additional, arbitrarily chosen bases were added to the PCR primers at their 3′ ends. These additional bases (by which primers are identified, *e.g.*, ATG or GGAG) overlap with genomic DNA beyond the restriction site, and amplify the subset of fragments that contain the additional nucleotides.

We used the same methods and extension primers (ATG, GGAG) as previously reported (Lopez and Knowlton, 1997; note, however, that in our earlier report, the GGAG primer was incorrectly listed as GAG). We also used primers with the following 3′ extensions: ATT, GAC, GTG, ATC, TGT, ACT, TTG, AGC, TAG, and ACGC. The PCR profile for all AFLP extension reactions was 94°C/45 s, 60°C/60 s, and 72°C/90 s for 30 cycles, using an MJ Research PTC-100 or PTC-200 thermocycler. Typically, a "preamplification" PCR was performed with an extension primer possessing one additional base (A, C, G or T) (Vos *et al.*, 1995). This reaction enriches for the subset of amplifiable templates possessing the extra nucleotide, improves the targeted band signal, and reduces background. The preamplification PCR was run with the same AFLP profile as above, but with fewer (20) cycles. However, this preamplification protocol did not improve the clarity of the patterns for the GGAG primer. The best electrophoretic resolution of PCR products was obtained with 1.2%–1.4% agarose/TBE gels (containing at least 50% Metaphor agarose, FMC) run at 5.4 V/cm. The agarose-based technique used here and in our previous study does not require radioactive nucleotides, is less toxic, and is relatively easy to perform (Mueller *et al.*, 1996; Lopez and Knowlton, 1997), although it yields fewer discrete bands per lane (6–12) than the original polyacrylamide gel electrophoresis (PAGE) method (Vos *et al.*, 1995) due to poorer resolution of fragments of less than 400 bp. All AFLP analyses shown here were performed more than once to ensure reproducibility, and AFLP-PCRs with no DNA added served as controls for contamination.

AFLP banding patterns and DNA sequences (see below) were analyzed with RFLPscan (Scanalytics), BLAST (Altschul *et al.*, 1990), and MAPD (Yuhki and O'Brien, 1990; Stephens *et al.*, 1992). Only bands in the 0.3–1.6 kb size range were considered, since variation in higher molecular weight bands is more difficult to interpret due to potentially inconsistent amplification of large DNA fragments and the possibility of incomplete restriction enzyme digestion. RFLPscan (Scanalytics) converted band patterns into binary presence/absence characters for each sample and computed distance estimates for pairwise comparisons based on band sharing (Nei and Li, 1979).

Cloning, Southern hybridization, and sequencing

Both gel-purified and cloned AFLP fragments were used as hybridization probes and as sequencing templates. Specific AFLP bands were dissected from low melting temperature agarose (NuSieve/Metaphor, FMC) gels, added to 200 μl of distilled H_2O, and melted at 65°C. When this DNA was used as a template in a "re-amplification" PCR with the original primer to obtain more material, PCR products were visualized on an agarose minigel to verify that a single band of the correct size had been amplified. Alternatively, AFLP fragments were cloned directly into pGEM-T vectors (Promega). Probes for Southern hybridizations were labeled with $\alpha[^{32}P]$-dCTP via nick-translation to a specific activity of 10^6–10^7 cpm/μg (Sambrook *et al.*, 1989).

After separation on agarose gels, AFLP products were blotted onto nylon membranes (Duralon, Stratagene) according to standard procedures (Southern, 1975; Sambrook *et al.*, 1989). Higher molecular weight fragments (> 1 kb) appeared to be transferred to membranes less efficiently than smaller fragments, probably because of the relatively high gel concentrations of agarose (1.2%–1.4%) that were used. After hybridization and stringent washing (in 0.1 X SSC and 0.5% SDS at 50°C) (Sambrook *et al.*, 1989), filters were exposed to Kodak XAR-2 X-ray film, generally for 2–3 days.

Informative fragments that were generated using the GGAG primer were either directly sequenced after cleaning the PCR product with QIAquick PCR purification kits (Quiagen), or sequenced from plasmid-cloned fragments purified with Wizard miniprep kits (Promega). Sequencing reactions were run on automated DNA sequencers (ABI 373A or 377, Perkin Elmer), initially using primers complementary to T7 or SP6 promoter regions, following the standard cycle sequencing protocols (ABI, Perkin Elmer) used previously (Lopez and Knowlton, 1997). The following primers were then designed and used to obtain complete sequences for the GGAG 880 and 920 bp fragments: 5′ CCCTGATCAGTATTTTGGG 3′ (880i), 5′ TTGGAATATTTGCCTTACCG 3′ (880f), and 5′ GGAGGGCTCTGTTATTCTATC 3′ (880r). The 880f primer (slightly internal to 880i) matches available *Montastraea* sequences, and when used with primer 880r yielded products of 837 or 804 bp.

Microsatellite analyses

The microsatellite locus Mfra-gtt1 was initially detected in a clone (tub29A) derived from *M. franksi* (no. 426) that was recovered while we were screening for taxonomically informative β-tubulin introns (Lopez and Knowlton, 1997). Its occurrence and polymorphism in other *Montastraea* species were determined by designing the following 2 oligonucleotide primers, which are complementary to the genomic sequences flanking Mfra-gttt1: Sput1f–5′ AAACA TACGG CCAGT GCTGG 3′ and Sput2rc – 5′ GAAAA GAGCA ATCTT TTGTA TGGTG 3′. The PCR profile used for Mfra-gttt1 amplification from genomic DNA was 94°C/40 s, 60°C/45 s, and 72°C/60 s for 30 cycles. All PCRs shown here were reproducible and included negative controls. The resolution of PCR products was better when 4.0% agarose (Metaphor, FMC) TBE gel electrophoresis was used, and banding patterns were confirmed by polyacrylamide gel (10%) electrophoresis using the entire PCR product (approximately 1 μg DNA).

Results

AFLP band patterns

Band patterns produced using the GGAG primer showed a clear diagnostic difference between *M. faveolata* and *M. franksi* (Fig. 1A), which confirms our previous results obtained with smaller sample sizes (Lopez and Knowlton, 1997). The 920 bp GGAG band was absent from, and the 880 bp band was present in, all 16 *M. faveolata* tested (including 6 previously analyzed), while the reciprocal pattern occurred in 15 *M. franksi* (including 7 previously analyzed). A third band, migrating at around 850 bp, may also occur at significantly different frequencies in the two taxa, but our sample sizes are too limited to test for this.

The ATG primer also provided evidence of genetic difference between *M. faveolata* and *M. franksi:* as previously reported (Lopez and Knowlton, 1997), the 630 band was characteristically present in the former and absent from the latter (Fig. 1B). In this case, however, increasing the sample size indicated that this difference between the species is not fixed: the 630 bp band was present in all 16 individuals of *M. faveolata* tested (including 7 from the previous study), but it also appeared in one individual of *M. franksi* (no. 19, lane 9). The remaining 14 *M. franksi* (including 6 previously studied) lacked this band.

In contrast to the clear differences separating *M. faveolata* from *M. franksi*, no diagnostic bands separated *M. franksi* and *M. annularis*. This was true, not only for the ATG (Fig. 1B) and GGAG primers (five *M. annularis* analyzed, data not shown), but also for 10 additional primers that were screened (data not shown). The ATT primer yielded band patterns with the strongest quantitative differences (Fig. 2), but the differences are not statistically significant by a chi-square test, once a Bonferroni correction (Rice, 1989) for the total number of bands examined is applied (see legend Fig. 2). Moreover, mean average percent difference (MAPD; Yuhki and O'Brien, 1990) in ATT band-sharing values among samples of *M. annularis* (28%) and among samples of *M. franksi* (22%) were very similar to the value calculated for interspecific comparisons between these taxa (27%).

Homology of bands

Southern hybridization with DNA probes derived from the 630 bp ATG bands provided further insights into the nature of genetic differences between *M. faveolata* and *M. franksi*. In general, results were better when the hybridization probes were derived from DNA clones. Multiple bands were labeled when probes were derived from gel-isolated ATG bands, suggesting that the 630 bp bands were contaminated with fragments of different molecular weight.

Southern hybridizations showed that the 630 bp ATG bands found in all *M. faveolata* and one *M. franksi* (no. 19) (Fig. 3A) are homologous (Fig. 3B). Moreover, another *M. franksi* (no. 20) possessed a higher molecular weight fragment that also hybridized to the 630 bp ATG probe (Fig. 3B). This larger fragment may be the same one visible in Figure 3A, and probably arose by one or more DNA insertions at the 630 bp locus. Unfortunately, similar Southern hybridizations using the diagnostic 880 GGAG fragment as a probe were unsuccessful due to our inability to use the preamplification protocol.

We therefore used DNA sequences to evaluate the homologies of the 880 and 920 bp GGAG bands. Partial DNA sequences were initially obtained from both 5′ and 3′ termini of the GGAG 880 (*M. faveolata*) and GGAG 920 (*M. franksi*) fragments. These preliminary sequences permitted the design of PCR primers by which the corresponding locus was amplified from genomic DNA. The GGAG 880 locus was amplified consistently from samples of *M. faveolata* (Fig. 4A), but a larger band appeared for *M. franksi* (Fig. 4A) and *M. annularis* (data not shown) when the same primers were used. DNA sequencing confirmed the homology of PCR products for 9 *M. franksi*, 6 *M. annularis*, and 7 *M. faveolata* (sequences deposited in Genbank AF110114-AF110129, AF112346-AF112351). Three insertions or deletions (22, 8, and 3 bp) constituted the primary differences between *M. faveolata* and the other two taxa (Fig. 4B), as would be expected from the estimated size differences in the 880 and 920 bp bands. There were also 5 nucleotide substitutions [4 transitions, 1 transversion in 837 bp within the GGAG 920 fragment (see methods); data not shown] that distinguished *M. faveolata* from *M. annularis* and *M. franksi*. The sequences exhibited d(AT) contents of 58%–64%, and did not resemble sequences in current databases (GenBank and EMBL; April 1998). The lack of significant open reading frames in the sequences suggests that they do not represent protein-encoding regions.

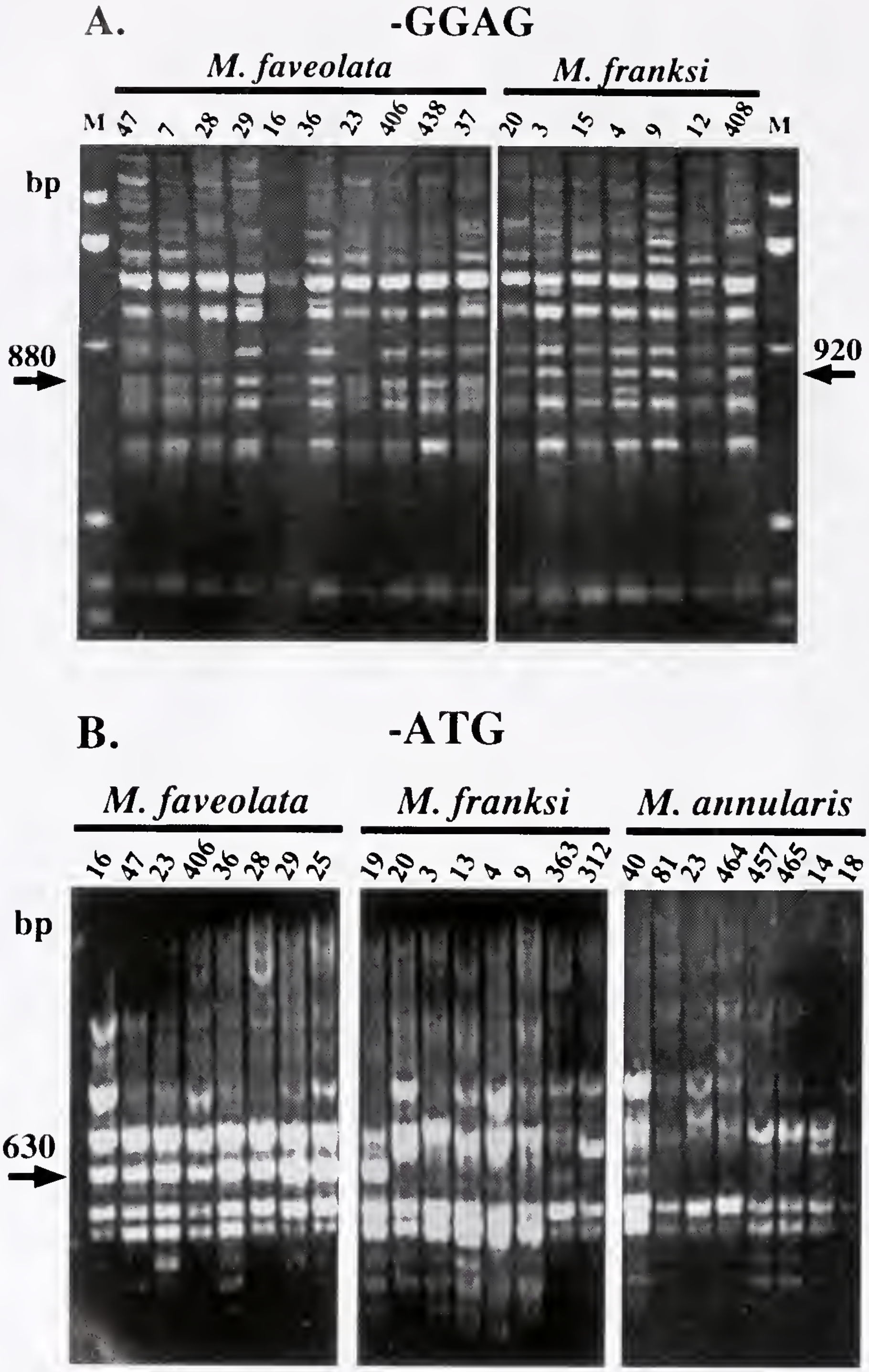
A.
-GGAG
M. faveolata
M. franksi
M
47
7
28
29
16
36
23
406
438
37
20
3
15
4
9
12
408
M
bp
880
920
B.
-ATG
M. faveolata
M. franksi
M. annularis
16
47
23
406
36
28
29
25
19
20
3
13
4
9
363
312
40
81
23
464
457
465
14
18
bp
630

Figure 1. AFLP band patterns. Samples are grouped by species, and individual sample numbers are indicated above each lane. A 1.0 kb ladder (Gibco/BRL, Bethesda) was used as the molecular weight standard. (A) AFLP patterns derived with the GGAG primer. Species-specific bands at 880 and 920 bp are indicated by arrows. (B) AFLP patterns derived with the ATG primer. The 630 bp band is indicated by an arrow.

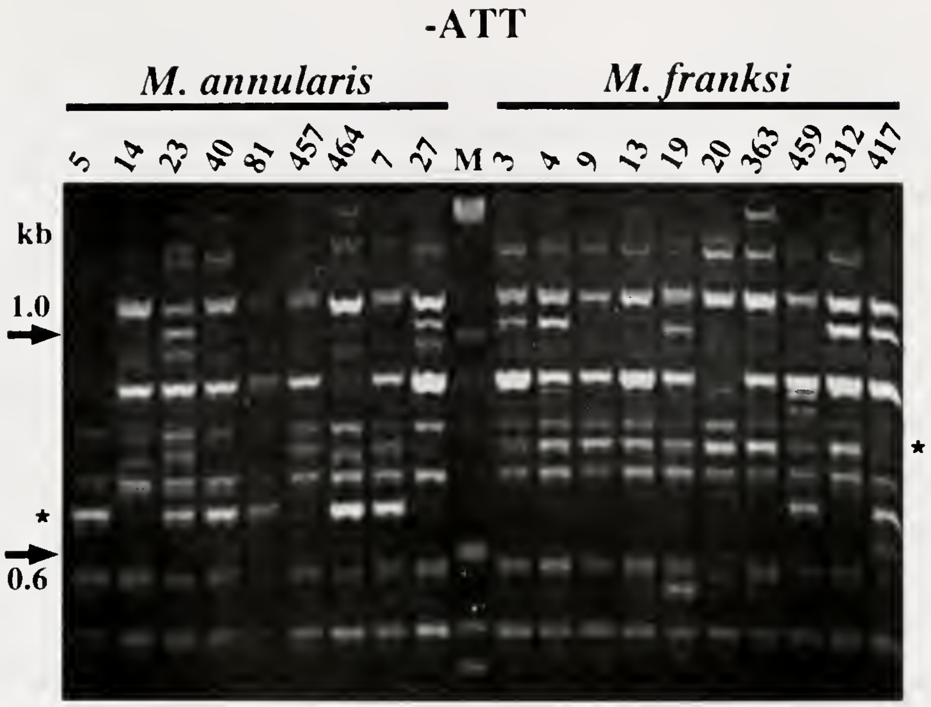

Figure 2. Comparison of *Montastraea franksi* and *M. annularis* AFLP patterns obtained with the ATT primer. Polymorphic bands showing the greatest frequency differences between the species are marked by asterisks. The most extreme frequency difference (band indicated by upper asterisk, present in 5 of 13 versus 12 of 13 individuals of *M. annularis* and *M. franksi*, respectively; not all samples shown) was individually significant (chi-square = 6.1, $P < 0.02$). However, this difference is not significant when a Bonferroni correction (Rice, 1989) for the total number of bands (18) is applied (P must be less than 0.003).

Comparisons of band patterns from gametes, somatic tissues, and zooxanthellae

The ATG patterns for DNA derived from sperm and from somatic tissue were generally consistent, and the taxonomically informative 630 bp band was conspicuous in analyses of somatic tissues from *M. faveolata* (Fig. 5A). Reproducibility for the GGAG primer was poorer due to our inability to use the preamplification protocol, but diagnostic GGAG bands at 920 and 880 bp were visible in analyzed samples of DNA from somatic tissues from *M. franksi* and *M. faveolata*, respectively (Fig. 5B). This suggests that AFLP analyses can be informative with somatic tissues, especially once diagnostic patterns have been established with sperm samples. The general lack of higher molecular weight AFLP bands from analyses of somatic tissue compared to those of gamete samples may be due to degradation during DNA purification of somatic samples (*e.g.*, McMillan *et al.*, 1998) or to the presence of contaminants that interfered with the reactions, but these bands were typically not scored. Some differences between somatic and gamete samples (*e.g.*, for *M. franksi* no. 467 in Fig. 5A) cannot currently be explained.

To determine how zooxanthella-derived bands in particular might confuse the interpretation of analyses of somatic tissues, we obtained AFLP bands from DNA purified from zooxanthella types A, B, and C from *Montastraea* (see Rowan and Knowlton, 1995) (Fig. 6). There may be some potential for confusion between the diagnostic 630 bp band in *M. faveolata* and similarly-sized bands from zooxanthella types A and B, although these zooxanthella bands may in fact be due to coral (animal) contamination. In general, the similarity of the gamete and somatic tissue samples (Fig. 5) and the difference between zooxanthella-enriched and zooxanthella-absent (sperm) samples (Fig. 6), suggest that for these corals, the AFLP technique primarily amplifies coral (animal) DNA from somatic tissue samples.

Microsatellite locus

Analysis of a clone from *M. franksi* derived from a PCR amplification product using primers for β-tubulin revealed a microsatellite locus (Mfra-gttt1) whose core repeat sequence (GTTT) was perfectly repeated 9 times (EMBL accession number AJ223626). It is similar (but not identical) to simple repeats in other scleractinian corals (McMillan *et al.*, 1991). Analysis of additional samples using the same primers revealed that a smaller allele (approximately 160 bp, its size presumably due to

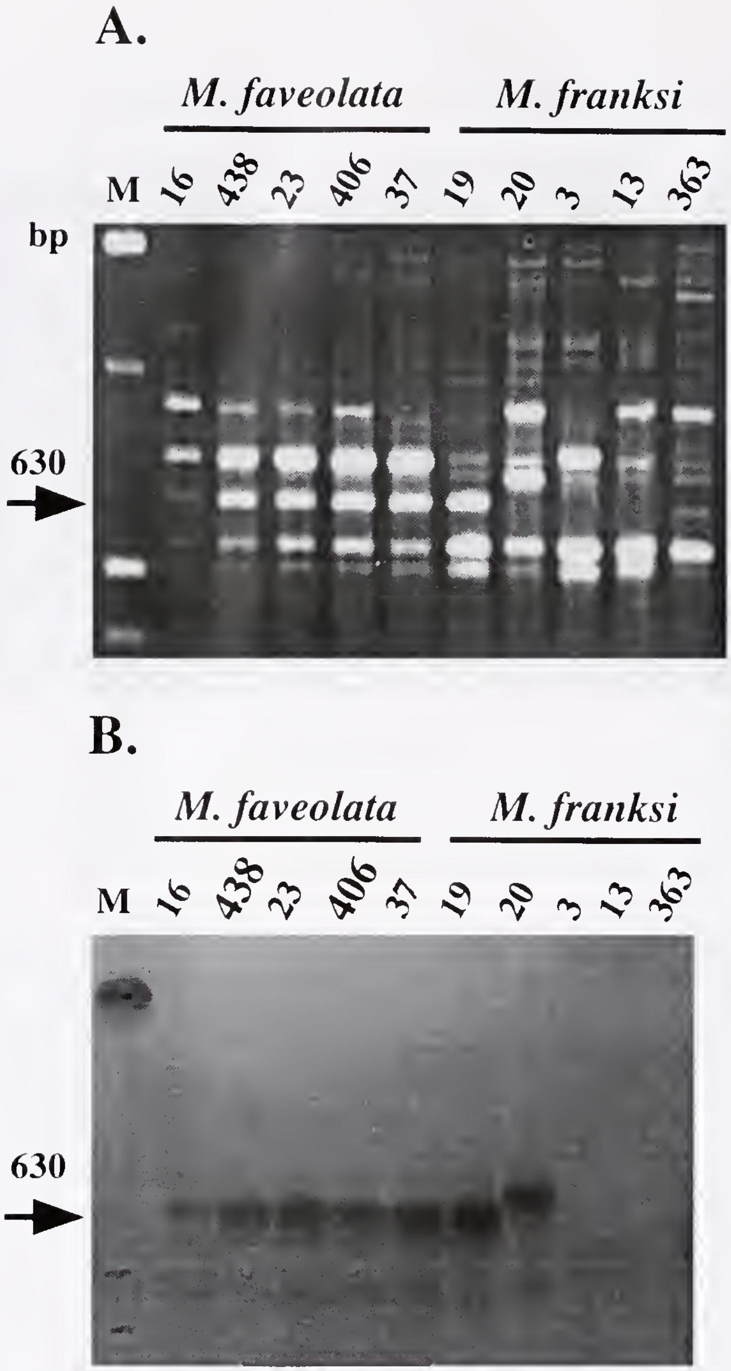
A.
M. faveolata
M. franksi
M
16
438
23
406
37
19
20
3
13
363
bp
630
B.
M. faveolata
M. franksi
M
16
438
23
406
37
19
20
3
13
363
630

Figure 3. Southern hybridization experiments with the ATG 630 bp fragment to determine band homologies. (A) Ethidium bromide-stained agarose gel used for Southern blotting, showing typical AFLP patterns obtained using the ATG primer. (B) Autoradiograph produced with probe for the ATG 630 bp fragment. A cloned 630 bp ATG fragment was radiolabeled and used for probing the filter of the gel in (A). This fragment also hybridized to the 1.6 kb fragment in the marker lane (M).

a loss of 2–3 repeat units) is the most common allele in both *M. franksi* and *M. annularis* (Fig. 7; Table I). Two individuals appeared to be heterozygous for the 160 bp and 169 bp alleles (*i.e.*, two bands amplified; data not shown). One sample (from *M. annularis* no. 27, Fig. 7) yielded three bands (160 bp, 169 bp, and an intermediate band migrating between them); this pattern suggests the presence of an additional locus, although it could be a

A.

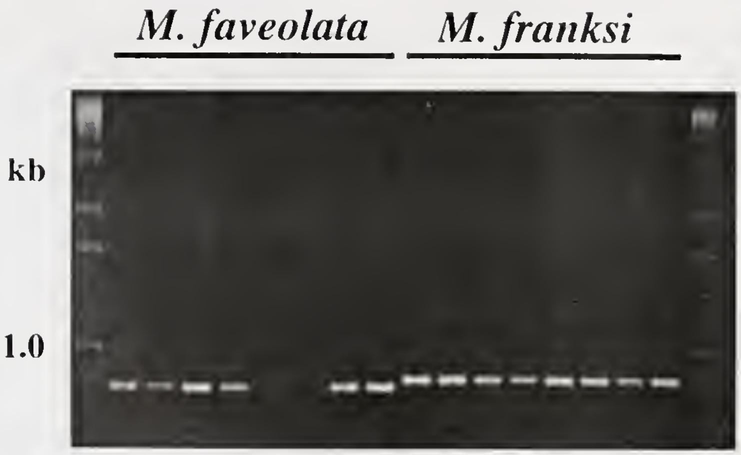

B.

```
                          131        141
                           |          |
M. franksi     ACCTATTTCCCTAAA ATTTCTCGC
M. franksi     ............... .........
M. franksi     ............... .........
M. annularis   ............... .........
M. annularis   ............... .........
M. faveolata   .-------------- --------.
M. faveolata   .-------------- --------.
M. faveolata   .-------------- --------.
M. faveolata   .-------------- --------.
M. faveolata   .-------------- --------.


               361       371   501       511
               |         |     |         |
M. franksi     GAGTTTAACAACT   AACCTTCTGCGTT
M. franksi     .....A.......   .............
M. franksi     .....A.......   .............
M. annularis   .....A.......   .............
M. annularis   .....A.......   .............
M. faveolata   .--------....   ....---......
M. faveolata   .--------....   ....---......
M. faveolata   .--------....   ....---......
M. faveolata   .--------....   ....---......
M. faveolata   .--------....   ....---......
```

Figure 4. Agarose gel and sequence alignments showing the differences between the 880 and 920 bp GGAG fragments. (A) Fragments amplified from genomic DNA of *Montastraea faveolata* and *M. franksi* using the *Montastraea*-biased primers. (B) Sequence alignment showing the regions that generate the difference in size of the 880 and 920 bp fragments.

PCR artifact. In contrast, most samples of *M. faveolata* yielded a higher molecular weight smear above 220 bp, rather than discrete 160 or 169 bp bands, when using the same primers and PCR conditions ("null" alleles, Fig. 7). Overall, this microsatellite locus suggests that genetic differences exist between *M. faveolata* and the other two taxa, but determining the precise nature of these differences would require further analyses.

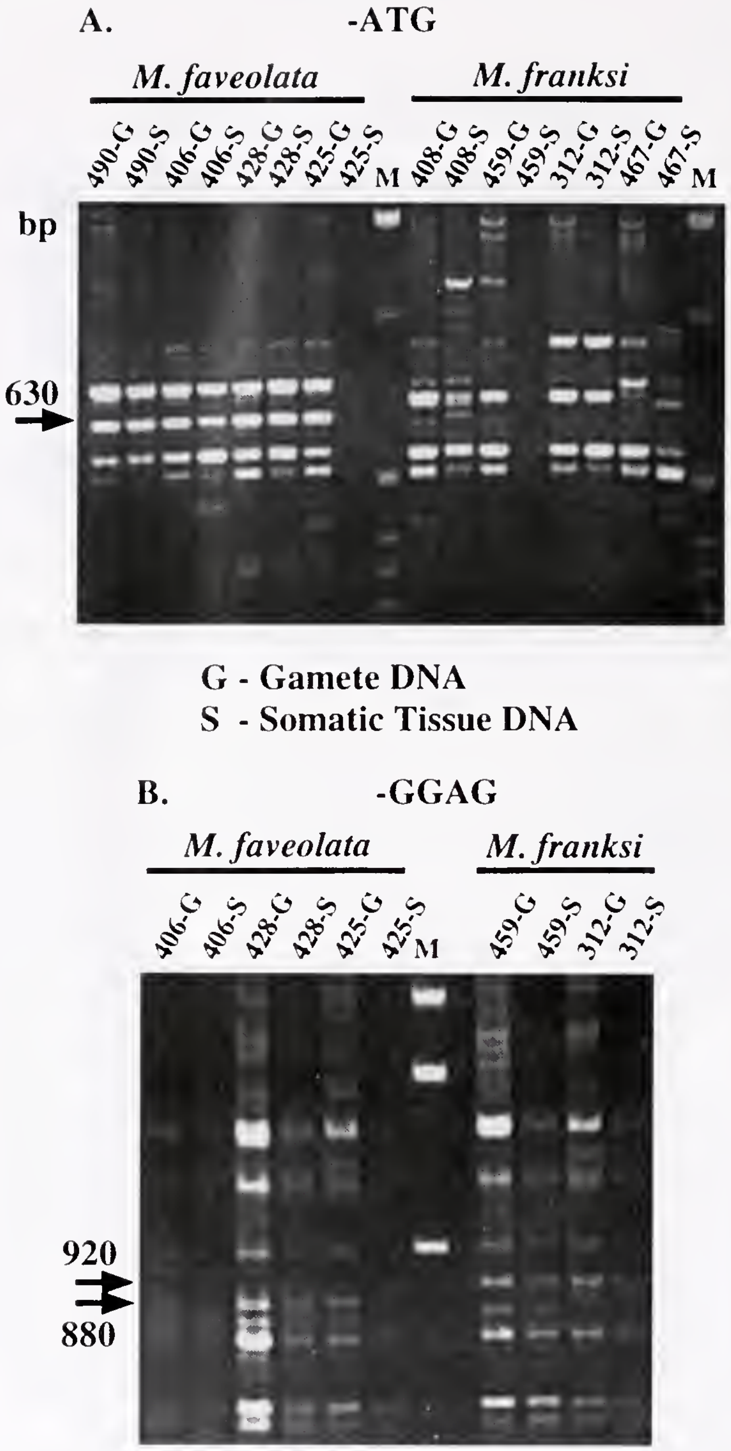
A.
-ATG
M. faveolata
M. franksi
490-G
490-S
406-G
406-S
428-G
428-S
425-G
425-S
M
408-G
408-S
459-G
459-S
312-G
312-S
467-G
467-S
M
bp
630
G - Gamete DNA
S - Somatic Tissue DNA
B.
-GGAG
M. faveolata
M. franksi
406-G
406-S
428-G
428-S
425-G
425-S
M
459-G
459-S
312-G
312-S
920
880

Figure 5. Comparison of AFLP patterns from gametic (G) and somatic (S) tissue samples. DNA derived from sperm and from somatic tissue of the same *Montastraea* colony were analyzed in parallel AFLP-PCRs, using identical conditions. (A) Results from ATG primer. (B) Results from GGAG primer. Diagnostic bands are identified by arrows.

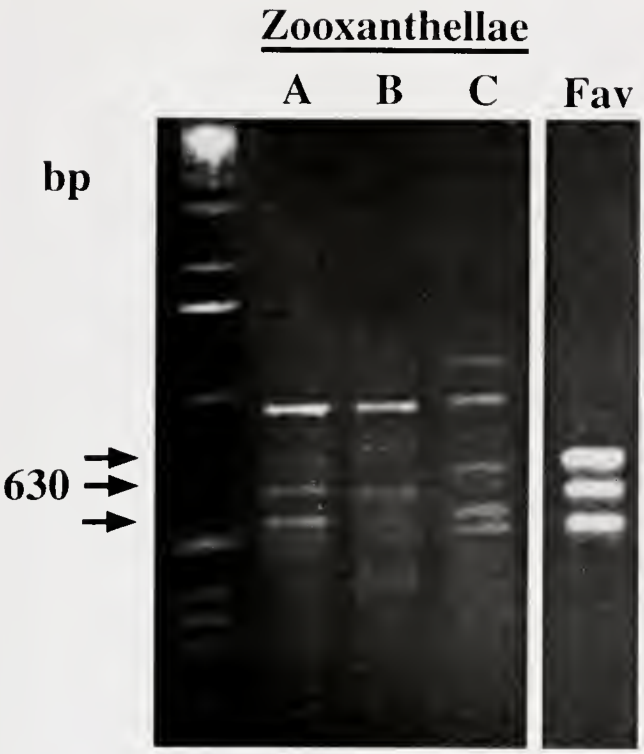

Figure 6. AFLP assay of zooxanthella samples. The ATG primer was used after PCR preamplification of zooxanthella templates (see methods). Identical conditions for AFLP analyses were used on both zooxanthellae and coral (*Montastraea faveolata*) DNA samples. Three faint bands (indicated by arrows) obtained from Type A zooxanthellae appear similar to the three dominant AFLP bands obtained from *M. faveolata* (550, 630, 750 bp) shown in Fig. 1B; these may be due to coral (animal) contamination of the zooxanthella DNA.

Table I

Mfra-gttt1 allele distributions in members of the Montastraea annularis *complex*

Species	Allele size*/pattern				
	160	169	160/169	Null	Total
M. franksi	8	1	1	1	11
M. annularis	7	2	1	1	11
M. faveolata	0	1	0	11	12

* Sizes indicated are approximate (see legend Fig. 7).

Discussion

Status of the three members of the Montastraea annularis *complex*

When the specific status of taxa in sympatry is questionable, multiple, independent, fixed differences provide compelling evidence for the lack of effective interbreeding (Avise and Ball, 1990). The reciprocal presence/absence pattern for the GGAG 880 and 920 bp bands appears to represent one such fixed difference between *M. faveolata* and the other two taxa. In addition, strong frequency differences at the ATG 630 locus and failure to amplify the 160 or 169 bp alleles at the microsatellite locus in most *M. faveolata* also point to the distinctiveness of this species. The significance of these genetic differences is further supported by other biological differences that distinguish the taxa (Tomascik, 1990; Hayes, 1990; Knowlton *et al.*, 1992; Van Veghel and Bak, 1993, 1994; Van Veghel, 1994; Van Veghel and Kahmann, 1994; Van Veghel and Bosscher, 1995; Van Veghel *et al.*, 1996; Weil and Knowlton, 1994; Szmant *et al.*, 1997; Knowlton *et al.*, 1997; Knowlton and Budd, unpubl.).

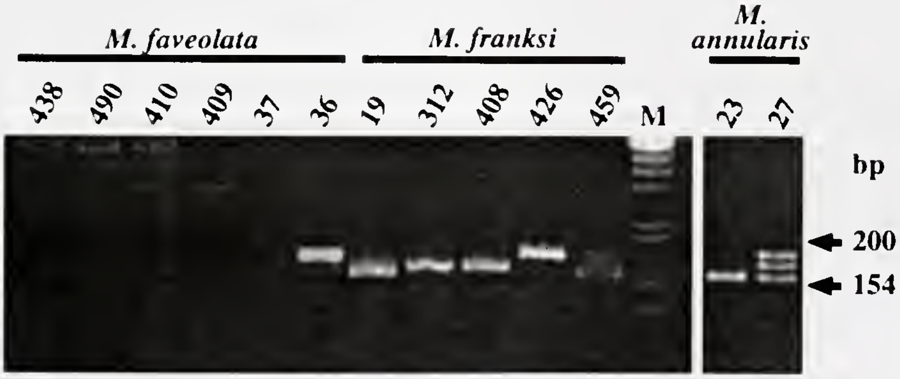

Figure 7. A subset of the *Montastraea* samples assayed for the Mfra-gttt1 microsatellite locus. Sample number and species identity for each coral colony are shown above gel. Sizes refer to two bands in the molecular weight markers (M). Representative "null" Mfra-gttt1 patterns are shown in the first five lanes. Samples from *M. annularis* were run on a separate gel. Samples from two individuals of *M. franksi* (nos. 312, 408) yielded bands that appear to be slightly larger than 160 bp; confirmation of their distinctiveness would require additional analysis.

The nature of a species boundary between *M. annularis* and *M. franksi* remains much more problematic. No technique used to date has revealed fixed genetic differences between them, despite marked differences in both aggressive behavior (Weil and Knowlton, 1994; Van Veghel and Bak, 1993) and the timing of spawning (Knowlton *et al.*, 1997; Szmant *et al.*, 1997). More than rare hybridization would presumably erode the predictable association between colony morphology and these other biological characteristics, but genetic evidence supporting this otherwise reasonable argument is lacking. Nevertheless, negative results for any single gene is weak evidence to support synonymizing species, particularly when, as is the case here, other types of data point to the existence of reproductive barriers. A sobering example of the limitations of negative genetic evidence is provided by Howard *et al.* (1997), who found only six species-specific markers distinguishing two species of oaks, despite having screened 700 10-bp primers.

Molecular characters also provide an ideal means for statistically analyzing the probability of encountering particular combinations of characters, including those that would be expected in an F1 hybrid (Lessios and Pearse, 1996; Boeklen and Howard, 1997; Suchanek *et al.*, 1997; Foltz, 1997). The only individual with an atypical allele for its species (*M. franksi* no. 19, with the ATG 630 bp band characteristic of *M. faveolata;* Fig. 1B) had the typical *M. franksi* band size for GGAG (fig. 2A in Lopez and Knowlton, 1997). This suggests that this individual is not an F1 hybrid, although this pattern could reflect introgression. Using these and additional loci to screen for hybrids in natural populations will allow us to determine whether Veron's (1995) proposal of frequent hybridization applies to this species complex. If F1 hybrids are not detected in large surveys, then the rare occurrence of atypical alleles at some loci probably reflects the fact that ancestral polymorphisms have not yet been completely sorted with respect to current species boundaries (Pamilo and Nei, 1988; Moore, 1995).

The finding of genetic differences between *M. faveolata* and the other two taxa in Panama should allow us to determine whether the same patterns occur at other locations within the range of these species. Of particular interest will be sites in the northern Caribbean. Fertilization studies in the Florida Keys do not reveal clear barriers between *M. faveolata* and the other taxa (Szmant *et al.*, 1997), in contrast to results from similar studies in Panama (Knowlton *et al.*, 1997; Levitan and Knowlton, pers. obs.). Occasional colonies that exhibit mosaic growth forms between *M. faveolata* and *M. annularis* have also been observed in both the Bahamas (Knowlton, pers. obs.) and the Dry Tortugas (E. Weil, pers. comm.). The same primers that amplified the Mfra-gttt1 microsatellite locus in Panama amplified a similar 169 bp band in two *Montastraea* colonies of uncertain taxonomic status from the Florida Keys, suggesting that at least some of the markers we have developed for corals from Panama will have broad geographic utility (Cook *et al.*, 1991).

Molecular genetic analyses of scleractinian corals

Until recently, protein electrophoresis was the primary tool for genetic studies of corals, primarily at the level of species (Ohlhorst, 1984; Ayre *et al.*, 1991; Weil, 1993; Potts *et al.*, 1993; Stobart and Benzie, 1994; Weil and Knowlton, 1994; Garthwaite *et al.*, 1994; Miller and Benzie, 1997) and population (Stoddart, 1984a, 1984b; Heyward and Stoddart, 1985; Willis and Ayre, 1985; Ayre and Willis, 1988; Hunter, 1993; Hellberg, 1994). More recently, DNA-based techniques have been used to determine higher level phylogenies (McMillan and Miller, 1990; McMillan *et al.*, 1991; Chen *et al.*, 1995; Veron *et al.*, 1996; Romano and Palumbi, 1996, 1997), and to analyze or recognize species and populations (McMillan and Miller, 1989; Beauchamp and Powers, 1996; Odorico and Miller, 1997; Lopez and Knowlton, 1997; Hunter *et al.*, 1997; Takabayashi *et al.*, 1998). This is, in principle, straightforward given the wide applicability of the methods; but in practice, the scleractinian coral genome has provided several surprises that remain poorly understood. For example, Romano and Palumbi (1996) used mitochondrial 16S rDNA sequences to define two distantly related clades, whose 29% sequence divergence implied a split predating the origin of coral skeletons 240 million years ago. Nevertheless, three individuals contained sequences from both of these highly divergent clades. Odorico and Miller (1997) also found highly divergent ITS and 5.8S nuclear rDNA sequences within single individuals of several *Acropora* species. These patterns could be interpreted as evidence for evolutionary reticulation. However, extensive inter-individual variation without intra-colony variation has also been reported (*e.g.*, 31% sequence variation among 12 individuals of *Stylophora pistillata;* Takabayashi *et al.*, 1998). Individual genes can also show quite different evolutionary patterns in different coral taxa: ITS sequences exhibit modest to considerable variability between congeneric species in *Acropora* (Odorico and Miller, 1997), *Porites* (Hunter *et al.*, 1997), and *Balanophyllia* (Beauchamp and Powers, 1996), but very little between members of the *Montastraea annularis* complex (Lopez and Knowlton, 1997; Szmant *et al.*, 1997). Identical 16S rDNA sequences for corals in different genera (Romano and Palumbi, 1996) are also surprising.

When genetic variation is low, sequencing individual genes may be less efficient than the use of approaches that screen broadly across the genome. Of these, analysis of AFLPs has considerable promise because it is straightforward, relatively inexpensive, and accessible. It is also probably more reproducible than RAPDs, and therefore more suitable for analyses of field samples (*e.g.*, Janssen *et al.*, 1996; Huys *et al.*, 1996; Majer *et al.*, 1996; Folkertsma *et* *al.*, 1996; this study). Many AFLP loci have already been shown to be inherited in a Mendelian fashion (Vos *et al.*, 1995), although like RAPDs they are dominant markers. Although allozymes remain a valuable tool because of their codominant inheritance and accessibility, the relatively small number of potential loci that can be reliably scored in scleractinians limits their usefulness for discriminating very similar species.

AFLP loci can also be further explored using the standard techniques of molecular biology. These more time-consuming and expensive steps are recommended whenever potential inherent biases in PCR-based methods have not been explored (Vos *et al.*, 1995). More detailed analysis is also essential for understanding the genetic basis of different band patterns and confirming which bands are homologous. The results of our studies of *Montastraea* support the importance of such additional analyses.

For example, the GGAG band pattern differences between *M. faveolata* and the other taxa could in principle have been due to a difference at one locus (resulting in change in fragment size), or differences at two loci (each with a visible band and a null allele). The ability of primers based on the 880 bp band to amplify what appears to be the 920 bp band and the homology of sequences from these amplifications support the former interpretation. When there are many differences between taxa, and distinguishing taxa is the only goal, then knowing the exact number of independent loci is perhaps not a serious issue. However, when there are relatively few loci that distinguish taxa (as is the case here), or when one wishes to recognize hybrids, understanding the basis of observed differences is particularly important.

Interpreting similarity between bands can be likewise complex due to the possibility of comigration of non-homologous fragments (Rieseburg, 1996; Grosberg *et al.*, 1996). Thus we cannot be sure that the AFLP bands shared between *M. annularis* and *M. franksi* are homologous, although this seems likely based on the overall genetic similarity of these two taxa (Van Veghel and Bak, 1993; Weil and Knowlton, 1994; this study). Assessing homology is particularly important in the interpretation of unusual banding patterns—for example, the ATG 630 bp band in a single individual of *M. franksi*, which was found to be homologous to the ATG 630 bp band characteristic of *M. faveolata*.

DNA-based methods for analysis of intraspecific gene flow will be especially difficult when species themselves are poorly defined. For *Montastraea*, there may be a narrow technical window between methods that can detect differences among species, and methods that can detect differences among populations or clones within species (*e.g.*, Coffroth, 1997; Sites and Crandall, 1997). This should be a high priority for future work, as effective conservation biology depends on determining whether regions are genetically interconnected to the extent predicted by current patterns (Roberts, 1997).

Acknowledgments

Early versions of this manuscript were improved by thoughtful discussions with J.C. Stephens and Tom Laughlin. Javier Jara, Juan Mate, and Rob Rowan helped collect the corals and sperm samples. The manuscript was improved by comments from Rob Rowan and anonymous reviewers. The Smithsonian Institution provided financial support. The Government of Panama (Instituto Nacional de Recursos Naturales Renovables and Recoursos Marinos) and the Kuna Nation granted permission for field work and collecting.

Literature Cited

Altschul, S. F., W. Gish, W. Miller, E. W. Myers, and D. J. Lipman. 1990. Basic local alignment search tool. *J. Mol. Biol.* **215:** 403–410.

Avise, J. C. 1994. *Molecular Markers, Natural History and Evolution.* Chapman and Hall, New York.

Avise, J. C., and R. M. Ball Jr. 1990. Principles of genealogical concordance in species concepts and biological taxonomy. *Oxford Surv. Evol. Biol.* **7:** 45–67.

Ayre, D. J., and B. L. Willis. 1988. Population structure in the coral *Pavona cactus:* clonal genotypes show little phenotypic plasticity. *Mar. Biol.* **99:** 495–505.

Ayre, D. J., J. E. N. Veron, and S. L. Dufty. 1991. The corals *Acropora palifera* and *Acropora cuneata* are genetically and ecologically distinct. *Coral Reefs* **10:** 13–18.

Beauchamp, K. A., and D. A. Powers. 1996. Sequence variation of the first internal spacer (ITS-1) of ribosomal DNA in ahermatypic corals from California. *Molec. Mar. Biol. Biotechnol.* **5:** 357–362.

Boecklen, W. J., and D. J. Howard. 1997. Genetic analysis of hybrid zones: numbers of markers and power of resolution. *Ecology* **78:** 2611–2616.

Chen, C. A., D. M. Odorico, M. Ten Lohuis, J. E. N. Veron, and D. J. Miller. 1995. Systematic relationships within the Anthozoa (Cnidaria: Anthozoa) using the 5′-end of the 28S rDNA. *Mol. Phylogenet. Evol.* **4:** 175–183.

Coffroth, M. A. 1997. Molecular approaches to the study of clonal organisms: deciphering the alphabet soup. *Proc. 8th Int. Coral Reef Symp.* **2:** 1603–1608.

Cook, C. B., J. V. Lopez, P. Eng, and E. M. Mueller. 1998. Geographic variation of reef corals in the *Montastraea annularis* complex: Florida vs. Panama. *Abstr. 26th Benthic Ecology Meet.* p. 27.

Cracraft, J. 1989. Speciation and its ontology: the empirical consequences of alternative species concepts for understanding patterns and processes of differentiation. Pp. 28–59 in *Speciation and Its Consequences.* D. Otte and J. A. Endler, eds. Sinauer, Sunderland, MA.

Folkertsma, R. T., J. N. A. M. R. van der Voort, K. E. de Groot, P. M. van Zandvoort, A. Schots, F. J. Gommers, J. Helder, and J. Bakker. 1996. Gene pool similarities of potato cyst nematode populations assessed by AFLP analysis. *Mol. Plant-Microbe Interact.* **9:** 47–54.

Foltz, D. W. 1997. Hybridization frequency is negatively correlated with divergence time of mitochondrial DNA haplotypes in a sea star (*Leptasterias* spp.) species complex. *Evolution* **51:** 283–288.

Garthwaite, R. L., D. C. Potts, J. E. N. Veron, and T. J. Done. 1994. Electrophoretic identification of poritid species (Anthozoa: Scleractinia). *Coral Reefs* **13:** 49–56.

Grosberg, R. K., D. R. Levitan, and B. B. Cameron. 1996. Characterization of genetic structure and genealogies using RAPD-PCR markers: A random primer for the novice and the nervous. Pp. 67–100 in *Molecular Zoology: Advances, Strategies and Protocols,* J. D. Ferraris and S. R. Palumbi, eds. Wiley-Liss, New York.

Hayes, J. A. 1990. Distribution, movement and impact of the corallivorous gastropod *Coralliophila abbreviata* (Lamarck) on a Panamanian patch reef. *J. Exp. Mar. Biol. Ecol.* **142:** 25–42.

Hellberg, M. E. 1994. Relationships between inferred levels of gene flow and geographic distance in a philopatric coral, *Balanophyllia elegans. Evolution* **48:** 1829–1854.

Heyward, A. J., and J. A. Stoddart. 1985. Genetic structure of two species of *Montipora* on a patch reef: conflicting results from electrophoresis and histocompatibility. *Mar. Biol.* **85:** 117–121.

Howard, D. J., R. W. Preszler, J. Williams, S. Fenchel, and W. J. Boecklen. 1997. How discrete are oak species? Insights from a hybrid zone between *Quercus grisea* and *Quercus gambelii. Evolution* **51:** 747–755.

Hunter, C. L. 1993. Genotypic variation and clonal structure in coral populations with different disturbance histories. *Evolution* **47:** 1213–1228.

Hunter, C., C. W. Morden, and C. M. Smith. 1997. The utility of ITS sequences in assessing relationships among zooxanthellae and corals. *Proc. 8th Int. Coral Reef Symp.* **2:** 1599–1602.

Huys, G., I. Kersters, R. Coopman, P. Janssen, and K. Kersters. 1996. Genotyping diversity among aeromonas isolates recovered from drinking water production plants as revealed by AFLP™ analysis. *Syst. Appl. Micro.* **19:** 428–435.

Janssen, P., R. Coopman, G. Huys, J. Swings, M. Bleeker, P. Vos, M. Zabeau, and K. Kersters. 1996. Evaluation of the DNA fingerprinting method AFLP as a new tool in bacterial taxonomy. *Microbiology* **142:** 1881–1893.

Jarne, P., and P. J. L. Lagoda. 1996. Microsatellites, from molecules to populations and back. *Trends Ecol. Evol.* **11:** 424–429.

Knowlton, N., and L. A. Weigt. 1997. Species of marine invertebrates: a comparison of the biological and phylogenetic species concepts. Pp. 199–219 in *Species: the Units of Biodiversity,* M. F. Claridge, H. A. Dawah, and M. R. Wilson, eds. Systematics Assoc. Spec. Vol. Ser. 54, Chapman and Hall, London.

Knowlton, N., E. Weil, L. A. Weigt, and H. M. Guzman. 1992. Sibling species in *Montastraea annularis,* coral bleaching, and the coral climate record. *Science* **255:** 330–333.

Knowlton, N., J. L. Mate, H. M. Guzman, R. Rowan, and J. Jara. 1997. Direct evidence for reproductive isolation among the three species of the *Montastraea annularis* complex in Central America (Panama, Honduras). *Mar. Biol.* **127:** 705–711.

Lessios, H. A., and J. S. Pearse. 1996. Hybridization and introgression between Indo-Pacific species of *Diadema. Mar. Biol.* **126:** 715–723.

Lopez, J. V., and N. Knowlton. 1997. Discrimination of species in the *Montastraea annularis* complex using multiple genetic loci. *Proc. 8th Int. Coral Reef Symp.* **2:** 1613–1618.

Majer, D., R. Mithen, B. G. Lewis, P. Vos, and R. P. Oliver. 1996. The use of AFLP fingerprinting for the detection of genetic variation in fungi. *Mycol. Res.* **100:** 1107–1111.

Mallet, J. 1995. A species definition for the Modern Synthesis. *Trends Ecol. Evol.* **10:** 294–299.

McMillan, J., and D. J. Miller. 1989. Restriction analysis and DNA hybridization applied to the resolution of *Acropora nobilis* from *Acropora formosa. Proc. 6th Intl. Coral Reef Symp.* **2:** 775–777.

McMillan, J., and D. J. Miller. 1990. Highly repeated DNA sequences in the scleractinian coral genus *Acropora:* evaluation of cloned repeats as taxonomic probes. *Mar. Biol.* **104:** 483–487.

McMillan, J., D. Yellowlees, A. Heyward, P. Harrison, and D. J. Miller. 1988. Preparation of high molecular weight DNA from hermatypic corals and its use for DNA hybridization and cloning. *Mar. Biol.* **98:** 271–276.

McMillan, J., T. Mahoney, J. E. N. Veron, and D. J. Miller. 1991. Nucleotide sequencing of highly repetitive DNA from seven species in the coral genus *Acropora* (Cnidaria: Scleractinia) implies a division contrary to morphological criteria. *Mar. Biol.* **110:** 323–327.

Miller, K., and R. Babcock. 1997. Conflicting morphological and reproductive species boundaries in the coral genus *Platygyra. Biol. Bull.* **192:** 98–110.

Miller, K. J., and J. A. H. Benzie. 1997. No clear genetic distinction between morphological species within the coral genus *Platygyra. Bull. Mar. Sci.* **61:** 907–917.

Moore, W. S. 1995. Inferring phylogenies from mtDNA variation: mitochondrial-gene trees versus nuclear-gene trees. *Evolution* **49:** 718–726.

Mueller, U. G., S. E. Lipari, and M. G. Milgroom. 1996. Amplified fragment length polymorphism (AFLP) fingerprinting of symbiotic fungi cultured by the fungus-growing ant *Cyphomyrmex minutus. Mol. Ecol.* **5:** 119–122.

Nei, M., and W. H. Li. 1979. Mathematical model for studying genetic variation in terms of restriction endonucleases. *Proc. Natl. Acad. Sci. USA* **76:** 5269–5273.

Odorico, D. M., and D. J. Miller. 1997. Variation in the ribosomal internal transcribed spacers and 5.8S rDNA among five species of *Acropora* (Cnidaria; Scleractinia): Patterns of variation consistent with reticulate evolution. *Mol. Biol. Evol.* **14:** 465–473.

Ohlhorst, S. L. 1984. The use of polyacrylamide gel electrophoresis in coral taxonomy. *Palaeont. Am.* **54:** 45–48.

Pamilo, P., and M. Nei. 1988. Relationships between gene trees and species trees. *Mol. Biol. Evol.* **5:** 568–583.

Potts, D. C., A. F. Budd, and R. L. Garthwaite. 1993. Soft tissue vs. skeletal approaches to species recognition and phylogeny reconstruction in corals. *Cour. Forsch.-Inst. Senckenberg* **164:** 221–231.

Rice, W. R. 1989. Analyzing tables of statistical tests. *Evolution* **43:** 223–225.

Rieseberg, L. H. 1996. Homology among RAPD fragments in interspecific comparisons. *Mol. Ecol.* **5:** 99–105.

Roberts, C. M. 1997. Connectivity and management of Caribbean coral reefs. *Science* **278:** 1454–1457.

Romano, S. L., and S. R. Palumbi. 1996. Evolution of scleractinian corals inferred from molecular systematics. *Science* **271:** 640–642.

Romano, S. L., and S. R. Palumbi. 1997. Molecular evolution of a portion of the mitochondrial 16s ribosomal gene region in scleractinian corals. *J. Mol. Evol.* **45:** 397–411.

Rowan, R., and N. Knowlton. 1995. Intraspecific diversity and ecological zonation in coral algal symbiosis. *Proc. Natl. Acad. Sci. USA* **92:** 2850–2853.

Rowan, R., and D. A. Powers. 1991. Molecular genetic identification of symbiotic dinoflagellates (zooxanthellae). *Mar. Ecol. Prog. Ser.* **71:** 65–73.

Sambrook, J., E. F. Fritsch, and T. Maniatis. 1989. *Molecular Cloning: A Laboratory Manual.* Cold Spring Harbor Laboratory, Cold Spring Harbor, NY.

Sites, J. W. Jr., and K. A. Crandall. 1997. Testing species boundaries in biodiversity studies. *Conserv. Biol.* **11:** 1289–1297.

Southern, E. M. 1975. Detection of specific sequences among DNA fragments separated by gel electrophoresis. *J. Mol. Biol.* **98:** 503–517.

Stephens, J. C., D. A. Gilbert, N. Yuhki, and S. J. O'Brien. 1992. Estimation of heterozygosity for single-probe multilocus DNA fingerprints. *Mol. Biol. Evol.* **9:** 729–743.

Stobart, B., and J. A. H. Benzie. 1994. Allozyme electrophoresis demonstrates that the scleractinian coral *Montipora digitata* is two species. *Mar. Biol.* **118:** 183–190.

Stoddart, J. A. 1984a. Genetic differentiation amongst populations of the coral *Pocillopora damicornis* off southwestern Australia. *Coral Reefs* **3:** 149–156.

Stoddart, J. A. 1984b. Genetical structure within populations of the coral *Pocillopora damicornis. Mar. Biol.* **81:** 19–30.

Suchanek, T. H., J. B. Geller, B. R. Kreiser, and J. B. Mitton. 1997. Zoogeographic distributions of the sibling species *Mytilus galloprovincialis* and *M. trossulus* (Bivalvia: Mytilidae) and their hybrids in the north Pacific. *Biol. Bull.* **193:** 187–194.

Szmant, A. 1991. Sexual reproduction by the Caribbean corals *Montastraea annularis* and *M. cavernosa. Mar. Ecol. Prog. Ser.* **74:** 13–25.

Szmant, A. M., E. Weil, M. W. Miller, and D. E. Colon. 1997. Hybridization within the species complex of the scleractinian coral *Montastraea annularis. Mar. Biol.* **129:** 561–572.

Takabayashi, M., D. Carter, S. Ward, and O. Hoegh-Guldberg. 1998. Inter- and intra-specific variability in rDNA sequence in the ITS region of corals. *Proc. Austral. Coral Reef Soc. 75th Ann. Conf.* 237–244.

Templeton, A. R. 1989. The meaning of species and speciation: a genetic perspective. Pp. 3–27 in *Speciation and its Consequences,* D. Otte and J. A. Endler, eds. Sinauer, Sunderland, MA.

Tomascik, T. 1990. Growth rates of two morphotypes of *Montastraea annularis* along a eutrophication gradient, Barbados, W. I. *Mar. Poll. Bull.* **21:** 376–380.

Van Veghel, M. L. J. 1994. Reproductive characteristics of the polymorphic Caribbean reef building coral *Montastraea annularis.* I. Gametogenesis and spawning behavior. *Mar. Ecol. Prog. Ser.* **109:** 209–219.

Van Veghel, M. L. J., and R. P. M. Bak. 1993. Intraspecific variation of a dominant Caribbean reef-building coral, *Montastraea annularis:* genetic, behavioral and morphometric aspects. *Mar. Ecol. Prog. Ser.* **92:** 255–265.

Van Veghel, M. L. J., and R. P. M. Bak. 1994. Reproductive characteristics of the polymorphic Caribbean reef-building coral *Montastraea annularis.* III. Reproduction in damaged and regenerating colonies. *Mar. Ecol. Prog. Ser.* **109:** 229–233.

Van Veghel, M. L. J., and H. Bosscher. 1995. Variation in linear growth and skeletal density within the polymorphic reef building coral *Montastraea annularis. Bull. Mar. Sci.* **56:** 902–908.

Van Veghel, M. L. J., and M. E. H. Kahmann. 1994. Reproductive characteristics of the polymorphic Caribbean reef building coral *Montastraea annularis.* II. Fecundity and colony structure. *Mar. Ecol. Prog. Ser.* **109:** 221–227.

Van Veghel, M. L. J., D. F. R. Cleary, and R. P. M. Bak. 1996. Interspecific interactions and competitive ability of the polymorphic reef-building coral *Montastraea annularis. Bull. Mar. Sci.* **58:** 792–803.

Veron, J. E. N. 1995. *Corals in Space and Time: The Biogeography and Evolution of the Scleractinia.* UNSW Press, Sydney, Australia.

Veron, J. E. N., D. M. Odorico, C. A. Chen, and D. J. Miller. 1996. Reassessing evolutionary relationships of scleractinian corals. *Coral Reefs* **15:** 1–9.

Vos, P., R. Hogers, M. Bleeker, M. Reijans, T. van de Lee, M. Hornes, A. Frijters, J. Pot, J. Peleman, M. Kuiper, and M. Zabeau. 1995. AFLP: a new technique for DNA fingerprinting. *Nucl. Acids Res.* **23:** 4407–4414.

Weil, E. 1993. Genetic and morphological variation in Caribbean and eastern Pacific *Porites* (Anthozoa, Scleractinia). Preliminary results. *Proc. 7th Inter. Coral Reef Symp.* **2:** 643–656.

Weil, E., and N. Knowlton. 1994. A multi-character analysis of the Caribbean coral *Montastraea annularis* (Ellis and Solander, 1786) and its two sibling species, *M. faveolata* (Ellis and Solander, 1786) and *M. franksi* (Gregory, 1895). *Bull. Mar. Sci.* **55:** 151–175.

Willis, B. L., and D. J. Ayre. 1985. Asexual reproduction and genetic determination of growth form in the coral *Pavona cactus:* biochemical genetic and immunologic evidence. *Oecologia* **65:** 516–525.

Willis, B. L., R. C. Babcock, P. L. Harrison, and C. C. Wallace. 1997. Experimental hybridization and breeding incompatibilities within the mating systems of mass spawning reef corals. *Coral Reefs* **16, Suppl.:** S53–S65.

Yuhki, N., and S. J. O'Brien. 1990. DNA variation of the mammalian major histocompatibility complex reflects genomic diversity and population history. *Proc. Natl. Acad. Sci. USA* **87:** 836–840.

Zabeau, M., and P. Vos. 1995. Selective restriction fragment amplification: a general method for DNA fingerprinting. European Patent Application, Publ # 0534858-A1, Office Europeen des Brevets, Paris.

Reference: *Biol. Bull.* **196:** 94–104. (February, 1999)

Ultraviolet Radiation and Distribution of the Solitary Ascidian *Corella inflata* (Huntsman)

BRIAN L. BINGHAM[1,*] AND NATHALIE B. REYNS[2]

[1] *Huxley College of Environmental Studies, Western Washington University, Bellingham, Washington 98225; and* [2] *Marine Sciences Research Center, State University of New York, Stony Brook, New York 11794*

Abstract. The solitary ascidian *Corella inflata* is a common fouling organism in many areas of Puget Sound and the San Juan Archipelago, Washington, USA. Despite its abundance, it is conspicuously absent from areas that receive direct sunlight. Previous work suggests that ascidians in unshaded habitats can be overgrown and killed by algal overgrowth. In this study, we tested the hypothesis that UV irradiation contributes to *C. inflata* distribution by killing individuals exposed to direct sunlight. To test this, we exposed *C. inflata* embryos, larvae, juveniles, and adults to UV irradiation and measured the responses. We also tested for UV-absorbing compounds in larvae, juveniles, and adults. In the laboratory, UV significantly damaged all life stages; the earliest stages were most vulnerable. A 3-week UV exposure significantly shortened adult life span. Juveniles suffered 100% mortality after only 3 days. Tadpole larvae decreased settlement and metamorphosis after 1 day of UV exposure, and embryos exhibited developmental abnormalities after only 30 minutes of exposure. None of the life-history stages had apparent UV-absorbing compounds. Given the vulnerability of this species to UV, we suggest that its unique life-history traits (*i.e.*, time of spawning, brooding behavior, length of larval life) help it persist in its preferred habitat and avoid dispersal into inappropriate, UV-exposed areas.

Introduction

Corella inflata (Huntsman) is a solitary ascidian common throughout Puget Sound, Washington, and in waters off the west coast of British Columbia. It occurs from the intertidal zone to 45 m (Van Name, 1945) but is most abundant on docks and pilings (Young, 1982). Adults, which may reach 5 cm in length, have a thin, transparent outer tunic. This is in marked contrast to the tough, opaque tunic that protects most other solitary ascidians.

Lambert (1968) studied a population of *C. inflata* in a Puget Sound marina for 12 months and observed mass mortality in the early spring. The mortality coincided with a period of heavy diatom growth, and Lambert suggested that smothering diatom mats were responsible for the ascidian deaths. This conclusion was supported by observations that mass mortality occurred only in areas exposed to full solar radiation; *C. inflata* in shaded habitats survived.

Recent research suggests that another factor may contribute to mortality of *C. inflata* in exposed areas. Increasing interest in the status of the stratospheric ozone layer has led to intense study of the deleterious effects of ultraviolet radiation (UV). Jokiel (1980) first demonstrated the damaging effects of UV radiation on tropical marine invertebrates (including ascidians). More recent work has shown that the UV-B portion of the spectrum (280–320 nm) is particularly lethal to marine bacteria, plankton, invertebrates, and fish (reviewed by Worrest, 1982; Hardy and Gucinski, 1989; see also Shick *et al.*, 1991; Karentz *et al.*, 1991; Karentz, 1994a, b). There are indications that marine invertebrate embryos and larvae may be particularly sensitive to solar radiation (Damkaer *et al.*, 1980; Pennington and Emlet, 1986; Biermann *et al.*, 1992; Adams and Shick, 1996).

The habitat (primarily shallow water) and anatomy (thin, transparent tunic) of *C. inflata* may make it particularly vulnerable to UV damage, and the effects may not be limited to adult animals. Unlike most solitary ascidians, *C. inflata* holds its embryos in a spacious brood chamber. The eggs are buoyant and float to the top of the chamber where there is potential for UV-induced damage during development.

Received 26 November 1997; accepted 6 November 1998.

[*] To whom correspondence should be addressed. E-mail: bingham@cc.wwu.edu

The purpose of this study was to determine how UV radiation affects *Corella inflata*. We examined field distributions of ascidians to determine whether population density was correlated with UV exposure. We measured the vulnerability of embryos, larvae, juveniles, and adults to UV damage. Finally, we examined larvae, juveniles, and adults for UV-absorbing compounds.

Materials and Methods

Field sampling

We selected docks in two marinas (Anacortes Marina and Skyline Marina) in Anacortes, Washington, for the field portion of this study. These marinas have similar construction designs, with docks that project out into a sheltered embayment. A roof shades inner dock slips, but outer slips are not covered and receive full sunlight. Because the docks rise and fall with the tides, they harbor diverse invertebrate communities including sponges, hydrozoans, polychaetes, barnacles, bivalves, bryozoans, and ascidians (particularly *Corella inflata*). Macroalgae are absent from most docks at both locations.

At each marina, we chose four nonadjacent slips (two shaded and two exposed) for detailed study. Five permanent sampling locations were marked at 2.5-m intervals along each slip. We measured *C. inflata* densities at each location by placing a 25 × 25 cm quadrat on the side of the slip just below the water's surface and counting all *C. inflata* individuals within the quadrat. We made counts in June and again in August, 1994.

To determine how the density of *C. inflata* related to UV exposure, we measured spectral irradiance 5 cm below the water's surface at each quadrat location. Measurements (from 300–700 nm at 2-nm intervals) were made with a LI-COR 1800UW spectroradiometer (see Kirk *et al.*, 1994, for a discussion of the measurement characteristics of this instrument) on a clear sunny day (15 July 1994) at 1300 h. We also measured light attenuation in the marinas by taking spectral scans at 50 cm and 1 m at several exposed quadrat locations. Finally, we went just outside the entrance to the Skyline Marina and measured light at 1-m intervals from the surface to 20 m. This allowed us to determine penetration of UV-A and UV-B in the local waters.

Because we could not measure the complete UV-B spectrum (from 280–320 nm) due to limitations of the instrument, we used a 2nd order regression of the data from 300–320 nm to extrapolate the curves from 280 to 300 nm. We then integrated the data files to get separate measurements of total UV-B (280–320 nm), UV-A (320–400 nm), and PAR (photosynthetically active radiation, 400–700 nm).

Because algal overgrowth could be a confounding factor in our sampling, we monitored algal growth at the study sites. We hung transparent acrylic strips (2-cm wide × 15-cm long) at all quadrat locations. After 6 weeks (1 July–15 August, 1994), they were collected and two 4-cm^2 areas, one at 5 cm and the other at 15 cm, were wiped with a GFF filter. We extracted the filters in 90% acetone for 24 h and made fluorometric readings of chlorophyll *a* (Parsons *et al.*, 1984). The two values were averaged to give a measurement of algal growth at each quadrat location.

Laboratory experiments

To measure the sensitivity of *C. inflata* to UV, we used an enclosed, flow-through seawater tank equipped with two UV bulbs (Q-Panel Company, UVB-313) and two cool-white fluorescent bulbs. A cellulose acetate bulb sheath filtered out wavelengths less than 290 nm. The tank was divided into two sections with nylon netting. The control section was covered by a UV-filtering shield (Atohaas North America, Plexiglas UF3, 3-mm thickness) that reflected wavelengths below 400 nm. To compare light in the two treatments, we measured the irradiance spectra in the shielded and unshielded portions of the tank (at 5-cm depth) with the spectroradiometer.

Adult sensitivity. To determine if UV exposure affects adult *C. inflata*, we placed 20 individuals in 240-ml polypropylene cups from which the bottoms had been removed and replaced with Nitex screen. A slit in a piece of open-cell foam attached to the inside wall of the cups held the ascidians in a normal position (horizontal with the excurrent siphon and brood chamber up; Young, 1988) but was flexible enough to allow normal feeding. The cups were randomly assigned to either UV-exposed ($n = 10$) or shielded ($n = 10$) treatments. Foam collars kept the cups floating with the adults about 3 cm below the surface of the water. The tank was placed on a 15:9 h light/dark cycle and survival was monitored for 22 days. Life spans (up to 22 days) in the two treatments were compared by one-way ANOVA. We set α at 0.05 for all statistical analyses and used Hartley's $F_{\max}$ test (Sokal and Rohlf, 1995) to test for homogenous variances before each analysis.

Juvenile sensitivity. We collected larvae by exposing adult *C. inflata* to bright light shortly after collection. Thirty larvae were placed in each of 12 roughened polystyrene petri dishes (100-mm diameter, 15-mm deep) and allowed to settle. Positions of the juveniles were marked with a permanent ink marker on the back of the dishes. We filled the dishes with fresh seawater and randomly assigned them to the UV-exposed ($n = 6$) or shielded ($n = 6$) treatments. Mortality was determined after 4 days of treatment. Because of unequal variances, we used a Kruskal-Wallis nonparametric ANOVA to compare treatments.

Larval sensitivity. Tadpole larvae were exposed to UV radiation to measure effects on settlement. Six petri dishes containing 30 newly released, swimming tadpole larvae were randomly assigned to the UV-exposed ($n = 3$) or shielded ($n = 3$) sections of the tank. Percent settlement in each treatment was determined after one light cycle (15 h UV exposure). Treatments were compared by one-way ANOVA.

We also subjected tadpole larvae to different periods of UV exposure to determine a damage threshold. Twenty-one replicate petri dishes (with 30 newly released tadpole larvae per dish) were prepared. Three dishes (the 0-exposure control) were placed in the shielded portion of the tank. The other 18 dishes were exposed to the UV light. At 30-min intervals, we moved three randomly chosen plates into the shielded portion of the tank until all plates had been moved over. Twenty-four hours later, percent settlement was determined for all plates. We analyzed the relationship between UV exposure time and percent settlement by simple linear regression.

Sensitivity of developing embryos. Approximately 75 adults were light shocked to obtain fertilized eggs. Eggs from all the adults were mixed and 30 were arbitrarily assigned to each of 21 petri dishes. The developing embryos were exposed to UV radiation in the experimental tank (in groups of three replicate dishes). Exposure intervals were staggered as described above to determine the threshold at which development becomes abnormal. After 24 h, all dishes were examined and the proportion of eggs that had (1) reached the tadpole stage, (2) arrested development at the morula stage, or (3) become abnormal at, or before, the 16-cell stage was determined. We used a chi-square test for independence to determine whether length of UV exposure affected the developmental stage the embryos reached. To avoid sacrificial pseudoreplication (Hurlburt, 1984), we analyzed only one randomly chosen replicate from each exposure period.

Outplants

To determine if recruiting *C. inflata* could survive in exposed areas of the marina where they were not usually found, newly settled ascidians were transplanted into the field. In the laboratory, 30 tadpole larvae were placed in 100-mm diameter petri dishes ($n = 20$) and allowed to settle. Settlement locations were marked on the back side of each dish with a permanent marker and five marked plates were hung vertically, front side out, on four slips in Skyline Marina (two shaded and two unshaded). After 6 days, we compared survival of the juveniles in the shaded and exposed treatments with a Kruskal-Wallis nonparametric ANOVA.

Recruitment

We monitored *C. inflata* recruitment to determine whether larvae ever colonize exposed docks. Six 100-mm diameter cement plates were hung from two shaded and two unshaded slips in Anacortes Marina and left in place from 8 July to 15 August, 1994. We then collected the plates, counted the recruits, and used correlation analysis to test for relationships between irradiance, algal growth, and adult density and number of recruits.

If algal overgrowth causes mortality of *C. inflata* at our site, larvae should avoid settling on algal-covered surfaces (such as those in exposed sites). We tested this by placing 15 roughened petri dishes (100-mm diameter) in Skyline Marina. Three of the dishes hung from a covered dock where darkness prevented algal growth. The remaining 12 dishes hung from a dock exposed to full sunlight. After 2 weeks, the exposed dishes had developed a layer of filamentous algae. We collected all the dishes and divided them among three treatments: no algal cover (3 dishes from the covered dock), 100% algal cover (3 dishes from the exposed dock), and 50% algal cover (9 exposed dishes that we carefully scraped to remove the algae from half of the bottom surface). The dishes were filled with fresh seawater and 30 *C. inflata* tadpole larvae were added to each. After 24 h, settlement in each dish was recorded. Settlement in 100% algal-covered dishes ($n = 3$) was compared to dishes with no algae ($n = 3$) with one-way ANOVA. We used a paired Student's t test to compare larval settlement in clean or algal-fouled halves of the scraped dishes ($n = 9$).

UV-absorbing compounds

To determine whether *C. inflata* has UV-absorbing substances, we extracted compounds from three large adults (between 1.5 and 2.5 cm long), five juveniles (less than 1.0 cm long), and the pooled tadpole larvae from 50–75 adults. The tunics were removed from the adults and analyzed separately from the bodies (we hypothesized that UV-absorbing compounds, if present, would be concentrated in the tunic). The bodies were carefully cleaned to remove all feces and gut material and ensure that only *C. inflata* compounds were measured. Tadpole larvae were collected by light shocking adults. We lyopholized and extracted the samples in 80% methanol as described by Karentz *et al.* (1991). Absorbance of the extracts was measured spectrophotometrically at 2-nm intervals from 280 to 400 nm.

The dry weights of the *C. inflata* samples were unequal (large tunics = 120 mg, large bodies = 100 mg, small tunics = 170 mg, small bodies = 100 mg, tadpole larvae = 120 mg). To permit direct comparison among the samples, we calculated relative absorptivity by the following equation.

$$\text{relative absorptivity} = \frac{\text{Measured absorbance}}{\text{path length (cm)} \times \left(\dfrac{\text{tissue dry weight (mg)}}{\text{solvent volume (ml)}}\right)}$$

This equation is derived from Beer's law (Skoog and

West, 1974) except that absorptivity in Beer's law is the molar absorptivity of a single absorbing substance. Since we do not know the composition of our extracts, we consider absorptivity in this case to be a relative measure.

To test the effectiveness of the tunic as a physical barrier to UV damage, we dissected the tunics from one juvenile and one adult *C. inflata,* placed them directly in the spectrophotometer light path and measured absorbance from 280 to 400 nm. By substituting tunic thickness ($\approx$900 μm) for path length and tunic density ($g \cdot cm^{-3}$) for the concentration measure in the above equation, we calculated relative absorptivities that were directly comparable to those measured with the extracts.

Results

Field sampling

Corella inflata was entirely restricted to shaded slips in both marinas, and densities decreased toward the slip ends where shading was less complete. At both marinas, there was a strong negative relationship between algal growth (as measured by Chl *a* concentration on acrylic strips) and *C. inflata* density and between UV irradiance and *C. inflata* density (Fig. 1). The relationship between *C. inflata* density and UV-B irradiance alone followed the same pattern and had similarly high correlations ($r = -0.88$, $P < 0.001$ for Anacortes Marina and $r = -0.68$, $P < 0.001$ for Skyline Marina). There was an apparent threshold in both irradiance and chlorophyll concentration above which few *C. inflata* individuals occurred. This threshold corresponded to the point at which slips were no longer shaded. There was essentially no change in densities of ascidians between the two sampling dates (June and August).

A vertical profile showed a logarithmic decrease in UV irradiance with depth (Fig. 2). UV-B was detected to 5 m. Levels of UV-B corresponding to threshold intensities for adult distributions in the marinas (Fig. 1) occurred at depths between 1.5 and 2 m. UV-A was measurable to 14 m.

Laboratory experiments

Light levels in our experimental tank differed significantly from those measured in the field. Although total UV-B irradiances were remarkably similar, total UV-A was 30 times lower in our tank than in the field; total PAR was 32 times lower (Table I). Closer examination of individual spectra reveals that tank and field light quality differed within these wavelength ranges. UV in the experimental tank was skewed to the more biologically damaging, low wavelengths (Fig. 3). Without a weighting function for this species, we cannot determine how this affected the experimental animals. It is likely, however, that the tank overemphasized low-wavelength UV-B effects and under-emphasized UV-A and PAR effects. The Plexiglas shield effectively removed all UV-B and UV-A from the shielded portion of the tank. The shield also caused an 8.5% drop in total PAR, with the greatest effect at wavelengths between 400 and 415 nm (Table I, Fig. 4).

Adult sensitivity. At irradiances present in the tank, UV damaged all *C. inflata* life-history stages. After 8 days, exposed adults became opaque and many were dead after 10 days; after 21 days, all exposed animals were dead. Control animals also experienced some mortality, probably due to handling. However, mortality rates were lower and leveled off after 17 days. The average life span of the UV-exposed adults (mean = 13.9 ± 1.2 d SD) was significantly lower than that of the shielded controls (18.0 ± 1.1 d, $F = 5.8$, $P = 0.02$) within the 21 days of the experiment. This result underestimates the true effect because the experiment was terminated at 22 days and many of the control animals were still living.

Juvenile sensitivity. UV exposure affected juveniles even more strongly than it did adults. In the laboratory, juveniles in the exposed treatment showed 100% mortality after only 4 days (controls had 57.0% ± 11% mortality, $H = 9.46$, $P = 0.002$). Similar results were seen in the field outplants. All juveniles had disappeared from dishes in the unshaded habitat after only 3–6 days, whereas 36.6% ± 8.3% of the shaded juveniles were still alive at the end of the experiment ($H = 7.27$, $P = 0.007$). Examination of the dishes in which the juveniles were outplanted revealed minimal algal growth, suggesting that overgrowth was not responsible for the mortality.

Larval sensitivity. Very few *C. inflata* larvae exposed to UV light settled successfully in the laboratory (2.3% ± 0.4% compared to 56.8% ± 0.8% for the shielded individuals, $F = 56.4$, $P = 0.001$). This underestimates the true effect because many larvae that had not settled in the shielded treatment were still actively swimming; all exposed larvae were dead. The effects of exposure were cumulative; as exposure time increased, settlement success decreased (Fig. 5).

Sensitivity of developing embryos. UV interfered with the normal development of *C. inflata* embryos (Fig. 6, χ^2 for one set of replicates = 303.48, $P < 0.001$). Even limited exposure had significant developmental consequences. After only 30 min of exposure, less than 20% of the embryos developed to tadpole stage. As exposure time increased, early cleavages became more abnormal, with many embryos failing to pass the 4- or 8-cell stages. No normal development occurred after 1.5 h of UV exposure.

Settlement and recruitment

Of 199 *C. inflata* individuals recruiting to plates in Anacortes Marina, 181 (90.9%) were on plates on shaded slips. The remaining 18 recruits on exposed plates were

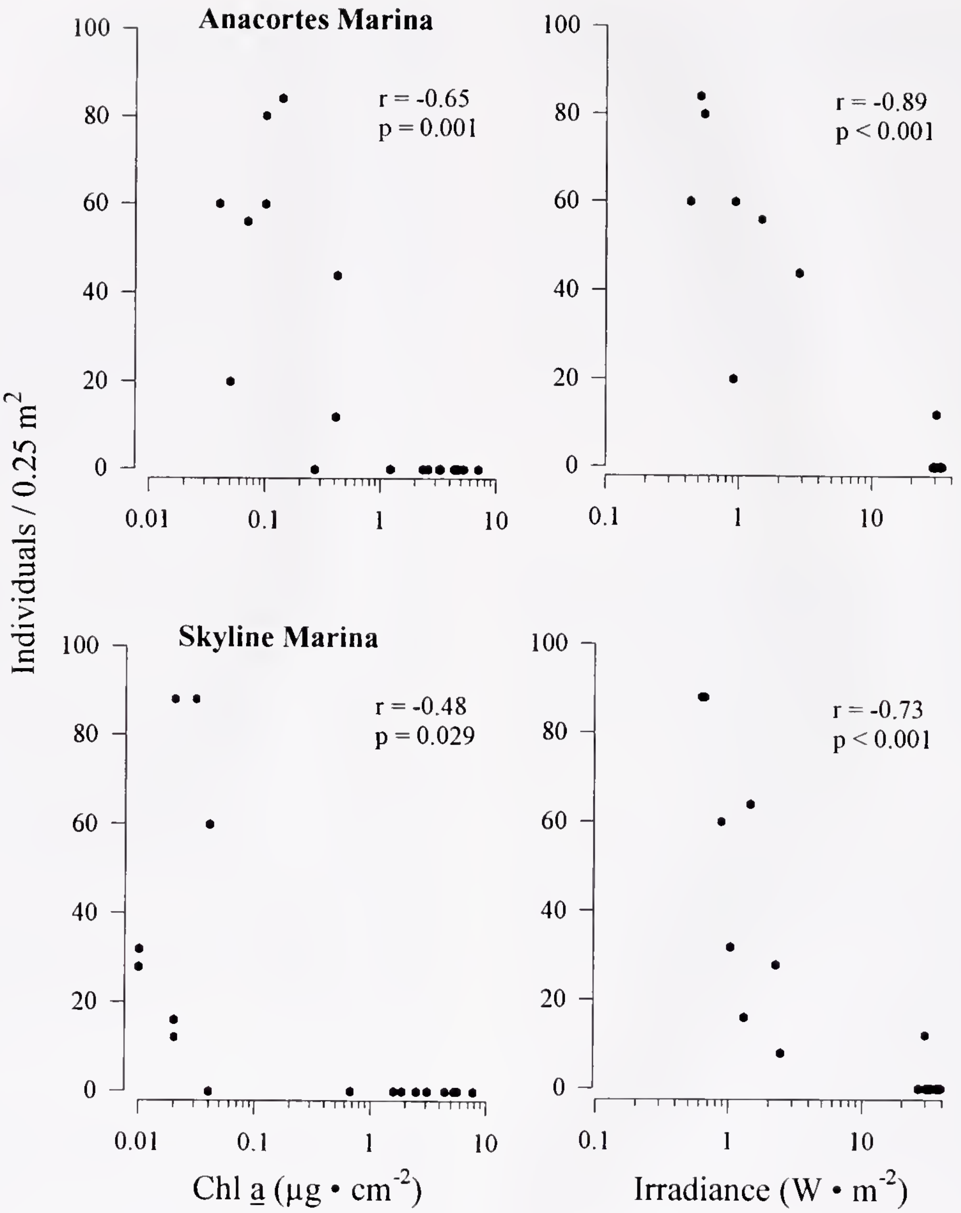

Figure 1. Density of *Corella inflata* in Anacortes and Skyline Marinas. Densities are plotted as a function of Chl *a* concentration (based on overgrowth of clear acrylic strips) and UV irradiance (300–400 nm). Correlation coefficients (*r*) and *P* values are shown.

on the lower edges where they were shaded by the plate itself.

In laboratory assays, a developed algal mat did not affect *C. inflata* settlement. Similar numbers of larvae settled successfully and metamorphosed on clean and algal-fouled surfaces, and larvae showed no preference for clean rather than algal-fouled surfaces when given a choice (Fig. 7). However, because of low replication, the power of these tests was low ($\beta = 0.65$ for the single choice and 0.24 for the preference experiment; Cohen, 1988). Levels of algal fouling in the dishes reached 0.08 μg Chl *a* · cm^{-2}.

UV-absorbing compounds

All methanol extracts showed minor absorptivity peaks in the UV range (Fig. 8). Tunic extracts absorbed much less UV than extracts of the bodies. Absorbance was greatest for the bodies of small specimens of *C. inflata*. Tadpole extracts showed a small peak at 290 nm. The peaks (λ_{max}) differed slightly among the samples, but all were between 294 and 300 nm. None fell within the wavelength range in which sunscreening mycosporine-like amino acids normally occur. The tunic provided little physical barrier to UV: absorptivi-

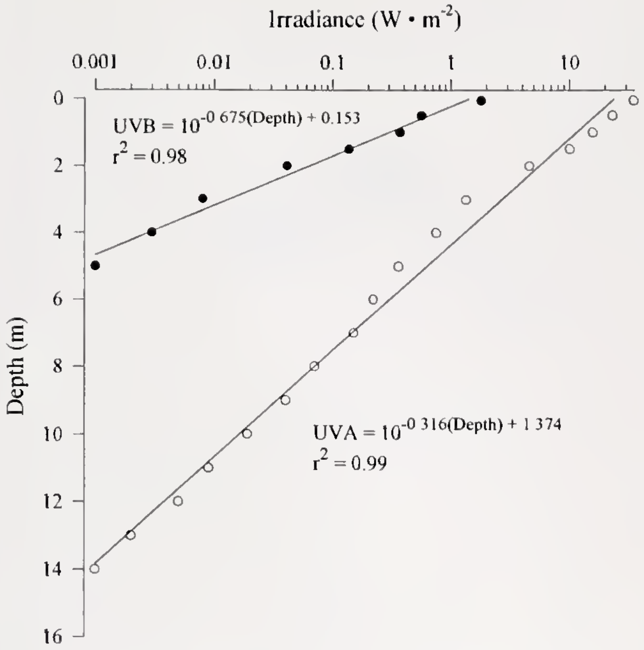

Figure 2. Penetration of UV-B (300–320 nm) and UV-A (320–400 nm) in the water column at the entrance to Skyline Marina. Simple regression lines and equations are shown. Measurements were made at 1300 h on 15 July 1994.

ties were only slightly above those seen in the chemical extracts (Fig. 8). For comparison, we calculated the relative absorptivity of mylar (a synthetic material that filters wavelengths <315 nm). Mylar relative absorptivity at 294 nm was 0.34.

Discussion

Unlike many Puget Sound ascidians, which occur primarily in subtidal benthic habitats, *Corella inflata* is found in greatest abundance on floating docks (Young, 1982). It is not normally found on fixed intertidal structures because it does not tolerate desiccation. The dock habitat may be a refuge from benthic predators that prefer this species to other ascidians that have thicker, heavier tunics (Young, 1985). However, although these artificial substrates may provide protection from predators, they expose *C. inflata* to hazards associated with high levels of solar radiation.

Young and Chia (1984) outplanted juveniles of *C. inflata* to subtidal locations at 4.5-m depths in shaded and unshaded dishes. Mortality was significantly higher in the unshaded dishes, presumably due to algal overgrowth (though this is still within the range to which UV penetrates; Fig. 2). Since algal overgrowth apparently can kill juveniles, we predicted that larvae should detect and avoid algal-filmed surfaces, particularly since larvae of many ascidian species show strong settlement specificity (reviewed by Svane and Young, 1989). In laboratory testing, however, larvae settled readily on surfaces that were covered with filamentous algae, sometimes attaching directly to the algae themselves.

Goodbody (1963) and Goodbody and Gibson (1974) outplanted juvenile *Ascidia nigra* (another solitary ascidian) to the field at depths of 1.2 and 2.1 m and measured cohort survival. They found very high mortality, particularly among individuals at the shallower depth. Mortality was significantly lower in shaded treatments, particularly at the 1.2-m depth. The authors hypothesized that one source of the mortality was smothering from accumulation of benthic diatoms or filamentous algae in the unshaded treatments. The mortality of the outplanted cohorts was highest within the first 15 days. Interestingly, the deep black pigmentation characteristic of adult *Ascidia nigra* does not develop until about the 15th day after larval settlement, and the authors noted that mortality decreased sharply after the pigment appeared (Goodbody and Gibson, 1974). Our results with *C. inflata* suggest that UV could be an alternative source of mortality for young ascidians in exposed habitats.

If the habitat of *C. inflata* makes this species vulnerable to UV damage—as suggested by our results—we expect it to show adaptations to avoid UV exposure in shallow-water habitats. Many organisms possess UV-absorbing, mycosporine-like amino acids (MAAs) that may prevent UV damage (reviewed by Karentz, 1994a). The Antarctic ascidian (*Molgula enodis*) contains seven MAAs (Karentz *et al.,* 1991) with distinct absorbance peaks around 330 nm; the Western Pacific *Halocynthia roretzi* contains a UV-absorbing sunscreen that absorbs maximally at 337 nm (Kobayashi *et al.,* 1981).

C. inflata absorptivities peaked between 290 and 300 nm, suggesting that MAAs are not responsible for the UV absorbance we measured. The body of this ascidian contains uric acid crystals that are deposited there as metabolic waste products (Lambert *et al.,* 1998). It is possible that uric acid provides some limited protection from UV damage (a uric acid absorbance peak occurs at 292 nm). Another possibility

Table I

Comparison of UV-B (300–320 nm), UV-A (320–400 nm), and PAR (400–700 nm) in Skyline Marina, Anacortes, WA, where Corella inflata *populations were monitored (15 July 1994) and in the tank where experiments were done (compare Fig. 3)*

Location	Depth (cm)	Intensity (W · m^{-2})*		
		UV-B	UV-A	PAR
Tank				
UV-exposed	5	1.10	1.12	9.99
Shielded	5	0.05	0.06	9.14
Marina	5	1.80	34.59	328.70
	50	0.56	23.02	248.00
	100	0.37	15.68	226.60

* Measured with a LI-COR 1800UW spectroradiometer.

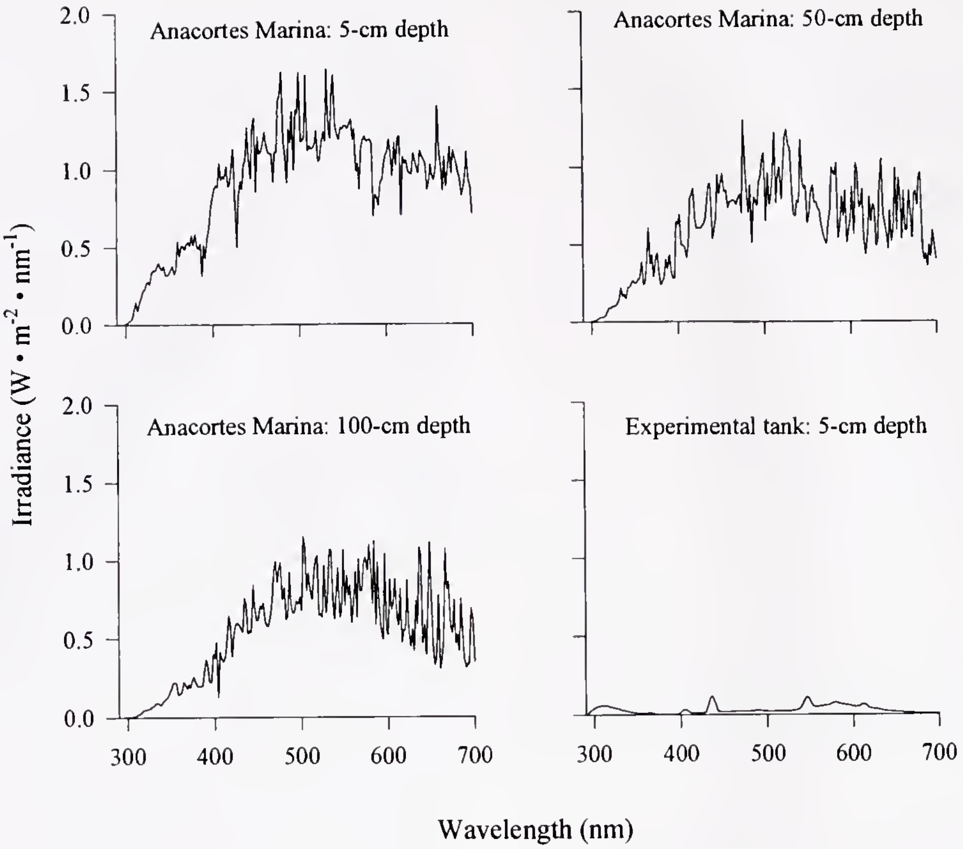

Figure 3. Irradiances at 5, 50, and 100 cm in Skyline Marina and in the flow-through seawater tank used for laboratory experiments (5-cm depth). Due to instrument constraints, we were unable to measure the UV-B below 300 nm. Lines on the figures between 290 and 300 nm are extrapolated second-order regressions from the data for 300 to 320 nm.

is that the absorbance we saw came from cell secretions known as "ornaments" (Cloney, 1990). Embryonic test cells produce ornaments that are deposited on the larval tunic of *C. inflata* and other ascidians (Cloney and Cavey, 1982; Cloney, 1994). The ornaments are composed largely of opal, a form of silicon dioxide (Monniot *et al.*, 1992). It is unlikely that the opal alone absorbs UV, but if the ornaments contain other UV-absorbing substances, they might provide larvae with some protection (R. A. Cloney, pers. comm.).

With little structural or chemical protection, *C. inflata* appears vulnerable to UV damage in all life-history stages. Embryos were the most vulnerable. Even short exposures caused developmental abnormalities; after only 30 min of laboratory UV exposure, many embryos arrested at the morula stage. This agrees with Jeffrey (1990), who also found that UV-irradiated ascidian embryos failed to gastrulate. Although embryos were most sensitive to UV, larvae, juveniles, and adults were also affected. We suggest that the unique life-history characteristics of *C. inflata* allow the populations to persist in shallow habitats despite this vulnerability.

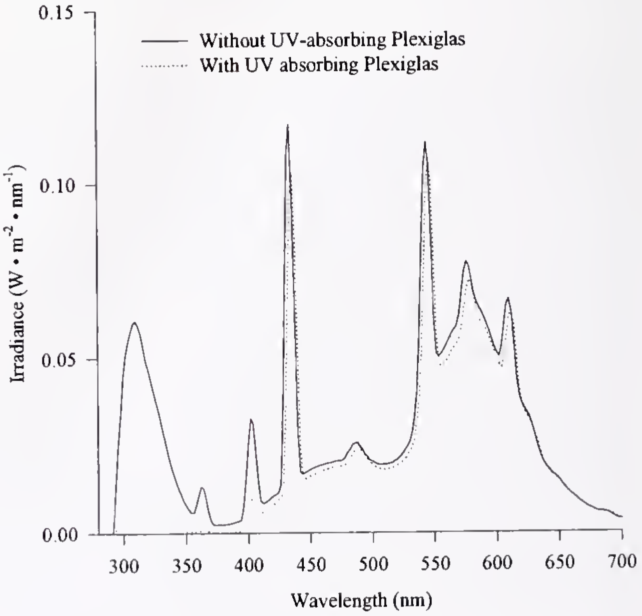

Figure 4. Irradiance spectra in the shielded and unshielded treatment portions of the experimental tank. Wavelengths from 290–300 nm are extrapolated second-order regressions from the data for 300 to 320 nm.

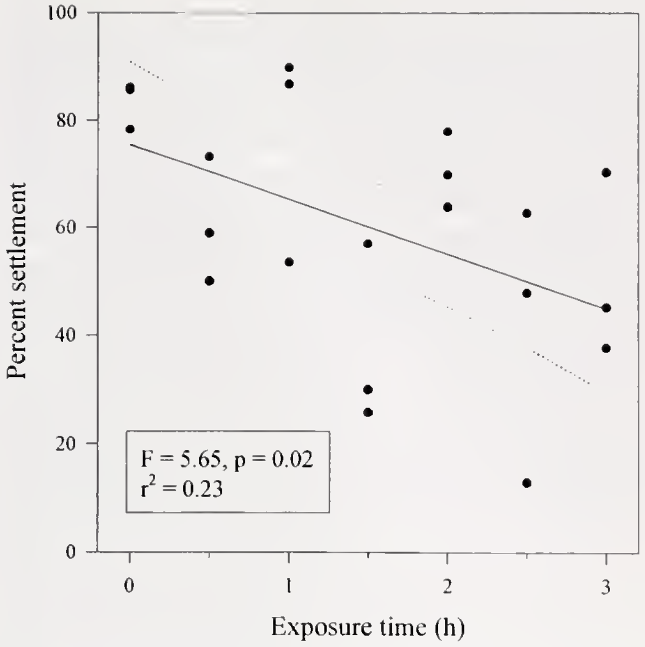

Figure 5. Cumulative effects of UV exposure on *Corella inflata* settlement. Exposures ranging from 0 to 3 h in 30-min intervals. A simple linear regression with a 95% confidence interval and regression statistics are shown.

C. inflata is one of a small number of solitary ascidians that brood their developing embryos. The hermaphroditic, self-fertile adult releases eggs just after dawn (Lambert *et al.*, 1995). If the eggs were freely released into the water, their ammonium-filled follicle cells (Lambert and Lambert, 1978) would carry them directly to the surface, where they would be exposed to full daytime sunlight during their development. Assuming that UV effects in the field are similar to those measured in the laboratory, our study suggests that this exposure could be fatal to the developing embryos.

Instead, *C. inflata* possesses an inflated atrium that functions as a brood chamber (Child, 1927). The horizontal, atrium-up position of the adults on the docks favors retention of the embryos within the chamber (Lambert, 1968; Young, 1988). The floating embryos hatch within the brood chamber after 24–26 h (Lambert *et al.*, 1995). Thus, the most vulnerable life stage is protected within the adult. Because adults persist only in shaded environments, this is a particularly safe environment for the embryos, even given the limited UV protection the adult tunic provides. Interestingly, *Corella willmeriana* and *Corella parallelogramma*, both free spawners, also have floating eggs (Hüus, 1939; Lambert *et al.*, 1981). Perhaps their early embryos are more resistant to UV damage than are those of *C. inflata*.

Until recently, it was thought that tadpoles were released from adult *C. inflata* soon after hatching. However, given that the eggs are produced in early morning and take about 24 h to develop, the larvae would be entering the environment when UV damage would be greatest, particularly since the larvae are apparently geonegative and swim toward the surface (Young, 1988).

Olson (1983) noted that larvae of the ascidian *Didemnum molle* are released near midday, when light levels are highest. This species contains a symbiotic cyanophyte (*Prochloron*) that is sensitive to both high and low light levels. Midday release permits larvae to choose an appropriate habitat while light levels are at their maximum. Newly released larvae swim briefly toward the surface, then descend to the bottom and settle (dispersal times were less than 10 min; Olson, 1983). The exposure time may be sufficiently brief, or the larvae sufficiently protected, that damage from UV does not occur.

C. inflata larvae can detect light but do not show phototaxis (Young, 1988), nor does light have a strong effect on settlement behavior (Young and Chia, 1985). Furthermore, larvae are incapable of detecting wavelengths below 425 nm (Young, 1982). Given these limitations, the larvae may be unable to use light as a cue to an appropriate settlement site (*i.e.*, one in which the sessile juvenile will not be killed by UV exposure).

Lambert *et al.* (1995) suggest that *C. inflata* tadpoles,

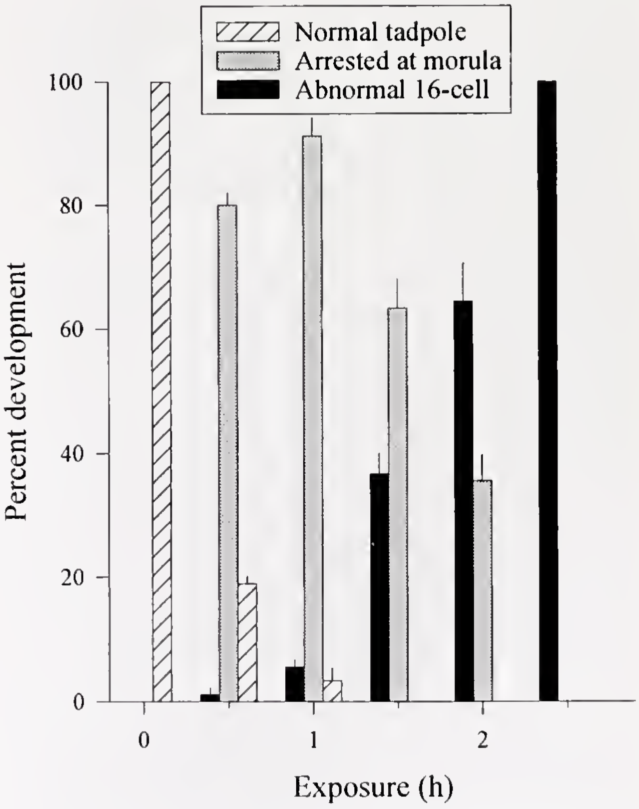

Figure 6. Effects of UV exposure on *Corella inflata* embryonic development. Morula stage is a solid ball of cleaved cells (probably 32–64 cells in this case). Standard errors are shown.

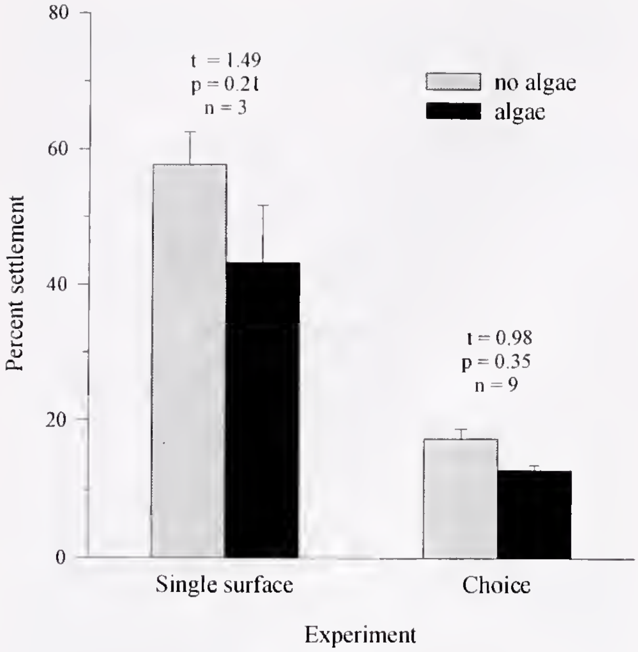

Figure 7. Effects of filamentous algae on *Corella inflata* settlement. There were no differences in settlement success on clean and fouled surfaces, nor did larvae choose clean surfaces over algal-fouled when given a choice (standard errors are shown).

which hatch in the early morning, are retained within the adult atrium for 12–17 h and released at night (they found swimming tadpoles in the atria of individuals collected at 2130 h). The larvae are competent to settle when released and probably settle near the adult that released them. Lambert (1968) described a settlement pattern of juvenile *C. inflata* clumped around adults.

Local settlement after a very brief planktonic period (in the dark) may improve the chances of survival for this species, which is apparently vulnerable to, but cannot detect, UV irradiation or algal overgrowth. This scenario is supported by our observation that, though adult *C. inflata* were abundant on the shaded undersides of exposed docks, no recruitment occurred to plates attached to the unshaded dock sides. Such highly localized recruitment has been described for a number of ascidian species (reviewed by Svane and Young, 1989). Note, however, that Cohen (1990) found significant genetic variability in *C. inflata* despite its self-fertility and short larval life. Outcrossing suggests that some dispersal of eggs or larvae is taking place.

C. inflata generally appears to follow a developmental scheme in which (1) embryos develop within the atrium of an adult in a shaded environment, (2) larvae hatch within the brood chamber and remain there throughout the daytime when UV effects are strongest, (3) competent larvae are released at night, and (4) the larvae quickly settle near the parent. This life-history pattern may allow *C. inflata* to opportunistically exploit floating-dock habitats in which other ascidians could not survive. For example, the range of *Corella willmeriana* overlaps that of *C. inflata*. These species are morphologically similar and have been confused by a number of authors (see Lambert *et al.*, 1981, for a review). However, *C. inflata* is found primarily on docks and pilings, whereas *C. willmeriana* is almost entirely restricted to deeper subtidal habitats; it is rare on docks (Lambert *et al.*, 1981). This distributional dichotomy is accompanied by a significant morphological difference: *C. willmeriana* does not have an inflated atrium and does not brood its young. The absence of these features may prevent it from invading the habitat *C. inflata* has successfully colonized.

At present, we do not know the relative importance of UV-B and UV-A to *C. inflata* distributions. The more damaging UV-B wavelengths penetrate to depths at which *C. inflata* occurs. However, UV-A intensities are much

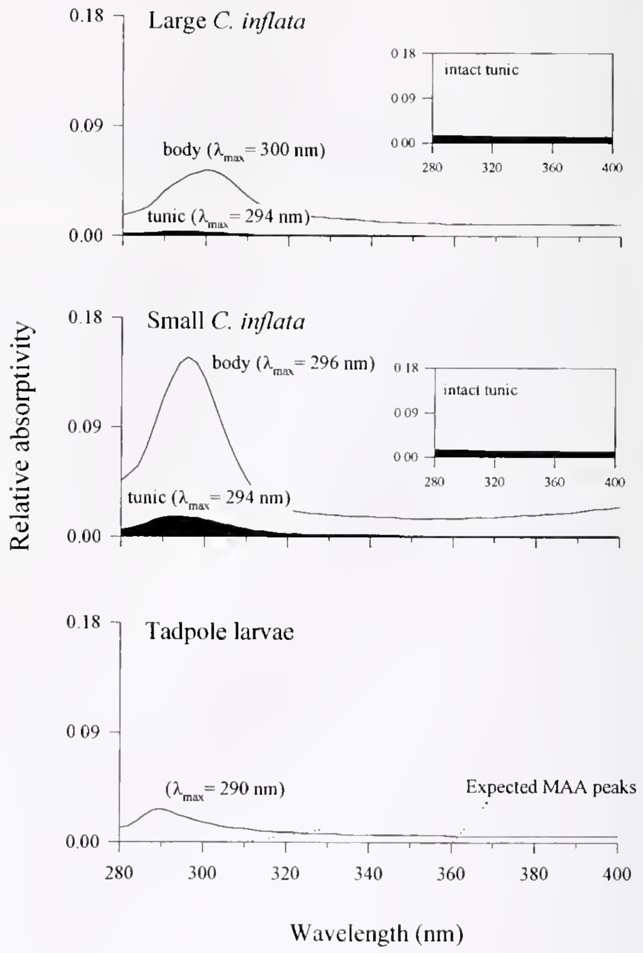

Figure 8. Relative absorptivities of *Corella inflata* extracts (80% methanol). Large individuals were >1.5 cm long; small individuals were <1.0 cm long. All gut contents were cleaned out during preparation to ensure that only *C. inflata* compounds were measured in the body samples. The area of normal mycosporine-like amino acid (MAA) absorbance peaks is indicated. Inset graphs are absorptivities for intact whole tunic. λ_{max} are maximum absorptivity peaks. See the text for absorptivity calculations.

higher, and it seems likely that those wavelengths also have a significant impact. The relative importance of UV-A, UV-B, and PAR to *C. inflata* populations merits further study. In our laboratory work, the UV/PAR ratios were higher than they would be under natural conditions. Many organisms possess DNA repair systems that are activated by short-wave visible light (reviewed by Mitchell and Karentz, 1993). If *C. inflata* has such systems, they may have been inoperable given the low PAR they received in our laboratory trials. The ideal way to test this possibility is to repeat the experiments under natural light in the field.

Whether UV effects are important for other ascidian species is unknown. Nearly 40 years ago, Endean (1961) suggested that pigmentation in the tunic of *Phallusia mamillata* protects that species from ultraviolet damage. To our knowledge, this has never been tested for *P. mamillata* or any other ascidian. Using a bacterial dosimeter, Karentz and Lutze (1990) detected significant UV-B radiation to 10 m and documented effects of irradiation to 20 and 30 m in Antarctic waters. Depth of UV penetration will depend on local conditions. However, in moderately clear, shallow waters, it is highly likely that UV will have significant ecological effects that may be detectable in life histories of the species that persist there.

Acknowledgments

We thank Steve Heywood and Gene McKeen for logistical assistance. Charley Lambert, Gretchen Lambert, Richard Cloney, and Jody Stecher provided unpublished information and/or valuable discussion and insight. We are also indebted to Deneb Karentz for patient guidance and suggestion. We appreciate the very helpful comments of two anonymous reviewers. The owners, staff, and residents of Anacortes, Cap Sante, Anchor Cove, and Skyline Marinas provided access to and use of their facilities. This work was supported by NSF grants OCE-9340328, USE-9650124, and USE-9151453.

Literature Cited

Adams, N. L., and J. M. Shick. 1996. Mycosporine-like amino acids provide protection against ultraviolet radiation in eggs of the green sea urchin *Strongylocentrotus droebachiensis. Photochem. Photobiol.* **64:** 149–158.

Biermann, C. H., G. O. Schinner, and R. R. Strathmann. 1992. Influence of solar radiation, microalgal fouling, and current on deposition site and survival of embryos of a dorid nudibranch gastropod. *Mar. Ecol. Prog. Ser.* **86:** 205–215.

Child, C. M. 1927. Developmental modification of the larval stage in the ascidian *Corella willmeriana. J. Morphol.* **44:** 467–517.

Cloney, R. A. 1990. Larval tunic and the function of the test cells in ascidians. *Acta Zool.* **71:** 151–159.

Cloney, R. A. 1994. Test cell secretions and their functions in ascidian development. Pp. 77–95 in *Development of Marine Invertebrates.* W. H. Wilson, S. A. Strickler, and G. L. Shinn, eds. Johns Hopkins University Press, Baltimore.

Cloney, R. A., and M. J. Cavey. 1982. Ascidian larval tunic: extraembryonic structures influence morphogenesis. *Cell Tissue Res.* **222:** 547–562.

Cohen, J. 1988. *Statistical Power Analysis for the Behavioral Sciences.* Earlbaum, Hillsdale, New Jersey. 567 pp.

Cohen, S. 1990. Outcrossing in field populations of two species of self-fertile ascidians. *J. Exp. Mar. Biol. Ecol.* **140:** 147–158.

Damkaer, D. M., D. B. Dey, G. A. Heron, and E. F. Prentice. 1980. Effects of UV-B radiation on near-surface zooplankton of Puget Sound. *Oecologia* **44:** 149–158.

Endean, R. 1961. The test of the ascidian, *Phallusia mammillata. Quart. J. Microsc. Soc.* **102:** 107–117.

Goodbody, I. 1963. The biology of *Ascidia nigra.* II. The development and survival of young ascidians. *Biol. Bull.* **124:** 31–44.

Goodbody, I., and J. Gibson. 1974. The biology of *Ascidia nigra* (Savigny) V. Survival in populations settled at different times of the year. *Biol. Bull.* **146:** 217–237.

Hardy, J., and H. Gucinski. 1989. Stratospheric ozone depletion: implications for marine ecosystems. *Oceanography,* **November 1989:** 18–21.

Hurlbert, S. H. 1984. Pseudoreplication and the design of ecological field experiments. *Ecol. Monogr.* **54:** 187–211.

Hüus, J. 1939. The effect of light on the spawning in ascidians. *Avh. Nor. Vidensk. Akad. Oslo. Mat. Naturvidensk. Kl.* **4:** 5–49.

Jeffrey, W. R. 1990. Ultraviolet irradiation during ooplasmic segregation prevents gastrulation, sensory cell induction, and axis formation in the ascidian embryo. *Dev. Biol.* **140:** 388–400.

Jokiel, P. L. 1980. Solar untraviolet radiation and coral reef epifauna. *Science* **207:** 1069–1071.

Karentz, D. 1994a. Ultraviolet tolerance mechanisms in Antarctic marine organisms. *Antarct. Res. Ser.* **62:** 93–110.

Karentz, D. 1994b. Prevention of ultraviolet radiation damage in Antarctic marine invertebrates. *NATO ASI Series I* **18:** 176–179.

Karentz, D., and L. H. Lutze. 1990. Evaluation of biologically harmful ultraviolet radiation in Antarctica with a biological dosimeter designed for aquatic environments. *Limnol. Oceanogr.* **35:** 549–561.

Karentz, D., F. S. McEuen, M. C. Land, and W. C. Dunlap. 1991. Survey of mycosporine-like amino acid compounds in Antarctic marine organisms: potential protection from ultraviolet exposure. *Mar. Biol.* **108:** 157–166.

Kirk, J. T. O., B. R. Hargreaves, D. P. Morris, R. B. Coffin, B. David, D. Grederickson, D. Karentz, D. R. S. Lean, M. P. Lesser, S. Madronich, J. H. Morrow, N. B. Nelson, and N. M. Scully. 1994. Measurements of UV-B radiation in two freshwater lakes: an instrument intercomparison. *Arch. Hydrobiol. Beih.* **43:** 71–99.

Kobayashi, J., H. Nakamura, and Y. Hirata. 1981. Isolation and structure of a UV-absorbing substance 337 from the ascidian *Halocynthia roretzi. Tetrahedron Lett.* **22:** 3001–3002.

Lambert, C. C., and G. Lambert. 1978. Tunicate eggs utilize ammonium ions for flotation. *Science* **200:** 64–65.

Lambert, C. C., I. M. Lambert, and G. Lambert. 1995. Brooding strategies in solitary ascidians: *Corella* species from north and south temperate waters. *Can. J. Zool.* **73:** 1666–1671.

Lambert, C. C., G. Lambert, G. Crundwell, and K. Kantardjieff. 1998. Uric acid accumulation in the solitary ascidian *Corella inflata. J. Exp. Zool.* **282:**323–331.

Lambert, G. 1968. The general ecology and growth of a solitary ascidian, *Corella willmeriana. Biol. Bull.* **135:** 296–307.

Lambert, G., C. C. Lambert, and D. P. Abbott. 1981. *Corella* species in the American Pacific Northwest: distinction of *C. inflata* Huntsman, 1912 from *C. willmeriana* Herdman, 1898 (Ascidiacea, Phlebobranchia). *Can. J. Zool.* **59:** 1493–1504.

Mitchell, D. L., and D. Karentz. 1993. The induction and repair of DNA photodamage in the environment. Pp. 345–377 in *Environmental*

UV Photobiology. A. R. Young, J. Moan, L. O. Björn, and W. Nultsch, eds. Plenum Press, New York.

Monniot, F., R. Martoja, M. Truchet, and F. Fröhlich. 1992. Opal in ascidians: a curious bioaccumulation in the ovary. *Mar. Biol.* **112:** 283–292.

Olson, R. R. 1983. Ascidian-*Prochloron* symbiosis: the role of larval photoadaptations in midday larval release and settlement. *Biol. Bull.* **165:** 221–240.

Parsons, T. R., Y. Maita, and C. M. Lalli. 1984. *A Manual of Chemical and Biological Methods for Seawater Analysis.* Pergamon Press, New York, New York. 173 pp.

Pennington, J. T., and R. B. Emlet. 1986. Ontogenetic and diel vertical migration of a planktonic echinoid larva, *Dendraster excentricus* (Eschscholtz): occurrence, causes, and probable consequences. *J. Exp. Mar. Biol. Ecol.* **104:** 69–95.

Shick, J. M., M. P. Lesser, and W. R. Stochaj. 1991. Ultraviolet radiation and photooxidative stress in zooxanthellate Anthozoa: the sea anemone *Phyllodiscus semoni* and the octocoral *Clavularia* sp. *Symbiosis* **10:** 145–173.

Skoog, D. A., and D. M. West. 1974. *Analytical Chemistry.* Holt, Rinehart, and Winston, New York. 598 pp.

Sokal, R. R., and F. J. Rohlf. 1995. *Biometry.* W. H. Freeman, New York. 887 pp.

Svane, I., and C. M. Young. 1989. The ecology and behaviour of ascidian larvae. *Oceanogr. Mar. Biol. Annu. Rev.* **27:** 45–90.

Van Name, W. 1945. North and South American ascidians. *Bull. Amer. Mus. Nat. Hist.* **84:** 1–476.

Worrest, R. C. 1982. Review of the literature concerning the impact of UV-B radiation upon marine organisms. Pp. 429–457 in *The Role of Solar Ultraviolet Radiation in Marine Ecosystems.* J. Calkins, ed. Plenum Press, NY.

Young, C. M. 1982. Larval behavior, predation, and early post-settlement mortality as determinants of spatial distribution in subtidal solitary ascidians of the San Juan Islands, Washington. Ph.D. dissertation, University of Alberta, Edmonton, Alberta, Canada, 260 pp.

Young, C. M. 1985. Abundance of subtidal solitary ascidians in the San Juan Islands, Washington, as influenced by food preferences of the predatory snail *Fusitriton oregonensis. Mar. Biol.* **84:** 309–321.

Young, C. M. 1988. Ascidian cannibalism correlates with larval behavior and adult distribution. *J. Exp. Mar. Biol. Ecol.* **117:** 9–26.

Young, C. M., and F. S. Chia. 1985. An experimental test of shadow response function in ascidian tadpoles. *J. Exp. Mar. Biol. Ecol.* **85:** 165–175.

Reference: *Biol. Bull.* **196:** 105–112. (February, 1999)

Time in Residence Affects Escape and Agonistic Behavior in Adult Male American Lobsters

S. I. CROMARTY*, J. MELLO, AND G. KASS-SIMON†

Biological Sciences Department, University of Rhode Island, 100 Flagg Road,
Kingston, Rhode Island 02881-0816

Abstract. Acquisition and retention of a shelter by a lobster are two of the variables that play a role in lobster agonistic interactions. Since shelter procurement and retention are important for lobster survival, behaviors related to this activity frequently outrank other daily behaviors (*e.g.*, searching for food). Here, we examine the effects of time in residence on the parameters of the escape response of the American lobster, *Homarus americanus*.

Adult male intermolt lobsters (Stage C_4) were placed in an experimental tank for three different time periods (one hour, 24 hours, and 48 hours). The probability of eliciting an escape response was inversely related to the time spent in the tank. Eighty percent of the animals in residence for 1 h tailflipped in response to a threat, whereas only 14% of the animals in residence for 48 h tailflipped.

There were also significant changes in some of the parameters of the escape response among animals in residence for 24 h compared to those in residence for 1 h. The number of tailflips and the distance traveled were reduced, although frequency, velocity, acceleration, force, and work factors were not significantly different.

Furthermore, with increased time in residence, lobsters switched from an avoidance or escape-prone behavior to an aggressive-prone behavior. Most of the animals in residence for 48 h approached and attacked a threat-stimulus rather than fleeing from it. On an empirically defined "index of aggressiveness," in which various behaviors were numerically ranked from least aggressive (0) to most aggressive (6), animals residing in the tank for 1 h had an average index value of 0.1 compared to a value of 5.0 for animals in residence for 48 h.

These findings are consonant with the suggestion that lobsters that have occupied a given space for an extended period of time take possession of the site and defend it instead of fleeing when threatened with a threat-inducing stimulus; it supports the idea that shelter retention increases aggressiveness and diminishes avoidance behaviors.

Introduction

Shelter selection by American lobsters, as they make the transition from their pelagic phase to a benthic existence, has been studied in detail (Cobb and Wahle, 1994; a review). Postlarval and early juvenile lobsters actively seek out cobble and boulder habitats for shelter—a habitat that offers the most protection from predators and conspecifics as well as protection against storm surges and rapid currents (Hudon, 1987; Abe *et al.*, 1988; Incze and Wahle, 1991; Wahle and Steneck, 1991, 1992). Such shelters may be limited in number since cobble and boulder habitats comprise only 10% of the sea-floor (Kelley, 1987)—the habitat that is most favored by lobsters. In addition, as lobsters grow (up to five orders of magnitude increase in body mass), their aggressiveness increases and their behavior becomes less cryptic, so crowding may become more of a problem (Cobb and Wahle, 1994).

Shelter procurement and retention may therefore be an important determinant of overall behavior in lobsters, with dominant individuals procuring and retaining the most favorable shelters, which in turn may be important for an individual's survival (Cobb, 1971; Stewart, 1972). Recently, Spanier and others (1998) assessed the behavior of juvenile American lobsters under predation risk in labora-

---

Received 22 July 1998; accepted 14 October 1998.

* Present address: Department of Neurobiology, Harvard Medical School, 220 Longwood Avenue, Boston, MA 02115. E-mail: Stuart_Cromarty@hms.harvard.edu

† To whom correspondence should be addressed. E-mail: avf101 @uriacc.uri.edu

Abbreviations: FEP, Fisher exact probability test; SS1, subsequent swims of first half; SS2, subsequent swims of second half.

tory settings. In the presence of a predator fish, the tautog, *Tautoga onitis*, the dominant lobster appeared to guard the available shelters; subdominant lobsters, which did not guard shelters, had a mortality rate seven times higher than that of dominant lobsters. Moreover, field observations by O'Neill and Cobb (1979) showed that intruders were less able to procure a shelter if the current resident had occupied it for a certain period of time.

In laboratory settings, factors that establish the dominance of an individual over other conspecifics and allow dominant individuals to have an advantage in procuring, capturing, and—more importantly—holding on to a suitable shelter include a greater carapace length and claw size (Scrivener, 1971), the sex of the individual (male), and molt stage (O'Neill and Cobb, 1979).

O'Neill and Cobb (1979) found that shelter familiarity did not affect shelter procurement or retention in the laboratory, but that in the field, lobsters already in a shelter were more likely to retain that shelter. On the other hand, American lobsters have been observed to display increased aggressiveness after being isolated in individual tanks (E. Kravitz, pers. comm. to S.C.), and during our earlier studies, we observed that it was harder to induce animals to tailflip after they had been kept for some time in isolated tanks.

Therefore, the question arises as to the extent to which an animal's time in residence is a significant determinant of its aggressive and avoidance behavior. To explore this question, we placed animals in an isolated experimental tank for periods of 1, 24, or 48 h and videotaped their responses to a nontactile threatening stimulus introduced into the tank.

We now present evidence that with increased time in residence, lobsters not only are less likely to flee from a threat, but also will confront it with increasing aggressiveness.

Materials and Methods

Procedures and experimental protocols are essentially the same as those described in Cromarty *et al.*, 1991, 1998), but are summarized here with relevant differences included.

Animals

Adult American lobsters (carapace length 78 to 84 mm) were obtained directly from an offshore lobster vessel fishing in Narragansett Bay, Rhode Island. Animals were housed at the Narragansett Bay Campus of the University of Rhode Island in separate, but connecting, tanks in a free-flow seawater system at ambient temperatures ranging from 16° to 22°C under a 14-h-light/10-h-dark illumination cycle. The animals were fed three times per week on a mixed diet of squid, crab, and fish, but were not fed for 48 h prior to an experiment. Six hours before an experiment, an animal was moved to the Kingston campus of the university, where it was placed in a holding tank (30 cm^3). The tank was supplied with its own air supply, and water was obtained from the same source used to supply the tanks at the URI Bay Campus.

Experiments

Experiments were conducted from May to October, to avoid possible seasonal differences in behavior. Lnenicka and Zhao (1991) documented seasonal differences in the physiology and morphology of crayfish neuromuscular terminals which suggested that lobster escape parameters might differ seasonally.

Experiments were carried out between 1200 and 1700 h in an aquarium filled with filtered recirculated seawater from Narragansett Bay. Salinity was measured before each experiment, and ranged between 29‰ and 33‰. Water was replaced or added as necessary to maintain salinity within this range. The experimental tank was kept between 18°C and 20°C by a Frigid Units AE-234 AG-602 chiller. The chiller was turned off before the start of the experiment. The experimental area consisted of an open-ended tank (1.0 m L × 0.3 m W × 0.3 m H) immersed in a larger main tank (2.2 m L × 0.75 m W × 0.91 m H). The layout was designed so that a threatening stimulus could be introduced at the open end of the experimental tank. A weighted wooden partition with a pulley acted as a blind—and a separation from the main tank—at the open end. To ensure that lobsters were initially at the closed, non-stimulus end, a light was placed at the open end, causing the lobster to move towards the darkened closed end. The partition was raised once the lobster had reached the closed end, while the light was moved to the *closed* non-stimulus end. This served to "push" the animal back towards the open (stimulus), now darkened, end. A piece of PVC tubing (0.15 m L × 0.10 m W) weighted to 1.45 kg with pebbles served as the threatening visual stimulus. The stimulus was raised above the open end and was released into the water at a preset distance of 10 cm (measured from the open edge of the tank to the lobster) whenever a lobster approached the open end after the designated residency period. One hour before the experiment, the physical condition of each animal was checked. Animals were used only if they moved around the tank or exhibited antennule flicking.

Cameras were placed in two positions (a Sony camcorder above the tank and a Panasonic WV-CD20 camera to the side), and experiments were recorded (Panasonic AG-6010 and Panasonic NV-8950) simultaneously from the vertical and horizontal perspectives. Video recordings of each lobster were analyzed frame-by-frame. For measurements of distance traveled, a metric grid divided into 0.5-cm units was painted onto the side of the experimental tank. Transparent overlays on the video monitor were later used to record the escape swimming distance of each animal. Distance traveled along the length of the tank was measured by using the position of the tip of the lobster's rostrum as a guide, and the number of tailflips was counted; time was automatically recorded on the videotape. An independent observer inspected all recordings and rejected runs in which the experimental parameters were not strictly adhered to (*e.g.*, cases in which the stimulus was released closer than 10 cm to the experimental animal).

After each experiment, the animal's molt stage was determined by examining cuticular changes and setal development in the pleopods (Aiken, 1973, 1980). Only stage C_4 (intermolt) animals were used, since probability of escape depends on the molt stage of each lobster (Cromarty *et al.*, 1991, 1995). Measurements of carapace length, cutter length, lobster weight and volume, temperature, and salinity were recorded at the end of each experimental trial.

Analysis of the escape response follows our previous protocol (Cromarty *et al.*, 1991, 1998). To analyze the escape parameters, the response was broken into two elements—the initial tailflip, henceforth called the "power swim," followed by the numerous subsequent tailflips, called "subsequent swims." (The number of subsequent swims in this study ranged from one to six.) A tailflip, or swim, is defined as beginning immediately after the start of abdominal flexion and ending at abdominal extension.

The following characteristics of the escape response were analyzed for each lobster: distance traveled (centimeters), number of tailflips, duration (seconds), frequency of tailflips (tailflips per second), velocity (meters per second), acceleration (meters per second squared), force (mass × acceleration), work (force × distance), distance swum per weight (meters per kilogram), and distance swum per lobster body length. The last two parameters were measured to determine whether individual lobster variability in weight and size could alter the significance of a parameter, even though weight and size were not significantly different (using an ANOVA) among the animals in the three resident periods.

As in previous analyses, in evaluating acceleration, the added-mass forces (Batchelor, 1967) that act on accelerating bodies in fluids were ignored since these are a multiple of mass and would act equally on all animals of the same weight (see Cromarty *et al.*, 1991). The analysis of the escape response is designed to reflect relative changes in lobster escape behavior and not the kinematic relationships investigated by other researchers (Batchelor, 1967; Daniel and Meyhöfer, 1989; Nauen and Shadwick, 1993).

Each of the escape parameters was analyzed for (1) the entire escape response; (2) the initial power swim; (3) the subsequent swims over the entire subsequent swimming distance; and (4) the subsequent swims in each half of that distance, since earlier experiments showed that there were differences in the total subsequent swimming distance traveled by lobsters. We therefore divided the distance traveled in the subsequent swims by half and analyzed each half (Cromarty *et al.*, 1991, 1998). Because the distances differed and because each distance was divided equally in half for each escape sequence for each animal, no data are available to compare distance traveled between the two halves of the subsequent swims for each residency group.

To quantify the degree of "aggression" in the post-stimulus behavior of each animal, we ranked this behavior on a scale of 0 to 6 and subjectively ordered behavior towards the stimulus as follows:

0 = back away, never approach
1 = approach but remain more than one bodylength away
2 = approach within one bodylength
3 = approach, touch
4 = approach, touch, grasp
5 = approach, touch, grasp, and tug/pull
6 = approach, touch and grasp, tug/pull, and an offensive tailflip

Statistical analysis

Differences in weight, carapace length, and cutter size among the three residency periods were determined by parametric analysis of variance (ANOVA). The Fisher exact probability test (FEP) was used to determine differences in the probabilities of escape among the three resident periods.

Due to a non-normal distribution of data, Kruskal-Wallis (KW) tests were run for all the escape parameters except the subsequent swims and the "aggression intensity index." The first and second halves of the subsequent swims were compared with a multiple analysis of variance (MANOVA) and a repeated measures follow-up test. A trend was considered to exist if the P value for a parameter ranged between $0.05 < P < 0.1$. Values were considered significant at $P \leq 0.05$ for all the statistical tests. Both ANOVAs and MANOVAs were run on SPSS software ver. 6.6.1 (SPSS Inc., Chicago).

Results

Weight (in grams)/carapace length (in millimeters)/cutter length (in millimeters)

There were no significant differences in the weights (mean ± SEM for all) of 1-h (415 ± 29), 24-h (414 ± 32), and 48-h (427 ± 31) resident lobsters (ANOVA, $F(2, 27) = 0.35$, $P = 0.71$). No significant differences were found in the carapace lengths of 1-h (78 ± 4.9), 24-h (79 ± 2), and 48-h (79 ± 3) resident lobsters (ANOVA, $F(2, 27) = 0.17$, $P = 0.84$); similarly there were no significant differences in the cutter lengths of 1-h (107 ± 3), 24-h (109 ± 3), and 48-h (108 ± 2) resident lobsters (ANOVA, $F(2, 27) = 0.69$, $P = 0.61$).

Effects of residence time on the probability of escape

Probability of escape. The probability of escape for animals in the three residence time periods is summarized in

Table I

Escape and post-threat behavior of animals in each residency period; some lobsters initially tailflipped and then re-approached the stimulus or re-approached and attacked it

	Immediate response		Secondary responses		
Residence period (h)	*n*	Tailflip	Back up	Approach only	Approach *and* Attack
1	10	8	9	1	0
24	13	8	6	7	5
48	7	1	0	7	7

Table I. Of the 1-h, 24-h, and 48-h resident lobsters, 8 out of 10, 8 out of 13, and 1 out of 7, respectively, escaped when the stimulus was introduced. These probabilities were significantly different (FEP, $P = 0.001$).

Escape parameters for one- and 24-hour resident male adult lobsters. Because only one lobster among the 48-h resident group could be induced to tailflip, only 1-h and 24-h residents were compared. Three lobsters in the 1-h resident period were not analyzed, because their gross swimming pattern deviated from a rectilinear motion; thus five 1-h lobsters and eight 24-h lobsters were used in the analyses.

Total escape response (initial power swim plus subsequent swims). One-hour resident lobsters swam farther (KW, $\chi^2 = 6.19$, $P = 0.012$) and took more tailflips (KW, $\chi^2 = 5.67$, $P = 0.017$) than did 24-hour resident animals (Fig. 1A, B, respectively). Distance-dependent parameters, such as distance traveled per body length and distance traveled per weight, were significantly shorter among the 24-h lobsters (KW, $P = 0.02$; Fig. 1C, D). Although time spent escaping, frequency of tailflips, velocity, acceleration, force, and work were not significantly different at the $P \leq 0.05$ level between the two groups (KW, $P > 0.05$), a trend at $0.05 < P < 0.10$ towards a decrease in time, frequency, and velocity was observed for the 24-h resident lobsters (Fig. 2A, B, and C).

Initial power swim. There was a significant decrease in the acceleration, force, and work of the power stroke in lobsters that were in residence for 24 h (KW, $P \leq 0.05$; Fig. 3A, B, and C) and a significant increase in the duration of the initial power stroke (KW, $P = 0.014$; Fig. 3D). A trend towards decreased distance traveled and lower velocity in the 24-h resident lobsters was observed (KW, $0.05 < P < 0.10$).

Total subsequent swims. Five males in the 1-h category and six males in the 24-h category were compared, since two lobsters in the 24-h resident period took only one tailflip with no subsequent swims. Significant differences in subsequent swim duration were found between animals in the 1-h to 24-h resident periods. Significant differences in subsequent swim duration (MANOVA, $F(1, 9) = 3.92$, $P = 0.04$), and number of tailflips (MANOVA, $F(1, 9) = 7.42$, $P = 0.02$) were found, with 24-h resident lobsters spending less time tailflipping and taking fewer tailflips (Fig. 4A, B).

Post-threat behavior

In the analysis of post-threat behaviors, the percentage of lobsters that re-approached the stimulus was 0% (0 out of 10), 54% (7 out of 13), and 100% (7 out of 7), in the residency periods of 1 h, 24 h, and 48 h, respectively (Table I). Of these, 0% (0 of 10) of the 1-h, 38% (5 of 13) of the 24-h, and 100% (7 of 7) of the 48-h lobsters approached *and* attacked the stimulus with high intensity after it had been

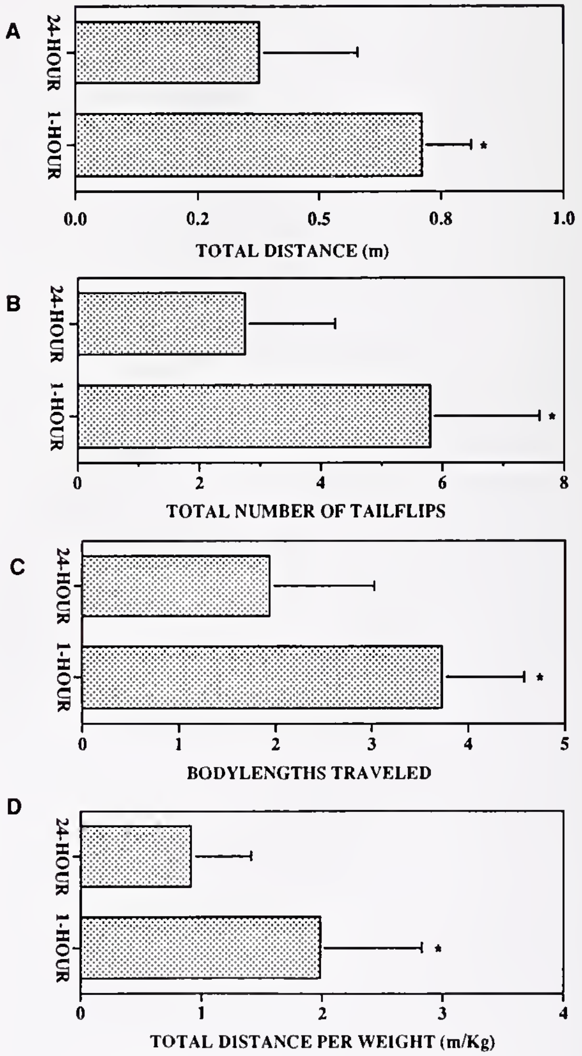

Figure 1. Parameters of the entire escape response exhibited by lobsters in residence for 1 h ($n = 5$) and 24 h ($n = 8$). An asterisk (*) indicates results that are significantly different at $P \leq 0.05$. (A) Mean distance traveled in meters (m). (B) Mean number of tailflips. (C) Mean distance traveled divided by lobster body length; represented as number of body lengths traveled. (D) Mean distance traveled in meters (m) divided by lobster weight in kilograms (kg).

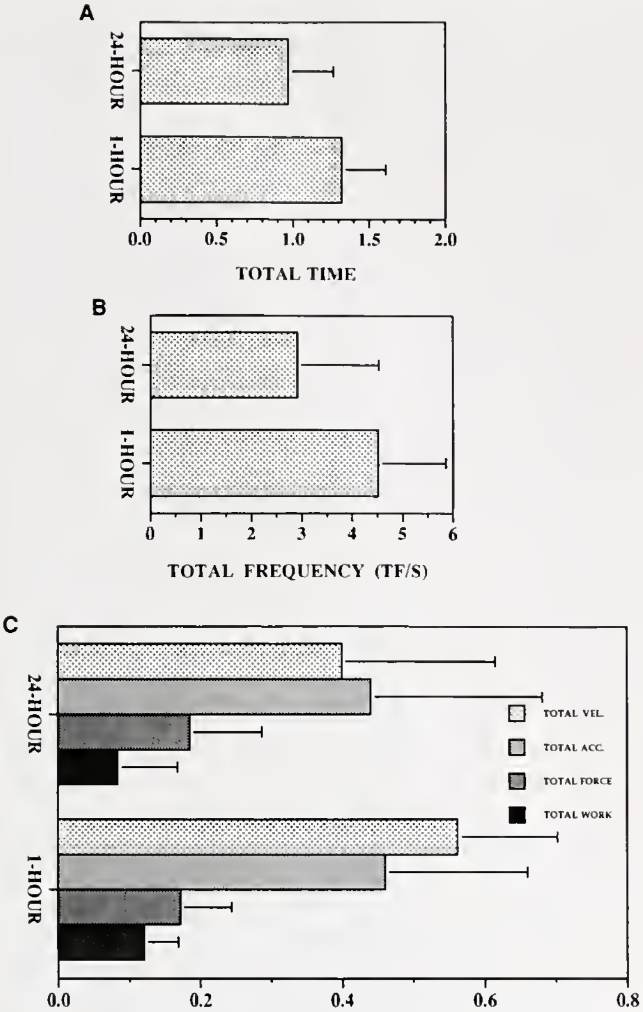

Figure 2. Parameters of the entire escape response exhibited by lobsters in residence for 1 h (n = 5) and 24 h (n = 8). (A) Mean time in seconds (s). (B) Mean frequency of tailflips in tailflips per second (TF s^{-1}). (C) Mean velocity in meters per second (m s^{-1}), acceleration in meters per second squared (m s^{-2}), force in newtons (kg m s^{-2}), and work in joules (J) of tailflips.

presented. On the aggression intensity index, (with predetermined levels of aggressive behavior, ranked from 0 to 6, see Methods), behavioral responses after the stimulus was introduced were statistically different (Fig. 5A–C), with lobsters in residence for 48 h displaying more intensively aggressive behaviors (average index of 5.0 ± 0.8) than those in residence for 24 h (average index of 2.1 ± 2.2; KW, $P = 0.03$) and 1 h (average index of 0.1 ± 0.3; $P = 0.006$).

Although it is possible that stress influenced these behaviors, no physical evidence of stress-related behavior was observed. Animals in all three residency periods exhibited typical active searching and antenna whipping behavior. (Lobsters that exhibit stress show no movement in the experimental tank and do not antenna whip [pers. obs.].) In addition, lobsters in the 48-h residency period showed a *distinct* change in behavior compared to the 24-h resident animal, exhibiting more grasping, pulling, and offensive tailflips. After the experiment, all animals (while still in the experimental tank) ate the food presented to them, indicating that they were not under stress, since sick or stressed animals avoid food altogether (pers. obs.).

Discussion

In this study, we have shown that lobsters residing in an experimental tank for 24 or 48 hours exhibit a reduced tendency to escape in response to a threat and an increase in post-threat aggressiveness.

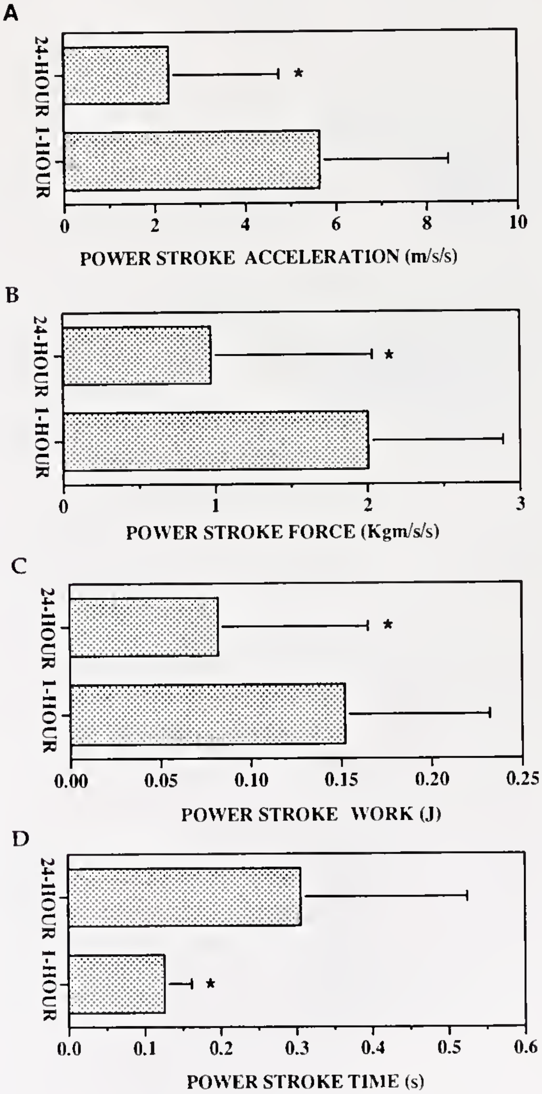

Figure 3. Parameters of the power stroke exhibited by lobsters in residence for 1 h (n = 5) and 24 h (n = 8). An asterisk (*) indicates results that are significantly different at $P \leq 0.05$. (A) Mean acceleration in meters per second squared (m s^{-2}). (B) Mean force in newtons (kg m s^{-2}). (C) Mean work in joules (J). (D) Mean duration in seconds (s).

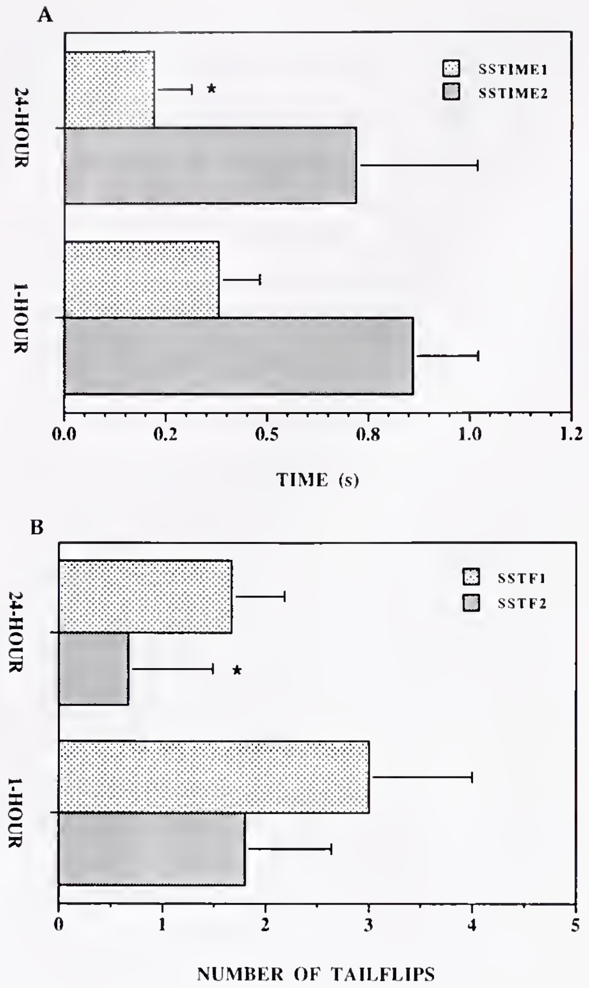

Figure 4. Parameters of subsequent swims of the escape response exhibited by lobsters in residence for 1 h ($n = 5$) and 24 h ($n = 8$). An asterisk (*) indicates results that are significantly different at $P \leq 0.05$. (A) Mean duration in seconds (s) for the first (SSTIME1) and second (SSTIME2) halves of the subsequent swimming distance. (B) Mean number of subsequent swims in the first (SSTF1) and second (SSTF2) halves of the subsequent swimming distance.

The measured parameters of the escape response (distance traveled, number of tailflips, acceleration, force, etc.) were all reduced in the 24-h residency group, while time spent escaping was increased. The efficacy of the initial power stroke was reduced, resulting in animals that appeared reluctant to escape. The power swim took longer to complete and the distance traveled was reduced, resulting in a lower initial velocity and acceleration (Figs. 1 and 2). Lobsters residing in the tank for 48 h simply did not tailflip, and therefore their escape response sequences could not be compared to those of 1-h and 24-h residency animals.

The post-stimulus behavior of the 24-h and 48-h resident lobsters was different from that of the 1-h residents. None of the latter attacked the stimulus, but 38% of the 24-h and 100% of the 48-h lobsters attacked the stimulus with high intensity, as reflected in the aggression intensity index. In particular, the 48-h resident lobsters exhibited the highest intensity of aggressive behaviors towards the stimulus (Fig. 5C). Therefore, as residency period was increased from 1 h to 48 h (in an experimental tank), escape behavior decreased and directed aggression towards the stimulus increased.

Our experiments were designed to test whether time in residence affects the probability that a lobster will respond with an escape response when threatened. Since animals tailflipped when initially caught and again when placed in the experimental tank, we tried to minimize handling by capturing them with a net (in their holding tanks) and then moving them directly to the experimental tank. To avoid handling-induced arousal, we did not re-handle 24-h and 48-h lobsters once they were placed in the experimental tank. In preliminary experiments we found that any attempt to recapture an animal caused it to tailflip wildly around the tank. In any event, although the interval between handling and presentation of a threat may have been different in the three groups, it is unlikely that a single prior handling would

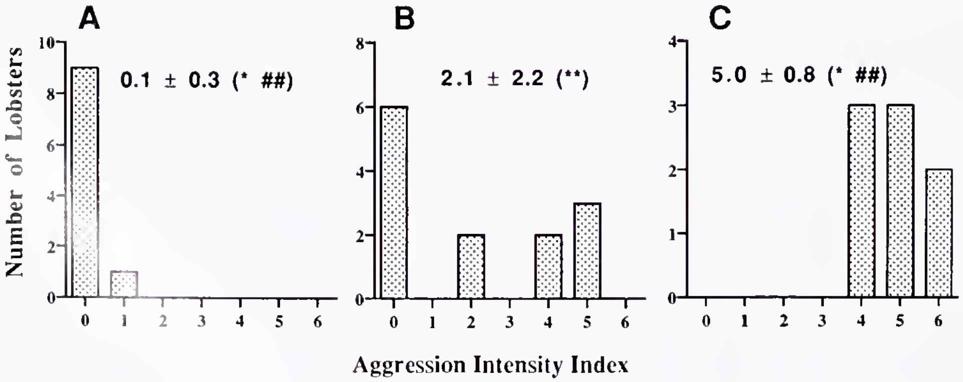

Figure 5. Average aggression intensity index of post-threat behaviors directed towards the stimulus by lobsters in residence for 1 h (A), 24 h (B), and 48 h (C). Index values range from 0 (back away, never approach) to 6 (grasp, pull, tug, and aggressive tailflip). The asterisks and number symbols indicate the level of significance: * 1 h < 24 h; $P = 0.03$; ## 1 h < 48 h; $P = 0.0006$; ** 24 h < 48 h; $P = 0.009$.

produce significant differences in the level of arousal in 24-h and 48-h residents.

Nonetheless, if prior handling contributed to the observed time-dependent reluctance to escape and increase in aggressiveness, then our findings suggest that an animal becomes more aggressive the longer it is left undisturbed in a site.

Many other factors appear to affect an animal's ability to procure and retain a shelter (O'Neill and Cobb, 1979). These include differences in dominance due to body length, weight, and claw size (Scrivener, 1971). Reproductive status is also important. In a related decapod, maternal female crayfish residents won 92% of their encounters with male intruders (Figler *et al.,* 1995). Gravid lobsters exhibit a distinct reduction in escape behavior and are more likely than males to attack an approaching stimulus (Cromarty *et al.,* 1998). Odor cues for discrimination of familiar and dominant lobsters (Karavanich and Atema, 1991, 1993, 1998a, b) and sex-identifying urine and molt signals in lobsters (Atema and Cowan, 1986), plus visual cues (Bruski and Dunham, 1987), are most likely important sensory cues for procuring and residing in a shelter. Crayfish rapidly learn to discriminate between changing spatial configurations (Sandeman and Varju, 1988; Varju and Sandeman, 1989; Basil and Sandeman, 1997) and, as shown by direct measurements of electrical heart activity (Shuranova and Burmistrov, 1995), are constantly sampling their surroundings (*i.e.,* predators or conspecific intruders, currents, shadows, food availability, etc.).

An important determinant in shelter retention may be social contact with conspecifics. Hoffman *et al.* (1975) showed that lobsters who were in visual contact with other animals or were communally housed were less aggressive. In this regard, Yeh *et al.* (1996, 1997) found that crayfish social status and social experience determine the effect of serotonergic modulation on the lateral giant motor neuron that mediates one form of escape behavior. Social isolation has also been found to cause dramatic increases in intraspecific aggression in mice (Valzelli, 1973).

In an early study, O'Neill and Cobb (1979) found that in the laboratory, shelter familiarity did not affect shelter procurement or retention, whereas in the field, resident lobsters were more likely to retain their shelters. These observed differences might have been due to the above-mentioned experimental conditions, *i.e.,* type and duration of the experimental housing of animals.

In our experimental conditions there were no other animals, no places to seek shelter, and only one avenue of escape. Therefore, an animal's immediate response under these circumstances may be considered to reflect and be driven by the differential effects of having been undisturbed in a familiar environment for different lengths of time. That is, our experiments seem to reveal that the patterns associated with either aggression and dominance, on the one hand, or avoidance and submission, on the other, become manifested as a function of how the animal assesses its own place in its immediate environment. This assessment then becomes a determinant of how an animal responds to other conspecifics and might be considered operationally as a "motivational state." A change in "motivational state" has recently been tested in the European hermit crab *Pagurus bernhardus* during agonistic encounters (Elwood *et al.,* 1998). This study showed that the duration and severity of the startle/threat response are inversely related to the "motivational state" of the animal to continue the previous activity, namely of fighting for a more suitable shelter inhabited by a conspecific.

In summary, our experiments indicate that time in residence and isolation are important physiological determinants of a lobster's behavior and can cause it to switch from an avoidance-prone to an aggression-prone state.

Acknowledgments

We thank Bill Mac Elroy for allowing us to collect nongravid and male animals while he was fishing offshore and Tom Angell of the Rhode Island Department of Environmental Management for collecting gravid animals offshore. (All lobsters were returned to the Bay after experimentation was completed.) Thanks to Dr. Mike Clancy and Ms. Kathy Castro for help in lobster collection and maintenance. Drs. Stanley Cobb and Frank Heppner kindly provided laboratory space and equipment. We also thank Ms. Malia Schwartz for critiquing an earlier draft of the manuscript. This research was supported by a Whitehall Foundation grant to G.K-S and Grant-in Aid of Research from Sigma Xi and Lerner Gray Grants for Marine Research to S.I.C.

Literature Cited

Able, K. W., K. L. Heck, M. P. Fahay, and C. T. Roman. 1988. Use of salt-marsh peat reefs by small juvenile lobsters on Cape Cod, Massachusetts. *Estuaries* **11:**83–86.

Aiken, D. E. 1973. Proecdysis, setal development, and molt prediction in the American lobster (*Homarus americanus*). *J. Fish. Res. Board Can.* **30:**1334–1337.

Aiken, D. E. 1980. Molting and growth. Pp. 91–163 in *The Biology and Management of Lobsters,* vol. 1, J. S. Cobb and B. F. Phillips, eds. Academic Press, New York.

Atema, J., and D. Cowan. 1986. Sex-identifying urine and molt signals in lobster (*Homarus americanus*). *J. Chem. Ecol.* **12:**2065–2080.

Basil, J., and D. Sandeman. 1997. Australian freshwater crayfish detect small spatial changes in their habitat using only tactile cues. *Soc. Neurosc. Abstr.* **23:**527.17.

Batchelor, G. K. 1967. *An Introduction to Fluid Dynamics.* Cambridge University Press, London.

Bruski, C. A., and D. W. Dunham. 1987. The importance of vision in agonistic communication of the crayfish *Orconectes rusticus.* I. An analysis of bout dynamics. *Behaviour* **63:**83–107.

Cobb, J. S. 1971. The shelter behavior of the American lobster, *Homarus americanus. Ecology* **52:**108–115.

Cobb, J. S., and R. A. Wahle. 1994. Early life history and recruitment processes of clawed lobsters. *Crustaceana* **67**:1–25.

Cromarty, S. I., J. S. Cobb, and G. Kass-Simon. 1991. Behavioral analysis of the escape response in juvenile American lobsters, *Homarus americanus* over the molt cycle. *J. Exp. Biol.* **158**:565–581.

Cromarty, S. I., J. S. Cobb, and G. Kass-Simon. 1995. Adult and juvenile lobsters (*Homarus americanus*), differ markedly in the neuromuscular physiology and behavior of the escape response over the molt cycle. *Soc. Neurosci. Abstr.* **25**:201.

Cromarty, S. I., J. Mello, and G. Kass-Simon. 1998. Behavioral analysis of escape behavior in male, and gravid and non-gravid, female lobsters. *Biol. Bull.* **194**:63–71.

Daniel, T. L., and E. Meyhöfer. 1989. Size limits in escape locomotion of caridean shrimp. *J. Exp. Biol.* **143**:245–265.

Elwood, R. W., K. E. Wood, M. B. Gallagher, and J. T. A. Dick. 1998. Probing motivational state during agonistic encounters in animals. *Nature* **393**:66–68.

Figler, M. H., M. Twum, J. E. Finkelstein, and H. V. S. Peeke. 1995. Maternal aggression in red swamp crayfish (*Procambarus clarkii*, Girard): The relation between reproductive status and outcome of aggressive encounters with male and female conspecifics. *Behaviour* **132**:107–125.

Hoffman, R. S., P. J. Dunham, and P. V. Kelly. 1975. Effect of water temperature and housing conditions upon the aggressive behavior of the lobster *Homarus americanus*. *J. Fish. Res. Board Can.* **32**:713–717.

Hudon, C. 1987. Ecology and growth of postlarval and juvenile lobster *Homarus americanus*, off îles de la Madeleine (Quebec). *Can. J. Fish. Aquat. Sci.* **50**:1422–1434.

Incze, L., and R. A. Wahle. 1991. Recruitment from pelagic to early benthic phase in lobsters (*Homarus americanus*). *Mar. Ecol. Progr. Ser.* **79**:77–87.

Karavanich, C., and J. Atema. 1991. Role of olfaction in recognition of dominance in the American lobster (*Homarus americanus*). *Biol. Bull.* **181**:359–360.

Karavanich, C., and J. Atema. 1993. Agonistic encounters in the American lobster, *Homarus americanus:* Do they remember their opponents? *Biol. Bull.* **185**:321–322.

Karavanich, C., and J. Atema. 1998a. Olfactory recognition of urine signals in dominance fights between male lobsters. *Behavior* **135**:719–730.

Karavanich, C., and J. Atema. 1998b. Individual recognition and memory in lobster dominance. *Anim. Behav.* **56**. (in press).

Kelley, J. 1987. A treatise on glaciated coast. Pp. 151–176 in *Sedimentary Environments Along Maine's Estuarine Coastline*, D. M. Fitzgerald and P. S. Rosen, eds. Academic Press, New York.

Lnenicka, G. A., and Y. Zhao. 1991. Seasonal differences in the physiology and morphology of crayfish motor terminals. *J. Neurobiol.* **22**:561–569.

Nauen, J. C., and R. E. Shadwick. 1993. Biomechanics of tail-flipping by the spiny lobster *Panulirus interruptus*. *Am. Zool.* **32(5)**:127A.

O'Neill, D. J., and J. S. Cobb. 1979. Some factors influencing the outcome of shelter competition in lobsters (*Homarus americanus*). *Mar. Behav. Physiol.* **6**:33–45.

Sandeman, D., and D. Varju. 1988. A behavioral study of tactile localisation in the crayfish *Cherax destructor*. *J. Comp. Physiol.* **163**: 525–536.

Scrivener, J. C. E. 1971. Agonistic behavior of the American lobster, *Homarus americanus* (Milne-Edwards). *Fish. Res. Bd. Can. Tech. Rep.* **235**:1–128.

Shuranova, Z. H., and I. U. Burmistrov. 1995. The orienting reaction in invertebrates. *Zh. Vyssh. Nerv. Deat. Im. IP. Pavola.* **45(3)**:510–520.

Spanier, E., T. P. McKenzie, J. S. Cobb, and M. Clancy. 1998. Behavior of juvenile American lobsters, *Homarus americanus*, under predation risk. *Mar. Biol.* **130**:397–406.

Stewart, L. L. 1972. The seasonal movements, population dynamics and ecology of the lobster, *Homarus americanus* (Milne Edwards) off Ram Island, Connecticut, Ph.D. Thesis, University of Connecticut, 152 pp.

Valzelli, L. 1973. The "isolation syndrome" in mice. *Psychopharmacologia* **31**:305–320.

Varju, D., and D. Sandeman. 1989. Tactile learning in a new habitat and spatial memory in the crayfish *Cherax destructor*. Page 21a in *Dynamics and Plasticity in Neuronal Systems*. N. Elsner and W. Singer, eds. Thieme, Stuttgart.

Wahle, R. A., and R. S. Steneck. 1991. Recruitment habitats and nursery grounds of the American lobster *Homarus americanus:* a demographic bottleneck. *Mar. Ecol. Progr. Ser.* **69**:231–243.

Wahle, R. A., and R. S. Steneck. 1992. Habitat restrictions in early benthic life: experiments on habitat selection and *in situ* predation with the American lobster. *J. Exp. Mar. Biol. Ecol.* **157**:91–114.

Yeh, S. R., R. A. Fricke, and D. H. Edwards. 1996. The effect of social experience on serotonergic modulation of the escape circuit of crayfish. *Science* **271**:366–369.

Yeh, S. R., B. E. Musolf, and D. H. Edwards. 1997. Neuronal adaptations to changes in the social dominance status of crayfish. *J. Neurosci.* **17**:697–708.

Reference: *Biol. Bull.* **196:** 113–120. (February, 1999)

Tunic Morphology and Cellulosic Components of Pyrosomas, Doliolids, and Salps (Thaliacea, Urochordata)

EUICHI HIROSE[1]*, SATOSHI KIMURA[2], TAKAO ITOH[2], AND JUN NISHIKAWA[3]

[1] *Department of Chemistry, Biology and Marine Science, Faculty of Science, University of the Ryukyus, Nishihara, Okinawa 903-0213, Japan;* [2] *Wood Research Institute, Kyoto University, Uji, Kyoto 611, Japan; and* [3] *Ocean Research Institute, University of Tokyo, Nakano, Tokyo 164-8639, Japan*

Abstract. The morphology and cellulosic composition of the tunic was studied in pelagic tunicates (3 pyrosomas, 2 doliolids, and 13 salps). The tunic is transparent and gelatinous, consisting of an electron-dense cuticular layer with a fibrous tunic matrix. The thickness and density of the cuticular layer and of the tunic matrix differ from species to species. In some salps, the cuticular layer has numerous minute protrusions that are structurally identical to those found in several ascidians. Free mesenchymal cells (tunic cells) are distributed in the tunic. Whereas the number of tunic cells in the pyrosomas is similar to that in ascidians, there are many fewer tunic cells in doliolids and salps. These differences may be caused by the different functions of the tunic in each group. The existence of cellulose in the tunic was confirmed using electron diffraction in all of the species studied thus far. Their diffractograms indicate that the cellulose microfibrils consist of nearly pure Iβ of the allomorph. These results show that tunic morphology and cellulosic composition are similar in ascidians and thaliaceans (pyrosomas, doliolids, and salps). The tunic is considered to be a homologous tissue in these animals, and their most recent common ancestor would have possessed this tissue.

Introduction

Members of the phylum Chordata are characterized by having a notochord during some stage of development. Urochordata (also called Tunicata) is one of three subphyla in the phylum Chordata. The name Tunicata is derived from the unique integumentary tissue, called the tunic, that entirely covers the epidermis. The Urochordata includes three classes; all of the species possess tunic in the classes Ascidiacea and Thaliacea, whereas the presence of tunic is not well documented in the class Appendicularia. The tunic is a peculiar tissue among metazoans because of its cellulosic components (De Leo *et al.,* 1977) and the presence of free-living cells (tunic cells) in the tunic, that is, outside the epidermis. To date, the biology and biochemistry of the tunic have been studied mainly in ascidians, sessile forms of tunicates, but they have not been well investigated in pelagic tunicates.

In ascidians, many types of tunic cells have been described, and they are involved in various biological functions, such as phagocytosis (De Leo *et al.,* 1981; Hirose *et al.,* 1994), conduction of impulses (Mackie and Singla, 1987), contractility of the tunic (Hirose and Ishii, 1995), bioluminescence (Aoki *et al.,* 1989; Chiba *et al.,* 1998), photosynthetic symbiosis (Hirose *et al.,* 1996b), and allorecognition (Hirose *et al.,* 1997c). The tunic is overlaid by a cuticular layer that sometimes has a subcuticular layer beneath it. In several ascidian species, the cuticular surface has numerous minute protrusions that are 100 nm high or less. Descriptions of the cuticular fine structures in 116 ascidian species indicate that the presence or absence of cuticular protrusions has phylogenetic significance (*cf.* Hirose *et al.,* 1997b). Little information has been accumulated on the tunic of pelagic tunicates, such as pyrosomas, doliolids, and salps (reviewed in Welsh, 1984, and Bone, 1998). In this study, we investigated the tunic morphology of thaliaceans, with special attention to the distribution of the tunic cells and the fine structure of the cuticule.

Received 8 June 1998; accepted 13 October 1998.

* To whom correspondence should be addressed. E-mail: euichi@sci.u-ryukyu.ac.jp

Almost all ascidians studied to date have been found to contain cellulose I microfibrils in the tunic (Yamamoto *et al.*, 1989; Van Daele *et al.*, 1992; Kimura and Itoh, 1996; Okamoto *et al.*, 1996). In pelagic tunicates, however, research has thus far shown cellulose I microfibrils with high crystallinity in the tunic of only one species of Salpidae, *Salpa fusiformis* (Belton *et al.*, 1989). It is not yet known whether other pelagic tunicates can make cellulose. Our study also focuses on the existence and characterization of cellulose in pelagic tunicates.

This report deals with the tunic morphology and cellulosic components of 18 thaliacean tunicates from all orders of Thaliacea. The results provide information valuable for better understanding the diversity and evolution of the tunic in conjunction with the phylogeny of tunicates.

Table 1

Tunic Cuticle Structures in Thaliacea

Species[a]	Cuticular protrusions[b]
Subclass Pyrosomata	
Order Pyrosomatida	
Family Pyrosomatidae	
Pyrostremma agassizi	–
Pyrosoma aherniosum	–
Pyrosoma atlanticum	–
Subclass Myosomata	
Order Doliolida (=Cyclomyaria)	
Family Doliolidae	
Dolioletta gegenbauri (gono.)	–
Doliolum nationalis (gono.)	0
Order Salpida (=Desmomyaria)	
Family Salpidae	
Cyclosalpa affinis (agg.)	N
Cyclosalpa polae (agg.)	0
Cyclosalpa quadriluminis forma *parallela* (agg.)	N
Iasis zonaria (agg.)	–
Metcalfina hexagona (sol.)	–
Pegea confoederata (agg.)	N
Salpa fusiformis (sol.)	–
Salpa fusiformis (agg.)	–
Thalia cicar (sol.)	0
Thalia democratica (sol.)	+
Thalia orientalis (sol.)	+
Thetys vagina (agg.)	+
Traustedtia multitentaculata (agg.)	0
Retteriella retracta (sol.)	N

[a] gono. = gonozooid; agg. = aggregate zooid; sol. = solitary zooid.

[b] 0 = cuticular layer was not observed clearly; N = cuticular layer was not observed (too lucent or bad preservation). A plus sign indicates the presence of minute protrusions. A minus sign indicates the absence of minute protrusion (the surface of the cuticle is flat).

Materials and Methods

Sample collection and fixation

We examined 3 species of pyrosomas, 2 species of doliolids, and 13 species of salps (see Table I), which were collected in several net tows taken southeast of Tokyo, Japan (34°11′–35°04′ N, 139°06′–143°32′ E). Apparently intact animals were sorted from the samples on board ship and prefixed immediately in 2.5% glutaraldehyde-0.45 *M* sucrose-0.1 *M* cacodylate (pH 7.4) at room temperature. Large species, such as *Thetys vagina*, *Salpa fusiformis*, and *Iasis zonaria*, were dissected in the fixation medium, and the tunic near a gill bar was used for the following examinations.

Microscopy for the observation of tunic morphology

After a brief rinse in 0.45 *M* sucrose-0.1 *M* cacodylate (pH 7.4), the specimens were postfixed in 1% osmium tetroxide-0.1 *M* cacodylate for 1.5 h, dehydrated through an ethanol series, cleared with *n*-butyl glycidyl ether, and embedded in low-viscosity epoxy resin. Thick sections were stained with 1% toluidine blue for light microscopy. Thin sections were double stained and examined in a Hitachi HS-9 transmission electron microscope at an accelerating voltage of 75 kV.

In some of the prefixed specimens, the tunic was isolated from the other tissues and observed using a light microscope equipped with Nomarski differential interference contrast (DIC) and phase contrast optics.

Microscopy for the analysis of cellulose fibers

To examine replicas of the cellulose fibers, the samples were treated with 5% KOH overnight at room temperature, followed by 2 h of bleaching in 0.34% $NaClO_2$, buffered at pH 4.9 in 50 m*M* acetate buffer, at 80°C. These treatments were repeated three times, at which point the tissue became completely white. The purified tunic samples were transferred to an acetyl cellulose film, air dried, then unidirectionally shadowed at 45° with platinum-carbon and coated with carbon at 2×10^{-4} Pa by a BAF 400D freeze-etch apparatus (Balzers, Liechtenstein). Replicas were cleaned in a 5% sodium dichromate-50% sulfuric acid mixture (w/v) and mounted on Formvar-coated copper grids for observation with a transmission electron microscope (JEOL, JEM-2000EXII) operating at an accelerating voltage of 100 kV.

For observation of the selected area electron diffraction, purified tunic samples were mounted on carbon-coated grids after homogenization with liquid nitrogen using mortar and pestle. The electron diffraction patterns were obtained with a JEM-2000EXII transmission electron microscope operating at an accelerating voltage of 100 kV.

Results

Tunic morphology

All of the species examined in this study have a transparent, gelatinous tunic that covers the epidermis (Fig. 1).

The hardness of the tunic varies among species. The tunic is very soft and fragile in some species, such as *Doliolum nationalis, Cyclosalpa polae, Pegea confoederata,* and *Retteriella retracta.* The soft tunic was usually only lightly stained in both light and electron microscopic preparations, suggesting that the structural components of the tunic are present in low density in these species. The thickness of the tunic also varies from one species to another: in some species it has a thickness of several millimeters or more (*e.g., Pyrosoma aherniosum, Metcalfina hexagona,* and *Thetys vagina*), whereas in others (*Dolioletta gegenbauri* and *Doliolum nationalis*) it is a thin sheath of 1–2 μm. However, the thickness we measured includes substantial error attributable to shrinkage of the specimens during fixation, embedding, and sectioning. In all of the species examined, bacteria were rarely found within the tunic.

In the salps and doliolids (species of the subclass Myosomata), we found many fewer tunic cells than in the ascidian species (Fig. 2A). The sparsely distributed tunic cells are amoeboid-shaped, with extending pseudopodia (Fig. 2, B and C). In contrast, the pyrosomas have many tunic cells of several types (Fig. 3), one of which forms a cellular network in the tunic (Fig. 4A). In histological sections, elongated forms of tunic cells that appear to correspond to cells of this network form a line (Fig. 4, B and C). The network probably occurs in a specific layer in the tunic.

Salps have two forms of zooids in their life cycle: solitary (asexual) and aggregate (sexual) zooids. We examined the tunic of both forms in *Salpa fusiformis.* Although the tunic shape differs between the two forms and the tunic is usually thicker in the solitary zooids, there are no prominent differences in the morphology of tunic cells or in the fine structure of the tunic cuticle.

Tunic cuticle

The tunic cuticle is an electron-dense layer covering the tunic matrix. In some of the species that have a very soft tunic, we could not clearly distinguish the cuticular layer or the tunic matrix, or both, in thick and thin sections (Table 1). Perhaps the stainability and electron density of the cuticular layer were too low to be detected or the tunic and cuticle were so fragile that they were poorly fixed or broken in these specimens.

The thickness of the cuticular layer is about 10–20 nm in 8 of 10 species in which we clearly observed the fine structure of the tunic cuticle (Fig. 5, A–E). The other two species, *Iasis zonaria* and *Thetys vagina,* have a cuticular layer of 0.5–1.0 μm thick, including a subcuticular layer (Fig. 5F). The minute cuticular protrusions (about 50 nm in height or less) were seen only in *Thalia democratica, Thalia orientalis,* and *Thetys vagina* (Fig. 5, E and F; Table 1). In general, when the tunic is harder, the cuticular layer is thicker and the fibrous components of the tunic matrix are stained more densely.

Cellulose fibers

Figure 6 shows replica images (A, C, E, and G) and electron diffractograms (B, D, F, and H) of purified tunic fibers in *Pyrosoma atlanticum* (A and B), *Doliolum nationalis* (C and D), *Iasis zonaria* (E and F), and *Pegea confoederata* (G and H). The electron diffractograms with three to five spots (110, $1\bar{1}0$, 200, 002, and 004) in each figure indicate that the tunic of pyrosomas, doliolids, and salps contains cellulose I microfibrils with high crystallinity. No super-lattice reflections originating from triclinic crystalline cellulose (Iα) were observed. In some specimens, a 002 reflection spot originating from monoclinic crystalline cellulose (Iβ) was clearly observed (Fig. 6D). The diffractograms obtained from *Pyrostremma agassizi, Dolioletta gegenbauri, Salpa fusiformis,* and *Retteriella retracta* are essentially identical to those shown in Figure 6. The 110 diffraction spot of *Pyrosoma atlanticum* was often stronger than $1\bar{1}0$ (Fig. 6B). *Pyrosoma atlanticum* and *Doliolum nationalis* have cellulose microfibrils of 20-nm mean width (Fig. 6, A and C), whereas the microfibrils of salps are 18-nm mean width (Fig. 6, E and G). Bundles with two to six cellulose microfibrils were often observed in specimens of *I. zonaria* and *P. confoederata* (Fig. 6, E and G, arrowheads).

Discussion

The functions of the tunic would be very different between benthic and pelagic forms of tunicates. In benthic environments, many organisms are concentrated at high densities and diversities, so the primary functions of the tunic of benthic tunicates would be protection against predators, including bacterial infections, and attachment to the substratum. The tunic might also assist in competition for space. Therefore, benthic tunicates would benefit from having a thick, hard tunic containing many tunic cells with a variety of functions that contribute to body protection. In contrast, pelagic tunicates do not need a tunic for settlement or for occupying space. Hard, heavy tunics like those possessed by ascidians would be unsuitable for maintaining the neutral buoyancy of pelagic tunicates, even though they might be protective. Moreover, since pelagic tunicates are heavily preyed upon by sight predators such as fish, a thin transparent tunic that transmits light would be a distinct advantage to the pelagic forms. Thus, it is reasonable for pelagic tunicates to posses relatively soft, fragile tunics.

Whereas the salps and doliolids examined in this study contained few tunic cells, pyrosomas had relatively high numbers of tunic cells, comparable to the numbers found in ascidians. If one assumes that tunic cells have evolved primarily for protection against predators and tend to be

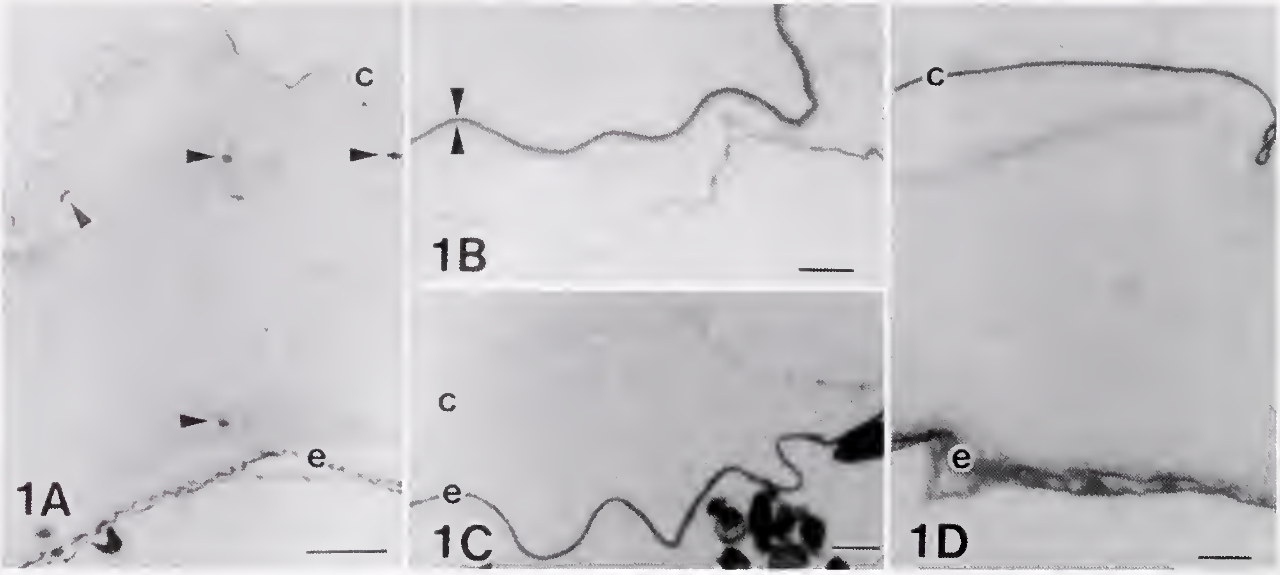
c
1A
e
1B
c
e
1C
c
e
1D

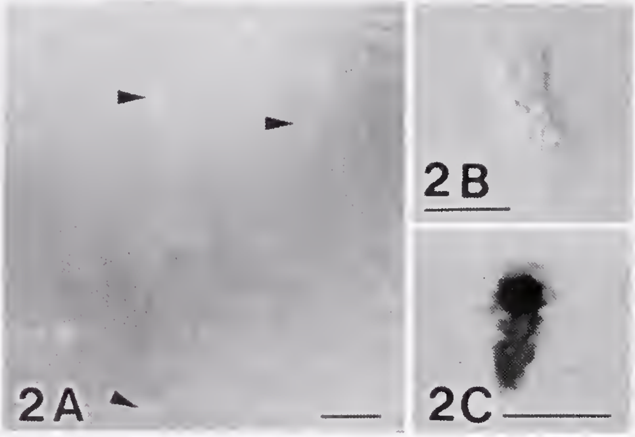
2A
2B
2C

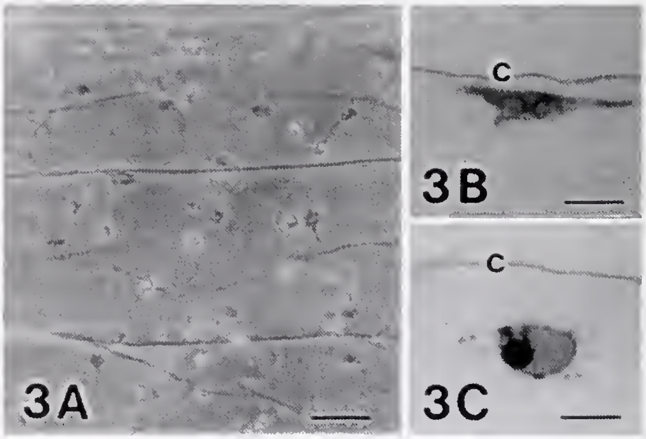
3A
c
3B
c
3C

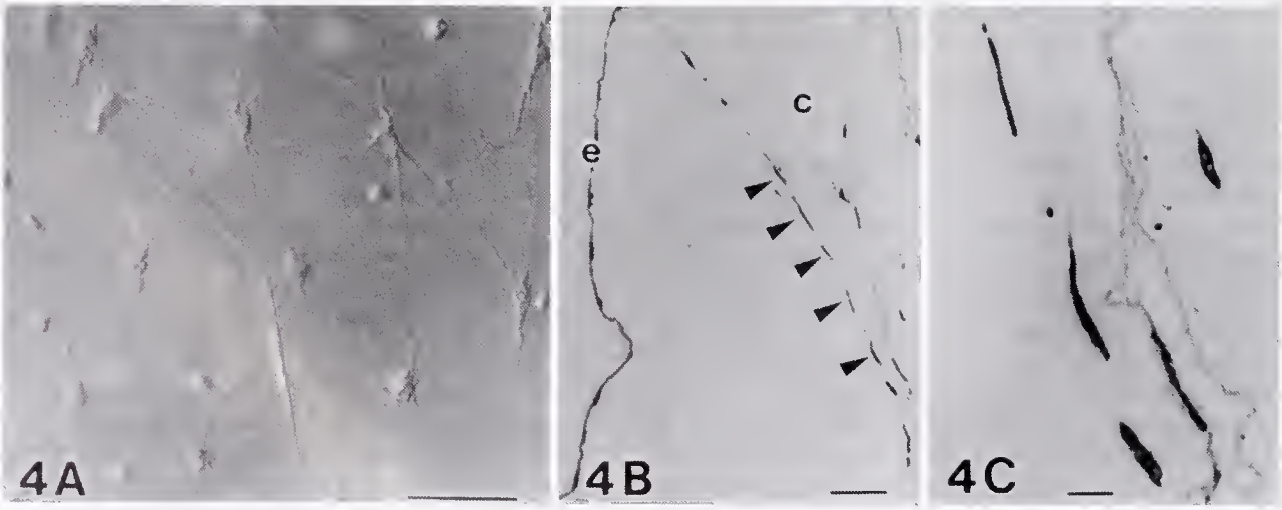
4A
e
c
4B
4C

Figure 1. Histological sections of the tunic stained with toluidine blue. The tunic matrix fills the space between the tunic cuticle (c) and the epidermis (e). (A) *Pyrosoma atlanticum.* Arrowheads indicate some tunic cells. (B) *Dolioletta gegenbauri* (gonozooid) has a very thin tunic layer (indicated by two arrowheads). (C) *Cyclosalpa polae* (aggregate zooid). (D) *Thalia orientalis* (solitary zooid). Scale bars = 50 μm (A), 10 μm (B–D).

Figure 2. Tunic cells of *Salpa fusiformis* (aggregate zooid). Tunic cells (arrowheads) are sparsely distributed in the tunic (A, phase contrast). Tunic cells are amoeboid-shaped with pseudopodia (B, Nomarski differential interference contrast; C, histological section). Scale bars = 50 μm (A), 10 μm (B and C).

Figure 3. Tunic cells of *Pyrostremma agassizi.* Several types of tunic cells are distributed in the tunic (A, Nomarski differential interference contrast; B and C, histological sections). c, tunic cuticle. Scale bars = 50 μm (A), 10 μm (B and C).

Figure 4. Multipolar tunic cells form a cellular network in the tunic of *Pyrostremma agassizi.* (A, Nomarski differential interference contrast). Tunic cells (arrowheads) forming a line are occasionally found in the tunic and probably correspond to the cellular network (B, histological section; C enlargement of B). c, tunic cuticle; e, epidermis. Scale bars = 50 μm (A and B), 10 μm (C).

well developed in animals that lack the ability to escape, these cells should be more important to pyrosomas than to doliolids and salps. Although all three groups use jet propulsion, pyrosomas swim slowly, using the water streams from the feeding currents of each zooid, whereas doliolids and salps swim quickly, using water pulses produced by the

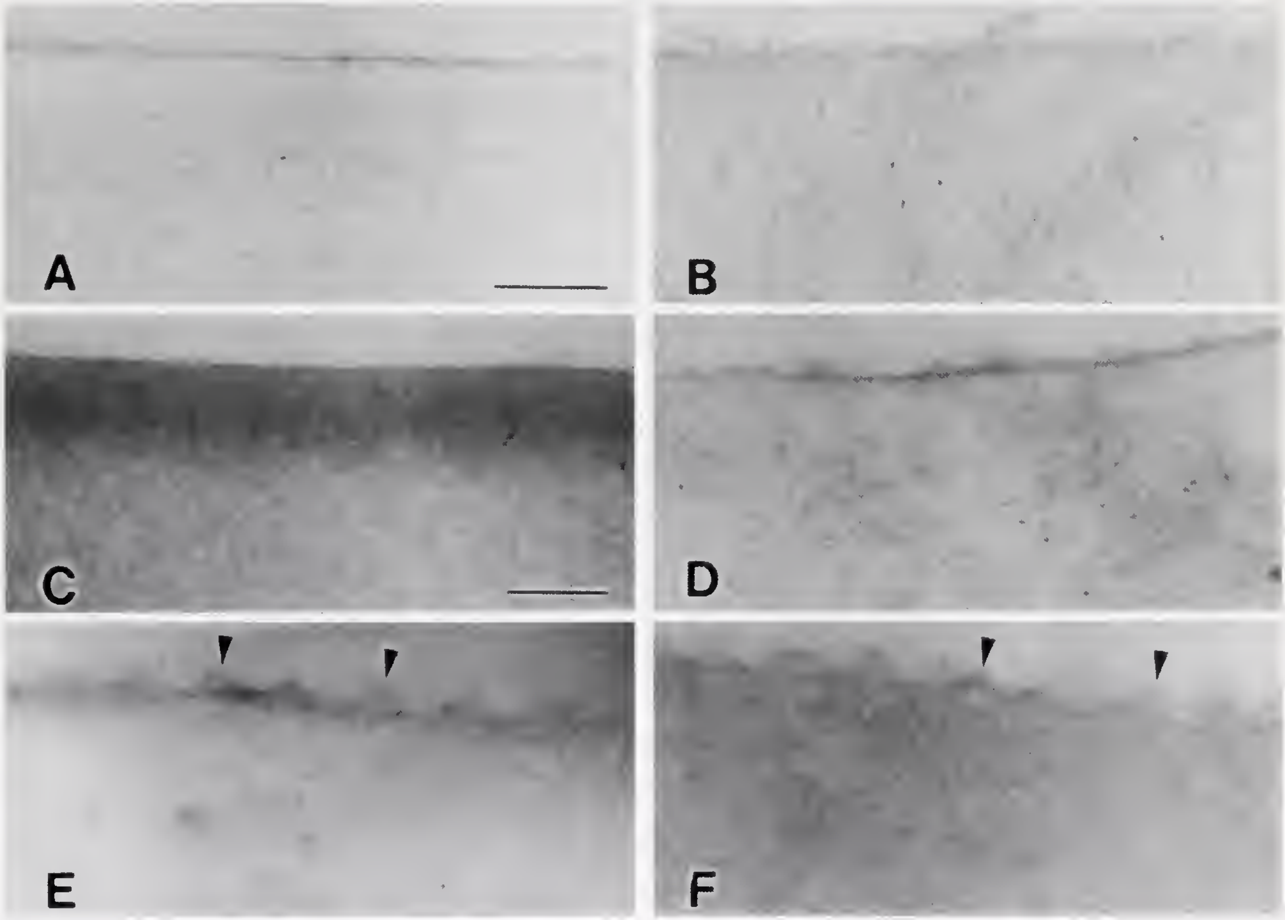

Figure 5. Transmission electron microscopy of the tunic cuticle of some thaliaceans. (A) *Pyrosoma atlanticum.* (B) *Dolioletta gegenbauri* (gonozooid). (C) *Iasis zonaria* (aggregate zooid). (D) *Metcalfina hexagona* (solitary zooid). (E) *Thalia democratica* (solitary zooid). (F) *Thetys vagina* (aggregate zooid). Arrowheads in E and F indicate cuticular protrusions. Magnifications of A, B, and D–F are identical. Scale bars = 0.2 μm (A), 1 μm (C).

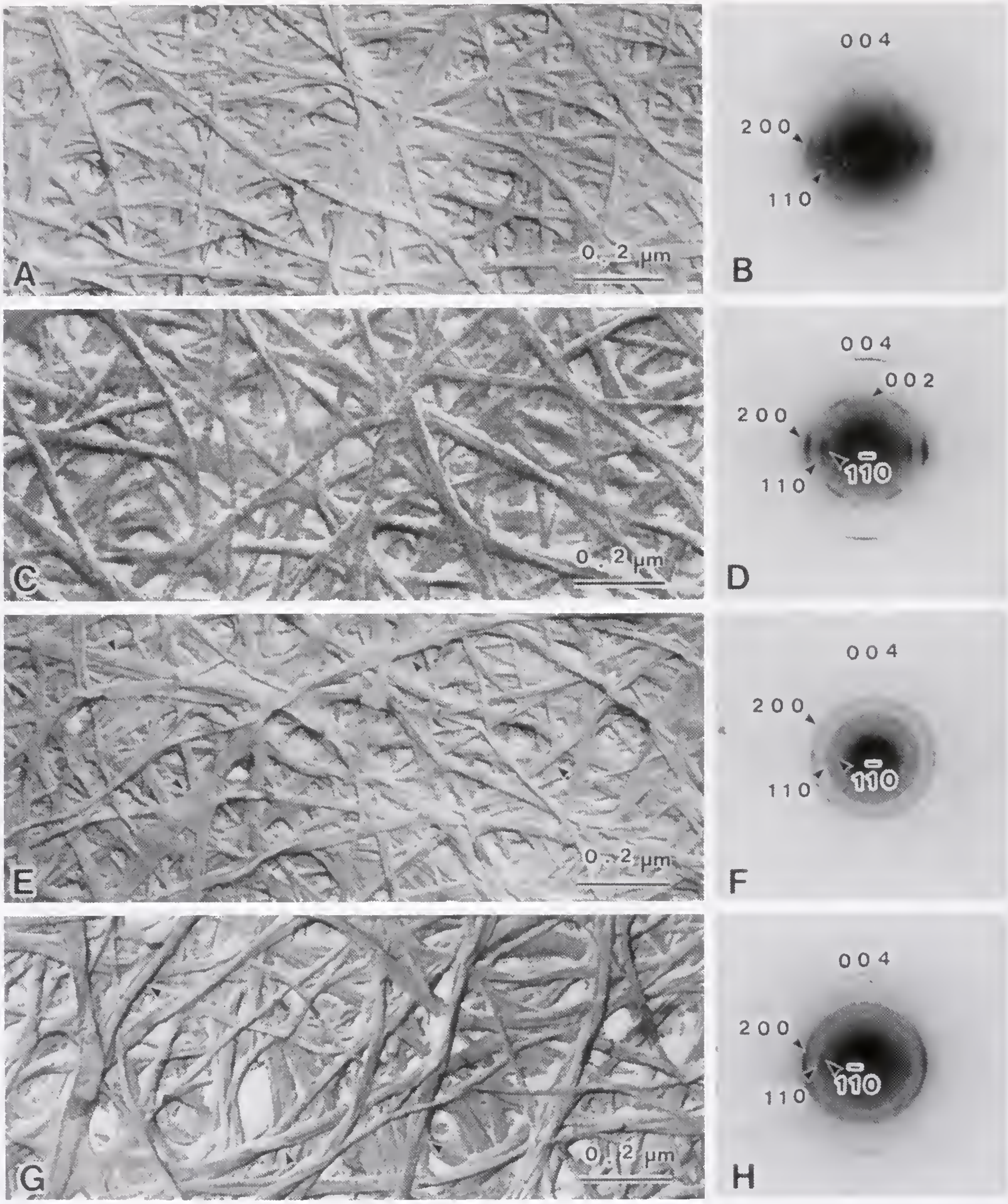

Figure 6. Replication images of purified cellulose microfibril (A, C, E, and G) and its electron diffractogram (B, D, F, and H) of *Pyrosoma atlanticum* (A and B), *Doliolum nationalis* (C and D), *Iasis zonaria* (E and F), and *Pegea confoederata* (G and H). All figures are of the same magnification. The diffractograms show that all specimens are composed of cellulose I microfibrils with high crystallinity. Bundles with two to six cellulose microfibrils were often observed in *I. zonaria* and *Pegea confoederata* (E and G, arrowheads).

rapid contraction of circular muscle bands responding to stimulation (*e.g.*, Bone and Trueman, 1983, 1984; Nishikawa and Terazaki, 1994; Bone, 1998).

The tunic cells in salps and doliolids have an amoeboid shape and many pseudopodia, characteristics that are suggestive of their motility within the tunic. Because they are very similar in morphology to the tunic phagocytes of some ascidians (*cf.* Hirose *et al.*, 1994, 1996a, b), these cells might be phagocytes. Among several types of tunic cells in pyrosomas, one type forms a cellular network. This network might facilitate coordination among the zooids in a colony. A cellular network has been described in the tunic of some colonial ascidians; it seems to be involved in impulse conduction (Mackie and Singla, 1987) and tunic contractility in response to wounding (Hirose and Ishii, 1995; Hirose *et al.*, 1997a). Although bacteria are often found within the tunic of some ascidians (*cf.* Hirose and Saito, 1992; Hirose *et al.*, 1996a), they are rarely found within the tunic of pelagic tunicates. Perhaps the tunic of the pelagic species contains some antibiotic substances, or maybe bacterial infections are less common in the habitat of the pelagic tunicates than in that of the sessile forms. If some tunic cells of pelagic tunicates are phagocytic, they may help to keep the tunic sterile.

To date, the fine structure of the tunic cuticle has been described in 116 ascidian species covering all of the families and subfamilies of the class Ascidiacea except for the phlebobranch families Octacnemidae and Plurellidae (Hirose *et al.*, 1990, 1992, 1997b). The presence of cuticular protrusions appears to have a phylogenetic significance in Ascidiacea, because there is a general stability of the character-state distribution (presence or absence) within the families or subfamilies in the traditional classification. The authors concluded that the common ancestor of ascidians lacked cuticular protrusions and that the protrusions possibly emerged independently in several lineages (Hirose *et al.*, 1997b). With respect to ascidian phylogeny, pelagic tunicates can be considered the "out-group." Our results tend to support this concept, because many of the examined species do not have cuticular protrusions. The common ancestor of tunicates probably did not have cuticular protrusions and this character may have been independently acquired in some lineages of ascidians and thaliaceans. If cuticular protrusions emerged repetitively and became fixed in certain tunicate lineages, these protrusions should have some adaptive purpose that is as yet unknown.

Using electron diffraction, the existence of cellulose was confirmed in the tunic of three groups of pelagic tunicates: pyrosomas, doliolids, and salps. The tunic of these pelagic tunicates consisted of cellulose I microfibrils with high crystallinity and large dimensions and belonging almost entirely to the cellulose Iβ allomorph. These features are similar to those of the cellulose found in ascidians (Yamamoto *et al.*, 1989; Van Daele *et al.*, 1992; Kimura and Itoh, 1996; Okamoto *et al.*, 1996), suggesting that cellulose synthetic ability is an inherited characteristic common to ascidians and thaliaceans. The tunic cellulose in thaliaceans may be synthesized by terminal complexes (TCs) in the plasma membrane of epidermal cells, as occurs in ascidians (Kimura and Itoh, 1996). The visualization of TCs in these thaliaceans is required for further discussion of the evolution of cellulose synthesis in tunicates.

In this study, we did not examine appendicularians, the other member of the pelagic tunicates. Adult appendicularians do not have integumentary tissue outside the epidermis, but they secrete a mucous substance that forms their "house," which is a feeding apparatus. In embryonic and juvenile stages, the entire animal is covered by an acellular membrane, but it is not certain whether the membrane is equivalent to the tunic (Fenaux, 1998).

The tunic is a synapomorphic character in tunicates, and it is generally believed to have evolved monophyletically. Our present results—demonstrating that the tunic morphology and cellulosic components are fundamentally the same in ascidians, pyrosomas, doliolids, and salps—are consistent with that view. The numbers of tunic cells in doliolids and salps are much smaller than those in ascidians and pyrosomas; this difference could reflect different functions of the tunic as an integumentary tissue. Thus, perhaps the tunic has become diversified in its properties and functions, thereby making it an attractive model for studying the evolution of adaptive tissue functions.

Acknowledgments

We thank the captain and the crews of R/V *Tansei Maru* of the Ocean Research Institute, University of Tokyo, for material collection at sea. We also wish to thank anonymous referees for their valuable comments and discussions. This study was supported by Grants-in-Aid for the Encouragement of Young Scientists to E. H. and S. K., by Grants-in-Aid for Research for the Future Program (JSPS-RFTF 96L00605) to T. I. from the Ministry of Education, Culture and Science of Japan, and by a predoctoral fellowship to S. K. from the Japanese Society for the Promotion of Science. The study was partly carried out at Shimoda Marine Research Center, University of Tsukuba (contribution #625).

Literature Cited

Aoki, M., K. Hashimoto, and H. Watanabe. 1989. The intrinsic origin of bioluminescence in the ascidian, *Clavelina miniata*. *Biol. Bull.* **176:** 57–62.

Belton P. S., S. F. Tanner, N. Cartier, and H. Chanzy. 1989. High-resolution solid-state ^{13}C nuclear magnetic resonance spectroscopy of tunicin, an animal cellulose. *Macromolecules* **22:** 1615–1617.

Bone, Q. 1998. *The Biology of the Pelagic Tunicate.* Oxford University Press. Oxford.

Bone, Q., and E. R. Trueman. 1983. Jet propulsion in salps (Tunicata: Thaliacea). *J. Zool. Lond.* **201:** 481–506.

Bone, Q., and E. R. Trueman. 1984. Jet propulsion in *Doliolum* (Tunicata: Thaliacea). *J. Exp. Mar. Biol. Ecol.* **76:** 105–118.

Chiba, K., M. Hoshi, M. Isobe, and E. Hirose. 1998. Bioluminescence in the tunic of the colonial ascidian, *Clavelina miniata:* Identification of luminous cells in vitro. *J. Exp. Zool.* **281:** 546–553.

De Leo, G., E. Patricolo, and G. D'Ancona Lunetta. 1977. Studies on the fibrous components of the test of *Ciona intestinalis* Linnaeus. I. Cellulose-like polysaccharide. *Acta Zool.* (Stockh.) **58:** 135–141.

De Leo, G., E. Patricolo, and G. Frittita. 1981. Fine structure of the tunic of *Ciona intestinalis* L. II. Tunic morphology, cell distribution and their functional importance. *Acta Zool.* (Stockh.) **62:** 259–271.

Fenaux, R. 1998. Life history of the Appendicularia. Pp. 151–159 in *The Biology of the Pelagic Tunicate,* Q. Bone, ed. Oxford University Press, Oxford.

Hirose, E., and T. Ishii. 1995. Microfilament contraction promotes rounding of tunic slices: an integumentary defense system in the colonial ascidian *Aplidium yamazii. Biol. Bull.* **189:** 29–35.

Hirose, E., and Y. Saito. 1992. Threadlike bacteria in the tunic of a botryllid ascidian. (Note). *Hiyoshi Rev. Natur. Sci. Keio Univ.* **12:** 108–110.

Hirose, E., Y. Saito, K. Hashimoto, and H. Watanabe. 1990. Minute protrusions of the cuticle: fine surface structures of the tunic in ascidians. *J. Morphol.* **204:** 67–73.

Hirose, E., T. Nishikawa, Y. Saito, and H. Watanabe. 1992. Minute protrusions of ascidian tunic cuticle: some implications for ascidian phylogeny. *Zool. Sci. (Tokyo)* **9:** 397–404.

Hirose, E., T. Ishii, Y. Saito, and Y. Taneda. 1994. Phagocytic activity of tunic cells in the compound ascidian *Aplidium yamazii* (Polyclinidae, Aplousobranchia). *Zool. Sci. (Tokyo)* **11:** 203–208.

Hirose, E., M. Aoki, and K. Chiba. 1996a. Fine structures of tunic cells and distribution of bacteria in the tunic of the luminescent ascidian *Clavelina miniata* (Ascidiacea, Urochordata). *Zool. Sci. (Tokyo)* **13:** 519–523.

Hirose, E., T. Maruyama, L. Cheng, and R. A. Lewin. 1996b. Intracellular symbiosis of a photosynthetic prokaryote, *Prochloron* sp., in a colonial ascidian. *Invertebr. Biol.* **115:** 343–348.

Hirose, E., T. Ishii, and Y. Taneda. 1997a. Two modes of tunic cuticle formation in a colonial ascidian *Aplidium yamazii,* responding to wounding. *Dev. Comp. Immunol.* **21:** 25–34.

Hirose, E., G. Lambert, T. Kusakabe, and T. Nishikawa. 1997b. Tunic cuticular protrusions in ascidians (Chordata, Tunicata): a perspective of their character-state distribution. *Zool. Sci. (Tokyo)* **14:** 683–689.

Hirose, E., Y. Saito, and H. Watanabe. 1997c. Subcuticular rejection: an advanced mode of the allogeneic rejection reaction in the compound ascidians, *Botrylloides simodensis* and *B. fuscus. Biol. Bull.* **192:** 53–61.

Kimura, S., and T. Itoh. 1996. New cellulose synthesizing complexes (terminal complexes) involved in animal cellulose biosynthesis in the tunicate *Metandrocarpa uedai. Protoplasma* **194:** 151–163.

Mackie, G. O., and C. L. Singla. 1987. Impulse propagation and contraction in the tunic of a compound ascidian. *Biol. Bull.* **173:** 188–204.

Nishikawa, J., and Terazaki, M. 1994. Measurement of swimming speed and pulse rate of salps using a video equipment. *Bull. Plankton Soc. Jpn.* **41:** 170–173.

Okamoto, T., J. Sugiyama, and T. Itoh. 1996. Structural diversity of ascidian cellulose. *Wood Res.* **83:** 27–29.

Van Daele, Y., J.-F. Revol, F. Gaill, and G. Goffinet. 1992. Characterization and supramolecular architecture of the cellulose-protein fibrils in the tunic of the sea peach (*Halocynthia papillosa,* Ascidiacea, Urochordata). *Biol. Cell* **76:** 87–96.

Welsh, U. 1984. Urochordata. Pp. 800–816 in *Biology of the Integument I. Invertebrates,* J. Bereiter-Hahn, A. G. Matoltsy, and K. S. Richards, eds. Springer-Verlag, Berlin.

Yamamoto, H., F. Horii, and A. Hirai. 1989. Structural changes of native cellulose crystals induced by annealing in aqueous alkaline and acid solutions at high temperatures. *Macromolecules* **22:** 4130–4132.

THE
BIOLOGICAL BULLETIN

APRIL 1999

APR 21 1999

Editor	MICHAEL J. GREENBERG	The Whitney Laboratory, University of Florida
Associate Editors	LOUIS E. BURNETT	Grice Marine Biological Laboratory, College of Charleston
	CHARLES D. DERBY	Georgia State University
	MICHAEL LABARBERA	University of Chicago
	RUDOLF A. RAFF	Indiana University
Section Editor	SHINYA INOUÉ, *Imaging and Microscopy*	Marine Biological Laboratory
Online Editors	JAMES A. BLAKE, *Keys to Marine Invertebrates of the Woods Hole Region*	ENSR Marine & Coastal Center, Woods Hole
	WILLIAM D. COHEN, *Marine Models Electronic Record and Compendia*	Hunter College, City University of New York
Editorial Board	PETER B. ARMSTRONG	University of California, Davis
	ANDREW R. CAMERON	California Institute of Technology
	ERNEST S. CHANG	University of California, Davis
	THOMAS H. DIETZ	Louisiana State University
	RICHARD B. EMLET	Oregon Institute of Marine Biology, Univ. of Oregon
	DAVID EPEL	Hopkins Marine Station, Stanford University
	GREGORY HINKLE	Cereon Genomics, Cambridge, Massachusetts
	MAKOTO KOBAYASHI	Hiroshima University of Economics, Japan
	DONAL T. MANAHAN	University of Southern California
	MARGARET MCFALL-NGAI	Kewalo Marine Laboratory, University of Hawaii
	MARK W. MILLER	Institute of Neurobiology, University of Puerto Rico
	TATSUO MOTOKAWA	Tokyo Institute of Technology, Japan
	YOSHITAKA NAGAHAMA	National Institute for Basic Biology, Japan
	SHERRY D. PAINTER	Marine Biomed. Inst., Univ. of Texas Medical Branch
	J. HERBERT WAITE	University of California, Santa Barbara
	RICHARD K. ZIMMER-FAUST	University of California, Los Angeles
Editorial Office	PAMELA CLAPP HINKLE	Managing Editor
	VICTORIA R. GIBSON	Staff Editor
	CAROL SCHACHINGER	Editorial Assistant
	PATRICIA BURNS	Subscription & Advertising Secretary

Published by
MARINE BIOLOGICAL LABORATORY
WOODS HOLE, MASSACHUSETTS

Cover

Cyanea capillata, the lion's mane jellyfish, is featured on our cover this month as an artistic memorandum to our readers that the *Keys to Marine Invertebrates of the Woods Hole Region,* edited by Ralph A. Smith (1964), are being revised online (see the Announcement on page 121). Moreover, the first segment of the revision has been completed; it is the section on Scyphozoa, authored by Dale Calder, who is at the Centre for Biodiversity and Conservation Biology of the Royal Ontario Museum in Toronto. The drawing on our cover—by Patrice Stephens-Bourgeault, also of the Royal Ontario Museum—is one of the plates from the new section. It is adapted from several sources, including a lithograph by Auguste Sonrel, drawn for Louis Agassiz, who published it in 1862.

Cyanea is a frequent visitor to the Woods Hole region during winter and spring, and occasionally in the summer. There may be two varieties that differ in size, color, and some minor morphological features. The larger version, found primarily in the North Atlantic, can attain a size of up to 2.5 m across the saucer-shaped bell with tentacles up to 40 m long. The tentacles of the medusa on our cover are contracted; if they were relaxed they would extend about six feet below the bottom of the journal.

When it is hunting, *Cyanea* sinks slowly, with its tentacles relaxed and spread out around it in a circular net. Its weapons are thousands of nematocysts, comprising euryteles and isorhizas, and its prey includes fishes and polychaete worms. Large arctic animals have a sting that can raise painful weals on humans, but are not known to be fatal—notwithstanding the assertion of Sherlock Holmes in "The Adventure of the Lion's Mane." Still, the nematocysts continue to be of interest to students of marine venoms.

Among Metazoa, the Cnidaria have the most primitive nervous systems, and these have been studied as an approach to the fundamental properties of neuronal mechanisms. *Cyanea capillata,* in particular, provides useful preparations with which to investigate synaptic transmission and ion channels. Most recently, these primitive animals have been found to have very conventional voltage-gated calcium channels, and continued investigation of these proteins will help us understand the relationship between structure and function in calcium channel subunits (see Jeziorsky *et al.* 1998. *J. Biol. Chem.* 273: 22792-99).

CONTENTS

Volume 196, No. 2: April 1999

Announcement: *Keys to Marine Invertebrates of the Woods Hole Region* . . . 121

RESEARCH NOTE

Ó Foighil, Diarmaid, Bruce A. Marshall, Thomas J. Hilbish, and Mario A. Pino
Trans-Pacific range extension by rafting is inferred for the flat oyster *Ostrea chilensis* . . . 122

NEUROBIOLOGY

Schmidt, Manfred, and Steffan Harzsch
Comparative analysis of neurogenesis in the central olfactory pathway of adult decapod crustaceans by *in vivo* BrdU-labeling . . . 127

PHYSIOLOGY

Frank, Tamara M.
Comparative study of temporal resolution in the visual systems of mesopelagic crustaceans . . . 137

Coughlin, David J., and Lawrence C. Rome
Muscle activity in steady swimming scup, *Stenotomus chrysops*, varies with fiber type and body position . . . 145

Khan, Hamid R., David A. Price, Karen E. Doble, Michael J. Greenberg, and A.S.M. Saleuddin
Osmoregulation and FMRFamide-related peptides in the salt marsh snail *Melampus bidentatus* (Say) (Mollusca: Pulmonata) . . . 153

BEHAVIORAL PHYSIOLOGY

McGaw, I.J., C.L. Reiber, and J.A. Guadagnoli
Behavioral physiology of four crab species in low salinity . . . 163

DEVELOPMENT AND REPRODUCTION

Vavra, Jay, and Donal T. Manahan
Protein metabolism in lecithotrophic larvae (Gastropoda: *Haliotis rufescens*) . . . 177

Biggers, William J., and Hans Laufer
Settlement and metamorphosis of *Capitella* larvae induced by juvenile hormone-active compounds is mediated by protein kinase C and ion channels . . . 187

Unuma, Tatsuya, Takeshi Yamamoto, and Toshio Akiyama
Effect of steroids on gonadal growth and gametogenesis in the juvenile Red Sea urchin *Pseudocentrotus depressus* . . . 199

ECOLOGY AND EVOLUTION

Okamura, Beth, and Julian C. Partridge
Suspension feeding adaptations to extreme flow environments in a marine bryozoan . . . 205

Schmidt, Hartmut, and Wilfried Westheide
Genetic relationships (RAPD-PCR) between geographically separated populations of the "cosmopolitan" interstitial polychaete *Hesionides gohari* (Hesionidae) and the evolutionary origin of the freshwater species *Hesionides riegerorum* . . . 216

THE BIOLOGICAL BULLETIN

THE BIOLOGICAL BULLETIN is published six times a year by the Marine Biological Laboratory, 7 MBL Street, Woods Hole, Massachusetts 02543.

Subscriptions and similar matter should be addressed to Subscription Manager, THE BIOLOGICAL BULLETIN, Marine Biological Laboratory, 7 MBL Street, Woods Hole, Massachusetts 02543. Subscription per year (six issues, two volumes): $205 for libraries; $95 for individuals. Subscription per volume (three issues): $102.50 for libraries; $47.50 for individuals. Back and single issues (subject to availability): $40 for libraries; $20 for individuals.

Communications relative to manuscripts should be sent to Michael J. Greenberg, Editor-in-Chief, or Pamela Clapp Hinkle, Managing Editor, at the Marine Biological Laboratory, 7 MBL Street, Woods Hole, Massachusetts 02543. Telephone: (508) 289-7428. FAX: 508-457-1924. E-mail: pclapp@mbl.edu.

http://www.mbl.edu/BiologicalBulletin/

The home page for the electronic companion to THE BIOLOGICAL BULLETIN—*the Marine Models Electronic Record*—and other BIOLOGICAL BULLETIN publications is available on the World Wide Web at the address shown above.

THE BIOLOGICAL BULLETIN is indexed in bibliographic services including *Index Medicus* and MEDLINE, *Chemical Abstracts, Current Contents, Elsevier BIOBASE/Current Awareness in Biological Sciences,* and *Geo Abstracts.*

Printed on acid free paper,
effective with Volume 180, Issue 1, 1991.

POSTMASTER: Send address changes to THE BIOLOGICAL BULLETIN, Marine Biological Laboratory,
7 MBL Street, Woods Hole, MA 02543.

Copyright © 1999, by the Marine Biological Laboratory

Periodicals postage paid at Woods Hole, MA, and additional mailing offices.
ISSN 0006-3185

INSTRUCTIONS TO AUTHORS

The Biological Bulletin accepts outstanding original research reports of general interest to biologists throughout the world. Papers are usually of intermediate length (10–40 manuscript pages). A limited number of solicited review papers may be accepted after formal review. A paper will usually appear within four months after its acceptance.

Very short, especially topical papers (less than 9 manuscript pages including tables, figures, and bibliography) will be published in a separate section entitled "Research Notes." A Research Note in *The Biological Bulletin* follows the format of similar notes in *Nature*. It should open with a summary paragraph of 150 to 200 words comprising the introduction and the conclusions. The rest of the text should continue on without subheadings, and there should be no more than 30 references. References should be referred to in the text by number, and listed in the Literature Cited section in the order that they appear in the text. Unlike references in *Nature,* references in the Research Notes section should conform in punctuation and arrangement to the style of recent issues of *The Biological Bulletin.* Materials and Methods should be incorporated into appropriate figure legends. See the article by Lohmann *et al.* (October 1990, Vol. **179:** 214–218) for sample style. A Research Note will usually appear within two months after its acceptance.

The Editorial Board requests that regular manuscripts conform to the requirements set below; those manuscripts that do not conform will be returned to authors for correction before review.

1. ***Manuscripts.*** Manuscripts, including figures, should be submitted in quadruplicate, with the originals clearly marked. (Xerox copies of photographs are not acceptable for review purposes.) The submission letter accompanying the manuscript should include a telephone number, a FAX number, and (if possible) an E-mail address for the corresponding author. The original manuscript must be typed in no smaller than 12 pitch or 10 point, using double spacing (*including* figure legends, footnotes, bibliography, etc.) on one side of 16- or 20-lb. bond paper, 8 by 11 inches. Please, no right justification. Manuscripts should be proofread carefully and errors corrected legibly in black ink. Pages should be numbered consecutively. Margins on all sides should be at least 1 inch (2.5 cm). Manuscripts should conform to the *Council of Biology Editors Style Manual,* 5th Edition (Council of Biology Editors, 1983) and to American spelling. Unusual abbreviations should be kept to a minimum and should be spelled out on first reference as well as defined in a footnote on the title page. Manuscripts should be divided into the following components: Title page, Abstract (of no more than 200 words), Introduction, Materials and Methods, Results, Discussion, Acknowledgments, Literature Cited, Tables, and Figure Legends. In addition, authors should supply a list of words and phrases under which the article should be indexed.

2. ***Title page.*** The title page consists of a condensed title or running head of no more than 35 letters and spaces, the manuscript title, authors' names and appropriate addresses, and footnotes listing present addresses, acknowledgments or contribution numbers, and explanation of unusual abbreviations.

3. ***Figures.*** The dimensions of the printed page, 7 by 9 inches, should be kept in mind in preparing figures for publication. We recommend that figures be about 1 times the linear dimensions of the final printing desired, and that the ratio of the largest to the smallest letter or number and of the thickest to the thinnest line not exceed 1:1.5. Explanatory matter generally should be included in legends, although axes should always be identified on the illustration itself. Figures should be prepared for reproduction as either line cuts or halftones. Figures to be reproduced as line cuts should be unmounted glossy photographic reproductions or drawn in black ink on white paper, good-quality tracing cloth or plastic, or blue-lined coordinate paper. Those to be reproduced as halftones should be mounted on board, with both designating numbers or letters and scale bars affixed directly to the figures. All figures should be numbered in consecutive order, with no distinction between text and plate figures and cited, in order, in the text. The author's name and an arrow indicating orientation should appear on the reverse side of all figures.

Color: The Biological Bulletin will publish color figures and plates, but must bill authors for the actual additional cost of printing in color. The process is expensive, so authors with more than one color image should—consistent with editorial concerns, especially citation of figures in order—combine them into a single plate to reduce the expense. On request, when supplied with a copy of a color illustration, the editorial staff will provide a pre-publication estimate of the printing cost.

4. ***Tables, footnotes, figure legends, etc.*** Authors should follow the style in a recent issue of *The Biological Bulletin* in preparing table headings, figure legends, and the like. Because of the high cost of setting tabular material in type, authors are asked to limit such material as much as possible. Tables, with their headings and footnotes, should be typed on separate sheets, numbered with consecutive Roman numerals, and placed after the Literature Cited. Figure legends should contain enough information to make the figure intelligible separate from the text. Legends should be typed double spaced, with consecutive Arabic numbers, on a separate sheet at the end of the paper. Footnotes should be limited to authors' current addresses, acknowledgments or contribution numbers, and explanation of unusual abbreviations. All such footnotes should appear on the title page. Footnotes are not normally permitted in the body of the text.

5. ***Literature cited.*** In the text, literature should be cited by the Harvard system, with papers by more than two authors cited as Jones *et al.*, 1980. Personal communications and material in preparation or in press should be cited in the text only, with author's initials and institutions, unless the material has been formally accepted and a volume number can be supplied. The list of references following the text should be headed Literature Cited, and must be typed double spaced on separate pages, conforming in punctuation and arrangement to the style of recent issues of *The Biological Bulletin*. Citations should include complete titles and inclusive pagination. Journal abbreviations should normally follow those of the U. S. A. Standards Institute (USASI), as adopted by BIOLOGICAL ABSTRACTS and CHEMICAL ABSTRACTS, with the minor differences set out below. The most generally useful list of biological journal titles is that published each year by BIOLOGICAL ABSTRACTS (BIOSIS List of Serials; the most recent issue). Foreign authors, and others who are accustomed to using THE WORLD LIST OF SCIENTIFIC PERIODICALS, may find a booklet published by the Biological Council of the U.K. (obtainable from the Institute of Biology, 41 Queen's Gate, London, S.W.7, England, U.K.) useful, since it sets out the WORLD LIST abbreviations for most biological journals with notes of the USASI abbreviations where these differ. CHEMICAL ABSTRACTS publishes quarterly supplements of additional abbreviations. The following points of reference style for THE BIOLOGICAL BULLETIN differ from USASI (or modified WORLD LIST) usage:

A. Journal abbreviations, and book titles, all underlined (for *italics*)

B. All components of abbreviations with initial capitals (not as European usage in WORLD LIST *e.g., J. Cell. Comp. Physiol.* NOT *J. cell. comp. Physiol.*)

C. *All* abbreviated components must be followed by a period, whole word components *must not* (*i.e., J. Cancer Res.*)

D. Space between all components (*e.g., J. Cell. Comp. Physiol.*, not *J.Cell.Comp.Physiol.*)

E. Unusual words in journal titles should be spelled out in full, rather than employing new abbreviations invented by the author. For example, use *Rit Vísindafjélags Islendinga* without abbreviation.

F. All single word journal titles in full (*e.g., Veliger, Ecology, Brain*).

G. The order of abbreviated components should be the same as the word order of the complete title (*i.e., Proc.* and *Trans.* placed where they appear, not transposed as in some BIOLOGICAL ABSTRACTS listings).

H. A few well-known international journals in their preferred forms rather than WORLD LIST or USASI usage (*e.g., Nature, Science, Evolution* NOT *Nature, Lond., Science, N.Y.; Evolution, Lancaster, Pa.*)

6. ***Reprints, page proofs, and charges.*** Authors of articles in black and white (no color figures) receive their first 50 reprints (without covers) free of charge. Color reprints and additional black-and-white reprints may be purchased; authors will receive order forms. Reprints normally will be delivered about 2 to 3 months after the issue date. Authors (or delegates for foreign authors) will receive page proofs of articles shortly before publication. They will be charged the current cost of printers' time for corrections to these (other than corrections of printers' or editors' errors). Other than these charges for authors' alterations, *The Biological Bulletin* does not have page charges.

Reference: *Biol. Bull.* **196:** 121. (April 1999)

ANNOUNCEMENT

Keys to Marine Invertebrates of the Woods Hole Region

The Biological Bulletin is undertaking a complete revision of Ralph Smith's classic handbook: *Keys to Marine Invertebrates of the Woods Hole Region.* This first revision will be carried out electronically, and will be directed and edited by James A. Blake (ENSR Marine and Coastal Center, Woods Hole). To date, the original edition of the *Keys* has been republished at <http://www.mbl.edu/html/BB/home.KK.html> for ready access. Moreover, a revised section on Cnidaria: Scyphozoa, by Dale Calder of the Centre for Biodiversity and Conservation Biology at the Royal Ontario Museum in Toronto, has now been completed, reviewed, and posted on the website, replacing the original section.

Keys to Marine Invertebrates of the Woods Hole Region grew out of the Systematics-Ecology Program, which operated at the Marine Biological Laboratory (MBL) during the 1960s. Melbourne R. Carriker, who directed this program, noted that illustrated, referenced, and indexed checklists and keys to the common organisms of the region were urgently needed by non-systematists in the scientific communities in and around Woods Hole. The region was defined to include collecting sites on both sides of Cape Cod, the islands of Martha's Vineyard, Nantucket, and the Elizabeth Islands, and the deeper waters of Cape Cod Bay, Nantucket Sound, Vineyard Sound, and Buzzards Bay—essentially all of southeastern New England.

The first response, in the 1960s, to the need for an invertebrate guide was a collection of looseleaf keys produced by the staff of the Invertebrate Zoology course at the MBL. These documents were added to or rewritten by a group of contributing experts, then compiled and edited by the late Ralph I. Smith, and published by the MBL in 1964. But the handbook that Smith produced was not intended to be an exhaustive survey of the rich and varied fauna of the Woods Hole Region; rather it was meant to provide the keys, illustrations, and glossaries that would facilitate a routine identification of those organisms commonly used in research and in classroom activities. Annotated species lists and bibliographies were also included as a guide to more comprehensive resources—or to specialists who could help with organisms that resisted identification. The *Keys* quickly became an important resource, and they are still used as a standard faunal reference.

The 1964 edition of the *Keys* was intended by Smith to be only the first of several editions, as the coverage was uneven, some especially microscopic or planktonic taxa were excluded, and some groups were represented only at higher taxonomic levels. Inaccuracies and lacunae were therefore expected, and revisions were invited. But no revisions were ever made, and from the standpoint of taxonomy, this manual is now hopelessly out of date.

Though the *Keys* are dated, their utility remains undiminished, and these considerations led the editors of *The Biological Bulletin* to essay the first revision in 35 years. Because the *Keys* (like any catalog) are composed of many independent sections, the unique advantages of online editing and publication are especially applicable to the project. For example, as a section, or even a subsection, is revised, the new key can be added at once to the online version of the manual. The updating can therefore proceed continuously and smoothly, even as the manual is being used. Moreover, because the *Keys* can be downloaded and printed in whole or in part, as necessary, the requirement for standard, printed, bound copies of a constantly changing product may be precluded.

Because few of the original contributors to the *Keys* are available to update their chapters, we have begun to search for scientists who are qualified and interested in revisiting existing chapters, or contributing new chapters for taxa not included in the 1964 edition. Unfortunately, we have not yet identified qualified systematists for some groups, reflecting the current lack of taxonomic expertise. Nevertheless, we hope to have the *Keys* substantially updated by the end of the year 2000, a fitting tribute, we think, to Ralph Smith and his contributing authors.

Anyone who would like to contribute to this project at any taxonomic level should contact James Blake directly. He can be reached at ENSR Marine and Coastal Center, 89 Water Street, Woods Hole, MA 02543; telephone 508-457-7900; e-mail jablake@ix.netcom.com.

—Michael J. Greenberg
Editor-in-Chief

Reference: *Biol. Bull.* **196:** 122–126. (April 1999)

Trans-Pacific Range Extension by Rafting Is Inferred for the Flat Oyster *Ostrea chilensis*

DIARMAID Ó FOIGHIL[1,*], BRUCE A. MARSHALL[2], THOMAS J. HILBISH[3], AND MARIO A. PINO[4]

[1] *Museum of Zoology and Department of Biology, University of Michigan, Ann Arbor, Michigan 48109-1079;* [2] *Museum of New Zealand, P.O. Box 467, Wellington, New Zealand;* [3] *Belle W. Baruch Institute, University of South Carolina, Columbia, South Carolina 29208; and* [4] *Instituto de Geociencias, Universidad Austral de Chile, Casilla 567, Valdivia, Chile*

Stretches of deep ocean are potent barriers to the dispersion of nearshore, benthic marine taxa. Such obstacles can be overcome, however, by species that have either a protracted pelagic larval development or a benthic life-history stage that can be transported by rafting (1, 2). The oyster *Ostrea chilensis* lacks an extended pelagic larval phase and has discrete populations in New Zealand and Chile that are separated by one of the largest extents (>7000 km) of open ocean on the planet. We tested competing dispersal hypotheses for this species by using ontogenetically informative, dated fossil and sub-fossil shell material, as well as molecular phylogenetic analyses. Our data show that dispersal by rafting is by far the most likely explanation for trans-Pacific range extension by this oyster, and we reject competing hypotheses of vicariance, anthropogenic introduction, and dispersal by ancestral lineages with extended larval development. The presence of *O. chilensis* in Chile is important because it clearly demonstrates that transoceanic range extension by rafting is potentially available to a significant fraction of nearshore marine biotas.

A prolonged pelagic larval phase facilitates the crossing of open-ocean barriers by nearshore benthic taxa (3, 4), and an evolutionarily important linkage has been proposed between this mode of development and a suite of species-level traits, including enhanced geographic range (5, 6). However, there are also many nearshore examples of individual species (7), clonal taxa (8, 9), and significant fractions of entire faunas (10) that lack significant pelagic larval development and have biogeographic ranges that span oceanic barriers to dispersal. Spontaneous rafting events, in which sessile life-history stages are passively transported on drifting objects, are common in the marine environment and have probably acted as an alternative long-distance dispersal mechanism for major subsections of shallow-water hard-bottom faunas over ecologically significant timescales (7–11). In the case of *individual* species, however, claims of long-distance range extension by rafting are usually confounded by the alternative possibilities of undocumented anthropogenic introductions that predate biotic surveys (12), or of transoceanic colonization by ancestral lineages having extended larval development, with the subsequent evolutionary loss of such larvae (13). In this study, we present a specific case of transoceanic range extension by rafting, possibly the first from which the alternative dispersal hypotheses can be excluded with confidence.

Ostrea chilensis is unique among oysters in lacking an obligate feeding pelagic (planktotrophic) larval development; larvae typically metamorphose less than 2 hours after their release from parental brood chambers (14). This greatly abbreviated pelagic phase is associated with a highly distinctive larval shell morphology (15) and is a derived condition among flat oysters (16). *O. chilensis* occurs in two regional populations separated by 7400 km of uninterrupted south Pacific Ocean (Fig. 1). It is found throughout the nearshore waters of New Zealand (including the Chatham Islands) to depths of 550 m (17) and also in the shallow subtidal zone of southern Chile (18). New Zealand and Chile share some relict Gondwanaland taxa (19), but this oyster does not qualify as such because it is unknown from pre-Holocene Chilean fossil strata (20), its appearance in the New Zealand Pliocene fossil record (21) greatly post-dates

---

Received 28 August 1998; accepted 14 January 1999.

* To whom correspondence should be addressed. E-mail: diarmaid@umich.edu

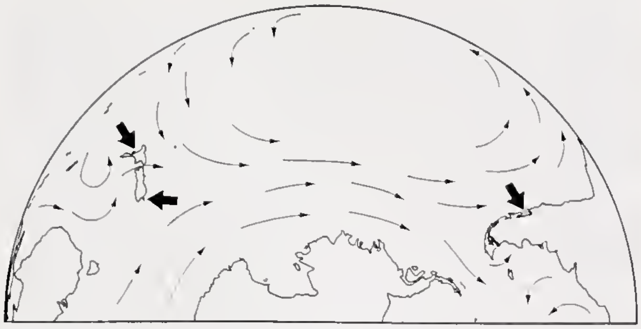

Figure 1. Polar View of the South Pacific showing *Ostrea chilensis* sampling locations (large arrows) for molecular analysis in New Zealand: Moturekareka Island, Hauraki Gulf (North Island), Foveaux Strait (South Island, 46°43′ S, 168°3′ E); and in Chile: Quempillén, Isla Chiloé. Small arrows show predominant surface circulation patterns.

the separation of New Zealand from Gondwanaland (22), and its New Zealand and Chilean populations are almost indistinguishable allozymically [genetic similarity = 0.991: a value of 1.0 indicates genetic identity (18)].

The fossil record suggests that the New Zealand population is ancestral, and it is speculated that the Chilean population was founded by rafted, post-metamorphic New Zealand oysters transported *via* the Antarctic circumpolar and Humboldt currents (18). Alternatively, Chilean populations might have been established by the transoceanic dispersal of ancestral New Zealand larvae with extended planktotrophic pelagic development, followed by independent losses of this developmental mode in both source and founder populations. The simplest hypothesis is that the Chilean population resulted from an undocumented human introduction event, a frequent occurrence for commercially important oysters (23, 24).

Samples of sub-fossil *O. chilensis* were collected for radiocarbon dating from the Raqi-Tubul estuary, a southern Chilean location where this species has been regarded as the sole native oyster (25). Radiocarbon age estimates (95% confidence intervals) of 953–1238 and 2998–3383 years before present (y BP) were obtained for specimens taken respectively from salt marsh sediments and from an oyster midden site (26). Some of the midden specimens had attached juvenile oysters (spat) that retained well-preserved larval shells (prodissoconchs) displaying the diagnostic morphological characteristics of this species of oyster (Fig. 2a). Unequivocal evidence for human settlement in New Zealand dates from about 850 y BP (27). The presence of significant populations of *O. chilensis* in South America 2000 years prior to this date precludes anthropogenic introduction as a credible explanation for transoceanic range extension in this species.

Although *O. chilensis* transversed the South Pacific without human intervention, the Chilean midden data do not reveal whether this occurred *via* planktotrophic larval dis-

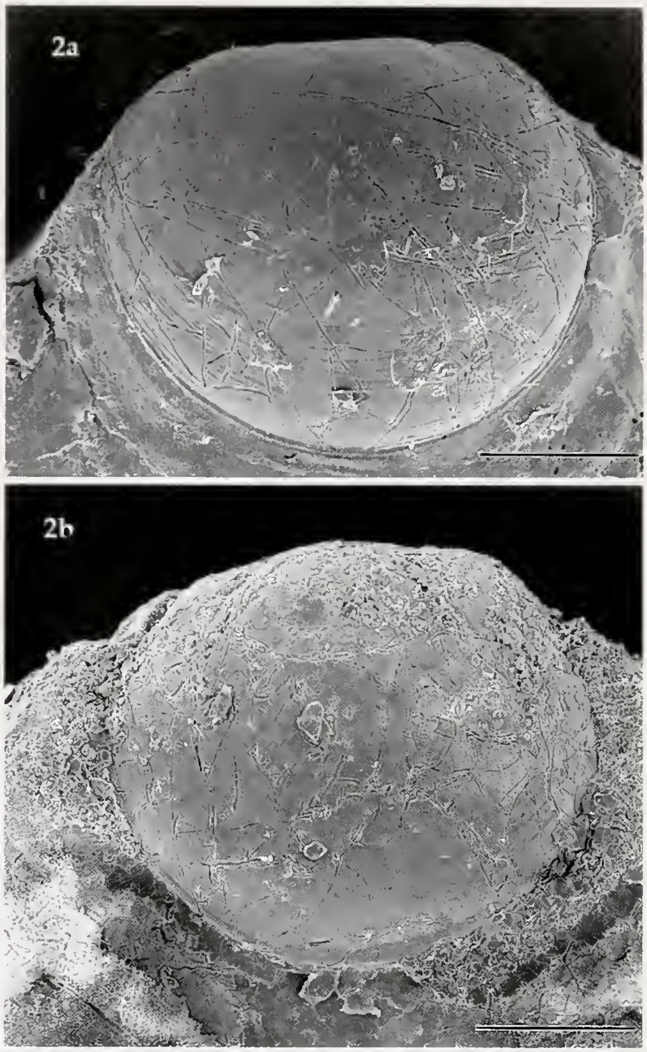

Figure 2. Scanning electron micrographs of prodissoconchs preserved on juvenile oyster shells from (2a) Chilean oyster midden sample radiocarbon-dated to 2998–3383 years y BP (95% probability), prodissoconch length = 469 μm (UMMZ 255348); (2b) New Zealand North Island upper Nukumaruan Stage (1.6–2.0 mya) strata, prodissoconch length = 470 μm (NMNZ M.42778). Both specimens display the non-umbonate, D-shaped, >425 μm in length, flattened prodissoconch valves diagnostic for *Ostrea chilensis* (15). Scale bars = 150 μm. Sub-fossil Chilean samples of *O. chilensis* were obtained by M. Pino at the Raqi-Tubul estuary (37°13′30″ S, 73°26′ W) in December 1996. Shell samples were recovered from a midden, predominantly (70%–80%) composed of oysters (26), situated 5 m above present sea level on the west slope of "La Isla" hill. Additional sub-fossil oyster shells were recovered from adjacent salt marsh sediments (1.5 m depth). Sub-fossil Chilean samples were subjected to radiocarbon dating analyses by Beta Analytic Inc, 4985 S.W. 74 Court, Miami, Florida 33155. New Zealand fossil flat oysters with characteristic *O. chilensis* prodissoconchs were sampled by B. A. Marshall and M. B. Willoughby from late Pliocene horizons on the north bank of Mangahao River, 1.5 km south of Mangahao, Wairarapa, North Island (map reference NZMS 260/462805). Prodissoconch samples were gold-coated and examined with a Hitachi S-3200N scanning electron microscope.

persal. Previous studies of fossil *O. chilensis* in New Zealand were based on adult shell morphology (21) and do not provide insights into when planktotrophic larval development was lost in this oyster lineage. We examined museum fossil holdings of *O. chilensis* and found individuals from North Island strata [late Pliocene, upper Nukumaruan Stage (1.6–2.0 mya)], with a prodissoconch structure identical to that of modern specimens (Fig. 2b). Earlier Pliocene specimens did not yield interpretable prodissoconchs, but the North Island populations of this species had fully evolved the present day nonplanktotrophic larval development prior to the Pleistocene. This is pertinent because molecular phylogenetic analysis of *O. chilensis* populations (Fig. 3) indicates that (1) a pronounced mitochondrial dichotomy exists among North and South Island samples, differing by 19 nucleotide substitutions (3.1% sequence divergence for a 609 nucleotide fragment of cytochrome oxidase I); (2) North Island and Chilean samples form sister lineages, differing by four nucleotide substitutions (0.6% sequence divergence); (3) ancestral North Island lineages were the probable source populations for trans-Pacific colonists.

Joint consideration of the fossil and molecular data allows a comparative evaluation of the two remaining dispersal hypotheses. Rafting is compatible with a single loss of planktotrophic larval development in a common ancestral lineage of *O. chilensis* and allows for a Pleistocene/Holocene trans-Pacific colonization event. Conversely, dispersal by planktotrophic larvae requires that trans-Pacific colonization be pre-Pleistocene, and that loss of such larvae (a condition unique to *O. chilensis* among the Ostreacea) occurred on three independent occasions after the respective branching of South Island, North Island, and (pre-Pleistocene and post-trans-Pacific colonization) Chilean lineages. This mechanism of dispersal also requires the assumption that putative ancestral larval cohorts were sufficiently long-lived and numerous to overcome mortality and (enormous) diffusion effects over a >7000-km linear dispersive pathway, and to recruit in viable breeding densities in Chile. Extant flat oyster species with planktotrophic larvae have pelagic periods ranging from 6 to 33 days (29). The effective dispersal distances [10 s–100 s of km (30)] calculated from these periods are insufficient for trans-Pacific coloni-

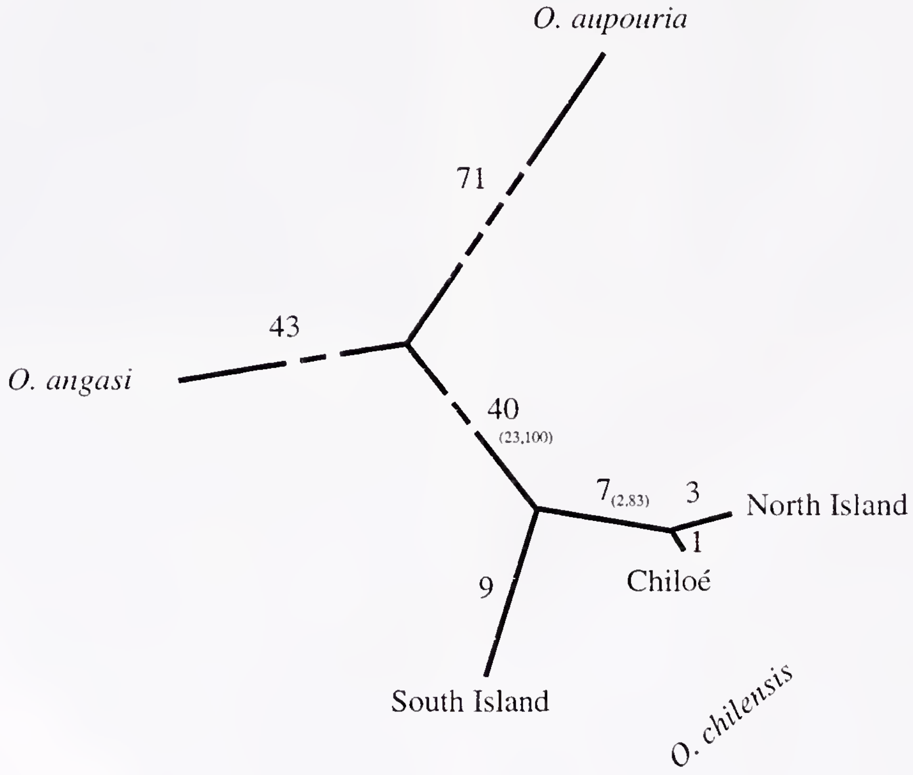

Figure 3. Most parsimonious tree (174 steps, CI = 0.948; RI = 0.775), obtained by an exhaustive search for optimal trees, based on an mt COI gene fragment [609 nucleotides, homologous to positions 52–669 of the chiton mt genome (28)] sequenced for New Zealand South Island (*n* = 12), New Zealand North Island (*n* = 13), and Chilean (Isla Chiloé, *n* = 16) samples of *Ostrea chilensis*. No intra-populational variation was observed. Regional flat oyster taxa, *O. aupouria* (New Zealand) and *O. angasi* (Australia), were employed as outgroups. The number of steps are indicated above each branch and brackets show, respectively, the decay index and bootstrap values supporting each node. Molecular techniques and phylogenetic analyses were as previously described (24), and GenBank accession numbers for the five haplotypes are AF112285-9.

zation, even if calculated for the most favorable oceanic currents: transoceanic, non-meandering flow rates of 125 cm · s^{-1} [<3600 km (31)]. On grounds of phylogenetic parsimony (Fig. 3), apparent absence of Pliocene/Pleistocene fossil specimens in Chile (20), and absence of exceptionally long-lived/teleplanic (2) larvae in flat oysters (29), the ancestral planktotrophic larval dispersal hypothesis is rejected as a plausible explanation for trans-Pacific range extension in *O. chilensis.*

We conclude that dispersal by rafting is by far the most likely explanation for the trans-Pacific range extension of *O. chilensis.* Pumice, an effective long-distance rafting vector for hard-bottom, shallow-water, suspension-feeding epibenthos (11), may have served as the transport platform, because very significant quantities of this buoyant material have been released by repeated eruptions of the North Island Taupo Volcanic Zone since the Pliocene (32). Further genetic characterization of the North Island and Chilean populations may uncover haplotypes common to both populations, a finding that would be necessary to entertain the possibility of continued trans-Pacific gene flow.

In principle, there may be no maximum dispersal distance for rafting organisms (7, 11), and the presence of *O. chilensis* in Chile highlights the existence of an alternative dispersal mechanism, of truly transoceanic scope, which is potentially available to many members of nearshore faunas (7–11). A broad cross-section of the North Island hard-bottom epibenthos was probably also rafted across the Pacific, including indirect developing species with an obligate planktotrophic larval stage. Rafted innocula of such taxa are less likely to have become established in Chile because an obligate extended pelagic larval phase would dilute population densities below the concentrations needed for reproductive success in the crucial initial generations of the new colonies (7–9, 11). However, careful analysis of Chilean taxa with reduced or absent pelagic larval development—including sponge, ascidian, cheilostome bryozoan and hydroid faunas (8)—may reveal additional cryptic rafted immigrants from New Zealand. Such taxa would have New Zealand sister lineages and might be identified by morphological or molecular characterization of epifaunal residues from Chilean midden shells that predate human settlement of New Zealand.

Our molecular results are in striking contrast to those from another oyster, *Crassostrea virginica*; this species undergoes a planktotrophic larval development, but it exhibits greater intraspecific genetic divergence values over a few hundred kilometers of contiguous southeastern Floridian coastline (33) than do North Island and Chilean populations of *O. chilensis.* The contrasting phylogeographic patterns of these developmentally heterogeneous oyster taxa indicate that assumptions of marine invertebrate genetic structuring based solely on extrapolations from pelagic larval periods may lead to spectacular error.

Acknowledgments

We are indebted to our colleagues who graciously provided ethanol-fixed oyster tissue samples: A. Jeffs, M. Barker, A. Frazer, O. Chaparro, J. Toro, R. Ward, and J. Nell. Manuscript drafts were improved by the comments of G. Paulay, T. Baumiller, W. Brown, S. Palumbi, and two anonymous reviewers. This study was supported by NSF award 9617689 to D. Ó Foighil.

Literature Cited

1. **Vermeij, G. J. 1987.** The dispersal barrier in the tropical Pacific: implications for molluscan speciation and extinction. *Evolution* **41:** 1046–1058.
2. **Scheltema, R. S. 1988.** Initial evidence for the transport of teleplanic larvae of benthic invertebrates across the east Pacific barrier. *Biol. Bull.* **174:** 145–156.
3. **Kohn, A. J., and F. E. Perron. 1994.** Life history and biogeography patterns in *Conus.* Oxford Biogeography Series. 9. Clarendon Press, Oxford. 110 pp.
4. **Lessios, H. A., B. D. Kessing, and D. R. Robertson. 1998.** Massive gene flow across the world's most potent marine biogeographic barrier. *Proc. R. Soc. Lond. B* **265:** 583–588.
5. **Jablonski, D. 1986.** Larval ecology and macroevolution in marine invertebrates. *Bull. Mar. Sci.* **39:** 565–587.
6. **Jablonski, D. 1987.** Heritability at the species level: analysis of geographic ranges of Cretaceous mollusks. *Science* **238:** 360–363.
7. **Johannesson, K. 1988.** The paradox of Rockall: why is a brooding gastropod (*Littorina saxatilis*) more widespread than one having a planktonic larval stage (*L. littorea*)? *Mar. Biol.* **99:** 507–513.
8. **Jackson, J. B. C. 1986.** Modes of dispersal of clonal benthic invertebrates: consequences for species' distributions and genetic structure of local populations. *Bull. Mar. Sci.* **39:** 588–606.
9. **Ó Foighil, D. 1989.** Planktotrophic larval development is associated with a restricted geographic range in *Lasaea,* a genus of brooding, hermaphroditic bivalves. *Mar. Biol.* **103:** 349–358.
10. **Davenport, J., and H. Macalister. 1996.** Environmental conditions and physiological tolerances of intertidal fauna in relation to shore zonation at Husvik, South Georgia. *J. Mar. Biol. Assoc. UK* **76:** 985–1002.
11. **Jokiel, P. L. 1990.** Transport of reef corals into the Great-Barrier Reef. *Nature* **347:** 665–667.
12. **Carlton, J. T., and J. Hodder. 1995.** Biogeography and dispersal of coastal marine organisms: experimental studies on a replica of a 16th-century sailing vessel. *Mar. Biol.* **121:** 721–730.
13. **Jablonski, D., and R. A. Lutz. 1983.** Larval ecology of marine benthic invertebrates: paleobiological implications. *Biol. Rev. Camb. Philos. Soc.* **58:** 21–89.
14. **Millar, R. H., and P. J. Hollis. 1963.** Abbreviated pelagic life of Chilean and New Zealand oysters. *Nature* **197:** 512–513.
15. **Chanley, P., and P. Dinamani. 1980.** Comparative descriptions of some oyster larvae from New Zealand and Chile, and a description of a new genus of oyster, *Tiostrea. N. Z. J. Mar. Freshwater Res.* **14:** 103–120.
16. **Jozefowitz, C. J., and D. Ó Foighil. 1998.** Molecular phylogenetic analysis of Southern Hemisphere flat oysters based on partial mitochondrial 16S rDNA gene sequences. *Mol. Phylogenet. Evol.* **10:**426–435.
17. **Jeffs, A. G., and R. G. Creese. 1996.** Overview and bibliography of research on the Chilean oyster *Tiostrea chilensis* (Phillippi, 1845) from New Zealand waters. *J. Shellfish Res.* **15:** 305–311.
18. **Buroker, N. E., P. Chanley, and P. Dinamani. 1983.** Systematic

status of two oyster populations of the genus *Tiostrea* from New Zealand and Chile. *Mar. Biol.* **77:** 191–200.

19. **Cooper, R. A., and P. R. Millener. 1993.** The New Zealand biota: historical background and new research. *TREE* **8:** 429–433.
20. **Herm, D. 1969.** Marines Pliozän und Pleistozän in Nord und Mittel-Chile unter besonderer Berücksichtigung der Entwicklung der Mollusken-faunen. *Zitteliana* **2:** 159 pp.
21. **Beu, A. G., and P. A. Maxwell. 1990.** Cenozoic Mollusca of New Zealand. *N. Z. Geol. Surv. Paleontol. Bull.* **58:** 336–341.
22. **Weissel, J. K., and D. E. Hayes. 1977.** Evolution of the Tasman Sea reappraised. *Earth Planet. Sci. Lett.* **36:** 77–84.
23. **Carlton, J. T., and R. Mann. 1996.** Transfers and world-wide introductions. Pp. 691–706 in *The Eastern Oyster* Crassostrea virginica, V. S. Kennedy, R. I. E. Newell, and A. F. Eble, eds. Maryland Sea Grant, College Park, Maryland.
24. **Ó Foighil, D., P. M. Gaffney, A. E. Wilbur, and T. J. Hilbish. 1998.** Mitochondrial cytochrome oxidase I gene sequences support an Asian origin for the Portuguese oyster, *Crassostrea angulata. Mar. Biol.* **131:** 497–503.
25. **Solis, I. F. 1967.** Observaciones biológicas en Ostras (*Ostrea chilensis* Philippi) de Pullinque. *Biol. Pesq.* (Chile) **2:** 51–82.
26. **Bustos, V., N. Vergara, and Z. Seguel. 1997.** Los conchales antrópicos de ostras en la micro-área de Raqui-Tubul del golfo de Arauco, Vii Región. Abstract, XIV Congreso Nacional de Arqueologiá Chilena, Copiapó, p. 41.
27. **McGlone, M. S., A. J. Anderson, and R. N. Holdaway. 1994.** An ecological approach to the Polynesian settlement of New Zealand. Pp. 136–163 in *The Origins of the First New Zealanders*, D. G. Sutton, ed. Auckland University Press, Auckland, NZ.
28. **Boore, J. L., and W. M. Brown. 1994.** Complete DNA sequence of the mitochondrial genome of the black chiton, *Katharina tunicata. Genetics* **138:** 423–443.
29. **Buroker, N. E. 1985.** Evolutionary patterns in the family Ostreidae: larviparous *vs.* oviparous. *J. Exp. Mar. Biol. Ecol.* **90:** 233–247.
30. **Okubo, A. 1971.** Oceanic diffusion diagrams. *Deep-Sea Res.* **18:** 789–802.
31. **Scheltema, R. S. 1992.** Passive dispersal of planktonic larvae and the biogeography of tropical sublittoral invertebrate species. Pp. 195–202 in *Marine Eutrophication and Population Dynamics. Proceedings of the 25th EMBS*, G. Colombo *et al.*, eds. Olsen and Olsen, Fredensborg, Denmark.
32. **Wilson, C. J. N., B. F. Houghton, and E. F. Lloyd. 1986.** Volcanic history and evolution of the Maroa-Taupo area, central North Island. Pp. 194–223 in *Late Cenozoic Volcanism in New Zealand*, I. E. M. Smith, ed. The Royal Society of New Zealand, Bulletin 23.
33. **Reeb, C. A., and J. C. Avise. 1990.** A genetic discontinuity in a continuously distributed species: mitochondrial DNA in the American oyster, *Crassostrea virginica. Genetics* **124:** 397–4.

Reference: *Biol. Bull.* **196:** 127–136. (April 1999)

Comparative Analysis of Neurogenesis in the Central Olfactory Pathway of Adult Decapod Crustaceans by *In Vivo* BrdU Labeling

MANFRED SCHMIDT[1,*] AND STEFFEN HARZSCH[2]

[1]*Zoologisches Institut und Zoologisches Museum, Neurophysiologie, Universität Hamburg, and Institut für Biologie, Technische Universität Berlin, Germany; and* [2]*Fakultät für Biologie, Neuroanatomie, Universität Bielefeld, Germany*

Abstract. To examine the distribution of neurogenesis in the central olfactory pathway of adult decapod crustaceans, we labeled, *in vivo,* six species of decapod crustaceans representing most infraorders (shrimps, spiny lobsters, clawed lobsters, crayfish, hermit crabs, true crabs) with the proliferation marker 5-bromo-2′-deoxyuridine (BrdU). In all tested species a group of small, neuron-like nuclei in the lateral soma clusters of the brain was labeled; the lateral soma clusters are composed of the cell bodies of ascending olfactory projection neurons. In only a few instances did groups of BrdU-positive nuclei also occur in the other soma clusters of the central olfactory pathway. In the spiny lobster (*Panulirus argus*), a group of small neuron-like nuclei was labeled in the medial soma clusters containing the cell bodies of local interneurons of the olfactory deutocerebrum. In the hermit crab (*Pagurus bernhardus*), and the true crab (*Cancer pagurus*), a group of small neuron-like nuclei was labeled in soma clusters located in the eyestalks. These soma clusters probably contain the cell bodies of local interneurons of the hemiellipsoid bodies, to which the olfactory projection neurons ascend. These results indicate that neurogenesis occurs among olfactory projection neurons in the adult brain. Among the other neuronal types of the central olfactory pathway, however, neurogenesis is restricted to specific taxa. The persistence of neurogenesis among the different neuronal types of the central olfactory pathway throughout adult life suggests an enormous structural plasticity of brain circuitry that may enable the long-lived decapod crustaceans to adapt to changing olfactory environments.

Introduction

It was commonly believed that neurogenesis is rare, if not totally absent, in the central nervous system of most adult animals (*e.g.*, Purves, 1988), although *de novo* generation of neurons occurs in the brain of adult birds (*e.g.*, Paton and Nottebohm, 1984), fish (*e.g.*, Raymond and Easter, 1983), and mammals (Kaplan and Hinds, 1977; Bayer, 1982; Kaplan *et al.*, 1985; Crespo *et al.*, 1986). During the last decade, the development of new techniques to label and culture proliferating cells fostered a surge of research that conclusively demonstrated neurogenesis in the adult mammalian brain (Corotto *et al.*, 1993; Luskin, 1993; Okano *et al.*, 1993; Morshead *et al.*, 1994; Kuhn *et al.*, 1996). Adult neurogenesis also occurs in the arthropod brain (Cayre *et al.*, 1994; Cayre *et al.*, 1996; Schmidt, 1997; Sandeman *et al.*, 1998). Thus, neurogenesis in the adult brain is now known to be a continuous process that contributes significantly to the neuronal population of specific brain areas.

In the mammalian brain, two regions in particular acquire new neurons throughout adult life: the dentate gyrus of the hippocampus (Bayer, 1982; Crespo *et al.*, 1986; Okano *et al.*, 1993; Kuhn *et al.*, 1996) and the olfactory bulb (Kaplan *et al.*, 1985; Corotto *et al.*, 1993; Luskin, 1993; Okano *et al.*, 1993). In the dentate gyrus, new granule cells develop from progenitor cells in the subgranular region (Crespo *et al.*, 1986; Okano *et al.*, 1993; Kuhn *et al.*, 1996). Although the rate of neurogenesis decreases significantly with age (Kuhn *et al.*, 1996), the number of granule cells increases continuously (Crespo *et al.*, 1986), indicating that cell death is rare. The olfactory bulb acquires local interneurons of dif-

Received 4 November 1997; accepted 6 January 1999.

* To whom correspondence should be addressed. Universität Hamburg, Zoologisches Institut und Zoologisches Museum, Neurophysiologie, Martin-Luther-King-Platz 3, 20146 Hamburg, Germany. E-mail: mschmidt@zoologie.uni-hamburg.de

ferent types (granule cells, periglomerular cells) almost linearly with age, although many of the new neurons do not survive, indicating a substantial turnover (Kaplan *et al.*, 1985; Corotto *et al.*, 1993; Luskin, 1993; Okano *et al.*, 1993). The new neurons in the olfactory bulb originate from constitutively proliferating cells in the subependymal zone of the lateral ventricles (Moreshead *et al.*, 1994), some of which migrate rostrally along a highly restricted pathway (the rostral migratory stream) and differentiate into neurons upon reaching the olfactory bulb (Luskin, 1993).

Evidence for neurogenesis in the adult arthropod brain was obtained in diverse insect species and in two species of decapod crustaceans, *Carcinus maenas* (shore crab) and *Cherax destructor* (Australian crayfish) (Bieber and Fuldner, 1979; Technau, 1984; Cayre *et al.*, 1994, 1996; Schmidt, 1997; Sandeman *et al.*, 1998). As in mammals, in arthropods adult neurogenesis is restricted to or prominent in specific brain areas. In adult insects, only the mushroom bodies, which represent the second stage of the central olfactory pathway and mediate olfactory learning and memory (see reviews by Davis, 1993; Menzel *et al.*, 1994), acquire new local interneurons, the Kenyon cells (Bieber and Fuldner, 1979; Technau, 1984; Cayre *et al.*, 1994, 1996). Surprisingly, only in some insect species do adults show neurogenesis of Kenyon cells (fly: *Drosophila melanogaster;* crickets: *Acheta domesticus, Gryllus bimaculatus, Gryllomorpha dalmatina;* beetles: *Aleochara curtula, Tenebrio molitor, Zophobas spec., Harmonia axyridis*), whereas other species (bee: *Apis mellifera;* locust: *Locusta migratoria;* cockroach: *Periplaneta americana*) do not (Bieber and Fuldner, 1979; Technau, 1984; Cayre *et al.*, 1994, 1996; Fahrbach *et al.*, 1995). In adult insects, neurogenesis appears to be driven by typically large neuroblasts or ganglion mother cells that continue to be mitotically active into the imaginal stage (Technau, 1984; Cayre *et al.*, 1994, 1996).

Evidence for adult neurogenesis in decapod crustaceans occurs in the central olfactory pathway (Schmidt, 1997; Sandeman *et al.*, 1998). In decapods, as in insects, this pathway is composed of two elements: bilateral glomerular neuropils of the deutocerebrum, where olfactory afferents transmit information onto local interneurons and projection neurons (antennal lobes in insects; olfactory lobes in decapods); and bilateral second-order neuropils of the protocerebrum, to which the projection neurons ascend (mushroom bodies in insects; hemiellipsoid bodies in decapods) (*e.g.*, Boeckh *et al.*, 1984; Blaustein *et al.*, 1988; Mellon *et al.*, 1992). In adult shore crabs (*Carcinus maenas*) and Australian crayfish (*Cherax destructor*). *in vivo* labeling with the thymidine analog 5-bromo-2′-deoxyuridine (BrdU) demonstrated neuronal proliferation in the lateral soma clusters (LC) containing the somata of olfactory projection neurons (Schmidt, 1997; Sandeman *et al.*, 1998). In *Carcinus maenas,* neuronal proliferation also occurred in clusters of cell bodies associated with the hemiellipsoid bodies (HBC) but not in the medial soma clusters (MC) containing the somata of local interneurons restricted to the olfactory deutocerebrum (Schmidt, 1997). In late juveniles of *Cherax destructor,* however, proliferation was detected in the MC (Sandeman *et al.*, 1998). In both analyzed species, proliferation in the LC is associated with a continuous linear increase in the number of mature olfactory projection neurons throughout the life span of postlarval animals (Schmidt, 1997; Sandeman *et al.*, 1998). In *Carcinus maenas,* the proliferating cells in the LC and the HBC are tightly packed in a very restricted area close to the respective neuropil, thus delineating these areas as proliferative zones. In location and morphology, the proliferating cells deviate considerably from typical neuroblasts or ganglion mother cells that are still mitotically active in the LCs of early crab juveniles (Harzsch and Dawirs, 1996). This indicates that neurogenesis in the central olfactory pathway of adult shore crabs occurs by a different mechanism than during embryonic and larval development.

In this study we ask whether the neurogenesis that has been observed in the central olfactory pathway of adult shore crabs (*Carcinus maenas*) and Australian crayfish (*Cherax destructor*) can be generalized to other decapod crustaceans. *In vivo* labeling with BrdU in six species representing most of the important decapod taxa (Caridea = shrimps, Palinura = spiny lobsters, Astacidea = clawed lobsters and crayfish, Anomura = hermit crabs, Brachyura = true crabs) revealed that proliferation among olfactory projection neurons is a common phenomenon in adult decapods. Significant differences between species exist in the occurrence of neurogenesis among local interneurons of the olfactory deutocerebrum and among neurons that probably represent local interneurons of the hemiellipsoid bodies. We conclude that the central olfactory pathway of decapod crustaceans retains a lifelong structural plasticity, whose regulation and physiological significance remains to be elucidated.

Materials and Methods

Experiments were performed on adult, sexually mature specimens (and in case of *Panulirus argus,* also on late juveniles) of six species of decapod crustaceans (Table 1). All animals were kept in tanks with running seawater or fresh water without feeding for at least 2 days prior to the experiments.

For *in vivo* labeling, 5-bromo-2′-deoxyuridine (BrdU) was injected into the hemolymph of experimental specimens (5 milligrams of BrdU per 100 gram of body weight in a 0.5% BrdU solution in the appropriate saline). After survival times of 6 to 24 h, the brains of the animals were fixed with Bodian # 2 fixative (90 ml 80% ethanol, 5 ml formol, 5 ml glacial acetic acid), for 1–4 h at room temperature. After rinsing in 0.1 *M* Sörensen phosphate buffer (SPB), the brains were embedded in gelatin and cut on a

Table I

Summary of decapod crustacean species investigated

Scientific name	Trivial name	Systematic status		n†	Carapace length (cm)	Weight (g)	Source of material
		Infraorder*	Family				
Sicyonia brevirostris	Rock shrimp	Penaeidea [Caridea]	Sicyonidae	3	—	15–17	Dr. J. Nunez, Whitney Laboratory, University of Florida
Panulirus argus	Caribbean spiny lobster	Palinura [Achelata]	Palinuridae	7	2.8–6.0	15–208	Dr. B. W. Ache, Whitney Laboratory, University of Florida
Homarus americanus	American lobster	Astacidea [Homarida]	Homaridae	5	11.0–13.5	500–750	Commercial supplier
Cherax destructor	Australian crayfish	Astacidea [Astacida]	Parastacidae	3	5.2–5.4	50–61	Commercial supplier
Pagurus bernhardus	Hermit crab	Anomura [Anomala]	Paguridae	5	1.6–2.8	3.5–29.7	Biologische Anstalt Helgoland
Cancer pagurus	Common crab	Brachyura [Brachyura]	Cancridae	5	10.2–16.0	167–688	Biologische Anstalt Helgoland

* Name according to Gruner (1993), followed [in brackets] by name according to terminology proposed in most recent investigations of decapod phylogeny by Sandeman *et al.*, (1993) and Scholtz and Richter (1995).

† n = number of specimens examined.

vibratome into serial sections with a thickness of 70 or 100 μm. After degelatinization in a warm water bath, incubation in 2 *N* HCl for 20 min, and rinsing (4 × 15 min) in SPB, the free-floating sections were incubated overnight in anti-BrdU ("Cell Proliferation Kit" from Boehringer or anti-BrdU containing nucleases from Amersham). Subsequently, sections were rinsed in SPB (4 × 30 min) and incubated for 4 h in goat anti-mouse CY3-labeled secondary antibody (Jackson Immunoresearch) diluted 1:100 in SPB. After final rinsing in SPB (4 × 30 min), the labeled sections were coverslipped in glycerol/SPB.

Sections were viewed and photographed using a microscope with bright-field optics and epifluorescence (Olympus BH-2 or IX-50). Despite increased section thickness (70 μm compared to the 20-μm-thick cryostat sections normally used in BrdU immunostainings of mammalian tissue), no problems with antibody penetration were encountered. Intensely labeled nuclei were detectable throughout the entire thickness of the vibratome sections. The method we used here for the *in vivo* BrdU-labeling was the same as in a previous study (Schmidt, 1997), where it was shown to be highly reliable since in all 16 shore crabs (*Carcinus maenas*) treated by this method, somata in the LC were distinctly labeled.

Results

In vivo labeling with BrdU resulted in the clear visualization of nuclei in soma clusters of the central olfactory pathway in most of the specimens. All tested species showed labeling of nuclei in the paired lateral soma clusters (LC; soma cluster # 10 according to Sandeman *et al.*, 1992) of the olfactory deutocerebrum (Figs. 1; 2a, b; 3a; 4; 5a, b; 6a). These clusters exclusively contain somata of ascending olfactory projection neurons (OPN). The BrdU-positive nuclei in the LC differed from other labeled nuclei that were present throughout almost all brain areas by their specific location, arrangement, and shape. The labeled nuclei in the LC always occurred as a tightly packed, string- or ball-like group that was located in the ventral part of the cluster directly adjacent to the neuropil of the olfactory lobe (OL). They were spherical and slightly smaller than were the

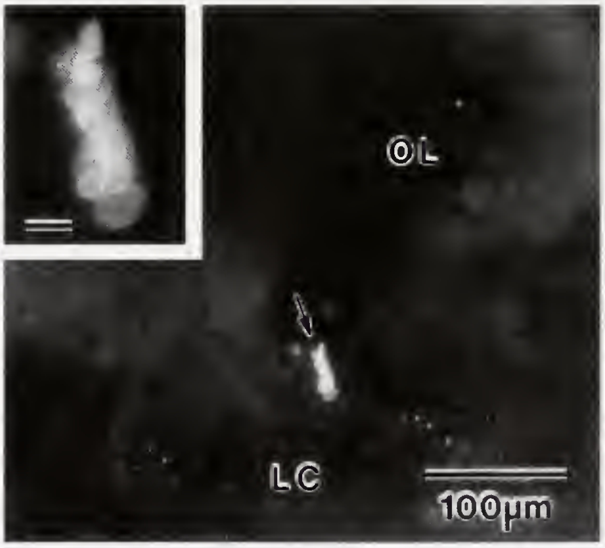

Figure 1. Proliferating cells in the central olfactory pathway of adult rock shrimp (*Sicyonia brevirostris:* Penaeidea [Caridea]; Sicyonidae) identified by *in vivo* BrdU-labeling. Light micrographs of vibratome sections. In the lateral soma cluster (LC) a compact, string-like group of small BrdU-positive nuclei (arrow) is located close to the neuropil of the olfactory lobe (OL). Inset: higher magnification shows spherical, and hence neuronal shape of labeled somata.

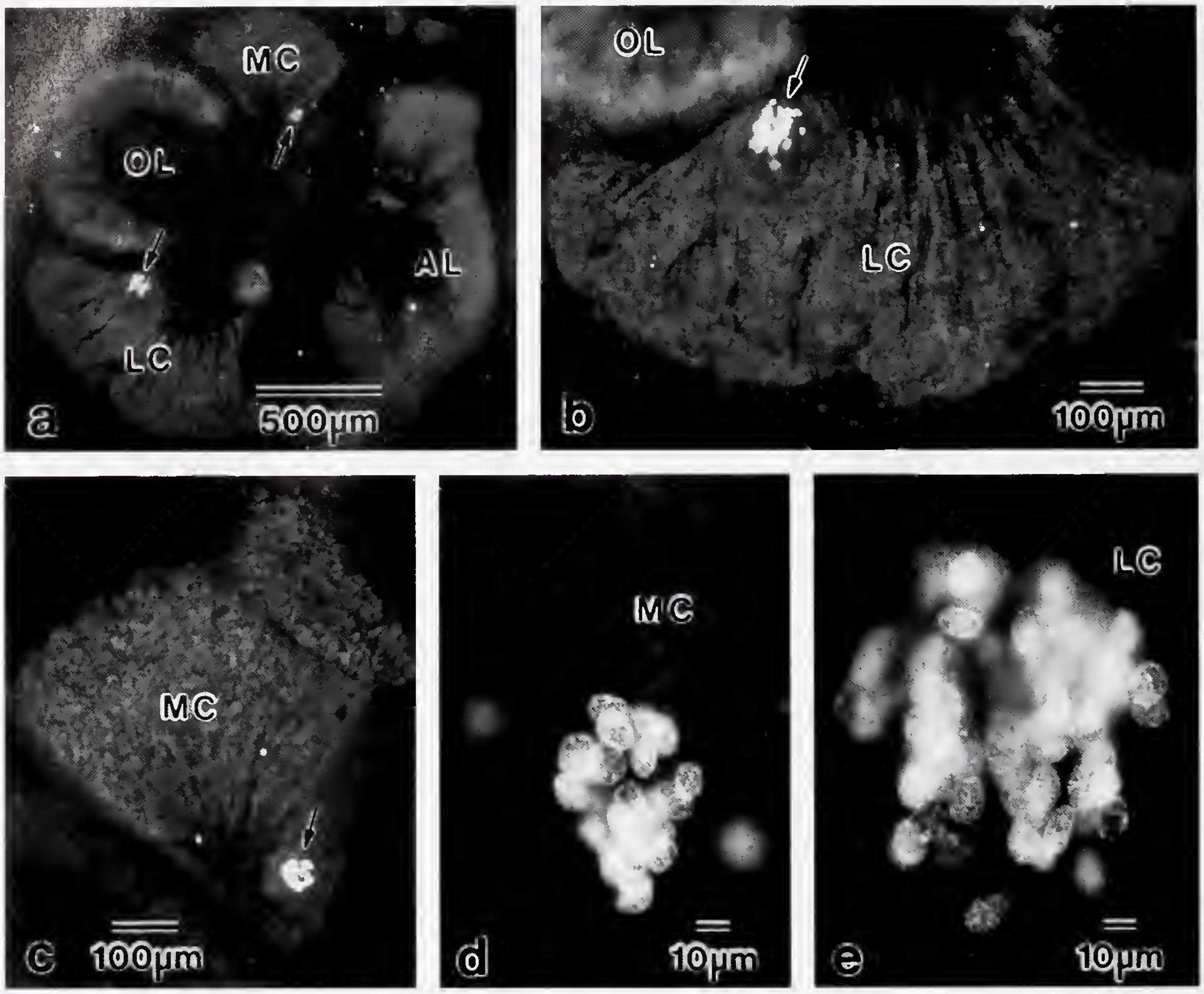

Figure 2. Proliferating cells in the central olfactory pathway of late juvenile (a–c; 49–57 g) and adult (d, e; 140 g) spiny lobster (*Panulirus argus*: Palinura [Achelata]; Palinuridae) identified by *in vivo* BrdU-labeling. Light micrographs of vibratome sections. (a) Overview of olfactory deutocerebrum (hemibrain). In the lateral soma cluster (LC) and the medial soma cluster (MC), a compact group of small BrdU-positive nuclei (arrows) is located close to the neuropil of the olfactory lobe (OL). Note presence of the large accessory lobe (AL). (b, e) BrdU-positive nuclei in the lateral soma cluster at higher magnification. Note spherical and hence neuronal shape of labeled nuclei in e. (c, d) BrdU-positive nuclei in the medial soma cluster at higher magnification. Note spherical and hence neuronal shape of labeled nuclei in d.

unlabeled nuclei of OPN somata located in the periphery of the LC (Fig. 2b, e).

For the species in which specimens of different size (and hence age) were tested (*Panulirus argus*, *Cancer pagurus*), only in *Cancer pagurus* did we find obvious differences in the number of BrdU-positive nuclei per LC between specimens. In *Cancer pagurus*, the LC of three large specimens (650–700 g and *ca.* 16 cm carapace width) showed no labeled somata or only some that were very weakly labeled (some nuclei belonging to other cell types were intensely labeled, showing that BrdU had been available for incorporation). However, typical groups of strongly BrdU-positive nuclei occurred in all LCs in two smaller, and hence younger, adults (160–200 g and 10–11 cm carapace width). In *Panulirus argus* (15–208 g and carapace length of 2.8–6 cm), we detected no obvious difference in the number of BrdU-positive nuclei per LC.

The number of BrdU-positive nuclei per LC differed considerably among species. In *Sicyonia brevirostris*, only a few nuclei (less then 15) per LC were BrdU-positive (Fig. 1). In *Cherax destructor* (Fig. 4), as well as in *Pagurus bernhardus* (Fig. 5) and *Cancer pagurus* (Fig. 6), the number of BrdU-positive nuclei per LC was somewhat higher (20 to 40). In *Homarus americanus* (Fig. 3a), about 50 nuclei per LC, and in *Panulirus argus* (Fig. 2a, b, e), more than 80 nuclei per LC were BrdU-positive.

Of the species included in this study, two (*Panulirus argus* and *Homarus americanus*) showed proliferation not only in the LC but also in the paired medial soma cluster (MC; soma clusters # 9 and 11 according to Sandeman *et*

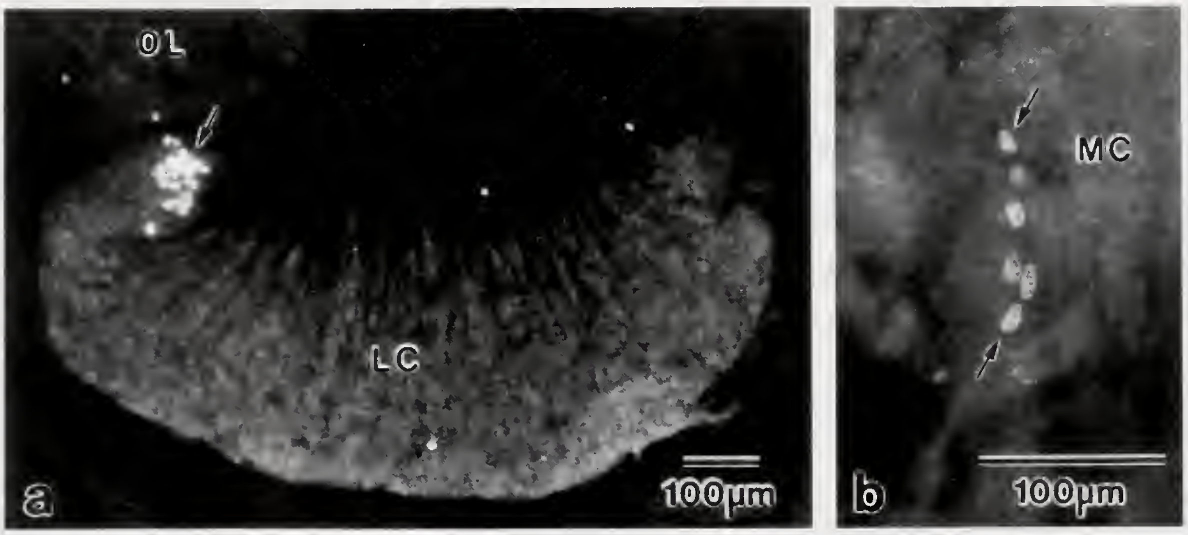

Figure 3. Proliferating cells in the central olfactory pathway of adult American lobster (*Homarus americanus:* Astacidea [Homarida]; Homaridae) identified by *in vivo* BrdU-labeling. Light micrographs of vibratome sections. (a) In the lateral soma cluster (LC), a compact group of small BrdU-positive nuclei (arrow) is located close to the neuropil of the olfactory lobe (OL). (b) In the medial soma cluster (MC) of this specimen, a string of slightly elongated nuclei is BrdU positive (arrows).

al., 1992) containing the cell bodies of local interneurons of the olfactory deutocerebrum (Figs. 2a, c, d, 3b). Only *Panulirus argus* showed a tightly packed group of BrdU-positive nuclei in the MCs in all tested specimens, which ranged from late juveniles to mid-sized sexually mature adults. In each case this group comprised 15–25 strongly labeled spherical nuclei that were slightly smaller than the nuclei of somata located in the periphery of the MC (Fig. 2c, d). The group of BrdU-positive nuclei was located in the ventralmost area of the MC adjacent to the neuropils of the olfactory and accessory lobes (Fig. 2a, c). In *Homarus americanus*, evidence for proliferation in the MC occurred in only two of five tested specimens. The MCs of these two animals contained a group of about 10 strongly BrdU-positive nuclei that were slightly elongated and arranged in a string transversing the cluster from its innermost aspect to the periphery (Fig. 3b).

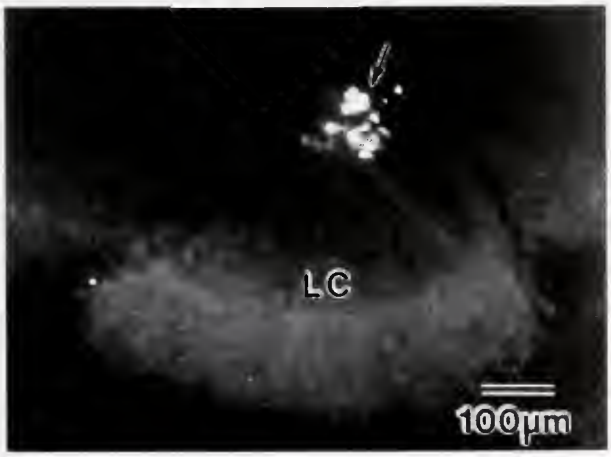

Figure 4. Proliferating cells in the central olfactory pathway of adult Australian crayfish (*Cherax destructor:* Astacidea [Astacida]; Parastacidae) identified by *in vivo* BrdU-labeling. Light micrograph of a vibratome section. A compact group of small BrdU-positive nuclei (arrow) is located in the LC close to the neuropils of the olfactory lobe and the accessory lobe.

Two of the species included in this study, the hermit crab (*Pagurus bernhardus*) and the true crab (*Cancer pagurus*), possessed BrdU-positive nuclei arranged in an obvious group in the LC and in a paired soma cluster adjacent to the hemiellipsoid body (HBC). The morphology of the neurons whose somata constitute the HBCs has not yet been elucidated, and it remains unclear whether they represent local interneurons of the hemiellipsoid bodies. In *Pagurus bernhardus*, the eyestalks ($n = 10$) of all specimens had a group of 6–15 BrdU-positive nuclei in the HBC (Fig. 5c). In only two of the eyestalks of the three large specimens of *Cancer pagurus* did we find a cluster of BrdU-positive nuclei in the HBC. In contrast, the eyestalks ($n = 4$) of the two smaller specimens contained a cluster of BrdU-positive nuclei in the HBC. In each case, the number of BrdU-positive nuclei ranged from 20 to 30 per HBC (Fig. 6b). The BrdU-positive nuclei in the HBC of *Pagurus bernhardus* and *Cancer pagurus* were spherical and slightly smaller than the nuclei of unlabeled somata in the periphery of the HBC. In each case, the group of BrdU-positive nuclei was located close to the HB neuropil. None of the other species had a group of BrdU-positive nuclei present in the HBC. This negative result is supported best by the spiny lobster (*Panulirus argus*), where 13 eyestalks were analyzed, and the rock

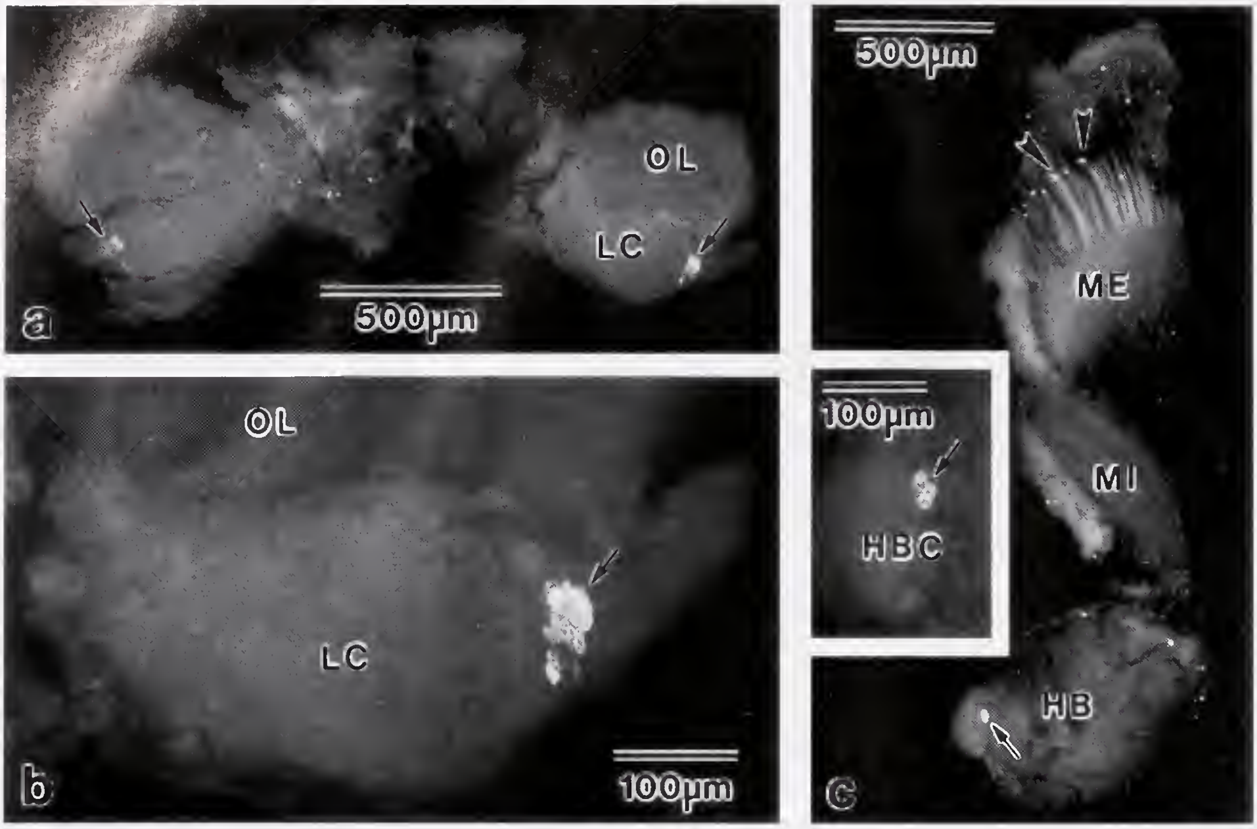

Figure 5. Proliferating cells in the central olfactory pathway of adult hermit crab (*Pagurus bernhardus:* Anomura [Anomala]; Paguridae) identified by *in vivo* BrdU-labeling. Light micrographs of vibratome sections. (a, b) Central brain. In the lateral soma clusters (LC), a compact group of small BrdU-positive nuclei (arrows) is located close to the neuropil of the olfactory lobe (OL). (c) Eyestalk ganglion. In the soma cluster (HBC) of the hemiellipsoid body (HB), a compact group of small BrdU-positive nuclei is located close to the HB neuropil. Note scattered BrdU-positive nuclei (arrowheads) in the soma clusters of visual neuropils (medulla interna = MI; medulla externa = ME). Inset: Higher magnification shows shows spherical and hence neuronal shape of BrdU-positive nuclei.

shrimp (*Sicyonia brevirostris*), where 5 eyestalks were analyzed. However, in all tested species, very few nuclei located in the HBC were labeled in most specimens; the same was true for other soma clusters of the eyestalk ganglia, especially the soma clusters of the three visual neuropils. Most of these BrdU-positive nuclei were either flat and elongated, and thus probably represent glial cells; or they were more spherical but clearly associated with arterioles passing through the soma clusters, and thus probably represent connective tissue cells constituting the wall of these hemolymph vessels. But some nuclei in soma clusters were spherical and not obviously associated with arterioles; thus they might represent neuronal precursor cells.

Discussion

We demonstrate by *in vivo* labeling with BrdU that mitotic activity in the neuronal soma clusters of the central olfactory pathway appears to be a common feature of adult decapod crustaceans; this result corroborates and substantially extends previous findings for juvenile and adult shore crabs (*Carcinus maenas*) and for the Australian crayfish (*Cherax destructor*) (Schmidt, 1997; Sandeman *et al.*, 1998). In all three studies the BrdU-positive nuclei in the soma clusters of the central olfactory pathway were small and almost spherical, and clearly resemble neurons. However, positive BrdU-labeling of neuron-like nuclei in soma clusters that are predominantly, but not exclusively, composed of neuronal cell bodies (the clusters also contain the somata of glial cells and of cells forming the walls of arterioles) is not conclusive evidence for the generation of new neurons, *i.e.*, neurogenesis. BrdU-labeling could be explained in several alternative ways: differentiation of proliferating cells into non-neuronal cells, programmed cell death shortly after birth of new cells, or DNA synthesis without subsequent mitosis. In the case of *Carcinus maenas*, however, various lines of evidence rule out these alternatives and thus strongly support the notion that proliferation in the soma clusters of the central olfactory pathway indeed

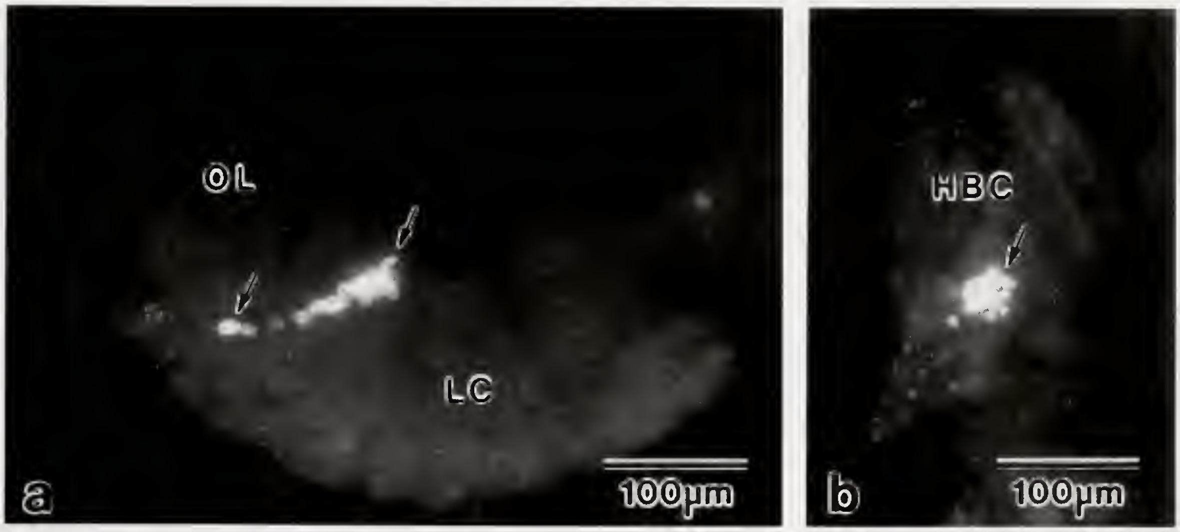

Figure 6. Proliferating cells in the central olfactory pathway of adult common crab (*Cancer pagurus:* Brachyura [Brachyura]; Cancridae) identified by *in vivo* BrdU-labeling. Light micrographs of vibratome sections. (a) Central brain. In the lateral soma cluster (LC), a compact group of small BrdU-positive nuclei (arrows) is located close to the neuropil of the olfactory lobe (OL). (b) Eyestalk ganglion. In the soma cluster (HBC) of the hemiellipsoid body, a compact group of small BrdU-positive nuclei is present (arrow).

reflects neurogenesis (Schmidt, 1997). This conclusion is substantially supported by the finding that in *Carcinus maenas* and in *Cherax destructor,* the olfactory projection neurons whose somata constitute the LCs increase continuously in number throughout juvenile and adult growth (Schmidt, 1997; Sandeman *et al.,* 1998). Throughout juvenile and adult life the number of olfactory projection neurons doubles in *Carcinus maenas* (from *ca.* 24,000 to *ca.* 48,000 per brain: Schmidt, 1997), and it approximately triples in *Cherax destructor* (from *ca.* 60,000 to *ca.* 180,000 per brain: Sandeman *et al.,* 1998). Thus, the generation of new olfactory projection neurons throughout juvenile and adult life appears to be well established in these species. The groups of proliferating cells in the respective soma clusters most likely reflect the cellular basis of this neuronal proliferation. We conclude that, at least for the LC, the occurrence of groups of BrdU-positive, neuron-like somata truly indicates neurogenesis, although a direct confirmation of this conclusion (for instance by double-labeling BrdU-positive cells with neuronal markers) is still lacking.

Another important issue is whether the occurrence of groups of BrdU-positive nuclei in the MC and the HBC can also be regarded as an indication of neurogenesis. At present the answer is uncertain, since counts of the respective neuron types have not yet been performed in the species we studied. Two lines of evidence support this assumption for the HBC. First, the BrdU-positive nuclei in the HBC are very similar in size, shape, and location (at the inside of the cluster, directly adjacent to the neuropil) to the BrdU-positive nuclei in the LC, in all three species in which they were found (this study; Schmidt, 1997). Second, in *Carcinus maenas,* groups of BrdU-positive neuron-like nuclei were present in the HBC after a long post-injection survival time (1 month), ruling out the possibilities that newly born cells collectively either undergo programmed cell death or differentiate into non-neuronal cells (Schmidt, 1997). For the MC, only the very similar size, shape, and location (also at the inside of the cluster, directly adjacent to the neuropil) of the BrdU-positive nuclei to the BrdU-positive nuclei in the LC supports the assumption that mitotic activity as shown by the BrdU-labeling in this study reflects neurogenesis. In a strict sense this argument applies only to the spiny lobster (*Panulirus argus*), in which BrdU-positive nuclei were consistently present in the MC and were indeed indistinguishable from their counterparts in the LC in terms of the above mentioned criteria. However, in the American lobster (*Homarus americanus*), where we also observed BrdU-positive nuclei in the MC, the situation is not as clear. BrdU-positive nuclei forming a group were present in the MCs in only two of the five tested specimens. Furthermore, the labeled nuclei were slightly elongated compared to the BrdU-positive nuclei of the LC, and the group they formed was neither compact nor located close to the OL/AL neuropil (as in the spiny lobster). Therefore it remains questionable whether the proliferating cells in the MC of *Homarus americanus* give rise to new neurons or to other cell types. The shape and arrangement of these BrdU-positive nuclei suggest that they might represent cells forming the wall of arterioles. Double labeling experiments with neuronal markers are necessary to clarify this point. Recently, the occurrence of BrdU-positive nuclei in the MC was reported for juveniles and adults of the Australian crayfish (*Cherax destructor*) (Sandeman *et al.,* 1998). Here we could not reproduce this result in the three adult specimens tested, and

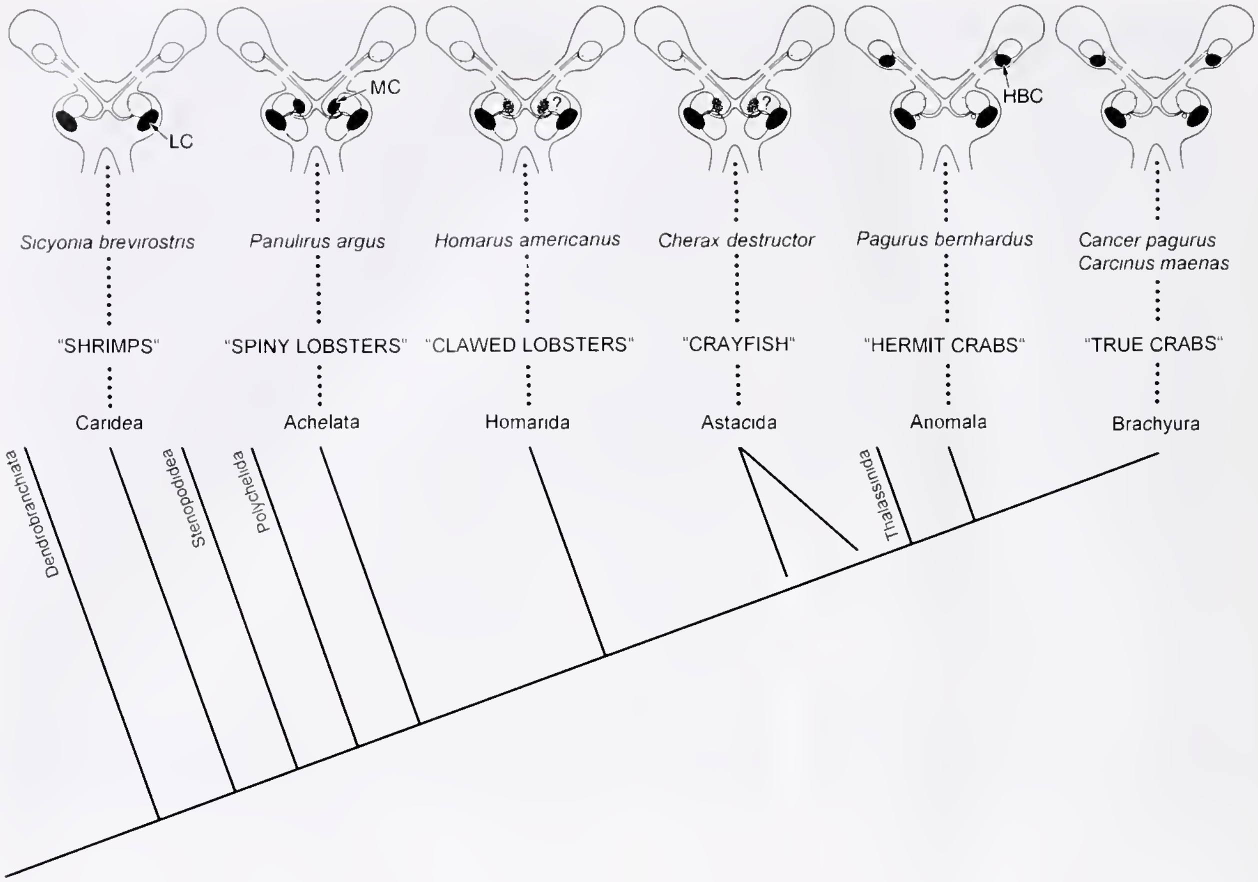
MC
LC
?
?
HBC
Sicyonia brevirostris
Panulirus argus
Homarus americanus
Cherax destructor
Pagurus bernhardus
Cancer pagurus
Carcinus maenas
"SHRIMPS"
"SPINY LOBSTERS"
"CLAWED LOBSTERS"
"CRAYFISH"
"HERMIT CRABS"
"TRUE CRABS"
Caridea
Achelata
Homarida
Astacida
Anomala
Brachyura
Dendrobranchiata
Stenopodidea
Polychelida
Thalassinida

Figure 7. Occurrence of neurogenesis in the central olfactory pathway of juvenile and adult decapod crustaceans. Decapod phylogeny and terminology of taxa are according to Sandeman *et al.*, (1993) and Scholtz and Richter (1995). Common names of taxa included in this study are given in parenthesis. Names of species studied to date (*Carcinus maenas* from Schmidt, 1997; *Cherax destructor* from Sandeman *et al.*, 1998, and from this study, all others from this study) are given in italics. Brain morphology highlights the central olfactory pathway with olfactory lobe, accessory lobe, hemiellipsoid body, the connecting olfactory globular tracts and associated soma clusters: lateral cluster (LC), medial cluster (MC), and hemiellipsoid body cluster (HBC). Soma clusters with typical groups of BrdU-positive nuclei are in black; in questionable cases they are dotted. Note that neuronal proliferation in the LC indicating neurogenesis among olfactory projection neurons is a common feature of adult decapod crustaceans. Proliferation in the other soma clusters of the central olfactory pathway (in the MC indicating neurogenesis among local interneurons of the olfactory deutocerebrum; in the HBC indicating neurogenesis among local interneurons of the hemiellipsoid body) appears to be linked to the occurrence (in spiny lobsters, clawed lobsters, and crayfish) and later reduction (in hermit crabs and true crabs) of the accessory lobe in the evolutionary history of decapods.

the reasons for this difference remain unclear. One possible explanation is that the adult animals tested by Sandeman *et al.*, (1998) were significantly younger than our specimens, since the position of the BrdU-positive nuclei of the adult illustrated in their report (in the center of the MC and at the outer edge of the LC) resembles the situation in early juveniles.

Our finding that no BrdU-positive somata were present in the LCs of three large adults of *Cancer pagurus* after an appropriate post-injection survival time (5.5 h) is the only instance so far of a negative result of this kind. In the previous study (Schmidt, 1997), all specimens of *Carcinus maenas* ($n = 16$), and in this study, all other specimens of *Cancer pagurus* ($n = 2$) as well as all specimens of the other species ($n = 20$) showed a typical group of BrdU-positive nuclei in each LC. This indicates that proliferation in the LC is a continuous process that apparently is not related to the molt cycle. That the negative result in *Cancer pagurus* occurred in very large and hence old adults suggests that, at least in some decapod species, the generation of new olfactory projection neurons may not continue for the entire life-span, but ceases in senescent animals. For some species of decapod crustaceans, enough growth data are available to allow absolute age to be estimated from body size. According to such estimates, the large specimens of *Cancer pagurus,* in which we did not detect BrdU-positive nuclei in the LC, were at least 7 years old; whereas the smaller adults, in which we found typical groups of BrdU-positive nuclei in each LC, were about 5 years old (Gruner, 1993). In comparison, the American lobsters that showed typical groups of BrdU-positive nuclei in each LC in our experiments were at least 8 and probably more than 10 years old (Hartnoll, 1982) and the largest specimen of *Panulirus argus* in our study that also showed normal proliferation in the LC was at least 5 years of age (Travis, 1954).

Common features of the proliferation in the soma clusters of the central olfactory pathway in adult decapod crustaceans include the very uniform relative size, the shape, and the location of the BrdU-positive nuclei (Schmidt, 1997; this study). In each case these nuclei are among the smallest of the respective soma clusters; they are mostly spherical and thus resemble neurons; and they are located in very restricted regions of the respective soma clusters close to the neuropil. These cells apparently represent a unique type of presumptive neuronal precursor cell differing in several aspects from the neuronal precursor cells that are active during embryonic and larval development of crustaceans and insects. The latter precursor cells are neuroblasts that differentiate from the ectoderm and ganglion mother cells that arise from the neuroblasts through a series of unequal mitoses; each produces two neurons by an equal mitosis (*e.g.*, Thomas *et al.*, 1984; Harzsch and Dawirs, 1994). Typically, neuroblasts and ganglion mother cells are considerably larger than terminally differentiated neurons, and they are located at the outer edge of the soma clusters formed by their mitotic activity (*e.g.*, Nordlander and Edwards, 1970; Ito and Hotta, 1992; Harzsch and Dawirs, 1994). The mitotically active precursor cells that were recently demonstrated in the LC of early postlarval crabs share these criteria and therefore are regarded as delayed ganglion mother cells (Harzsch and Dawirs, 1996). We did not find BrdU-positive nuclei resembling typical large neuroblasts or ganglion mother cells in any specimen, indicating that the mitotic activity of these cells ceases during juvenile development.

Since BrdU-positive groups of nuclei were detected in the LC of all tested species representing the major infraorders of decapod crustaceans (Fig. 7), we conclude that proliferation in the LC—and hence neurogenesis of olfactory projection neurons—most likely represents a general principle common to the brain of late juvenile and adult decapod crustaceans. In contrast, neurogenesis of local interneurons of the olfactory deutocerebrum and of neurons whose somata constitute the hemiellipsoid body clusters clearly is not a common feature among adult decapod crustaceans, since evidence for neuronal proliferation in the MC and in the HBC, respectively, occurs only in some of the tested species. In the case of the MC, we found clear evidence for neuronal proliferation only in the spiny lobster (*Panulirus argus*). Although we detected BrdU-positive nuclei in the MCs of two American lobsters (*Homarus americanus*), it remains questionable whether they represent neuronal precursor cells. Proliferation has recently been reported (Sandeman *et al.*, 1998) in the MCs of the Australian crayfish (*Cherax destructor*), but we were unable to reproduce this result. In the case of the HBC, on the other hand, evidence for neurogenesis (*i.e.*, clustered BrdU-positive, neuron-like nuclei) occurs only in the brachyuran crabs *Carcinus maenas* (Schmidt, 1997) and *Cancer pagurus* and in the hermit crab *Pagurus bernhardus*. Clearly, not enough species have been tested to exclude simple species-specific differences as the basis of this variability. However, it is striking that presumptive neurogenesis of local interneurons of the olfactory deutocerebrum appears to be restricted to species with accessory lobes (Fig. 7)—that is, glomerular neuropils of the deutocerebrum connected to the olfactory lobes (Schmidt and Ache, 1997)—whereas neurogenesis of neurons residing in the HBC occurs only in species in which the accessory lobes are thought to be reduced secondarily (Scholtz and Richter, 1995; Sandeman *et al.*, 1993).

Clearly, the function of adult neurogenesis in decapod crustaceans and other animals remains to be determined. From the studies in decapod crustaceans, as well as from those in vertebrates and insects, it emerges that adult neurogenesis is either limited to or is at least very prominent in the central olfactory pathway (*e.g.*, Kaplan *et al.*, 1985; Corotto *et al.*, 1993; Luskin, 1993; Okano *et al.*, 1993; Cayre *et al.*, 1994, 1996; Schmidt, 1997). The olfactory pathway also is the only sensory pathway in which primary receptor neurons show a lifelong, continuous turnover. This has been known for vertebrates including mammals for many years (*e.g.*, Graziadei, 1973) and recently was also found for a decapod crustacean, *Cherax destructor* (Sandeman and Sandeman, 1996). It seems reasonable to speculate that neurogenesis in the olfactory pathway of the adult brain may be linked to the continuous turnover of olfactory receptor neurons in the periphery. This could allow a lifelong "adaptation" of the olfactory system to ever-changing olfactory environments and would be advantageous for long-lived animals such as most vertebrates and decapod crustaceans.

Acknowledgments

This study was supported in part by grants from the Deutsche Forschungsgemeinschaft (Schm 738/4-1; Ha 2540/1-1). We wish to thank Dr. B. W. Ache (Whitney Laboratory, University of Florida) for providing lab space and spiny lobsters, and Dr. J. Nunez (Whitney Laboratory, University of Florida) for providing rock shrimp.

Literature Cited

Bayer, S. A. 1982. Changes in the total number of dentate granule cells in juvenile and adult rats: a correlated volumetric and 3H-thymidine autoradiographic study. *Exp. Brain Res.* **46:** 315–323.

Bieber, M., and D. Fuldner. 1979. Brain growth during the adult stage of a holometabolous insect. *Naturwissenschaften* **66:** 426.

Blaustein, D. N., C. D. Derby, R. B. Simmons, and A. C. Beall. 1988. Structure of the brain and medulla terminalis of the spiny lobster *Panulirus argus* and the crayfish *Procambarus clarkii*, with an emphasis on olfactory centers. *J. Crust. Biol.* **8:** 493–519.

Boeckh, J., K. D. Ernst, H. Sass, and U. Waldow. 1984. Anatomical and physiological characteristics of individual neurons in the central antennal pathway of insects. *J. Insect Physiol.* **30:** 15–26.

Cayre, M., C. Strambi, and A. Strambi. 1994. Neurogenesis in an adult insect brain and its hormonal control. *Nature* **368:** 57–59.

Cayre, M., C. Strambi, P. Charpin, R. Augier, M. R. Meyer, J. S. Edwards, and A. Strambi. 1996. Neurogenesis in adult insect mushroom bodies. *J. Comp. Neurol.* **371:** 300–310.

Corotto, F. S., J. A. Henegar, and J. A. Maruniak. 1993. Neurogenesis persists in the subependymal layer of the adult mouse brain. *Neurosci. Lett.* **149:** 111–114.

Crespo, D., B. B. Stanfield, and W. M. Cowan. 1986. Evidence that late-generated granule cells do not simply replace earlier formed neurons in the rat dentate gyrus. *Exp. Brain Res.* **62:** 541–548.

Davis, R. L. 1993. Mushroom bodies and *Drosophila* learning. *Neuron* **11:** 1–14.

Fahrbach, S. E., J. L. Strande, and G. E. Robinson. 1995. Neurogenesis is absent in the brains of adult honey bees and does not explain behavioral neuroplasticity. *Neurosci. Lett.* **197:** 145–148.

Graziadei, P. P. C. 1973. Cell dynamics in the olfactory mucosa. *Tissue Cell* **5:** 113–131.

Gruner, H.-E., ed. 1993. *Lehrbuch der speziellen Zoologie. Band 1: Wirbellose Tiere. 4. Teil: Arthropoda (ohne Insecta).* Gustav Fischer Verlag, Stuttgart.

Hartnoll, R. G. 1982. Growth. Pp. 111–196 in *The Biology of Crustacea. Vol. 2. Embryology, Morphology, and Genetics,* L. G. Abele, ed. Academic Press, New York.

Harzsch, S., and R. R. Dawirs. 1994. Neurogenesis in larval stages of the spider crab *Hyas araneus* (Decapoda, Brachyura): proliferation of neuroblasts in the ventral nerve cord. *Roux's Arch. Dev. Biol.* **204:** 93–100.

Harzsch, S., and R. R. Dawirs. 1996. Neurogenesis in the developing crab brain: postembryonic generation of neurons persists beyond metamorphosis. *J. Neurobiol.* **29:** 384–398.

Ito, K., and Y. Hotta. 1992. Proliferation pattern of postembryonic neuroblasts in the brain of *Drosophila melanogaster. Dev. Biol.* **149:** 134–148.

Kaplan, M. S., and J. W. Hinds. 1977. Neurogenesis in the adult rat: electron microscopic analysis of light radioautographs. *Science* **197:** 1092–1094.

Kaplan, M. S., N. A. McNelly, and J. W. Hinds. 1985. Population dynamics of adult-formed granule neurons of the rat olfactory bulb. *J. Comp. Neurol.* **239:** 117–125.

Kuhn, H. G., H. Dickinson-Anson, and F. H. Gage. 1996. Neurogenesis in the dentate gyrus of the adult rat: age-related decrease of neuronal progenitor proliferation. *J. Neurosci.* **16:** 2027–2033.

Luskin, M. B. 1993. Restricted proliferation and migration of postnatally generated neurons derived from the subventricular zone. *Neuron* **11:** 173–189.

Mellon, D., Jr., V. Alones, and M. D. Lawrence. 1992. Anatomy and fine structure of neurons in the deutocerebral projection pathway of the crayfish olfactory system. *J. Comp. Neurol.* **321:** 93–111.

Menzel, R., C. Durst, J. Erber, S. Eichmüller, M. Hammer, H. Hildebrandt, J. Mauelshagen, U. Müller, H. Rosenboom, J. Rybak, S. Schäfer, and A. Scheidler. 1994. The mushroom bodies in the honeybee: from molecules to behavior. Pp. 81–102 in *Fortschritte der Zoologie, Vol. 39. Neural Basis of Behavioural Adaptations,* K. Schildberger and N. Elsner, eds. Gustav Fischer Verlag, New York.

Morshead, C. M., B. A. Reynolds, C. G. Craig, M. W. McBurney, W. A. Staines, D. Morassutti, S. Weiss, and D. Van der Kooy. 1994. Neural stem cells in the adult mammalian forebrain: a relatively quiescent subpopulation of subependymal cells. *Neuron* **13:** 1071–1082.

Nordlander, R. H., and J. S. Edwards. 1970. Postembryonic brain development in the monarch butterfly, *Danaus plexippus plexippus* L. III. Morphogenesis of centers other than the optic lobes. *Wilhelm Roux' Arch.* **164:** 247–260.

Okano, H. J., D. W. Pfaff, and R. B. Gibbs. 1993. RB and Cdc2 expression in brain: correlations with ^{3}H-thymidine incorporation and neurogenesis. *J. Neurosci.* **13:** 2930–2938.

Paton, J. A., and F. N. Nottebohm. 1984. Neurons generated in the adult brain are recruited into functional circuits. *Science* **225:** 1046–1048.

Purves, D. 1988. *Body and Brain. A Trophic Theory of Neuronal Connections.* Harvard University Press, Cambridge.

Raymond, P. A., and S. S. Easter, Jr. 1983. Postembryonic growth of the optic tectum in goldfish. I. Location of germinal cells and numbers of neurons produced. *J. Neurosci.* **3:** 1077–1091.

Sandeman, R. E., and D. C. Sandeman. 1996. Pre- and postembryonic development, growth and turnover of olfactory receptor neurons in crayfish antennules. *J. Exp. Biol.* **199:** 2409–2418.

Sandeman, D., R. Sandeman, C. Derby, and M. Schmidt. 1992. Morphology of the brain of crayfish, crabs, and spiny lobsters: a common nomenclature for homologous structures. *Biol. Bull.* **183:** 304–326.

Sandeman, D. C., G. Scholtz, and R. E. Sandeman. 1993. Brain evolution in decapod Crustacea. *J. Exp. Zool.* **265:** 112–133.

Sandeman, R., D. Clarke, D. Sandeman, and M. Manly. 1998. Growth-related and antennular amputation-induced changes in the olfactory centers of crayfish brain. *J. Neurosci.* **18:** 6195–6206.

Schmidt, M. 1997. Continuous neurogenesis in the olfactory brain of adult shore crabs, *Carcinus maenas. Brain Res.* **762:** 131–143.

Schmidt, M., and B. W. Ache. 1997. Immunocytochemical analysis of glomerular regionalization and neuronal diversity in the olfactory deutocerebrum of the spiny lobster. *Cell Tissue Res.* **287:** 541–563.

Scholtz, G., and S. Richter. 1995. Phylogenetic systematics of the reptantian Decapoda (Crustacea, Malacostraca). *Zool. J. Linn. Soc.* **113:** 289–328.

Technau, G. M. 1984. Fiber number in the mushroom bodies of adult *Drosophila melanogaster* depends on age, sex and experience. *J. Neurogenet.* **1:** 113–126.

Thomas, J. B., M. J. Bastiani, M. Bate, and C. S. Goodman. 1984. From grasshopper to *Drosophila:* a common plan for neuronal development. *Nature* **310:** 203–207.

Travis, D. F. 1954. The molting cycle of the spiny lobster *Panulirus argus* Latreille. I. Molting and growth in laboratory-maintained individuals. *Biol. Bull.* **107:** 433–450.

Reference: *Biol. Bull.* **196:** 137–144. (April 1999)

Comparative Study of Temporal Resolution in the Visual Systems of Mesopelagic Crustaceans

TAMARA M. FRANK

Harbor Branch Oceanographic Institution, 5600 U.S. 1 N, Ft. Pierce, Florida 34946

Abstract. The temporal characteristics of the visual systems of eight species of mesopelagic crustaceans were studied using the electroretinogram (ERG). Experiments were conducted on shipboard, using dark-captured specimens collected off the south coast of Cuba. As one would expect based on the relative intensity differences in their light environments, the deepest living species, *Systellaspis debilis* and *Sergia filictum*, have low maximum critical flicker fusion frequencies (CFFs) of 21–25 Hz, whereas the shallower living species *Oplophorus gracilirostris* and *Janicella spinacauda* have higher maximum CFFs (31–32 Hz). One of the shallowest living species, *Funchalia villosa*, has an unusually low maximum CFF (24 Hz), which may be a function of working with a dark-adapted eye. Two of the bilobed euphausiid species, *Nematobrachion flexipes* and *N. sexspinosus*, have very high maximum CFFs (44–57 Hz), comparable to those of surface-dwelling crabs, even though they live between 400 and 600 m. The maximum CFF of *Stylocheiron maximum*, a shallower living bilobed euphausiid, is only 36 Hz, indicating that maximum CFF among the euphausiids cannot be correlated with depth of occurrence. The unusually high flicker fusion frequency of the deeper living euphausiids may be correlated to their preference for bioluminescent prey.

Introduction

Autrum's studies of insect photoreceptors in the 1950s gave rise to the idea that the response dynamics of the retina match the habitat and lifestyle of the organism. In these classic studies, he established that the eyes of rapidly moving day-active species have better temporal resolution, as indicated by flicker fusion frequencies of 200–300 Hz, than the eyes of slower moving night-active forms, with flicker fusion frequencies of 10–20 Hz (Autrum, 1950, 1958; Autrum and Stöcker, 1952). These extracellular studies, using the electroretinogram (ERG), which is the summed mass response from a large number of receptor cells, were later supported by studies on the intracellular responses of single cells (Howard *et al.*, 1984; de Souza and Ventura, 1989). Since the light environment of mesopelagic crustaceans is similar to that of nocturnal insects, one might predict that they would also have fairly low temporal resolution, and that temporal resolution would be correlated with daytime depth of occurrence. Although the spatial resolution, which is a function of the structure and optics of photoreceptors, has been studied in a number of mesopelagic species (see Cronin, 1986; Land, 1990, for review), the temporal resolution, which is a function of the membrane properties of the receptor cells themselves (see Weckström and Laughlin, 1995, for review), has received little attention. As shown by the theoretical analysis of Srinivasan and Bernard (1975), visual acuity is dependent on both the spatial resolution and the temporal resolution of the eye, because for most organisms, visual targets are rarely stationary. Either the organisms themselves are actively moving, so the environment is in motion with respect to their photoreceptors, or their photoreceptors are moving because of muscle tremor or nystagmus. Srinivasan and Bernard (1975) determined that at angular velocities (of the object with respect to the organism viewing it) above a critical value, spatial resolution is more dependent on the temporal properties of the photoreceptor cells than on the structural optics of the eye. Therefore, for any comprehensive analysis of the visual system of an organism, both the spatial and temporal characteristics of the photoreceptor need to be studied.

Studies on temporal resolution in mesopelagic organisms are rare, due to the difficulties in collecting visually competent organisms and keeping them alive during transport back to shore-based labs. The only published study on the temporal characteristics of the visual systems of mesope-

Received 4 June 1998; accepted 9 December 1998.

lagic organisms is by Moeller and Case (1995), in which they demonstrated that two species of deep-sea crustaceans have very low flicker fusion frequencies (8–12 Hz), compared to much higher maximum flicker fusion frequencies (50–60 Hz) for shallow-water crabs (Bröcker, 1935; Crozier and Wolf, 1939). However, Moeller and Case (1995) measured the critical flicker fusion frequency at threshold light intensities, which is difficult to compare between species because (1) the threshold sensitivity of a crustacean eye measured using the ERG technique varies considerably from preparation to preparation (pers. obs.), and (2) critical flicker fusion frequency is dependent upon the intensity of the stimulus light (Bröcker, 1935; Crozier and Wolf, 1939; Crozier *et al.*, 1939). A less problematic characteristic to use for comparative studies of temporal resolution is the *maximum* critical flicker fusion frequency. This is the maximum flicker rate that the eye is capable of following at any light intensity. In the current study, the maximum critical flicker fusion frequencies of the photoreceptors of eight species of mesopelagic crustaceans from a variety of depths (250–900 m) were examined using ERG recordings. The results of these experiments indicate that several species from this dim light environment have surprisingly high maximum flicker fusion rates. These unusually high rates do not appear to be a function of depth of occurrence, but rather, appear to be more closely correlated with the bioluminescence of the preferred prey.

Materials and Methods

Animal collections

The crustacean species used in this study (Table 1) were collected off the south coast of Cuba on a research cruise aboard the RV *Seward Johnson*, with a 2.4 × 1.8 m Tucker trawl fitted with a thermally insulated, light-tight closing collecting container (cod-end). The light-tight cod-end was closed at depth, ensuring that the organisms inside were not exposed to damaging light levels at the surface, as studies have demonstrated that even low levels of light can cause permanent structural and physiological damage to the photoreceptors of light-sensitive species (Loew, 1976; Nilsson and Lindström, 1983; Frank and Case, 1988b). Once at the surface, the cod-end was detached from the net and carried into a light-tight room, where it was opened and species were sorted under dim red light. Specimens were maintained in chilled (8°C), aerated seawater in 1-qt containers, which were placed inside light-tight boxes. All trawling was conducted between the hours of 2200 and 0500.

Table 1

Daytime depth distribution of crustaceans in this study

Species	Depth (m)*
Family Euphausiacidae	
Stylocheiron maximum	250–500 (1)
Nematobrachion sexspinosus	400–600 (1)
Nematobrachion flexipes	450–600 (1)
Family Oplophoridae	
Janicella spinacauda	500–600 (2)
Oplophorus gracilirostris	500–650 (2)
Systellaspis debilis	600–900 (2)
Family Penaeidae	
Funchalia villosa	300–500 (3)
Family Sergestidae	
Sergia filictum	600–900 (4)

* Numbers in parentheses indicate the source of the data: (1) Roger, 1978; (2) Hopkins *et al.*, 1989; (3) Hopkins *et al.*, 1994; (4) Flock and Hopkins, 1992.

Electrophysiological recordings

The species in this study ranged in size from 20 mm body length (the euphausiids and *Janicella spinacauda*) to 80 mm body length (*Oplophorus gracilirostris*). They were mounted on an acrylic plastic holder and suspended in a chilled (8°C) seawater bath with the dorsal surface of the eyes just above the level of the water. In this configuration, which allowed their pleopods to remain free to generate respiratory water currents around the gills, the crustaceans remained alive and healthy for the duration of experiments lasting up to 12 h. A tungsten microelectrode (10 μm tip; F. Haer and Co.) was placed subcorneally in the left eye. A reference electrode was placed in the right eye, which was then covered with black petroleum jelly (petroleum jelly mixed with black oil-based paint) to block all light input to this eye. This differential recording technique was used so that background noise was subtracted from the signal before amplification. A silver chloride electrode grounded the water bath. Electrodes were placed in the eyes under dim red light (>650 nm; Wratten Filter 79B). Signals were amplified with a Haer Microelectrode Amplifier (Model × Cell-3) used in conjunction with a high-impedance probe to eliminate electrode polarization artifacts (Kugel, 1977). Low-frequency filters were set to minimal filtering (0.01–0.1 Hz) to minimize distortion of the AC-amplified signal. Data were digitized using a program written in LabView (National Instruments, Inc.), and stored to disk for later analysis.

This study was conducted on shipboard because the organisms used will not survive transport to a shore-based laboratory. Due to the difficulties inherent in working on a moving and rolling vessel, only extracellular electrophysiology was possible.

Light stimuli

Test flashes of 490 nm light from an American Instruments SA monochromator (Model H-20) were delivered to the eye *via* a fused silica light guide, positioned so the circle of light at the output was larger than the eye. A piece of lens tissue between the light guide and the eye served as a diffuser. Flash duration was controlled by a Uniblitz shutter (Model T132) under computer control, such that a 50% duty cycle (50:50 light:dark ratio) was maintained. Irradiance was controlled with a neutral-density wheel driven by a stepper motor under computer control, and calibrated with a UDT optometer (United Detector Technology Model S370) and radiometric probe with point calibrations provided by UDT.

Procedure

Although mesopelagic crustaceans are relatively insensitive to red light (Frank and Case, 1988a), the dim red preparation light did produce a small degree of light adaptation. Therefore, after electrode placement, the specimen was dark-adapted until the response to a test flash, given every 5 min, had not changed for 1 h, indicating that the eye was in its fully dark-adapted condition. A flickering light stimulus of 1.5-s duration was then presented to the dark-adapted eye. To ensure that every flicker stimulus was presented to a fully dark-adapted eye, a dim 100-ms test flash that elicited a 50-μV response (the smallest response reliably discernible from background noise) in the fully dark-adapted eye was presented to the eye after every flicker stimulus, and the eye was allowed to re-dark-adapt until the test flash response had recovered to 50 μV, before the next flicker stimulus was presented. The flicker rate for subsequent stimuli was increased until critical flicker fusion was achieved; this is defined as the point at which the eye can no longer produce a modulated electrical signal that remains in phase with the flickering light. Irradiance was then increased by one log unit, and the flicker rate of the stimulus light was increased until fusion was again achieved. Maximum critical flicker fusion frequency (CFF) is defined as the point at which further increases in irradiance do not result in a faster flicker fusion frequency. All maximum CFFs are in reference to dark-adapted eyes.

The responses to single 100-ms flashes of 490-nm light of varying irradiances were also measured, starting from irradiances generating a threshold response, and continuing to the point at which further increases in irradiance produced no further increases in response amplitude. In some preparations, the response was not saturated at the maximum stimulus light irradiance. For those preparations in which response saturation was reached, the log I_{10} was determined; this is the log of the stimulus irradiance eliciting a response that is 10% of the maximum amplitude. The log I_{10} was used as an estimate of the relative sensitivity of the photoreceptors (after de Souza and Ventura, 1989).

For all species, latencies were measured using a response amplitude that was 10% of the maximum response. Response latency is defined as the time from the start of the light stimulus to the start of the ERG.

Results

The critical flicker fusion frequency measured *via* the extracellular electroretinogram is dependent on a variety of factors, namely adaptational state, background intensity, stimulus intensity, and the subtended visual angle of the source. In this study, all factors, with the exception of the stimulus intensity, were equal for all the species: they were all completely dark-adapted before being presented with a flickering light stimulus, the background intensity was 0, and the eye was always bathed with a circle of light that was larger than the eye itself. The only variable factor was the stimulus intensity. Although the irradiance of the light source was calibrated, the response to the light stimulus depended on the position of the electrode in the eye, so that a 100-μV response might be generated by a dim stimulus in one specimen and a brighter stimulus in another specimen of the same species. As shown in Figure 1, the CFF depended on irradiance level, with lower irradiances evoking lower CFFs and higher irradiances evoking higher CFFs. Therefore, to ensure that the same parameter was measured for all species in this comparative study, the maximum CFF, which is the highest flicker rate that the eye is capable of following at any intensity, was used.

Maximum critical fusion frequency

The maximum CFFs were measured for eight species of mesopelagic crustaceans from a variety of depths (Table I).

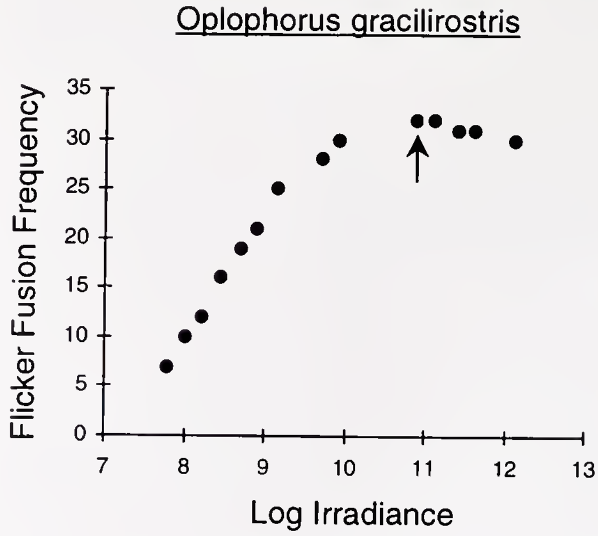

Figure 1. Flicker fusion frequency (Hz) as a function of irradiance (photons cm^{-2} s^{-1}) for *Oplophorus gracilirostris*. Flicker fusion frequency increases as the irradiance increases, up to the maximum critical flicker fusion frequency (arrow), the point at which further increases in irradiance do not result in a more rapid flicker fusion frequency.

Three species, *Sergia filictum, Systellaspis debilis,* and *Funchalia villosa,* had relatively low maximum CFFs, between 20 and 25 Hz (Table II), as one would expect from species coming from a very low light environment. A representative example of an ERG is shown for *Systellaspis debilis* in Figure 2A. Three species, *Oplophorus gracilirostris, Janicella spinacauda,* and *Stylocheiron maximum,* had somewhat higher rates, between 31 and 36 Hz; and two species, *Nematobrachion flexipes* and *Nematobrachion sexspinosus,* had extremely high CFFs, considering their dim light environment, of 44 and 57 respectively (Table II). A representative example of an ERG for *N. sexspinosus* is shown in Figure 2B.

Sensitivity

The overall sensitivity of the eye was estimated by determining the log of the irradiance (log I_{10}) required to produce a response that was 10% of the amplitude of the maximum response the eye was capable of generating. In several preparations, the maximum response was not seen, and the log I_{10} could not be determined. As shown in Table II, there is a trend towards lower sensitivity to light as the response dynamics of the eye speeds up. *Systellaspis debilis,* the species with the lowest maximum CFF, had, according to the log I_{10}, the most sensitive eye, while *N. sexspinosus,* the species with the highest maximum CFF, has the lowest sensitivity to light.

Response latency

As an indicator of the speed of transduction in the photoreceptors of the various species, latency from the start of the light stimulus to the start of the photoreceptor response was measured, using a response amplitude that was 10% of the maximum amplitude. Species with lower flicker fusion frequencies also have longer latencies, indicative of slower eyes, and species with higher flicker fusion frequencies have eyes with much faster response dynamics (Table II).

Table II

Mean values for temporal resolution (max CFF), sensitivity (Log I_{10}) and response latencies obtained from ERG data

Species	Max CFF (Hz)	Log I_{10} (photons cm^{-2} s^{-1})	Latency (ms)
Systellaspis debilis	21 (±0.6; *n* = 4)	8.9 (±0.06)	58 (±6.9)
Funchalia villosa	24 (±0.5; *n* = 2)	9.3 (±0.0)	75 (±2.0)
Sergia filictum	25 (*n* = 1)	NA	NA
Janicella spinacauda	[illegible] (±0.3; *n* = 3)	9.4 (±0.06)	49 (±3.5)
Oplophorus gracilirostris	32 ([illegible]; *n* = 2)	9.4 (±0.09)	42 (±5.5)
Stylocheiron maximum	36 (*n* [illegible])	10.0	42
Nematobrachion flexipes	44 (±1.0; *n* = 2)	10.2 (±0.38)	22 (±0.5)
Nematobrachion sexspinosus	56 (±2.0; *n* = 4)	10.8 (±0.18; *n* = 2)	16 (±2.5)

Species are ranked by max CFF, from lowest to highest. Standard errors and number of specimens tested are in parenthesis.

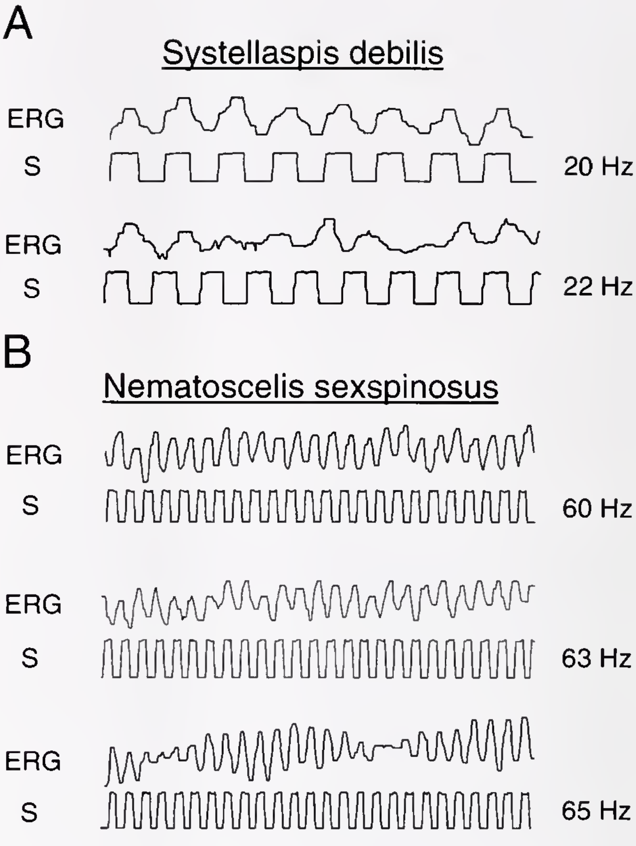

Figure 2. Representative examples of species with low and high flicker fusion frequencies. ERG designates the response recorded from the eye; S designates the flickering light stimulus. The data shown are from the last 0.4 s of the 2-s stimulus pulse. (A) The ERG from *Systellaspis debilis* was able to follow the stimulus light at 20 Hz cycle for cycle; at 22 Hz, the ERG response was lagging behind the light stimulus and "missing" cycles. (B) The ERG from *Nematoscelis sexspinosus* was able to follow the stimulus light at 60 Hz. At 63 Hz, the ERG appears to be in phase with the stimulus light, but careful examination of the data shows that 25 flashes of light were given, but only 23 responses were produced. By 65 Hz, the lag is even greater, and the ERG is clearly "missing" cycles. The CFF of this specimen is 60 Hz, since this is the last recorded frequency at which the ERG was able to match, cycle for cycle, the phase of the stimulus light.

Discussion

The vertical distributions of the species examined in this study have not been determined for the south coast of Cuba. The vertical distribution data in Table I are for the Gulf of Mexico, except for the euphausiids. Since Gulf of Mexico water originates in the Caribbean Sea (Nowlin, 1971), and both areas have Jerlov's Type I or IA water (Jerlov, 1976), it is likely that these two areas would have similar species assemblages and distribution patterns. The abundance of the three species of euphausiids in this study was extremely low in the Gulf of Mexico (Kinsey and Hopkins, 1994), as it was off the coast of Cuba (pers. obs.), and comprehensive data on depth distribution are not available for these areas. The data presented in the table are for the tropical Pacific, where Jerlov's Type 1 or 1A water is also present. The depth distributions of nine relatively abundant euphausiid species in the Gulf of Mexico (Kinsey and Hopkins, 1994) were compared with those provided by Roger (1978) for the same species in the tropical Pacific, and the depth ranges proved to be the same in the two areas. Therefore, it is likely that the data presented for the vertical distribution of *Nematobrachion flexipes, N. sexspinosus,* and *Stylocheiron maximum* in the tropical Pacific would also apply to the Gulf of Mexico.

Depth vs. critical flicker fusion

Shallower depth ranges do not necessarily mean a brighter light environment: an organism found at 300 m in murky water might see significantly less light than an organism found at 500 m in very transparent water. However, in this study, the depth of occurrence is an indication of relative light intensity, as the water is all Jerlov's Type 1 or 1A (Jerlov, 1976). Most of the species in this study live below 400 m. At 400 m during the day, in Jerlov's type 1 water, downwelling ambient light has been reduced to less than 0.0001% of the surface irradiance (Jerlov, 1976). This is about as bright as the moonlight seen by nocturnal insects, in that light from a full moon is 0.0001% of daytime illumination (Munz and McFarland, 1973; Land, 1981). Therefore, one would expect mesopelagic crustaceans to have relatively low maximum CFFs, indicative of low temporal resolution, as has been found in nocturnal insects (Autrum, 1950, 1958, 1984; Howard *et al.*, 1984; de Souza and Ventura, 1989; Laughlin and Weckström, 1993). In addition, one might expect the deepest dwelling species, which live in the dimmest light, to have the lowest maximum CFFs. This is certainly the case for the two deepest living species in this study—an oplophorid, *Systellaspis debilis,* and a sergestid, *Sergia filictum*—which have maximum CFFs of 20–25 Hz (Fig. 3), equivalent to those of the nocturnal slow moving insects studied by Autrum (1950, 1958). *Oplophorus gracilirostris* and *Janicella spinacauda* are in the same family as *S. debilis,* but have higher maximum CFFs—between 31–32 Hz. Their daytime depth range is about 100 m shallower than that of *S. debilis* (Fig. 3), so a higher maximum CFF is not unexpected. A previous study by Moeller and Case (1995) reports a critical flicker fusion frequency of 12 Hz for *Oplophorus spinosus,* which has a depth distribution similar to that of *O. gracilirostris.* However, those authors were using a light that was only 1 log unit above the irradiance that produced a threshold response, and as shown by Figure 1, a much lower critical flicker fusion frequency would result from such a dim light stimulus.

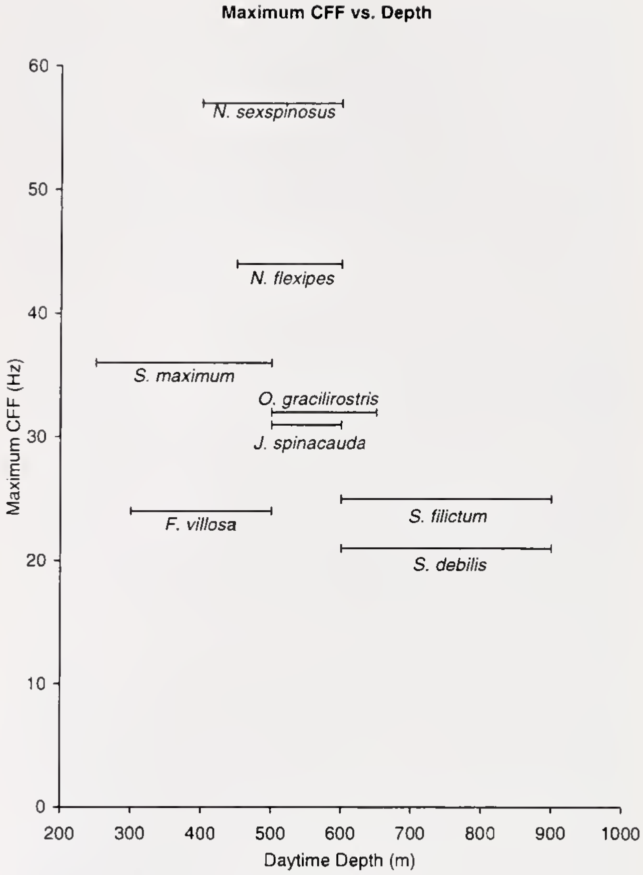

Figure 3. Maximum critical flicker fusion frequency (CFF) as a function of daytime depth distribution for the eight species in this study.

At first glance, the very low maximum CFF of the penaeid, *Funchalia villosa,* is somewhat puzzling. It is one of the shallowest living species, and also possesses an eye with a fairly high spatial resolution (Herring and Roe, 1988). High spatial resolution is usually correlated with a higher light environment, and is also associated with a comparatively higher temporal resolution (Srinivasan and Bernard, 1975). However, these measurements of maximum CFF were made in a completely dark-adapted eye; the eye of *F. villosa,* which is of the superposition type, possesses migrating screening pigments, which changes the eye from a spatially acute, apposition-like eye during the day to an eye with less spatial resolution, but greater sensitivity, at night (Herring and Roe, 1988). Maximum CFF is known to be higher in the light-adapted vs. the dark-adapted eyes of shallow-water crustaceans that possess mobile screening pigments (Crozier and Wolf, 1939; Crozier *et al.*, 1939; Bröcker, 1935), but mobile screening pigments are usually not found in mesopelagic species (see Hallberg and Elofsson, 1989, for review). *F. villosa* appears to be an exception to this rule. Looking at the other species in this study, the screening pigments in the photoreceptors of *Oplophorus spinosus* (Welsh and Chace, 1937; Land, 1976; Gaten *et al.*, 1992), a close relative of *O. gracilirostris* with the same depth distribution, and *Systellaspis debilis* (Gaten *et al.*, 1992) do not appear to be mobile. Although some species of sergestids may possess screening pigments (Welsh and Chace, 1938), it is not known whether these are mobile. Chun (1896), Zimmer (1956), and Meyer-Rochow and Walsh (1978) found no evidence of the migration of screening pigments in euphausiid eyes, and while Kampa (1965) indicates that some migration does occur, Land *et al.* (1979) conclude that this migration is not of sufficient magnitude to affect the spatial resolution of the eye. It remains to be seen whether *F. villosa*, whose spatial resolution is clearly higher when its screening pigments are in the light-adapted position, will also demonstrate a higher temporal resolution under light adaptation that is more consistent with its daytime depth distribution. Future studies will include determining the temporal resolution of *F. villosa*, as well as that of other species without migrating screening pigments, under light-adapted conditions.

The three euphausiid species in this study (*Nematobrachion sexspinosus, N. flexipes*, and *Stylocheiron maximum*) all have bilobed eyes, and Chun (1896) determined (morphologically) that the upper lobe, which is oriented upwards toward the brighter downwelling light, has higher spatial resolution than the lower lobe, which is oriented downwards towards dimmer upwelling light. Due to limitations set by working on shipboard, the responses from receptor cells in the upper lobe could not be isolated from responses from receptor cells in the lower lobe. Therefore, it remains to be determined whether the temporal resolution differs between the two lobes. However, it is clear that two of these species, *N. sexspinosus* and *N. flexipes*, have the highest maximum CFFs of all the species in this study, comparable to CFFs reported for shallow-water crabs (Bröcker, 1935; Crozier and Wolf, 1939). This is unexpected, because their daytime depths of occurrence are in the middle of the depth distribution for the eight species in the study (Fig. 3). These two species live at a depth at which the downwelling light intensity is roughly the same as that experienced by nocturnal insects under a full moon (see above), yet they have a substantially higher maximum CFF (40–60 Hz) than most nocturnal insects (10–20 Hz; Autrum, 1950, 1958). Laughlin and Weckstrom (1993) demonstrated that the benefits of high temporal resolution are limited for nocturnal, generally slow moving insects, and that the metabolic price for improving the temporal bandwidth of vision is substantial. In addition to the metabolic expense, fast photoreceptors have a lower sensitivity than slow photoreceptors (Laughlin, 1990), which would be a distinct disadvantage to organisms living in a light-limited environment. However, these conclusions were drawn for terrestrial organisms, and other factors must be taken into account in the oceanic realm.

Critical flicker fusion and bioluminescence

Although the crustaceans in this study share the same light regime as nocturnal insects with respect to background illumination, many of their prey are bioluminescent. Bioluminescence, which is very rare in the terrestrial environment, is an extremely common phenomenon in the oceanic realm. In the mesopelagic zone (200–900 m), luminescence has been found in up to 75% of the fish species (Herring and Morin, 1978) and 79% of the shrimp species (Herring, 1976). Nocturnal terrestrial insects must image dark objects against a dimly lit background, so a higher temporal resolution, with the resulting decrease in contrast sensitivity, would be a considerable disadvantage. In the ocean, it might be advantageous for predatory carnivorous species to sacrifice sensitivity for the ability to more accurately track a glowing or flashing prey item.

All euphausiid species with bilobed eyes possess an extremely elongated second or third thoracic leg, some with clawlike chelae at the end, which is hypothesized to be an adaptation for active carnivorous feeding (Mauchline and Fisher, 1969). If some of these species specialized in capturing bioluminescent prey, the greater contrast between a bioluminescent prey item against a dim background *vs.* a dark prey item against a dim background would make it advantageous for these species to sacrifice sensitivity (and hence contrast detection) in return for greater temporal resolution (and hence tracking ability). This rationale would likewise explain the puzzling result that *Stylocheiron maximum*, which is also a bilobed euphausiid with an elongated thoracic appendage, has the shallowest depth distribution of the three euphausiid species but also the lowest maximum CFF (Fig. 3). *S. maximum* eats primarily copepods in the genera *Oithona*, which is nonluminescent, and *Oncaea*, of which only one species is known to be bioluminescent (see Herring, 1985, for review), and this bioluminescent species is not present in the Gulf of Mexico (Kinsey and Hopkins, 1994). Since the biomass and species distribution off Cuba is similar to that of the Gulf of Mexico, it is likely that *S. maximum* is eating primarily nonbioluminescent prey in Cuban waters as well. On the other hand, the primary prey item of *N. sexspinosus* and *N. flexipes*, the two species with the highest critical flicker fusion frequencies, is an active bioluminescent copepod called *Pleuromamma* (Hu, 1978; Kinsey and Hopkins, 1994), all species of which emit some form of bioluminescent spew (see Herring, 1985, for review). To further support the argument that this visual adaptation is driven by bioluminescence, the *Nematobrachion* species, as mentioned above, have a deeper depth range than *S. maximum*, but possess a less sensitive eye, according to the log I_{10} values (Table II). Following Autrum's hypothesis, one would predict that the organism from the dimmer light regime would have the more sensitive eye with slower response dynamics (assuming similar activity levels). However, because the *Nematobrachion* species are specializing in bioluminescent prey, the advantages of a higher temporal resolution might outweigh the advantages of a more sensitive eye.

Other species, however, might benefit from having an eye with lower temporal resolution. If the preferred bioluminescent prey were a slow moving item that glowed, such as some species of gelatinous zooplankton, or marine snow colonized by bioluminescent bacteria, an eye with a lower temporal resolution—assuming this meant a longer integration time (see below)—would actually be advantageous. This benefit would only apply to a dim "slow" signal, such as a glow or a flash with a slow rise time; a brief dim flash with a rapid rise time would be equally difficult to detect by either slow or fast photoreceptors (for a comprehensive discussion of frequency coding, see Laughlin, 1981; Laughlin and Weckström, 1993).

As stated above, the advantage of possessing an eye with a lower flicker fusion frequency depends on the assumption that a lower CFF is correlated with a longer integration time. The integration times of the eyes of the species in this study have not been measured, but de Souza and Ventura (1989) found that critical duration, another temporal characteristic of a photoreceptor that is determined electrophysiologically, is directly related to integration time, so that a long critical duration indicates a long integration time. Since the maximum CFF can be equated to the reciprocal of the critical duration (Matin, 1968), the low CFFs of most of the crustaceans in this study (the *Nematobrachion* species being the exception) indicate that they possess photoreceptors with fairly long integration times, and therefore might be well adapted for detecting dim, glowing bioluminescence. The conclusion that eyes with lower CFFs have slower response dynamics is supported by the latency data, in that the eyes with lower maximum CFFs also have longer response latencies (Table II).

In conclusion, it appears that while the mesopelagic light environment is similar to that of nocturnal insects with respect to background light, the temporal resolutions of several species found in this environment are substantially higher than would have been predicted on the basis of background light alone. In addition, the hypothesis that temporal resolution would be correlated with daytime depth distribution is not supported by these data. However, this preliminary study indicates that when bioluminescence is taken into account, Autrum's hypothesis that the response dynamics of the retina match the habitat and lifestyle of the organism appears to be valid in the oceanic realm as well as in the terrestrial environment.

Acknowledgments

I thank Discovery Channel for allowing me to participate on their expedition off the coast of Cuba, and the captain and crew of the RV *Seward Johnson* for their great assistance with animal collection. I also thank Dr. Simon Laughlin for his valuable advice, and Dr. Edith Widder, Dr. Sönke Johnsen, and Ms. Erin Fisher for their helpful comments on the manuscript. Additional funding for this work was provided by NSF Grant No. #OCE-9313972 to T. M. Frank and E. A. Widder. Harbor Branch Oceanographic Institution Contribution #1270.

Literature Cited

Autrum, H. 1950. Die Belichtungspotentiale und das Sehen der Insekten (Untersuchungen an *Calliphora* und *Dixippus*). *Z. Vergleich. Physiol.* **32:** 176–227.

Autrum, H. 1958. Electrophysiological analysis of the visual systems in insects. *Exp. Cell Res.* **5:** 426–439.

Autrum, H. 1984. Comparative physiology of invertebrates: Hearing and vision. Pages 1–19 in *Foundations of Sensory Science. Vol 1*, W. W. Dawson and J. M. Enoch, eds. Springer-Verlag, Berlin.

Autrum, H., and M. Stöcker. 1952. Über optische Verschmelzungsfrequenzen und stroboskopisches Sehen bei Insekten. *Biol. Zentr.* **71:** 129–152.

Bröcker, H. 1935. Untersuchungen über das Sehvermögen der Einsiedlerkrebse. *Zool. Jahrb. Abt. Allgem. Zool. Physiol. Tiere* **55:** 399–430.

Chun, C. 1896. Atlantis: Biologische Studien über pelagische Organismen. *Zoologica* **7:** 1–260.

Cronin, T. W. 1986. Photoreception in marine invertebrates. *Am. Zool.* **26:** 403–415.

Crozier, W. J., and E. Wolf. 1939. The flicker response contour for the crayfish. *J. Gen. Physiol.* **23:** 1–10.

Crozier, W. J., E. Wolf, and G. Zerrahn-Wolf. 1939. The flicker response contour for the isopod *Asellus*. *J. Gen. Physiol.* **22:** 451–462.

de Souza, J. M., and D. F. Ventura. 1989. Comparative study of temporal summation and response form in hymenopteran photoreceptors. *J. Comp. Physiol.* **165:** 237–245.

Flock, M. E., and T. L. Hopkins. 1992. Species composition, vertical distribution, and food habits of the sergestid shrimp assemblage in the eastern Gulf of Mexico. *J. Crust. Biol.* **12:** 210–223.

Frank, T. M., and J. F. Case. 1988a. Visual spectral sensitivities of bioluminescent deep-sea crustaceans. *Biol. Bull.* **175:** 261–273.

Frank, T. M., and J. F. Case. 1988b. Visual spectral sensitivities of the bioluminescent deep-sea mysid, *Gnathophausia ingens*. *Biol. Bull.* **175:** 274–284.

Galen, E., P. M. J. Shelton, and P. J. Herring. 1992. Regional morphological variations in the compound eyes of certain mesopelagic shrimps in relation to their habitat. *J. Mar. Biol. Ass. UK* **72:** 61–75.

Hallberg, E., and R. Elofsson. 1989. Construction of the pigment shelf of the crustacean compound eye: A review. *J. Crust. Biol.* **9:** 359–372.

Herring, P. J. 1976. Bioluminescence in decapod crustacea. *J. Mar. Biol. Ass. UK* **56:** 1029–1047.

Herring, P. J. 1985. Bioluminescence in the Crustacea. *J. Crust. Biol.* **5:** 557–573.

Herring, P. J., and J. G. Morin. 1978. Bioluminescence in fishes. Pp. 273–239 in *Bioluminescence in Action*, P. J. Herring, ed. Academic Press, New York.

Herring, P. J., and H. S. J. Roe. 1988. The photoecology of pelagic oceanic decapods. *Symp. Zool. Soc. Lond.* **59:** 263–290.

Hopkins, T. L., J. V. Gartner, and M. E. Flock. 1989. The caridean shrimp (Decapoda: Natantia) assemblage in the mesopelagic zone of the eastern Gulf of Mexico. *Bull. Mar. Sci.* **45:** 1–14.

Hopkins, T. L., M. E. Flock, J. V. Gartner, Jr., and J. J. Torres. 1994. Structure and trophic ecology of a low latitude midwater decapod and mysid assemblage. *Mar. Ecol. Prog. Ser.* **109:** 143–156.

Howard, J., A. Dubs, and R. Payne. 1984. The dynamics of phototransduction in insects. A comparative study. *J. Comp. Physiol.* **154A:** 707–718.

Hu, V. J. H. 1978. Relationships between vertical migration and diet in four species of euphausiids. *Limnol. Oceanog.* **23:** 296–306.

Jerlov, N. G. 1976. *Marine Optics.* Elsevier, Amsterdam.

Kampa, E. M. 1965. The euphausiid eye—a re-evaluation. *Vision Res.* **5:** 475–481.

Kinsey, S. T., and T. L. Hopkins. 1994. Trophic strategies of euphausiids in a low-latitude system. *Mar. Biol.* **118:** 651–661.

Kugel, M. 1977. The time course of the electroretinogram of compound eyes in insects and its dependence on special recording conditions. *J. Exp. Biol.* **71:** 1–6.

Land, M. F. 1976. Superposition images are formed by reflection in the eyes of some oceanic decapod crustacea. *Nature* **263:** 764–765.

Land, M. F. 1981. Optics and vision in invertebrates. Pp. 471–592 in *Handbook of Sensory Physiology, Vol VII/6B,* H. Autrum, ed. Springer-Verlag, Berlin.

Land, M. F. 1990. Optics of the eyes of marine animals. Pp. 149–166 in *Light and Life in the Sea,* P. J. Herring, A. K. Campbell, M. Whitfield, and M. Maddock, eds. Cambridge Univ. Press, Cambridge.

Land, M. F., F. A. Burton, and V. B. Meyer-Rochow. 1979. The optical geometry of euphausiid eyes. *J. Comp. Physiol.* **130:** 49–62.

Laughlin, S. B. 1981. Neural principles in the peripheral visual systems of invertebrates. Pages 133–280 in *Handbook of Sensory Physiology. Vol. VII/6B,* H. Autrum, ed. Springer-Verlag, Berlin.

Laughlin, S. B. 1990. Invertebrate vision at low luminances. Pp. 223–250 in *Night Vision,* R. F. Hess, L. T. Sharpe, and K. Nordby, eds. Cambridge Univ. Press, Cambridge.

Laughlin, S. B., and M. Weckstrom. 1993. Fast and slow photoreceptors—a comparative study of the functional diversity of coding and conductances in the Diptera. *J. Comp. Physiol.* **172:** 593–609.

Loew, E. R. 1976. Light and photoreceptor degeneration in the Norway lobster, *Nephrops norvegicus (L.). Proc. Roy. Soc. Lond.* **193B:** 31–44.

Matin, L. 1968. Critical duration, the differential luminance threshold, critical flicker frequency and visual adaptation: a theoretical treatment. *J. Opt. Soc. Am.* **58:** 404–415.

Mauchline, J., and L. R. Fisher. 1969. The biology of euphausiids. Pages 1–454 in *Advances in Marine Biology. Vol. 7,* R. S. Russel and M. Yonge, eds. Academic Press, London.

Meyer-Rochow, V. B., and S. Walsh. 1978. The eyes of mesopelagic crustaceans. III. *Thysanopoda tricuspidata* (Euphausiacea). *Cell Tiss. Res.* **195:** 59–79.

Moeller, J. F., and J. F. Case. 1995. Temporal adaptation in visual systems of deep-sea crustaceans. *Mar. Biol.* **123:** 47–54.

Munz, F. W., and W. N. McFarland. 1973. The significance of spectral position in the rhodopsins of tropical marine fishes. *Vision Res.* **13:** 1829–1874.

Nilsson, H. L., and M. Lindström. 1983. Retinal damage and sensitivity loss of a light-sensitive crustacean compound eye (*Cirolana borealis*); electron microscopy and electrophysiology. *J. Exp. Biol.* **107:** 277–292.

Nowlin, W. D. 1971. Water masses and general circulation of the Gulf of Mexico. *Oceanol. Int.* **6:** 28–33.

Roger, C. 1978. *Bioecological Sheets on Tropical Pacific Euphausiids.* Orstom, Paris.

Srinivasan, M. V., and G. D. Bernard. 1975. The effect of motion on visual acuity of the compound eye: A theoretical analysis. *Vision Res.* **15:** 515–525.

Weckström, M., and S. B. Laughlin. 1995. Visual ecology and voltage-gated ion channels in insect photoreceptors. *Trends Neurosci.* **18:** 17–21.

Welsh, J. H., and F. A. Chace, Jr. 1937. Eyes of deep sea crustaceans. I. Acanthephyridae. *Biol. Bull.* **72:** 57–74.

Welsh, J. H., and F. A. Chace, Jr. 1938. Eyes of deep sea crustaceans. II. Sergestidae. *Biol. Bull.* **74:** 364–375.

Zimmer, C. 1956. Euphausiacea. Pages 1–286 in *Bronns Klassen des Tierreichs, Bd. 5,* H. E. Gruner, ed. Geest and Portig, Leipzig.

Reference: *Biol. Bull.* **196:** 145–152. (April 1999)

Muscle Activity in Steady Swimming Scup, *Stenotomus chrysops,* Varies With Fiber Type and Body Position

DAVID J. COUGHLIN[1] AND LAWRENCE C. ROME[2]

[1]*Science Division, Widener University, One University Place, Chester, Pennsylvania 19013; and*
[2]*University of Pennsylvania, Department of Biology, Leidy Laboratory, Philadelphia, Pennsylvania, 19104, and Coastal Research Laboratory, Woods Hole Oceanographic Institution, Woods Hole, Massachusetts 02543*

Abstract. The red and pink aerobic muscle fibers are used to power steady swimming in fishes. We examined red and pink muscle recruitment and function during swimming in scup, *Stenotomus chrysops,* through electromyography and high-speed ciné. Computer analysis of electromyograms (EMGs) allowed determination of initial speed of muscle recruitment and duty cycle and phase of muscle electromyographic activity for both fiber types. This analysis was carried out for three longitudinal positions over a range of swimming speeds. Fiber type and longitudinal position both affected swimming speed of initial recruitment. Posterior muscle is recruited at the lowest swimming speed, whereas more anterior muscle is not initially recruited until higher speeds. At more anterior positions, the initial recruitment of pink muscle occurs at a higher swimming speed than the recruitment of red muscle. The duty cycle of pink muscle EMG activity is significantly shorter than that of red muscle, reflecting a difference in the onset time of activation during each cycle of length change: pink muscle onset time follows that of red. The different patterns of usage of red and pink muscle reflect differences in their contraction kinetics. Because pink muscle generates force more rapidly than red muscle, it can be activated later in each tailbeat cycle. Pink muscle is used to augment red muscle power production at higher swimming speeds, allowing a higher aerobically based steady swimming speed than that possible by red muscle alone.

Received 26 August 1998; accepted 22 January 1999.
Email: coughlin@pop1.science.widener.edu

Introduction

Steady swimming in teleosts is powered by aerobic muscle fibers (Rome *et al.,* 1984; Bone, 1989), including the slow-twitch red muscle and the intermediate-twitch pink muscle (Coughlin and Rome, 1996). These muscle fibers are arranged in relatively thin longitudinal bands, with the pink muscle medial to the red muscle. During steady swimming, red muscle is used at the lowest swimming speeds (Rome *et al.,* 1984). Pink muscle reportedly is not recruited until intermediate swimming speeds (Johnston *et al.,* 1977). At the maximum steady swimming speed, both red and pink muscle are recruited (Coughlin and Rome, 1996).

Muscle function and power production in a steadily swimming fish have recently been detailed for scup (Rome *et al.,* 1993; Coughlin and Rome, 1996; Coughlin *et al.,* 1996). These studies have employed the workloop technique (Josephson, 1985) to examine power production by isolated muscle bundles activated using patterns of muscle length change and muscle stimulation that had been recorded *in vivo* from swimming fish. At the maximum steady swimming speed (the highest speed before white muscle recruitment), scup generate most of the power for swimming by using the aerobic muscle fibers of the posterior myotomes (Rome *et al.,* 1993; Coughlin and Rome, 1996).

Coughlin *et al.* (1996) found several differences between the contraction kinetics of red and pink muscle. First, pink muscle has faster kinetics than red muscle. In isometric contractions, the rates of activation and relaxation of pink muscle are about twice those of red muscle. These rates will influence power production by each muscle type, and therefore, they may affect how the muscle is recruited and activated in a swimming fish. During oscillatory activity such as swimming, muscle must alternately be activated and relax during each tailbeat cycle. The muscle is activated to generate force during shortening and must relax at the end of shortening to minimize the "negative" work done on the muscle to lengthen it. For most fish muscle, activation occurs during the lengthening phase, giving the muscle time to generate force so that force peaks as shortening begins. Because pink muscle activates more quickly than red muscle, the onset of pink muscle stimulation can lag behind that of red muscle during each cycle of length change, as we have previously found at maximal swimming speeds (Coughlin and Rome, 1996). This appeared to help minimize the negative work that is due to a high force level at the end of lengthening. Finally, because the offset of red and pink muscle electromyographic activity during each cycle of length change occurs at the same time, this also resulted in the EMG duty cycle of pink being less than that of red muscle at the highest aerobic swimming speed. In this study, we analyze whether these patterns of recruitment occur at submaximal steady swimming speeds as well.

Under optimized conditions of oscillatory activity and at oscillation frequencies greater than 4 Hz, pink muscle produces more mass-specific power than red muscle. However, at low frequencies of oscillation, isolated scup pink muscle shows a marked reduction in power production compared to red muscle. In workloop experiments at oscillation frequencies below 4 Hz, force levels drop rapidly in pink muscle during the shortening phase of each length change. The mechanistic reasons for this drop in force during shortening at low frequencies are not known (Coughlin *et al.*, 1996), but this observation leads to a prediction that pink muscle should not be recruited at low swimming speeds that correspond to relatively low tailbeat frequencies.

In this study, we used electromyography to record the activity of red, pink, and white muscle in swimming scup over a range of steady swimming speeds. We examined the effects of swimming speed, longitudinal position on the fish, and fiber type on muscle electromyographic activity parameters such as swimming speed of initial recruitment, relative phase of red and pink muscle activation, and duration of electromyographic activity. Also, for a limited number of swimming speeds, the phase of EMG relative to the cycle of length change could be determined. Data collected permit an analysis of how pink and red muscle are used during steady swimming in scup over a range of speeds.

Materials and Methods

Scup, collected in June 1994 at Cape Cod, Massachusetts (n = 12, length ± SD = 21.8 ± 1.4 cm), swam in a recirculating water treadmill (Rome *et al.*, 1990). Electromyograms (EMGs) were recorded from fish swimming at speeds ranging from 1.5 to 3 body lengths (BL) per second at 10°C (~30 to 60 cm s^{-1}) and from 2.5 to 4.25 BL per second at 20°C (~50–85 cm s^{-1}). These are the ranges of steady, aerobic swimming speeds exhibited by these fish. For each temperature, the fish would not reliably swim at lower speeds, and swimming at higher speeds was "unsteady," indicating anaerobic activity due to the recruitment of white muscle.

For each fish, EMGs were recorded simultaneously from red and pink muscle at one of three longitudinal positions along the fish: the ANT-1, ANT-2, and MID positions, which are defined as 28%, 40%, and 55% of the total length from the anterior tip or snout (Rome *et al.*, 1993). Recordings were not made in the POST position (70%), because this position had no distinct layer of pink muscle (Zhang *et al.*, 1996). When possible, recordings were made from two positions simultaneously (Table I). In addition, white muscle recordings were made at the ANT-2 position in all fish. The recording technique has been previously detailed (Rome *et al.*, 1990, 1992). Fish were anesthetized with tricaine methanosulfate (MS-222) at a dosage of 50 mg l^{-1}. They were maintained during the surgical procedure with regulated respiratory current pumped across their gills. A hypodermic needle was used to insert twisted wire (Teflon-coated Medwire) bipolar electrodes into the muscle. All wires were sutured at their point of entry and collectively near the back of the dorsal fin. Fish recovered quickly from anesthesia when returned to the holding tank. Fish were swum 24 h after surgery at either 10° or 20°C. Fish swum at two temperatures were allowed to adjust to a change of temperature for 48 h. Grass amplifiers filtered the electromyographic signal with a bandwidth of 10 to 3000 Hz and a 60-Hz notch filter. The placement of electrodes into either

Table I

Specimens and conditions used for electromyographic recordings of the swimming musculature of scup

Fish number	Total length (cm)	Aerobic fiber position	Temperature (°C)
2	23.1	ANT-1	20
4	21.0	ANT-2, MID	20
7	22.2	ANT-2, MID	20
8	23.2	ANT-2	20
9	20.3	ANT-1	20
10	22.0	ANT-1, ANT-2	20
11	21.1	ANT-1, MID	20
19	23.7	ANT-2, MID	10, 20
20	23.6	ANT-2, MID	10, 20
22	19.7	ANT-1, ANT-2	10, 20
24	20.5	ANT-2, MID	10
25	21.0	ANT-1, ANT-2	10

For all fish, white muscle activity was recorded at ANT-2. For each fish, the aerobic muscle fibers (red and pink) were recorded at one or two positions for one or two temperatures. For each position and fiber type, electromyographic activity was analyzed for a minimum of four tailbeat cycles.

the thin pink layer or the overlying red muscle was verified through dissection after each experiment. Also, the nature of the signal indicated that cross-talk between red and pink muscle recordings was not occurring. The pink and red muscle EMG waveforms at one position were not the same.

The EMGs from swimming fish were analyzed using custom macros in DATAPAC software. The semi-automated analysis of the EMG computer files permitted characterization of bursts of electromyographic activity. For each muscle fiber type at each longitudinal position, several variables relating to muscle activity were measured at each swimming speed. First, swimming speed of initial recruitment, or the minimum speed at which bursts of activity could be detected, was determined for each fiber type at each position. Bursts were identified by an algorithm that examined the first derivative at each point in a rectified EMG trace. For each rectified trace, a threshold was set to distinguish the slowly varying background noise from the spikes of electromyographic activity. Spikes were identified as points in the trace that exceeded this threshold, and each burst was then identified as a string of consecutive spikes.

Burst duration, or the length of each electromyographic burst, was expressed as duty cycle, the duration of muscle activity as a proportion of the period of tailbeat oscillation. The relative timing of the onset of activity in red and pink muscle in each tailbeat cycle was also analyzed. The phase difference between the times of activity onset in red and pink muscle was determined for each fish at each longitudinal position for each swimming speed. Phase difference was expressed as a proportion of the oscillation period. Positive values indicate that the activity of red muscle occurred before that of pink muscle; negative values indicate that pink muscle activity had an earlier onset.

For swimming at 2.5 and 4.0 BL s^{-1} at 20°C, patterns of muscle length change were also determined. The fish were filmed from above with high-speed ciné. The films were synchronized with the EMG traces (Rome, 1995). Body curvature and the associated muscle length change characteristics, including the amplitude and frequency of muscle oscillation, were then determined from the films (Rome *et al.*, 1992, 1993; Coughlin and Rome, 1996). For these swimming bouts, the relative phase of the electromyographic activity with respect to the muscle length change was calculated for both fiber types. Phase was defined as the timing of the electrical activity with respect to the beginning of muscle shortening (maximum length) and was determined separately for red and pink muscle as previously reported (Coughlin and Rome, 1996). The phase was expressed as a proportion of the period of tailbeat oscillation and is similar to the On-β shift reported by Jayne and Lauder (1995, 1996).

Results

As swimming speed increased, so did tailbeat frequency (Fig. 1). For swimming at both 10° and 20°C, the increase of tailbeat frequency with swimming speed is well fit by a linear regression for the range of steady swimming speeds. The swimming speed at which initial muscle recruitment occurred varied significantly with both muscle fiber type and longitudinal position (Table II). At 20°C, muscle from more posterior positions was recruited at a lower swimming speed than muscle from anterior positions. At the MID position, red muscle and pink muscle were initially recruited at the lowest steady swimming speed, 2.5 BL s^{-1} (Fig. 2). At the ANT-2 position, red muscle was also recruited at the lowest steady swimming speed, but pink muscle was not recruited until at least 3.0 BL s^{-1}, and not until 4.0 BL s^{-1} in some fish (Fig. 2). At the ANT-1 position, red muscle was initially recruited at 2.5-3.0 BL s^{-1}, whereas pink muscle was not initially recruited until an average of almost 4 BL s^{-1}. Similar trends hold for 10°C. Both red muscle and pink muscle at the MID position were initially recruited at the lowest steady swimming speed, 1.5 BL s^{-1} (Fig. 3). At the ANT-2 position red muscle was also recruited at this speed, but the swimming speed of initial recruitment for pink muscle was significantly faster (1.9 BL s^{-1}, $t = 3.67$, $P = 0.021$ with df = 4, Fig. 3). At the ANT-1 position, sample size was limited ($n = 2$). In these fish, red

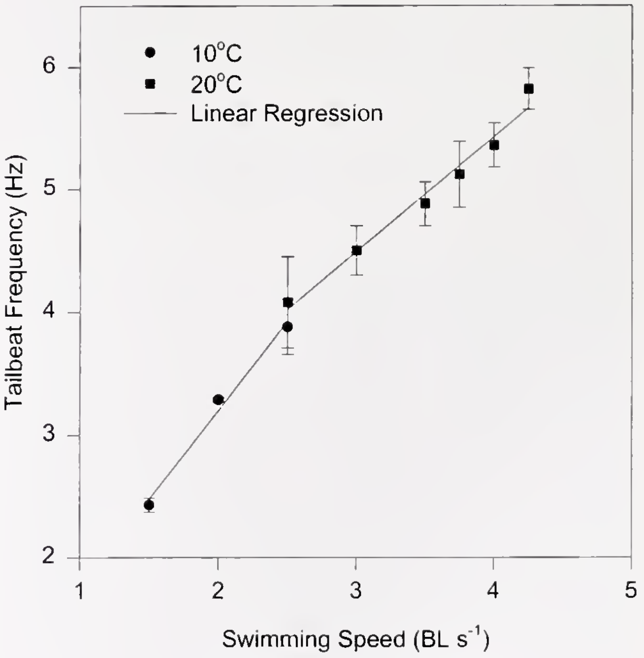

Figure 1. Tailbeat frequency as a function of swimming speed at two temperatures. The regression equations are as follows: tailbeat frequency = 0.30 + 1.45 (swim speed), $r^2 = 0.99$ and $P = 0.012$ at 10°C; and tailbeat frequency = 1.679 + 0.938 (swim speed), $r^2 = 0.97$ and $P < 0.001$ at 20°C.

Table II

Swimming speed (in body lengths per second ± SE) at which aerobic muscle in swimming scup is initially recruited varies with both fiber type and longitudinal position

Fiber type	Longitudinal Position ANT-1 ($n = 5$)	 ANT-2 ($n = 7$)	 MID ($n = 5$)	 POST ($n = 5$)
Pink	3.8 ± 0.1	3.3 ± 0.2	2.6 ± 0.1	—
Red	2.7 ± 0.1	2.5 ± 0.0	2.5 ± 0.0	2.5 ± 0.0*

Initial recruitment speeds were determined at 20°C through automated analysis of EMG bursts; the recruitment speed for a given position and fiber type is the minimum speed at which bursts were detected. Sample size (n) is given for each position. Longitudinal position ($F = 15.4$, $P < 0.001$) and fiber type ($F = 48.9$, $P < 0.001$) both had an effect on recruitment speed. There was also an interactive effect (longitudinal position × fiber type; $F = 8.3$, $P = 0.001$).

* There is no identifiable pink muscle layer at the POST position, just a scattered distribution of pink muscle fibers within the red muscle layer (Zhang *et al.*, 1996). The value given for red muscle represents unpublished data.

muscle was initially recruited at 2.0 BL s^{-1}, and pink muscle was not recruited until 2.25 BL s^{-1}. White muscle recruitment (at the ANT-2 position) was observed in all fish at a speed of 4.5 BL s^{-1} at 20°C and at a speed of 3.0 BL s^{-1} at 10°C.

The stimulation of red muscle during each tailbeat cycle occurred at the same time as or just prior to stimulation of pink muscle for most swimming conditions at 20°C (Fig. 4, Table III). Phase difference (red *vs.* pink) was positive for all three positions at 4 BL s^{-1}. This was true for the MID position at all swimming speeds. However, at lower swimming speeds, the time of electromyographic activity onset for pink and red muscle was the same for the more anterior positions; that is, the phase difference of red and pink muscle was near zero (Fig. 4). Swimming speed and longitudinal position significantly affected the onset time for red *vs.* pink muscle during each tailbeat cycle (two-way ANOVA: for swimming speed, $F = 3.484$, $P = 0.009$; for longitudinal position, $F = 3.640$, $P = 0.028$). Pink muscle and red muscle are both activated prior to the beginning of shortening during each cycle of length change (Table III). The onset time for red muscle is before that of pink muscle, as described above. The phases of red and pink muscle are closest to one another at anterior positions and at lower swimming speeds. Generally similar results were obtained for swimming at 10°C, but sample sizes were limited at that temperature.

The duty cycle of muscle activity during swimming at 20°C was affected significantly by fiber type ($F = 4.34$, $P = 0.04$; Table III). Red muscle had longer duty cycles than pink muscle. When data from the POST position are included, duty cycle was significantly affected by longitudinal position ($F = 12.571$, $P < 0.001$). This agrees with many other studies, such as Jayne and Lauder (1995) on bass, Wardle and Videler (1993) for both mackerel and saithe, and Rome *et al.* (1993) for scup red muscle.

Discussion

The recruitment and activity of aerobic swimming muscle depends on several variables: the type of muscle fiber, the longitudinal position on the fish, and the swimming speed. Pink muscle, with its faster kinetics, is used differently than red muscle. Whereas red muscle is active at most positions at all swimming speeds, pink muscle activity is restricted on the basis of both longitudinal position and swimming speed.

Swimming speed of initial recruitment and duty cycle

Fiber type affects the patterns of recruitment during swimming. Initial recruitment of pink muscle occurs at swimming speeds the same as or higher than recruitment speed of red muscle for all longitudinal positions. Pink muscle recruitment occurs at the lowest swimming speeds for the MID position only; at other positions, pink muscle is initially recruited at higher speeds than red muscle. Pink muscle is used minimally at low swimming speeds, when the tailbeat frequency and the frequency of oscillation of muscle are lowest. This correlates with the low power output of pink muscle at low oscillation frequencies.

Aerobic muscle recruitment is also affected by longitudinal position on the fish. Positions more posterior on the fish body are recruited before anterior ones, particularly for pink muscle. Although pink muscle generally is recruited at the lowest steady swimming speed at the MID position, it is not recruited until higher swimming speeds at more anterior positions. At ANT-1, pink muscle is not consistently recruited until the near-maximum steady swimming speed. The pattern is less obvious for red muscle. At the lowest steady swimming speed, red muscle was active at the POST (Rome, unpubl. data), MID, and ANT-2 positions. At ANT-1, red muscle was not always recruited at the minimum steady swimming speed. This pattern makes sense from a functional viewpoint. ANT-1 pink muscle and red muscle undergo very low strain during swimming, even when the muscle is recruited. For instance, although all aerobic muscle fibers are recruited at 4.0 BL s^{-1} in scup, red muscle strain is around ±2.0% for the ANT-1 position (Rome *et al.*, 1993), and red and pink muscle strain at the ANT-2 position is less than ±3% (Table III). At low swimming speeds, the combination of low strain and low oscillation frequency limits power production by the aerobic muscle (Coughlin and Rome, 1996). Power output of cyclically active muscle is a function of work per cycle and cycle frequency. If work per cycle is limited by very low muscle strain and if cycle frequency is low, power output will be low as well. In scup, the anterior aerobic musculature (pink

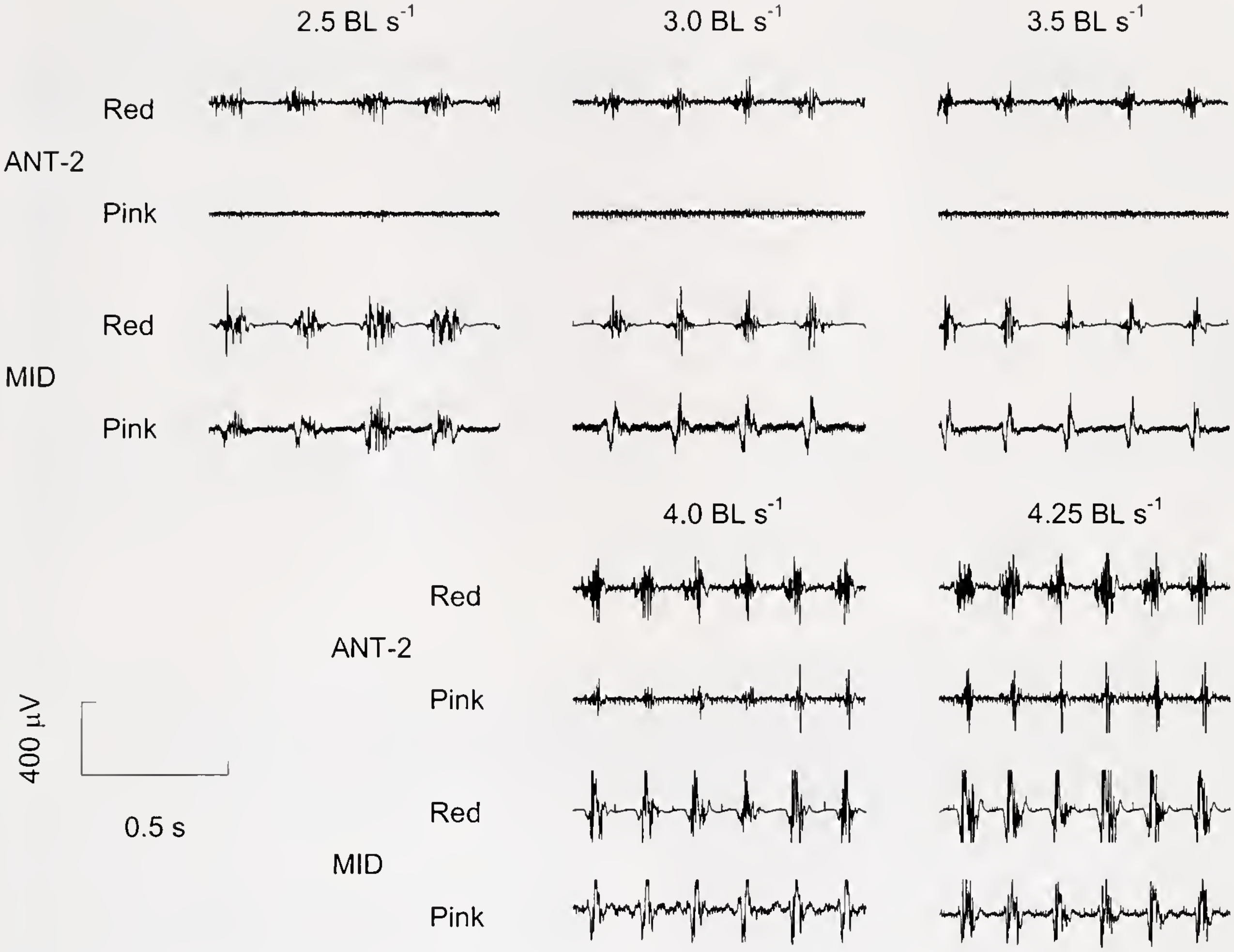

Figure 2. Electromyograms from red (R) and pink (P) muscle at the ANT-2 and MID positions for a scup swimming at 20°C. Each trace is 1.0 s long. BL = body length. In this fish, both red and pink muscle are recruited at a swimming speed of 2.5 BL s^{-1} at the MID position. Red muscle at the ANT-2 position is recruited at this speed as well, although pink muscle at the ANT-2 position is not recruited until 4.0 BL s^{-1} (as determined by computer-driven burst analysis).

and, to a lesser extent, red muscle) is not consistently recruited at low swimming speeds when power production would be low or negative.

A recent report on muscle function in swimming eels (Gillis, 1998) describes a pattern of recruitment for red muscle similar to that in scup. Posterior red muscle is recruited at the lowest steady swimming speeds, and red muscle from more anterior positions is initially recruited at higher steady swimming speeds.

The results presented here for recruitment of red, pink, and white muscle in scup agree in a general sense with the work of Johnston and colleagues. Johnston *et al.* (1977) reported that pink muscle recruitment occurs at swimming speeds intermediate between those of red and white muscle. This seems to be due to the intermediate kinetics of pink muscle relative to the slower red and the faster white muscle (Coughlin *et al.*, 1996). In scup, the initial speed of pink muscle recruitment is most clearly intermediate at the ANT-2 position (Table II). At the MID position, recruitment of red and pink muscle occurs at the same swimming speed. At the ANT-1 position, pink muscle is often not recruited until the maximum steady swimming speed, just before recruitment of white muscle. That red and pink muscle at one longitudinal position can be recruited to power swimming independently raises an interesting question about the innervation patterns of the aerobic swimming musculature.

Fiber type has a significant effect on duty cycle. For most swimming speeds and at most positions, the duty cycle of red muscle is longer than that of pink muscle. The simultaneous offset of electromyographic activity for red and pink fibers in scup holds true across the range of swimming speeds reported here. Interestingly, the approximately simultaneous offset of all red muscle on one side of the fish has been observed in a number of fish species, such as scup

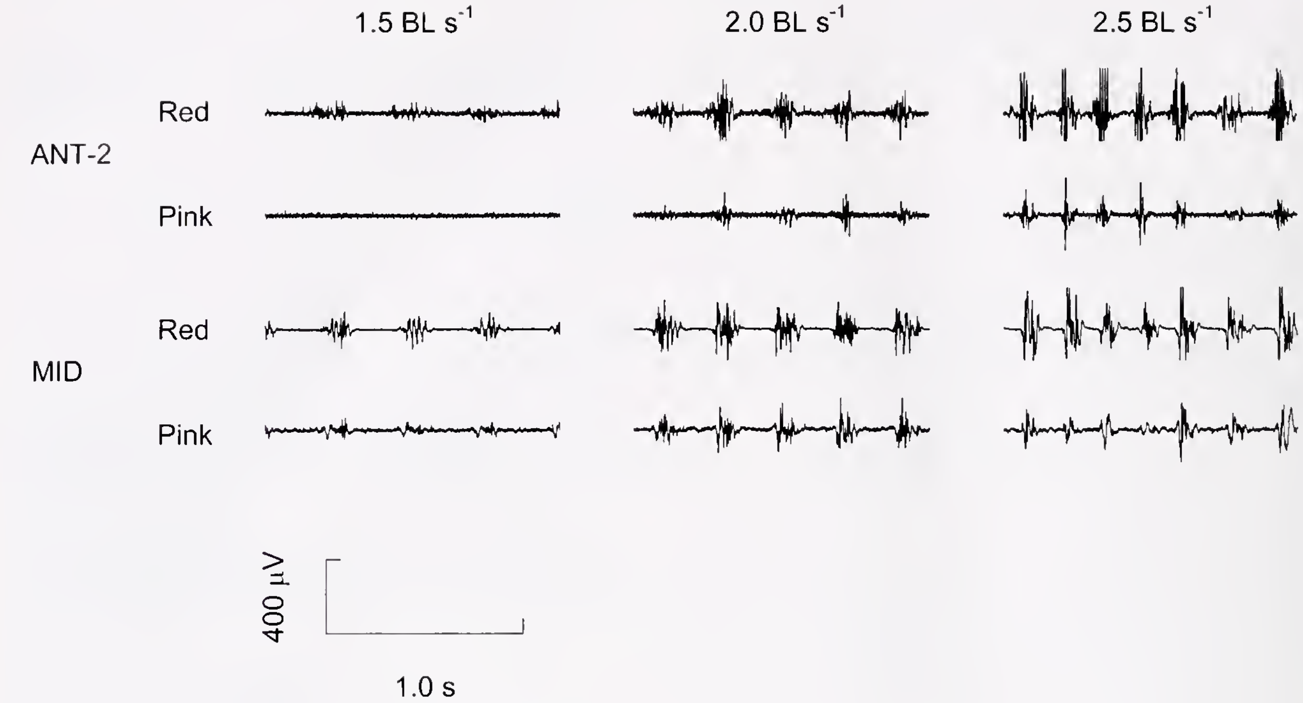

Figure 3. Electromyograms from red (R) and pink (P) muscle at the ANT-2 and MID positions for a scup swimming at 10°C. Each trace is 1.5 s long. BL = body length. In this fish, both pink and red muscle are recruited at a swimming speed of 1.5 BL s^{-1} at the MID position, although pink muscle recruitment is relatively weak. At the ANT-2 position, red muscle is weakly recruited at 1.5 BL s^{-1}, but pink muscle is not recruited until 2.0 BL s^{-1} (as determined by computer-driven burst analysis).

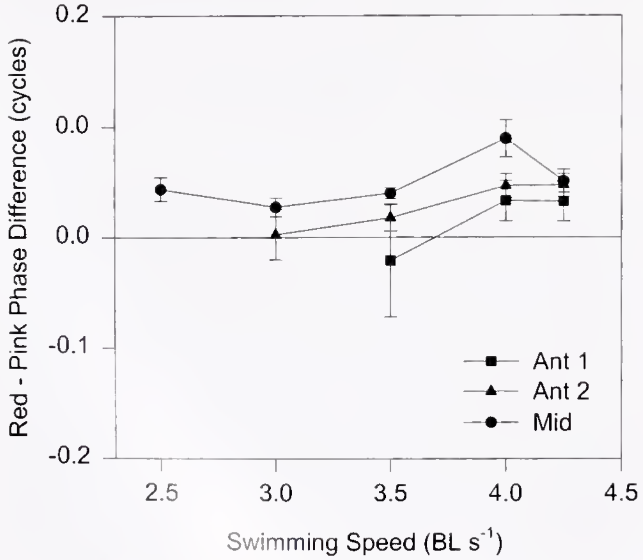

Figure 4. Phase difference of red and pink muscle for three longitudinal positions across the range of steady swimming speeds at 20°C. The difference in the timing of onset electromyographic activity in red and pink muscle during each length change cycle is expressed as a proportion of the period of one cycle. Positive values of relative phase indicated that red muscle is stimulated before pink muscle during each length change cycle.

(Rome *et al.*, 1993; Coughlin and Rome, 1996), carp (van Leeuwen *et al.*, 1990), bass (Jayne and Lauder, 1995), and mackerel and saithe (Wardle and Videler, 1993). Alternatively, more elongate fish that swim with greater body curvature do not have a simultaneous offset of the red muscle electromyographic activity. Instead, the offset of red muscle activation progresses from anterior to posterior, just as the wave of the onset of activation progresses (Wardle *et al.*, 1995; Hammond *et al.*, 1998). Not enough is known about the nervous control of swimming muscle activity to explain the variety of aerobic fiber activation patterns seen in swimming fish.

Phase of muscle activity

Both red muscle and pink muscle are activated prior to muscle shortening for most swimming conditions, such that there is a negative phase shift of electromyographic activity relative to shortening. This agrees with most previous work on red muscle in steady swimming fish such as bass (Jayne and Lauder, 1995, 1996), mackerel and saithe (Wardle and Videler, 1993), carp (van Leeuwen *et al.*, 1990; van Leeuwen, 1995), eel (Williams *et al.*, 1989; Wardle *et al.*, 1995), adult rainbow trout (Hammond *et al.*, 1998), and with previous work on scup (Rome *et al.*, 1993). All of these

Table III

Patterns of in vivo *muscle activity for scup swimming at 2.5 and 4 BL s^{-1} at 20°C with a tailbeat frequency of 4.0 and 6.0 Hz, respectively*

		2.5 BL s^{-1}		4.0 BL s^{-1}	
	Fiber type	ANT-2 (*n* = 4)	MID (*n* = 3)	ANT-2 (*n* = 9)	MID (*n* = 4)
Strain	Pink	3.69 ± 0.31	4.06 ± 0.20	2.62*	3.43*
	Red	3.6*	5.5*	2.9*	4.8*
Duty cycle	Pink	0.310 ± 0.062	0.367 ± 0.021	0.412 ± 0.021	0.331 ± 0.037
	Red	0.395 ± 0.040	0.403 ± 0.040	0.421 ± 0.016	0.391 ± 0.014
Phase	Pink	−14.5 ± 11.4 (−0.040)	−52.1 ± 26.4 (−0.145)	−14.5* (−0.040)	−17.6* (−0.049)
	Red	−16.1 ± 20.7 (−0.045)	−65.2 ± 27.7 (−0.181)	−32.7* (−0.091)	−40.8* (−0.113)

Strain is the ± percent change in muscle length during the oscillatory length change cycle. Duty cycle is the duration of the burst of electromyographic activity during each oscillatory cycle expressed as a proportion of the oscillation period. Phase is the timing of the onset of the activity burst relative to the onset of shortening, expressed in degrees (one oscillation cycle = 360°). Negative values indicate muscle activity preceding muscle shortening. For comparison, phase expressed as a proportion of the period oscillation is provided in parentheses. Data are not provided for the ANT-1 position because the data set for that position at 2.5 BL s^{-1} is not complete. Sample size (*n*) is given in parentheses at the top of each column.

* Red muscle data from Rome *et al.* (1993); pink muscle data from Coughlin and Rome (1996).

studies report results similar to those presented here—a smaller phase shift for red muscle at more anterior positions. In a few fish, such as rainbow trout smolts (Williams *et al.*, 1989) and, at some swimming speeds, bass (Johnson *et al.*, 1994; Jayne and Lauder, 1995), a positive phase of red muscle activity has been reported for anterior positions. In these fish, muscle shortening occurs prior to muscle stimulation. In general, this was not observed in scup, although for a few fish, red muscle at the ANT-1 position did have a positive phase at low swimming speeds (unpubl. data). However, technical difficulties inherent in measurements of the muscle length change at this position lead to considerable uncertainty of the phase.

For rainbow trout, at least, a positive phase shift of muscle activation results in net negative power production (Coughlin and Burdick, 1996). Anterior muscle that undergoes either a very small negative phase shift or a positive phase shift will not contribute significantly to powering swimming (Rome *et al.*, 1993; Coughlin and Rome, 1996). For this reason, Hammond *et al.* (1998) suggest that the phase data from Williams *et al.* (1989) cannot reflect red muscle activity during steady swimming in trout. However, the many species of fish that show a relatively low negative phase in the anterior red muscle probably swim similarly to scup: most of the power is generated by the posterior musculature. Curiously, the data of Gillis (1998) suggest the same may be true for eels: at low steady swimming speeds, only the posterior red muscle is recruited to power swimming; the anteriormost red muscle is not recruited until the highest steady swimming speeds. Furthermore, when it is recruited, the negative phase shift is smaller than in posterior muscle (Gillis, 1998). This small negative phase shift may limit power production by anterior eel red muscle during swimming and, therefore, be associated with the lack of recruitment of this muscle at lower swimming speeds.

No previous research has reported on the relative phase differences in the stimulation of the aerobic muscle fibers of fish during each length change cycle of swimming. During each cycle of length change, pink muscle is stimulated after red muscle consistently (Fig. 4), except in the more anterior positions at lower swimming speeds. This correlates with the faster activation kinetics of pink muscle (Coughlin *et al.*, 1996): since it activates more rapidly, its stimulation can occur nearer to the onset of muscle shortening. Otherwise, it would reach high force levels while the muscle was still lengthening and might then generate net negative work during the length change cycle. Jayne and Lauder (1994) report similar results for red and white muscle in bass swimming at high, unsteady speeds. In those fish, white muscle stimulation lagged behind red muscle stimulation at a given longitudinal position. However, the lag between red and white activation was the same for both anterior and posterior positions; this finding differs from our results. We found that the phase difference between red and pink muscle increased at the more posterior positions of steady swimming scup.

Pink muscle function in swimming fish

Pink muscle is employed effectively by swimming scup. At maximal steady swimming speeds at both 10° and 20°C, pink muscle is heavily recruited and allows fish to swim steadily at speeds greater than possible with red muscle alone. At swimming speeds at which the performance of red muscle is near maximal, pink muscle produces considerable power for swimming (Coughlin and Rome, 1996). In addition, across a range of swimming speeds, the activation patterns of pink muscle (*i.e.* the delayed onset of activation) are well timed to take advantage of this muscle's faster rate of activation. At submaximal swimming speeds, the pink muscle at anterior body positions is a relatively ineffective source of power, and its recruitment is correspondingly limited.

Acknowledgments

We thank D. Leavitt, B. Lancaster, and B. Tripp and the rest of the staff of the Coastal Research Center at the Woods Hole Oceanographic Institution for facilitating our work. We thank Linh Nguyen for laboratory assistance. This work was supported by NIH AR38404 and NSF IBN-9514383 to LCR and by an NIH postdoctoral fellowship to DJC.

Literature Cited

Bone, Q. 1989. Evolutionary patterns of axial muscle systems in some invertebrates and fish. *Am. Zool.* **29:** 5–18.

Coughlin, D. J., and J. W. Burdick. 1996. Muscle mechanics and power production in swimming rainbow trout, *Oncorhynchus mykiss*. *Am. Zool.* **36:** 61A.

Coughlin, D. J., and L. C. Rome. 1996. The roles of pink and red muscle in powering steady swimming in scup, *Stenotomus chrysops*. *Am. Zool.* **36:** 666–677.

Coughlin, D. J., G. Zhang, and L. C. Rome. 1996. Contraction dynamics and power production of pink muscle of scup (*Stenotomus chrysops*). *J. Exp. Biol.* **199:** 2703–2712.

Gillis, G. B. 1998. Neuromuscular control of anguilliform locomotion: patterns of red and white muscle activity during swimming in the American eel *Anguilla rostrata*. *J. Exp. Biol.* **201:** 3245–3256.

Hammond, L., J. D. Altringham, and C. S. Wardle. 1998. Myotomal slow muscle function of rainbow trout, *Oncorhynchus mykiss* during steady swimming. *J. Exp. Biol.* **201:** 1659–1671.

Jayne, B. C., and G. V. Lauder. 1994. How swimming fish use slow and fast muscle fibers: implications for models of vertebrate muscle recruitment. *J. Comp. Physiol. A* **175:** 123–131.

Jayne, B. C., and G. V. Lauder. 1995. Red muscle motor patterns during steady swimming in largemouth bass: effects of speed and correlation with axial kinematics. *J. Exp. Biol.* **198:** 657–670.

Jayne, B. C., and G. V. Lauder. 1996. New data on axial locomotion in fishes: how speed affects diversity of kinematics and motor patterns. *Am. Zool.* **36:** 642–655.

Johnson, T. P., D. A. Syme, B. C. Jayne, G. V. Lauder, and A. F. Bennett. 1994. Modeling red muscle power output during steady and unsteady swimming in largemouth bass. *Am. J. Physiol.* **267:** R481–R488.

Johnston, I. A., W. Davison, and G. Goldspink. 1977. Energy metabolism of carp swimming muscles. *J. Comp. Physiol.* **114:** 203–216.

Josephson, R. K. 1985. Mechanical power output from striated muscle during cyclical contraction. *J. Exp. Biol.* **114:** 493–512.

Rome, L. C. 1995. A device for synchronizing biomechanical data to ciné film. *J. Biomech.* **28:** 333–338.

Rome, L. C., P. T. Loughna, and G. Goldspink. 1984. Muscle fiber recruitment as a function of swim speed and muscle temperature in carp. *Am. J. Physiol.* **247:** R272–R270.

Rome, L. C., R. P. Funke, and R. M. Alexander. 1990. The influence of temperature on muscle velocity and sustained performance in swimming carp. *J. Exp. Biol.* **154:** 163–178.

Rome, L. C., I. Choi, G. Lutz, and A. A. Sosnicki. 1992. The influence of temperature on muscle function in fast swimming scup. I. Shortening velocity and muscle recruitment during swimming. *J. Exp. Biol.* **163:** 259–274.

Rome, L. C., D. Swank, and D. Corda. 1993. How fish power swimming. *Science* **261:** 340–343.

van Leeuwen, J. L. 1995. The action of muscles in swimming fish. *Exp. Physiol.* **80:** 177–191.

van Leeuwen, J. L., M. J. M. Lankheet, H. A. Akster, and J. W. M. Osse. 1990. Function of red axial muscles of carp (*Cyprinus carpio*): recruitment and normalized power output during swimming in different modes. *J. Zool. (Lond.)* **220:** 123–145.

Wardle, C. S., and J. J. Videler. 1993. The timing of the electromyogram in the lateral myotomes of mackerel and saithe at different swimming speeds. *J. Fish Biol.* **42:** 347–359.

Wardle, C. S., J. J. Videler, and J. D. Altringham. 1995. Tuning in to fish swimming waves: body form, swimming mode and muscle function. *J. Exp. Biol.* **198:** 1629–1636.

Williams, T. L., S. Grillner, V. V. Smoljaninov, P. Wallen, S. Kashin, and S. Rossignol. 1989. Locomotion in lamprey and trout: relative timing of activation and movement. *J. Exp. Biol.* **143:** 559–566.

Zhang, G., D. M. Swank, and L. C. Rome. 1996. Quantitative distribution of muscle fiber types in the scup. *J. Morph.* **229:** 71–81.

Reference: *Biol. Bull.* **196:** 153–162. (April 1999)

Osmoregulation and FMRFamide-Related Peptides in the Salt Marsh Snail *Melampus bidentatus* (Say) (Mollusca: Pulmonata)

HAMID R. KHAN[1,*], DAVID A. PRICE[2], KAREN E. DOBLE[2], MICHAEL J. GREENBERG[2], AND A.S.M. SALEUDDIN[1]

[1]*Department of Biology, York University, Toronto, Ontario, Canada M3J 1P3; and*
[2]*Whitney Laboratory, University of Florida, St. Augustine, Florida 32086*

Abstract. The pulmonate snail *Melampus bidentatus* occupies the high intertidal zone of salt marshes in a nearly terrestrial environment. The hemolymph osmolarity of the snails collected in the field paralleled that of the adjacent water and was affected by the tides and precipitation. The snails initially gained or lost weight when submerged in hypo- or hyperosmotic media, respectively, but returned to their original weight after 24 h. The content of their immunoreactive (IR)-*F*MRF*a*mide-*R*elated *P*eptide*s* (FaRPs) was measured in various tissues by radioimmunoassay, and IR-FaRPs were found in every tissue analyzed. The subesophageal part of the central nervous system (CNS) contained more IR-FaRPs than the supraesophageal part, and the kidney and the tissues of the reproductive tract contained more than other peripheral tissues. The levels of IR-FaRPs in the CNS, kidney, and hemolymph were higher in snails that were immersed in higher concentrations of seawater. Many IR neurons are present in all ganglia of the CNS except the pleural ganglia, and IR neurites are extensively distributed within the CNS and its connective tissue sheath. The visceral nerve from the visceral ganglion is immunoreactive and could be seen to innervate the kidney, which contains IR-varicosities. An osmoregulatory role for the FaRPs is suggested.

Introduction

Melampus bidentatus is a common amphibious pulmonate snail. Its habitat is the high intertidal zone of salt marshes, and it ranges from Nova Scotia, Canada, to the coast of the Gulf of Mexico in Texas (Apley, 1970; Hilbish, 1981). *Melampus* belongs to the primitive family Ellobiidae and is believed to be related to an ancestral marine strain that colonized the intertidal habitat, giving rise to the land snails and then to the freshwater snails (Morton, 1955; Russell-Hunter, 1978). Environmental factors such as temperature, salinity, and tides are extremely variable in the high littoral habitat. But the adult snails are adapted to this variation, and can survive for several days at temperature extremes of −12°C to 40°C, submergence in 25%–100% seawater, and desiccation at 0% relative humidity for 27–36 h (Price, 1980; McMahon and Russell-Hunter, 1981). Although adults of *M. bidentatus* can endure a terrestrial life, its planktonic veliger larvae are restricted to the aquatic habitat of estuaries (Russell-Hunter *et al.*, 1972).

The natural history of *M. bidentatus* suggests that in estuarine and semiterrestrial molluscs, osmotic and volume regulation must be particularly responsive. Moreover, scattered evidence suggests that the family of neuropeptides related to FMRFamide is involved in this regulation. First, in a freshwater pulmonate snail, *Helisoma duryi*, FMRFamide causes water retention in the kidney *in vitro* (Saleuddin *et al.*, 1992). Further, the level of immunoreactive, FMRFamide-related peptides (IR-FaRPs) in the kidney of *Helisoma trivolvis* kept in hypoosmotic medium is lower than that in the kidneys of snails kept in isosmotic medium (Madrid *et al.*, 1994). The IR-FaRPs have also been localized in the kidneys of the terrestrial pulmonate snail *Helix*

Received 7 January 1998; accepted 27 January 1999.

* To whom correspondence should be addressed. E-mail: hamid@turing.sci.yorku.ca

Abbreviations: One-letter abbreviations of the amino acids are used to state the peptide sequences. ASW, artificial seawater; BSA, bovine serum albumin; CNS, central nervous system; FaRPs, *F*MRF*a*mide-*r*elated *p*eptide*s*; IM, incubation medium; IR, immunoreactive; NGS, normal goat serum; PBS, phosphate-buffered saline; RIA, radioimmunoassay.

aspersa (Lehman and Price, 1987), and in the central nervous system (CNS) of the veligers of *M. bidentatus* (Moffett, 1992). Finally, the regulation of hypoosmotic cell volume by cardiac muscles of the clam *Mercenaria mercenaria* is potentiated by FMRFamide (Deaton, 1990).

Since *M. bidentatus* inhabits highly variable osmotic conditions, it is an appropriate species with which to further test the proposal that the FaRPs have a role in osmoregulation. In this paper, we have studied, both in the field and the laboratory, the influence of the ambient osmotic concentration on that of the hemolymph. We have then compared the levels of IR-FaRPs in the CNS, hemolymph, and kidney of snails maintained in media of different osmotic concentrations. We also report IR-FaRP-staining of neurites in the kidney, and of neurons in the CNS of adult snails.

Materials and Methods

Animals and media

During January to April, *M. bidentatus* adults (shell lengths, 10.0 ± 2.0 mm) were collected at random from an area 100 m × 20 m in a salt marsh on the Matanzas river estuary near Crescent Beach, Florida (29°40′ N : 81°13′ W). Experiments with the freshly collected snails were performed nearby, at the Whitney Laboratory of the University of Florida. At York University, the animals were maintained at 22°C, 95% relative humidity, and a photoperiod of 14 h light to 10 h dark, in glass tanks (30 cm L × 15 cm W × 20 cm H) covered with nylon screens. The floor of each tank was covered with a layer of crushed oyster shells (poultry feed) graded in thickness from 0.5 cm at one end of the tank to 3.0 cm at the other. A volume of 50% artificial seawater (ASW; Instant Ocean, Aquarium Systems, Ohio) was added to cover about one-third of the crushed oyster shells. Slanted against the walls of each tank were 4–6 broken, irregularly shaped pieces of clay plant-pot (about 10 cm in diameter). Most snails crawled to terrestrial conditions above the water level on the walls of the tank and on the dark side of the moist pieces of clay plant-pot. Distilled water was added daily to maintain osmolarity and water level, and the snails were fed fish-food and boiled lettuce *ad libitem*. The snails were acclimated to laboratory conditions for at least 2 weeks before experimentation.

The kidney is embedded just under the dorsal surface of the mantle tissue, and the CNS is located under the skin, between the tentacles. Before dissection, the snails were chilled on ice for 5–10 min, which reduced their movements and mucus secretion; no other anesthetic was used. Deshelled snails were pinned on a dish lined with Sylgard (Dow Corning, Canada) and dissected in filtered isosmotic ASW. We adjusted the osmolarity of the ASW with distilled water to be isosmotic with that of the hemolymph, which varies with the medium or relative humidity (described later). The kidney and CNS were removed from a snail within 3–5 min, and were used for FaRP studies.

Osmotic conditions

Snails that had been maintained under terrestrial conditions (described above) were submerged for various periods (maximum, 4 days; minimum 3 h) in 10%, 50%, or 100% ASW (dilutions made with distilled water) in 250-ml plastic containers, each with a nylon screen. The levels of IR-FaRPs were measured (described later) after 24 h of osmotic treatments. Hemolymph was collected as follows. The snails were pricked in the head area with a sharp needle. Each animal was then quickly placed in a 0.5-ml polypropylene microcentrifuge tube with a hole in its bottom. This tube was then placed in a larger (1.5 ml) polypropylene microcentrifuge tube. The nested tubes and the snail were spun at 500 × *g* for 2–5 s. Then the inner tube containing the snail was removed, and the outer tube containing the hemolymph was spun for an additional 5 min. About 30–50 μl of hemolymph could be collected from each snail. The osmotic pressures of 10-μl samples were measured in a Wescor Model 5300 vapor pressure osmometer (Logan, Utah). After the bleeding, all of the snails fed and lived for many days thereafter. To measure the effects of osmotic water exchange on weight, the snails were weighed with a Mettler AE163 balance after the visible water and mucus had been removed from their shells and feet with adsorbent tissue.

Radioimmunoassay

Pulmonate molluscs contain two major classes of FaRPs: the tetra-FaRPs (FMRFamide and FLRFamide) and the hepta-FaRPs (XDP[F/Y]LRFamide, where the N-terminal residue X is pQ, S, N, or G). The hepta-FaRP analog with the glycyl residue occurs only in snails of the subclass Basommatophora (like *M. bidentatus*), and these animals lack the analog with the pyroglutamic acid (pQ) residue, which occurs only in stylommatophorans (Price *et al.*, 1987a, b). To ensure that all of the FaRPs would be detected, we used S253 antiserum in the radioimmunoassay (RIA). The antiserum was raised to thyroglobulin-peptide (synthetic analog YGGFMRFamide) conjugate in a rabbit. It has high affinities for both FMRFamide and GDPFLRFamide, and was used in the assays at a dilution of 1:10,000. Iodinated pQYPFLRFamide was used as tracer (for details see: Price *et al.*, 1990; Lesser and Greenberg, 1993).

The protocol of Madrid *et al.* (1994) was followed in processing the tissues. After dissection, each tissue sample was placed in a plastic tube (1.5 ml) containing HPLC grade acetone (1 part tissue: 4 parts acetone) and frozen immediately at −80°C for at least 24 h. The acetone extracts were spun for 5 min at 5,000 × *g*, and the supernatants were collected and then dried in a Speed-Vac centrifuge. Each pellet was dissolved in 100 μl RIA buffer [0.01 *M* sodium phosphate with 1% bovine serum albumin (BSA), 0.9% sodium chloride, 0.01% merthiolate, and 0.025 *M* sodium EDTA]. Aliquots of 10 μl were placed in glass tubes to which 100 μl tracer (10,000 cpm) (in RIA buffer) and 100 μl diluted antiserum (in RIA buffer) were added. The tubes were stored at 4°C overnight; on the following morning, 1.0 ml charcoal suspension (0.25% charcoal, 0.025% dextran, 0.01% merthiolate in 0.1 *M* sodium phosphate, pH 7.5) was added to each tube. After 10 min, the mixture was centrifuged at 2500 × *g* for 15 min at 4°C, and the supernatant was counted in an LKB MiniGamma counter. All statistical comparisons were made with a one-way analysis of variance (ANOVA); when the ANOVA showed a significant difference, the effect was followed with the Bonferroni multiple comparison post test using a statistical software package (InStat, GraphPad Software, San Diego, California).

Immunocytochemistry

Isolated CNS and kidney tissues from animals in laboratory terrestrial condition were either embedded in paraffin and sectioned, or examined in whole mount. Sections were prepared as follows. The tissues were fixed for 12–18 h in modified Bouin-Hollande [7% picric acid, 2.5% copper acetate, 2% formaldehyde (freshly prepared from paraformaldehyde), and 1.5% glacial acetic acid, in phosphate-buffered saline (PBS) (0.2 *M* NaCl, 0.003 *M* KCl, 0.002 *M* KH_2PO_4, 0.02 *M* Na_2HPO_4, 0.001 *M* $CaCl_2$, 0.001 *M* $MgCl_2$, pH 7.5)], then dehydrated in graded ethanol solutions and embedded in paraffin. Serial sections (10 μm) were cut and mounted on coverslips (22 mm × 22 mm) coated with 0.5% gelatin, 0.5% chrome alum, and 0.01% formaldehyde. The deparaffinized sections were treated with 100% methanol and 0.1% H_2O_2 for 5 min, hydrated in a graded series of ethanol solutions, kept 30 min in an incubation medium (IM) consisting of PBS containing 2% Triton × 100 (Sigma Chem., St. Louis, MO), 5% normal goat serum (NGS), and 1% BSA. The sections were incubated for 1 h at 22°C with hepta-FaRP-specific CK antiserum, which was raised in a rabbit to the peptide CKQDPFLRFGK (a gift from Dr. G.A. Cottrell, University of St. Andrews, Scotland) (Cottrell *et al.*, 1994). The primary antiserum was diluted 1:200 in IM. After many rinses in IM for 10 min, the sections were incubated for 1 h at 22°C in fluorescein-conjugated goat antirabbit-serum (Sigma) diluted 1:80 in IM (secondary antibody). The coverslips were rinsed well in PBS and mounted on glass slides in 5% polyvinyl alcohol, 30% glycerol, and 0.1% phenylenediamine in PBS (mounting medium).

Whole mounts were prepared as follows. The tissues were treated with proteases before and after fixation (Longley and Longley, 1986). The tissues were first treated in 0.05% pronase in isosmotic saline for 10 min, then fixed in Bouin-Hollande (see above) for 12 h. After fixation, the tissues were rinsed in saline for 10 min, then treated in 0.1% trypsin in saline for 30 min, and rinsed well in saline for 10 min. A preincubation in IM for 6–12 h at 4°C was followed by incubation in primary antibody (hepta-FaRP-specific CK antiserum; 1:200 in IM) for 24 h. After rinsing several times in 1% Triton X 100 in PBS for 1 h, the tissues were incubated in secondary antibody (1:80 in IM) for 6 h, followed by repeated rinses in IM. When whole-mount tissues were incubated for more than 60 min, this was done in the dark at 4°C. The tissues were mounted in mounting medium (see above) between two coverslips (one rectangular, 60 mm × 22 mm; and one circular, 18 mm). To prevent tissue distortion, the weight of the coverslip was supported by four pieces of broken coverslip (~0.5 mm diameter). The larger coverslip was affixed with adhesive tape on an aluminum slide (36 mm × 80 mm × 1 mm) with a central 25-mm circular window. The smaller circular coverslip was placed face down in this window, so these preparations could be flipped for viewing from either side.

For controls, either pre-immune rabbit serum (1: 200 in IM) or IM alone was used in the primary incubation; in either case, the tissues were then stained with secondary antibody as described above. The controls showed no staining. The specimens were viewed and photographed with either a Leitz epifluorescence microscope or a Bio-Rad MRC 600 confocal microscope. The IR-FaRP cells were mapped from the serial sections and from whole-mount images, and were measured with the calibration marker from the confocal images.

Results

Osmoregulation

The high-tide location of the marsh where *M. bidentatus* was collected has an uneven surface with a shallow slope, and contains abundant decaying organic matter of plant and animal origin. The osmolarity and pH of the waters in the habitat varied with time and location in the observation area. During the sunny days of April, the average osmolarities were 1200 ± 26 mosm/kg H_2O (mean ± standard error of mean, $n = 50$) (range = 1015–1650 mosm/kg H_2O), and the pH ranged from 6.0–7.2; at 1200–1400 h, the ambient air temperature was 31 ± 4°C, and the soil surface and water temperatures were 34.2 ± 1.3°C. At the same time, the tidal seawater coming through the Matanzas inlet had a consistent osmolarity of 980 ± 5 mosm/kg H_2O, a temperature of 22 ± 2°C, and a pH of 7.5 ± 0.1. The variables that altered the osmolarities of the water in the habitat and hemolymph of snails were tide, temperature, and precipitation. Most snails in the field were out of the water, on grass stems or higher points of the uneven ground, while a much smaller number were creeping and feeding underwater. The osmolarities of the hemolymph of snails from different locations and conditions and during high and low tides were measured within 30 min after collection and compared with the osmolarities of the adjacent media. The hemolymph osmolarities ranged from 1100 to 1500 mosm/kg H_2O and appeared to parallel that of the adjacent medium. A few hours of heavy rainfall reduced the osmolarity of the water in the habitat to 750 ± 40 mosm/kg H_2O; the hemolymph osmolarities also declined to 850 ± 50 mosm/kg H_2O. Most snails in the laboratory crawled to the dry parts of the tank (see methods section) and stayed away from the water; thus they sought terrestrial conditions. But a few snails were also seen feeding and crawling underwater. The hemolymph osmolarity of the laboratory snails that sought terrestrial conditions was much lower (450 ± 25 mosm/kg H_2O) than that of field snails (1200 ± 100 mosm/kg H_2O) collected away from the water. When laboratory snails from terrestrial conditions were held for 24 h in 10% or 50% ASW, the osmolarity of the hemolymph paralleled, and was about 150 mosm/kg H_2O hyperosmotic to, that of the medium. Snails in 10% and 50% ASW gained weight during the first 3–6 h, but over 24 h, gradually returned towards their original weight. In contrast, snails kept in 100% ASW for 24 h first lost weight and then returned towards their original weight (Fig. 1).

Table I.

Immunoreactive FaRP content detected by S253 antiserum in various tissues of animals from terrestrial condition in laboratory

Tissue	IR-FaRP content (picomol)
Buccal ganglia*	1.2 ± 0.40a
Cerebral ganglia*	4.0 ± 0.70a
Pedal ganglia*	19.1 ± 7.0 b
Visceral and parietal ganglia*	13.50 ± 6.0 b
Heart*	1.07 ± 0.40a
Hemolymph (50 μl)	0.35 ± 0.10a
Buccal mass	0.20 ± 0.07a
Foot	0.22 ± 0.09a
Digestive gland	0.36 ± 0.08a
Intestine	0.12 ± 0.03a
Kidney	3.45 ± 0.36a
Mantle	1.28 ± 0.20a
Ovotestis	1.10 ± 0.60a
Penis complex	3.55 ± 0.08a
Skin	0.40 ± 0.20a
Vulva/vagina complex	4.20 ± 2.00a

For tissues marked with an asterisk (*), which are very small and difficult to handle for weighing, the IR-FaRP content is expressed as picomole/tissue; in all other tissues the content is expressed as picomole/mg tissue ($n = 5$; mean ± standard error of mean). The values followed by different letters (a or b) are significantly different ($P < 0.05$, $F = 5.05$) from each other, whereas the values sharing same letters (a or b) are not.

Levels of IR-FaRPs

Immunoreactive-FaRPs were detected in every tissue studied; the CNS had higher levels than the other organs. The supraesophageal portion of the CNS (the buccal and cerebral ganglia) had lower levels of IR-FaRPs than the subesophageal portion (the pedal, parietal, and visceral ganglia) (Table I).

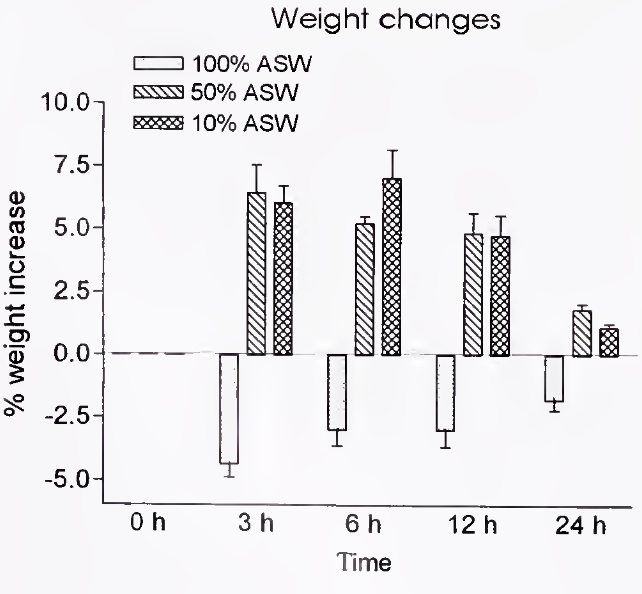

Figure 1. Time course of weight changes of snails acclimated under laboratory conditions and subsequently submerged in 10%, 50%, and 100% ASW ($n = 10$; mean ± standard error of mean).

The levels of IR-FaRP in the CNS, hemolymph, and kidney varied with the ambient osmotic conditions. In all three tissues, the levels of IR-FaRPs were correspondingly reduced in lower salinities, and the highest levels were always in terrestrial conditions. The CNS of animals submerged in 10% ASW for 24 h had levels of IR-FaRPs that were 80% lower than those in the terrestrial condition (Fig. 2). In hemolymph, the 10% ASW condition reduced the levels of IR-FaRPs by 77% compared to the terrestrial condition (Fig. 3). In kidney tissues, the 10% ASW condition reduced IR-FaRP levels by 64% compared to the terrestrial condition (Fig. 4).

Immunocytochemistry

Like other dextral gastropods, *M. bidentatus* retains only its right kidney. A whole mount of the kidney reveals IR-staining of axons with varicosities; moreover, such staining and varicosities are restricted to the kidney, and none are present in the surrounding mantle tissue (Fig. 5). Longitudinal sections of the kidney also show localized IR-staining at the periphery (Fig. 6). Some aggregation of varicosities appear as intense staining. No IR-cell bodies were seen in the kidney.

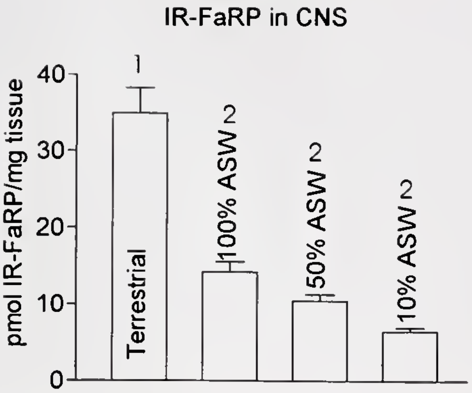

②

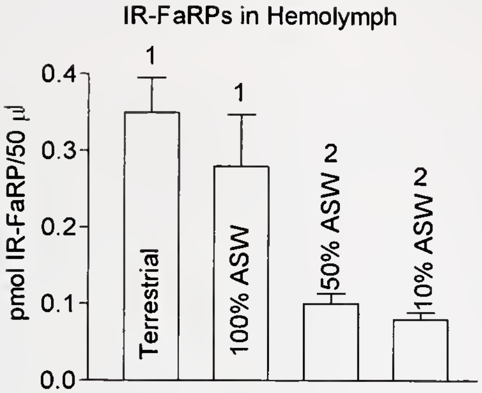

③

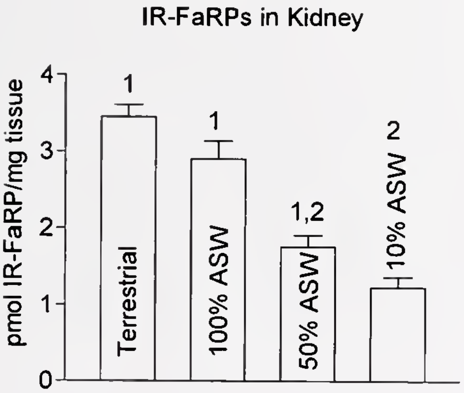

④

Figure 2. IR-FaRPs in the CNS. Note that the level of IR-FaRPs in the terrestrial condition is higher than that in the three ASW conditions ($P < 0.05$ for 100% ASW and 50% ASW; $P < 0.01$ for 10% ASW. $F = 18.02$) ($n = 5$; mean ± standard error of mean).

Figure 3. IR-FaRPs in the hemolymph. The levels of IR-FaRPs in the terrestrial and 100% ASW conditions are significantly greater than those in 50% and 10% ASW conditions ($P < 0.01$ and $P < 0.001$, respectively. $F = 10.50$) ($n = 5$; mean ± standard error of mean).

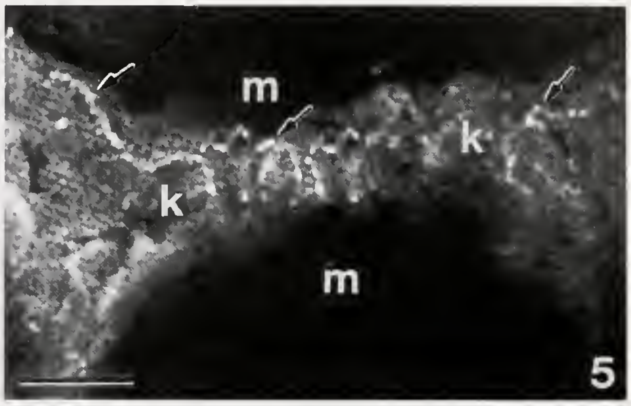

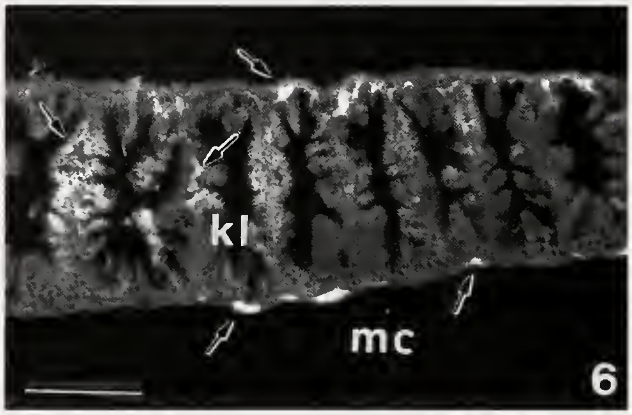

Figure 5. Optical section of the whole mount of the kidney (k) and adjacent mantle (m) tissue showing IR-fibers and varicosities (arrows) in the kidney. Scale bar: 50 µm

Figure 6. Longitudinal section of the kidney showing IR-staining (thin arrows) possibly as innervations to smooth muscles within the kidney tissue and also in the periphery. kl, kidney lumen; mc, mantle cavity. Scale bar: 300 µm..

The distribution of IR-neurons in the CNS is mapped in Figure 7. All commissures, connectives, and major nerves in the CNS display IR-fibers, and all ganglia except the pleurals contain IR-cell bodies. Visceral and right parietal ganglia contain both large (20 ± 5 µm) and small (10 ± 5 µm) IR-neurons, whereas mostly small and only a few large IR-neurons are found in the cerebral and pedal ganglia (Figs. 7–9, 12).

Cerebral ganglia. Two groups of large (20 ± 5 µm) and small (10 ± 5 µm) IR-neurons are present at the anterior and posterior location of the cerebral commissure (Figs. 7–9). The middle part of each cerebral ganglion contains a large (20 ± 5 µm) IR-cell surrounded by small IR-cells (Fig. 9). In the lateral lobes, 2–4 large (20 ± 3 µm) cells and 8–12 small (12 ± 4 µm) IR-cells are seen (Figs. 7, 10).

Figure 4. IR-FaRPs as detected by antiserum S253 in the kidney. The level of IR-FaRPs in the terrestrial condition is significantly ($P < 0.05$. $F = 8.17$) higher than that of 10% ASW ($n = 5$; mean ± standard error of mean).

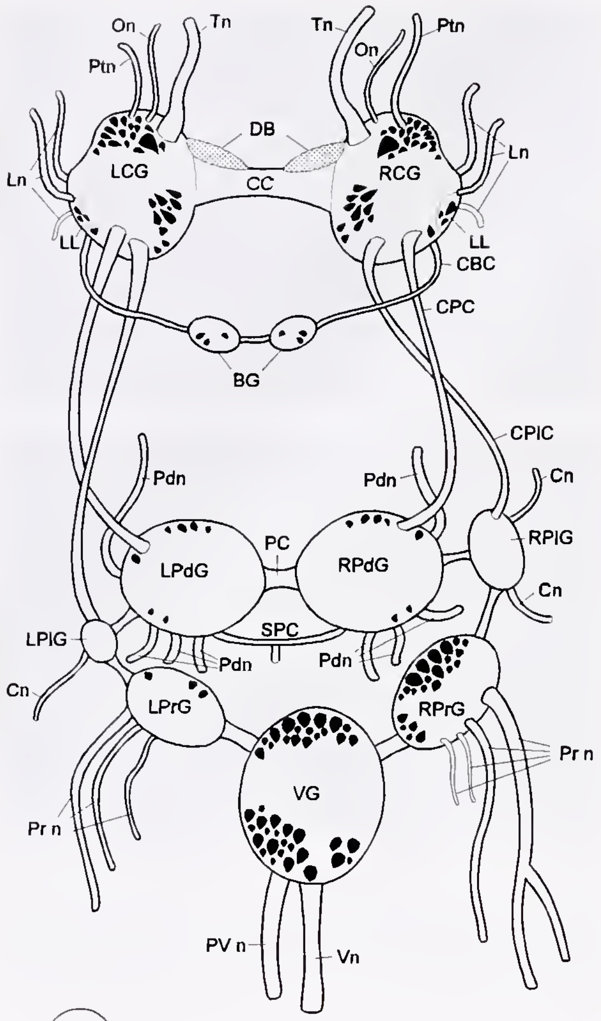

7

Figure 7. Showing the schematic distribution of the IR-cells in the CNS. BG, buccal ganglia; CBC, cerebro-buccal connective; CC, cerebral commissure; Cn, cutaneous nerve; CPC, cerebro-pedal connective; CPIC, cerebro-pleural connective; DB, dorsal bodies; LCG, left cerebral ganglion; LL, lateral lobe; Ln, labial nerves; LPdG, left pedal ganglion; LPIG, left pleural ganglion; LPrG, left parietal ganglion; On, optic nerve; PC, pedal commissure; Pdn, pedal nerve; Ptn, peritentacular nerve; Prn, parietal nerves; PVn, parieto-visceral nerve; RCG, right cerebral ganglion; RPdG, right pedal ganglion; RPIG, right pleural ganglion; RPrG, right parietal ganglion; SPC, sub-pedal commissure; Tn, tentacular nerve; VG, visceral ganglion; Vn, visceral nerve. Not to scale.

Buccal ganglia. In each buccal ganglion, 3 intermediate sized (18 ± 2 μm) IR-cells, and many IR-fibers and varicosities are seen (Fig. 11).

Pedal ganglia. Groups of 6–10 small IR-neurons are seen at the periphery of each pedal ganglion (Figs. 7, 12).

Parietal and visceral ganglia. More large and small IR-cells were seen in the right parietal and visceral ganglia than in any other ganglion (Figs. 7, 13). The left parietal ganglion contains only small IR-neurons (Fig. 7). The IR-cells are arranged in anterior and posterior groups in both ganglia (Figs. 7, 14). Numerous IR-neurites emanate from the CNS into the surrounding connective tissue and appear to terminate in varicosities (Fig. 15).

Discussion

In both the field and the laboratory, most individuals of *M. bidentatus* were emergent, living under semiterrestrial conditions. But some members of the population were always submerged, suggesting that they crawl in and out of water intermittently. The osmotic concentration of the hemolymph was correlated with that of the adjacent aqueous medium. Moreover, IR-FaRPs are present in the CNS, kidney, and hemolymph, and the levels of these peptides are also correlated with the osmotic concentration of the ambient medium.

Osmoregulation and kidney

When the osmolarity of the external medium changes, the hemolymph osmolarity of *M. bidentatus* also changes due to inward and outward movements of water from its body. Such conditions must be offset by various adjustments: regulation of urine production by its kidney is one of them. The IR-staining of the kidney was seen as a diffuse pattern on the kidney cells, as an intense localized pattern in areas with neural arborizations and varicosities, and in other small areas that are probably bundles of smooth muscles. The smooth muscles of the kidney of the basommatophoran snail *Helisoma duryi* are innervated by FMRFamide-immunoreactive axons (Saleuddin *et al.*, 1992). In this species the *in vitro* contraction of kidney tissues was influenced by FaRPs (unpubl. obs., A.S.M. Saleuddin). The FaRPs are well known for their contractile activity on visceral and smooth muscles in various species. They are also known to regulate salivary glands and ion channels (Bulloch *et al.*, 1988; Green *et al.*, 1994; Price and Greenberg, 1994; Lingueglia *et al.*, 1995). In the pulmonate kidney they are probably involved in regulating smooth muscle contractions for peristalsis and the production of hydrostatic pressure for urine formation, as well as in regulating ion channels for selective secretion and reabsorption of ions from urine.

Osmoregulation and IR-FaRP levels

The CNS and hemolymph displayed the highest and lowest levels of IR-FaRPs, respectively. Organs containing involuntary muscles, such as the reproductive tracts and kidney, have high levels of IR-FaRPs. These organs apparently receive FaRPs through direct innervation by neurons from the CNS. Thus, in these target tissues, the FaRPs may act as neuromodulators or as paracrine agents. Numerous IR-FaRP processes terminating in varicosities in the connective tissue around the CNS may constitute a diffuse

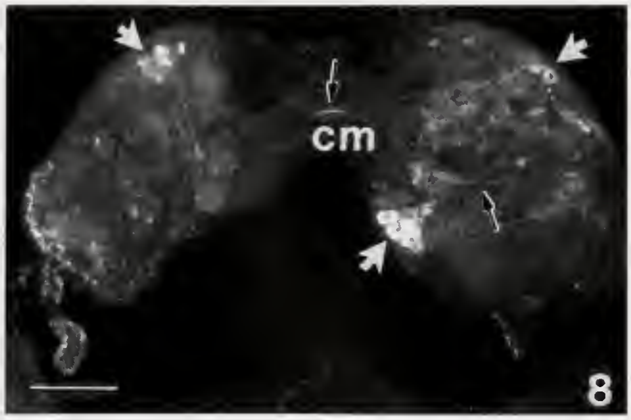

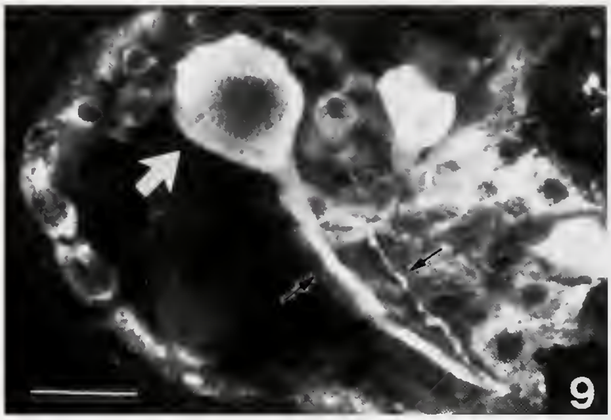

Figure 8. Groups of IR-cells (large arrows) in a cross section of the left and right cerebral ganglia; thin arrows point to IR-material in the commissure (cm) and neuropile. Scale bar: 100 μm.

Figure 9. Optical section of the left cerebral ganglion showing a large IR-cell (large arrow) among small IR-FMRFamide cells and their neurites (small arrows). Scale bar: 20 μm.

neurohemal area and account for the hemolymph IR-FaRP levels.

The levels of IR-FaRPs in the CNS, hemolymph, and kidney varied under different osmotic conditions. The IR-FaRP levels were reduced in hypoosmotic conditions compared with those in hyperosmotic or terrestrial conditions. Terrestrial or hyperosmotic salt-water conditions produced threats of desiccation and salt loading in snails, whereas hypoosmotic conditions had the opposite effect. The changes of IR-FaRP levels in the tissues of *M. bidentatus* by osmotic conditions may reflect osmoregulation by the snail. Since IR-FaRP levels increased in the CNS, hemolymph, and kidney under conditions of increased water losses such as in terrestrial or 100% ASW conditions, the FaRPs may have an antidiuretic function. *In vitro* culture of the kidney tissues of *Helisoma* with synthetic FMRFamide increased its intracellular water uptake, and FMRFamide has been suggested to have an antidiuretic role (Saleuddin *et al.*, 1992; Madrid *et al.*, 1994). Antidiuretic and diuretic activities of FMRFamide and GDPFLRFamide respectively have been demonstrated in nephridia of a leech (Salzet *et al.*, 1994). Basommatophoran pulmonates such as *Melampus* contain GDPFLRFamide (unpub. obs., D. A. Price). Both tetra- and hepta-FaRPs are present in the osmoregulatory tissues of *Helisoma* (Madrid *et al.*, 1994). The tetra- and hepta-FaRPs are expressed in exclusive neurons and may have different actions in a target tissue (Greenberg and Price, 1992; Benjamin and Burke, 1994; Price and Greenberg, 1994). The precise mechanism of the tetra- and hepta-FaRP actions in molluscan kidneys awaits future studies. In molluscs, osmoregulation by the kidney appears to be a combined effect of many physiological systems regulated by different hormones. In *Lymnaea stagnalis*, a neuropeptide that stimulates sodium uptake by the skin has been sequenced; furthermore, axons that release immunoreactive sodium-influx-stimulating peptides are present in this snail (De With *et al.*, 1994). In *Aplysia californica*, R15α1 neuropeptide causes water retention, thus having an osmoregulatory role (Weiss *et al.*, 1989). Additionally, in this species various kidney functions are modulated by L10 and LUQ neurons, and the latter neurons are immunoreactive to FMRFamide (Koester and Alevizos, 1989; Giardino *et al.*, 1996). Such systems include increased circulation of hemolymph for ultrafiltration, subsequent secretion and reabsorption of ions and organic matters, and expulsion of final urine (Khan and Saleuddin, 1979). Bioassay studies assessing the effects of FaRPs on kidney functions will enhance understanding of hormonal control of osmoregulation.

Location of IR-FaRP cells

The neurosecretory cells of the CNS of *M. bidentatus* have been described by using histochemical staining (Price, 1977; Ridgway, 1987). The IR-FaRP cells described in this paper are some of these neurosecretory cells; their pattern of distribution is basically similar to that of other basommatophoran pulmonates such as *Lymnaea stagnalis* and *Helisoma duryi* (Schot and Boer, 1982; Buckett *et al.*, 1990; Murphy *et al.*, 1985; Saleuddin *et al.*, 1992). In the cerebral ganglia of *M. bidentatus*, the IR-cells are present in groups located anteriorly and posteriorly. Similar groups are also seen in the cerebral ganglia of *H. duryi* near the endocrine growth-regulating mediodorsal cells and the ovulation-regulating caudodorsal cells. In the latter species, however, an additional large group of small IR-cells is seen in the left cerebral extension; such cells are absent in the corresponding location in *M. bidentatus*. The lateral lobes of the cerebral ganglia of *M. bidentatus* contain several large and small IR-cells, whereas those of *H. duryi* contain only two IR-cells, and those of *L. stagnalis* have none (Saleuddin *et* *al.*, 1992; Schot and Boer, 1982). The lateral lobes of *L. stagnalis* and *H. duryi* are known to regulate both growth and reproductive centers of the CNS (for review, see Saleuddin *et al.*, 1994; Saleuddin and Ashton, 1996). In the buccal ganglia of *M. bidentatus*, three IR-cells have been seen; in those of *H. duryi* two cells occur; and in those of *H.*

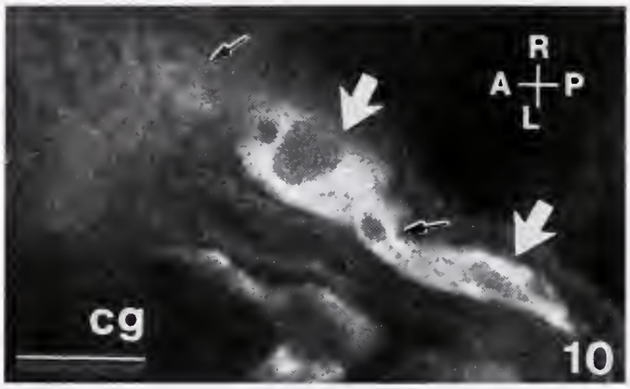

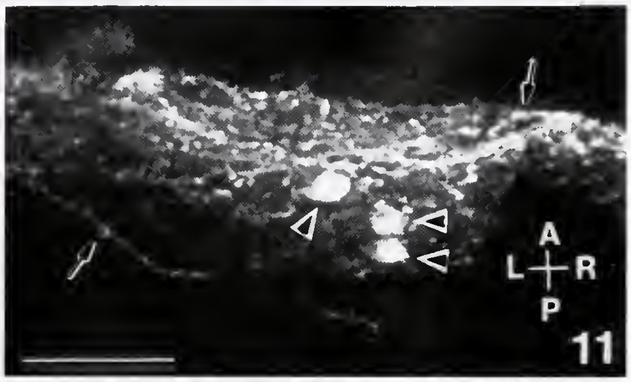

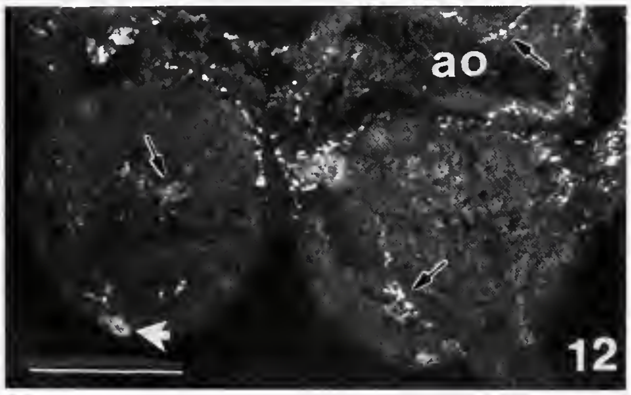

Figure 10. Optical section of the right lateral lobe and a part of right cerebral ganglion (cg) showing large (large arrows) and small (small arrows) IR-cells. Note that the large cells are intensely stained and the small cells are less intensely stained; the cells can be recognized by the lack of staining in their nuclei. Orientation of the tissue is shown by the two axes showing anterior (A) to posterior (P), and left (L) to right (R) sides. Scale bar: 20 μm.

Figure 11. Three cells (arrow heads) and many IR-neurites and varicosities (thin arrows) are shown in the whole mount of right buccal ganglion. Orientation of the tissue is shown by the axes showing anterior (A) to posterior (P), and left (L) to right (R) sides. Scale bar: 50 μm.

Figure 12. Cross section of the pedal ganglia showing a small IR-cell (large arrow) and many IR-neurites (thin arrows). ao, aorta. Scale bar: 250 μm.

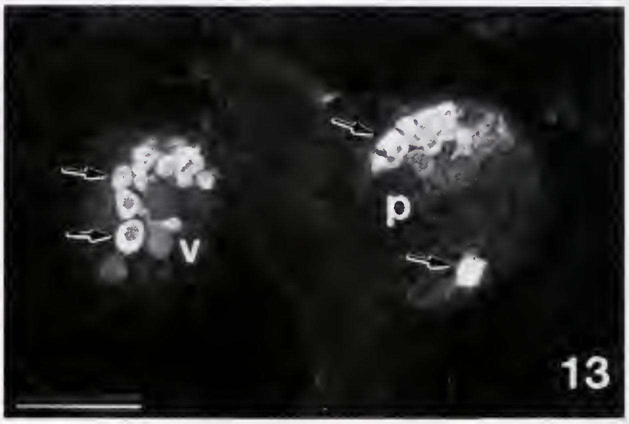

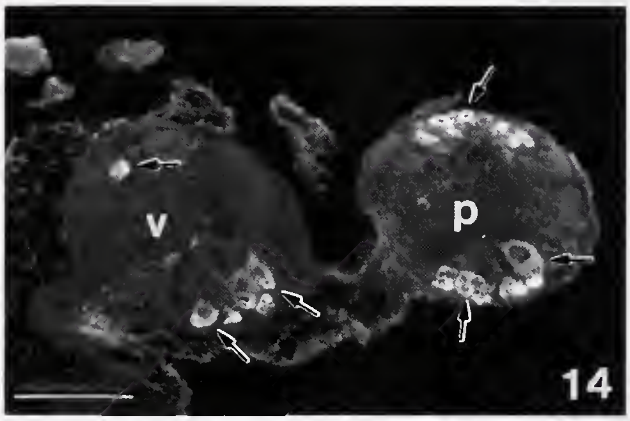

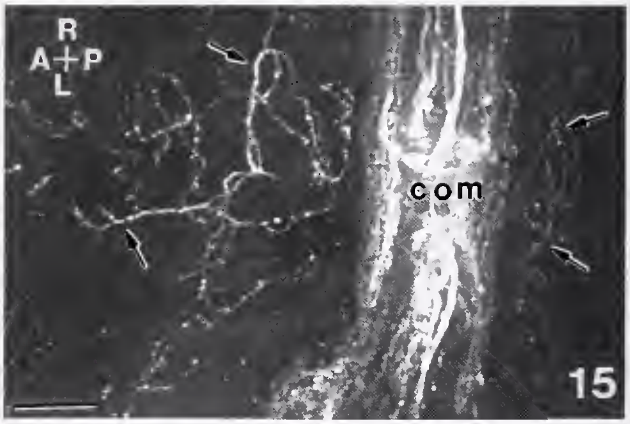

Figure 13. Cross section of the anterior region of the visceral (v) and mid region of the right parietal (p) ganglia showing IR-cells (thin arrows). Scale bar: 50 μm.

Figure 14. Cross section of the mid region of the visceral (v) and posterior region of the right parietal (p) ganglia showing IR-cells (thin arrows). Scale bar: 50 μm.

Figure 15. Whole mount of the cerebral commissure (com) showing extensive IR-neurites and varicosities within the connective in adjacent area (arrows). Orientation of the tissue is shown by the two axes showing anterior (A) to posterior (P), and left (L) to right (R) sides. Scale bar: 50 μm.

trivolvis about 30 smaller cells have been seen (Murphy *et al.*, 1985; Saleuddin *et al.*, 1992). The IR-cells in the parietal and visceral ganglia of *M. bidentatus* are arranged in anterior and posterior groups, which appear to be similar to those in *H. duryi* and *L. stagnalis* (Schot and Boer, 1982; Buckett *et al.*, 1990; Saleuddin *et al.*, 1992). The location of IR-cells in the bassommatophoran pulmonates such as *H. duryi* and *L. stagnalis* is close to or within important endocrine centers that regulate growth and reproduction, and the lateral lobes of the cerebral ganglia that regulate both growth and reproduction. Numerous IR-fibers emanate from the CNS and terminate as varicosities in the nearby connective tissue, suggesting that the FaRPs are released into the hemolymph that perfuses the CNS. The FaRPs may also participate in regulating other endocrine centers of the CNS.

Acknowledgments

This study was supported by grants from York University (to HRK), NSERC, Canada (to ASMS), and NIH, USA (to MJG). We thank Dr. B. G. Loughton, York University, for his helpful comments on the manuscript and Ms. Mary-Lou Ashton, York University, for her technical help.

Literature Cited

Apley, M. L. 1970. Field studies on life history, gonadal cycle and reproductive periodicity in *Melampus bidentatus* (Pulmonata: Ellobiidae). *Malacologia* **10:** 381–397.

Benjamin, P. R., and J. F. Burke. 1994. Alternative mRNA splicing of the FMRFamide gene and its role in neuropeptidergic signaling in a defined neural network. *Bioessays* **16:** 335–342.

Buckett, K. J., M. Peters, G. J. Dockray, J. van Minnen, and P. R. Benjamin. 1990. Regulation of heartbeat in *Lymnaea* by motor neurons containing FMRFamide-like peptides. *J. Neurophysiol.* **63:** 1426–1435.

Bulloch, A. G. M., D. A. Price, A. D. Murphy, T. D. Lee, and H. N. Bowes. 1988. FMRFamide peptides in *Helisoma:* identification and physiological actions at a peripheral synapse. *J. Neurosci.* **8:** 3459–3469.

Cottrell, G. A., E. M. Lutz, D. A. Price, and J. Sommerville. 1994. N-terminally extended FMRFamide related peptides of *Helix aspersa:* processing of the precursor protein and distribution of the released peptides. *Mol. Cell. Neurosci.* **5:** 632–641.

Deaton, L. E. 1990. Potentiation of hypoosmotic cellular volume regulation in the quahog, *Mercenaria mercenaria*, by 5-hydroxytryptamine, FMRFamide, and phorbol esters. *Biol. Bull.* **178:** 260–266.

De With, N. D., H. H. Boer, A. B. Smit, and R. C. Van Der Schors. 1994. Neurosecretory yellow cells and hydromineral regulation in the pulmonate freshwater snail *Lymnaea stagnalis*. Pp. 81–84 in *Perspectives in Comparative Endocrinology*, K. G. Davey, R. E. Peter, and S. S. Tobe, eds. National Research Council of Canada, Ottawa.

Giardino, N. D., R. S. Aloyz, M. Zollinger, and M. W. Miller. 1996. L5-67 and LUQ-1 peptide precursors of *Aplysia californica:* distribution and localization of immunoreactivity in the central nervous system and in peripheral tissues. *J. Comp. Neurol.* **374:** 230–245.

Green, K. A., S. W. P. Falconer, and G. A. Cottrell. 1994. The neuropeptide Phe-Met-Arg-Phe-NH_2 (FMRFamide) directly gates two ion channels in an identified *Helix* neurone. *Pflügers Arch.* **428:** 232–240.

Greenberg, M. J., and D. A. Price. 1992. Relationships among the FMRFamide-like peptides. *Prog. Brain Res.* **92:** 25–37.

Hilbish, T. J. 1981. Latitudinal variation in freezing tolerance of *Melampus bidentatus* (Say) (Gastropoda: Pulmonata). *J. Exp. Mar. Biol. Ecol.* **52:** 283–297.

Khan, H. R., and A. S. M. Saleuddin. 1979. Effects of osmotic changes and neurosecretory extracts on kidney ultrastructure in the freshwater pulmonate *Helisoma*. *Can. J. Zool.* **57:** 1256–1270.

Koester, J., and A. Alevizos. 1989. Innervation of the kidney of *Aplysia* by L10 and LUQ cells, and an identified peripheral motoneuron. *J. Neurosci.* **9:** 4078–4088.

Lehman, H. K., and D. A. Price. 1987. Localization of FMRFamide-like peptides in the snail *Helix aspersa*. *J. Exp. Biol.* **131:** 37–53.

Lesser, W., and M. J. Greenberg. 1993. Cardiac regulation by endogenous small cardioactive peptides and FMRFamide-related peptides in the snail *Helix aspersa*. *J. Exp. Biol.* **178:** 205–230.

Lingueglia, E., G. Champigny, M. Lazdunski, and P. Barbry. 1995. Cloning of the amiloride sensitive FMRFamide peptide-gated sodium channel. *Nature* **378:** 730–733.

Longley, R. D., and A. J. Longley. 1986. Serotonin immunoreactivity of neurons in the gastropod *Aplysia californica*. *J. Neurobiol.* **17:** 339–358.

Madrid, K. P., D. A. Price, M. J. Greenberg, H. R. Khan, and A. S. M. Saleuddin. 1994. FMRFamide-related peptides from the kidney of the snail, *Helisoma trivolvis*. *Peptides* **15:** 31–36.

McMahon, R. F., and W. D. Russell-Hunter. 1981. The effects of physical variables and acclimation on survival and oxygen consumption in the high littoral salt-marsh snail, *Melampus bidentatus* Say. *Biol. Bull.* **161:** 246–269.

Moffett, S. B. 1992. Patterns of neurotransmitter-like immunoreactivity in veligers of the pulmonate gastropod *Melampus bidentatus*. *Am. Zool.* **32:** 131A.

Morton, J. E. 1955. The evolution of Ellobiidae with a discussion on the origin of the Pulmonata. *Proc. Zool. Soc. Lond.* **125:** 127–168.

Murphy, A. D., K. Lukowiak, and W. K. Stell. 1985. Peptidergic modulation of patterned motor activity in identified neurons of *Helisoma*. *Proc. Natl. Acad. Sci. USA* **82:** 7160–7166.

Price, C. H. 1977. Morphology and histology of the central nervous system and neurosecretory cells in *Melampus bidentatus* Say (Gastropoda: Pulmonata). *Trans. Am. Micros. Soc.* **96:** 295–312.

Price, C. H. 1980. Water relations and physiological ecology of the salt marsh snail, *Melampus bidentatus* Say. *J. Exp. Mar. Biol. Ecol.* **45:** 51–67.

Price, D. A., and M. J. Greenberg. 1994. Comparative aspects of FMRFamide gene organization in molluscs. *Neth. J. Zool.* **44:** 421–431.

Price, D. A., N. W. Davies, K. E. Doble, and M. J. Greenberg. 1987a. The variety and distribution of FMRFamide-related peptides in molluscs. *Zool. Sci.* **4:** 395–410.

Price, D. A., C. G. Cobb, K. E. Doble, J. K. Kline, and M. J. Greenberg. 1987b. Evidence for a novel FMRFamide-related heptapeptide in the pulmonate snail *Siphonaria pectinata*. *Peptides* **8:** 533–538.

Price, D. A., W. Lesser, T. D. Lee, K. E. Doble, and M. J. Greenberg. 1990. Seven FMRFamide-related and two SCP-related cardioactive peptides from *Helix*. *J. Exp. Biol.* **154:** 421–437.

Ridgway, R. L. 1987. Alcian blue-alcian yellow mapping of neurosecretory cells in the central nervous system of the salt marsh pulmonate snail *Melampus bidentatus*. *Comp. Biochem. Physiol.* **87A:** 295–303.

Russell-Hunter, W. D. 1978. Ecology of freshwater pulmonates. Pp. 335–383 in *Pulmonates*, Vol. 2A, V. Fretter and J. F. Peake, eds. Academic Press, New York.

Russell-Hunter, W. D., M. L. Apley, and R. D. Hunter. 1972. Early life-history of *Melampus* and the significance of semilunar synchrony. *Biol. Bull.* **129:** 623–656.

Saleuddin, A. S. M., and M. L. Ashton. 1996. Neuronal pathways of three neurosecretory cells from the lateral lobes in *Helisoma* (Mollusca): innervation of the dorsal body. *Tissue Cell* **28:** 5362.

Saleuddin, A. S. M., H. R. Khan, M. L. Ashton, and B. Griffond. 1992. Immunocytochemical localization of FMRFamide in the central nervous system and the kidney of *Helisoma duryi* (Mollusca): its possible antidiuretic role. *Tissue Cell* **24:** 179–189.

Saleuddin, A. S. M., S. T. Mukai, and H. R. Khan. 1994. Molluscan endocrine structures associated with the central nervous system. Pp. 257–263 in *Perspectives in Comparative Endocrinology*, K. G. Davey, R. E. Peter, and S. S. Tobe, eds. National Research Council of Canada, Ottawa.

Salzet, M., P. Bulet, C. Wattez, and J. Malecha. 1994. FMRFamide-related peptides in the sex segmental ganglia of the pharyngobdellid leech *Erpobdella octoculata*. Identification and involvement in the control of hydric balance. *Eur. J. Biochem.* **221:** 269–275.

Schot, L. P. C., and H. H. Boer. 1982. Immunocytochemical demonstration of peptidergic cells in the pond snail *Lymnaea stagnalis* with an antiserum to the molluscan cardioactive tetrapeptide FMRFamide. *Cell Tissue Res.* **225:** 347–354.

Weiss, K. R., H. Bayley, P. E. Lloyd, R. Tenenbaum, M. A. Gainowicz Kolks, E. C. Cropper, S. C. Rosen, and I. Kupfferman. 1989. Purification and sequencing of neuropeptides contained in neuron R15 of *Aplysia californica*. *Proc. Natl. Acad. Sci. USA* **86:** 2913–2917.

Reference: *Biol. Bull.* **196:** 163–176. (April 1999)

Behavioral Physiology of Four Crab Species in Low Salinity

I. J. MCGAW, C. L. REIBER, AND J. A. GUADAGNOLI

Department of Biological Sciences, University of Nevada, Las Vegas, 4505 Maryland Parkway,
Las Vegas, Nevada 89154-4004

Abstract. Reports focusing on the behavioral responses of crabs to exposure to low salinity have involved choice chamber experiments or quantification of changes in activity. In addition to describing changes in locomotor activity in four species of crabs of differing osmoregulatory ability, the present study describes six behaviors: increased movement of the mouthparts, cleaning of the mouthparts with the chelae, cleaning of the antennae and antennules with the maxillipeds, flicking of the antennae, retraction of the antennules, and extension of the abdomen. *Callinectes sapidus* and *Carcinus maenas* are classed as efficient osmoregulators, and in general, showed an increase in these behaviors with decreasing salinity. *Cancer magister,* a weak regulator, and *Libinia emarginata,* an osmoconformer, exhibited these behaviors to a lesser degree and became inactive in the lower salinities, tending to adopt an isolation-type response. The differences in behaviors between the species correlated closely with previously reported changes in cardiovascular function and hemolymph flow. These overt reactions are discussed in relation to the osmoregulatory physiology and ecology of each crab species.

Introduction

The osmoregulatory physiology of a number of crustacean species has been studied extensively during the past four decades (see Mantel and Farmer, 1983; Pequeux, 1995, for references). There are few reports on behavioral reactions to salinity variation, and these have involved either salinity choice experiments or quantification of locomotor activity.

The anomuran crab *Porcellana platycheles* displays discriminatory behavior in low salinity, but only outside its limits of physiological tolerance. In choice chamber experiments, this species shows rapid avoidance of salinities below 40% seawater (SW), but cannot distinguish between pairs of salinities above 40% SW (Davenport, 1972; Davenport and Wankowski, 1973). The amphipod *Corophium volutator* has a preference for salinities in the range of 10–30 ppt (30–90% SW), but only discriminates between pairs of salinities outside this range (McLusky, 1970). Comparable behavioral reactions are reported for *Marinogammarus marinus,* which has a preferred salinity range of 80%–100% SW, although it is able to survive in more dilute concentrations (Bettison and Davenport, 1976). *Carcinus maenas,* the green shore crab, increases its locomotor activity in low salinity, a behavior defined as halokinesis (Taylor and Naylor, 1977; Thomas *et al.,* 1981; Bolt and Naylor, 1985; Ameyaw-Akumfi and Naylor, 1987). Its preferred salinity range, as determined by choice chamber experiments, is 27–41 ppt (82–125% SW; Thomas *et al.,* 1981) or 17–40 ppt (51–121% SW; Ameyaw-Akumfi and Naylor, 1987), and it is able to discriminate between salinities separated by a difference as little as 0.5 ppt (McGaw, 1991). In addition, salinity choice behavior in this species is affected by the coloration of the individual and by prior acclimation salinity (McGaw and Naylor, 1992a), as well as by the availability of shelter (McGaw and Naylor, 1992b). Low salinity is also known to re-entrain and modulate the endogenous tidal locomotor rhythm in this species (Bolt and Naylor, 1985; McGaw and Naylor, 1992c).

A number of other species can control the osmotic pressure of body fluids by behavioral selection of different salinities. The coconut crab *Birgus latro* (Gross, 1995), the lined shore crab *Pachygrapsus crassipes* (Gross, 1957), and the hermit crab *Pagurus bernhardus* (Davenport *et al.,* 1980) all show modulation of behavior in response to

Received 16 July 1998; accepted 11 January 1999.
Abbreviations: SW = seawater, CW = carapace width.
E-mail: imcgaw@ccmail.nevada.edu

changes in the concentration of their body fluids. In contrast, the mud crab *Scylla serrata,* which is able to survive in salinities from 2 ppt to 42 ppt (3–127% SW), shows no discriminatory behavior between salinities in this range (Davenport and Wong, 1987).

These behaviors ensure that the crab either escapes from unfavorable conditions or moves to a compatible salinity range. In either case, short-term changes in the behavior will ultimately prevent the crab from expending energy during longer term alterations in physiology associated with regulation of the internal body fluid concentrations. Behavioral reactions, therefore, appear to be closely related to the physiological ability of an individual to osmoregulate.

In this paper, we describe several behaviors exhibited in response to low salinity by four crab species of varying osmoregulatory abilities. The blue crab *Callinectes sapidus* is a very efficient osmoregulator (Tan and Van Engel, 1966; Lynch *et al.,* 1973) and can live in a range of salinities from hypersaline lagoons to fresh water (Hedgpeth, 1967; Mangum and Amende, 1972). Male crabs are more efficient osmoregulators and extend further into estuaries than female or juvenile crabs (Haefner and Schuster, 1964; Hines *et al.,* 1987). The green shore crab *Carcinus maenas* is classed as an efficient hyperosmoregulator (Rankin and Davenport, 1981); it is able to tolerate exposure to salinities as low as 5 ppt (Broekhuysen, 1936), and can even withstand short-term exposure to fresh water (McGaw and Naylor, 1992c). The salinity tolerance of this species is related to the coloration of the individual, which is indicative of intermolt duration (McGaw *et al.,* 1992). Red-colored individuals are poorer osmoregulators than green ones (Reid *et al.,* 1989; Rasmussen and Bjerregaard, 1995) and are absent from estuaries (McGaw and Naylor, 1992c). The Dungeness crab *Cancer magister* is a large and commercially important species on the west coast of North America. It lives in sandy and muddy bays, and although it occurs in estuaries, it is classed as a weak osmoregulator (Jones, 1941; Engelhardt and Dehnel, 1973; Hunter and Rudy, 1975) and cannot survive in salinities below 12 ppt (36% SW; Cleaver, 1957). The spider crab *Libinia emarginata* is found in rocky and muddy bays on the eastern seaboard of North America. It is classed as an osmoconformer and can survive exposure to 40% SW if acclimated slowly (Gilles, 1970), although the lower range of tolerance is nearer 75%–80% SW (Cornell, 1980).

The aim of the present study was to determine whether crab behaviors vary with salinity and time and to compare the responses of the four species. In addition, possible explanations for these overt reactions are discussed in relation to the physiology and ecology of each species.

Materials and Methods

Adult male crabs (intermolt stage) of each species were maintained separately, in a recirculating artificial seawater system (Instant Ocean) at 1000–1050 mOsm (considered as 100% seawater, salinity = 33 ppt), and fed fish twice weekly. Blue crabs (*Callinectes sapidus*) of 12–16 cm carapace width (CW) were obtained from Gulf Specimen Marine Labs, Panacea, Florida, and kept at a temperature of 18°–20°C. Green shore crabs (*Carcinus maenas*), 4–7 cm CW (green color only), and spider crabs (*Libinia emarginata*), 2–4 cm CW, were purchased from the Marine Biological Laboratory, Woods Hole, Massachusetts, and maintained at a temperature of 13°–15°C. Dungeness crabs (*Cancer magister*), 16–20 cm CW, were purchased from a local fish market and held at 11°–13°C.

The osmoregulatory ability of the crabs was determined by acclimating eight crabs of each species to seawater concentrations of 100%, 75%, 50%, and 25%. Acclimation times were 24 h, with one exception: in 25% SW the acclimation time for *Libinia emarginata* was 10 h due to high mortality. Blood samples were taken by withdrawing a small amount of hemolymph from the arthrodial membranes between the walking legs. Osmolality was measured on a vapor pressure osmometer (Westcor Inc 5100B).

Behavioral experiments were carried out in 10-gallon aquaria with filtered aerated seawater and a layer of gravel in the bottom. Temperatures were similar to those in the holding tanks, and the salinity was changed by adding a known volume of distilled water (of the same temperature), over a 15-minute period. The behavior of the crabs was observed for a total of 3 h. Seven separate behaviors were observed, and these occurred to varying degrees, depending on the salinity and species of crab. (1) Locomotor activity: This was the only behavior that has been described previously in relation to low salinity. In the present study, locomotor activity was quantified each time the crab changed location horizontally, or vertically as it attempted to escape the aquarium. (2) Movement of mouth parts: The third maxillipeds were opened and closed in a side-to-side motion, which was counted as one event. At the same time, the palps of the maxillipeds were moved independently, and there was rapid flicking of all the exopodites of the mouth parts. (3) Cleaning of mouth parts: The 3rd maxillipeds and exopodites of the mouth parts were scraped by the chelae; usually one chela at a time was used. (4) Cleaning of antennae/antennules: Both the antennae and antennules were cleaned; they were folded down towards the maxillipeds and the palps were scraped along the length a number of times. (5) Flicking of antennae: The antennae were flicked up and down, independently of each other; each separate movement was counted as an event. (6) Percentage time of antennule retraction: The antennules made continuous rapid flicking movements while extended, but for periods of time they would be folded backwards into a depression in the carapace; the approximate percentage of time the antennules were retracted was recorded. (7) Percentage time of abdomen extension: This behavior was usually observed when the crab raised itself up on its legs. Initially, the last abdominal segment was opened and closed; subsequently, the entire abdomen was opened, exposing the hindgut and rectum. The crab would then either keep the abdomen open, or open and close it in a slow and regular motion.

These behaviors were recorded for 1 min at set time intervals in constant light, over a 3-h period. This time period was chosen because choice chamber experiments have shown that salinity choice is usually completed within 2–3h (Thomas *et al.*, 1981; Ameyaw-Akumfi and Naylor, 1987). A total of 16 crabs of each species were monitored in separate experiments in 100%, 75%, 50%, and 25% seawater.

Similar *P* values were obtained with Friedman's nonparametric ANOVA and with standard repeated measures ANOVA on normalized data. The latter test was therefore used because it allowed significant interactions to be followed up with Student-Newman-Keuls tests on pairwise comparisons of each salinity.

Results

There was a difference in osmoregulatory ability between each of the four crab species (Fig. 1). *Callinectes sapidus* was the most efficient osmoregulator, and even in 100% seawater its hemolymph osmolality was higher than that of the other species. The hemolymph osmolality of each species was similar in 75% seawater, but in 50% and 25% SW, there was a gradation. *Callinectes sapidus* had the highest mean hemolymph osmolality of 690 mOsm. *Libinia emarginata* was an osmoconformer with a hemolymph osmolality close to that of the ambient seawater. The osmoregulatory ability of *Carcinus maenas* and *Cancer magister* lay in between these two extremes, with the former being the more efficient osmoregulator.

Locomotor activity increased in all four species as the salinity decreased (Fig. 2). In *Callinectes sapidus*, there was a large variation between individual crabs. Although there was a strong trend towards greater activity in low salinity, at the end of the 3 h-test period (not shown) there was no statistically significant difference in activity levels ($F = 1.21$, $P > 0.05$; Table I). Locomotor activity was more

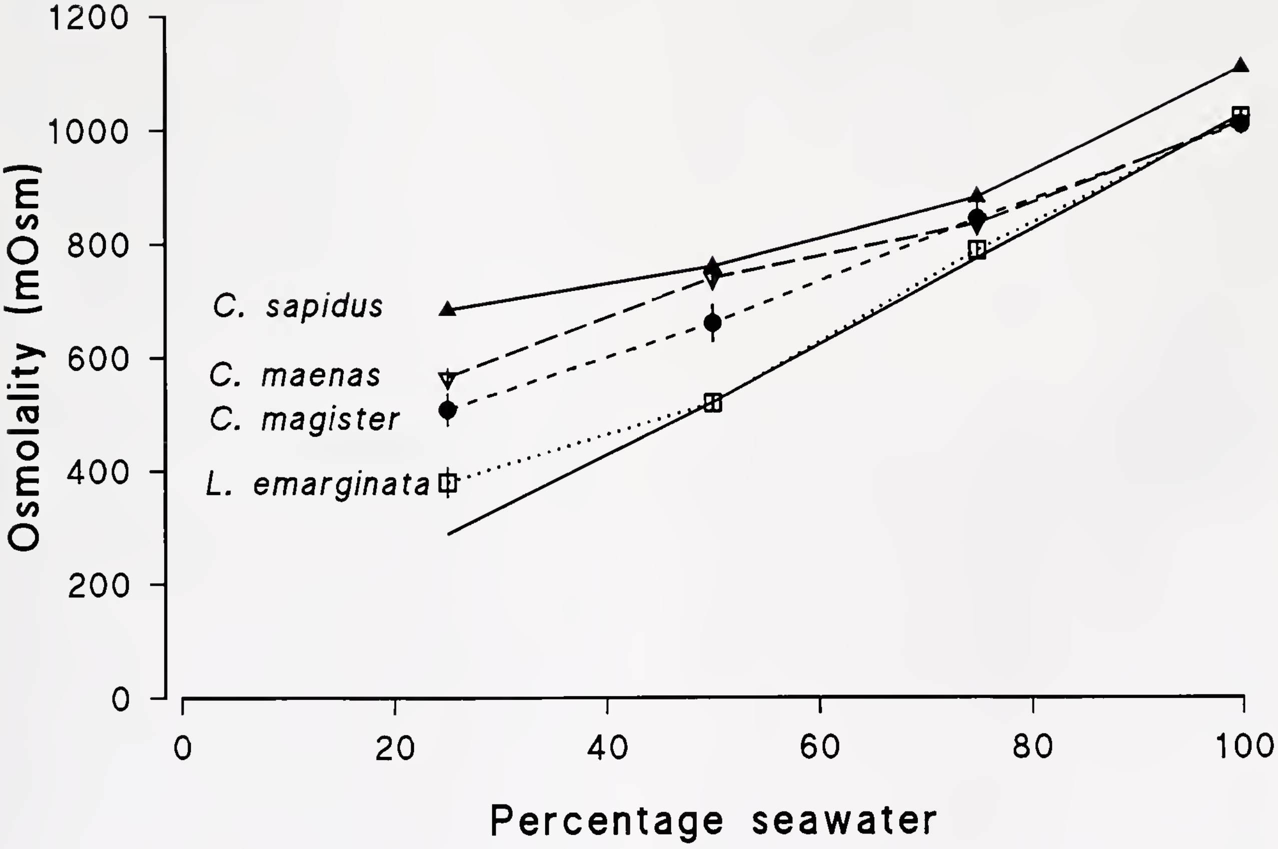

Figure 1. Hemolymph osmolality (mean ± SEM) of 8 male *Callinectes sapidus, Carcinus maenas, Cancer magister,* and *Libinia emarginata* in seawater concentrations of 100%–25%, shown in relation to iso-osmotic line for each seawater concentration.

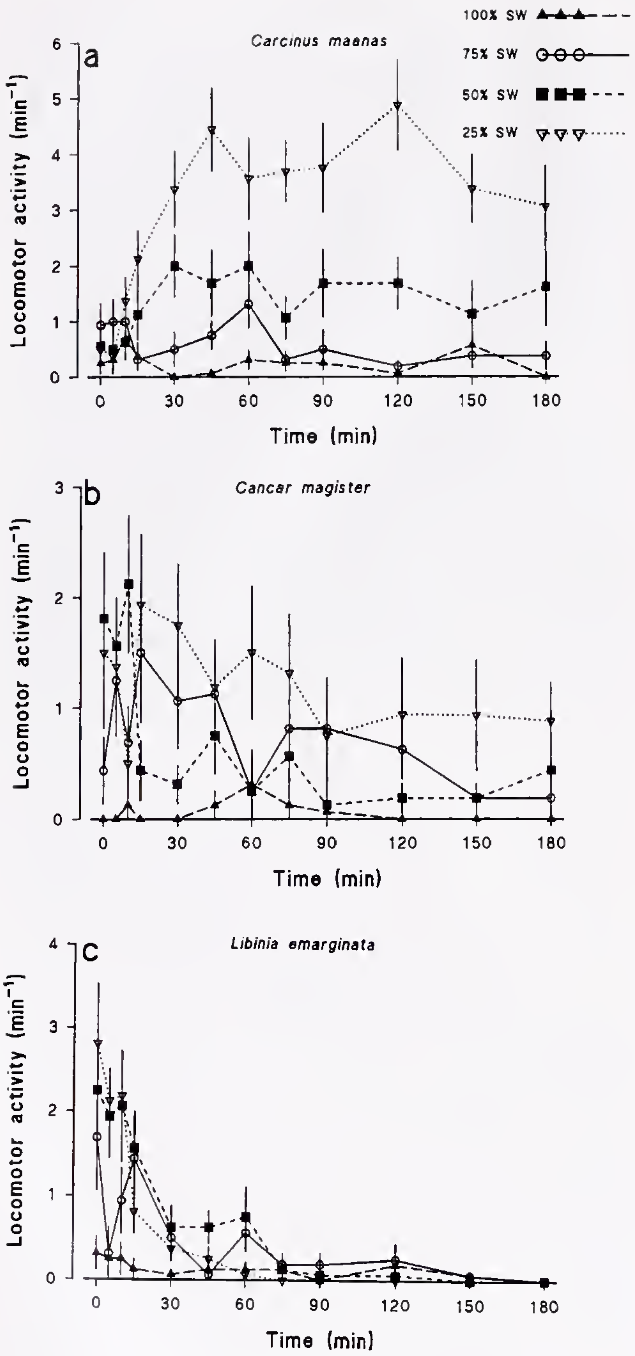

Figure 2. Locomotor activity of 16 crabs (mean ± SEM) during 3-h exposure to seawater concentrations of 100%, 75%, 50%, and 25% seawater; (a) *Carcinus maenas*, (b) *Cancer magister*, and (c) *Libinia emarginata*.

pronounced in *Carcinus maenas*. There was a significant increase after 15–30 min in 50% and 25% seawater (Fig. 2a; $F = 22.45$, $P < 0.000$), and activity remained elevated above levels in 100% and 75% seawater, for the duration of the experiment. Both *Cancer magister* (Fig 2b) and *Libinia emarginata* (Fig. 2c) showed an immediate and significant increase in activity as the salinity was lowered ($F = 7.46$ and 7.60, $P < 0.000$). However, the pattern was somewhat different than in *Callinectes sapidus* and *Carcinus maenas*. The activity levels of *Cancer magister* declined during the first hour of low-salinity exposure, and *Libinia emarginata* was largely inactive after 45 min. Individuals of both species buried themselves in the gravel and moved infrequently thereafter.

Each species also responded to a decrease in salinity with an increase in frequency of mouthpart movements; each set of mouthpart movements (3–8 movements per set) was associated with a ventilatory reversal (not shown). In *Callinectes sapidus*, there was a clear increase in mouthpart movements as the seawater was lowered to 25% (Fig. 3a; $F = 23.29$, $P < 0.000$). In 100% seawater this species only occasionally opened its mouthparts, but in 50% and 25% seawater the frequency of mouthpart movements was elevated for the 3-h experimental period. *Carcinus maenas* exhibited a similar behavior pattern, with increasing mouthpart movements in the lower salinities (Fig. 3b; $F = 20.11$, $P < 0.000$). In 50% and 25% SW there was a significant increase in frequency of mouthpart movements compared to levels in 100% and 75% SW (Table 1); this was maintained for the duration of the experiment. In *Cancer magister* (Fig. 3c), there was a significant increase in mouthpart movements in all salinities below 100% seawater ($F = 4.55$, $P < 0.01$); but unlike *Callinectes sapidus* and *Carcinus maenas*, *Cancer magister* did not maintain the increase. The number of mouthpart movements quickly declined, reaching levels equivalent to those in 100% SW after 30–45 min. In *Libinia emarginata* (Fig. 3d), a similar trend was observed, with a short-term increase in frequency of mouthpart movements in 25% SW ($F = 3.25$, $P < 0.05$), which decreased within an hour to levels comparable to those in 100% SW. The overall trend was a decrease in the frequency of mouthpart movements with decreasing osmoregulatory ability of each crab species (Fig. 1, Fig. 3a–d).

The crabs used their chelae to scrape the third maxillipeds and exopodites of the mouthparts; this behavior was only observed during the first hour of low-salinity exposure. Both *Callinectes sapidus* (Fig. 4a) and *Carcinus maenas* (Fig. 4b) cleaned their mouthparts only in the lowest salinity tested (25% SW; $F = 12.26$ and 11.65, $P < 0.000$). In *Callinectes sapidus* this behavior stopped after 90 min (Fig. 4a), whereas in *Carcinus maenas* it was not observed after 45 min (Fig. 4b). Only a small percentage of *Cancer magister* individuals actually cleaned their mouthparts (Fig. 4c), and the increase in this behavior was significant only in 50% seawater ($F = 4.6$, $P < 0.01$; Table I). *Libinia emarginata* (Fig. 4d) showed a significant increase in mouthpart cleaning in 50% and 25% SW ($F = 13.37$, $P < 0.000$; Table

Table I

Student-Newman-Keuls pairwise tests for significant differences in behavior of each crab species, between each of the four salinities tested

	Percentage Seawater Comparison					
	100 *vs* 75	100 *vs* 50	100 *vs* 25	75 *vs* 50	75 *vs* 25	50 *vs* 25
Callinectes sapidus						
Locomotor activity	NS	NS	NS	NS	NS	NS
Mouthpart movement	NS	*	*	*	*	*
Mouthpart cleaning	NS	NS	*	NS	*	*
Antennae cleaning	NS	*	*	NS	*	NS
Antennae flicking	NS	NS	NS	NS	NS	NS
Antennule retraction	*	*	*	NS	NS	NS
Abdomen extension	NS	NS	NS	NS	NS	NS
Carcinus maenas						
Locomotor activity	NS	*	*	NS	*	*
Mouthpart movement	NS	*	*	*	*	NS
Mouthpart cleaning	NS	NS	*	NS	*	*
Antennae cleaning	*	*	*	*	*	NS
Antennae flicking	*	*	*	NS	NS	NS
Antennule retraction	NS	*	NS	NS	NS	NS
Abdomen extension	NS	NS	*	NS	*	*
Cancer magister						
Locomotor activity	*	*	*	NS	NS	NS
Mouthpart movement	*	*	*	NS	NS	NS
Mouthpart cleaning	NS	*	NS	NS	NS	*
Antennae cleaning	NS	NS	NS	NS	NS	NS
Antennae flicking	NS	NS	*	NS	NS	NS
Antennule retraction	*	*	*	*	*	*
Abdomen extension	NS	NS	*	NS	*	*
Libinia emarginata						
Locomotor activity	*	*	*	NS	NS	NS
Mouthpart movement	NS	NS	*	NS	NS	NS
Mouthpart cleaning	NS	*	*	*	*	*
Antennae cleaning	NS	NS	NS	NS	NS	NS
Antennae flicking	NS	NS	NS	NS	NS	NS
Antennule retraction	*	*	*	NS	NS	NS
Abdomen extension	NS	NS	*	NS	*	*

NS = not significant; * = significant ($P < 0.05$).

I), and as with the other species, this behavior ceased after 45 min.

Both *Callinectes sapidus* (Fig. 5a) and *Carcinus maenas* (Fig. 5b) cleaned the antennae and antennules with the palps of the third maxillipeds, and this behavior increased with decreasing salinity ($F = 10.85$ and 11.86, $P < 0.000$). *Callinectes sapidus* showed an increase in frequency of cleaning in 50% and 25% SW, whereas *Carcinus maenas* increased antennae and antennule cleaning in 75% SW, as well as in the two lowest salinities (Table I). Antennae or antennule cleaning essentially did not occur in *Cancer magister* or *Libinia emarginata* (not shown): only one or two individuals of each species exhibited this behavior, hence the insignificant value ($P > 0.05$).

In *Callinectes sapidus* the antennae were flicked up and down, on average, 2–3 times per minute, and this did not change with salinity (Table I; $F = 2.35$, $P > 0.05$). There was also no significant change in antennae flicking in *Libinia emarginata* ($F = 0.83$, $P > 0.05$), since this behavior was only observed in two individuals in 25% SW. In *Carcinus maenas* there was an increase in antennae flicking in all salinities below 100% SW ($F = 7.04$, $P < 0.000$; Table I), which increased in frequency as the salinity decreased. In *Cancer magister*, there was a similar increase in frequency of antennae flicking; however, rates were significantly elevated only in 25% SW ($F = 3.04$, $P < 0.05$; Table I). In each case there was a large variation in this behavior between each of the salinities.

The antennules of all the crabs were flicked rapidly while orientated in different directions, but were also retracted into the carapace for periods of time. In 100% SW each species retracted the antennae for about 5–20 s of every minute (10%–30%), but distinct differences between the species occurred in the lower salinities (Fig. 6). *Callinectes sapidus* (Fig. 6a) retracted its antennules upon initial exposure to 25% SW, but after 10 min the antennules were rarely

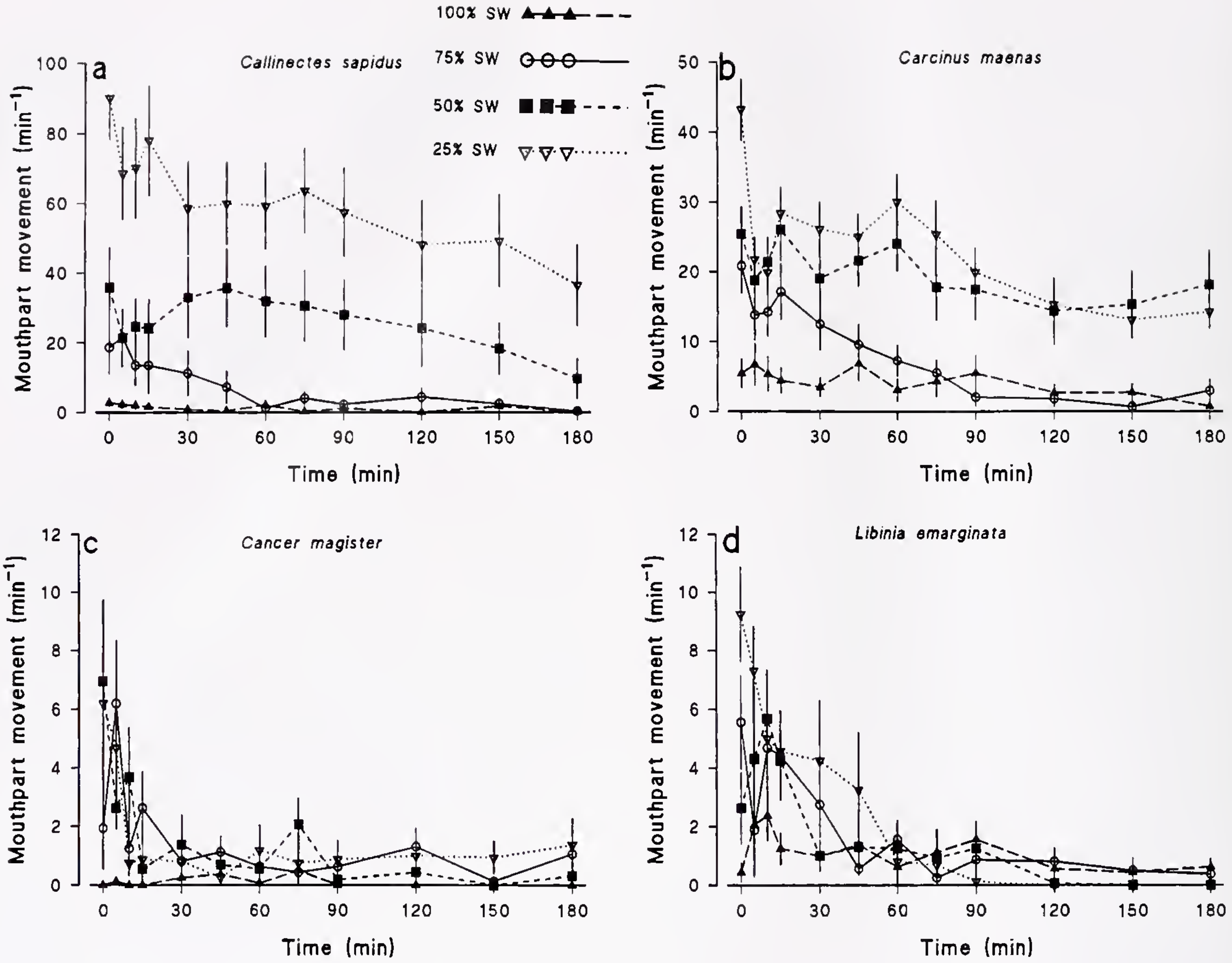

Figure 3. Mouthpart movements of 16 crabs (mean ± SEM) during 3-h exposure to seawater concentrations of 100%, 75%, 50%, and 25% seawater: (a) *Callinectes sapidus*, (b) *Carcinus maenas*, (c) *Cancer magister*, and (d) *Libinia emarginata*.

retracted; in 75% and 50% SW the antennules remained extended for the entire experimental period ($F = 24.24$, $P < 0.000$). Although the pattern was similar in *Carcinus maenas* (Fig. 6b), with the antennules exposed for longer periods in all salinities below 100%, this was statistically significant only in 50% SW ($F = 4.48$, $P < 0.01$). In *Cancer magister* and *Libinia emarginata*, the opposite response was seen: in low salinities the animals retracted the antennules. *Cancer magister* (Fig. 6c) showed a stepwise and significant increase in antennule retraction ($F = 27.32$, $P < 0.000$) in decreasing salinities, with the antennules more-or-less retracted for 100% of the time in 25% SW. *Libinia emarginata* (Fig. 6d) also retracted the antennules to a greater degree (60%–80% of the time) in all salinities below 100% SW ($F = 33.88$, $P < 0.000$), but there was no significant difference in retraction times between 75%, 50%, and 25% SW, as occurred in *Cancer magister* (Fig. 6c).

Crabs extended their abdomens in 50% and 25% SW only, although this behavior was also observed in some animals when returned to 100% SW in the holding tanks. *Callinectes sapidus* did not extend the abdomen to any significant degree ($F = 1.77$, $P > 0.05$): only three animals were observed to extend the last segment of the abdomen in 25% SW, for short periods of time (not shown). *Carcinus maenas* extended the entire abdomen during the first hour in 25% SW and to a lesser degree in 50% SW (Fig. 7a), and this was usually accompanied by slow fanning movements of the abdomen; however, this was significantly different from control levels only in 25% SW ($F = 12.03$, $P < 0.000$). *Cancer magister* (Fig. 7b) also extended the abdomen in 50% and 25% SW, although the time course for this behavior was more erratic. Again, this behavior was only significantly different from the control in 25% SW ($F = 9.95$, $P < 0.000$). Abdomen extension increased steadily ($F = 12.35$, $P < 0.000$) in *Libinia emarginata* (Fig 7c) after 1 h exposure to 25% SW. This appeared to be a passive

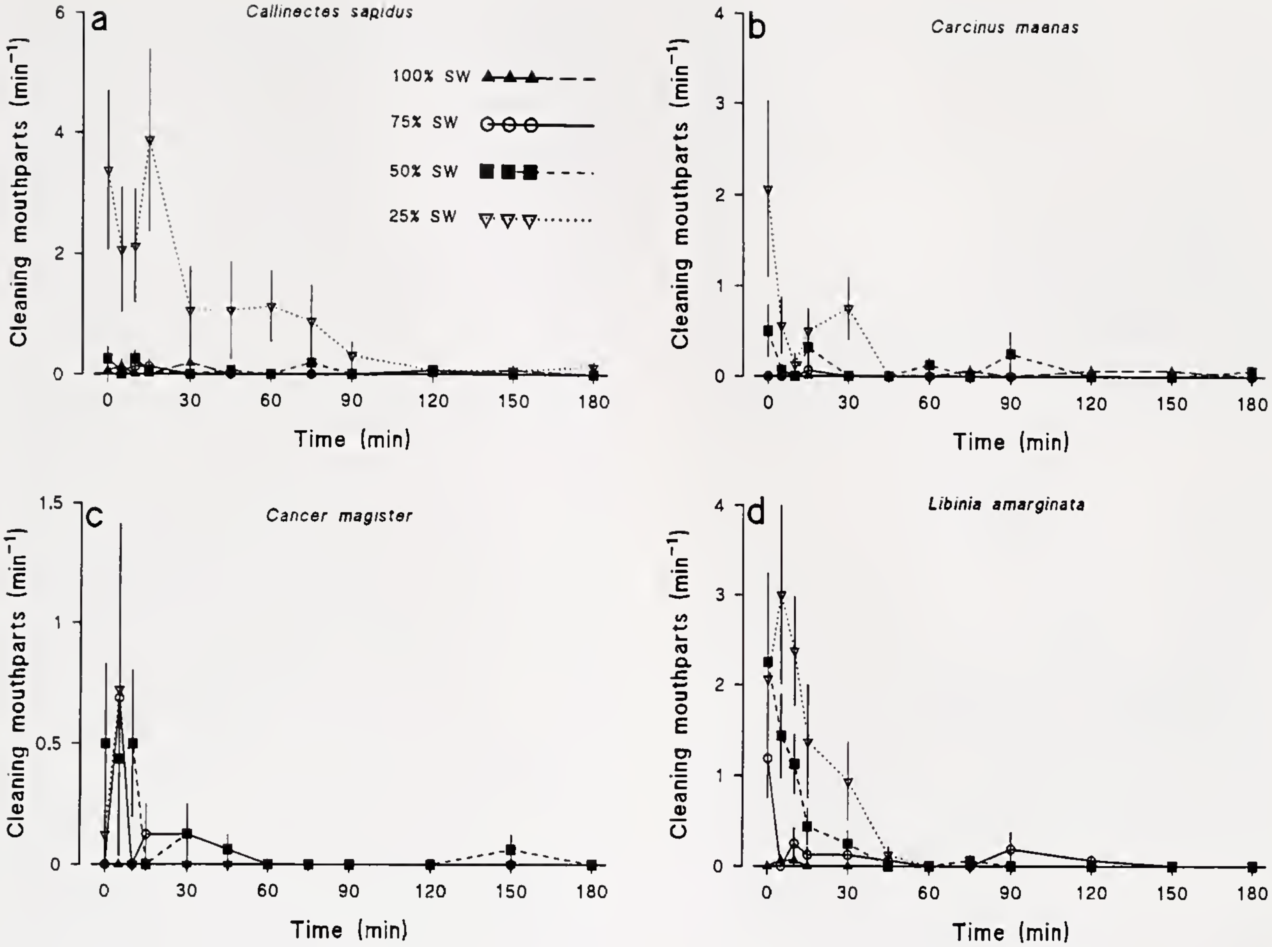

Figure 4. Cleaning of the mouthparts in 16 crabs (mean ± SEM) during 3-h exposure to 100%, 75%, 50%, and 25% seawater: (a) *Callinectes sapidus*, (b) *Carcinus maenas*, (c) *Cancer magister*, and (d) *Libinia emarginata*.

process, rather than the extension and fanning of the abdomen seen in the other species.

Discussion

Callinectes sapidus hyper-regulated its body fluids in all salinities, including 100% SW (Fig. 1); this has been reported previously (Tan and Van Engel, 1966). In all the other species, hemolymph was iso-osmotic with 100% SW. *Carcinus maenas*, which is classed as an efficient osmoregulator, had hemolymph osmolality levels (Fig. 1) similar to previous reports (Lucu *et al.*, 1973; Rankin and Davenport, 1981). All *Carcinus* used in the present study were green-colored male crabs. Red-colored individuals, which are in a prolonged intermolt (McGaw *et al.*, 1992), are poorer osmoregulators (Reid *et al.*, 1989; McGaw, 1991) and have different behavioral responses to low salinity (McGaw and Naylor, 1992a, c). *Cancer magister* is classed as a weak osmoregulator (Jones, 1941) and the levels of hemolymph osmolality reported here (Fig. 1) agree closely with the data of Hunter and Rudy (1975). *Cancer magister* is able to survive in salinities as low as 12 ppt (36% SW; Cleaver, 1957); however, in the present study all survived short-term exposure (24 h) to 25% SW (8 ppt) (Fig. 1). *Libinia emarginata* is an osmoconformer, with ion levels closely following those of the external medium (Gilles, 1970). This was also seen in the present study (Fig. 1), except in the lowest salinity. *Libinia emarginata* can withstand dilution of the medium only to 40% SW (Gilles, 1970). Mortality was high after 12-h exposure to 25% SW, and the short acclimation time (10 h) used would not have allowed hemolymph osmolality to decline to stable levels (Fig. 1).

Most reports on the activity of crabs in low salinity pertain to *Carcinus*. Taylor and Naylor (1977) report that *Carcinus maenas* responds to a lowering of salinity with an increase in locomotor activity, defined as halokinesis. This has been confirmed by a number of other studies (Taylor *et*

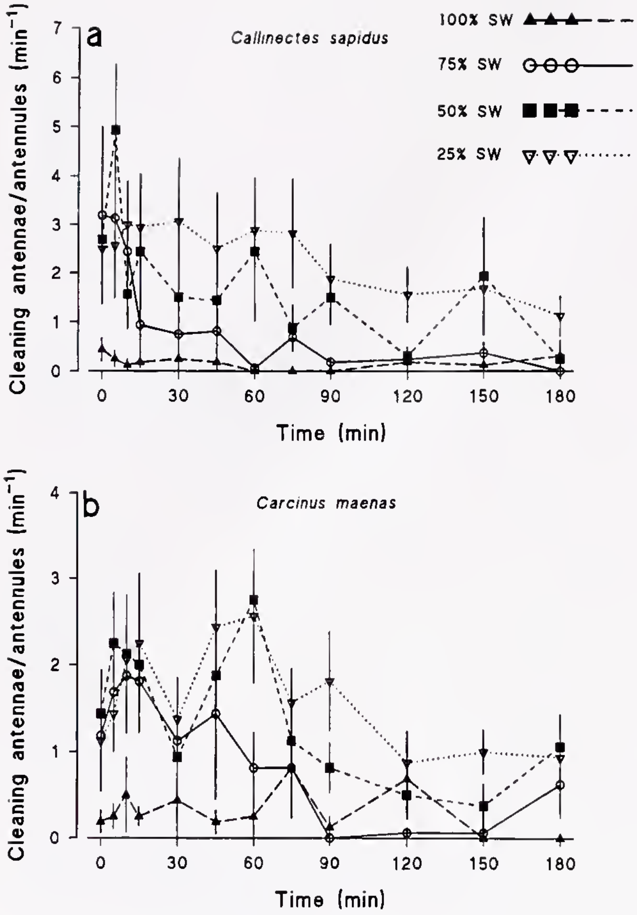

Figure 5. Antennae/antennule cleaning of 16 crabs (mean ± SEM) during 3 h in 100%, 75%, 50%, and 25% seawater: (a) *Callinectes sapidus*, (b) *Carcinus maenas*.

al., 1977; Thomas *et al.*, 1981; Bolt and Naylor, 1985; Ameyaw-Akumfi and Naylor, 1987; Warman *et al.*, 1991); such behavior enables the crab to escape deleterious salinities. In the present study, this increase in activity was not shown by all the crab species (Fig. 2b, c). Although *Callinectes sapidus* responded to a decrease in salinity with an increase in activity, this increase proved to be statistically insignificant. This species can live for extended periods in fresh water (Mangum and Amende, 1972), and therefore an escape response would be unnecessary. Likewise, the mud crab *Scylla serrata*, which can survive in 2 ppt salinity (Hill, 1979), shows no increase in activity and no preference for a particular medium (Davenport and Wong, 1987). *Carcinus maenas* showed a clear increase in locomotor activity with decreasing salinity (Fig. 2a), thus confirming the previous reports. Activity levels were noticeably higher in 25% SW, probably because this salinity approaches the lower limits of tolerance for the species (Broekhuysen, 1936). *Cancer magister* showed an increase in locomotor activity in all salinity below 100% SW, but this behavior was different than that exhibited by *Callinectes sapidus* and *Carcinus maenas*. About half of the animals ceased activity soon after salinity reduction, remaining motionless with the eyes and antennae retracted; the majority of individuals were inactive after 60–90 min (Fig. 2b). This behavior was more pronounced in *Libinia emarginata* (Fig. 2c); these crabs were active for only 30–60 min before ceasing activity. This was not due to water loading and impairment of movement as it is in porcelain crabs (Davenport, 1972), since inactive *Cancer magister* and *Libinia emarginata* reacted aggressively and resumed activity when probed with a glass rod.

This difference in locomotor activity between the species is echoed in their cardiovascular responses to low salinity. *Callinectes sapidus* reacts to a dilution of the medium with an immediate increase in heart rate and cardiac output, which eventually leads to increased venous return through the gills (McGaw and Reiber, 1998). Likewise, *Carcinas maenas*, which also exhibits increased locomotor activity, shows an increase in heart rate (Hume and Berlind, 1976; Taylor, 1977) as well as in calculated cardiac output and gill blood flow (Spaargaren, 1974, 1982). Although *Cancer magister* increases heart rate in 50% SW, cardiac stroke volume actually decreases, leading to a substantial decrease in cardiac output and gill blood flow (McGaw and McMahon, 1996). Cornell (1993, 1974) reports a corresponding decrease in heart rate (and presumably cardiac output) of *Libinia emarginata* in low salinity. In addition, hemolymph flow to the muscles of the legs *via* the sternal artery (Pearson, 1908; McLaughlin, 1983) increases in *Callinectes sapidus* (McGaw and Reiber, 1998), possibly reflecting increased metabolic demand of the locomotory muscles (Fig. 2a). In contrast, hemolymph flow through the sternal artery of *Cancer magister* decreases (McGaw and McMahon, 1996), as does activity after 60 min (Fig. 2b). In crabs, differential hemolymph flow and changes in cardiac function are controlled by pericardial hormones (Airriess and McMahon, 1992; McGaw and McMahon, 1995, 1999; McGaw *et al.*, 1994a, 1995) and possibly by neurohormones from the X-organ complex (McGaw and McMahon, 1998). A variety of neurohormones are known to have multiple effects on the osmoregulatory physiology of crustaceans, including modulation of cardiovascular parameters (see Kamemoto, 1976; Pequeux, 1995).

There were distinct differences in movement of the mouthparts (third maxillipeds and exopodites) between each of the species (Fig. 3). Each set of maxilliped movements corresponds to a ventilatory reversal (McGaw, unpubl. data), with water being taken in through the mouth, directed backwards towards the posterior gills, and ejected through the Milne Edwards opening at the base of the legs (Arudpragasam and Naylor, 1964, 1966; Hughes *et al.*, 1969). The exact function of these reversals is not known, but they are thought to aid in clearing the gill chambers of debris as well as irrigating the posterior gills (Arudpragasam and Naylor,

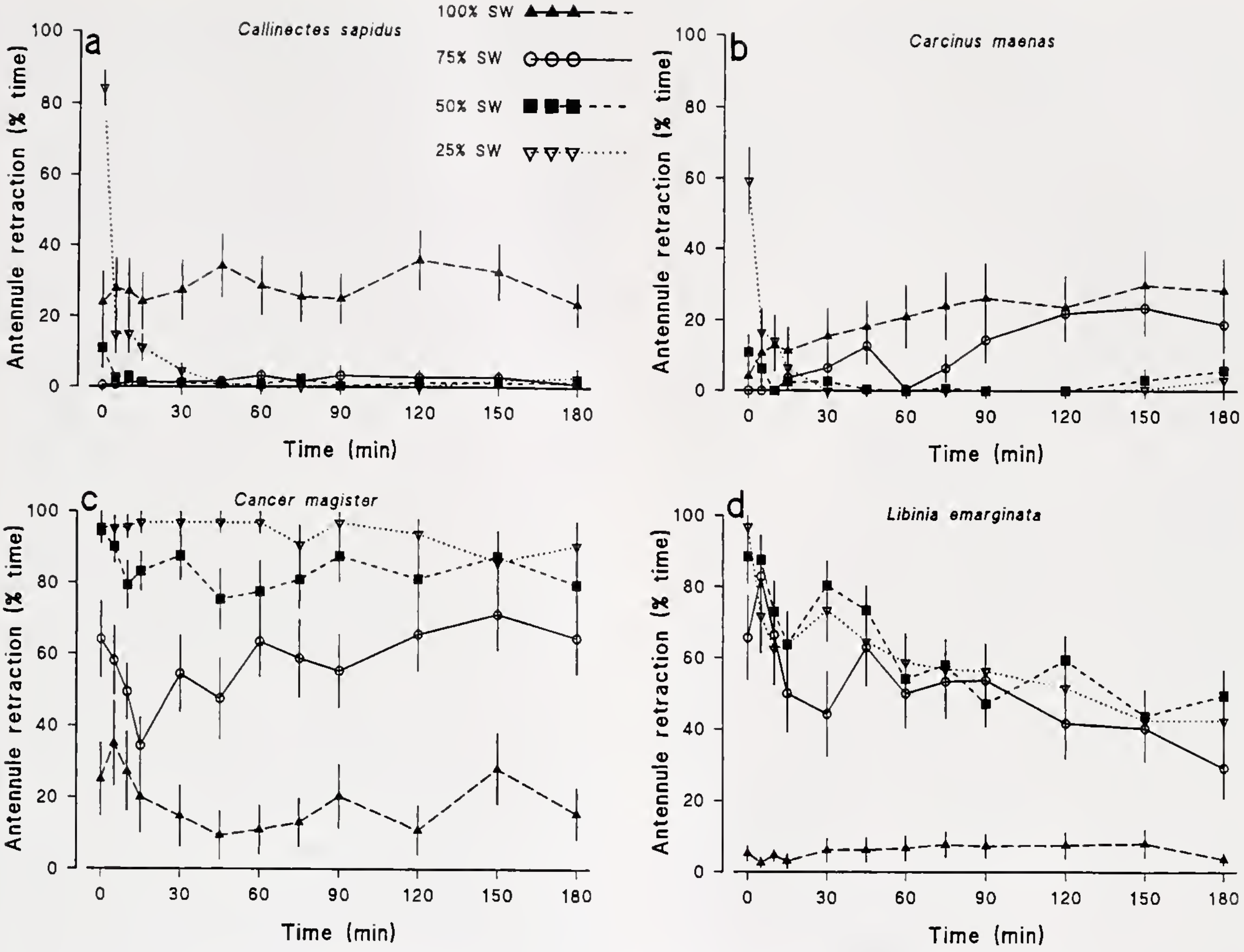

Figure 6. Percentage time of antennule retraction of 16 crabs (mean ± SEM) during 3 h in seawater concentrations ranging from 100%–25%: (a) *Callinectes sapidus*, (b) *Carcinus maenas*, (c) *Cancer magister*, and (d) *Libinia emarginata*.

1964, 1966). Evidence suggests that the posterior gills have the highest Na-K-ATPase activity (Florkin and Schoffeniels, 1969; Neufeld *et al.*, 1980; Siebers *et al.*, 1982, 1983, 1985, 1986), and therefore a ventilatory reversal would bring water into contact with the pumps of the posterior gills, enhancing active ion uptake. In support of this concept, *Callinectes sapidus*, which is the most efficient osmoregulator tested, exhibits the highest frequency of mouthpart movements (and hence ventilatory reversals; Fig. 3a), and this behavior decreases with the declining osmoregulatory ability of the species (Fig. 3), with the weak osmoregulator *Cancer magister* (Fig. 3c) and the stenohaline *Libinia emarginata* (Fig. 3d) showing substantially less ventilatory reversals than the two efficient osmoregulators (Fig. 3a, b). In addition, both *Callinectes sapidus* (Fig. 3a) and *Carcinus maenas* (Fig. 3b) showed a stepwise increase in mouthpart movements with decreasing salinity; this increase was sustained in 50% and 25% SW, for the 3-h experimental period. In both *Cancer magister* and *Libinia emarginata* (Fig. 3c, d; Table I), mouthpart movements increased only during the first 30 min. Thereafter, the crabs kept the mouthparts sealed, isolating the branchial chamber. This sealing of the branchial chambers has been reported previously for *Cancer magister* (Sugarman *et al.*, 1980). Isolation of the branchial chambers, in conjunction with a decrease in gill blood flow *via* a reduced cardiac output (McGaw and McMahon, 1996; Cornell, 1973, 1974), would help reduce the gradient for water uptake and diffusive salt loss.

There are also differences in hemolymph flow to the muscles of the mouthparts, which are supplied by the sternal artery and branches of the anterolateral arteries (Pearson, 1908; McLaughlin, 1983). In *Callinectes sapidus*, hemolymph flow through the sternal artery and anterolateral arteries is elevated for 2–4 h in 25% SW (McGaw and Reiber, 1998), which corresponds to the period of increased mouthpart movement (Fig. 3a). In contrast, blood flow through the sternal artery and anterolateral arteries of *Cancer magister* decreases (McGaw and McMahon, 1996), and

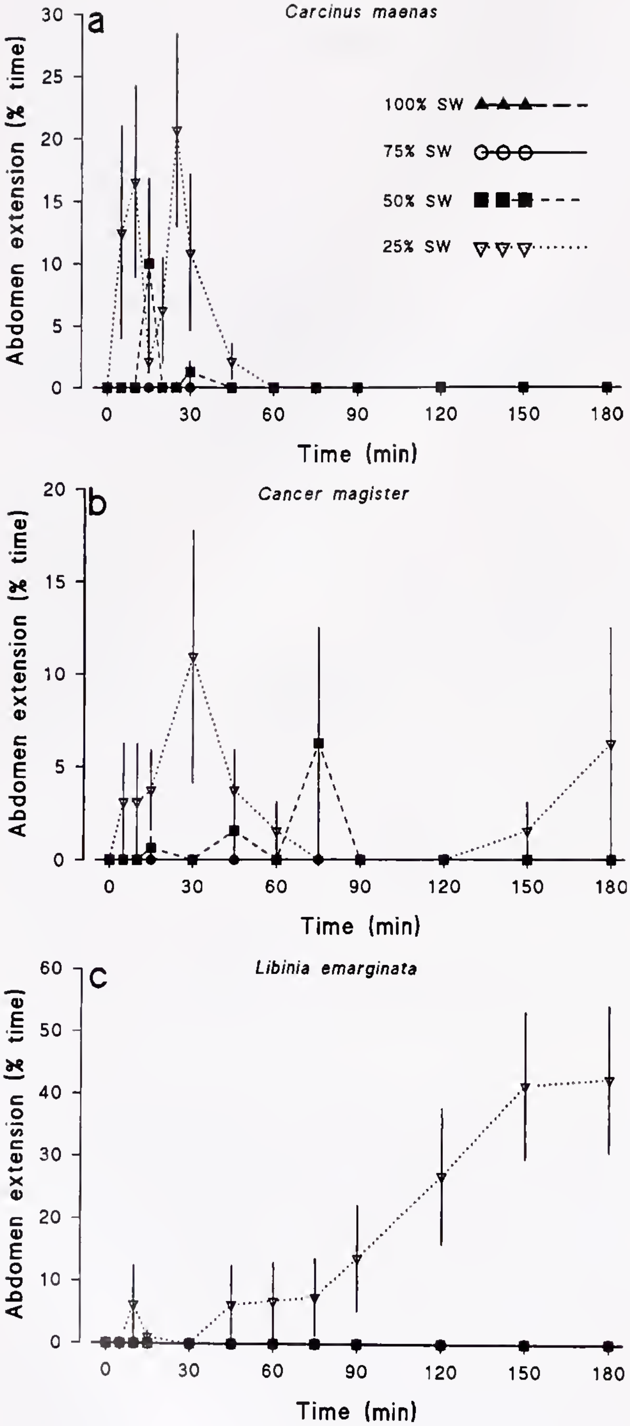

Figure 7. Mean abdomen extension (% time) of 16 crabs during a 3-h period in 100%–25% seawater concentrations: (a) *Carcinus maenas*, (b) *Cancer magister*, and (c) *Libinia emarginata*.

this parallels the rapid decrease in the number of mouthpart movements seen in this species after 15 min in low salinity (Fig. 3c).

All species of crabs cleaned their mouthparts with the chelae (Fig. 4); this occurred only during the first hour of low-salinity exposure, and was most evident in the lowest salinity tested. The reasons for this behavior are unclear, but the short time period suggests that it could be a startle response to the initial salinity change, possibly due to irritation of the setae of the mouthparts, which have a chemosensory function (Shelton and Laverack, 1970). This behavior was evident only in 25% SW in both *Callinectes sapidus* (Fig. 4a) and *Carcinus maenas* (Fig. 4b), but became more pronounced in 50% SW in the other two species. Although *Cancer magister* (Fig. 4c) cleaned the mouthparts more often in all salinities below 100%, the frequency of this behavior was low and it was statistically significant only in 50% SW. *Libinia emarginata* (Fig. 4d) showed a significant increase (Table I) in mouthpart cleaning in both 50% and 25% SW.

Differences in hemolymph flow are again observed between the species. *Callinectes sapidus* shows an increase in hemolymph delivered to the chelae *via* the sternal artery (McGaw and Reiber, 1998), which correlates with their increased use. *Cancer magister,* in contrast, shows a reduced blood flow through the sternal artery (McGaw and McMahon, 1996). Only four individual *Cancer magister* were observed to clean their mouthparts, hence the low mean frequency (0.5 min^{-1}; Fig. 4c). This would explain why the increase in flow that occurs in *Callinectes sapidus* is not evident in *Cancer magister.*

In both the efficient osmoregulators, *Callinectes sapidus* and *Carcinus maenas* (Fig. 5a, b), there was a stepwise increase in cleaning of the antennae and antennules with decreasing salinity (Table I). This behavior was not observed in the weak osmoregulator *Cancer magister* or the stenohaline *Libinia emarginata* (Table I). Recent evidence (Gleeson *et al.*, 1996, 1997) shows that the dendrites in the olfactory sensilla of the antennules of blue crabs are osmotically ablated in low salinity. Cleaning of the antennules (Fig. 5a) may be the response to the sensory loss or irritation resulting from the osmotic destruction of the dendrites. Cleaning of the antennules ceases after a number of hours in low salinity (Fig. 5), possibly allowing for their regeneration, which takes 48–96 h (Gleeson *et al.*, 1996). Changes in hemolymph flow to the muscles of the mouthparts, *via* the sternal and anterolateral arteries, compare closely with their use. *Callinectes sapidus* shows an increase in hemolymph flow through these vessels for 2–4 h after low-salinity exposure (McGaw and Rieber, 1998), whereas *Cancer magister*, which doesn't clean the antennae with the mouthparts (Table I), has about a 50% decrease in hemolymph flow during 6 h of exposure to 50% SW (McGaw and McMahon, 1996).

In conclusion, the increase in hemolymph flow through the anterolateral and sternal arteries of *Callinectes sapidus* (McGaw and McMahon, 1998), and the concurrent decrease in the same arteries of *Cancer magister* (McGaw and Mc-

Mahon, 1996), is a result of change in blood demand, probably caused by a combination of alterations in mouthpart movement and in mouthpart and antennae/antennule cleaning, with changes in locomotor activity having a lesser effect (Figs. 2–5).

The antennae and antennules of crustaceans have been implicated as having a chemosensory role in salinity detection (Krijgsman and Krijgsman, 1954; Lagerspetz and Mattila, 1961; Van Weel and Christofferson, 1966; Davenport, 1972; Tazaki, 1975; Gleeson *et al.,* 1996, 1997). Both the antennae and antennules were flicked up and down during the experiments. Although *Callinectes sapidus* flicked the antennae, there was no change in rate with salinity (Table 1). In *Libinia emarginata,* the antennae were small and rarely moved. There was a slight increase in antennae flicking of *Cancer magister,* but only in the lowest salinity. *Carcinus maenas* was the only species to show a significant increase in all lowered salinities (Table 1). However, with such variability within and between the species, it is hard to draw conclusions as to the role of the antennae in salinity detection; indeed, only a few papers cite the antennae as the sites of salinity reception (Lagerspetz and Mattila, 1961; Tazaki, 1975).

The percentage of time that the antennules were folded back into the carapace was recorded because flicking was too rapid to allow accurate determination of rate. *Callinectes sapidus* and *Carcinus maenas* exhibited similar behaviors (Fig. 6a, b): in 100% SW the antennules were retracted for 20%–25% of time; in the lowest salinity tested (25% SW) they were retracted during the initial salinity change-over period, but remained extended thereafter (Fig. 6a, b); in 50% and to a degree in 75% SW the antennules were rarely retracted. The opposite pattern was observed in the other two species. In 100% SW the retraction times were somewhat similar to those of *Callinectes sapidus* and *Carcinus maenas*; but in *Cancer magister* there was an increase in retraction with decreasing salinity, to the point that the antennules were retracted for nearly 100% of the time in 25% SW (Fig. 6c). In *Libinia emarginata,* too, there was an increase in retraction time in all salinities below 100% SW (Fig. 6d). Possibly these two species avoid low-salinity exposure with an isolation-type response. These results, as well as other behavioral and physiological work (Krijgsman and Krijgsman, 1954; Van Weel and Christofferson, 1966; Davenport, 1972; Sugarman *et al.,* 1980; Gleeson *et al.,* 1996, 1997), suggest that the antennules are more important than the antennae for salinity detection. In addition to the antennae and antennules, crabs possess hair-peg organs on many areas of the carapace, and these could be also be used for salinity detection (Schmidt, 1989).

Extension and flicking of the antennules of *Callinectes sapidus* is paralleled by increased hemolymph flow through the anterior aorta (McGaw and Reiber, 1998), which supplies these structures (Pearson, 1908; McLaughlin, 1983), and by a decrease in flow in the same artery of *Cancer magister* (McGaw and McMahon, 1996). When *Cancer magister* was returned to 100% SW, the antennules were extended again and rapidly flicked from side to side, and flow through the anterior aorta also increased at this time (McGaw and McMahon, 1996).

A number of individuals of each species were observed extending the abdomen for short periods or fanning it up and down. This behavior was not statistically significant in *Callinectes sapidus,* since only three crabs opened the last segment of the abdomen (Table 1). *Carcinus maenas* (Fig. 7a) and *Cancer magister* (Fig. 7b) increased abdomen extension in 50% and 25% SW, although it proved to be significant only in 25% SW (Table 1). *Libinia emarginata* also extended the abdomen (Fig. 7c) but it wasn't considered to be the same active behavior involving fanning and retraction. It occurred later in the experiment, increased progressively, and was probably caused by swelling of the tissues due to increased water loading. Extending the abdomen brings the soft tissues of the hindgut and rectum into direct contact with the water. Crustaceans and other arthropods can use the hindgut for osmotic and ionic regulation (Heeg and Cannone, 1966; Kamemoto, 1976; Malley, 1977; Phillips *et al.,* 1986; Audsley *et al.,* 1992); abdomen extension could, therefore, function as an additional means of ion uptake in low salinity.

There are also interspecific changes in blood flow to the abdomen and hindgut, which is perfused by the posterior aorta (Pearson, 1908; McLaughlin, 1983). *Callinectes sapidus* shows no change in hemolymph flow through this artery upon salinity reduction. In contrast, an increase in flow through the posterior aorta of *Cancer magister* occurs during low-salinity exposure, and on return to 100% SW (McGaw and McMahon, 1996). In *Cancer magister,* abdomen extension occurs in low salinity and for short periods upon return to 100% SW. Increased blood flow would supply the extensor muscles of the abdomen and may also aid in ion exchange across the hindgut.

Previous work on behavioral reactions of crabs to low salinity is largely confined to efficient osmoregulators, which show active avoidance of low salinity, changes in physiology, or both. These efficient hyperosmotic regulators actively uptake ions from the environment across their gills and eliminate excess water gained by osmosis, through the production of an iso-osmotic (to the hemolymph) urine (Pequeux, 1995). The hyperosmoregulating crabs (*Callinectes sapidus, Carcinus maenas*) responded to a decrease in salinity with an increase in activity, which may serve as an initial escape response (Fig. 2a, b). In addition, a number of other behavioral mechanisms may enhance the ability of these species to tolerate the low-salinity exposure. An increase in mouthpart movements (Fig. 3a, b) was correlated with ventilatory reversals that may increase the efficiency of ion exchange between the water and the posterior gills.

Chemoreceptors on the antennae and antennules were moved through the water during low-salinity exposure (cleaning and percentage time of antennule retraction, Figs. 5–6, a, b) and appear to be actively sensing the environment. In contrast, the strategy of the weak regulator (*Cancer magister*) and the osmoconformer (*Libinia emarginata*), after a short escape attempt, was to become quiescent and essentially isolate the main osmoregulatory organs, the gills, by decreasing passage of water through the branchial chambers. In addition to this isolation response, the chemoreception ability appears to have been compromised by the reduction in salinity, and the crabs no longer sampled the water by active movement of the antennules (Fig. 6c, d). Since most salinity variation is linked to the daily tidal changes, short-term isolation mechanisms may help reduce energy expenditure associated with escape responses or active regulation of the body fluids.

Many of the behaviors documented in the present study can be directly correlated with changes in the cardiovascular and osmoregulatory physiology. Previous reports on the inherent variability and discrepancies between studies of crustacean cardiovascular dynamics (Spaargaren, 1974; Hume and Berlind, 1976; Cumberlidge and Uglow, 1977; Taylor *et al.*, 1977; McGaw *et al.*, 1994b) are paralleled by intraspecific differences in behavior; as reported in the present study, a percentage of animals of each species exhibit a specific behavior, but some individuals may not. The causes of these discrepancies are unclear, but could be subtle differences such as intermolt duration or hormonal state, which can affect physiological ability (Reid *et al.*, 1989; McGaw and Naylor, 1992a, c; McGaw *et al.*, 1994b). The present study underscores the importance of studying behavioral reactions in conjunction with physiological measurements. Moreover, it provides evidence that well-studied gross physiological mechanisms to compensate for disturbances are linked with more subtle, behaviorally related modulations.

Acknowledgments

This work was supported by the Aquatic Biology Program at UNLV. We also thank Nicole Laundrie for help with data collection.

Literature Cited

Airriess, C. N., and B. R. McMahon. 1992. Aminergic modulation of circulatory performance in the crab *Cancer magister*. Pp. 123–131 in *Comparative Physiology*. R. B. Hill, K. Kuwasawa, B. R. McMahon, and T. Kuramoto, eds. Karger, Basel.

Ameyaw-Akumfi, C., and E. Naylor. 1987. Spontaneous and induced components of salinity preference behaviour in *Carcinus maenas*. *Mar. Ecol. Prog. Ser.* **37:** 153–158.

Arudpragasam, K. D., and E. Naylor. 1964. Gill ventilation and the role of reversed respiratory currents in *Carcinus maenas*. *J. Exp. Biol.* **41:** 299–307.

Arudpragasam, K. D., and E. Naylor. 1966. Patterns of gill ventilation in some decapod Crustacea. *J. Zool. Lond.* **150:** 401–411.

Audsley, N., C. McIntosh, and J. E. Phillips. 1992. Actions of ion-transport peptide from locust corpus cardiacum on several hindgut transport processes. *J. Exp. Biol.* **173:** 275–288.

Bettison, J. C., and J. Davenport. 1976. Salinity preference in gammarid amphipods with special reference to *Marinogammarus marinus*. *J. Mar. Biol. Assoc. UK* **56:** 135–142.

Bolt, S. L. R., and E. Naylor. 1985. Interaction of endogenous and exogenous factors controlling the locomotor activity rhythms in *Carcinus* exposed to tidal salinity cycles. *J. Exp. Mar. Biol. Ecol.* **85:** 47–56.

Broekhuysen, G. J. 1936. On development, growth and distribution of *Carcinus maenas*. *Arch. Neerl. Zool.* **2:** 257–399.

Cleaver, F. C. 1957. Preliminary results of coastal (*Cancer magister*) investigation. *Department of Fisheries, Washington State Biological Report* **49A:** 47–52.

Cornell, J. C. 1973. A reduction in water permeability in response to a dilute medium in the stenohaline crab *Libinia emarginata* (Brachyura, Majidae). *Biol. Bull.* **145:** 430–431.

Cornell, J. C. 1974. A reduction in water exchange rates in an osmoconforming crab. *Am. Zool.* **14:** 1259.

Cornell, J. C. 1980. Salt and water balance in two marine spider crabs, *Libinia emarginata* and *Pugettia producta*. III. Some factors involved in short-term adaptation to a dilute medium. *Biol. Bull.* **158:** 16–25.

Cumberlidge, N., and R. F. Uglow. 1977. Heart and scaphognathite activity in the shore crab *Carcinus maenas*. *J. Exp. Mar. Biol. Ecol.* **28:** 87–107.

Davenport, J. 1972. Salinity tolerance and preference in the porcelain crabs. *Mar. Behav. Physiol.* **1:** 1123–1128.

Davenport, J., and J. Wankowski. 1973. Pre-immersion salinity choice behaviour in *Porcellana platycheles*. *Mar. Biol.* **22:** 313–316.

Davenport, J., and T. M. Wong. 1987. Responses of adult mud crabs *Scylla serrata* to salinity and low oxygen tension. *Comp. Biochem. Physiol.* **86A:** 43–47.

Davenport, J., P. L. Busschots, and D. F. Cawthorne. 1980. The influence of salinity on the distribution, behaviour and oxygen uptake of the hermit crab *Pagurus bernhardus*. *J. Mar. Biol. Assoc. UK* **60:** 127–134.

Englehardt, F. R., and P. A. Dehnel. 1973. Ionic regulation in the Pacific edible crab *Cancer magister*. *Can. J. Zool.* **51:** 735–743.

Florkin, M., and E. Schoffeniels. 1969. Anisosmotic extracellular and isosmotic intracellular regulations as examples of physiological radiations of biochemical systems. Pp. 112–163 in *Molecular Approaches to Ecology*. Academic Press, New York.

Gilles, R. 1970. Osmoregulation in the stenohaline crab *Libinia emarginata*. *Arch. Physiol. Biochim.* **112:** 43–62.

Gleeson, R. A., L. M. McDowell, and H. C. Aldrich. 1996. Structure of the aesthetic (olfactory) sensilla of the blue crab, *Callinectes sapidus*: transformations as a function of salinity. *Cell Tissue Res.* **284:** 279–288.

Gleeson, R. A., M. G. Wheatly, and C. L. Reiber. 1997. Perireceptor mechanisms sustaining olfaction at low salinities: insight from the euryhaline blue crab *Callinectes sapidus*. *J. Exp. Biol.* **200:** 445–456.

Gross, W. J. 1955. Aspects of osmoregulation in crabs showing the terrestrial habit. *Am. Nat.* **89:** 205–222.

Gross, W. J. 1957. A behavioral mechanism for osmotic regulation in a semi-terrestrial crab. *Biol. Bull.* **113:** 168–174.

Haefner, P. A., and C. N. Schuster. 1964. Length increments during terminal molt of the female blue crab *Callinectes sapidus* in different salinity environments. *Chesapeake Sci.* **5:** 114–118.

Hedgpeth, J. 1967. Ecological aspects of the Laguna Madre, a hypersaline estuary. Pp. 408–419 in *Estuaries*, G. H. Lauff, ed. American Association for Advancement of Science, Washington, DC.

Heeg, J., and A. J. Cannone. 1966. Osmoregulation by means of a hitherto unsuspected organ in two grapsid crabs. *Zool Afr.* **2:** 127–129.

Hill, B. J. 1979. Biology of the crab *Scylla serrata* (Forskal) in the St Lucia system. *Trans R. Soc. S. Afr.* **44:** 55–62.

Hines, A. H., R. N. Lipcius, and A. M. Haddon. 1987. Population dynamics and habitat partitioning by size, sex and molt stage of blue crabs *Callinectes sapidus*, in a subestuary of central Chesapeake Bay. *Mar. Ecol. Prog. Ser.* **36:** 55–64.

Hughes, G. M., B. Knights, and C. A. Scammell. 1969. The distribution of PO_2 and hydrostatic pressure changes within the branchial chambers in relation to gill ventilation of the shore crab *Carcinus maenas* L. *J. Exp. Biol.* **51:** 203–220.

Hume, R. I., and A. Berlind. 1976. Heart and scaphognathite changes in a euryhaline crab *Carcinus maenas* exposed to a dilute medium. *Biol. Bull.* **150:** 241–254.

Hunter, K. C., and P. P. Rudy. 1976. Osmotic and ionic regulation in the Dungeness crab *Cancer magister* (Dana). *Comp. Biochem. Physiol.* **51A:** 439–447.

Jones, L. L. 1941. Osmotic regulation in several crabs of the Pacific coast of North America. *J. Cell. Comp. Physiol.* **18:** 79–91.

Kamemoto, F. I. 1976. Neuroendocrinology of osmoregulation in decapod Crustacea. *Am. Zool.* **6:** 141–150.

Krijgsman, B. J., and N. E. Krijgsman. 1954. Osmorezeption in *Jasus lalandii. Z. Vgl. Physiol.* **37:** 78–81.

Lagerspetz, K., and M. Mattila. 1961. Salinity reactions of some fresh and brackish water crustaceans. *Biol. Bull.* **120:** 44–53.

Lucu, C., D. Siebers, and K. R. Sperling. 1973. Comparison of osmoregulation between Adriatic and North Sea *Carcinus. Mar. Biol.* **22:** 85–95.

Lynch, M. P., K. L. Webb, and W. A. Van Engel. 1973. Variations in serum constituents of the blue crab *Callinectes sapidus.* Chloride and osmotic concentration. *Comp. Biochem. Physiol.* **44A:** 719–734.

Malley, D. F. 1977. Salt and water balance of the spiny lobster, *Panuliris argus*: the role of the gut. *J. Exp. Biol.* **70:** 231–245.

Mantel, L. H., and L. L. Farmer. 1983. Osmotic and ionic regulation. Pp. 54–142 in *Biology of Crustacea. Vol. 5. Internal Anatomy and Physiological Regulation*, L. H. Mantel, ed. Academic Press, New York.

Mangum, C. P., and L. M. Amende. 1972. Blood osmotic concentration of blue crabs (*Callinectes sapidus*) found in freshwater. *Chesapeake Sci.* **13:** 318–320.

McGaw, I. J. 1991. Behavioural responses of the shore crab *Carcinus maenas* to salinity variation. Ph.D. Thesis, University of Wales.

McGaw, I. J., and B. R. McMahon. 1995. The FMRFamide-related peptides F1 and F2 alter hemolymph distribution and cardiac output in the crab *Cancer magister. Biol. Bull.* **188:** 186–196.

McGaw, I. J., and B. R. McMahon. 1996. Cardiovascular responses resulting from variation in external salinity in the Dungeness crab *Cancer magister. Physiol. Zool.* **69:** 1384–1401.

McGaw, I. J., and B. R. McMahon. 1998. Endogenous rhythms of haemolymph flow and cardiac performance in the crab *Cancer magister. J. Exp. Mar. Biol. Ecol.* **224:** 127–142.

McGaw, I. J., and B. R. McMahon. 1999. Actions of putative cardioinhibitory substances on the *in vivo* decapod crustacean cardiovascular system. *J. Crust. Biol.* (in press).

McGaw, I. J., and E. Naylor. 1992a. Salinity preference of the shore crab *Carcinus maenas* in relation to coloration during intermoult and to prior acclimation. *J. Exp. Mar. Biol. Ecol.* **155:** 145–159.

McGaw, I. J., and E. Naylor. 1992b. The effect of shelter on salinity preference behaviour of the shore crab *Carcinus maenas. Mar. Behav. Physiol.* **21:** 145–152.

McGaw, I. J., and E. Naylor. 1992c. Distribution and rhythmic locomotor patterns of estuarine and open shore populations of *Carcinus maenas. J. Mar. Biol. Assoc. UK* **72:** 599–609.

McGaw, I. J., and C. L. Reiber. 1998. Circulatory modification in the blue crab *Callinectes sapidus*, during exposure and acclimation to low salinity. *Comp. Biochem. Physiol.* **121A:** 67–76.

McGaw, I. J., M. J. Kaiser, E. Naylor, and R. N. Hughes. 1992. Intra-specific morphological variation related to the moult-cycle in colour forms of the shore crab *Carcinus maenas. J. Zool. (Lond.)* **228:** 351–359.

McGaw, I. J., C. N. Airriess, and B. R. McMahon. 1994a. Peptidergic modulation of cardiovascular dynamics in the Dungeness crab *Cancer magister. J. Comp. Physiol.* **164:** 103–111.

McGaw, I. J., C. N. Airriess, and B. R. McMahon. 1994b. Patterns of haemolymph flow variation in decapod crustaceans. *Mar. Biol.* **121:** 53–60.

McGaw, I. J., J. L. Wilkens, B. R. McMahon, and C. N. Airriess. 1995. Crustacean cardioexcitatory peptides may inhibit the heart *in vivo. J. Exp. Biol.* **198:** 2547–2550.

McLaughlin, P. A. 1983. Internal anatomy. Pp. 1–41 in *Biology of the Crustacea. Vol. 5. Internal Anatomy and Physiological Regulation*, L. H. Mantel, ed. Academic Press, New York.

McLusky, D. S. 1970. Salinity preference in *Corophium volutator. J. Mar. Biol. Assoc. UK* **50:** 747–752.

Neufeld, G. J., C. W. Holliday, and J. B. Pritchard. 1980. Salinity adaptation of gill Na,K-ATPase in the blue crab, *Callinectes sapidus. J. Exp. Zool.* **211:** 215–224.

Pearson, J. 1908. *Cancer* (the edible crab). *Proc. Trans. Liverpool Biol. Soc.* **22:** 291–499.

Pequeux, A. 1995. Osmotic regulation in crustaceans. *J. Crustac. Biol.* **15:** 1–60.

Phillips, J. E., J. Hanrahan, M. Chamberlin, and R. B. Thomson. 1986. Mechanisms of control of reabsorption in insect hindgut. *Adv. Insect Physiol.* **19:** 329–422.

Rankin, J. C., and J. Davenport. 1981. *Animal Osmoregulation: Tertiary Level Biology.* Blackie and Son, Glasgow.

Rasmussen, A. D., and P. Bjerregaard. 1995. The effect of salinity and calcium concentration on the apparent water permeability of *Cherax destructor, Astacus astacus* and *Carcinus maenas* (Decapoda, Crustacea). *Comp. Biochem. Physiol.* **111A:** 171–175.

Reid, D. G., P. Abello, I. J. McGaw, and E. Naylor. 1989. Phenotypic variation in sympatric crab populations. Pp. 89–96 in *Phenotypic Responses and Individuality in Aquatic Ectotherms*, J. C. Aldrich, ed. JAPAGA Ashford, Wicklow, Ireland.

Schmidt, M. 1989. The hair-peg organs of the shore crab, *Carcinus maenas* (Crustacea, Decapoda): ultrastructure and function properties of sensilla sensitive to changes in seawater concentration. *Cell Tissue Res.* **257:** 609–621.

Shelton, R. G., and M. S. Laverack. 1970. Receptor hair structure and function in the lobster *Homarus gammarus* (L.). *J. Exp. Mar. Biol. Ecol.* **4:** 201–210.

Siebers, D., K. Leweck, H. Markus, and A. Winkler. 1982. Sodium regulation in the shore crab *Carcinus maenas* as related to ambient salinity. *Mar. Biol.* **69:** 37–43.

Siebers, D., A. Winkler, K. Leweck, and A. Madian. 1983. Regulation of sodium in the shore crab *Carcinus maenas*, adapted to environments of constant and changing salinities. *Helgol. Meeresunters.* **36:** 303–312.

Siebers, D., A. Winkler, C. Lucu, G. Thiedens, and D. Weichert. 1985. Na-K-ATPase generates an active transport potential in the gills of the hyperregulating shore crab *Carcinus maenas. Mar. Biol.* **87:** 185–192.

Siebers, D., C. Lucu, A. Winkler, L. Dalla Venezia, and H. Wille. 1986. Active uptake of sodium in the gills of the hyperregulating shore crab *Carcinus maenas. Helgol. Meersunters.* **40:** 151–160.

Spaargaren, D. H. 1974. Measurements of the relative rate of blood flow in the shore crab *Carcinus maenas* at different temperatures and salinities. *Neth. J. Sea Res* **8:** 398–406.

Spaargaren, D. H. 1982. Cardiac output in the crab. *Carcinus maenas*

(L.) in relation to solute exchange and osmotic pressure. *Mar. Biol. Lett.* **3:** 231–240.

Sugarman, P. C., W. H. Pearson, and D. L. Woodruff. 1980. Detection of thresholds and behavioral responses to salinity changes by the Dungeness crab *Cancer magister. Am. Zool.* **20:** 922.

Tan, E. C., and W. A. Van Engel. 1966. Osmoregulation in the adult blue crab *Callinectes sapidus,* Rathbun. *Chesapeake Sci.* **7:** 30–35.

Taylor, A. C. 1977. Respiratory responses of *Carcinus maenas* to changes in environmental salinity. *J. Exp. Mar. Biol. Ecol.* **29:** 197–210.

Taylor, A. C., and E. Naylor. 1977. Entrainment of the locomotor rhythm of *Carcinus maenas* by cycles of salinity change. *J. Mar. Biol. Assoc. UK* **57:** 273–277.

Taylor, E. W., P. J. Butler, and A. Al-Wassia. 1977. The effect of a decrease in salinity on respiration, osmoregulation and activity in the shore crab *Carcinus maenas* at different acclimation temperatures. *J. Comp. Physiol.* **119:** 155–170.

Tazaki, K. 1975. Sensory units responsive to osmotic stimuli in the antennae of the spiny lobster, *Panuliris japonicus. Comp. Biochem. Physiol.* **51A:** 647–653.

Thomas, N. J., T. A. Lasiak, and E. Naylor. 1981. Salinity preference behaviour in *Carcinus. Mar. Behav. Physiol.* **7:** 277–282.

Van-Weel, P. B., and J. P. Christofferson, 1966. Electrophysiological studies on various stimuli in the antennulae of certain crabs. *Physiol. Zool.* **39:** 317–325.

Warman, C. G., P. Abello, and E. Naylor. 1991. Behavioural responses of *Carcinus mediterraneus* Czernaivsky, 1884, to changes in salinity. *Sci. Mar.* **55:** 637–643.

Reference: *Biol. Bull.* **196:** 177–186. (April 1999)

Protein Metabolism in Lecithotrophic Larvae (Gastropoda: *Haliotis rufescens*)

JAY VAVRA AND DONAL T. MANAHAN*

Department of Biological Sciences, University of Southern California,
Los Angeles, California 90089-0371

Abstract. Rates of protein depletion, synthesis, and turnover were measured in larvae of the abalone *Haliotis rufescens* as an approach to understanding macromolecular metabolism during lecithotrophic development. Protein content decreased linearly during development to metamorphic competence, with 34% of the initial protein in eggs depleted during the 8-day larval life span. Fractional rates of protein synthesis (percentage of total body-protein synthesized per day) decreased during development, from 40% (1-day-old trochophore larva) to 14% (7-day-old veliger larva). Separation of proteins by one-dimensional gel electrophoresis showed that protein pools in larvae are dominated by two high-molecular-weight protein classes (88 and 121 kDa). When the proteins of 1- and 3-day-old larvae were labeled with a mixture of ^{35}S-methionine and cysteine, the pattern on two-dimensional gels showed that the turnover process (protein synthesis and degradation) involved hundreds of different proteins. The energy gained from loss of protein could account for 20% of the protein turnover rates for trochophore larvae and 79% of the lower turnover costs for late-stage veligers. Lecithotrophic larvae of *H. rufescens* maintained high biosynthetic activities, with up to 40% of their whole-body protein being turned over each day. Such dynamic processes during development of nonfeeding larvae would contribute significantly to maintenance metabolism.

Introduction

Nonfeeding (lecithotrophic) larval forms are widely represented in the life cycles of many marine invertebrate taxa (Thorson, 1950; Strathmann, 1978; Pearse, 1994). Nevertheless, our understanding of metabolic processes during lecithotrophic larval development is very limited compared to what is known about metabolism and the dynamics of biosynthetic processes in species with planktotrophic development (*e.g.,* protein synthesis in sea urchin embryos: Goustin and Wilt, 1981; Bedard and Brandhorst, 1983). Most studies of the biochemistry and physiology of lecithotrophic larvae have focused on the composition of energy reserves in the early stages of development (Turner and Rutherford, 1976; Jaeckle and Manahan, 1989a; Anger, 1996). The importance of maternally endowed energy supply to larval life span has also been studied (Shilling and Manahan, 1994; Ben-David-Zaslow and Benayahu, 1998), as have respiration rates and amino acid transport (Jaeckle and Manahan, 1989a, b; Shilling *et al.*, 1996; Hoegh-Guldberg and Emlet, 1997).

The aim of this study is to quantify the energetics of protein degradation and synthesis (turnover) in a lecithotrophic larval form. Protein metabolism was chosen as the focus of this study because protein, not lipid, has been reported (Jaeckle and Manahan, 1989a) to be the major endogenous energy reserve utilized by larvae of *Haliotis rufescens* (red abalone), a species with lecithotrophic development.

Materials and Methods

Larval culture

Adult abalone (*Haliotis rufescens*) were spawned and fertilized at a commercial hatchery (Ab Lab, Port Hueneme, California). All cultures were started using gametes from 1 male and 2–3 females (different adults were used for each culture). Zygotes and larvae were maintained at 14–15°C in unstirred, UV-irradiated seawater that had been passed through a 5-μm (pore size) filter; the larvae were reared on

---

Received 28 May 1998; accepted 6 January 1999.

* To whom correspondence should be addressed. E-mail: manahan@usc.edu

80-μm mesh screens. Under these culturing conditions, it took 6–8 days for larvae to reach metamorphic competence, as determined by ability to undergo metamorphosis when induced with γ-aminobutyric acid (GABA).

Change in total protein

Throughout development, samples (Culture 1, $n = 4$–5 independent samples; Culture 2, $n = 3$ independent samples) containing 50–75 individuals were taken for measurement of protein content (Bradford assay, 1976; as modified by Jaeckle and Manahan, 1989a). The rate of protein loss during development was calculated from the linear regression of total protein per individual with time, during the period from egg to metamorphic competence. Protein content of eggs (day zero) was determined only for Culture 1.

Rates of amino acid transport

To determine absolute rates of protein synthesis, rates of amino acid transport by larvae were measured during the ^{14}C-labeling experiments (see Manahan, 1983, for methods). All physiological rates were measured at 15° ± 0.1°C. Each transport assay used 5000 larvae in 10 ml of filtered (pore size 0.2 μm) seawater to which was added 1 μCi ml^{-1} of ^{14}C-(U)-glycine (New England Nuclear; 110 μCi μmol^{-1}). The rate of isotope transport was measured (500 μl sample every 2–3 min) during a 16–18-min exposure of larvae to 9 μM glycine in seawater.

Rates of protein synthesis

A modified radioisotope-labeling protocol, based on that of Fry and Gross (1970) for sea urchin embryos, was used to measure absolute rates of protein synthesis in abalone larvae. Our modifications included trace labeling over a short time interval (<18 min) to minimize possible effects of perturbations, caused by high transport rates of exogenous ^{14}C-labeled amino acid, of the free amino acid pool. A short exposure also avoided the interconversion of ^{14}C-glycine, the tracer used in our measurements, into other amino acids (confirmed by analysis with high-performance liquid chromatgraphy, HPLC). Short experiments also minimized any effects from protein degradation (*i.e.*, reutilization of ^{14}C-labeled amino acids due to protein breakdown). Glycine was used as the tracer because it is transported at a high rate and is a measurable fraction of the free amino acid pool in larvae of *H. rufescens* (Fig. 1). These characteristics allowed for accurate HPLC measurement of the change, with time, in the specific activity of glycine in the free amino acid pools of larvae (Fig. 2A). Also, glycine in acid-hydrolyzed, whole-body protein extracts of *H. rufescens* larvae (Table 1) could be measured with HPLC; this value is required for calculation of absolute rates of protein synthesis (see below).

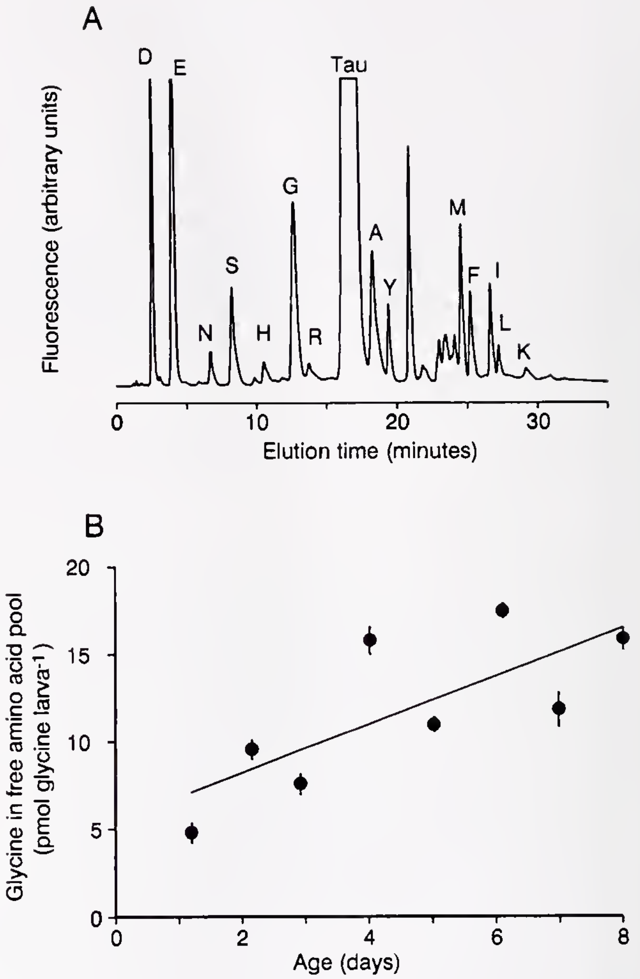

Figure 1. Glycine in the free amino acid pool of larvae of *Haliotis rufescens.* (A) Chromatogram showing the separation of amino acids extracted from 3-day-old veliger larvae by reverse-phase high-performance liquid chromatography: D, aspartic acid; E, glutamic acid; N, asparagine; S, serine; H, histidine; G, glycine; R, arginine; Tau, taurine; A, alanine; Y, tyrosine; M, methionine; F, phenylalanine; I, isoleucine; L, leucine; K, lysine (unknown peaks are unlabeled). (B) Change in the amount of glycine in free amino acid pools through larval development. Error bars represent ± 1 SE of the mean ($n = 6$ for each stage). The equation for the linear regression is pmol glycine larva^{-1} = $1.51x + 5.16$; where x = age in days ($r^2 = 0.50$; $n = 48$).

Rates of protein synthesis were determined by measuring the rate of incorporation of ^{14}C-glycine into protein [defined as the 5% trichloroacetic acid (TCA)-insoluble fraction of larval homogenates, shell included]. For measurements from the free amino acid pools, the intracellular contents of larvae were extracted overnight into 70% ethanol. The specific activity of glycine was then determined with HPLC (Welborn and Manahan, 1995) for each larval stage studied. After detection of fluorescence (*i.e.*, moles of glycine: Fig. 1A, B), post-column samples of eluent were collected every 30 s (LKB fraction collector) and mixed with scintillation cocktail to determine the amount of radioactivity in the

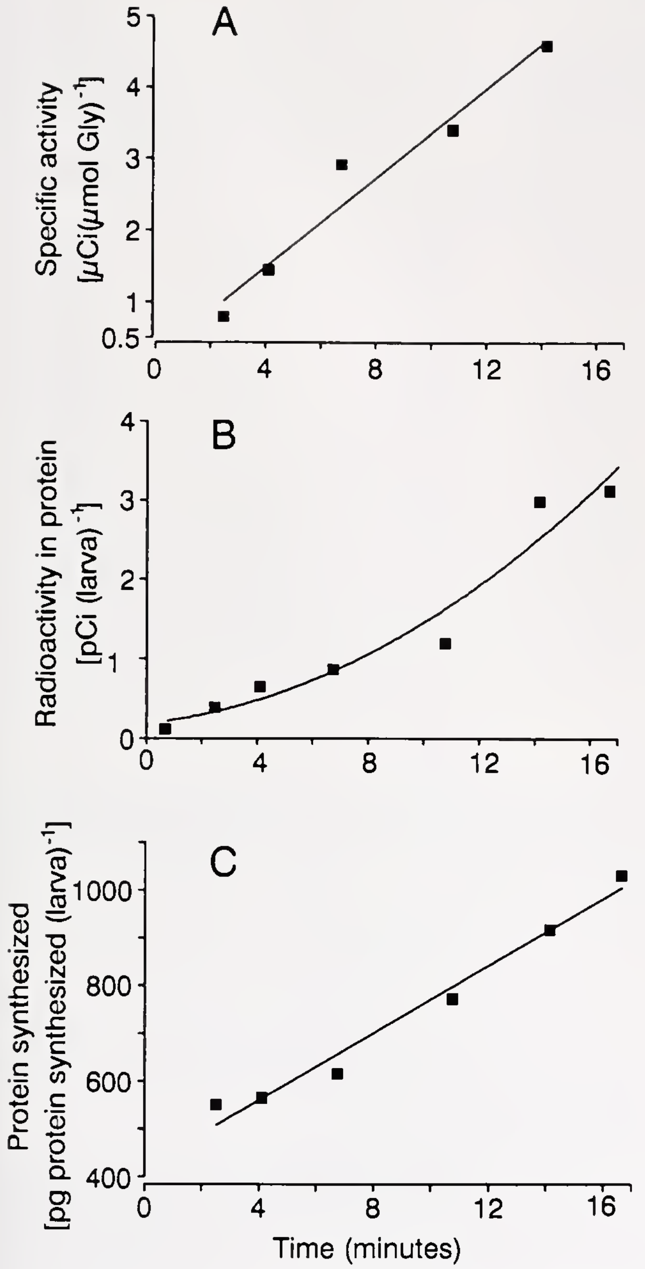

Figure 2. Determination of the absolute rate of protein synthesis in 7-day-old veliger larvae of *Haliotis rufescens.* (A) Specific activity of intracellular glycine in the free amino acid pool following transport of ^{14}C-glycine. Each point represents the specific activity determined by high-performance liquid chromatography using fluorescence detection (moles of glycine) and measurement by liquid scintillation counting of radioactivity in the glycine peak collected from the chromatographic eluent. (B) Radioactivity in the trichloroacetic acid (TCA)-insoluble fraction (protein). (C) Rate of protein synthesis after correcting the TCA-insoluble fraction for the change in intracellular specific activity of ^{14}C-glycine, the mole percent of glycine in protein, and the average mole-percent corrected molecular weight of amino acids in larval protein (Table I).

glycine peak. All measurements of radioactivity (as counts per min, CPM) were corrected for quenching and converted to total disintegrations per min (DPM). By correcting for the change in the specific activity of glycine in the free amino acid pool (Fig. 2A), the incorporation rate of ^{14}C-glycine (Fig. 2B) could be converted to the total amount of glycine incorporated into protein (both ^{12}C- and ^{14}C-glycine). The value for the incorporation of total glycine into protein was then converted to an absolute rate of protein synthesis (Fig. 2C) by determining the mole-percent of glycine in larval protein and the mole-percent-corrected molecular weight of all amino acids in larval protein of *H. rufescens* (Table I). The components required for the calculation of the absolute rate of protein synthesis are

$$k_s = \frac{MW_p}{S_m} \times \frac{d}{dt}\left(\frac{S_p}{S_{faa}}\right)$$

where k_s is the rate of protein synthesis, MW_p is the mole-percent-corrected molecular weight of amino acids in larval protein, S_m is the mole-fraction of glycine in protein, S_p is the amount of radioactivity in protein, and S_{faa} is the specific activity of glycine in the free amino acid pool, which changed during the time course of exposure to isotope (Fig. 2A). The above equation was solved for each sampling time interval during which the incorporation of ^{14}C-glycine into protein was measured (Fig. 2B).

Patterns of protein synthesis

For the analysis of the electrophoretic patterns of protein synthesis, each labeling experiment used 10,000–15,000 larvae in 14 ml of filtered seawater with 200 μCi of ^{35}S-methionine/cysteine (1100–1200 Ci mmol^{-1}, New England Nuclear). Non-radiolabeled methionine was added to seawater (final concentration of 500 n*M*) to increase substrate concentration and, hence, transport rates. After a 3-h incubation, unincorporated isotope was removed with three successive seawater washes after the larvae were pelleted in 15-ml conical tubes with a hand centrifuge. Protein samples for electrophoresis were prepared by ultrasonicating embryos or larvae in 50 m*M* Tris-HCl at pH 7.2. Samples were kept on ice during this process to prevent any rise in temperature. Homogenates were centrifuged to remove larval shell (30 min at 15,000 × *g*, 4°C) prior to electrophoresis. The amount of ^{35}S-methionine/cysteine incorporated into protein was determined by TCA (5%) precipitation of 10-μl aliquots ($n = 2$) of the homogenate. Tissue solubilizer (0.5 ml, Scintigest, Fisher Co.) was added to these precipitates before the radioactivity was counted. These data were required for loading of equal amounts of radioactivity on each gel to permit comparisons of different larval stages (see Results). The amount of protein loaded on each gel was also determined.

Table I

Amino acid composition (mole-percent) of proteins in larval stages of Haliotis rufescens

Amino acid	Age (days after fertilization)						Mean (± SEM)
	2	3	4	5	6	8	
Glutamic acid & Glutamine*	9.9	10.0/10.6	8.6	10.5/10.5	10.7/10.5	10.5	10.2 (0.2)
Alanine	8.4	8.3/8.0	9.0	9.1/8.1	8.1/8.3	8.4	8.4 (0.1)
Glycine	7.0	7.5/7.7	9.9	8.2/8.1	8.0/7.8	8.1	8.0 (0.2)
Aspartic acid & Asparagine*	7.4	7.2/7.3	7.9	6.3/6.4	7.8/7.9	7.6	7.3 (0.2)
Lysine	6.5	6.7/6.5	6.2	6.9/8.1	6.8/7.7	7.4	7.0 (0.2)
Serine	7.0	7.2/7.1	6.3	7.2/7.1	6.9/6.7	7.1	7.0 (0.1)
Leucine	6.8	6.8/6.7	6.8	6.6/7.4	6.6/6.8	6.2	6.8 (0.1)
Valine	6.4	6.9/6.9	6.3	7.2/7.0	6.3/6.2	5.7	6.5 (0.2)
Isoleucine	6.8	6.8/6.7	6.8	3.9/7.4	6.6/6.8	6.2	6.5 (0.3)
Threonine	6.4	5.9/7.0	6.2	6.3/5.4	5.8/5.5	5.6	6.0 (0.2)
Arginine	6.0	6.1/5.7	5.8	6.5/5.8	5.8/5.7	6.2	6.0 (0.1)
Proline	5.9	6.4/5.8	5.2	5.1/5.8	5.0/4.8	4.9	5.4 (0.2)
Tyrosine	4.7	4.0/3.9	5.0	4.0/3.3	4.7/4.6	4.4	4.3 (0.2)
Phenylalanine	3.9	4.0/3.8	3.9	4.0/4.7	4.2/4.2	4.0	4.1 (0.1)
Methionine	3.6	2.8/3.3	3.3	6.1/2.7	3.5/3.3	4.4	3.7 (0.3)
Histidine	2.4	2.6/2.3	1.9	1.7/1.6	2.5/2.4	2.2	2.2 (0.1)
Cysteine	0.8	0.9/0.8	0.8	0.3/0.7	0.8/0.7	1.2	0.8 (0.1)
Mole-percent corrected MW_p†	136.1	135.6/135.1	133.7	134.9/135.0	136.2/136.5	136.8	135.5 (0.3)

All values are calculated as mole percents; where two values are separated by a slash (*e.g.*, 10.0/10.6), this represents two replicate chromatographic analyses for that sample.

* During acid hydrolysis, asparagine and glutamine form aspartic acid and glutamic acid, respectively.

† Mole-percent corrected molecular weights (MW_p) represent the average molecular weight of amino acids in larval protein determined by multiplying each mole percent value by the appropriate molecular weight (*e.g.*, glycine: 0.08 * 75.1 g mol^{-1}), and then taking the sum of all of the mole-percent corrected molecular weights of each amino acid.

Protein extracts of larvae were separated with one- and two-dimensional polyacrylamide gel electrophoresis (PAGE). One-dimensional sodium dodecyl sulfate (SDS)-PAGE was conducted according to Laemlli (1970), with equal amounts of radiolabeled protein (1×10^6 DPM) loaded per lane, totaling about 30 μg protein. The proteins resolved by electrophoresis were stained with Coomassie brilliant blue (Biorad) and were exposed to X-ray film (XOMAT AR, Eastman Kodak) for 24 h. Two-dimensional gel electrophoresis was conducted with pre-cast gels on the Multiphor system (LKB-Pharmacia) following the manufacturer's protocol for the first dimension Immobiline Dry Strip Kit and the second dimension ExcelGel SDS (LKB-Pharmacia: publication 18-1038-63, edition AA). For two-dimensional gels, samples were loaded with equal amounts of radiolabeled protein (3×10^6 DPM), totaling about 100 μg protein per loading. The two-dimensional gels of the different larval stages, each loaded with equivalent amounts of radioactivity, were exposed to X-ray film for an identical time period (8 days).

Results

Change in total protein

There was a linear decrease in protein during development of *Haliotis rufescens* (Fig. 3). The rate of protein loss was not statistically different between Culture 1 (23.7 ± 5.7 ng day^{-1} [± 1 SE of the slope]) and Culture 2 (22.5 ± 5.7 ng day^{-1}); ANOVA: $F_{[1,59]}$ for comparison of slopes = $0.17^{\text{n.s.}}$ and for comparison of y-intercepts = $0.17^{\text{n.s}}$. All data were combined to calculate a rate of protein loss from egg to metamorphic competence (nanograms of protein per larva = $-21.2\,x + 498.6$, where x = age in days; SE of slope = 3.52; n = 68). By the end of larval development, 8-day-old larvae still had 66% of their initial (egg) protein content (from regression analysis, Table II).

Glycine transport

Larvae had higher rates of glycine transport near metamorphosis (Culture 1: day 6 = 9.6 pmol glycine larva^{-1} h^{-1}; Culture 2: day 8 = 9.3 pmol glycine larva^{-1} h^{-1}; Fig.

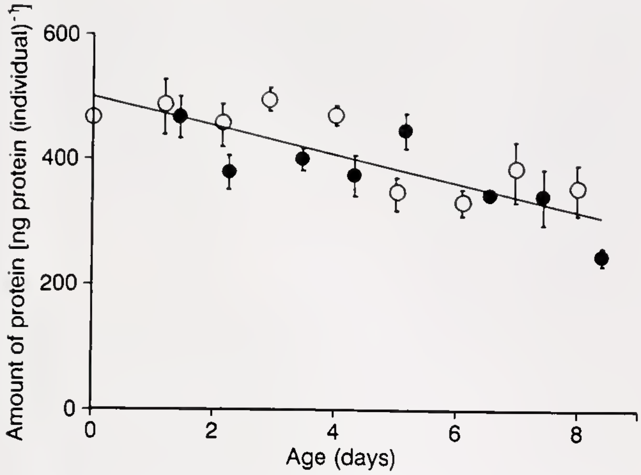

Figure 3. Total protein content during development of *Haliotis rufescens*. Data from two cultures are shown: Culture 1 (n = 4–5 independent samples per data point; ○) and Culture 2 (n = 3 independent samples per data point; ●). Protein content of eggs was determined only for Culture 1. Rates of protein loss were not statistically different between cultures (see text), and all data were combined to calculate the rate of protein loss during development: ng protein individual^{-1} = $-21.2\,x + 498.6$, where x = age in days (SE of slope = 3.52, n = 68). Error bars are ±1 SEM.

4). Combining all glycine transport data for both cultures revealed that transport rates were significantly higher at metamorphic competence (based on larvae before and after day 6; $t_{[24]} = 2.81$, $P < 0.005$).

Table II

Protein synthesis and fractional rates of protein turnover during larval development of Haliotis rufescens

Age (days)	Total protein (ng larva^{-1})	Protein synthesis rate (ng protein synthesized larva^{-1} day^{-1})	Fractional rates of protein turnover (% total protein synthesized day^{-1})
1	477	193	40
2	456	150	33
3	435	115	26
4	414	87	21
5	393	67	17
6	371	54	15
7	350	49	14

Total protein amounts (nanograms of protein per larva) were calculated from the least-squares linear regression of the change in protein content calculated for two different cultures during development (Fig. 3: ng protein larva^{-1} = $-21.2\,x + 498.6$, where x = age in days). Changes in the absolute rate of protein synthesis during development were calculated from the second-order polynomial (Fig. 5: ng protein synthesized day^{-1} = $3.76\,x^2 - 54.09\,x + 243.52$, where x = age in days). Fractional rates of protein turnover (percentage of whole-body protein synthesized per larva per day) were calculated from the ratio of the rate of protein synthesis to total protein content at the corresponding stage of development.

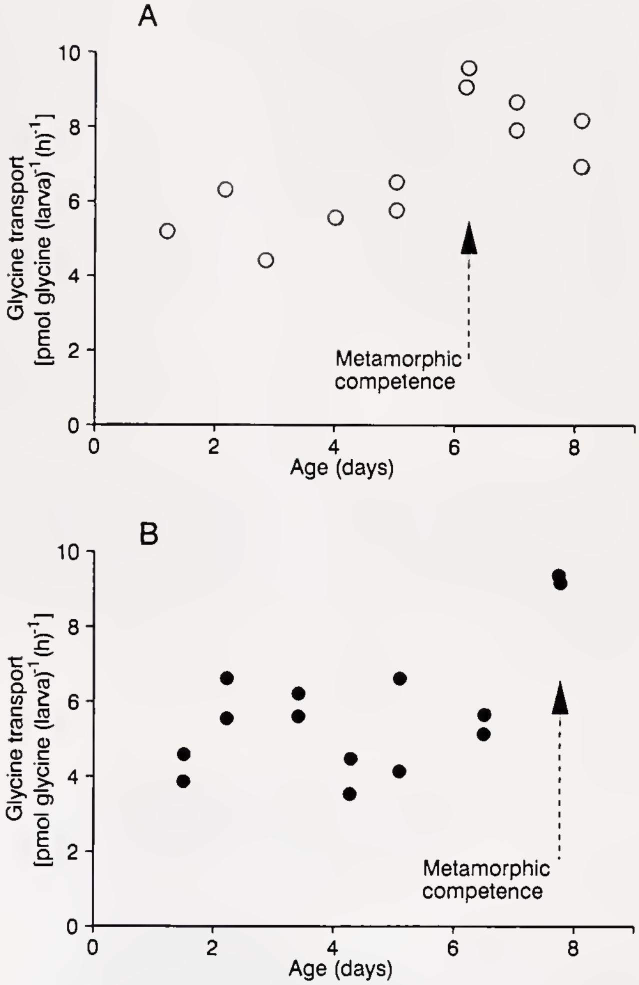

Figure 4. Transport of ^{14}C-glycine (9 μM) from seawater by larvae of *Haliotis rufescens*. Each data point represents the rate of transport calculated from a regression of a separate time-course experiment (4–5 samples per experiment, with about 250 larvae per sample; all assays had r^2 values > 0.96). Data are shown for two cultures: Culture 1 (A) and Culture 2 (B). Arrows show the time when metamorphic competency was reached for larvae from each culture.

Glycine content in free amino acid pools and protein

The amount of glycine in the free amino acid pool increased significantly during development (ANOVA: $F_{[1,46]} = 45.43$, $P < 0.0005$; Fig. 1B). The linear increase in glycine during larval development is represented by the following equation: picomoles of glycine per larva = $1.51\,x + 5.16$, where x = age in days ($r^2 = 0.50$; $n = 48$). Over the larval life span, glycine only represented about 1% of the total free amino acid pool (see Fig. 1A), with taurine being the dominant amino acid. The mole-percent of glycine in protein did not change during development (from glycine data in Table I: ANOVA of the regression slope of protein-glycine over time was not significantly different from zero, $F_{[1,7]} = 0.44^{\text{n.s.}}$). The mean mole-percent of

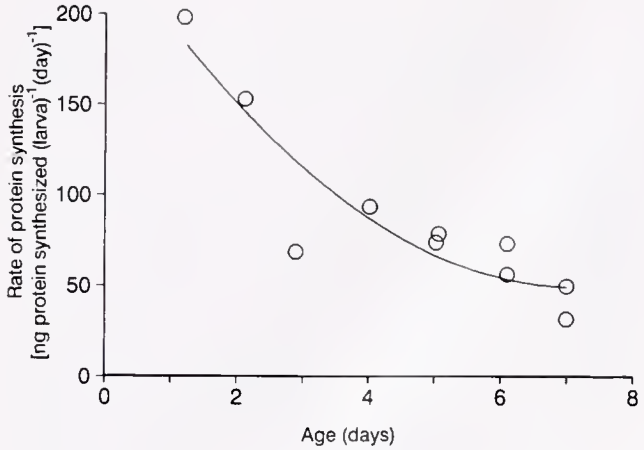

Figure 5. Absolute rates of protein synthesis during larval development of *Haliotis rufescens*. Each data point represents a rate of protein synthesis determined from the slope of a separate time-course experiment, based on multiple samples (as in Fig. 2). The decrease in protein synthesis with development was fitted to a second-order polynomial: ng protein synthesized larva^{-1} day^{-1} = $3.76x^2 - 54.09x + 243.52$, where x = age in days.

glycine in the proteins of 2- to 8-day-old larvae was 8.0% (±0.2 SEM), and this value was used for all calculations of protein synthesis rates. The mole-percent corrected molecular weight of amino acids in larval protein ranged from 133.7 to 136.8 g amino acid mol^{-1}, with a mean value of 135.5 (±0.3, SEM) used for all calculations (Table I).

Rates of protein synthesis

Rates of protein synthesis decreased during development, from 193 to 49 ng protein synthesized larva^{-1} day^{-1} (calculated from analysis given in Table II of data shown in Fig. 5). The decrease was nonlinear and was best described by a second-order polynomial (nanograms of protein synthesized per larva = $3.76x^2 - 54.09x + 243.52$, where x = age in days). The fractional rate of protein synthesis, expressed as the percentage of total whole-body protein synthesized per day, also showed a steady decline through larval development and decreased from 40% (1-day-old) to 14% (7-day-old) (Table II: comparison of total protein content per larva and absolute rate of protein synthesis).

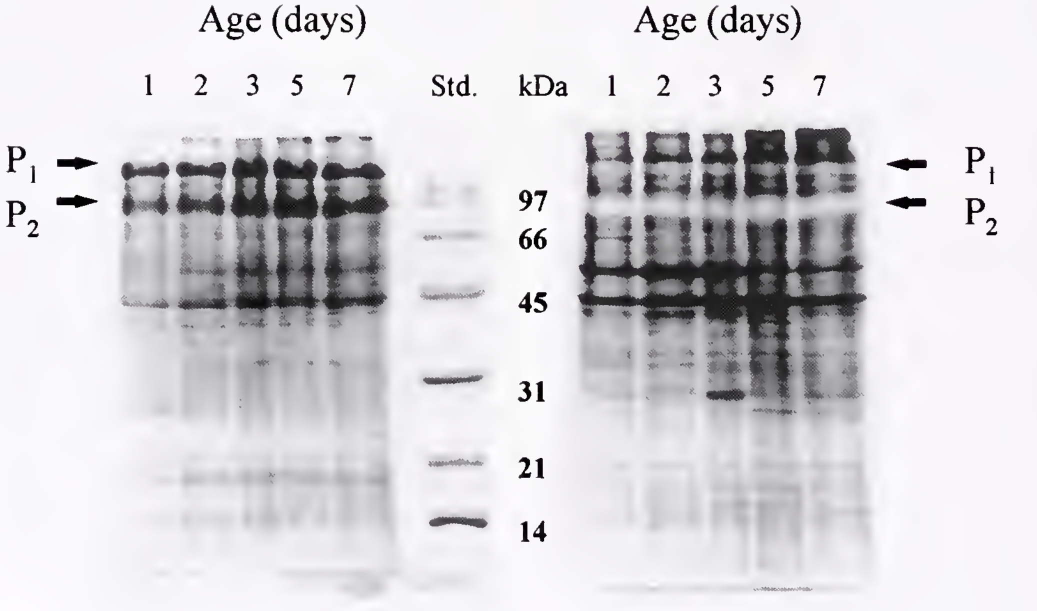

A. Coomassie-stained gel showing protein classes

B. Autoradiogram showing ^{35}S incoporation into protein

Figure 6. One-dimensional sodium dodecyl sulfate polyacrylamide gel electrophoretic analysis of total soluble proteins in larvae of *Haliotis rufescens*. (A) Coomassie-stained protein pools. (B) Corresponding autoradiogram of proteins labeled with ^{35}S-methionine/cysteine (*i.e.*, newly synthesized proteins). Each lane contains a different larval stage (day 1, 2, 3, 5, and 7) and equal radioactivity (1×10^6 DPM loaded per lane). Bands marked P_1 and P_2 are high-molecular-weight proteins present at each stage of larval development as shown in the Coomassie-stained gel (A) and are not radiolabeled in the autoradiogram (B). Molecular-weight standards are represented with markers from 97 to 14 kDa.

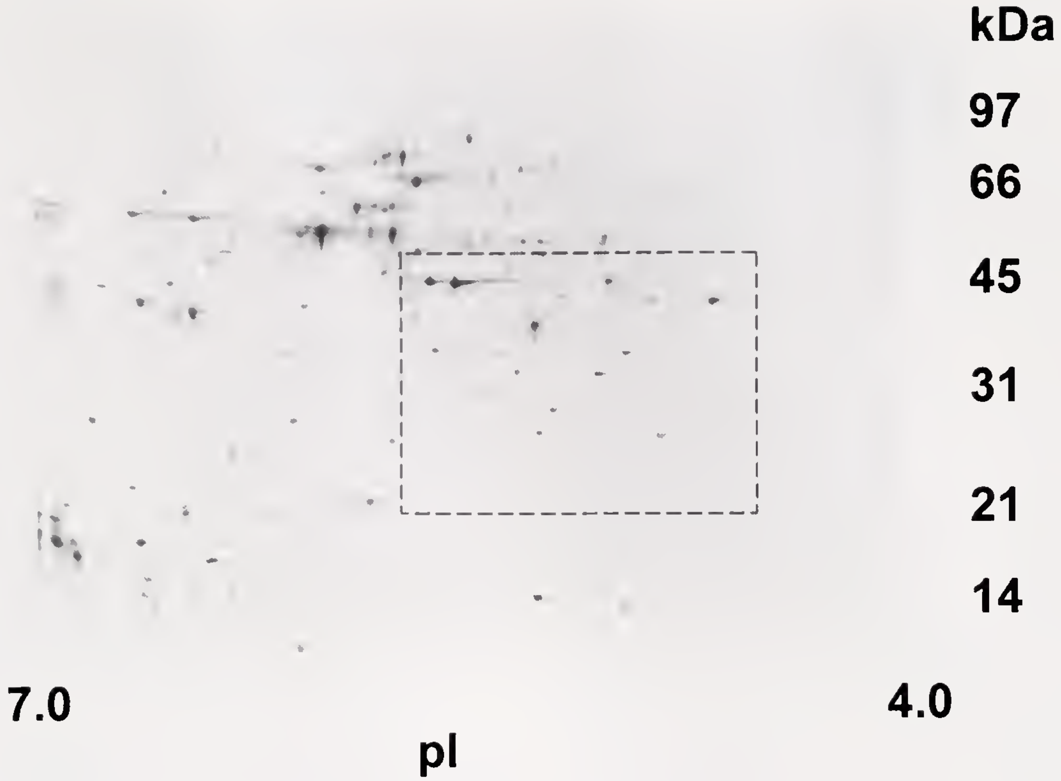

Figure 7. Autoradiogram of proteins in 3-day-old veliger larvae of *Haliotis rufescens* labeled with ^{35}S-methionine/cysteine and separated by two-dimensional gel electrophoresis. Area bounded by the dashed box is displayed in expanded form in Figure 8B. Molecular-weight standards correspond to Coomassie-stained gel (not shown) with markers from 97 to 14 kDa. Isoelectric points (pI) fall within a linear pH gradient from 7.0 to 4.0.

Patterns of protein synthesis

At the analytical resolution of one-dimensional gel electrophoresis, similar patterns of Coomassie-stained proteins were evident during development (1- to 7-day-old larvae). Two classes of high-molecular-weight protein (Fig. 6A: labeled as P_1 and P_2 at 121 and 88 kDa, respectively) dominated the Coomassie-stained protein pool at each larval stage analyzed. The patterns of the existing pool of proteins (Fig. 6A: Coomassie-stained proteins) were different than those of the newly synthesized proteins (Fig. 6B: autoradiogram of labeled proteins), with no detectable synthesis of the two high-molecular-weight protein classes at any larval stage (note lack of signal in Fig. 6B autoradiogram for P_1 and P_2).

The patterns of synthesis of individual proteins were compared, using two-dimensional gel electrophoresis (Figs. 7, 8), for the trochophore stage (1-day-old) and a veliger stage (3-day-old). The two-dimensional separation resolved over 300 proteins that were being synthesized in larvae (Fig. 7). The results of a qualitative analysis (visual absence or presence) are given in Figure 8 to show some of the different proteins being synthesized by 1- and 3-day-old larvae. The main point illustrated in Figures 7 and 8 is that protein synthesis in these larval forms is not limited to any single group (MW or pI) of proteins, but involves many proteins and complex patterns.

Discussion

Larval stages of *Haliotis rufescens* lost protein reserves continuously during development (Fig. 3). By day 8, veligers that were competent to metamorphose contained 34% less protein than the egg. The average daily loss of protein was 21.2 ng protein larva^{-1} day^{-1} (average rate of both cultures, Fig. 3), equivalent to 509 μJ day^{-1} (24.0 kJ g^{-1} protein; Gnaiger, 1983). During this period of protein loss, the absolute rates of protein synthesis decreased fourfold, from 193 to 49 ng protein synthesized larva^{-1} day^{-1} for 1-day-old trochophores and 7-day-old veliger larvae, respectively (Fig. 5; Table II). Note that the rate of protein loss was linear with time (Fig. 3), whereas the decrease in the rate of protein synthesis was nonlinear (Fig. 5). The relationship of these ontogenetic changes in protein loss and synthesis was analyzed further by calculating the fractional rates of protein synthesis during development. When

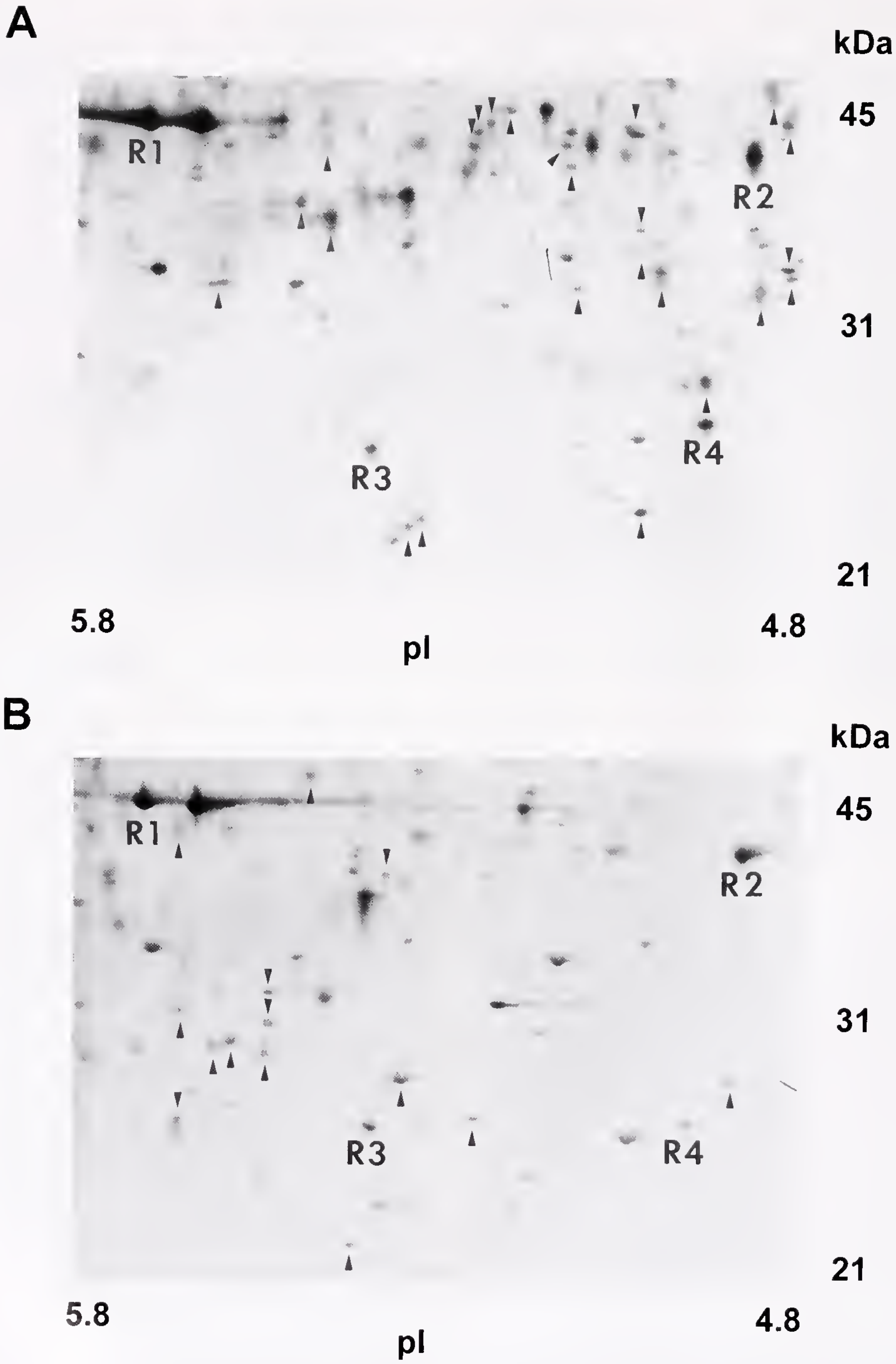

Figure 8. Autoradiograms of two-dimensional separation of ^{35}S-labeled proteins in (A) 1-day-old trochophore larvae and (B) 3-day-old veliger larvae of *Haliotis rufescens* (see Fig. 7 for the entire two-dimensional pattern of protein synthesis for the veliger stage). Each gel was loaded with equal radioactivity (3×10^6 DPM) and exposed to X-ray film for 8 days. Four different proteins that were labeled in each developmental stage are marked as reference points (R1–R4) for comparison of proteins in each gel. Arrows show proteins synthesized at one stage but not the other (by visual comparison of overlaid autoradiograms of trochophore and veliger). Orientation of arrows is not intended to indicate greater or lesser amounts of protein, just presence or absence. Molecular-weight standards correspond to Coomassie-stained gel (not shown) with markers from 45 to 21 kDa. Isoelectric points (pI) fall within a linear pH gradient from 5.8 to 4.8.

expressed as the percentage of a larva's total (whole-body) protein content that was synthesized per day, the fractional rates ranged from 40% (1-day-old trochophore) to 14% (7-day-old veliger) (Table II). These rates of synthesis represent the turnover rates of whole-body protein in larvae of *H. rufescens*. When there is no net deposition (growth) of total protein, as in the lecithotrophic larvae of *H. rufescens*, the rate of protein synthesis is the measure of the rate of protein turnover (Waterlow *et al.*, 1978). Protein turnover, the continual breakdown and replacement of cellular proteins, is a significant component of maintenance metabolism in adult marine invertebrates (Hawkins, 1991). Few data are available in the literature for rates of protein turnover during development of marine invertebrates, making comparisons with our own data difficult. However, Berg and Mertes (1970) measured a rate of protein turnover in sea urchin embryos (*Lytechinus anamesus* at 19°C) of 23% day^{-1}, a value that falls within the range we determined for larvae of *H. rufescens* (14%–40% at 15°C, Table II). These synthesis rates in abalone larvae are not limited to a few specific proteins. The electrophoretic patterns of protein synthesis showed widespread incorporation of ^{35}S-label, indicating a high synthesis rate of multiple proteins (Figs. 6B, 7, 8), as has been found in developing stages of other species of marine invertebrates (*e.g.*, sea urchin embryos: Bedard and Brandhorst, 1983). These complex patterns of synthesis show that many proteins are involved with the synthesis side of the turnover process (synthesis and degradation). The specific proteins that are degraded to provide the precursors for new synthesis have not been identified in this study, but the lack of synthesis of two high-molecular-weight proteins (Fig. 6B: P1 and P2 at 88 and 121 kDa, respectively) suggests that these proteins might be degraded to support the new synthesis of other proteins. Amino acids dissolved in seawater are unlikely to have been a source of precursors for synthesis in our experiments, because the very high numbers of larvae (500 ml^{-1}) that we used would have quickly depleted any substrates present at low concentration in natural seawater.

The energy cost of protein turnover (= synthesis) in larvae of *H. rufescens* can be calculated for comparison with the energy made available from the degradation of protein (Fig. 3). The cost of protein synthesis appears to be constant in different animals and stages of development [*e.g.*, Reeds *et al.*, 1985: mammal = 11.52 ± 1.12 J (mg protein synthesized)$^{-1}$; Hawkins *et al.*, 1989: juvenile marine bivalve = 11.38 ± 8.88 J (mg protein synthesized)$^{-1}$; Vavra *et al.*, unpubl.: veliger larvae of the bivalve *Crassostrea gigas* = 13.2 ± 4.2 J (mg protein synthesized)$^{-1}$]. Using our value for molluscan larvae, the protein turnover rate measured for trochophore larvae of *H. rufescens* of 193 ng protein would equate to a requirement of 2548 μJ larva^{-1} day^{-1}, decreasing in late-stage veliger larvae (7-day-old) to 647 μJ larva^{-1} day^{-1} (turnover rate of 49 ng protein; Table II). The energy gained from the loss of protein (24.0 kJ g^{-1}) during development of *H. rufescens* was constant at 509 μJ day^{-1}. Assuming complete oxidation of the protein depleted, this input of energy from the loss of protein could account for only 20% (509/2548) of the cost of protein turnover in 1-day-old larvae. Obviously, during early development most of the costs of protein turnover have to be supplied from sources other than protein degradation. However, later in development (near metamorphosis) when rates of protein turnover decrease, the energy made available from protein reserves could account for a large percentage (79%) of the costs of turnover.

Protein turnover plays a major role in establishing the metabolic rate and physiological state of animals (Waterlow *et al.*, 1978; Reeds *et al.*, 1985; Hawkins, 1991). For lecithotrophic larval forms, little is known about rates of macromolecular synthesis during nonfeeding development. Our findings with larvae of *H. rufescens* show that these processes proceed at a high rate and undergo dynamic ontogenetic changes, with up to 40% of a larva's whole-body protein being turned over per day compared to depletion rates of only 4%–6%. If abalone larvae are typical of other lecithotrophs, at least in their biochemical and physiological activities, then biosynthetic rates in nonfeeding larval forms may be much higher than expected.

Acknowledgments

We thank John McMullen and Mike Machuzak of the Ab Lab (Port Hueneme, California) for supplying animals and supporting this project. Our thanks also to Nicholas Appelmans for his help in rearing the larvae. This research was supported by a grant from NOAA, Office of Sea Grant (U.S.C. Sea Grant) and by a grant from the Office of Naval Research (N00014-90-J-1740).

Literature Cited

Anger, K. 1996. Physiological and biochemical changes during larval development and early juvenile growth in the northern stone crab, *Lithodes maja* (Decapoda: Anomura). *Mar. Biol.* **126:** 283–296.

Bedard, P. A., and B. P. Brandhorst. 1983. Patterns of protein synthesis and metabolism during sea urchin embryogenesis. *Dev. Biol.* **96:** 74–83.

Ben-David-Zaslow, R., and Y. Benayahu. 1998. Competence and longevity in planulae of several soft corals. *Mar. Ecol. Prog. Ser.* **163:** 235–243.

Berg, W. E., and D. H. Mertes. 1970. Rates of synthesis and degradation of protein in the sea urchin embryo. *Exp. Cell Res.* **60:** 218–224.

Bradford, M. 1976. A rapid and sensitive method for the quantitation of microgram quantities of protein utilizing the principle of protein-dye binding. *Anal. Biochem.* **72:** 248–254.

Fry, B. J., and P. R. Gross. 1970. Patterns and rates of protein synthesis in sea urchin embryos: I. Uptake and incorporation of amino acids during the first cleavage cycle. *Dev. Biol.* **21:** 105–124.

Gnaiger, E. 1983. Calculation of energetic and biochemical equivalents of respiratory oxygen consumption. Pp. 337–345 in *Polarographic Oxygen Sensors*, E. Gnaiger and H. Forstner, eds. Springer-Verlag, Berlin.

Goustin, A. S., and F. H. Wilt. 1981. Protein synthesis, polyribosomes, and peptide elongation in early development of *Strongylocentrotus purpuratus*. *Dev. Biol.* **82:** 32–40.

Hawkins, A. J. S. 1991. Protein turnover: a functional appraisal. *Funct. Ecol.* **5:** 222–233.

Hawkins, A. J. S., J. Widdows, and B. L. Bayne. 1989. The relevance of whole-body protein metabolism to measured costs of maintenance and growth in *Mytilus edulis*. *Physiol. Zool.* **62:** 745–763.

Hoegh-Guldberg, O., and R. B. Emlet. 1997. Energy use during the development of a lecithotrophic and a planktotrophic echinoid. *Biol. Bull.* **192:** 27–40.

Jaeckle, W. B., and D. T. Manahan. 1989a. Growth and energy imbalance during the development of a lecithotrophic molluscan larva (*Haliotis rufescens*). *Biol. Bull.* **177:** 237–246.

Jaeckle, W. B., and D. T. Manahan. 1989b. Feeding by a "nonfeeding" larva: uptake of dissolved amino acids from seawater by lecithotrophic larvae of the gastropod *Haliotis rufescens*. *Mar. Biol.* **103:** 87–94.

Laemmli, U. K. 1970. Cleavage of structural proteins during the assembly of the head of bacteriophage T4. *Nature* **227:** 680–685.

Manahan, D. T. 1983. The uptake and metabolism of dissolved amino acids by bivalve larvae. *Biol. Bull.* **164:** 236–250.

Pearse, J. S. 1994. Cold-water echinoderms break "Thorson's Rule." Pp. 26–43 in *Reproduction, Larval Biology, and Recruitment in the Deep-sea Benthos*, K. J. Eckleharger and C. M. Young, eds. Columbia University Press, New York.

Reeds, P. J., M. F. Fuller, and B. A. Nicholson. 1985. Metabolic basis of energy expenditure with particular reference to protein. Pp. 46–57 in *Substrate and Energy Metabolism*, J. S. Garrow and D. Halliday, eds. John Libbey, London.

Shilling, F. M., and D. T. Manahan. 1994. Energy metabolism and amino acid transport during early development of antarctic and temperate echinoderms. *Biol. Bull.* **187:** 398–407.

Shilling, F. M., O. Hoegh-Guldberg, and D. T. Manahan. 1996. Sources of energy for increased metabolic demand during metamorphosis of the abalone *Haliotis rufescens* (Mollusca). *Biol. Bull.* **191:** 402–412.

Strathmann, R. R. 1978. The evolution and loss of feeding larval stages of marine invertebrates. *Evolution* **32:** 894–906.

Thorson, G. 1950. Reproductive and larval ecology of marine bottom invertebrates. *Biol. Rev.* **25:** 1–45.

Turner, R. L., and J. C. Rutherford. 1976. Organic, inorganic, and caloric composition of eggs, pentactulae, and adults of the brooding sea cucumber *Cucumaria curata* Cowles (Echinodermata: Holothuroidea). *J. Exp. Mar. Biol. Ecol.* **24:** 49–60.

Waterlow, J. C., P. J. Garlick, and D. J. Millard. 1978. *Protein Turnover in Mammalian Tissues and in the Whole Body*. North-Holland, Amsterdam.

Welborn, J. R., and D. T. Manahan. 1995. Taurine metabolism in larvae of marine molluscs (Bivalvia, Gastropoda). *J. Exp. Biol.* **198:** 1791–1799.

Reference: *Biol. Bull.* **196:** 187–198. (April 1999)

Settlement and Metamorphosis of *Capitella* Larvae Induced by Juvenile Hormone-Active Compounds Is Mediated by Protein Kinase C and Ion Channels

WILLIAM J. BIGGERS[1] AND HANS LAUFER[1,2,*]

[1]*Department of Molecular and Cell Biology, The University of Connecticut, Storrs, Connecticut 06268;*
and [2]*The Marine Biological Laboratory, Woods Hole, Massachusetts 02543*

Abstract. The signal transduction pathway by which juvenile hormone-active compounds induce settlement and metamorphosis of metatrochophore larvae of the polychaete annelid *Capitella* sp. I was investigated. The known protein kinase C (PKC) activator phorbol-12,13-dibutyrate was an active inducer of settlement and metamorphosis, whereas H-7, an inhibitor of PKC, inhibited settlement and metamorphosis in response to juvenile hormone III (JH III). JH III and methyl farnesoate (MF) also directly activated, *in vitro*, both a PKC-like enzyme present in *Capitella* homogenates and PKC purified from rat brain. In addition, binding studies using the fluorescent PKC inhibitor RIM-1 revealed the presence of a PKC-like enzyme in intact *Capitella* larvae and juveniles. Settlement and metamorphosis of the larvae was also stimulated by membrane-depolarizing concentrations of KCl. This response to KCl was inhibited by tetraethylammonium. The potassium channel blocker 4-aminopyridine induced settlement and metamorphosis, whereas settlement and metamorphosis in response to JH III was inhibited by the potassium channel ionophore nigericin. Settlement and metamorphosis induced by JH III was inhibited by the calcium channel blockers Ni^{2+}, Zn^{2+}, and verapamil, whereas settlement and metamorphosis was induced by the calcium ionophore A23187. These results suggest that in mediating this response, juvenile hormones may cause activation of PKC, leading to subsequent modulation of potassium and calcium channels.

Introduction

The chemoreception by marine invertebrate larvae of chemical "cues" that are present in the ocean environment and induce settlement and metamorphosis is important for the recognition of habitats that favor growth and reproduction (Chia and Rice, 1978; Rittschof and Bonaventura, 1986; Scheuer, 1990). These settlement signals appear to be specific for different species, as evidenced by findings that larvae of the abalone *Haliotis rufescens* respond to specific chemicals in red algae (Morse *et al.*, 1984), larvae of the nudibranch *Phestilla sibogae* respond to chemicals in corals (Hadfield, 1978, 1984), larvae of the polychaete annelid *Phragmatopoma californica* respond to chemicals present in the burrows of adult worms (Pawlik, 1988, 1990; Jensen and Morse, 1990), and larvae of the sand dollars *Dendraster excentricus* (Burke, 1984) and *Echinarachnius parma* (Pearce and Scheibling, 1990) respond to chemicals produced by adult sand dollars.

In previous studies, we have found that juvenile hormones (JH), which are known morphogens that regulate reproduction and development of insects and crustaceans (Laufer and Borst, 1983, 1988; Laufer *et al.*, 1987), as well as chemicals with juvenile hormone activity in insect cuticle bioassays, are able to induce settlement and metamorphosis of metatrochophore larvae of the polychaete annelid *Capitella* sp. I (Biggers and Laufer, 1992, 1996), which is a subspecies member of the *Capitella* polychaete complex (Grassle and Grassle, 1976). In nature, larvae of *Capitella* sp. I are stimulated to settle and metamorphose (Fig. 1) when they come into contact with chemical inducers present in sediments (Butman *et al.*, 1988), although the identity of these chemicals remains in debate (Cuomo, 1985; Dubilier, 1987), they appear to have JH-activity (Biggers, 1994).

We have now investigated the signal transduction process through which the *Capitella* larvae respond to JH-active compounds. Our results presented in this paper indicate that JH-active compounds stimulate settlement and metamor-

Received 6 August 1998; accepted 29 December 1998.

* To whom correspondence should be addressed.

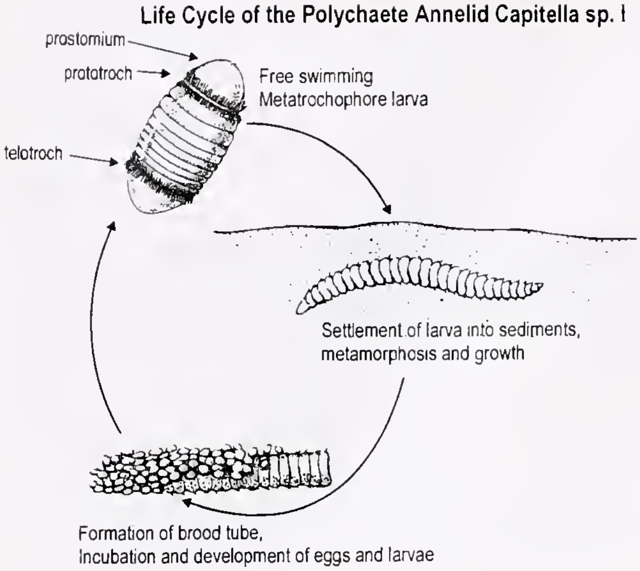
Life Cycle of the Polychaete Annelid Capitella sp. I
prostomium
prototroch
Free swimming
Metatrochophore larva
telotroch
Settlement of larva into sediments,
metamorphosis and growth
Formation of brood tube,
Incubation and development of eggs and larvae

Figure 1. Diagram of the life cycle and metamorphosis of *Capitella* sp. I larvae. In parental brood tubes, trochophore larvae develop into segmented metatrochophore larvae. After hatching and release from the brood tubes, in response to chemical settlement cues, swimming metatrochophore larvae settle and metamorphose into juvenile worms by losing their cilia needed for swimming and developing capillary setae and hooded hooks necessary for crawling through sediments.

phosis of these larvae through the activation of protein kinase C (PKC) and subsequent modulation of ion channels.

Materials and Methods

Capitella *larval settlement bioassays*

Stock cultures of *Capitella* sp. I were maintained at 18°C in large plastic containers containing artificial seawater (Utikem Co.) and washed sea sand (Fisher Scientific) and were fed Tetramin fish food flakes. Brood tubes containing adult females along with their developing eggs and larvae were then separated from the cultures and placed into 60-mm glass petri dishes containing seawater. The dishes were checked daily for hatched, swimming metatrochophore larvae to be used for bioassays. All test chemicals, except for methyl farnesoate (MF) which was synthesized in our laboratory, were purchased from Sigma Chem. Co. Stock solutions of juvenile hormone III (JH III), MF, phorbol-12,13 dibutyrate (PDBU), 1-(5-isoquinolinyl-sulfonyl)-2-methylpiperazine (H-7), arachidonic acid, elaidic acid, verapamil, 4-aminopyridine, and nigericin were prepared in 95% ethanol. Stock solutions of KCl, $NiCl_2$, $ZnCl_2$, and tetraethylammonium chloride (TEA) were prepared in distilled water. Settlement and metamorphosis bioassays were conducted at 18°C using 60-mm glass petri dishes that were pre-baked at 250°C to remove contaminants (Biggers and Laufer, 1996). For the assays, 10 to 100 μl of the test chemical stock solutions were added by micropipet into petri dishes containing 10 metatrochophore larvae less than 1 day old (1 day post-release), and 10 ml of artificial seawater. The dishes were then observed. After 1 h, the amount of settlement and metamorphosis was assessed by placing each dish under a dissecting microscope and counting the number of settled larvae crawling on the bottom of the dish. Metamorphosis after 1 hour was also more critically assessed by using a compound microscope and noting the loss of cilia, elongation, and development of capillary setae.

Protein kinase C assays

Assays for the presence of protein kinase C were carried out essentially as described by Yasuda *et al.* (1990), by measuring phosphorylation of an 11-residue synthetic peptide from myelin basic protein (MBP_{4-14}). This method is specific for measurement of PKC, and permits selective measurement in crude tissue preparations. The PKC assay was first standardized using purified rat brain PKC (calcium and phospholipid dependent) from Calbiochem Co. Phosphorylation of MBP_{4-14} was measured using 2–10 ng of enzyme, and over a time period of 30 min. Reactions were carried out in plastic Eppendorf tubes, with 50-μl reaction mixtures containing 20 m*M* Tris/HCl, pH 7.5, 5 m*M* magnesium acetate, 100 μM $CaCl_2$, 25 μM MBP_{4-14} (Sigma Chem. Co.), 50 ng diolein and 500 ng phosphatidylserine, 2–10 ng of rat brain PKC, and 10 μM ATP (containing $5-6 \times 10^5$ CPM gamma ^{32}P-ATP). Reactions were started by addition of enzyme, and incubations were carried out at 30°C for up to 30 min. The reactions were then stopped by placing the tubes on ice and spotting the reaction mixtures onto P-81 anion exchange paper discs (Whatman Co.), which were then immediately immersed in 75 m*M* H_3PO_4, and washed eight times in 100 ml of the same solution. The filter discs were placed in Ecolume cocktail for analysis with a scintillation counter. Other PKC assays using rat brain PKC were carried out in the same manner, except with the replacement of diolein and phosphatidylserine with test chemicals as indicated.

PKC activity in *Capitella* larval homogenates was determined in the same manner, except with the inclusion of the larval homogenates (20–100 μg protein) instead of the rat brain PKC. *Capitella* larvae were collected within 1 day of release from the brood tubes, and were frozen at −20°C. After thawing, the larvae were centrifuged at 5000 rpm for 1 min in a microfuge, the seawater was discarded, and larval homogenates were prepared by homogenizing 1000 larvae in 1 ml 20 m*M* Tris/HCL, pH 7.5, containing 0.5 m*M* phenylmethylsulfonyl fluoride (protease inhibitor) using small glass homogenizers. The homogenates were then centrifuged in a microfuge at 5000 rpm for 1 min to remove large cellular debris, and the PKC activity of the supernatant was assessed as previously described for studies with rat brain PKC. Protein concentrations of supernatants were determined using a microprotein assay (Sigma Chem. Co.) and a standard curve of increasing concentrations of bovine serum albumin.

Localization of PKC by RIM-1 analysis

Rhodamine-conjugated bisindolylmaleimide (RIM-1) (Calbiochem), a fluorescent PKC inhibitor (Chen and Poenie, 1993), was used to visually locate PKC in *Capitella* larvae and juveniles. Metatrochophore larvae less than 1 day old and 1-day-old juveniles were briefly exposed for 1 min at room temperature to 200 nm RIM-1 in seawater (100 μl) in depression slides covered with aluminum foil. Larvae or juveniles were then fixed in 2% formaldehyde containing seawater for 15 min, transferred into methanol for 15 min to permeabilize the membranes, and then transferred three times (5 min each wash) into 1 ml fresh seawater to rinse away excess unbound RIM-1. Fixed larvae or juveniles were then transferred in 10% glycerol-seawater onto microscope slides and visualized by either light microscopy or fluorescent microscopy with a Nikon confocal fluorescent microscope equipped with a rhodamine filter.

Results

Effects of protein kinase C modulators on larval settlement and metamorphosis

We have previously found that the juvenile hormones MF, JH I, and JH III, as well as compounds with juvenile hormone activity in insect cuticle bioassays, including arachidonic acid, are able to induce settlement and metamorphosis of *Capitella* sp. I metatrochophore larvae (Biggers and Laufer, 1992).

The first indication that the larvae sense the presence of JH III in the seawater is the onset of excited swimming. This response, which is typical of normal settlement behavior (Butman *et al.*, 1988; Pechenik and Cerulli, 1991), is faster than normal, with intermittent spiral-corkscrew movements, gradual body elongation, and periodic touching of the bottom of the petri dish. The larvae then settle and metamorphose into normal juvenile worms within 1 h. Both MF and JH III are very potent inducers of settlement and metamorphosis of the *Capitella* larvae at micromolar concentrations, whereas control larvae do not start to spontaneously settle and metamorphose until after 24 h (Fig. 2).

In preliminary investigations of the signal transduction process that mediates JH-induced settlement and metamorphosis of the *Capitella* larvae, we found compounds that elevate intracellular cAMP concentrations to be ineffective inducers of settlement and metamorphosis, indicating that cAMP does not act as a second messenger in this signal transduction process (Biggers and Laufer, 1992).

Based upon the ability of JH I, JH III, and arachidonic acid to activate PKC in other species including insects (Yamamoto *et al.*, 1988; Holian *et al.*, 1989; Sevala and Davey, 1989; Shearman *et al.*, 1989a; Shinomura *et al.*, 1991), and on reports that PKC activation is involved in the mediation of settlement and metamorphosis of other species of marine invertebrate larvae (Muller, 1985; Baxter and Morse, 1987; Leitz and Klingman, 1990; Morse, 1990), we further investigated the involvement of PKC activation in mediating settlement and metamorphosis of the *Capitella* larvae by testing the effects of other known PKC modulators. The phorbol ester phorbol-12,13-dibutyrate (PDBU) is a well-studied activator of PKC, and PKC has been found to be the actual cellular receptor for PDBU in some cells (Castagna *et al.*, 1982; Vandenbark *et al.*, 1984). Experiments with PDBU on the *Capitella* larvae showed that it is also a very potent inducer of settlement and metamorphosis (Fig. 3A), indicating that PKC activation is involved in mediating this process.

The effect of a PKC inhibitor was next studied to determine if it could inhibit settlement and metamorphosis induced by JH. The PKC inhibitor 1-(5-isoquinolinyl-sulfonyl)-2-methylpiperazine, abbreviated H-7 (Hidaka *et al.*, 1984), caused a concentration-dependent inhibition of *Capitella* settlement and metamorphosis induced by 25 μM JH III, when the larvae were pre-exposed to H-7 for 3 h (Fig. 3B). This result again indicates the involvement of PKC activation in mediating the effects of JH on settlement and metamorphosis.

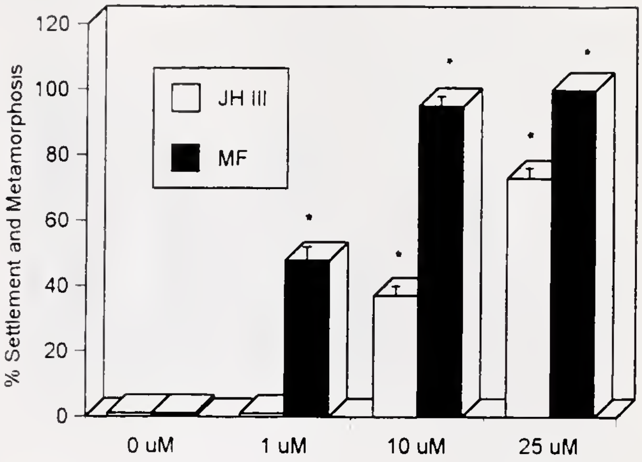

Figure 2. Concentration-dependent stimulatory effects of juvenile hormone III (JH III) and methyl farnesoate (MF) on *Capitella* larval settlement. Metatrochophore larvae, less than 1 day after release from parental brood tubes, were exposed to several concentrations of JH III or MF in seawater, ranging from 1 to 25 μM. Percent settlement and metamorphosis is shown for each concentration after 1 h. Each bar represents the percent settlement and metamorphosis for each concentration (mean ± SEM, $n = 6$, representing 60 larvae/concentration). Controls (0 μM) received 50 μl 95% ethanol. Asterisks indicate significant differences ($P < 0.001$, $F > 50$) between control and experimental values at each concentration tested by one-way ANOVA with a Bonferroni correction for multiple comparisons where $\alpha = 0.017$.

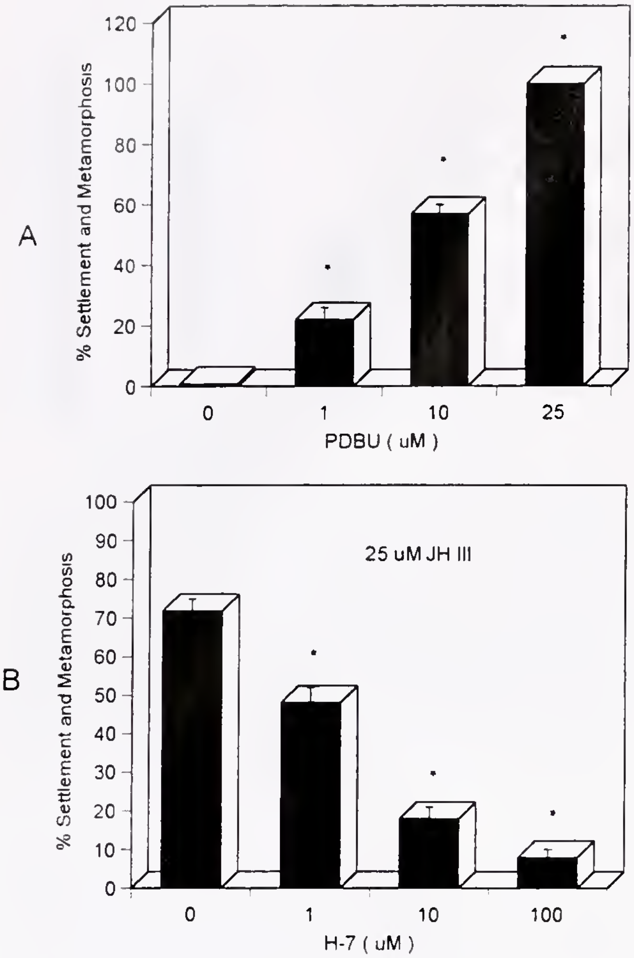

Figure 3. Effects of protein kinase C (PKC) modulators on larval settlement and metamorphosis. (A) Induction of settlement and metamorphosis by 12,13 dibutyrate (PDBU): *Capitella* metatrochophore larvae, less than 1 day after release, were exposed to the PKC activator phorbol PDBU added to the seawater at concentrations ranging from 1 to 25 μM, and settlement and metamorphosis was noted after 1 h. Controls received 50 μl 95% ethanol. Bars represent the percent settlement and metamorphosis for each concentration (mean ± SEM, $n = 6$, representing 60 larvae/concentration). Asterisks indicate significant differences ($P < 0.001$, $F > 25$) between control and experimental values at each concentration tested by one-way ANOVA with a Bonferroni correction for multiple comparisons where $\alpha = 0.017$. (B) Inhibition of juvenile hormone (JH) III-induced settlement and metamorphosis by H-7. *Capitella* metatrochophore larvae, less than 1 day after release, were pre-exposed for 3 h to concentrations of H-7, a PKC inhibitor, in seawater ranging from 1 to 100 μM, before being exposed to JH III (20 μM) for 1 h. Controls (0 μM) received 100 μl 95% ethanol followed by JH III. Bars represent the percent settlement and metamorphosis for each concentration after the 4-h time period (mean ± SEM, $n = 6$, representing 60 larvae/concentration). Asterisks same as in (A).

Activation of a protein kinase C-like enzyme in Capitella *larvae by JH-active chemicals*

Although PKC is considered to be a ubiquitous enzyme present throughout the animal kingdom and has been found in marine sponges (Muller *et al.*, 1987) and *Dictyostelium discoideum* (Jimenez *et al.*, 1989; Luderus *et al.*, 1989), its presence in polychaetes has so far not been documented. The presence of a PKC-like enzyme in *Capitella* larvae was therefore investigated, as was also the ability of JH-active compounds to activate this enzyme. In these investigations, we used an assay specific for PKC. Developed by Yasuda *et al.* (1990), this assay is based upon the specific phosphorylation by PKC of an 11-amino acid peptide sequence of myelin basic protein, which is not phosphorylated by either cAMP-dependent protein kinase (PKA), casein kinases I and II, Ca^{2+}/calmodulin-dependent protein kinase II, or phosphorylase kinase. The results demonstrate that a PKC-like enzyme does exist in *Capitella* (Fig. 4). PKC activity was linear for up to 15 min for homogenate concentrations up to 100 μg (Fig. 4A, B). The specific activity of PKC in the larval homogenates was calculated as being 6.7 fmoles ^{32}P-incorporated per minute per microgram of protein. Incubations were also done without the PKC substrate MBP_{4-14} to monitor endogenous larval protein phosphorylation, of which only a very small amount could be detected.

Experiments were next conducted to determine whether

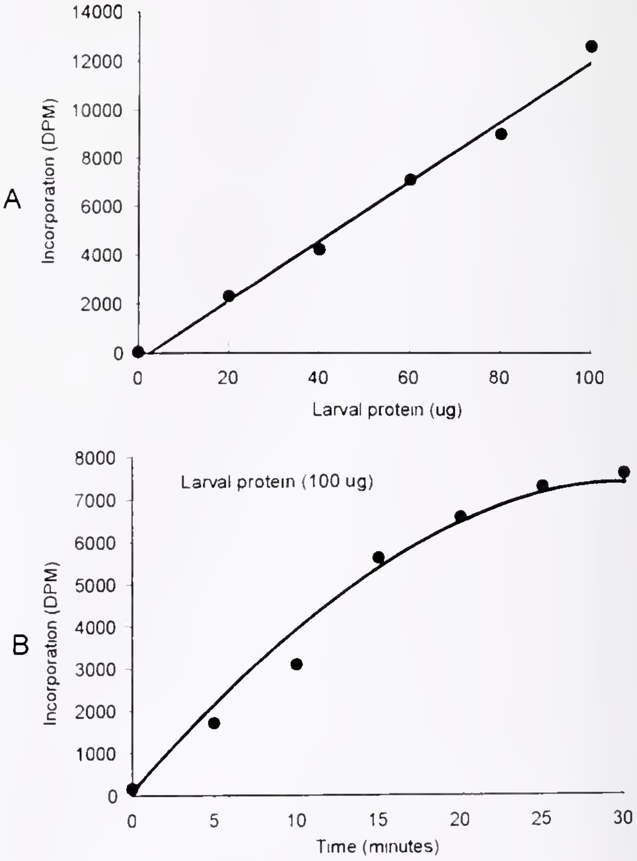

Figure 4. Protein kinase C (PKC) activity in *Capitella* larvae. PKC activity was detected in larval homogenates after activation with phosphatidylserine and diolein. ^{32}P-incorporation into MBP_{4-14} was linear with increasing protein concentrations ranging from 20 to 100 μg (A) and was also linear for 15 min using 100 μg protein (B).

the PKC-like enzyme present in the *Capitella* larvae could be activated by JH-active compounds. Incubations were carried out using 100 μg of the larval homogenates for 15 min at 30°C in the presence of either phosphatidylserine/diolein (PS/DO), 10 μM arachidonic acid (AA), 10 μM JH III, 10 μM MF, or 10 μM elaidic acid (EA). The results of this experiment indicate that JH III, MF, and AA are able to activate *Capitella* PKC *in vitro* (Fig. 5A). In comparison with activation by PS/DO, arachidonic acid was the strongest activator (94% activation), followed by MF (73% activation) and JH III (51% activation). Elaidic acid, a trans-isomer of oleic acid that does not activate rat brain PKC (Shearman *et al.*, 1989a) and does not induce settlement and metamorphosis of the *Capitella* larvae, did not activate the *Capitella* PKC. These results therefore again indicate the involvement of PKC activation in mediating settlement and metamorphosis of the *Capitella* larvae.

Since it is possible that the crude larval homogenates contain enzymes, receptors, and substrates of the diacylglycerol pathway, such as phospholipase C and guanine-binding proteins through which indirect activation of PKC may occur, we also tested whether JH could directly activate a purified preparation of rat brain PKC. Polyunsaturated fatty acids such as arachidonic acid can activate bovine brain PKC (Shearman *et al.*, 1989a) and rat brain PKC (Holian *et al.*, 1989; Shinomura *et al.*, 1991); therefore, juvenile hormones might also be able to cross species lines and activate rat brain PKC. Incubations were carried out using 5 ng purified rat brain PKC (Calbiochem Co.) in the presence of either PS/DO, 10 μM AA, 10 μM JH III, 10 μM MF, or 10 μM EA, at 37°C for 15 min. The results show that insect juvenile hormones and the crustacean juvenile hormone MF are able to directly activate rat brain PKC in the absence of phosphatidylserine and diolein (Fig. 5B). Arachidonic acid was the most potent activator tested (93% activation relative to PS/DO), whereas elaidic acid was inactive, confirming earlier work reported by Shearman *et al.* (1989a). MF caused 59% activation of the rat brain PKC and was more active than JH III (28% activation).

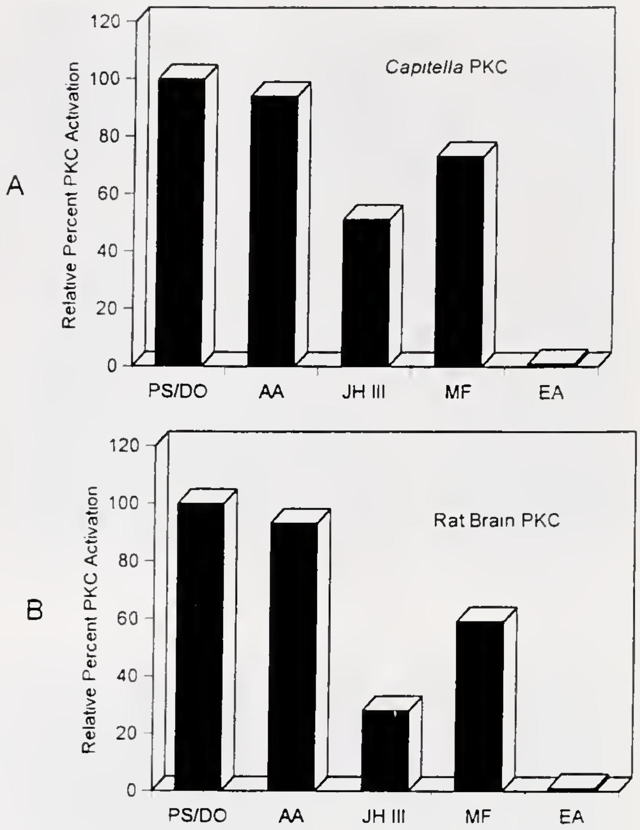

Figure 5. Activation of an enzyme resembling protein kinase C (PKC) in *Capitella* larval homogenates and purified rat brain PKC by JH-active chemicals. (A) Activation of the PKC-like enzyme present in larvae. PKC assays using *Capitella* larval homogenates were carried out in the presence of either phosphatidylserine/diolein (PS/DO), 10 μM arachidonic acid (AA), 10 μM juvenile hormone (JH) III, 10 μM *trans, trans* methyl farnesoate (MF), or 10 μM elaidic acid (EA). Incorporation of ^{32}P into MBP_{4-14} for AA, JH III, MF, and EA is shown expressed as the percentage incorporation relative to that found for the control (PS/DO). (B) Activation of purified rat brain PKC. PKC assays using 5 ng purified rat brain PKC were carried out in the presence of either phosphatidylserine/diolein (PS/DO), 10 μM arachidonic acid (AA), 10 μM JH III, 10 μM *trans, trans* methyl farnesoate (MF), or 10 μM elaidic acid (EA). Incorporation of ^{32}P into MBP_{4-14} for AA, JH III, MF, and EA is shown expressed as the percentage incorporation relative to that found for the control (PS/DO).

Localization of PKC in Capitella *by RIM-1*

To visualize the location of PKC in the *Capitella* larvae and juveniles and to identify possible chemosensory cells that would rapidly take up external chemicals or chemicals in the environment, larvae and juveniles were briefly (1 min) exposed to a fluorescently labeled protein kinase C inhibitor, rhodamine-conjugated bisindolylmaleimide (RIM-1), which has proven useful as a fluorescent probe for PKC (Chen and Poenie, 1993). After exposure to this inhibitor, the larvae or juveniles were fixed, permeabilized, rinsed to remove excess unbound RIM-1, and viewed under a fluorescent microscope. In metatrochophore larvae, distinct cells in the ciliary bands of the prototroch and telotroch and isolated cells in the apical region of the prostomium and the rest of the body displayed RIM-1 binding, indicating that these cells possess PKC (Fig. 6B). Juvenile *Capitella* exposed in the same manner displayed RIM-1 binding to cells in the apical region of the prostomium and scattered throughout the rest of the body (Fig. 6D). These results provide more evidence for the presence of a PKC-like enzyme in *Capitella* larvae and juveniles, and are consistent with a chemosensory function for apical cells in regions of the prostomium as previously noted by Eckelbarger and Grassle (1987).

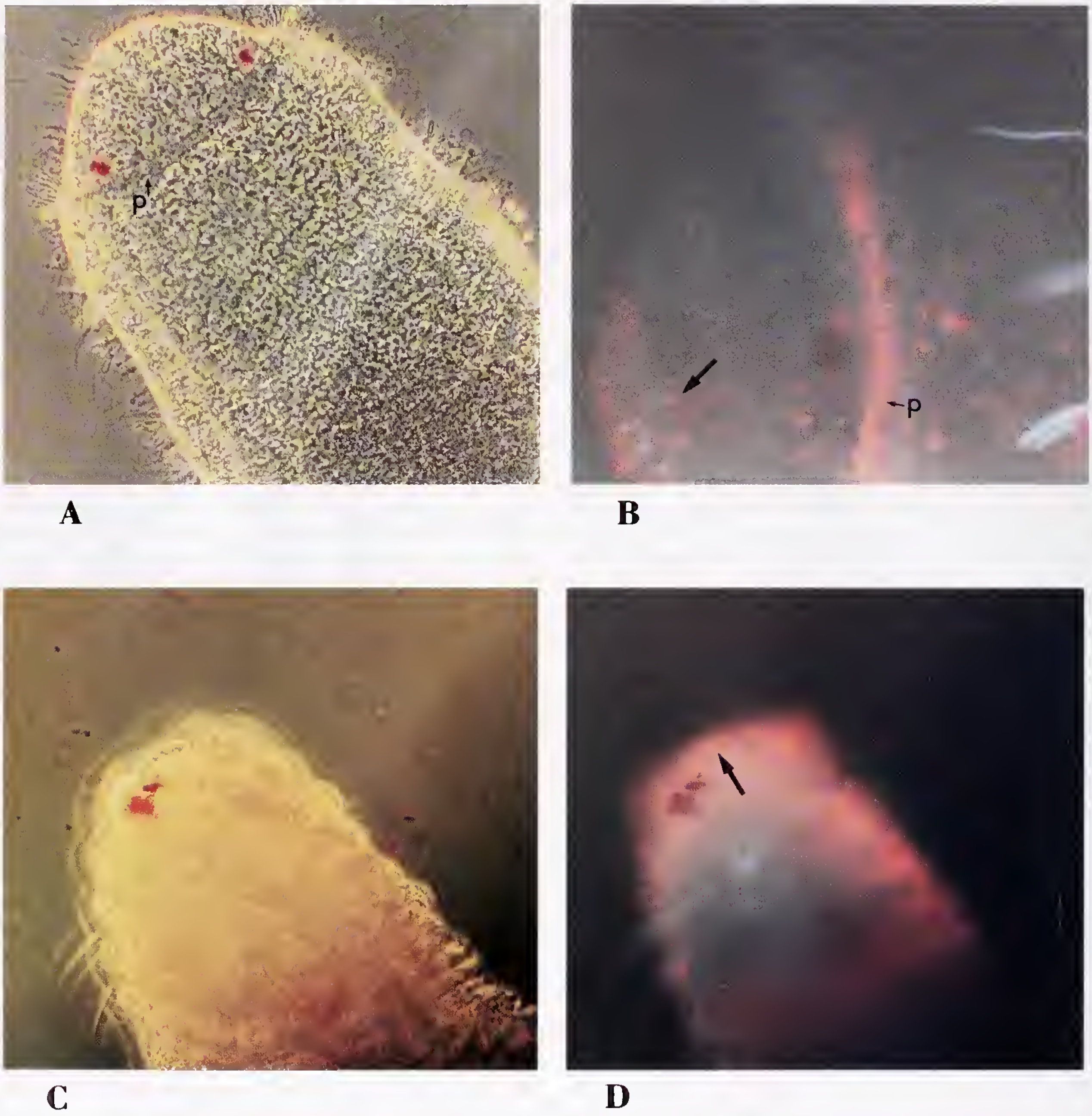

Figure 6. Localization of protein kinase C (PKC) in *Capitella* by RIM-1 analysis. Metatrochophore larvae less than 1 day after release from parental brood tubes and 1-day-old juveniles were exposed for 1 min to RIM-1, a rhodamine-conjugated PKC inhibitor. (A) Light microscopy of metatrochophore larva (400×). (B) Fluorescence microscopy of metatrochophore larva showing binding of RIM-1 to ciliary cells of the prototroch (p) as well as isolated apical cells located in the prostomium (arrow) (800×). (C) Light microscopy of juvenile *Capitella* prostomium (400×). (D) Fluorescence microscopy of juvenile *Capitella* prostomium showing binding of RIM-1 to apical cells (arrow) (400×).

Effects of potassium channel modulators

In mediating cellular responses, PKC activation has in many cases been found to result in the modulation of potassium and calcium channels (Kaczmarek, 1987; Shearman *et al.*, 1989b). The involvement of potassium channels in mediating the settlement and metamorphosis of several types of marine invertebrate larvae has also been previously demonstrated (Baloun and Morse, 1984; Yool *et al.*, 1986; Leitz and Klingman, 1990; Carpizo-Ituarte and Hadfield,

Table I

Effects of ion channel modulators on settlement and metamorphosis of Capitella *sp. I larvae*

Chemical	% Larvae settled and metamorphosed (after 1 h)
Potassium channel modulators	
KCl (20 m*M*)	100
KCl (20 m*M*) + TEA (100 m*M*)	5
4-Aminopyridine (100 μM)	100
JH III (38 μM)	100
JH III (38 μM) + nigericin (500 ng/ml)	0
Calcium channel modulators	
A23187 (400 n*M*)	100
JH III (38 μM)	100
JH III (38 μM) + $NiCl_2$ (10 m*M*)	0
JH III (38 μM) + $ZnCl_2$ (10 m*M*)	0
JH III (38 μM) + Verapamil (17 μM)	0

JH = juvenile hormone.

1998). Studies were therefore carried out to determine if the modulation of potassium channels may also mediate settlement and metamorphosis of the *Capitella* larvae. Increased external KCl concentrations in the seawater induced settlement and metamorphosis of the *Capitella* larvae in a concentration-dependent manner, with an added concentration of 20 m*M* (30 m*M* total including seawater) inducing 100% settlement and metamorphosis in 1 h (Table I). These effects of KCl appear to be mediated by K^+ ions and not Cl^- since addition of NaCl had no effect on settlement and metamorphosis. The effect of tetraethylammonium chloride (TEA), a known blocker of potassium currents, was next studied to determine its effect on settlement and metamorphosis. TEA did not induce settlement and metamorphosis of the *Capitella* larvae, but instead inhibited the stimulatory response of the larvae to KCl, with a concentration of 100 m*M* TEA almost completely inhibiting settlement and metamorphosis (Table I). Settlement and metamorphosis of the *Capitella* larvae was, however, stimulated in a concentration-dependent manner by 4-aminopyridine (4-AP), another potassium channel blocker, which blocks outward rectifying potassium currents. A concentration of 100 μM 4-AP stimulated 100% settlement and metamorphosis of the larvae within 1 h (Table I). The effects of the potassium channel ionophore, nigericin, was next studied. Pre-exposure of the larvae to nigericin for 30 min inhibited the response of the larvae to JH III in a concentration-dependent manner, with 500 ng/ml nigericin causing 100% inhibition of settlement and metamorphosis in response to JH III in 1 h (Table I).

Effects of calcium channel modulators

Calcium channels are in many cases activated in response to membrane depolarization and in response to PKC activators (Kaczmarek, 1987; Shearman *et al.*, 1989b). Calcium channel modulators were therefore studied for their effects on settlement and metamorphosis of the *Capitella* larvae. Pre-exposure of the larvae to the known calcium channel blockers Ni^{2+} at a concentration of 10 m*M*, Zn^{2+} at a concentration of 10 m*M*, and verapamil at a concentration of 17 μM completely inhibited the settlement- and metamorphosis-inducing effects of JH III (Table I). Next, to determine whether an influx of calcium could stimulate settlement and metamorphosis, the effect of the calcium channel ionophore A23187 was tested. A23187 proved to have a potent, concentration-dependent effect on larval settlement and metamorphosis (Fig. 7), with a concentration of 400 n*M* stimulating 100% of the larvae to settle and metamorphose in 1 h (Table I). These results therefore suggest that JH III activation of PKC may lead to the opening of calcium channels.

Discussion

The ability of juvenile hormones and compounds with JH activity to induce settlement and metamorphosis in *Capitella* larvae raises the possibility that these compounds may act on the larvae through a mechanism similar to that by which they affect insect metamorphosis and reproduction. In insects, juvenile hormones have multiple mechanisms for regulating metamorphosis and reproduction. For example, they may act through nuclear receptors and transcriptional regulation (Jones *et al.*, 1993; Palli *et al.*, 1994; Jones and

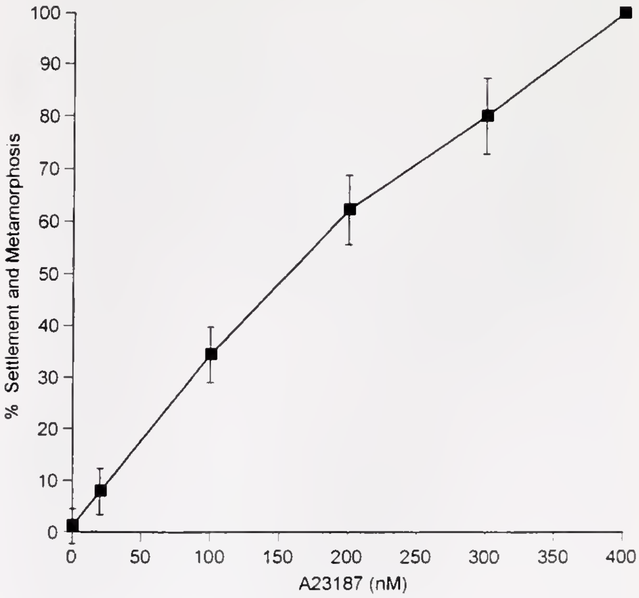

Figure 7. Effect of the calcium ionophore A23187 on settlement and metamorphosis of *Capitella* larvae. Metatrochophore larvae less than 1 day after release, exposed for 1 h to concentrations of A23187 ranging from 25 to 400 n*M* in seawater, were stimulated to settle and metamorphose in a concentration-dependent manner.

Sharp, 1997), or by affecting mRNA stability (Jones *et al.*, 1993) and mRNA translation (Ilan *et al.*, 1972). JH I affects follicle cell patency in *Rhodnius prolixus* through—another well-studied mechanism (Sevala and Davey, 1989)—a signal transduction cascade involving a membrane receptor, activation of PKC, and the subsequent activation of a Na/K-ATPase. Other studies (Yamamoto *et al.*, 1988) have demonstrated that PKC activation and opening of calcium channels is involved in the mechanism by which JH III induces protein synthesis in *Drosophila* male accessory glands. Our studies indicate that PKC activation and ion channel modulation are also involved in the process of chemosensory signal transduction by which JH and compounds with JH activity induce settlement and metamorphosis of larvae of *Capitella* sp. I.

In addition to JH I and JH III, other known activators of PKC can also induce settlement of *Capitella* larvae. One example is arachidonic acid, which has shown JH activity in insect cuticle bioassays (Slama, 1962) and strongly activates PKC from bovine brain (Shearman *et al.*, 1989a) and rat brain (Holian *et al.*, 1989; Shinomura *et al.*, 1991). The potency of the phorbol ester PDBU in inducing settling and metamorphosis of *Capitella* larvae (Fig. 3A) is particularly good evidence for the activation of a protein kinase C-like enzyme, since it is well established that PDBU directly activates PKC in mammalian tissues (Castagna *et al.*, 1982; Nishizuka, 1984; Vandenbark *et al.*, 1984; Parker *et al.*, 1986). The PKC inhibitor H-7 is able to inhibit the settlement and metamorphosis effects of JH III (Fig. 3B). Although H-7 at higher concentrations also inhibits other protein kinases such as cyclic AMP-dependent protein kinase (PKA) (Hidaka *et al.*, 1984), the effects of H-7 on the *Capitella* larvae are probably due to the inhibition of PKC and not PKA, since PDBU, which induces settlement and metamorphosis, activates only PKC and not PKA (Castagna *et al.*, 1982).

PKC is regarded as a ubiquitous enzyme present throughout the animal kingdom (Nishizuka, 1984), having been demonstrated in *Dictyostelium* (Luderus *et al.*, 1989; Jimenez *et al.*, 1989) and sponges (Muller *et al.*, 1987) as well as in mammalian tissues. Other studies have also demonstrated that PKC activation is involved in the signal transduction processes that mediate settlement and metamorphosis of marine invertebrate larvae of the coelenterate *Hydractinia* (Muller, 1985; Leitz and Klingman, 1990) and the mollusc *Haliotis rufescens* (Baxter and Morse, 1987; Morse, 1990). It is therefore likely that *Capitella* also possesses a PKC-like enzyme that is involved in mediating larval settlement and metamorphosis. Our data indicate that *Capitella* does possess such an enzyme, since crude homogenates of the larvae show PKC activity in a selective PKC assay (Fig. 4). More studies are needed to further characterize the enzyme and determine its requirement for calcium.

JH appears to activate PKC in the *Capitella* larvae directly, much like the mechanism of action of phorbol esters. Our results show that MF, JH III, and arachidonic acid can, *in vitro*, directly activate the PKC-like enzyme in *Capitella* as well as purified PKC from rat brain in the complete absence of the normal membrane inducers phosphatidyl serine and diacylglycerol (Fig. 5). These data therefore indicate that juvenile hormones, as well as JH-active compounds such as arachidonic acid, are able to bind to the lipid-binding site in PKC (Parker *et al.*, 1986; Ziesel, 1993). This is perhaps not surprising given that phorbol esters and juvenile hormones are both terpenoid compounds: phorbol esters are diterpenoids and juvenile hormones are sesquiterpenoids.

In sensing JH-active compounds in the seawater, these lipophilic compounds presumably pass through the membrane of ciliary epithelial chemosensory cells similar to those reported to transduce chemical signals for settlement and metamorphosis in larvae of the abalone *Haliotis* (Trapido-Rosenthal and Morse, 1986), the cnidarian *Hydractinia* (Schwoerer-Bohning *et al.*, 1990), the polychaete *Phragmatopoma californica* (Amieva *et al.*, 1987), and the sea star *Luidia senegalensis* (Komatsu *et al.*, 1991). Our studies with the fluorescent PKC inhibitor RIM-1 provide more evidence that *Capitella* larvae possess a PKC-like enzyme and that PKC is present in chemosensory cells. The RIM-1 presumably was able to directly enter chemosensory cells of the larvae that allow rapid uptake of external chemicals, since the larvae were exposed to RIM-1 only briefly (1 min). The intense RIM-1 binding in isolated cells of the prostomium (Fig. 6) may represent the presence of PKC in apical cilia that are thought, on the basis of evidence from electron microscopy (Eckelbarger and Grassle, 1987) to serve a chemosensory function. However, entry of RIM-1 into the larvae through other processes cannot be ruled out, since RIM-1 binding was found in cells throughout the body, especially in ciliary cells of the prototroch and telotroch, and in both metatrochophore larvae and juveniles.

It is likely that JH-active compounds, after passing through the membrane of chemosensory cells, bind with an inactive PKC present in the cytosol, which, as in other species (Nishizuka, 1984), then becomes active and is translocated to the membrane. It is evident from our studies that micromolar concentrations of JH-active compounds are able to activate PKC and thereby induce settlement and metamorphosis. Concentrations of 10 μM JH III, MF, and arachidonic acid activate both *Capitella* PKC and rat brain PKC (Fig. 4), and the same concentrations of these chemicals dissolved in the seawater also induce settlement and metamorphosis of the larvae. The inability of elaidic acid to activate PKC *in vitro* and to induce settlement and metamorphosis is further evidence that PKC activation is involved in mediating settlement and metamorphosis of the *Capitella* larvae.

In *Capitella* larvae, PKC activation may cause several

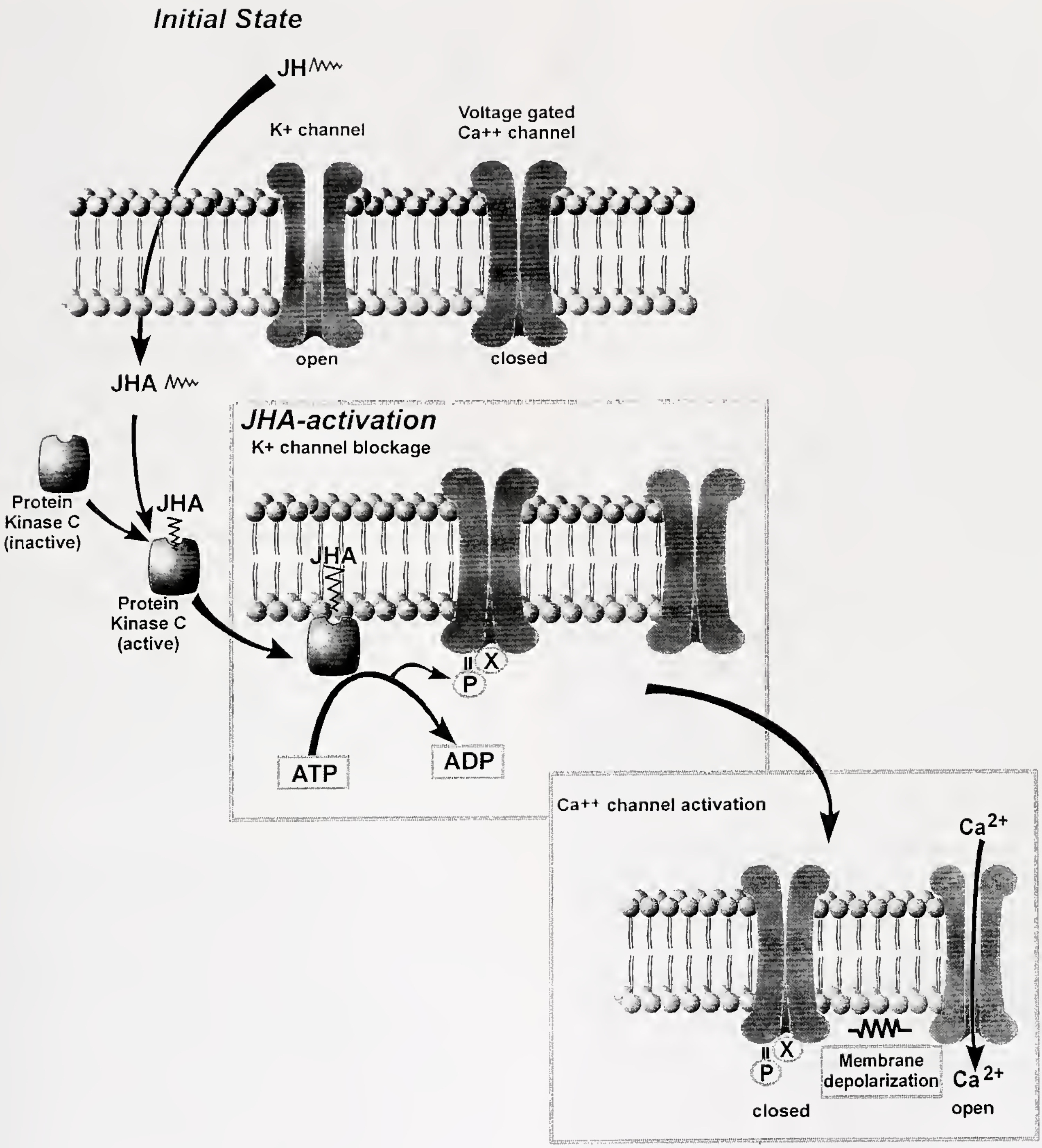
Initial State
JH
K+ channel
Voltage gated Ca++ channel
open
closed
JHA
Protein Kinase C (inactive)
JHA
Protein Kinase C (active)
JHA-activation
K+ channel blockage
JHA
X
P
ATP
ADP
Ca++ channel activation
Ca2+
X
P
Membrane depolarization
Ca 2+
closed
open

Figure 8. Model for the juvenile hormone (JH) signal-transduction pathway in *Capitella* sp. I larvae. In this proposed model, JH induces settlement and metamorphosis by directly interacting with and activating cytosolic protein kinase C (PKC), which acts as the cellular receptor in the larval chemosensory cells. This activation of PKC then causes the closure of potassium channels by phosphorylation, invoking membrane depolarization, and the subsequent opening of voltage-activated calcium channels. PKC and calcium may in subsequent steps activate transcription factors and protein kinases, leading to changes in gene activity, and also cause neurotransmitter release.

cellular events that transduce the external JH signal and lead to settlement and metamorphosis. One well-characterized effect of PKC activation is the modulation of ion transporters such as a Na+/K+ ATPase (Ilenchuk and Davey, 1987; Sevala and Davey, 1989), Na+/H+ exchangers (Berridge, 1984), and ion channels (Kaczmarek, 1987; Shearman *et al.*, 1989b). The modulation of potassium channels, resulting in membrane depolarization and neural relay of external chemical settlement cues, has been demonstrated to be involved with the settlement and metamorphosis of several types of marine invertebrate larvae, including those of the abalone *Haliotis rufescens* (Baloun and Morse, 1984), the nudibranch *Phestilla sibogae* and the prosobranch *Astraea undosa* (Yool *et al.*, 1986), the cnidarian *Hydractinia* (Leitz and Klingman, 1990), and the polychaetes *Phragmatopoma californica* (Yool *et al.*, 1986), and *Hydroides elegans* (Carpizo-Ituarte and Hadfield, 1998). Pheromone reception by insects and non-insect species has also in some instances been demonstrated to be mediated by PKC activation and the concommitant modulation of ion channel activity (Zufall and Hatt, 1991; Stengl, 1993). Like those studies, our investigations suggest that ion channel modulation is also involved. We found that the addition of excess KCl to the seawater stimulated settlement and metamorphosis, whereas this effect was negated by simultaneous addition of the potassium channel blocker tetraethylammonium chloride (TEA). These results indicate that TEA blocks settlement and metamorphosis by preventing the entry of excess potassium. These results are similar to those reported by Carpizo-Ituarte and Hadfield (1998) in their investigations with larvae of the polychaete *Hydroides elegans*. TEA did not induce settlement and metamorphosis of the *Capitella* larvae at the concentrations tested; however, the larvae were induced to settle and metamophose in response to another potassium channel blocker, 4-aminopyridine (4-AP), which causes blockage of outward rectifying potassium currents (Alkon *et al.*, 1986). These data indicate that blockage of outward rectifying potassium channels can induce settlement and metamorphosis of the *Capitella* larvae. Since studies by Leitz and Klingman (1990) demonstrated that potassium channel closure was involved in mediating settlement and metamorphosis of *Hydractinia* larvae in response to PKC-activating diacylglycerols, we tested the possibility that JH induces settlement of the *Capitella* larvae through closure of potassium channels in response to PKC activation. Our findings that the potassium channel ionophore nigericin inhibits settlement and metamorphosis induced by JH III and that 4-AP can directly stimulate settlement and metamorphosis provide evidence that JH stimulates settlement and metamorphosis through the closure of potassium channels.

Since potassium channel closure may cause membrane depolarization, it is possible that voltage-gated calcium channels are activated during this process and participate in mediating settlement and metamorphosis. Our studies support this idea, since the calcium channel blockers Ni^{2+}, Zn^{2+}, and verapamil inhibited settlement and metamorphosis induced by JH III, whereas the calcium channel ionophore A23187 induced settlement and metamorphosis.

Our interpretation of these data is that juvenile hormones and JH-active chemicals induce settlement and metamorphosis of *Capitella* larvae through activation of PKC, which causes closure of potassium channels; the reduced efflux of potassium depolarizes the membranes of the chemoreceptor cells, leading to the opening of voltage-activated calcium channels (Fig. 8). In eliciting metamorphosis, PKC activation by JH may activate transcription factors such as nuclear factor-kB (NF-kB) or stimulate the mitogen-activated protein kinase (MAP-kinase) pathway. Membrane depolarization and calcium influx in PC12 cells has been demonstrated to activate the MAP kinase pathway (Rosen *et al.*, 1994; Rosen and Greenberg, 1996). PKC modulation also plays a role in regulating neural differentiation of *Xenopus* (Durston and Otte, 1991), epithelial patterning in *Hydra* (Shenk and Steele, 1993), and skin morphogenesis in chickens (Noveen *et al.*, 1995). The molecular mechanisms by which PKC and calcium may be regulating settlement and metamorphosis of the *Capitella* larvae are now the subject of our ongoing research.

Acknowledgments

The authors thank Dr. Judith Grassle at Rutgers University for kindly supplying cultures of *Capitella* sp. I, Dr. David Knecht at the University of Connecticut for help and use of the fluorescent microscope, and Mrs. Mary Jane Spring of the University of Connecticut for providing illustrations. This research was supported in part by a research fellowship to WJB from the Marine Science Institute of the University of Connecticut and by the Sea Grant College Program, NOAA.

Literature Cited

Alkon, D. L., M. Kubota, J. T. Neary, S. Naito, D. Coulter, and H. Rasmussen. 1986. C-kinase activation prolongs Ca^{2+}-dependent inactivation of K^+ currents. *Biochem. Biophys. Res. Commun.* **134:** 1245–1253.

Amieva, M. R., C. G. Reed, and J. R. Pawlik. 1987. Ultrastructure and behavior of the larva of *Phragmatopoma californica* (Polychaeta: Sabellariidae): identification of sensory organs potentially involved in substrate selection. *Mar. Biol.* **95:** 259–266.

Baloun, A. J., and D. E. Morse. 1984. Ionic control of settlement and metamorphosis in larval *Haliotis rufescens* (Gastropoda). *Biol. Bull.* **167:** 124–138.

Baxter, G., and D. E. Morse. 1987. G protein and diacylglycerol regulate metamorphosis of planktonic molluscan larvae. *Proc. Natl. Acad. Sci. USA* **84:** 1867–1870.

Berridge, M. J. 1984. Inositol trisphosphate and diacylglycerol as second messengers. *Biochem. J.* **220:** 345–360.

Biggers, W. J. 1994. Effects of juvenile hormone-active compounds on larval settlement and metamorphosis of the polychaete annelid *Capitella* sp. I. Dissertation, University of Connecticut, Storrs, CT.

Biggers, W. J., and H. Laufer. 1992. Chemical induction of settlement and metamorphosis of *Capitella capitata* sp. I (polychaeta) larvae by juvenile hormone-active compounds. *Invert. Reprod. Dev.* **22:** 39–46.

Biggers, W. J., and H. Laufer. 1996. Detection of juvenile hormone-active compounds by larvae of the marine annelid *Capitella* sp. I. *Arch. Insect Biochem. Physiol.* **32:** 475–484.

Burke, R. D. 1984. Pheromonal control of metamorphosis in the Pacific sand dollar, *Dendraster excentricus. Science* **225:** 442–443.

Butman, C. A., J. P. Grassle, and C. M. Webb. 1988. Substrate choices made by marine larvae settling in still water and in a flume flow. *Nature* **333:** 771–773.

Carpizo-Ituarte, E., and M. G. Hadfield. 1998. Stimulation of metamorphosis in the polychaete *Hydroides elegans* Haswell (Serpulidae). *Biol. Bull.* **194:** 14–24.

Castagna, M., Y. Takai, K. Kaibuchi, K. Sano, U. Kikkawa, and Y. Nishizuka. 1982. Direct activation of calcium-activated, phospholipid-dependent protein kinase C by tumor-promoting phorbol esters. *J. Biol. Chem.* **257:** 7847–7851.

Chen, C.-S., and M. Poenie. 1993. New fluorescent probes for protein kinase C. *J. Biol. Chem.* **268:** 15812–15822.

Chia, F. S., and M. E. Rice, eds. 1978. *Settlement and Metamorphosis of Marine Invertebrate Larvae.* Elsevier, New York.

Cuomo, M. C. 1985. Sulfide as a larval settlement cue for *Capitella* sp. I. *Biogeochemistry* **1:** 169–181.

Dubilier, N. 1987. H_2S- A settlement cue or toxic substance for *Capitella* sp. I larvae? *Biol. Bull.* **174:** 30–38.

Durston, A. J., and A. P. Otte. 1991. A hierarchy of signals mediates neural induction in *Xenopus laevis.* Pp. 109–127 in *Cell-Cell Interactions in Early Development,* J. Gerhart, ed. Wiley-Liss, New York.

Eckelbarger, K. J., and J. P. Grassle. 1987. Interspecific variation in genital spine, sperm, and larval morphology in six sibling species of *Capitella. Biol. Soc. Wash. Bull.* **7:** 62–76.

Grassle, J. P., and J. F. Grassle. 1976. Sibling species in the marine pollution indicator *Capitella* (Polychaeta). *Science* **192:** 567–569.

Hadfield, M. G. 1978. Metamorphosis in marine molluscan larvae: an analysis of stimulus and response. Pp. 165–175 in *Settlement and Metamorphosis of Marine Invertebrate Larvae,* F. S. Chia and M. E. Rice, eds., Elsevier, New York.

Hadfield, M. G. 1984. Settlement requirements of molluscan larvae: new data on chemical and genetic roles. *Aquaculture* **39:** 283–298.

Hidaka, H., M. Inagaki, S. Kawamoto, and Y. Sasaki. 1984. Isoquinolinesulfonamides, novel and potent inhibitors of cyclic nucleotide dependent protein kinase and protein kinase C. *Biochemistry* **23:** 5036–5041.

Holian, O., R. Kumar, and L. M. Nyhus. 1989. Fatty acyl esters potentiate fatty acid induced activation of protein kinase C. *Biochem. Biophys. Res. Commun.* **160:** 1110–1116.

Ilan, J., J. Ilan, and N. Patel. 1972. Regulation of messenger RNA translation mediated by juvenile hormone. Pp. 43–68 in *Insect Juvenile Hormones, Chemistry and Action,* J. Menn and M. Beroza, eds. Academic Press, New York.

Ilenchuk, T. T., and K. G. Davey. 1987. Effects of various compounds on Na/K-ATPase activity, JH I binding capacity and patency response in follicles of *Rhodnius prolixus. Insect Biochem.* **17:** 1085–1088.

Jensen, R. A., and D. E. Morse. 1990. Chemically induced metamorphosis of polychaete larvae in both the laboratory and ocean environment. *J. Chem. Ecol.* **16:** 911–930.

Jimenez, B., A. Pestana, and M. Fernandez-Renart. 1989. A phospholipid-stimulated protein kinase from *Dictyostelium discoideum. Biochem. J.* **260:** 557–561.

Jones, G., and P. A. Sharp. 1997. Ultraspiracle: an invertebrate nuclear receptor for juvenile hormones. *Proc. Nat. Acad. Sci. USA* **94:** 13499–13503.

Jones, G., V. Venkataraman, M. Manczak, and D. Schelling. 1993. Juvenile hormone action to suppress gene transcription and influence message stability. *Dev. Gen.* **14:** 323–332.

Kaczmarek, L. K. 1987. The role of protein kinase C in the regulation of ion channels and neurotransmitter release. *Trends Neurosci.* **10:** 30–34.

Komatsu, M., F.-S. Chia, and R. Koss. 1991. Sensory neurons of the bipinnaria larva of the sea star, *Luidia senegalensis. Invertebr. Reprod. Dev.* **19:** 203–211.

Laufer, H., and D. W. Borst. 1983. Juvenile hormone and its mechanism of action. Pp. 203–216 in *Invertebrate Endocrinology, Vol. 1, Endocrinology of Insects,* R. G. H. Downer and H. Laufer, eds., Alan Liss, New York.

Laufer, H., and D. W. Borst. 1988. Juvenile hormone in crustacea. Pp. 305–313 in *Invertebrate Endocrinology, Vol. 2, Endocrinology of Selected Invertebrate Types,* H. Laufer and R. G. H. Downer, eds., Alan Liss, New York.

Laufer, H., D. Borst, F. Baker, C. Carrasco, M. Sinkus, C. Reuter, L. Tsai, and D. Schooley. 1987. Identification of a juvenile hormone-like compound in a crustacean. *Science* **235:** 202–205.

Leitz, T., and G. Klingman. 1990. Metamorphosis in *Hydractinia:* studies with activators and inhibitors aiming at protein kinase C and potassium channels. *Roux's Arch. Dev. Biol.* **199:** 107–113.

Luderus, M. E. E., R. G. van der Most, A. Otte, and R. van Driel. 1989. A protein kinase C-related enzyme activity in *Dictyostelium discoideum. FEBS Lett.* **253:** 71–75.

Morse, A. N. C., C. A. Froyd, and D. E. Morse. 1984. Molecules from cyanobacteria and red algae that induce larval settlement and metamorphosis in the mollusc *Haliotis rufescens. Mar. Biol.* **81:** 293–298.

Morse, D. E. 1990. Recent progress in larval settlement and metamorphosis: closing the gaps between molecular biology and ecology. *Bull. Mar. Sci.* **46:** 465–483.

Muller, W. A. 1985. Tumor-promoting phorbol esters induce metamorphosis and multiple head formation in the hydroid *Hydractinia. Differentiation* **29:** 216–222.

Muller, W. E. G., M. Rottmann, B. Diehl-Seifert, B. Kurelec, G. Uhlenbruck, and H. C. Schroder. 1987. Role of the aggregation factor in the regulation of phosphoinositide metabolism in sponges. *J. Biol. Chem.* **262:** 9850–9858.

Nishizuka, Y. 1984. The role of protein kinase C in cell surface signal transduction and tumour promotion. *Nature* **308:** 693–698.

Noveen, A., T.-X. Jiang, and C.-M. Chuong. 1995. Protein kinase A and protein kinase C modulators have reciprocal effects on mesenchymal condensation during skin appendage morphogenesis. *Dev. Biol.* **171:** 677–693.

Palli, S. R., K. Touhara, J.-P. Charles, B. C. Bonning, J. K. Atkinson, S. C. Trowell, K. Hiruma, W. G. Goodman, T. Kyriakides, G. D. Prestwich, B. D. Hammock, and L. M. Riddiford. 1994. A nuclear juvenile hormone-binding protein from larvae of *Manduca sexta:* a putative receptor for the metamorphic action of juvenile hormone. *Proc. Natl. Acad. Sci. USA* **91:** 6191–6195.

Parker, P. J., L. Coussens, N. Totty, L. Rhee, S. Young, E. Chen, S. Stabel, M. Waterfield, and A. Ullrich. 1986. The complete primary structure of protein kinase C- the major phorbol ester receptor. *Science* **233:** 853–866.

Pawlik, J. R. 1988. Larval settlement and metamorphosis of Sabellariid polychaetes, with reference to *Phragmatopoma lapidosa,* a reef-building species, and *Sabellaria floridensis,* a non-gregarious species. *Bull. Mar. Sci.* **43:** 41–60.

Pawlik, J. R. 1990. Natural and artificial induction of metamorphosis of *Phragmatopoma lapidosa californica* (Polychaeta: Sabellariidae), with a critical look at the effects of bioactive compounds on marine invertebrate larvae. *Bull. Mar. Sci.* **46:** 512–536.

Pearce, C. M., and R. E. Scheibling. 1990. Induction of settlement and metamorphosis in the sand dollar *Echinarachnius parma:* evidence for an adult-associated factor. *Mar. Biol.* **107:** 363–369.

Pechenik, J. A., and T. R. Cerulli. 1991. Influence of delayed metamorphosis on survival, growth, and reproduction of the marine polychaete *Capitella* sp. I. *J. Exp. Mar. Biol. Ecol.* **151:** 17–27.

Rittschof, D., and J. Bonaventura. 1986. Macromolecular cues in marine systems. *J. Chem. Ecol.* **12:** 1013–1023.

Rosen, L. B., and M. E. Greenberg. 1996. Stimulation of growth factor receptor signal transduction by activation of voltage-sensitive calcium channels. *Proc. Natl. Acad. Sci. USA* **93:** 1113–1118.

Rosen, L. B., D. D. Ginty, M. J. Weber, and M. E. Greenberg. 1994. Membrane depolarization and calcium influx stimulate MEK and MAP kinase via activation of Ras. *Neuron* **12:** 1207–1221.

Scheuer, P. J. 1990. Chemical communication of marine invertebrates. *Bioscience* **27:** 664–668.

Schwoerer-Bohning, B., M. Kroiher, and W. A. Muller. 1990. Signal transmission and covert prepattern in the metamorphosis of *Hydractinia echinata* (Hydrozoa). *Roux's Arch. Dev. Biol.* **198:** 245–251.

Sevala, V. L., and K. G. Davey. 1989. Action of juvenile hormone on the follicle cells of *Rhodnius prolixus:* evidence for a novel regulatory mechanism involving protein kinase C. *Experientia* **45:** 355–356.

Shearman, M. S., Z. Naor, K. Sekiguchi, A. Kishimoto, and Y. Nishizuka. 1989a. Selective activation of the g-subspecies of protein kinase C from bovine cerebellum by arachidonic acid and its lipoxygenase metabolites. *FEBS Lett.* **243:** 177–182.

Shearman, M. S., K. Sekiguchi, and Y. Nishizuka. 1989b. Modulation of ion channel activity: a key function of the protein kinase C enzyme family. *Pharmacol. Rev.* **41:** 211–237.

Shenk, M. A., and R. E. Steele. 1993. Homeobox genes and epithelial patterning in *Hydra.* Pp. 231–240 in *Molecular Basis of Morphogenesis,* M. Bernfield, ed. Wiley-Liss, New York.

Shinomura, T., Y. Asaoka, M. Oka, K. Yoshida, and Y. Nishizuka. 1991. Synergistic action of diacylglycerol and unsaturated fatty acid for protein kinase C activation: its possible implications. *Proc. Natl. Acad. Sci. USA* **88:** 5149–5153.

Slama, K. 1962. The juvenile hormone like effect of fatty acids, fatty alcohols, and some other compounds in insect metamorphosis. *Acta. Entom. Bohemoslav.* **59:** 323–340.

Stengl, M. 1993. Intracellular-messenger-mediated cation channels in cultured olfactory receptor neurons. *J. Exp. Biol.* **178:** 125–147.

Trapido-Rosenthal, H. G., and D. E. Morse. 1986. Availability of chemosensory receptors is down-regulated by habituation of larvae to a morphogenetic signal. *Proc. Natl. Acad. Sci. USA* **83:** 7658–7662.

Vandenbark, G. R., L. J. Kuhn, and J. E. Niedel. 1984. Possible mechanism of phorbol diester-induced maturation of human promyelocytic leukemia cells. *J. Clin. Invest.* **73:** 448–457.

Yamamoto, K., A. Chadarevian, and M. Pellegrini. 1988. Juvenile hormone action mediated in male accessory glands of *Drosophila* by calcium and kinase C. *Science* **239:** 916–918.

Yasuda, I., A. Kishimoto, S.-I. Tanaka, M. Tominaga, A. Sakurai, and Y. Nishizuka. 1990. A synthetic peptide substrate for selective assay of protein kinase C. *Biochem. Biophys. Res. Commun.* **166:** 1220–1227.

Yool, A. J., S. M. Grau, M. G. Hadfield, R. A. Jensen, D. A. Markell, and D. E. Morse. 1986. Excess potassium induces larval metamorphosis in four marine invertebrate species. *Biol. Bull.* **170:** 255–266.

Ziesel, S. 1993. Choline phospholipids: signal transduction and carcinogenesis. *FASEB J.* **7:** 551–557.

Zufall, F., and H. Hatt. 1991. Dual activation of a sex pheromone-dependent ion channel from insect olfactory dendrites by protein kinase C activators and cyclic GMP. *Proc. Natl. Acad. Sci. USA* **88:** 8520–8524.

Reference: *Biol. Bull.* **196:** 199–204. (April 1999)

Effect of Steroids on Gonadal Growth and Gametogenesis in the Juvenile Red Sea Urchin *Pseudocentrotus depressus*

TATSUYA UNUMA[1,*], TAKESHI YAMAMOTO[2], AND TOSHIO AKIYAMA[3]

[1] *National Research Institute of Aquaculture, Nansei, Mie 516-0193, Japan;*
[2] *Inland Station, National Research Institute of Aquaculture, Tamaki, Mie 519-0423, Japan; and*
[3] *National Research Institute of Fisheries Science, Fukuura, Kanazawa, Yokohama 236-8648, Japan*

Abstract. Red sea urchins, 10 months old, were fed for 30 days on a casein-based diet containing progesterone, androstenedione, testosterone, estrone, or estradiol-17β. The mean gonad indices of male animals in the androstenedione- and the estrone-treated groups were significantly higher than those in the control group, suggesting that these steroids promote gonadal growth in male animals. Histological observations indicated that spermatogenesis in the estrone-treated group was also promoted compared to that in the control group. In contrast, female urchins were not obviously affected by the steroid-treated diets, probably because yearling female *P. depressus* are not otherwise ready to carry out gametogenesis. We conclude that androstenedione, estrone, and possibly their derivatives, are involved in the reproduction of male *P. depressus*.

Introduction

Sex-related steroids, which have regulatory functions in vertebrate reproduction, are also found in echinoderms. The roles and actions of steroids in starfish have been investigated often: *e.g.*, biosynthesis and metabolism (Schoenmakers, 1979; Schoenmakers and Voogt, 1980, 1981; Voogt and Van Rheenen, 1986; Voogt *et al.*, 1986, 1990, 1991a, b; Hines *et al.*, 1992a); seasonal variations in steroid levels (Schoenmakers and Dieleman, 1981; Voogt and Dieleman, 1984; Xu and Barker, 1990; Xu, 1991; Hines *et al.*, 1992b); and the effects of steroid injections (Schoenmakers *et al.*, 1981; Takahashi, 1982a, b; Barker and Xu, 1993). These previous reports suggest that steroids are involved in the reproduction of starfish.

The importance of steroids in sea urchin reproduction is less well known. Estradiol-17β induced the synthesis of a novel protein in the coelomocytes of *Dendraster excentricus* and *Strongylocentrotus purpuratus in vitro* (Harrington and Ozaki, 1986). Levels of estradiol-17β and progesterone were determined in the testes and ovaries of *Eucidaris tribuloides* every 3 months during the annual reproductive cycle (Hines *et al.*, 1992c). Oral administration of estrone increased the body weight of *Pseudocentrotus depressus*, the red sea urchin (Unuma *et al.*, 1996a). However, we are just beginning to understand the relationship between steroids and the reproduction of sea urchins.

In *P. depressus*, gonadal growth occurs from spring to late autumn, preceding and also during gametogenesis. This growth is mainly due to the accumulation of nutrients by the nutritive phagocytes that occupy the lumina of the gonads of both sexes. Gametogenesis normally begins in September or October, and gonads are filled with mature gametes in November or December (unpubl. data). To investigate the effect of steroids on gonadal growth and gametogenesis, we fed sex-related steroids to *P. depressus*. Casein-based diets containing progesterone, androstenedione, testosterone, estrone, or estradiol-17β were prepared and fed to juvenile red sea urchins for 30 days beginning in early September.

Materials and Methods

Animals

Individuals of *P. depressus* were hatched and reared at the Fukuoka Prefectural Fish Farming Center and were transferred to the Nansei Station of the National Research

Received 21 October 1997; accepted 25 January 1999.

* Author to whom correspondence should be addressed. E-mail: unuma@nria.affrc.go.jp

Table I

Composition of the experimental diets

Casein	30 g
Sodium alginate	30 g
Dextrin	20 g
Cellulose	5 g
Pollock viscera oil	5 g
Mineral mix[1]	4 g
Soybean lecithin	3 g
Vitamin mix[2]	2.3 g
Choline chloride	0.59 g
L(+)-Ascorbic acid	0.1 g
β-Carotene	0.01 g
Ethanol with steroid[3]	2 ml
Water	120 ml

[1] U. S. P. XII salt mixture with trace elements (Halver, 1957).

[2] Contains each vitamin corresponding to 44% of the premix reported by the National Research Council (1973).

[3] The dissolved steroid is one of the following: progesterone, androstenedione, testosterone, estrone, or estradiol-17β (2 m*M*). Control diet lacks steroid.

Institute of Aquaculture, Mie, Japan, in May 1993. These individuals, 6 months old, were kept in a 1000-liter tank supplied with sand-filtered seawater at 30 l · min^{-1} and were reared on kelp (*Eisenia bicyclis*) for 4 months until used in the feeding experiments. Before these experiments, 20 urchins were sacrificed and their gonads were examined. The average gonad index (GI) was 0.87%, and all the gonads were in Stage 0 as determined by histological observations. The stages of maturation are defined below.

Experimental diets

The experimental diets were formulated according to Akiyama *et al.* (1997) with some slight modifications (Table I). On a dry weight basis, 25% of the diet was protein from casein, the sole protein source. Five test diets, each containing a steroid, and a control diet that lacked steroid were tested. Progesterone, (+)-4-androstene-3,17-dione (androstenedione), testosterone, estrone, and estradiol-17β (Wako Pure Chemical Industries, Ltd., Tokyo) were dissolved in ethanol and added to the diet to make a concentration of 1.8×10^{-8} mol · g^{-1} wet weight of diet. Only ethanol was added to the control diet. The ingredients were mixed thoroughly, shaped into a cookie-like form (about 50 mm in diameter) and then soaked in 5% $CaCl_2$ solution for 10 min (Akiyama *et al.*, 1997). The prepared test diets were kept at −20°C until used.

Feeding procedure

The feeding experiments were conducted from 6 September to 6 October. Three hundred urchins, 20 mm in test diameter and 3.8 g in body weight, were divided into six experimental groups, each containing 50 urchins; five groups were each given one of the steroid diets, and one group was given the control diet. Each group was placed in two rectangular acrylic tanks (50 × 20 × 30 cm, holding 20 liter of water), with 25 individuals per tank. Sand-filtered seawater was supplied to the tanks at the rate of 0.7 l · min^{-1}. During the experimental period, the water temperature gradually decreased from 25°C to 21°C. Sea urchins in each tank were given an excess of the experimental diets (7–10 g per tank) every other day and were allowed to feed to satiation. Uneaten diets were collected and weighed before new diets were given. Food intake for each tank was estimated based on the decrease in weight of the diet. After 30 days of feeding, body weight and gonad weight were measured for all animals. Gonad index (GI) was calculated from the following formula.

GI (%) = 100 × gonad wet weight/body wet weight

Daily food consumption was calculated for each tank using the following formula.

Daily food consumption (%) = 100 × food intake/[(initial body weight + final body weight)/2] × rearing period (days)

Histological observations

Small pieces of gonad from each animal were fixed in Bouin's solution, embedded in paraffin, and sectioned at 10 μm. The sections were stained with hematoxylin and eosin, and then observed by light microscopy to determine the sex and gametogenic stage of the gonads. The gonadal maturity of each animal was assessed according to the six-stage classification of Fuji (1960), with some slight modifications (Unuma *et al.*, 1996b) as follows (see Fig. 1).

Stage 0 (neuter): No obvious germ cells are observed, and sexes are unidentifiable. The gonadal lumina are filled with nutritive phagocytes.

Stage 1 (developing virgin): A few small oocytes or small clusters of spermatogonia are present at the periphery of gonads otherwise filled with nutritive phagocytes.

Stage 2 (growing): The gonads contain rows of spermatogonia or of oocytes at the periphery. The center of the gonads still contain nutritive phagocytes.

Stage 3 (pre-mature): In the center of the gonad, nutritive phagocytes are replaced with spermatozoa or ripe ova.

Stage 4 (mature): The gonadal lumina are filled with ripe ova or spermatozoa. Nutritive phagocytes are recognized only at the periphery of gonads.

Stage 5 (spent): Gonadal lumina are almost empty, with a few relict ova or small masses of relict spermatozoa. Nutritive phagocytes are recognized at the periphery of gonads.

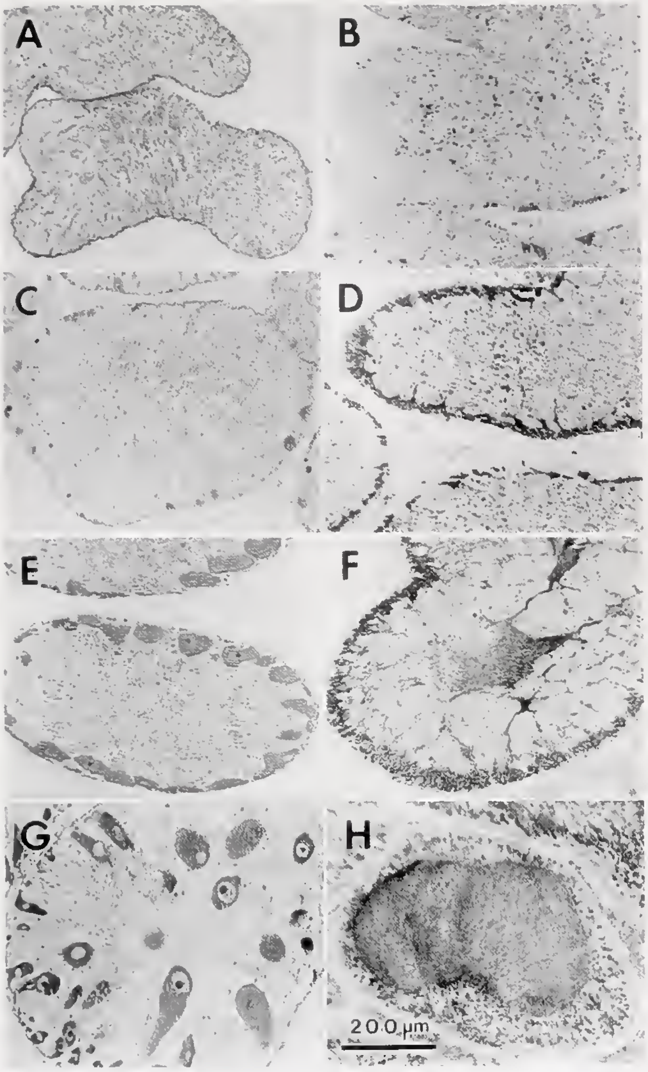

Figure 1. Classification of gonadal maturity in *Pseudocentrotus depressus*. Only the stages observed in this study are shown. B, D, F, H: male; C, E, G: female. (A) Stage 0: No obvious germ cells are observed, and sex is unidentifiable. (B, C) Stage 1: Small clusters of spermatogonia or a few young oocytes are present at the periphery of the gonad. (D, E) Stage 2: The gonads contain rows of spermatogonia or of oocytes. (F, G) Stage 3: In the center of the lumina, nutritive phagocytes are replaced with spermatozoa or ripe ova. (H) Stage 4: The gonadal lumina are filled with spermatozoa. Scale bar: 200 μm.

Statistical analysis

The mean values of GI and daily food consumption were compared using unpaired Student's t tests between the steroid-treated groups and the control group, after comparison of the variances using F test.

The Mann-Whitney U test was used to compare the distribution of the maturational stages of gonads between the steroid-fed groups and the control group.

Results

Gonad index

No mortality occurred during these experiments. Moreover, sex could be determined by histological observations in all but three animals. One specimen in each of the progesterone-, androstenedione-, and testosterone-treatment groups was neuter, and these three cases were omitted when average GIs were calculated for each sex.

Figure 2 shows the mean GI values for each sex after the 30-day feeding trial. In male animals, the mean GI of the control group was 4.87%. The androstenedione- and estrone-treated groups showed significantly higher values than the control group, 6.22% ($P < 0.05$) and 6.94% ($P < 0.001$), respectively. The values in the progesterone-, the testosterone-, and the estradiol-17β-treated groups were not significantly different from the control group.

Unlike the male animals, the female animals had similar mean GI values from all groups; in particular, no significant difference was found between the steroid-treated groups and the control group.

Maturational stages of gonads

Frequencies of the maturational stages of gonads for each sex are shown in Figure 3. In males, the percentages of Stages 1, 2, and 3 in the control group were 32%, 54% and 14%, respectively. In all the steroid-treated groups except that treated with estrone, the percentage of each stage was similar to that in the control group. In the estrone-treated group, however, the percentage of Stage 1 was only 4% (one-eighth that of the control group) and that of Stage 3 was 31% (more than twice that of the control group). The distribution of maturational stages in the estrone-treated group was significantly different ($P < 0.05$) from that of the

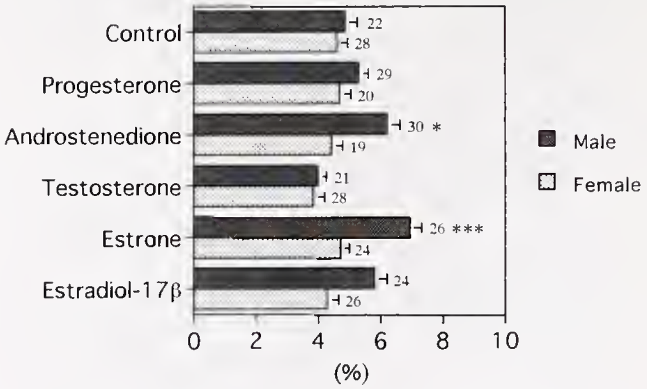

Figure 2. Gonad index of male and female *Pseudocentrotus depressus* fed diets containing steroids. Values represent the mean ± SE. Numerals in the graph indicate the number of individuals. Values with asterisks are significantly different from the control of the same sex (*, $P < 0.05$; ***, $P < 0.001$).

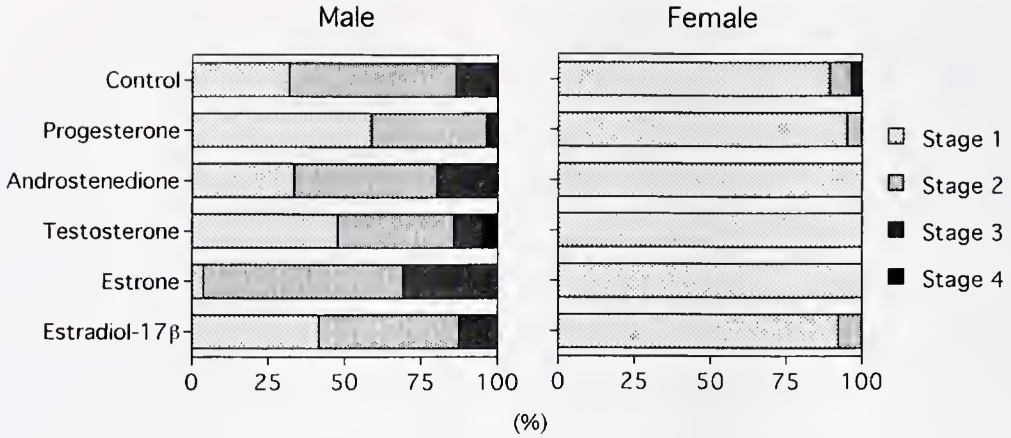

Figure 3. Frequencies of the maturational stages of gonads for male and female *Pseudocentrotus depressus* fed diets containing steroids. The frequencies for male animals in the estrone-treated group are significantly different from those in the control group ($P < 0.05$).

control group. This suggests that spermatogenesis was promoted in the estrone-treated group.

In the females from all groups, most of the gonads were in Stage 1, with no specific difference observed between the steroid-treated and control groups.

Daily food consumption

The mean daily consumption, based on wet matter, for duplicate tanks are shown in Table II. The androstenedione- and the estrone-treated groups showed higher values than the control group, but this difference was not significant.

Discussion

In this study of *P. depressus*, the responses of males and females to orally administered steroids was markedly different. In males, the mean GIs in the androstenedione- and the estrone-treated groups were significantly elevated compared to that in the control group, suggesting that androstenedione and estrone promoted gonadal growth. In these two groups, daily food consumption was higher than in the control group. The mobilization of nutrients from the food into the testes may have been enhanced in these steroid-fed groups.

Unlike males, female animals were not affected by the steroids tested in this study. Unuma *et al.* (1996b) cultured *P. depressus* for one year, from an age of 8 months to 20 months, and during this period most of the females remained immature throughout the annual reproductive cycle, but most of the males commenced gametogenesis. Yearling female red sea urchins thus probably cannot carry out gametogenesis. We think this is the main reason that the female animals did not respond to the steroids in this study.

In both sexes of the sea urchin, the nutritive phagocytes in the gonad are the main site for storage of nutrients required for gametogenesis (Walker, 1982). Nutrients derived from ingested food are assimilated into storage in the nutritive phagocytes before and also during gametogenesis (Takashima, 1976). We suppose that, in this study, androstenedione and estrone promoted the accumulation of nutrients by the nutritive phagocytes. But as gametogenesis progresses, the nutritive phagocytes shrink and lose their nutrient reserves. Therefore, it is difficult to compare the total amount of nutrients accumulated by the nutritive phagocytes of animals that are in different gonadal stages.

Sea urchins are unlike other oviparous animals in that yolk protein is not female specific. The yolk protein accumulates in the nutritive phagocytes as a nutrient source for gametogenesis, not only in females (Ozaki *et al.*, 1986), but also in males (Unuma *et al.*, 1998). Shyu *et al.* (1987) identified, in the sea urchin *Strongylocentrotus purpuratus*, a DNA sequence closely resembling the estrogen-responsive element of vertebrates near the gene of the yolk protein precursor, called vitellogenin. This suggests that vitelloge-

Table II

Daily consumption by Pseudocentrotus depressus *of diets containing steroids*

Diet	Daily consumption (%)[1]
Control	1.985 ± 0.043
Progesterone	1.987 ± 0.002
Androstenedione	2.188 ± 0.073
Testosterone	2.098 ± 0.139
Estrone	2.164 ± 0.026
Estradiol-17β	1.991 ± 0.047

[1] Calculated as 100 × food intake/[(initial body weight + final body weight)/2] × rearing period (days). Values represent the mean ± SE of duplicate tanks. None of these values in steroidal groups is significantly different from that in the control group.

nin synthesis may be controlled by steroids in sea urchins, as it is controlled in oviparous vertebrates by estrogens (Wallace, 1985), and in insects by ecdysteroids (Hagedorn, 1985). In this study, the accumulation of nutrients into the nutritive phagocytes may have been enhanced by the steroids through the synthesis of vitellogenin.

In sea stars of both sexes, estrogens may promote biosynthesis of protein in the pyloric caeca and its subsequent mobilization into the gonads (Schoenmakers and Dieleman, 1981; Voogt and Dieleman, 1984; Voogt *et al.*, 1985; Xu and Barker, 1990). Takahashi (1982a) reported that daily injections of androstenedione and estrone over a 16-day period induced gonadal growth in female *Asterina pectinifera*, whereas progesterone, testosterone, and estradiol-17β did not. Takahashi's results are similar to our observations for male *P. depressus*. Takahashi supposed that androstenedione was metabolized to estrone, which then affected the mobilization of proteins into the ovaries. However, little information is available on the biosynthesis of estrogen from androgens in echinoderms (Hines *et al.*, 1992a). Whether androstenedione itself has the potential to promote gonadal growth in echinoderms must be determined in future studies.

The relationship between steroids and gametogenesis in sea stars has been the concern of several reports. Estrone injections over a 5-day period increased the number of male germ cells in *A. pectinifera* (Takahashi, 1982b). Increases in estrone levels in the testes were observed at the onset of testicular growth in *Asterias rubens* (Voogt and Dieleman, 1984) and in *Sclerasterias mollis* (Xu, 1991). Transient increases in estradiol-17β levels in the testes occurred coincidently with mitotic proliferation of spermatogonia in *Asterias vulgaris* (Hines *et al.*, 1992b). In *A. vulgaris*, after a pretreatment with progesterone, estradiol-17β stimulated spermatogonial mitosis *in vitro* (Marsh and Walker, 1995). These reports suggest that, in sea stars, estrogens are responsible for initiating spermatogenesis through the stimulation of spermatogonial proliferation. In the current feeding experiment, spermatogenesis was promoted in the estrone-treated group. This result suggests that, in sea urchins, estrone is important for the initiation of spermatogenesis, as reported in sea stars. Our conclusion in this study is that androstenedione, estrone, and possibly their derivatives, are probably involved in the reproduction of sea urchins through the control of gonadal growth and gametogenesis.

Acknowledgments

We are grateful to the Fukuoka Prefectural Fish Farming Center for providing the experimental *P. depressus* seedlings.

Literature Cited

Akiyama, T., T. Unuma, T. Yamamoto, H. Furuita, and K. Konishi. 1997. An evaluation of amino acid sources and binders in semipurified diet for red sea urchin *Pseudocentrotus depressus*. *Fish. Sci.* **63:** 881–886.

Barker, M. F., and R. A. Xu. 1993. Effects of estrogens on gametogenesis and steroid levels in the ovaries and pyloric caeca of *Sclerasterias mollis* (Echinodermata: Asteroidea). *Invertebr. Reprod. Dev.* **24:** 53–58.

Fuji, A. 1960. Studies on the biology of the sea urchin. I. Superficial and histological gonadal changes in gametogenic process of two sea urchins, *Strongylocentrotus nudus* and *S. intermedius*. *Bull. Fac. Fish. Hokkaido Univ.* **11:** 1–14.

Hagedorn, H. H. 1985. The role of ecdysteroids in reproduction. Pp. 205–262 in *Comprehensive Insect Physiology, Biochemistry and Pharmacology*, G. A. Kerkut and L. I. Gilbert, eds. Pergamon Press, Oxford.

Halver, J. E. 1957. Nutrition of salmonid fishes III. Water soluble vitamin requirement of chinook salmon. *J. Nutr.* **62:** 225–243.

Harrington, F. L., and H. Ozaki. 1986. The effect of estrogen on protein synthesis in echinoid coelomocytes. *Comp. Biochem. Physiol.* **84B:** 417–421.

Hines, G. A., S. A. Watts, C. W. Walker, and P. A. Voogt. 1992a. Androgen metabolism in somatic and germinal tissues of the sea star *Asterias vulgaris*. *Comp. Biochem. Physiol.* **102B:** 521–526.

Hines, G. A., S. A. Watts, S. A. Sower, and C. W. Walker. 1992b. Sex steroid levels in the testes, ovaries, and pyloric ceaca during gametogenesis in the sea star *Asterias vulgaris*. *Gen. Comp. Endocrinol.* **87:** 451–460.

Hines, G. A., J. B. McClintock, and S. A. Watts. 1992c. Levels of estradiol and progesterone in male and female *Eucidaris tribuloides* (Echinodermata: Echinoidea) over an annual gametogenic cycle. *Fla. Sci.* **55**(2): 85–91.

Marsh, A. G., and C. W. Walker. 1995. Effect of estradiol and progesterone on c-myc expression in the sea star testis and the seasonal regulation of spermatogenesis. *Mol. Reprod. Dev.* **40:** 62–68.

National Research Council. 1973. *Nutrient Requirements of Trout, Salmon, and Catfish.* National Academy of Science, Washington, DC.

Ozaki, H., O. Moriya, and F. E. Harrington. 1986. A glycoprotein in the accessory cell of the echinoid ovary and its role in vitellogenesis. *Roux's Arch. Dev. Biol.* **195:** 74–79.

Schoenmakers, H. J. N. 1979. *In vitro* biosynthesis of steroids from cholesterol by the ovaries and pyloric caeca of the starfish *Asterias rubens*. *Comp. Biochem. Physiol.* **63B:** 179–184.

Schoenmakers, H. J. N., and S. J. Dieleman. 1981. Progesterone and estrone levels in the ovaries, pyloric ceca, and perivisceral fluid during the annual reproductive cycle of starfish, *Asterias rubens*. *Gen. Comp. Endocrinol.* **43:** 63–70.

Schoenmakers, H. J. N., and P. A. Voogt. 1980. *In vitro* biosynthesis of steroids from progesterone by the ovaries and pyloric ceca of the starfish *Asterias rubens*. *Gen. Comp. Endocrinol.* **41:** 408–416.

Schoenmakers, H. J. N., and P. A. Voogt. 1981. *In vitro* biosynthesis of steroids from androstenedione by the ovaries and pyloric caeca of the starfish *Asterias rubens*. *Gen. Comp. Endocrinol.* **45:** 242–248.

Schoenmakers, H. J. N., C. G. Van Bohemen, and S. J. Dieleman. 1981. Effects of oestradiol-17β on the ovaries of the starfish *Asterias rubens*. *Dev. Growth Differ.* **23**(2): 125–135.

Shyu, A.-B., T. Blumenthal, and R. A. Raff. 1987. A single gene encoding vitellogenin in the sea urchin *Strongylocentrotus purpuratus*: sequence at the 5′ end. *Nucleic Acids Res.* **15:** 10405–10417.

Takahashi, N. 1982a. The relation between injection of steroids and ovarian protein amounts in the starfish *Asterina pectinifera*. *Bull. Jpn. Soc. Sci. Fish.* **48:** 509–511.

Takahashi, N. 1982b. Effect of injection of steroids on the starfish testes *Asterina pectinifera*. *Bull. Jpn. Soc. Sci. Fish.* **48:** 513–515.

Takashima, Y. 1976. Ultrastructure of nurse cells and oogenesis in the sea urchin. *Gunma Symp. Endocrinol.* **13:** 105–127.

Unuma, T., T. Yamamoto, and T. Akiyama. 1996a. Effects of oral administration of steroids on the growth of juvenile sea urchin, *Pseudocentrotus depressus. Suisanzoshoku* **44**(1): 79–83.

Unuma, T., K. Konishi, H. Furuita, T. Yamamoto, and T. Akiyama. 1996b. Seasonal changes in gonads of cultured and wild red sea urchin, *Pseudocentrotus depressus. Suisanzoshoku* **44**(2): 169–175.

Unuma, T., T. Suzuki, T. Kurokawa, T. Yamamoto, and T. Akiyama. 1998. A protein identical to the yolk protein is stored in the testis in male red sea urchin, *Pseudocentrotus depressus. Biol. Bull.* **194:** 92–97.

Voogt, P. A., and S. J. Dieleman. 1984. Progesterone and oestrone levels in the gonads and pyloric caeca of the male sea star *Asterias rubens:* a comparison with the corresponding levels in the female sea star. *Comp. Biochem. Physiol.* **79A:** 635–639.

Voogt, P. A., and J. W. A. Van Rheenen. 1986. Androstenedione metabolism in the sea star *Asterias rubens* L. studied in homogenates and intact tissue: biosynthesis of the novel steroid fatty-acyl testosterone. *Comp. Biochem. Physiol.* **85B:** 497–502.

Voogt, P. A., J. J. S. Broertjes, and R. C. H. M. Oudejans. 1985. Vitellogenesis in sea star: physiological and metabolic implications. *Comp. Biochem. Physiol.* **80A:** 141–147.

Voogt, P. A., J. W. A. Van Rheenen, J. G. D. Lambert, and B. F. De Groot. 1986. Effects of different experimental conditions on progesterone metabolism in the sea star *Asterias rubens* L. *Comp. Biochem. Physiol.* **84B:** 397–402.

Voogt, P. A., P. J. Den Besten, and M. Jansen. 1990. The Δ 5-pathway in steroid metabolism in the sea star *Asterias rubens* L. *Comp. Biochem. Physiol.* **97B:** 555–562.

Voogt, P. A., P. J. Den Besten, and M. Jansen. 1991a. Steroid metabolism in relation to the reproductive cycle in *Asterias rubens* L. *Comp. Biochem. Physiol.* **99B:** 77–82.

Voogt, P. A., S. Van Ieperen, M. B. J. C. B. Van Rooyen, H. J. Wynne, and M. Jansen. 1991b. Effect of photoperiod on steroid metabolism in the sea star *Asterias rubens* L. *Comp. Biochem. Physiol.* **100B:** 37–43.

Walker, C. W. 1982. Nutrition of gametes. Pp. 449–468 in *Echinoderm Nutrition,* M. Jangoux and J. M. Lawrence, eds. A. A. Balkema, Rotterdam.

Wallace, R. A. 1985. Vitellogenesis and oocyte growth in nonmammalian vertebrates. Pp. 127–177 in *Developmental Biology,* L. W. Browder, ed. Plenum Press, New York.

Xu, R. A. 1991. Annual changes in the steroid levels in the testis and the pyloric caeca of *Sclerasterias mollis* (Hutton) (Echinodermata: Asteroidea) during the reproductive cycle. *Invertebr. Reprod. Dev.* **20:** 147–152.

Xu, R. A., and M. F. Barker. 1990. Annual changes in the steroid levels in the ovaries and the pyloric caeca of *Sclerasterias mollis* (Echinodermata: Asteroidea) during the reproductive cycle. *Comp. Biochem. Physiol.* **95A:** 127–134.

Reference: *Biol. Bull.* **196:** 205–215. (April 1999)

Suspension Feeding Adaptations to Extreme Flow Environments in a Marine Bryozoan

BETH OKAMURA* AND JULIAN C. PARTRIDGE

School of Biological Sciences, University of Bristol, Woodland Road, Bristol BS8 1UG, UK

Abstract. We describe the effects of extreme flow on the growth and morphology of a bryozoan, *Membranipora membranacea*, encrusting laminarian fronds in the Rapids of Lough Hyne (=Ine), County Cork, Ireland. An ultrasonic current meter was used to characterize ambient flow regimes at the level of the algal canopy over a complete tidal cycle at three sites within the Rapids. Colonies collected from sites exposed to different flows showed a trend towards miniaturization with increased flow: the zooids were less elongate, the lophophores were smaller in diameter and had fewer tentacles, and the distances between excurrent jets were shorter. These morphological changes probably place feeding surfaces into slower flow regimes of the boundary layer. Similar growth rates of colonies at sites differing in flow provide evidence that this miniaturization is adaptive and that bryozoans are capable of adopting appropriate morphological responses to varying environmental regimes. Such plasticity should be considered when assessing feeding from different flow regimes because particular colonies may be adapted to a limited and specific range of flow conditions.

Introduction

Many aquatic organisms, ranging from microbes to whales, have the ability to collect food particles from the water column. Whereas mobile suspension feeders collect particles by actively swimming through the water, sessile suspension feeders rely on the movement of water to carry food resources to their feeding surfaces. In both cases, the potential food available is determined by the flux of particles past feeding surfaces, which is a function of particle concentration and the rate at which these particles are encountered by the feeding surfaces. All else being equal, increased flow will increase the flux of food to sessile suspension feeders. It will also result in increased turbulent mixing of the surrounding water, which reduces depletion of food particles near feeding surfaces (Wildish and Kristmanson, 1979; Patterson, 1984; Fréchette and Bourget, 1985; Fréchette *et al.*, 1989).

Despite these benefits of flow, too much flow will eventually be detrimental, as indicated by a decline in feeding rates at higher flows in a variety of suspension feeders (*e.g.*, Okamura, 1984, 1985, 1992; McFadden, 1986; Best, 1988; Leonard *et al.*, 1988; Sponaugle and LaBarbera, 1991; Eckman and Duggins, 1993; Anthony, 1997). These declines are explained by deformation of filtering structures that reduces surface areas for particle capture, drag effects that reduce efficiency of handling or processing particles, adverse pressure gradients that inhibit effective processing of water in feeding, or a combination of these factors (Eckman and Duggins, 1993). These considerations suggest that sessile suspension feeders may avoid extreme flow conditions by (1) not feeding during inappropriate flow conditions, (2) colonizing appropriate flow habitats, or (3) employing flow-dependent morphological responses that allow them to exploit particular flow microhabitats.

A number of studies have examined the effects of flow on growth and feeding of active suspension feeders including bivalves (*e.g.*, Kirby-Smith, 1972; Eckman *et al.*, 1989; Grizzle *et al.*, 1992; Lenihan *et al.*, 1996; Judge and Craig, 1997), barnacles (Eckman and Duggins, 1993), bryozoans (Okamura, 1984, 1985, 1990; Eckman and Duggins, 1993; Grünbaum, 1995), and serpulids (Eckman and Duggins, 1993), although only one study has demonstrated that the effect of flow on feeding translates into flow effects on growth (Okamura, 1992). Except in sponges, whose morphologies vary with exposure to flow (Wilkinson and Vace-

Received 26 May 1998; accepted 11 January 1999.

* Current address: School of Animal and Microbial Sciences, The University of Reading, Whiteknights, PO Box 228, Reading, RG6 6AJ, UK. E-mail: b.okamura@reading.ac.uk

let, 1979; Palumbi, 1984), the morphological responses to flow of active suspension feeders have received little attention.

Studies of cnidarians indicate that morphological changes can enable passive suspension feeders to exploit a range of flow environments. For instance, individuals of the sea anemone *Anthopleura xanthogrammica* are found in flow conditions ranging from exposed intertidal surge channels to protected crevices. Koehl (1977) showed that variation in the shapes of anemones resulted in exposure to similar flow forces in these two types of habitats. Thus taller anemones in protected habitats encountered flows as fast as those experienced by squat anemones in surge channels because squat anemones hide in the reduced flow regimes of the benthic boundary layer, whereas tall anemones extend into the freestream flow regime beyond that layer. Similarly, Anthony (1997) reported large individuals of the anemone *Metridium senile* to occur in regions of low currents and small individuals in narrow channels with greatly increased current speeds. He found that feeding rates were dependent on anemone size and hence were related to habitat. Large anemones thus experienced an inhibition in feeding at increased flows, but the feeding rate of small anemones was unaffected. These studies indicate that plasticity in body size and shape may allow anemones to avoid the feeding inhibition that occurs in faster flows by ensuring that feeding surfaces experience similar flow microhabitats even though the anemones may be found in strikingly different flow macrohabitats.

Here we address how flow affects the growth rates and the associated morphological responses of an active suspension feeder by studying colonies of the bryozoan *Membranipora membranacea* along a gradient of extremely rapid flow in a tidal channel in southwest Ireland.

Materials and Methods

The study system

The Rapids of Lough Hyne (=Ine) (County Cork, Ireland) present an ideal site for studying growth and morphological variation along an environmental gradient of flow. In the Rapids, tidal water is forced to flow through a relatively narrow channel that connects an inland marine lough with the sea (Fig. 1). Flows reach highest speeds in the narrowest and shallowest region of the Rapids known as the "Sill," which is about 1 m deep at low water and is bordered on the west by a seawall. The site is subject to simple flows with no confounding wave action; near-maximal flows are maintained during much of the inflow and outflow periods, and the period of slack water is of very short duration (Bassindale *et al.*, 1948; data reported here). Organisms living in the Rapids are thus subjected to highly predictable flow regimes, the characteristics of which are determined principally by their location within the Rapids channel. However, other than flow, environmental conditions are similar in different stretches of the Rapids because a large tidal volume is forced through the relative short and narrow region of the Rapids. Thus organisms within the Rapids will be subject to similar temperatures, salinities, food particle concentrations, etc.

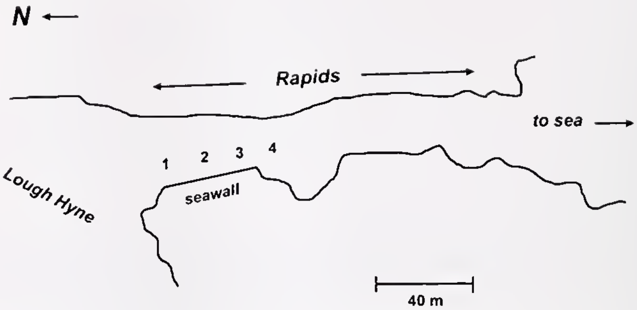

Figure 1. Schematic of the Rapids of Lough Hyne showing sites where flow measurements and growth studies were conducted (Sites 1–3) and from which colonies were collected for morphometric studies (Sites 1–4).

Membranipora is an epifaunal bryozoan that specializes in encrusting the fronds of macroalgae, forming sheetlike colonies that grow rapidly (Seed, 1976) and can attain large sizes. *M. membranacea* is common on fronds of the laminarians *Laminaria digitata* and *Saccorhiza polyschides*, both of which grow in the Rapids area. Because these macroalgal fronds are highly flexible, colonies of *M. membranacea* will experience unidirectional flows as the fronds flex and become extended by incoming and outgoing tidal currents.

Flow measurements

We characterized the ambient flow regime at the canopy level of algal fronds at three sites along the Rapids by using an ultrasonic current meter (Minilab Model SD-12) that measured the velocity of flow in three dimensions with a resolution of 1 mm s^{-1}. Because of the strength of flow through the Rapids it was necessary to securely deploy the flow probe to ensure it was not displaced downstream or its orientation disturbed. We did this by attaching the probe to an aluminum pole fastened to the end of a ladder that extended outwards over the Rapids from a solid seawall. The aluminum pole and attached probe were lowered from the end of the ladder directly into the Rapids so that the probe was measuring flows at the level of the algal canopy. The ladder itself was weighed down with boulders, and we maintained the probe in a vertical position with a rope that was attached to the aluminum pole and held taut from an upstream position during flow measurements. This set-up was sufficient to ensure that the flow probe maintained a constant position in the face of strong tidal flows. The probe itself was placed in a cylindrical wire cage (diameter = 10 cm, height = 17 cm; mesh thickness = 0.2 cm; gap size =

1.7 cm) to protect it from water-borne objects. The caging may have contributed to the turbulence levels measured in the study, but such effects are greatest in low-energy environments (Nowell and Jumars, 1984) that are not characteristic of the Lough Hyne Rapids.

Measurement sites were chosen to represent a gradient of flow through the Rapids area in which *M. membranacea* colonies were growing on laminarian fronds (see Fig. 1). The exact location of measurements was determined by the availability of reasonably flat stretches of the seawall where a stable probe-and-ladder apparatus could be set up. Flows at each of the three sites were measured about 1 m from the wall, at the level of the algal canopy. Data collected represent instantaneous flow readings taken every second over a series of 5-min periods for each site over a complete tidal cycle. After each 5-min period, the probe and its ladder support were moved to the next site and reassembled to monitor for a further 5-min period. It should be noted that this sampling scheme may underestimate turbulence by overlooking high-frequency turbulent fluctuations over very short time scales. However, some of these fluctuations should be reflected in overall turbulence estimates because they contribute to the level of variation in flow that is sampled by the 300 or so data points accumulated over a 5-min period.

Our sampling regime provided an overall measure of flow at each site during both the inflow and the following outflow periods of a tidal cycle. We began monitoring flows at the end of the short slack-water phase when the laminarian fronds were observed to flop over with the incoming tide. The measurements were taken on 20 August 1995 during a period of neap tides and thus represent minimal ranges of tidal flow at the three sites.

Data on flow in the x (along the length of the Rapids), y (across the Rapids), and z (vertical) dimensions were used to determine the overall mean velocities and turbulent kinetic energy densities for each 5-min period. Overall mean velocities for each sampling period were calculated as the mean of individual determinations of $(u^2 + v^2 + w^2)^{1/2}$ sampled once per second over the 5-min period (where u, v, and w represent the flow velocities in the x, y and z directions). Turbulent kinetic energy density (joules per cubic meter; Clifford and French, 1993) summarizes the turbulent fluctuations in all three dimensions and was calculated by the equation

$$E = \frac{1}{2}\rho(\sigma_u{}^2 + \sigma_v{}^2 + \sigma_w{}^2)$$

using $\rho = 1.025$ kg · m^{-3} (the density of seawater) and $o_u{}^2$, $o_v{}^2$ and $o_w{}^2$ the variances of the three components of flow over the 5-min periods of sampling in the x, y, and z directions.

Bryozoan responses to flow

We monitored growth rates of relatively small colonies of *M. membranacea* growing on fronds in the three sites in which flows were assessed. To ensure independence, we mapped and photographed only one colony per frond segment to monitor its growth. The frond segments containing the mapped colonies were marked by attaching cable ties to the mapped colonies. We attached a small piece of orange surveyor's tape to the cable tie, which helped us to relocate colonies. We chose colonies that were relatively isolated from other colonies on the frond segment and therefore would be unobstructed in growth. We mapped and photographed 8 colonies in Sites 1 and 2, and 13 colonies in Site 3. Because we were restricted to working in the Rapids during the short period of slow flow around the time of slack water, we required two consecutive days (17 and 18 August 1995) to set up the growth experiments. All colonies were allowed to grow for 10 days, and were then collected and rephotographed. The seawater temperature measured midway through the growth experiments was 19°C.

To assess morphological responses to flow, colonies were collected from within 1 m of the three sites at which flow was monitored. We also collected colonies from a fourth site at which flows were not measured because we could not securely deploy the probe in such rapid flow conditions. In the laboratory, a dissection microscope was used for morphometric measurements, which were accurate to the nearest 20 μm. For each colony we measured lengths, maximum widths (Fig. 2), lophophore diameters, and number of tentacles per lophophore of seven haphazardly chosen zooids. We avoided measuring zooids that are produced at early stages of colony development and had not yet achieved normal size, and the smaller zooids that develop initially in lineal series of zooids that are produced through bifurcation from a parental lineal series. We determined interchimney distances as the distance between the centers of neighboring chimneys (Fig. 3). Chimneys represent regions where excurrents are jetted away from colony surfaces. We collected a fresh set of colonies from each site for these measurements; this ensured that the colonies were behaving normally and that the extended arrays of lophophores made the chimneys clearly visible. We attempted to measure nine interchimney distances per colony, although in a small number of cases fewer than nine were available for measurement.

We determined the relative densities of colonies in the three sites by assessing the percent cover of *M. membranacea* on three *Laminaria* and three *Saccorhiza* plants from each of the three sites. We randomly selected three fronds per plant and measured the percent cover of *M. membranacea* along a line transect running the lengths of the fronds.

We ensured that the data collected conformed to the assumptions of all statistical analyses used. If assumptions of variance homogeneity in ANOVA could not be met through transformation of the data, we employed the non-parametric Kruskal-Wallis test. Morphometric analyses used mean values per colony as individual data points and are therefore reported as overall mean values. This approach allowed us to test specifically the overall differences in colonies from different sites, but it overlooks additional information on intra-colony levels of variation within and between sites.

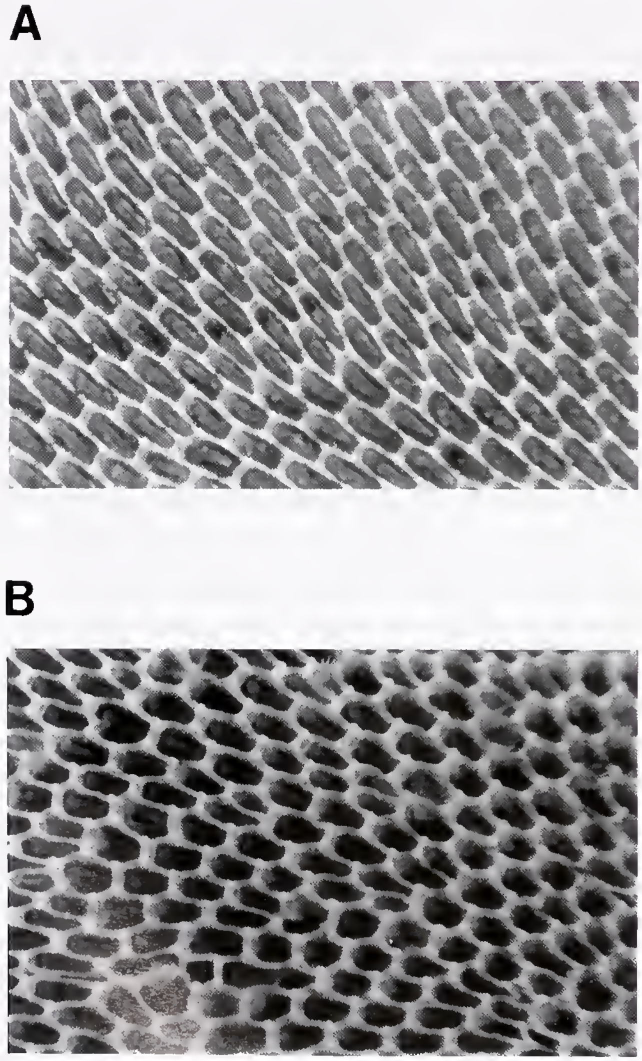

Figure 2. *Membranipora membranacea* colonies collected from slower and faster flow sites showing flow-associated variation in zooid shapes. (A) Zooids produced in colonies growing in slower flows assume elongate, nearly rectangular shapes. Note that zooid lengths were measured as the distance from the midline of distal edges of the end walls of contiguous zooids in lineal series, and zooid widths were measured as the maximum width observed between lateral zooidal walls (see Materials and Methods for discussion of choosing zooids for measurement). (B) Zooids produced in colonies growing in fast flows assume more hexagonal shapes and often possess wavering walls. Magnification = × 10.

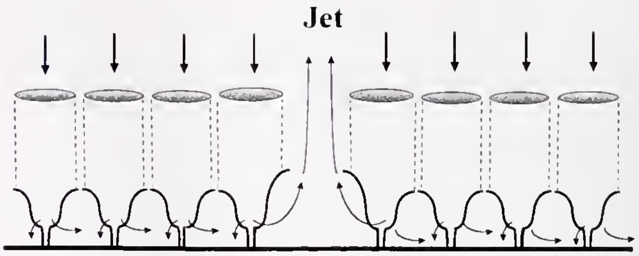

Figure 3. Schematic depiction of ciliary-driven movement of water (shown by arrows) over colony of *Membranipora membranacea.* Ciliary feeding currents produce feeding zones through which water is drawn into the lophophore. Water exits the bases of lophophores between the tentacles. Because lophophores are closely spaced, this excurrent flow is directed below the array of extended lophophores until it finds a gap, or chimney, where lophophores are not extended; it then escapes through this gap as a jet from colony surfaces. The relatively high velocity of the excurrent jet carries excurrents to some height above the colony surface, which minimizes refiltration since jets are then carried away by boundary layer flow (Lidgard, 1981).

Results

Flow measurements

Flows differed at the three sites as expected, with Site 1 consistently experiencing the lowest flow speeds and Site 3 the highest (Fig. 4). The period of inflow (into Lough Hyne) was much shorter, and thus higher flows were sustained, than during the longer period of slower outflow. The upper plot of Figure 4 shows the overall mean velocities in the x, y, and z directions. In nearly all cases apart from several instances around the time of slack water, the major contributor to flow was in the x (downstream) direction due to the incoming and outgoing flows, as can be seen by the ranges of flows in each direction for each site during the inflow and outflow periods (Table 1). Turbulent kinetic energy density was consistently highest in Site 3 and lowest in Site 1 (see Fig. 4, lower panel), as might be expected from the flow velocities at the three sites, and was greater during inflow.

Bryozoan responses to flow

M. membranacea showed morphological variation for several traits along the flow gradient. Mean zooid lengths decreased from Sites 1 to 4, in association with the increase in mean (and maximum) flow velocities at these sites, although this trend was not quite significant (Kruskal-Wallis test: $H_{\text{adj}} = 7.491$, df = 3, $0.05 < P < 0.10$; Fig. 5a). There was no change in mean zooid widths among the four sites (Kruskal-Wallis test: $H_{\text{adj}} = 0.184$, df = 3, $P \gg 0.05$; Fig. 5b). Mean zooid elongation (zooid length/zooid width) significantly decreased with increased flow ($F_{3,30} = 4.106$, $P = 0.015$; Fig. 6a), but mean zooid areas (zooid length × zooid width) did not differ among the four sites ($F_{3,30} = 1.411$, $P = 0.259$; Fig. 6b). These results indicate that zooids become less elongate largely through a decrease in

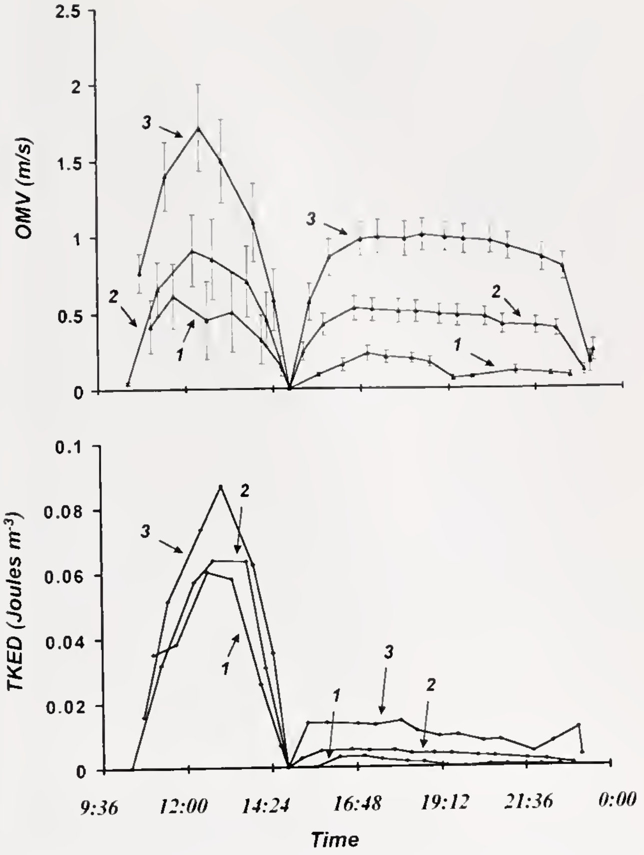

Figure 4. Two characterizations of ambient flow regimes at the algal canopy level for Sites 1–3. Sites are denoted by numbers, with arrows pointing to relevant data. Overall mean velocities (OMV) are plotted in the top graph and were calculated from flow measurements in the *x*, *y*, and *z* directions over 5-min intervals during inflow (from 1024–1450) and outflow (from 1513–2311) at Sites 1–3 (see Fig. 1). Bars represent one standard deviation. Values of turbulent kinetic energy density (TKED) are shown in the lower graph. See Materials and Methods section for details on flow measurements and characterization of the flow regimes.

length. There must also, however, be some slight increase in width—even though zooid width on its own did not vary significantly among sites (but see trend towards increasing width with increased flows; Fig. 5b)—since less elongate zooids in sites exposed to faster flows have areas similar to those of zooids in slower flow sites. Although we made no explicit attempt to compare zooid shapes, other than assessing zooid elongation, it was apparent that zooids in colonies exposed to the extremely rapid flows at Site 4 were irregular in outline. They were more hexagonal, often with wavering walls, than the normal elongate, fairly rectangular zooid with straight walls (see Fig. 2). This suggests that calculations based on data for maximum length and width may overestimate the zooid areas of colonies under conditions of very rapid flows. Such irregularly shaped zooids may be a character indicative of exposure to flow in *M. membranacea*.

Table 1

Ranges of mean velocities measured in the x, y, and z directions denoted as u, v, and w measured at Sites 1–3 during inflow and outflow tidal periods

Tidal Period	Site	Mean u (m s^{-1})	Mean v (m s^{-1})	Mean w (m s^{-1})
	1	0.082–0.564	0.023–0.126	0.002–0.117
Inflow	2	0.411–0.866	(−0.026)–0.133	0.028–0.191
	3	0.548–1.652	0.022–0.186	0.199–0.436
	1	(−0.056)–0.133	0.013–0.178	(−0.0004)–0.052
Outflow	2	0.089–0.485	0.053–0.181	0.018–0.082
	3	(−0.230)–0.954	0.057–0.351	0.024–0.245

Data represent minimum and maximum values obtained over all 5-minute sampling periods conducted at each site during inflow and outflow.

The mean diameter of lophophores decreased significantly with increased flow (Kruskal-Wallis test: $H_{\text{adj}} = 13.657$, df = 3, $P < 0.005$; Fig. 7a). Coupled with the decrease in lophophore diameter was a decrease in the number of tentacles per lophophore ($G = 48.388$, df = 6, $P < 0.001$) (Fig. 8). Frequency analysis on data for number

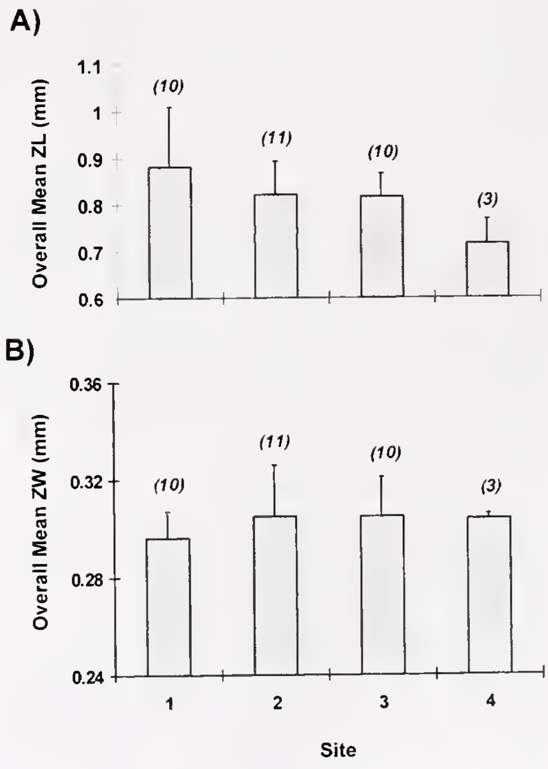

Figure 5. (A) Overall mean zooid lengths (ZL) per colony from colonies collected from Sites 1–4. (B) Overall mean zooid widths (ZW) per colony from colonies collected from Sites 1–4. Bars represent one standard deviation; *n* values in parentheses.

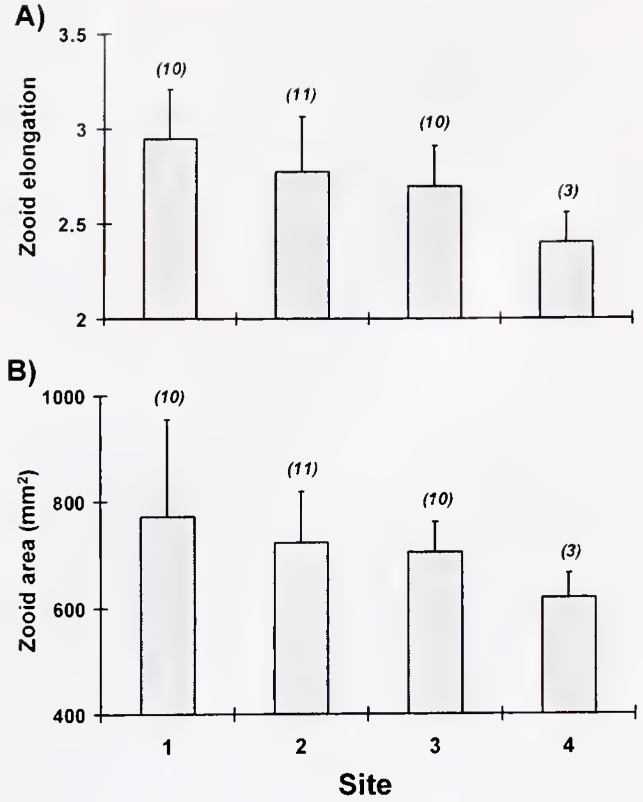

Figure 6. (A) Overall mean zooid elongation (zooid length/zooid width) per colony from colonies collected from Sites 1–4. (B) Overall mean zooid area (zooid length × zooid width) per colony from colonies collected from Sites 1–4. Bars represent one standard deviation; *n* values in parentheses.

of tentacles per lophophore entailed pooling frequencies in the highest and lowest categories to avoid low expected values. Such pooling ensured that no more than 20% (in our case 8.33%) of expected values were less than 5 (in our case one expected value was 3.5) and therefore that the sampling distribution provided a good approximation of the χ^2 distribution (Cochran, 1954, cited in Siegel and Castellan, 1988). Smaller lophophores with fewer tentacles should also be shorter, although we made no direct measurements of lophophore height. This expectation is supported by the positive relationship between tentacle number and lophophore height in Best and Thorpe's study (1986) of a variety of British bryozoan species, including *Membranipora*, as well as Ryland's overall finding (1975) that all lophophore parameters are related to lophophore size and therefore are intercorrelated. We also found significant decreases in mean interchimney distances along the flow gradient ($F_{3,29}$ = 39.442, $P < 0.001$; analysis on log-transformed data to ensure homogeneity of variances; see Fig. 7b). Thus, as ambient flows increase, colonies produce less elongate zooids with smaller lophophores, and excurrent flows travel shorter distances below these more closely spaced and smaller lophophores before they are ejected as jets from colony surfaces.

For monitoring growth rates, we were able to relocate 6 of the 8 colonies photographed in Site 1, and 7 of the 8 colonies photographed in Site 2, but we failed to find any of the 13 colonies photographed in Site 3. We noted that the holes punched for attaching cable ties to algal fronds were often beginning to split along the length of the fronds, presumably due to drag forces, causing the cable ties to cut through and split apart the fronds. Indeed, in several instances we re-attached the cable ties to different locations on fronds when we noticed these splits developing. Thus it is likely that the drag forces in Site 3 were great enough to result in the loss of all cable ties and surveyor's tape used to mark the mapped and photographed colonies.

ANOVA indicated no significant differences in the initial sizes of colonies retrieved for growth analysis (Site 1: mean initial colony size = 317.5 mm^2, SD = 186.1, n = 6; Site 2: mean initial colony size = 368.4 mm^2, SD = 240.7, n = 7; $F_{1,11}$ = 0.1802, P = 0.6794). Analysis of the growth increments of these colonies revealed no significant differences in the difference between mean final and initial col-

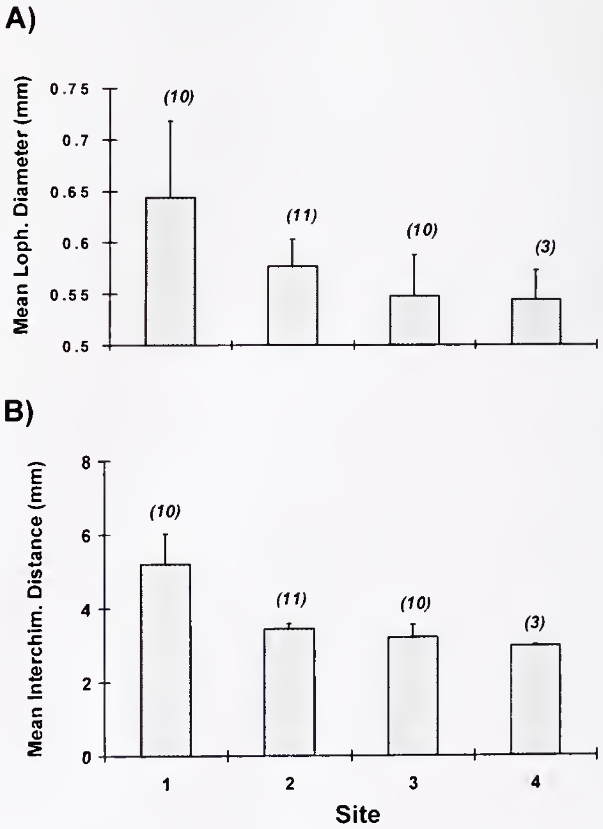

Figure 7. (A) Overall mean lophophore (Loph.) diameter per colony from colonies collected from Sites 1–4. (B) Overall mean interchimney (Interchim.) distances per colony from colonies collected from Sites 1–4. Bars represent one standard deviation; *n* values in parentheses.

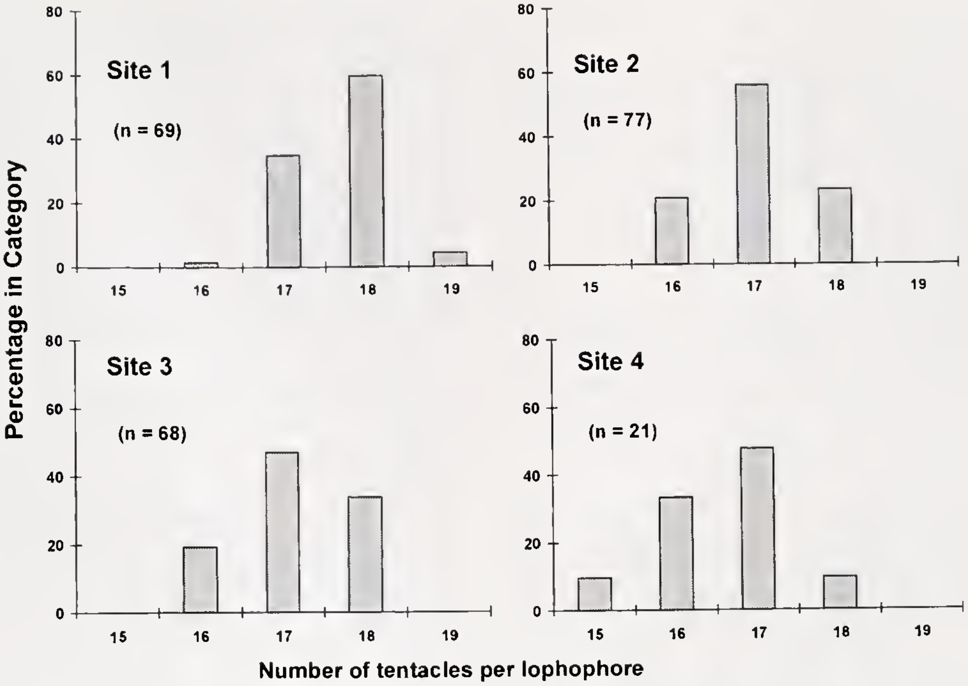

Figure 8. Percentages of lophophores with different numbers of tentacles in colonies collected from Sites 1–4.

ony sizes over the period of study ($F_{1,11}$ = 0.385, P = 0.548; Fig. 9). Thus, although colonies showed a progressive miniaturization by producing smaller, more closely spaced lophophores with increased flow, there was no apparent effect of flow on growth rates at the two sites in which we were able to assess growth. It is unfortunate that our inability to relocate colonies in Site 3 meant we could not determine the extent to which flow continues to have no effect on growth; nevertheless, it is notable that decreases in zooid length and elongation, lophophore diameter, and number of tentacles per lophophore continue along the entire flow gradient of the four sites. Since we did not retrieve any colonies from Site 3 for growth assessment and did not attempt growth studies at Site 4, it is not clear whether the irregularly shaped zooids are associated with poor growth rates in more extreme flows.

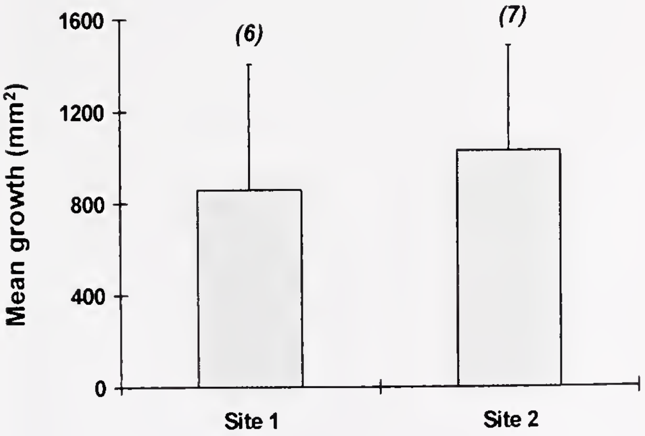

Figure 9. Mean growth increments of colonies over 10 days in Sites 1 and 2. Growth measured as final colony size minus initial colony size. Bars represent standard deviation; *n* values in parentheses.

Concurrent with the miniaturization of colonies with increased flow was a decrease in percent cover (Fig. 10). ANOVA on arcsine-transformed data showed highly significant differences in cover between Sites 1 and 2 ($F_{1,37}$ = 34.548, $P \ll 0.001$). We excluded Site 3 from the analysis as nearly all fronds had zero percent cover and we could find no transformation to meet the requirement of homogeneity of variance in ANOVA.

Discussion

Adaptive miniaturization in response to ambient flow

Our study indicates that encrusting bryozoans respond to increased flow regimes by morphological changes that result in the miniaturization of sheetlike colonies. This response parallels that of anemones in which individuals become smaller or squatter in more exposed conditions. Such flow-modulated alterations in size and shape are probably beneficial because they should place feeding surfaces into the slower flow regimes of the boundary layer, thus allowing individuals to avoid excessive flows that are detrimental to feeding. Equivalent growth rates for *M. mem-*

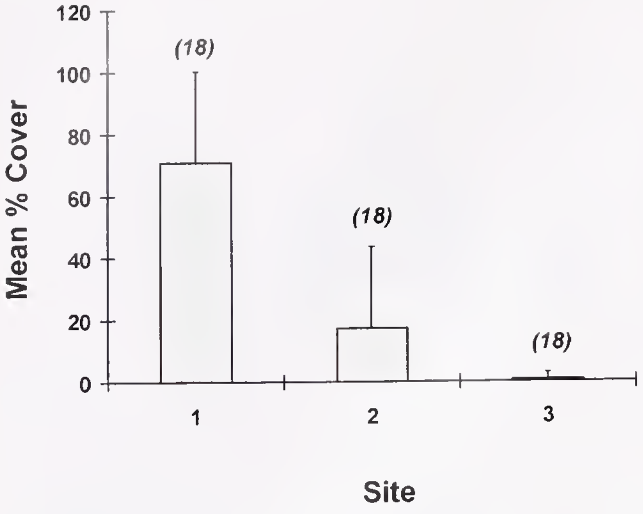

Figure 10. Mean percentage cover of laminarian fronds by *Membranipora membranacea* colonies in Sites 1–3. Bars represent one standard deviation; *n* values in parentheses.

branacea colonies growing in Sites 1 and 2 suggest that these morphological changes are adaptive, in that they are expressed in colonies that achieve similar growth rates under different flow conditions, presumably because of similar rates of feeding. At some point, boundary layers will become so thin that further miniaturization is not feasible; however, the continuous decline in size shown by *M. membranacea* colonies over the four sites studied suggests that this critical point had not been reached.

Previous field investigations have obtained evidence that increased turbulence can have beneficial effects on growth (Wildish and Kristmanson, 1979; Patterson, 1984; Fréchette and Bourget, 1985; Fréchette *et al.*, 1989). However, while increased levels of turbulent kinetic energy density characterized the ambient flow regimes measured at the level of the algal canopy at Site 2, these were not reflected in increased growth rates of *M. membranacea* colonies. It may be that the bryozoans themselves do not experience the higher turbulence because the flexibility of algal fronds in response to three-dimensional flows, and the thickness of the boundary layer, reduces the relative movements of water over frond surfaces. Although Koehl and Alberte (1988) found that increased blade flapping in *Nereocystis luetkeana*, the giant bull kelp, stirs water near the blade surface, this effect was greatest at slow ambient flows and is unlikely to apply to the extreme flow conditions experienced by laminarian fronds in Lough Hyne. Alternatively, turbulence may have had no effect on growth in our study if food levels were not limiting.

It is notable that the percent cover of *M. membranacea* colonies decreased dramatically along the flow gradient: values near 100% on some fronds in Site 1 declined to 0% on most fronds by Site 3. Beyond Site 4, where flow velocities were very great (and not measured), no colonies were evident. These patterns could reflect pre-settlement, settlement, or post-settlement events. The lack of colony development in sites exposed to extremely fast flows may be due to detrimental effects of flow on feeding that can no longer be overcome by increased miniaturization. It is also conceivable that larvae settle at much lower rates with increased exposure to flow, either because they actively choose not to settle or because drag forces prevent most of them from adhering to frond substrata. Yet another explanation—that the higher cover in Site 1 results from differential settlement patterns controlled by proximity to a source population of larvae within Lough Hyne—is unlikely because the larvae of *M. membranacea* are long-lived planktotrophs.

Our finding that growth rates were equivalent at Sites 1 and 2 contrasts with Eckman and Duggins' study (1993) in which the growth of very young colonies of *M. membranacea* was reduced at increased flows through pipes. This lack of concordance might be explained by several factors. First, the flows experienced by colonies within pipes could have been greater than those experienced by colonies in the Rapids since the former were growing on acrylic plastic strips whose edges were oriented into the flow through the center of the pipes and which were 2 cm long in the along-stream dimension. However, calculations of turbulent boundary layer thicknesses (Vogel, 1981) for the two studies suggest that this was not the case. Turbulent boundary layer thicknesses for slow (mean flow = 0.02 m s^{-1}) and fast (mean flow = 0.15 m s^{-1}) flows in pipes were 21 mm and 14 mm respectively, assuming a downstream distance of 10 mm from the leading edge of their plastic growth strips. Corresponding thicknesses in Lough Hyne would range from 28 mm to 21 mm for slow (mean flow = 0.22 m s^{-1}; Fig. 4) and fast (mean flow = 0.87 m s^{-1}; Fig. 4) flows respectively, assuming a downstream distance of 0.5 m from the leading edge of fronds to the colonies. This indicates that in all situations, boundary layer thicknesses were much greater than the heights of lophophores; colonies were thus hidden from mainstream flows in both studies. The variation in growth may therefore be related to differences in the steepness of the velocity gradients within these boundary layers.

A second, and probably equally important, difference in the two studies is that Eckman and Duggins assessed the growth of juvenile colonies that were less than 2 mm in diameter at the start of the experiments (and hence were probably at the stage of having from 2–8 zooids). Colonies in our studies were not at an early astogenetic stage but had already become established in the field. These differences are illustrated by the very different growth rates in the two studies. Mean growth rates of the small colonies in Eckman and Duggins' study ranged from about 5 to 20 mm^2 d^{-1} (see fig. 4 in Eckman and Duggins, 1993) while the equivalent mean growth rates of the larger colonies in our study were 86 mm^2 d^{-1} (SD = 55 mm^2 d^{-1}) in Site 1 and 103 mm^2 d^{-1} (SD = 45 mm^2 d^{-1}) in Site 2. It may be that early stages of colony development are more sensitive to flow conditions in microhabitats because arrays of lophophores and excurrent jets are not yet developed. Eckman and Duggins (1993) obtained large differences in growth rates in replicates for each of the two slower flow speeds studied (fig. 4, Eckman and Duggins, 1993). If the higher values obtained for each of these replicates are regarded as outliers due to anomalous conditions in these pipes, there is much less suggestion of a flow effect on growth across the range of the five flow speeds studied. Nevertheless, since at some point drag forces must begin to inhibit feeding, flow will eventually limit growth as Eckman and Duggins' evidence indicates. We feel the most likely explanation for our contrasting results is that colonies differed in developmental stages and experienced different velocity gradients within boundary layer microhabitats.

Other consequences of ambient flow regimes

As discussed above, miniaturization appears to be an effective means of achieving similar growth rates when colonies happen to become established in sites exposed to rapid flows. However, another consequence of living in such sites is that colonies occur at reduced densities. Thus they will experience a reduction in intraspecific competition for space, allowing individual colonies to attain larger size; it was certainly notable that, at high percent cover, colonies tended to be smaller, although we did not collect data to document this.

A possible detrimental effect of low cover is a reduction in the likelihood of achieving fertilization. *M. membranacea* releases sperm packets into the water column, where they become entrained by feeding currents. Once within the lophophore region they gain access to maternal zooids through specialized intertentacular organs of the lophophore, and subsequently effect internal fertilization of eggs within maternal zooids (Temkin, 1994). Although proximity to neighboring colonies may increase fertilization success, it is also possible that release of sperm packets into the rapid and turbulent flows in the Rapids swamps this effect, particularly since sites of high and low density are within meters of each other. We have no data on the reproductive output of colonies growing in the different ambient flow conditions to resolve this issue. Although miniaturization allows similar growth rates, it could conceivably inhibit or promote reproduction if more or less energy were allocated to growth. Also unknown is the extent to which these effects may be offset or otherwise influenced by the possibility of reaching larger colony sizes due to decreased intraspecific competition for space.

Colony hydraulics

Venting of excurrent flows as jets through chimney regions allows *M. membranacea* to avoid or at least reduce refiltering of particle-depleted water. Chimneys in *M. membranacea* represent small regions in which zooids degenerate and are not replaced. Thus the potential contribution to feeding made by these zooids is sacrificed, presumably because the energetic gain conferred by minimizing refiltration exceeds the cost of zooid degeneration (Lidgard, 1981). One mechanism postulated to explain the formation of chimneys is that chimneys develop when the pressure beneath the extended array of lophophores becomes greater than the array can withstand (Dick, 1987). The decrease in interchimney distances that accompanies the miniaturization of zooids in *M. membranacea* is consistent with this explanation. Smaller and shorter lophophores provide less space for excurrent water below the lophophore array. Thus, pressure develops more quickly and excurrents must be vented sooner. The notably regular spacing of chimneys in *M. membranacea* is also consistent with a hypothesis of pressure build-up under the lophophore sheet (Dick, 1987).

This postulated mechanism of pressure build-up provides a simple explanation for how *M. membranacea* can maintain functional colony-wide hydraulics across a range of ambient flow conditions, as suggested by the evidence presented here. The explanation that chimneys arise at particular developmental stages in colonies (*i.e.*, are astogenetically determined) is less satisfactory. If chimneys are astogenetically determined, interchimney distances might be expected not to vary when growth is equivalent. However, while growth for colonies at Sites 1 and 2 was not significantly different, chimneys were produced much more frequently in Site 2.

Implications of study

We have found that bryozoans show flow-dependent morphologies that result in a miniaturization of colonies with exposure to rapid flows. These morphological changes likely promote exposure to similar flow microhabitats, thereby allowing the maintainenance of similar rates of feeding, and hence growth, at least up to a point. For several reasons, we suggest that these morphological changes are the result of phenotypic plasticity rather than selection for colonies with particular morphologies. Firstly, tidal flushing through the Rapids ensures that algal fronds will be subject to recruitment by the same larval pool. Secondly, there is evidence that flow regime limits active choice in habitat selection by larvae (Butman, 1987), and as all sites were subject to considerable flow, it is unlikely that larvae could discriminate amongst them. Thirdly, post-recruitment interactions are also unlikely to have selected for certain types. Colonies were chosen to be free from overgrowth interactions, and there was no evidence of predation.

The only obvious factor that could result in post-settlement mortality was flow regime itself: increased flow could have selected for miniaturized colonies. Unfortunately, we did not conduct transplant experiments; thus selection cannot be distinguished from phenotypic plasticity. However, in general, algal fronds should offer great variation in exposure to flow for encrusting bryozoans: as fronds grow, the colonies are placed in different positions both along the length of the frond and in the water column. This is particularly true since larvae of *M. membranacea* preferentially recruit to the younger regions of laminarian fronds, near the holdfasts of the plants (Brumbaugh *et al.*, 1994). Furthermore, colonies may be buffered from flows when they are growing on dense fronds within macroalgal stands but may be more exposed to flows when growing on fronds along the edges of stands. These arguments suggest that genetic specialization to narrow ranges of flow regimes is an unlikely strategy to have evolved. Rather, colonies should be able to tolerate a wide range of flow conditions since it cannot be predicted what conditions will be encountered during their lifetime. This tolerance can be achieved by phenotypic plasticity.

In the Introduction, we cited some of the many studies of feeding from flow for a variety of suspension feeders; these have provided important insights about feeding opportunities (*e.g.*, increased turbulent mixing) and constraints (*e.g.*, increased drag forces) presented by increased flow. However, a common practice in these studies has been to assess feeding across a range of flows by suspension feeders collected from particular sites (but see Okamura, 1992, and Anthony, 1997). Hence flow-dependent feeding rates of suspension feeders which themselves inhabit a range of flow environments have received little investigation, and therefore the extent to which suspension feeders may be locally adapted to flow conditions is poorly known. Thus, although studies to date reveal important information about the general effects of flow on feeding for a given situation, their results may not depict what happens in the real world since they do not take into account the longer term responses to flow by the animals in the field. However, even if many suspension feeders show plasticity in growth in response to flow, flow and feeding studies of suspension feeders collected from relatively restricted ranges of flow environments are nonetheless informative. Such studies should provide predictions about what kinds of morphological change might be adaptive under different flow conditions and may lead to insights about the significance and consequences of observed morphological variation.

Acknowledgments

We thank Linda Teagle for her great help in setting up and collecting data using the ultrasonic flow meter and for assisting in the field; Allison Myles for help collecting colonies during the short periods of low flow in the Rapids; the Department of Zoology of the University College Cork for laboratory space; and the National Parks & Wildlife Service, Office of Public Works, Dublin, for permission to work at Lough Hyne. This work was partially supported by a grant from the Royal Society to B. Okamura, which provided funds to purchase the ultrasonic flow meter. Comments from two anonymous referees have helped to improve the manuscript.

Literature Cited

Anthony, K. R. N. 1997. Prey capture by the sea anemone *Metridium senile* (L.): effects of body size, flow regime, and upstream neighbors. *Biol. Bull.* **192:** 73–86.

Bassindale, R., F. J. Ebling, J. A. Kitching, and R. D. Purchon. 1948. The ecology of Lough Ine Rapids with special reference to water currents. I. Introduction to hydrography. *J. Ecol.* **36:** 305–322.

Best, B. A. 1988. Passive suspension feeding in a sea pen: effects of ambient flow on volume rate and filtering efficiency. *Biol. Bull.* **175:** 332–342.

Best, M. A., and J. P. Thorpe. 1986. Effects of food concentration on feeding current velocity in six species of marine Bryozoa. *Mar. Biol.* **93:** 255–262.

Brumbaugh, D. R., J. M. West, J. L. Hintz, and F. E. Anderson. 1994. Determinants of recruitment by an epiphytic marine bryozoan: field manipulations of flow and host quality. Pp. 287–301 in *Reproduction and Development of Marine Invertebrates*, W. H. Wilson, Jr., S. A. Stricker, and G. L. Shinn, eds. The Johns Hopkins University Press, Baltimore, MD.

Butman, C. A. 1987. Larval settlement of soft-sediment invertebrates: the spatial scales of pattern explained by active habitat selection and the emerging role of hydrodynamical processes. *Oceanogr. Mar. Biol. Annu. Rev.* **25:** 113–165.

Clifford, N. J., and J. R. French. 1993. Monitoring and modelling turbulent flows: historical and contemporary perspectives. Pp. 1–34 in *Turbulence: Perspectives in Flow and Sediment Transport*, N. J. Clifford, J. R. French, and J. Hardisty, eds. John Wiley, Chichester, UK.

Dick, M. H. 1987. A proposed mechanism for chimney formation in encrusting bryozoan colonies. Pp. 73–80 in *Bryozoa: Present and Past*, J. R. P. Ross, ed. Western Washington University, Bellingham, WA.

Eckman, J. E., and D. O. Duggins. 1993. Effects of flow speed on growth of benthic suspension feeders. *Biol. Bull.* **185:** 28–41.

Eckman, J. E., C. H. Peterson, and J. A. Cahalan. 1989. Effects of flow speed, turbulence, and orientation on growth of juvenile bay scallops *Argopecten irradians concentricus* (Say). *J. Exp. Mar. Biol. Ecol.* **132:** 123–130.

Fréchette, M., and E. Bourget. 1985. Food-limited growth of *Mytilus edulis* (L.) in relation to the benthic boundary layer. *Can. J. Fish. Aquat. Sci.* **42:** 1166–1170.

Fréchette, M., C. A. Butman, and W. R. Geyer. 1989. The importance of boundary-layer flows in supplying phytoplankton to the benthic suspension feeder, *Mytilus edulis* L. *Limnol. Oceanogr.* **34:** 19–36.

Grizzle, R. E., R. Langdon, and W. H. Howell. 1992. Growth responses of suspension-feeding bivalve molluscs to changes in water flow: differences between siphonate and non-siphonate taxa. *J. Exp. Mar. Biol. Ecol.* **162:** 213–228.

Grünbaum, D. 1995. A model of feeding currents in encrusting bryozoans shows interference between zooids within a colony. *J. Theor. Biol.* **174:** 409–425.

Judge, M. L., and S. F. Craig. 1997. Positive flow dependence in the initial colonization of a fouling community: results from *in situ* water current manipulations. *J. Exp. Mar. Biol. Ecol.* **210:** 209–222.

Kirby-Smith, W. W. 1972. Growth of the bay scallop: the influence of experimental water currents. *J. Exp. Mar. Biol. Ecol.* **8:** 7–18.

Koehl, M. A. R. 1977. Effects of sea anemones on the flow forces they encounter. *J. Exp. Biol.* **69:** 87–105.

Koehl, M. A. R., and R. S. Alberte. 1988. Flow, flapping, and photosynthesis of *Nereocystis luetkeana:* a functional comparison of undulate and flat blade morphologies. *Mar. Biol.* **99:** 435–444.

Lenihan, H. S., C. H. Peterson, and J. M. Allen. 1996. Does flow speed also have a direct effect on growth of active suspension-feeders: an experimental test on oysters. *Limnol. Oceanogr.* **41:** 1359–1366.

Leonard, A. B., J. R. Strickler, and N. D. Holland. 1988. Effects of current speed on filtration during suspension feeding in *Oligometra serripinna* (Echinodermata: Crinoidea). *Mar. Biol.* **97:** 111–126.

Lidgard, S. 1981. Water flow, feeding, and colony form in an encrusting cheilostome. Pp. 135–142 in *Recent and Fossil Bryozoa,* G. P. Larwood and C. Nielsen, eds. Olsen and Olsen, Fredensborg, Denmark.

McFadden, C. S. 1986. Colony fission increases particle capture rates of a soft coral: advantages of being a small colony. *J. Exp. Mar. Biol. Ecol.* **103:** 1–20.

Nowell, A. R. M., and P. A. Jumars. 1984. Flow environments of aquatic benthos. *Annu. Rev. Ecol. Syst.* **15:** 303–328.

Okamura, B. 1984. The effects of ambient flow velocity, colony size, and upstream colonies on the feeding success of Bryozoa. I. *Bugula stolonifera* Ryland, an arborescent species. *J. Exp. Mar. Biol. Ecol.* **83:** 179–193.

Okamura, B. 1985. The effects of ambient flow velocity, colony size, and upstream colonies on the feeding success of Bryozoa. II. *Conopeum reticulum* (Linnaeus), an encrusting species. *J. Exp. Mar. Biol. Ecol.* **89:** 69–80.

Okamura, B. 1990. Particle size, flow velocity, and suspension-feeding by the erect bryozoans *Bugula neritina* and *B. stolonifera. Mar. Biol.* **105:** 33–38.

Okamura, B. 1992. Microhabitat variation and patterns of colony growth and feeding in a marine bryozoan. *Ecology* **73:** 1502–1513.

Palumbi, S. R. 1984. Tactics of acclimation: morphological changes of sponges in an unpredictable environment. *Science* **225:** 1478–1480.

Patterson, M. R. 1984. Patterns of whole colony prey capture in the octocoral, *Alcyonium siderium. Biol. Bull.* **167:** 613–629.

Ryland, J. S. 1975. Parameters of the lophophore in relation to population structure in a bryozoan community. Pp. 363–393 in *Proceedings of the 9th European Marine Biology Symposium,* H. Barnes, ed. Aberdeen University Press, Aberdeen, Scotland.

Seed, R. 1976. Observations on the ecology of *Membranipora* (Bryozoa) and a major predator *Doridella steinbergae* (Nudibranchiata) along the fronds of *Laminaria saccharina* at Friday Harbor, Washington. *J. Exp. Biol. Mar. Ecol.* **24:** 1–17.

Siegel, S., and N. J. Castellan, Jr. 1988. *Nonparametric Statistics for the Behavioral Sciences.* McGraw-Hill, New York. 399 pp.

Sponaugle, S., and M. LaBarbera. 1991. Drag-induced deformation: a functional feeding strategy in two species of gorgonians. *J. Exp. Mar. Biol. Ecol.* **148:** 121–134.

Temkin, M. H. 1994. Gamete spawning and fertilization in the gymnolaemate bryozoan *Membranipora membranacea. Biol. Bull.* **187:** 143–155.

Vogel, S. 1981. *Life in Moving Fluids: the Physical Biology of Flow,* Princeton University Press, Princeton, NJ. 352 pp.

Wildish, D. J., and D. D. Kristmanson. 1979. Tidal energy and sublittoral macrobenthic animals in estuaries. *J. Fish. Res. Board Can.* **36:** 1197–1206.

Wilkinson, C. R., and J. Vacelet. 1979. Transplantation of marine sponges to different conditions of light and current. *J. Exp. Mar. Biol. Ecol.* **37:** 91–104.

Reference: *Biol. Bull.* **196:** 216–226. (April 1999)

Genetic Relationships (RAPD-PCR) Between Geographically Separated Populations of the "Cosmopolitan" Interstitial Polychaete *Hesionides gohari* (Hesionidae) and the Evolutionary Origin of the Freshwater Species *Hesionides riegerorum*

HARTMUT SCHMIDT AND WILFRIED WESTHEIDE*

Spezielle Zoologie, Biology/Chemistry, University of Osnabrück, 49069 Osnabrück, Germany

Abstract. In an analysis of the population genetics of the tiny meiofaunal polychaete *Hesionides gohari,* the RAPD-PCR method was applied to 49 specimens from 7 collecting sites far apart on three continents: French Atlantic coast, Mediterranean (Majorca, Giglio, Crete), Red Sea, Indian Ocean (Phuket), and U.S. Atlantic coast (Florida). In the band patterns produced with 14 arbitrary decamer primers, 496 genetic characters were detected. Genetic distances between the *H. gohari* populations vary between 0.55 and 0.70. The data were evaluated by three cluster programs; in the almost congruent phenograms, three clades were found with high bootstrap values: (1) European Atlantic–Mediterranean–Red Sea, (2) Indian Ocean, (3) Western Atlantic. In all cluster analyses, *Hesionides riegerorum* from a U.S. east coast river system is shown as genetically nearest to the Florida specimens of *H. gohari,* making it most probable that this freshwater species of the genus originated from a Western Atlantic *H. gohari* population. The genetic distances detected between the *H. gohari* specimens from the three continents are almost identical to those found between morphologically similar interstitial polychaete species pairs. Thus, the degree of genetic consistency is considered not to be high enough to corroborate the notion of a cosmopolitan distribution pattern, but rather suggests that the three clades represent different species.

Introduction

The many species of *Hesionides* Friedrich, 1937, are highly characteristic meiofaunal polychaetes with a great variety of morphological, reproductive, and behavioral adaptations to the habitat of interstitial crevices in marine surf-beaten sand beaches (Westheide, 1967, 1971, 1984). Several of the *Hesionides* species are known to be characterized by another peculiarity of the marine interstitial fauna—a broad geographic distribution, comprising intertidal localities throughout the world (Westheide, 1971; Sterrer, 1973; Giere, 1993). Within the genus, *H. arenaria* Friedrich, 1937, and *H. gohari* Hartmann-Schröder, 1960, appear to have the most cosmopolitan distribution (Westheide, 1977); they occur on all continents except Antarctica. *H. gohari* was discovered by Adolf Remane in littoral sands near Ghardaqa (today: Hurghada) in the Red Sea (Remane and Schulz, 1964); it was described by Hartmann-Schröder (1960). Westheide (1970, 1972a, 1972b) investigated the morphology, reproductive biology, and local distribution pattern of populations occurring in beaches of northern Tunisia (Mediterranean Sea).

This tiny species (max. length 1.5 mm) is typical of warm seas and has a range extending as far north as Arcachon, on the Atlantic coast of France (Westheide, 1972/73). New localities for the species are still being recorded worldwide (Hartmann-Schröder, 1991; Westheide, 1992). Its most characteristic diagnostic features are considered to be its length, the proportions of the head appendages, the position of penis papillae, the dentation of notopodial chaetae, and especially the shape of the anal appendages. Among the other *Hesionides* species of comparable size, one inhabits

---

Received 9 September 1998; accepted 29 January 1999.

* To whom correspondence should be addressed. E-mail: westheide@mail.biologie.uni-osnabrueck.de

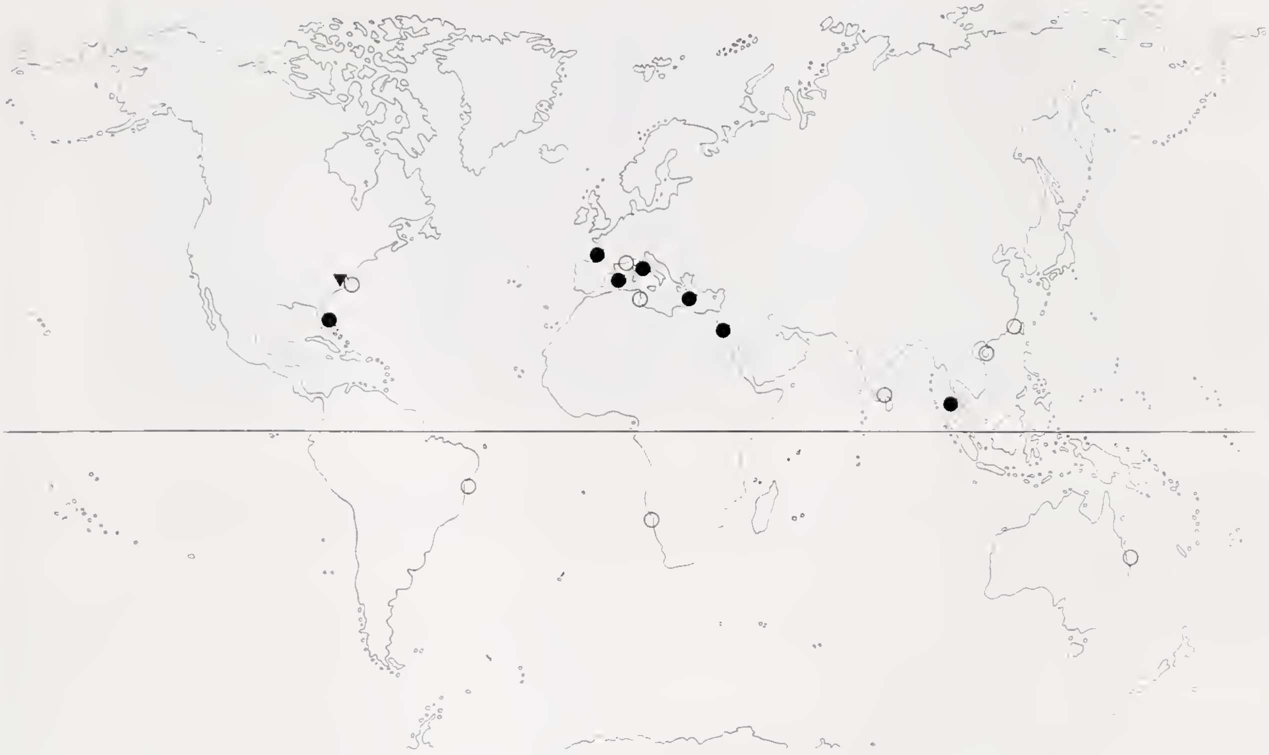

Figure 1. Records (open circles) and sampling sites (solid circles) for *Hesionides gohari* and sampling site for *H. riegerorum* (triangle).

fresh water, *H. riegerorum* Westheide, 1979; it can be distinguished from *H. gohari* by various morphological features.

The demonstrated almost cosmopolitan distribution of these *Hesionides* species, together with that of many other species of various meiofaunal taxa, gave rise to a still-controversial hypothesis of Sterrer (1973) (see also Rao, 1972) based on the notion that speciation of these forms is extraordinarily slow. It is postulated that they were already present on an old supercontinent and were distributed over their present vast range by the drifting apart of the continental plates. This explanation could apply only if the genetic changes in the separated populations were relatively small over long periods of time, and mostly had no effect on the phenotype. Such minimal genetic variability can be explained by assuming a complete constancy of the ecological factors in the habitat of these animals, the sand beaches. Sterrer's hypothesis appeared necessary because long-range, transoceanic dispersal of these meiofaunal organisms seemed inconceivable: they are not capable of active swimming and, with few exceptions, have no larval dispersal stages.

However, it gradually became evident that, even without dispersal stages, many of these species do succeed in colonizing geologically young islands far from any coast (Westheide, 1991); furthermore, dispersal of meiofaunal individuals in the seawater column along shores has been observed and demonstrated experimentally (Hagerman and Rieger, 1981; Palmer, 1988; Armonies, 1989). These observations led to the proposal that the cosmopolitan distribution pattern is ascribable not to geologically ancient processes but rather to occasional contemporary events (Sterrer, 1973; Gerlach, 1977) involving long-range dispersal by birds, on drifting material, or in ballast sand or tanks in ships.

Lately, arguments for one or the other view have been supported by genetic investigations. Todaro *et al.* (1996) expressed the conviction, based on their restriction-fragment length polymorphism analyses, that the proposed cosmopolitan species *Xenotrichula intermedia* (Gastrotricha), apparently present both in the Mediterranean Sea and along the coast of North America (Ruppert, 1977), consists of more than one taxon. Similarly, with RAPD-PCR (random applied polymorphic DNA-polymerase chain reaction) Soosten *et al.* (1998) found genetic differences between specimens of the polychaete *Petitia amphophthalma* from Europe and North America, although these differences are considerably smaller than those between certain morphologically distinct species of other taxa. In the present study of *Hesionides gohari* collected from seven intertidal localities on three continents (Europe, North America, Southeast Asia; Fig. 1), the RAPD-PCR method was likewise chosen, to evaluate the results obtained for *P. amphophthalma* with

Table I

Collection information for H. gohari *and* H. riegerorum

Species	Locality			Abbreviation	Number of specimens
H. gohari	Atlantic Ocean	France	Arcachon (intertidal)	A	11
H. gohari	Mediterreanean Sea	Spain, Majorca	Palma (subtidal)	M	8
H. gohari	Mediterranean Sea	Italy, Giglio	Campese (subtidal)	G	8
H. gohari	Mediterranean Sea	Greece, Crete	Heraklion (intertidal)	C	8
H. gohari	Red Sea	Egypt	Hurghada (intertidal)	H	4
H. gohari	Indian Ocean	Thailand	Phuket (intertidal)	T	4
H. gohari	Atlantic Ocean	Florida	Ft. Pierce (intertidal)	F	6
H. riegerorum	Chowan River	North Carolina	Edenhouse (riverbank)	NC	5

those of other cosmopolitan species studied in our laboratory (Schmidt and Westheide, 1998; Schmidt unpubl. results). For general advantages of the RAPD-PCR method in molecular systematic and ecological studies, see Hadrys *et al.* (1992), Schierwater (1995), and Schirmacher *et al.* (1998).

Materials and Methods

A total of 49 individuals of *Hesionides gohari* Hartmann-Schröder, 1960, from seven localities and 5 specimens of *H. riegerorum* Westheide, 1979, from North Carolina were examined genetically (Table I). The meiofaunal animals were extracted from small samples of sand by the magnesium chloride method (Westheide, 1990). After sorting and washing in doubly distilled water, the specimens were either frozen in LTE-buffer at −60°C or dried at temperatures below 90°C. Both methods of preservation guaranteed reproducible results even when samples were stored for months prior to actual DNA isolation.

Total DNA was isolated by a modification of the method of Kocher *et al.* (1989). The DNA was extracted from frozen tissues (−70°C) in 1.5-ml microtubes by digestion in 100 μl 100 mM Tris HCl, pH 8.0, 10 mM EDTA, 100 mM NaCl, 0.1% SDS, 50 mM dithiothreitol and proteinase K (0.5 μg/ml) incubated for 2 h at 50°C in a heating block. SDS was precipitated by 40 μl 3 M potassium acetate cooled down to 0°C for 10 min. The DNA was purified by extracting once with 150 μl phenol/chloroform/isoamyl alcohol (25:24:1, saturated with 10 mM Tris, pH 8.0, and 1 mM EDTA) and once with 150 μl chloroform/isoamyl alcohol (24:1). After precipitation with 150 μl 100% isopropanol, the DNA was washed with 100 μl 70% ethanol (both refrigerated at 0°C). The phases were separated by centrifugation at 14,000 rpm for 10 min at 4°C. The dried DNA was dissolved in 1 mM Tris HCl, pH 8.0, plus 0.1 mM EDTA and stored at 4°C.

Fourteen arbitrary 10-mer primers from Operon Technologies (Alameda, California) listed in Table II were used for PCR amplification following the recipes reported by Williams *et al.* (1990) with minor modifications. PCR was done in a total reaction volume of 25 μl with the following compounds: 10 mM Tris HCl, pH 8.3; 50 mM KCl; 2 mM $MgCl_2$; 1% Triton X-100; 100 μM each of dATP, dCTP, dGTP, and dTTP (Boeringer); 5 pM decamer primer; 1–5 ng DNA; and 0.4 U Tbr Polymerase (Biometra Prime Zyme™ Polymerase). Controls were run with no template DNA. Amplification was done simultaneously by two thermocyclers: Perkin Elmer Cetus DNA thermal cycler 480 and Biometra personal cycler 48. All synthesized fragments patterns were comparable. Each PCR cycle consisted of denaturation for 1 min at 94°C, hybridization for 1 min at 36°C, and extension for 2 min at 72°C. This cycle was repeated 45 times followed by a paused file at 4°C. Fastest available transitions between temperatures were employed in each case. Reaction products were separated by electrophoresis in 1.5% agarose gels buffered in 1× TBE (0.045 M Tris-borate, 1 mM EDTA) at 3 V/cm for 2.5 h, stained with ethidium bromide, and documented under UV light. As size markers, 100-base-pair DNA ladders were used (from Life

Table II

Decamer primers and their sequences used in this study (all primers from Operon Technologies, Inc., Alameda, CA)

Primer	Primer sequence 5′ to 3′	Molecular weight
OPB-01	GTTTCGCTCC	2961
OPB-02	TGATCCCTGG	3010
OPB-03	CATCCCCCTG	2915
OPB-04	GGACTGGAGT	3099
OPB-05	TGCGCCCTTC	2946
OPB-06	TGCTCTGCCC	2946
OPB-07	GGTGACGCAG	3048
OPB-08	GTCCACACGG	3004
OPB-10	CTGCTGGGAC	3035
OPB-11	GTAGACCCGT	3019
OPB-12	CCTTGACGCA	2779
OPB-15	GGAGGGTGTT	3130
OPB-17	AGGGAACGAG	3117
OPB-18	CCACAGCAGT	2988

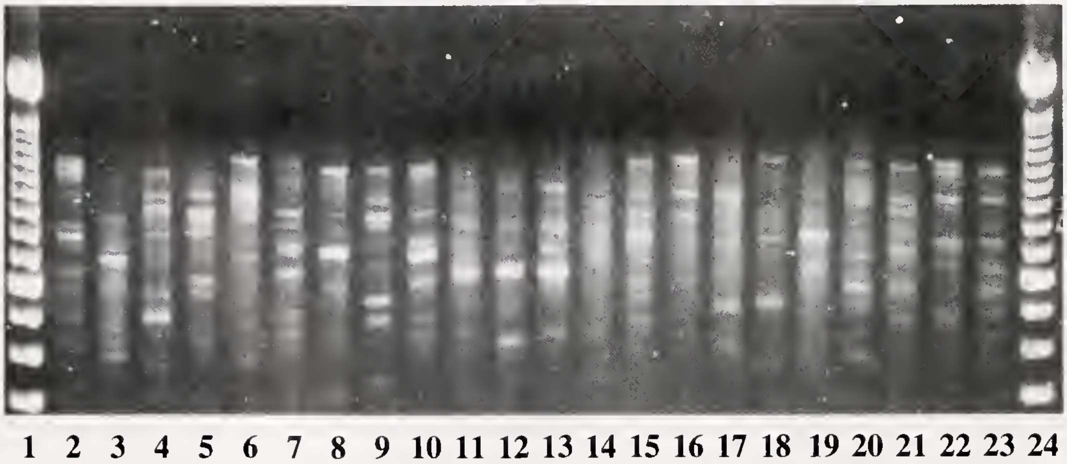

Figure 2. RAPD fingerprinting of *Hesionides gohari* specimens from Phuket (2, 3), Florida (8–11), Crete (12–15), Giglio (16–18), Arcachon (19–23), and *H. riegerorum* specimens from North Carolina (4–7); 1 and 24; 100 bp marker. Primer OPB 6.

Technologies, Inc., Berlin, Germany, or Pharmacia Biotech, Uppsala, Sweden). The reproducibility of the data was checked at regular intervals on different levels throughout all three parallel experiment lines. First, at the beginning of each series the optimal DNA concentration for PCR was determined for the individual animal, by testing the PCR with three DNA concentrations per animal (*ca.* 1 ng, 3 ng, and 10 ng per 25 μl reaction volume). In pilot experiments with larger annelids, it became clear that the results were reproducible with up to 25 ng/25 μl reaction volume. With DNA concentrations as high as *ca.* 50 ng/25 μl reaction volume, reproducibility was distinctly worse. A further increase in DNA concentration (to over 100 ng/25 μl reaction volume) brought the PCR to a complete halt, so that no specific DNA fragments could be detected. Reproducibility was tested further throughout each test series by running the same experiment twice in parallel reactions. In addition, for each series one reaction was carried out with a "blind" sample lacking DNA, to check the possibility of contamination with foreign DNA. We also looked for differences in the amplification patterns that might derive from the use of different thermocyclers (Büscher *et al.*, 1993; He *et al.*, 1994) or preservation methods (drying or deep-freezing), but found none.

The detected amplification product patterns were examined visually for monomorphic and polymorphic markers (Hadrys *et al.*, 1992). The degrees of polymorphism are given in percentages. The banding patterns were then translated into a 0/1-matrix (0 for absence, 1 for presence of a specific DNA marker) and fed into the cluster analysis program TREECON 1.2 (Peer and Wachter, 1994), which also transformed the data into distance values in percentages (Nei and Li, 1979). Cluster analyses were carried out by UPGMA (unweighted pair-group method using arithmetic averages; Sneath and Sokal, 1973), single linkage (Sneath and Sokal, 1973), and neighbor joining (Saitou and Nei, 1987) including bootstrap proportions (Felsenstein, 1985).

Results

For the seven sampled populations of *H. gohari* and one population of *H. riegerorum*, with 14 different primers a total of 496 different DNA fragments were detected, ranging in length from 150 bp to 1900 bp (*e.g.*, Fig. 2).

The calculated degree of polymorphism is similarly high in all the populations tested: for Arcachon, 96%; Giglio, 94%; Majorca, 95%; Crete, 94%; Hurghada, 89%; Phuket, 89%; Florida, 97%; and for *H. riegerorum* of North Carolina, 86%, the lowest value. For none of the European populations, nor for the population at the Red Sea, could diagnostic DNA fragments be detected. However, if the European and Egyptian animals are considered as a single group, its members are found to exhibit 33 common polymorphic characters that are absent from the individuals living in Thailand and Florida. With few exceptions, characters present in the animals from Thailand are the same as those found in the European and Egyptian individuals. Three diagnostic and five polymorphic DNA fragments were observed in the Phuket population only. Only one characteristic polymorphic character was detectable in the animals from Florida, and none of the primers revealed diagnostic DNA fragments. A surprising result was obtained by comparing the population of *H. riegerorum* with those of *H. gohari*. Although this freshwater species can be distinguished from the *H. gohari* populations by 12 diagnostic DNA fragments and 9 polymorphic characters, all other DNA bands are common to the two groups. There is an especially close match with the animals of the Florida population: of the 191 shared characters, 39 polymorphic DNA fragments are present only in these individuals. The

Table III

Comparison of genetic distances generated from RAPD data (after Nei and Li, 1979) within and between the seven Hesionides gohari *populations and the sole population of* Hesionides riegerorum

Locality	Arcachon	Giglio	Majorca	Crete	Hurghada	Florida	Phuket	N. Carolina *H. rieg.*
Arcachon	$\bar{x} = 0.53$ 0.43–0.6							
Giglio	$\bar{x} = 0.57$ 0.48–0.67	$\bar{x} = 0.50$ 0.38–0.61						
Majorca	$\bar{x} = 0.58$ 0.51–0.66	$\bar{x} = 0.55$ 0.43–0.67	$\bar{x} = 0.53$ 0.45–0.61					
Crete	$\bar{x} = 0.56$ 0.48–0.63	$\bar{x} = 0.55$ 0.46–0.65	$\bar{x} = 0.55$ 0.47–0.61	$\bar{x} = 0.50$ 0.37–0.58				
Hurghada	$\bar{x} = 0.60$ 0.5–0.68	$\bar{x} = 0.59$ 0.53–0.64	$\bar{x} = 0.61$ 0.54–0.69	$\bar{x} = 0.6$ 0.54–0.68	$\bar{x} = 0.51$ 0.46–0.61			
Florida	$\bar{x} = 0.70$ 0.63–0.78	$\bar{x} = 0.70$ 0.6–0.77	$\bar{x} = 0.68$ 0.59–0.75	$\bar{x} = 0.68$ 0.62–0.75	$\bar{x} = 0.70$ 0.65–0.76	$\bar{x} = 0.58$ 0.51–0.56		
Phuket	$\bar{x} = 0.68$ 0.62–0.76	$\bar{x} = 0.65$ 0.56–0.75	$\bar{x} = 0.68$ 0.6–0.73	$\bar{x} = 0.64$ 0.57–0.74	$\bar{x} = 0.69$ 0.62–0.76	$\bar{x} = 0.70$ 0.64–0.77	$\bar{x} = 0.50$ 0.47–0.53	
N. Carolina *H. rieg.*	$\bar{x} = 0.78$ 0.73–0.86	$\bar{x} = 0.79$ 0.70–0.87	$\bar{x} = 0.78$ 0.69–0.78	$\bar{x} = 0.77$ 0.71–0.83	$\bar{x} = 0.77$ 0.72–0.83	$\bar{x} = 0.68$ 0.56–0.77	$\bar{x} = 0.75$ 0.70–0.81	$\bar{x} = 0.40$ 0.28–0.47

Values are means ($\bar{x}$) followed by min/max ranges.

average genetic distances and the range of variation within and between the seven *H. gohari* populations are shown in Table III, as is their genetic relation to the population of *H. riegerorum* in North Carolina.

The genetic distance values within the European, Egyptian, and Thai populations are roughly the same, but a somewhat higher value was obtained for the animals from Florida. The genetic distances among the individuals of *H. riegerorum* are distinctly less than the values for all the *H. gohari* populations. The European populations, including the animals from Hurghada, bear the closest genetic resemblance to one another, and each of them is about the same distance away from the population of Thailand and from that of Florida. Comparison between *H. riegerorum* and the *H. gohari* populations gave an unexpected result (Table III): whereas *H. riegerorum* is, unsurprisingly, relatively distant genetically from the populations of Europe, Egypt, and Thailand, its genetic distance from the population of Florida is less.

These findings become particularly clear when the associated phenograms are constructed (Figs. 3–5). With all three analytical procedures, the individuals of the following geographic regions form groupings with high bootstrap values: (1) European Atlantic coast (Arcachon)–Mediterranean (Majorca, Giglio and Crete)–Red Sea; (2) Indian Ocean (Phuket); (3) Western Atlantic coast (Florida); (4) *H. riegerorum* (Chowan River, North Carolina). The European *H. gohari*, including the individuals from the Red Sea, form a common cluster in the phenograms, the common root of which has a bootstrap value ranging from 76 (single linkage) to a maximum of 98 (UPGMA).

Only with UPGMA (see Fig. 3) can the animals from the Red Sea be distinguished as a cluster (bootstrap value <70); with neighbor joining (Fig. 4) and single linkage (Fig. 5) they fall within the European cluster but still form a bootstrap-supported cluster of Red Sea animals. The individuals from the French Atlantic coast form a common cluster (bootstrap value <70) only with UPGMA, and this cluster lies between the Mediterranean populations. In all the trees, the animals from Thailand are separate from the European-Egyptian group.

All cluster analyses distinguish *H. riegerorum* from the *H. gohari* of Florida, but together, the Florida *H. gohari* and the *H. riegerorum* always form a cluster that is separate from the individuals of the *H. gohari* populations. That is, according to the present results, animals living in regions close together geographically are genetically more similar, although they belong to two morphologically distinct species, than individuals that are considered to be of the same species but originate in regions far apart from one another.

Discussion

The European populations of *H. gohari* treated in the present study (from Arcachon into the Mediterranean region) are relatively similar genetically, in some cases forming intermingled clusters, but clustering differently in the different analyses. It is therefore extremely likely that these individuals belong to a single species. The animals from the Red Sea form a distinct cluster in only one of these analyses; treated with either of the two other procedures, the four individuals in this sample are positioned among the Euro-

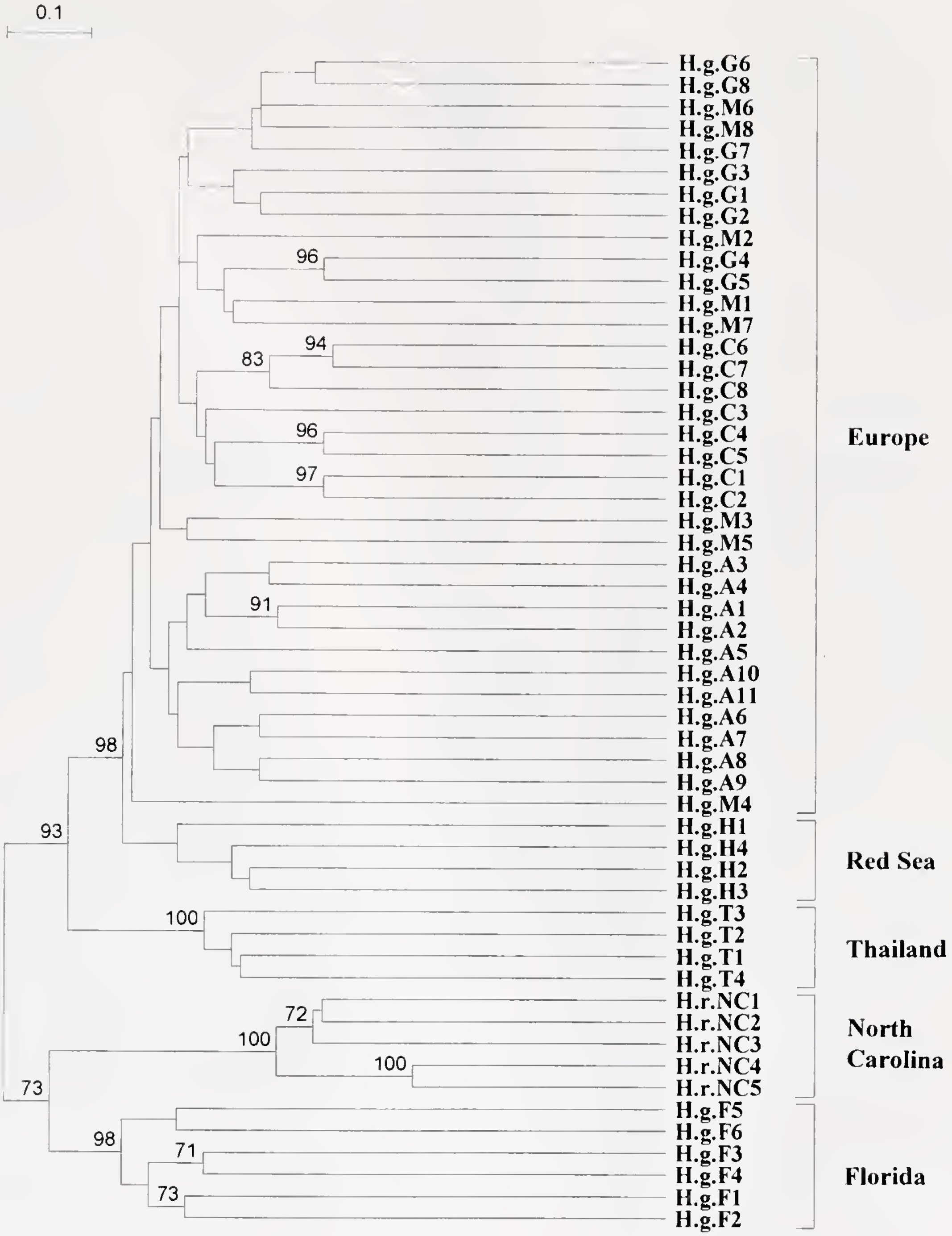
0.1
H.g.G6
H.g.G8
H.g.M6
H.g.M8
H.g.G7
H.g.G3
H.g.G1
H.g.G2
H.g.M2
H.g.G4
H.g.G5
H.g.M1
H.g.M7
H.g.C6
H.g.C7
H.g.C8
H.g.C3
H.g.C4
H.g.C5
H.g.C1
H.g.C2
H.g.M3
H.g.M5
H.g.A3
H.g.A4
H.g.A1
H.g.A2
H.g.A5
H.g.A10
H.g.A11
H.g.A6
H.g.A7
H.g.A8
H.g.A9
H.g.M4
H.g.H1
H.g.H4
H.g.H2
H.g.H3
H.g.T3
H.g.T2
H.g.T1
H.g.T4
H.r.NC1
H.r.NC2
H.r.NC3
H.r.NC4
H.r.NC5
H.g.F5
H.g.F6
H.g.F3
H.g.F4
H.g.F1
H.g.F2
Europe
Red Sea
Thailand
North Carolina
Florida
96
94
83
96
97
91
98
93
100
72
100
100
73
98
71
73

Figure 3. UPGMA phenogram of *Hesionides riegerorum* specimens (H. r.) from North Carolina (NC) and *H. gohari* specimens (H. g.) from the local populations in Arcachon (A), Giglio, Mediterranean (G), Majorca, Mediterranean (M), Crete, Mediterranean (C), Hurghada, Red Sea (H), Florida (F), Phuket, Thailand (T). Only bootstrap values above 70 are indicated.

pean individuals. Their genetic distances are generally not much different from those within the European group, so that they too are very probably members of the same species. The fact that the Red Sea site where they were collected, Hurghada, is the type locality of *Hesionides gohari* Hartmann-Schröder, 1960, presumably makes it highly likely that all animals of this cluster are of this species.

The relatively slight genetic distance between Red Sea animals and Mediterranean animals indicates either that gene exchange occurred between previously isolated popu-

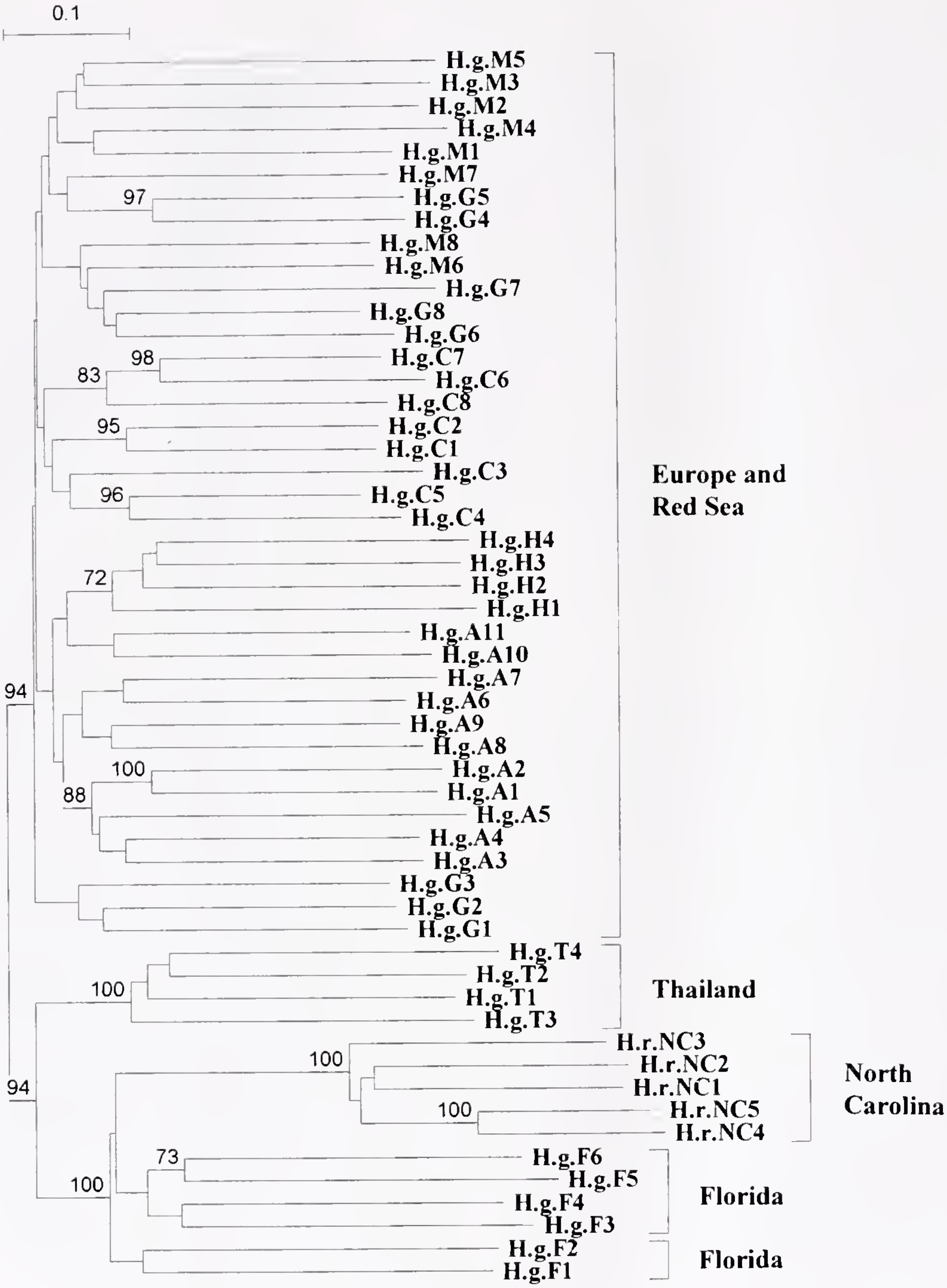
0.1
H.g.M5
H.g.M3
H.g.M2
H.g.M4
H.g.M1
H.g.M7
97
H.g.G5
H.g.G4
H.g.M8
H.g.M6
H.g.G7
H.g.G8
H.g.G6
98
H.g.C7
83
H.g.C6
H.g.C8
95
H.g.C2
H.g.C1
H.g.C3
96
H.g.C5
H.g.C4
H.g.H4
H.g.H3
72
H.g.H2
H.g.H1
H.g.A11
H.g.A10
94
H.g.A7
H.g.A6
H.g.A9
H.g.A8
100
H.g.A2
88
H.g.A1
H.g.A5
H.g.A4
H.g.A3
H.g.G3
H.g.G2
H.g.G1
Europe and Red Sea
H.g.T4
H.g.T2
100
H.g.T1
H.g.T3
Thailand
100
H.r.NC3
H.r.NC2
94
H.r.NC1
100
H.r.NC5
H.r.NC4
North Carolina
73
H.g.F6
H.g.F5
100
H.g.F4
H.g.F3
Florida
H.g.F2
H.g.F1
Florida

Figure 4. Neighbor-joining phenogram of *Hesionides riegerorum* specimens (H. r.) from North Carolina (NC) and *H. gohari* specimens (H. g.) from the local populations in Arcachon (A), Giglio, Mediterranean (G), Majorca, Mediterranean (M), Crete, Mediterranean (C), Hurghada, Red Sea (H), Florida (F), Phuket, Thailand (T). Only bootstrap values above 70 are indicated.

lations in these two regions after the two seas were joined by the construction of the Suez Canal, or that one population was isolated from the other by migrating through the Canal after it was opened. The latter possibility is likely, but it is hard to decide whether the migration was from the Red Sea into the Mediterranean and on to the Atlantic (Lessepsian migration; Por, 1978) or in the other direction. No finds from areas further east, between Hurghada and Thailand,

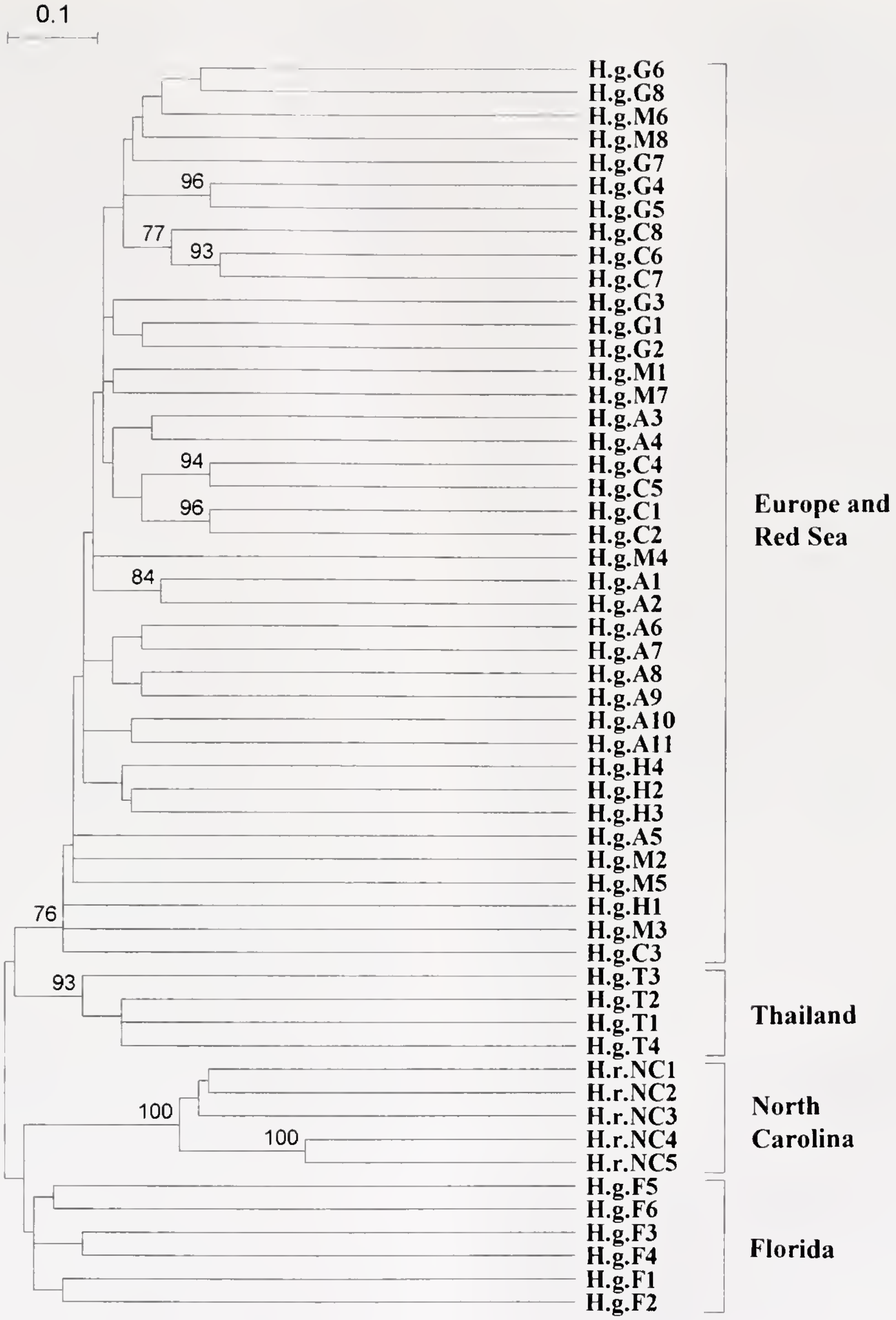
0.1
H.g.G6
H.g.G8
H.g.M6
H.g.M8
H.g.G7
96
H.g.G4
H.g.G5
77
H.g.C8
93
H.g.C6
H.g.C7
H.g.G3
H.g.G1
H.g.G2
H.g.M1
H.g.M7
H.g.A3
H.g.A4
94
H.g.C4
H.g.C5
96
H.g.C1
H.g.C2
H.g.M4
84
H.g.A1
H.g.A2
H.g.A6
H.g.A7
H.g.A8
H.g.A9
H.g.A10
H.g.A11
H.g.H4
H.g.H2
H.g.H3
H.g.A5
H.g.M2
H.g.M5
76
H.g.H1
H.g.M3
H.g.C3
93
H.g.T3
H.g.T2
H.g.T1
H.g.T4
H.r.NC1
H.r.NC2
100
H.r.NC3
100
H.r.NC4
H.r.NC5
H.g.F5
H.g.F6
H.g.F3
H.g.F4
H.g.F1
H.g.F2
Europe and Red Sea
Thailand
North Carolina
Florida

Figure 5. Single-linkage phenogram of *Hesionides riegerorum* specimens (H. r.) from North Carolina (NC) and *H. gohari* specimens (H. g.) from the local populations in Arcachon (A), Giglio, Mediterranean (G), Majorca, Mediterranean (M), Crete, Mediterranean (C), Hurghada, Red Sea (H), Florida (F), Phuket, Thailand (T). Only bootstrap values above 70 are indicated.

have yet been analyzed. Migration from the Red Sea would probably imply that in a very short time, about 100 years, the species extended its range through the entire Mediterranean Sea to the Atlantic. Immigrations of polychaetes can occur extremely rapidly, as has been demonstrated for species of *Marenzelleria* that became distributed in the North and Baltic Seas within a decade (Bastrop *et al.*, 1997); however, these spionids have long-lived pelagic larvae

(Bochert, 1997), whereas *H. gohari* is thought to undergo direct development (Westheide, 1970). Along-shore migration is presumably a general feature of the latter species, but the rate of geographic expansion achieved by this means is unknown.

H. gohari is considered to be one of the many cosmopolitan interstitial polychaete species (Westheide, 1971; Sterrer, 1973; Westheide and Rao, 1977; Riser, 1981; Giere, 1993; Soosten *et al.*, 1998). As yet no morphological distinctions have been found among individuals from the most diverse of the earth's marine regions (see Fig. 1), so that the species must temporarily be regarded as distributed worldwide on the coasts of warm seas (Westheide, 1977; Hartmann-Schröder, 1991) provided that a morphological species concept is applied. In the present genetic study, all the cluster analyses employed show clear differences between the animals in the regions (1) European Atlantic/Mediterranean/Red Sea, (2) Indian Ocean, and (3) Western Atlantic (North America). Whether the observed genetic distances reflect species differences—that is, reproductive barriers—cannot be decided on the basis of current observations. In another cosmopolitan morphospecies, *Petitia amphophthalma* Siewing, 1956 (Syllidae), the distances found by RAPD analyses between North American and European animals correspond to the values found here: 0.60–0.66 (Soosten *et al.*, 1998). However, similar distance values (after Nei and Li, 1979) of geographically separated but morphologically differentiated pairs of interstitial polychaete species have been revealed by RAPD analyses as well: *Nerilla antennata* Schmidt, 1848–*N. mediterranea* Schlieper, 1925 (Nerillidae): 0.74–0.77 (Schmidt and Westheide, 1998); *Microphthalmus carolinensis* Westheide and Rieger, 1987–*M. nahantensis* Westheide and Rieger, 1987: 0.77 (unpubl. data). Schirmacher *et al.* (1998) found a distance value of only 0.17 between two enchytraeid sibling species. Thus the notion of *H. gohari* representing a cosmopolitan species will have to be abandoned.

It is remarkable in this connection that the Florida population, identified as *H. gohari*, in all analyses formed a sibling cluster with the freshwater species *H. riegerorum* Westheide, 1979. These animals are the nearest neighbors geographically to the latter species, with recorded finds on the East Coast of the United States in Florida (Westheide, 1995) and North Carolina; that is, they live only about 100 km away from the habitat of the freshwater species, which so far has been found only at a site in the sandy bank of the Chowan River in North Carolina. When *H. riegerorum* was first described, mention was made of its close morphological resemblance to *H. gohari* (Westheide, 1979). There is much evidence that the freshwater form separated from the neighboring marine *Hesionides* population on the seacoast. The genetic distance between *H. riegerorum* and the marine *Hesionides* individuals on the Florida coast is appreciable, although considerably less than that between the latter and the *gohari* individuals from Thailand or Europe. But whereas the freshwater species is also clearly distinguishable morphologically (*e.g.*, by the different notopodial chaetae, penis papillae, and anal lobes; Westheide, 1979), no such diagnostic characters have yet been identified for the populations classified as *H. gohari*. The small geographic distance between the new freshwater species and its marine population of origin has evidently produced morphological character shifts, some of which may act as isolating mechanisms—for instance, the differently positioned and shaped penis papillae on the prostomium (see also Westheide, 1984, fig. 8). In contrast, the large geographic distance separating the European/Egyptian, Thai, and North American individuals from one another is correlated with genetic distinctions but not with any morphological ones that can readily be discerned, perhaps because of the stability of this marine habitat.

To continue to regard all these populations as belonging to a single species, *H. gohari*, is problematic. They would then constitute something like a paraphylum (Lorenzen, 1976), with one population (Florida) more closely related to the distinct sibling species (*H. riegerorum*) than to the other populations. As soon as possible, therefore, at least the North American "*H. gohari*" should be given the status of a separate species. However, we prefer not to undertake its description until the animals on the coast of the United States have been further examined in a specific search for morphological diagnostic characters, so that the practical taxonomic work will not be hampered by a species analysis based exclusively on genetic tests and on the geographic situation.

Regarding Sterrer's (1973) hypothesis, it is irrelevant whether these genetically derived clades represent distinct species or merely populations of a single, and hence indeed cosmopolitan, species. Testing this question, however, demands a larger number of specimens from different sites separated by oceans and sequencing techniques.

Acknowledgments

Special thanks for the provision of working facilities are due to Mr. Somsak Chullasorn and Dr. Anuwat Nateewathana (Phuket Marine Biological Center), Dr. Mary Rice (Smithsonian Institution at Harbor Branch, Ft. Pierce, Florida), Dr. Charles H. Petersen and Hal Summerson (Marine Science Institute, Morehead City, North Carolina). Dr. Claude Cazaux (Laboratoire Marine, Institut Universitaire de Biologie marine de Bordeaux, Arcachon), and Mrs. Martina Übel (Institut für Marine Biologie, Giglio). Among the various people who helped in the collection of the specimens, we especially thank Cornelia von Soosten, Monika C. Müller, and Alice Westheide. We gratefully acknowledge

preparation and typing of the manuscript by Mrs. Anna Stein and Mrs. Andrea Noël.

Literature Cited

Armonies, W. 1989. Meiofaunal emergence from intertidal sediment measured in the field: significant contribution to nocturnal planktonic biomass in shallow waters. *Helgol. Meeresunters.* **43:** 29–43.

Bastrop, R., M. Röhner, C. Sturmbauer, and K. Jürss. 1997. Where did *Marenzelleria* spp. (Polychaeta: Spionidae) in Europe come from? *Aquat. Ecol.* **31:** 119–136.

Bochert, R. 1997. *Marenzelleria viridis* (Polychaeta: Spionidae): a review of its reproduction. *Aquat. Ecol.* **31:** 163–175.

Büscher, N., E. Zyprian, and R. Blaich. 1993. Identification of grapewine cultivars by DNA analyses: pitfalls of random amplified polymorphic DNA techniques using 10mer primers. *Vitis* **32:** 187–188.

Felsenstein, J. 1985. Confidence limits on phylogenies: an approach using the bootstrap. *Evolution* **39:** 7778–7783.

Gerlach, S. A. 1977. Means of meiofauna dispersal. In *The Meiofauna Species in Time and Space.* W. Sterrer and P. Ax, eds. Workshop Symposium, Bermuda, 1975. *Mikrofauna Meeresboden* **61:** 89–103.

Giere, O. 1993. *Meiobenthology. The Microscopic Fauna in Aquatic Sediments.* Springer, Berlin.

Hadrys, H., M. Balick, and B. Schierwater. 1992. Application of random amplified polymorphic DNA (RAPD) in molecular ecology. *Mol. Ecol.* **1:** 55–63.

Hagerman, G. M., and R. M. Rieger. 1981. Dispersal of benthic meiofauna by wave and current action in Bogue Sound, North Carolina, USA. *Pubbl. Stn. Zool. Napoli (I. Mar. Ecol.)* **2:** 245–270.

Hartmann-Schröder, G. 1960. Polychaeten aus dem Roten Meer. *Kieler Meeresforsch.* **16:** 69–125.

Hartmann-Schröder, G. 1991. Die Polychaeten der subtropisch-tropischen bis tropischen Ostküste Australiens zwischen Maclean (New South Wales) und Gladstone (Queensland) sowie von Heron Island (Großes Barrier Riff). In: G. Hartmann-Schröder and G. Hartmann. Zur Kenntnis des Eulitorals der australischen Küsten unter besonderer Berücksichtigung der Polychaeten und Ostracoden. Teil 16. *Mitt. Hambg. Zool Mus. Inst.* **88:** 17–71.

He, Q., M. K. Viljanen, and J. Mertsola. 1994. Effects of thermocyclers and primers on the reproducibility of banding patterns in random amplified polymorphic DNA analysis. *Mol. Cell. Probes* **8:** 155–160.

Kocher, T. D., W. K. Thomas, A. Meyer, S. V. Edwards, S. Pääbo, F. X. Villablanca, and A. C. Wilson. 1989. Dynamics of mitochondrial DNA evolution in animals amplification and sequencing with conserved primers. *Proc. Natl. Acad. Sci. USA* **86:** 6196–6200.

Lorenzen, S. 1976. Zur Theorie der phylogenetischen Systematik. *Verh. Dtsch. Zool. Ges.* **1976:** 228.

Nei, M., and W. H. Li. 1979. Mathematical model for studying genetic variation in terms of restriction endonucleases. *Genetics* **76:** 5269–5273.

Palmer, M. A. 1988. Dispersal of marine meiofauna: a review and conceptual model explaining passive transport and active emergence with implications for recruitment. *Mar. Ecol. Prog. Ser.* **48:** 81–91.

Peer, Y. van de, and R. de Wachter. 1994. TREECON for Windows: a software package for the construction and drawing of evolutionary trees for the Microsoft Windows environment. *Comput. Appl. Biosci.* **10:** 569–570.

Por, F. D. 1978. *Lessepsian Migration. The Influx of Red Sea Biota into the Mediterranean by Way of the Suez Canal.* Springer, Berlin 228 pp.

Rao, G. C. 1972. On the geographical distribution of interstitial fauna of marine sand. *Proc. Indian Natl. Sci. Acad.* **38B:** 164–178.

Remane, A., and E. Schulz. 1964. Strandzonen des Roten Meeres und ihre Tierwelt. *Kieler Meeresforsch.* **20:** 5–17.

Riser, N. W. 1981. The aberrant polychaete *Stygocapitella* from some American beaches. *Wasmann J. Biol.* **38:** 10–17.

Ruppert, E. E. 1977. Zoogeography and speciation in marine Gastrotricha. in *The Meiofauna Species in Time and Space.* W. Sterrer and P. Ax, eds. Workshop Symposium, Bermuda, 1975. *Mikrofauna Meeresboden* **61:** 231–251.

Saitou, N., and M. Nei. 1987. The neighbour joining method. A new method for reconstructing phylogenetic trees. *Mol. Biol. Evol.* **4:** 406–425.

Schierwater, B. 1995. Arbitrarily amplified DNA in systematics and phylogenetics. *Electrophoresis* **16:** 1643–1647.

Schirmacher, A., H. Schmidt, and W. Westheide. 1998. RAPD-PCR investigations on sibling species of terrestrial *Enchytraeus* (Annelida: Oligochaeta). *Biochem. Syst. Ecol.* **26:** 27–36.

Schmidt, H., and W. Westheide. 1998. RAPD-PCR experiments confirm the distinction between three morphologically similar species of *Nerilla* (Polychaeta: Nerillidae). *Zool. Anz.* **26:** 277–285.

Sneath, P. H. A., and R. R. Sokal. 1973. *Numerical Taxonomy.* W. H. Freeman, San Francisco.

Soosten, C. von, H. Schmidt, and W. Westheide. 1998. Genetic variability and relationships among geographically widely separated populations of *Petitia amphophthalma* (Polychaeta: Syllidae): Results from RAPD-PCR investigations. *Mar. Biol.* **131:** 659–669.

Sterrer, W. 1973. Plate tectonics as a mechanism for dispersal and speciation in interstitial sand fauna. *Neth. J. Sea Res.* **7:** 200–222.

Todaro, M. A., J. W. Fleeger, Y. P. Hu, A. W. Hrincevich, and D. W. Foltz. 1996. Are meiofaunal species cosmopolitan? Morphological and molecular analysis of *Xenotrichula intermedia* (Gastrotricha: Chaetonotida). *Mar. Biol.* **125:** 735–742.

Westheide, W. 1967. Monographie der Gattungen *Hesionides* Friedrich und *Microphthalmus* Mecznikow (Polychaeta). Ein Beitrag zu Organisation und Biologie psammobionter Polychaeten. *Z. Morph. Tiere* **61:** 1–159.

Westheide, W. 1970. Zur Organisation, Biologie und Ökologie des interstitellen Polychaeten *Hesionides gohari* Hartmann-Schröder (Hesionidae). *Mikrofauna Meeresboden* **3:** 1–37.

Westheide, W. 1971. Interstitial Polychaeta (excluding Annelida). *Smithson. Contrib. Zool.* **76:** 57–70.

Westheide, W. 1972/73. Nouvelles récoltes d'annélides interstitielles dans les plages sableuses du Bassin d'Arcachon. *Vie Milieu Serie A* **23:** 365–370.

Westheide, W. 1972a. Räumliche und zeitliche Differenzierungen im Verteilungsmuster der marinen Interstitialfauna. *Verh. Dtsch. Zool. Ges.* **1971:** 23–32.

Westheide, W. 1972b. La faune des Polychètes et des Archiannélides dans les plages sableuse à ressac de la côte méditerranéenne de la Tunisie. *Bull. Inst. Natl. Sci. Tech. Oceanogr. Peche, Salammbo* **2:** 449–468.

Westheide, W. 1977. The geographic distribution of interstitial polychaetes. In *The Meiofauna Species in Time and Space.* W. Sterrer and P. Ax, eds. Workshop Symposium, Bermuda, 1975. *Mikrofauna Meeresboden* **61:** 287–302.

Westheide, W. 1979. *Hesionides riegerorum* n. sp., a new interstitial freshwater polychaete form the United States. *Int. Rev. Gesamten Hydrobiol.* **64:** 273–280.

Westheide, W. 1984. The concept of reproduction in polychaetes with small body size: adaptations in interstitial species. In *Polychaete Reproduction,* A. Fischer and H.-D. Pfannenstiel, eds. *Fortsch. Zool.* **29:**265–287.

Westheide, W. 1990. Polychaetes: Interstitial Families. In *Synopsis of the British Fauna (New series)* No. 44, D. M. Kermack and R. S. K. Barnes, eds. Universal Book Services/W. Backhuys, Oegstgeest, The Netherlands.

Westheide, W. 1991. The meiofauna of the Galapagos. A review. Pp.

37–73 in *Galapagos Marine invertebrates. Taxonomy, Biogeography, and Evolution in Darwin's Islands,* M. J. James, ed. Plenum, New York.

Westheide, W. 1992. Neue interstitielle Polychaeten (Hesionidae, Dorvilleidae) aus dem Litoral des Golfs von Bengalen. *Microfauna Mar.* **7:** 147–157.

Westheide, W. 1995. *Pisione hartmannschroederae* sp.n. (Polychaeta: Pisionidae) from a Florida sand beach. *Mitt. Hambg. Zool. Inst.* **92:** 77–84.

Westheide, W., and G. G. Rao. 1977. On some species of the genus *Hesionides* (Polychaeta, Hesionidae from Indian sandy beaches. *Cah. Biol. Mar.* **18:** 275–287.

Westheide, W., and R. M. Rieger. 1987. Systematics of the amphiatlantic *Microphthalmus-listensis*-species-group (Polychaeta: Hesionidae): facts and concepts for reconstruction of phylogeny and speciation. *Z. Zool. Syst. Evolutionsforsch.* **25:** 12–39.

Williams, J. G. K., A. R. Kubelik, K. J. Livak, J. A. Rafalski, and S. V. Tingey. 1990. DNA polymorphisms amplified by arbitrary primers are useful as genetic markers. *Nucleic Acids Res.* **18:** 6531–6535.

THE
BIOLOGICAL BULLETIN

JUNE 1999

JUN 23 1999

Editor	Michael J. Greenberg	The Whitney Laboratory, University of Florida
Associate Editors	Louis E. Burnett	Grice Marine Biological Laboratory, College of Charleston
	Charles D. Derby	Georgia State University
	Michael LaBarbera	University of Chicago
	Rudolf A. Raff	Indiana University
Section Editor	Shinya Inoué, *Imaging and Microscopy*	Marine Biological Laboratory
Online Editors	James A. Blake, *Keys to Marine Invertebrates of the Woods Hole Region*	ENSR Marine & Coastal Center, Woods Hole
	William D. Cohen, *Marine Models Electronic Record and Compendia*	Hunter College, City University of New York
Editorial Board	Peter B. Armstrong	University of California, Davis
	R. Andrew Cameron	California Institute of Technology
	Ernest S. Chang	Bodega Marine Lab., University of California, Davis
	Thomas H. Dietz	Louisiana State University
	Richard B. Emlet	Oregon Institute of Marine Biology, Univ. of Oregon
	David Epel	Hopkins Marine Station, Stanford University
	Gregory Hinkle	Cereon Genomics, Cambridge, Massachusetts
	Makoto Kobayashi	Hiroshima University of Economics, Japan
	Donal T. Manahan	University of Southern California
	Margaret McFall-Ngai	Kewalo Marine Laboratory, University of Hawaii
	Mark W. Miller	Institute of Neurobiology, University of Puerto Rico
	Tatsuo Motokawa	Tokyo Institute of Technology, Japan
	Yoshitaka Nagahama	National Institute for Basic Biology, Japan
	Sherry D. Painter	Marine Biomed. Inst., Univ. of Texas Medical Branch
	J. Herbert Waite	University of California, Santa Barbara
	Richard K. Zimmer-Faust	University of California, Los Angeles
Editorial Office	Pamela Clapp Hinkle	Managing Editor
	Victoria R. Gibson	Staff Editor
	Carol Schachinger	Editorial Assistant
	Patricia Burns	Subscription & Advertising Secretary

Published by
Marine Biological Laboratory
Woods Hole, Massachusetts

Cover

The illustration on the cover—comprising a DNA molecule, the earth, and a distant ringed planet—highlights the publication, in this issue (p. 303), of the proceedings of a workshop entitled *Evolution: A Molecular Point of View.* The workshop was held in Woods Hole, late in 1997, at the Marine Biological Laboratory; it dealt broadly with the origin and evolution of organic molecules; the evolution of genes, genomes and metabolic capacities; the phylogeny of early life forms (prokaryotes and ancestral eukaryotes); and the effect of changing environments on these processes.

The workshop was sponsored and funded by NASA through its Center for Advanced Studies in the Space Life Sciences at the MBL. Indeed, this forward looking agency has, for more than four decades, been stimulating interest in, and supporting studies of, the origin and evolution of life as general phenomena in our solar system and beyond. Largely as a result of these efforts, such studies are now in the mainstream of science.

Readers should know that the cover illustration is actually the logo of the Woods Hole Astrobiology Program, whose goals are similar to those of NASA and the workshop. This program, which includes projects at both the MBL and the Woods Hole Oceanographic Institution, is itself a node in a network of related programs constituting a nationwide virtual Astrobiology Institute organized recently by NASA.

CONTENTS

Volume 196, No. 3: June 1999

Catherine Henley (1922–1999) 227

DEVELOPMENT AND REPRODUCTION

Moran, A.L.
Intracapsular feeding by embryos of the gastropod genus *Littorina* 229

Pennington, J. Timothy, Mario N. Tamburri, and James P. Barry
Development, temperature tolerance, and settlement preference of embryos and larvae of the articulate brachiopod *Laqueus californianus* 245

PHYSIOLOGY

Goffredi, Shana K., Peter R. Girguis, James J. Childress, and Nicole T. Desaulniers
Physiological functioning of carbonic anhydrase in the hydrothermal vent tubeworm *Riftia pachyptila*. . . 257

ECOLOGY AND EVOLUTION

Maas, Paula A. Y., Gregory D. O'Mullan, Richard A. Lutz, and Robert C. Vrijenhoek
Genetic and morphometric characterization of mussels (Bivalvia: Mytilidae) from Mid-Atlantic hydrothermal vents. 265

Davidson, Seana K., and Margo G. Haygood
Identification of sibling species of the bryozoan *Bugula neritina* that produce different anticancer bryostatins and harbor distinct strains of the bacterial symbiont "*Candidatus* Endobugula sertula" 273

Palmer, A. Richard, Graeme M. Taylor, and Anise Barton
Cuticle strength and the size-dependence of safety factors in *Cancer* crab claws 281

Steele, Craig, Carol Skinner, Catherine Steele, Philip Alberstadt, and Candice Mathewson
Organization of chemically activated food search behavior in *Procambarus clarkii* Girard and *Orconectes rusticus* Girard crayfishes 295

EVOLUTION: A MOLECULAR POINT OF VIEW

Sogin, Mitchell
Introduction 307

Chang, Sherwood
Planetary environments and the origin of life 308

Ferris, James P.
Prebiotic synthesis on minerals: bridging the prebiotic and RNA worlds 311

Ellington, Andrew D.
Molecular origins and the null hypothesis: motifs from our Maker? 315

Huang, Faqing, Zhili Yang, and Mike Yarus
Self-capping RNA catalysts derived from selection-amplification 320

Bartel, David P.
Creation and evolution of new ribozymes. 322

Landweber, Laura F.
The evolution of cellular computing 324

Weiner, Alan M., and Nancy Maizels
The genomic tag hypothesis: modern viruses as molecular fossils of ancient strategies for genomic replication, and clues regarding the origin of protein synthesis. 327

Maizels, Nancy, Alan M. Weiner, Dongxian Yue, and Pei-Yong Shi
New evidence for the genomic tag hypothesis: archael CCA-adding enzymes and tDNA substrates . . . 331

Ibba, M., A. W. Curnow, J. Bono, P. A. Rosa, C. R. Woese, and D. Söll
Archaeal aminoacyl-tRNA synthesis: unique determinants of a universal genetic code?. 335

Sharp, Paul M., Elizabeth Bailes, David L. Robertson, Feng Gao, and Beatrice H. Hahn
Origins and evolution of AIDS viruses 338

Felsenstein, Joseph
Coalescents, phylogenies, and likelihoods. 343

Cummings, Michael P., Sarah P. Otto, and John Wakeley
Genes and other samples of DNA sequence data for phylogenetic inference 345

Schopf, J. William
Deep divisions in the tree of life—what does the fossil record reveal? 351

Doolittle, Russell F., Da-Fei Feng, and Glen Cho
Determining divergence times with protein clocks. . 356

Gogarten, J. Peter, Ryan D. Murphey, and Lorraine Olendzenski
Horizontal gene transfer: pitfalls and promises 359

DeLong, Edward F., Christa Schleper, Robert Feldman, and Ronald V. Swanson
Application of genomics for understanding the evolution of hyperthermophilic and nonthermophilic Crenarchaeota 363

Reysenback, A.-L., S. Seitzinger, J. Kirshtein, and E. McLaughlin
Molecular constraints on a high-temperature evolution of early life. 367

Forterre, Patrick, and Hervé Philippe
The Last Universal Common Ancestor (LUCA): simple or complex?. 373

Doolittle, W. Ford
Rethinking the origin of eukaryotes 378

Patterson, David J., Alastair G. B. Simpson, and Nimalika Weerkaoon
Free-living flagellates from anoxic habitats and the assembly of the eukaryotic cell 381

Clark, C. Graham
The effect of secondary loss on our views of eukaryotic evolution. 385

Hasegawa, Masami, and Tetsuo Hashimoto
Phylogenetic position of amitochondriate protists in the evolution of eukaryotes. 389

Cavalier-Smith T.
Zooflagellate phylogeny and the systematics of protozoa 393

Douglas, Susan E.
Evolutionary history of plastids 397

Gray, Michael W., Gertraud Burger, Robert Cedergren, G. Brian Golding, Claude Lemieux, David Sankoff, Monique Turmel, and Franz Lang
A genomics approach to mitochondrial evolution . . 400

Redfield, Rosemary J.
The problem of the evolution of sex 404

Bode, Hans, Daniel Martinez, M. Andrew Shenk, Kerry Smith, Robert Steele, and Ulrich Technau
Evolution of head development 408

Mohr, Scott, Jim Freeman, Tom Plasterer, and Temple Smith
Patterns of mitochondrial DNA strand asymmetry correlate with phylogeny. 411

Margulis, Lynn, Michael Dolan, and Ricardo Guerrero
The molecular tangled bank: not seeing the phylogenies for the trees 413

Concluding Remarks 415
List of Participants 417

* * *

Index for Volume 196 421

CONTENTS
for Volume 196

No. 1, February 1999

PHYSIOLOGY

Dudgeon, Steve, Andreas Wagner, J. Rimas Vaišnys, and Leo W. Buss
Dynamics of gastrovascular circulation in the hydrozoan *Podocoryne carnea:* the one-polyp case 1

Kelly, Robert H., and Paul H. Yancey
High contents of trimethylamine oxide correlating with depth in deep-sea teleost fishes, skates, and decapod crustaceans 18

Beaven, Amy E., and Kennedy T. Paynter
Acidification of the phagosome in *Crassostrea virginica* hemocytes following engulfment of zymosan 26

Smith, Andrew M., Tonya J. Quick, and Rachel L. St. Peter
Differences in the composition of adhesive and non-adhesive mucus from the limpet *Lottia limatula* 34

Kawaii, Satoru, Keiji Yamashita, Mitsuyo Nakai, Miyuki Takahashi, and Nobuhiro Fusetani
Calcium-dependence of settlement and nematocyst discharge in actinulae of the hydroid *Tubularia mesembryanthemum* 45

RESEARCH NOTE

Tapley, David W., Garry R. Buettner, and J. Malcolm Shick
Free radicals and chemiluminescence as products of the spontaneous oxidation of sulfide in seawater, and their biological implications 52

DEVELOPMENT AND REPRODUCTION

Froggett, Stephan J., and Esther M. Leise
Metamorphosis in the marine snail *Ilyanassa obsoleta*, yes or NO? 57

Stewart-Savage, J., Bradley J. Wagstaff, and Philip O. Yund
Developmental basis of phenotypic variation in egg production in a colonial ascidian: primary oocyte production versus oocyte development 63

Schwarz, Jodi A., David A. Krupp, and Virginia M. Weis
Late larval development and onset of symbiosis in the scleractinian coral *Fungia scutaria* 70

ECOLOGY AND EVOLUTION

Lopez, Jose V., Ralf Kersanach, Stephen A. Rehner, and Nancy Knowlton
Molecular determination of species boundaries in corals: genetic analysis of the *Montastraea annularis* complex using amplified fragment length polymorphisms and a microsatellite marker 80

Bingham, Brian L., and Nathalie Reyns
Ultraviolet radiation and distribution of the solitary ascidian *Corella inflata* (Huntsman) 94

NEUROBIOLOGY AND BEHAVIOR

Cromarty, S.I., J. Mello, and G. Kass-Simon
Time in residence affects escape and agonistic behavior in adult male American lobsters 105

ULTRASTRUCTURE

Hirose, Euichi, Satoshi Kimura, Takao Itoh, and Jun Nishikawa
Tunic morphology and cellulosic components of pyrosomas, doliolids, and salps (Thaliacea, Urochordata) 113

No. 2, April 1999

Announcement: *Keys to Marine Invertebrates of the Woods Hole Region* 121

RESEARCH NOTE

Ó Foighil, Diarmaid, Bruce A. Marshall, Thomas J. Hilbish, and Mario A. Pino
Trans-Pacific range extension by rafting is inferred for the flat oyster *Ostrea chilensis* 122

NEUROBIOLOGY

Schmidt, Manfred, and Steffan Harzsch
Comparative analysis of neurogenesis in the central olfactory pathway of adult decapod crustaceans by *in vivo* BrdU-labeling 127

PHYSIOLOGY

Frank, Tamara M.
Comparative study of temporal resolution in the visual systems of mesopelagic crustaceans 137
Coughlin, David J., and Lawrence C. Rome
Muscle activity in steady swimming scup, *Stenotomus chrysops*, varies with fiber type and body position ... 145
Khan, Hamid R., David A. Price, Karen E. Doble, Michael J. Greenberg, and A.S.M. Saleuddin
Osmoregulation and FMRFamide-related peptides in the salt marsh snail *Melampus bidentatus* (Say) (Mollusca: Pulmonata) 153

BEHAVIORAL PHYSIOLOGY

McGaw, I.J., C.L. Reiber, and J.A. Guadagnoli
Behavioral physiology of four crab species in low salinity 163

DEVELOPMENT AND REPRODUCTION

Vavra, Jay, and Donal T. Manahan
Protein metabolism in lecithotrophic larvae (Gastropoda: *Haliotis rufescens*) 177
Biggers, William J., and Hans Laufer
Settlement and metamorphosis of *Capitella* larvae induced by juvenile hormone-active compounds is mediated by protein kinase C and ion channels 187
Unuma, Tatsuya, Takeshi Yamamoto, and Toshio Akiyama
Effect of steroids on gonadal growth and gametogenesis in the juvenile Red Sea urchin *Pseudocentrotus depressus* 199

ECOLOGY AND EVOLUTION

Okamura, Beth, and Julian C. Partridge
Suspension feeding adaptations to extreme flow environments in a marine bryozoan 205
Schmidt, Hartmut, and Wilfried Westheide
Genetic relationships (RAPD-PCR) between geographically separated populations of the "cosmopolitan" interstitial polychaete *Hesionides gohari* (Hesionidae) and the evolutionary origin of the freshwater species *Hesionides riegerorum* 216

No. 3, June 1999

Catherine Henley (1922–1999) 227

DEVELOPMENT AND REPRODUCTION

Moran, A.L.
Intracapsular feeding by embryos of the gastropod genus *Littorina* 229
Pennington, J. Ti othy, Mario N. Tamburri, and James P. Barry
Development, temperature tolerance, and settlement preference of embryos and larvae of the articulate brachiopod *Laqueus californianus* 245

PHYSIOLOGY

Goffredi, Shana K., Peter R. Girguis, James J. Childress, and Nicole T. Desaulniers
Physiological functioning of carbonic anhydrase in the hydrothermal vent tubeworm *Riftia pachyptila*. . . 257

ECOLOGY AND EVOLUTION

Maas, Paula A. Y., Gregory D. O'Mullan, Richard A. Lutz, and Robert C. Vrijenhoek
Genetic and morphometric characterization of mussels (Bivalvia: Mytilidae) from Mid-Atlantic hydrothermal vents 265
Davidson, Seana K., and Margo G. Haygood
Identification of sibling species fo the bryozoan *Bugula neritina* that produce different anticancer bryostatins and harbor distinct strains fo the bacterial symbiont "*Candidatus* Endobugula sertula" 273
Palmer, A. Richard, Graeme M. Taylor, and Anise Barton
Cuticle strength and the size-dependence of safety factors in *Cancer* crab claws 281
Steele, Craig, Carol Skinner, Catherine Steele, Philip Alberstadt, and Candice Mathewson
Organization of chemically activated food search beharior in *Procambarus clarkii* Girard and *Orconectes rusticus* Girard crayfishes 295

EVOLUTION: A MOLECULAR POINT OF VIEW

Sogin, Mitchell
Introduction 307
Chang, Sherwood
Planetary environments and the origin of life 308
Ferris, James P.
Prebiotic synthesis on mineral: bridging the prebiotic and RNA worlds 311
Ellington, Andrew D.
Molecular origins and the null hypothesis: motifs from our Maker? 315

Huang, Faqing, Zhili Yang, and Mike Yarus
Self-capping RNA catalysts derived from selection-amplification 320
Bartel, David P.
Creation adn evolution of new ribozymes. 322
Landweber, Laura F.
The evolution of cellular computing 324
Weiner, Alan M., and Nancy Maizels
The genomic tag hypothesis: modern viruses as molecular fossils of ancient strategies for genomic replication, and clues regarding the origin of protein synthesis. 327
Maizels, Nancy, Alan M. Weiner, Dongxian Yue, and Pei-Yong Shi
New evidence for the genomic tag hypothesis: archael CCA-adding enzymes and tDNA substrates . . . 331
Ibba, M., A. W. Curnow, J. Bono, P. A. Rosa, C. R. Woese, and D. Söll
Archaeal aminoacyl-tRNA synthesis: unique determinants of a universal genetic code?. 335
Sharp, Paul M., Elizabeth Bailes, David L. Robertson, Feng Gao, and Beatrice H. Hahn
Origins and evolution of AIDS viruses 338
Felsenstein, Joseph
Coalescents, phylogenies, and likelihoods. 343
Cummings, Michael P., Sarah P. Otto, and John Wakeley
Genes and other samples of DNA sequence data for phylogenetic inference 345
Schopf, J. William
Deep divisions in the tree of life—what does the fossil record reveal? 351
Doolittle, Russell F., Da-Fei Feng, and Glen Cho
Determining divergence times with protein clocks. . 356
Gogarten, J. Peter, Ryan D. Murphey, and Lorraine Olendzenski
Horizontal gene transfer: pitfalls and promises 359
DeLong, Edward F., Christa Schleper, Robert Feldman, and Ronald V. Swanson
Application of genomics for understanding the evolution of hyperthemophilic and nonthermophilic Crenarchaeota 363
Reysenback, A.-L., S. Seitzinger, J. Kirshtein, and E. McLaughlin
Molecular constraints on a high-temperature evolution of early life. 367
Forterre, Patrick, and Hervé Philippe
The Last Universal Common Ancestor (LUCA): simple or complex?. 373
Doolittle, W. Ford
Rethinking the origin of eukaryotes 378
Patterson, David J., Alastair G. B. Simpson, and Nimalika Weerkaoon
Free-living flagellates from anoxic habitats and the assembly of the eukaryotic cell 381
Clark, C. Graham
The effect of secondary loss on our views of eukaryotic evolution. 385
Hasegawa, Masami, and Tetsuo Hashimoto
Phylogenetic position of amitochondriate protists in the evolution of eukaryotes. 389
Cavalier-Smith T.
Zooflagellate phylogeny and the systematics of protozoa 393
Douglas, Susan E.
Evolutionary history of plastids 397
Gray, Michael W., Gertraud Burger, Robert Cedergren, G. Brian Golding, Claude Lemieux, David Sankoff, Monique Turmel, and Franz Lang
A genomics approach to mitochondrial evolution . . 400
Redfield, Rosemary J.
The problem of the evolution of sex 404
Bode, Hans, Daniel Martinez, M. Andrew Shenk, Kerry Smith, Robert Steele, and Ulrich Technau
Evolution of head development 408
Mohr, Scott, Jim Freeman, Tom Plasterer, and Temple Smith
Patterns of mitochondrial DNA strand asymmetry correlate with phylogeny 411
Margulis, Lynn, Michael Dolan, and Ricardo Guerrero
The molecular tangled bank: not seeing the phylogenies for the trees 413

Concluding remarks 415
List of participants. 417

* * *

Index for Volume 196 421

Reference: *Biol. Bull.* **196:** 227. (June 1999)

Catherine Henley (1922–1999)

We note, with regret, the passing, this year, of Dr. Catherine Henley, whose life and scientific career were closely linked to the Marine Biological Laboratory and, especially, to *The Biological Bulletin.*

Dr. Henley was born in Quantico, Virginia, to Regina Knowles and John Ralph Henley, a colonel in the U.S. Marine Corps. Like all military families, the Henleys moved frequently, so during her early years, their daughter had the experience of living in many different places in the world. Henley received her AB degree in 1943 from the University of North Carolina at Chapel Hill, the MS from Johns Hopkins in 1947 (with B. H. Willier), and returned to UNC for the Ph.D., which was completed in 1949 with D. P. Costello.

It was as an undergraduate in Chapel Hill that Henley met Prof. Donald P. Costello, the teacher and mentor who would provide the connection to the Marine Biological Laboratory. In the summer of 1944, she came to Woods Hole as a student in the Embryology course, in which Costello was an instructor. As it happened, this was only the first in a series of more than 30 MBL summers; she would return as a Lab Assistant in the Embryology course (1945–47), as an independent investigator (1950–1976), and finally, as a Trustee of the Laboratory (1971–79). As a Trustee, she is especially remembered for her outspoken espousal of the cause of the non-scientific staff of the Laboratory.

From our perspective, Henley's most significant service at the MBL was to *The Biological Bulletin.* In 1950, when Costello assumed the editorship of this journal, Henley joined him as Assistant to the Editor. The two of them brought out the *Bulletin* together, migrating with it, each year, between Woods Hole and North Carolina. Their lab space on the first floor of the Lillie building bulged with files and manuscripts, but they enjoyed the view of Great Harbor and of the passing scene and goings on in sundial park. In 1968, they retired from their leadership of the journal, and in the annual report of 1968, the MBL acknowledged its "deep sense of gratitude" for their service to *The Biological Bulletin.* From 1969 to 1979, Henley continued to serve the *Bulletin* as a member of the Editorial Board.

Henley was a member of the Zoology faculty for many years at UNC; she taught there and carried out her research, according to the season, at Chapel Hill or Woods Hole. Her fields were embryology and cytology, and she and Costello collaborated for more than 20 years on studies of gamete physiology, chromatin condensation, patterns of microtubules in invertebrate sperm, and related matters. Dozens of papers and abstracts about their work were published in *The Biological Bulletin* alone. Probably their most lasting contribution was a manual: *Methods for Obtaining and Handling Marine Eggs and Embryos,* which was first published by the MBL in 1957 and then revised (Costello and Henley, 1971). This manual is being republished online by Biological Bulletin Publications and provides most of the data for an online compendium about the breeding seasons and eggs of Woods Hole species (Cohen, 1999).

Henley's life began to change significantly in 1975. She left the University of North Carolina to administer the peer review of grant proposals at the National Institutes of Health, the institution that had been the major supporter of her research. The following year, 1976, was her last as a summer researcher at the MBL, and she retired from the NIH in 1990.

On February 19, 1999, at the age of 76, Catherine Henley, afflicted with cancer, died in her home at Carolina Meadows, Chapel Hill.

Literature Cited

Cohen, W. D. 1999. Egg characteristics and breeding season for Woods Hole species. In *Biological Bulletin Compendia.* [Online]. Biological Bulletin Publications. Available: http://www.mbl.edu/BiologicalBulletin/ [1999, June].

Costello, D. P., and C. Henley, 1971. *Methods for Obtaining and Handling Marine Eggs and Embryos,* 2nd ed. Marine Biological Laboratory, Woods Hole, MA.

Reference: *Biol. Bull.* **196:** 229–244. (June 1999)

Intracapsular Feeding by Embryos of the Gastropod Genus *Littorina*

A. L. MORAN[1]

Oregon Institute of Marine Biology, University of Oregon, Charleston, Oregon 97420

Abstract. Many gastropod species develop within egg capsules within which larvae are provided with extraembryonic nutrients. Species with encapsulated development frequently have transitory embryonic organs, such as "larval kidneys," that may represent specializations for consumption of intracapsular nutrition. Larvae of *Littorina* species with nonplanktonic, encapsulated development consume intracapsular albumen, but they lack obvious morphological modifications for albumen consumption. To determine the mechanism and location of protein uptake, larvae of seven species of *Littorina* (*L. keenae, L. littorea, L. plena, L. saxatilis, L. scutulata, L. sitkana, L. subrotundata*) were exposed to solutions of either fluorescently labeled protein (FITC-bovine serum albumen) or ferritin. Under fluorescence microscopy, larvae of all species with encapsulated, nonplanktonic development displayed strong regional affinity for FITC in the ciliated cells of the velum, whereas hatched larvae of planktotrophic *Littorina* species did not. Transmission electron microscopy of epithelial cells of nonplanktotrophic veligers exposed to ferritin supported the interpretation that localized affinity for labeled protein indicated endocytotic protein uptake. Planktotrophic *Littorina* and *Littorina* with encapsulated, nonplanktonic development were shown to share equivalent velar width/larval length ratios during early embryonic development, whereas a literature search suggested that in other nonplanktotrophic prosobranchs the velum is relatively smaller than in planktotrophs. Retention of a large velum in *Littorina* that develop entirely within egg capsules may facilitate feeding on intracapsular protein, in the absence of specialized assimilative organs found in other species with encapsulated development.

Introduction

Marine invertebrates exhibit a remarkable variety of reproductive and developmental modes both within and among taxa, and this variation provides a powerful comparative means of studying the integration of development, life history, and evolution. One of the best-known dichotomies in invertebrate development is between species with larvae that must feed in the plankton to grow and attain metamorphic competence (*planktotrophic*), and species that reach competence without feeding in the plankton (*nonplanktotrophic*) (Thorson, 1946; Jablonski and Lutz, 1983; Strathmann, 1985). Another important distinction can be made between species with entirely planktonic development, and species that spend all or part of development in egg capsules (*planktonic, encapsulated nonplanktonic,* and *mixed* development, respectively) (Thorson, 1946; Pechenik, 1979; Perron, 1981).

Larvae of many species with encapsulated, nonplanktonic development are morphologically similar to larvae of related planktotrophic species, and retain structures that presumably had an ancestral role in larval swimming and feeding. For example, larvae of most gastropod molluscs with nonplanktonic, encapsulated development possess a velum (*e.g.*, Fretter and Graham, 1962; Buckland-Nicks *et al.*, 1973; Strathmann, 1978; Hadfield and Iaea, 1989), which is the primary larval structure that planktotrophic molluscan larvae use in swimming and food collection (Strathmann and Leise, 1979). The velum may be smaller in species that lack free-living larvae than in planktotrophic species (Jägersten, 1972; Webber, 1977; Rivest, 1983; but see Hadfield and Iaea, 1989), and it may have different patterns of ciliation (*e.g.*, Lyons and Spight, 1973; Hadfield and Iaea, 1989). These changes in gastropod larval morphology have been interpreted as the loss of complex, ancestral planktotrophic features due to relaxation of stabilizing selection, and as functional modifications that en-

Received 9 September 1997; accepted 12 February 1999.

[1] Present address: Friday Harbor Laboratories, University of Washington, 620 University Road, Friday Harbor, WA 98250. Email: moran@fhl.washington.edu

hance performance during development in the egg capsule (Fretter and Graham, 1962; Lyons and Spight, 1973; Hadfield and Iaea, 1989).

Egg capsules protect offspring (Shuto, 1974; Spight, 1977; Pechenik, 1984; Hawkins and Hutchinson, 1988; Rawlings, 1990, 1996) and retain progeny within suitable adult habitat (Wells and Wells, 1962; Chapman, 1965; Pechenik, 1979); in many species, capsules also provide a nutrient-rich environment for developing embryos (Fretter and Graham, 1962; Fioroni, 1977, 1988). Larvae of many gastropods with mixed or entirely encapsulated development have transitory structures that may represent specializations for consumption of nutritive materials such as albumen or nurse eggs (Portmann, 1955; Portmann and Sandmeier, 1965; Cather and Tompa, 1972; Lyons and Spight, 1973; Rivest, 1983, 1992; Rivest and Strathmann, 1995). However, in many species the mechanisms of consumption of intracapsular nutrition are poorly known. Likewise, the extent to which planktotrophic larval characters have been modified in species with nonplanktonic, encapsulated larvae is not fully understood, and has not previously been addressed by comparing closely related taxa with contrasting developmental modes.

The gastropod genus *Littorina*, the periwinkle snails, contains ~19 species found in the high-shore zone throughout the northern Atlantic and Pacific oceans (Reid, 1989; Reid *et al.*, 1996). The genus contains both planktotrophic and nonplanktotrophic species (see Reid, 1989, for review); molecular phylogenetic evidence supports planktotrophy as the ancestral state within the genus (see Rumbak *et al.*, 1994). All species of *Littorina* undergo early development in egg capsules. Planktotrophic species have "mixed" development: early developmental stages are contained in complex pelagic capsules (Fig. 1A), within which each larva is encased in an individual egg envelope (Fig. 1A) from which it emerges just prior to hatching from the capsule as a swimming, planktotrophic veliger. Other species lack a planktonic stage altogether, metamorphosing from veligers to juveniles within benthic or brooded egg masses. Egg capsules of these nonplanktotrophic species are filled with granular albumen (Fig. 1B) that larvae consume during development (Buckland-Nicks *et al.*, 1973). *Littorina* veligers have been reported to lack albumen-absorbing larval kidneys (Rivest, 1981; 1992), and the site and mechanism of albumen consumption in encapsulated embryos and larvae of nonplanktotrophic *Littorina* species have not been established.

The objectives of this study were to (1) determine the location of nutrient assimilation by larvae of encapsulated, nonplanktonic species in the gastropod genus *Littorina*; (2) investigate the extent to which congeneric planktotrophs share similar patterns of assimilation; and (3) compare the larval functional feeding morphologies of planktotrophic *Littorina* and their congeners that develop entirely within egg capsules.

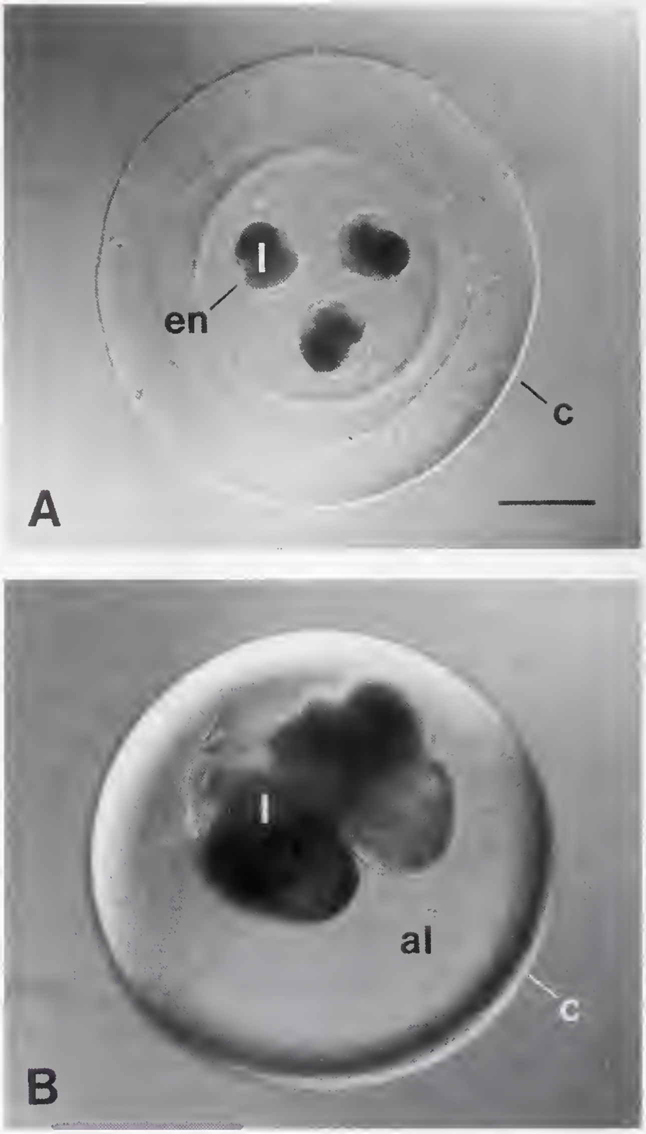

Figure 1. (A) Planktonic egg capsule of *Littorina scutulata*, a species with planktotrophic development, containing three prehatching veliger-stage larvae surrounded by individual egg envelopes. (B) Albumen-filled capsule of *Littorina saxatilis*, a species with encapsulated, nonplanktonic development. Capsule was removed from the oviduct of a gravid female. al, albumen; c, capsule; l, larva; en, egg envelope. Scale bar = 200 μm.

Materials and Methods

Terminology

Because the words *embryo* and *larva* can have multiple interpretations in taxa with complex life histories, I use the terminology for early developmental stages as defined by McEdward and Janies (1993). *Embryo* refers to developmental stages from fertilized egg to gastrula; *larva* describes any premetamorphic stage with recognizable larval features (*e.g.*, the prototroch), regardless of whether stages are free-living or not.

Spawning and larval rearing

Seven *Littorina* species were used in these experiments: four planktotrophs (*L. littorea* (Linnaeus, 1758), *L. keenae* Rosewater, 1978, *L. plena* Gould 1849, *L. scutulata* Gould, 1849) and three species with encapsulated, nonplanktonic development (*L. saxatilis* (Olivi, 1792), *L. sitkana* Philippi, 1846, *L. subrotundata* (Carpenter, 1864)) (Table I). Egg capsules of planktotrophic species and species with benthic egg masses (*L. sitkana, L. subrotundata*) were obtained by placing live, freshly collected adult animals into mesh-walled containers (<1 mm diameter mesh size), and immersing the containers in vigorously aerated seawater for 1 to 7 days. Egg capsules of the nonplanktotrophic species *L. saxatilis,* which broods larvae to metamorphosis in the oviduct, were obtained by cracking adult animals with needle-nose pliers and removing capsules from the brood chamber.

Larvae of planktotrophic species were reared at concentrations of about one larva per milliliter in 0.45 μm filtered seawater changed every 4 days. Planktotrophic larvae were fed *ad libitum* on a mixture of the single-celled algae *Isochrysis galbani* (CCMP #1324 [T-ISO]) and *Dunaliella tertiolecta* (CCMP #1320 [DUN]). Egg masses of species with encapsulated, nonplanktonic development were maintained in glass dishes of filtered (0.45 μm) seawater at 12°C.

Fluorescence microscopy

To test for regions of affinity for labeled albumen protein, embryos and larvae of three species with encapsulated, nonplanktonic development (*L. saxatilis, L. sitkana, L. subrotundata*) were removed from their capsules at developmental stages from early cleavage to metamorphosis. Fine forceps were used to free embryos and larvae from capsules. Veliger larvae of four planktotrophic species (*L. littorea, L. planaxis, L. plena, L. scutulata*) were examined both before and after they hatched from the egg capsule. Because the egg envelope that surrounded earlier developmental stages of planktotrophs could not be removed without damage to developing larvae, early larval stages of one planktotrophic species (*L. plena*) were exposed to test solutions while they were still in the egg envelope.

Embryos and larvae were placed in solutions of bovine serum albumen labeled with fluoroscein isothiocyanate (FITC-BSA, Sigma #A-9771), a solution useful for demonstrating receptor-mediated endocytosis of proteins (Rivest, 1992; Rivest and Strathmann, 1995). FITC-BSA was also made in the laboratory from commercially available BSA and FITC (Sigma #F-7250) using the methods of Rivest (1981). To remove unconjugated FITC, FITC-BSA was dialyzed for 24 h against several changes of filtered (0.45 μm) seawater or treated with excess charcoal for 30 min (Rivest, 1981).

Embryos and larvae were placed in test solutions of 10–1000 μg/ml FITC-BSA in filtered seawater at 12°C for 15 min to 24 h, then rinsed in filtered seawater for periods ranging from 1 to 48 h. Controls were exposed to test solutions containing filtered seawater only, unlabeled BSA, or unconjugated FITC. Experimental and control embryos and larvae were examined with an Olympus epifluorescence microscope fitted with an FITC filter set (Omega Optics stock number XF23, excitation maximum 485 nm, emission 535 nm).

Transmission electron microscopy

To identify regions active in protein uptake, veligers of one species with encapsulated, nonplanktonic development

Table I

Species, development and collection information for Littorina *utilized in this study*

Species, Authority	Mode[1]	Collection locality	Collection habitat
Littorina littorea (Linnaeus, 1758)	P	Woods Hole, MA Mystic, CT	Rocky shoreline
Littorina keenae Rosewater, 1978	P	Monterey, CA	Rocky shoreline
Littorina plena Gould, 1849	P	Charleston, OR	Rocky shoreline
Littorina scutulata Gould, 1849	P	Charleston, OR Monterey, CA	Protected estuary Rocky shoreline
Littorina saxatilis (Olivi, 1792)	NP	Woods Hole, MA Mystic, CT	Rocky shoreline
Littorina sitkana Philippi, 1846	NP	Charleston, OR Friday Harbor, WA	Estuarine marsh Rocky shoreline
Littorina subrotundata (Carpenter, 1864)	NP	Charleston, OR	Estuarine marsh

[1] P = planktotrophic, NP = nonplanktotrophic.

(*L. sitkana*) were removed from their capsules and prepared for transmission electron microscopy, using the methods of Rivest and Strathmann (1995) with minor modifications. Larvae were placed for 10 min in a solution of 0.05% osmium tetroxide and 3% glutaraldehyde in 0.1 *M* (pH 7.35) phosphate buffer, with the osmolarity raised to 990 mOsM with sucrose. Next, larvae were placed in a solution of 3% glutaraldehyde in 0.1 *M* phosphate buffer with the osmolarity raised to 990 mOsM with sucrose for 1 h, after which an equal volume of 10% EDTA was added (to dissolve the shell) and larvae were fixed for another hour. Larvae were postfixed for 1 h at room temperature in 2% osmium tetroxide in 1.25% sodium bicarbonate, then dehydrated in an ethanol series. Finally, specimens were exchanged in propylene oxide, embedded in epoxy resin, and thin sections were cut on a Reichert Ultracut E ultramicrotome. Sections were picked up on Butvar films on 200-μm hex grids, stained with uranyl acetate and lead citrate (after Reynolds, 1963), and examined with a Philips CM 12 electron microscope.

To determine whether protein was assimilated into velar cells, some larvae were exposed to a solution of 1 mg/ml ferritin (Sigma catalog #F4503) in filtered seawater for 12 h and rinsed in seawater for 2 h prior to fixation. Ferritin is an electron-dense protein useful as a marker for endocytosis (Rivest, 1981). Five ferritin-exposed larvae and four controls were examined with transmission electron microscopy.

Measurement of velar aspect ratios

Freshly laid egg capsules of *L. plena* (planktotrophic) were transferred to filtered seawater and reared at room temperature. When larvae had reached the veliger stage (judged by the appearance of the velum), one larva was haphazardly chosen from each capsule. Brooded capsules of one species with encapsulated, nonplanktonic development (*L. saxatilis*) were removed from the adult, and several veligers from each brood were haphazardly chosen for measurements. Velar width and total length were measured on each larva, and dimensions of these measurements are shown in Figure 2. Larvae were traced with a camera lucida attached to a compound microscope, and measurements were made using a SummaSketch II digitizing pad and the software package SigmaScan for Windows (Jandel Corporation). To control for developmental stage, only early veligers of *L. saxatilis* (lacking well-developed tentacles or propodia, similar in degree of development to prehatching *L. plena*) were measured.

To compare the relative size of the velum and to compensate for size differences between larvae of the two species, the "velar aspect ratio" (VAR) was calculated by dividing velar width by total length of each larva. VARs were calculated for 64 *L. plena* and 60 *L. saxatilis* veligers. To compare VARs of other planktotrophic and nonplanktotrophic prosobranch gastropods, the literature was searched to find drawings or photographs of prosobranch veligers from many taxa. Images were chosen based on two criteria, developmental stage and orientation. Because comparisons of *Littorina* with different developmental modes were made when both species were fully developed, but early, veligers (see above), I selected images of planktotrophic species if the larvae were described as prehatching or newly hatched, and I rejected images of nonplanktotrophic species if the larvae were described as mature or near hatching. If multiple stages were pictured, I used the earliest veliger stage. Images were used only if both the full width of the velum and the length of the larva were depicted. However, because orientation varied considerably among images, measurements of length were necessarily somewhat subjective.

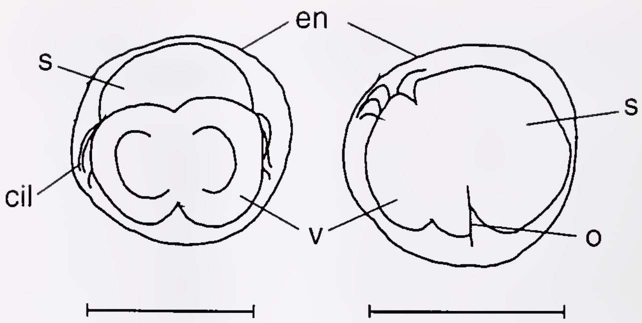

Figure 2. Camera lucida drawings of a prehatching larva of *Littorina plena* indicating measured dimensions: velar width (left on figure; apical view of larva) and larval length (right; lateral view). en, egg envelope; cil, cilia of velum; o, operculum; s, shell; v, velum). Larval length bar (on right) = 110 μm.

The velar aspect ratio of each image was measured with a SummaSketch II digitizing pad and SigmaScan for Windows software as described above for *Littorina*. If an image included a scale bar, it was used to calibrate measurements; otherwise, the aspect ratio was measured without units.

Ideally, statistical analyses would take into account the degrees of phylogenetic relatedness among all taxa; failure to do so may artificially inflate the sample size and hence the degrees of freedom (Martins and Hansen, 1996). Although there has been much recent interest in higher gastropod phylogeny (*e.g.*, Bieler, 1992; Ponder and Lindberg, 1996; Ponder and Lindberg, 1997), there is little consensus regarding relationships at or above the family level (Harasewych *et al.*, 1997; Ponder and Lindberg, 1997). Therefore, for the purposes of this study, species were not considered individually but were sorted by family. VARs were averaged within families if measurements were made on more than one species in a family, and average VARs were graphed for comparison of planktotrophs and nonplanktotrophs. Six families in this data set were represented by both planktotrophic and nonplanktotrophic species, presumably representing six independent losses of planktotrophy.

To compare velar sizes among developmental modes, mean VARs of planktotrophs and nonplanktotrophs of these six families were compared by using a paired Student's *t* test.

Measurement of cilia length

To determine whether ciliary length and growth differed between species with contrasting developmental modes, freshly spawned egg capsules of three planktotrophs (*L. keenae, L. plena, L. scutulata*) and egg masses of one species with encapsulated, nonplanktonic development (*L. sitkana*) were collected, transferred to filtered seawater, and reared at 12°C. Planktotrophs were observed from first cleavage through hatching; they were initially examined every 2–3 h and at intervals of about 1 d or longer in later development. The nonplanktotrophs, which developed more slowly, were observed from first cleavage through reaching a fully formed veliger; they were initially examined daily and during later development at intervals of several days. Larvae were immobilized under a coverslip and examined on a compound microscope equipped with a camera lucida. The cilia were drawn at their greatest extensions and the images were then digitized (as described for velar aspect ratios) to measure greatest length. In addition, veligers of *L. saxatilis* were removed from their capsules and placed in seawater to determine whether larvae could swim.

Results

Fluorescence microscopy

Encapsulated, nonplanktonic developers. None of the experimental eggs or embryos exhibited FITC fluorescence after exposure to FITC-BSA, prior to the trochophore stage. In all species with encapsulated, nonplanktonic development (*Littorina saxatilis, L. sitkana, L. subrotundata*), FITC-BSA fluorescence was first seen at the trochophore stage, when it was confined to the ciliated cells of the prototrochal band (prototroch; Fig. 3A, B). At the late trochophore stage (before the appearance of eyespots, foot, or the larval shell) and the veliger stage (with shell, foot, eyespots), FITC fluorescence was confined to the ciliated cells of the developing velum (Fig. 4A, B), which are derived from the ciliated cells of the prototroch (Fretter and Graham, 1962). Fluorescence was not evident in other cells of the pretrochal region or in the developing structures of the head (tentacles, eyespots; Fig. 5A–D). Fluorescence was seen in the ciliated cells of the velum of larvae exposed to FITC-BSA throughout development, until the velum was resorbed prior to hatching. FITC fluorescence in these cells was concentrated in small (<2 μm) vacuoles visible inside cells (Fig. 6).

In addition to the ciliated cells of the velum, three other larval regions showed FITC-BSA fluorescence. In older larvae with a well-developed foot, the ciliated cells of the rejection band of the foot fluoresced in a manner qualitatively similar to prototrochal/velar fluorescence. Small, isolated points of fluorescence, similar to the vacuoles seen in prototrochal/velar cells, were occasionally seen in the mantle and other parts of the foot as well. In mature veligers of all nonplanktotrophs, two small areas of FITC fluorescence appeared just posterior to the ciliated band of the velum on either side of the head (Fig. 7; "larval kidneys"). These areas autofluoresced in control larvae, but the intensity of autofluorescence was low and varied considerably among larvae. In mature, fully formed veligers and in posthatching juveniles, FITC fluorescence appeared in the gut as well (Fig. 8A, B). Newly hatched juveniles did not exhibit FITC fluorescence except in the gut.

Control embryos and larvae did not fluoresce when exposed to filtered seawater only or to BSA in filtered seawater, except for autofluorescence in the operculum and larval kidneys. Larvae exposed to unconjugated FITC displayed FITC fluorescence in multiple regions including the foot, shell gland, viscera, and velum, probably due to adherence of FITC to cell proteins. FITC fluorescence faded in most areas when larvae were rinsed in filtered seawater for >24 h. Unconjugated FITC also adhered to the shell and operculum of mature larvae.

Planktotrophs. Among larvae of four planktotrophic species exposed to test solutions containing FITC-BSA at the stage of emerging from the egg envelope (but prior to hatching from the egg capsule), none showed fluorescence in the velum (Fig. 9A, B). The planktotrophic *L. plena* did not exhibit FITC-BSA fluorescence at any stage when larvae in their egg envelopes were soaked overnight in FITC-BSA solutions, suggesting that either (1) the egg envelope is not permeable to large proteins (molecular weight of BSA is about 88,000 kDa), or (2) if the envelope is permeable to proteins, early stages do not exhibit affinity at a visually detectable level. Egg capsules of planktotrophic species contained a gel-like material outside the egg envelopes (Fig. 1A). However, this material did not appear to be protein-rich because no schleiren lines were seen when capsules were opened in seawater. Hatched veligers of all four planktotrophs exhibited fluorescence in the gut after exposure to FITC-BSA solutions (Fig. 9A, B). Control larvae exposed to filtered seawater only or to BSA in seawater showed autofluorescence in the operculum only.

Transmission electron microscopy

The ciliated cells of the velum of larvae exposed to ferritin contained numerous endosomes 1–5 μm in diameter filled with an electron-dense material that was by far the darkest material in unstained sections (Fig. 10A). This material was identified as ferritin because it consisted of densely packed particles of uniform shape about 7–8 nm in diameter (Fig. 10B), consistent with the size and appearance

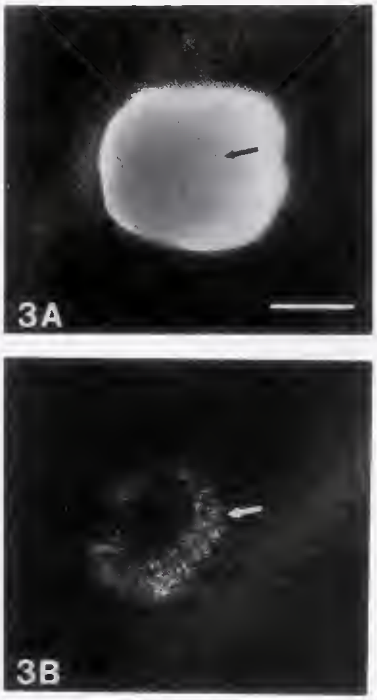

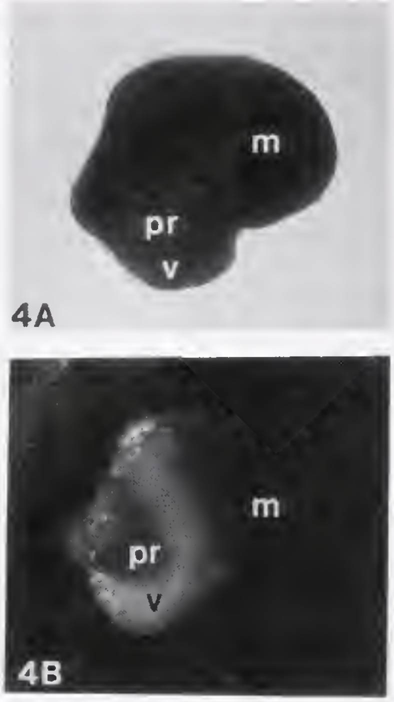

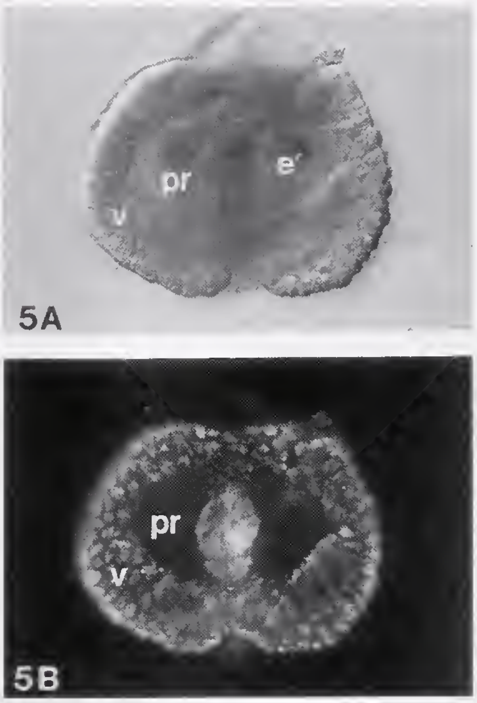

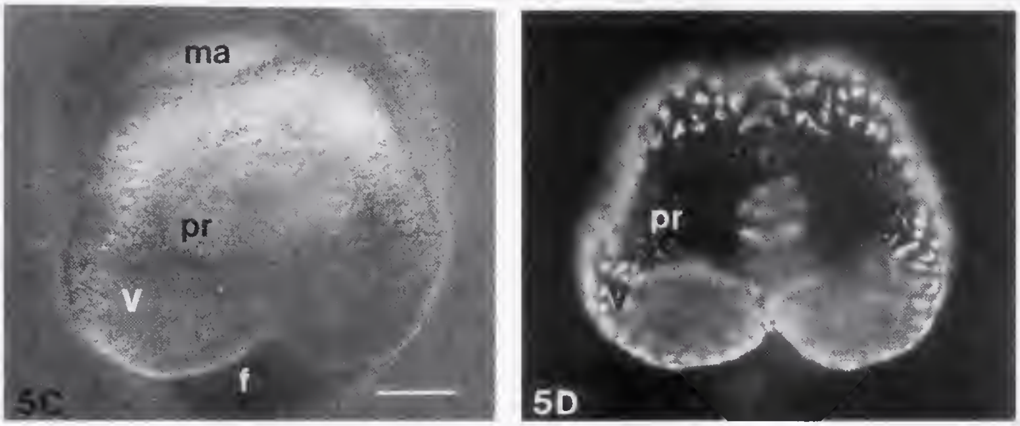

Figure 3. (A) Excapsulated trochophore larva of *Littorina saxatilis*, viewed obliquely from the apical end under transmitted light (dark field). Larva was exposed to fluorescently labeled albumen for 12 h. Arrow indicates position of prototroch (cilia are not visible). (B) Same larva viewed with epifluorescence microscopy and FITC filter set. Only the cells of the prototroch (arrow) are fluorescent, indicating localized affinity for FITC-labeled albumen. Scale bar = 70 μm.

Figure 4. (A) Excapsulated early veliger of *Littorina saxatilis* viewed from the side under transmitted light (bright field). Larva has been exposed to fluorescently labeled albumen for 12 h. (B) Same larva viewed with epifluorescence microscopy and FITC filter set. Only the ciliated cells of the velum are fluorescent; no fluorescence appears in the pretrochal region or visceral mass. m, visceral mass; pr, pretrochal region; v, velum (v is positioned on ciliated band). Scale bar (on Fig. 3) = 70 μm.

Figure 5. (A) Velum of excapsulated, mature veliger of *Littorina saxatilis* (viscera and foot have been removed) viewed under transmitted light (bright field). Larva was exposed to fluorescently labeled albumen for 12 h. (B) Same partial larva, viewed with epifluorescence microscopy and an FITC filter set. The ciliated velar cells are brightly fluorescent, whereas the pretrochal region exhibits no fluorescence. The fluorescent area in the center of the velum is continuous with the ciliated band of velar cells, and may represent cells of the apical plate (see Raven, 1958, pp. 143–145) or an extension of the ciliated band. (C) Excapsulated, mature veliger of *Littorina sitkana*, viewed head-on under transmitted light and epi-illumination. Larva was exposed to fluorescently labeled albumen for 12 h. (D) Same larva, viewed with epifluorescence microscopy and FITC filter set. Ciliated velar cells are brightly fluorescent, and some fluorescence can be seen (out of focus) in the ciliated rejection band of the foot. No fluorescence is seen in the pretrochal region or mantle. e, eyespot; f, foot; ma, mantle; pr, pretrochal region; v, velum (v is positioned on ciliated band). Scale bars: A–B (on Fig. 3A) = 70 μm, C–D (on Fig. 5C) = 50 μm.

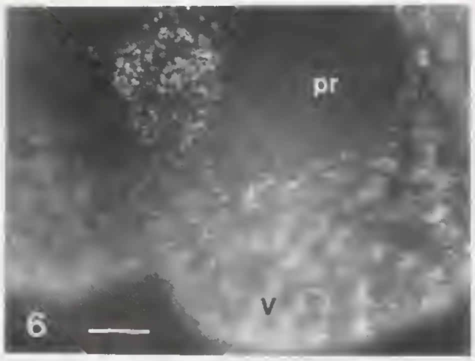

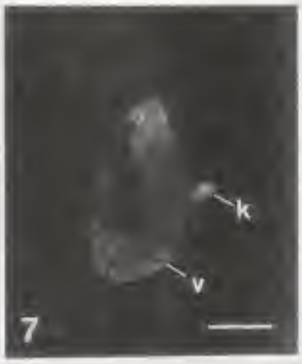

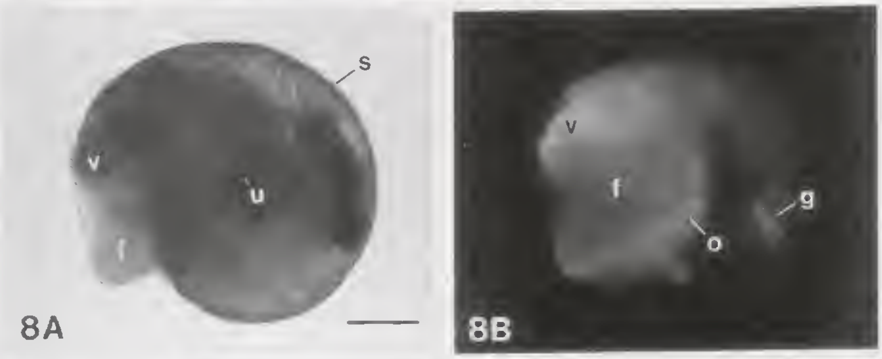

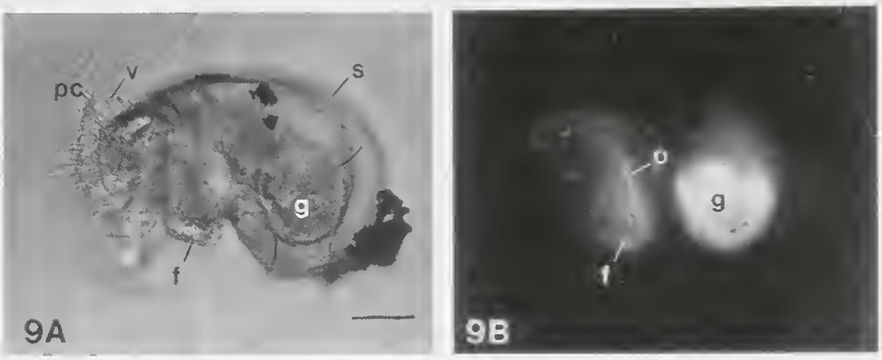

Figure 6. High-magnification view of velum of mature *Littorina saxatilis* larva viewed with epifluorescence microscopy (FITC filter set). Larva was exposed to fluorescently labeled albumen for 12 h. Fluorescence appears in the ciliated band of velar cells but not the pretrochal region. Fluorescence is concentrated in small (<2 μm) vacuoles within the prototrochal cells. pr, pretrochal region; v, velum (positioned on ciliated band). Scale bar = 20 μm.

Figure 7. Veliger of *Littorina saxatilis*, exposed to FITC-BSA and viewed laterally under fluorescent light with FITC filter set. The orientation of this larva is similar to Fig. 3. Immediately posterior to the ciliated band is one of two symmetrically positioned fluorescent regions (larval kidneys) that were found in fully formed veligers. k, larval kidney; v, velum. Scale bar = 75 μm.

Figure 8. (A) Mature veliger of *Littorina saxatilis*, close to hatching, viewed under transmitted light. Larva was exposed to fluorescently labeled albumen for 12 h. (B) Same larva viewed under fluorescent light with FITC filter set. Fluorescence can be seen in the ciliated cells of the velum, the autofluorescent operculum, and in a short region of the gut. The dim illumination of the foot is due to light reflected from the operculum. f, foot; g, gut; o, operculum; s, shell; u, umbilicus; v, velum. Scale bar = 150 μm.

Figure 9. (A) Newly hatched veliger of *Littorina plena* (planktotroph), viewed under transmitted light. Larva was exposed to fluorescently labeled albumen for 12 h. (B) Same larva viewed under fluorescent light with FITC filter set, showing strong FITC fluorescence in the gut. The operculum is autofluorescent, and the foot is dimly illuminated by light reflected from the operculum. Note absence of fluorescence in the velum. f, foot; g, gut; o, operculum; pc, prototrochal cilia; s, shell; v, velum. Scale bar = 25 μm.

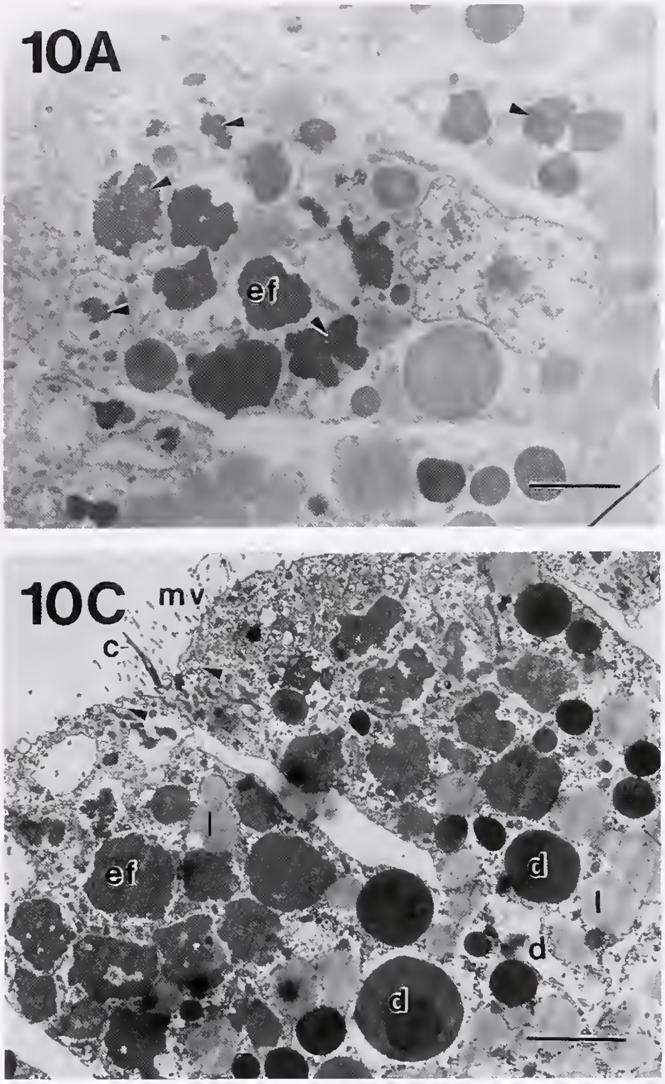

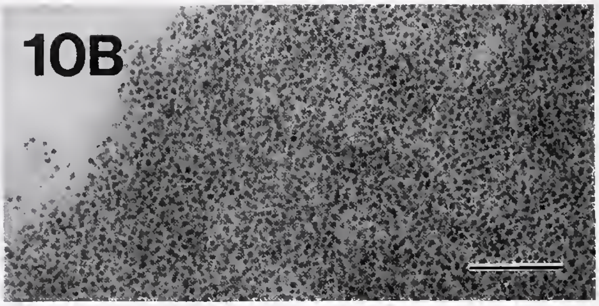

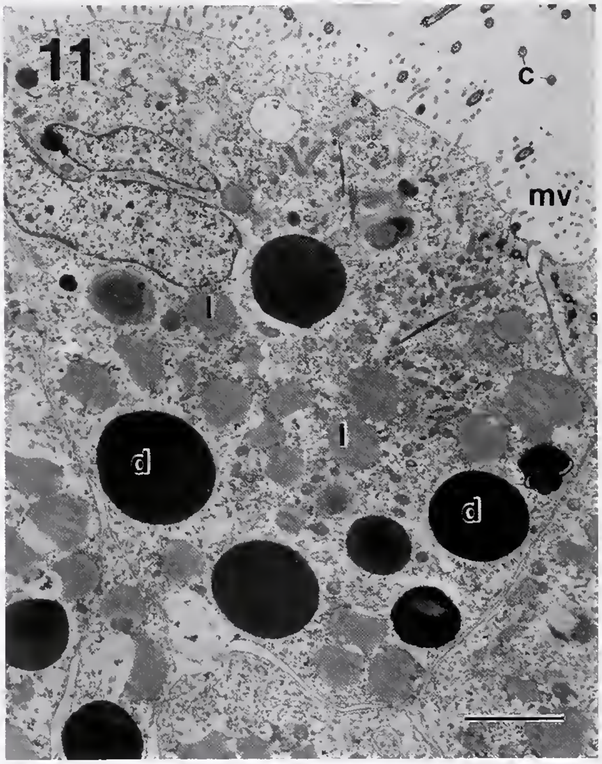

Figure 10. Transmission electron micrographs of the velum of *Littorina sitkana* exposed to ferritin for 12 h. (A) Unstained section of a ciliated cell of the velum. The plasma membrane is to the upper left. Cells contain numerous irregularly shaped endosomes 1–5 μm in diameter that are filled with a dark (electron-dense) granular material. One endosome is labeled, and other concentrations of ferritin are indicated with arrows. (B) High-magnification view of the electron-dense material contained within the endosomes in (A), identified as ferritin by its uniform shape and size (approximately 8 nm diameter, consistent with the size of ferritin molecules) and its absence from control larvae. (C) Stained section of a larva exposed to ferritin, with probable endocytotic vesicles (arrows), light body (tentatively identified as lipid), dark body (tentatively identified as yolk), and numerous endosomes (one is labeled) similar in size, shape, and appearance to endosomes appearing in the unstained section shown in (A). Endosomes in (C) contain the same granular material as those in (A). Note that in the stained section, endosomes and dark bodies are similar in electron density. Exterior of the larva is to the upper left. c, cilium; d, dark body; ef, endosome containing electron-dense material (ferritin); l, light body; mv, microvilli. Scale bars; A, 4 μm; B, 100 nm; C, 4 μm.

Figure 11. Transmission electron micrograph of ciliated cells of the velum of a *Littorina sitkana* larva removed from the egg capsule and soaked in filtered seawater for 12 h prior to fixation; larva NOT exposed to ferritin. Cilia, numerous microvilli, light bodies, and dark bodies are labeled. Note that dark bodies are the most electron-dense material in this section, and that ferritin-containing endosomes are lacking. Exterior of the larva is to the upper right. c, cilium; d, dark body; l, light body; mv, microvilli. Scale bar = 3 μm.

of the electron-dense core of ferritin molecules (Gider *et al.*, 1995). Ferritin-filled endosomes were also abundant in stained sections of ferritin-exposed larvae (Fig. 10C). Other distinctive features of stained sections of velar cells were numerous microvilli and invaginations at the cell surface (Fig. 10C), small (0.1–0.3 μm in diameter) vesicles immediately inside the cell surface (Fig. 10C), "light bodies" tentatively identified as lipid, and "dark bodies" tentatively identified as yolk on the basis of the lack of a surrounding membrane (Fig. 10C).

Ciliated velar cells of larvae not exposed to ferritin contained many similar features, including surface cilia and microvilli and light and dark bodies (Fig. 11). Sections of control larvae were distinguished by the absence of ferritin-filled endosomes; ferritin or ferritin-like electron-dense material was not seen in velar sections of any of four control larvae examined.

At higher magnification, the cell membrane of ciliated velar cells of larvae exposed to ferritin appeared to be endocytotically active. Probable endocytotic profiles were evident in the plasma membrane (Fig. 12A), and ferritin-filled endosomes appeared immediately inside the cells (Fig. 12A, 12A inset). Nonciliated epithelial cells of ferritin-exposed larvae shared some features with ciliated cells of the velum and foot, including the presence of microvilli and light bodies. However, ferritin was not present in these cells (Fig. 12B) even when ciliated and nonciliated cells were immediately adjacent to each other, as in ciliated and nonciliated areas of the foot (Fig. 12C).

Velar aspect ratios

The velar aspect ratios (VARs) of early *Littorina saxatilis* (nonplanktotroph) veligers were not significantly different from the velar aspect ratio of prehatching *L. plena* (planktotroph) veligers (Student's two-sample t test, $P = 0.77$; Fig. 13A). The VARs of planktotrophs from the literature were generally greater than VARs of confamilial nonplanktotrophs, although there was considerable overlap (Table II; Fig. 13B). VARs of planktotrophs were significantly greater than nonplanktotrophs when average VARs were compared among planktotrophs and nonplanktotrophs from within six families (Fig. 13B; paired Student's t test, $P = 0.02$).

Cilia length

Velar cilia of planktotrophic *Littorina* larvae grew faster than cilia of *L. sitkana*, and reached a much greater total length (Fig. 14). Observations of cilia length in additional species with encapsulated, nonplanktonic development (*L. saxatilis, L. subrotundata*) were consistent with this pattern. The velum of these species bore cilia that appeared to be simple rather than compound, and when removed from their egg capsules, veligers of these species rotated on the bottom of the dish but did not swim.

Discussion

Two lines of evidence indicate that the ciliated cells of the velum and foot of *Littorina* with encapsulated, nonplanktonic development are active in localized uptake of capsular proteins. First, these cells fluoresced brightly after exposure to fluorescently labeled albumen, clearly indicating regional affinity for labeled protein. Affinity strongly suggested uptake, because fluorescently labeled vacuoles were interspersed with cell structures such as lipid droplets in optical sections. Second, ciliated cells of the velum and rejection band of the foot of larvae exposed to ferritin solutions contained large amounts of electron-dense material identifiable as ferritin by the size of molecules, whereas adjacent areas of the foot did not contain ferritin; likewise, no ferritin was seen in control larvae. The absence of ferritin from nonciliated cells of the foot (which did not fluoresce after exposure to FITC-BSA) further supports the hypothesis that regional FITC-BSA fluorescence indicates localized uptake of intracapsular albumen.

Other larval structures have been associated with the endocytotic uptake of capsular proteins by gastropods. These include the larval kidneys of many prosobranch species (Rivest, 1992), the "pedal cell complex" of neritoideans (Rivest and Strathmann, 1995), and the podocyst of some pulmonates (Cather and Tompa, 1972), all of which assimilate protein *via* receptor-mediated endocytosis (Cather and Tompa, 1972; Rivest, 1981, 1992; Rivest and Strathmann, 1995). Structures such as the pedal cell complex and larval kidneys are unique to encapsulated larval forms, and in species with mixed development these structures are resorbed before or soon after hatching (Rivest, 1992; Rivest and Strathmann, 1995). Thus, it has been proposed that such structures may have evolved to facilitate intracapsular development by enhancing capsular nutrient uptake (Rivest, 1992; Rivest and Strathmann, 1995) or respiration (Cather and Tompa, 1972; Rivest and Strathmann, 1995). The velum, in contrast, is an ancestral structure that is present in all *Littorina* and functions in swimming and particle capture in planktotrophic species; therefore, intracapsular protein uptake by the velum of nonplanktotrophic *Littorina* likely represents an exaptation of an ancestral character to the evolutionarily novel (within the genus) condition of developing to metamorphosis in the egg capsule.

In many taxa, egg capsules provide a nutrient-rich environment for developing embryos (Rivest and Strathmann, 1995), in addition to other functions such as protecting offspring from environmental stress and predation (Shuto, 1974; Spight, 1977; Pechenik, 1984; Hawkins and Hutchinson, 1988; Rawlings, 1990, 1996) and retaining progeny within suitable adult habitat (Wells and Wells, 1962; Chapman, 1965; Pechenik, 1979). Albumen is a common nutrient source among gastropods, and in many taxa albumen is rich in proteins, carbohydrates, or free amino acids (Hörstmann, 1956; De Mahieu *et al.*, 1974; Rivest, 1992; Stöckmann-Bosbach and Althoff, 1989; Penchaszadeh and Rincón, 1996). Albumen has been implicated in larval nutrition through a decline in nutrient content of the fluid during development, and by a correlated increase in larval lipid and

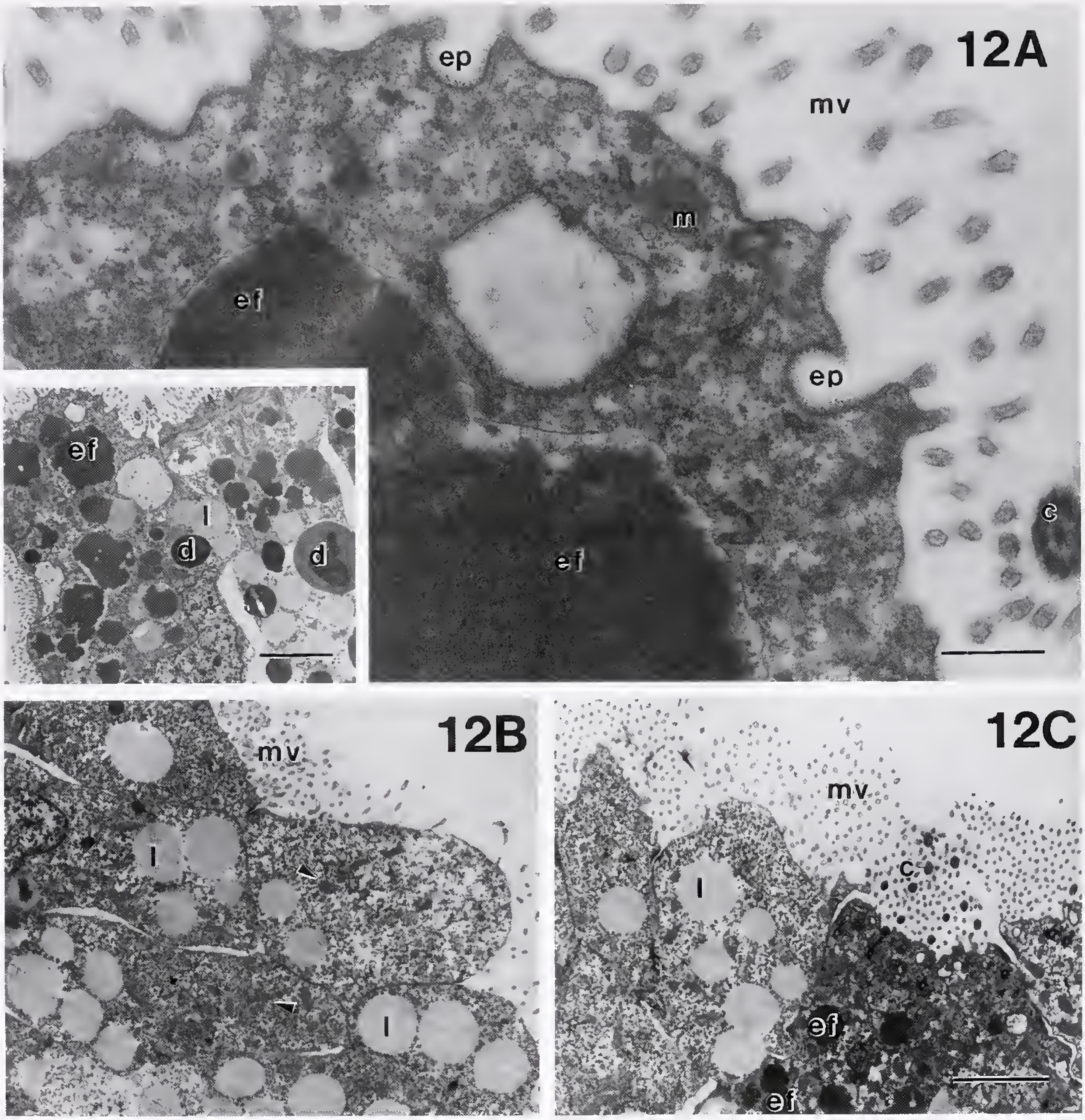

Figure 12. Transmission electron micrographs of sections from the velum and foot of *Littorina sitkana* larvae exposed to ferritin for 12 h. (A) High-magnification view of cell surface of a prototrochal cell of the velum, showing a prototrochal cilium, surface microvilli, a mitochondrion, and an endosome containing electron-dense material (ferritin). Two endocytotic profiles are evident at the cell surface membrane. Inset; lower magnification view of the same area of the larva. Magnified area shown in 12A is the upper left corner of the inset. (B) Cells from the foot of larva exposed to ferritin for 12 h. Cells contain light bodies and mitochondria (arrows). Numerous microvilli are visible on the cell surface, but cilia are not evident. Cells contain no ferritin. (C) Cells from the foot of a second larva also exposed to ferritin for 12 h. This image shows the junction of two cell types, from the ciliated rejection band of the foot (right) and adjacent, nonciliated foot cells (left). Ferritin-containing endosomes are visible in the ciliated cells but are not seen in adjacent, nonciliated cells. c, cilium; d, dark body; ef, endosome containing ferritin; ep, endocytotic profile; l, light body; mv, microvilli; m, mitochondrion. Scale bars; A, 0.5 μm; A inset, 5 μm; B and C, 3 μm.

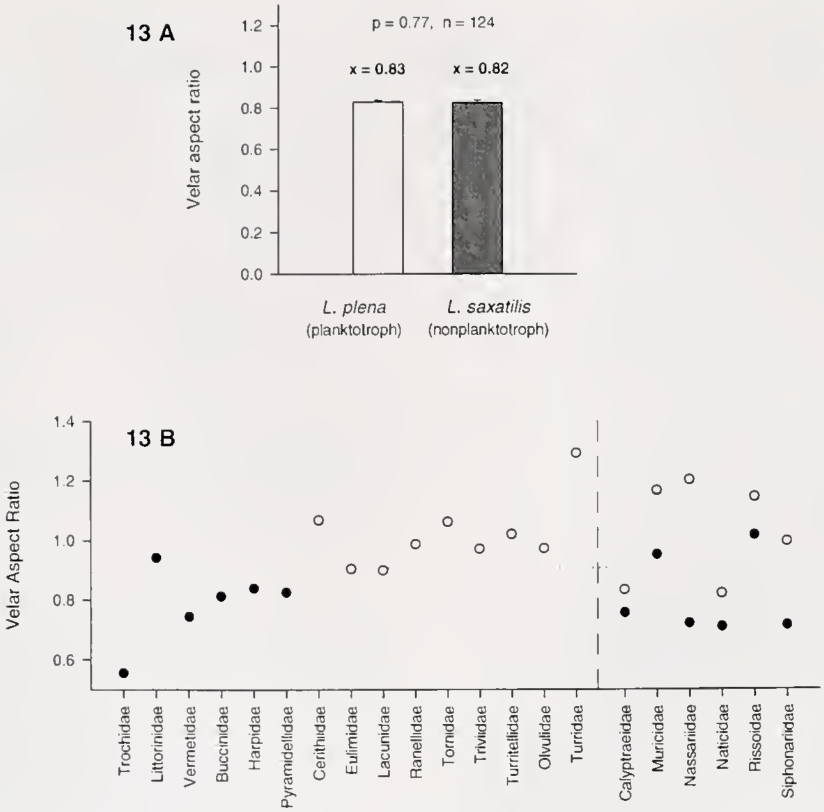

Figure 13. (A) Mean velar aspect ratios of 64 early veligers of *Littorina plena* (planktotroph, open bar) and 60 early *L. saxatilis* veligers (nonplanktotroph; shaded bar). Error bars are 95% confidence intervals. (B) Mean velar aspect ratios of planktotrophs (open circles) and nonplanktotrophs (closed circles) from 21 gastropod families. Error bars are not shown because most families are represented by single species (see Table I). The six families to the right of the vertical dotted line are represented by both planktotrophic and nonplanktotrophic species. The horizontal dotted line represents the mean velar aspect ratio of all families combined.

protein content (Hörstmann, 1956; Morrill, 1964; Raven, 1972; Morrill *et al.*, 1976; Taylor, 1983). Considerable increases in larval size are also correlated with disappearance of capsular albumen in many gastropod taxa (Rasmussen, 1951; Buckland-Nicks *et al.*, 1973; Clark *et al.*, 1979; Clark and Jensen, 1981; Losse and Greven, 1993). The nutritive importance of albumen varies in different taxa, depending on egg size, volume of albumen, nutritive content of albumen, and the presence or absence of additional food sources such as nurse eggs (Pechenik *et al.*, 1984; Miloslavich, 1996; Penchaszadeh and Rincón, 1996).

Intracapsular albumen is thought to be of nutritive importance to developing *Littorina* with encapsulated, nonplanktonic development for two reasons. First, albumen of one species, *L. saxatilis*, is dominated by a single protein of molecular weight 80,000 kDa that disappears from the intracapsular fluid during development (Losse and Greven, 1993). Second, larvae of these species increase in size during development; Buckland-Nicks *et al.* (1973) reported that *L. sitkana* increases from an egg size of 175 μm to a hatching length of 575 μm, presumably due to consumption of albumen. Velar albumen assimilation is likely to be important to larval nutrition, because the surface area of the velum is a large proportion of the larval surface area during early development (see Fig. 4). In addition, assimilation by the cells that will form the velum begins early in development, prior to the development of other structures implicated in assimilation (the foot, gut, and larval kidneys). Assimilation *via* the foot and gut may be of greater importance later in development, when the velum is being resorbed. Larval kidneys are unlikely to be as important in protein assimilation as other structures; their small size and dim fluorescence after exposure to FITC-BSA, which may account for previous reports of their absence in *Littorina sitkana* (Rivest, 1981, 1992), suggests that assimilation by the larval kidneys is negligible relative to velar assimilation.

The velum may take up other substances in addition to proteins. Losse and Greven (1993) noted considerable fluorescence in the gut, hepatopancreas, and velum of *L. saxatilis* veligers exposed to FITC-labeled dextrans, and the intracapsular fluid of some gastropods contains carbohydrates and free amino acids that may be nutritive (*e.g.*,

Table II

Taxa utilized in comparisons of velar aspect ratios among planktotrophs and nonplanktotrophs

Family	Genus/Species	Mode[1]	VAR[2]	References
Buccinidae	*Engoniophos unicinctus*	NP	1.205	Miloslavich and Penchaszadeh, 1994
	Neptunea antiqua	NP	0.418	Pearce and Thorson, 1967
Calyptraeidae	*Calyptraea chinensis*	NP	1.074	Lebour, 1936
	Calyptraea trochiformis	NP	0.779	Cañete and Ambler, 1992
	Crepidula adunca	NP	0.47	Moritz, 1939
	Crepidula fornicata	P	0.834	Fretter and Graham, 1962
Cerithiidae	*Cerithiopsis tubercularis*	P	0.924	Lebour, 1993a
	Cerithiopsis barleei	P	1.135	Lebour, 1993a
	Triphora perversa	P	1.144	Lebour, 1993a
Eulimidae	*Eulima distorta*	P	0.829	Thorson, 1946
	Pelseneeria stylifera	P	0.982	Thorson, 1946
Harpidae	*Morum onuscus*	NP	0.839	Hughes, 1990
Lacunidae	*Lacuna vincta*	P	0.900	Lebour, 1937
Littorinidae	*Bembicium vittatum*	NP	0.943	Black *et al.*, 1994
Muricidae	*Chicoreous ramosus*	NP	1.599	Soliman, 1991
	Concholepas concholepas	P	1.169	DiSalvo, 1988
	Nucella lapilus	NP	0.817	Fretter and Graham, 1962
	Nucella lamellosa	NP	0.880	Lyons and Spight, 1973
	Nucella crassilabrum	NP	0.625	Gallardo, 1979
	Nucella canaliculata	NP	0.780	Lyons and Spight, 1973
	Nucella emarginata	NP	0.861	Lyons and Spight, 1973
	Trophon muricatus	NP	1.102	Lebour, 1936
Nassariidae	*Bullia digitalis*	NP	0.720	da Silva and Brown, 1985
	Nassarius incrassatus	P	1.150	Lebour, 1931a
	Nassarius reticulatus	P	1.257	Lebour, 1931a
Naticidae	*Natica catena*	NP	0.574	Thorson, 1946
	Natica (Lunatida) pallida	NP	0.843	Thorson, 1946
	Natica (Lunatida) nitida	P	0.822	Thorson, 1946
Olvulidae	*Simnia barbarensis*	P	0.973	Main, 1974
Pyramidellidae	*Boonea (Odostomia) impressa*	NP	0.825	White *et al.*, 1985
Ranellidae	*Cabestana spengleri*	P	0.987	Reidel, 1992
Rissoidae	*Cingula semicostata*	NP	1.018	Lebour, 1934
	Rissoa sarsii	P	1.134	Lebour, 1934
	Rissoa membranacea	P	1.000	Lebour, 1934
	Rissoa parva	P	1.247	Lebour, 1934
	Rissoa guerini	P	1.202	Lebour, 1934
Tornidae	*Tornus subcarinatus*	P	1.064	Lebour, 1936
Triviidae	*Trivia europa*	P	0.971	Lebour, 1931b
Trochidae	*Calliostoma granulatum*	NP	0.707	Ramón, 1990
	Margarites helicinus	NP	0.393	Holyoak, 1988
	Tegula funebratis	NP	0.566	Moran, 1997
Turritellidae	*Turritella communis*	P	1.022	Kennedy and Keegan, 1992
Turridae	*Haedropleura septangularis*	P	1.205	Lebour, 1936
	Philbertia (Comarmondia) gracilis	P	1.380	Lebour, 1993b
Vermetidae	*Dendropoma corrodens*	NP	0.612	Miloslavich and Penchaszadeh, 1992
	Vermetus sp.	NP	0.875	Miloslavich and Penchaszadeh, 1992
Siphonariidae	*Siphonaria serrata*	NP	0.731	Chambers and McQuaid, 1994
	Siphonaria concinna	P	0.996	Chambers and McQuaid, 1994
Trimusculidae	*Trimusculus conica*	NP	0.696	Haven, 1973

[1] P = planktotrophic; NP = nonplanktotrophic.

[2] Velar aspect ratio.

Hörstmann, 1956, for *Lymnaea stagnalis*). However, the presence of other potentially nutritive substances such as carbohydrates or lipids in the capsular fluid of *Littorina* has not been established.

Unlike the velum of species of *Littorina* with encapsulated, nonplanktonic development, the velum of planktotrophs does not appear to play a substantial role in the assimilation of intracapsular proteins. None of four plank-

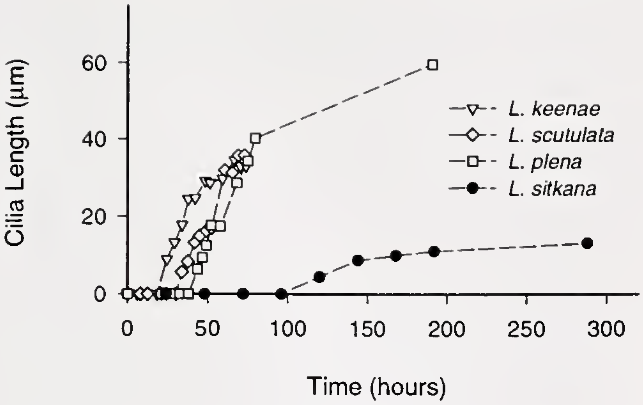

Figure 14. Lengths of the longest velar cilia over partial development of three planktotrophic (open symbols) *Littorina* and one *Littorina* with encapsulated, nonplanktonic development (filled circles). Cilia length units are micrometers and time units are hours, beginning at spawning of each species (time 0).

totrophic species exhibited localized affinity for FITC-BSA in the velum after larvae emerged from the egg envelope (pictured in Fig. 1). Preemergent larvae (still in the egg envelope) did not fluoresce after being soaked in FITC-BSA solutions, and one interpretation of these data is that larvae of planktotrophic species lack FITC-BSA affinity at this stage. A second possibility is that the egg envelope is not permeable to FITC-BSA, in which case preemergent larvae were never directly exposed to labeled protein. However, if the egg envelope is impermeable to large proteins, protein assimilation is certainly unlikely to be of nutritive importance to larvae contained in the very limited space within the egg envelope (see Fig. 1). Likewise, planktotrophs did not exhibit localized velar FITC-BSA affinity upon hatching from the egg envelope into the capsule space (when they would have access to any intracapsular protein) or after hatching from the egg capsule. Therefore, although at this point velar protein affinity cannot be conclusively ruled out for all stages of planktotrophic development, the velum of planktotrophs certainly does not function as a large assimilative surface for intracapsular proteins as it does in *Littorina* with encapsulated, nonplanktonic development.

Larvae of many planktotrophic marine invertebrate taxa have the ability to take up nutrients from seawater in the form of dissolved organic matter (DOM). Among molluscs, this ability has been demonstrated in bivalves (Manahan, 1983) and in the gastropod *Haliotis rufescens* (Jaeckle and Manahan, 1989). The primary site of DOM uptake in veliger larvae is the velum (Manahan and Crisp, 1983); however, because marine larvae take up DOM *via* carrier-mediated pathways (Wright and Manahan, 1989), this process is probably not homologous to velar protein uptake. Among gastropods, albumen is generally consumed by endocytosis (Elbers and Bluemink, 1960; Fioroni, 1977; Rivest, 1981; Rivest, 1992; Rivest and Strathmann, 1995).

Planktotrophy is the ancestral state in *Littorina*, so the presence of protein uptake by the larval epithelium of *Littorina* species with encapsulated, nonplanktonic development suggests that planktotrophic larvae may share a similar capability, although at a much lower level. The FITC-BSA assay used in this study and others (*e.g.*, Rivest, 1992; Rivest and Strathmann, 1995) may not be sufficiently sensitive to detect such low levels of protein endocytosis.

The evolutionary transition from planktotrophy to nonplanktotrophy is often accompanied by modifications to ancestral planktotrophic feeding characters (Strathmann, 1978). Such modifications have been viewed both as losses of complex structures that occur with the loss of planktotrophic larval feeding (Strathmann, 1978), and as novel features that enhance other aspects of nonfeeding larval performance (*e.g.*, swimming; Emlet, 1994). In gastropods, encapsulation of larvae is often associated with altered ciliary and velar morphology (Jägersten, 1972; Webber, 1977; Hadfield and Iaea, 1989). This study documents that compared to their planktotrophic congeners, veligers of *Littorina* with encapsulated, nonplanktonic development have shorter prototrochal cilia and cannot swim in seawater. Reductions in cilia length may be due to relaxation of selection for swimming and particle capture or, alternatively, to selection pressures associated with intracapsular development. Functions of prototrochal cilia in encapsulated larvae might include (1) rotating larvae to enhance oxygen diffusion through benthic, gelatinous egg masses (Hunter and Vogel, 1986; but see Strathmann and Strathmann, 1995), (2) feeding on nurse eggs (Lyons and Spight, 1973; Fioroni, 1988), or (3) stirring fluids to enhance feeding on intracapsular albumen. In the confined and more viscous environment of the egg capsule, short cilia may function better than long cilia in feeding on intracapsular nutrition or in rotating larvae.

The presence of recognizable planktotrophic larval feeding structures (such as the velum) in nonplanktotrophic species is commonly accepted as evidence of descent from a planktotrophic ancestor, and is one of many independent lines of evidence that support planktotrophy as the ancestral state in caenogastropods (Haszprunar *et al.*, 1995). Although various authors have remarked that encapsulated, nonplanktonic veligers have reduced velar lobes (*e.g.*, Jägersten, 1972; Webber, 1977; Rivest and Strathmann, 1995), possibly because the velum is no longer necessary for swimming and feeding (Jägersten, 1972), very few studies have addressed this issue in a comparative or quantitative context. The present study supports the general observation that during early development, gastropods with nonplanktotrophic development have smaller velar lobes than confamilial planktotrophs. Yet, degree of velar loss varies considerably: at one end of the range are species whose larvae never develop a velum (*e.g.*, Penchaszadeh and Rincón, 1996) and at the other are genera such as *Littorina* in which planktotrophs and nonplanktotrophs have velums that are proportionally equivalent in early development. Retention of the velum may be attributed to several causes, including morphogenetic or other developmental constraints and an evolutionarily recent loss of planktotrophy. However, the lack of a velum in some species (*e.g.*, Penchaszadeh and Rincón, 1996) argues that the presence of velar lobes may not be necessary for prosobranch morphogenesis, and the second hypothesis has yet to be tested in a comparative, historical context. A third possibility is that nonplanktotrophs that retain a large velum do so in part because the velum has been coopted to perform specific functions in the egg capsule, such as feeding on nurse eggs (*e.g.*, Fioroni and Sandmeier, 1964) or providing a respiratory surface (Fretter and Graham, 1962). In *Littorina* with encapsulated, nonplanktonic development the velum performs a third and previously undescribed function, assimilation of intracapsular albumen. A large velum may be an advantage because it provides a large surface for assimilation of capsule proteins.

In summary, the velum of *Littorina* species with encapsulated, nonplanktonic development is active in endocytotic albumen assimilation. In contrast, affinity for labeled albumen was not seen in the velum of planktotrophic *Littorina* species. This suggests that, since their loss of planktotrophy, the former species have undergone evolutionary changes that enhance assimilation of intracapsular nutrients. The feeding morphologies of *Littorina* veligers differ in some ways, depending on developmental mode: species with encapsulated, nonplanktonic development have prototrochal cilia that are much shorter and grow more slowly, and the larvae cannot swim when removed from the egg capsule. However, the velar apparatuses of two *Littorina* species with contrasting development are comparable in size during early development. A survey of prosobranch gastropods suggests a general trend towards reduction in the relative size of the velum in nonplanktotrophic species. The size of the velum of *Littorina* with encapsulated, nonplanktonic development may be retained in part because of the velum's role in assimilation of intracapsular proteins.

Acknowledgments

I thank E. Schabtach and T. Schroeder for invaluable and generous assistance with TEM; S. Balser, B. Bradshaw, R. Emlet, W. Jaeckle, P. Marko, E. Martins, A. Shanks, and four anonymous reviewers for valuable comments on methods and the manuscript; J. Carlton, M. Ryan, and N. Terwilliger for technical advice; B. Butler for help with reference material; and L. Crumrine and A. Kuzirian for providing biological specimens. I also thank the faculty and staff of the Oregon Institute of Marine Biology where this study was largely performed. This research was supported by grants from Sigma Xi and the Lerner-Gray Fund for Marine Research to A. Moran, by NSF Grant OCE-9416590 to R. Emlet, and by the Friday Harbor Laboratories.

Literature Cited

Bieler, R. 1992. Gastropod phylogeny and systematics. *Annu. Rev. Ecol. Syst.* **23:** 311–338.

Black, R., S. J. Turner, and M. S. Johnson. 1994. The early life history of *Bembicium vittatum* Philippi, 1846 (Gastropoda: Littorinidae). *Veliger* **37:** 393–399.

Buckland-Nicks, J., F.-S. Chia, and S. Behrens. 1973. Oviposition and development of two intertidal snails, *Littorina sitkana* and *Littorina scutulata*. *Can. J. Zool.* **51:** 359–365.

Cañete, J. I., and R. P. Ambler. 1992. Desarollo intracapsular del gastrópodo comestible *Calyptraea (Trochita) trochiformis* (Born, 1778), en Chile. *Rev. Chil. Hist. Nat.* **65:** 255–266.

Cather, J., and A. S. Tompa. 1972. The podocyst in pulmonate evolution. *Malacol. Rev.* **5:** 1–3.

Chambers, R. J., and C. D. McQuaid. 1994. Notes on the taxonomy, spawn and larval development of South African species of the intertidal limpet *Siphonaria* (Gastropoda, Pulmonata). *J. Molluscan Stud.* **60:** 263–275.

Chapman, G. 1965. The egg cocoons of *Scoloplos armiger* O. F. Müller. *Biol. Bull.* **128:** 189–197.

Clark, K. B., and K. R. Jensen. 1981. A comparison of egg size, capsule size and development patterns in the order Ascoglossa (Sacoglossa) (Mollusca: Opisthobranchia). *Int. J. Invertebr. Reprod.* **3:** 57–64.

Clark, K. B., M. Busacca, and H. Stirts. 1979. Nutritional aspects of development of the ascoglossan *Elysia cauze*. Pp. 11–24 in *Reproductive Ecology of Marine Invertebrates,* S. E. Stancyk, ed. University of Carolina Press, Columbia, SC.

da Silva, F. M., and A. C. Brown. 1985. Egg capsules and veligers of the whelk *Bullia digitalis* (Gastropoda: Nassariidae). *Veliger* **8:** 200–203.

De Mahieu, G., P. E. Penchaszadeh, and A. B. Casal. 1974. Algunos aspectos de las variaciones de proteínas y aminoácidos libres totales del líquido intracapsular en relación al desarollo embrionario en *Adelomelon brasiliana* (Lamarck, 1811) (Gastropoda, Prosobranchia, Volutidae). *Cah. Biol. Mar.* **15:** 215–227.

DiSalvo, L. H. 1988. Observations on the larval and post-metamorphic life of *Concholepas concholepas* (Brugière, 1789) in laboratory culture. *Veliger* **30:** 358–368.

Elbers, P. F., and J. G. Bluemink. 1960. Pinocytosis in the developing egg of *Limnaea stagnalis*. *Expt. Cell. Res.* **21:** 619–622.

Emlet, R. B. 1994. Body form and patterns of ciliation in nonfeeding larvae of echinoderms—functional solutions to swimming in the plankton. *Am. Zool.* **34:** 570–585.

Fioroni, P. 1977. On the peripheric resorption of albumen in gastropods and its significance for general embryology. *Zool. Jahrb., Abt. Anat. Ontog. Tiere* **98:** 181–202.

Fioroni, V. P. 1988. Die Prosbranchier-Entwicklung mit Nähreiern. *Zool. Anz.* **221:** 201–247.

Fioroni, V. P., and E. Sandmeier. 1964. Über eine neue Art der Nähreibewältigung bei Prosobranchierveligern. *Vie Milieu* (suppl.) 17.

Fretter, V., and A. Graham. 1962. *British Prosobranch Molluscs.* Ray Society, London.

Gallardo, C. S. 1979. Developmental patterns and adaptations for reproduction in *Nucella crassilabrum* and other muricacean gastropods. *Biol. Bull.* **157:** 453–463.

Gider, S., D. D. Awschalom, T. Douglas, S. Mann, and M. Chaparala. 1995. Classical and quantum magnetic phenomena in natural and artificial ferritin proteins. *Science* **268:** 77–79.

Hadfield, M. G., and D. K. Iaea. 1989. Velum of encapsulated veligers of *Petaloconchus* (Gastropoda), and the problem of re-evolution of planktotrophic larvae. *Bull. Mar. Sci.* **45:** 377–386.

Harasewych, M. G., S. L. Adamkewicz, J. A. Blake, D. Saudek, T. Spriggs, and C. J. Bult. 1997. Neogastropod phylogeny: a molecular perspective. *J. Molluscan Stud.* **63:** 327–351.

Haszprunar, G., L. v. Salvini-Plawen, and R. M. Rieger. 1995. Larval planktotrophy—a primitive trait in the Bilateria? *Acta Zool.* **76:** 141–154.

Haven, N. 1973. Reproduction, development and feeding of the Australian marine pulmonate, *Trimusculus (Gadina) conica. Veliger* **16:** 61–65.

Hawkins, L. E., and S. Hutchinson. 1988. Egg capsule structure and hatching mechanism of *Ocenebra erinacea* (L.) (Prosobranchia: Muricidae). *J. Exp. Mar. Biol. Ecol.* **119:** 269–283.

Holynak, A. R. 1988. Spawning, egg mass formation and larval development of the trochid gastropod *Margarites helicinus* (Fabricius). *Veliger* **31:** 111–112.

Hörstmann, H. J. 1956. Der Galktogengehalt der Eier von *Lymnaea stagnalis* L. während der Embryonalentwicklung. *Biochem. Z.* **328:** 342–347.

Hughes, R. N. 1990. Larval development of *Morum onuscus* (L.) (Gastropoda: Harpidae). *J. Molluscan Stud.* **56:** 1–8.

Hunter, T., and S. Vogel. 1986. Spinning embryos enhance diffusion through gelatinous egg masses. *J. Exp. Mar. Biol. Ecol.* **96:** 303–308.

Jablonski, D., and R. A. Lutz. 1983. Larval ecology of marine invertebrates: paleobiological implications. *Biol. Rev. Camb. Philos. Soc.* **58:** 21–89.

Jaeckle, W. B., and D. T. Manahan. 1989. Feeding by a "nonfeeding" larva: uptake of dissolved amino acids from seawater by lecithotrophic larvae of the gastropod *Haliotis rufescens. Mar. Biol.* **103:** 87–94.

Jägersten, G. 1972. *Evolution of the Metazoan Life Cycle.* Academic Press, New York. 282 pp.

Kennedy, J. J., and B. F. Keegan. 1992. The encapsular developmental sequence of the mesogastropod *Turritella communis* (Gastropoda: Turritellidae). *J. Mar. Biol. Assoc. UK* **72:** 783–805.

Lebour, M. V. 1931a. The larval stages of *Nassarius reticulatus* and *Nassarius incrassatus. J. Mar. Biol. Assoc. UK* **17:** 797–818.

Lebour, M. V. 1931b. The larval stages of *Trivia europa. J. Mar. Biol. Assoc. UK* **17:** 819–831.

Lebour, M. V. 1933a. The eggs and larvae of *Philbertia gracilis* (Montagu). *J. Mar. Biol. Assoc. UK* **18:** 507–510.

Lebour, M. V. 1993b. The life histories of *Cerithiopsis tubercularis* (Montagu), *C. barleei* Jeffreys and *Triphora perversa* (L.). *J. Mar. Biol. Assoc. UK* **18:** 491–506.

Lebour, M. V. 1934. Rissoid larvae as food of the young herring. The eggs and larvae of the Plymouth Rissoidae. *J. Mar. Biol. Assoc. UK* **19:** 523–539.

Lebour, M. V. 1936. Notes on the eggs and larvae of some Plymouth prosobranchs. *J. Mar. Biol. Assoc. UK* **20:** 547–565.

Lebour, M. V. 1937. The eggs and larvae of British prosobranchs with special reference to those living in the plankton. *J. Mar. Biol. Assoc. UK* **22:** 105–166.

Losse, G., and H. Greven. 1993. Structure, composition and permeability of the egg covering in the viviparous prosobranch gastropod *Littorina saxatilis. Invertebr. Reprod. Dev.* **24:** 225–235.

Lyons, A., and T. M. Spight. 1973. Diversity of feeding mechanisms among embryos of Pacific Northwest *Thais. Veliger* **16:** 189–194.

Main, K. L. 1974. The early development of two ovulid snails, *Simnia aequalis* and *Simnia barbarensis. Veliger* **24:** 252–258.

Manahan, D. T. 1983. The uptake and metabolism of dissolved organic amino acids by bivalve larvae. *Biol. Bull.* **164:** 236–250.

Manahan, D. T., and D. J. Crisp. 1983. Autoradiographic studies on the uptake of dissolved amino acids by bivalve larvae. *J. Mar. Biol. Assoc. UK* **63:** 673–682.

Martins, E. P., and T. F. Hansen. 1996. The statistical analysis of interspecific data: a review and evaluation of phylogenetic comparative methods. Pp. 22–75 in *Phylogenies and the Comparative Method in Animal Behavior*, E. P. Martins, ed. Oxford University Press, New York.

McEdward, L. R., and D. A. Janies. 1993. Life cycle evolution in asteroids: What is a larva? *Biol. Bull.* **184:** 255–268.

Miloslavich, P. 1996. Nurse-egg feeding prosobranchs: a comparative biochemical and electrophoretic analysis of eggs and hatchlings. *Am. Malacol. Bull.* **13:** 37–46.

Miloslavich, P., and P. E. Penchaszadeh. 1992. Reproductive biology of *Vermetus* sp. and *Dendropoma corrodens* (Orbigny, 1942): two vermetid gastropods from the southern Caribbean. *Veliger* **35:** 78–88.

Miloslavich, P., and P. E. Penchaszadeh. 1994. Spawn and larval development of *Engoniophos unicinctus* (Say, 1825) (Gastropoda: Prosobranchia) from the southern Caribbean Sea. *Veliger* **37:** 425–429.

Moran, A. L. 1997. Spawning and larval development of the black turban snail *Tegula funebralis* (Prosobranchia, Trochidae). *Mar. Biol.* **128:** 107–114.

Moritz, C. E. 1939. Organogenesis in *Crepdula adunca* Sowerby. *Univ. Calif. Publ. Zool.* **43:** 217–248.

Morrill, J. B. 1964. Protein content and dipeptidase activity of normal and cobalt-treated embryos of *Limnaea palustris. Acta Embryol. Morphol. Exp.* **7:** 131–142.

Morrill, J. B., R. W. Rubin, and M. Grandi. 1976. Protein synthesis and differentiation during pulmonate development. *Am. Zool.* **16:** 547–562.

Pearce, J. B., and G. T. Thorson. 1967. The feeding and reproductive biology of the red whelk, *Neptunea antiqua* (L.) (Gastropoda, Prosobranchia). *Ophelia* **4:** 277–314.

Pechenik, J. A. 1979. Role of encapsulation in invertebrate life histories. *Am. Nat.* **114:** 859–870.

Pechenik, J. A. 1984. Egg capsules of *Nucella lapillus* protect against low-salinity stress. *J. Exp. Mar. Biol. Ecol.* **63:** 195–208.

Pechenik, J. A., S. C. Chang, and A. Lord. 1984. Encapsulated development of the marine prosobranch gastropod *Nucella lapillus. Mar. Biol.* **78:** 223–229.

Penchaszadeh, P. E., and A. Rincón. 1996. Egg capsules and development of *Prunum prunum* (Gmelin, 1791) (Prosobranchia: Marginellidae) from the Venezuelan Caribbean. *Veliger* **39:** 83–86.

Perron, F. E. 1981. The partitioning of reproductive energy between ova and protective capsules in marine gastropods of the genus *Conus. Am. Nat.* **118:** 110–118.

Ponder, W. F., and D. R. Lindberg. 1996. Gastropod phylogeny—challenges for the 90s. Pp. 135–154 in *Origin and Evolutionary Radiation of the Mollusca*, J. Taylor, ed. Oxford University Press, Oxford.

Ponder, W. F., and D. R. Lindberg. 1997. Towards a phylogeny of gastropod molluscs—an analysis using morphological characters. *Zool. J. Linn. Soc.* **119:** 83–265.

Portmann, A. 1955. La métamorphosis "abritée" de *Fusus* (Gast., Prosobranchs). *Rev. Suisse Zool.* **62:** 236–252.

Portmann, A., and E. Sandmeier. 1965. Die Entwicklung von Vorderdarm, Macromeren und Enddarm unter dem Einfluss von Nähreiern bei *Buccinum, Murex* und *Nucella* (Gastropoda, Prosobranchia). *Rev. Suisse Zool.* **72:** 187–204.

Ramón, M. 1990. Spawning and development of *Calliostoma granulatum* in the Mediterranean Sea. *J. Mar. Biol. Assoc. UK* **70:** 321–328.

Rasmussen, E. 1951. Faunistic and biological notes on marine invertebrates II. The eggs and larvae of some Danish marine gastropods. *Vidensk. Medd. Naturhist. Foren.* **113:** 201–249.

Raven, C. P. 1958. *Morphogenesis: The Analysis of Molluscan Development.* Pergamon Press, London.

Raven, C. P. 1972. Chemical embryology of Mollusca. Pp. 155–185 in

Chemical Zoology, Vol VII: Mollusca. M. Florkin and B. T. Scheer, eds. Academic Press, New York.

Rawlings, T. A. 1990. Associations between egg capsule morphology and predation among populations of the marine gastropod, *Nucella emarginata. Biol. Bull.* **179:** 312–325.

Rawlings, T. A. 1996. Shields against ultraviolet radiation—an additional protective role for the egg capsules of benthic marine gastropods. *Mar. Ecol. Prog. Ser.* **136:** 81–95.

Reid, D. G. 1989. The comparative morphology, phylogeny and evolution of the gastropod family Littorinidae. *Philos. Trans. R. Soc. Lond. B* **324:** 1–110.

Reid, D. G., E. Rumbak, and R. H. Thomas. 1996. DNA, morphology and fossils: phylogeny and evolutionary rates of the gastropod genus *Littorina. Philos. Trans. R. Soc. Lond. B* **351:** 877–895.

Reynolds, E. S. 1963. The use of lead citrate at high pH as an electron-opaque stain in electron microscopy. *J. Cell Biol.* **17:** 208–211.

Riedel, F. 1992. A re-evaluation of the ontogeny of *Cabestana spengleri* (Perry, 1811) (Gastropoda: Tonnoidea: Ranellidae). *Veliger* **35:** 111–121.

Rivest, B. R. 1981. Nurse egg consumption and the uptake of albumen in the embryonic nutrition of marine snails. Ph.D. dissertation, University of Washington, Seattle.

Rivest, B. R. 1983. Development and the influence of nurse egg allotment on hatching size in *Searlesia dira* (Reeve, 1846) (Prosobranchia, Buccinidae). *J. Exp. Mar. Biol. Ecol.* **69:** 217–241.

Rivest, B. R. 1992. Studies on the structure and function of the larval kidney complex of prosobranch gastropods. *Biol. Bull.* **182:** 305–325.

Rivest, B. R., and R. R. Strathmann. 1995. Uptake of protein by an independently evolved transitory cell complex in encapsulated embryos of neritoidean gastropods. Pp. 166–176 in *Reproduction and Development of Marine Invertebrates,* W. H. Wilson, S. A. Strickler, and G. L. Shinn, eds. Johns Hopkins University Press, Baltimore, MD.

Rumbak, E., D. G. Reid, and R. H. Thomas. 1994. Reconstruction of phylogeny of 11 species of *Littorina* (Gastropoda, Littorinidae) using mitochondrial DNA sequence data. *Nautilus* **108 (Suppl. 2):** 91–97.

Shuto, T. 1974. Larval ecology of prosobranch gastropods and its bearing on biogeography and paleontology. *Lethaia* **7:** 39–256.

Soliman, G. N. 1991. A comparative review of the spawning, development and metamorphosis of prosobranch and opisthobranch gastropods with special reference to those from the northwestern Red Sea. *Malacologia* **32:** 257–272.

Spight, T. M. 1977. Do intertidal snails spawn in the right places? *Evolution* **31:** 682–691.

Stöckman-Bosbach, R., and J. Althoff. 1989. A correlated morphological and biochemical study of capsular fluid of *Nucella lapillus* (Gastropoda: Prosobranchia: Muricidae). *Mar. Biol.* **102:** 283–289.

Strathmann, R. R. 1978. The evolution and loss of feeding larval stages in marine invertebrates. *Evolution* **32:** 894–906.

Strathmann, R. R. 1985. Feeding and non-feeding larval development and life-history evolution in marine invertebrates. *Annu. Rev. Ecol. Syst.* **16:** 339–361.

Strathmann, R. R., and E. Leise. 1979. On feeding mechanisms and clearance rates of molluscan veligers. *Biol. Bull.* **157:** 524–535.

Strathmann, R. R., and M. F. Strathmann. 1995. Oxygen supply and limits on aggregation of embryos. *J. Mar. Biol. Assoc. UK* **75:** 413–428.

Taylor, H. H. 1983. The ionic properties of the capsular fluid bathing embryos of *Lymnaea stagnalis* and *Biomphalaria sudanica* (Mollusca: Pulmonata). *J. Exp. Biol.* **59:** 543–564.

Thorson, G. 1946. Reproduction and larval development of Danish marine bottom invertebrates. *Medd. Komm. Dan. Fisk-og. Havunders, Ser. Plankton* **4:** 1–52.

Webber, H. H. 1977. Gastropoda: Prosobranchia. Pp. 1–97 (Chap. 1) in *Reproduction of Marine Invertebrates,* Vol. IV, A. C. Giese and J. S. Pearse, eds. Academic Press, New York. 369 pp.

Wells, H. W., and M. J. Wells. 1962. The distinction between *Acteucina candei* and *Retusa canaliculata. Nautilus* **75:** 87–93.

White, M. E., C. L. Kitting, and E. N. Powell. 1985. Aspects of reproduction, larval development, and morphometrics in the pyramidellid *Boonea impressa* (= *Odostomia impressa*) (Gastropoda: Opisthobranchia). *Veliger* **28:** 37–51.

Wright, S. H., and D. T. Manahan. 1989. Integumental nutrient uptake by aquatic organisms. *Annu. Rev. Physiol.* **51:** 585–600.

Reference: *Biol. Bull.* **196:** 245–256. (June 1999)

Development, Temperature Tolerance, and Settlement Preference of Embryos and Larvae of the Articulate Brachiopod *Laqueus californianus*

J. TIMOTHY PENNINGTON*, MARIO N. TAMBURRI, AND JAMES P. BARRY

Monterey Bay Aquarium Research Institute, 7700 Sandholdt Road, Moss Landing, California 95039

Abstract. Populations of the articulate brachiopod *Laqueus californianus* occur in dense single-species aggregations near the continental shelf/slope break (100-200 m) in Monterey Bay, California. The development of embryos and larvae of *L. californianus* has been examined by scanning electron microscopy. Fertilizable eggs are 130-140 μm in diameter, and sperm are unmodified. Cleavage is holoblastic and radial. At 10°C an up-swimming blastula develops by 18-h, and gastrulation occurs within 24-38 h. The embryo elongates on a new larval axis and the blastopore closes by 72 h. A trilobed articulate brachiopod larva forms by day 3-4, and a metamorphically competent larva with attachment disk is attained in 7 days. Competent larvae swim downwards.

Effects of temperature on larval survival and development rate have also been examined. Larvae die within 1 day at 25°C. At 20°C, development appears normal but results in spontaneous abnormal settlement of larvae 5-6 days old. At 15°, 10°, and 5°C, most larvae achieve competence in 5, 7, and 9 days, respectively. Many larvae survive for 71 days at 10° and 15°C.

Patterns of larval settlement vary among substrates, but larvae show strong preference for shells of living conspecific adults. Settlement and metamorphosis can occur within 24 h upon exposure of larvae to substrate.

Introduction

The Brachiopoda compose a major part of the fossil record (~30,000 described species), yet the biology of extant brachiopods (~280 species) is understood poorly relative to that of other macrofaunal invertebrates (Rudwick, 1970; James *et al.*, 1992). This lack of knowledge exists in part because brachiopods often inhabit cryptic or inaccessible habitats and are rarely conspicuous members of communities that attract the attention of zoologists and ecologists. The dense communities of epifaunal brachiopods that dominated level-bottom, shallow-water habitats prior to the Permo-Triassic extinction are largely absent from recent seas (reviewed by Thayer, 1986; Rudwick, 1970), and numerous attempts have been made to explain this shift in abundance and diversity (Stanley, 1977; Vermeij, 1977; Gould and Calloway, 1980; Gilmour, 1981; Thayer, 1981, 1985, 1986; Valentine and Jablonski, 1983a; Law and Thayer, 1991; Rhodes and Thayer, 1991; Thayer and Allmon, 1991; Rhodes and Thompson, 1993). The present-day Brachiopoda are typically regarded as a relic phylum, with extant species living in relic or marginal habitats (James *et al.*, 1992; Rhodes and Thompson, 1993).

A striking exception to this pattern occurs in Monterey Bay, California, where populations of the articulate brachiopod *Laqueus californianus* (Koch 1848, Terebratellacea) are found as dense epifaunal 'beds' at the outer margin of the continental shelf (100-200 m; Fig. 1A-B). These aggregations occur near rock outcrops associated with the San Gregorio fault zone, but the brachiopods are also abundant on nearby mud bottoms where individuals are attached to both living and dead shells of conspecifics (Fig. 1C). Research on *L. californianus* is limited, and little information is available concerning its reproductive biology.

This paper presents (1) a description of *L. californianus* embryos and larvae as examined by scanning electron microscopy (SEM), (2) data from assays of the effects of temperature on larval survival and development rate, and (3) results of experiments on substrate preference during larval settlement. The work constitutes part of an ongoing investigation of the biology and community ecology of the *L.*

Received 29 October 1998; accepted 19 February 1999.

* E-mail: peti@mbari.org

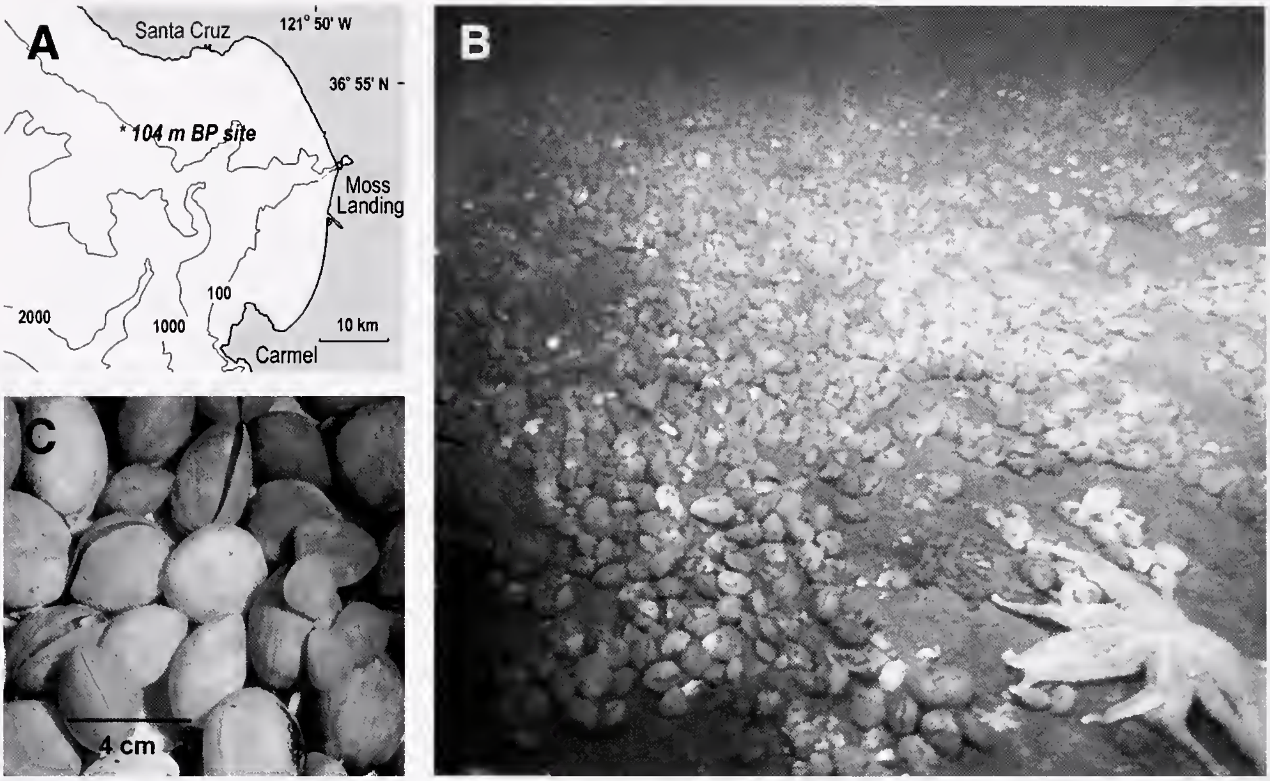

Figure 1. Collection site and habitat of *Laqueus californianus.* (A) Map of Monterey Bay, Monterey Submarine Canyon, and continental shelf and slope in central California. Contours in meters; the shelf/slope break is ~120 m deep. Brachiopods were collected from beds at 104 m in northern Monterey Bay ('104 m BP site'). (B) Submarine view of the 104 m BP site. All brachiopods are *L. californianus;* the asteroid is *Rathbunaster californicus* and is ~35 cm in diameter. Brachiopods occur on rock or nearby as beds extending over soft substrate; individual aggregations range from $<1/m^2$ to $\sim 100/m^2$. (C) Detail of an aggregation similar to that in B. Small brachiopods are commonly attached to larger individuals.

californianus beds in Monterey Bay—assemblages that are reminiscent of the fossil brachiopod 'reefs' described in the paleontological literature.

Materials and Methods

Collection

Adult *Laqueus californianus* were collected at a depth of 104 m by the R/V *Point Lobos* and the remotely operated vehicle (ROV) *Ventana* at the head of Cabrillo Canyon at the continental shelf/slope break in northern Monterey Bay, California (Fig. 1A). Collections were obtained with a suction sampler because most animals were attached to living or dead brachiopod shells (Fig. 1B) and were readily dislodged from the seafloor. Upon recovery of the ROV, brachiopods were placed in coolers and transported to the Monterey Bay Aquarium Research Institute (MBARI) at Moss Landing, California (Fig. 1A), and placed in a recirculating seawater system at 10°C. Adults are hardy and have been held unfed for many months prior to use in embryological work.

Gametes and rearing

Culture methods were adapted from those in Reed (1987) as developed by Long (1964) for other articulate brachiopods. All embryological and larval work was performed in filtered (5 μm) seawater obtained from surface waters in mid-Monterey Bay; embryos and larvae did not survive in recirculated seawater.

Oocytes were obtained by pressing and washing dissected ovaries through 0.5-mm nylon mesh. Oocyte suspensions were washed several times in seawater and allowed to stand overnight to undergo germinal vesicle breakdown and to shed follicle cells prior to fertilization. Sperm were stripped from testes as above and induced to swim by addition of 0.5 *M* Trisma base buffer solution to the sperm suspension (20% Trisma base:sperm suspension; pH 9; 5-30 min). Once sperm were verified motile under the microscope, oocytes were fertilized by adding ~1% by volume of faintly milky sperm suspension. Excess sperm was washed from cultures after 30 min.

Embryos and larvae were cultured in unstirred glass beakers or gallon jars at densities of 1-10 larvae/ml. Seawater was changed daily for the first 3 days and every other day thereafter. After one day, healthy up-swimming embryos were decanted from unfertilized eggs and poorly swimming embryos at the bottom of culture vessels.

Microscopy

Aliquots of gametes, embryos, larvae, and juveniles were examined with an ISI WB-6 scanning electron microscope at 10 Kv. The samples were prepared using Karnovsky's fixative (Gold, 1976), postfixation in 1% seawater-buffered osmium, dehydration though an acetone series, critical point drying, and sputter coating with gold/palladium.

Temperature effects

Two experiments were conducted to determine survivorship and development rate as a function of temperature. Survival of larvae as a function of temperature was evaluated in assays exposing 2-day-old gastrulae to five temperatures. Capped vials containing embryos were placed in water baths at 5°, 10°, 15°, 20°, and 25°C, ±0.5°C (three replicate vials for each temperature, each vial containing 10 gastrulae and 10 ml of filtered seawater). Surviving larvae were counted daily. To minimize handling errors, culture water was not changed. The effect of temperature on development rate of larvae was assessed by rearing several hundred 2-day-old gastrulae in beakers held at the above temperatures. These larvae were scored daily for developmental stage, behavior, and general health, but were not counted. Culture water in these beakers was changed every other day.

Settlement substrate preference

Two experiments were performed to evaluate the settlement preferences of competent larvae. One experiment provided eight settlement substrates to larvae: (1) carbonate rock, (2) frosted microscope slide, (3) unidentified sedimentary rock collected from the Monterey Submarine Canyon, (4) clam shell (*Tresus nuttallii*), (5) dead, air-dried (>1 month) *L. californianus* shell, (6) dead, air-dried *L. californianus* pedicle, (7) dead, air-dried *L. californianus* shell subsequently "conditioned" in seawater for several days prior to the experiment, and (8) small (~1 cm length) live *L. californianus*. Shells in treatment (7) presumably developed a living microflora during conditioning. In this experiment, 150 competent larvae (7 days old; 10°C culture) were pipetted into each of forty 20-ml polyethylene wells. Potential settlement substrates were added to each well (~1 cm^2 exposed surface area each; five replicate wells/substrate type), and the wells placed on a shaker table (25 rpm) in a dark 10°C cold room. Larvae attached to the substrates were counted after 3 days.

A second experiment was conducted to replicate portions of the above experiment and to assess the effect of rugosity (grooves; *cf.* Wisely, 1969) and surface-bound conspecific chemical cues in larval substrate preference. Treatments in this experiment included conditioned substrates (as described above) and substrates "painted" with brachiopod extract. Painted substrates were coated five times with a solvent extract of whole *L. californianus* (five adult *L. californianus* extracted in 300 ml 100% acetone for 1 month) and allowed to air-dry > 1 week before use. Substrate treatments were (1) no substrate added, (2) painted rugose cockle shell (*Clinocardium nuttallii*), (3) unpainted rugose cockle shell, (4) painted smooth clam shell (*Tresus nuttallii*), (5) unpainted smooth clam shell, (6) painted frosted microscope slide, (7) unpainted frosted microscope slide, (8) painted smooth microscope slide, (9) unpainted smooth microscope slide, (10) conditioned smooth microscope slide, (11) conditioned rugose cockle shell, (12) dead air-dried bryozoan test (*Membranipora membranacea*), (13) dead air-dried *L. californianus* pedicle, and (14) living *L. californianus*. Thirty competent larvae (7 day-old; 10°C culture) were counted into each of forty-two 10-ml polystyrene wells. Substrates were added (three wells for each substrate type), and the wells were held in the coldroom for 24 h, after which any settled larvae were counted.

Counts in each experiment were square-root transformed to satisfy assumptions of normality and equal variance, and subsequently analyzed by ANOVA and Bonferroni *t*-tests (SigmaStat). Data from treatments in which no larvae settled were lumped into one group; because assumptions of normality and variance could not be satisfied, these data were analyzed by nonparametric ANOVA and Dunn's test (SigmaStat).

Results

Obtaining gametes

Gonads were almost always present in animals >20-25 mm in length (maximum size is ~45 mm long). Sex was not distinguishable externally, but was noted for 67 dissected adults. Of these, 44% were female, which is not significantly different than 50% (Z-test, $P = 0.4$). No hermaphroditism or brooding was observed. Season of reproduction remains uncertain since collections have been sporadic and few ($n = 5$). Both ovaries and testes typically appear plump following collection. Testes almost always contain at least some mature spermatozoa, and ovaries some full-size oocytes. However, oocytes from none of the field collections were immediately fertilizable, but matured when held several months in the laboratory. The most successful larval cultures were obtained in spring.

Fertilizable oocytes were 130-140 μm in diameter and surrounded by follicle cells (Fig. 2A). In such oocytes the

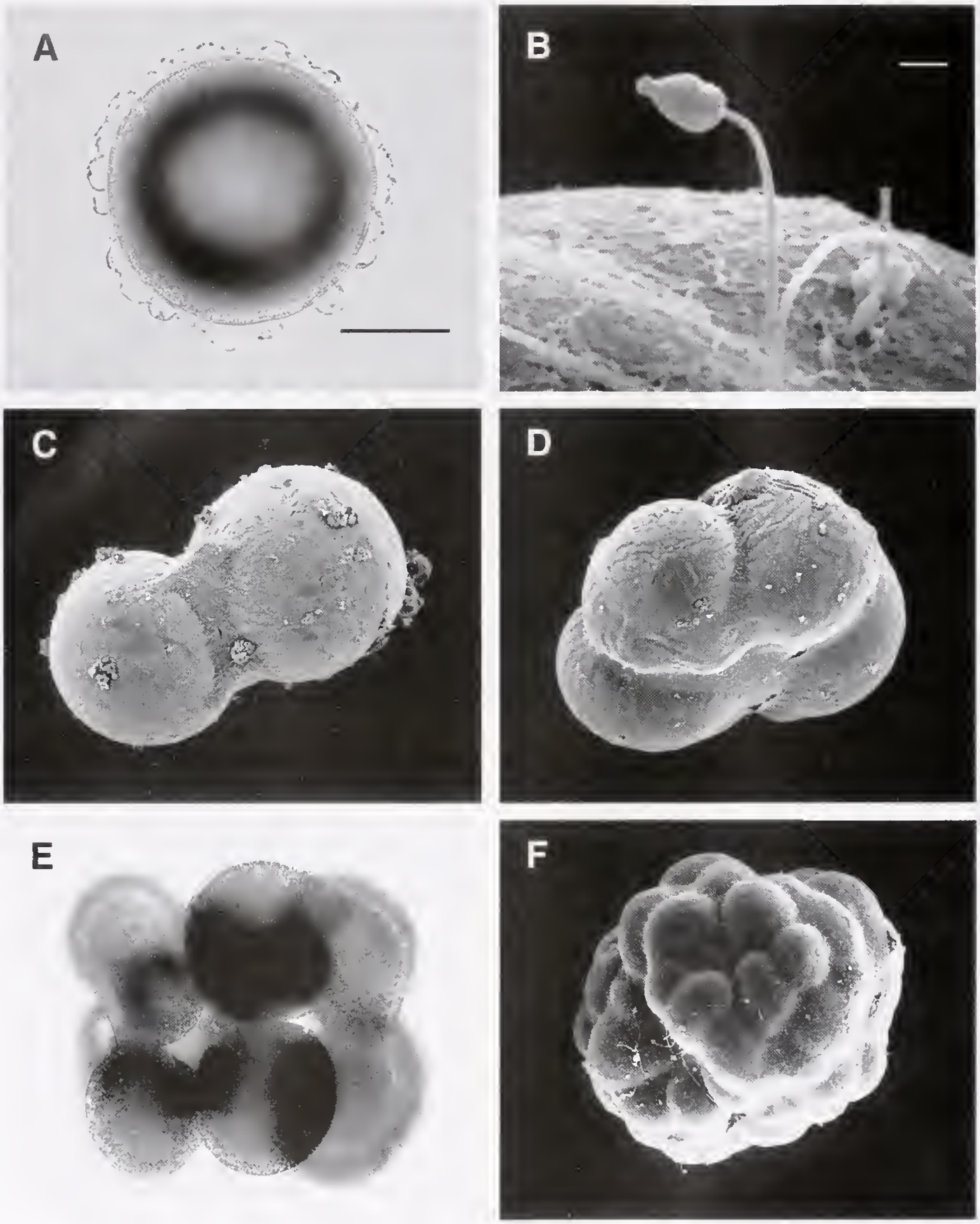

Figure 2. Early development of *Laqueus californianus.* (A) Freshly stripped oocyte. Light area in center is the germinal vesicle (nucleus) obscured by yolk; follicle cells at the periphery of oocyte slough off prior to fertilization. Scale bar, 50 μm. (B) Spermatozoan on embryo surface. Scale bar, 1 μm. (C) Two-cell embryo, with prominent extracellular membrane and a few follicle cells. Polar bodies not apparent. Scale as in A. (D) Four-cell stage. Scale as in A. (E) Eight-cell stage, showing radial arrangement of blastomeres. Small blastomere in upper left is probably abnormal. Scale as in A. (F) Late cleavage, with overlying blastomeres apparently pressed by egg membrane into furrows between cells beneath. Scale as in A.

germinal vesicle (visible as a translucent area in the salmon-colored egg cytoplasm; Fig. 2A; see Stricker and Folsom, 1997) disappeared overnight, as did follicle cells. Unfertilizable immature oocytes were more firmly attached to the ovary and when stripped were usually recognizable by a large surface dimple that probably marks the site of attachment to the ovarian wall.

Sperm heads and midpiece together are 2 μm long with head and midpiece visible (Fig. 2B); their tails are 40-45 μm long.

Development

Embryos. A developmental schedule for *L. californianus* at 10°C is presented in Table I. Cleavage is holoblastic, equal, and radial (Fig. 2C-E). First cleavage occurs at 3 h post-fertilization, and subsequent cleavages follow at 1-h intervals until cell counts become problematic after the fourth cleavage. Polar bodies were looked for but not recognized (*cf.* Freeman, 1993a). A thick egg membrane (~2 μm; visible in Fig. 2A, C, E) appears to press blastomeres into the furrows of underlying cells in later cleavage stages (Fig. 2F).

A hollow blastula forms by 12 h (Fig. 3A) and becomes ciliated by 18 h post-fertilization. Over the next several hours, embryos swim to the surface of cultures, spiraling with a clockwise rotation (anterior view). Blastulae occasionally stop swimming when they contact the water surface. Over 20-34 h, embryos gastrulate. The blastopore opens widely at the posterior, as defined by direction of swimming (Fig. 3B-C). By 48 h, embryos flatten and elongate ("wedge" embryos; Fig. 3D-E) and the swimming axis shifts such that, relative to swimming direction (arrows in Fig. 3B, D-F), the blastopore becomes ventrolateral. At this time an apical tuft of cilia appears (Fig. 3D, but not visible in Fig. 3E-F) on the thicker and new anterior end of the wedge embryo. During this time the blastopore also elongates and begins to fill with cells (Fig. 3D) from the posterior forwards. By 72 h the blastopore is closed.

Larvae. From 80-96 h (day 3-4) the swimming embryos differentiate into larvae 150 μm long, with apical, mantle, and pedicle lobes (Figs. 3F, 4A). The apical tuft is prominent (Fig. 4A), and dorsal and ventrolateral pairs of setal bundles develop from the posterior margin of the mantle lobe (Fig. 4C). The mantle lobe is ciliated sparsely, but ciliation of the apical and pedicle lobes remains uniform. From 96-128 h (day 4-5; Fig. 4B) the setae lengthen, ciliation is lost from the pedicle lobe, and cilia at the margin of the apical lobe form a well-defined locomotory band. Viewed from anterior, swimming larvae rotate slowly clockwise while metachronal waves pass counterclockwise through cilia of the locomotory band. As viewed through a dissecting microscope in culture bowls, larvae swim ~1 mm/s. They remain near the surface, and if disturbed can stop swimming, spread their setae, and sink; they do not swim backwards. Side, top, or bottom illumination produces no obvious photobehavior, and no pigment or eyespots are visible by light microscopy or SEM. Near the end of this period (120-128 h; day 5), the apical tuft disappears (Fig. 4B). By 145 h (day 6), the pedicle lobe begins to appear conical, and the ventral side of the mantle lobe begins to grow posteriorly to partially cover the pedicle lobe. At this time a small percentage of larvae begin to swim downwards, and many display distinctive, apparently muscular lateral flexions of the apical lobe while swimming. By 168 h (day 7; Fig. 4D-E), the ventral margin of the mantle lobe has become extended as a prominent skirt partly covering the pedicle lobe, a posteriorly directed ventral band of cilia develops on the mantle lobe, and a concave depression (the "attachment disk") forms at the terminus of the pedicle lobe (Fig. 4E). Most larvae leave the surface of cultures by 168 h and are found swimming obliquely downwards at the bottom of culture bowls. Such larvae swim, without rotating, and press the anteroventral surface of the apical lobe against the substrate. We used the presence of an attachment disk (Fig. 4E) to indicate metamorphic competence in the temperature and settlement substrate preference experiments described below.

Table I

Developmental schedule of Laqueus californianus *at 10°C.*

Hour (Day)	Event	Hour (Day)	Event
0 (0)	Insemination	48 (2)	Wedge larva; apical tuft; blastopore elongating
3 (0)	1st cleavage (2-cell)		
4 (0)	2nd cleavage (4-cell)	72 (3)	Blastopore closed
5 (0)	3rd cleavage (8-cell)	80 (3)	Lobe differentiation begins; setae appear
6 (0)	4th cleavage (16-cell)		
12 (0)	Unciliated blastula	96 (4)	Early trilobed larva
18 (0)	Ciliated blastula; upswimming begins	128 (5)	Full trilobed larva; apical tuft lost
26 (1)	Gastrulation begins	154 (6)	Pedicle lobe conical; some downswimming
34 (1)	Gastrula; large open blastopore	168 (7)	Competent larva; attachment disk complete; downswimming

Metamorphosis. Several hundred larvae successfully metamorphosed in culture, although most did not settle. Many larvae also underwent abnormal or incomplete metamorphoses. Complete metamorphosis includes cementation of the pedicle lobe attachment disk to the substrate, reversal of the mantle lobe anteriorly (Fig. 5A) so that it encloses the apical lobe (Fig. 5B), and growth of adult shell valves on the now exterior surfaces of the mantle lobe (Fig. 5B). Metamorphosis of individual larvae has not been directly followed but occurs within 24 h of addition of appropriate substrate. Larval setae are not shed immediately. Juveniles that metamorphosed normally have survived to 115 days in culture, reaching a shell diameter of ~400 μm before death.

Temperature

In an assay of survival over a range of temperature (results not figured), no embryos or larvae survived 1 day at 25°C; about 15% survived to day 7 at 20° and 15°C, when

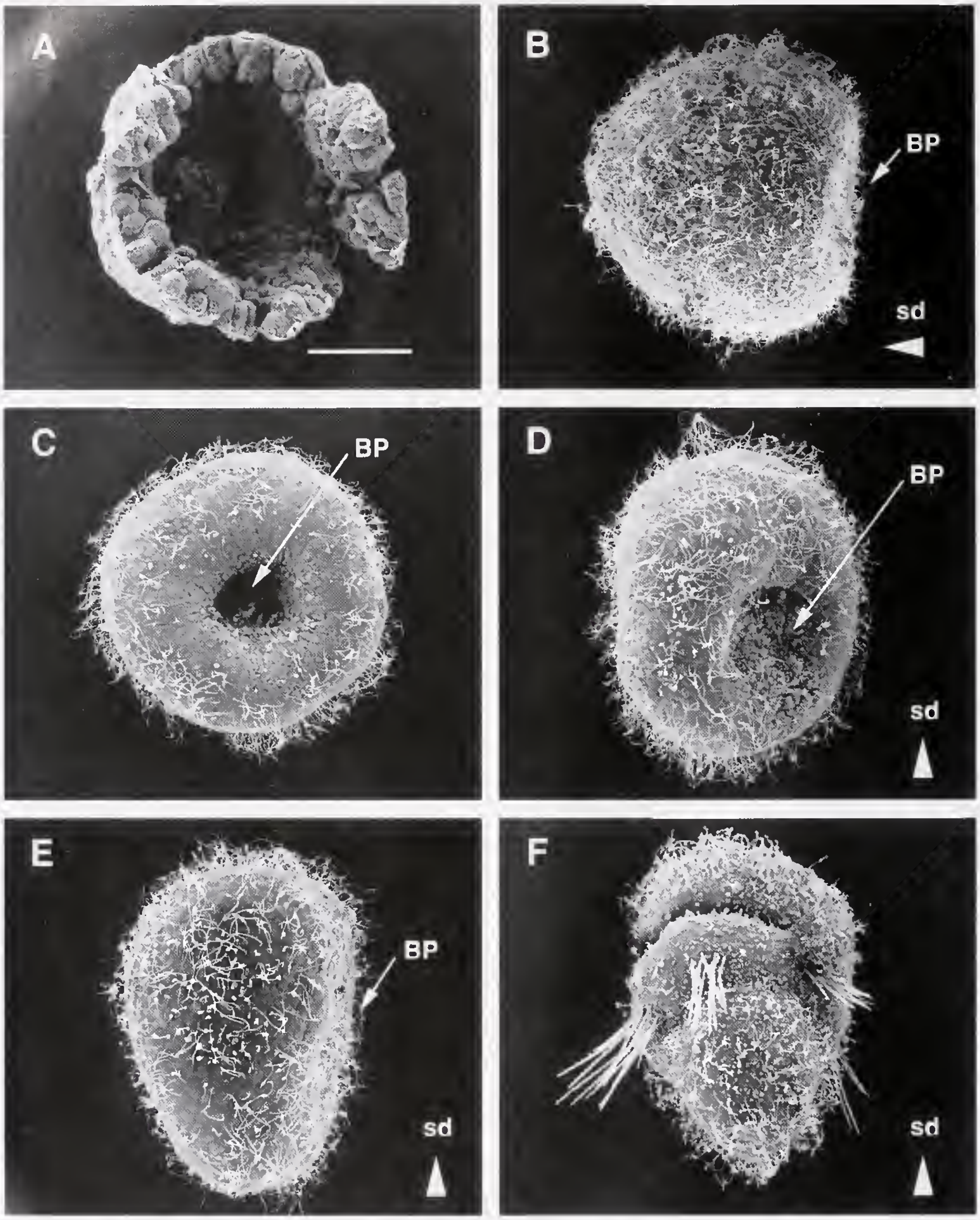

Figure 3. Late embryos and early larva of *Laqueus californianus*. (A) Broken 18-h-old blastula. Blastomeres are rounded, not yet ciliated, and ~1 layer thick beneath the egg membrane. Blastocoel is spacious and hollow. Scale bar, 50 μm; A-F to same scale. (B-C) Lateral and posterior views of 34-h-old gastrulae. Embryos are ciliated and swim to the surface of cultures with blastopore ('BP') trailing (arrows 'sd' indicate swimming direction). Blastopore open to archenteron. (D-E) Oblique ventral and lateral views of 48-h-old 'wedge' embryos. Blastopore fills with cells and closes by the first larval stage. Swimming direction changes (arrows 'sd') such that the blastopore becomes ventrolateral. An apical tuft develops (visible in D but not E-F) at the new anterior of the embryo. (F) Dorsolateral view of 80-h-old (3-day) early larva, with apical (top), mantle (middle), and pedicle (bottom) lobes differentiating. Pair of short dorsal setal bundles in foreground, and longer ventrolateral bundles to left and behind larva. Mantle lobe unciliated.

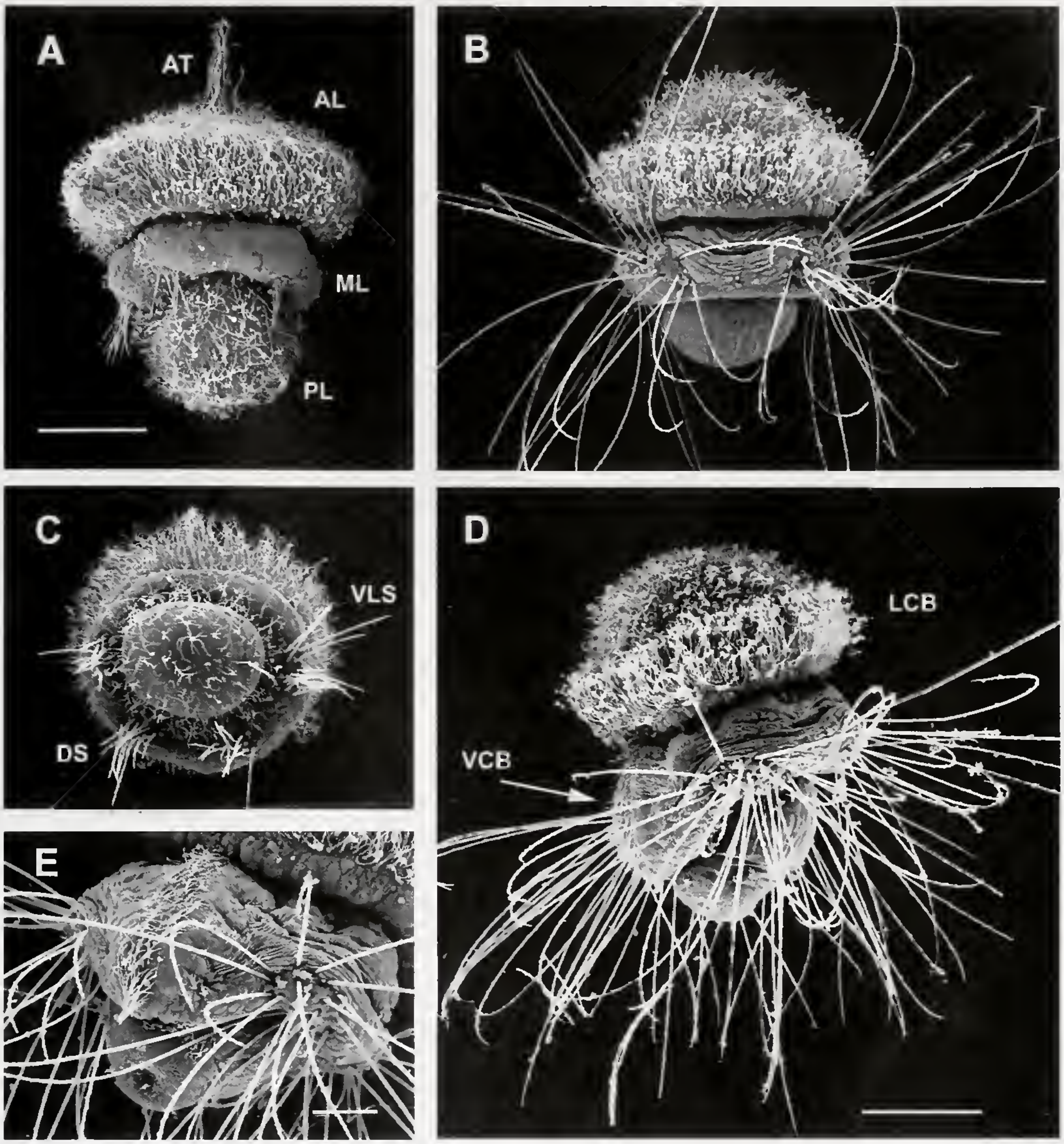

Figure 4. Larvae of *Laqueus californianus*. (A) Dorsal view of 96-h-old early larva. Apical lobe ('AL') uniformly ciliated except for prominent apical tuft ('AT'), mantle lobe ('ML') unciliated with short dorsal setal bundles and the left ventrolateral bundle visible, and pedicle lobe ('PL') rounded and ciliated. Scale bar, 50 μm. (B) Dorsal view of 128-h-old larva. Band of locomotory cilia differentiating on margins of apical lobe; the balls at tips of many cilia are probably fixation artifacts. Apical tuft cilia are present at this stage but not preserved on this specimen. Setae of mantle lobe erected, as when swimming larva is disturbed. Pedicle lobe has lost its cilia but is still rounded. Scale as in A. (C) Posterior view of 4-day-old early larva as in A. Pedicle lobe rounded and sparsely ciliated, ventrolateral ('VLS') and dorsal ('DS') setal bundles pairs on mantle lobe, and cilia on apical lobe. Scale as in A. (D) Lateral view of 168-h-old metamorphically competent larva. Locomotory ciliated band ('LCB') on apical lobe; the apical tuft of cilia is absent in competent larvae. Ventral ciliated band ('VCB') now present on mantle lobe. Pedicle lobe partially enclosed by mantle lobe; the attachment disk has formed on its distal tip. Scale bar, 45 μm. (E) Oblique ventral view of mantle and pedicle lobes of competent larva, showing ventral ciliated band and attachment disk. Scale bar, 20 μm.

these treatments were terminated; and about 80% of embryos or larvae held at 10° and 5°C survived to day 11 of the experiment. Most mortality occurred in the first 24-48 h, suggesting that either (a) late embryos (gastrulae and wedge embryos) were more sensitive to higher temperatures than larvae, or (b) lack of water changes produced the observed mortality at higher temperatures.

In a second assay, development rate increased with tem-

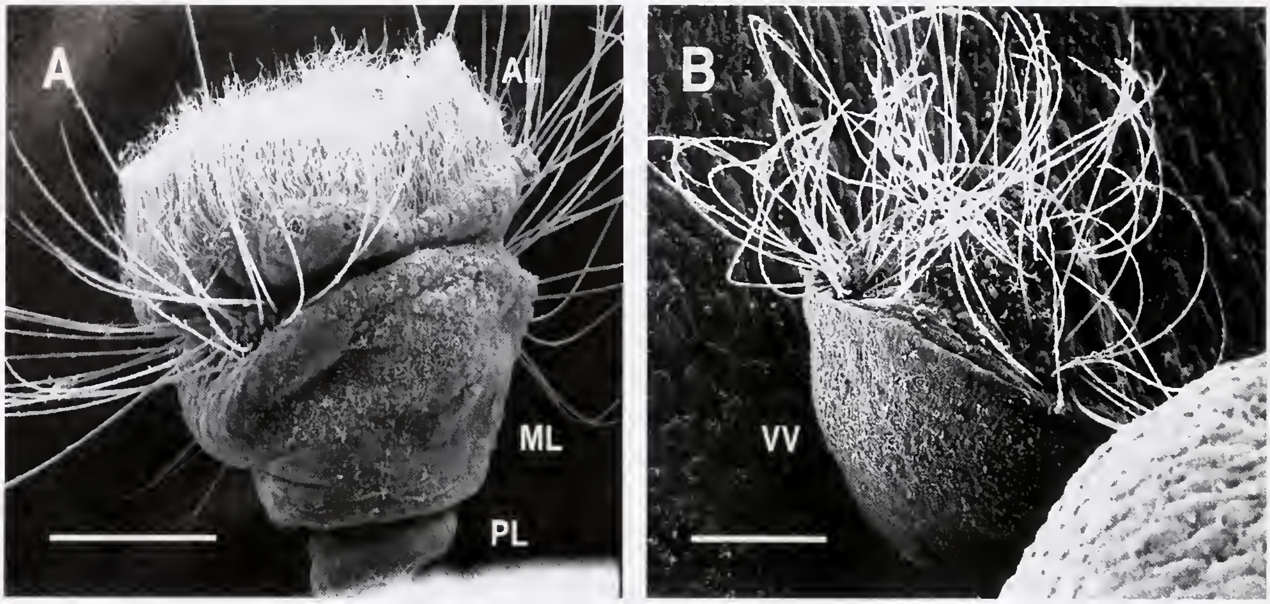

Figure 5. Metamorphosis of *Laqueus californianus.* (A) Larva undergoing mantle reversal in the first stages of metamorphosis. Mantle lobe ('ML') is beginning reversal to enclose the apical lobe ('AL'). 'PL' = pedicle lobe; scale bar, 50 μm. (B) Normal metamorphosis. Mantle reversal complete and apical lobe enclosed; shell valves secreted; 'VV' = ventral valve; scale bar, 50 μm.

perature within survival limits (Table II). Embryos held at 25°C did not develop and swam near the bottom of dishes on day 1 of the experiment. All were dead by day 2. Embryos moved from 25° to 10°C on day 1 survived for several days but did not develop. At 20°C, embryos developed into early larvae by day 1 but swam abnormally at the bottom of dishes, and by day 2 appeared competent to metamorphose. On day 3-4, most larvae cemented to the bottom of the glass culture dish but did not metamorphose (larvae 5-6 days old). Instead the mantle and pedicle lobes

Table II

Temperature effects on development rate and swimming behavior of Laqueus californianus.

Temp (°C)	Observation	Day of experiment (Age of larva)						
		1 (3)	2 (4)	3 (5)	4 (6)	5 (7)	6 (8)	7 (9)
5	Stage	Gastrula w/ AT	Early TL w/ AT	Early TL w/ AT	Full TL w/ AT	Full TL w/o AT	Full TL w/o AT	Competent
	Swim	~All up	~All up	~50% up	~50% up	Most near bottom	Most near bottom	Most near bottom
10	Stage	Gastrula w/ AT	Full TL w/ AT	Full TL w/o AT	Full TL w/ AT	Competent	Competent	Competent
	Swim	~All up	~All up	~50% up	~30% up	~20% up	~20% up	Most near bottom
15	Stage	Early TL w/ AT	Full TL w/o AT	Competent	Competent	Competent	Competent	Competent
	Swim	~All up	~50% up	~30% up	~20% up	Most near bottom	Most near bottom	Most near bottom
20	Stage	Early TL w/ AT	Competent	~70% abnormal settlement	~100% abnormal settlement	Abnormal-Terminate		
	Swim	Most near bottom	Most near bottom					
25	Stage	Gastrula w/o AT	Dead-Terminate					
	Swim	Most near bottom						

Abbreviations: AT, apical ciliary tuft; Competent, metamorphically competent larva; TL, trilobed larva.

became abnormally tall so that the apical lobe came to rest on a thin stalk ~300 μm off the bottom. This treatment was terminated on day 5. Embryos and larvae developed normally and with little mortality at 15°, 10°, and 5°C, with accelerated development at higher temperatures. Thus at 15°C, larvae became competent on day 3 of the experiment (larvae 5 days old), whereas larvae at 5°C did not become competent until day 7 (larvae 9 days old). Embryos and larvae at these temperatures swam normally at the surface of cultures, but at or near the time of attaining metamorphic competence they moved to the bottom of dishes. No larvae metamorphosed, but many survived at 10° and 15°C until day 69, when the experiment was terminated (larvae 71 days old). The higher survival of larvae in 15° and 20°C water compared to larvae in the temperature:survival assay was probably due to frequent water changes in this experiment.

Settlement substrate preference

In the first larval settlement experiment very few larvae settled on carbonate rocks, microscope slides, rocks from brachiopod habitat in the Monterey Submarine Canyon, clam shells, and dead, air-dried *L. californianus* shells (Fig. 6A). A moderate but significantly ($P < 0.05$) higher percentage settled on dead, air-dried *L. californianus* pedicles and dead, air-dried but conditioned *L. californianus* shells. In addition, a number of larvae settled on pieces of dead, air-dried bryozoan test that were inadvertently included with two of the clam-shell treatments (these settlers were scored separately and the data treated as replicates). Nevertheless, by far the largest percentage ($P < 0.05$) settled on living *L. californianus* shells. These results indicate that significantly more larvae settled on conspecifics, and further, that shells of living brachiopods were most highly preferred.

Results from the second settlement experiment confirm that larvae preferred shells of live conspecific brachiopods (Fig. 6B; $P < 0.05$), and indicate that larvae had a low preference for substrates that were conditioned or painted with brachiopod extract. These latter treatments received no settlement, and their counts were lumped in the 'other' category (Fig 6B).

Several additional experiments (data not presented) produced results consistent with those above. However, in many cases settled larvae, as scored in all settlement experiments, failed to undergo complete metamorphosis (see *Metamorphosis*, above).

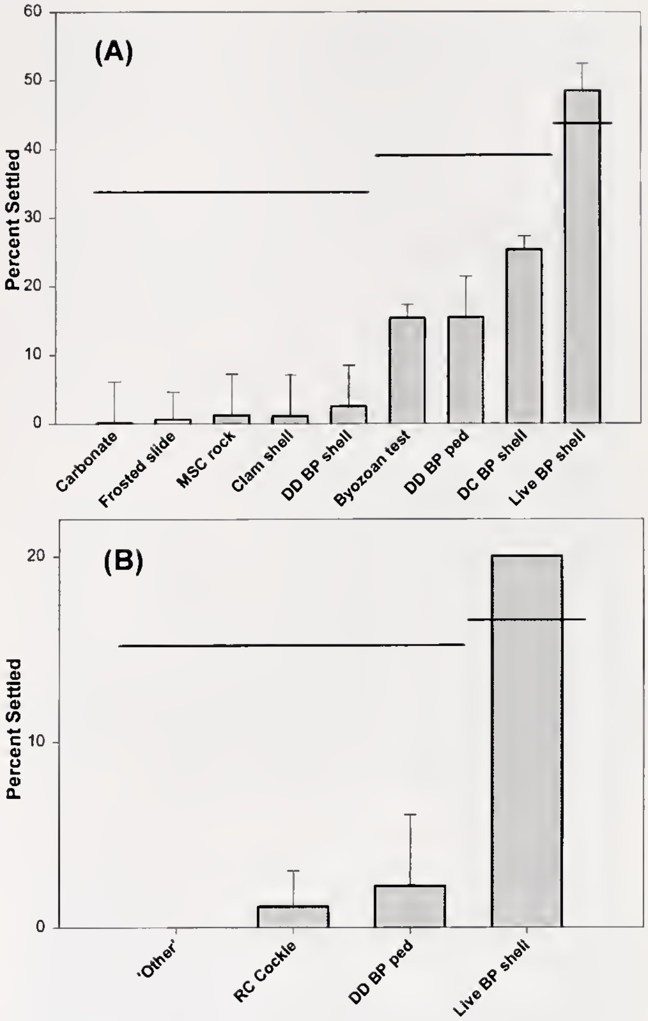

Figure 6. Mean percentage of larvae settling in substrate preference surveys. In both (A) and (B), *Laqueus californianus* larvae strongly preferred living *L. californianus* shells. Competent larvae were exposed to the various substrates and scored for settlement only; most larvae did not undergo normal metamorphosis in these experiments. Lines over histograms group nonsignificantly different treatments ($P > 0.05$); error bars are one standard deviation. Treatment substrata are detailed in Methods. Abbreviations are (A) 'MSC rock', rock collected from a brachiopod habitat in Monterey Submarine Canyon; 'DD BP shell', shell from dead, air-dried *L. californianus;* 'Bryozoan', unidentified bryozoan test; 'DD BP Ped', dead, air-dried *L. californianus* pedicles; 'DC BP shell', shell from dead, air-dried *L. californianus* conditioned in seawater; 'Live BP shell', living *L. californianus;* and (B) 'Other', 11 substratum treatments in which no larvae settled; 'RC Cockle', rugose cockle shell conditioned in seawater; 'DD BP Ped', dead, air-dried *L. californianus* pedicles; 'Live BP shell', living *L. californianus*.

Discussion

Environmental setting and adult habitat

Adult *Laqueus californianus* occur in dense epifaunal beds near the outer margin of the continental shelf in northern Monterey Bay (100-200 m; Fig. 1A-C). These beds are near carbonate rock outcrops associated with the San Gregorio fault zone (Dan Orange, University of California at Santa Cruz, pers. comm.), but often extend over or occur on near-horizontal soft sediment (Fig. 1B) where individual brachiopods are attached to either living or dead brachiopod shells (Fig. 1C) lying on mud. Other aggregations of *L.*

californianus have been observed on the continental shelf a few kilometers north of Monterey Bay, and Mattox (1955) dredged masses of adults from 60-240 m off Santa Catalina Island. Tunnicliffe and Wilson (1988) found abundant populations of *L. californianus* on vertical rock walls in British Columbia. *L. californianus* ranges from Alaska to southern California and also occurs in the Sea of Japan (Bernard, 1972; Tunnicliffe and Wilson, 1988). The species is typically found at depths <200 m (Hertlein and Grant, 1944), but is common in the intertidal zone of British Columbia (Bernard, 1972), and shell fragments have been dredged from 1570 m off the Monterey Peninsula (Dall, 1920). *L. californianus* is also common on rock walls in the Monterey Submarine Canyon to at least 800 m (Barry, unpubl), where it occurs as scattered individuals intermixed with the more ovate form *Laqueus californianus* var. *vancouveriensis.* The taxonomic status of this latter form is uncertain, but our observations of its distribution are in accord with the deeper, non-aggregated occurrence of *L. californianus* var. *vancouveriensis* reported by other authors (Hertlein and Grant, 1944; Mattox, 1955; Bernard, 1972; Tunnicliffe and Wilson, 1988). *Terebratulina crossei* also occurs in the Monterey Submarine Canyon, and the inarticulate *Glottidia albida* occurs in soft substrates on the continental shelves of Monterey Bay (Zimmer and Haderlie, 1980).

Development

Embryos and larvae. Development of *L. californianus* is similar to that of another north Pacific terebratellacean, *Terebratalia transversa* (Long, 1964; Stricker and Reed, 1985a,b,c; Long and Stricker, 1991; Freeman, 1993a,b). The eggs of *L. californianus* are smaller than those of *T. transversa* (135 *vs.* 150 μm diameter), and the sperm tails of *L. californianus* spermatozoa are longer (45 *vs.* 30 μm). Reed (1987) states that *L. californianus* eggs are 170 μm in diameter, larger than observed in this study. Cleavage and embryogenesis appear nearly identical, although we have not identified polar bodies in *L. californianus* embryos. Larvae of the two species are also similar, although *L. californianus* larvae are smaller (150 μm *vs.* 200 μm in length), do not develop pigmented eyespots, and lack vesiculated cells at the posterior margin of the apical lobe.

The developmental schedule of *L. californianus* is slower than that of *T. transversa.* At 12°-13°C, *T. transversa* reaches metamorphic competence in 4 days (Freeman, 1993a), whereas *L. californianus* takes 7 days to achieve competence at 10°C and 5 days at 15°C (Table I). We have maintained *L. californianus* larvae in culture for 71 days, which to our knowledge, is the longest recorded for articulate brachiopod larvae (also see Peck and Robinson, 1994, for a description of 45-day-old larvae of *Liothyrella uva* in the Antarctic). We do not know over what portion of this period *L. californianus* larvae remain competent to settle and metamorphose.

Development among articulate brachiopods is highly conservative (reviewed by Chuang, 1990; Long and Stricker, 1991; James *et al.*, 1992), and development in *L. californianus* is similar to that of other terebratellaceans and articulate brachiopods in general.

Metamorphosis. Metamorphosis in *L. californianus* is similar to that described for *T. transversa* and other articulates (reviewed by Long and Stricker, 1991; Chuang, 1990). However, many larvae in our cultures metamorphosed incompletely and did not proceed to develop normally. The anterior end of the apical lobe of such animals developed an ectodermal invagination (not illustrated) that is strikingly similar to stomodeal invaginations reported for other species by previous authors (Percival, 1944, 1960; Mano, 1960; Franzen, 1969). We have not followed the fate of this invagination in these abnormal individuals. Incomplete metamorphosis appears to be fairly common among articulate larvae (Percival, 1960; Freeman, 1993b) and in our cultures is probably a laboratory artifact associated with quality of eggs, culture seawater, or substratum.

Larval and recruitment biology

Depth-regulatory behavior. Changes in swimming direction associated with larval stage observed for *L. californianus* are similar to that known for a number of other articulate larvae (*Calloria inconspicua*–Percival, 1944; Doherty, 1979; Chuang, 1996; *Frenulina sanguinolenta*–Mano, 1960; *Terebratulina septentrionalis*–Noble *et al.*, 1976; *Terebratulina retusa*–James *et al.*, 1992). Such behavior has been attributed to phototaxis (*e.g.*, reviews by Long and Stricker, 1991; James *et al.*, 1992), and late larvae of many species develop putative eyespots (reviewed by Chuang, 1990). *L. californianus* larvae, however, do not have eyespots and show no obvious photobehavior in response to vertically or horizontally directed lights; their vertical swimming behaviors are probably geotactic.

Most invertebrate larvae exhibit depth-regulatory swimming (see Mileikovsky, 1973; Chia *et al.*, 1984), with young larvae typically swimming up in the water column and older larvae swimming or sinking downwards (Thorson, 1964; Young and Chia, 1988). Off central California where surface temperatures are <20°C (J.T. Pennington and F.P. Chavez, unpubl. data), *L. californianus* can develop at surface temperatures (Table II). At 1 mm/s (see Results), larvae might swim to the surface in ~28 h from brachiopod beds at 100 m. Such larvae could spend several days near the surface and could easily be dispersed dozens of kilometers by currents (see Breaker and Broenkow, 1994); the faster development at surface temperatures (Table II) should also be advantageous in terms of predation and other time-dependent sources of mortality (Rumrill, 1990). This scenario contradicts the notion that articulate larvae are so short-lived that they must have very limited dispersal (Rudwick, 1970; James *et al.*, 1992), resulting in patchy meter-scale distributions of adults (especially brooding species; see Noble *et al.*, 1976; reviewed by James *et al.*, 1992). If *L. californianus* larvae can delay metamorphosis for long periods, as may be suggested by their 71-day survival in culture, widespread dispersal could occur, which could have implications for arguments concerning evolutionary rates (*cf.* Jablonski and Lutz, 1983; Valentine and Jablonski, 1983b). We plan to conduct field experiments to confirm the possibility that *L. californianus* larvae migrate to and from the surface during the course of their development, and to determine how long the larvae remain competent to settle and metamorphose.

Settlement. Late larvae of *L. californianus* swim to the bottom of cultures and engage in what may be a 'searching' behavior. In this behavior, the larvae swim, not rotating as do younger larvae, with the anteroventral surface of the apical lobe pressed against or in proximity (within micrometers) to the substrate. This anteroventral surface is at or near the leading edge of the site of blastopore closure (*e.g.*, the possible site of the adult mouth; Long and Stricker, 1991), and it is possible that the larvae are 'tasting' potential settlement sites. Similar behaviors occur among other articulate species (reviewed by Long and Stricker, 1991; James *et al.*, 1992; Chuang, 1990, 1996). Percival (1960) additionally described late larvae of *Notosaria* (= *Tegulorhyncha*) *nigricans* 'running about' the substrate by means of the ventral ciliated band.

We have not observed larvae in the act of settlement (cementation to substrate), but substrate-choice experiments (Fig. 6A-B) indicate that larvae settle preferentially on shells of living *L. californianus.* They also settle in moderate numbers on nonliving brachiopod shell and pedicle, but prefer conditioned (biofilmed) shell. Gregarious settlement is not uncommon among articulates (reviewed by Long and Stricker, 1991; James *et al.*, 1992), but has usually been inferred from distribution of juvenile recruits. Conditioned substrates, presumably colonized by microfauna, are also known to facilitate brachiopod settlement (Percival, 1960). The finding that the larvae strongly prefer living conspecific substrate, however, is new, though both Percival (1960) and Freeman (1993b) noted that live or freshly smashed conspecific shells were effective inducers of metamorphosis in *N. nigricans* and *T. transversa,* respectively. The settlement-inducing cues remain unknown—substrates treated with a brachiopod extract were apparently unattractive. Gregarious settlement would appear to be adaptive in Monterey Bay, where the brachiopod beds are largely composed of living animals cemented to each other and onto dead shell material imbedded in sediment underlying the beds (Fig. 1B-C). Larvae settling on live rather than dead shells should stand less chance of burial (but on gregariousness also see Doherty, 1979; James *et al.*, 1992). Almost certainly, preferential settlement of larvae on living conspecifics is one factor that promotes formation and maintenance of the *L. californianus* beds in Monterey Bay.

Acknowledgments

We thank D. Orange, who discovered the brachiopod beds; the crew and pilots of the R/V *Point Lobos* and the ROV *Ventana;* P. Whaling for patient collection; J. and T. Pennington for assistance with culture; K. Buck and J. Krupp for assistance with SEM; and the David and Lucile Packard Foundation for financial support.

Literature Cited

Bernard, F. R. 1972. The living Brachiopoda of British Columbia. *Syesis* **5:** 73–82.

Breaker, L. C., and W. W. Broenkow. 1994. The circulation of Monterey Bay and related processes. *Oceanogr. Mar. Biol. Annu. Rev.* **32:** 1–64.

Chia, F. S., J. Buckland-Nicks, and C. M. Young. 1984. Locomotion of marine invertebrate larvae: a review. *Can. J. Zool.* **62:** 1205–1222.

Chuang, S. H. 1990. Brachiopoda. Pp. 211–254 in *Reproductive Biology of Invertebrates. Vol. VI, Fertilisation, Development and Parental Care,* K. G. and R. G. Adiyodi, eds. John Wiley, New York.

Chuang, S. H. 1996. The embryonic, larval and early postlarval development of the terebratellid brachiopod *Calloria inconspicua* (Sowerby). *J. R. Soc. N. Z.* **26:** 119–137.

Dall, W. H. 1920. Annotated list of the recent Brachiopoda in the collection of the United States National Museum, with descriptions of thirty-three new forms. *Proc. U.S. Natl. Mus.* **57:** 261–377.

Doherty, P. J. 1979. A demographic study of a subtidal population of the New Zealand articulate brachiopod *Terebratella inconspicua. Mar. Biol.* **52:** 331–342.

Franzen, A. 1969. On larval development and metamorphosis in *Terebratulina* Brachiopoda. *Zool. Bidr. Upp.* **38:** 155–174.

Freeman, G. 1993a. Regional specification during embryogenesis in the articulate brachiopod *Terebratalia. Dev. Biol.* **160:** 196–213.

Freeman, G. 1993b. Metamorphosis in the brachiopod *Terebratalia:* evidence for a role of calcium channel function and the dissociation of shell formation from settlement. *Biol. Bull.* **184:** 15–24.

Gilmour, T. H. J. 1981. Food-collecting and waste-rejecting mechanisms in *Glottidia pyramidata* and the persistence of Lingulacean inarticulate brachiopods in the fossil record. *Can J. Zool.* **59:** 1539–1547.

Gold, K. 1976. Methods for preserving tintinnids. Pp. 236–239 in *Zooplankton Fixation and Preservation.* H. F. Steedman, ed. UNESCO, Paris.

Gould, S. J., and C. B. Calloway. 1980. Clams and brachiopods— ships that pass in the night. *Paleobiology* **6:** 383–396.

Hertlein, L. G., and U. S. Grant. 1944. The cenozoic Brachiopoda of western North America. *Publ. UCLA Math. Phys. Sci.* **3:** 1–236.

Jablonksi, D., and R. A. Lutz. 1983. Larval ecology of marine benthic invertebrates: paleobiological implications. *Biol. Rev.* **58:** 21–89.

James, M. A., A. D. Ansell, M. J. Collins, G. B. Curry, L. S. Peck, and M. C. Rhodes. 1992. Biology of living brachiopods. *Adv. Mar. Biol.* **28:** 175–387.

Law, R. H., and C. W. Thayer. 1991. Articulate fecundity in the phanerozoic: Steady state or what? Pp. 183–190 in *Brachiopods Through Time.* D.I. McKinnon, D. E. Lee, and J. D. Campbell, eds. Balkema, Rotterdam.

Long, J. A. 1964. The embryology of three species representing three superfamilies of articulate Brachiopoda. Ph.D. Dissertation, University of Washington, Seattle. 185 pp.

Long, J. A., and S. A. Stricker. 1991. Brachiopoda. Pp. 47–84 in *Reproduction in Marine Invertebrates, Vol. 6, Echinoderms and Lophophorates.* A. C. Giese, J. S. Pearse, and V. B. Pearse, eds. Boxwood Press, Palo Alto, CA.

Mano, R. 1960. On the metamorphosis of the brachiopod *Frenulina sanguinolenta* (Gmelin). *Bull. Mar. Biol. Stn. Asamushi* **10:** 171–175.

Mattox, N. T. 1955. Observations on the brachiopod communities near Santa Catalina Island. Pp. 73–86 in *Essays in the Natural Sciences in Honor of Captain Allan Hancock.* University of Southern California Press, Los Angeles.

Mileikovsky, S. A. 1973. Speed of active movement of pelagic larvae of marine bottom invertebrates and their ability to regulate their vertical position. *Mar. Biol.* **23:** 11–17.

Noble, J. P. A., A. Logan, and G. R. Webb. 1976. The recent *Terebratulina* community in the rocky subtidal zone of the Bay of Fundy, Canada. *Lethaia* **9:** 1–17.

Peck, L. S., and K. Robinson. 1994. Pelagic larval development in the brooding Antarctic brachiopod *Liothyrella uva. Mar. Biol.* **120:** 279–286.

Percival, E. 1944. A contribution to the life-history of the brachiopod *Terebratella inconspicua* Sowerby. *Trans. R. Soc. N. Z.* **74:** 1–23.

Percival, E. 1960. A contribution to the life-history of the brachiopod *Tegulorhynchia nigricans. Q. J. Microsc. Sci.* **101:** 439–458.

Reed, C. G. 1987. Phylum Brachiopoda. Pp. 486–493 in *Reproduction and Development of Marine Invertebrates of the Northern Pacific Coast,* M. F. Strathmann, ed. University of Washington Press, Seattle.

Rhodes, M. C., and C. W. Thayer. 1991. Effects of turbidity on suspension feeding: Are brachiopods better than bivalves? Pp. 191–196 in *Brachiopods Through Time.* D. I. McKinnon, D. E. Lee, and J. D. Campbell, eds. Balkema, Rotterdam.

Rhodes, M. C., and R. J. Thompson. 1993. Comparative physiology of suspension-feeding in living brachiopods and bivalves: evolutionary implications. *Paleobiology* **19:** 322–334.

Rudwick, M. J. S. 1970. *Living and Fossil Brachiopods.* Hutchinson, London. 199 pp.

Rumrill, S. S. 1990. Natural mortality of marine invertebrate larvae. *Ophelia* **32:** 163–198.

Stanley, S. M. 1977. Trends, rates and patterns of evolution in the Bivalvia. Pp 209–250 in *Patterns of Evolution.* A. Hallam, ed. Elsevier, Amsterdam.

Stricker, S. A., and M. W. Folsom. 1997. Oocyte maturation in the brachiopod *Terebratalia transversa:* role of follicle cell-oocyte attachments during ovulation and germinal vesicle breakdown. *Biol. Bull.* **193:** 324–340.

Stricker, S. A., and C. G. Reed. 1985a. The ontogeny of shell secretion in *Terebratalia transversa* (Brachiopoda, Articulata). I. Development of the mantle. *J. Morphol.* **183:** 233–250.

Stricker, S. A., and C. G. Reed. 1985b. The ontogeny of shell secretion in *Terebratalia transversa* (Brachiopoda, Articulata). II. Formation of the protegulum and juvenile shell. *J. Morphol.* **183:** 251–272.

Stricker, S. A., and C. G. Reed. 1985c. Development of the pedicle in the articulate brachiopod *Terebratalia transversa* (Brachiopoda, Terebratulida). *Zoomorphology* **105:** 253–264.

Thayer, C. W. 1981. Ecology of living brachiopods. Pp. 110–126 in *Lophophorates. Notes for a Short Course.* J. T. Dutro, Jr., and R. S. Boardman, eds. University of Tennessee, Knoxville. Publication EO1-1040-006-89.

Thayer, C. W. 1985. Brachiopods versus mussels: competition, predation, and palatability. *Science* **228:** 1527–1528.

Thayer, C. W. 1986. Are brachiopods better than bivalves? Mechanisms of turbidity tolerance and their interaction with feeding in articulates. *Paleobiology* **12:** 161–174.

Thayer, C. W., and R. A. Allmon. 1991. Unpalatable thecideid brachiopods from Palau: ecological and evolutionary implications. Pp. 253–260 in *Brachiopods Through Time.* D. I. McKinnon, D. E. Lee, and J. D. Campbell, eds. Balkema, Rotterdam.

Thorson, G. 1964. Light as an ecological factor in the dispersal and settlement of larvae of marine bottom invertebrates. *Ophelia:* **1:** 167–208.

Tunnicliffe, V., and K. Wilson. 1988. Brachiopod populations: distribution in fjords of British Columbia (Canada) and tolerance of low oxygen concentrations. *Mar. Ecol. Prog. Ser.* **47:** 117–128.

Valentine, J. W., and D. Jablonski. 1983a. Larval adaptations and patterns of brachiopod diversity through time. *Evolution* **37:** 1052–1061.

Valentine, J. W., and D. Jablonski. 1983b. Speciation in the shallow sea: general patterns and biogeographic controls. Pp. 201–226 in *Evolution, Time and Space: The Emergence of the Biosphere.* R. W. Sims, J. H. Price, and P. E. S. Whalley, eds. Academic Press, New York.

Vermeij, G. J. 1977. The Mesozoic marine revolution: evidence from snails, predators and grazers. *Paleobiology* **3:** 245–258.

Wisely, B. 1969. Preferential settlement in concavities by the brachiopod *Waltonia inconspicua. N. Z. J. Mar. Freshwater Res.* **3:** 273–280.

Young, C. M., and F. S. Chia. 1987. Abundance and distribution of pelagic larvae as influenced by predation, behavior, and hydrographic factors. Pp. 385–464 in *Reproduction of Marine Invertebrates, Vol. IX.* A. C. Giese, J. S. Pearse, and V. B. Pearse, eds. Blackwell Scientific, Palo Alto, CA.

Zimmer, R. L., and E. C. Haderlie. 1980. Brachiopoda and phoronida. Pp. 108–114 in *Intertidal Invertebrates of California.* R. H. Morris, D. P. Abbott, and E. C. Haderlie, eds. Stanford University Press, Stanford, CA.

Reference: *Biol. Bull.* **196:** 257–264. (June 1999)

Physiological Functioning of Carbonic Anhydrase in the Hydrothermal Vent Tubeworm *Riftia Pachyptila*

SHANA K. GOFFREDI*, PETER R. GIRGUIS, JAMES J. CHILDRESS,
AND NICOLE T. DESAULNIERS

*Marine Science Institute and Department of Ecology, Evolution and Marine Biology,
University of California, Santa Barbara, California 93106*

Abstract. On the basis of our experiments, it is clear that carbonic anhydrase (CA) plays an important role in the CO_2-concentrating mechanisms in *Riftia pachyptila.* Plume tissue from freshly collected animals had the highest CA activity, 253.7 ± 36.0 μmol CO_2 min^{-1} g^{-1} wet wt, and trophosome activity averaged 109.4 ± 17.9 μmol CO_2 min^{-1} g^{-1} wet wt. Exposure of living worms to ethoxyzolamide, a carbonic anhydrase inhibitor, resulted in a 99% decrease in CA activity (from 103.9 ± 38.6 to 0.7 ± 0.2 μmol CO_2 min^{-1} g^{-1} wet wt in the plume tissue and 57.6 ± 17.9 to 0.04 ± 0.11 μmol CO_2 min^{-1} g^{-1} wet wt in the trophosome) and essentially a complete cessation of ΣCO_2 uptake. High concentrations of CA appear to facilitate the equilibration between inorganic carbon (C_i) in the external and internal environments, greatly enhancing the diffusion of CO_2 into the animal. In summary, *R. pachyptila* demonstrates very effective acquisition of inorganic carbon from the environment, thereby providing the symbionts with large amounts of CO_2. This effective acquisition is made possible by three factors: extremely effective pH regulation, a large external pool of CO_2, and, described in this paper, high levels of carbonic anhydrase.

Introduction

The giant hydrothermal vent tubeworm *Riftia pachyptila* has an unusual mode of existence, relying primarily upon its symbionts for nutrition. These symbiotic bacteria have been shown to fix only CO_2, yet they have a low affinity for it (K_m for CO_2 = 21–35 μmol l^{-1}; Scott *et al.*, 1994). *R. pachyptila* must, therefore, supply inorganic carbon to the bacteria, which are far removed from the external medium, at high rates and at concentrations sufficient to support its extremely high growth rates (up to 3 ft y^{-1}; Lutz *et al.*, 1994). Net rates of carbon fixation in *R. pachyptila* can be quite high, and the acquisition of inorganic carbon (C_i) *via* CO_2 diffusion has been documented (Childress *et al.*, 1991; Goffredi *et al.*, 1997). Although the P_{CO_2} in the vent environment is higher than in most seawater environments, these animals appear to use carbon-concentrating mechanisms for C_i uptake. Although the worms use binding proteins (hemoglobins) to concentrate oxygen and sulfide internally, there is no evidence that proteins in the extracellular fluids bind either CO_2 or HCO_3^- (Arp *et al.*, 1985, 1987; Childress *et al.*, 1991, 1993; Kochevar *et al.*, 1993; Toulmond *et al.*, 1994). Thus, other concentrating mechanisms must be responsible for the internal accumulation of inorganic carbon.

Many organisms have evolved carbon-concentrating mechanisms that create gradients favoring the internal movement of CO_2, either by increasing the external CO_2 pool or by decreasing the internal CO_2 pool, to aid in the acquisition of CO_2 (Raven, 1991). Carbonic anhydrase (CA) can function in this capacity and has proven to be very important for marine autotrophs. CA, the enzyme that catalyzes the interconversion between carbon dioxide (CO_2) and bicarbonate (HCO_3^-), is widespread among organisms. Since its discovery in the 1930s, CA has been shown to participate in a variety of physiological and biochemical processes, although it is still most commonly known for aiding in CO_2 elimination in metazoans (Meldrum and Roughton, 1933; Maren, 1967; Burnett, 1984; Burnett and McMahon, 1985; Henry 1987, 1988). In addition to CO_2 elimination, however, CA plays an important role in the

---

Received 29 July 1998; accepted 16 March 1999.

* Present address: Monterey Bay Aquarium Research Institute, 7700 Sandholdt Rd., P.O. Box 628, Moss Landing, CA 95039. E-mail: goffredi@mbari.org

uptake of C_i in aquatic photosynthetic organisms, including a variety of marine plants, algae, eubacteria, and cyanobacteria, as well as in invertebrate hosts of photosynthetic symbionts, including corals, anemones, and clams (Maren, 1967; Lucas and Berry, 1985; Badger, 1987; Weis *et al.*, 1989; Weis, 1991).

Recently, high levels of CA activity have also been measured in the gas-exchange and symbiont-containing tissues of vesicomyid clams, mytilid mussels, and vestimentiferan tube worms from sulfide-rich environments, including hydrothermal vents and cold seeps (Kochevar and Childress, 1996). It has been suggested that CA in these hosts of chemoautotrophic symbionts is important for the uptake of inorganic carbon, as it is for hosts of photosynthetic symbionts (Kochevar, 1992; Kochevar *et al.*, 1993; Kochevar and Childress, 1996). Of all the hosts of chemosynthetic symbionts measured in previous studies, the vent tubeworm, *Riftia pachyptila*, has demonstrated the highest CA activity, especially in the plume (the primary gas-exchange tissue), and the trophosome tissue (the specialized organ in which the bacteria are housed in the trunk of the worm) (Kochevar *et al.*, 1993; Kochevar and Childress, 1996).

The purpose of this project was to determine the physiological functioning of CA in the *R. pachyptila* symbiosis. Based on the assumption that CA in the worm's plume is involved in concentrating C_i from the external environment into the animal, our goal was to provide evidence of the actual *in vivo* functioning of CA in the uptake process. We further assumed that CA enhances CO_2 movement into the worm and that inhibition of CA activity would reduce the rate of CO_2 diffusion, thus lowering the CO_2 uptake rate and internal CO_2 level in *R. pachyptila*. To test these hypotheses, we analyzed the uptake of CO_2 by these animals in the presence and absence of the membrane-permeable carbonic anhydrase inhibitor ethoxyzolamine (EZ). We chose EZ because it has a high *in vivo* stability as well as a high affinity for CA (Holder and Hayes, 1965; Maren, 1967, 1977).

Materials and Methods

Collections

Individuals of *R. pachyptila* were collected at an average depth of 2600 m by submersible during research expeditions to 9°N (9°50′N, 104°18′W) and 13°N (12°48′N, 103°57′W) along the East Pacific Rise in 1994 and 1996. Animals were brought to the surface in a temperature-insulated container and transferred to cold seawater (5°C) in a refrigerated van on board ship. Worms were then sorted to be used either for experiments on living animals (described below) or for immediate measurements of physiological parameters. Live-animal experiments were initiated within 2 h of surfacing. Worms labeled "freshly collected" in this text were dissected in less than 4 h after collection from the sea floor (see Goffredi *et al.*, 1997, for dissection techniques). Tissue and blood samples were stored at −70°C for assays of CA activity.

Analytical methods

ΣCO_2 and ΣH_2S of body fluids and large-vessel water samples were measured in 0.5-ml aliquots with a Hewlett Packard 5880A gas chromatograph (GC) (Childress *et al.*, 1984; "Σ" is used to indicate total concentrations, including all ionic species present). Body fluid pH values were measured with a thermostatted (10°C) Radiometer BMS-2 blood pH analyzer equipped with a G299A capillary pH electrode. All values are given as mean ± standard error.

Carbonic anhydrase activity was measured using the protocol described in Weis *et al.* (1989). Briefly, tissue samples were homogenized in 10 × vol of chilled 25 mmol l^{-1} veronal buffer (25 mmol l^{-1} barbital buffer, 5 mmol l^{-1} EDTA, 5 mmol l^{-1} dithiothreitol, and 10 mmol l^{-1} $MgSO_4$, pH 8) and centrifuged for 10 min at 1200 × *g*. Homogenates were stored on ice and 1-ml aliquots were transferred to test tubes for assay. This homogenate was combined with 1 ml 50 mmol l^{-1} veronal buffer solution and 1 ml CO_2-saturated distilled water. The rate of pH change following the addition of CO_2-saturated distilled water was monitored over time. As a control to determine nonspecific changes in pH, the assay was performed on boiled homogenate. The difference between the boiled and non-boiled sample was considered CA activity (and was measured in triplicate). CA activity was measured as Δ pH min^{-1} $weight^{-1}$; however, to facilitate comparison between the rates of CO_2 conversion and the rates of CO_2 uptake, we converted these units to μmol CO_2 min^{-1} $weight^{-1}$ by assuming 0.351 Δ pH min^{-1} $weight^{-1} \approx 1$ μmol CO_2 converted to $HCO_3^- + H^+$ min^{-1} $weight^{-1}$, a factor previously determined by Kochevar and Childress (1996). Protein concentration in crude homogenates was determined spectrophotometrically by the Lowry method, with bovine serum albumin as the standard (Lowry *et al.*, 1951).

Internal vs. external parameter experiments

Experiments in which we were concerned with comparing internal versus external parameters, such as pH and ΣCO_2, were carried out in vessels with a capacity of 6 l to accommodate large worms (see Goffredi *et al.*, 1997 for further details). Use of large (14–42 cm in length and 10–80 g) worms was necessary to measure internal parameters in both vascular and coelomic fluids, as well as in tissues. Seawater was taken from two reservoir tanks, 200 l and 75 l, and pumped by high-pressure, diaphragm metering pumps through the vessels at flow rates ranging from 4 to 12 l h^{-1}, at pressures around 21.5 MPa. All worms in these experiments were first maintained in aquaria with flowing surface seawater (ΣCO_2 = 2.1 mmol l^{-1}, P_{CO_2} = 0.04 kPa, pH = 8.2, at 8°C). Low internal levels of ΣCO_2, which resulted from maintenance in surface seawater, were necessary to measure the uptake rates of CO_2 over time. Decrease in extracellular ΣCO_2 was monitored over periods of 2–4 days, after which the animals were transferred to experimental vessels.

Experimental water conditions were similar to *in situ* vent conditions of 3.98 ± 0.12 mmol l^{-1} ΣCO_2, 0.15 ± 0.02 mmol l^{-1} ΣH_2S, 0.26 ± 0.03 mmol l^{-1} O_2, 0.38 ± 0.02 mmol l^{-1} N_2, and pH 6.0 ± 0.1. Water ΣCO_2, O_2, and N_2 were controlled by bubbling gases directly into a gas equilibration column, which fed the high-pressure pumps, which supplied the vessels (see diagram in Kochevar *et al.*, 1992; Goffredi *et al.*, 1997). Sulfide concentrations were controlled by continuously pumping anaerobic solutions of sodium sulfide (30–50 mmol l^{-1}) into the gas equilibration column. To stabilize and control the pH, 10 mmol l^{-1} MOPS (3-[*N*-morpholino]propanesulfonic acid) or MES (2-[*N*-morpholino]ethanesulfonic acid) buffer was added to the sulfide solutions. Pressure gauges and sample ports were connected to the vessel outflow to allow monitoring of pressure and water conditions.

Control worms (n = 5) were those animals kept in the above conditions without exposure to inhibitors. Inhibitor-exposed worms (n = 5) were those animals initially maintained in the same manner as for the control worms, and transferred to the same experimental conditions; however, once inside the experimental vessels they were exposed to ethoxyzolamide, a specific inhibitor of carbonic anhydrase (final concentration of 0.8–0.9 mmol l^{-1} in the surrounding water; Holder and Hayes, 1965; Maren, 1967, 1977). EZ was first dissolved in pH 13 seawater (at 4–5 mmol l^{-1} concentrations) and introduced into the vessels over a 1-h time period *via* metering pumps. The flow rate determined the final concentration. Worms were sacrificed at times between 0 and 6 h for the determination of tissue CA and vascular blood and coelomic fluid pH and ΣCO_2.

Flux experiments

For experiments in which we measured metabolite fluxes, we used a smaller flow-through, high-pressure respirometry system (Kochevar *et al.*, 1992). Individuals of *R. pachyptila*, ranging in size from 2 to 10 g, were maintained in a high-pressure vessel (volume = 350 ml). A second aquarium, which did not contain worms, was used as a control. In a gas equilibration column, seawater was bubbled with gas mixes of CO_2, H_2S, O_2, and N_2, which were controlled by a gas flow controller (Sierra Instruments Inc.; Kochevar *et al.*, 1992). Dissolved gas concentrations of 3.11 ± 0.32 mmol l^{-1} ΣCO_2, 0.37 ± 0.03 mmol l^{-1} ΣH_2S, 0.40 ± 0.03 mmol l^{-1} O_2, and 0.35 ± 0.02 mmol l^{-1} N_2 were achieved. A seawater pH of 6.25 ± 0.13 was maintained by a proportional pH controller (Cole-Parmer, Inc.). From the equilibration column, seawater was pumped into the vessels *via* high-pressure pumps, at 12.5 ± 1.0 ml min^{-1}, and maintained at 27.5 MPa *via* gas-charged back pressure valves (Circle Seal Controls, Inc.). A pair of pneumatically actuated 4-port valves (VALCO, Inc.) were used to direct the effluent streams (one at a time) to a gas extraction system, where the effluent was acidified and stripped of dissolved gases. Dissolved gas concentrations were measured using a residual gas analyzer (Hiden Analytical), and pH was measured using a double-junction pH electrode. The minimum flux of CO_2, H_2S, and O_2 discernible by this technique is 0.9 μmol g^{-1} h^{-1}, and 0.4 μmol g^{-1} h^{-1}, respectively. The difference in C_i, oxygen, and sulfide concentrations between the experimental and control vessels were used to calculate the flux rates.

To test the effects of EZ on C_i flux, the worms were first maintained under the conditions described above until they showed signs of autotrophy (stable net C_i uptake), after about 20 h. In this study, we use the word *autotrophy* strictly with respect to carbon. EZ was then added at a concentration of 2 mmol l^{-1} to the surrounding seawater. At the end of the experiment, which lasted approximately 4 days, the worms were weighed and dissected. Tissues were kept in liquid nitrogen for later determination of CA activity.

Results

Freshly collected animals

Plume tissue from freshly collected animals had a CA activity of 253.7 ± 36.0 μmol CO_2 min^{-1} g^{-1} wet wt; trophosome activity averaged 109.4 ± 17.9 μmol CO_2 min^{-1} g^{-1} wet wt. (Table I). Both body wall and vestimentum had much lower values, which is in agreement with previous research (Table I; Kochevar and Childress, 1996). Protein values for plume and trophosome tissue averaged 87.7 ± 6.3 mg g^{-1} (n = 27) and 124.7 ± 9.9 mg g^{-1} (n = 16), respectively. Thus, protein-specific CA activities for plume and trophosome were measured to be 4.0 ± 0.9 μmol

Table I

Carbonic anhydrase activities in Riftia pachyptila

Sample	n	CA activity (μmol CO_2 min^{-1} g^{-1} wet wt)
Plume	38	253.7 ± 36.0
Trophosome	39	109.4 ± 17.9
Body wall	17	5.4 ± 0.6
Vestimentum	6	2.3 ± 0.7

Carbonic anhydrase activity (mean ± SE) for *Riftia pachyptila* collected at 9° and 13°N along the East Pacific Rise. CA activity was measured using the protocol described in Weis *et al.* (1989).

CO_2 min^{-1} mg protein^{-1} ($n = 27$) and 0.8 ± 0.2 μmol CO_2 min^{-1} mg protein^{-1} ($n = 16$), respectively.

Internal vs. external parameter experiments

All experimental worms were first kept in maintenance vessels with surface seawater conditions, and monitored until extracellular fluid ΣCO_2 was reduced to a low value (<10 mmol l^{-1}; about 2–4 days). When control worms were subsequently exposed to flowing water with an average ΣCO_2 of 3.98 ± 0.12 mmol l^{-1} and P_{CO_2} of 5.8 ± 0.6 kPa (typical vent conditions), they demonstrated an increase in extracellular fluid ΣCO_2 (Fig. 1a, b). The rate of increase in internal ΣCO_2, from 0 to 6 h, was 4.1 mmol l^{-1}h^{-1} for coelomic fluid and 4.8 mmol l^{-1}h^{-1} for vascular blood. Despite this increase in internal ΣCO_2, there was no change in the pH of either coelomic fluid or vascular blood; values averaged 7.21 ± 0.07 and 7.04 ± 0.07, respectively, during the 6-h time period (Fig. 1c, d).

Worms exposed to EZ were kept in the same overall water conditions as the control worms, with an additional 1 h exposure to 0.8–0.9 mmol l^{-1} EZ. These worms, when placed in typical vent conditions (*i.e.*, high ΣCO_2 and P_{CO_2}), did not accumulate internal ΣCO_2 as rapidly as the control worms (0.8 mmol l^{-1} h^{-1} and 0.0 mmol l^{-1} h^{-1} for coelomic fluid and vascular blood, respectively; Fig. 1a, b). The decreased rate of ΣCO_2 accumulation for vascular blood in the EZ-exposed worms was significantly less than that of the control worms ($P = 0.032$, ANCOVA; Fig. 1b). EZ-exposed worms, like the control worms, showed no change in the pH of either coelomic fluid or vascular blood during the experiment (7.15 ± 0.09 and 7.07 ± 0.01, respectively), and neither was significantly different from that of the control worms ($P = 0.47$ and $P = 0.72$, respectively, Mann-Whitney U test; Fig. 1c, d).

EZ exposure also resulted in a decrease in CA activity of about 99%: from 103.9 ± 38.6 to 0.7 ± 0.2 μmol CO_2 min^{-1} g^{-1} wet wt in the plume tissue and 57.6 ± 17.9 to 0.04 ± 0.11 μmol CO_2 min^{-1} g^{-1} wet wt in the trophosome (Table II).

Flux experiments

For convention, since we are referring to materials that are consumed from the surrounding water, any flux that occurs from the environment into the worm is expressed as a negative value, and any flux that occurs from the worm into the environment is expressed as a positive value. Ini-

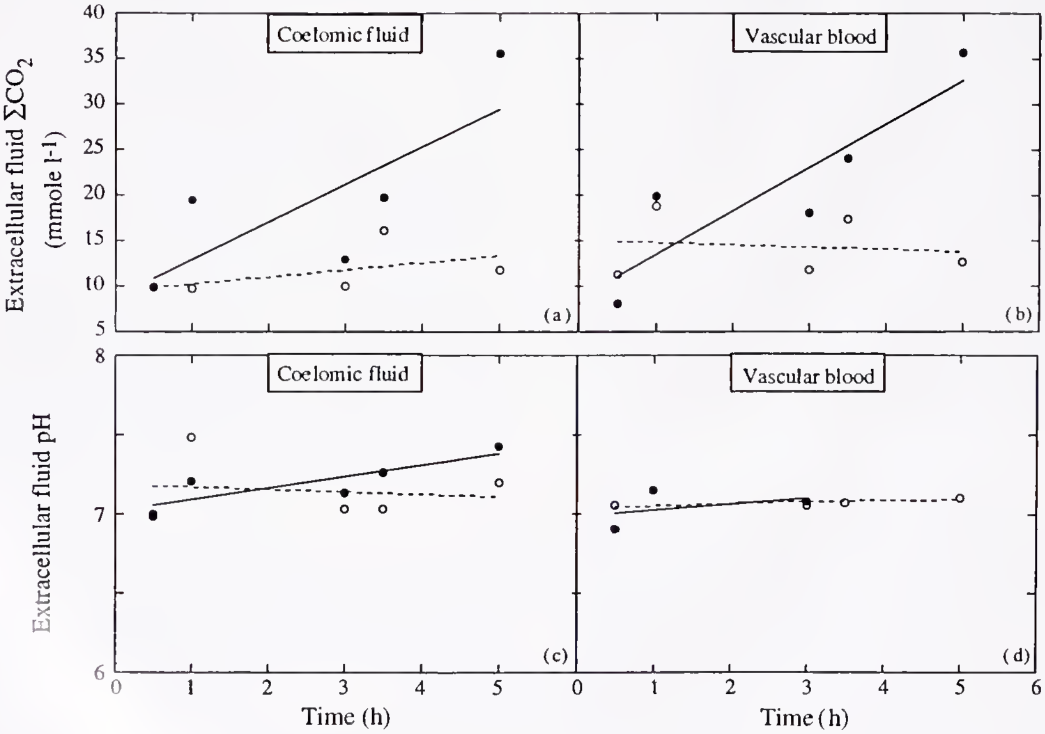

Figure 1 Coelomic fluid ΣCO_2 (a) and pH (c), and vascular blood ΣCO_2 (b) and pH (d), over time for *Riftia pachyptila* exposed to 3.98 ± 0.12 mmol l^{-1} ΣCO_2, 0.15 ± 0.02 mmol l^{-1} ΣH_2S, 0.26 ± 0.03 mmol l^{-1} O_2, 0.38 ± 0.02 mmol l^{-1} N_2, and a pH of 6.0 ± 0.1. Each point represents a single animal sacrificed at the indicated time. Closed symbols represent control worms ($n = 5$) and open symbols represent worms exposed to ethoxyzolamide ($n = 5$). Lines are drawn to show correlations (the only significant regression correlations ($P < 0.05$), showing changes over time, are for both control worm coelomic fluid and vascular blood ΣCO_2).

Table II

Effect of ethoxyzolamide on carbonic anhydrase activity in the tubeworm Riftia pachyptila

Experiment	Sample	Plume CA activity (μmol CO_2 min^{-1} g^{-1} wet wt)	Trophosome CA activity (μmol CO_2 min^{-1} g^{-1} wet wt)
Internal parameters	Control worms	103.9 ± 38.6 (5)	57.6 ± 17.9 (5)
	EZ-exposed worms	0.7 ± 0.2 (5)	0.04 ± 0.11 (5)
Flux	Control worms	82.8 ± 6.7 (2)	50.9 ± 2.1 (2)
	EZ-exposed worms	0.1 ± 0.2 (3)	0.2 ± 0.2 (3)

Carbonic anhydrase activity (mean ± SE; *n* in parentheses) for *Riftia pachyptila* in Internal *vs.* External parameter experiments and Flux experiments, with and without *in vivo* exposure to ethoxyzolamide (EZ), a carbonic anhydrase inhibitor (EZ = 0.8–0.9 mmol l^{-1} in Internal *vs.* External parameter experiments and 2 mmol l^{-1} in Flux experiments). CA activity was measured using the protocol described in Weis *et al.* (1989).

tially, the worms exhibited a net production of inorganic carbon for about 3 h (8.6 ± 0.4 μmol CO_2 g^{-1} h^{-1}; Table III, Fig. 2a). Shortly thereafter, the worms showed signs of autotrophy, indicated by net acquisition of inorganic carbon, which, again, is expressed as a negative flux rate (−12.9 ± 0.5 μmol CO_2 g^{-1} h^{-1}; Table III, Fig. 2a). During net C_i acquisition, both oxygen and sulfide uptake rates increased slightly—by 5.7% and 6.8%, respectively (Table III, Fig. 2b).

Exposure to EZ resulted in a rapid change from C_i acquisition to production (from −12.9 ± 0.5 to 8.2 ± 0.5 μmol CO_2 g^{-1} h^{-1}; Fig. 2a). The resulting net inorganic carbon production rate was similar to that seen at the beginning of the experiment (P = 0.40, Mann-Whitney U-test; Fig. 2a). EZ exposure also resulted in about a 99% decrease in CA activity: from 82.8 ± 6.7 to 0.1 ± 0.2 μmol CO_2 min^{-1} g^{-1} wet wt in the plume tissue and 50.9 ± 2.1 to 0.2 ± 0.2 μmol CO_2 min^{-1} g^{-1} wet wt in the trophosome (Table II). Following the addition of EZ, the worms continued to produce C_i for 3 h. During this time, however, there was a significant trend towards the re-establishment of C_i acquisition ($P < 0.0001$, Kendall rank, Fig. 2a). At the observed rate of increase, it was calculated that C_i acquisition could have been resumed within 6 h, assuming that CA inhibition was irreversible and that the return to acquisition was *via* passive diffusion.

Exposure to EZ also resulted in a transient decrease (*ca.* 50 min) in the rates of O_2 and H_2S uptake (from −16.0 to −12.2 μmol g^{-1} h^{-1} and −8.8 to −5.0 μmol g^{-1} h^{-1}, respectively; Fig. 2b). This decrease coincided with the worms retracting into their tubes, a short-term response in which the plume (the primary respiratory surface) is withdrawn from direct contact with the surrounding seawater. This often occurs when conditions are rapidly changed, and it results in a short-term (less than 60 min) decrease in flux rates. Both oxygen and sulfide flux rates returned to at least 95% of their previous values after 50 min (P = 0.54 and P = 0.58, respectively, Mann-Whitney U test).

Discussion

Previous studies have indicated the involvement of CA in the *R. pachyptila* symbiosis. These studies have included the measurement of CA activities in various tissues as well as the characterization of the enzyme (or enzymes), including size, kinetics, and subunit composition (Kochevar *et al.*, 1993; Kochevar and Childress, 1996). In this study, we have examined not only the levels of CA activity in these animals but also the specific functioning of this enzyme in this symbiotic association as a whole.

Carbonic anhydrase inhibition—ethoxyzolamide

In a past attempt to inhibit CA in *R. pachyptila,* Goffredi *et al.* (1997) demonstrated that exposure to sulfanilamide, another specific inhibitor of carbonic anhydrase, resulted in no significant change in coelomic fluid ΣCO_2, pH, or P_{CO_2} values. In addition, plume and trophosome samples taken from worms exposed to sulfanilamide showed no significant difference in CA activity from control worms. This is not surprising considering that sulfanilamide is a very weak, membrane-impermeable inhibitor of carbonic anhydrase, with a weak affinity for the enzyme (Maren, 1967).

Ethoxyzolamide, on the other hand, has a high affinity for carbonic anhydrase (Holder and Hayes, 1965; Maren, 1967, 1977). Exposure to EZ in our experiments resulted in a complete inhibition of CA in the trophosome and plume, a

Table III

Inorganic carbon, oxygen, and sulfide fluxes in Riftia pachyptila: *pre- and post-ethoxyzolamide (EZ) treatment*

Metabolite	Pre-autotrophic flux (μmol g^{-1} h^{-1})	Autotrophic flux (μmol g^{-1} h^{-1})	Post EZ treatment flux (μmol g^{-1} h^{-1})
Inorganic carbon	8.6 ± 0.4*	−12.9 ± 0.5	8.2 ± 0.5*
Sulfide	−8.9 ± 0.3	−9.6 ± 0.2	−9.0 ± 0.3
Oxygen	−15.9 ± 0.3	−16.9 ± 0.4	−16.0 ± 0.3

Inorganic carbon, oxygen, and sulfide fluxes (μmol g^{-1} h^{-1}) in *Riftia pachyptila* (mean ± SE, taken from Figure 2), preceding autotrophy (average over 191 min), during autotrophy (147 min), and after (post) treatment with the carbonic anhydrase inhibitor ethoxyzolamide (EZ; 205 min). The word "autotrophy" is used strictly with respect to carbon and represents a net uptake of C_i. A negative flux denotes net acquisition; a positive flux denotes net production. Asterisks denote mean fluxes of inorganic carbon that are not significantly different from one another (Mann-Whitney U test).

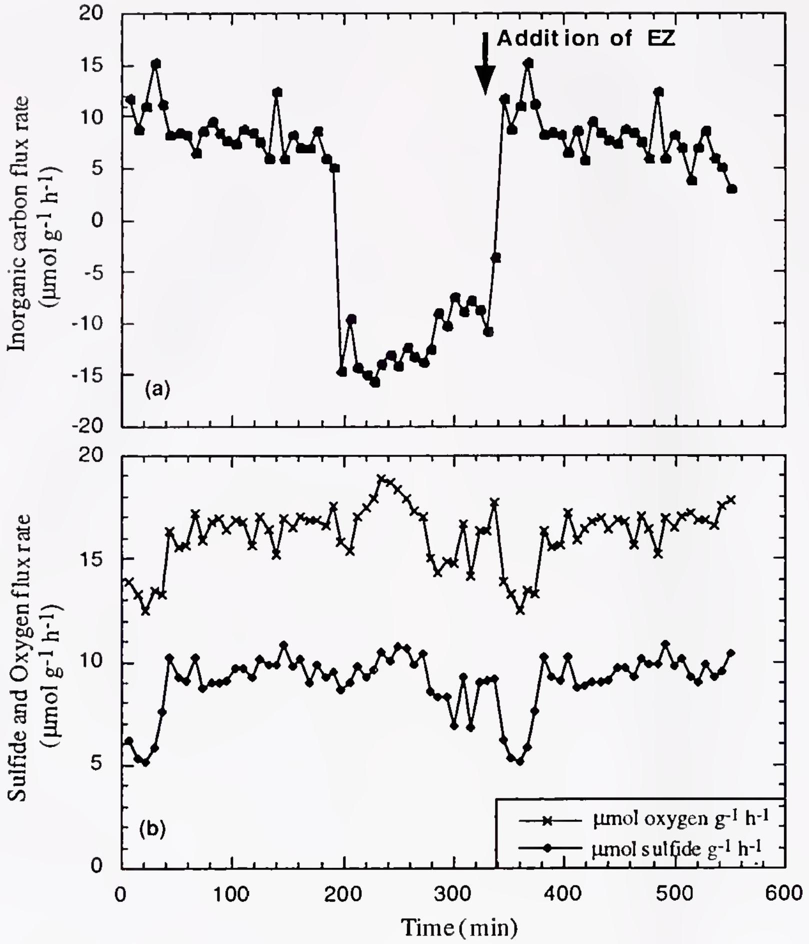

Figure 2. Plot of inorganic carbon (a) and sulfide and oxygen flux rates (b) in *Riftia pachyptila*. Each point represents the values measured at the time indicated (the entire trace represents results from one animal). Water conditions of 3.11 ± 0.32 mmol l^{-1} ΣCO_2, 0.37 ± 0.03 mmol l^{-1} ΣH_2S, 0.40 ± 0.03 mmol l^{-1} O_2, and pH of 6.25 ± 0.13 were maintained. In plot 2a, *acquisition* refers to a net uptake of inorganic carbon, and *production* refers to a net elimination of inorganic carbon. When the worm demonstrated net acquisition of inorganic carbon (*autotrophy*), ethoxyzolamide, an inhibitor of carbonic anhydrase, was added to the aquaria (2 mmol l^{-1}, arrow).

decreased rate of coelomic fluid ΣCO_2 uptake, and a complete shutdown in the movement of ΣCO_2 into vascular blood. The inhibition of CA by EZ, and the subsequent effect on carbon acquisition rates, demonstrates the importance of CA in maintaining an efficient net influx of inorganic carbon. It is interesting that the inhibition of CA by EZ resulted in net rates of CO_2 production that are similar to the pre-autotrophic rates of CO_2 production. In these experiments, freshly captured worms typically do not exhibit net inorganic carbon acquisition for the first 20 h. Thus, the net production of CO_2 during the first few hours represents CO_2 production from both host and symbiont respiration. CO_2 resulting from the metabolic processes within the association is, most likely, insufficient to meet the carbon need of the bacteria. Therefore, the acquisition of C_i from the environment is employed to help fulfill this demand, and we see this as a rather large net uptake of CO_2. Inhibition of CA results in similar rates of CO_2 production, indicating a nearly complete disruption of the carbon-concentrating system.

Until recently, it was thought that EZ was a specific inhibitor of CA, with no known properties other than CA inhibition. EZ, however, has also been suggested to inhibit proton pumps as well as CA (Maren, 1967; Harvey and Ehrenfeld, 1988). It has been demonstrated that these animals may use proton pumps to maintain an extracellular pH that is elevated in relation to the environment (Goffredi *et al.*, 1997). This creates a gradient for the inward movement of CO_2 because CO_2 demonstrates a strong pH-dependent dissociation with a pK of 6.1 (*i.e.*, the pH value at which the ratio of CO_2:HCO_3^- is 1:1; Raven, 1984; Dickson and Millero, 1987). For this reason, CO_2, the dominant chemical species *in situ* due to the acidic external pH (5–6), diffuses into the animal, which maintains an extracellular pH of

7.1–7.5 (Childress *et al.*, 1984, 1991; Goffredi *et al.*, 1997). For *R. pachyptila*, a change in the pH gradient between the internal and external environments, *via* the inhibition of proton pumps, could drastically impair ability to take up CO_2. EZ exposure in our experiments, however, did not result in significant changes in extracellular pH, indicating that EZ was not impairing extracellular pH control by inhibition of proton elimination. In previous studies, proton-pump inhibitors eliminated this pH regulation and resulted in very significant acidification of extracellular fluids with a corresponding reduction in ΣCO_2 concentrations at a given PCO_2. The fact that the EZ-inhibited worms showed no reduction in extracellular fluid pH, under conditions in which worms treated with other proton pump inhibitors showed very significant decreases, strongly suggests that EZ did not inhibit the relevant proton ATPases (Goffredi *et al.*, 1999). Thus, after a period of exposure to elevated P_{CO_2}, the lower extracellular ΣCO_2 and lower rates of C_i accumulation in the extracellular fluids are almost certainly due to a lower rate of movement of C_i into the extracellular fluid. Inhibition of CA is the most likely cause of this reduced rate of movement; therefore based on these results, we believe that EZ acted primarily upon carbonic anhydrase.

In our flux experiments, the addition of EZ resulted in an initial decrease in net acquisition of C_i. After the onset of inhibition, however, there was a significant trend towards restoration of net C_i acquisition over time. The initial decrease in net C_i acquisition was presumably caused by the permanent inhibition of CA by EZ; however, this inhibition did not significantly affect the extracellular pH. Under normal conditions (*i.e.*, without an inhibitor), CA is apparently essential for facilitating C_i uptake at the CO_2 gradient that exists when the worm exhibits autotrophy. However, with the complete inhibition of CA, this gradient is no longer sufficient for the net uptake of CO_2. We would expect, therefore, that as the EZ-exposed *R. pachyptila* depletes the vascular and coelomic C_i pools, the increasing CO_2 gradient would lead to an eventual reduction of net C_i production, as seen in our experiments. About 20% of the total C_i acquisition (heterotrophic C_i production − autotrophic C_i uptake) by *R. pachyptila* had been recovered at 4 h following the addition of EZ. To determine the rates that would have been achieved without the functioning of CA, longer experiments would have been necessary.

Carbon-concentrating mechanisms

Judging from the results of our animal metabolism experiments, it appears that CA plays an important role in the CO_2-concentrating mechanism in *R. pachyptila*. Prior studies have addressed the importance of proton elimination in maintaining a diffusion gradient for the influx of CO_2 (Goffredi *et al.*, 1997). The elevated extracellular pH maintained by these worms allows for C_i to be concentrated in the extracellular fluid above external levels, *via* two mechanisms. The process of pumping protons into the surrounding medium, which has been demonstrated in *R. pachyptila*, increases the free CO_2 concentration externally, which creates a larger external pool of CO_2 available to diffuse inward (Raven, 1991; Girguis and Childress, 1996). Secondly, the actual pH gradient maintained between the internal (pH 7.3) and external environments (pH 6.0) acts to concentrate C_i internally by shifting the internal C_i equilibrium towards HCO_3^-. Under steady-state conditions, the interconversion of CO_2 to bicarbonate at the plume must be reversed in the trophosome because CO_2 is the species of C_i utilized by the symbionts of *R. pachyptila* (Scott *et al.*, 1994). Thus, the gradient for diffusion must ultimately be created by C_i consumption by the symbionts. This provides the "driving force" for the passive influx of CO_2 but does not expedite the conversion of CO_2 into bicarbonate.

By speeding the interconversion between CO_2 and HCO_3^-, CA helps to maximize the effectiveness of CO_2 movement into the plume, through the animal, to the symbionts, allowing for very effective acquisition of inorganic carbon from the environment. Although CO_2 transport at the water/epithelium interface is accomplished by diffusion of dissolved CO_2, an important role for CA in the equilibration between C_i in the external and internal environments is likely, given its high concentrations and the high rates of inorganic carbon uptake. It appears that both the maintenance of a strong pH gradient and high levels of carbonic anhydrase work in concert to rapidly concentrate C_i in this animal, thus providing the symbionts with an abundance of CO_2. Ability to maintain these conditions is apparently a further specialization of *Riftia pachyptila* for supporting autotrophic endosymbionts.

Acknowledgments

Funding for this project was provided by NSF grants OCE-9301374 (J.J.C.) and OCE-9632861 (J.J.C.). The authors thank the captains and crew of the RV *New Horizon*, RV *Atlantis II*, RV *Nadir*, RV *Wecoma*, DSRV *Alvin*, and DSRV *Nautile*. We also thank Dr. F. Lallier, Dr. R. Lee, S. Powell, J. Freytag, and J. Smith for technical support at sea and Dr. R. Kochevar, Dr. R. Trench, and Dr. J. Company for helpful suggestions on the manuscript. Finally, we'd like to thank Dr. L. Mullineaux and Dr. F. Gaill, chief scientists on the HERO 94 and HOT 96 expeditions, respectively.

Literature Cited

Arp, A. J., J. J. Childress, and C. R. Fisher, Jr. 1985. Blood gas transport in *Riftia pachyptila*. *Bull. Biol. Soc. Wash.* **6:** 289–300.

Arp, A. J., J. J. Childress, and R. D. Vetter. 1987. The sulphide-binding protein in the blood of the vestimentiferan tube-worm, *Riftia pachyptila*, is the extracellular haemoglobin. *J. Exp. Biol.* **128:** 139–158.

Badger, M. R. 1987. The CO_2-concentrating mechanism in aquatic phototrophs. Pp. 219–274 in *The Biochemistry of Plants: A Comprehensive Treatise*, Vol. 10, M. D. Hatch and N. K. Broadman, eds. Academic Press, New York.

Burnett, L. E. 1984. CO_2 excretion across isolated perfused crab gills: facilitation by carbonic anhydrase. *Am. Zool.* **24:** 253–264.

Burnett, L. E., and B. R. McMahon. 1985. Facilitation of CO_2 excretion by carbonic anhydrase located on the surface of the basal membrane of crab gill epithelium. *Respir. Physiol.* **62:** 341–348.

Childress, J. J., A. J. Arp, and C. R. Fisher, Jr. 1984. Metabolic and blood characteristics of the hydrothermal vent tube worm *Riftia pachyptila. Mar. Biol.* **83:** 109–124.

Childress, J. J., C. R. Fisher, J. A. Favuzzi, R. E. Kochevar, N. K. Sanders, and A. M. Alayse. 1991. Sulfide-driven autotrophic balance in the bacterial symbiont-containing hydrothermal vent tubeworm, *Riftia pachyptila* Jones. *Biol. Bull.* **180:** 135–153.

Childress, J. J., R. Lee, N. K. Sanders, H. Felbeck, D. Oros, A. Toulmond, D. Desbruyéres, M. C. Kennicutt II, and J. Brooks. 1993. Inorganic carbon uptake in hydrothermal vent tubeworms facilitated by high environmental pCO_2. *Nature* **362:** 147–149.

Dickson, A. G., and F. J. Millero. 1987. A comparison of the equilibrium constants for the dissociation of carbonic acid in sea water media. *Deep-Sea Res.* **34:** 1733–1743.

Girguis, P. R., and J. J. Childress. 1996. Proton equivalent ion flux in *R. pachyptila.* (Annual Meeting of the Society for Integrative and Comparative Biologists, Albuquerque, New Mexico, USA, December 26–30, 1996). *Am. Zool.* **36(5):** 64A.

Goffredi, S. K., J. J. Childress, N. T. Desaulniers, R. W. Lee, F. H. Lallier, and D. Hammond. 1997. Inorganic carbon acquisition by the hydrothermal vent tubeworm *Riftia pachyptila* depends upon high external P_{CO_2} and upon proton elimination by the worm. *J. Exp. Biol.* **200:** 883–896.

Goffredi, S. K., J. J. Childress, F. H. Lallier, and N. T. Desaulniers. 1999. The internal ion composition of the hydrothermal vent tubeworm *Riftia pachyptila:* evidence for the elimination of SO_4^{2-} and H^+ and for a Cl^-/HCO_3^- shift. *Phys. Zool.* **72** (in press).

Harvey, B. J., and J. Ehrenfeld. 1988. Epithelial pH and ion transport regulation by proton pumps and exchangers. Pp. 139–164 in *Proton Passage Across Cell Membranes.* G. Bock and J. Marsh, eds. John Wiley, Chichester, UK.

Henry, R. P. 1987. Membrane-associated carbonic anhydrase in gills of the blue crab, *Callinectes sapidus. Am. J. Physiol.* **252:** R966–R971.

Henry, R. P. 1988. Multiple functions of carbonic anhydrase in the crustacean gill. *J. Exp. Zool.* **248:** 19–24.

Holder, L. B., and S. L. Hayes. 1965. Diffusion of sulfonamides in aqueous buffers and into red cells. *Mol. Pharmacol.* **1:** 266–279.

Kochevar, R. E. 1992. Carbonic anhydrase in the giant hydrothermal vent tubeworm *Riftia pachyptila* Jones and other deep-sea chemoautotrophic symbioses. Ph.D. dissertation, University of California, Santa Barbara. 103 pp.

Kochevar, R. E., and J. J. Childress. 1996. Carbonic anhydrase in deep-sea chemoautotrophic symbioses. *Mar. Biol.* **125:** 375–383.

Kochevar, R. E., J. J. Childress, C. R. Fisher, and L. Minnich. 1992. The methane mussel: roles of symbiont and host in the metabolic utilization of methane. *Mar. Biol.* **112:** 389–401.

Kochevar, R. E., N. S. Govind, and J. J. Childress. 1993. Identification and characterization of two carbonic anhydrases from the hydrothermal vent tube-worm *Riftia pachyptila* Jones. *Mol. Mar. Biol. Biotechnol.* **2:** 10–19.

Lowry, O. H., N. J. Rosebrough, L. Farr, and R. J. Randall. 1951. Protein measurement with the Folin Phenol Reagent. *J. Biol. Chem.* **193:** 267–275.

Lucas, W. J., and J. A. Berry. 1985. Inorganic carbon transport in aquatic photosynthetic organisms. *Physiol. Plant.* **65:** 539–543.

Lutz, R. A., T. M. Shank, D. J. Fornari, R. M. Haymon, M. D. Lilley, K. L. Von Damm, and D. Desbruyéres. 1994. Rapid growth at deep-sea vents. *Nature* **371:** 663–664.

Maren, T. H. 1967. Carbonic anhydrase: chemistry, physiology, and inhibition. *Physiol. Rev.* **47:** 595–779.

Maren, T. H. 1977. Use of inhibitors in physiological studies of carbonic anhydrase. *Am. J. Physiol.* **232:** F291–F297.

Meldrum, N. U., and F. J. W. Roughton. 1933. Carbonic anhydrase: Its preparation and properties. *J. Physiol.* **80:** 113–142.

Raven, J. A. 1984. *Energetics and Transport in Aquatic Plants.* A. R. Liss, New York.

Raven, J. A. 1991. Implications of inorganic carbon utilization: ecology, evolution, and geochemistry. *Can. J. Bot.* **69:** 908–924.

Scott, K. M., C. R. Fisher, J. S. Vodenichar, E. R. Nix, and E. Minnich. 1994. Inorganic carbon and temperature requirements for autotrophic carbon fixation by the chemoautotrophic symbionts of the giant hydrothermal vent tube worm, *Riftia pachyptila. Physiol. Zool.* **67:** 617–638.

Toulmond, A., F. H. Lallier, J. de Frescheville, J. J. Childress, R. Lee, N. K. Sanders, and D. Desbruyéres. 1994. Unusual carbon dioxide-combining properties of body fluids in the hydrothermal vent tubeworm *Riftia pachyptila. Deep-Sea Res.* **41:** 1447–1456.

Weis, V. M. 1991. The induction of carbonic anhydrase in the symbiotic sea anemone *Aiptasia pulchella. Biol. Bull.* **180:** 496–504.

Weis, V. M., G. J. Smith, and L. Muscatine. 1989. A "CO_2 supply" mechanism in zooxanthellate cnidarians: role of carbonic anhydrase. *Mar. Biol.* **100:** 195–202.

Reference: *Biol. Bull.* **196:** 265–272. (June 1999)

Genetic and Morphometric Characterization of Mussels (Bivalvia: Mytilidae) From Mid-Atlantic Hydrothermal Vents

PAULA A. Y. MAAS*, GREGORY D. O'MULLAN, RICHARD A. LUTZ, AND ROBERT C. VRIJENHOEK

Center for Theoretical and Applied Genetics and Institute of Marine and Coastal Sciences, Rutgers University, New Brunswick, New Jersey 08901

Abstract. Mussels were collected from deep-sea hydrothermal vents along the Mid-Atlantic Ridge. Specimens from the Snake Pit site were previously identified genetically and anatomically as *Bathymodiolus puteoserpentis*, but the relationships of mussels from other sites (Logatchev and Lucky Strike) were unclear. Molecular genetic and morphological techniques were used to assess differences among these mussel populations. The results indicate that the range for *B. puteoserpentis* extends from Snake Pit to Logatchev, and that an unnamed second species, *B.* n. sp., occurs at Lucky Strike. Analysis of mitochondrial NADH dehydrogenase subunit 4 (ND4) revealed 13% sequence divergence between the two species. Nei's genetic distance (*D*) based on 14 allozyme loci was 0.112. A multivariate morphometric analysis yielded a canonical discriminant function that correctly identified individuals from these sites to species 95% of the time.

Introduction

Modioliform mussels that depend wholly or in part on symbiotic bacteria for their nutriment are common constituents of biological communities associated with deep-sea hydrothermal vents and cold-water sulfide/hydrocarbon seeps throughout the world. Eight species of these mussels were known to occur in vent and seep environments in the Atlantic and Pacific Oceans (Desbruyères and Segonzac, 1997). Recently, five new species, including one new genus, were described from hydrocarbon seeps in the Gulf of Mexico (GOM) (Gustafson *et al.*, 1998). The new GOM species were first identified in an allozyme study aimed at describing genetic diversity in these mytilids (Craddock *et al.*, 1995a). This study also recognized two genetically distinct populations of mussels from the Mid-Atlantic Ridge (MAR; Fig. 1). The degree of divergence between mussels from the Snake Pit (23°22′N) and Lucky Strike (37°17′N) localities (Nei's $D = 1.179$) led the authors to suggest that two distinct species occupied the MAR. Von Cosel and coworkers (1994) described the mussels from Snake Pit as a new species, *Bathymodiolus puteoserpentis.* On the basis of morphological comparisons, they subsequently suggested that mussels from Lucky Strike should be recognized as a distinct species, but to date the Lucky Strike mussels remain unnamed (von Cosel *et al.*, 1997). We refer to the second MAR species as *B.* n. sp. for the present purposes. Von Cosel *et al.* (1997, p. 146) also suggested that mussels from the southernmost MAR locality (Logatchev; 14°45′N) "belong to another new species, which is however extremely close to *B. puteoserpentis* . . . only an electrophoretic analysis could determine the distance between this new (*e.g.*, Logatchev) species and *B. puteoserpentis.*"

The purpose of this study was to clarify evolutionary relationships among these MAR mussels. We examined mitochondrial DNA sequences and allozyme variation in new samples collected from Lucky Strike, Snake Pit, and Logatchev during July 1997 (Fig. 1; Table 1). We clearly show that the Logatchev population and *B. puteoserpentis* are genetically identical and do not warrant separation as distinct species. In addition, we clarify the genetic distances between the two known Mid-Atlantic Ridge species.

Received 30 November 1998; accepted 9 March 1999.

* To whom correspondence should be addressed. Center for Theoretical and Applied Genetics, Room 318, Rutgers, the State University of New Jersey, 71 Dudley Road, New Brunswick, New Jersey 08901-8521. E-mail: maas@aesop.rutgers.edu

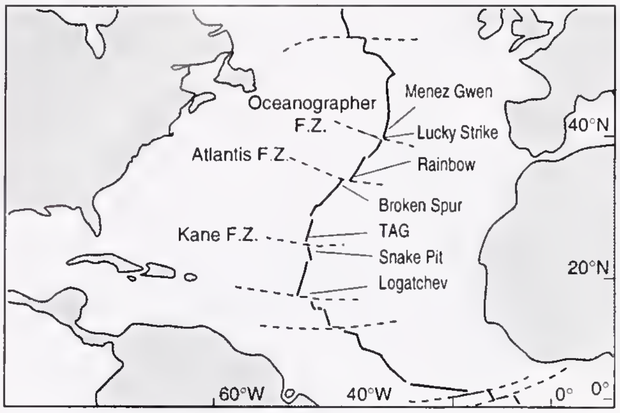

Figure 1. Geographic locations of *Bathymodiolus* collection sites along the Mid-Atlantic Ridge. Major fracture zones (F.Z.) are shown.

Materials and Methods

Specimens

Using the deep submergence vehicle *Alvin's* mechanical claw, samples were collected along the MAR (Fig. 1, Table I) in July 1997. Once aboard the support vessel *Atlantis*, we placed the specimens in 4°C filtered seawater. Mytilids were then either dissected or frozen whole. For dissected specimens, gill, mantle, adductor muscle, and tissue mass were frozen at −70°C in labeled bags; shells were then measured and labeled. All samples were brought back to Rutgers University on dry ice and stored at −80°C until they were prepared for genetic analysis.

DNA extraction, polymerase chain reaction, and sequencing

Whole cellular DNA was isolated by digesting 0.05–0.1 g of frozen tissue following a hexadecyl-trimethyl-ammonium bromide (CTAB) protocol (Doyle and Dickson, 1987), followed by a phenol extraction and ethanol precipitation (Sambrook *et al.*, 1989). Purified nucleic acids were rehydrated in 1X TE buffer (10 m*M* Tris-HCl, pH 7.5; 1 m*M* EDTA) to a final concentration of 100–500 ng/μl and stored for short periods at 4°C and for longer periods at −20°C.

An approximately 710-bp region of the mitochondria was amplified using primers designed to amplify ND4-L in fish. Arg BL (5′-CAA gAC CCT TgA TTT Cgg CTC A-3′) is in the tRNA arginine (Bielawski and Gold, 1996) and NAP 2H (5′-Tgg AgC TTC TAC gTg A/ggC TTT-3′) is within ND4 itself (Arevalo *et al.*, 1994). Comparison of the resulting sequences *via* BLASTN (Altschul *et al.*, 1990) and BLASTP (Altschul *et al.*, 1997) searches of GenBank sequences indicated that these primers amplified tRNA-Met, tRNA-Val, and the first third of ND4 in *Bathymodiolus*. The 50-μl amplification reaction contained 100–500 ng template DNA, 2.5 m*M* $MgCl_2$, 20 μM dNTP (5 μM each nucleotide), 0.4 μM of each primer, 1.5 units *Taq* polymerase, and 5 μl 10× buffer (Promega, Madison, WI). The polymerase chain reaction (PCR) profile (95°C/45s, 56°C/45s, 72°C/min) continued for 35 cycles, with an initial denaturation at 95°C/2 min and a final extension at 72°C/7 min. Negative controls were included with each set of amplifications.

PCR product (5 μl) from each set of reactions was viewed on a 1% agarose gel stained with ethidium bromide, and the remaining 45 μl was extracted once with chloroform/isoamyl alcohol (24:1) and precipitated with 22.5 μl 8 *M* ammonium acetate (pH 5.8) and 90 μl cold 100% ethanol. Sequencing reactions were performed for each individual with both the heavy and light strand primers used for amplification. We used 60–70 ng of template DNA in a 10-μl sequencing reaction containing 4.25 μl FS mix (Applied Biosystems, Foster City, CA), 0.2 μM primer, and sterile distilled H_2O. The cycle-sequencing profile (95°C/30 s, 50°C/15 s, 60°C/4 min) continued for 25 cycles. Electrophoretic separations of the sequencing reactions were performed on a Perkin-Elmer ABI 373 DNA sequencer (Foster City, CA).

The 507-bp ND4 sequence was edited and aligned in Auto Assembler (ver. 1.4.0, Applied Biosystems) and Sequence Navigator (ver. 1.0.1, Applied Biosystems). Trans-

Table 1

Mussel samples collected during July 1997 along the Mid-Atlantic Ridge (MAR)

Location	Latitude Longitude	*Alvin* Dive number	Depth (m)	Species	*n* Sequenced	*n* RFLP	*n* Allozymes	*n* Morphology
Lucky Strike	37°17′N 32°15′W	A3120	1710	*Bathymodiolus* n. sp.	5	11	27	123
Snake Pit	23°22′N 44°56′W	A3129	3480	*B. puteoserpentis*	3	9	30	40
Logatchev	14°45′N 44°58′W	A3133 A3131	3080	*B. puteoserpentis*	5	11	34	113

n is the number of individuals used for each type of analysis.

Table II

Enzyme buffer combinations used in allozyme electrophoresis

Enzyme	Loci	Buffer system
Aspartate aminotransferase	*Aat*	B
Isocitarte dehydrogenase	*Idh*	B
Leucine aminopeptidase	*Lap*	C and D
Malate dehydrogenase	*Mdh*-1, *Mdh*-2	A
Malic enzyme	*Me*	B
Mannose-6-phosphate isomerase	*Mpi*	D
D-Octopine dehydrogenase	*Opdh*	C
Peptidase LG, LGG	*Pep*-gl, *Pep*-lgg	A and D
Phosphoglucose isomerase	*Pgi*	A and D
Phosphoglucomutase	*Pgm*	B and D
6-Phosphogluconate dehydrogenase	*Pgd*	B and D
Superoxide dismutase	*Sod*	C

Buffer A (AP 6.0), B (TC 6.0), C (TVB 8.0) and D (TC 7.0).

lation and amino acid alignments were performed in ESEE (Cabot and Beckenbach, 1989). Genetic distances were calculated in MEGA (Kumar *et al.*, 1994). Due to a large bias in nucleotide base composition, pairwise nucleotide sequence divergence was estimated with the Tajima-Nei distance algorithm (Tajima and Nei, 1984). GenBank accession numbers are AF128534 and AF128533 for haplotypes A1 (*B.* n. sp.) and B1 (*B. puteoserpentis*), respectively.

Restriction fragment length polymorphism analysis

The sequences were used to identify a restriction enzyme, *Cac*8 I, which produced diagnostic restriction band patterns for the two mitochondrial haplotypes A1 and B1. ND4 product was obtained by PCR as described above; 10 μl was digested with 1 μl of *Cac*8 I and 2 μl of the appropriate buffer (New England Biolabs, Beverly, MA) and 7 μl sterile distilled water for a total volume of 20 μl for 1 h at 37°C. Digestions were separated by electrophoresis on a 2% agarose gel containing ethidium bromide. The gel was viewed and photographed under UV light.

Allozymes

About 0.2 g of tissue from the mantle was removed and homogenized in two volumes of grinding buffer (0.05 *M* Tris/20% glycerol, pH 8.0) and spun at 15,000 × *g* for 10 min to remove tissue debris. The supernatant fluid was inserted into a preformed well in a 12.5% starch gel (StarchArt, Smithville, TX). We used four buffer systems that were previously shown to resolve polymorphic enzymes in these mytilids (Craddock *et al.*, 1995a), Buffer A (AP 6), Buffer B (TC 6), Buffer C (TVB 8), and Buffer D (TC 7). Horizontal starch gels were used to assess variation at 14 loci (Table II) following standard protocols (Murphy *et al.*, 1990). To confirm allelic identities, samples were run on multiple gels after the loading order was varied.

Population genetic analyses were performed with programs BIOSYS-1 (Swofford and Selander, 1981) and DISPAN (Ota, 1993). Nei's *D* (Nei, 1978) was estimated from electromorph-frequency data. Agreement with random mating expectations was determined by the "exact HW test" (Guo and Thompson, 1992). *F* statistics were estimated by the method of Nei (Nei, 1977), and heterogeneity among samples was assessed by contingency chi-squared analysis.

Morphology

On board the support vessel, all specimens were measured using a hand-held electric caliper accurate to 0.01 mm. Six shell measurements (Fig. 2) were recorded: A, anterior length (the distance from the anterior shell margin to the anterior edge of umbo); G, ligament length; H, shell height; L, shell length; W, width of shell valves; and U, umbo length (the distance from the anterior edge of umbo to the posterior shell margin). Linear regressions and principal components analysis of morphological data were performed in JMP (SAS Institute, 1986), and discriminant analysis was performed in SAS (SAS Institute, 1997). All variables were natural log transformed prior to multivariate analyses.

Results

Mitochondrial DNA sequences

The DNA fragment used for this study included sequences for two transfer RNAs (200 bp) and the first third of the ND4 gene. The tandemly arranged tRNAs presented problems for alignment of the sequences. Thus for the present study, we used sequences only for the first 507 bp of the protein coding ND4 gene. Altogether, we examined sequences from 13 specimens collected at the three MAR locations (Table I). Six unique ND4 sequences could be assigned to two major haplotypes (A and B) that corresponded to morphospecies *B.* n. sp. and *B. puteoserpentis*, respectively (Fig. 3). On average, the two major haplotypes differed at 13% of the 507 bp (Table III), including 14 inferred amino acid substitutions. Haplotype A included

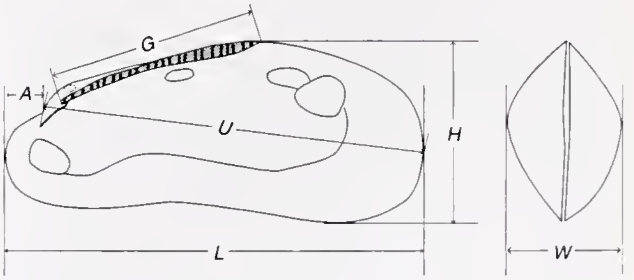

Figure 2. Diagram depicting shell measurements. A, anterior length (distance from anterior shell margin to anterior edge of umbo); H, shell height; L, shell length; G, ligament length; U, umbo length (distance from anterior edge of umbo to posterior shell margin); W, width of shell valves.

A.

```
ATG TGT ATA GTG CTT TTA GGG GTT TTA GGG GTT CTA GAG GTA TCG GTT GCT GGC   54
TTT TCT TTG CTT GGG GTG CTA GCT ATG CCT TTG TTT CTG TCC GGA AGG TGC TCT  108
GAA ATA AAC GGT ATG TTT AAT TTG GAT TTT TCG GGG CAG ACT CTG GTA ATT CTT  162
AGA ATC TAT ATC AGT TTT TTA ATA TTA ATG GGG AGG GTC ACA GTG TCT CGG TTT  216
AGT GCA TTT AAT AGG CTT ATT GTT TGC ATT GGT GCT TTG TTG GTC GGT GCC TTT  270
AGT GTT AGG GTT ACT TTC CTT TTC TTC GTT CTT TTT GAG GGC GTT TTG TTT CCC  324
ACT TTG CTG TTA ATT GTT GGA TGG GGG TAC CAG CCG GAG CGT TTA CAG GCA GTT  378
GTT TAT ATA GTT ATT TAC ACT GTT ATA GGG TCC CTA CCC CTT TTA TAT GGC TTG  432
GGA AAA CTT TAT TTT CAT GAC GGG AGA GAC AAT TTA TTT AGG TTG GAA TTT GTT  486
CTT GAC AAA AGT ATT TTA AGG                                              507
```

B.

```
                       11111111111111122222222222223333344444444444455
         234557789999990001234455788891233566777881445600112233578900
         425453851345692567851817437906858157069182251058176925644212

A1 (3)   CGATCTCCTACTTCATATGCAGTGTGCGGCCGATTTCCACTTGTTTGAATCTAGAATTCT
A2 (1)   ...........................................................C
A3 (1)   ...C........................................................

B1 (3,3) TTGCTCTTCGTCCAGCTCATGACACATAATTAGCGCTTGTCCTAGGAGCCTCGAGGGCT.
B2 (0,1) ..................................................C.........
B3 (0,1) .................................T..........................
AA Δ      *  *      *    * *   **    *  *** *   *                *
```

C.

```
             11334556788896
             19263034904942

A1,2,3 (5)   GLLTSAVVVIVSAF

B1,2   (3,4) VFSSNTIMIVAAVV
B3     (0,1) ..........V...
```

Figure 3. Mitochondrial ND4 haplotypes of the *Bathymodiolus* mussels on the Mid-Atlantic Ridge. Haplotype A corresponds to *B.* n. sp. and haplotype B to *B. puteoserpentis*. For haplotype A, numbers in parenthesis indicate the number of sequences for the Lucky Strike site. For haplotype B, the first number in parenthesis is the number from the Snake Pit site and the second is the number from the Logatchev site. (A) complete sequence for *B. puteoserpentis*, haplotype B1; (B) Nucleotide positions that differ between haplotypes; * indicates non-synonomous substitutions; (C) presumptive amino acid residues that differ between them.

three minor variants that differed by one (A1, A2) or two (A2, A3) synonymous substitutions. Haplotype B included variants that differed from each other by one synonymous substitution (B1, B2) and differed from a third (B3) by one non-synonymous substitution. The percentage sequence divergence within the two major haplotypes was 0.27%.

Population survey (PCR-RFLP)

Given small sample sizes, the mtDNA sequence information did not exclude the possibility of the alternative haplotype also occurring at these putatively monotypic localities. To increase the sample size, we used a six-base cutter enzyme, *Cac*8 I, that produced diagnostic fragment profiles for each major haplotype (Fig. 4). With the added RFLP information, our samples were increased to 12–16 individuals per locality (Table I), 31 specimens total. No additional variation was found within localities.

Allozymes

To quantify within-locality variation, we examined 14 allozyme loci (Table II) that previously were used to discriminate among the MAR mytilid species (Craddock *et al.*, 1995a). Hardy-Weinberg testing of 10 to 11 polymophic loci in each population revealed no significant deviations

Table III

Genetic distances and standard errors (in parentheses) between Mid-Atlantic Ridge Bathymodiolus *species*

	Lucky Strike	Snake Pit	Logatchev
Lucky Strike	0.0027	0.1325	0.1307
	(0.0023)	(0.0186)	(0.0184)
Snake Pit	**0.110**	0.0000	0.0020
	(0.085)	(0.0000)	(0.0020)
Logatchev	**0.114**	**0.000**	0.0027
	(0.088)	**(0.001)**	(0.0023)

Plain type: Average nucleic acid distances within and among populations for a 507-bp fragment of mitochondrial ND4. Boldface type: Nei's D based on 14 polymorphic allozyme loci.

from random mating expectations after application of a sequential Bonferroni adjustment (Rice, 1989). The multilocus observed heterozygosity (H_{obs}; Table IV) approximately equaled the expected value (H_{exp}), revealing no pattern of systematic deviation from random mating.

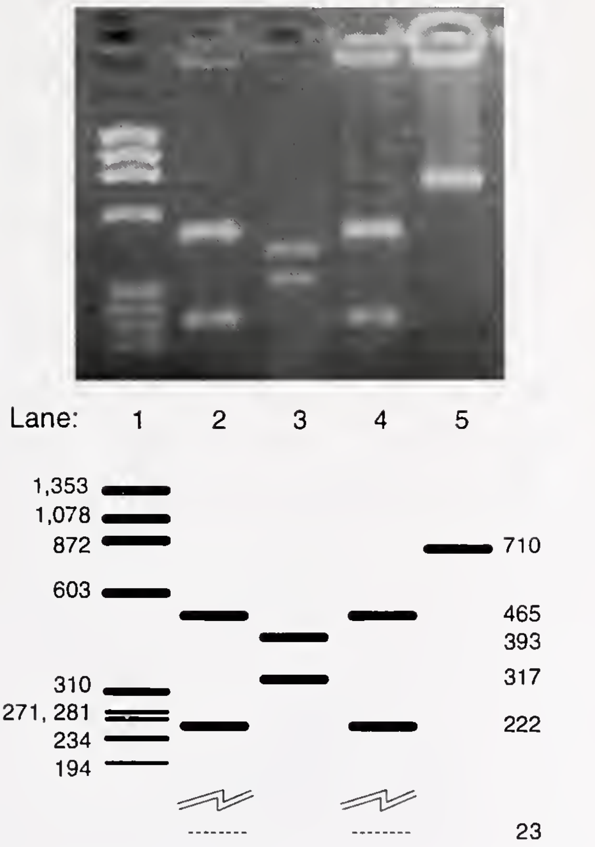

Figure 4. Restriction fragment banding pattern of the two Mid-Atlantic Ridge *Bathymodiolus* haplotypes upon digestion of the mitochondrial ND4 PCR fragment with *Cac* 81. Lanes from left to right are (1) *Phi-X Hind* III ladder; (2) Snake Pit; (3) Lucky Strike; (4) Logatchev; (5) uncut PCR fragment.

Table IV

Allozyme diversity in Mid-Atlantic Ridge Bathymodiolus *species*

Site	n	P_{95}	H_{obs}	H_{exp}
Lucky Strike	26.1	64.29	0.256 (SE0.069)	0.242 (SE0.062)
Snake Pit	29.7	50	0.150 (SE0.045)	0.161 (SE0.052)
Logatchev	33.2	42.86	0.133 (SE0.043)	0.146 (SE0.049)

n = mean sample size; P_{95} = percentage of polymorphic loci (95% criteria); H_{obs} and H_{exp} = observed and expected mean heterozygosity per sample (standard errors in parentheses).

Craddock *et al.* (1995a) did not identify intraspecific polymorphisms in an earlier study that examined 26 gene loci in two mussels from Lucky Strike and two from Snake Pit. Techniques used in this earlier study were optimized to show interspecific differences between more divergent mussel species from the Gulf of Mexico, and thus failed to identify intraspecific variation within the MAR samples. The present study used techniques that were optimized to show the interspecific allozyme differences between *B. puteoserpentis* and *B.* n. sp. Using a subset of 14 loci reported by Craddock *et al.* (1995a), we found a high percentage of polymorphism in each population sample (Table IV). Interspecific monomorphic loci were not examined in this study; thus, the present estimates of polymorphism and heterozygosity should not be used in comparative analyses of genetic diversity.

Nei's (1978) genetic distances (D values) were estimated between the mussel populations from the three locations (Table III). The D value between the Logatchev and Snake Pit samples of *B. puteoserpentis* was 0.00, and the average D value between the two *B. puteoserpentis* samples and *B.* n. sp. was 0.112. The interspecific value is much lower than that reported by Craddock *et al.* (1995a) because the smaller sample sizes used in the previous study resulted in the mistaken interpretation of intraspecific differences as interspecific. We are currently developing a larger array of allozyme and DNA genetic markers to undertake a hierarchical analysis of genetic diversity and intraspecific gene flow among MAR mussel populations.

Morphology

We performed a principal components analysis to assess overall character correlations (Table V) for the six shell characters measured (Fig. 2). The first two rotated axes (PC-1, PC-2) encapsulated 98.5% of the total variance. Covariates of overall size loaded highly on PC-1, and the length of shell anterior to the beak (A) loaded highly on PC-2. A PC-2 component based on similar character loadings was useful for distinguishing among modioliform species from the Gulf of Mexico (Gustafson *et al.*, 1998). Nevertheless, considerable overlap remains between the

Table V

Correlation matrix of six morphological characters (natural log transformed) from Mid-Atlantic Ridge Bathymodiolus *species*

Variable	L	H	W	A	G	U	PC-1	PC-2
L	1.000	0.971	0.973	0.897	0.986	0.997	0.825	−0.527
H		1.000	0.964	0.921	0.959	0.962	0.710	−0.594
W			1.000	0.910	0.966	0.966	0.752	−0.571
A				1.000	0.891	0.872	0.507	−0.847
G					1.000	0.984	0.830	−0.530
U						1.000	0.853	−0.482

The PC-1 and PC-2 columns represent loadings of each character from the first two Varimax rotated principal component axes. L = shell length, H = shell height, W = width of shell valves, A = anterior length, G = ligament length, and U = umbo length (see Fig. 4).

two MAR species (Fig. 5). To develop a more useful morphological diagnostic, we performed a stepwise discriminant analysis with the six shell measurements. Four variables, when used in a canonical discriminant analysis, result in correct identification of individuals with respect to species 95% of the time (Fig. 6). The discriminant equation for the canonical value, C, is

$$C = 1.12 \ln A - 38.16 \ln U + 34.39 \ln L + 4.71 \ln H.$$

Values of $C < 5.5$ were classified as *B.* n. sp., and $C > 6.5$ are *B. puteoserpentis.* Values in the range $5.5 \geq C > 6.5$ could not be assigned to either species, due to the 5% overlap in canonical value distributions. In addition, two *B.* n. sp. individuals had values greater than 6.5.

Discussion

Von Cosel *et al.* (1997) raised doubts about the specific status of newly discovered mussels from the Logatchev locality on the Mid-Atlantic Ridge; the misgivings were based on the morphological affinity between these mussels and *B. puteoserpentis* from the Snake Pit locality. The authors' recommendation of a genetic analysis to resolve relationships between these populations was warranted, as the present study identified no substantial genetic divergence between the two. Despite the observation of considerable allozyme polymorphism within the two populations, Nei's D between them was zero. The mtDNA haplotypes found at the two sites also revealed no evidence for differentiation; sequence divergence averaged 0.2%. Finally, a multivariate analysis of shell morphometrics provided no

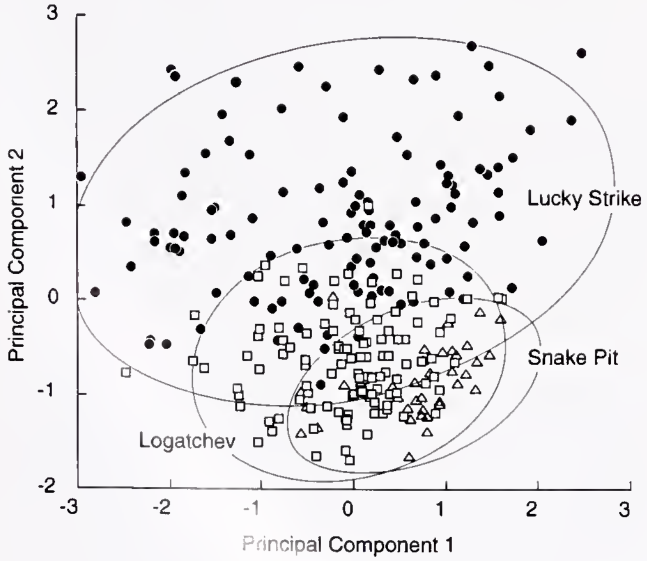

Figure 5. Scatter plot of the first two Varimax rotated principal components (PC-1 and PC-2) for shell measurements of Mid-Atlantic Ridge *Bathymodiolus*. Ellipses encompass 95% confidence limits for each species. Open triangles, *Bathymodiolus puteoserpentis* from the Snake Pit locality; open squares, *Bathymodiolus puteoserpentis* from the Logatchev locality; closed circles, *Bathymodiolus* n.sp. from the Lucky Strike.

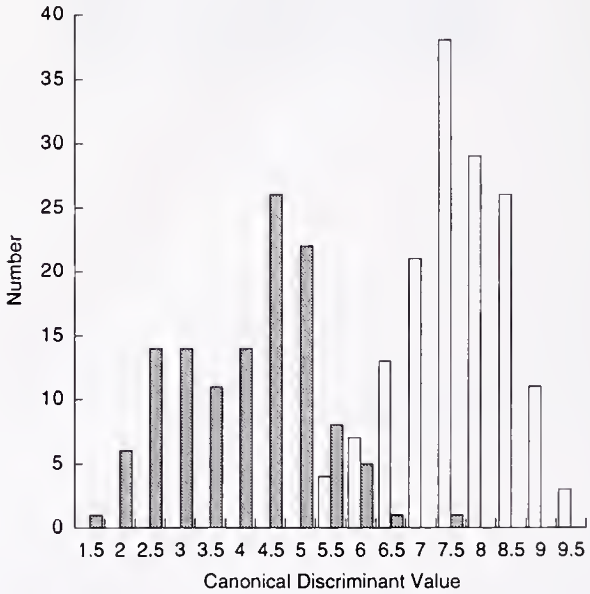

Figure 6. Histogram of the canonical discriminant value for Mid-Atlantic Ridge *Bathymodiolus. Bathymodiolus puteoserpentis* = white bars; *Bathymodiolus* n.sp. = shaded bars.

basis for separating the two *B. puteoserpentis* samples. Clearly, mussels from the Logatchev locality should be considered *B. puteoserpentis.*

The present genetic and morphometric analyses are consistent with recognition of *B. puteoserpentis* and *B.* n. sp. as distinct species. These mytilids typically express extreme morphological variability that may result from living in microhabitats that differ greatly in temperature and water chemistry (von Cosel *et al.*, 1997). Although we found some overlap in morphometric characteristics of the two species, discriminant analysis provided a useful basis for separating them 95% of the time. Dubious individuals, and possibly intergrades, can be identified with the application of molecular methods. First, mtDNA haplotypes based on a 507-bp portion of the mitochondrial ND4 gene unequivocally distinguished between the two species. Sequence divergence between *B. puteoserpentis* and *B.* n. sp. was 13%. This value is consistent with interspecific levels of divergence found in parallel studies of other deep-sea modioliform species (Maas *et al.*, unpubl. data).

In contrast, the present degree of allozyme divergence between *B. puteoserpentis* and *B.* n. sp. ($D = 0.112$) was low compared to an earlier report ($D = 1.179$) for mussels from Snake Pit (*B. puteoserpentis*) and Lucky Strike (*B.* n. sp.), (Craddock *et al.*, 1995a). This discrepancy can be explained by the larger sample sizes in the present study. Although the "number of individuals to be used for estimating genetic distances can also be very small if the genetic distance is large and the average heterozygosity of the two species compared is low" (Nei, 1978, p. 583), these criteria were not met in the light of present information. We found that heterozygosity was high and genetic distance was low; therefore, the earlier study confounded intraspecific variation with interspecific differences.

We are currently using the ND4 haplotypes to better define the ranges of *B. puteoserpentis* and *B.* n. sp. from additional MAR localities (Fig. 1). Preliminary data indicate that *B.* n. sp. is present at northern localities including the Menez Gwen, Lucky Strike, and Rainbow hydrothermal vent fields, and that *B. puteoserpentis* occurs at southern localities including Snake Pit and Logatchev. Preliminary mitochondrial information indicates that both species may occur at an intermediate locality, Broken Spur; however, additional work with allozymes is needed to determine whether the two species intergrade at this site. Several ecological factors contribute to separation of the two MAR species. The northern localities with *B.* n. sp. are at shallower depths, ranging from 869 m to 2303 m; the southern localities, with *B. puteoserpentis*, are at greater depths, ranging from 3080 m to 3480 m (Table 1). Ridge offsets associated with transform faults create barriers to dispersal and prevent mixing of some deep-sea vent species (Van Dover, 1990). Three transform faults (Oceanographer at 35°N, Atlantis at 30°N, and Kane at 24°N) may slow dispersal between the northern and southern localities. It is worth noting that the Broken Spur site (29°10′N) occurs between the Atlantis and Kane Transform Faults, and that it may contain both MAR species, but mussels were very rare at Broken Spur in 1997. We found no mussels at the nearby TAG hydrothermal mound, although a few were previously observed there. It is possible that this intermediate zone (35°N to 24°N) provides an unsuitable habitat for either species of mussel, although other vent-endemic fauna (*e.g., Rimicaris exoculata*) are abundant at these sites (Van Dover, 1995).

Ridge offsets do not appear to provide significant barriers to dispersal for most vent organisms with a free-swimming larval stage (Vrijenhoek, 1997). For example, in the eastern Pacific, the mussel *Bathymodiolus thermophilus* and the vesicomyid clam *Calyptogena magnifica* showed relatively little differentiation and high rates of gene flow among sites along the East Pacific Rise and Galapagos Rift (Craddock *et al.,* 1995b; Karl *et al.,* 1996). All the eastern Pacific sites occurred at about the same depth (~2500 m), however. Because we have no reason to believe that the Mid-Atlantic mussels' dispersal abilities differ from those of *B. thermophilus,* it is possible that depth may provide a more fundamental barrier to dispersal than ridge offsets. We are currently engaged in a more detailed study of gene flow and dispersal in the MAR mytilids.

Acknowledgments

We thank the crews and pilots of the R/V *Atlantis* and the DSV *Alvin* for their collection efforts and technical support. We also thank all the scientists aboard R/V *Atlantis* during MAR 97 for their assistance in the mytilid specimen preparation "assembly line." We are indebted to John Gold for graciously providing primers. This work was supported by NSF grants (OCE-9529819 and OCE-9633131), an NIH grant (PHSTW00735-01), and an internal grant for undergraduate research from the Rutgers University Biodiversity Center. This is contribution no. 99-04 of the Institute of Marine and Coastal Sciences, and New Jersey Agricultural Experiment Station Publication No. D-32104-1-99.

Literature Cited

Altschul, S. F., W. Gish, W. Miller, E. W. Myers, and D. J. Lipman. 1990. Basic local alignment search tool. *J. Mol. Biol.* **215:** 403–410.

Altschul, S. F., T. L. Madden, A. A. Schaffer, Z. Zhang, W. Miller, and D. J. Lipman. 1997. Gapped BLAST and PSI-BLAST: a new generation of protein database search programs. *Nucleic Acids Res.* **25:** 3389–3402.

Arevalo, E., S. K. Davis, and J. W. J. Sites. 1994. Mitochondrial DNA sequence divergence and phylogenetic relationships among eight chromosome races of the *Sceloperus grammicus* complex (Phrynosomatidae) in Central Mexico. *Syst. Biol.* **43:** 387–418.

Bielawski, J. P., and J. R. Gold. 1996. Unequal synonymous substitution rates within and between two protein-coding mitochondrial genes. *Mol. Biol. Evol.* **13:** 880–992.

Cabot, E. L., and A. T. Beckenbach. 1989. Simultaneous editing of multiple nucleic acid and protein sequences with ESEE, v. 3.0. *CABIOS* **5:** 233–234.

Craddock, C., W. R. Hoeh, R. G. Gustafson, R. A. Lutz, J. Hashimoto, and R. J. Vrijenhoek. 1995a. Evolutionary relationships among deep-sea mytilids (Bivalvia: Mytilidae) from hydrothermal vents and cold-water methane/sulfide seeps. *Mar. Biol.* **121:** 477–485.

Craddock, C., W. R. Hoeh, R. A. Lutz, and R. C. Vrijenhoek. 1995b. Extensive gene flow in the deep-sea hydrothermal vent mytilid *Bathymodiolus thermophilus*. *Mar. Biol.* **124:** 137–146.

Desbruyères, D., and M. Segonzac. 1997. InterRidge News. *Handbook of Deep-Sea Hydrothermal Vent Fauna.* Éditions IFREMER, Brest, France.

Doyle, J. J., and E. Dickson. 1987. Preservation of plant samples for DNA restriction endonuclease analysis. *Taxon* **36:** 715–722.

Gun, S. W., and E. A. Thompson. 1992. Performing the exact test of Hardy-Weinberg proportions for multiple alleles. *Biometrics* **48:** 361–372.

Gustafson, R. G., R. D. Turner, R. A. Lutz, and R. C. Vrijenhoek. 1998. A new genus and five species of mussels (Bivalvia, Mytilidae) from deep-sea sulfide/hydrocarbon seeps in the Gulf of Mexico. *Malacologia* **40:** 63–113.

Karl, S. A., S. J. Schutz, D. Desbruyères, R. A. Lutz, and R. C. Vrijenhoek. 1996. Molecular analysis of gene flow in the hydrothermal-vent clam *Calyptogena magnifica*. *Mol. Mar. Biol. Biotechnol.* **5:** 193–202.

Kumar, S., K. Tamura, and M. Nei. 1994. MEGA: Molecular Evolutionary Genetics Analysis software for microcomputers, v. 1.01. *CABIOS* **10:** 189–191.

Murphy, R. W., J. W. Sites Jr., D. G. Buth, and C. H. Houfler. 1990. Proteins I: Isozyme electrophoresis. Pp. 45–126 in *Molecular Systematics*, D. Hillis and C. Moritz, eds. Sinauer Associates, Sunderland, MA.

Nei, M. 1977. F-statistics and analysis of gene diversity in subdivided populations. *Ann. Hum. Genet.* **41:** 225–233.

Nei, M. 1978. Estimation of average heterozygosity and genetic distance from a small number of individuals. *Genetics* **89:** 583–590.

Ota, T. 1993. *DISPAN: Genetic Distance and Phylogenetic Analysis.* Pennsylvania State University, University Park.

Rice, W. R. 1989. Analyzing tables of statistical tests. *Evolution* **43:** 223–225.

Sambrook, J., E. F. Fritsch, and T. Maniatis. 1989. *Molecular Cloning, A Laboratory Manual.* Cold Spring Harbor Press, Cold Spring Harbor, NY.

SAS Institute. 1986. *JMP User's Guide.* SAS Institute, Cary, NC.

SAS Institute. 1997. *SAS System for the Mac OS for Power PC.* SAS Institute, Cary, NC.

Swofford, D. L., and R. K. Selander. 1981. BIOSYS-1: a FORTRAN program for the comprehensive analysis of electrophoretic data in population genetics and systematics. *J. Hered.* **72:** 281–283.

Tajima, F., and M. Nei. 1984. Estimation of evolutionary distance between nucleotide sequences. *Mol. Biol. Evol.* 269–285.

Van Dover, C. L. 1990. Biogeography of hydrothermal vent communities along seafloor spreading centers. *Trends Ecol. Evol.* **5:** 242–246.

Van Dover, C. L. 1995. Ecology of Mid-Atlantic Ridge hydrothermal vents. Pp. 257–294 in *Hydrothermal Vents and Processes*, L. M. Parson, C. L. Walker, and D. R. Dixon, eds. The Geological Society, London.

von Cosel, R., B. Métivier, and J. Hashimoto. 1994. Three new species of *Bathymodiolus* (Bivalvia: Mytilidae) from hydrothermal vents in the Lau Basin and the Fiji Basin, Western Pacific, and the Snake Pit Area, Mid-Atlantic Ridge. *Veliger* **37:** 374–392.

von Cosel, R., T. Comtet, and E. Krylova. 1997. Two new species of *Bathymodiolus* from hydrothermal vents on the Mid-Atlantic Ridge. *Cah. Biol. Mar.* **38:** 145–146.

Vrijenhoek, R. C. 1997. Gene flow and genetic diversity in naturally fragmented metapopulations of deep-sea hydrothermal vent animals. *J. Hered.* **88:** 285–293.

Reference: *Biol. Bull.* **196:** 273–280. (June 1999)

Identification of Sibling Species of the Bryozoan *Bugula neritina* That Produce Different Anticancer Bryostatins and Harbor Distinct Strains of the Bacterial Symbiont "*Candidatus* Endobugula sertula"

SEANA K. DAVIDSON AND MARGO G. HAYGOOD*

Marine Biology Research Division and Center for Marine Biotechnology and Biomedicine,
Scripps Institution of Oceanography, UCSD, La Jolla, California 92093-0202

Abstract. Although the cosmopolitan marine bryozoan *Bugula neritina* is recognized as a single species, natural products from this bryozoan vary among populations. *B. neritina* is the source of the anticancer drug candidate bryostatin 1, but it also produces other bryostatins, and different populations contain different bryostatins. We defined two chemotypes on the basis of previous studies: chemotype O contains bryostatins with an octa-2,4-dienoate substituent (including bryostatin 1), as well as other bryostatins; chemotype M lacks bryostatins with the octa-2,4-dienoate substituent. *B. neritina* contains a symbiotic γ-proteobacterium "*Candidatus* Endobugula sertula," and it has been proposed that bryostatins may be synthesized by bacterial symbionts. In this study, *B. neritina* populations along the California coast were sampled for genetic variation and bryostatin content. Colonies that differ in chemotype also differ genetically by 8% in the mitochondrial cytochrome *c* oxidase subunit 1 (CO 1) gene; this difference is sufficient to suggest that the chemotypes represent different species. Each species contains a distinct strain of "*E. sertula*" that differs at four nucleotide sites in the small subunit ribosomal RNA (SSU rRNA) gene. These results indicate that the chemotypes have a genetic basis rather than an environmental cause. Gene sequences from an Atlantic sample matched sequences from the California chemotype M colonies, suggesting that this type may be cosmopolitan due to transport on boat hulls.

Introduction

The recognition of sibling species throughout the world oceans has gained attention in recent years (Knowlton, 1993; Knowlton and Jackson, 1994; Muricy *et al.*, 1996; Palumbi, 1996). The identification of species that are difficult to distinguish by morphology alone is clearly important to understanding the ecology of a system. This has been demonstrated in studies of the coral *Montastraea annularis* and symbiotic dinoflagellates, which until recently were treated as a single species of coral and a single symbiont (Knowlton *et al.*, 1997; Knowlton *et al.*, 1992). Distinguishing these species is essential to understanding patterns of bleaching and interpreting data regarding environmental degradation and global climate changes (Knowlton *et al.*, 1992; Rowan *et al.*, 1997). In designing research programs, distinguishing sibling species is critical to understanding the biology of a system since these species can differ in their physiology and behavior in ways that affect their relationships and geographic distributions. If multiple species are treated as one species, we are likely to misinterpret the cause of observed patterns. Secondary metabolite chemistry is another character that probably varies among sibling species. The ability to distinguish closely related but apparently identical marine invertebrate species is critical to bioprospecting for pharmaceuticals from the sea and understanding the chemical ecology of the community. One of the obstacles in efforts to find potential drugs is the inconsistent recovery of compounds from different collections of the same organism. This has proven especially troublesome in work with sponges, and for certain species of sponges there is genetic evidence of extensive cryptic speciation (Muricy *et al.*, 1996). Christophersen attributed geographic variation

Received 6 October 1998; accepted 10 February 1999.

* To whom correspondence should be addressed. E-mail: mhaygood@ucsd.edu

in bioactive compounds from some bryozoans to environmental factors (Christophersen, 1991). However, in this study we show that a variation in chemistry from the common marine bryozoan *Bugula neritina* is most likely due to genetic differences.

B. neritina is a common member of fouling communities on boat docks, boat hulls, and submerged rocks. This species has been treated as a single species throughout its cosmopolitan temperate range, although there are consistent chemistry differences among populations (Pettit, 1991). Some features of the biology of *B. neritina* could promote divergence between populations separated by long distances. The dispersal of the larvae is limited, which hinders mixing between populations by larval dispersal alone (Keough, 1989; Wendt, 1996). Larvae are brooded on the colony until they are ready to be released, are nonfeeding, and spend only a few hours in the water column before settling. On the other hand, settlement of these organisms on boat hulls and floating debris allows wide dispersal and mixing between populations separated by long distances.

B. neritina is commonly studied in the laboratory and in field studies because of its abundance and the ease with which larvae can be collected and induced to settle in the laboratory. In recent years, attention has focused on the chemistry of this invertebrate. *B. neritina* produces a series of cyclic macrolides, the bryostatins, which have cytotoxic properties including action against certain cancer cell lines. There are currently 18 different described bryostatins; all have in common the bryopyran ring but vary at two substituent sites (Fig. 1). The structural similarity between the bryostatins and compounds produced by bacteria has led to the proposal that the bryostatins are produced by bacterial symbionts (Anthoni *et al.*, 1990). Bacterial symbionts are borne inside the larvae (Woollacott, 1981); these are γ-proteobacteria named "*Candidatus* Endobugula sertula" (Haygood and Davidson, 1997). These bacteria have not been cultivated; *Candidatus* is a taxonomic status used for bacteria when it is not possible to deposit a type strain (Murray and Stackebrandt, 1995).

Clinical research efforts have concentrated on bryostatin 1,

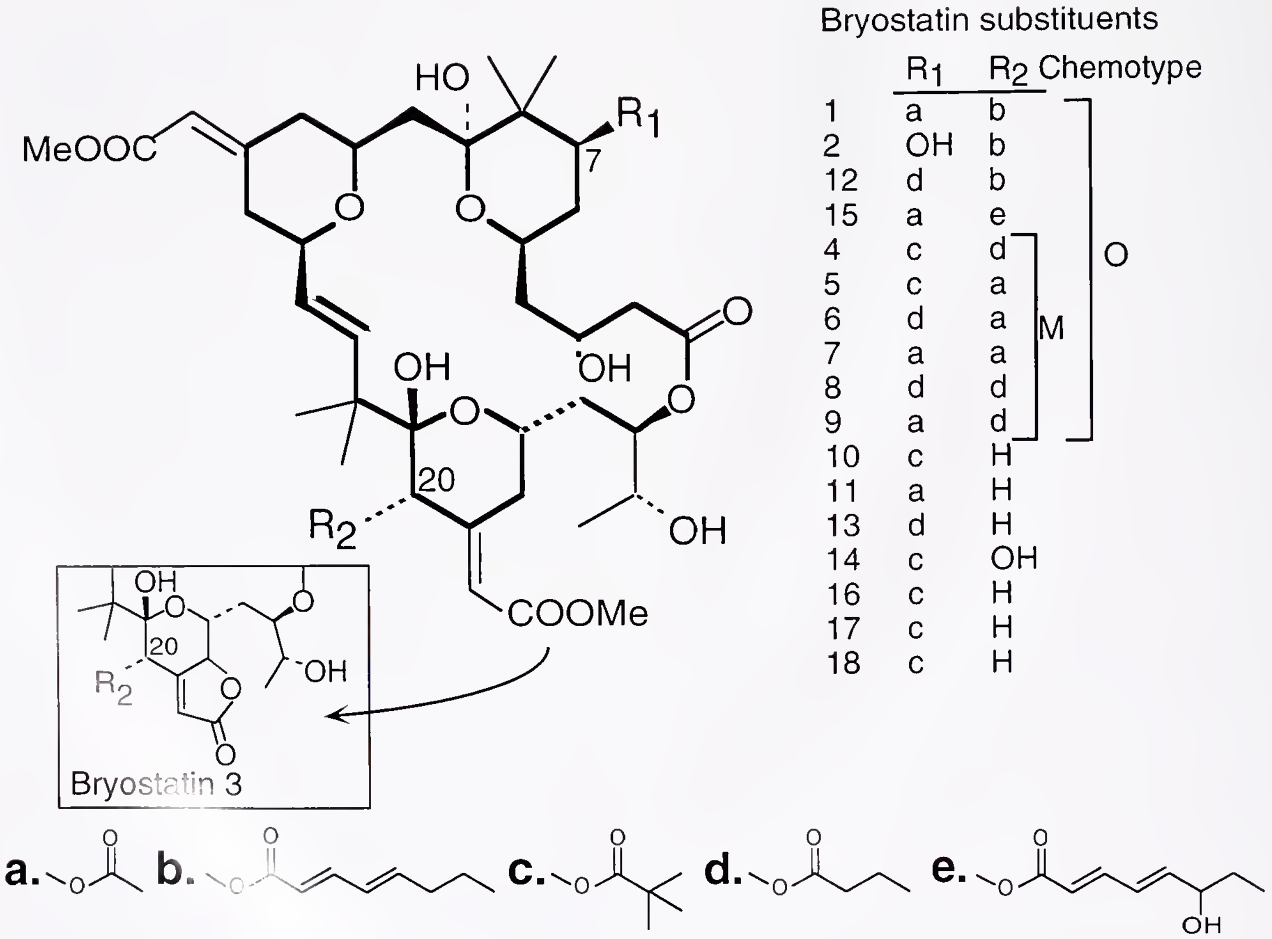

Bryostatin substituents

	R1	R2	Chemotype	
1	a	b		O
2	OH	b		
12	d	b		
15	a	e		
4	c	d	M	
5	c	a		
6	d	a		
7	a	a		
8	d	d		
9	a	d		
10	c	H		
11	a	H		
13	d	H		
14	c	OH		
16	c	H		
17	c	H		
18	c	H		

Figure 1. Structure of bryostatins. The bryopyran ring is in bold. The bryostatins of chemotypes M and O are bracketed.

which is in Phase II clinical trials for the treatment of leukemias, lymphomas, melanomas, and solid tumors (Pluda *et al.*, 1996). Pettit and colleagues observed that bryostatin 1 was found in *B. neritina* samples from California, but not from the Gulf of Mexico (Pettit, 1991). In more extensive work in Southern California, Mendola observed that bryostatin 1 is typically found in deeper samples, but is absent from shallow populations (D. Mendola, pers. comm.). We have defined two bryostatin chemotypes, O and M, on the basis of the observations of Pettit and colleagues in California and Gulf of Mexico populations (Pettit, 1991, Fig. 1). Chemotype O (octa-2,4-dienoate) contains bryostatins with an octa-2,4-dienoate ester at C-20 (bryostatins 1-3, 12, and 15) and small amounts of the minor bryostatins 4-9. The presence of bryostatins 1, 2, or 3 is diagnostic of chemotype O. Chemotype M (minor) contains the minor bryostatins 4-9 only, and lacks the octa-2,4-dienoate ester at C-20. The presence of minor bryostatins and the absence of bryostatins 1, 2, or 3 is diagnostic of chemotype M. Because the occurrence of bryostatins 10-18 is not well characterized, they are not included in the chemotype descriptions.

To investigate the relationship between chemotype and genetic variation in *B. neritina*, three characters were analyzed in samples from 13 locations at various depths along the California coast (Fig. 2), and from one Atlantic location (North Carolina): (1) bacterial symbiont small subunit ribosomal RNA gene sequence (SSU rRNA), (2) host bryozoan mitochondrial cytochrome *c* oxidase subunit 1 gene sequence (CO 1), and (3) bryostatin content.

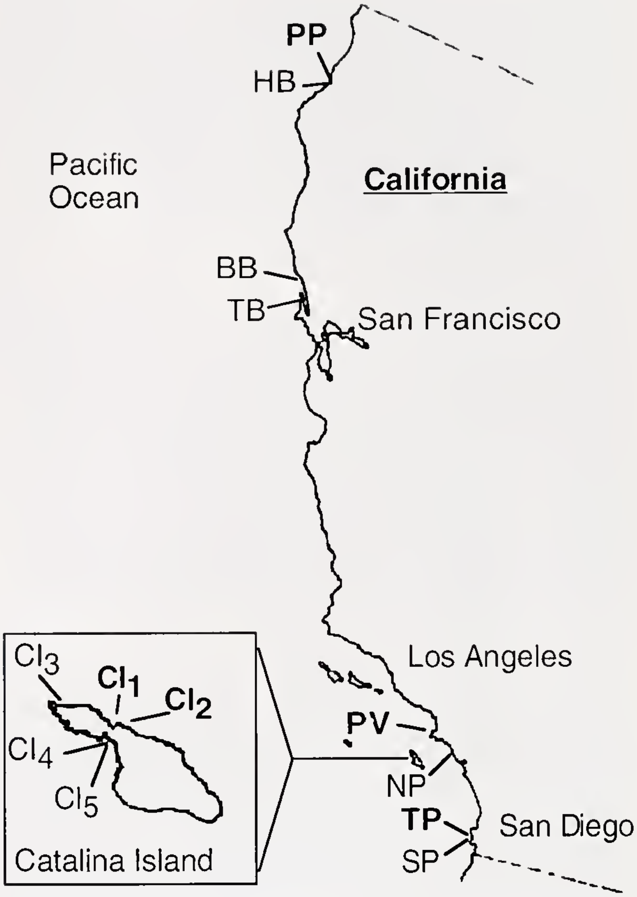

Figure 2. Sampling locations along the California coast. Locations labeled in bold are deeper than 9 m; locations in plain text are shallower than 9 m. Abbreviated site names are designated in Figure 4.

Materials and Methods

Sampling regime

Colonies of *B. neritina* were collected by hand, off docks or subtidally using scuba, along the California coast from Humboldt Bay to San Diego (Fig. 2). *B. neritina* was collected from different depths (ranging from surface to 24 m) at the same location when possible, and at nearby locations in most cases. In addition, one sample was collected in the Atlantic Ocean, from a settling panel array in Beaufort, North Carolina. Samples for chemical analysis were frozen live or dried in the field, then stored frozen at −20° or −80°C. At each site, individual colonies were selected for DNA analysis; these were immediately placed in 95% ethanol in the field and kept cool until stored at −20°C.

DNA extraction, polymerase chain reaction, and sequencing

DNA was extracted from individual colonies by using the QIAGEN QIAamp tissue kit and following the instructions for tissue. To avoid contaminating parent-colony DNA with progeny DNA, only the portions of a colony lacking ovicells, which contain larvae, were used. If necessary, ovicells were removed with forceps before DNA was extracted.

Polymerase chain reaction (PCR), using symbiont-specific primers and conditions described in Haygood and Davidson (1997), was used to amplify about 1060 bp of the "*E. sertula*" SSU rRNA gene. Approximately 710 bp of the bryozoan mitochondrial cytochrome *c* oxidase subunit 1 gene (CO 1) was amplified using primers and conditions described in Folmer *et al.*, 1994. Taq polymerase (Boehringer Mannheim) and included buffer were used for all reactions.

Sequencing was performed using the Applied Biosystems, Inc. (ABI) Prism ready reaction kit FS using guidelines provided by ABI, and reaction products were analyzed on an ABI 373A automated sequencer. The SSU rRNA gene was sequenced using symbiont-specific and universal eubacterial SSU rRNA primers (Haygood and Davidson, 1997; Lane, 1990). The CO I gene was sequenced using the amplification primers. Sequences were aligned in AssemblyLign (Kodak), and differences were counted and compared against the total base pair count to calculate percentage differences. PAUP was used for maximum parsimony phylogenetic analysis (Swofford, 1990), with a transversion cost of 2 relative to transition. Position 365 was excluded from the analysis due to a possible sequencing artifact. A heuristic search was conducted with 10 starting trees created by random addition, and one best tree was found; bootstrap resampling was done 100 times.

Nhe*I restriction digest*

A sequence difference in the SSU rRNA gene between two detected strains of "*E. sertula*" allows rapid identification of strain type by digestion with *Nhe*I (see Fig. 3). The *Nhe*I restriction enzyme cuts only the amplified SSU rRNA gene from one strain (type D) into two fragments. The SSU rRNA gene amplification products were cleaned using the QIAGEN QIAquick PCR purification kit, then digested with *Nhe*I (Boehringer Mannheim) and analyzed by agarose gel electrophoresis.

Bryostatin content analysis

Bryostatin content analyses were performed by Dr. M. Koleck of SAIC-Frederick, under contract to the National Cancer Institute. *B. neritina* samples, 50-90 grams wet weight from each sample site, were sent frozen to SAIC-Frederick, where they were lyophilized, extracted, and analyzed for bryostatin using high-pressure liquid chromotography (HPLC) (Schaufelberger *et al.*, 1990). A portion of each dried sample was removed for extraction and HPLC analysis. Subsample size was 5 g except for samples HB1 (4.44 g) and HB2 (3.47 g). A Rainin-Microsorb column (3 μm C-18, 100 × 4.6 mm I.D.) and corresponding precolumn (15 × 4.6 mm I.D.) were used for HPLC separations. The system includes a Waters 600 E system controller, a Waters 715 Ultra Wisp sample processor, and a Waters 996 photodiode array detector. The mobile phase was aqueous 78% MeCN, UV, at 1 ml/min. Samples were dissolved in MeOH (2 ml). All sample solutions were filtered through Anotop 0.2-μm filters prior to injection (10 μl).

A bryostatin 1 standard was used to establish a bryostatin 1 standard curve to determine the amount of bryostatin 1 in each sample (data not shown). The National Cancer Institute (NCI) standard method for bryostatin analysis was established on the basis of HPLC retention times, absorbance spectra, and phorbol dibutyrate displacement assays of peaks from many *B. neritina* samples. Co-injections of bryostatin 1, 2, and 3 standards confirmed the validity of the method. The results of extensive analysis of *B. neritina* samples has shown that retention times and absorbance spectra are sufficient to identify bryostatins (David Newman, NCI, pers. comm.). The presence of bryostatins 1, 2, and 3 was determined by the appearance of peaks at established HPLC retention times (~11.3, ~5.2, and ~8.1 min respectively) and confirmed by absorption spectra for these peaks scanned from 200 to 600 nm. The diagnostic UV absorbance peaks for the bryostatins that contain the octa-2,4-dienoate ester are at 230 nm and 265 nm.

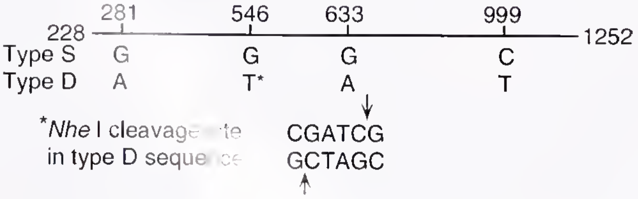

Figure 3. Polymorphic sites in the SSU rRNA gene of "*Endobugula sertula*" strains D and S. The fragment represented results from PCR amplification of the SSU rRNA gene using the symbiont specific primers from Haygood and Davidson (1997). Nucleotide numbers are based on alignment with *E. coli* SSU rRNA gene.

The presence of the minor bryostatins was determined, but individual minor bryostatins were not identified. The minor bryostatins (4-11) each have different HPLC retention times and similar absorbance peaks at 230 nm but not at 265. Most of the common minor bryostatin HPLC peaks are observed at ~9.8 min and ~6.5 min retention. If HPLC peaks cannot be confirmed by the absorbance spectra, the bryostatin in question is scored as not detected.

Chemotypes were assigned as follows: if the minor bryostatins were detected in the absence of bryostatins 1-3, chemotype M was assigned. If bryostatins 1-3 were detected, chemotype O was assigned. In chemotype O *B. neritina*, bryostatins 1-3 are found at much higher levels than the minor bryostatins 4-9 (Pettit, 1991). Thus if minor bryostatins are detectable and bryostatins 1-3 are absent, the sample can be assigned to chemotype M with confidence.

Results

Symbiont strain analysis

The "*E. sertula*" SSU rRNA sequences from populations in Southern California, Northern California, and North Carolina (Atlantic) were identical except for consistent differences at four nucleotide sites within the 1024 bp sequenced from seven locations (Fig. 3). These differences are fixed, not base-paired with each other; they divide the samples into two strains, D (deep) and S (shallow). One of these polymorphisms fell within a restriction enzyme recognition site such that digestion of the SSU rRNA gene amplification product with *Nhe*I could be used to screen individual *B. neritina* colonies for "*E. sertula*" strain (Fig. 3). In Southern California, colonies from sites less than a mile apart were found to have different strains: strain S at sites shallower than 9 m and strain D at sites deeper than 9 m (Figs. 2, 4). In Northern California, colonies containing strain D symbiont were found on the same docks (HB2, Humboldt Bay, Woodley Marina) and shallow rocks

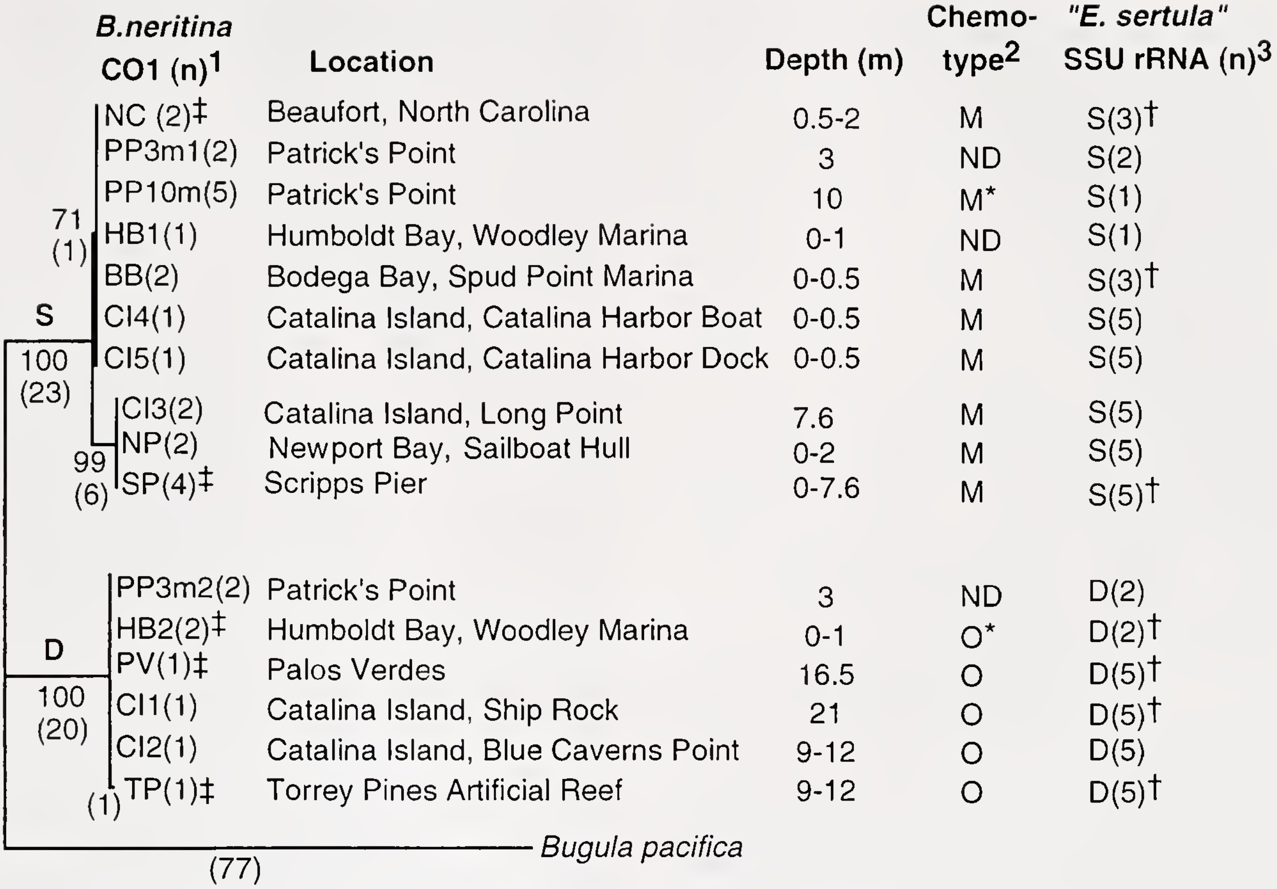

B.neritina CO1 (n)^1	Location	Depth (m)	Chemo-type^2	"*E. sertula*" SSU rRNA (n)^3
NC (2)‡	Beaufort, North Carolina	0.5-2	M	S(3)†
PP3m1(2)	Patrick's Point	3	ND	S(2)
PP10m(5)	Patrick's Point	10	M*	S(1)
HB1(1)	Humboldt Bay, Woodley Marina	0-1	ND	S(1)
BB(2)	Bodega Bay, Spud Point Marina	0-0.5	M	S(3)†
CI4(1)	Catalina Island, Catalina Harbor Boat	0-0.5	M	S(5)
CI5(1)	Catalina Island, Catalina Harbor Dock	0-0.5	M	S(5)
CI3(2)	Catalina Island, Long Point	7.6	M	S(5)
NP(2)	Newport Bay, Sailboat Hull	0-2	M	S(5)
SP(4)‡	Scripps Pier	0-7.6	M	S(5)†
PP3m2(2)	Patrick's Point	3	ND	D(2)
HB2(2)‡	Humboldt Bay, Woodley Marina	0-1	O*	D(2)†
PV(1)‡	Palos Verdes	16.5	O	D(5)†
CI1(1)	Catalina Island, Ship Rock	21	O	D(5)†
CI2(1)	Catalina Island, Blue Caverns Point	9-12	O	D(5)
TP(1)‡	Torrey Pines Artificial Reef	9-12	O	D(5)†

Figure 4. Summary of results. ^{1}Phylogenetic relationships among *Bugula neritina* CO I genes based on 480 nucleotides. *Bugula pacifica* is selected as the outgroup. Horizontal branch lengths are proportional to the number of steps separating groups. Numbers show the bootstrap support of the labeled nodes. Numbers in parentheses indicate the number of steps between nodes. ‡ 638 bp sequenced on both strands. ^{2}M, minor bryostatins detected; O, bryostatins 1-3 and minor bryostatins detected; * tentative, based on HPLC retention times and very weak absorbance spectra for bryostatin 3 and minors; ND, bryostatins not detected. ^{3}"*E. sertula*" SSU rRNA genotype determined by *Nhe*I digestion as shown in Fig. 2. † genotypes confirmed by sequencing.

(PP3m2, Patrick's Point, 3 m) as colonies containing the strain S symbiont (HB1 and PP3m1). In Bodega Bay (BB) and Tomales Bay (TB; not shown in Fig. 4 or 5, sequence data similar to BB) only the strain S symbiont was detected. To date, both strains of "*E. sertula*" have not been found within the same colony of *B. neritina*.

Host bryozoan CO I gene sequence analysis

At most locations sampled, a single "*E. sertula*" strain was detected within the *B. neritina* population. For sequence analysis of the CO I genes, a region of 480 nucleotides was examined. For locations shown to contain a single "*E. sertula*" strain, one or two samples were sequenced, on the assumption that hosts with similar genotypes would contain similar "*E. sertula*" strains. In the case of Northern California, where both symbiont types were detected at the same location, the CO I gene was sequenced from two colonies of each representative type to ensure detection of differences between the hosts. To confirm the accuracy of using the single-stranded CO I sequence, five samples (each from a different site) were sequenced for 638 bp on both strands; all showed similar results. Two distinct lineages (D and S) of *B. neritina* were found. The difference between the two was 8.1% for the 480-bp region (Figs. 4, 5) and 9.1% over 638 bp (data not shown). Additional sequence differences were detected within the type S *B. neritina*, distinguishing two groups that are much more closely related. Both S types were found in Southern California. At Catalina Island, both S_1 and S_2 were present, showing that these two genotypes are present in the same area and at similar depths.

Colonies of CO I genotype D contained "*E. sertula*" strain D, and colonies of CO I genotype S contained "*E. sertula*" strain S.

```
                 4 28 37 43 44 52 85 88 91 100 103 106 121 130 157 172 190 191 199 202 206 217 223 236 268 271 284 298 304 307 313 316 322 325 328 337 349 361 367 394 415 418 427 436 469
       S1 NC     CGTTTTCAACATCTCTATCGCTTGTAATAGGTAGACTGCATCAACC
          PP3m1  ..............................................
          PP10m  ..............................................
Type      HB1    ..............................................
 S        BB     ..............................................
          CI4    ..............................................
          CI5    ..............................................
       S2 CI3    ........G...T..C..........G.GA...G..........
          NP     ........G...T..C..........G.GA...G..........
          SP     ........G...T..C..........G.GA...G..........
          HB2    TA.CCCTG.TGA.CA.GCGATCAACG.C.AAGGA.TAATGCTGGTT
          PP3m2  TA.CCCTG.TGA.CA.GCGATCAACG.C.AAGGA.TAATGCTGGTT
Type      PV     TA.CCCTG.TGA.CA.GCGATCAACG.C.AAGGA.TAATGCTGGTT
 D        CI1    TA.CCCTG.TGA.CA.GCGATCAACG.C.AAGGA.TAATGCTGGTT
          CI2    TA.CCCTG.TGA.CA.GCGATCAACG.C.AAGGA.TAATGCTGGTT
          TP     TACCCCTG.TGA.CA.GCGATCAACG.C.AAGGA.TAATGCTGGTT
```

Figure 5. *Bugula neritina* cytochrome *c* oxidase subunit I gene alignment showing only the variable sites. Sequence corresponds to position 1521-1990 in the published *Drosophila yakuba* mitochondrial genome sequence (Clary and Wolstenholme, 1985) with nucleotide position number noted above. The brackets indicate sequences for *B. neritina* varieties type D and S, including the differences within type S as S_1 and S_2.

Bryostatin content analysis

Bryostatin analysis by HPLC showed that bryostatins of chemotype O (bryostatin 1-3) were detected consistently in *B. neritina* collections from deeper than 9 m in Southern California, and the minor bryostatins of chemotype M (bryostatins 4-9) were detected in *B. neritina* from shallower than 9 m (Figs. 2, 4). Several of these populations have been sampled repeatedly for bryostatin analysis for other studies as well as for this paper and have given consistent results.

At sites farthest north, separation of chemotypes by depth was not apparent, but this result must be interpreted with caution because the chemistry data from *B. neritina* taken in the Humboldt area are ambiguous. HPLC peaks indicative of minor bryostatins, but no peaks for bryostatin 1, 2, or 3, were detected in a *B. neritina* sample from deeper than 9 m (PP10m, Patrick's Point, submerged rocks outside of Humboldt Bay); these findings are indicative of chemotype M. Absorbance spectra were weak, but consistent with minor bryostatins. This sample had CO I type S and "*E. sertula*" strain S. One of the dock samples from Humboldt Bay (HB2) yielded HPLC peaks at the correct retention times for bryostatins 1, 2, and 3, and the minor bryostatins, indicating chemotype O. However, the absorbance spectra were too weak (bryostatin 3), or possibly were obscured by compounds in overlapping peaks, to positively confirm the bryostatin identification. For these two Northern California samples, chemotype designations are tentative due to lack of clear confirmation by absorbance spectra.

Consistently, the collections of *B. neritina* with type D CO I genotype and strain D "*E. sertula*" contained the bryostatins of chemotype O. Those samples with genotype S host and symbiont contained bryostatins of chemotype M.

Discussion

In this study we identified two types (D and S), probably species, of the marine bryozoan nominal species *Bugula neritina* that differ in their mitochondrial CO I sequences by approximately 8%. Each type harbors a distinct strain of the bacterial symbiont "*E. sertula*" and has a characteristic chemistry profile. Both of these *B. neritina*/"*E. sertula*" associations produce bryostatins, but only type D contains the additional bryostatins 1-3, characterized by the octa-2,4-dienoate ester at C-20 of the bryopyran ring (Fig. 1). We found that, without exception, the type D *B. neritina* lineage contains strain D "*E. sertula*" and chemotype O bryostatins. The type S *B. neritina* lineage contains strain S "*E. sertula*" and bryostatins of chemotype M (Fig. 4).

In Southern California, the two types of *B. neritina* were found in the same areas but at different depths (transition at about 9 m). In Northern California, colonies containing type D host and symbiont were found on the same docks (Humboldt Bay) and shallow 3-m rocks (Patrick's Point) as colonies containing the type S host and symbiont. This pattern suggests that the two types are separated by an environmental parameter such as temperature, as has been found in some other marine invertebrates (Hellberg, 1998;

Knowlton, 1993). In Southern California, where the two types are separated, surface waters become several degrees warmer in the spring through early fall. In Northern California, however, the surface remains much cooler. Additional research must be conducted before any conclusions can be drawn regarding the cause of the separation. The North Carolina *B. neritina* matches the type S *B. neritina* in California. The predominance of type S on boat docks and hulls and its appearance in both the Atlantic and Pacific indicates that this genotype of *B. neritina* is transported on boat hulls and may have a worldwide distribution mediated by human transport. The type D genotype, however, has a more restricted distribution that relies on larval dispersal and promotes divergence between widely separated populations. Additional samples from deep locations in the Atlantic and other areas will be valuable in confirming this hypothesis. The type S may have a broader temperature tolerance or other characters, such as better pigment protection from UV, that allow it to survive conditions it may experience on boat hulls. Taken together, these data suggest that two sympatric species of *B. neritina* exist in California.

A serendipitous experiment provided evidence that the type D *B. neritina* does not colonize shallow habitats in Southern California even if type D larvae are introduced there. *B. neritina* is a normal inhabitant of the Scripps Pier, La Jolla, California. Over a period of 3 years, larvae from Palos Verdes parent stock (consistently chemotype O and type D genotype) collected at about 16.5 m have been poured into the water around the pier as a consequence of aquaculture research. Cumulatively, these releases, each lasting 2 weeks and taking place three or four times yearly from spring through fall, put hundreds of thousands of larvae into the water. In November 1997, about a month after the end of the summer season of larval release, samples were taken from the Scripps Pier pilings in an attempt to detect any type D *B. neritina* that may have become established over the 3-year period. At the time, the only *B. neritina* present were located at the bottoms of the pilings (4.5-7.5 m). The colonies were small (5 cm tall), which matched expected colony size for the settlement dates of the recently released larvae. Collections were taken from each northern piling along a transect from just below the location of release out to the end of the pier. Five colonies from each of the six pilings sampled were tested for symbiont genotype. Strain D symbionts were not detected in any of the samples. All the sequences and *Nhe*I digests of the SSU rRNA "*E. sertula*" gene taken from previous pier samples over 3 years have been strain S. The host bryozoan CO I gene was sequenced from two individuals, and these sequences matched type S. Bryostatin analysis of each of the pier samples and of previous collections revealed only the bryostatins of chemotype M, consistent with the genotype found. These results suggest that the type D *B. neritina* is not able to establish a major population on the pier.

The finding that chemotypes O and M occur in distinct lineages of *B. neritina* indicates that there is a genetic basis for patterns of bryostatin synthesis. Previous experimental work has shown that bryostatins do not accumulate from the diet (Thompson and Mendola, 1993), but did not rule out the influence of other environmental factors in determining the types of constituents used in bryostatin synthesis. A type D shallow sample (HB2) probably contains chemotype O bryostatins (by HPLC retention times), whereas a type S sample at 10 m (PP10m) does not, and is probably chemotype M. If so, these samples strengthen the argument that bryostatin substituents are determined by genetic capabilities and not by environmental factors associated with depth. It is possible that the chemotype differences are due to the different strains of "*E. sertula*" in the two types, to a difference in the host bryozoan, or to an additional unknown bacterium. In any case, one *B. neritina*/"*E. sertula*" mutualism is capable of making the octa-2,4-dienoate substituents of bryostatins 1-3, 12, and 15, and the other is not. It is also possible that there are additional genotypes of *B. neritina*/"*E. sertula*," and new bryostatins may be discovered in areas that remain to be sampled.

In some cases the consistent re-isolation of natural products from marine invertebrates has been problematic, possibly because of difficulty in distinguishing closely related species or subspecies. On the other hand, geographic variation in bioactive compounds from a few bryozoans has been attributed to environmental factors (Christophersen, 1991). The present study provides evidence that invertebrate sibling species can contain different natural products, and it illustrates that distinguishing variants is important to ensure consistency in natural product chemistry. Variations in secondary metabolite chemistry should be included among the reasons, discussed by Knowlton and Jackson (1994), that proper taxonomy is critical to understanding the diversity, evolution, and ecology of a system. Molecular characterization provides a powerful tool for this endeavor. The chemistry, chemical ecology, and biology of variants may differ slightly but significantly, as in the case of *B. neritina*, where the genotypes are indistinguishable in the field, but one produces the commercially important compound and the other does not. Moreover, these chemical differences may determine the predators to which the colonies are susceptible. It is possible that these or other subtle chemical differences affect chemical defense and thus influence the ecology of the bryozoan.

Genbank Accessions #s: PP3m1, AF061429; PP3m2, AF061430; PP10ml, AF061431; HB1, AF061427; HB2, AF061428; BB, AF061426; CI1, AF061417; CI2, AF061418; CI3, AF061419; CI4, AF061420; CI5, AF061421; PV, AF061422; NP, AF061423; TP AF061424; SP, AF061425; NC, AF061432; *B. pacifica*, AF061433.

Acknowledgments

We thank those who helped collect samples, especially CalBioMarine Technologies, Inc., Dr. L. V. Basch, Ron McConnaughey, Dr. Dan Rittschof, and Dr. Ron LeValley. Mary Koleck of SAIC-Frederick, Maryland, provided bryostatin analyses sponsored by the National Cancer Institute through a grant to CalBioMarine Technologies, Inc. Ron Burton provided advice regarding the population genetic survey.

This paper is funded by a grant from the National Sea Grant College Program, National Oceanic and Atmospheric Administration, U.S. Department of Commerce, under grant number NA66RG0477; by project number R/MP-61 through the California Sea Grant College System; and in part by the California State Resources Agency. The views expressed herein are those of the authors and do not necessarily reflect the views of NOAA or any of its sub-agencies. The U.S. Government is authorized to reproduce and distribute for governmental purposes.

Literature Cited

Anthoni, U., P. H. Nielsen, M. Perieira, and C. Christophersen. 1990. Bryozoan secondary metabolites: a chemotaxonomical challenge. *Comp. Biochem. Physiol.* **96B:** 431–437.

Christophersen, C. 1991. Evolution in molecular structure and adaptive variance in metabolism. *Comp. Biochem. Physiol.* **98B:** 427–432.

Clary, D. O., and D. R. Wolstenholme. 1985. The mitochondrial DNA molecule of *Drosophila yakuba:* nucleotide sequence, gene organization and genetic code. *J. Mol. Evol.* **22:** 252–271.

Folmer, O., M. Black, R. Hoeh, R. Lutz, and R. Vrijenhoek. 1994. DNA primers for amplification of mitochondrial cytochrome *c* oxidase subunit I from diverse metazoan invertebrates. *Mol. Mar. Biol. Biotechnol.* **3:** 294–299.

Haygood, M. G., and D. K. Davidson. 1997. Small subunit ribosomal RNA genes and *in situ* hybridization of the bacterial symbionts in the larvae of the bryozoan *Bugula neritina* and proposal of "*Candidatus* Endobugula sertula." *Appl. Environ. Microbiol.* **63:** 4612–4616.

Hellberg, M. E. 1998. Sympatric sea shells along the sea's shore: the geography of speciation in the marine gastropod *Tegula. Evolution* **52:** 1311–1324.

Keough, M. J. 1989. Dispersal of the bryozoan *Bugula neritina* and effects of adults on newly metamorphosed juveniles. *Mar. Ecol. Prog. Ser.* **57:** 163–171.

Knowlton, N. 1993. Sibling species in the sea. *Annu. Rev. Ecol. Syst.* **24:** 189–216.

Knowlton, N., and J. B. C. Jackson. 1994. New taxonomy and niche partitioning on coral reefs: jack of all trades or master of some? *Trends Ecol. Evol.* **9:** 7–9.

Knowlton, N., E. Weil, L. A. Weigt, and H. M. Guzman. 1992. Sibling species in *Montastraea annularis,* coral bleaching, and the coral climate record. *Science* **255:** 330–333.

Knowlton, N., J. L. Mate, H. M. Guzman, and R. Rowan. 1997. Direct evidence for reproductive isolation among the three species of the *Montastraea annularis* complex in Central America (Panama and Honduras). *Mar. Biol.* **127:** 705–711.

Lane, D. S. 1990. 16S and 23S rRNA sequencing. Pp. 115-148 in *Nucleic Acid Techniques in Bacterial Systematics.* E. Stackebrandt and M. Goodfellow, eds. John Wiley, New York.

Muricy, G., A. M. Sole-Cava, J. P. Thorpe, and N. Boury-Esnault. 1996. Genetic evidence for extensive cryptic speciation in the subtidal sponge *Plankina trilopha* (Porifera: Demospongiae: Homoscleromorpha) from the Western Mediterranean. *Mar. Ecol. Prog. Ser.* **138:** 181–187.

Murray, R. G. E., and E. Stackebrandt. 1995. Taxonomic Note: Implementation of the provisional status *Candidatus* for incompletely described procaryotes. *Int. J. Syst. Bacteriol.* **45:** 186–187.

Palumbi, S. R. 1996. What can molecular genetics contribute to marine biogeography? An urchin's tail. *J. Exp. Mar. Biol. Ecol.* **203:** 75-92.

Pettit, G. R. 1991. The bryostatins. *Prog. Chem. Org. Nat. Prod.* **57:** 153–195.

Pluda, J. M., B. D. Cheson, and P. H. Phillips. 1996. Clinical trials referral resource. Clinical trials using bryostatin-1. *Oncology (Huntingt)* **10:** 740–742.

Rowan, R., N. Knowlton, A. Baker and J. Jara. 1997. Landscape ecology of algal symbionts creates variation in episodes of coral bleaching. *Nature* **388:** 265–269.

Schaufelberger, D. E., A. B. Alvarado, P. Andrews, and J. A. Beutler. 1990. Detection and quantitation of bryostatin 1 and 2 in *Bugula neritina* by combined high-performance liquid chromatography and ^{3}H-phorbol dibutyrate displacement. *J. Liq. Chromatogr.* **13:** 583–598.

Swofford, D. L. 1990. PAUP: *Phylogenetic Analysis Using Parsimony, 3.0.* Ill. Nat. Hist. Surv., Champaign, Illinois.

Thompson, J., and D. Mendola. 1993. *Aquacultural Production of Bryostatin 1: Non-confidential Results of the Phase 1 Project.* Small Business IR Report, CalBioMarine Technologies, Inc., Carlsbad, California.

Wendt, D. E. 1996. Effect of larval swimming duration on success of metamorphosis and size of the ancestrular lophophore in *Bugula neritina* (Bryozoa). *Biol. Bull.* **191:** 224–233.

Woollacott, R. M. 1981. Association of bacteria with bryozoan larvae. *Mar. Biol.* **65:** 155–158.

Reference: *Biol. Bull.* **196:** 281–294. (June 1999)

Cuticle Strength and the Size-Dependence of Safety Factors in *Cancer* Crab Claws

A. RICHARD PALMER*, GRAEME M. TAYLOR, AND ANISE BARTON

Department of Biological Sciences, University of Alberta, Edmonton, Alberta T6G 2E9, Canada; and Bamfield Marine Station, Bamfield, British Columbia V0R 1B0, Canada

Abstract. The surprising incidence of nonlethal skeletal fractures implies that many organisms operate near their upper performance limits, yet we know little about the loads at which biological structures break or about the material properties of those structures. In addition, biologically realistic estimates of how closely normal maximal loads approach breaking strengths (*i.e.*, safety factors) remain elusive. We measured cuticular breaking strength (a material property) and safety factors (breaking force/maximum biting force) for intact claws of six species of predatory *Cancer* crabs (Crustacea, Brachyura). Cuticular breaking stresses in *Cancer* claws (40–120 MN m^{-2}) exceeded those reported for the carapace of shore crabs (*Carcinus*) and swimming crabs (*Scylla*), but were similar to published values for the claws of stone crabs (*Menippe*). Cuticular breaking strength increased towards the tip of the pollex (fixed finger), correlated with visible changes in the claw cuticle, but decreased with increasing claw size. Safety factors of the pollex varied within and among *Cancer* species and ranged from 2 to 7. Safety factors increased with increasing claw size ($\propto$manus length$^{0.6}$), due to proportionally thicker cuticle ($\propto$manus length$^{1.31 \pm 0.078}$) and proportionally lower maximum biting forces ($\propto$manus length$^{1.49 \pm 0.082}$). Why larger crabs have proportionally lower biting forces remains an important unsolved problem. The higher safety factors of larger claws appear adaptive, however, since costs of failure and unpredictability of cuticle strength increase with increasing size. Patterns of intraspecific size-dependence offer an attractive test of whether safety factors vary adaptively. A brief review of the literature suggests that positive size-dependence often signals adaptive variation in safety factors, whereas negative size-dependence may signal the action of constraints on growth or form.

Introduction

Rather unexpectedly, structures as diverse as mollusc shells (Vermeij, 1982; Brandwood, 1985), crab claws (Juanes and Hartwick, 1990; Taylor *et al.*, in press), the teeth of living and extinct carnivorous mammals (Van Valkenburgh, 1988; Van Valkenburgh and Hertel, 1993), the antlers of ungulates (Kitchener, 1991), and the limbs of birds and mammals (Buikstra, 1975; Currey, 1984; Brandwood *et al.*, 1986) exhibit high rates of nonlethal failure in natural populations. The skeletons of many organisms therefore appear to operate near their upper performance limits under normal living conditions, and safety factors (*e.g.*, the ratio of breaking strength to maximum load) should be under constant pressure to evolve. Yet enhanced durability bears a price and, like most attributes of organisms, must reflect a balance between the benefits of increased performance and the costs of construction, maintenance, and possible failure (Alexander, 1982).

Because explicit predictions exist for how safety factors should vary under different situations (Alexander, 1981, 1997), tests may be conducted to assess how closely biological structures approach theoretical design optima. Compared to analyses of among-species differences, those of size-dependent variation within species offer even more rigorous tests because fewer potentially confounding factors vary and predictions are therefore more precise (Currey, 1977; Niklas, 1994). For example, for the brachyuran crabs we studied, larger crabs should exhibit higher claw safety factors for several reasons: (a) stress cracks and wear have more time to accumulate between molts, which increases the unpredictability of claw strength in larger crabs, (b) the negative ecological impact of lost or damaged claws (Juanes

---

Received 11 August 1998; accepted 25 March 1999.

* To whom correspondence should be addressed. E-mail: rich.palmer@ualberta.ca

and Smith, 1995) will be more prolonged or severe for larger crabs, and (c) larger crabs may experience a greater range of extreme forces because claws are used increasingly for aggression (Juanes and Smith, 1995).

Intraspecific size-dependence of safety factors may also reveal unexpected geometrical or ontogenetic constraints that preclude an optimal design. For example, if cuticle thickness varies in proportion to body mass within a species, the critical buckling loads of walking legs in smaller insects must greatly exceed the likely maximal loads experienced to ensure an appropriate critical buckling load at larger body size (Prang, 1977). Similarly, the stems of small horsetails, *Equisetum,* are mechanically "overbuilt" by roughly 10 times compared to larger plants (Niklas, 1989). In both of these examples of narrow, tubular support systems, mechanical and growth considerations appear to conflict.

Unfortunately, biologically realistic distributions of strength and, particularly, load are difficult to measure with confidence for most structures, so estimates of safety factors of individual organisms are often indirect. Typically, safety factors are estimated either (a) by computing or measuring maximal loads on aggregate samples and then comparing these to standard estimates of material properties or theoretical estimates of failure strengths (Alexander, 1981; Biewener, 1990; Niklas, 1994; Biewener and Dial, 1995; Claussen and Maycock, 1995), or (b) by computing an average maximum load and an average breaking force measured on different samples of individuals (Lowell, 1985, 1987; Friedland and Denny, 1995). Crab claws offer a particularly attractive opportunity for direct study of the intraspecific size-dependence of safety factors because both maximal closing forces and breaking forces can be measured on an individual claw. In addition, because the entire cuticle is assembled anew following a molt, the intermolt interval may be considered a "lifetime" for a claw (Taylor *et al.,* in press) in the same way as ungulate antlers that are also renewed annually (Kitchener, 1991). Therefore, we could examine intraspecific variation that would otherwise not be apparent using indirect approaches.

We examined the size-dependence of safety factors in the claws of six closely related species of *Cancer* crabs, to test whether safety factors varied in a manner more consistent with adaptation or constraint: do claw safety factors increase with increasing crab size—as would be expected because of increased unpredictability of cuticle strength, increased costs of failure, and possibly increased unpredictability of load distribution (Juanes and Smith, 1995)—or do they decrease with increasing crab size, because geometric or ontogenetic constraints associated with the growth of "external" tubular support systems yield structures that must be disproportionately strong at smaller sizes to retain function at larger sizes, as suggested for insect legs (Prang, 1977) and the shoots of horsetails (Niklas, 1989).

Throughout the paper, we apply the verb *to bite* to the action of claws. Although most commonly used in reference to mouthparts, we invoke it here because anyone attacked by a large crab would surely exclaim that they had been bitten rather than squeezed, grasped, pinched, or nipped, and because in carnivorous brachyuran crabs claws function to crush prey, or to tear apart the flesh, much like vertebrate jaws.

Materials and Methods

Experimental animals

Crabs collected from various shallow-water sites near Bamfield, British Columbia, Canada (see Table 1 for size ranges) were held in running seawater aquaria and fed shucked mussels daily (*Mytilus* spp.). Biting forces of claws were measured within 7 days of collection, as maximum force and consistency declined with time in the laboratory (G. M. Taylor, unpubl. obs.). Crabs with damaged or regenerating claws were not used, nor were crabs suspected to be early or late intermolt (Taylor *et al.,* unpubl. obs.) because biting forces (Kaiser *et al.,* 1990) and cuticle properties (Horst and Freeman, 1993) may vary substantially over the intermolt interval.

To minimize among-investigator variation, GMT mea-

Table I

Crab size, load position, and number of bites obtained per claw for six species of Cancer *crabs*

Species	n_t	Carapace width (mm) Mean (SE, min., max.)	n_c	Load position (SE)*	Mean # bites per claw (SE)
C. antennarius	14	76.1 (3.20, 56.4, 99.1)	28	0.89 (0.005)	7.8 (0.07)
C. branneri	8	51.0 (1.30, 44.9, 55.5)	16	0.92 (0.003)	6.9 (0.48)
C. gracilis	9	91.4 (3.13, 74.9, 103.8)	18	0.94 (0.002)	7.1 (0.75)
C. magister	[illegible]	122.6 (2.58, 111.4, 139.2)	23	0.94 (0.004)	7.8 (0.42)
C. oregonensis	15	33.1 (0.76, 29.4, 39.9)	30	0.86 (0.004)	7.4 (0.18)
C. productus	16	89.6 (6.26, 60.1, 130.1)	31	0.91 (0.006)	8.3 (0.20)

n_t = number of individual crabs, n_c = number of claws for which biting force measurements were obtained; not all claws were included in all analyses (see Methods).

* Position at which biting force or breaking strength was measured, expressed as a proportion of the pollex length (line d–e, Fig. 1).

sured biting force in all cases and AB measured claw morphometrics and breaking strengths.

Biting force measurements

Crabs were encouraged to grasp a force gauge with their claw and bite as hard as possible while held firmly in the air by the proximal portions of both chelipeds so other movement would not affect the biting force measurements. The pollex (fixed finger) was inserted into a lower fixed steel ring, and the dactyl into an upper ring mounted on a flexible 2-mm-thick steel beam bearing two strain gauges (Bean BAE-13-250BB-350TE; 350Ω) that were connected to a Wheatstone bridge and a chart recorder. The rings were positioned at the same point for all claws: just inside the tip of the dactyl and pollex, distal to the first tooth (*i.e.,* the same position as the load when breaking the claw, Fig. 1, Table I). To ensure comparable biting forces among claws of different size, the distance between the inner margins of the rings was adjusted to about 60% of the maximum gape at this position for each claw. Before and after each session of 7–10 crabs, deflections of the upper ring were calibrated with five known weights (4.6–112 N) that exceeded the full range of observed maximum biting forces. The average of these two curves was used to digitize calibrated biting forces after each session.

Biting forces were measured for both claws of each crab in succession. To avoid possible biases, the first measurement alternated between the right and left claw on successive trials. At most, two measurements were obtained per claw per day, separated by at least 4 h. Mean number of trials per claw varied from 6.9–8.3 among species (Table I); claws with fewer than four trials were excluded from the analyses. Though median-maximum biting force exhibited less statistical noise, the allometric coefficient was statistically indistinguishable from that for extreme-maximum biting force (see Table Ve *versus* Vf), so extreme-maximum biting forces were used to permit comparison with previously published values.

Morphometry and breaking force

Claw and cuticle dimensions (Fig. 1) were digitized with a Summagraphics drawing tablet (20 dots/mm resolution) from enlarged (8–12×), calibrated camera lucida drawings of autotomized claws (Wild M5A dissecting microscope with a 0.3× reducing lens, if necessary). This method is accurate to within ±1% (Smith and Palmer, 1994).

Claws were broken within 1 h of autotomy and held in seawater or kept wet continuously until broken. Breaking forces were typically measured within 2–3 days of the last biting force, and never more 14 days after the last biting force. To obtain breaking forces, claws were clamped rigidly, and a container was suspended from the tip of the pollex by a loop of 4 mm diam. steel wire (Fig. 1). Lead weights to about 80% of the estimated breaking force were gently added, and then sand was poured into the container at a constant rate (approx. 5 g/s) until the claw broke. The container and contents were then weighed to the nearest gram.

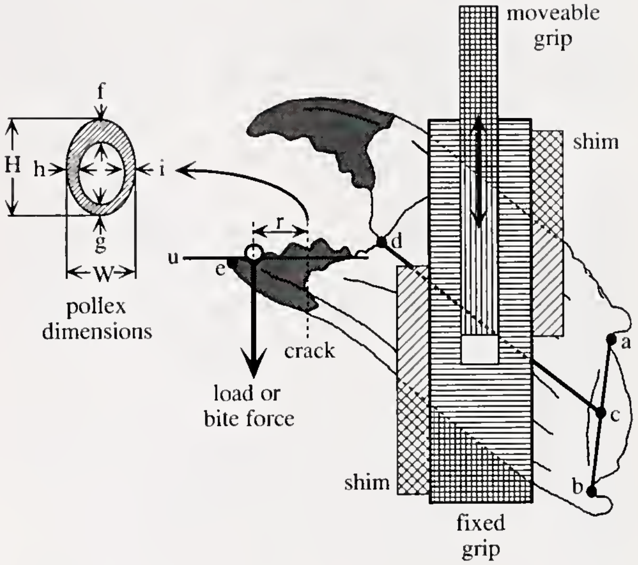

Figure 1. Clamping orientation and dimensions of a *Cancer* claw. (a) and (b) are the dorsal and ventral hinge points of the manus, and (c) is the midpoint between them. *Manus length*: line-segment (c)–(d) (*i.e.*, chela length excluding the pollex). *Pollex (= fixed finger) length*: line-segment (d)–(e). *Moment of the load at failure*: the double-headed arrow labeled r. Moveable (vertical shading) and fixed (horizontal shading) pieces of acrylic plastic (Plexiglas) gripped the claw at about the midpoint of the manus, and softer wooden shims (angled-shading) reduced the risk of twisting and unwanted damage to claws under load; cross-hatching indicates the acrylic or shim was solid at that point. These acrylic pieces and shims had notches cut in them to fit either the right or left claw as snugly as possible (not visible in the figure as they were parallel to the plane of view). Claws were aligned so the load was oriented perpendicular to the *gum line* (= occlusal surface) of the pollex (line u; a best-fit line through the bases of the teeth). The load was applied just inside the tip of the pollex (open circle). Pollex height (*H*) and width (*W*), as well as cuticle thickness at the dorsal (*f*), ventral (*g*), medial (*h*) and lateral (*i*) margins, was measured at the point of fracture (*crack*) in a plane parallel to the load vector and perpendicular to the long axis of the pollex.

After the claw failed, the location of the load wire and the fracture margin were recorded on each claw drawing. Cuticle thickness at the point of failure was measured by orienting the fracture surface of the broken pollex towards the viewer so that the line of sight was parallel to the occlusal surface of the pollex (line u, Fig. 1). Pollex width (*W*), as well as cuticle thickness at the dorsal (*f*), ventral (*g*), medial (*h*) and lateral (*i*) margins, was digitized from enlarged drawings of this orientation. In addition, the height of the pollex immediately below the point of crack initiation and perpendicular to the occlusal surface was also digitized (*H*, along the vertical dashed line labeled *crack*, Fig. 1). The actual fracture plane was not always perpendicular to the occlusal surface, so stresses were calculated twice, once using all the data and once using only breaks that were within ±30° of the vertical dashed line labeled *crack* (Fig. 1).

Analyses

Regression analyses and analyses of variance were conducted with StatViewII (ver. 1.03, Abacus Concepts). Tests for differences in slopes between sexes and among species, and common slopes, were computed by means of analysis of covariance (ANCOVA; SuperANOVA ver. 1.11, Abacus Concepts).

Ultimate stress (σ_b, MN m^{-2}) of the cuticle surface at the point of fracture—*extreme fiber stress* in the engineering literature—was estimated using the linearly elastic theory (Biewener, 1982)

$$\sigma_b = F_b r c I^{-1} \qquad \text{(Equation 1)}$$

where

F_b = breaking force (in newtons, N).

r = moment arm (center of the load wire to the point of crack initiation, in mm; Fig. 1).

c = distance from the neutral axis of the pollex to the upper surface ($H/2$, where H = height of the pollex parallel to the load vector immediately below the point of crack initiation, in mm; Fig. 1). Ideally, c should be computed from the centroid (the presumed neutral axis) of the pollex cuticle in a plane perpendicular to the occlusal surface at the point of crack initiation, but we did not have sufficiently detailed measurements of the distribution of cuticle to do this, so we assumed that the neutral axis was at the midpoint of the cross-section of the pollex (H, Fig. 1).

I = second moment of area (mm^4) computed parallel to the load vector immediately below the point of crack initiation as $I = (I_u + I_l)/2$, where $I_u = (\pi/64)\{(WH^3) - [(W - h - i)(H - 2f)^3]\}$ and $I_l = (\pi/64)\{(WH^3) - [(W - h - i)(H - h - i)^3]\}$ (see Fig. 1 for cuticle dimensions and Alexander (1983) for the formula). I was computed separately for the upper (I_u) and lower (I_l) half of the cross section of the pollex because the upper cuticle margin was roughly twice as thick as that of the sides or bottom. Side thicknesses (h and i of Fig. 1) instead of measured bottom thickness (g) were used to compute I_l because bottom thickness varied with fracture angle, and because in claws where the bottom thickness could be measured reliably, it did not differ from the side thickness (data not shown).

Ultimate stress (σ_b) could not be computed for all claws for which we obtained safety factors because a few claws broke at the base of the pollex adjacent to the opening where the dactyl inserted, so dimension (f) could not be measured.

Breaking force variability of different sized crabs was assessed by (a) computing residuals from a least-squares linear regression of untransformed breaking force (Y) on untransformed manus length (X) for each species separately (sexes were pooled), (b) dividing the sample for each species into two roughly equal-sized groups (smaller and larger) based on carapace width, and (c) conducting a Levene's test on the absolute values of the residuals (2-way ANOVA: species × size group). This analysis was also repeated using log-transformed variables.

Least-squares linear regressions were used to obtain coefficients of allometry throughout the analyses, even though such coefficients may be underestimated as the goodness-of-fit to a line declines (LaBarbera, 1989). They were nonetheless preferred over alternative Model II regressions in our study for two reasons. First, the uncontrolled variation in the dependent variable was substantially greater than that in the independent variable (*e.g.*, see Tables II and IV), so a Model I analysis was more appropriate. Second, we wished to compare both slopes and intercepts among species by ANCOVA (*e.g.*, Tables III and V below), and the validity of P values from such comparisons based on Model II regressions is open to question.

The statistical significance of differences between pairs of model coefficients was computed using two-sample t tests for unequal sample sizes (Sokal and Rohlf, 1995).

Results

Breaking force and breaking-force variability

Although claws broke at many different locations along the pollex, most breaks fell either towards the base (0.2–0.4 of standardized pollex length), near the proximal margin of the tanned cuticle (the black ends to the fingers of many brachyuran crab claws), or towards the tip (0.6–0.8 of standardized pollex length, Fig. 2a). Nonetheless, even though pollex diameter varied substantially from the base to the tip, the location of the break had no effect on the force at which the pollex broke after controlling statistically for the effects of claw size (Fig. 2a). Only 5 claws out of 141 shattered along the lower margin of the pollex, as would occur when failure was due to local buckling (Wainwright *et al.*, 1976), and these were excluded from the analyses.

The fracture plane, however, was not always perpendicular to the upper pollex surface (*i.e.*, parallel to the load vector). Most commonly, cracks deflected proximally towards the pollex base. In some cases, the fracture plane deviated by more than 30° from the load vector. Such cracks tended to be concentrated towards the tip of the pollex and yielded somewhat more variable estimates of breaking strength (Fig. 2b).

Larger crabs exhibited significantly more variable break-

Table II

Size-dependence of pollex cuticle-strength for claws from six species of Cancer *crabs*

Species	n	Slope (SE)	Intercept (SE)	P	r
a) log(ultimate stress, MN m^{-2}) (Y) *vs.* standardized pollex position (X) (see Fig. 2b for data)					
1. *C. antennarius*	28	0.178 (0.0953)	1.715 (0.0200)	0.073	0.344
2. *C. branneri*	12	0.427 (0.1537)	1.817 (0.0325)	0.019	0.660
3. *C. gracilis*	12	0.195 (0.1100)	1.684 (0.0285)	0.106	0.490
4. *C. magister*	17	0.262 (0.2060)	1.630 (0.0563)	0.223	0.312
5. *C. oregonensis*	28	0.198 (0.1334)	1.712 (0.0256)	0.151	0.279
6. *C. productus*	28	0.618 (0.1363)	1.377 (0.0250)	<0.001	0.664
7. All pooled	125	0.213 (0.0582)	1.702 (0.0136)	<0.001	0.313
8. All pooled*	60	0.178 (0.0971)	1.716 (0.0171)	0.073	0.234
9. All pooled†	125	0.162 (0.0478)	−0.095 (0.0112)	0.001	0.292
b) log(ultimate stress, MN m^{-2}) (Y) *vs.* log(manus length, mm) (X) (see Fig. 3 for data)					
1. *C. antennarius*	28	−0.615 (0.2023)	2.642 (0.0183)	0.005	0.512
2. *C. branneri*	12	−1.123 (0.8404)	3.352 (0.0399)	0.211	0.389
3. *C. gracilis*	12	−0.433 (0.4542)	2.408 (0.0313)	0.363	0.289
4. *C. magister*	17	−1.146 (1.3504)	3.562 (0.0578)	0.409	0.214
5. *C. oregonensis*	28	−0.575 (0.7015)	2.448 (0.0263)	0.420	0.159
6. *C. productus*	28	−0.811 (0.1776)	2.926 (0.0250)	<0.001	0.667
7. All combined‡	125	−0.751 (0.1447)	2.842 (0.2042)	<0.001	0.573
8. All combined‡,§	125	−0.624 (0.1352)	0.820 (0.1908)	<0.001	0.591

Least-squares linear regression equations. n = number of individual crabs; SE = standard error; r = correlation coefficient.

* Excluding claws that broke at more than 30° from the load vector (Fig. 2b).

† Based on residuals from separate regressions of log(ultimate stress) *versus* log(manus length) for each species.

‡ Common slope from a one-factor ANCOVA with species as the grouping variable.

§ ANCOVA recomputed using residuals from a single regression of log(ultimate stress) *versus* standardized pollex position for all species combined.

ing forces (P = 0.036, Levene's test), but this difference was not significant when computed for log-transformed size and biting force (P = 0.67). Therefore in absolute terms, breaking forces were more variable for larger claws, but the variability appeared to be proportional to claw size.

Under natural conditions, claws may fail mechanically in ways other than the breakage of the pollex that we examined in this study. For example, claws might fail because the dactyl tip breaks, rather than the tip of the pollex, or because the dactyl condyles become disarticulated from their sockets. Among the 81 injured claws we observed in field-collected crabs, the dactyl tip was broken more frequently than the pollex tip (46 *versus* 33), however none exhibited a dislocated dactyl. Disarticulated dactyls are occasionally observed in field-collected crabs (G. M. Taylor, unpubl. obs.), but this mode of failure appears quite rare. Therefore we believe our study has focused on the most biologically relevant form of claw failure: fracture of one of the fingers.

Cuticle strength of claws—patterns

Although breaking force did not vary along the pollex, the ultimate stress (force per unit area, σ_b)—a measure of the ability of claw cuticular material to resist failure in tension—did (Fig. 2b). When data for all species were considered together, ultimate stress increased distally from a mean of 53 at 0.1 to a mean of 78 MN m^{-2} at 0.9 of the standardized pollex length (Fig. 2b; $P < 0.001$, Table IIa-7). Ultimate stress (σ_b) of claws that fractured along a line deviating by more than 30° from the load vector (Fig. 2b) was somewhat more variable because of increased uncertainty about the true cuticle thicknesses below the site of crack initiation. However, exclusion of these points did not significantly alter the slope or intercept of this relationship (P = 0.75; compare row a-8 to row a-7 in Table II). Because ultimate stress (σ_b) declined with increasing claw size (see below), the effect of claw size might have confounded the effect of crack location. Here again, though, an analysis of the residuals, where residuals were computed separately for each species from a regression of log(ultimate stress) *versus* log(manus length), also yielded a slope that did not differ significantly from the original untransformed data (P = 0.50; compare row a-9 to a-7 in Table II). Slopes of this relationship appeared to vary among species (rows a1–a6, Table II); however, these differences were not significant statistically (P = 0.2; see Table Va). Therefore, regardless of how the analysis was conducted, the cuticle was nearly 50% stronger at the pollex tip than at the base (0.9 *versus* 0.1 of standardized pollex length, respectively).

For all six *Cancer* species, breaking or ultimate stress (σ_b) declined with increasing claw size (Fig. 3, Table IIb). This decline was significant statistically only for *C. antennarius* and *C. productus* (Table IIb-1,6) when species were

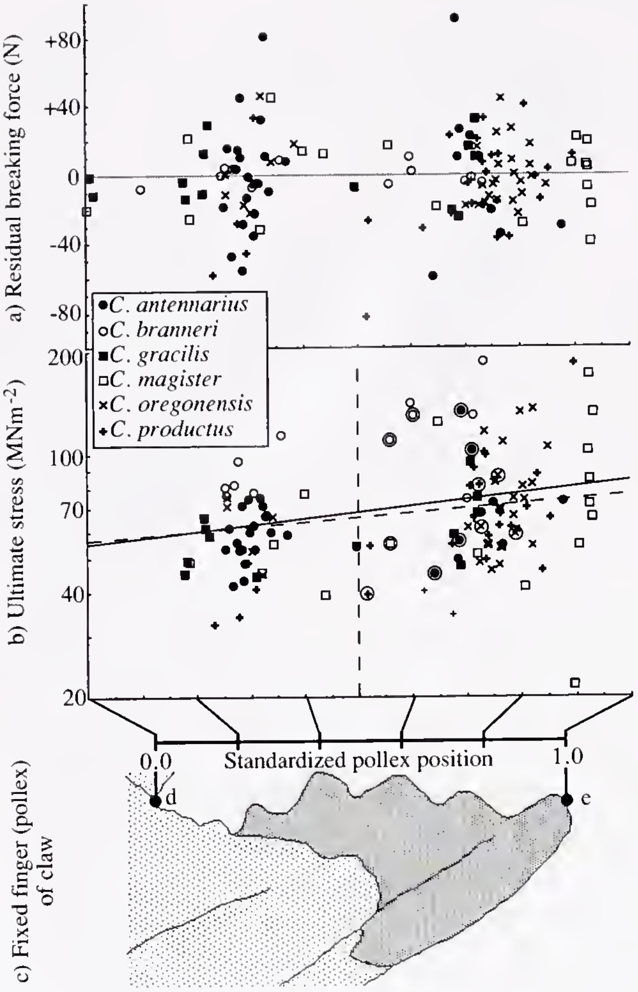

Figure 2. (a) Deviation of breaking force from that expected for a given claw size (manus length), and (b) the computed ultimate stress (σ_b; meganewtons per meter squared, MN m^{-2}) at which the cuticle failed, both as a function of standardized position along the upper margin of the pollex between the insertion point of the closer apodeme (landmark d) and the tip (landmark e) for six species of *Cancer* crabs. (c) The pollex, or fixed finger, of a *C. productus* claw illustrating how *standardized position* was determined; claws of other *Cancer* species differ in shape and number of teeth (Nations, 1975). The darker portion of the finger is often black in life, and both harder and stronger (Melnick *et al.*, 1996). Points surrounded by circles above 0.5 standardized pollex length indicate claws for which the fracture plane did *not* deviate by more than 30° from the load vector (see methods). The solid line in (b) indicates a least-squares linear regression through all the data, whereas the dashed line applies only to claws for which the fracture plane did *not* deviate by more than 30° from the load vector (see Table IIa7,8 for regression statistics).

analyzed separately because of the smaller size ranges for the other species. However, a 1-factor ANCOVA with species as the grouping variable revealed that slopes did not differ significantly among species ($P = 0.96$; see Table Vb) and that the common slope was highly significant ($P < 0.001$) (Table IIb-7). To control for possible effects of crack location (Fig. 2b), an ANCOVA was also conducted on residuals from the regression of Table IIa-7. This too revealed no significant difference in slopes among species ($P = 0.97$; see Table Vb). The common slope from ANCOVA was also highly significant statistically ($P < 0.001$) and did not differ significantly from the slope obtained for the original untransformed data ($P = 0.52$; compare row b-8 to b-7 in Table II). Therefore, regardless of how the analysis was conducted, cuticle strength decreased by approximately 40% with a doubling of claw size (measured as manus length).

This decline was not simply an artifact of our computations for intact claws; if it were, all claws should fall upon the same regression line, and *C. oregonensis* clearly does not (Fig. 3). This decline was also not an artifact of using manus length as the arbitrary measure of claw size, because nearly identical results were obtained using total claw wet weight as the covariate (results not shown).

Finally, size-adjusted breaking or ultimate stress (σ_b) differed up to twofold among *Cancer* species ($P < 0.001$, ANCOVA; Table III). For a given claw size, *C. magister* had the strongest pollex cuticle and *C. oregonensis* the weakest. *Post-hoc* tests, however, revealed that most of the statistical support for interspecific variation arose from the unusually low value for *C. oregonensis*, although *C. magister* did differ from *C. antennarius* when standardized by manus length. Unfortunately, we cannot say with much confidence whether the significantly lower cuticle strength of *C. oregonensis* would also obtain for pristine, unworn claws because *C. oregonensis* are undoubtedly older, for a given body size, than the other *Cancer* species and their claws may simply have accumulated more fatigue or wear in the field prior to measurement.

Differences in our estimates of cuticle strength among

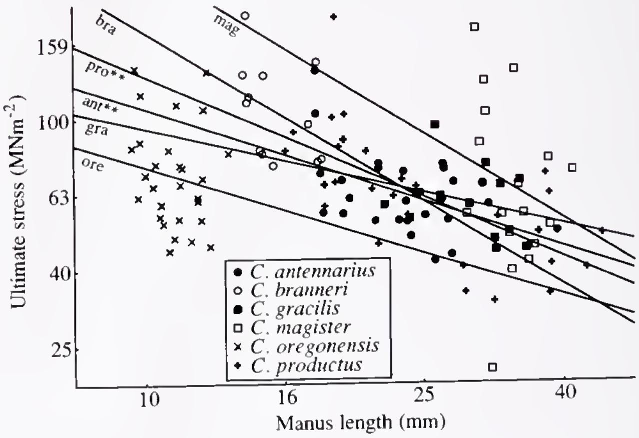

Figure 3. Cuticle ultimate stress (σ_b; meganewtons per meter squared, MN m^{-2}) as a function of claw size (manus length, mm) for six species of *Cancer* crabs. Solid lines indicate least-squares linear regressions for each species. See Table II for statistics. **$P < 0.01$. Note that both axes are on a logarithmic scale. Three-letter abbreviations adjacent to each line indicate the first three letters of each species' name.

Table III

Average, size-adjusted pollex cuticle-strength for claws from six species of Cancer *crabs*

Species	Mean (SE)* log(ultimate stress)	Detransformed mean ultimate stress (MN m^{-2})			
		By length*	Post-hoc†	By weight‡	Post-hoc†
C. magister	1.967 (0.0444)	92.7	a	80.7	a
C. branneri	1.919 (0.0434)	83.0	ab	83.6	a
C. gracilis	1.884 (0.0447)	76.6	ab	70.2	a
C. productus	1.851 (0.0281)	71.0	ab	66.1	a
C. antennarius	1.839 (0.0271)	69	b	71.7	a
C. oregonensis	1.641 (0.0474)	43.8	c	50.8	b

* Adjusted means (± SE) from a one-factor ANCOVA (species was the grouping factor; see Table IIb-7 for regression statistics) for a common manus length of 20.9 mm. Differences among adjusted means were highly significant ($P < 0.001$).

† Results from a Tukey-Kramer post-hoc test (Sokal and Rohlf, 1995) on adjusted means (prior to detransformation); letters indicate means that were not significantly different from each other at a table-wide significance level of 0.05.

‡ Detransformed means for a standard claw wet weight of 3.6 g from a similar one-factor ANCOVA using claw weight as opposed to manus length as the covariate (regression statistics not shown).

species were potentially complicated by differences in cuticle thickness. Even though *C. oregonensis* claws have a much larger area of black cuticle at the pollex tip (G. M. Taylor, unpubl. obs.), and even though this material is probably considerably stronger than cuticle on the remainder of the claw (Melnick *et al.,* 1996; this study), *C. oregonensis* claws exhibited the lowest cuticle strength of all the *Cancer* species we examined (Table III). *C. oregonensis* also had the thickest cuticle on the occlusal surface of the pollex (1.9 mm). It was nearly 2.5 times thicker than that of *C. magister* (0.7 mm), which had the highest cuticle strength (adjusted means from ANCOVA for a standard manus length of 20.9 mm, data and analysis not shown). Because the tanned and harder cuticle at the pollex tip forms only the outermost layer of the cuticle, and an additional layer of "normal" cuticle appears to lie underneath it (G. M. Taylor, unpubl. obs.), our estimates of cuticle strength, which were based on the total thickness of the cuticle, may underestimate the actual strength of this tanned cuticle and therefore potentially confound some of the differences we observed among species.

Cuticle strength of claws—assumptions

To compute ultimate tensile strength of cuticle based on failure of intact claws, we were obliged to make several simplifying assumptions. The indirect method we used, based on linearly elastic theory applied to cantilevered beams (Young, 1989), assumes (I) that the pollex, or fixed finger, of the claw exhibited a constant cross-section along its length; (II) that the cuticle is isotropic and homogeneous; (III) that shape variation along the length of the pollex, such as caused by teeth, does not create local points of stress concentration; and (IV) that tensile strength was less than compressive strength (*i.e.,* that the cuticle failed in tension).

The taper of the pollex (violation of assumption I) undoubtedly introduced some error; however, Young (1989, p. 181) notes that tapers of 30°–40°, similar to those observed in the pollex of *Cancer* claws, would cause extreme fiber stress to be overestimated by only 5%–10%, so although our estimates of tensile strength may be somewhat high, this overestimate should be less than 10%.

Crustacean cuticle is undoubtedly neither isotropic nor homogeneous (violation of assumption II), because of its composite structure (Wainwright *et al.,* 1976). In addition, the stronger tanned material found at the tips of the fingers of many brachyuran crab claws (Melnick *et al.,* 1996) is limited to the outer layer of the cuticle in *Cancer* crabs (G. M. Taylor, unpubl. obs.). Unfortunately, we cannot assess how these attributes influenced our estimates. This assumption, however, also applies to estimates of cuticle strength that others have made on the basis of excised pieces of cuticle (Wainwright *et al.,* 1976; Melnick *et al.,* 1996).

Rather surprisingly, cracks did not appear to start preferentially at the base of adjacent teeth where stress might be expected to be concentrated (violation of assumption III); for example, for 22 of the 136 breaks we observed, cracks started at a point between the tip and base of a tooth, rather than at the top (where wear would have been greatest) or the base of a tooth (where fatigue might have been highest). In addition, breaking force exhibited no apparent predictable variation along the length of the pollex, other than to increase towards the tip (Fig. 2a).

Finally, we were confident that the pollex failed in tension on the upper surface (assumption IV) because all but five of 141 claw tips fractured cleanly in one piece, indicating failure in tension of the upper margin, rather than buckling of the lower margin as observed in crab walking legs (Hahn and LaBarbera, 1993). Therefore, in spite of the

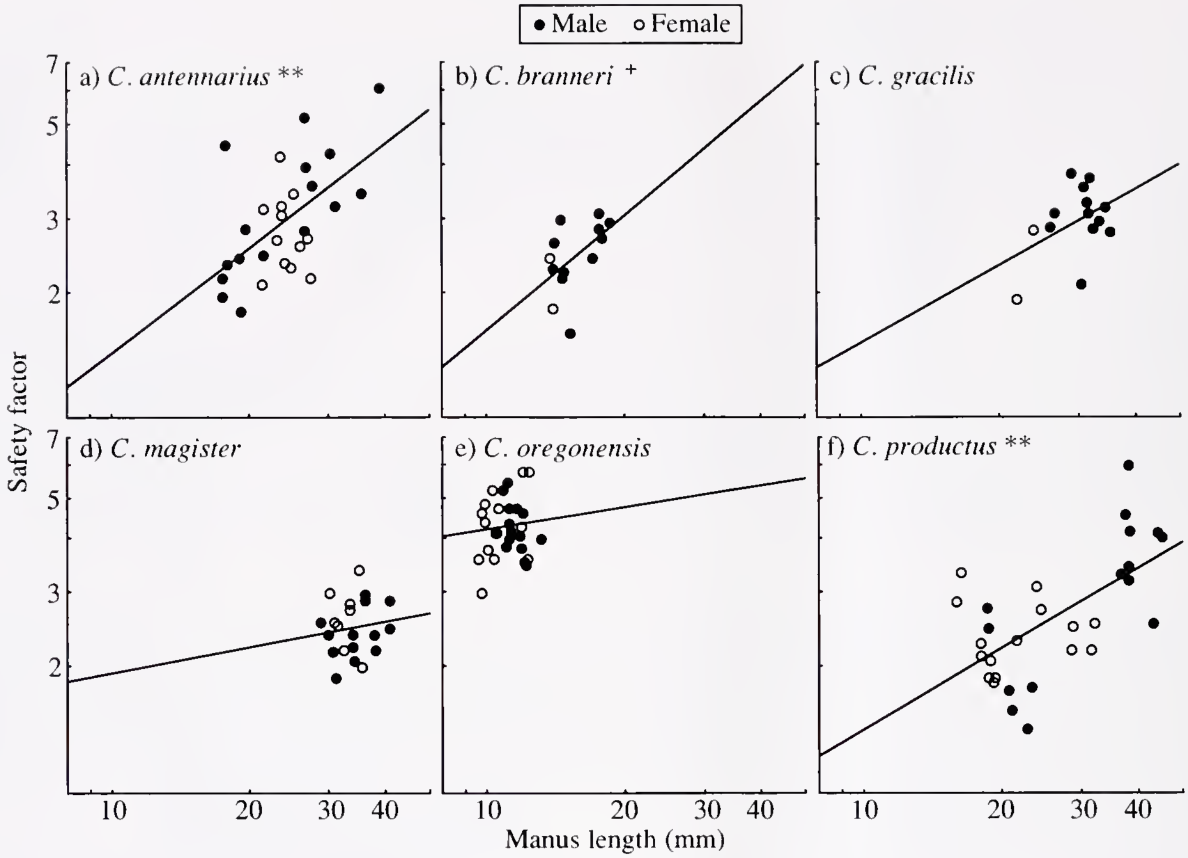

Figure 4. Size-dependence of claw safety factors [breaking force (N)/extreme-maximum biting force (N)] for six species of *Cancer* crabs. Each point represents an individual claw. Lines indicate least-squares linear regressions [see Table IVa for regression statistics and Table Vc for ANCOVA results; $+P < 0.07$, $^{**}P < 0.005$]. Note that both axes are on a logarithmic scale.

potential errors introduced by estimating material properties from the behavior of a complex, intact structure, we believe our estimates are biologically realistic.

Safety-factor allometry

Pollex safety factors increased with increasing claw size for all six *Cancer* species, regardless of whether manus length (Fig. 4, Table IVa) or claw wet weight (Table IVb) was used as the measure of claw size. This increase was highly significant statistically for the two species for which the range of sizes was the largest ($P \leq 0.002$; *C. antennarius* and *C. productus*), and nearly significant for a third species ($P \leq 0.072$; *C. branneri*) (Table IV). Although the intercepts differed among species (see below), the slopes did not differ significantly (Table Vc,d), so we were justified in computing a common slope (*i.e.*, coefficient of allometry) by ANCOVA.

When all six species of *Cancer* crabs were analyzed simultaneously by ANCOVA, claw safety factors increased $\propto$manus length$^{0.65 \pm 0.094}$ (mean ± SE) or $\propto$claw wet weight$^{0.22 \pm 0.030}$ (Fig. 4, Table Vc,d). Viewed another way, the allometric coefficients for maximum biting force were significantly less than for breaking force. Maximum biting force increased $\propto$manus length$^{1.49 \pm 0.082}$ (Table Vf), while breaking force increased $\propto$manus length$^{2.13 \pm 0.0814}$ (Table Vg), yielding a difference in the coefficients of 0.64 ($= 2.13 - 1.49$). Therefore, regardless of how they were computed, safety factors increased approximately $\propto$manus length$^{0.6}$. If breaking force and biting force varied isometrically, then the scaling coefficient for safety factors (a ratio of the two) should have been zero, so the observed coefficient was significantly greater than expected for isometry. Size-adjusted safety factors also differed among species (Taylor *et al.*, in press).

Both relatively thicker cuticle and relatively weaker biting forces contributed to the higher safety factors of larger *Cancer* claws. When all six species were analyzed together, lateral cuticle thickness of the pollex (dimensions *h* and *i*, Fig. 1) increased $\propto$manus length$^{1.31 \pm 0.078}$ (Table Vh), so cuticle cross-sectional area would increase $\propto$manus

Table IV

Size-dependence of pollex safety-factors for claws from six species of Cancer *crabs*

Species	n	Slope (SE)	Intercept (SE)	P	r
a) log(safety factor) (Y) *vs.* log(manus length, mm) (X)					
1. *C. antennarius*	28	0.827 (0.2393)	−0.673 (0.0215)	0.002	0.561
2. *C. branneri*	13	0.900 (0.4513)	−0.692 (0.0230)	0.072	0.515
3. *C. gracilis*	14	0.609 (0.3645)	−0.430 (0.0228)	0.121	0.434
4. *C. magister*	21	0.203 (0.3507)	0.079 (0.0153)	0.570	0.132
5. *C. oregonensis*	30	0.178 (0.3646)	0.446 (0.0138)	0.630	0.092
6. *C. productus*	30	0.633 (0.1520)	−0.483 (0.0223)	<0.001	0.618
b) log(safety factor) (Y) *vs.* log(claw wet wt., g) (X)					
1. *C. antennarius*	28	0.247 (0.0734)	0.269 (0.0218)	0.002	0.551
2. *C. branneri*	13	0.307 (0.1514)	0.328 (0.0230)	0.067	0.522
3. *C. gracilis*	14	0.211 (0.1400)	0.282 (0.0233)	0.157	0.399
4. *C. magister*	21	0.103 (0.1175)	0.292 (0.0150)	0.392	0.197
5. *C. oregonensis*	30	0.060 (0.1138)	0.633 (0.0138)	0.599	0.100
6. *C. productus*	30	0.216 (0.0485)	0.256 (0.0218)	<0.001	0.645

Least-squares linear regression equations; slopes correspond to coefficients of allometry. Safety factor = ratio of breaking force/maximum bite force; isometry for safety factors should be 0 (see text). SE = standard error; r = correlation coefficient.

length$^{2.6}$. Since breaking force should scale $\propto$cross-sectional area for linearly elastic structures loaded in bending and of constant material properties and shape (see Eq. 1 in Methods), this coefficient significantly exceeded that for breaking force ($\propto$manus length$^{2.13}$; $P < 0.001$). Furthermore, because of the longer time between molts, the cuticle of larger claws in our samples would likely have accumulated more stress cracks and wear than smaller ones, so the

Table V

Overall size-dependence of mechanical and morphological attributes of Cancer *crab claws*

Slope$_{\text{comm}}$ (SE)	Range (n_s)*	r^2_{comm}	P	P_{sp}
a) log(ultimate stress, MN m^{-2}) (Y) *vs.* standardized pollex position (X)				
0.30 (0.059)	0.43–0.62 (2)	0.32	<0.001	0.20
0.21 (0.055)†	(none significant)	0.11	<0.001	0.98
b) log(ultimate stress, MN m^{-2}) (Y) *vs.* log(manus length, mm) (X)				
−0.75 (0.144)	−0.81−−0.62 (2)	0.32	<0.001	0.96
−0.62 (0.135)†	−0.64−−0.58 (2)	0.35	<0.001	0.97
c) log(safety factor) (Y) *vs.* log(manus length, mm) (X)				
0.65 (0.094)	0.63–0.83 (2)	0.58	<0.001	0.72
d) log(safety factor) (Y) *vs.* log(claw wet wt., g) (X)				
0.22 (0.030)	0.22–0.25 (2)	0.59	<0.001	0.83
e) log(median-maximum biting force, n) (Y) *vs.* log(manus length, mm) (X)				
1.52 (0.072)	0.95–2.21 (6)	0.90	<0.001	0.045
f) log(extreme-maximum biting force, n) (Y) *vs.* log(manus length, mm) (X)				
1.49 (0.082)	0.93–2.36 (6)	0.88	<0.001	0.081
g) log(breaking force, n) (Y) *vs.* log(manus length, mm) (X)				
2.13 (0.081)	1.54–2.54 (5)	0.88	<0.001	0.35
h) log(lateral cuticle thickness of pollex‡, mm) (Y) *vs.* log(manus length, mm) (X)				
1.31 (0.078)	1.20–1.92 (5)	0.76	<0.001	<0.001

$n = 136$ claws (usually two per crab) for all analyses except a and b, for which $n = 125$. Safety factor = ratio of breaking force/maximum bite force. Slope$_{\text{comm}}$ = common slope from a one-factor ANCOVA (species was the grouping factor); expected slopes for isometry relative to manus length are 1.0 for ultimate stress (b), 0.0 for safety factors (c, d), 2.0 for biting force (e, f), 2.0 for breaking force (g), and 1.0 for cuticle thickness (see text). SE = standard error. n_s = number of statistically significant slopes for individual *Cancer* species out of six. r^2_{comm} = coefficient of determination for common slope from ANCOVA. P = probability that the common slope did not differ from zero. P_{sp} = probability that slopes did not differ among species.

* Range of slopes among species exhibiting a significant slope.

† The same ANCOVA design but conducted on residuals obtained separately for each species from the regressions in Table II.

‡ Average of dimensions h and i in Fig. 1. See Tables II, III and IV for regression statistics for individual species.

observed coefficient of 2.13 probably underestimates that for pristine claws. Therefore, the allometric increase in cuticle thickness alone would be sufficient to yield a significant positive allometry for safety factors in pristine claws, even if relative biting force did not decline with increasing size; we would thus expect an even higher positive allometry than the 0.6 actually observed had we been able to use pristine claws.

The lower-than-expected scaling coefficient for maximum biting force was not an artifact of size-dependence in our measurement protocol, because (a) the gape angle at which biting force was measured was kept constant for all claw sizes, (b) the location of the load wire scaled isometrically ($\propto$manus length$^{0.96\pm0.025}$) (data not shown), (c) the transducers were recalibrated before and after each set of measurements, and (d) the scaling coefficients did not differ among species, even though average claw length differed among species by more than threefold. Nor was it due to size-dependent changes in mechanical advantage. In all but one species, mechanical advantage did not vary significantly with size. In *C. productus,* mechanical advantage actually increased with increasing size, so the lower-than-expected coefficient of allometry for maximum biting force was even more puzzling.

Potential limitations due to small sample sizes and narrow size ranges

Coefficients of allometry based on small sample sizes or narrow size ranges can be misleading because of statistical uncertainties (LaBarbera, 1989). For only two species we studied did the size range approach or exceed a factor of two (*C. antennarius* and *C. productus*) and, perhaps unsurprisingly, we most commonly obtained statistically significant associations with claw size for these two species (Tables II and IV). We may thus be premature in concluding that safety factors increase allometrically, and in the same fashion, in all six *Cancer* species.

In spite of small sample sizes and size ranges for four species (Table IV), coefficients of allometry for safety factors were nonetheless positive for all six species, and the slope was nearly significant for one of the remaining species ($P \leq 0.072$, *C. branneri*). In addition, we could not reject the hypothesis that the slopes were statistically indistinguishable using ANCOVA (Table Vc,d), even for the species for which we had reasonable size ranges. Therefore, with the present data we are obliged to accept the simpler hypothesis that safety factors increase similarly with increasing claw size for all six *Cancer* species.

Discussion

Cuticle strength in Cancer *crab claws*

In spite of the functional significance of claws (Warner, 1977; Brown *et al.*, 1979; Seed and Hughes, 1995) and the impact that claw failure has on feeding ability (Juanes and Hartwick, 1990; Juanes and Smith, 1995), little is known about their mechanical properties other than biting force or mechanical advantage (Warner and Jones, 1976; Elner, 1978; Elner and Campbell, 1981; Blundon, 1988; Kaiser *et al.*, 1990; Levinton and Judge, 1993; Levinton *et al.*, 1995; Preston *et al.*, 1996). In addition, we are aware of only three reports of tensile strength in crustacean cuticle, and only one was for claw cuticle. The tensile strength of carapace cuticle reported for two portunid crabs is approximately 30 MN m^{-2} [Wainwright *et al.* (1976, Table 5.3) for *Carcinus maenas,* and Hepburn *et al.* (1975) for *Scylla serrata*], and Melnick *et al.* (1996) report fracture strength in three-point bending of 109 MN m^{-2} in the black cuticle of the claw tips and 32 MN m^{-2} ($n = 10$) in the lighter-colored cuticle of the manus in the stone crab (*Menippe mercenaria*). Although we computed stress on intact claws, as opposed to excised pieces of cuticle loaded in three-point bending, our estimates of breaking strength in *Cancer* claws (40–120 MN m^{-2}) nonetheless agree quite well with those of Melnick *et al.* (1996), in spite of the simplifying assumptions we were obliged to make (see *Cuticle strength of claws—assumptions* in the Results).

Our results (Fig. 2b, Table IIa) also support the conclusion of Melnick *et al.* (1996) that the distal cuticle on the fingers of brachyuran claws, often black in color, is a stronger material than other claw cuticle. This stronger material towards the claw tip ensures that the force at which the pollex breaks remains roughly constant along its length (Fig. 2a), even though the cross-sectional area declines distally. It may also increase the abrasion resistance of the claw tip, since crabs forced to feed for extended times on hard-shelled prey often exhibit severe wear of the teeth and tip of both the dactyl and pollex (A. R. Palmer, unpubl. obs.). Material properties of the claw cuticle therefore appear finely tuned to the mechanical demands placed upon it.

Within- and among-species variation in cuticle strength

Unlike previous studies of cuticular properties, our experiments were designed to assess cuticle-strength variation as a function of claw size, both within and among closely related crab species. Somewhat surprisingly, cuticle strength decreased with increasing claw size both within and among the six *Cancer* species we examined (Fig. 3).

Two observations suggest that this decline may reflect increased wear and fatigue that larger claws experienced before we measured breaking strengths. First, the intermolt interval increases with increasing size in *Cancer* crabs (Orensanz and Gallucci, 1988) and although we attempted to use crabs in mid-intermolt throughout, larger crabs may have been further away from their most recent molt and their claws may thus have experienced more wear or fatigue. Second, *C. oregonensis,* whose claws exhibited generally lower cuticle strength for a given claw size (Fig. 3), matures at a considerably smaller body size (<25 mm carapace width) than the other *Cancer* species we studied (generally >60 mm carapace width; Orensanz and Gallucci, 1988). Here again, because intermolt intervals are longer for older crabs, claws of *C. oregonensis* may have accumulated more wear or fatigue before we measured their breaking strength than did similar-sized claws in presumably younger individuals of the other species. Regardless of the cause of this relationship, conclusions about differences in cuticle strength among species must take into account the effect of claw size.

Indeed, after controlling for the effects of claw size, cuticle strength varied by up to 100% among the six *Cancer* species we examined (Table III). Even though potentially confounded by differences in cuticle thickness (see *Cuticle strength of claws—patterns* in the Results), these interspecific differences in size-adjusted cuticle strength correlated significantly with interspecific differences in size-adjusted safety factors (Taylor *et al.*, in press): species with weaker cuticle had higher safety factors ($n = 6$, $r = 0.92$, $P = 0.008$ when standardized by manus length, and $r = 0.82$, $P = 0.045$ when standardized by claw weight). Therefore, differences in safety factors among species appear to have evolved at least in part in response to differences in mechanical properties of their cuticle.

Allometry of skeletal safety factors in crab claws

The higher safety factors we observed in larger claws of all six *Cancer* species were consistent with theoretical predictions. Larger claws were expected to have larger safety factors because (a) unpredictability of claw strength should increase in larger crabs due to the longer time to accumulate stress cracks and wear between molts, (b) the costs of lost or damaged claws (Juanes and Smith, 1995) will be more prolonged or severe for larger crabs, and (c) larger crabs probably experience a greater range of extreme forces because the claws are used increasingly for aggression (Juanes and Smith, 1995). Thus this size-dependence appears adaptive.

But why does maximum muscle stress, which has the biggest impact on the size-dependence of safety factors, decline with increasing claw size? Similar declines with increasing claw size in stone crabs (Blundon, 1988), male fiddler crabs (Levinton and Judge, 1993), and lobsters (Elner and Campbell, 1981) suggest a general pattern that remains a significant unsolved phenomenon in claw mechanics and evolution. Perhaps larger crabs actively restrain the maximum stress they generate to avoid damaging their claws. Alternatively, larger claws may generate lower stresses because of some as-yet-unidentified physiological constraints. The former would support our interpretation that higher safety factors in larger claws are adaptive, whereas the latter would not.

The scaling relation between maximum force and a linear claw dimension might possibly be influenced by the bipinnate arrangement of muscles in crustacean limbs (Warner and Jones, 1976), but we believe this is unlikely. In bipinnate muscles, twice as many muscle fibers attach per unit area of apodeme (the crustacean tendon) because they attach on both sides. Bipinnate muscles therefore generate more force per unit volume than do linear muscles (Goldspink, 1977). In addition, muscle fibers attach to the apodeme at an angle, so their per-fiber contribution to the final biting force is less than in typical vertebrate skeletal muscle, where fibers lie roughly parallel to the tendon (Goldspink, 1977). Nonetheless, these two factors affect only the force produced *per unit area of apodeme*. They do not affect the expected allometric relation between maximum force and claw length unless they too vary allometrically. Maximum biting force should therefore still increase $\propto$apodeme area (*i.e.*, $\propto$claw length$^{2.0}$) for bipinnate muscles, just as it should for linear muscles.

The higher safety factors we observed in larger claws did not appear to affect the probability of failure in the field. Among the six *Cancer* species we examined, 9.2% of crabs had injured claws and 28.9% were missing or regenerating one or both claws ($n = 671$). As injuries leading to death would have been under-represented, actual injury rates were probably higher. Significantly, in the two species for which we had adequate sample sizes, the incidence of neither regenerating nor injured claws varied significantly with claw size: $P = 0.44$ and 0.94 respectively for *C. productus* ($n = 285$ crabs: one or both claws missing or regenerating = 33.0%, or injured = 8.4%) and *C. gracilis* ($n = 99$ crabs: one or both claws missing or regenerating = 41.4%, or injured = 17.2%) (Taylor *et al.*, in press). However, because larger claws should accumulate more wear during their longer intermolt intervals and thus be more likely to fail, their higher safety factors nonetheless appear to have reduced the probability of failure to levels similar to those of smaller crabs.

Allometry of skeletal safety factors in other taxa

In other taxa, safety factors vary in many ways with increasing body size or age. As body size or age increases within species, safety factors may either increase, decrease, or exhibit a U-shaped pattern (Table VIa). Within many mollusc species, shell weight or thickness increases disproportionately with increasing body size (Currey, 1977; Palmer, 1981, 1992), suggesting that safety factors also increase with body size (Preston *et al.*, 1996) since the sizes of shell-breaking predators, and hence potential load distribution, should remain about the same. Only for bovid horns

Table VI

Dependence of safety factors on size or age in various taxa and structures

	Safety factor			
Taxon and trait	Load type		Dependence*	Reference
a) Intraspecific variation				
Human female long bones	locomotion	A	decrease†	Biewener (1993)
Bovid horns	fighting	S/A	none‡	Kitchener (1991)
Spider walking legs	locomotion	S/A	decrease	Prang (1977)
Cockroach walking legs	locomotion	S/A	decrease	Prang (1977)
Crab claws	biting force	S/A	increase§	This study
Mollusc shells	breaking force	S/A	increase¶	Preston *et al.* (1996, see text)
Kelp stipe	wave stress	S	none	Friedland and Denny (1995)
Equisetum stems	self-loading	S	decrease	Niklas (1989)
Shade-intolerant tree trunks	self-loading	S/A	decrease	King (1991)
Early-successional tree trunks	self-loading	S/A	decrease	Claussen and Maycock (1995)
Shade-tolerant tree trunks	self-loading	S/A	U-shaped	King (1991)
Late-successional tree trunks	self-loading	S/A	U-shaped	Claussen and Maycock (1995)
b) Interspecific variation				
Mammalian long bones	locomotion	S	none#	Biewener (1990)
Tree trunks	self-loading	S	none¶	McMahon and Kronauer (1976)
Tree trunks	self-loading	S	none**	Niklas (1994)
Various nonwoody plant stems	self-loading	S	decrease††	Niklas (1994)
Herbaceous plant stems	self-loading	S	decrease§§	Niklas (1995)

* S = explicitly tests for size-dependence; A = explicitly tests for age-dependence; S/A = size- and age-dependence confounded.

† Due to osteoporosis; inferred assuming load distributions were not age-dependent.

‡ True for 8 species.

§ True for 6 species.

¶ True for many species.

# Interspecific variation over >3 orders of magnitude of body mass.

** True for 56 species.

†† True for multiple species: mossess (n = 40), pteridophytes (n = 16), dicot herbs (n = 120), palms (n = 17).

§§ True for 76 species.

do safety factors appear not to change with increasing body size (Kitchener, 1991).

Rather few extensive studies of interspecific variation have been conducted, but safety factors appear to vary less with size among species of mammals and trees than within species (Table VIb). Only for nonwoody plants and palm trees do safety factors appear to vary substantially with size among species.

These patterns raise an obvious question: to what extent is intraspecific variation in safety factors adaptive? Although the data are too few to draw any generalities with confidence, the patterns in Table VIa suggest that increases in safety factors with increasing size may more commonly reflect adaptive variation (the outcome of selection for genotypes that specifically induce changes in safety factors), whereas decreases in safety factors may signal some form of constraint (nonadaptive variation resulting from peculiarities of the ways in which organisms grow). The evidence for crab claws seems clear: longer intermolt intervals at larger size, increased variability in cuticle strength due to wear and fatigue, and increased cost of failure should all favor higher safety factors (this study). Similarly, for many molluscs and other organisms whose defensive skeletons permit an *escape in size* (Paine, 1976; Palmer, 1990), larger size results in lower vulnerability; therefore, higher safety factors appear adaptive.

In contrast, safety factors decline with increasing size in the walking legs of insects and arachnids (Prang, 1977) and in the *rind-core* type stems of many nonwoody plants (Niklas, 1989, 1995). Indeed, for both arthropod limbs (Currey, 1967) and rind-core type plant stems (Niklas, 1994), mechanical limits to strength appear to determine the upper limit to body size, which strongly implies that safety factors decline with increasing proximity to a critical size and that this decline is not adaptive. One might also expect the safety factors of long bones in the walking legs of large-bodied vertebrates to decline nonadaptively with increasing body size, because of an unavoidable tradeoff between the mechanically necessary allometric increases in cross-sectional area required to support a greater body mass and the increased cost of producing and transporting heavier skeletal elements (Schmidt-Nielsen, 1984). Similarly, any time the future contribution to fitness declines with increasing size or age, safety factors might decrease nonadaptively, as observed in the long bones of human females (Table VIa; Biewener, 1993).

Two relations in the preceding discussion require additional comment. First, the argument for adaptive size-dependence in the safety factors of molluscan shells is not entirely untainted by potential constraints. In marine gastropods, and probably in many heavily skeletonized marine invertebrates, the maximum rate of body growth at small size may be constrained by the maximum rate of calcification, which in turn may be limited by the physical chemistry of crystal growth (Palmer, 1981). This *calcification-rate constraint* imposes a cruel tradeoff on small individuals: rapid growth is incompatible with increased skeletal defense. So, while the increase in relative shell thickness with increasing size observed in so many molluscs is likely to be adaptive, because it reduces vulnerability to shell-breaking predators, the lower relative shell weight at small size, which is responsible for the observed trend, may be strongly influenced by the calcification-rate constraint. Therefore, perhaps unsurprisingly, not all positive correlations between safety factors and body size may arise for purely adaptive reasons.

Second, whereas declines in safety factors with increasing size may typically signal some kind of constraint, such declines might be adaptive under unusual situations in which controlled failure may enhance fitness. For example, fragmentation of corals may actually promote dispersal and colonization (Highsmith, 1982), but at small size competitive interactions may favor larger colonies (Sebens, 1983). Under these conditions, selection should favor reduced vulnerability to fragmentation at small size but enhanced vulnerability at larger size. Clearly, this type of adaptive decline in safety factors would be limited to colonial organisms.

Acknowledgments

We thank J. Ackerman, L. Hammond, S. Zaklan, and two referees for comments on the manuscript; M. W. Palmer and L. Bach for advice on the calculations of ultimate stress; D. Arsenault, S. Zaklan, and B. Penney for discussion; and the staff at the Bamfield Marine Station for help with several aspects of this study. This research was supported by NSERC Operating Grant A7245 to ARP.

Literature Cited

Alexander, R. M. 1981. Factors of safety in the structure of animals. *Sci. Prog.* **67:** 109–130.

Alexander, R. M. 1982. *Optima for Animals.* Arnold, London. 112 pp.

Alexander, R. M. 1983. *Animal Mechanics.* Blackwell, London. 301 pp.

Alexander, R. M. 1997. A theory of mixed chains applied to safety factors in biological systems. *J. Theor. Biol.* **184:** 247–252.

Biewener, A. A. 1982. Bone strength in small mammals and bipedal birds: Do safety factors change with body size? *J. Exp. Biol.* **98:** 289–301.

Biewener, A. A. 1990. Biomechanics of mammalian terrestrial locomotion. *Science* **250:** 1097–1103.

Biewener, A. A. 1993. Safety factors in bone strength. *Calcif. Tissue Int.* **53 (Suppl):** S68–S74.

Biewener, A. A., and K. P. Dial. 1995. *In vivo* strain in the humerus of pigeons (*Columba livia*) during flight. *J. Morphol.* **225:** 61–75.

Blundon, J. A. 1988. Morphology and muscle stress of chelae of temperate and tropical stone crabs *Menippe mercenaria. J. Zool. (Lond.)* **215:** 663–673.

Brandwood, A. 1985. The effects of environment upon shell construction and strength in the rough periwinkle *Littorina rudis* Maton (Mollusca: Gastropoda). *J. Zool. (Lond.)* **A206:** 551–565.

Brandwood, A., A. S. Jayes, and R. M. Alexander. 1986. Incidence of healed fractures in the skeletons of birds, molluscs and primates. *J. Zool. (Lond.)* **208:** 55–62.

Brown, S. C., S. R. Cassuto, and R. W. Loos. 1979. Biomechanics of chelipeds in some decapod crustaceans. *J. Zool. (Lond.)* **188:** 143–159.

Buikstra, J. E. 1975. Healed fractures in *Macaca mulatta*: Age, sex, and symmetry. *Folia Primatol.* **23:** 140–148.

Claussen, J. W., and C. R. Maycock. 1995. Stem allometry in a north Queensland tropical rainforest. *Biotropica* **27:** 421–426.

Currey, J. D. 1967. The failure of exoskeletons and endoskeletons. *J. Morphol.* **123:** 1–16.

Currey, J. D. 1977. Problems of scaling in the skeleton. Pp. 153–167 in *Scale Effects in Animal Locomotion.* T. J. Pedley, ed. Academic Press, New York.

Currey, J. D. 1984. *The Mechanical Adaptations of Bone.* Princeton University Press, Princeton. 294 pp.

Elner, R. W. 1978. The mechanics of predation by the shore crab, *Carcinus maenas* (L.), on the edible mussel, *Mytilus edulis* L. *Oecologia (Berl.)* **36:** 333–344.

Elner, R. W., and A. Campbell. 1981. Force, function and mechanical advantage in the chelae of the American lobster *Homarus americanus* (Decapoda: Crustacea). *J. Zool. (Lond.)* **193:** 269–286.

Friedland, M. T., and M. W. Denny. 1995. Surviving hydrodynamic forces in a wave-swept environment: Consequences of morphology in the feather boa kelp, *Egregia menziesii* (Turner). *J. Exp. Mar. Biol. Ecol.* **190:** 109–133.

Goldspink, G. 1977. Design of muscles in relation to locomotion. Pp. 1–22 in *Mechanics and Energetics of Animal Locomotion,* R. M. Alexander and G. Goldspink, eds. Chapman and Hall, New York.

Hahn, K., and M. LaBarbera. 1993. Failure of limb segments in the blue crab, *Callinectes sapidus* (Crustacea: Malacostraca). *Comp. Biochem. Physiol.* **105A:** 735–739.

Hepburn, H. R., I. Joffe, N. Green, and K. J. Nelson. 1975. Mechanical properties of a crab shell. *Comp. Biochem. Physiol.* **50A:** 551–554.

Highsmith, R. C. 1982. Reproduction by fragmentation in corals. *Mar. Ecol. Prog. Ser.* **7:** 207–226.

Horst, M. N., and J. A. Freeman. eds. 1993. *The Crustacean Integument. Morphology and Biochemistry.* CRC Press, Ann Arbor, Michigan.

Juanes, F., and E. B. Hartwick. 1990. Prey size selection in Dungeness crabs: The effect of claw damage. *Ecology* **71:** 744–758.

Juanes, F., and L. D. S. Smith. 1995. The ecological consequences of limb damage and loss in decapod crustaceans: A review and prospectus. *J. Exp. Mar. Biol. Ecol.* **193:** 197–223.

Kaiser, M. J., R. N. Hughes, and D. G. Reid. 1990. Chelal morphometry, prey-size selection and aggressive competition in green and red forms of *Carcinus maenas* (L.). *J. Exp. Mar. Biol. Ecol.* **140:** 121–134.

King, D. A. 1991. Tree size. *Natl. Geogr. Res.* **7:** 342–351.

Kitchener, A. C. 1991. The evolution and mechanical design of horns and antlers. Pp. 229–253 in *Biomechanics in Evolution,* J. M. V. Rayner and R. J. Wooton, eds. Cambridge University Press, New York.

LaBarbera, M. 1989. Analyzing body size as a factor in ecology and evolution. *Annu. Rev. Ecol. Syst.* **20:** 97–117.

Levinton, J. S., and M. L. Judge. 1993. The relationship of closing force to body size for the major claw of *Uca pugnax* (Decapoda: Ocypodidae). *Funct. Ecol.* **7:** 339–345.

Levinton, J. S., M. L. Judge, and J. P. Kurdziel. 1995. Functional differences between the major and minor claws of fiddler crabs (*Uca*, family Ocypodidae, order Decapoda, subphylum Crustacea): A result of selection or developmental constraint. *J. Exp. Mar. Biol. Ecol.* **193:** 147–160.

Lowell, R. B. 1985. Selection for increased safety factors of biological structures as environmental unpredictability increases. *Science* **228:** 1009–1011.

Lowell, R. B. 1987. Safety factors of tropical versus temperate limpet shells: Multiple selection pressures on a single structure. *Evolution* **41:** 638–650.

McMahon, T. A., and R. E. Kronauer. 1976. Tree structure: Deducing the principle of mechanical design. *J. Theor. Biol.* **59:** 443–466.

Melnick, C. A., Z. Chen, and J. J. Mecholsky. 1996. Hardness and toughness of exoskeleton material in the stone crab, *Menippe mercenaria*. *J. Mater. Res.* **11:** 2903–2907.

Nations, J. D. 1975. The genus *Cancer* (Crustacea: Brachyura): Systematics, biogeography and fossil record. *Nat. Hist. Mus. Los. Angel. Cty. Sci. Bull.* **23:** 1–104.

Niklas, K. J. 1989. Safety factors in vertical stems: Evidence from *Equisetum hyemale*. *Evolution* **43:** 1625–1636.

Niklas, K. J. 1994. The allometry of safety factors for plant height. *Am. J. Bot.* **81:** 345–351.

Niklas, K. J. 1995. Plant height and the properties of some herbaceous stems. *Ann. Bot.* **75:** 133–142.

Orensanz, J. M., and V. F. Gallucci. 1988. Comparative study of postlarval life-history schedules in four sympatric species of Cancer (Decapoda: Brachyura: Cancridae). *J. Crustac. Biol.* **8:** 187–220.

Paine, R. T. 1976. Size-limited predation: An observational and experimental approach with the *Mytilus-Pisaster* interaction. *Ecology* **57:** 858–873.

Palmer, A. R. 1981. Do carbonate skeletons limit the rate of body growth? *Nature* **292:** 150–152.

Palmer, A. R. 1990. Predator size, prey size, and the scaling of vulnerability: Hatchling gastropods *vs.* barnacles. *Ecology* **71:** 759–775.

Palmer, A. R. 1992. Intraspecific variation in three species of rocky shore gastropods from Hong Kong: correlations among habitats and a comparison with temperate species. Pp. 649–691 in *Proceedings of the Fourth International Marine Biological Workshop. Vol. 1. General Proceedings.*, B. Morton, ed. Hong Kong University Press, Hong Kong.

Prang, H. D. 1977. The scaling and mechanics of arthropod exoskeletons. Pp. 169–181 in *Scale Effects in Animal Locomotion*, T. J. Pedley, ed. Academic Press, New York.

Preston, S. J., I. C. Review, J. F. Orr, and D. Roberts. 1996. A comparison of the strength of gastropod shells with forces generated by crab predators. *J. Zool. (Lond.)* **238:** 181–193.

Schmidt-Nielsen, K. 1984. *Scaling: Why is Animal Size so Important?* Cambridge University Press, New York. 241 pp.

Sebens, K. P. 1983. Size structure and growth rates in population of colonial and solitary invertebrates. *Workshop on Coral Reef Ecology* **1:** 9–15.

Seed, R., and R. N. Hughes. 1995. Criteria for prey-selection in molluscivorous crabs with contrasting claw morphologies. *J. Exp. Mar. Biol. Ecol.* **42:** 25–40.

Smith, L. D., and A. R. Palmer. 1994. Effects of manipulated diet on size and performance of brachyuran crab claws. *Science* **264:** 710–712.

Sokal, R. R., and F. J. Rohlf. 1995. *Biometry*. Freeman, New York. 887 pp.

Taylor, G. M., A. R. Palmer, and A. Barton. Variation in safety factors of claws within and among six species of *Cancer* crabs (Decapoda: Brachyura). *Biol. J. Linn. Soc.* (accepted).

Van Valkenburgh, B. 1988. Incidence of tooth breakage among large, predatory mammals. *Am. Nat.* **131:** 291–302.

Van Valkenburgh, B., and F. Hertel. 1993. Tough times at La Brea: Tooth breakage in large carnivores of the late Pleistocene. *Science* **261:** 456–459.

Vermeij, G. J. 1982. Unsuccessful predation and evolution. *Am. Nat.* **120:** 701–720.

Wainwright, S. A., W. D. Biggs, J. D. Currey, and J. M. Gosline. 1976. *Mechanical Design in Organisms*. Arnold, London. 423 pp.

Warner, G. F. 1977. *The Biology of Crabs*. Paul Elek Ltd., London. 202 pp.

Warner, G. F., and A. R. Jones. 1976. Leverage and muscle type in crab chelae (Crustacea: Brachyura). *J. Zool. (Lond.)* **180:** 57–68.

Young, W. C. 1989. *Roark's Formulas for Stress and Strain*. McGraw-Hill, New York.

Reference: *Biol. Bull.* **196:** 295–302. (June 1999)

Organization of Chemically Activated Food Search Behavior in *Procambarus clarkii* Girard and *Orconectes rusticus* Girard Crayfishes

CRAIG STEELE*, CAROL SKINNER, CATHERINE STEELE, PHILIP ALBERSTADT, AND CANDICE MATHEWSON

Department of Biology and Health Services, Edinboro University, Edinboro, Pennsylvania 16444

Abstract. The feeding responses of decapod crustaceans to chemical stimuli have most often been evaluated in terms of one defining act, ignoring the organization of the behavior. To gain greater insight into foraging behavior, we considered the organization of food-search behavior in evaluating the responses of two species of crayfishes to a feeding stimulant. We also examined the effects of food deprivation on the behavioral organization and whether a behavioral dichotomy exists between food search and feeding behavior in these species.

Individual crayfish of the species *Procambarus clarkii* and *Orconectes rusticus* were presented with infusions of a feeding stimulant consisting of a supernatant leachate of 100 ml water and 1 g of fish flakes. The stimulant was injected with a syringe and small-bore plastic infusion tubing into the center of a behavioral arena 25 cm square and 15 cm deep. Total injection time was 20 s. Experimental groups were presented with either the full-strength leachate (100%) or one of five dilutions: 75%, 50%, 25%, 10%, or 0% (controls) of full-strength. The feeding stimulant was presented either the day after the crayfish were fed or after one week of food deprivation. We analyzed three components of food-search behavior—detection, probing (near-field search), and locomotion (far-field, or distant, search)—recording the order of occurrence and the latency time to initiation for each behavior.

When presented with the stimulus following regular feeding, both species responded to concentrations ≥50% full-strength with probing behavior (near-field search) prior to locomotion, and to concentrations <50% full-strength with locomotion prior to, or even in the absence of, probing. Detection always occurred first. These results indicate that chemical stimuli preferentially activate distant food search in both species and that a behavioral dichotomy exists between food search and feeding behavior. One week of food deprivation had no effect on the organization of food-search behavior in *P. clarkii;* however, groups of unfed *O. rusticus* presented with 25% and 10% full-strength concentrations probed prior to locomotion, indicating a change in behavioral organization.

Introduction

Most animals must forage efficiently to optimize both growth and survival (Werner and Mittelbach, 1981; Zimmer-Faust, 1987). An animal that can, from a distance, sense the quality and quantity of food and estimate the effort required to capture it has an advantage. This is especially true in low-light benthic environments because such an ability reduces the time spent choosing food, maximizing the net rate of energy or nutrient gain (*e.g.*, Hughs, 1979; Erichsen *et al.*, 1980; Orians, 1981; Peckarsky, 1984; Zimmer-Faust, 1987).

Many studies have demonstrated that chemical stimuli elicit food-search behavior in decapod crustaceans, often in the absence of other sensory cues (*e.g.*, McLeese, 1970, 1973; Shelton and Mackie, 1971; Mackie, 1973; Hindley, 1975; Derby and Atema, 1982, 1988; Rittschof, 1982; Tierney and Atema, 1986, 1988; Hazlett, 1994; Wilman *et al.*, 1994). In laboratory experiments, visual and tactile prey stimuli are often ineffective, whereas prey odors elicit food-search behavior (*e.g.*, Schembri, 1981; Derby and Atema, 1982; Zimmer-Faust and Case, 1982; Tierney and Atema, 1988; Hazlett, 1994; Wilman *et al.*, 1994). However, crayfish may require experience and learning to associate a particular odor with food (Hazlett, 1994). Foragers are influenced by food-specific chemical stimuli that are essen-

Received 8 December 1997; accepted 19 March 1999.

* E-mail: csteele@edinboro.edu

tial for activating and orienting food search (Bell and Tobin, 1982; Tierney and Atema, 1988; Momot, 1995).

Chemical stimuli can influence decapod crustacean foraging by activating far-field (distant) food searching preferentially (*e.g.*, Hazlett, 1971a, b; McLeese, 1973; Atema, 1977; Pearson *et al.*, 1979; Reeder and Ache, 1980). In this behavioral model, chemical concentration may be important in relating distance to food: dilute concentrations of food odor may be interpreted as originating from distant food sources. This model assumes that locomotion (far-field food search) is the primary response to low-concentration chemical stimuli, and that appetitive feeding (near-field search, indicated by probing the substrate) is the primary response to high-concentration chemical stimuli, resulting in a behavioral dichotomy between food search and feeding (Atema, 1977).

An alternative model has been developed from studies on marine crustaceans. Evidence from experiments on many species of marine decapods indicates that response to chemical stimuli activates near-field (nearby) rather than distant food search, regardless of the concentration of the chemical stimuli. Low concentrations of food odor activate substrate probing (appetitive feeding), and only higher concentrations active locomotion. Food search is thus primarily organized to obtain nearby food items, implying that there is no behavioral dichotomy between food search and feeding (*e.g.*, Zimmer-Faust and Case, 1982, 1983; Zimmer-Faust *et al.*, 1984; Zimmer-Faust, 1987; see review, Zimmer-Faust and Case, 1982).

Crustacean feeding responses are often evaluated in terms of one specific defining act in response to a chemical stimulus (*e.g.*, Zimmer-Faust and Case, 1982; Johnson and Atema, 1986; Tierney and Atema, 1988), or to several unrelated behavioral acts (Wilman *et al.*, 1994). These methods of categorizing behavior simplify data collection, analysis, and interpretation, but ignore the structural organization of behavior (Zimmer-Faust and Case, 1982). Greater insight into an animal's foraging behavior may be gained through studying the structural organization of food search (Zimmer-Faust and Case, 1982, 1983; Zimmer-Faust *et al.*, 1984; Zimmer-Faust, 1987).

Wilman *et al.*, (1994) examined the responses of three *Orconectes* congeners to the odor of fish carrion and live predaceous fish (as food). They found that *Orconectes rusticus* Girard is more responsive than either *O. propinquus* Girard or *O. virilis* Hagen to these food odors and speculated that such differential chemoreception is contributing to the success of *O. rusticus* in its invasion of northern Wisconsin lakes, where it is replacing the other two species. Differential chemoreception toward food odors should also be important across genera in species invasions. *Procambarus clarkii* Girard is an exotic invader in nearby Ohio and is replacing *O. rusticus* in certain areas of its range (Norrocky, 1983). If *P. clarkii* is more responsive than *O. rusticus* to food odors, then *P. clarkii* may be able to locate food more quickly and increase its feeding rate compared to *O. rusticus*.

We quantitatively investigated the organization of food-search behavior in the crayfishes *P. clarkii* and *O. rusticus*. The objectives of our study were to (1) evaluate the sequence of food-search behavior in both species; (2) determine the effects of food deprivation on the organization of food search and feeding in these crayfishes; (3) determine whether a behavioral dichotomy exists between their food search and feeding behavior; and (4) examine the comparative responsives of both species to the feeding stimulant.

Materials and Methods

Experimental animals and maintenance conditions

Ninety-six adult, intermolt, Form II (nonbreeding) crayfish of each species were used in the experiments. All crayfish were >6 cm in total length from rostrum to tail (caudal edge of telson). *Procambarus clarkii* was commercially raised and was obtained from Waubun Laboratories (Schriever, LA). *Orconectes rusticus* was captured from local streams in Erie County, Pennsylvania. Crayfish were held in 25-liter species-specific community aquaria (23° ± 1°C) for at least one week prior to experimentation. Each aquarium contained an average of four to six crayfish, a gravel bottom, a filter, aeration, and sufficient cover material to provide each individual with shelter. A window in the laboratory provided natural photoperiod. Crayfish were fed TetraMin fish flakes, *ad libitum*, daily; they were not fed during experiments. Water was changed in the aquaria weekly. All animals were tested for their behavioral responses to chemical feeding stimuli within 2 weeks after the initial 1-week adjustment period.

Experimental procedures

The 96 crayfish of each species were divided randomly into two experimental series (48 crayfish of each species in each experimental series) of six treatment groups ($n = 8$ per group) per series. They were placed individually into opaque, white plastic behavioral arenas measuring 25 × 25 × 15 cm (length, width, depth) to examine their responses to one of six chemical conditions. Gravel covered the bottom of each arena to a depth of 2.5 cm, displacing 800 ml. Thus each arena held 8.5 liters of laboratory water (tap water treated with NovAqua to remove chlorine and heavy metals).

No crayfish was tested more than once. Both sexes were used in all experiments, with the exception of ovigerous females. Responding to food odor is a basic behavior; there was no *a priori* reason to suspect that male and female crayfish might differ in their responses.

After placement into the arena, the crayfish were given 1 h to adjust to it. For our bioassay, it was essential that the animals were inactive when the chemical feeding stimulant was infused into the arena. All animals were inactive after this 1-h adjustment period; none had to be removed from the study.

For each trial, an individual crayfish was presented with an infusion of 10 ml of a freshly prepared solution of a chemical feeding stimulant (food odor) or with 10 ml of laboratory water (controls). The stock solution of feeding stimulant consisted of a leachate of 100 ml of laboratory water and 1 g of TetraMin fish flakes. The water and fish flakes were mixed for 5 min in a 250-ml beaker. The supernatant leachate was then poured off into a second beaker. A previous study by Steele *et al.* (1992) demonstrated that this leachate formulation elicits an unambiguous feeding response by crayfish of both species used in the present study.

The 10 ml of leachate was injected by hand into the center of the arena within 20 s (injection rate, 0.5 ml s^{-1}) using a 10-ml hypodermic syringe and small-bore plastic infusion tubing. The infusion tubing was buried beneath the gravel in the arena. It curved upwards to the vertical in the center of the arena, with the end just below the gravel surface. Dye studies indicated that injected chemicals diffused through an arena within 45 s from the beginning of infusion.

Following the adjustment period, the animals in the treatment groups of both species were presented either with the undiluted leachate, full-strength concentration (100%), or with one of five other concentrations: 75%, 50%, 25%, 10%, or 0% (controls) of full-strength. Concentrations were of injected leachate prior to dilution in the arena water. Controls served as indicators of spontaneous detection responses to water flow from injections (rheotaxis) and spontaneous probing and locomotion in the absence of chemical cues. Crayfish were presented with these chemical infusions either the day following regular feeding (Experimental Series I) or after one week of food deprivation (Experimental Series II). All experiments were conducted between 0800 and 1600 h from 14 August through 3 October 1996.

A Sony Hi8 video camera (Model CCD-V701) was mounted above the arena and each animal's behavior was videotaped during each trial. Videotaping began 1 min prior to chemical infusion and continued for 5 min after the end of the infusion. Three components of food-search behavior were analyzed from the videotapes: detection, probing, and locomotion (Itagaki and Thorpe, 1981; Zimmer-Faust and Case, 1982; Zimmer-Faust *et al.*, 1984; Tierny and Atema, 1986). These behaviors are defined in Table I. For each behavior, the numbers of crayfish engaging in it, its rank order of occurrence, and the latency to its initiation (to the nearest 0.1 s) were recorded for each trial. For those groups in which probing preceded locomotion, the total time (to nearest 0.1 s) each crayfish spent probing the gravel was calculated from the initiation of probing to the initiation of locomotion.

Statistical analyses

A *G* test for independence, with Williams' correction for 2 × 2 contingency tables (Sokal and Rohlf, 1981), was used in analyzing the number of crayfish responding to a food-odor concentration compared to laboratory water controls. Because responses to the five food-odor concentrations were compared to the control results, we used a significance level of 0.01 for each comparison to achieve a maximum experimentwise error of 0.05. The Mann-Whitney *U* test (Sokal and Rohlf, 1981; Rohlf and Sokal, 1981) was used to compare behavioral response times following regular feeding and after food deprivation between the same treatment concentrations between species, and to compare the times of initiation of each behavior and the total times spent probing for each concentration of chemical feeding stimulant following regular feeding between the species. The Kruskal-Wallis one-way rank ANOVA (Rohlf and Sokal, 1981; Sokal and Rohlf, 1981) was used to compare behavioral response times following regular feeding and after food deprivation among treatment concentrations within a spe-

Table I

Definitions of behavioral elements in crayfish food-search behavior

Behavior	Definition
Detection behavior	
Lower antennule	Antennules directed downward or held parallel to the body.
Near-field search	
Leg probing	Any non-locomotor movement of a pereiopod (ambulatory leg) which rakes a dactyl across the substratum, inserts it into the substratum, or elevates it above the substratum.
Chela probing	Any non-locomotor movement of the first pereiopod which rakes a chela across the substratum, inserts it into the substratum, or elevates it above the substratum.
Digging	Leg probing and chela probing.
Far-field search	
Walking	Lateral or anterior movement of the body a distance greater than one carapace length.
Climbing	Cephalothorax angled above the substratum, with at least four walking legs not in contact with the substratum.
Locomotion	Gross body movement (walking and climbing).

cies, and to compare the times of initiation of each behavior and the total times spent probing for each concentration of chemical feeding stimulant following regular feeding with the responses following food deprivation within each species. Where the Kruskal-Wallis analysis indicated significance in the data, a nonparametric multiple comparison test based on the Student-Newman-Keuls (SNK) test was used for all pairwise comparisons (Glantz, 1997).

Results

Numbers responding to chemical stimuli

Except for the detection component, the responses of both fed and food deprived *P. clarkii* to food odors $\geq 25\%$ full-strength are significantly greater ($P < 0.01$, at least) than the responses of the controls to laboratory water (Table II). In most instances where significant differences occurred, all individuals in the experimental groups exhibited a response to the food odors. Of the control individuals, both fed and food-deprived, half or fewer exhibited detection or locomotion behaviors, and none exhibited probing, in response to injections of laboratory water (Table II).

Both fed and food-deprived *O. rusticus* responded to food odors $\geq 25\%$ full-strength in significantly greater numbers than the controls responded to laboratory water (Table II). In all instances where significant differences occurred, all individuals in the experimental groups exhibited a response to the food odors (Table II). Fewer *O. rusticus* controls responded than did *P. clarkii* controls; as with *P. clarkii*, *O. rusticus* controls responded with detection or locomotion behaviors, none with probing (Table II).

Types of responses to chemical stimuli—regularly fed groups

For all regularly fed individuals of both *P. clarkii* and *O. rusticus*, concentrations $\geq 50\%$ full-strength of the chemical feeding stimulant induced first detection, then probing (defined as near-field search), and lastly, locomotion (defined as far-field search) (Table III). In contrast, concentrations $<50\%$ full-strength induced first detection, then locomotion prior to—or even in the absence of—probing in those individuals responding (Table III). Initiation of locomotion in both species at stimulant concentrations $\geq 50\%$ full-strength was delayed considerably by intensive probing, compared to experimental groups receiving $<50\%$ full-strength injections of feeding stimulant (Table IV).

The time to initiate a food-search behavior following the start of odor injection was compared across stimulant concentrations for each species and between species for similar stimulant concentrations. The results of Kruskal-Wallis and Mann-Whitney U tests for all comparisons are summarized here, and in Table IV.

Within species. For *P. clarkii*, response times were significantly different with respect to detection, probing, and locomotion for stimulant concentrations $\geq 50\%$ full-strength compared with lesser concentrations. The results of Kruskal-Wallis analyses indicated significant differences in the times of detection ($H_{\text{corrected}} = 30.252$; $P < 0.001$), probing ($H_{\text{corrected}} = 28.317$; $P < 0.001$), and locomotion ($H_{\text{corrected}} = 32.029$; $P < 0.001$) among the experimental groups receiving the different stimulant concentrations. Results of the nonparamentric comparisons indicated that responses at 100%, 75%, and 50% full-strength were not

Table II

Behavioral responses (numbers of crayfish responding) of P. clarkii *and* O. rusticus *to chemical feeding stimuli following regular feeding and food deprivation*

Food odor conc. (% full-strength)	Regular Feeding			Food Deprivation		
	Detection	Probing	Locomotion	Detection	Probing	Locomotion
Procambarus clarkii						
100	8	8***	8*	8	8***	8*
75	8	8***	8*	8	8***	8*
50	8	8***	8*	8	8***	8*
25	8	8***	8*	8	8***	8*
10	4	4	4	8	8***	8*
0	4	0	2	3	0	2
Orconectes rusticus						
100	8**	8***	8**	8*	8***	8*
75	8**	8***	8**	8*	8***	8*
50	8**	8***	8**	8*	8***	8*
25	8**	8***	8**	8*	8***	8*
10	6	5	5	5	5	5
0	1	0	1	2	0	2

Responses that are significant compared to controls (G-test with Williams' Correction) are marked with asterisks: * $P < 0.01$; ** $P < 0.005$; *** $P < 0.001$. All others are not significant ($P > 0.01$).

Table III

Ranked order of initiation (1st, 2nd, 3rd) of behaviors after chemical stimulus infusion for Procambarus clarkii *and* Orconectes rusticus *crayfish following regular feeding and following one week's food deprivation*

		Following regular feeding						Following food deprivation					
		P. clarkii			*O. rusticus*			*P. clarkii*			*O. rusticus*		
Food odor conc. (% full-strength)	Behavior	1st	2nd	3rd	1st	2nd	3rd	1st	2nd	3rd	1st	2nd	3rd
100	Detection	8	0	0	8	0	0	8	0	0	8	0	0
	Probing	0	8	0	0	8	0	0	8	0	0	8	0
	Locomotion	0	0	8	0	0	8	0	0	8	0	0	8
75	Detection	8	0	0	8	0	0	8	0	0	8	0	0
	Probing	0	8	0	0	8	0	0	8	0	0	8	0
	Locomotion	0	0	8	0	0	8	0	0	8	0	0	8
50	Detection	8	0	0	8	0	0	8	0	0	8	0	0
	Probing	0	8	0	0	8	0	0	8	0	0	8	0
	Locomotion	0	0	8	0	0	8	0	0	8	0	0	8
25	Detection	8	0	0	8	0	0	8	0	0	8	0	0
	Probing	0	0	8	0	0	8	0	0	8	0	0	8
	Locomotion	0	8	0	0	8	0	0	8	0	0	8	0
10	Detection	4	0	0	6	0	0	4	0	0	5	0	0
	Probing	0	0	4	0	0	5	0	0	4	0	5	0
	Locomotion	0	4	0	0	5	0	0	4	0	0	0	5
0	Detection	4	0	0	1	0	0	3	0	0	2	0	0
(Controls)	Probing	0	0	0	0	0	0	0	0	0	0	0	0
	Locomotion	0	2	0	0	1	0	0	2	0	0	2	0

significantly different from each other ($\alpha > 0.05$), but were significantly different from responses at 25% and 10% full-strength (which were not significantly different from each other; $\alpha > 0.05$) for detection, ($\alpha = 0.05$), probing ($\alpha = 0.01$), and locomotion ($\alpha = 0.05$).

Although the pattern of response latency was slightly different for *O. rusticus* across stimulant concentrations, there was, in general, also a significant difference in the response times for each behavior at stimulant concentrations ≥50% full-strength compared to responses at concentrations <50% full strength. Kruskal-Wallis analyses indicated significant differences in the times of initiation of detection ($H_{\text{corrected}} = 32.699$; $P < 0.001$), probing ($H_{\text{corrected}} = 35.077$; $P < 0.001$), and locomotion ($H_{\text{corrected}} = 28.189$; $P < 0.001$) among the experimental groups receiving the different stimulant concentrations. Nonparametric comparisons indicated that for detection and probing, responses at 100% full-strength were significantly different from re-

Table IV

Comparisons of mean initiation time(s) of behavior after chemical stimulus injection for Procambarus clarkii *and* Orconectes rusticus *crayfish following regular feeding*

	Detection			Probing			Locomotion		
Food odor conc. (% of full-strength)	*P. clarkii*	*O. rusticus*	*P-value*	*P. clarkii*	*O. rusticus*	*P-value*	*P. clarkii*	*O. rusticus*	*P-value*
100	11.7	14.0	NS	15.7	17.0	NS	148.3	31.2	***
	(4.62)	(4.62)		(5.03)	(5.06)		(20.72)	(4.54)	
	11.3	20.0	***	15.7	30.5	**	136.7	45.4	**
	(1.53)	(0.90)		(3.06)	(9.37)		(13.80)	(10.16)	
50	9.5	19.6	**	16.3	23.9	*	108.0	36.9	**
	(3.50)	(3.81)		(6.81)	(2.95)		(13.46)	(2.66)	
25	25.0	28.4	NS	46.9	50.8	NS	31.8	32.3	NS
	(5.97)	(6.37)		(7.51)	(3.22)		(7.31)	(7.10)	
10	34.6	48.6	NS	50.8	68.8	NS	43.6	55.9	NS
	(9.90)	(8.71)		(7.07)	(9.20)		(2.83)	(3.05)	

Times are measured from start of odor infusion. Standard deviation is given in parentheses. Significance levels for Mann-Whitney U tests comparing responses between species: * $P < 0.05$; ** $P < 0.025$; *** $P < 0.001$; NS, not significant ($P > 0.05$).

Table V

Comparisons of mean initiation time(s) of behavior after chemical stimulus infusion for Procambarus clarkii *and* Orconectes rusticus *crayfish following one week's food deprivation*

Food odor conc. (% of full-strength)	Detection			Probing			Locomotion		
	P. clarkii	*O. rusticus*	*P-value*	*P. clarkii*	*O. rusticus*	*P-value*	*P. clarkii*	*O. rusticus*	*P-value*
100	11.6 (1.70)	17.4 (6.68)	*	13.0 (1.56)	22.3 (5.50)	**	120.0 (9.90)	33.8 (8.42)	**
75	10.0 (2.83)	21.8 (2.31)	*	12.8 (5.23)	30.8 (2.08)	*	137.1 (10.21)	41.3 (2.52)	*
50	12.6 (4.57)	24.5 (2.60)	***	14.8 (5.24)	31.2 (1.04)	***	117.2 (18.40)	44.1 (3.50)	***
25	22.9 (10.2)	26.1 (1.62)	NS	37.8 (12.2)	29.4 (1.47)	NC	29.2 (9.66)	39.7 (5.78)	NC
10	41.3 (11.20)	51.9 (3.96)	*	58.1 (18.70)	55.7 (1.72)	NC	52.5 (17.71)	69.4 (8.62)	NC

Times are measured from start of odor infusion. Standard deviation is given in parentheses. Significance levels for Mann-Whitney U tests comparing responses between species: * $P < 0.05$; ** $P < 0.025$; *** $P < 0.001$; NS, not significant ($P > 0.05$); NC, Not Calculated, since these responses had different ranked orders of occurrence following food deprivation.

sponses at all other concentrations of leachate ($\alpha = 0.05$), and responses at 75% and 50% full-strength were not significantly different from each other ($\alpha > 0.05$) but were significantly different ($\alpha = 0.05$) from responses at 25% and 10% full-strength (which were not significantly different from each other; $\alpha > 0.05$). For locomotion, responses at 100%, 75%, 50%, and 25% full-strength were not significantly different from one another, but were significantly different ($\alpha = 0.05$) from responses at 10% full-strength.

Between species. In seven out of nine comparisons between *P. clarkii* and *O. rusticus* at stimulant concentrations ≥50% full-strength, the responses were significantly different (Mann-Whitney U test, $P < 0.05$–0.01; Table IV). Except for responses to 100% full-strength stimulant, *P. clarkii* detected the feeding stimulant and began probing the gravel significantly sooner than did *O. rusticus*. Locomotion in *P. clarkii* was significantly delayed compared to *O. rusticus* due to the increased amount of time *P. clarkii* spent probing the gravel (mean ± SD: 132.6 ± 42.41 s at 100%; 121 ± 14.11 s at 75%; 91.7 ± 29.26 s at 50% full-strength) compared with *O. rusticus* (mean ± SD: 14.2 ± 2.92 s at 100%; 14.9 ± 0.95 s at 75%; 13.0 ± 0.61 s at 50% full-strength). Results of Mann-Whitney U tests were significant for all comparisons at $P < 0.01$ (Table IV). At stimulant concentrations <50% full-strength, there were no significant differences in any behavioral responses between the species (Mann-Whitney U tests, $P > 0.05$; Table IV).

Types of responses to chemical stimuli–food-deprived groups

One week of food deprivation had no effect on the organization of food search in *P. clarkii* (Table III). As with the regularly fed groups, concentrations ≥50% full-strength of the chemical feeding stimulant induced first detection, then probing and, lastly, locomotion. Concentrations <50% full-strength induced first detection and then locomotion prior to probing in those individuals responding.

In *O. rusticus*, however, one week of food deprivation altered the organization of food search for those groups presented with 25% and 10% full-strength concentrations of the feeding stimulant (Table III). As with their conspecifics presented with greater concentrations, they now initiated probing (near-field search) prior to locomotion.

The times of initiation of food-search behaviors after stimulus injection following one week of food deprivation were compared between species at similar concentrations and within species for all concentrations. The results of Kruskal-Wallis and Mann-Whitney U tests are summarized here and in Table V.

Within species. For food-deprived *P. clarkii*, the patterns of latency for detection, probing, and locomotion for all odor concentrations were no different from those of the regularly fed groups, with significant latency differences at concentrations <50% full-strength (compare Tables IV and V). The results of Kruskal-Wallis analyses indicated significant differences in the times of initiation of detection ($H_{\text{corrected}} = 30.427$; $P < 0.001$), probing ($H_{\text{corrected}} = 29.155$; $P < 0.001$), and locomotion ($H_{\text{corrected}} = 29.674$; $P < 0.001$) among the experimental groups receiving the different stimulant concentrations. Results of the nonparamentric comparisons indicated that responses at 100%, 75%, and 50% full-strength were not significantly different from each other ($\alpha < 0.05$), but were significantly different from responses at 25% and 10% full-strength (which were not significantly different from each other; $\alpha > 0.05$) for detection, ($\alpha = 0.01$), probing ($\alpha = 0.01$), and locomotion ($\alpha = 0.05$).

Food-deprived *O. rusticus* displayed fewer differences in latencies for the initiation of food-search behaviors than did the regularly fed groups. The only significant time differences were seen at the 10% full-strength concentration (compare Tables IV and V). Kruskal-Wallis analyses indicated significant differences in the times of initiation of detection ($H_{\text{corrected}} = 22.069$; $P < 0.001$), probing ($H_{\text{corrected}} = 25.678$; $P < 0.001$), and locomotion ($H_{\text{corrected}} = 21.377$; $P < 0.001$) among the experimental groups receiving the different stimulant concentrations. Nonparametric comparisons indicated that for detection, probing, and locomotion, responses at 100%, 75%, 50%, and 25% full-strength were not significantly different from one another, but were significantly different ($\alpha = 0.05$) from responses at 10% full-strength.

Between species. The results of comparisons were similar to those following regular feeding (Table IV), except that now the responses of *P. clarkii* differed significantly from those of *O. rusticus* for every behavior at stimulant concentrations ≥50% full-strength; *P. clarkii* detected the feeding stimulant and probed significantly sooner than did *O. rusticus* (Table V). As in the regularly fed groups, locomotion in *P. clarkii* was significantly delayed compared to *O. rusticus* due to the time spent probing the gravel by *P. clarkii.* At all three stimulant concentrations ≥50% full-strength, *P. clarkii* probed the gravel significantly longer before initiating locomotion (mean ± SD: 107.0 ± 8.34 s at 100%; 124.3 ± 5.23 s at 75%; 102.4 ± 35.06 s at 50% full-strength) than did *O. rusticus* (mean ± SD: 11.5 ± 5.85 s at 100%; 10.5 ± 1.50 s at 75%; 12.9 ± 2.59 s at 50% full-strength) (Mann-Whitney *U* test, $P < 0.01$ for all comparisons; Table V). Due to the altered order of initiation of locomotion and probing in *O. rusticus* presented with ≤25% full-strength stimulant (Table III), interspecific comparisons for the initiation times were not calculated. At the 10% full-strength concentration, food-deprived *P. clarkii* detected the stimulus significantly sooner than did food-deprived *O. rusticus* (Table V).

Discussion

As expected, both *Procambarus clarkii* and *Orconectes rusticus* crayfishes responded to the feeding stimulant, suggesting that chemoreception is used in the foraging strategy of both species. The results indicate that low concentrations of chemical feeding stimuli preferentially activated far-field (distant) food search in both species following regular feeding. Appetitive feeding (near-field search, or probing the substrate) always occurred before locomotion (far-field, or distant search) in response to high-concentration stimuli (≥50% full-strength), indicating that a behavioral dichotomy exists between food search and feeding behavior in these species. Detection always occurred first. Thus, there is a linear organization of these behavioral components of food-search behavior.

Our results differ from those of experiments with a variety of marine decapod crustaceans. Those studies indicate that chemical feeding stimuli selectively activate near-field (nearby) rather than distant food search, regardless of the stimulus concentration. In those studies, lesser concentrations of food odor activated substrate probing (appetitive feeding), and only greater concentrations of food odor activated locomotion. Thus, food search in those species is primarily organized to obtain nearby food items, implying that there is no behavioral dichotomy between food search and feeding (*e.g.*, Zimmer-Faust and Case, 1982, 1983; Zimmer-Faust *et al.*, 1984; Zimmer-Faust, 1987; see review in Zimmer-Faust and Case, 1982).

One week of food deprivation had no effect on the organization of food search and feeding in *P. clarkii* for either rank order of occurrence or latency to initiation of any of the components of food-search behavior. One week of food deprivation, however, did affect the organization of food search and feeding in *O. rusticus* for those crayfish presented with 25% and 10% full-strength concentrations. Crayfish in these groups now initiated probing prior to locomotion (a reversal of previous behavior). In natural situations this behavior would appear not to be adaptive given the low probability of finding food nearby. Otherwise, there were no statistically significant effects of food deprivation on the behavioral responses of either species.

Perhaps the behavior of *O. rusticus* presented with the low-concentration feeding stimulants following one week of food deprivation is not as maladaptive as it first appears. It could be that food deprivation has made the animals less selective in their foraging strategy, and that any concentration of food odor is sufficient to initiate appetitive feeding behavior prior to locomotion. Perhaps food deprivation leads individual *O. rusticus* to interpret low-concentration food odors as originating from small nearby food items (*sensu* Reeder and Ache, 1980; Zimmer-Faust and Case, 1982). Under those conditions the behavior might represent an adaptive foraging strategy for this species. In addition, freshwater crayfishes (as well as marine decapods) locomote spontaneously; thus chemical induction of locomotion may not always be necessary for "distant" foraging to occur (Zimmer-Faust and Case, 1983).

For stimulant concentrations of 50% and 75% full-strength, *P. clarkii* detected the feeding stimulant and began probing significantly sooner than *O. rusticus,* both following regular feeding and after food deprivation (see Tables IV and V). The initiation of locomotion in *P. clarkii* was significantly delayed compared to *O. rusticus* due to the time the former spent probing the gravel. At all three stimulant concentrations ≥50% full-strength, *P. clarkii* probed the gravel significantly longer before initiating locomotion than did *O. rusticus* (see Tables IV and V, and Results). *Procambarus clarkii,* therefore, appears to be significantly more responsive to moderate concentrations of food odors, at least in this experimental situation, than does *O. rusticus* for all three behavioral components of food search behavior. We speculate that such differential chemoreception in response to food odors could contribute to the invasion success of *P. clarkii* by allowing crayfish of this species to detect economically significant food items more quickly.

Acknowledgments

This research was funded by a grant from the Faculty Professional Development Council, Pennsylvania State System of Higher Education, to C. Steele and C. Skinner. Portions of the results were presented at the following conferences: Pennsylvania Aquarium Consortium Environmental Conference II, 4–6 October 1996, Gannon University, Erie, PA; 106th Annual Meeting, Ohio Academy of Science, 4–6 April 1997, Bowling Green State University, Bowling Green, OH; Pennsylvania Natural History Conference, 25–27 April 1997, Powdermill Biological Station, Rector, PA.

Literature Cited

Atema, J. 1977. Functional separation of smell and taste in fish and crustacea. Pp. 165–173 in *Olfaction and Taste, Vol. 6,* J. LeMagnen and P. MacLeod, eds. Information Retrieval, London.

Bell, W. J., and T. R. Tobin. 1982. Chemo-orientation. *Biol. Rev.* **57:**1319–1324.

Derby, C., and J. Atema. 1982. The function of chemo- and mechanoreceptors in lobster (*Homarus americanus*) feeding behavior. *J. Exp. Biol.* **98:**317–327.

Derby, C., and J. Atema. 1988. Chemoreceptor cells in aquatic invertebrates: peripheral mechanisms of chemical signal processing in decapod crustaceans. Pp. 365–386 in *Sensory Biology of Aquatic Animals,* J. Atema, R. R. Fay, A. N. Popper, and W. N. Tavolga, eds. Springer-Verlag, New York.

Erichsen, J. T., J. R. Krebs, and A. I. Houston. 1980. Optimal foraging and cryptic prey. *J. Anim. Ecol.* **49:**271–276.

Glantz, S. A. 1997. *Primer of Biostatistics.* 4th ed. McGraw-Hill, New York. Pp. 350–351.

Hazlett, B. A. 1971a. Antennule chemosensitivity in marine decapod crustacea. *J. Anim. Morphol. Physiol.* **18:**1–10.

Hazlett, B. A. 1971b. Chemical and chemotactic stimulation of feeding behavior in hermit crab, *Petrochirus diogenes. Comp. Biochem. Physiol.* **39A:**665–670.

Hazlett, B. A. 1994. Crayfish feeding responses to zebra mussels depend on microorganisms and learning. *J. Chem. Ecol.* **20:**2623–2630.

Hindley, J. P. R. 1975. The detection, location and recognition of food by juvenile banana prawns, *Panaeus merguiensis* de Man. *Mar. Behav. Physiol.* **3:**193–210.

Hughs, R. N. 1979. Optimal diets under the energy maximization premise: the effects of recognition time and learning. *Am. Nat.* **113:** 209–221.

Itagaki, H., and J. H. Thorpe. 1981. Laboratory experiments to determine if crayfish can communicate chemically in a flow-through system. *J. Chem. Ecol.* **7:**115–126.

Johnson, B. R., and J. Atema. 1986. Chemical stimulants for a component of feeding behavior in the common gulf-weed shrimp *Leander tenuicornis* (Say). *Biol. Bull.* **170:**1–10.

Mackie, A. M. 1973. The chemical basis of food detection in the lobster *Homarus gammarus. Mar. Biol.* **15:**103–108.

McLeese, D. W. 1970. Detection of dissolved substances by the American lobster (*Homarus americanus*) and olfactory attraction between lobsters. *J. Fish Res. Board Can.* **27:**1371–1378.

McLeese, D. W. 1973. Orientation of lobsters (*Homarus americanus*) to odor. *J. Fish Res. Board Can.* **30:**838–840.

Momot, W. T. 1995. Redefining the role of crayfish in aquatic ecosystems. *Rev. Fish. Sci.* **3**(1):33–63.

Norrocky, M. J. 1983. *Procambarus* (*Scapulicambarus*) *clarkii* (Girard, 1952): the red swamp crayfish in Ohio. *Ohio J. Sci.* **46:**75–82.

Orians, G. H. 1981. Foraging behavior and the evolution of discriminatory abilities. Pp. 389–405 in *Foraging Behavior,* A. C. Kamil, and T. D. Sargent, eds. Garland Press, New York.

Pearson, W. H., P. C. Sugarman, D. L. Woodruff, and B. L. Olla. 1979. Thresholds for detection and feeding behavior in the Dungeness crab, *Cancer magister* (Dana). *J. Exp. Mar. Biol. Ecol.* **39:**65–78.

Peckarsky, B. I. 1984. Predator-prey interactions among aquatic insects. Pp. 196–254 in *The Ecology of Aquatic Insects,* V. H. Resh, and D. M. Rosenberg, eds. Praeger Publishers, New York.

Reeder, P. B., and B. W. Ache. 1980. Chemotaxis in the Florida spiny lobster, *Panulirus argus. Anim. Behav.* **28:**831–839.

Rittschof, D. 1982. Chemical attraction of hermit crabs and other attendants to simulated gastropod predation sites. *J. Chem. Ecol.* **6:**103–118.

Rohlf, F. J., and R. R. Sokal. 1981. *Statistical Tables.* 2nd ed. Freeman, San Francisco. Pp. 98; 185–190.

Schembri, P. J. 1981. Feeding in *Ebalia tuberosa* (Pennant) (Crustacea: Decapoda: Leucosiidae). *J. Exp. Mar. Biol. Ecol.* **55:**1–10.

Shelton, R. G. J., and A. M. Mackie. 1971. Studies on the chemical preferences of the shore crab, *Carcinus maenas* (L.). *J. Exp. Mar. Biol. Ecol.* **7:**41–49.

Sokal, R. R., and F. J. Rohlf. 1981. *Biometry,* 2nd ed. W. H. Freeman, San Francisco. Pp. 74; 438–439; 704–716.

Steele, C. W., S. Strickler-Shaw, and D. H. Taylor. 1992. Attraction of crayfishes *Procambarus clarkii, Orconectes rusticus* and *Cambarus bartoni* to a feeding stimulant and its suppression by a blend of metals. *Environ. Toxicol. Chem.* **11:**1323–1329.

Tierney, A. J., and J. Atema. 1986. Effects of acidification on the behavioral responses of crayfishes (*Orconectes virilis* and *Procambarus acutus*) to chemical stimuli. *Aquat. Toxicol.* **9:**1–11.

Tierney, A. J., and J. Atema. 1988. Behavioral responses of crayfish (*Orconectes virilis* and *Orconectes rusticus*) to chemical feeding stimulants. *J. Chem. Ecol.* **14**(**1**)**:**123–133.

Werner, E. E., and G. G. Mittelbach. 1981. Optimal foraging: field tests of diet choice and habitat switching. *Am. Zool.* **21:**813–829.

Wilman, E. J., A. M. Hill, and D. M. Lodge. 1994. Response of three crayfish congeners (*Orconectes* spp.) to odors of fish carrion and live predatory fish. *Am. Midl. Nat.* **132:**44–54.

Zimmer-Faust, R. K. 1987. Crustacean chemical perception: Towards a theory on optimal chemoreception. *Biol. Bull.* **172:**10–29.

Zimmer-Faust, R. K., and J. F. Case. 1982. Organization of food search in the kelp crab, *Pugettia producta* (Randall). *J. Exp. Mar. Biol. Ecol.* **57:**237–255.

Zimmer-Faust, R. K., and J. F. Case. 1983. A proposed dual role of odor in foraging by the California spiny lobster, *Panulirus interruptus* (Randall). *Biol. Bull.* **164:**341–353.

Zimmer-Faust, R. K., J. E. Tyre, W. C. Michel, and J. F. Case. 1984. Chemical mediation of appetitive feeding in a marine decapod crustacean: the importance of suppression and synergism. *Biol. Bull.* **167:** 339–353.

EVOLUTION:
A MOLECULAR POINT OF VIEW

Proceedings
of a workshop
sponsored by
THE CENTER FOR ADVANCED STUDIES
IN THE SPACE LIFE SCIENCES
AT THE MBL

24–26 October 1997

Marine Biological Laboratory,
Woods Hole, Massachusetts

Funded by THE NATIONAL AERONAUTICS AND SPACE ADMINISTRATION under Cooperative Agreement NCC 2-896. Reprints of this symposium can be obtained from the NASA Center for Advanced Studies in the Space Life Sciences, 7 MBL Street, Woods Hole, MA 02543, Tel. 508-289-7199.

CONTENTS

Evolution: a Molecular Point of View

Sogin, Mitchell
Introduction 307
Chang, Sherwood
Planetary environments and the origin of life 308
Ferris, James P.
Prebiotic synthesis on minerals: bridging the prebiotic and RNA worlds 311
Ellington, Andrew D.
Molecular origins and the null hypothesis: motifs from our Maker? 315
Huang, Faqing, Zhili Yang, and Mike Yarus
Self-capping RNA catalysts derived from selection-amplification 320
Bartel, David P.
Creation and evolution of new ribozymes. 322
Landweber, Laura F.
The evolution of cellular computing 324
Weiner, Alan M., and Nancy Maizels
The genomic tag hypothesis: modern viruses as molecular fossils of ancient strategies for genomic replication, and clues regarding the origin of protein synthesis. . . 327
Maizels, Nancy, Alan M. Weiner, Dongxian Yue, and Pei-Yong Shi
New evidence for the genomic tag hypothesis: archael CCA-adding enzymes and tDNA substrates . . . 331
Ibba, M., A.W. Curnow, J. Bono, P.A. Rosa, C.R. Woese, and D. Söll
Archaeal aminoacyl-tRNA synthesis: unique determinants of a universal genetic code?. 335
Sharp, Paul M., Elizabeth Bailes, David L. Robertson, Feng Gao, and Beatrice H. Hahn
Origins and evolution of AIDS viruses 338
Felsenstein, Joseph
Coalescents, phylogenies, and likelihoods. 343
Cummings, Michael P., Sarah P. Otto, and John Wakeley
Genes and other samples of DNA sequence data for phylogenetic inference 345
Schopf, J. William
Deep divisions in the tree of life—what does the fossil record reveal? 351
Doolittle, Russell F., Da-Fei Feng, and Glen Cho
Determining divergence times with protein clocks. . 356
Gogarten, J. Peter, Ryan D. Murphey, and Lorraine Olendzenski
Horizontal gene transfer: pitfalls and promises 359
DeLong, Edward F., Christa Schleper, Robert Feldman, and Ronald V. Swanson
Application of genomics for understanding the evolution of hyperthermophilic and nonthermophilic Crenarchaeota. 363
Reysenbach, A.-L., S. Seitzinger, J. Kirshtein, and E. McLaughlin
Molecular constraints on a high-temperature evolution of early life. 367
Forterre, Patrick, and Hervé Philippe
The Last Universal Common Ancestor (LUCA): simple or complex?. 373
Doolittle, W. Ford
Rethinking the origin of eukaryotes 378
Patterson, David J., Alastair G.B. Simpson, and Nimalika Weerkaoon
Free-living flagellates from anoxic habitats and the assembly of the eukaryotic cell 381
Clark, C. Graham
The effect of secondary loss on our views of eukaryotic evolution. 385
Hasegawa, Masami, and Tetsuo Hashimoto
Phylogenetic position of amitochondriate protists in the evolution of eukaryotes. 389
Cavalier-Smith, T.
Zooflagellate phylogeny and the systematics of protozoa 393
Douglas, Susan E.
Evolutionary history of plastids 397
Gray, Michael W., Gertraud Burger, Robert Cedergren, G. Brian Golding, Claude Lemieux, David Sankoff, Monique Turmel, and Franz Lang
A genomics approach to mitochondrial evolution . . 400
Redfield, Rosemary J.
The problem of the evolution of sex 404
Bode, Hans, Daniel Martinez, M. Andrew Shenk, Kerry Smith, Robert Steele, and Ulrich Technau
Evolution of head development 408
Mohr, Scott, Jim Freeman, Tom Plasterer, and Temple Smith
Patterns of mitochondrial DNA strand asymmetry correlate with phylogeny. 411
Margulis, Lynn, Michael Dolan, and Ricardo Guerrero
The molecular tangled bank: not seeing the phylogenies for the trees 413

CONCLUDING REMARKS 415

LIST OF PARTICIPANTS 417

Reference: *Biol. Bull.* **196:** 307. (June 1999)

Introductory Remarks

MITCHELL L. SOGIN

Josephine Bay Paul Center, Marine Biological Laboratory, 7 MBL Street, Woods Hole, Massachusetts 02543-1015

Molecular Evolution is a broad field, with a conceptual base that should unify biology. Some of the speakers at this meeting will talk about topics with which you may not be very familiar. These speakers are for the most part biologists who study the evolution of genes, genomes, and metabolic capacities.

We are holding a meeting on molecular evolution at the MBL, first because we have interests in the Woods Hole community, and also because NASA has played a historical role in evolutionary biology. The original charter for NASA included a mission for the agency to search for extraterrestrial life, or to at least understand how life might have arisen on this planet. From the very beginning, NASA has always been interested in this particular topic. I would like to argue that, if it hadn't been for the money that NASA put into evolutionary biology, major advances that have occurred in this field, particularly as mediated through molecular evolution, would not have occurred in the time that they did occur. One exemplary advance is the discovery of Archaebacteria by Carl Woese.

NASA is now proposing to expand support for evolutionary biology with the formation of an Astrobiology Institute. Astrobiology deals with the cosmic evolution of biogenic compounds—prebiotic evolution. From my perspective, this is an interesting new field because it addresses the early evolution of life and the evolution of advanced life.

NASA will need a lot of guidance and help in establishing this Institute. The participants at this meeting have been invited to talk about Astrobiology and the kinds of areas that NASA might support.

This paper was originally presented at a workshop titled *Evolution: A Molecular Point of View*. The workshop, which was held at the Marine Biological Laboratory, Woods Hole, Massachusetts, from 24–26 October 1997, was sponsored by the Center for Advanced Studies in the Space Life Sciences at MBL and funded by the National Aeronautics and Space Administration under Cooperative Agreement NCC 2-896.

Reference: *Biol. Bull.* **196:** 308–310. (June 1999)

Planetary Environments and the Origin of Life

SHERWOOD CHANG

Exobiology Branch, NASA Ames Research Center, Moffett Field, California 94035

As a consequence of advances in modeling planet formation processes, Earth is now thought to have formed hot, rather than cold, with core formation occurring during accretion. The atmosphere and oceans formed early, and although the climate was probably hot early on, the variation of surface temperature over time is largely unknown. Depending on the redox state of the mantle and that of impacting bodies, the atmosphere could have been weakly or strongly reducing overall, with perturbations caused by impacts. Seawater composition and redox state would have been governed primarily by circulation through hydrothermal systems. Out of this planetary context, life emerged at least 3.85 billion years ago (1), less than 600 million years after the period of planetary accretion.

Equable conditions for prebiotic evolution could have existed as early as 4.4 billion years ago. But these conditions were interrupted by major short-term perturbations in surface environments caused by a declining flux of impactors. Although giant impactors undoubtedly constrained the timing of life's origin, quantitative statements about when the clock was set await a stronger consensus on impactor fluxes and more refined theoretical models. Organic matter that survived impacts or was synthesized in impacts would have augmented the inventory of compounds produced endogenously in surface environments (2). But the fate of organic matter in large (>1 km) projectiles is poorly understood, and all estimates of the survival or synthesis rates from such impacts are highly uncertain (Fig. 1). At the other extreme, impactors in the 10–50 μm range (interplanetary dust particles), derived from comets and asteroids, would have decelerated gently in the upper atmosphere and are thought to have provided a substantial flux of organic matter early on (3).

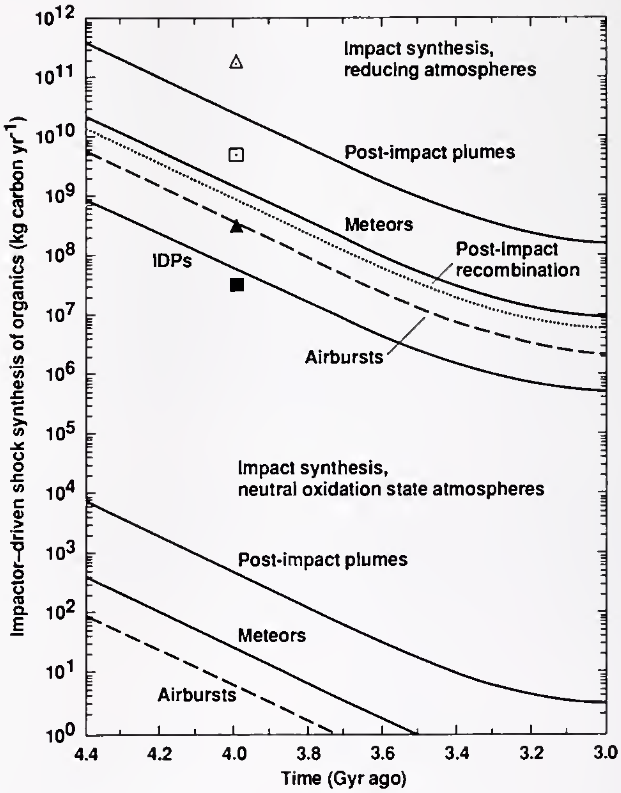

Figure 1. Rates of impact shock synthesis, exogenous delivery, and endogenous production of organic carbon as a function of time. Upper set of curves for a reducing atmosphere: CH_4 + (N_2 or NH_3) + H_2O; lower set for neutral redox atmosphere: $CO_2 + N_2 + H_2O$. Dashed lines indicate upper bounds, and the dotted line represents a poorly understood estimate that may be independent of atmospheric redox state. Open triangle and square, respectively, indicate production rates from lightning and UV (absorption by H_2S) in a highly reduced atmosphere; filled symbols apply to neutral atmospheres (absorption by CO_2). (After Chyba and Sagan, 1992.)

The geological record indicates the presence of carbon

This paper was originally presented at a workshop titled *Evolution: A Molecular Point of View*. The workshop, which was held at the Marine Biological Laboratory, Woods Hole, Massachusetts, from 24–26 October 1997, was sponsored by the Center for Advanced Studies in the Space Life Sciences at MBL and funded by the National Aeronautics and Space Administration under Cooperative Agreement NCC 2-896.

dioxide in the atmosphere as long ago as 3.8 billion years, but it is mute with respect to methane or carbon monoxide. If organic matter had to form in the atmosphere, theory and experiment indicate that productivity in atmospheres dominated by carbon dioxide would have been orders of magnitude lower than in those dominated by the reduced gaseous forms of carbon (Fig. 1). If the atmosphere has been only mildly reducing since the end of the major epoch of accretion at ~4.4 Ga, the apparent lack of strong atmospheric sources of hydrogen cyanide, formaldehyde, and ammonia poses a serious challenge for theories of prebiotic evolution, which require these key chemical intermediates for synthesis of more complex organic compounds (4). While the oxidation state of the prebiotic atmosphere remains controversial, little question exists about the reduced state of the early ocean. Only recently, however, have researchers begun exploring its potential for organic synthesis.

Environments at phase boundaries between gas, solid, and liquid states would appear to be highly favorable for prebiotic evolution and the origin of life, provided that they contain suitable sources of energy. These criteria are met by marine hydrothermal systems, intertidal regions, and the wind mixed layer of the ocean. These regions are ubiquitous, geophysically active boundary regions far from equilibrium, with gradients in properties maintained by physical and chemical energy fluxes. Within these environments, small-scale interfacial regions are provided by aerosols, volcanic and extraterrestrial dust, hydrothermal minerals, chemical precipitates, and vesicle-like structures of organic or mineral chemical composition. Inasmuch as life itself must have emerged as a phase-bounded system, the ability of an environment to form, dissipate, and reform small-scale interfaces (structures) must have been a prerequisite for the origin of life. In any such locale, however, there must be processes that offset the hazards of dilution, burial, and secondary decomposition of the compounds which are destined to be the molecular building blocks of life.

Decades of laboratory experimentation have been devoted to demonstrating steps in the prebiotic synthesis of the precursors of proteins, nucleic acids, and membranes. Yet, many uncertainties—about the monomers that were necessary and the manner of their production—remain. These uncertainties persist in some measure because most model syntheses suffer from dubious geochemical plausibility. The bulk of this work has also been carried out within the context of a canonical scenario for a stepwise progression toward the origin of life, from simple reactive compounds, to monomeric building blocks of proteins and nucleic acids, to the biopolymers themselves, to replicating systems. The validity of such a scenario has been largely accepted on faith, and alternatives merit experimental and theoretical exploration.

Literature Cited

1. **Mojzsis S., G. Arrhenius, K. D. McKeegan, T. M. Harrison, A. P. Nutman, and C. R. L. Friend. 1996.** Evidence for life on Earth before 3,800 million years ago. *Nature* **385:** 55–59.
2. **Chyba, C. F., and C. Sagan. 1992.** Endogenous production, exogenous delivery, and impact-shock synthesis of organic molecules: an inventory for the origins of life. *Nature* **355:** 125–131.
3. **Anders, A. 1989.** Pre-biotic organic matter from comets and asteroids. *Nature* **342:** 255–256.
4. **Chang, S. 1993.** Prebiotic synthesis in planetary environments. Pp. 259–299 in *The Chemistry of Life's Origins*, J. M. Greenberg *et al.*, eds. Kluwer Academic, Dordrecht, The Netherlands.

Discussion

YARUS: You have said that the reductive scenario might be rescued, but put in jail. That is, it might apply for short times, following certain impacts. What are those impacts? Are they at all probable?

CHANG: My response to your first statement is, "Yes." But "held captive" is probably a better term. "Held captive," probably, until more information is available on how the interior of the earth works. That has to do with how long, if ever, the early earth was able to maintain an atmosphere that was in equilibrium with metallic iron in the upper mantle or the core. A second point to consider is the prospect that some impactors were iron asteroids, or that the surface rock of the early earth still contained metallic iron during the prebiotic evolution era. In both cases the hot gases added to the atmosphere by vaporization of projectile and target during hypervelocity impact would have been substantially reduced. The carbon originally in these materials would have been converted to carbon monoxide. The larger and more iron-rich the projectile, the larger the amount of carbon monoxide that would have been generated. It is likely that much of the iron in earth's core was derived from iron-rich asteroids, and impacts with such objects must have continued after core formation since we continue to recover iron meteorites today. Those are the possibilities if organic synthesis must take place in a reduced atmosphere. On the other hand, I suggest that organic synthesis need not take place in the atmosphere. Drs. Wächtershäuser and Shock (1, 2) would like to convince you that considerable organic synthesis can take place in hydrothermal systems. However, that issue is not resolved.

Ellington: In your presentation, it seemed you were implying that polymer catalysts arose prior to polymer replication. Where do you think polymer replication fits in with the evolution of catalysis?

Chang: I'm not sure that I believe that polymer catalysis was important. Perhaps catalysis was important, but catalysis can take place without polymers. Short oligonucleotides and short peptides can be catalytic. In addition, the very surface of a membrane may be catalytic. Catalysis has to emerge before polymer replication. One might even argue that polymer replication is preceded by oligomer replication, and oligomer replication can then evolve chemically in conjunction with the evolution of catalytic function. I think that the development of catalytic functions and of the information system needed for replication is a single process. I believe the replication system is an emergent property of catalysis which may have its beginnings at the level of short oligomers.

Guerrero: In your presentation, you showed the presence of a subsurface biosphere. I see this as a critical issue. We now know that microbes live in granite and in basalt at a depth of 2 km, which implies the possibility that life occurs at these depths on other planets. Before we recognized microbial life at these depths, we were limited to the "photosphere," the well-lit surface of the planet. We know high pressure can be tolerated. The possibility of the origin of life in the deep subsurface, at high pressure, and in the absence of light from any star has increased. This changes our scenarios.

Chang: I don't disagree with you. I think that the hydrothermal systems are especially interesting and that the subsurface systems are somewhat less interesting. From my perspective as a physical organic chemist, I think we will finally discover that the organisms inhabiting subsurface biospheres never arose there, but rather colonized those extreme environments. If that is true, then I'm not sure that the granitic or basaltic subsurface environments are particularly interesting for the origin of life. On the other hand, those subsurface systems do appear to have liquid water and a continuous source of energy: hydrogen and CO_2 are present and can be coupled.

Literature Cited

1. **Wächtershäuser, G. 1988.** Before enzymes and templates: theory of surface metabolism. *Microbiol. Rev.* **52:** 452–484.
2. **Shock, E. 1992.** Chemical environments of submarine hydrothermal systems. *Origins Life Evol. Biosphere* **22:** 67–107.

Reference: *Biol. Bull.* **196:** 311–314. (June 1999)

Prebiotic Synthesis on Minerals: Bridging the Prebiotic and RNA Worlds

JAMES P. FERRIS

Department of Chemistry, Rensselaer Polytechnic Institute, Troy, New York 12180

An array of experimental findings suggest that the simple molecules required for the origin of life may have been available on the primitive Earth. The well-known Miller-Urey electric discharge experiment yields HCN, amino acids, and carboxylic acids (1). Carbonaceous meteorites contain over 70 amino acids, some heterocyclic compounds, including purines, and carboxylic acids. Other organics may have been synthesized under the reducing conditions present in hydrothermal systems (2). Although some of these organics may have been present on the primitive Earth, there is no agreement on which was the most important for their formation. The Miller-Urey experiment requires the presence of either hydrogen gas or reduced carbon and hydrogen compounds, such as methane, carbon monoxide, and ammonia, in the atmosphere of the primitive Earth. Most geochemists believe that the Earth's crust was not reducing when life originated, so the volcanic emissions that resulted in the primitive atmosphere were also not reducing. The notion that comets, meteorites, and asteroids delivered reduced organics to the surface of the primitive Earth is not favored by those who believe that, when these bodies hit the Earth's atmosphere, the organic compounds present on them would have been pyrolyzed. The hydrothermal synthesis of reduced organics is a relatively new hypothesis that is just now undergoing experimental evaluation.

Assuming that the requisite starting materials were available on the primitive Earth (2), and providing conditions that plausibly occurred at that time, I have undertaken to investigate how monomers, particularly mononucleotides, may have condensed to biopolymers (*i.e.,* polynucleotides). Some studies suggest that mononucleotides could have formed from the simpler molecules present on the primitive Earth. Oro (3) first reported the synthesis of adenine from concentrated solutions of HCN and ammonia. These studies could be extended to more dilute solutions of HCN (0.01 *M*) with the aid of a photochemical rearrangement of a tetramer of HCN (Fig. 1) (3). The imidazole intermediates formed in the synthesis of adenine were demonstrated to be intermediates in the synthesis of an array of other purines. The pyrimidines uracil and orotic acid are formed directly from HCN, whereas uracil and cytosine are formed from cyanoacetylene (Fig. 2) (3). As noted previously, carbonaceous meteorites were also a potential source of purines.

The reaction of these bases with ribose to form nucleosides has been investigated (1). Purine nucleosides are formed in low yield in the reaction with ribose when the mixture is heated in the dry state in the presence of the divalent ions (Fig. 3, equation 1). Pyrimidine nucleosides are not formed under these reaction conditions. The condensation of formaldehyde to ribose is not an efficient reaction, but the condensation of glycolaldehyde phosphate and formaldehyde to the 2,4-diphosphate of ribose does proceed efficiently (4). The phosphorylation of nucleosides to nucleotides proceeds under dry heating conditions (Fig. 3, equation 2). Many of these proposed prebiotic reactions do not proceed efficiently, and we must still determine whether other synthetic conditions will lead to more convincing prebiotic routes. Our investigation of the prebiotic synthesis of RNA is based on the assumption that the polymerization of monomers to polymers proceeded on mineral surfaces. This assumption is made because there is no evidence that long biopolymers form spontaneously in aqueous solution in the absence of enzymes (5). Minerals could have served as prototypical enzymes by selectively adsorbing organics from a mixture of other compounds and

---

This paper was originally presented at a workshop titled *Evolution: A Molecular Point of View*. The workshop, which was held at the Marine Biological Laboratory, Woods Hole, Massachusetts, from 24–26 October 1997, was sponsored by the Center for Advanced Studies in the Space Life Sciences at MBL and funded by the National Aeronautics and Space Administration under Cooperative Agreement NCC 2-896.

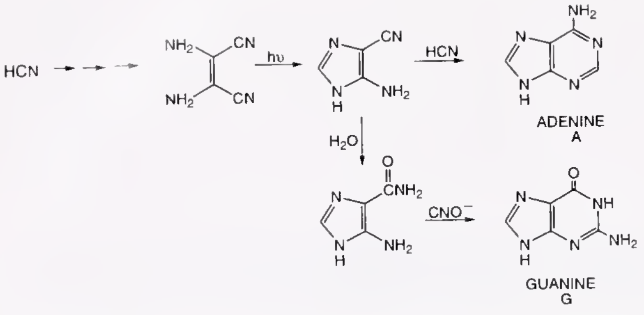

Figure 1. Pathways for the prebiotic synthesis of purines from dilute solutions of HCN.

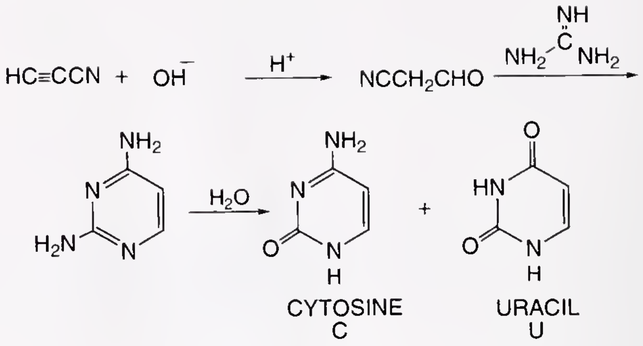

Figure 2. Formation of pyrimidines from cyanoacetylene.

catalyzing the self-condensation of these monomers to oligomers. In initial studies, dimers and trimers were formed by the carbodiimide-mediated reaction of 5′-mononucleotides on montmorillonite (1). Polynucleotides were obtained by the reaction of an aqueous solution of the 5′-phosphorimidazolides of mononucleotides (ImpN, Fig. 4, equation 1) on montmorillonite (6–8; Kawamura and Ferris, unpubl. data). The phosphorimidazolides of adenosine, inosine, cytidine, and uracil yielded oligomers containing 10–15 monomer units, whereas hexamers were the longest oligomers formed from ImpG.

In addition to catalyzing phosphodiester bond formation, montmorillonite also influences the regiochemistry of the phosphodiester link produced. The nucleotides of the purines adenine and hypoxanthine yield mainly 3′,5′-linked phosphodiester bonds (67% and 90%, respectively), while the pyrimidine nucleotides of uracil and cytosine yielded predominantly 2′,5′-linked nucleotides (50%–75%). The dimers and trimers formed from the reaction of ImpN in the absence of montmorillonite contain about 90% 2′,5′-linkages.

The regioselectivity for phosphodiester bond formation also varies with the activating group used. The use of 1-methyladenine or 4-dimethylaminopyridine as activating groups (Fig. 4, line 2) results in the formation of oligomers in which 90% of the phosphodiester bonds are 3′,5′-linked (9, 10).

One of the tenets of the proposed RNA world is that the sequence information of the RNA formed by prebiotic processes was preserved by template-directed synthesis (11). We tested this tenet by using the heterogeneous oligo(C)s formed by montmorillonite catalysis as templates for the

ROUTES TO NUCLEOSIDES AND NUCLEOTIDES

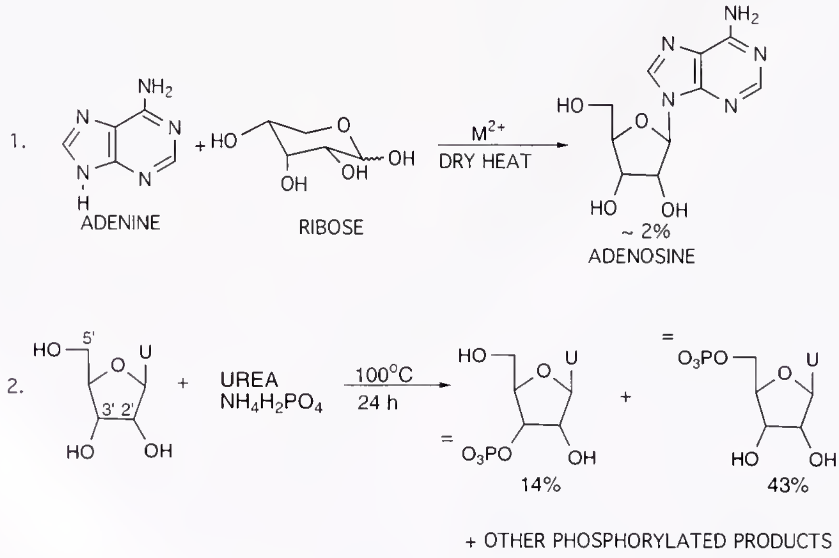

Figure 3. Routes to nucleosides and nucleotides. (1) A proposed prebiotic synthesis of adenosine. (2) Phosphorylation of the nucleoside uridine.

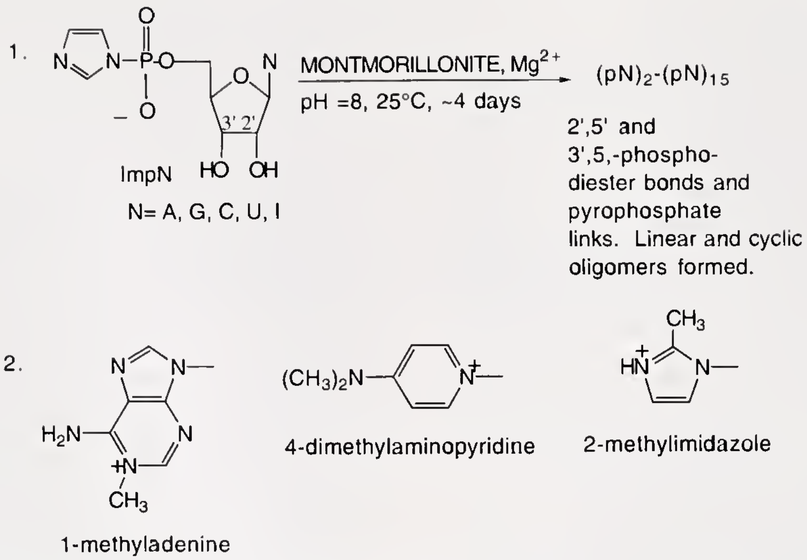

Figure 4. (1) Reaction of the phosphorimidazolides of nucleosides on montmorillonite. (2) Phosphate activating groups with the site of binding to the phosphate indicated.

formation of the complementary oligo(G)s. These oligo(C)s contain mainly 2′,5′-links along with 3′,5′- and pyrophosphates bonds (7); in addition, both straight-chain and cyclic oligomers are present as products. The complementary oligo(G)s were formed when the heterogeneous template was treated with 5′-GMP activated by 2-methylimidazole (Fig. 4, line 2). Both 2′,5′- and 3′,5-linked oligo(G)'s were formed in this template-directed synthesis. Even when all the 3′,5′-links were removed from the oligo(C)s, a template that directed the synthesis of the complementary oligo(G)s still resulted. Thus, the information content of the heterogeneous oligomers formed by mineral catalysis or by other prebiotic routes could have been maintained by template-directed synthesis.

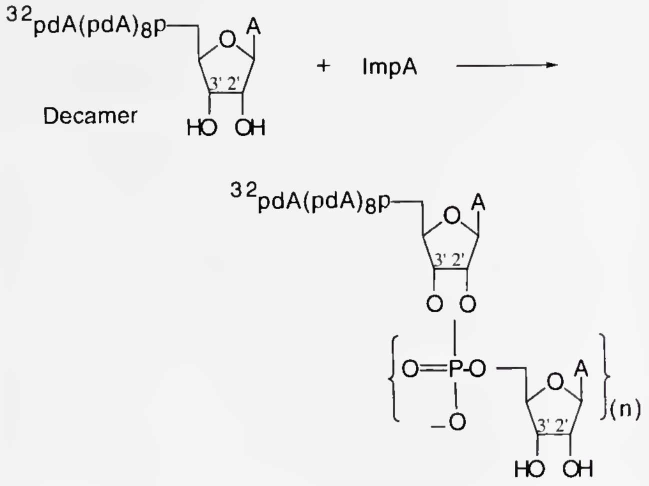

Figure 5. The reaction of ImpA with a decamer bound to montmorillonite.

The other characteristic of the proposed RNA world would have been its ability to catalyze the reactions of other organics. It is not likely that the 10-15-mers formed by clay mineral catalysis have sufficient 3-dimensional tertiary structure to bind and catalyze the reactions of other RNAs. But oligo(A)s as long as 50 mers could be made in 14 days in so-called "feeding reactions," where an activated monomer (ImpA) was added daily to a decameric primer bound to the montmorillonite (Fig. 5) (12). Oligomers with a median number of 30 bases and as long as 50 bases were detected as reaction products. These oligomers may be long enough to exhibit catalytic activity (13, 14). This experiment suggests that long oligomers may have been formed on the primitive Earth by activated monomers reacting with short oligomers bound to the surface of a catalytic mineral. What remains to be done is to prepare, on montmorillonite, oligomers containing two or more complementary bases in a feeding reaction, and to test the mixture of polynucleotides that forms for catalytic activity. If catalysis is found in this experiment, we will have demonstrated that RNAs possessing the two essential elements for the RNA world—information storage and catalysis—form from simple monomers.

Acknowledgments

I thank my skillful collaborators, listed in the references, who supplied many of the ideas and most of the experimental studies outlined in this review. The research was supported by NSF grant CHE-9619149 and, in part, by NASA grant NAG 5-4557.

Literature Cited

1. **Ferris, J. P. 1987.** Prebiotic synthesis—problems and challenges. *Cold Spring Harbor Symposia on Quantitative Biology* **52:** 29–35.
2. **Ferris, J. P. 1992.** Marine hydrothermal systems and the origin of life: chemical markers of prebiotic chemistry in hydrothermal systems. *Origins Life Evol. Biosphere* **22:** 109–134.
3. **Ferris, J. P., and W. J. Hagan, Jr. 1984.** HCN and chemical evolution: the possible role of cyano compounds in prebiotic synthesis. *Tetrahedron* **40:** 1093–1120.
4. **Eschenmoser, A. 1994.** Chemistry of potentially prebiological natural products. *Origins Life Evol. Biosphere* **24:** 389–423.
5. **Ferris, J. P. 1993.** Catalysis and prebiotic RNA synthesis. *Origins Life Evol. Biosphere* **23:** 307–315.
6. **Ferris, J. P., and G. Ertem. 1993.** Montmorillonite catalysis of RNA oligomer formation in aqueous solution. A model for the prebiotic formation of RNA. *J. Am. Chem. Soc.* **115:** 12270–12275.
7. **Ertem, G., and J. P. Ferris. 1997.** Template-directed synthesis using heterogeneous templates produced by montmorillonite catalysis. A possible bridge between the prebiotic and RNA worlds. *J. Am. Chem. Soc.* **119:** 7197–7201.
8. **Ding, P. Z., K. Kawamura, and J. P. Ferris. 1996.** Oligomerization of uridine phosphorimidazolides on montmorillonite: a model for the prebiotic synthesis of RNA on minerals. *Origins Life Evol. Biosphere* **26:** 151–171.
9. **Prabahar, K. J., T. D. Cole, and J. P. Ferris. 1994.** Effect of phosphate activating group on oligonucleotide formation on montmorillonite: the regioselective formation of 3′,5′-linked oligoadenylates. *J. Am. Chem. Soc.* **116:** 10914–10920.
10. **Prabahar, K. J., and J. P. Ferris. 1997.** Adenine derivatives as phosphate-activating groups for the regioselective formation of 3′,5′-linked oligoadenylates on montmorillonite: possible phosphate-activating groups for the prebiotic synthesis of RNA. *J. Am. Chem. Soc.* **119:** 4330–4337.
11. **Gilbert, W. 1986.** The RNA world. *Nature* **319:** 618.
12. **Ferris, J. P., A. R. Hill, Jr., R. Liu, and L. E. Orgel. 1996.** Synthesis of long prebiotic oligomers on mineral surfaces. *Nature* **381:** 59–61.
13. **Joyce, G. F., and L. E. Orgel. 1993.** Prospects for understanding the origin of the RNA World. Pp. 1–25 in *The RNA World*, R. F. Gesteland and J. F. Atkins, eds. Cold Spring Harbor Laboratory Press, Cold Spring Harbor, New York.
14. **Szostak, J. W., and A. D. Ellington. 1993.** *In vitro* selection of functional RNA sequences. Pp. 511–53 in *The RNA World*, R. F. Gesteland and J. F. Atkins, eds. Cold Spring Harbor Laboratory Press, Cold Spring Harbor, New York.

Discussion

FORTERRE: Have you, or do you plan to, do the same kind of experiment that you have described at different temperatures? Specifically, are you planning to look at high temperature? RNA is a very thermolabile molecule, which presents a problem for the hypothesis that life originated at very high temperature. We have shown that DNA is stabilized against thermodegradation by physiological salt concentrations (1), but we don't know how RNA behaves at high temperature in the presence of clay or salt.

FERRIS: We've done the RNA synthesis at high temperature. The reaction is not strongly temperature dependent. I've done some work on the stability of RNAs on clays that can catalyze formation and breakdown. Pyrimidine-containing RNAs tend to break down more readily than those containing purine. I can't say much more than that about stability.

REYSENBACH: Have you looked at lower pH conditions?

FERRIS: At lower pH, with the activated phosphates that we use, a competing reaction occurs. The basic leaving groups become protonated, and the rate of hydrolytic reaction of these activated derivatives becomes greater; this causes a competing hydrolysis of the activating group at lower pHs.

UNIDENTIFIED: Why have you neglected the roles of the natural polyamines in these syntheses?

FERRIS: The polyamines will bind exceedingly strongly to the clay, especially if the clay has somewhat acidic surfaces. We haven't necessarily neglected polyamines, we just haven't gotten around to them. Orgel and co-workers (2, 3, 4) have looked at the 2′, 3′-cyclic phosphate of nucleotides in anhydrous conditions in the presence of ethylenediamine and similar polyamines. They find that the cyclic phosphates will polymerize in the absence of water, whereas the reaction does not proceed efficiently in the presence of water.

ELLINGTON: Why are you focusing on monomer addition rather than oligomer ligation?

FERRIS: We find that monomer addition works very well. On the other hand, our preliminary studies on ligation reactions, where we hooked dimers together using carbodiimide, didn't work very well. The latter reaction tended to hook the phosphates together to form pyrophosphate linkages.

Literature Cited

1. **Marguet, T., and P. Forterre. 1994.** DNA stability at temperatures typical for hyperthermophiles. *Nucl. Acid. Res.* **22:** 1681–1686.
2. **Renz, M., R. Lohrmann, and L. E. Orgel. 1971.** Catalysts for the polymerization of adenosine cyclic 2′,3′-phosphate on a Poly (U) template. *Biochim. Biophys. Acta* **240:** 463–471.
3. **Verlander, M. S., R. Lohrmann, and L. E. Orgel. 1973.** Catalysts for the self-polymerization of adenosine cyclic 2′,3′-phosphate. *J. Mol. Evol.* **2:** 303–306.
4. **Verlander, M. S., and L. E. Orgel. 1974.** Analysis of high molecular weight material from the polymerization of adenosine cyclic 2′,3′-phosphate. *J. Mol. Evol.* **3:** 115–120.

Reference: *Biol. Bull.* **196:** 315–319. (June 1999)

Molecular Origins and the Null Hypothesis: Motifs From Our Maker?

ANDREW D. ELLINGTON

Department of Chemistry, University of Texas at Austin, Austin, Texas 78712

A comparative examination of the sequences and functions of molecules can reveal clues as to their origins. However, the unity of modern biochemistry makes it likely that most extant molecules descend from an organismal singularity known as the progenote, the last common ancestor of modern life. The progenote was already complex, containing a variety of enzymes and cofactors; multiple metabolic pathways; and replication, transcription, and translation apparatuses. Because nucleic acids and nucleic acid cofactors are prevalent in basal metabolic processes ranging from redox reactions to translation, one of the progenote's predecessors has been hypothesized to have lived in an "RNA world" in which ribozymes, rather than protein enzymes, catalyzed most biochemical transformations. Further support for the existence of an RNA world has been garnered from the discovery of catalytic RNAs, and from experiments in which functional nucleic acids have been selected from random sequence populations. If functional nucleic acids or ribozymes are present in nature, or are relatively easy to generate by *in vitro* selection—the argument goes—then similar functional nucleic acids or ribozymes could have also existed during the evolution of an RNA world. In some cases though, these arguments are carried further, and it is claimed that, not only are natural or unnatural RNA molecules doppelgangers of ancient RNAs, but sequence or structural motifs that exist in modern RNA molecules are identical to those that existed in a putative RNA world. These claims should in all instances be evaluated in relation to the null hypothesis: that modern, functional RNAs may have arisen by chance and thus either have no historical connection to the RNA world, or at best have no connection that can be experimentally tested. Several popular vignettes of the RNA world, in which modern RNAs are claimed to descend from their forebears, will be examined in light of the null hypothesis.

Vignette #1: The tRNA tag hypothesis and the origin of replication

Transfer RNA is one of the biochemical features held in common by all modern life forms, and it has been persuasively argued that tRNA is a remnant of the RNA world. However, given that translation did not, by definition, occur in an all-RNA world, the primordial role of tRNA is unclear. Weiner and Maizels (1, 2, 3) have suggested that tRNA may have served as a "tag" for signaling or initiating replication, much as it does in many modern viruses. While this is a plausible argument, it is no more plausible than many other explanations that could also be put forth for the origins of tRNA. For example, tRNAs could have, with equal plausibility, arisen in the context of a primitive translation apparatus for the preparation of non-catalytic peptides, such as the polyglutamate tails of folate cofactors. Or tRNAs could have served as carriers for amino acids involved in the biosynthesis of other cofactors, such as the glutamate tRNAs that currently act as the precursors for porphyrins in some organisms.

In an attempt to support the hypothesis that tRNA tags may have existed in the RNA world, Weiner and Maizels have suggested that modern, viral tRNA tags are direct descendents of those that may have existed in the RNA world. This hypothesis needs to be examined in light of the null hypothesis: that modern, viral tRNA tags were invented by opportunistic viruses at some time following the reign of ribozymes. I suggest that the null hypothesis has at least as much, if not more, logical force than the notion that tRNAs served as replication tags. Viruses frequently exploit cellu-

---

This paper was originally presented at a workshop titled *Evolution: A Molecular Point of View*. The workshop, which was held at the Marine Biological Laboratory, Woods Hole, Massachusetts, from 24–26 October 1997, was sponsored by the Center for Advanced Studies in the Space Life Sciences at MBL and funded by the National Aeronautics and Space Administration under Cooperative Agreement NCC 2-896.

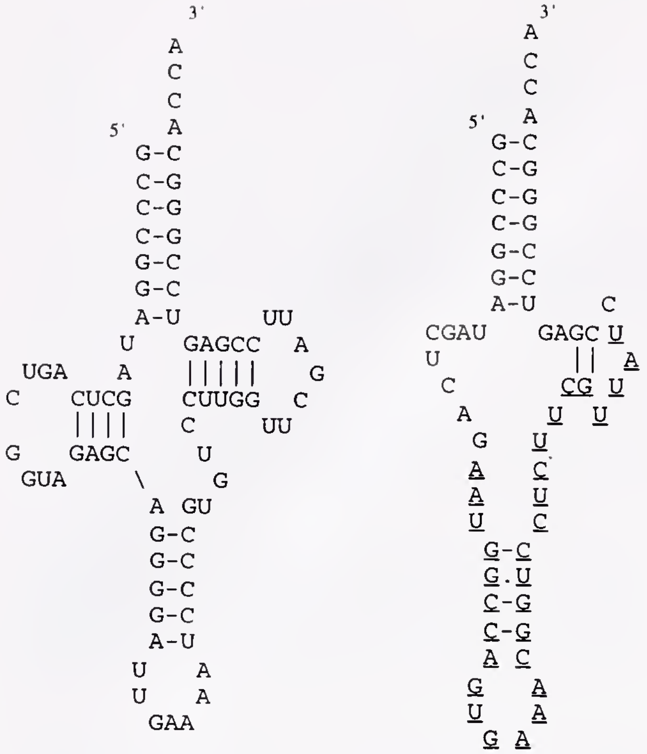

Figure 1. Natural and unnatural substrates for tRNA synthetases. On the left is *E. coli* phenylalanyl tRNA. On the right is an RNA molecule selected to bind *E. coli* phenylalanine tRNA synthetase. Residues that were originally present in the random-sequence region are underlined. Redrawn from Peterson *et al.* (7).

lar metabolism by interacting with, or altering, the functions of cellular metabolites or proteins. If a virus were to invent an RNA molecule that could be used to exploit cellular metabolism, then one of the most obvious targets would be the most abundant RNA molecule in the cell: tRNA. Moreover, if the tRNA tags on viruses were invented by viruses, rather than descending directly from a primordial RNA world, then it might be expected that the tags would be quite different in sequence and structure than the conserved and canonical cloverleaf of tRNA. This is, in fact, the case: many viral tags contain sequences and structures, such as pseudoknots, that have not, so far, been identified in the cellular world (4, 5). In addition, selection experiments have demonstrated the relative ease of generating RNA molecules that can interact with tRNA synthetases and other proteins that bind tRNA, and yet do not contain the sequences and structures that signify cellular tRNAs (6, 7; Fig. 1). Although cellular tRNAs certainly perform more functions than RNAs that have merely been selected to bind proteins and thus may be subject to more sequence constraints, this is also true when cellular tRNAs and viral tags are compared. Thus, although the existence of a plausible explanation for the origins of tRNA would no doubt expand our knowledge of the RNA world and the origin of protein biosynthesis, the tRNA tag hypothesis cannot be claimed to be more likely than the null hypothesis: that viruses invented their tRNA tags.

Vignette #2: Arginine-binding sites and the origin of the genetic code

Anti-arginine aptamers have been selected from random-sequence populations (8, 9). Analyses of the functional sequences within these aptamers suggested that there was an unusual preponderance of sequence triplets that corresponded to arginine codons. This apparent statistical correlation was used to advance the hypothesis that direct interactions between arginine and an arginine codon were somehow involved in the evolution of the genetic code itself. The route by which an arginine codon may have become an aminoacylated tRNA is uncertain. Moreover, such a process seems mechanistically implausible; for example, it is unclear how an original, direct association between codon and amino acid could have become the rather indirect association between codon and amino acid that is mediated by an aminoacylated tRNA (10). Nevertheless, the notion that amino acid:RNA interactions drove the formation of the genetic code can be separately evaluated in comparison with the null hypothesis: that the apparent preponderance of amino acid:RNA interactions is either nonexistent or an anomaly. To ferret out the details behind the supposed correlation requires a deeper insight into how selection experiments are conducted. The anti-arginine aptamers that contained a preponderance of arginine codons were selected from an RNA population with a relatively short (25 residue) random-sequence tract. The selected sequences were predicted to form secondary structures that would include the constant sequence regions at the termini of the pool; in other words, the functional arginine-binding site was presented not in the context of random sequence, but in the context of an arbitrary, predetermined sequence. If the constant sequence, in fact, skewed the anti-arginine aptamers to include presumptive arginine codons, then other selections, in which the constant region did not play as large a role, should reveal this. In fact, subsequent selections for anti-arginine aptamers yielded binding species with affinities for arginine that were higher, with functional sequences and structures that were drawn solely from the original random-sequence tract, but with functional sequences containing no apparent predominance of arginine codons (11, 12). Thus, while it would be interesting to know whether the genetic code is more than the "frozen accident" that Crick hypothesized, selection experiments provide no evidentiary basis for such a speculation.

Vignette #3: Anti-aminoglycoside aptamers and the origin of the ribosome

Aminoglycoside antibiotics have long been known to bind to ribosomal RNA (rRNA). More recently, some aminoglycoside antibiotics have been shown to bind to ribozymes. This has led some researchers to suggest that the aminoglycoside antibiotic-binding sites on the ribosome are related to the aminoglycoside antibiotic-binding sites on ribozymes, and thus that ribozymes and ribosomal RNA are somehow historically related (13). As with the previous vignettes, the plausibility of this argument turns on the competing plausibility of the null hypothesis: that the occurrence of aminoglycoside-binding sites on ribosomal RNA and ribozymes is coincidental. In essence, these competing hypotheses can be reduced to the question of whether there are few or many ways for RNA to bind aminoglycosides. To answer this question, Lato *et al.* (14) selected anti-aminoglycoside aptamers with affinities and specificities for the aminoglycosides lividomycin and kanamycin that are similar to those observed for rRNA. When the selected populations were characterized, it was discovered that there were literally millions and perhaps billions of unique ways to form aminoglycoside-binding sites. In other words, it was unclear whether a functional relationship (aminoglycoside binding) was, in fact, an accurate predictor of a historic relationship. Rather, the functional relationship could have readily existed even if the aminoglycoside-binding sites on ribosomal RNA and ribozymes were quite independently derived. Overall, this latter interpretation is also most consistent with the hypothesis that aminoglycosides were invented by bacteria to bind rRNA, rather than *vice versa.* To the extent that aminoglycosides evolved as biochemical weapons and were targeted to the translation apparatuses of many different organisms, then many different RNAs, including non-ribosomal RNAs such as ribozymes, should be able to bind to them.

These three vignettes highlight a disturbing trend in modern thinking about abiogenesis and the evolution of metabolism. We can now bring increasingly powerful techniques and methods to bear on experimental problems that affect our understanding of the origins of life. However, the results of these experiments are often interpreted as being proof of a particular scenario, rather than as general support for a more vague view of our origins. While it would be extremely exciting to establish that the RNA world evolved according to a particular scenario, it is unfortunately unlikely that sequence minutiae have remained unchanged and unscathed following a several billion year journey through multiple different types of organisms and biochemistries. Much of the comparative biochemistry of the RNA world was lost at the transition to protein-based catalysis, and again later during the ascendance of the progenote. Thus, just as paleontologists and anthropologists are cautious in interpreting an incomplete fossil record, molecular biologists should be similarly circumspect in interpreting a molecular fossil record that continues to undergo change and is open to many interpretations. In many instances, despite the exuberance of the Discussion sections of papers, we will likely have to forever remain agnostics about the true nature of the RNA world.

Literature Cited

1. **Weiner, A. M., and N. Maizels. 1987.** 3′ terminal tRNA-like structures tag genomic RNA molecules for replication: implications for the origin of protein synthesis. *Proc. Natl. Acad. Sci. USA* **84:** 7383–7387.
2. **Maizels, N., and A. M. Weiner. 1993.** The genomic tag hypothesis: modern viruses are molecular fossils of ancient strategies for genomic replication. Pp. 577–602 in *The RNA World,* R. F. Gesteland and J. F. Atkins, eds. Cold Spring Harbor Laboratory Press, Cold Spring Harbor, New York.
3. **Maizels, N., and A. M. Weiner. 1994.** Phylogeny from function: evidence from the molecular fossil record that tRNA originated in replication, not translation. *Proc. Natl. Acad. Sci. USA* **91:** 6729–6734.
4. **Haenni, A. L., S. Jnshi, and F. Chapeville. 1982.** tRNA-like structures in the genomes of RNA viruses. *Prog. Nucleic Acid Res. Mol. Biol.* **27:** 85–104.
5. **Guerrier-Takada, C., A. van Belkum, C. W. Pleij, and S. Altman. 1988.** Novel reactions of RNase P with a tRNA-like structure in turnip yellow mosaic virus RNA. *Cell* **53:** 267–272.
6. **Peterson, E. T., J. Blank, M. Sprinzl, and O. C. Uhlenbeck. 1993.** Selection for active *E. coli* tRNA (Phe) variants from a randomized library using two proteins. *EMBO J.* **12:** 2959–2967.
7. **Peterson, E. T., T. Pan, J. Coleman, and O. C. Uhlenbeck. 1994.** *In vitro* selection of small RNAs that bind to *Escherichia coli* phenylalanyl-tRNA synthetase. *J. Mol. Biol.* **242:** 186–192.
8. **Connell, G. J., M. Illangesekare, and M. Yarus. 1993.** Three small ribooligonucleotides with specific arginine sites. *Biochemistry* **32:** 5497–5502.
9. **Connell, G. J., and M. Yarus. 1994.** RNAs with dual specificity and dual RNAs with similar specificity. *Science* **262:** 1137–1141.
10. **Hirao, I., and A. D. Ellington. 1995.** Re-creating the RNA world. *Curr. Biol.* **5:** 1017–1022.
11. **Famulok, M. 1994.** Molecular recognition of amino acids by RNA-aptamers: an L-citrulline binding RNA motif and its evolution into an L-arginine binder. *J. Am. Chem. Soc.* **116:** 1698–1706.
12. **Osborne, S. E., and A. D. Ellington. 1997.** Nucleic acid selection and the challenge of combinatorial chemistry. *Chem. Rev.* **97:** 349–370.
13. **Schroeder, R., B. Streicher, and H. Wank. 1993.** Splice-site selection and decoding: Are they related? *Science* **260:** 1443–1444.
14. **Lato, S. M., A. R. Boles, and A. D. Ellingtnn. 1995.** *In vitro* selection of RNA lectins: using combinatorial chemistry to interpret ribozyme evolution. *Chem. Biol.* **2:** 291–303.

Discussion

Landweber: Why did you analyze the pool of cyclic aptamers after only four rounds of selection? Isn't that going to force the result that you will find a lot of sequence diversity? If you went further, just a few would have actually survived.

Ellington: We selected the pool until it had characteristics, binding constants, similar to those of the ribosome. We wanted to ask, "What was the universe of sequences that could bind aminoglycosides like the ribosome?" That pool, containing a million to a billion sequences, was composed of sequences that could all bind like the ribosome, with about the same dissociation constant. If we had pushed that pool further, we could have worked it down to one sequence. That's what people who work on *in vitro* selection do. However, we wanted to ask the evolutionary question, rather than the molecular recognition question, for that particular set of results.

Yarus: Regarding the idea of codons in amino acid binding sites, I recently counted these up, and there are, in sites published and unpublished, 13 codons at 11 sites. I think the hypothesis of a connection between these and the genetic code is still alive. My general comment is that randomness being captured by evolution is not an unknown biological scenario, it is precisely the Darwinian scenario. Finding that randomness can generate patterns that are later found to be selected during evolution is usually counted in favor of the relevance of those structures, rather than against it, as you seem to propose.

Ellington: The point I am trying to make is that, given a large number of potential scenarios, how does one choose from amongst them? All we have to look at are the modern descendants, which may or may not be related to what occurred in antiquity. To the extent that there were many other possibilities, we must be agnostics about whether the modern structures had any of our wonderful hypothesized roles in antiquity. I'm not an atheist about this. I am an agnostic, trying to encourage other people to be agnostic about models.

Yarus: It strikes me that there are things that fail your test that cannot be generated by randomness, and must therefore be eliminated as evolutionary material. I feel quite differently. Rather than finding that oligos are precise, haven't you found that there might be a sort of a Grisham's Law, where largely inaccurate results drive out the accurate things? In other words, have you done competitions?

Ellington: No, but we would like to do that with more delimited pools; for example where one of the positions is ribose *versus* xylose. We are going to do competitions to see whether there could be the selective purification that I have hypothesized.

Ibba: I would like to present another null hypothesis. The RNAs you select, that bind synthetases, don't look like tRNAs because I believe that most of them weren't actually functioning tRNAs. They're not actually charged.

Ellington: That is correct. In order to rescue the tRNA tag hypothesis, one must hypothesize that there are a very limited number of RNA-like molecules that could actually function as tRNAs and be charged. The tRNA tags don't actually function as tRNAs in the sense that they go into the ribosome; they are just charged. A testable prediction of the tag hypothesis is that there should be very few charged tRNA structures. If there are very few potential charged tRNA structures derived from randomness, one could conclude that virus tags are, in fact, somewhat unique.

Weiner: You can ask that question in a different way. If some motif is easy to invent, that could actually lead to its perpetuation. For example, if two molecules interact and one of them is easy to invent, then others can arise which also interact with the same partner. Co-evolution allows the repeated selection of a particular motif. Your question is, "Could something like that arise *de novo*?" That is different from an interactive system, where one part of it may have a molecular memory of the other part, allowing more such parts to arise. We would never say that there is a linear physical descent from the beginning to today. We would say that this kind of structure was invented by biology and then perpetuated by co-evolution.

Ellington: I agree. The real question is, "What is the information content of the interaction?" If the information content is relatively limited, either in a direct selection or in a co-evolutionary perspective, and if molecules must have historically been funneled a certain way, then that's support for a particular hypothesis. I'm trying to point out whether there are many ways to generate these sort of tags. If these tags just happen to be lying around because a virus invents a tRNA-like molecule, tRNA is the most prevalent RNA molecule in the cell, and it could have been so four years ago or four billion years ago. If there is no way to distinguish between those possibilities, then the aspects of the tag hypothesis are less predictive than they could be.

Maizels: Have you tested whether these little RNAs that bind tyrosyl synthetase also bind any of the other enzymes involved in tRNA metabolism, including RNaseP and CCA-adding enzyme?

Ellington: That is a similar sort of question.

Maizels: No, it is not a similar question. If you are only looking at a single trait, you are not really asking the question that you are stating. tRNAs have multiple properties. You can't say that you have assayed for a property of tRNA when you haven't assayed for the whole spectrum of properties of tRNAs. I think this is also true of looking for the arginine recognition. You are turning this into an extremely simplified and reductionist approach and pretending that this gives you an answer, which it doesn't.

ELLINGTON: Perhaps I should modify my statement to say, it is relatively easy to generate molecules that have a particular portion of tRNA-like function, which is the ability to bind to a synthetase. It is currently unknown what the universe of answers is for RNA molecules that can both bind tRNA, recharge and interact with RNaseP.

MAIZELS: . . . and interact with about four other enzymes with tRNA-like molecules.

ELLINGTON: Olke Uhlenbeck (1) has conducted experiments looking at binding both to synthetase and to EFTu and has found that there were a fairly wide range of sequences that could do so. Tao Pan (2) reported a large variety of sequences that can interact with ribonucleaseP. We haven't done the sequential experiments, but whenever it has been done individually, or even in just a single sequential (EFTu and tRNA synthetase) way, the answer remains the same. Rather than tRNA molecules being so delimited in function that they must be an ancient relic, there seem to be too many sequences that allow function; so I cannot believe that RNA tags are anything other than modern viral inventions.

Literature Cited

1. **Peterson, E. T., J. Black, M. Sprinzl, and O. Uhlenbeck. 1993.** Selection for active *E. coli* tRNAPhe variants from a randomized library using two proteins. *EMBO J.* **12:** 2959–2967.
2. **Pan, T. 1995.** Novel RNA substrates for the ribozyme from *Bacillus subtilis* ribonuclease P identified by *in vitro* selection. *Biochemistry* **34:** 8458–8464.

Reference: *Biol. Bull.* **196:** 320–321. (June 1999)

Self-Capping RNA Catalysts Derived From Selection-Amplification

FAQING HUANG, ZHILI YANG, AND MIKE YARUS

Department of Molecular, Cellular, and Developmental Biology, University of Colorado, Boulder, Colorado 80309-0347

The reactions of nucleoside 5′ triphosphates are among the most widespread (and therefore ancient) of the reactions of modern biochemistry. To study RNA enzymes that catalyze an important class of such reactions, we devised a new selection for RNAs that labilize their $\beta\gamma$ phosphates. We select RNAs that circularize in the presence of T4 RNA ligase, a reaction that requires a free 5′ α-phosphate and therefore indicates release of the $\beta\gamma$ phosphates present in every transcript. Unexpectedly, free phosphates were found to react readily at the α-phosphate of such RNAs. This was emphasized by further selection for RNAs that self-link to the free triphosphate of UTP-agarose. The most prevalent ribozyme (40% of the final, doubly-selected pool) has been characterized.

The uniform product of all such reactions is released pyrophosphate, and the RNA product has the attacking phosphate linked to the 5′ α-phosphate of the catalytic RNA. Thus, reaction with free GDP yields pyrophosphate plus a congener of the eukaryotic message cap (1):

$$\text{ppG} + \text{ppp(5}'\text{)GRNA} \rightarrow \text{pp}_i + \text{G(5}'\text{)ppp(5}'\text{)GRNA}$$

The cap structure has been proven by release of the cap from the catalyst, and by comparison with the cap released from an *in vitro* RNA transcript after initiation with *bona fide* GpppG_{OH}. Accordingly, the eukaryotic message cap may have been devised in an RNA world, by RNA catalysts.

The reaction with attacking phosphate nucleophiles can be almost indefinitely generalized (2). The self-capping RNA will react with any nucleoside 3′ phosphate, any NMP, any NDP, NTP, or NtetraP to yield caps of varied structure. Even other 5′ pRNAs react, though with low yields, to yield unique double molecules with diverging polarity: RNA(5′)pp(5′)RNA. The attacking nucleophile need not be a nucleotide, because phosphoarginine and phosphogluconate can also cap an RNA catalyst.

Most interestingly, phosphorylated enzyme cofactors react well, yielding RNAs to which the chemical capabilities of (for example) thiamine pyrophosphate or Cofactor A have been precisely linked. These cofactor reactions may be useful in recreating a generation of cofactor-containing RNA catalysts that might have been the progenitors of the modern cofactors themselves.

The self-capping RNA is a metalloenzyme, optimally active in a very simple buffered calcium solution over a broad range of pH. There is an exceptionally strong calcium-binding site, at which barium or strontium (or even magnesium) competes (the ribozyme is inactivated). The evolved capping activity exists side-by-side with the initially selected pyrophosphatase activity (attack of water at the α-phosphate, accelerated 1.7×10^5-fold or more (3) over the initial randomized pool), with a cap hydrolysis activity (attack of water, though more slowly, at the α-phosphate of the capped RNA), and with a cap exchange activity (attack of a phosphate nucleophile at the α-phosphate of an initially capped RNA).

The kinetics of the RNA reactions show some unusual qualities: notably, the sum of the rates of hydrolysis and capping (reaction with phosphates *in trans*) is a constant whose value is determined by the temperature and phosphate concentration. This points to the formation of an intermediate that can be rapidly captured by either water or an attacking cap. The sum of these two reactions always adds up to the rate at which the 5′-reactive form of the RNA is generated. The nature of this reactive intermediate is unknown at present.

This paper was originally presented at a workshop titled *Evolution: A Molecular Point of View*. The workshop, which was held at the Marine Biological Laboratory, Woods Hole, Massachusetts, from 24–26 October 1997, was sponsored by the Center for Advanced Studies in the Space Life Sciences at MBL and funded by the National Aeronautics and Space Administration under Cooperative Agreement NCC 2-896.

As consequences of the properties of this RNA, both the message cap and the phosphorylated nucleoside cofactors can be plausibly incorporated into accounts of RNA metabolism in an RNA world. Furthermore, the broad substrate specificity of the RNA suggests that it might be made the catalytic subunit in a series of ribozymes, the specificities of which are determined by a second RNA to constitute, for example, a multimeric RNA replicase.

Literature Cited

1. **Huang, F., and M. Yarus. 1997.** 5′ RNA self-capping from guanosine diphosphate. *Biochemistry* **36:** 6557–6563.
2. **Huang, F., and M. Yarus. 1997.** Versatile 5′ phosphoryl coupling of small and large molecules to an RNA. *Proc. Nat. Acad. Sci. USA* **94:** 8965–8969.
3. **Huang, F., and M. Yarus. 1997.** A calcium-metalloribozyme with autodecapping and pyrophosphatase activities. *Biochemistry* **36:** 14107–14119.

Discussion

BARTEL: It is fascinating that this enzyme, born to hydrolyze its α, β-phosphoranhydride, would prefer to catalyze this attack using a phosphate. Is there a way of making sense out of that?

YARUS: Yes. This has to do with the special affinities of calcium and phosphates. I think the Michaelis complex for the capping reactions are phosphates sandwiched between calciums, derived from the site for the original leaving group, pyrophosphate. All of the capping reactions are present because such a complex is there to capture this transition state, which was selected for hydrolysis. The calcium-terminal phosphate complex is crucial to reactivity.

FERRIS: This capping reaction is a common process even without a ribozyme. In all of our reactions we tend to have a chemical reaction on the end of caps of this type as a by-product. This is a general process.

YARUS: Jim (Ferris), you use artificially activated nucleotides. The reaction that you are talking about, cap formation, is not detectable as a spontaneous reaction in our pools. Thus, using activation with the biological leaving group, pyrophosphate, capping is not spontaneous or general.

FERRIS: I would agree. If you were discussing this in an origin of life context, what's artificial and what isn't artificial is a big question. Whether the pyrophosphate or some other leaving group was there is not known. It is also not known if pyrophosphate was actually a prebiotic activating group.

ELLINGTON: You quoted Harold White as saying that these ribonucleotide cofactors exist (1). You then point out that the pyrophosphate linkages in ribo cofactors may be equally fundamental, because they may be vestiges of linkages to ancient catalysts. A prediction from that argument would be that the covalently linked cofactors are going to be better catalysts than the noncovalently linked ones. Normally this would present a problem. The reason for having NAD as a diffusible cofactor rather than nicotinamide amino acid is that one doesn't want it to diffuse. Under your scenario, you can attach the ribozyme, make it a better catalyst, and then it can be de-attached to go and be recycled elsewhere.

YARUS: That's correct. I predict that, in fact, the covalently linked cofactors will be more effective because they are just more precise and more available. RNA and cofactor functionality need not be wasted by putting the cofactors into an enveloping binding site.

Literature Cited

1. **White, H. B., III. 1976.** Coenzymes as fossils of an earlier metabolic state. *J. Mol. Evol.* **1:** 101–104.

Reference: *Biol. Bull.* **196:** 322–323. (June 1999)

Creation and Evolution of New Ribozymes

DAVID P. BARTEL

Whitehead Institute for Biomedical Research and Department of Biology, MIT, 9 Cambridge Center, Cambridge, Massachusetts 02142

To better understand the basic properties of RNA as a catalyst, and to determine whether these properties are compatible with the RNA world scenario, we have been isolating new RNA catalysts (ribozymes) from large pools of random RNA sequences (1, 2). Supplementing the meager number of known types of ribozymes found in nature with these artificial ribozymes permits a more complete understanding of RNA catalysis and allows us to address questions related to the origins of biocatalysis, such as the activity, size, and distribution of catalysts in sequence space (3).

The hypothesis that certain RNA molecules may be able to catalyze RNA replication is central to the RNA world scenario (4). In support of this idea, we have generated an RNA that synthesizes RNA using the same reaction as that employed by protein enzymes that catalyze RNA polymerization (5). In the presence of the appropriate template RNA and nucleoside triphosphates, the ribozyme extends an RNA primer by the successive addition of up to six mononucleotides. The ribozyme shows significant template fidelity; extension by nucleotides complementary to the template is generally 30 times faster than that by a mismatched nucleotide. This ribozyme will serve as a starting point in efforts to evolve ribozymes capable of more extensive and accurate polymerization.

Among the most challenging questions for the RNA world hypothesis is, What would have been the source of the RNA nucleotides? Forming the glycosidic link between the nucleoside bases and ribose is thought to be the most difficult step in prebiotic nucleotide synthesis (4). The presumed scarcity of RNA nucleotides on the prebiotic earth has led many to the view that life did not begin with the RNA world, but instead originated with a "pre-RNA" world. During the transition to an RNA world, ribozymes would have had to assume the responsibility for synthesizing nucleotides. We will describe our exploration of ability of RNA to synthesize uridine, one of the four RNA building blocks, using uracil and PRPP, an activated form of ribose (6).

The experiments described thus far have started with random sequences and worked toward activities thought to have been important in the RNA world. It might also be possible to start with contemporary sequences and to work back toward an activity of the RNA world. We tested whether this "retro-evolution" approach could be a useful tool for exploring the origin and function of the small nuclear RNAs (snRNAs) of the mammalian spliceosome.

In the vertebrate nucleus, splicing is performed by the spliceosome, a ribosome-sized complex that contains mostly protein, but also includes, at various stages of the reaction, five snRNAs. It has been proposed that the contemporary spliceosome descended from an RNA-only enzyme, and that some of the snRNAs may still catalyze the transesterification reactions involved in splicing. However, when assayed without protein, the snRNAs have shown no hint of catalytic activity. An *in vitro* selection experiment was designed to simultaneously examine more than 10^{14} snRNA variants for their ability to promote RNA processing reactions, including the type of transesterification reaction executed by spliceosomes (7). Four different activities were initially isolated. Even though the selection criteria were designed to be optimally satisfied by a reaction equivalent to the second step of splicing, none of the ribozymes promoted this reaction. Of the ribozymes isolated, the most notable were a ribozyme with a three-step reaction pathway similar to that of tRNA splicing, and a ribozyme that promotes a previously undescribed and relatively difficult transesterification reaction.

This paper was originally presented at a workshop titled *Evolution: A Molecular Point of View*. The workshop, which was held at the Marine Biological Laboratory, Woods Hole, Massachusetts, from 24–26 October 1997, was sponsored by the Center for Advanced Studies in the Space Life Sciences at MBL and funded by the National Aeronautics and Space Administration under Cooperative Agreement NCC 2-896.

Literature Cited

1. **Bartel, D. P., and J. W. Szostak. 1993.** Isolation of new ribozymes from a large pool of random sequences. *Science* **261:** 1411–1418.
2. **Williams, K. P., and D. P. Bartel. 1996.** *In vitro* selection of catalytic RNA. Pp. 367–381 in *Catalytic RNA*, F. Eckstein and D. M. J. Lilley, eds. Springer-Verlag, Berlin.
3. **Ekland, E. H., J. W. Szostak, and D. P. Bartel. 1995.** Structurally complex and highly active RNA ligases derived from random RNA sequences. *Science* **269:** 364–370.
4. **Joyce, G. F., and L. E. Orgel. 1993.** Prospects for understanding the origin of the RNA world. Pp. 1–25 in *The RNA World*, R. Gestland and J. Atkins, eds. Cold Spring Harbor Press, Cold Spring Harbor, NY.
5. **Ekland, E. H., and D. P. Bartel. 1996.** RNA-catalysed RNA polymerization using nucleoside triphosphates. *Nature* **382:** 373–376.
6. **Unrau, P. J., and D. P. Bartel. 1998.** RNA-catalyzed nucleotide synthesis. *Nature* **395:** 260–263.
7. **Tuschl, T., P. A. Sharp, and D. P. Bartel. 1998.** Selection *in vitro* of novel ribozymes from partially randomized U2 and U6 snRNA library. *EMBO J.* **17:**2637–2650.

Discussion

MARGULIS: You mentioned that, in addition to the original work by Tom Cech on a ribozyme from *Tetrahymena*, a ciliate, there are six other naturally occurring ribozymes. What are the other six?

BARTEL: The seven known motifs that I was referring to include the self-splicing intron found by Tom Cech, another type of self-splicing intron termed the group II self-splicing intron, which catalyzes splicing with lariat formation.

MARGULIS: Pardon me, what biological material do the group II introns come from?

BARTEL: The group II introns are primarily from chloroplasts and mitochondria, although they have been found in some bacteria. They are mobile elements that insert themselves into genomes, so they can spread horizontally. To continue, there are four types of self-cleaving motifs: the hammerhead, the hairpin, the vsRNA, and the hepatitis delta ribozyme. These four self-splicing introns catalyze reactions involving self-cleavage with a cyclic phosphate. There is, finally, the seventh ribozyme, RNaseP, which is ubiquitous and trims off the 5′ end of tRNAs. This ribozyme is present as a ribonucleoprotein. However, the bacterial RNAseP RNA, by itself, catalyzes the reaction quite efficiently.

IBBA: Since many of these RNA catalyst activities that you can select *in vitro* are so effective, why do you think so few of them have been retained in contemporary organisms?

BARTEL: It is difficult to say. Most of the very efficient reactions that we have seen involve oligonucleotide substrates, yet *in vivo* there are many protein-catalyzed reactions that involve substrates much smaller than oligonucleotides. One possible explanation is that it is much harder for RNA to use small-molecule substrates. There is no question that protein, with the added functionality, is a great catalytic biopolymer. The big question is, to what degree can RNA match protein, particularly when RNA is given cofactors?

WEINER: Your ability to make a real RNA replicase is absolutely amazing, but it doesn't keep going and going and going. Why do you think that is the case?

BARTEL: I hesitate to call it a real RNA replicase for that reason. I tried to point out where it runs into base pairing between the template and the ribozyme, so the same interactions that it uses to bind the template inhibit further polymerization. I believe that is the main reason it doesn't keep going.

ELLINGTON: Given that you provided the spliceosome with every opportunity to return to its RNA roots and it didn't, would you care to comment on the hypothesis that the spliceosome was once all RNA?

BARTEL: Just because we weren't able to access the catalytic activity of the spliceosome doesn't mean that it isn't currently RNA catalyzed. On the other hand, the last phosphodiester transfer reaction that I described was more difficult chemically to do than the phosphodiester transfer reactions catalyzed by the spliceosome.

LANDWEBER: Are there many modified nucleosides in the spliceosome? That could be the missing feature.

BARTEL: Yes, there are some that are highly conserved. I'm not sure if there are any that are absolutely conserved.

LANDWEBER: In order for a ribozyme that consists of pyrimidines to fill in a missing step in the origin of life, an all-purine ribozyme would be required first to synthesize pyrimidines.

BARTEL: That is correct. This ribozyme presents a chicken and egg problem. Just as the first replicase molecule could not have made itself, the first molecule that synthesized pyrimidines could not have made the monomers from which it was constituted. Most people who are talking about the RNA world don't think about it as the origin of life. Instead, there is this so-called pre-RNA world that gave rise to the RNA world, presumably by facilitating synthesis of RNA monomers and oligomers needed to begin the transition to the RNA world. Nevertheless, later in the transition to an RNA world, RNA would have required the ability to make its own nucleotides. The concentration of nucleotides in the early earth would have been very, very low.

UNIDENTIFIED: Have you confirmed the glycosidic bond?

BARTEL: Yes, we have confirmed this with digestions, and subsequent analyses where we have compared the product to known standards. It always co-migrates exactly with the known standard.

Reference: *Biol. Bull.* **196:** 324–326. (June 1999)

The Evolution of Cellular Computing

LAURA F. LANDWEBER

Department of Ecology and Evolutionary Biology, Princeton University, Princeton, New Jersey 08544

How do cells and nature "compute"? They read and "rewrite" DNA all the time, by processes that modify sequence at the DNA or RNA level. In 1994, Leonard Adleman reported an elegant solution to a seven-city traveling salesman problem using DNA. This launched the new field of DNA computers, which in a few years has grown to international scope. However, unknown to Adleman and his field, two ciliated protozoans of the genus *Oxytricha* had solved a much harder problem several million years earlier.

Ciliates possess two or more dimorphic nuclei: an active somatic macronucleus and a transcriptionally inert germline micronucleus. The genomic copies of some genes in the germline micronucleus of hypotrichous ciliates are crippled by the presence of intervening non-coding DNA sequence elements (internally eliminated sequences, or IESs) which must be removed before a functional copy can be assembled in the somatic macronucleus. Even more surprising, the coding DNA segments (macronuclear destined sequences, or MDSs) in *Oxytricha* species are sometimes present in a jumbled order relative to their mature position in the macronuclear copy. For example, in *O. nova*, the micronuclear copy of the genes for Actin 1, α-telomere binding protein, and DNA polymerase α must be reordered, and the intervening DNA sequences removed, to construct functional macronuclear genes. Most impressive, probably, is the gene encoding DNA polymerase α in *O. trifallax*, which is apparently scrambled in 50 or more pieces in its germline nucleus (1). Destined to unscramble its micronuclear genes by putting the pieces together again, *O. trifallax* routinely solves a complicated path problem while unscrambling several of its micronuclear genes, therefore rewriting its somatic genome (Fig. 1). This is an astounding feat of DNA computation, especially as 50-city path problems are often classified as hard problems in computer science. The developing macronuclear "computer" apparently relies on the information contained in short repeat sequences to act as guides in homologous recombination, again similar in design to Adleman's solution of a mathematical problem (2). Other structural components of the ciliate chromatin presumably play an important role.

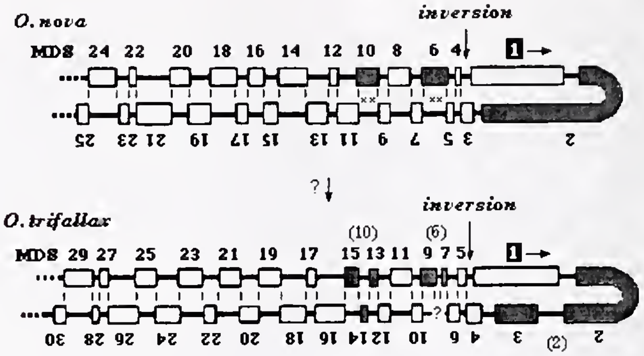

Figure 1. Model for the accumulation of scrambled macronuclear destined sequences (MDSs) in a gene with an inversion. Short vertical lines indicate recombination junctions between scrambled MDSs. MDS 1 contains the 5′ end of the gene, which must be assembled in a linear order. MDS 10 in *Oxytricha nova* can give rise to three new MDSs (13–15) in *O. trifallax*, one scrambled on the inverted strand, by two spontaneous intramolecular recombination events (x's) in the folded orientation shown. *O. nova* MDS 6 can give rise to *O. trifallax* MDSs 7–9 (MDS 8, shaded, is only 6 bp and has not been identified in Hoffman and Prescott (1)). *O. trifallax* non-scrambled MDSs 2 and 3 could be generated by the insertion of an IES in *O. nova* MDS 2 (similar to a model suggested by M. DuBois in Hoffman and Prescott (1)).

We have recently discovered scrambling in the gene encoding DNA polymerase α in the micronucleus of a different ciliate, *Stylonychia lemnae*, which enjoys the benefit of a working transfection system (3). The "scrambled genes" in ciliates offer a unique system with which to study the origin of a complex genetic mechanism and the role of inversions as catalysts of acrobatic gene rearrangements

---

This paper was originally presented at a workshop titled *Evolution: A Molecular Point of View*. The workshop, which was held at the Marine Biological Laboratory, Woods Hole, Massachusetts, from 24–26 October 1997, was sponsored by the Center for Advanced Studies in the Space Life Sciences at MBL and funded by the National Aeronautics and Space Administration under Cooperative Agreement NCC 2-896.

during evolution (Fig. 1). The complex scrambling pattern of DNA polymerase α is possibly the closest analog in nature of a hard path problem. Alternate splicing could be viewed as another path problem. The isolation of functional nucleic acid molecules, such as ribozymes, from random sequence pools is a different kind of molecular computation (4).

We have also studied RNA editing, which is another cellular paradigm for nucleic acid computers. RNA editing, the modification of RNA sequences by addition, deletion, or substitution of bases, is found in a wide variety of eukaryotes, from parasitic protozoa to humans.

This remarkable process alters the sequence of messenger RNA before its translation into protein, such that the resulting protein sequence often differs dramatically from the original gene sequence, which sometimes does not encode a protein at all. For example, in kinetoplastid protozoa, RNA editing by addition and deletion of literally *hundreds* of uridine residues creates initiation and termination codons, alters the structural features of transcripts, and creates over 90% of the amino-acid codons (5). Driven by small guide RNA sequences, RNA editing is another example of a cellular process that uses sequence pairing to convert seemingly disordered sequences into a functional coding sequence: a truly RNA-based computer. Together, RNA editing and gene unscrambling provide an array of potentially usable paradigms for writing and rewriting DNA.

Our current effort in this field is directed toward (1) recoding DNA in the laboratory; and (2) understanding how cells unscramble DNA, how this process has arisen, and how the "programs" are written. Do they decode the message by following the shortest unscrambling path, or by following a more circuitous but equally effective route, as in the case of RNA editing. Also, how error prone is the unscrambling process? Together, the stunning acrobatics of DNA, such as scrambling or editing, give proof to the versatility of nucleic acids and their potential use in solving biological problems of computation.

Acknowledgments

The author thanks Richard Lipton (6), David Prescott, Hans Lipps, and members of her laboratory, especially Dirk Faulhammer and Laura Katz, for discussion. L.F.L. is a Burroughs-Wellcome Fund New Investigator in Molecular Parasitology.

Literature Cited

1. **Hoffman, D. C., and D. M. Prescott. 1997.** Evolution of internal eliminated segments and scrambling in the micronuclear gene encoding DNA polymerase a in two *Oxytricha* species. *Nucleic Acids Res.* **25:** 1883–1889.
2. **Adleman, L. M. 1994.** Molecular computation of solutions to combinatorial problems. *Science* **266:** 1021–1024.
3. **Wen, J., C. Eder, and H. J. Lipps. 1995.** The processing of macronuclear-destined DNA sequences microinjected into the macronuclear anlagen of the hypotrichous ciliate *Stylonychia lemnae*. *Nucleic Acids Res.* **23:** 1704–1709.
4. **Bartel, D. P., and J. W. Szostak. 1993.** Isolation of new ribozymes from a large pool of random sequences. *Science* **261:** 1411–1418.
5. **Landweber, L. F., and W. Gilbert. 1993.** RNA editing as a novel source of genetic variation. *Nature* **363:** 179–182.
6. **Lipton, R. J. 1995.** DNA solution of hard computational problems. *Science* **268:** 542–545.

Discussion

MARGULIS: My question concerns intracellular selection. During macronuclear differentiation, are the incorrect sequences actually made, selected, and corrected to begin with, or are they just not made? Or does recombination occur from the beginning?

LANDWEBER: The recombination occurs during 40 hours or so of macronuclear development in hypotrichous ciliates.

MARGULIS: Is it made wrong and then selected?

LANDWEBER: We don't know the answer yet to that question. One can either find the solution, or interpret the solution readout by simply analyzing PCR products and seeing which MDSs are connected in the final solution. One of the next experiments I have planned is to look at which MDSs are connected throughout the developing macronucleus.

MARGULIS: Didn't you show a simplified diagram of *Paramecium aurelia*, illustrating conjugation (sex) in these organisms? I wondered if you really have new genetic data for *Oxytricha* and *Stylonychia* sexual systems.

LANDWEBER: The life-cycle illustration derived from *Oxytricha* but was just a textbook example. *Stylonychia* are useful because they are very amenable to study, and we have plenty of details, at least at the molecular level, but we don't really know the details at the cellular level.

REDFIELD: Larry Klobutcher and Glenn Herrick (1) have presented evidence that transposable elements have played a role in generating this situation which the descrambling then solved.

LANDWEBER: We don't see any sequence relationship between these excised sequences and transposable elements. But in some classes of excised sequences, particularly in *Euplotes*, you do see such similarities. This leads to one model for how information was inserted into what were originally intact genes. It means that some classes of excised sequences could have certainly come from mobile DNA.

CAVALIER-SMITH: I don't think that you should call the DNA that is eliminated in the macronucleus "junk DNA," because that designation begs the question of whether it has a non-coding function. If it is just called non-coding DNA, then we can decide what its function is, or indeed, whether it has a function. I think it has, of course, as skeletal DNA.

LANDWEBER: I agree. It might have some specific function in the micronucleus, but the DNA is transcriptionally inert in the micronucleus and absent from the macronucleus. DNA elimination is a way of amplifying and selecting only those sequences that are absolutely required to be in the macronucleus, and in that sense it's truly elegant.

WEINER: Since these genes presumably began in the right order and were then scrambled, there must be a driving force. Presumably the first scramble happens, and then the others follow one by one. Could you comment on this?

LANDWEBER: There may not be a selective force that maintains scrambling, but it does take place, so it parallels an argument I have used before for RNA editing. There certainly doesn't seem to be a selective explanation for why RNA editing would be so extensive and so rampant that over 90% of the codons in some trypanosome genes are created by RNA editing. Nor is there a selective argument as to why a gene should be so disassembled in the micronucleus, where it is inert anyway. I think the case is more strongly along the lines of overactive recombination machinery, so that rampant DNA recombination is available to take an intact gene and to pull it apart into various pieces. The idea is that there is some destructive force operating at a very high level and re-assembling genes into these scrambled patterns without an adaptive explanation for why such an event would take place. I think that scrambling is simply introduced by natural forces that operate on the micronuclear DNA, since the genes aren't even turned on until the pattern is entirely unscrambled.

BARTEL: You say that you are able to transform these organisms. Have you taken an unscrambled gene and put it in the macronucleus to determine if it is functional?

LANDWEBER: Hans Lipps's lab in Witten, Germany, has successfully injected DNA into the developing macronucleus and shown that it is *partially* processed and stably retained in the macronucleus (2), but we have not yet tried scrambled genes in any form.

YARUS: The even/odd character of the gene is accounted for beautifully by the model of DNA folding back; but is it not true that, even in the same organism, there are intercalated sections which are gloriously baroque? One knows that, at the molecular level, this flamboyant distribution of DNA must be an optional feature of the mechanism, and that there must be some deeper aspects of the mechanism that drive unscrambling.

LANDWEBER: It could be. One could speculate about it; and perhaps this snapback pattern with an inversion might have something to do with the chromatin and physical chemistry of the DNA. Maybe there is quadruplex DNA somewhere actually holding these strands together. I don't want to speculate too far on that, but I think that an inversion between any of these segments not only makes the unscrambling much easier, and acts as a catalyst by aiding the unscrambling, but also acts as a catalyst for more scrambling to evolve by clamping together these two portions of DNA, which can then continue to recombine. Only very little sequence similarity between any two junctions is required for recombination to take place, and this would introduce more scrambling.

Literature Cited

1. **Klobutcher, L. A., and G. Herrick. 1997.** Developmental genome reorganization in ciliated protozoa: the transposon link. *Prog. Nucleic Acid Res. Mol. Biol.* **56:** 1–62.
2. **Wen, J., C. Maercker, and H. J. Lipps. 1996.** Sequential excision of internal eliminated DNA sequences in the differentiating macronucleus of the hypotrichous ciliate *Stylonychia lemnae*. *Nucleic Acids Res.* **24:** 4415–4419.

Reference: *Biol. Bull.* **196:** 327–330. (June 1999)

The Genomic Tag Hypothesis: Modern Viruses as Molecular Fossils of Ancient Strategies for Genomic Replication, and Clues Regarding the Origin of Protein Synthesis

ALAN M. WEINER AND NANCY MAIZELS

Departments of Molecular Biophysics and Biochemistry, and of Genetics, Yale University School of Medicine, New Haven, Connecticut 06520-8024

Although tRNA is best known as a component of the translation apparatus, tRNA and tRNA-like molecules also play key roles—either as template or as primer—in a wide variety of replicative processes. These processes include replication of single-stranded RNA viruses of bacteria, plants, and possibly mammals; replication of duplex DNA plasmids of fungal mitochondria; replication of retroviral and pararetroviral genomes; and replication of modern chromosomal telomeres. Consider the following two obvious examples. First, the 3′ end of many eubacterial and plant single-stranded RNA viruses resembles the "top half" (acceptor stem/loop) of tRNA, with a stem/loop structure immediately followed by the 3′ terminal sequence CCA. This tRNA-like structure functions as the template for initiation of RNA replication. In fact, some of these tRNA-like structures are so similar to *bona fide* tRNA that they can be aminoacylated by the corresponding aminocyl-tRNA synthetases. Second, the replication of most retroviral RNA genomes begins with annealing of a mature tRNA to the primer binding site on genomic RNA; reverse transcriptase then uses the tRNA as primer to copy the RNA genome into the first strand of DNA. Thus in each case tRNA or a tRNA-like structure plays a role in initiation of RNA replication, but in one instance it functions as template and in the other as primer. Is this pure coincidence, or does it suggest descent from a common ancestral function? No conclusions could be drawn from just two examples, but many more instances are known in which tRNA plays a role in replication, and many of these examples appear to provide "missing links," or connections, between one replicative strategy and another.

How did tRNA come to have so many different roles in replication? One possibility is that tRNA or tRNA-like structures have been repeatedly and independently borrowed from translation to serve *ad hoc* roles in replication. Alternatively, tRNA or tRNA-like structures may be widespread in modern replication because tRNA played a central role in the replication of ancient RNA genomes, a role that was then both conserved and subtly transformed as genomes evolved from single-stranded RNA to duplex DNA. We have proposed that tRNA-like structural motifs first evolved as 3′ terminal structures that tagged RNA genomes for replication in the RNA world *before* the advent of protein synthesis (1). This simple "genomic tag hypothesis" then enabled us to build a compelling phylogeny showing how the role of tRNA in replication is likely to have evolved as RNA genomes in an RNA world gave rise first to retroelements (genomes in transition from an RNA to a DNA world) and finally to contemporary DNA genomes (2–5).

The phylogeny we have proposed for the evolution of tRNA in replication is shown in Figure 1. This phylogeny has clear implications for the origin of protein synthesis, because at least one key component of the translation apparatus—tRNA itself—would have evolved as a component of the *replication* machinery before the advent of templated

---

This paper was originally presented at a workshop titled *Evolution: A Molecular Point of View*. The workshop, which was held at the Marine Biological Laboratory, Woods Hole, Massachusetts, from 24–26 October 1997, was sponsored by the Center for Advanced Studies in the Space Life Sciences at MBL and funded by the National Aeronautics and Space Administration under Cooperative Agreement NCC 2-896.

protein synthesis. Moreover, it is not difficult to imagine that tRNA aminoacylation activity might also have evolved in the RNA world to regulate RNA replication, perhaps to identify mature genomes in need of replication, or to withdraw genomes from the replicative pool so that they might serve other structural or catalytic functions. Thus both tRNA and tRNA charging could have evolved before templated protein synthesis (1).

So many wild and fantastic views of evolution have been advanced over the ages that biologists tend to be shy about advocating phylogenies that cannot be backed up by rigorous quantitative analysis. Unfortunately, fear of the unquantifiable has now become a major obstacle to understanding the rich historical and evolutionary implications of the wealth of contemporary information about the structure and function of biological macromolecules. The eminent philosopher Sir Karl Popper argued in his youth that nothing could be "science" unless it was falsifiable. With the wisdom of later years, however, Popper invented a new term, "explanatory power," as a criterion for judging ideas that organize data in new and provocative patterns, but are not easily falsifiable. We suggest that the genomic tag hypothesis has just this kind of explanatory power: without the hypothesis, one must believe that tRNA has been repeatedly borrowed, adapted, and exapted for a host of roles in replication, but that these events have not occurred in any necessary order, and have nothing to do with the widely accepted evolution of genomes from RNA to DNA.

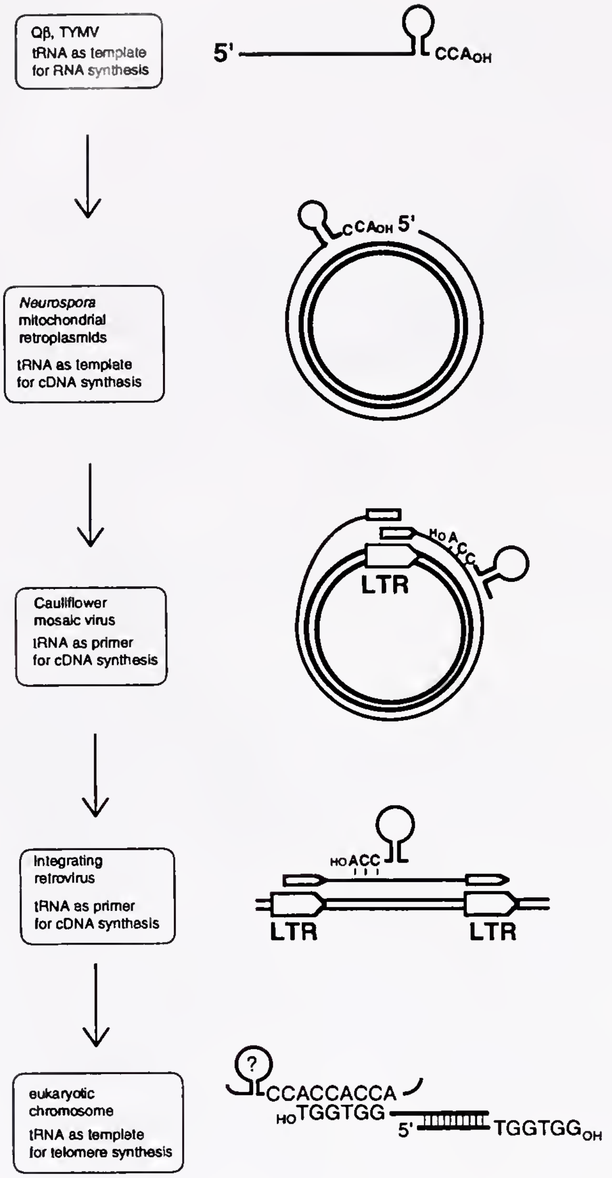
Qβ, TYMV
tRNA as template for RNA synthesis
5'
CCA$_{OH}$
CCA$_{OH}$ 5'
Neurospora mitochondrial retroplasmids
tRNA as template for cDNA synthesis
LTR
HOACC
Cauliflower mosaic virus
tRNA as primer for cDNA synthesis
HOACC
LTR
LTR
Integrating retrovirus
tRNA as primer for cDNA synthesis
?
CCACCACCA
HOTGGTGG
5'
TGGTGG$_{OH}$
eukaryotic chromosome
tRNA as template for telomere synthesis

Figure 1. A functional phylogeny for the origin of tRNA in replication. We propose that tRNA first evolved as a 3′ terminal genomic tag in single-stranded RNA genomes where it served as *template* for initiation of RNA synthesis. The genomic tag is preserved in transitional replication strategies, where it serves as template for initiation of DNA synthesis on single-stranded RNA genomes. Eventually, the genomic tag was transformed into the *primer* for initiation of DNA synthesis in retroviral-like replication strategies. The ends of modern eukaryotic chromosomes are repaired by telomerase, a specialized reverse transcriptase that adds GT-rich repeats to the 3′ end of chromosomal DNA using a built-in, CA-rich, tRNA-like RNA as template. This tRNA-like template can be viewed as a stolen genomic tag, and the addition of GT-rich sequences as repeated abortive initiation of replication on a genomic RNA (*cf.* retroplasmid above).

Literature Cited

1. **Weiner, A. M., and N. Maizels. 1987.** 3′ terminal tRNA-like structures tag genomic RNA molecules for replication: implications for the origin of protein synthesis. *Proc. Natl. Acad. Sci. USA* **84:** 7383–7387.
2. **Maizels, N., and A. M. Weiner. 1993.** The genomic tag hypothesis: modern viruses as molecular fossils of ancient strategies for genomic replication. Pp. 577–602 in *The RNA World,* 2nd ed. R. F. Gesteland and J. F. Atkins, eds. Cold Spring Harbor Press, Cold Spring Harbor, NY.
3. **Maizels, N., and A. M. Weiner. 1993.** The genomic tag hypothesis: what molecular fossils tell us about the evolution of tRNA. Pp. 79–111 in *The RNA World,* 2nd ed. R. F. Gesteland and J. F. Atkins, eds. Cold Spring Harbor Press, Cold Spring Harbor, NY.
4. **Weiner, A. M., and N. Maizels. 1994.** Unlocking the secrets of retroviral evolution. *Curr. Biol.* **4:** 560–563.
5. **Maizels, N., and A. M. Weiner. 1994.** Phylogeny from function: evidence from the molecular fossil record that tRNA originated in replication, not translation. *Proc. Natl. Acad. Sci. USA* **91:** 6729–6734.

Discussion

Cavalier-Smith: I don't think tRNA is as essential to the end replication process as you have suggested, because there are so many different ways in which that problem has been solved. I also doubt that the telomere sites are related to the tRNA mechanism that you discussed, partly because the telomere sequences that are most like this CCA are relatively derived within the protozoan tree; *i.e.,* those of ciliates and *Saccharomyces.* The more broadly distributed sequences do not have a CCA sequence within them; therefore, the sequence that you are assuming to be ancestral is probably not.

Weiner: I disagree. The fact is that C and A are the predominant nucleotides in all telomeres that have been examined from organisms great and small.

Redfield: You have developed a nice story. How are you going to test it? How will you distinguish between these things being there because they descended from an ancestor, or being there because it's really easy to invent things this way? What you need are features that are arbitrary, unnecessary, and presumably present only because they're ancestral—features that would not be there if they just arose by accident. Have you identified such features?

Weiner: I don't believe that studying the history of things that are unnecessary is the right way to go about biology. We look for things which are conserved and ask where they came from. If you're asking for us to identify something that's truly arbitrary and has been preserved for the last three billion years, that's a tall order and I'm not quite sure how to fill it. I think you have to look at conserved things. We would argue that we're looking at structures involved in initiation of replication, and that property is shared. Everyone is happy to be a cladist and to score the dimensions of a clamshell, but if we say that all these structures were involved in initiation of replication, then the reaction is: What does that have to do with anything? If they are all the same structure involved in the initiation of replication, surely that qualifies at some level as a similarity.

When we came up with these ideas in 1987 (1), there were a couple of things that weren't known. For example, it wasn't known that telomerase was a reverse transcriptase with an RNA template. It wasn't known at all that the retroplasmid existed. We came up with an idea that has turned out to be robust in the light of some pretty amazing discoveries by others. We can't go out and do some definitive experiment to determine the truth, but there has been some heavy support which is utterly consistent with the approach that we have suggested for looking at replication.

Yarus: The genomic tag hypothesis assigns to the tRNA-like structure the function of replication solely. What does one then make of modern RNA genomes, like the plant viruses which are still aminoacylated? Are they not easier to explain as captured pieces of the translation apparatus than by the genomic tag hypothesis, in which aminoacylation would have no function and should therefore have been lost during evolution?

Weiner: tRNA interacts with many enzymes, synthetases, RNaseP, modifying enzymes, EFTu, peptidohydrolase. Any virus that uses a tRNA-like structure in replication will have to relate to some enzymes and not to others. If a virus with a tRNA at its 3′ end were recognized by RNaseP, that would be the end of the virus because RNaseP would chop the tag off the genome. It's a difficult path for anything to use a tRNA as part of its genome because it can interact with some enzymes but not others. I don't think we know enough to say whether aminoacylation of a plant virus is necessary for its replication or is simply an evolutionary accident which persists because the structure that the 3′ terminus needs to be recognized in replication is also a structure that is recognized by an enzyme that happens to aminoacylate the terminus.

Forterre: I agree with most of what you have said about the origin of viruses, except I think that this hypothesis is not only true for RNA viruses but also applies to DNA viruses. DNA viruses probably also came from very ancient times, maybe before the separation of the three domains (2).

Olsen: How would you portray the history of the three other components of the Qβ replicase in this?

Weiner: Qβ replicase is a heterotetramer composed of EFTu, EFTs, ribosomal protein S1 and the virally encoded replicase subunit. The replicase is very nonspecific—it basically copies anything, and the other proteins are believed to somehow give it specificity. The trouble is that no one has been able to show that inactivating the ability of Tu to bind tRNA will inactivate the ability of those proteins to target the replicase. I don't really know the answer, but I think it does say that replication activity and replication recognition can be physically separated yet function as a unit.

Olsen: It's just that all three of those other subunits of the heterotetramer come from the translation apparatus.

Weiner: Yes. Once you have tRNA it is hard to imagine that it would not interact with the translation apparatus. After all, as we see it, tRNA gave birth to the translation apparatus.

Ellington: You said that glyceraldehyde-3-phosphate dehydrogenase is not a social enzyme. However, it interacts with its substrate, glyceraldehyde-3-phosphate, and with 1,3-diphosphoglycerate, both of which are absolutely fixed. There is not a lot of mutability to glyceraldehyde-3-phosphate. This brings up the question of dealing with substrates, tRNAs that are highly mutable: doesn't that make it much more difficult to discern the origins of things like tRNA synthetases by your hypothesis, than things like glyceraldehyde-3-phosphate dehydrogenase? In other words, since glyceraldehyde-3-phosphate dehydrogenase is social with an immutable molecule, wouldn't you expect that its phylogeny and history are much better established than those of a molecule that is social and socializes with a promiscuous and mutable molecule like tRNA?

WEINER: In order to interact with a small substrate molecule, only certain residues at the active site would have to be fixed, and even that recognition could be achieved in different ways. If we are talking about a macromolecule that interacts in a major way with another macromolecule, there may be fewer ways accommodation is possible that don't alter or destroy the functions of both molecules.

Literature Cited

1. **Weiner, A. M., and N. Maizels. 1987.** 3′ terminal tRNA-like structures tag genomic RNA molecules for replication: implications for the origin of protein synthesis. *Proc. Natl. Acad. Sci. USA* **84:** 7383–7387.
2. **Forterre, P. 1992.** Pp. 221–234 in *Frontiers of Life,* J. K. Tran Thanh Van, J. C. Mounolou, J. Shneider, and C. McKay, eds. Editions Frontieres, Gif-sur-Yvette, France.

Reference: *Biol. Bull.* **196:** 331–334. (June 1999)

New Evidence for the Genomic Tag Hypothesis: Archaeal CCA-Adding Enzymes and tDNA Substrates

NANCY MAIZELS, ALAN M. WEINER, DONGXIAN YUE AND PEI-YONG SHI

Departments of Molecular Biophysics and Biochemistry, and of Genetics, Yale University School of Medicine, New Haven, Connecticut 06520-8024

The CCA-adding enzyme [ATP(CTP):tRNA nucleotidyl transferase] catalyzes the addition and regeneration of the 3′ terminal CCA sequence of tRNAs. The enzyme adds the sequence CCA one nucleotide at a time to the 3′-terminus of tRNA, using CTP and ATP as precursors, and can utilize tRNA substrates lacking one, two, or all three terminal nucleotides. The 3′ terminal CCA is encoded in all tRNA genes of some eubacteria (*Escherichia coli, Mycoplasma genitalium*), in about half the tRNA genes of other eubacteria (*Bacillus subtilis*) and Archaea (1–3), but only very rarely in eukaryotes (4). The CCA-adding enzyme thus functions mainly as a "repair" enzyme in a subset of eubacteria, but as an essential biosynthetic enzyme in most eubacteria, as well as in all known Archaea and eukaryotes. As expected, the enzyme is essential for viability in the budding yeast *Saccharomyces cerevisiae* where CCA is not encoded (5), but it is partially dispensable in *E. coli* where CCA is encoded (6).

We have argued that molecular structure and function can provide compelling evidence for descent from a common ancestor, and that careful inspection of the structure and function of contemporary biological molecules can yield highly informative, intellectually rigorous, functional phylogenies despite the absence of conventionally quantifiable traits. Based on the many different roles that tRNA is known to play in RNA and DNA replication, we have presented one such functional phylogeny showing how these diverse roles of tRNA in replication are likely to have evolved from an RNA to the DNA world (7–10; and see Weiner and Maizels, pp. 327–330, these proceedings). If tRNA-like structures corresponding to the top half of tRNA (the acceptor stem/loop; see Fig. 1) served as genomic tags at the 3′ end of RNA genomes in an RNA world, the CCA-adding activity may have served as the original telomerase to regenerate 3′ termini during replication, and might thus be present in all three living kingdoms. We therefore asked whether Archaea also have a CCA-adding activity, and if so whether it was related to that found in eubacteria and eukaryotes. We purified, cloned, and expressed the enzyme from the thermophile *Sulfolobus shibatae* (11), and identified homologs in the published genomic sequences of *Methanococcus jannaschii* (1), *Methanobacter thermoautotrophicum* (2), and *Archaeoglobus fulgidus* (3).

Our phylogenetic analysis of the eubacterial, eukaryal, and archaeal CCA-adding enzymes shows that all known CCA-adding enzymes do indeed belong to a single nucleotidyltransferase superfamily, as might be expected if this activity was present in the last common ancestor of contemporary organisms. Intriguingly, we were able to divide this superfamily into three subfamilies: class I contains the archaeal CCA-adding enzyme, eukaryotic poly(A) polymerases, and DNA polymerase β; class II contains eubacterial and eukaryotic CCA-adding enzymes, and eubacterial poly(A) polymerases; and class III contains eubacterial polynucleotide phosphorylases (11). These data suggest that CCA-adding and poly(A) polymerase activities were able to interconvert early in evolution, with the CCA-adding enzyme degenerating into a simple poly(A) polymerase, or poly(A) polymerase acquiring the additional specificity required to synthesize a defined sequence of defined length.

tRNA consists of two coaxially stacked helices which appear to be independent structural and functional domains: the top half contains the acceptor stem and the TψC stem-loop, and the bottom half contains the D stem-loop and the

---

This paper was originally presented at a workshop titled *Evolution: A Molecular Point of View*. The workshop, which was held at the Marine Biological Laboratory, Woods Hole, Massachusetts, from 24–26 October 1997, was sponsored by the Center for Advanced Studies in the Space Life Sciences at MBL and funded by the National Aeronautics and Space Administration under Cooperative Agreement NCC 2-896.

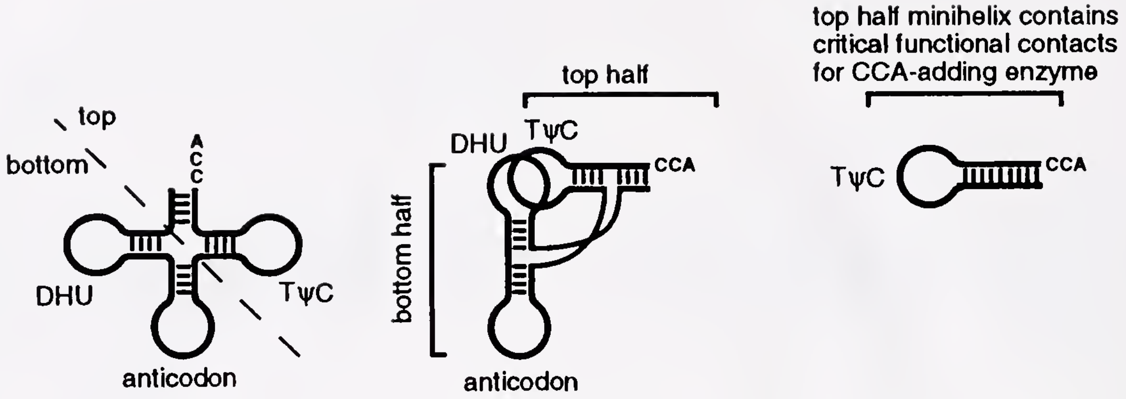
top
bottom
A
C
C
DHU
TψC
anticodon
top half
DHU
TψC
CCA
bottom half
anticodon
top half minihelix contains critical functional contacts for CCA-adding enzyme
TψC
CCA

Figure 1. The top half of tRNA is an independent structural and functional domain, which may have evolved independently from the bottom half. Shown is the traditional cloverleaf diagram of tRNA structure (left); a diagram which illustrates the coaxial stack of the dihydrouracil (DHU) and anticodon stems (center); and a diagram which illustrates the top half minihelices which are good substrates for the CCA-adding enzyme (right) (19).

anticodon stem-loop (Fig. 1). Based upon the widespread roles of *top-half* tRNA-like structures in replication of contemporary RNA genomes, we have suggested that the top-half domain had an independent and more ancient origin than the anticodon domain (2, 4). The separable interactions of the top half and anticodon domains with the 23S and 16S rRNAs, respectively, also led Noller to suggest that these domains of tRNA evolved independently (12). Schimmel *et al.* (13) reached similar conclusions by a very different route, based on the modular interaction of tRNA synthetases with the top and bottom halves of tRNA. The top-half domain, sometimes referred to as a tRNA "minihelix," has been shown to provide the determinants necessary for specific charging by aminoacyl tRNA synthetases (14, 15); for interaction with elongation factor Tu (16); for 5′ processing by RNase P (17); and for distinguishing elongator from initiator tRNA (18). However, it had not been established whether top-half minihelices could function as substrates for the CCA-adding enzyme.

We have recently carried out two sorts of experiments designed to ask whether the top-half domain of tRNA has the necessary determinants for efficient CCA addition, and whether critical contacts between the tRNA and the CCA-adding enzyme lie within this domain. By analyzing CCA-addition to synthetic DNA oligonucleotides corresponding to the top half of tRNA, we have shown that the CCA-adding enzyme will efficiently and specifically add a CCA terminus to minihelices (19). CCA addition to the tDNA minihelices requires a 2′ as well as a 3′ OH at the 3′ terminus of the tDNA. Addition depends on the length of the base-paired stem and is facilitated by, but is not dependent upon, the TψC loop. By footprinting analysis, we have defined the specific phosphates recognized by the CCA-adding enzyme in tRNA, and we have shown that most of these contacts are within the top-half domain (20). The fact that the top half of tRNA contains determinants for specific addition by the CCA-adding enzyme, itself an ancient activity present in all three living kingdoms (11), provides additional experimental support for the hypothesis that the top-half domain of tRNA evolved independently from the bottom half.

Literature Cited

1. **Bult, C. J., O. White, G. J. Olsen, L. Zhou, R. D. Fleischmann, G. G. Sutton, J. A. Blake, L. M. FitzGerald, R. A. Clayton, J. D. Gocayne, A. R. Kerlavage, B. A. Dougherty, J. F. Tomb, M. D. Adams, C. I. Reich, R. Overbeek, E. F. Kirkness, K. G. Weinstock, J. M. Merrick, A. Glodek, J. L. Scott, N. S. M. Geoghagen, and J. C. Venter. 1996.** Complete genome sequence of the methanogenic archaeon, *Methanococcus jannaschii. Science* **273:** 1058–1073.
2. **Smith, D. R., L. A. Doucette-Stamm, C. Deloughery, H. Lee, J. Dubois, T. Aldredge, R. Bashirzadeh, D. Blakely, R. Cook, K. Gilbert, D. Harrison, L. Hoang, P. Keagle, W. Lumm, B. Pothier, D. Qiu, R. Spadafora, R. Vicaire, Y. Wang, J. Wierzbowski, R. Gibson, N. Jiwani, A. Caruso, D. Bush, J. N. Reeve, *et al.* 1997.** Complete genome sequence of *Methanobacterium thermoautotrophicum* deltaH: functional analysis and comparative genomics. *J. Bacteriol.* **179:** 7135–7155.
3. **Klenk, H. P., R. A. Clayton, J. F. Tomb, O. White, K. E. Nelson, K. A. Ketchum, R. J. Dodson, M. Gwinn, E. K. Hickey, J. D. Peterson, D. L. Richardson, A. R. Kerlavage, D. E. Graham, N. C. Kyrpides, R. D. Fleischmann, J. Quackenbush, N. H. Lee, G. G. Sutton, S. Gill, E. F. Kirknes, B. A. Dougherty, K. McKenney, M. D. Adams, B. Loftus, J. C. Venter, *et al.* 1997.** The complete genome sequence of the hyperthermophile, sulphate-reducing archaeon *Archaeoglobis fulgidus. Nature* **390:** 364–370.
4. **Mewes, H. W., K. Albermann, M. Bahr, D. Frishman, A. Gleissner, J. Hani, K. Heumann, K. Kleine, A. Maierl, S. G. Oliver, F. Pfeiffer, and A. Zollner. 1997.** Overview of the yeast genome. *Nature* **387:** 7–65.
5. **Aebi, M., G. Kirchner, J. Y. Chen, U. Vijayraghavan, A. Jacobson, N. C. Martin, and J. Abelson. 1990.** Isolation of a temperature-sensitive mutant with an altered tRNA nucleotidyltransferase and cloning of the gene encoding tRNA nucleotidyltransferase in the yeast *Saccharomyces cerevisiae. J. Biol. Chem.* **265:** 16216–16220.

6. **Zhu, L., and M. P. Deutscher. 1987.** tRNA nucleotidyltransferase is not essential for *Escherichia coli* viability. *EMBO J.* **6:** 2473–2477.
7. **Weiner, A. M., and N. Maizels. 1987.** 3′ terminal tRNA-like structures tag genomic RNA molecules for replication: implications for the origin of protein synthesis. *Proc. Natl. Acad. Sci. USA* **84:** 7383–7387.
8. **Maizels, N., and A. M. Weiner. 1993.** The genomic tag hypothesis: modern viruses as molecular fossils of ancient strategies for genomic replication. Pp. 577–602 in *The RNA World,* R. F. Gesteland and J. F. Atkins, eds. Cold Spring Harbor Press, Cold Spring Harbor, NY.
9. **Weiner, A. M., and N. Maizels. 1994.** Unlocking the secrets of retroviral evolution. *Curr. Biol.* **4:** 560–563.
10. **Maizels, N., and A. M. Weiner. 1994.** Phylogeny from function: evidence from the molecular fossil record that tRNA originated in replication, not translation. *Proc. Natl. Acad. Sci. USA* **91:** 6729–6734.
11. **Yue, D., N. Maizels, and A. M. Weiner. 1996.** CCA-adding enzymes and poly(A) polymerases are all members of the same nucleotidyltransferase superfamily: characterization of the CCA-adding enzyme from the archaeal hyperthermophile *Sulfolobus shibatae. RNA* **2:** 895–908.
12. **H. F. Noller. 1993.** On the origin of the ribosome: coevolution of subdomains of tRNA and rRNA. Pp. 137–156 in *The RNA World,* R. F. Gesteland and J. F. Atkins, eds. Cold Spring Harbor Press, Cold Spring Harbor, NY.
13. **Schimmel, P., R. Giegé, D. Moras, and S. Yokoyama. 1993.** An operational RNA code for amino acids and possible relationship to genetic code. *Proc. Natl. Acad. Sci. USA* **90:** 8763–8768.
14. **Shi, J.-P., S. A. Martinis, and P. Schimmel. 1992.** RNA tetraloops as minimalist structures for aminoacylation. *Biochemistry* **31:** 4931–4936.
15. **Schimmel, P., and L. R. D. Pouplana. 1995.** Transfer RNA: from minihelix to genetic code. *Cell* **81:** 983–986.
16. **J. Rudinger, J. B. Blechschmidt, S. Ribeiro, and M. Sprinzl. 1994.** Minimalist aminoacylated RNAs as efficient substrates for elongation factor Tu. *Biochemistry* **33:** 5682–5688.
17. **McClain, W. H., C. Guerrier-Takada, and S. Altman. 1987.** Model substrates for an RNA enzyme. *Science* **238:** 527–530.
18. **Puglisi, E. V., J. D. Puglisi, J. R. Williamson, and U. L. RajBhandary. 1994.** NMR analysis of tRNA acceptor stem microhelices: discriminator base change affects tRNA conformation at the 3′ end. *Proc. Natl. Acad. Sci. USA* **91:** 11467–11471.
19. **Shi, P.-Y., A. M. Weiner, and N. Maizels. 1998.** A top-half tDNA minihelix is a good substrate for the eubacterial CCA-adding enzyme. *RNA* **4:** 276–284.
20. **Shi, P.-Y., N. Maizels, and A. M. Weiner. 1998.** CCA addition by tRNA nucleotidyltransferase: polymerization without translocation? *EMBO J.* **17:** 3197–3206.

Discussion

GUERRERO: You have stated that the sequence of events depicted in one of your slides was demonstrated by the fossil record. Is this a real observation, a metaphor, or just wishful thinking?

MAIZELS: We are seeing the top half of the tRNA in the fossil record, and I believe that the synthetase determinants constitute a molecular fossil record. After that, you could postulate any order that you want.

FORTERRE: Did you screen archaeal genomes for genes homologous to the *Sulfolobus shibatae* CCA-adding enzymes, or for other CCA-adding enzymes?

MAIZELS: We showed that there was only one CCA-adding activity in *Sulfolobus* (1). There might have been two, or even thirty—nobody had looked. We made antibodies against purified recombinant protein and showed that antibodies against this single enzyme destroyed all CCA-adding activity in the cell extract. We have also looked through the newly sequenced archael genomes as they have appeared and found good homologs. Thus far genomics is consistent with the picture we are showing.

FORTERRE: Do you find homologs to the bacterial and eukaryotic CCA-adding enzymes in those genomes?

MAIZELS: We haven't found anything that looks like a class II enzyme, only the class I enzyme so far, but we have found poly-A addition enzymes that look like they are in the other class. Those two activities are even possibly interchangeable.

YUE: You have shown data which suggest that binding of arginine by RNA can evolve quite readily. Why do you suppose the primitive tRNA molecule would have gone on to associate with other amino acids if use of arginine was sufficient to allow it to readily associate with other RNAs and catalyze replication?

MAIZELS: Is your question, why go beyond arginine?

YUE: Yes, why bother with other amino acids, why bother with all twenty?

MAIZELS: Have you seen any arginine-based worlds yet? That's the best answer that I can give.

RONNEBERG: It seems that what you are showing is that this CCA-adding enzyme is very ancient and goes back perhaps to the last common ancestor. How can you use protein homology to show something about a world in which proteins did not exist?

MAIZELS: We're not using the protein homology to go back beyond the last common ancestor at all. We are using the existence of the activity to go back beyond the last common ancestor and into the RNA world. We suggest that there was an RNA-based enzyme that was able to add CCA. Looking at the sequences, one could argue that, while the CCA-adding enzymes in Archea are related to those in the two other kingdoms, they are also characteristically different. Is that telling us something about how things got shuffled around in early evolution? I don't think the data really answer that yet, especially considering all we know about horizontal transfer among these genomes.

Bartel: You're making the argument that because all these enzymes that recognize tRNA interact primarily with the top minihelix, that minihelix is therefore more ancient. But virtually all of these enzymes also catalyze their chemistry at the minihelix. Have you looked at an enzyme that catalyzes a reaction elsewhere on the tRNA—for example, the one that makes the Y base in the anticodon loop? If that enzyme recognized only the anticodon loop, it wouldn't support your argument. On the other hand, if it recognized both the minihelix and the anticodon loop, then that may bolster your argument because it's recognizing the entire tRNA.

Maizels: If such an enzyme recognized only the anticodon loop, I don't think it would contradict our hypothesis at all. If that enzyme catalyzed a reaction somewhere on the anticodon loop and could recognize only the anticodon loop, that enzyme could be indicative of the independent origin of the anticodon domain. That would be very interesting.

Bartel: That is correct.

Maizels: I'm not saying that there wasn't some other completely ancient parallel lineage that produced the anticodon loop–but it would have to be a lineage that we know nothing about yet. We believe that there is evidence that the lineage that produced the top-half minihelix of tRNA is ancient. At the same time, not only is there no evidence for the antiquity of the anticodon loop, but all current evidence is most consistent with the possibility that it evolved subsequent to the top half.

Cavalier-Smith: What observations would refute the genomic tag hypothesis?

Maizels: If we had found that the CCA-adding enzyme recognized the entire tRNA, that would have been fairly discouraging. Altman's (2) lab did an experiment in which they asked if RNaseP from *E. coli* was able to recognize the 3′ termini of the plant viruses that have CCA ends and tRNA-like structures. They may have set out to do that experiment as a way of disproving the genomic tag hypothesis. In any case, the experiment supports the hypothesis. They got the amazing result that *E. coli* RNAse P, which had diverged from the plants a long, long time ago, was able to insert a nick at the 3′ termini of plant viruses, suggesting that there is strong conservation of the 3′ tRNA-like structures, even though they are currently living in entirely different evolutionary milieus and have been separated for a very long time. If we could think of an experiment to refute the model, we would do the experiment.

Literature Cited

1. **Yue, D., N. Maizels, and A. M. Weiner. 1996.** CCA-adding enzymes and poly(A) polymerases are all members of the same nucleotidyltransferase superfamily: characterization of the CCA-adding enzyme from the archael hyperthermophile *Sulfolubus shibatae*. *RNA* **2:** 895–908.
2. **Guerrier-Takada, C., A. van Belkum, C. W. Pleij, and S. Altman. 1998.** Novel reactions of RNAse P with a tRNA-like structure in turnip yellow mosaic virus RNA. *Cell* **53:** 267–272.

Reference: *Biol. Bull.* **196:** 335–337. (June 1999)

Archaeal Aminoacyl-tRNA Synthesis: Unique Determinants of a Universal Genetic Code?

M. IBBA[1], A. W. CURNOW[1], J. BONO[2], P. A. ROSA[2], C. R. WOESE[3], AND D. SÖLL[1]

[1]*Department of Molecular Biophysics and Biochemistry, Yale University, New Haven, Connecticut, 06520-8114;* [2]*Laboratory of Microbial Structure and Function, Rocky Mountain Laboratories of the NIAID, National Institutes of Health, Hamilton, Montana 59840; and* [3]*Department of Microbiology, University of Illinois, Champaign-Urbana, Illinois 61801*

The accurate synthesis of aminoacyl-tRNAs is essential for faithful translation of the genetic code and is assumed to be one of the most highly conserved processes in biology. Recently, this dogmatic view has been called into question by the sequences of a number of archaeal genomes; for example, the genomic sequence of *Methanococcus jannaschii* does not contain open reading frames (ORFs) encoding homologs of the asparaginyl-, cysteinyl-, glutaminyl-, and lysyl-tRNA synthetases (1–3). Furthermore, the full complement of aminoacyl-tRNAs necessary for translation is not entirely formed by the aminoacyl-tRNA synthetases (AARS). In a significant number of cases, the AARSs activate a non-cognate amino acid, and the generation of the correct aminoacyl-tRNA pair is brought about subsequently by a second protein. The use of such pathways for the formation of Gln-tRNA^{Gln} (*via* Glu-tRNA^{Gln}) and Sec-tRNA^{Sec} (*via* Ser-tRNA^{Sec}) is well documented in all the living kingdoms (4, 5). Moreover, in several Archaea, an additional aminoacyl-tRNA, Asn-tRNA^{Asn}, is also formed by transformation of a mischarged tRNA rather than by direct aminoacylation with asparaginyl-tRNA synthetase. Biochemical evidence indicates that aspartyl-tRNA synthetase initially synthesizes Asp-tRNA^{Asn}, which is subsequently converted to Asn-tRNA^{Asn} in a distinct tRNA-dependent transamidation reaction (6).

The use of two-step (indirect) aminoacylation pathways for the formation of Asn-tRNA^{Asn} and Gln-tRNA^{Gln} in some organisms circumvents the need for the enzymes that catalyze one-step formation of these molecules, the asparaginyl- (AsnRS) and glutaminyl-tRNA synthetases (GlnRS) respectively. Consequently, it is not surprising that genes encoding these enzymes have not been found in the completed genomic sequences of organisms that employ one or both of the indirect pathways. However, in addition to lacking AsnRS and GlnRS, the genomic sequences of the euryarchaeons *M. jannaschii* and *Methanobacterium thermoautotrophicum* do not contain homologs of known cysteinyl- (CysRS) or lysyl-tRNA synthetases (1–3). Although no adequate explanation yet exists for the apparent absence of CysRS, several members of the Archaea, including *M. jannaschii,* do contain a functional lysyl-tRNA synthetase (LysRS) that has, however, no resemblance to known bacterial or eukaryal LysRSs or any other sequences in the public database (7). This is in contrast to all other AARSs, which are highly conserved throughout the living kingdom. The high degree of conservation is exemplified by the invariant classification of AARSs into one of two classes defined by the presence of characteristic amino acid sequence motifs and topologically distinct nucleotide binding folds (8). This is not true of the recently identified archaeal LysRSs, which are class I-type AARSs and are thus easily distinguished from their known bacterial and eukaryal counterparts, which are class II enzymes. Although this novel type of LysRS was initially assumed to be confined to certain Archaea, continued genomic sequencing efforts have suggested that it may also occur in some bacteria. This was confirmed by the cloning of a gene encoding a functional archaeal-type LysRS from the Lyme disease spirochete *Borrelia burgdorferi* (9). The spirochetes are a phylogenetically distinct bacterial group, and the existence of

---

This paper was originally presented at a workshop titled *Evolution: A Molecular Point of View*. The workshop, which was held at the Marine Biological Laboratory, Woods Hole, Massachusetts, from 24–26 October 1997, was sponsored by the Center for Advanced Studies in the Space Life Sciences at MBL and funded by the National Aeronautics and Space Administration under Cooperative Agreement NCC 2-896.

archaeal-type genes in these organisms raises doubts about our understanding of their evolutionary origin and development.

Our data raise several evolutionary questions, and the first is about the aminoacyl-tRNA synthetases themselves. If these enzymes are not evolving as orthologs despite the orthology of the translation apparatus [and the constancy of genetic code, with exceptions that are relatively recent compared to the findings at issue (10)], then we must compare the relation between evolution of the aminoacyl-tRNA synthetases and that of translation in general and the structure of the genetic code in particular. It appears that, at the time that the universal ancestor of all life gave rise to the primary lineages, the aminoacyl-tRNA synthetases had not achieved as settled an evolutionary condition as is generally assumed. Second, if the existing universal phylogeny is indeed representative of organismal lineages, then our data speak to the general issue of which functions in the cell were firmly established when the universal ancestor gave rise to the primary lineages.

Acknowledgments

We thank The Institute for Genomic Research for availability of sequence data before publication. This study was supported by a grant from the NIGMS (to DS).

Literature Cited

1. **Bult, C. J., O. White, G. J. Olsen, L. Zhou, R. D. Fleischmann, G. G. Sutton, J. A. Blake, L. M. FitzGerald, R. A. Clayton, J. D. Gocayne, A. R. Kerlavage, B. A. Dougherty, J. F. Tomb, M. D. Adams, C. I. Reich, R. Overbeek, E. F. Kirkness, K. G. Weinstock, J. M. Merrick, A. Glodek, J. L. Scott, N. S. M. Geoghagen, F. Weidman, J. L. Fuhrmann, D. Nguyen, T. R. Utterback, J. M. Kelley, J. D. Peterson, P. W. Sadow, M. C. Hanna, M. D. Cotton, K. M. Roberts, M. A. Hurst, B. P. Kaine, M. Borodovsky, H.-P. Klenk, C. M. Fraser, H. O. Smith, C. R. Woese, and C. J. Venter. 1996.** Complete genome sequence of the methanogenic archaeon, *Methanococcus jannaschii*. *Science* **273:** 1058–1073.
2. **Ibba, M., A. W. Curnow, and D. Söll. 1997.** Aminoacyl-tRNA synthesis: divergent routes to a common goal. *Trends Biochem. Sci.* **22:** 39–42.
3. **Dennis, P. P. 1997.** Ancient ciphers: translation in Archaea. *Cell* **89:** 1007–1010.
4. **Curnow, A. W., K. W. Hong, R. Yuan, S. I. Kim, O. Martins, W. Winkler, T. M. Henkin, and D. Söll. 1997.** Glu-tRNA$^{\mathrm{Gln}}$ amidotransferase: a novel heterotrimeric enzyme required for correct decoding of glutamine codons during translation. *Proc. Natl. Acad. Sci. USA* **94:** 11819–11826.
5. **Baron, C., and A. Böck. 1995.** The selenocysteine-inserting tRNA species: structure and function. Pp. 529–544 in *tRNA: Structure, Biosynthesis, and Function*, D. Söll and U. L. RajBhandary, eds. ASM Press, Washington, DC.
6. **Curnow, A. W., M. Ibba, and D. Söll. 1996.** tRNA-dependent asparagine formation. *Nature* **382:** 589–590.
7. **Ibba, M., S. Morgan, A. W. Curnow, D. R. Pridmore, U. C. Vothknecht, W. Gardner, W. Lin, C. R. Woese, and D. Söll. 1997.** A euryarchaeal lysyl-tRNA synthetase: resemblance to class I synthetases. *Science* **278:** 1119–1122.
8. **Arnez, J. G., and D. Moras. 1997.** Structural and functional considerations of the aminoacylation reaction. *Trends Biochem. Sci.* **22:** 211–216.
9. **Ibba, M., J. L. Bono, P. A. Rosa, and D. Söll. 1997.** Archaeal-type lysyl-tRNA synthetase in the Lyme disease spirochete *Borrelia burgdorferi*. *Proc. Natl. Acad. Sci. USA* **94:** 14383–14388.
10. **Watanabe, K., and S. Osawa. 1995.** tRNA sequences and variations in the genetic code. Pp. 225–250 in *tRNA: Structure, Biosynthesis, and Function*, D. Söll and U. L. RajBhandary, eds. ASM Press, Washington, DC.

Discussion

OLSEN: How to explain the absence of a cysteinyl-tRNA synthetase?

IBBA: That's still a question for us. There are a number of possibilities that one could easily envisage. The most obvious of these is the existence of a seleno-cysteine like pathway. However, this would raise the question of how the cell would achieve the specificity that it needs, since it is very hard to distinguish between seleno-cysteine and cysteine when both are present as free amino acids. We have examined this possibility and find no evidence of it. We think that the problem could be, as with the LysRS, that it's a non-recognizable CysRS. Here is a possibility; if we look carefully through the genomic sequence, we find three PheRS subunits, whereas we know there are only two subunits in PheRS. In fact, one of these three subunits could be CysRS. Another possibility is that there is some vastly complex editing reaction that results in cysteine synthesis in the active site; but I don't see how that would work. We are now testing our assumption that there is a CysRS among the three subunits.

ELLINGTON: Have you considered a third hypothesis, that coming out of the last common ancestor, we weren't quite rid of all of the vestiges of the RNA world, and that in the common ancestor tRNA, charged tRNAs were all made in the same way by ribozymes? Then during the divergence past the progenote, we could have had selective replacement by the protein enzymes.

IBBA: The problem with that hypothesis is that the selectivity for different amino acid is insufficient in an RNA context. Mike Yarus showed that the selectivity between valine and isoleucine is less than one to two hundred. In comparison, the isoleucyl tRNA synthetase can only discriminate at a level of one to two hundred, but then uses the full power of a protein to edit out valine. Consequently I don't think that a full complement of aminoacyl tRNAs could be made by ribozymes. Of course, a very limited complement is possible, but I don't think that the required discrimination is achievable with an RNA.

Ellington: That's a different question, and I think there are a lot of people who might disagree with that.

Cavalier-Smith: I didn't understand why, in your second scenario for the lysyl-tRNA synthetase, you suggested gene transfer rather than a change in the specificity of an amino-acyl tRNA synthetase.

Ibba: I'm hedging my bets at the moment. In the glutamine and glutamate cases, it's very easy to envisage which synthetase arises from another by looking at the sequences and by looking at the specificity. Our best candidate here would be that LysRS arose as a duplication of ArgR—also a Class I synthetase. ArgRS has some unique biochemistry, and we have begun to see lots of that in the LysRS. Therefore, it is possible that there was a duplication and diversification of ArgRS to give the class I LysRS, followed by loss of the class II type of LysRS.

Reference: *Biol. Bull.* **196:** 338–342. (June 1999)

Origins and Evolution of AIDS Viruses

PAUL M. SHARP[1], ELIZABETH BAILES[1], DAVID L. ROBERTSON[1], FENG GAO[2], AND BEATRICE H. HAHN[2]

[1]*Institute of Genetics, University of Nottingham, Queens Medical Centre, Nottingham NG7 2UH, UK;*
and [2]*Departments of Medicine and Microbiology, University of Alabama at Birmingham,*
Birmingham, Alabama 35294

Acquired immune deficiency syndrome (AIDS) can be caused by either of two retroviruses, known as human immunodeficiency virus types 1 and 2 (HIV-1 and HIV-2). Related viruses have been isolated from a number of other primate species; these have been termed simian immunodeficiency viruses (SIV), although in their natural hosts they do not appear to cause disease. Since complete or partial sequences have been determined for very large numbers of both HIVs and SIVs, and because they exhibit an extraordinary degree of sequence diversity, these viruses provide an interesting and challenging model system in which to study molecular evolution. Furthermore, the results obtained provide interesting insights into the origins of AIDS, and have important practical implications for understanding and tackling the ongoing AIDS epidemic.

The HIVs and SIVs belong to the lentivirus family of retroviruses. As with all retroviruses, the HIV (or SIV) virion contains two copies of an RNA genome about 10 kb in length, and encoding three major genes *gag*, *pol*, and *env*. While lentiviruses have been isolated from a number of different orders of mammals, in phylogenetic analyses of the Gag, Pol or Env proteins the primate viruses form a discrete clade within the lentivirus radiation (1). Within this cluster of primate lentiviruses, the phylogenetic relationships among the viruses (Fig. 1) show little correspondence with the phylogenetic relationships of their hosts. This indicates that the viruses must have been the subject of numerous cross-species transmissions (2). In particular, the two human viruses HIV-1 and HIV-2 are not closely related to each other. Rather, HIV-1 is closely related to a virus found in chimpanzees (SIV_{CPZ}; each SIV is given a subscript denoting the species of origin), while HIV-2 is closely related to SIV from sooty mangabeys (SIV_{SM}). Since humans appear to have become infected with these viruses only recently, they are inferred to be the recipients of the cross-species transmissions. Closer examination of the phylogenetic relationships among these viruses indicates that both HIV-1 and HIV-2 have arisen on more than one occasion.

The origins of HIV-2 seem quite clear. HIV-2 first became evident, and is still most common, in individuals from West Africa. Sooty mangabeys (*Cercocebus torquatus atys*) are indigenous to the same geographic area and are infected with SIV_{SM} at high rates in the wild. Apparently, humans have become infected with a virus from sooty mangabeys in rural West Africa, where these monkeys are commonly hunted for food and kept as pets. Diverse HIV-2 sequences fall into (so far) six discrete phylogenetic lineages, which have been termed subtypes A–F (3, 4, 5). These HIV-2 lineages are not more closely related to one another than to examples of SIV_{SM} (6). Instead, the HIV-2 and SIV_{SM} lineages are phylogenetically interspersed (Fig. 2). This indicates that the different lineages of HIV-2 cannot all be due to a single cross-species transfer: in fact, it may be that each of the subtypes arose from a separate transmission from sooty mangabey to human (2, 5).

The origins of HIV-1 remain uncertain. Since SIV_{CPZ} is closely related to HIV-1, we might speculate that HIV-1 was the result of cross-species transmission from chimpanzees. However, there is little information on the prevalence of SIV infection in chimpanzees: as yet, only four examples of SIV_{CPZ} have been reported, and many chimpanzees have been found to be seronegative. In those primate species where high levels of SIV infection have been found in the

---

This paper was originally presented at a workshop titled *Evolution: A Molecular Point of View*. The workshop, which was held at the Marine Biological Laboratory, Woods Hole, Massachusetts, from 24–26 October 1997, was sponsored by the Center for Advanced Studies in the Space Life Sciences at MBL and funded by the National Aeronautics and Space Administration under Cooperative Agreement NCC 2-896.

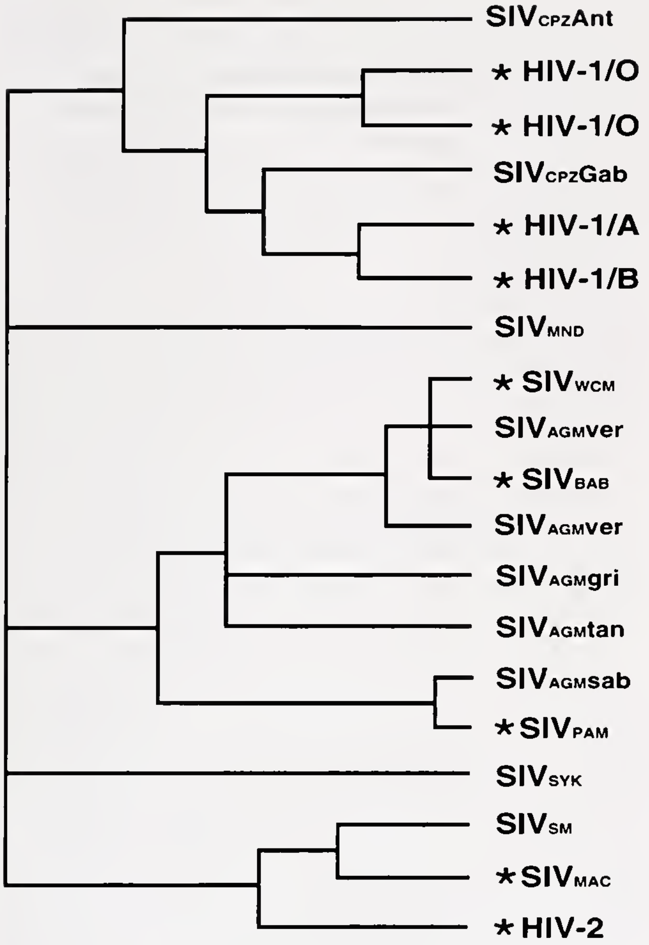

Figure 1. Schematic diagram summarizing the phylogenetic relationships among primate lentiviruses. The simian immunodeficiency viruses (SIV) have a subscript denoting the species from which they were isolated: these are chimpanzee (CPZ), mandrill (MND), white-crowned mangabey (WCM), African green monkey (AGM), baboon (BAB), patas monkey (PAM), Sykes' monkey (SYK), sooty mangabey (SM), and macaque (MAC). There are four species of African green monkeys, *i.e.*, vervet, grivet, tantalus, and sabaeus monkeys; viruses from each exhibit similar levels of diversity to that shown for the two examples of SIV$_{\mathrm{AGM}}$ver. For HIV-1, representatives of the O group, and of the A and B subtypes of the M group, are shown. This composite phylogeny was adapted from Jin *et al.* (19), Sharp *et al.* (15), Vanden Haesevelde *et al.* (27), and Bibollet-Ruche *et al.* (8). See Figure 2 for more detail of the relationships among HIV-2, SIV$_{\mathrm{SM}}$ and SIV$_{\mathrm{MAC}}$. Asterisks indicate viruses inferred to have arisen from recent cross-species transmissions.

wild, namely sooty mangabeys and African green monkeys (the *Cercopithecus aethiops* super-species), it is primarily adults that are seropositive, leading to the hypothesis that SIV is normally transmitted through sexual activity. The vast majority of chimpanzees that have been tested were taken from the wild as juveniles or bred in captivity; and so higher rates of SIV infection might be found if wild adult chimpanzees were tested. On balance, chimpanzees seem the most likely direct source of HIV-1, but it cannot be ruled out that both humans and chimpanzees have acquired a virus from a third species, presumably a small African monkey (2).

Sequences have been determined for isolates of HIV-1 from all over the world. These viruses fall into two quite distinct phylogenetic clusters, which have been termed groups M and O. Viruses from the M group are (by far) the most numerous and the most geographically widespread. The O group contains only viruses isolated from individuals originating from, or with epidemiological links to, the area of central Africa around Cameroon. Full-length sequences have been determined for only two of the isolates of SIV$_{\mathrm{CPZ}}$, one from Gabon (Gab) and one from Zaire (Ant). As with SIV$_{\mathrm{SM}}$ and HIV-2, the SIV$_{\mathrm{CPZ}}$ and HIV-1 lineages are interspersed (Fig. 1). Thus, unless we hypothesize that SIV$_{\mathrm{CPZ}}$Gab resulted from human-to-chimpanzee transmission (which seems most unlikely), the HIV-1 groups M and O must have arisen through separate cross-species transmissions (whether or not the source was chimpanzees).

The inference that SIVs have been transmitted to humans on numerous occasions need not be surprising, especially given evidence that transmission between different species

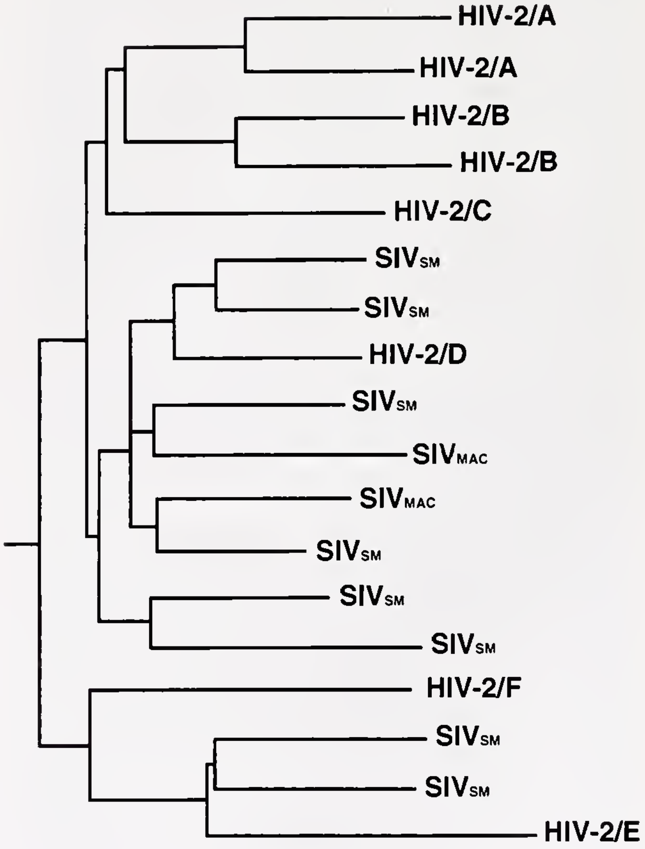

Figure 2. Phylogenetic relationships of HIV-2, SIV$_{\mathrm{SM}}$, and SIV$_{\mathrm{MAC}}$. For HIV-2, just two examples of the A and B subtypes are shown, to represent the extent of sequence diversity known within these clades; for subtypes C–F, only single examples are known as yet. Adapted from Gao *et al.* (4), and Chen *et al.* (5, 6).

of monkeys has also occurred both in the wild and in captivity. For example, SIVs have been found in wild-living yellow baboons (*Papio hamadryas cynocephalus*) in Tanzania (7) and patas monkeys (*Erythrocebus patas*) in Senegal (8). These species do not appear to be normally infected with SIV. In each case, phylogenetic analyses indicated that the viruses were closely related to $\mathrm{SIV}_{\mathrm{AGM}}$ from the local species of African green monkey, namely, vervet monkeys in East Africa and sabaeus monkeys in West Africa (Fig. 1). A white crowned mangabey (*Cercocebus torquatus lunulatus*) was also found to be infected with a virus closely related to $\mathrm{SIV}_{\mathrm{AGM}}$ from vervet monkeys (9), but this transmission most likely occurred in captivity (2). In addition to HIV-2, other viruses closely related to $\mathrm{SIV}_{\mathrm{SM}}$ have been isolated from rhesus macaques (*Macaca mulatta*), stump-tailed macaques (*M. arctoides*), and pig-tailed macaques (*M. nemestrina*); macaques are not naturally infected with SIV, and it seems that these animals were infected from sooty mangabeys in captivity.

Subsequent to their transmission to humans, the HIVs have accumulated considerable sequence diversity. This reflects a very rapid rate of evolution, caused primarily by two features of the viral replicative enzyme, reverse transcriptase. The first of these properties is a lack of proofreading functions, leading to a mutation rate of around 3.4×10^{-5} nucleotide changes per site per replication cycle (10). In an early analysis of the evolution of HIV-1, the rate of synonymous nucleotide substitution was estimated to be around 10×10^{-3} substitutions per site per year (11). This is remarkably consistent with recent estimates of about 300 replication cycles per year during HIV-1 infection (12, 13), and suggests that the great majority of synonymous substitutions are neutral. Note that these substitution rates are extremely fast: about six orders of magnitude faster than those seen in the nuclear genes of the viruses' primate hosts (14). Nonsynonymous nucleotide substitution rates in HIV-1 are not much slower, at about 2×10^{-3} substitutions per site per year in *gag* and *pol*, and 5×10^{-3} substitutions per site per year in *env* (11).

For the most numerous (M) group of HIV-1, phylogenetic analyses place viruses within distinct subclades, which have been called subtypes. So far, 10 subtypes (A–I) have been proposed. These subtypes are approximately equidistant from one another, with the exception of subtypes B and D, which are somewhat closer to one another (15). Since there is no evidence that these subtypes, unlike those of HIV-2, represent separate cross-species origins, the cause of this phylogenetic substructure remains unclear. There are geographical patterns: most subtypes are common in sub-Saharan Africa, where HIV-1 originated, but only particular subtypes are frequently found in other parts of the world. The strains of HIV-1 first isolated in North America and Europe fall within subtype B, which is still by far the most common in those regions, but is rare in sub-Saharan Africa. Apparently, subtype B originated with the successful invasion of North America by a single initial virus, related to subtype D. The (earlier) origins of the other subtypes may have been due to similar chance epidemiological events in Africa. As a consequence of the rapid rate of nonsynonymous substitution in HIV-1, the Env proteins of these different subtypes now exhibit about 25% sequence divergence, even though the M group probably arose only within the last 50 years or so.

The second way in which reverse transcriptase contributes to sequence diversity is through its propensity to "hop" between the two available RNA templates, causing recombination. For several years, there was a widespread belief that individuals could not become infected with more than one HIV-1 strain. If this were true, then although some sequence diversity does build up during the course of infection, recombination would only occur among rather similar sequences. However, among the first African isolates of HIV-1, was one, MAL, which appeared to be a recombinant of highly divergent viruses (11). After extensive sequence data became available for non-subtype B viruses from around the world, it became apparent that a significant fraction (perhaps 10%) of characterized HIV-1 group M strains have mosaic genomes due to recombination between different subtypes (16). This indicates that infection with multiple strains of HIV-1 can occur, and indeed such cases have been found (*e.g.,* 17). It also implies that recombination has a significant impact on the generation of diversity in HIV-1, bringing together new combinations of quite divergent sequences, and perhaps enabling evolutionary "leaps" that are not achievable by simple accumulation of substitutions. In this context, note that in Thailand, where AIDS started as two distinct epidemics due to viruses of subtypes B (spreading among injecting drug users) and E (spreading heterosexually), over recent years the proportion of HIV-1 that are subtype E has increased dramatically. These "subtype E" viruses are, in fact, descendants of a recombination between subtypes A and E, that probably occurred in Central Africa (18). Whether the success of "subtype E" viruses in Thailand is merely an epidemiological phenomenon, or is due to an increased fitness (transmissibility) of these recombinant viruses, is not known.

Evidence for recombination has also been seen in other primate lentiviruses. The strain of $\mathrm{SIV}_{\mathrm{AGM}}$ found in sabaeus monkeys appears to be the result of a relatively ancient recombination event between $\mathrm{SIV}_{\mathrm{AGM}}$ and $\mathrm{SIV}_{\mathrm{SM}}$ from sooty mangabeys (19). Investigations of the diversity of $\mathrm{SIV}_{\mathrm{AGM}}$ from wild sabaeus monkeys (20) and of $\mathrm{SIV}_{\mathrm{SM}}$ from wild sooty mangabeys (6) have each provided an example of an apparently mosaic virus generated by more recent recombination. Among HIV-2 strains, one (FA) appears to be a recombinant of two subtype A viruses (4), while another (7312A) is a mosaic of genomic regions from subtypes A and B (3, 21), and thus is a combination of sequences that probably evolved after separate transmissions from sooty mangabeys to humans (see above).

The above recombination events were homologous in the sense that they involved an exchange of genomic segments. A nonhomologous recombination event that was responsible for the generation of an additional gene also seems to have occurred early in the evolution of the SIV_{SM}/HIV-2 lineage. All of the primate lentiviruses have a *vpr* gene, but members of the SIV_{SM}/HIV-2 lineage are unique in also having an adjacent related gene, *vpx*. While *vpx* could have arisen through duplication of *vpr* within the SIV_{SM} genome, phylogenetic analyses suggest that it is more closely related to the *vpr* gene of SIV_{AGM}, leading to the suggestion that *vpx* was acquired through a nonhomologous recombination event (22).

If we are to understand fully the molecular evolution of these primate lentiviruses, we must be able to place a time scale on their phylogeny. Since there is no reason to believe that HIV-2 or the SIVs evolve at rates significantly different from HIV-1, it would be tempting to use the molecular clock described above to extrapolate across the entire primate lentivirus phylogeny. That would lead us to estimate that the common ancestor of the entire group existed within the last 150–200 years (23). However, the four different species of African green monkeys within the *C. aethiops* super-species—including grivet and tantalus monkeys, as well as the vervet and sabaeus monkeys mentioned above—are each infected with their own variety of SIV (19, 24). This probably indicates that, within this part of the viral phylogeny, evolution has been host-dependent, and therefore that an ancestral SIV_{AGM} was present in the common ancestor of the African green monkeys, which may have existed more than a million years ago. Because our estimate of the rate of evolution seems reasonably accurate, this suggests that current views of the extent of substitution that has occurred during the divergence of the SIV/HIV lineages are gross underestimates. Standard methods of estimating the evolutionary distance between two sequences tend to ignore variation across sites in the rate of substitution, and consequently underestimate evolutionary distance. Two different approaches to this problem have recently been applied to HIV-1 (25, 26), and they indicate that distances within the M group of HIV-1 may have been underestimated by a factor of two. The extent of underestimation becomes far more serious when more divergent sequences are considered, and we now suspect that the discrepancy of four orders of magnitude alluded to above may be explicable!

Acknowledgments

This work was supported in part by grants from the National Institutes of Health (NO1 AI35170 and AI85338; to B.H.H.).

Literature Cited

1. **Sharp, P. M., C. J. Burgess, and B. H. Hahn. 1995.** The molecular evolution of the human immunodeficiency viruses. Pp. 438–454 in *Molecular Basis of Virus Evolution*, A. J. Gibbs, C. H. Calisher, and F. Garcia-Arenal, eds. Cambridge University Press, Cambridge.
2. **Sharp, P. M., D. L. Robertson, and B. H. Hahn. 1995.** Cross-species transmission and recombination of "AIDS" viruses. *Phil. Trans. Roy. Soc. London B* **349:** 41–47.
3. **Gao, F., L. Yue, A. T. White, P. G. Pappas, J. Barchue, A. P. Hanson, B. M. Greene, P. M. Sharp, G. M. Shaw, and B. H. Hahn. 1992.** Human infection by genetically diverse SIV_{SM}-related HIV-2 in West Africa. *Nature* **358:** 495–499.
4. **Gao, F., L. Yue, D. L. Robertson, S. C. Hill, H. Hui, R. J. Biggar, A. E. Neequaye, T. M. Whelan, D. D. Ho, G. M. Shaw, P. M. Sharp, and B. H. Hahn. 1994.** Genetic diversity of human immunodeficiency virus type 2: evidence for distinct sequence subtypes with differences in virus biology. *J. Virol.* **68:** 7433–7447.
5. **Chen, Z. W., A. Luckay, D. L. Sodora, P. Telfer, P. Reed, A. Gettie, J. M. Kanu, R. F. Sadek, J. Yee, D. D. Ho, L. Zhang, and P. A. Marx. 1997.** Human immunodeficiency virus type 2 (HIV-2) seroprevalence and characterization of a distinct HIV-2 genetic subtype from the natural range of simian immunodeficiency virus-infected sooty mangabeys. *J. Virol.* **71:** 3953–3960.
6. **Chen, Z. W., P. Telfer, A. Gettie, P. Reed, L. Zhang, D. D. Ho, and P. A. Marx. 1996.** Genetic characterization of new West African simian immunodeficiency virus SIVsm: geographic clustering of household-derived SIV strains with human immunodeficiency virus type 2 subtypes and genetically diverse viruses from a single feral sooty mangabey troop. *J. Virol.* **70:** 3617–3627.
7. **Jin, M. J., J. Rogers, J. E. Phillips-Conroy, J. S. Allan, R. C. Desrosiers, G. M. Shaw, P. M. Sharp, and B. H. Hahn. 1994.** Infection of a yellow baboon with simian immunodeficiency virus from African green monkeys: evidence for cross-species transmission in the wild. *J. Virol.* **68:** 8454–8460.
8. **Bibollet-Ruche, F., A. Galat-Luong, G. Cuny, P. Sarni-Manchado, G. Galat, J.-P. Durand, X. Pourrut, and F. Veas. 1996.** Simian immunodeficiency virus infection in a patas monkey (*Erythrocebus patas*): evidence for cross-species transmission from African green monkeys (*Cercopithecus aethiops sabaeus*) in the wild. *J. Gen. Virol.* **77:** 773–781.
9. **Tomonaga, K., J. Katahira, M. Fukasawa, M. A. Hassan, M. Kawamura, H. Akari, T. Miura, T. Goto, M. Nakai, M. Suleman, M. Isahakia, and M. Hayami. 1993.** Isolation and characterization of simian immunodeficiency virus from African white-crowned mangabey monkeys (*Cercocebus torquatus lunulatus*). *Arch. Virol.* **129:** 77–92.
10. **Mansky, L. M., and H. M. Temin. 1995.** Lower *in vivo* mutation rate of human immunodeficiency virus type 1 than that predicted from the fidelity of purified reverse transcriptase. *J. Virol.* **69:** 5087–5094.
11. **Li, W.-H., M. Tanimura, and P. M. Sharp. 1988.** Rates and dates of divergence between AIDS virus nucleotide sequences. *Mol. Biol. Evol.* **5:** 313–330.
12. **Wei, X., S. K. Ghosh, M. E. Taylor, V. A. Johnson, E. A. Emini, P. Deutsch, J. D. Lifson, S. Bonhoeffer, M. A. Nowak, B. H. Hahn, M. S. Saag, and G. M. Shaw. 1995.** Viral dynamics in HIV-1 infection. *Nature* **73:** 117–122.
13. **Perelson, A. S., A. U. Neumann, M. Markowitz, J. M. Leonard, and D. D. Ho. 1996.** HIV-1 dynamics *in vivo:* virion clearance rate, infected cell lifespan, and viral generation time. *Science* **271:** 1582–1586.
14. **Li, W.-H., M. Tanimura, and P. M. Sharp. 1987.** An evaluation of the molecular clock hypothesis using mammalian DNA sequences. *J. Mol. Evol.* **25:** 330–342.
15. **Sharp, P. M., D. L. Robertson, F. Gao, and B. H. Hahn. 1994.**

Origins and diversity of human immunodeficiency viruses. *AIDS* **8:** S27–S42.

16. **Robertson, D. L., P. M. Sharp, F. E. McCutchan, and B. H. Hahn. 1995.** Recombination in HIV-1. *Nature* **374:** 124–126.
17. **Salminen, M. O., J. K. Carr, D. L. Robertson, P. Hegerich, D. Gotte, C. Koch, E. Sanders-Buell, F. Gao, P. M. Sharp, B. H. Hahn, D. S. Burke, and F. E. McCutchan. 1997.** Evolution and probable transmission of intersubtype recombinant human immunodeficiency virus type 1 in a Zambian couple. *J. Virol.* **71:** 2647–2655.
18. **Gao, F., D. L. Robertson, S. G. Morrison, H. Hui, S. Craig, J. Decker, P. N. Fultz, M. Girard, G. M. Shaw, B. H. Hahn, and P. M. Sharp. 1996.** The heterosexual human immunodeficiency virus type 1 epidemic in Thailand is caused by an intersubtype (A/E) recombinant of African origin. *J. Virol.* **70:** 7013–7029.
19. **Jin, M. J., H. Hui, D. L. Robertson, M. C. Muller, F. Barre-Sinoussi, V. M. Hirsch, J. S. Allan, G. M. Shaw, P. M. Sharp, and B. H. Hahn. 1994.** Mosaic genome structure of simian immunodeficiency virus from West African green monkeys. *EMBO J.* **13:** 2935–2947.
20. **Bibollet-Ruche, F., C. Brengues, A. Galat-Luong, G. Galat, X. Pourrut, N. Vidal, F. Veas, J.-P. Durand, and G. Cuny. 1997.** Genetic diversity of simian immunodeficiency viruses from West African green monkeys: evidence of multiple genotypes within populations from the same geographic locale. *J. Virol.* **71:** 307–313.
21. **Robertson, D. L., B. H. Hahn, and P. M. Sharp. 1995.** Recombination in AIDS viruses. *J. Mol. Evol.* **40:** 249–259.
22. **Sharp, P. M., E. Bailes, M. Stevenson, M. Emerman, and B. H. Hahn. 1996.** Gene acquisition in HIV and SIV. *Nature* **383:** 586–587.
23. **Sharp, P. M., and W.-H. Li. 1988.** Understanding the origins of AIDS viruses. *Nature* **336:** 315.
24. **Soares, M., D. L. Robertson, H. Hui, J. S. Allan, G. M. Shaw, and B. H. Hahn. 1997.** A full-length and replication-competent proviral clone of SIV$_{AGM}$ from tantalus monkeys. *Virology* **228:** 394–399.
25. **Van de Peer, Y., W. Janssens, L. Hendryckx, K. Fransen, G. van der Groen, and R. De Wachter. 1996.** Phylogenetic analysis of the *env* gene of HIV-1 isolates taking into account individual nucleotide substitution rates. *AIDS* **10:** 1485–1494.
26. **Leitner, T., S. Kumar, and J. Albert. 1997.** Tempo and mode of nucleotide substitutions in *gag* and *env* gene fragments in human immunodeficiency virus type 1 populations with a known transmission history. *J. Virol.* **71:** 4761–4770.
27. **Vanden Haesevelde, M. M., M. Peeters, G. Jannes, W. Janssens, G. van der Groen, P. M. Sharp, and E. Saman. 1996.** Sequence analysis of a highly divergent HIV-1 related lentivirus isolated from a wild captured chimpanzee. *Virology* **221:** 346–350.

Discussion

KUHLMAN: Why not suggest that there is a grossly unequal variation in the clock along lineages, instead of supposing that there is this grossly unequal rate of substitution across sites?

SHARP: We've known of this apparent paradox for several years, and our explanation, until very recently, was that the clock may be quite variable. However, there is no reason to think that a retrovirus should evolve at a significantly slower rate than HIV-1. It has been suggested that the SIVs may evolve slowly because they're in a natural host, where they are not causing disease. Typically, when a human is first infected with the virus, the viral population within the individual is quite homogenous. The very fast rate of evolution then results in a quasi-species evolving within an individual. The amount of diversity within a quasi-species of a monkey appears to be about the same as for a human, suggesting a very similar rate of evolution for the monkey quasi-species. Estimated rates of evolution for other quite distinct retroviruses are no more than an order of magnitude slower, if that.

RUSS DOOLITTLE: The retrovirus data suggest one reason why things should slow down considerably. When viruses become endogenous and incorporated as part of the genome, and are not infectious, they retreat by many orders of magnitude to the typical or vertical rate. If these viruses are later re-awakened by some opportunistic mode, they can then resume the fast track.

SHARP: You are absolutely right. If these viruses ever became endogenous, that would drop their rate of evolution by five or six orders of magnitude, and this would explain the data immediately. However, there is no sign that these lentiviruses become endogenous in humans or other primates. In the case of the African green monkeys, the adults are infected with the virus, and they are SIV positive. They are re-infected in every generation as they become sexually mature. Your proposal would provide us with a lovely simple explanation, but it doesn't seem to work.

ROTHSCHILD: Has anyone looked for an AIDS virus in mummies from North Africa? This could give an idea of time.

SHARP: Jaap Goudsmit has described searches of this type in his book (1). Unfortunately they didn't find anything.

Literature Cited

1. **Goudsmit, Jaap. 1997.** *Viral Sex: The Nature of Aids.* Oxford University Press, Oxford.

Reference: *Biol. Bull.* **196:** 343–344. (June 1999)

Coalescents, Phylogenies, and Likelihoods

JOSEPH FELSENSTEIN

Department of Genetics, University of Washington, Box 357360, Seattle, Washington 98195-7360

When phylogenies get down below the species level, they turn into coalescents. Individual genetic loci then have genealogies that are, in the absence of recombination, trees. But as one moves along the genome, recombination moves branches and changes the trees, with the result that other loci more than a few kilobases away usually have very different trees. Between species their trees of ancestry are very similar; the difference in their behavior within and between species is an indication that there really is something different, and nonarbitrary, about the species level. When one looks at the problems of estimation involving these trees, one can get overly involved in estimating the tree itself. But the interest in doing so is limited, as there may be a million completely different coalescent trees for different parts of the genome. Furthermore, the number of varying sites available for estimating each is quite limited, so that each is poorly estimated. The solution to this quandary is to realize that the genealogies are generated by a random process of genetic drift, possibly with other evolutionary forces intervening. What we need to know is not the trees themselves, but the parameters of these evolutionary forces and of population structure, such as effective population size, migration rates, population growth rates.

The coalescent process defined by J.F.C. Kingman (1, 2) was the foundation of this theory. Coalescent likelihood methods have been developed by two groups, ours and Griffiths and Tavaré's. The two approaches use the same statistical methods and models, and differ mostly in the computational methods. The likelihood for a population sample is the sum over all possible genealogies, summing the probability of that genealogy given the parameters, multiplied by the probability of the sample of sequences given the genealogy. The number of genealogies is infinitely large, and even their shapes occur in very large numbers. The solution both groups have adopted to calculating these integrals is to sample randomly from the possible genealogies, but with the sampling directed mostly toward genealogies that have a good chance of contributing substantially to the likelihood. This is an "importance sampling" method of Monte Carlo integration. The approach that my colleagues Mary Kuhner, Jon Yamato, Peter Beerli, and I have taken (3) is to use Markov Chain Monte Carlo sampling, where one starts with a tree and modifies it randomly, using an acceptance-rejection method (the Metropolis-Hastings method) to wander among possible trees. The result, after an hour or two of computer time, is a sample of perhaps 2000 trees out of 100,000 visited. The sampling uses approximate trial values of the parameters, and allows us to calculate likelihood surfaces for nearby parameter values from one series of sampling runs.

The method seems to work, and can be extended in a number of interesting ways. Like Griffiths and Tavaré (4, 5, 6), who are the pioneers here, we can treat cases of exponential population growth, migration structure, and recombination (7, 8). The latter is particularly important, as it enables the use of nuclear gene sequences. Combining all these models will be a challenge; rather than produce separate computer programs to handle all possible combinations of evolutionary forces, it may be better to use object-oriented programming languages such as C++ to produce a program that asks the user to describe the desired situation, and then links together the appropriate set of modules to sample genealogies for it. We have started distributing individual programs in our LAMARC package (at http://evolution.genetics.washington.edu/lamarc.html). For the moment these are stand-alone programs.

Two extensions that are particularly interesting are a method for handling natural selection and one for handling samples of sequences in historical time. Some cases of extremely strong selection can be treated, using methods

---

This paper was originally presented at a workshop titled *Evolution: A Molecular Point of View*. The workshop, which was held at the Marine Biological Laboratory, Woods Hole, Massachusetts, from 24–26 October 1997, was sponsored by the Center for Advanced Studies in the Space Life Sciences at MBL and funded by the National Aeronautics and Space Administration under Cooperative Agreement NCC 2-896.

developed by Richard Hudson and Norman Kaplan (9, 10). Recently Claudia Neuhauser and Steven Krone (11, 12) have made major progress in formulating coalescents for natural selection. We propose another method for handling natural selection that may complement theirs, using a randomly sampled history of the frequencies of the selected alleles. For historical samples, such as work on ancient DNA, or work on the progress of HIV infections within a single patient, we can also formulate coalescent likelihood methods. Any two of the generation time, the effective population size, and the mutation rate can then be estimated, given the other. If one is known, all three can be estimated.

Literature Cited

1. **Kingman, J. F. C. 1982.** The coalescent. *Stochastic Process. Applic.* **13:** 235–248.
2. **Kingman, J. F. C. 1982.** On the genealogy of large populations. Pp. 27–43 in *Essays in Statistical Science,* J. Gani and E. J. Hannan, eds. Applied Probability Trust, London.
3. **Kuhner, M. K., J. Yamato, and J. Felsenstein. 1995.** Estimating effective population size and mutation rate from sequence data using Metropolis-Hastings sampling. *Genetics* **140:** 1421–1430.
4. **Griffiths, R. C., and S. Tavaré. 1994.** Ancestral inference in population genetics. *Stat. Sci.* **9:** 307–319.
5. **Griffiths, R. C., and S. Tavaré. 1994.** Sampling theory for neutral alleles in a varying environment. *Philos. Trans. R. Soc. Lond. B Biol. Sci.* **344:** 403–410.
6. **Griffiths, R. C., and P. Marjoram. 1996.** Ancestral inference from samples of DNA sequences with recombination. *J. Computational Biol.* **3:** 479–502.
7. **Kuhner, M. K., J. Yamato, and J. Felsenstein. 1997.** Applications of Metropolis-Hastings genealogy sampling. Pp. 183–192 in *Progress in Population Genetics and Human Evolution,* P. Donnelly and S. Tavaré, eds. IMA Volumes in Mathematics and its Applications, Vol. 87. Springer Verlag, Berlin.
8. **Kuhner, M. K., J. Yamato, and J. Felsenstein. 1998.** Maximum likelihood estimation of population growth rates based on the coalescent. *Genetics* **149:** 429–434.
9. **Hudson, R. R., and N. L. Kaplan. 1988.** The coalescent process in models with selection and recombination. *Genetics* **120:** 831–840.
10. **Kaplan, N. L., T. Darden, and R. R. Hudson. 1988.** The coalescent process in models with selection. *Genetics* **120:** 819–829.
11. **Neuhauser, C., and S. M. Krone. 1997.** The genealogy of samples in models with selection. *Genetics* **145:** 519–534.
12. **Krone, S. M., and C. Neuhauser. 1997.** Ancestral processes with selection. *Theor. Popul. Biol.* **51:** 210–237.

Discussion

UNRAU: Given that you have taken migration into account in your model, to what extent do you believe random breeding is representative of human beings?

FELSENSTEIN: It's not at all representative. In the long run we would like to be able to handle data such as the mitochondrial Eve data set (1). We would have to take into account geographic structure, population growth, migration events, and historical events. One of the hypotheses we want to consider is colonization of Eurasia from Africa by a small group of people. The complexities of doing so are very daunting. We would approximate the complex genetic patterns in Europe and Asia by a few simple populations. Our reason for choosing this approach is that high rates of migration tend to scramble the lineages very thoroughly. Anything with a migration rate above the reciprocal of the effect of population size is enough to scramble things. Consequently, we will not need to model all the details of every invasion of Europe by barbarians on horseback in order to get things to fit approximately.

Literature Cited

1. **Cann, R. L., M. Stoneking, and A. C. Wilson. 1987.** Mitochondrial DNA and human evolution. *Nature* **325:** 31–36.

Reference: *Biol. Bull.* **196:** 345–350. (June 1999)

Genes and Other Samples of DNA Sequence Data for Phylogenetic Inference

MICHAEL P. CUMMINGS[1,*], SARAH P. OTTO[2], AND JOHN WAKELEY[3,†]

[1] *Department of Botany and Plant Sciences, University of California, Riverside, California 92521-1024;*
[2] *Department of Zoology, University of British Columbia, 6270 University Blvd. Vancouver,*
British Columbia V6T 1Z4, Canada; and [3] *Department of Ecology, Evolution & Natural Resources,*
Nelson Hall, Rutgers University, P.O. Box 1059, Piscataway, New Jersey 08855-1059

One of the most basic uses of DNA sequence data in the study of evolution is as a source of information for inferring evolutionary history. Where homology may be difficult to establish, particularly in comparisons of phylogenetic lineages that have diverged relatively early, DNA sequence data may offer distinct advantages over other data, such as morphology. However, DNA sequence data may present its own difficulties, and the sampling properties of DNA sequence data are not well characterized.

To better understand the sampling properties of DNA sequence data in phylogenetic analysis, a series of computational experiments were performed using complete mitochondrial genomes from 10 vertebrate species. These taxa were cow, *Bos taurus;* carp, *Cyprinus carpio;* chicken, *Gallus gallus;* human, *Homo sapiens;* loach, *Crossostoma lacustre;* mouse, *Mus musculus;* rat, *Rattus norvegicus;* harbor seal, *Phoca vitulina;* fin whale, *Balenoptera physalus;* and frog, *Xenopus laevis.* For this study, the mitochondrial genome has some distinct advantages:

1. A number of complete genome sequences are available.
2. A complete genome represents an entire population of sites in a statistical sense.
3. It has a simple history with little or no recombination.
4. It is a convenient size for analysis.
5. It is widely used in systematic studies.

The complete DNA sequences from the mitochondrial genomes of these organisms, exclusive of the control region, were aligned gene by gene and assembled into a data set of 16,075 sites. These data formed the basis of phylogenetic analyses using three methods of phylogenetic tree construction: maximum likelihood (1), parsimony (2), and neighbor-joining (3). These three methods were chosen in part because of their widespread use, but mainly to ascertain whether observed patterns seen were specific to the tree construction methodology or were more general properties of DNA sequence data sampling. Further details of the analyses are given in Cummings *et al.* (4).

As definable and recognizable units, genes represent the most common currency by which DNA sequences are considered; and for reasons related to history, function, and experimental utility, most DNA sequences used in phylogenetic study are, in whole or in part, gene sequences. Therefore, the first question considered was, Do individual genes provide an accurate estimate of whole-genome results?

For these experiments the sequences of all the major genes (those exclusive of tRNA genes) were analyzed by the three phylogenetic methods. Analysis of the complete genomes results in a single common and unambiguously supported tree (Fig. 1), and thus the gene trees could be directly compared to a common tree.

---

[*] Current address: The Josephine Bay Paul Center for Comparative Molecular Biology and Evolution, Marine Biological Laboratory, 7 MBL Street, Woods Hole, MA 02543-1015.

[†] Current address: Department of Organismic and Evolutionary Biology, The Biological Laboratories, 16 Divinity Avenue, Harvard University, Cambridge, MA 02318.

This paper was originally presented at a workshop titled *Evolution: A Molecular Point of View.* The workshop, which was held at the Marine Biological Laboratory, Woods Hole, Massachusetts, from 24–26 October 1997, was sponsored by the Center for Advanced Studies in the Space Life Sciences at MBL and funded by the National Aeronautics and Space Administration under Cooperative Agreement NCC 2-896.

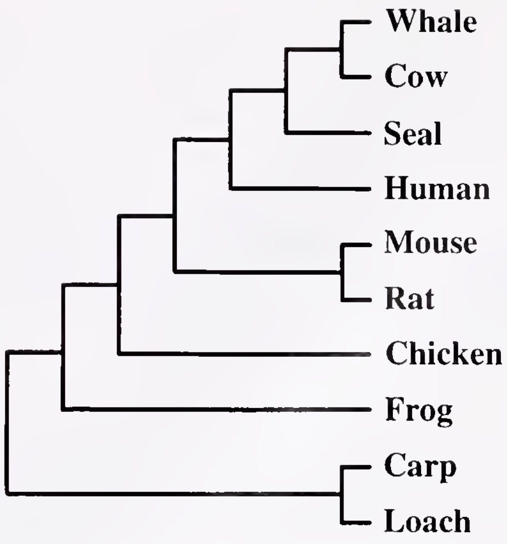

Figure 1. Tree of phylogenetic relationships based on the entire mitochondrial genome, exclusive of the control region, as inferred using maximum likelihood, parsimony, and neighbor-joining.

The major observations from these gene-based experiments were as follows:

1. Few trees inferred from individual genes are identical to the whole-genome tree (3–5 out of 15 genes, depending on the tree construction method; Table I).
2. Twenty different trees were inferred from individual gene sequences across all three construction methods.
3. No single alternative tree was commonly found.
4. No gene sequence gave the same tree for all three methods.
5. Labile branches were not restricted to one part of the tree; *e.g.*, both shallow and deep relationships were unstable (see also references 4 and 5).

There appeared to be some crude relationship between the length of a gene and its chance of leading to a tree identical to the whole-genome tree; indeed, only one gene less than 1111 bp (COIII, 785 bp) gave a tree identical to the whole-genome tree (Table I).

The next question was, If individual gene sequences are not good samples, then how many sites are needed? The answer to this question was obtained simultaneously with the answer to a closely related question, Does it matter how sites are sampled? To answer these questions, two types of random samples were collected and analyzed, and the resulting trees were compared to the whole-genome tree. One sampling scheme is similar to the method of data collection in empirical studies; a site defines one end of a sequence region, and adjacent bases are determined to produce a contiguous sequence (Fig. 2A). This involves the collection of n contiguous sites (where $n = 1000, 2000, 3000, \ldots, 8000$) starting from a random nucleotide position in the genome. The second sampling scheme also involved the collection of n sites, but the sites were individually and independently sampled, without replacement, from random locations throughout the genome (Fig. 2B). By examining multiple collections (1024) of each different sample size, we can determine how many sites are needed to produce a tree identical to that of the whole genome with any chosen level of probability. Simultaneously, by examining the two different sampling schemes, we can determine whether contiguous sites are independently and identically distributed (i.i.d.). Knowing whether contiguous sites are i.i.d. is important, because i.i.d. is a basic assumption of the bootstrap (6), which is a common means of evaluating confidence limits of inferred phylogenetic relationships (7). The reference point in the experiments with these sampling schemes was again the whole-genome tree, but this time each set of samples was evaluated with regard to the proportion of the sample that produced a tree identical to the whole genome tree.

The exact results of these experiments were dependent on the method of tree construction, but several general patterns were evident. The two most fundamental were that many sites are required to have a high probability of producing a tree identical to the whole genome tree, and that samples of contiguous sites do not perform as well as samples of sites

Table I

Results of gene-based sampling experiments

		Phylogenetic Inference Method*		
Gene	Length (bp)	Likelihood	Parsimony	Neighbor-Joining
ATPase8	207			
NADH4L	297			
NADH3	350			
NADH6	561			
ATPase6	687			
COII	705			
COIII	785	×	×	
NADH1	981			
NADH2	1047			
12S rRNA	1111	×	×	
CYTB	1149	×		
NADH4	1387		×	×
COI	1560	×		
16S rRNA	1786	×		×
NADH5	1860			×
Number of distinct topologies		9	12	9

* The symbol × denotes that the topology of the gene tree was identical to that of the genome tree; absence of a symbol means that some other topology was inferred for that gene-method combination (see reference 4 for the alternative gene trees).

that are individually and independently chosen. The observation that the two sampling schemes produce different results is evidence that contiguous sequence data do not meet the i.i.d. assumption.

Taken over the entire study, the principal conclusions are that individual gene sequences are not sufficient samples from which to infer the phylogeny of these taxa; and that contiguous DNA sequence data are not i.i.d. and hence do not meet the basic assumption of the bootstrap. More detail and elaboration of these and other points can be found in references 4 and 5.

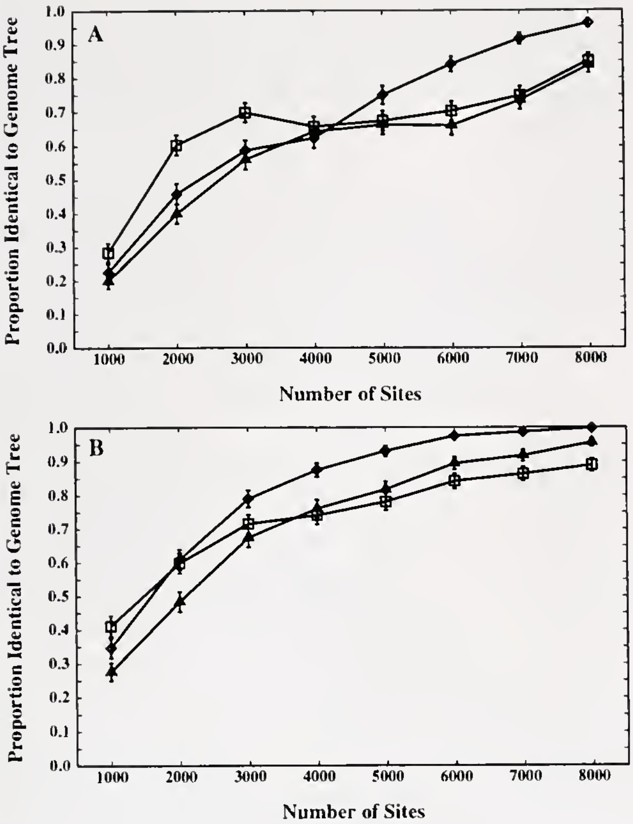

Figure 2. Proportion of trees identical to the whole-genome tree inferred from different sampling schemes. Data points represent mean of 1024 samples of the indicated size, error bars denote 95% confidence intervals for the mean, diamonds represent maximum likelihood, triangles represent parsimony, and squares represent neighbor-joining. (A) Samples of contiguous sites beginning at random locations. (B) Samples of sites individually and independently chosen without replacement from random locations throughout the genome.

Literature Cited

1. **Felsenstein, J. 1981.** Evolutionary trees from DNA sequences: a maximum likelihood approach. *J. Mol. Evol.* **17:** 368–376.
2. **Fitch, W. M. 1971.** Toward defining the course of evolution: minimal change for a specific tree topology. *Syst. Biol.* **20:** 406–416.
3. **Saitou, N., and M. Nei. 1987.** The neighbor-joining method: a new method for reconstructing phylogenetic trees. *Mol. Biol. Evol.* **4:** 406–425.
4. **Cummings, M. P., S. P. Otto, and J. Wakeley. 1995.** Sampling properties of DNA sequence data in phylogenetic analysis. *Mol. Biol. Evol.* **12:** 814–822.
5. **Otto, S. P., M. P. Cummings, and J. Wakeley. 1996.** Inferring phylogenies from DNA sequence data: the effects of sampling. Pp. 103–115 in *New Uses for New Phylogenies*, P. H. Harvey, A. J. Leigh Brown, J. Maynard Smith, and S. Nee, eds. Oxford University Press.
6. **Efron, B. 1979.** Bootstrap methods: another look at the jacknife. *Ann. Statist.* **7:** 1–26.
7. **Felsenstein, J. 1985.** Confidence limits on phylogenies: an approach using the bootstrap. *Evolution* **39:** 783–791.

Discussion

LANDWEBER: Marty Kreitman developed a sequencing method (1) that used a battery of four-cutter restriction enzymes to recognize, on average, 20% of the genome, at best. Your work suggests that method could be resurrected. If one surveyed a 5 kb region with a battery of four-cutter restriction enzymes, that might be better than sequencing 1000 bases of DNA.

CUMMINGS: Kreitman's method of four-cutter analysis ended up being an expensive, laborious method of approximating sequencing. You could only look at a small region at a time using the four-cutter restriction enzymes. When you have to look at a larger region, it does not work out very well. To get at the issue you raise, we considered doing simulated restriction analyses of this whole genome data set. Assuming that there is no problem in establishing homology between fragments, the answer is already in the results presented. The results of a four-cutter approach will, at best, fall between the curve of sequencing everything completely randomly (see Fig. 2B) and the curve for sequencing contiguously (see Fig. 2A). You are not going to do any better than sequencing random sites throughout the whole genome. Any design that is chosen will, at best, simply place the results between those two curves. For example, you want to know the best design and are only going to sequence 1 kb and have to decide between sequencing a single 1 kb region; 2 × 500 bp regions; or 10 × 100 bp regions. On average, you are better off with 10 × 100 bp regions than with a single contiguous stretch of sequence. I think this gets at the issue.

KATZ: You showed a discouraging table from the individual genes and how they were wrong so often. Did you do any calculation of the branch collapsing? How many steps away is this? We would be a lot more upset if you had fish and humans coming out as sister taxa than if you had changes within mammals.

CUMMINGS: The topological differences covered a pretty broad range, but the implications depend on the metric used. One characteristic of the metric of Robinson and Foulds (2) is that when one taxon is placed on the other end of the tree, relative to the reference tree, the whole tree must be collapsed. Among the notable consistent features in the 20 trees of this study were that the two fish always occurred together as sister taxa, and the two rodents were always together. The relationships among the amniotes and the basic relationships within the mammals showed differences.

SHARP: Do you ever use codons to make these trees?

CUMMINGS: Yes. We split the 11 kb of protein coding sequence from these mitochondrial genomes into first positions, second positions, and third positions of codons. We then analyzed random samples within those three groups separately. It is known, *a priori*, that the second codon position is by far the most conserved position, followed by the first position; and the third position is the most variable (3). One can generate very good trees from just third positions alone, if one uses maximum likelihood. In fact, if you take second positions using parsimony (which are the best for parsimony, because they are the most conserved, having evolved at the slowest rate) and plot the rate of convergence in terms of the portion of trees that are identical to the whole-genome tree based on increasing sample size, and then repeat this with third positions using maximum likelihood, the two curves are quite similar (Fig. 3). The whole notion that third positions are random noise is fallacious. Substitutions proceed in such a way that there is appreciable phylogenetic signal just in third positions alone.

SHARP: That cannot be true.

CUMMINGS: It is true; we have done the experiments (4, 5). Third positions are saturated, in that on average each has undergone one or more substitution events. However, these changes are not random in any true sense. Third positions are only noise, from a practical standpoint, for some methods of phylogenetic analysis. For other methods, such as maximum likelihood, third positions contain a significant amount of information.

KATZ: What is the effect of linkage in broadening your conclusions? Would your expectations change if we were looking at nuclear genes, where there are genes that are not physically linked to one another?

CUMMINGS: Then you get into what Joe (Felsenstein) presented at this meeting (Felsenstein, these proceedings, pp. 343–344)—that different genes can have different histories—and that is why

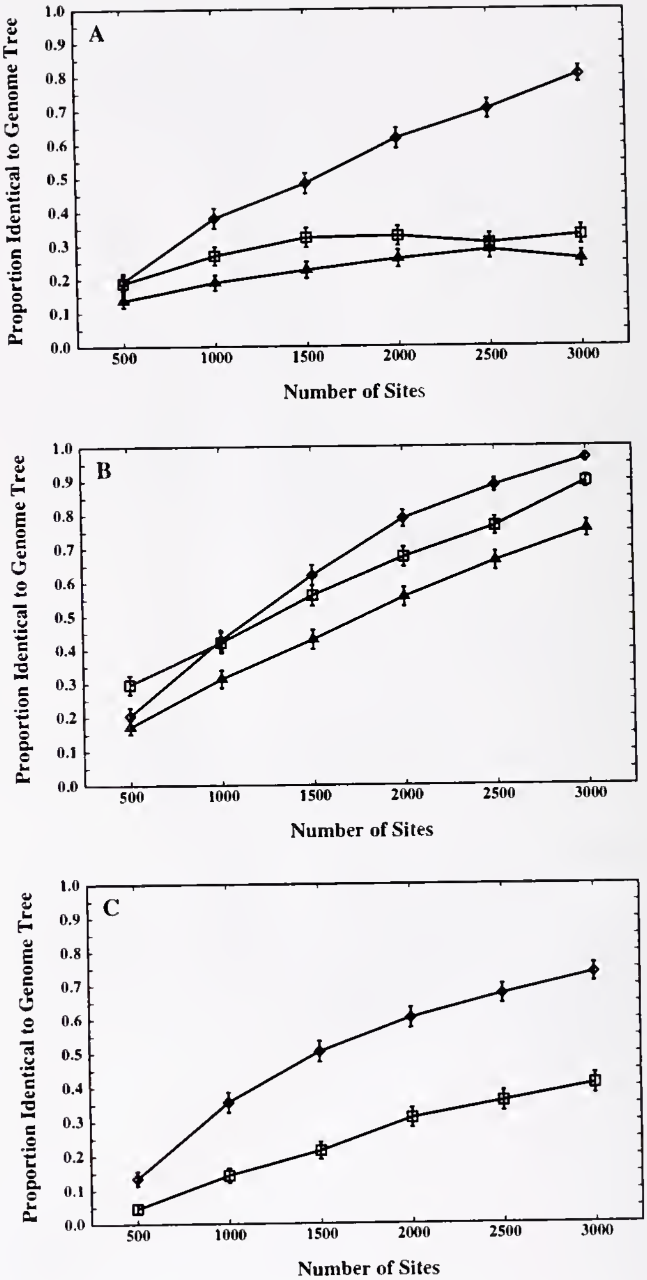

Figure 3. Proportion of trees identical to the whole-genome tree inferred from samples of sites from each codon position class. Data points represent means of 1024 samples of the indicated size, error bars denote 95% confidence intervals for the mean, diamonds represent maximum likelihood, triangles represent parsimony, and squares represent neighbor-joining. (A) First position of codons. (B) Second position of codons. (C) Third position of codons. For third positions analyzed by parsimony, the performance of the branch and bound search approximates an exhaustive search due to the high level of homoplasy in the third position data; consequently this method required an unacceptable length of time to find the shortest tree. Preliminary analyses indicated that for all sample sizes, the number of equally parsimonious trees is generally quite large ($>10^5$), and the resulting proportion of trees identical to the genome tree was very small ($<10^{-5}$).

we wanted to use mitochondrial genomes. An advantage of the mitochondrial genome is that every gene within it has the same history. In this work we are looking at differences in history as inferred from a collection of sites and not at true differences in history. Every site has the same history for the mitochondrial genome.

Forterre: Do you assume that the complete tree, which mixes all these wrong trees, can become a good tree?

Cummings: Yes, but there are two ways to look at that. First of all, this is the largest data set ever used in an analysis of these taxa, and it is the best estimate that we have. Secondly, this is the mitochondrial tree, and we are not going to get any more mitochondrial data than the complete genome. One could also say that whether the whole mitochondrial genome tree is really the right tree or not is unimportant. If we do not believe that the whole-genome tree is correct, but we really do think that, for example, the one from cytochrome oxidase subunit two (COII) inferred from neighbor-joining is really the correct tree, what do we do? We disagree with the largest sample that we have available to address the question. If we cast the whole-genome result aside and say that a smaller, seemingly arbitrarily chosen sample is better than the whole genome, I think we are in trouble.

Felsenstein: There is a method that allows the bootstrap to cope with samples that have certain kinds of departure from independent and identically distributed assumption. That is the block bootstrap of Hans Künsch (6). What it does is to say, "Suppose the problem is that neighboring sites (sites within a certain distance of each other) are correlated either in rate or in the particular process." We will then sample a random place and take a block of ten sites starting there, and take a number of samples which is one-tenth as great. Instead of sampling a thousand sites out of a thousand, we will sample a hundred blocks of ten. Have you tried that method, and would it help the bootstrap be a more accurate indication of the variation?

Cummings: No, we have not done experiments along the lines you suggest. This does point out something that is not so dramatic here in the maximum likelihood curves, but can be seen to a greater extent in the neighbor-joining curves. In the curves presented for all analytical methods there is a phenomenon happening at a large scale in these genomes that happened repeatedly in a very consistent manner. In neighbor-joining, for example, at about 3000 sites, it reaches a little peak and then dips. This means that a worse estimate of relationships is obtained on average using 4000 or 5000 sites than with 3000 sites (see Fig. 2A). One must increase the sample of sites to 6000 sites before one gets as good an estimate as with 3000. There is a large-scale phenomenon happening when we take contiguous blocks of 3000, 4000, 5000, 6000 sites. It is unclear, even if a program for your (Felsenstein) suggested method were available, what the appropriate block-size values should be. One might use such a program to explore a range of values to see at what scale variability happens in a particular genome. Based on work of many people (7), all sorts of patterns will occur within codons, for example. There will also be all sorts of interactions on many different levels (8). The scale at which one has to sample sequences to meet the assumptions of the bootstrap is not clear. Furthermore, it is unclear how much the assumption is violated, and whether it makes much difference in terms of bootstrap values and interpretation.

Olsen: You have asserted that it would be better to take 10 blocks of 100 nucleotides. Did you actually attempt that in simulation?

Cummings: No, but you know that, on average, it is going to be approximately between the results from sampling contiguous sites (Fig. 2A) and from sampling sites individually and independently (Fig. 2B).

Olsen: I understand that it has to fall between them. The question is, is it a significant step toward independence or is it false security?

Cummings: It depends on how secure you want to be. The only way you can sequence is by taking contiguous blocks. Again, on average you will get better estimates of phylogenetic relationships if you are able to collect samples from different regions of the genome. Although we have not done the experiment you suggest, again, the results will fall between the two curves (Fig. 2).

Olsen: As a comment, or a reaction, you certainly chose to put a negative spin on your presentation. You tried to recap at the end, but saying that you got twenty different trees out of two million possible is still certainly a small subset. It is particularly depressing in terms of not telling us how far those departures were in terms of either your measure, or symmetric difference, or any of the tree metrics available.

Cummings: All those twenty trees are published (4). One has to choose which particular differences are important, and which are not. Whether the results of a phylogenetic analysis are important depends on your question. I cannot say whether it is a big difference or not; I am not going to make a decision arbitrarily about whether something is important for a particular question. As an aside, I would like to acknowledge that part of the computer code that we used for this work was based, in part, upon code written by Gary (Olsen), Joe (Felsenstein), and their collaborators. My coauthors and I highly modified the code for our purposes. We certainly benefited greatly from their programs.

Sharp: If you had taken the human sequence out of your tree, the rest of it would be unambiguous. We think we are absolutely certain what the relationships between those species would have been if the human were out.

Cummings: That is not true.

Sharp: What would be in question?

Cummings: The relationships that are labile were not restricted to any one part of the tree.

Sharp: That is not my point; I am referring to morphology and everything else. We know the two fish are closer to one another than they are to us. I do not think you are ever going to overturn that. We know that the same is true for the two rodents. You said that you do not care if you get the right tree or not. I am just saying that if you remove the human sequence, we would know what the right tree was that you were aiming towards.

CUMMINGS: Are you saying that primates were the only disputed group in that tree?

SHARP: The relationship of primates, artiodactyls plus cetaceans and rodents, that would be the only unambiguous one. My question concerns a very similar piece of work by Nei and coworkers who looked at complete mitochondrial sequences and compared their results with an examination of individual genes. I am not sure how your work differs from theirs. I remember that they were far more optimistic in their conclusions and seemed to get the right answer far more often.

CUMMINGS: The paper from Masatoshi Nei's group was an extension of our study in some respects and different in others. Among the differences are restricting examination to protein coding genes; including additional mitochondrial genomes available at the time; and using more tree-reconstruction methods. You can read both papers and interpret them. It depends on what is important to you, whether you think the results are really negative, or if I have put a negative spin on it.

SHARP: My question concerns results, not viewpoints. At least in their paper, they reported what was honestly found. They got the right answer for the majority of genes, and did not just use the three methods that you used.

CUMMINGS: No, their results were not that appreciably different from ours. Are you referring to the paper by Russo *et al.* (9)? Where the two studies were similar in design, they came out with largely the same results.

KUNKEL: Do you have a better model with nuclear genes, or do your results (where you have these twenty different trees) suggest that you need to modify the model?

CUMMINGS: I assume that you are referring to the use of mitochondrial genomes as a model system to address the questions in our study. Would one get a different answer if one were to use complete bacterial genomes, or data with more genes to choose from? If we made experimental design choices, now that there are more vertebrate mitochondrial genome sequences, we would probably get a slightly different answer, although the same general trends would hold. The taxa in this study were convenient; they were the first ten mitochondrial genomes, the only ones available at the time, the only complete non-recombining genomes, and ten was a convenient number to deal with because it provided a lot of variation. A lot of possibilities.

We are all interested in evolutionary history, and do the best we can. The study just shows that how badly one does, or how well one does, depends on how you look at it. For most trees, it does not take very much data to get very close to getting most relationships right. However, it takes a lot of sequence to get it all perfect. Whether that is horrible or great depends on your perspective.

FELSENSTEIN: The alternatives that you gave, of taking a thousand bases or ten chunks of one hundred, aren't very economically realistic. People who sequence (and I've never sequenced anything, I hasten to add; nor will I) tell me that to get four hundred in a chunk instead of one hundred is not much more effort. Can you give us an idea of what the real tradeoff might be? It looks to me, at any rate, that simply counting bases is not going to give you the real choices that you are faced with.

CUMMINGS: I think the overriding concerns, as someone who has sequenced quite a lot, are experimental considerations and convenience. If I were doing the sequencing, I would sequence contiguous chunks. In many cases you are faced with what you are given. I do not think there is a general answer to your question. One cannot say that one is best off sequencing a particular number of blocks each of a particular number of sites. Each situation is going to be different and the experimental design is going to be dictated by practical concerns.

Literature Cited

1. **Kreitman, M., and M. Aguade. 1986.** Genetic uniformity in two populations of *Drosophila melanogaster* as revealed by filter hybridization of four-nucleotide-recognizing restriction enzyme digests. *Proc. Natl. Acad. Sci. USA* **83:** 3562–3566.
2. **Robinson, D. F., and L. R. Foulds. 1981.** Comparison of phylogenetic trees. *Math. Biosci.* **53:** 131–147.
3. **Nei, M. 1987.** *Molecular Evolutionary Genetics.* Columbia University Press, New York.
4. **Cummings, M. P., S. P. Otto, and J. Wakeley. 1995.** Sampling properties of DNA sequence data in phylogenetic analysis. *Mol. Biol. Evol.* **12:** 814–822.
5. **Otto, S. P., M. P. Cummings, and J. Wakeley. 1996.** Inferring phylogenies from DNA sequence data: the effects of sampling. Pp. 103–115 in *New Uses for New Phylogenies.* P. H. Harvey, A. J. Leigh Brown, J. Maynard Smith, and S. Nee, eds. Oxford University Press.
6. **Künsch, H. R. 1989.** The jackknife and the bootstrap for general stationary observations. *Ann. Stat.* **17:** 1217–1241.
7. **Grantham, R., C. Gautier, M. Gouy, R. Mercier, and A. Pave. 1980.** Codon catalog usage and the genome hypothesis. *Nucleic Acids Res.* **8:** r49–r62.
8. **Peng, C.-K., S. V. Buldyrev, A. L. Goldberger, S. Havlin, F. Sciortino, M. Simons, and H. E. Stanley. 1992.** Long-range correlations in nucleotide sequences. *Nature* **356:** 168–170.
9. **Russo, C. A. M., N. Takezaki, and M. Nei. 1996.** Efficiencies of different genes and different tree-building methods in recovering a known vertebrate phylogeny. *Mol. Biol. Evol.* **13:** 525–536.

Reference: *Biol. Bull.* **196:** 351–355. (June 1999)

Deep Divisions in the Tree of Life—What Does the Fossil Record Reveal?

J. WILLIAM SCHOPF

IGPP Center for the Study of Evolution and the Origin of Life, Department of Earth and Space Sciences, and Molecular Biology Institute, University of California, Los Angeles, California 90095-1567

Dating early evolution by the fossil record

Accurate dating of the antiquity of the major biologic lineages has been a long-standing goal in Precambrian paleobiology (1, 2, 3). This is a young field, however, and the early fossil record is too incompletely known to provide precise answers. Moreover, even in the best circumstances, fossils and associated geological and geochemical indicators of biologic activity (that is, "paleobiologic" evidence) can establish only a minimum age for a lineage, not how much earlier the lineage actually existed. Bearing these caveats in mind, data currently available indicate that stromatolitic microbial ecosystems, evidently including cyanobacteria and other members of the bacterial domain, were extant ~3500 Ma ago (4, 5); methanogenic archaeans by ~2800 Ma ago (6, 7); and gram-negative sulfate-reducing bacteria as early as ~2700 Ma ago (8) and possibly earlier (9).

Timing early evolution by the amino acid "clock"

Another way to address this problem has been proposed by Doolittle *et al.* (10). They reasoned that a molecular "clock" that would date the times of lineage emergence might be established by comparing the sequences of amino acids in proteins of the same families in diverse groups of organisms. Their study was thorough: It took into account fast and slowly evolving lineages and compared 531 amino acid sequences in 57 families in enzymatic proteins from 15 major groups of organisms. Their analysis yielded an internally consistent, amino acid-based tree in which the branches are all more or less the same length and have a branching order in good agreement with the 16S rRNA Tree of Life.

The discrepancy and the challenge

Strangely, however, the Doolittle *et al.* (10) clock meshes not at all well with the known Precambrian fossil record. Because paleobiologic evidence can yield only a minimum date for the emergence of a biologic lineage, the molecular clock would be expected to have yielded ages that are older than those documented by fossils. Yet the Doolittle *et al.* study concluded that all early evolving lineages originated at younger, not older, ages than those indicated by paleobiology, and the differences are substantial. For example, the amino acid data suggest that cyanobacteria originated about 1500 Ma ago, two billion years later than the time inferred from fossil evidence. The origins of gram-negative bacteria and methane-producing archaeans are placed a billion or more years later than indicated by paleobiology. And the "last common ancestor" is dated at only ~2000 Ma ago, whereas cellular fossils having morphologies indistinguishable from modern microbes are present in rocks nearly 3500 Ma old (4, 5).

Something is amiss. Perhaps the ancient fossils have been misinterpreted and are actually unrelated to present-day lineages. Or perhaps, like rRNA tress, the amino acid data yield reliable evidence only of the order of branching of evolution, not the timing of that branching. Whatever the answer, the discrepancies between the molecular clock and evidence from the rock record are too great and too consistent to be ignored. The challenge at hand is to unify these competing lines of evidence. Toward that end, assessment is made here of what now seems known, and what is not, from the available fossil data.

How can the challenge be met?

As Darwin pointed out in *On The Origin of Species*, there is only one court of last resort by which to decipher the timing

---

This paper was originally presented at a workshop titled *Evolution: A Molecular Point of View*. The workshop, which was held at the Marine Biological Laboratory, Woods Hole, Massachusetts, from 24–26 October 1997, was sponsored by the Center for Advanced Studies in the Space Life Sciences at MBL and funded by the National Aeronautics and Space Administration under Cooperative Agreement NCC 2-896.

and course of the evolutionary progression—the fossil record. Much progress has been made toward uncovering the early record, but much more remains to be accomplished.

How common the fossils of any biologic group are can be measured by what are called taxonomic occurrences—the number of species belonging to a given group that are known to be present in formally recognized geologic units. For example, 10 species of fossil cyanobacteria in each of three named geologic formations adds up to 30 taxonomic occurrences. More than 4000 such occurrences of fossil microbes are known from Precambrian rocks (11, 12, 13), but the Precambrian encompasses such an enormous span of Earth history that the known fossil record nevertheless remains meager. Even Precambrian cyanobacteria, the best documented branch of early life, have a scanty fossil record: For chroococcacean (spheroidal) species, the record amounts to fewer than 50 taxonomic occurrences per 50-Ma-long interval; and for filament-forming oscillatoriaceans, fewer than two dozen (11). Moreover, the record is uneven. As shown in Figure 1, it extends to nearly 3500 Ma ago but is woefully inadequate in rock units older than about 2200 Ma—mainly because rather few rocks from this time have survived to the present, and most of these have experienced the fossil-destroying heat and pressure of metamorphism (but also because most workers have chosen to

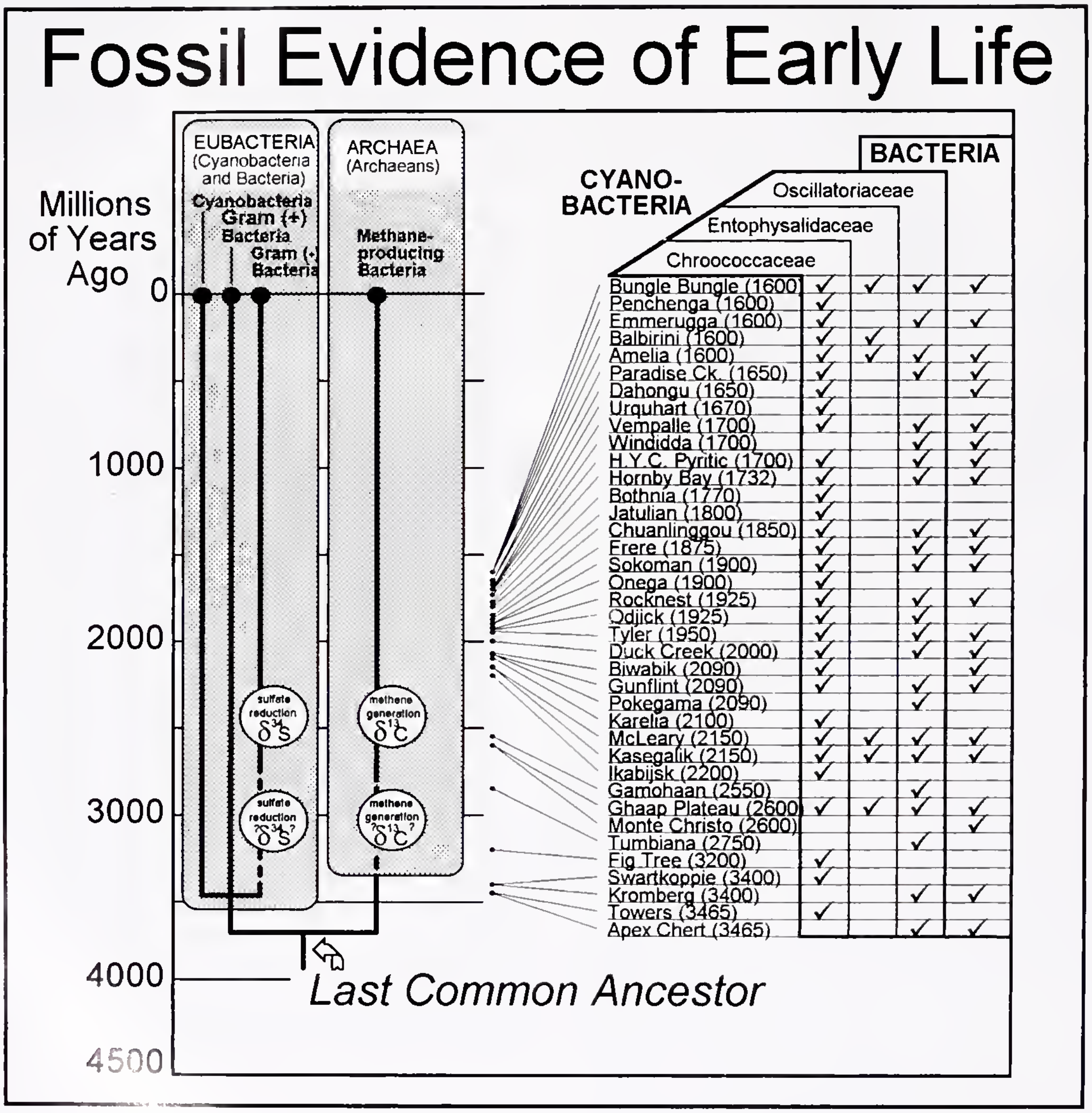
Fossil Evidence of Early Life
Millions of Years Ago
0
1000
2000
3000
4000
4500
EUBACTERIA (Cyanobacteria and Bacteria)
Cyanobacteria
Gram (+) Bacteria
Gram (+ Bacteria
ARCHAEA (Archaeans)
Methane-producing Bacteria
sulfate reduction $\delta^{34}S$
sulfate reduction $?\delta^{34}S?$
methane generation $\delta^{13}C$
methane generation $?\delta^{13}C?$
Last Common Ancestor
CYANO-BACTERIA
BACTERIA

	Chroococcaceae	Entophysalidaceae	Oscillatoriaceae	BACTERIA
Bungle Bungle (1600)	✓	✓	✓	✓
Penchenga (1600)	✓			
Emmerugga (1600)	✓		✓	✓
Balbirini (1600)	✓	✓		
Amelia (1600)	✓	✓	✓	✓
Paradise Ck. (1650)	✓		✓	✓
Dahongu (1650)	✓			✓
Urquhart (1670)	✓			
Vempalle (1700)	✓		✓	✓
Windidda (1700)			✓	✓
H.Y.C. Pyritic (1700)	✓		✓	✓
Hornby Bay (1732)	✓		✓	✓
Bothnia (1770)	✓			
Jatulian (1800)	✓			
Chuanlinggou (1850)	✓		✓	✓
Frere (1875)	✓		✓	✓
Sokoman (1900)	✓		✓	✓
Onega (1900)	✓			
Rocknest (1925)	✓		✓	✓
Odjick (1925)	✓		✓	
Tyler (1950)	✓		✓	✓
Duck Creek (2000)	✓		✓	✓
Biwabik (2090)	✓			✓
Gunflint (2090)	✓		✓	✓
Pokegama (2090)			✓	
Karelia (2100)	✓			
McLeary (2150)	✓	✓	✓	✓
Kasegalik (2150)	✓	✓	✓	✓
Ikabijsk (2200)	✓			
Gamohaan (2550)			✓	
Ghaap Plateau (2600)	✓	✓	✓	✓
Monte Christo (2600)				✓
Tumbiana (2750)			✓	
Fig Tree (3200)	✓			
Swartkoppie (3400)	✓			
Kromberg (3400)			✓	✓
Towers (3465)	✓			
Apex Chert (3465)			✓	✓

Figure 1. Timeline of prokaryotic history inferred from the known Precambrian paleobiologic record. Fossil representatives of three families of cyanobacteria (Chroococcaceae, Entophysalidaceae, and Oscillatoriaceae) and diverse noncyanobacterial prokaryotes ("bacteria") have been identified in the listed 38 geologic units older than 1600 Ma (13, 14, 21).

hunt the younger terrains, where well-preserved fossils are plentiful and it is easier to make good finds).

To be accepted as *bona fide*, ancient microfossils must be structurally preserved biogenic remnants that are indigenous to and syngenetic with the primary deposition of sedimentary rocks of known stratigraphic and geographic source and established age (5, 14). At present, only 26 taxonomic occurrences of microfossils older than ~2200 Ma meet these criteria: eight from the ~2550-Ma-old Transvaal Supergroup of South Africa (15, 16, 17); two from the ~2750-Ma-old Fortescuse Group of Western Australia (14); three from the ~3400-Ma-old Onverwacht Group of the eastern Transvaal, South Africa (18, 19); and 13 from ~3465-Ma-old units of the Warrawoona Group of Western Australia—two from the Towers Formation (20) and 11 from bedded cherts of the Apex Basalt (4, 5).

So, there is an obvious immediate need for careful paleobiologic studies of additional rock units older than about 2200 Ma. Fossils of this age are almost all charred and deformed, often nearly beyond recognition, so the work is not easy—and to be of value, studies must be done with care. But the potential rewards are great, and without more fossils to fill the gap between the Apex assemblage and those at the beginning of the more or less continuous fossil record 2200 Ma ago, sorting out the pathway of life's earliest development will remain difficult.

The molecular biology of living organisms can also be expected to hold key evidence. All organisms alive today are a product of the past, and it must be true that their genetic and biochemical makeups hold clues to their evolutionary history—not only of evolutionary relations, but of the timing of divergences as well. Doolittle *et al.* (10) cannot have been mistaken in searching proteins for those relations and that timing. And rRNA trees also should, eventually, prove useful for determining the times of lineage divergences. The problem today is to solve the riddle of reading the molecular evolutionary clock. Ultimately, this problem will be solved, and when it is, the molecular evidence will be shown to mesh with the fossil record—both, after all, deal with the same evolutionary progression, the same history of life!

Literature Cited

1. **Schopf, J. W. 1970.** Precambrian micro-organisms and evolutionary events prior to the origin of vascular plants. *Biol. Rev. Camb. Philos. Soc.* **45:** 651–688.
2. **Schopf, J. W., J. M. Hayes, and M. R. Walter. 1983.** Evolution of Earth's earliest ecosystems: recent progress and unsolved problems. Pp. 361–384 in *Earth's Earliest Biosphere, Its Origin and Evolution*, J. W. Schopf, ed. Princeton University Press, Princeton, NJ.
3. **Schopf, J. W. 1992.** Times of origin and earliest evidence of major biologic groups. Pp. 587–593 in *The Proterozoic Biosphere, a Multidisciplinary Study*, J. W. Schopf and C. Klein, eds. Cambridge University Press, New York.
4. **Schopf, J. W. 1992.** Paleobiology of the Archean. Pp. 25–39 in *The Proterozoic Biosphere, a Multidisciplinary Study*, J. W. Schopf and C. Klein, eds. Cambridge University Press, New York.
5. **Schopf, J. W. 1993.** Microfossils of the Early Archean Apex chert: new evidence of the antiquity of life. *Science* **260:** 640–646.
6. **Hayes, J. M. 1983.** Geochemical evidence bearing on the origin of aerobiosis, a speculative hypothesis. Pp. 291–301 in *Earth's Earliest Biosphere, Its Origin and Evolution*, J. W. Schopf, ed. Princeton University Press, Princeton, NJ.
7. **Hayes, J. M. 1994.** Global methanotrophy at the Archean-Proterozoic transition. Pp. 220–236 in *Early Life on Earth*, S. Bengtson, ed. Columbia University Press, New York.
8. **Schidlowski, M., J. M. Hayes, and I. R. Kaplan. 1983.** Isotopic inferences of ancient biochemistries: carbon, sulfur, hydrogen, and nitrogen. Pp. 149–186 in *Earth's Earliest Biosphere, Its Origin and Evolution*, J. W. Schopf, ed. Princeton University Press, Princeton, NJ.
9. **Ohmoto, H., T. Kakegawa, and D. R. Lowe. 1993.** 3.4-billion-year-old biogenic pyrites from Barberton, South Africa: sulfur isotope evidence. *Nature* **262:** 555–557.
10. **Doolittle, R. F., D.-F. Feng, S. Tsang, G. Cho, and E. Little. 1996.** Determining divergence times of the major kingdoms of living organisms with a protein clock. *Science* **271:** 470–477.
11. **Schopf, J. W. 1992.** Proterozoic prokaryotes: affinities, geologic distribution, and evolutionary trends. Pp. 195–218 in *The Proterozoic Biosphere, a Multidisciplinary Study*, J. W. Schopf and C. Klein, eds. Cambridge University Press, New York.
12. **Schopf, J. W. 1992.** Informal revised classification of Proterozoic microfossils. Pp. 1119–1168 in *The Proterozoic Biosphere, a Multidisciplinary Study*, J. W. Schopf and C. Klein, eds. Cambridge University Press, New York.
13. **Mendelson, C. V., and J. W. Schopf. 1992.** Proterozoic and selected Early Cambrian microfossils and microfossil-like objects. Pp. 865–951 in *The Proterozoic Biosphere, a Multidisciplinary Study*, J. W. Schopf and C. Klein, eds. Cambridge University Press, New York.
14. **Schopf, J. W., and M. R. Walter. 1983.** Archean microfossils: new evidence of ancient microbes. Pp. 214–239 in *Earth's Earliest Biosphere, Its Origin and Evolution*, J. W. Schopf, ed. Princeton University Press, Princeton NJ.
15. **Klein, C., J. N. Beukes, and J. W. Schopf. 1987.** Filamentous microfossils in the Early Proterozoic Transvaal Supergroup: their morphology, significance, and paleoenvironmental setting. *Precambrian Res.* **36:** 81–94.
16. **Altermann, W., and J. W. Schopf. 1995.** Microfossils from the Neoarchean Campbell Group, Griqualand West Sequence of the Transvaal Supergroup, and their paleoenvironmental and evolutionary implications. *Precambrian Res.* **75:** 65–90.
17. **Lanier, W. P. 1986.** Approximate growth rates of Early Proterozoic microstromatolites as deduced by biomass productivity. *Palaios* **1:** 525–542.
18. **Walsh, M. M., and D. R. Lowe. 1985.** Filamentous microfossils from the 3,500-Myr-old Onverwacht Group, Barberton Mountain Land, South Africa. *Nature* **314:** 530–532.
19. **Walsh, M. M. 1992.** Microfossils and probable microfossils from the early Archean Onverwacht Group, Barberton Mountain Land, South Africa. *Precambrian Res.* **54:** 271–293.
20. **Schopf, J. W., and B. M. Packer. 1987.** Early Archean (3.3-billion to 3.5-billion-year-old) microfossils from the Warrawoona Group, Australia. *Science* **237:** 70–73.
21. **Hofmann, H. J., and J. W. Schopf. 1983.** Early Proterozoic microfossils. Pp. 321–360 in *Earth's Earliest Biosphere, Its Origin and Evolution*, J. W. Schopf, ed. Princeton University Press, Princeton, NJ.

Discussion

ELLINGTON: Do you ever find fossils that you can't identify?

SCHOPF: Absolutely. Recall, for a moment, the recent claims for ancient life on Mars (1), the finding of objects that some call fossils—are they truly fossils; are they remnants of Martian life? If one doesn't find them wholly convincing, then the question is, What if Martian life really was bizarre, was substantially different from that on Earth; could its fossil remains be identified as being an organism? The answer is, Yes! The experiment has already been done, because it turns out that in Earth rocks at 1.8 billion years, even 2.2, 2.3, 2.4 billion years, there are indeed "bizarre" taxa. One example is the genus *Eosphaera*. *Eosphaera* is about 20 micrometers in diameter and it was clearly a planktonic organism. But its morphology is unlike anything living today. Another example is a fossil called *Kakabekia umbellata*. There hasn't been a good study done on it, but the specimens look really strange—something like chocolate-covered peanuts, each with a Japanese umbrella coming out of the top. They're plenty bizarre, yet they certainly are remnants of organisms.

ELLINGTON: Do all of these fossils that are born and then die have lineages? They are not just isolated incidents; they are lineages?

SCHOPF: Yes, in the case I just mentioned, *Kakabekia* spans about 600 million years. *Eosphaera* spans at least 300 million years. Those are two examples, and there are others.

GUERRERO: You mentioned that metamorphic rocks can yield carbon isotope fractionations typical of photosynthesis. Such results are not valid to prove evidence of life.

SCHOPF: Under conditions of severe metamorphic alteration, ^{12}C to ^{13}C bonds can break and the isotopic signal can be reset. In carbonates, the carbonate carbon gets lighter, due to exchange reactions, and the organic matter gets heavier. Manfred Schidlowski (2) studied the organic matter and carbonates in a set of rocks that are around 3.8 billion years in age. Because he noticed that they showed less fractionation than that in younger geologic materials, he tried to extrapolate back to their original compositions, arguing that the extrapolation provided evidence of photosynthesis because the isotopic signature had been reset by metamorphism. Both that work and more recent work by Steven Mojzsis (3) and others have the same sort of problem: namely, the isotopic signals in these rocks have probably been reset. That there was photosynthesis going on as early as 3.8 billion years ago is a plausible supposition, but one doesn't know for sure what the original isotopic composition was. It can only be guessed.

GUERRERO: Based on isotope fractionation values, overlap exists where oxygenic and anoxygenic photosynthesizers cannot be discriminated; and at the same time, overlap occurs between photosynthesizers and methanogenetic bacteria. The highest values of methanogens are in the same ranges as the lowest values of anoxygenic photosynthesis. In any given sample, therefore, one cannot preclude the possible presence of methanogenic bacteria.

SCHOPF: I think you are entirely correct. If I understood you, the carbon isotopic data seem to be suggesting that archaeans, photosynthetic bacteria, and I think probably cyanobacteria, were present all the way back to 3.5 billion years ago. Based on the data available, the various relative proportions and contributions to the carbon cycle are very difficult to sort out. But that's what the signals look like; and it's even more complicated than that, because isotopic fractionation in photosynthesis is sensitive to the head pressure of CO_2. If there was a lot more CO_2 in the early atmosphere, as David DesMarais and lots of other folks think is likely, then fractionation would be higher, up to as much as, say, 35, 36 parts per thousand through photosynthesis.

DESMARAIS: We've done a recent study (4) and found that this metamorphic isotope shift is a lot less than we had previously thought. Also, Naraoka *et al.* (5) have calculated that a considerable amount of abiotic graphite could have been formed. Therefore, we might be observing a dual origin of reduced carbon (abiotic and biotic) in some of these highly metamorphosed rocks. Thus, future efforts to explore further inside the highly resistant apatite grains for chemical and isotopic remnants of an early biosphere will be a very important venture.

MARGULIS: Did you make a comment implying that you have direct evidence that sulfate reduction had already evolved more than 3 billion years ago? Might you please tell use about those data?

SCHOPF: According to those who have interpreted and studied the isotopic record in detail, there is consensus that sulfate reduction extends back to 2.7 or 2.8 billion years ago. In addition, there is a paper (6) that reported sulfate to sulfide, ^{32}S to ^{34}S ratios from the Barberton Mountainland, near the kingdom of Swaziland in South Africa, in rocks going back to 3.4 billion years. The authors claim that those data indicate the presence of sulfate reducers that early.

REDFIELD: You've shown pictures of something old, and something modern, and how they look the same. It arouses the same skepticism that I have toward electron micrographs. We are really good at pattern matching. I'd like a quick example of something that gets discarded; where you say, No.

SCHOPF: Something that is discarded because it is not a fossil, or something that is discarded because it's not a cyanobacterium?

REDFIELD: The latter.

SCHOPF: There are many examples; for instance, one from the 3.5-billion-year-old Apex Chert—cellular filaments that are only half a micrometer in diameter. I think those are probably noncyanobacterial microbes, not cyanobacteria; and I think that because I've done morphometric analyses of a large number of taxa, both modern and fossil. I've looked at literally hundreds of varieties and species reported in the literature (as referenced in this paper), and plotted them in many ways. There are ten different morphometric characters that I can get out of the fossils, and those are the same characteristic features on which cyanobacteria and most other prokaryotes have traditionally been identified. What I am really saying is that, if a particular fossil microbe were alive today, it would have features like 90% or more of one group, and unlike the great majority of another group. There is always a little overlap. I've done the morphometric analyses both of the fossils and of the modern groups; and those analyses, plus the isotopes, are virtually the only data available. So that's the way that I have to approach the problem. The strategy has been to use modern biology as the basis by which to trace fossil lineages back through time.

Literature Cited

1. **McKay, D. S., E. K. Gibson, Jr., K. L. Thomas-Keprta, H. Vali, C. S. Romanek, S. J. Clemett, X. D. F. Chiller, C. R. Maechling, and R. N. Zare. 1996.** Search for past life on Mars: possible relic biogenic activity in Martian meteorite ALH84001. *Science* **273:** 924–930.
2. **Schidlowski, M. 1988.** A 3,800-million-year isotopic record of life from carbon in sedimentary rocks. *Nature* **333:** 313–318.
3. **Mojzsis, S. J., G. Arrhenius, K. D. McKeegan, T. M. Harrison, A. P. Nutman, and C. R. Friend. 1996.** Evidence for life on Earth before 3,800 million years ago. *Nature* **384:** 55–59.
4. **DesMarais, D. J. 1997.** Isotopic evolution of the biogeochemical carbon cycle during the Proterozoic Eon. *Org. Geochem.* **27:** 185–193.
5. **Naraoka, H., M. Ohtake, S. Maruyama, and H. Ohmoto.** Nonbiogenic graphite in 3.8 Ga metamorphic rocks from the Isua district, Greenland. *Chem. Geol.* (in press).
6. **Ohmoto, H., T. Kakegawa, and D. R. Lowe. 1993.** 3.4-billion-year-old biogenic pyrites from Barberton, South Africa: Sulfur isotope evidence. *Science* **262:** 555–557.

Reference: *Biol. Bull.* **196:** 356–358. (June 1999)

Determining Divergence Times With Protein Clocks

RUSSELL F. DOOLITTLE, DA-FEI FENG, AND GLEN CHO

Center for Molecular Genetics, University of California, San Diego, La Jolla, California 92093-0634

Recently, we conducted a study of divergence times of the major groups of organisms as gauged by amino acid sequence comparison of 57 sets of enzymes encompassing 531 sequences (1). Among the main results we reported was a divergence time for prokaryotes and eukaryotes of only slightly more than two billion years ago. In line with this result, the average resemblance of these enzymes between Bacteria (a.k.a. eubacteria) and Eukarya (a.k.a. eukaryotes) was 37% identity. The recency of this divergence time was criticized by others on several grounds, particularly with regard to the way we converted sequence-based distances into evolutionary time. We had used a modified Poisson relationship and applied a *post-hoc* correction factor. The distance data were themselves calibrated on the basis of divergence times drawn from the fossil record and mostly involved sequences from vertebrate animals.

The study has now been expanded and the data reanalyzed with a distance measure that corrects for both constraints on amino acid interchange and variation in substitution rate at different sites (2). The validity of the method was checked by an in-depth simulation study (3). Beyond that, the number of enzyme sets compared was increased to 64 and the total number of sequences used was 823 (4). Interestingly, the average sequence resemblance between Bacteria and Eukarya held steady at 37% identity.

The study was greatly enriched by the availability of complete genome sequences for several eubacteria and an archaebacterium. The latter not only expanded the data set but also had a great impact on the interpretation of certain aspects of the data. As it happens, the majority of the archaebacterial sequences are not consistent with currently accepted views of the Tree of Life which cluster the archaebacteria (Archaea) with eukaryotes (Eukarya). Instead, Archaea are either outliers or mixed in with eubacterial orthologs.

In our first study (1) we had simply used the bulk data in our comparison of Archaea, Bacteria, and Eukarya. In the light of the new data, it is now clear that this was overly simplistic. Accordingly, we divided those enzyme sets for which representation was available for all three major groups of life into three classes, dependent on the best phylogeny obtained with each set of sequences. Group A (n = 8) consisted of those enzymes in which Archaea and Eukarya were nearest neighbors; group B (n = 17) was composed of those enzymes in which Bacteria and Eukarya were clustered; and group C (n = 13) had Archaea and Bacteria clustered. The most relevant of these groups for determining divergence times involving Eukarya are groups A and B. The resemblances of sequences from these two groups are shown in Table I.

Group A sequences of Archaea and Eukarya average 41% identity, but group B sequences are only 31% identical

Table I

Resemblances of different sets of enzymes sequences between various groups of organism

	Enzyme Group A (n = 8)	Enzyme Group B (n = 17)
Main Tree of Life		
Archaea *vs.* Bacteria	36	32
Bacteria *vs.* Eukarya	32	42
Archaea *vs.* Eukarya	41	31
Within Bacteria		
Gram-positive *vs.* gram-negative	46	42
Gram-positive *vs.* cyanobacteria	42	46
Gram-negative *vs.* cyanobacteria	41	41

This paper was originally presented at a workshop titled *Evolution: A Molecular Point of View.* The workshop, which was held at the Marine Biological Laboratory, Woods Hole, Massachusetts, from 24–26 October 1997, was sponsored by the Center for Advanced Studies in the Space Life Sciences at MBL and funded by the National Aeronautics and Space Administration under Cooperative Agreement NCC 2-896.

(Table 1). The inverse holds true for comparisons of Bacteria and Eukarya. The resemblance data also make it very clear that three major groups of Bacteria—the cyanobacteria, the gram-positives, and the gram-negatives—are much more similar to each other than any of them is to either Archaea or Eukarya.

The simplest explanation for these degrees of similarity is to postulate that many of these enzyme sequences were carried into eukaryotes by early eubacterial endosymbionts about two billion years ago, only very shortly after or even coincident with the divergence of Eukarya and Archaea. The strong resemblances of these same enzymes among the major eubacterial groups suggest that the cyanobacteria, gram-positive and gram-negative eubacteria also diverged at about the same time, whereas the much greater differences between archaebacterial and eubacterial sequences indicate these two groups may have diverged between three and four billion years ago.

Literature Cited

1. **Doolittle, R. F., D.-F. Feng, S. Tsang, G. Cho, and E. Little. 1996.** Determining divergence times of the major kingdoms of living organisms with a protein clock. *Science* **271**:470–476.
2. **Grishin, N. V. 1995.** Estimation of the number of amino acid substitutions per site when the substitution rate varies among sites. *J. Mol. Evol.* **41**:675–679.
3. **Feng, D.-F., and R. F. Doolittle. 1997.** Converting amino acid alignment scores into measures of evolutionary time: a simulation study of various relationships. *J. Mol. Evol.* **44**:361–370.
4. **Feng, D.-F., G. Cho, and R. F. Doolittle. 1997.** Determining divergence times with a protein clock: update and reevaluation. *Proc. Natl. Acad. Sci. USA* **94**:13028–13033.

Discussion

GOGARTEN: Could you comment on the finding that some heterocyst-forming cyanobacteria date back to about 2 billion years? When I looked at the phylogeny of the cyanobacteria, it appeared that this branch emerges about halfway through cyanobacterial evolution. If one agrees with Andy Knoll's (1) finding that microfossils from between 1.5 to 2 billion years are indeed heterocyst-forming cyanobacteria, this would directly contradict your finding that cyanobacteria originate at 2 billion years.

R. DOOLITTLE: Knoll's finding would also have to explain how a large set of orthologous enzymes from Archaea could differ in time by almost twice as much as the cyanobacteria. If you take all of the cyanobacteria compared with other bacteria, they average about 42% identity. Compare those same enzymes with archaebacteria and it drops to 31 or 32 or 33, way back further in time. Anyone who wants to push all of the cyanobacteria back in time has to proportionally push the archaebacteria back to the same degree.

GOGARTEN: That is exactly what you find when you assume a more extreme among-site rate variation than reflected in Grishin's formula (2). When one uses a gamma distribution with an alpha smaller than one, (which corresponds to the alpha that we estimated for many protein families (3)), all the data move back much further in time. This suggests either that substitution rates were not constant throughout early evolution, or that life evolved somewhere else before it arrived on this planet (4).

R. DOOLITTLE: I would like to talk about the Grishin formula. At this meeting you have heard a lot about alpha distributions and alpha factors and gamma distributions. Grishin has a formula by which you can actually look at a set of sequences and see what the phyletic range is—you build the tree and then count the number of different substitutions along the tree. Of course, the more taxa you have represented the better, and you can actually see what the distribution is among the sites. Take an enzyme, triophosphate isomerase, for just a small distribution of 21 taxa. Some fraction of the sites didn't change at all, and some other fraction of the sites had 16 different substitutions along the way. One can test the Grishin formula in a simulation, which we did and have published (5). One can impose the actual distributions without guessing. You can take your model and for each enzyme put the particular distribution that you see when you make a large-scale phylogeny. When you do that, you find that the Grishin formula is linear with time. You keep track of time in a simulation by the number of mutational events; there are some instances where it tends to *overcorrect*. I don't think that pushing this argument about making some more extreme distribution in the Grishin is valid.

This work is in print (5), and we are ready to defend it. I think the Grishin formula is a good clocking mechanism to use if you have lots of sequences. Clearly you don't want to look at single trees; you want to look at them when you put a lot of them together.

DESMARAIS: I didn't get a clear sense as to where the actual connection to absolute time is made. How does that calibration work?

R. DOOLITTLE: The extrapolation is based on the vertebrate fossil record. The calibration was based on the rates of change for the same enzymes, calculated the same way, based on the vertebrate fossil record. We performed numerous checks on the slopes, doing omit tests, for example, in which we leave out any given timepoint to see if it changes the slope; or weighting it depending on the number of contributants and so forth. The slope is certainly very good over the vertebrate time course, and a large part of our study was devoted to the major groups of eukaryotes. Certainly that should be without challenge; at any rate, that's where the time came from.

YARUS: When there is a collision between methods previously thought to give reliable information, maybe we ought to take it as an opportunity to believe both.

R. DOOLITTLE: In showing his rendering of our trees, Bill (Schopf) should also have pointed out that on that left side, all our divisions for the eukaryotes are much deeper than his divisions based on the fossil record for the eukaryotes. Differences appear only as you go into probing the relationship of the eukaryotes, the archebacteria, and the eubacteria. Our tree is more robust and deeper for those divergences on the eukaryote side. His (Schopf's) are all squeezed up at the top. Ours are all twice as far into the past. I think if you look at that carefully, it's a little bit of a red herring.

Literature Cited

1. **Golubic, S., V. N. Sergeev, and A. H. Knoll. 1995.** Mesoproterozoic Archaeoellipsoides: akinetes of heterocystous cyanobacteria. *Letaia* **28:** 285–298.
2. **Grishin, N. V. 1995.** Estimation of the number of amino acid substitutions per site when the substitution rate varies among sites. *J. Mol. Evol.* **41:**675–679.
3. **Gogarten, J. P., L. Olendzenski, E. Hilario, C. Simon, and K. E. Holzinger. 1996.** Dating the cenancestor of organisms. *Science* **274:** 1750–1751.
4. **Secker, J., P. S. Wesson, and J. R. Lepock. 1996.** Astrophysical and biological constraints on radiopanspermia. *J. R. Astron. Soc. Can.* **90:**184–192.
5. **Feng, D.-F., and R. F. Doolittle. 1997.** Converting amino acid alignment scores into measures of evolutionary time: A simulation study of various relationships. *J. Mol. Evol.* **44:**361–370.

Reference: *Biol. Bull.* **196:** 359–362. (June 1999)

Horizontal Gene Transfer: Pitfalls and Promises

J. PETER GOGARTEN, RYAN D. MURPHEY, AND LORRAINE OLENDZENSKI

Department of Molecular and Cell Biology, University of Connecticut, Storrs, Connecticut 06269-3044

Phylogenetic reconstruction from protein or nucleic acid sequence families provides information on the evolution of individual genes. In contrast to the assumed bifurcating, tree-like evolution of genes, organismal evolution is characterized by the exchange of genetic information between organisms and even by the fusion of formerly independent lines of descent (1). The invocation of horizontal gene transfer events is often regarded as a last-ditch attempt by systematists to reconcile conflicting phylogenies constructed from different markers. In general, however, organismal evolution is clearly visible as the majority consensus of a number of molecular phylogenies, and transfer events can be recognized in phylogenies constructed from one or several markers whose topologies deviate from that of the consensus.

Often it is difficult to decide whether conflicts between molecular phylogenies are due to actual events in evolution (horizontal gene transfer or gene duplications [see 2]), or due to artifacts generated during phylogenetic reconstruction. For example, investigation of the maximum likelihood landscape of 18S rRNA and V-ATPase A-subunit phylogenies suggests that the grouping of microsporidia either with the fungi (3, 4, 5) or close to the root of the archaeal domain (*e.g.*, 6, 7, 8) probably represents an artifact in the 18S rRNA data analyses and not another case of horizontal transfer.

Although the recognition of horizontal transfer as a major factor in prokaryotic evolution (*e.g.*, 9, 10, 11, 12) certainly complicates the interpretation of molecular phylogenies, it also allows synchronization of different parts of the universal tree of life, and thus might provide the key to the detection of periods of rapid substitutions. Two examples will be presented of attempts to extract organismal evolution from conflicting molecular phylogenies. One concerns the finding of archaeal genes in Deinococcaceae, the other the finding of bacterial genes in Archaea.

Thermus and *Deinococcus* both have an archaeal-type coupling factor ATPase (13, 14, 15); in contrast, most of the other molecular markers available clearly indicate that the group comprising *Thermus* and *Deinococcus* species is an early branching lineage within the Bacteria (*e.g.*, 16, 17). Reflecting this majority consensus, *Thermus* and *Deinococcus* can be considered as Bacteria that branch off before the major bacterial lineages evolved in an at present ill-resolved radiation. However, in addition to the archaeal-type coupling factor ATPase, the malic acid dehydrogenases found in Deinococcaceae do not group with the typical bacterial homologs, but closer to the eukaryotes. The interpretation of the malic acid dehydrogenase phylogenies is complicated by potential switches in substrate specificities between lactic and malic acid dehydrogenases. Nevertheless, these results prompted us to look for additional archaeal genes in *Thermus ruber*. A genomic library of *Thermus ruber* was screened with labeled genomic DNA from the archaeon *Thermoplasma acidophilum*. One of the clones that showed stronger cross reactivity to the archaeal probe encodes a prolyl tRNA synthetase. Phylogenetic analysis of this sequence and its homolog from *Deinococcus radiodurans*, obtained through The Institute for Genomic Research at http://www.TIGR.org/, reveals that the prolyl tRNA synthetase from Deinococcaceae groups with the eucaryal and archaeal homologs and not with the typical bacterial prolyl tRNA synthases (Fig. 1). Distance, parsimony, and quartet puzzling analyses show similar tree topologies. These trees suggest two major types of prolyl tRNA synthetases: a bacterial type and a eukaryotic/archaeal type (see ref. 18 for an in-depth comparison of the bacterial and eucaryal types). The majority of bacteria form a group that also includes *Candida* and *Saccharomyces* sequences, which may be of mitochondrial origin. Grouping with the archaeal and eu-

This paper was originally presented at a workshop titled *Evolution: A Molecular Point of View*. The workshop, which was held at the Marine Biological Laboratory, Woods Hole, Massachusetts, from 24–26 October 1997, was sponsored by the Center for Advanced Studies in the Space Life Sciences at MBL and funded by the National Aeronautics and Space Administration under Cooperative Agreement NCC 2-896.

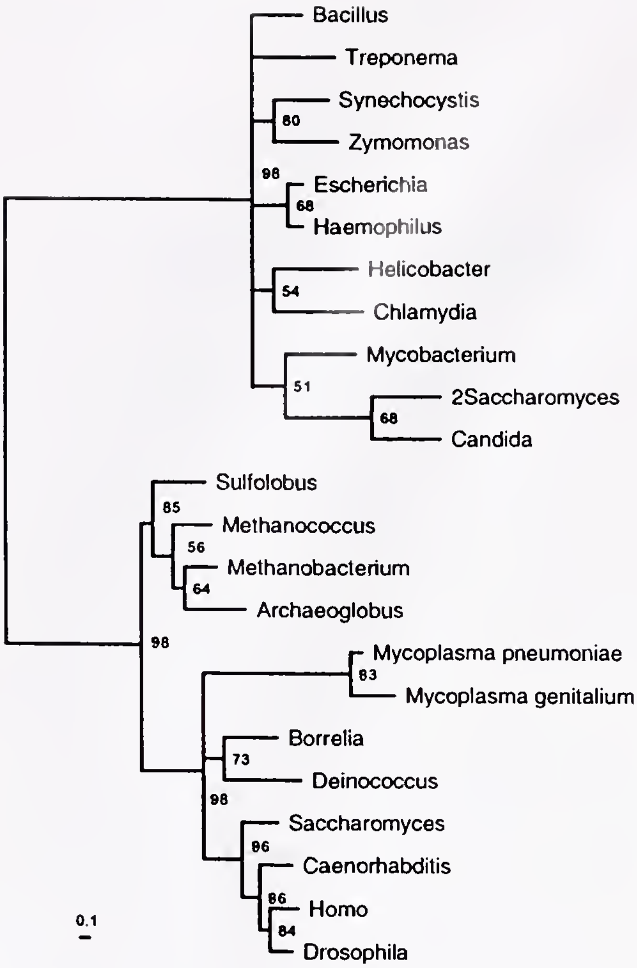

Figure 1. Quartet puzzling analysis (21) of prolyl tRNA synthetase amino acid sequences. Sequences were aligned using the profile alignment option of ClustalX with default parameters (22). Numbers reflect quartet puzzling support values for each node. Nodes with values of less than 50% have been collapsed. Analysis was corrected for among site rate variation using the Gamma distribution (=1.97). All sequences were obtained from GenBank except those of *Deinococcus* and *Treponema*, which were obtained through BLAST search from The Institute for Genomic Research, and *Sulfolobus*, which was kindly provided by Mark Regan and Christoph Sensen, Institute for Marine Biosciences, Dalhousie University, Halifax, Nova Scotia.

karyotic sequences are the bacteria *Deinococcus, Borrelia,* and *Mycoplasma.* All three of these bacteria appear to have acquired a eukaryotic/archaeal-type prolyl tRNA synthetase. The finding that the gene encoding prolyl tRNA synthetase in *Sulfolobus sulfotaricus* is located immediately downstream from the operon encoding the archaeal coupling factor ATPase (Mark Regan and Christoph Sensen, Dalhousie University; pers. comm.) suggests that these genes could have been transferred simultaneously before the evolutionary divergence of *Deinococcus* and *Thermus.* Interestingly, *Borrelia* and *Treponema,* both spirochetes, each have a different prolyl tRNA synthetase type. *Borrelia* possesses a eukaryotic/archaeal type, whereas *Treponema* has the type found more commonly in other bacteria.

One noteworthy exception from using the majority consensus as backbone for the organismal phylogeny are the Archaea. Although many characters clearly characterize the Archaea as a group that is distinct from the Bacteria (2), recent complete genome analyses confirm earlier observations that many (44%) archaeal genes are very similar to their bacterial homologs, whereas only 13% are more similar to their eukaryotic homologs (19). If gene families are analyzed in more detail, the archaeal genes are found to group within the bacterial domain, and the different archaeal genes do not even cluster together (2). Thus the majority consensus does not show Archaea and Bacteria to be sister groups and would dissolve both the Archaea and the Bacteria into paraphyletic groups. In contrast, most genes involved in genome structure, transcription, translation, and chemiosmotic coupling clearly set the Archaea apart from the Bacteria. In this case the backbone of our preliminary organismal phylogeny reflects those markers less prone to horizontal gene transfer, and explains the presence of many genes in the Archaea that are bacterial in character as the result of horizontal gene transfer. The fact that so many genes found in the archaeal genomes appear to be bacterial in character raises the question of how these genes were transferred. Initially, a single horizontal transfer event of a major portion of the genome was considered (1, 19); however, comparison of individual gene families suggests at least several transfer events, each involving a subset of the total complement of genes transferred (20).

Acknowledgments

This work was supported through the NASA-Exobiology program.

Literature Cited

1. **Gogarten, J. P. 1995.** The early evolution of cellular life. *Trends Ecol. Evol.* **10:** 147–151.
2. **Gogarten, J. P., E. Hilario, and L. Olendzenski. 1996.** Gene duplications and horizontal gene transfer during early evolution. Pp. 267–292 in *Evolution of Microbial Life, Society for General Microbiology,* D. McL. Roberts, P. Sharp, G. Alderson, and M. Collins, eds., University Press, Cambridge, UK.
3. **Edlind, T. D., J. Li, G. S. Visvesvara, M. H. Vodkin, G. L. McLaughlin, and S. K. Katiyar. 1996.** Phylogenetic analysis of beta-tubulin sequences from amitochondrial protozoa. *Mol. Phylogenet. Evol.* **5:** 359–367.
4. **Keeling, P. J., and W. F. Doolittle. 1996.** Alpha-tubulin from early-diverging eukaryotic lineages and the evolution of the tubulin family. *Mol. Biol. Evol.* **13:** 1297–1305.
5. **Müller, M. 1997.** What are the Microsporidia? *Parasitol. Today* **13:** 455–456.
6. **Sogin, M. L., J. H. Gunderson, H. J. Elwood, R. A. Alonso, and D. A. Peattie. 1989.** Phylogenetic meaning of the kingdom concept: an unusual ribosomal RNA from *Giardia lamblia. Science* **243:** 75–77.

7. **Sogin, M. L. 1991.** Early evolution and the origin of eukaryotes. *Curr. Opin. Genet. Dev.* **1:** 457–463.
8. **Kamaishi, T., T. Hashimoto, Y. Nakamura, F. Nakamura, S. Murata, N. Okada, K. Okamoto, M. Shimizu, and M. Hasegawa. 1996.** Protein phylogeny of translation elongation factor EF-1 alpha suggests microsporidians are extremely ancient eukaryotes. *J. Mol. Evol.* **42:** 257–263.
9. **Lorenz, M. G., and W. Wackernagel. 1994.** Bacterial gene transfer by natural genetic transformation in the environment. *Microbiol. Rev.* **58:** 563–602.
10. **Lawrence, J. G., and H. Ochman. 1997.** Amelioration of bacterial genomes: rates of change and exchange. *J. Mol. Evol.* **44:** 383–397.
11. **Herrick, J. B., K. G. Stuart-Keil, W. C. Ghiorse, and E. L. Madsen. 1997.** Natural horizontal transfer of a naphthalene dioxygenase gene between bacteria native to a coal tar-contaminated field site. *Appl. Environ. Microbiol.* **63:** 2330–2337.
12. **Lawrence, J. G., and J. R. Roth. 1996.** Selfish operons: horizontal transfer may drive the evolution of gene clusters. *Genetics* **143:** 1843–1860.
13. **Yokoyama, K., T. Oshima, and M. Yoshida. 1990.** *Thermus thermophilus* membrane-associated ATPase: indication of a eubacterial V-type ATPase. *J. Biol. Chem.* **265:** 21946–21950.
14. **Tsutsumi, S., K. Denda, K. Yokoyama, T. Oshima, T. Date, and M. Yoshida. 1991.** Molecular cloning of genes encoding major two subunits of a eubacterial V-Type ATPase from *Thermus thermophilus. Biochim. Biophys. Acta* **1098:** 13–20.
15. **Gogarten, J. P., T. Starke, H. Kibak, J. Fichmann, and L. Taiz. 1992.** Evolution and isoforms of V-ATPase subunits. *J. Exp. Biol.* **172:** 137–147.
16. **C. R. Woese. 1987.** Bacterial evolution. *Microbiol. Rev.* **51:** 221–271.
17. **Hensel, R., W. Demharter, O. Kandler, M. Kroppenstedt, and E. Stackebrandt. 1986.** Chemotaxonomic and molecular-genetic studies of the genus *Thermus:* evidence for a phylogenetic relationship of *Thermus aquaticus* and *Thermus ruber* to the genus *Deinococcus. Int. J. Syst Bacteriol.* **36:** 444–453.
18. **Stehlin, C., B. Burke, F. Yang, H. Liu, K. Shiba, and K. Musier-Forsyth. 1998.** Species-specific differences in the operational RNA code for aminoacylation of tRNAPro. *Biochemistry* **9:** 8605–8613.
19. **Koonin, E. V., A. R. Mushegian, M. Y. Galperin, and D. R. Walker. 1997.** Comparison of archaeal and bacterial genomes: computer analysis of protein sequences predicts novel functions and suggests a chimeric origin for the archaea. *Mol. Microbiol.* **25:** 619–637.
20. **Olendzenski L., E. Hilario, and J. P. Gogarten. 1998.** Horizontal gene transfer and fusing lines of descent: the Archaebacteria—a chimera? Pp 349–362 in *Horizontal Gene Transfer,* M. Syvanen and C. Kado, eds., Chapman and Hall, London.
21. **Strimmer, K., and A. von Haeseler. 1996.** Quartet puzzling: a quartet maximum likelihood method for reconstructing tree topologies. *Mol. Biol. Evol.* **13:** 964–969.
22. **Thompson, J. D., T. J. Gibson, F. Plewniak, F. Jeanmougin, and D. G. Higgins. 1997.** The ClustalX windows interface: flexible strategies for multiple sequence alignment aided by quality analysis tools. *Nucleic Acids Res.* **24:** 4876–4882.

Discussion

ELLINGTON: It seems that phylogeneticists assume that all genes work the same way in all organisms. Is there a possibility that different biochemical usages, even of something as common as malate dehydrogenase, could lead to convergent evolution, and that convergence would appear as if it were horizontal transfer?

GOGARTEN: At least in theory this seems a viable alternative. However, if one examines actual data, one rarely finds instances of convergent evolution. There are instances of convergent substitutions in lineages that independently evolved in extreme environments, for example, high-salt environments (1). A more serious problem for phylogeneticists is that if an enzyme evolves to perform a different function, one often observes faster substitution rates. That does not constitute convergent evolution in itself, but the accelerated rates of evolution can lead to long-branch attraction artifacts (2), which might look very much like convergent evolution. An example might be the ATPase catalytic subunit in *Borrelia.* When this enzyme was transferred from one domain to another, it had to adjust to the different cellular environment and therefore might have had much higher substitution rates.

MARGULIS: When you moved microsporidians like *Nosema* and others in with the fungi and showed maximum likelihood data, you said that *Giardia* is then no longer the deepest branch (oldest ancestor). What is the deepest branching eukaryotic lineage?

GOGARTEN: The tree that according to a distance matrix analysis best described the V-ATPase catalytic subunit evolution had *Giardia* as the deepest and the microsporidia as the second deepest branch within the protists. When we moved the microsporidia into the fungi, we found that the resulting tree actually had a higher likelihood than the starting tree. However, when we moved *Giardia* away from the bottom of the tree, the likelihood dropped significantly. Thus, based on the V-ATPase sequences, *Giardia* still appears to be the deepest branch (3). We also looked at the 18S rRNA tree, and found that both the microsporidia and *Giardia* are highly supported as deep branches within the eukaryotic domain. However, when we moved the branch leading to the microsporidia throughout the eukaryotic domain, we found a second relative likelihood maximum when the microsporidia are part of the eukaryotic crown group. Thus, although the absolute maxima in the likelihood landscape are found with very different tree topologies, we found a dual affinity for the microsporidia for both the ATPase catalytic subunits and the 18S rRNAs. This suggests that ribosomal rRNAs and proteins had the same phylogenetic history. The reason that we find two very different tree topologies is probably due to problems associated with phylogenetic reconstruction.

KUHLMAN: You said that spirochetes have an archaeal-type ATPase. It was reported earlier in this meeting that they also have this archael-type lysyl tRNA synthetase. Is there any evidence from other genes that the spirochetes and the *Deinococcaceae* are really a natural group? Am I correct that this suggests there is one transfer?

GOGARTEN: I agree with you that one possible solution is to group the *Deinococcaceae* and the spirochaetes together. One then needs to postulate only a single horizontal transfer event. However, if one takes a closer look at the different gene trees, things are not so straightforward. Spirochaetes and *Deinococcaceae* both have the archaeal/vacuolar-type ATPase; in the case of the prolyl tRNA synthetase, the Deinococcaceae and *Borellia* have the archaeal/eucaryal-type enzyme, but *Treponema* has the bacterial type. In the case of the lysyl tRNA synthetase (4) the spirochaetes have the archaeal type of enzyme, but *Deinococcus* does not. One possible explanation for these observations is that a single interdomain transfer took place just before the split between spirochaetes and Deinococcaceae, and that different subsets of genes were completely integrated into the genomes of the different lines of descent. The radiation that gave rise to the different bacterial kingdoms appears as a very rapid event. I think we are fooling ourselves if we believe that 16S rRNA or ATPases would reliably resolve this radiation. If you construct a tree, some groups are slightly closer together for one marker and further apart for another. I wouldn't be surprised if spirochaetes and *Deinococcaceae* actually turn out to group together.

CAVALIER-SMITH: I agree with your final comment. On the other hand, I think it is even worse than you have implied. The logic of rooting the tree by reciprocal rooting of duplicate proteins is good, but in practice, it's probably a lot more difficult than is often thought. In general, the outgroup is a very long branch that is likely to introduce systematic bias into the rooting. Therefore I am more skeptical than most that we really can root the tree of life from the molecular trees.

GOGARTEN: We only have data which suggest that the root is placed between all of the eubacteria on one side and the archaea and eukaryotes on the other. The branches are long, and it could be that there are some problems with long branches. Based on our simulations, I don't have the impression that artifacts due to long branches would be so big as to pull out the root from inside the bacterial domain. However, this is clearly an important question that warrants further careful analysis. The reason I placed the root between the eubacteria and the archaea/eukaryotes is that this is the place suggested by the currently available data.

Literature Cited

1. **Gandbhir, M., I. Rasched, P. Marliere, and R. Mutzel. 1995.** Convergent evolution of amino acid usage in archaebacterial and eubacterial lineages adapted to high salt. *Res. Microbiol.* **146:** 113–120.
2. **Felsenstein, J. 1978.** Cases in which parsimony and compatability methods will be positively misleading. *Syst. Zool.* **27:** 401–410.
3. **Hilario, E., and J. P. Gogarten. 1998.** The prokaryote to eukaryote transition reflected in the evolution of the V/F/A-ATPase catalytic and proteolipid subunits. *J. Mol. Evol.* **46:** 703–715.
4. **Ibba, M., J. L. Bono, P. A. Rosa, and D. Söll. 1997.** Archaeal-type lysyl-tRNA synthetase in the Lyme disease spirochete *Borrelia burgdorferi. Proc. Natl. Acad. Sci. USA* **94:** 14383–14388.

Reference: *Biol. Bull.* **196:** 363–366. (June 1999)

Application of Genomics for Understanding the Evolution of Hyperthermophilic and Nonthermophilic Crenarchaeota

EDWARD F. DELONG[1], CHRISTA SCHLEPER[2], ROBERT FELDMAN[3], AND RONALD V. SWANSON[3]

[1] *Monterey Bay Aquarium Research Institute, Moss Landing, California 95039;*
[2] *Marine Science Institute, University of California Santa Barbara, Santa Barbara, California 93106;*
and [3] *Diversa Corporation, San Diego, California 92121*

Analysis of small subunit rRNAs retrieved from mixed microbial populations has provided a framework for understanding global microbial diversity (1). These molecular phylogenetic analyses have revealed the presence of previously undetected species and lineages in a wide variety of microbial habitats, and placed newly discovered microbial groups on a universal phylogenetic map. These studies also show that some microbial groups, undetected by traditional cultivation approaches, are major components of natural microbial communities.

Whole genome sequencing, developed over the past several years, has been so successful that more than 40 prokaryotic genome projects have either been completed or are under way. New genome technologies also offer novel avenues for characterization of uncultivated prokaryotes. Since the main requirement for such an approach is the availability of high-quality genomic DNA (readily isolated from environmental samples), large genomic fragments of uncultivated organisms from mixed populations can, in theory, be isolated and characterized using developing genomic techniques. Application of "environmental genomics" could provide access to gene organization, evolution, and physiological potential of novel uncultivated microorganisms. The archived genomes of uncultivated microbial types also become reagents, which could be used for expressing proteins, determining protein structure and function, isolating enzymes, and dissecting metabolic pathways relevant to energy, bioremediation, and biotechnological applications. For the first time, microbial groups previously defined solely by rRNA gene phylogenies can in theory be characterized by their genomic and functional potential.

As part of a collaborative effort, our laboratory is using genomic technologies to investigate the evolution of an as-yet uncultivated archaeal group, the nonthermophilic crenarchaeotes. The domain *Archaea* comprises two kingdoms, the *Euryarchaeota* and *Crenarchaeota* (2). Cultured crenarchaeotes currently hold the record for growth at high temperature. Previously, crenarchaeotes were thought to live mainly at temperatures above about 70°C. Recent molecular phylogenetic surveys show, however, that crenarchaeotes are diverse, abundant, and ubiquitous in a variety of low-temperature habitats (Fig. 1). For instance, in temperate subsurface coastal marine waters and polar seas, planktonic Crenarchaeota make up an estimated 10% to 30% of the prokaryotic biomass contained in these vast habitats (3). Nonthermophilic crenarchaeotes also occur in the guts of deep-sea invertebrates recovered from abyssal depths in the Atlantic Ocean. Furthermore, the uncultivated psychrophilic or mesophilic Crenarchaeota are not restricted to marine habitats. Crenarchaeotes thrive in a wide array of freshwater and terrestrial habitats, including rice paddies, forest soils, agricultural soil, and a variety of freshwater lake sediments (see ref. 1 for a review).

In less than five years, the concept of Crenarchaeota has expanded from an ecologically restricted, obligately thermophilic group, to a kingdom that is cosmopolitan, abundant, and spans the temperature limits of life (Fig. 1).

This paper was originally presented at a workshop titled *Evolution: A Molecular Point of View*. The workshop, which was held at the Marine Biological Laboratory, Woods Hole, Massachusetts, from 24–26 October 1997, was sponsored by the Center for Advanced Studies in the Space Life Sciences at MBL and funded by the National Aeronautics and Space Administration under Cooperative Agreement NCC 2-896.

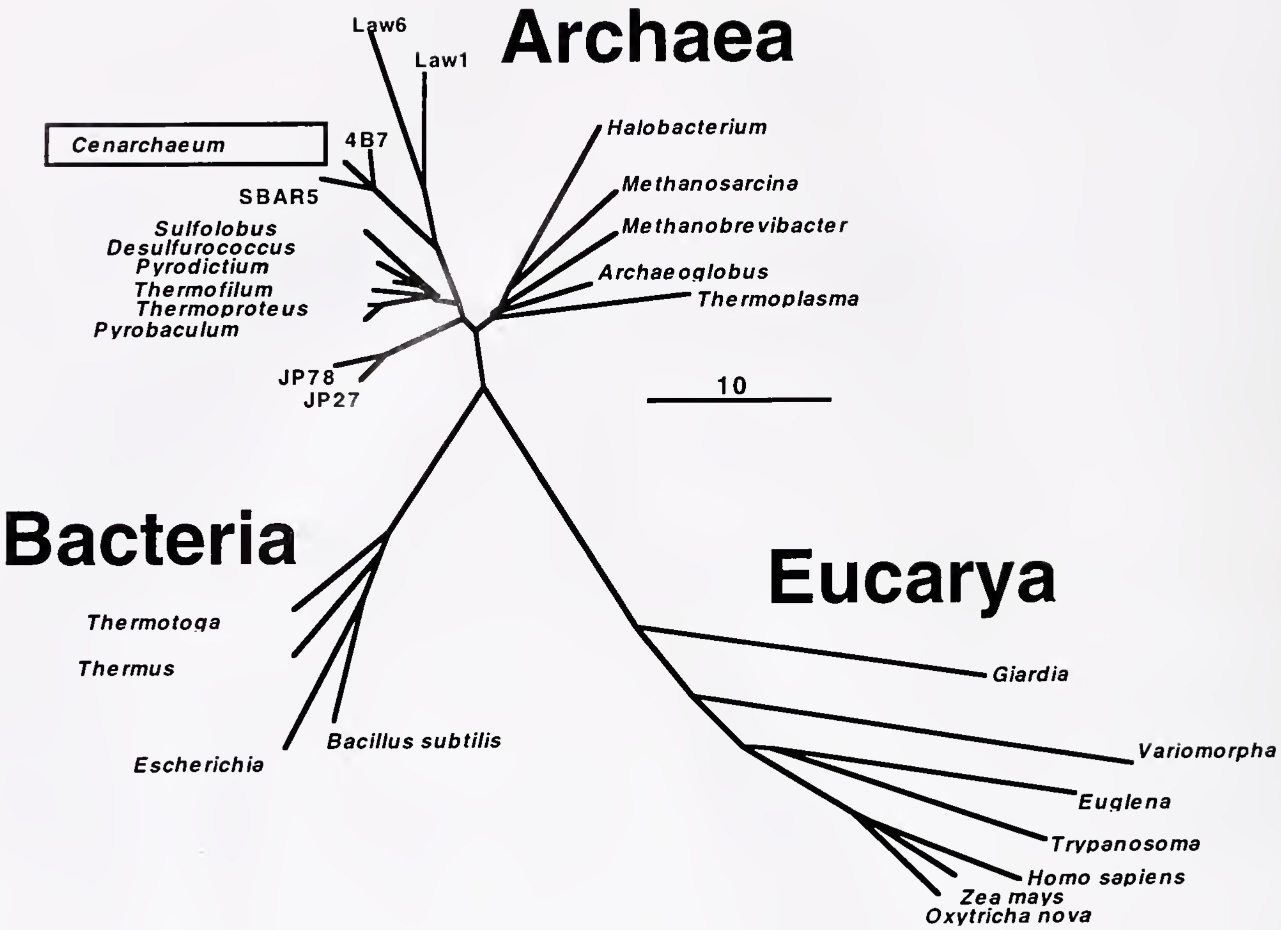
Archaea
Law6
Law1
Cenarchaeum
4B7
SBAR5
Sulfolobus
Desulfurococcus
Pyrodictium
Thermofilum
Thermoproteus
Pyrobaculum
JP78
JP27
Halobacterium
Methanosarcina
Methanobrevibacter
Archaeoglobus
Thermoplasma
10
Bacteria
Thermotoga
Thermus
Escherichia
Bacillus subtilis
Eucarya
Giardia
Variomorpha
Euglena
Trypanosoma
Homo sapiens
Zea mays
Oxytricha nova

Figure 1. Tree of life inferred from 16S rRNA gene sequences showing the phylogenetic position of *Cenarchaeum symbiosum.* In addition to *C. symbiosum,* low-temperature, uncultivated crenarchaeotes are represented by the lineages SBAR5, 4B7, Law6, Law1. pSL12 is a cloned 16S rRNA gene fragment recovered from a Yellowstone hot spring microorganism, and is specifically related to the nonthermophilic Crenarchaeota (4).

Crenarchaeotes apparently originated in hot environments, as suggested by recent molecular ecological surveys of Archaea in hot springs (4). Ribosomal RNA clones obtained from Yellowstone hot springs (*e.g.,* pSL12, Fig. 1; (1, 4)) are specifically affiliated with, but basal in phylogenetic trees to, the nonthermophilic crenarchaeotes (SBAR5, 4B7, Law1, Law6, Fig. 1; (3)). These data suggest that one or more specific lineages of hyperthermophilic crenarchaeotes adaptively radiated into colder habitats, giving rise to contemporary nonthermophilic Crenarchaeota. Despite the intensive efforts of several investigators, nonthermophilic crenarchaeotes have resisted isolation and cultivation.

The physiological, biochemical, and genetic properties of this abundant, ubiquitous, and potentially biogeochemically significant group remain unknown.

We recently discovered and began preliminary work on a tractable system aimed at whole genome sequencing of an uncultivated psychrophilic crenarchaeote. Specifically, high densities of a single species of psychrophilic, symbiotic crenarchaeon, *Cenarchaeum symbiosum,* were discovered within the tissues of its host, the marine sponge *Axinella mexicana* (5). The discovery of this sponge-archaeal association conclusively demonstrated that marine Crenarchaeota thrive at temperatures at least as low as 10°C.

The sponge-crenarchaeal symbiosis provides an excellent, and currently the most tractable, opportunity for genomic analysis of nonthermophilic crenarchaeotes. Initial work has included construction of several "fosmid" libraries prepared from partially purified *C. symbiosum* cell fractions. Briefly, the host cells were mechanically and enzymatically disrupted to release the *C. symbiosum* symbiont cells. The symbionts were then purified by differential centrifugation, followed by cell fractionation and purification on Percoll gradients. High molecular weight chromosomal DNA was prepared from the archaeal-enriched cell fraction. Partial digests of the DNA with Sau3A were ligated into the fosmid vector, using standard methods, to prepare the fosmid library.

Two fosmid libraries were constructed from enriched cell preparations. One yielded, from 10,236 total clones, seven fosmids containing *C. symbiosum* small subunit rRNA genes. The second fosmid library was prepared after improvement of cell fractionation techniques and from 2100 total recombinants yielded eight archaeal ssu rRNA-containing fosmids. The insert sizes ranged from 30 to 40 kbp. Several fosmids have been mapped as overlapping contiguous sequence segments (contigs) by RFLP, Southern analysis, sequence tagged site mapping (STS), and sequencing of the insert termini. Shotgun cloning and sequencing of fosmid inserts have yielded >50 kb of contiguous *C. symbiosum* genomic sequence already completed, and 100 kbp in progress (6). We are continuing to identify contigs in these two libraries using STS mapping of contig termini. Other archaeal "nucleation sites" in the libraries are also being identified by multiplex screening with PCR primers designed from conserved archaeal genes. One example includes the identification of the archaeal recA homolog in fosmids from the *C. symbiosum* libraries (7). In total, our ability to produce high-quality libraries from the *C. symbiosum* genome, and to identify contigs for genomic sequencing efforts, demonstrates the feasibility of the approach.

The guanine-plus-cytosine content of the *C. symbiosum* genome is about 56%, as judged by approximately 100 kbp of sequence data generated so far. Genes appear as densely packed in *C. symbiosum* as they are in other sequenced archaeal genomes. Ribosomal rRNA gene order, spacer regions, and structure are most similar to those of hyperthermophilic Crenarchaeota. Deduced amino acid sequences of proteins of *C. symbiosum*, including the DNA polymerase, TATA-binding protein (TBP), and glutamate semialdehyde aminotransferase, all share highest sequence similarity with archaeal homologs. A number of eukarya-like regulatory, transcriptional, and translational features that generally distinguish Archaea from Bacteria are also present in the *C. symbiosum* genome. Finally, although many of the protein-encoding genes of *C. symbiosum* are most similar to those of cultivated hyperthermophiles, our genomic analyses have led to expression studies which have revealed that *C. symbiosum* proteins are not thermostable (8).

Literature Cited

1. **Pace, N. R. 1997.** A molecular view of microbial diversity and the biosphere. *Science* **276:** 734–740.
2. **Woese, C. R. 1987.** Bacterial evolution. *Microbiol. Rev.* **51:** 221–271.
3. **DeLong, E. F. 1992.** Archaea in coastal marine environments. *Proc. Natl. Acad. Sci. USA* **89:** 5685–5689.
4. **Barns, S. M., C. F. Delwiche, J. D. Palmer, and N. R. Pace. 1996.** Perspectives on archaeal diversity, thermophily, and monophyly from environmental rRNA sequences. *Proc. Natl. Acad. Sci. USA* **93:** 9188–9193.
5. **Preston, C. M., K. Y. Wu, T. F. Molinski, and E. F. DeLong. 1996.** A psychrophilic crenarchaeon inhabits a marine sponge: *Cenarchaeum symbiosum* gen. nov., sp. nov. *Proc. Natl. Acad. Sci. USA* **93:** 6241–6246.
6. **Schleper, C., C. M. Preston, R. A. Feldman, K. Y. Wu, E. F. DeLong, and R. V. Swanson. 1998.** Genomic analysis reveals chromosomal variation in natural populations of the uncultured psychrophilic archaeon *Cenarchaeum symbiosum*. *J. Bacteriol.* **180:** 5003–5009.
7. **Sandler, S. J., P. Hugenholtz, C. Schleper, E. F. DeLong, N. R. Pace, and A. J. Clark. 1999.** Diversity of radA genes from cultured and uncultured Archaea: comparative analysis of their putative RadA proteins and their use as a phylogenetic marker. *J. Bacteriol.* **181:** 907–915.
8. **Schleper, C., R. Swanson, E. Mathur, and E. F. DeLong. 1997.** Characterization of a DNA polymerase from the uncultivated psychrophilic archaeon *Cenarchaeum symbiosum*. *J. Bacteriol.* **179:** 7803–7811.

Discussion

FORTERRE: Since the Crenarchaeota are so widely distributed, not only in water and in soil, etc., presumably they should also be in humans. Do you know if anyone has looked for this organism in the human bowel?

DELONG: Several groups are looking for these organisms. I don't think there is any reason that one can state empirically why they wouldn't be involved in other symbiotic associations.

LEADBETTER: Have you done the electron microscopy on these organisms? I'm impressed by the compactness and conciseness of the DAPI stain and the exclusion of your probe. Might there be a membrane around that nuclear material?

DELONG: The best system that we have had to look at is the sponge, but getting sections on that sponge is difficult. We now know from improved methods for *in situ* hybridization that there is a morphology in the planktonic types. When you use a specific probe, the planktonic types have exactly that same morphology, with a region where the DAPI stains that excludes the oligoprobes; those light up outside. *Planctomyces* is actually a prokaryote (1) that has been shown to have some kind of a membrane associated with it.

MARGULIS: The prokaryote with the nucleoid membrane is *Gemmata obscuriglobus*, studied by Fuerst and his colleagues (1, 2).

DELONG: You are correct. They appear to have membrane associated with the nuclei.

ELLINGTON: As you continue to accumulate data about the cyclophilic and mesophilic Archaebacteria, is it possible that the hyperthermophiles will be the derived group?

DELONG: I don't think that one can exclude that possibility at present.

ELLINGTON: The membrane lipids in the cyclophilic Archaebacteria seem to accumulate ring structures. Could that serve the same purpose as unsaturation in normal fatty acid lipids to increase membrane fluidity?

DELONG: It probably doesn't; it's almost the opposite in *Sulfolobus*. Membrane lipids get more and more rings as growth temperature rises. There are things that we don't understand about archaeal membranes. It turns out that biophysical studies do not reveal nice clean phase transitions within archaeal membranes as is seen with ester-linked fatty acid membranes of eukaryotes and eubacteria. What is going on with temperature and these ether-linked phytanyl lipid structures is not entirely clear.

WEINER: A couple of years ago, there was a report of phage in the ocean (3), also at very high concentrations, making the ocean look like a big petri plate. Have you ever looked for phage in your samples also?

DELONG: This is a big issue in microbial ecology. We haven't looked at it ourselves.

MARGULIS: Have you seen any ester linkages in the lipids of any of your Crenarchaeota?

DELONG: We can't answer that question at this time, because all of the organisms we have looked at so far are in one way, shape or form, mixed populations, that include bacteria with ester-linked fatty acid containing lipids. We have found tetraethers associated with the low temperature crenarchaea, but cannot say for certain what else might be there.

Literature Cited

1. **Fuerst, J. A., and R. I. Webb. 1991.** Membrane-bounded nucleoid in the eubacterium *Gemmata obscuriglobus. Proc. Natl. Acad. Sci. USA* **88:** 8184–8188.
2. **Margulis, L. 1993.** *Symbiosis in Cell Evolution,* 2nd ed. W. H. Freeman, New York.
3. **Proctor, L. M. 1997.** Advances in the study of marine viruses. *Microsc. Res. Tech.* **37:** 136–161.

Reference: *Biol. Bull.* **196:** 367–372. (June 1999)

Molecular Constraints on a High-Temperature Evolution of Early Life

A.-L. REYSENBACH[1,2], S. SEITZINGER[2], J. KIRSHTEIN[1,2], AND E. MCLAUGHLIN[2]

[1]*Department of Biochemistry and Microbiology or* [2]*Institute of Marine and Coastal Sciences,*
Cook College, Rutgers University, New Brunswick, New Jersey 08903

The debate over the early evolution of life remains complex and diverse. Inferences about the early evolution of life can be obtained essentially from the physical (atmospheric, geological) and biological (fossil and molecular) records. Compelling theories toward a high-temperature early evolution of life in environments analogous to present-day geothermal and submarine hydrothermal vents are receiving more attention. If life did originate in such an environment (1, 2, 3), the prevailing niche should be very similar to that of early earth—namely, hot and reducing (4, 2)—and possibly the first metabolic pathways required these conditions. In the reducing atmosphere of geothermal systems, chemolithoautotrophy is a prevalent process among the thermophilic microorganisms, and therefore a chemolithoautotrophic origin for life at elevated temperatures (3, 5) is a tantalizing theory. Furthermore, some "signatures" or biomarkers from this early development in life's origins may still prevail today. Yet whether life on Earth first evolved in hydrothermal environments (6, 7) or merely survived the heat generated by the early meteoritic bombardments remains an open question.

The molecular record. Unlike macroorganisms, the microbial fossil record is sparse, and difficult to interpret. Therefore, many of the microbial evolutionary relationships are left to the molecular record. Phylogenies based on the small subunit rRNAs (and other molecules) have placed all life in three primary lineages, namely, the Archaea, Bacteria, and Eucarya (8). Although the root of this three-domain tree remains debatable (9), compelling evidence based on gene duplication data (10, 7) places thermophilic representatives on all the deeply branching lineages of the prokaryotes. These data suggest thermophily as closest to the ancestral state of extant life. Therefore, it is conceivable that life may have originated under elevated temperatures such as those encountered at hydrothermal vents, with the deepest lineages representing modern-day analogs of early life.

The disconnect between early assembly (for example, the proposed evolution of RNA (see Ellington, pp. 315–319 and Bartel, pp. 322–323, these proceedings)) and extant life is large. If indeed life did originate, develop, and thrive in a high-temperature, reducing environment, then does an analogous environment exist today? If so, what extant organisms inhabit these "ancestral niches"? Do they provide clues for early metabolic pathways? What are the molecular constraints for life in such an environment? We will revisit theories of early evolution of life in the light of recent data on microbial diversity and activity in high-temperature geothermal environments.

Microbial diversity at high temperatures

Although novel thermophilic isolates from hydrothermal vents have increased exponentially in the past decade (11), and the upper temperature limit for life is continually challenged (113°; 12), the ecology and diversity of these high-temperature microbial communities is relatively poorly studied. Recent advances in molecular phylogenetic techniques based on the small subunit rRNA (16S rRNA) have provided an alternative and more comprehensive framework for the study of microbial communities. This approach has been used to study microbial diversity at high-temperature hydrothermal vents, with results that have implications pivotal to our understanding of evolution of all the domains of

---

This paper was originally presented at a workshop titled *Evolution: A Molecular Point of View*. The workshop, which was held at the Marine Biological Laboratory, Woods Hole, Massachusetts, from 24–26 October 1997, was sponsored by the Center for Advanced Studies in the Space Life Sciences at MBL and funded by the National Aeronautics and Space Administration under Cooperative Agreement NCC 2-896.

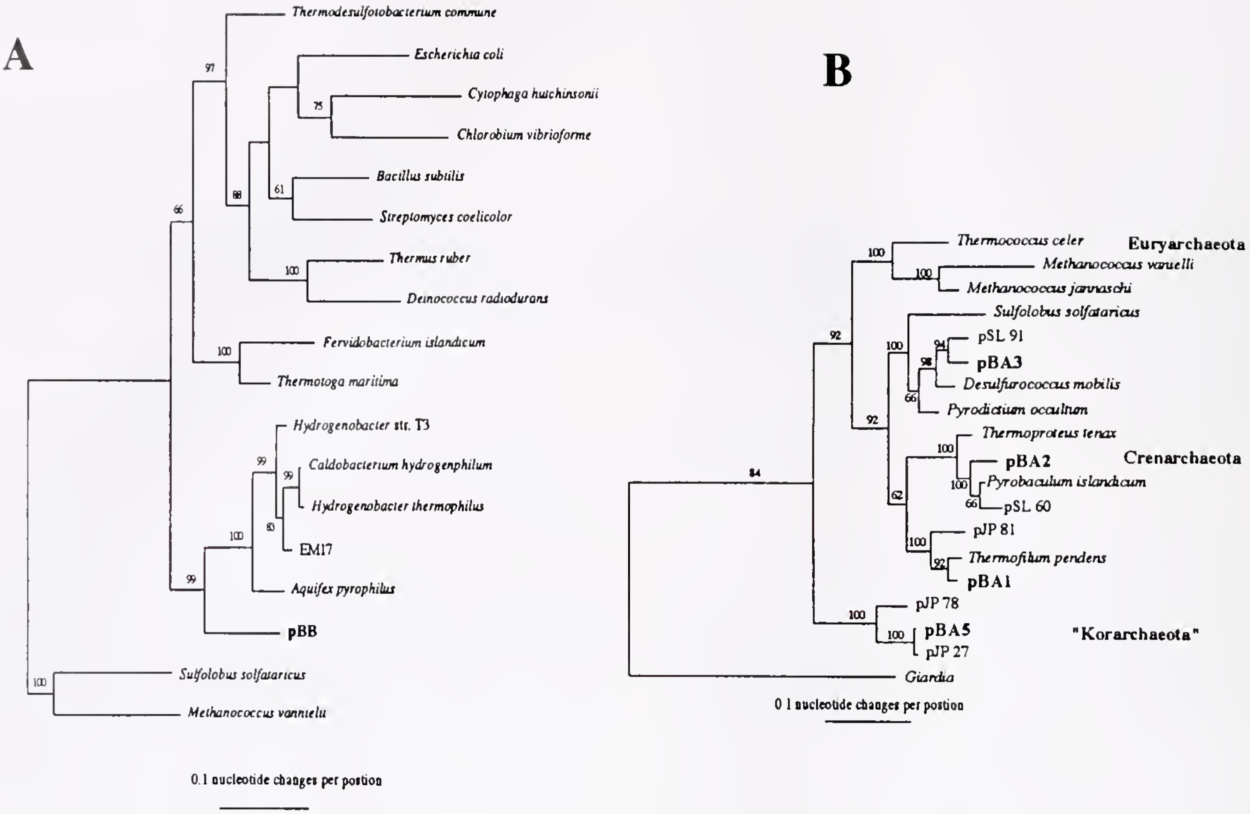
A
Thermodesulfobacterium commune
Escherichia coli
Cytophaga hutchinsonii
Chlorobium vibrioforme
Bacillus subtilis
Streptomyces coelicolor
Thermus ruber
Deinococcus radiodurans
Fervidobacterium islandicum
Thermotoga maritima
Hydrogenobacter str. T3
Caldobacterium hydrogenphilum
Hydrogenobacter thermophilus
EM17
Aquifex pyrophilus
pBB
Sulfolobus solfataricus
Methanococcus vannielii
0.1 nucleotide changes per postion
B
Thermococcus celer
Methanococcus vanuelli
Methanococcus jannaschi
Euryarchaeota
Sulfolobus solfataricus
pSL 91
pBA3
Desulfurococcus mobilis
Pyrodictium occultum
Thermoproteus tenax
pBA2
Pyrobaculum islandicum
pSL 60
Crenarchaeota
pJP 81
Thermofilum pendens
pBA1
pJP 78
pBA5
pJP 27
"Korarchaeota"
Giardia
0.1 nucleotide changes per postion

Figure 1. Maximum likelihood phylogenetic trees of (**A**) bacterial rDNA gene clone (pBB) and (**B**) archaeal rDNA gene clones (pBA1, 2, 3, 5) obtained from an 83°C sample at Calcite Springs, Yellowstone National Park. The trees were generated using fastDNAml, using the generalized two-parameter model of evolution. The scale bar represents the number of fixed mutations per nucleotide position. The numbers at the branch nodes are bootstrap values based on 100 bootstrap resampling.

life (Archaea, Bacteria, and Eucarya) and to the origins of life (13, 14, 15, 16, 17).

The microbial diversity from two thermal springs in Yellowstone National Park was determined as described previously (13). DNA was extracted from samples, and the 16S rRNA genes were amplified using either an archaeal-specific or a bacterial-specific forward primer (4F-5′-TCCGGTTGATCCCGCCRG-3′ or 8F-5′-AGAGTTTGATCCTGGCTCAG-3′, respectively) and a corresponding universal reverse primer (1492R-5′-GGTTACCTTGTTACGACTT-3′). The PCR products were purified and cloned, and unique clones were sequenced using an automated sequencer (ABI 377). The sequences were aligned with a subset of sequences from Genbank and the Ribosomal Database (RDP). Phylogenetic trees were constructed by maximum likelihood analysis using fastDNAml. Analyses of the microbial diversity of these thermal springs revealed a plethora of novel archaeal and bacterial sequences (*phylotypes*), most notably some of the deepest lineages within the Bacteria and Archaea and a proposed new kingdom within the Archaea, the Korarchaeota (14, 15, 18, 19). Recently we have reported another member of the Korarchaeota from an 83°C sample from Calcite Springs, Yellowstone National Park. This community is much less complex (five phylotypes were detected; Fig. 1) than the community associated with the highly mixed Obsidian Pool, where the Korarchaeota were first reported (14). Furthermore, the dominant phylotype, and the only bacterial phylotype reported, from the Calcite Spring study is a deeply branching filamentous organism that dominantes (in biomass) the communities of Calcite Springs, from ~63°C to 84°C (16, 25). Based on *in situ* hybridization using fluorescein-labeled oligonucleotide probes specific for the dominant bacterial phylotypes, this group represented 90%–95% of the community. This phylotype has been obtained from the Obsidian Pool community (19), from a stream near Obsidian Pool, and from terrestrial thermal springs at Furnas, Azores (20). Furthermore, preliminary results from a diversity analysis of a community obtained from a deep-sea hydrothermal vent site on the Mid-Atlantic Ridge (Snake Pit, 23°N 45′ W) produced the first report of members of relatives of the Aquificales from deep-sea vents (17, 20) (Fig. 2). Therefore, these

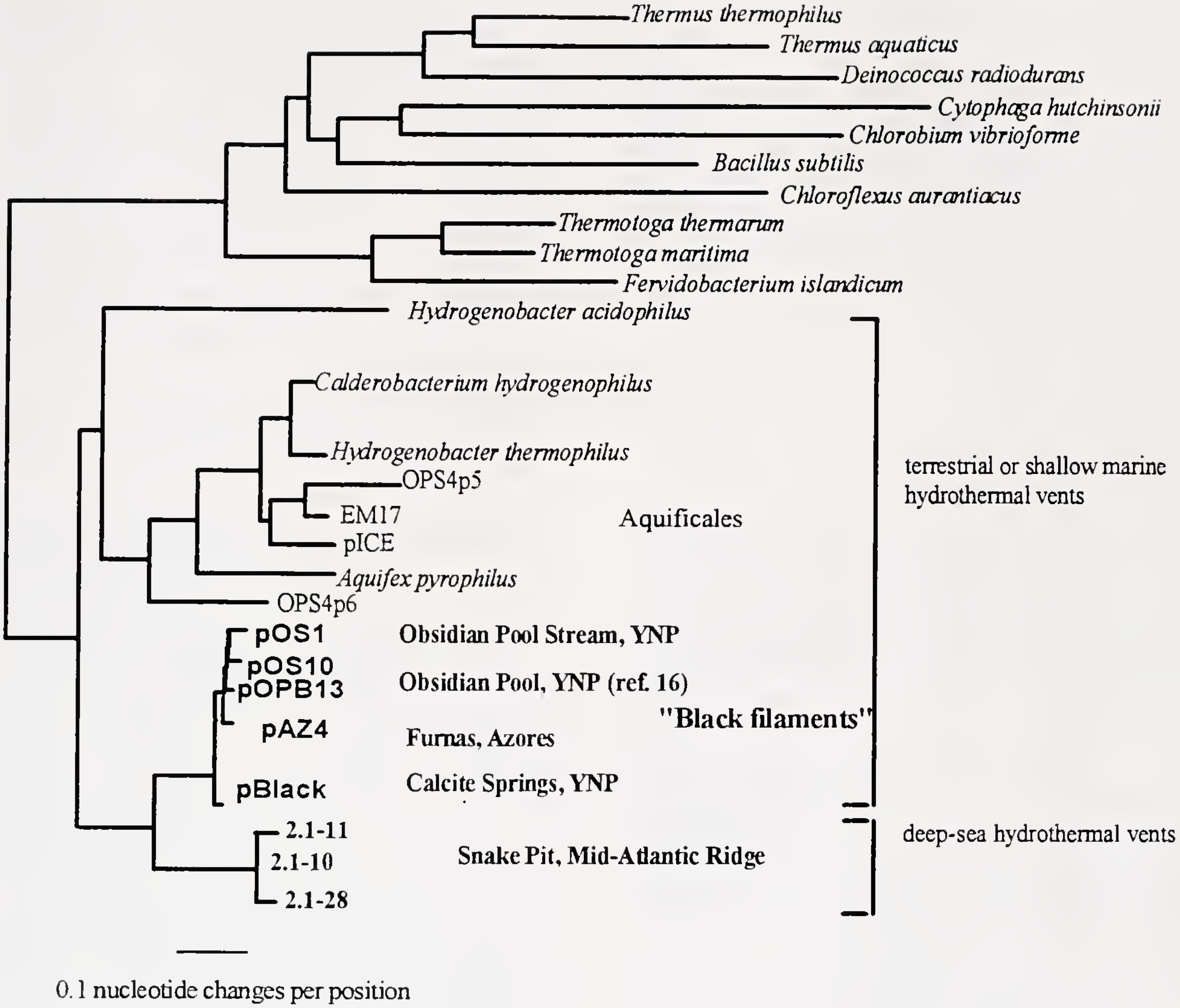
Thermus thermophilus
Thermus aquaticus
Deinococcus radiodurans
Cytophaga hutchinsonii
Chlorobium vibrioforme
Bacillus subtilis
Chloroflexus aurantiacus
Thermotoga thermarum
Thermotoga maritima
Fervidobacterium islandicum
Hydrogenobacter acidophilus
Calderobacterium hydrogenophilus
Hydrogenobacter thermophilus
OPS4p5
EM17
pICE
Aquificales
Aquifex pyrophilus
OPS4p6
terrestrial or shallow marine hydrothermal vents
pOS1
Obsidian Pool Stream, YNP
pOS10
pOPB13
Obsidian Pool, YNP (ref. 16)
"Black filaments"
pAZ4
Furnas, Azores
pBlack
Calcite Springs, YNP
2.1-11
2.1-10
2.1-28
Snake Pit, Mid-Atlantic Ridge
deep-sea hydrothermal vents
0.1 nucleotide changes per position

Figure 2. A distance phylogenetic tree of rDNAs including the deeply branching "black filamentous organisms" rDNAs obtained from Calcite Springs, Obsidian Pool, a stream near Obsidian Pool (all in Yellowstone National Park); the hot springs at Furnas, Azores; and samples obtained from a deep-sea hydrothermal vent on the Mid-Atlantic Ridge. Many clones with very similar sequences (98% similar or more) were obtained; for clarity, not all are depicted. Clones designated OPS are from the stream at Obsidian Pool. pICE was obtained from a sample in Iceland, and EM 17 is the pink filamentous organism from Octopus Spring, Yellowstone National Park (13).

bacterial phylotypes are important members of these near-neutral, sulfidic, and iron-rich environments.

Preliminary *in situ* measurements of biological activity associated with the communities at Calcite Springs are suggestive of significant chemoautotrophic activity as measured by radioactive bicarbonate incorporation. Hydrogen consumption in these communities is several-fold higher than that observed for deep-sea hydrothermal communities. Members of the community are able to reduce iron and precipitate an iron mineral within the periplasmic space. The surrounding black-gray banded rocks at Calcite Springs are rich calcite, aragonite, and iron-sulfur minerals, including pyrite (Reysenbach and Onstott, unpubl. data). If a chemoautotrophic origin of life relied on energy generated through pyrite formation from FeS and H_2S (3, 5), and considering that CH_3SH (a precursor of acetic acid) is formed by the reduction of CO_2 with FeS and H_2S (21), the conditions at geothermal springs such as Calcite Springs may be good models to test the high-temperature milieu for the early evolution of life.

The molecular and fossil record—an alternative hypothesis?

That iron reduction occurs in these geothermal environments and is associated with direct or indirect biologically precipitated iron oxides such as magnetite may have implications for the origins of banded iron formations (BIFs) in the Archaea. A number of models for a biological role in BIFs have been proposed (22, 23, 24). Recent theories about the potential role of anoxygenic phototrophs in BIFs are tantalizing but not conclusive (25, 26, 27). Furthermore, mesophilic iron reducers have been implicated in BIFs (28, 29). If the early evolution of life occurred in hot-spring-like environments, and given that iron reduction (this study) and iron oxidation (30) are associated with some of the deepest phylogenetic lineages that occur in these environments, might these organisms not be responsible in part for the Archean BIFs? Since some of the oldest known microfossils from the early Archean (~3.0 to ~3.5 Ga-old) (31, 32) have been postulated to be cyanobacterial in origin, perhaps Archean hydrothermally derived deposits may reveal some interesting microfossils analogous to the thermophilic black filamentous organisms that thrive in iron-rich, sulfidic near-neutral geothermal springs.

Acknowledgments

These ideas have been stimulated and inspired by many, including Terry Beveridge, T. C. Onstott, Everett Shock, and Bev Pierson. Much credit goes to Norman Pace, in whose lab the Calcite study was initiated and who made the foray into the microbial forest possible.

Literature Cited

1. **Baross, J. A., and S. E. Hoffman. 1985.** Submarine hydrothermal vent and associated gradient environment as sites for the origin and evolution of life. *Origins Life* **15:** 327–345.
2. **Pace, N. R. 1991.** Origin of life—facing up to the physical setting. *Cell* **65:** 531–533.
3. **Wachtershauser, G. 1988.** Pyrite formation, the first energy source for life: a hypothesis. *Syst. Appl. Microbiol.* **10:** 207–210.
4. **Holland, H. D. 1984.** *The Chemical Evolution of the Atmosphere and Oceans,* p. 582. Princeton University Press, Princeton, New Jersey.
5. **Wachtershauser, G. 1990.** Evolution of first metabolic cycles. *Proc. Natl. Acad. Sci. USA* **87:** 200–204.
6. **Forterre, P. 1996.** A hot topic: the origin of hyperthermophiles. *Cell* **85:** 789–792.
7. **Gogarten-Boekels, M., E. Hilario, and J. P. Gogarten. 1995.** The effects of heavy bombardment on the early evolution—the emergence of the three domains of life. *Origins Life* **25:** 251–264.
8. **Woese, C. R., O. Kandler, and M. L. Wheelis. 1990.** Towards a natural system of organisms: proposal for the domains Archaea, Bacteria, Eucarya. *Proc. Natl. Acad. Sci. USA* **84:** 4576–4579.
9. **Doolittle, W. F., and J. R. Brown. 1994.** Tempo, mode, the progenote, and the universal root. *Proc. Natl. Acad. Sci. USA* **91:** 6721–6728.
10. **Iwabe, N., K. Kuma, M. Hasegawa, S. Osawa, and T. Miyata. 1989.** Evolutionary relationship of archaebacteria, eubacteria and eukaryotes inferred from phylogenetic trees of duplicated genes. *Proc. Natl. Acad. Sci. USA* **86:** 9355–9359.
11. **Stetter, K. O. 1986.** Diversity of extremely thermophilic archaebacteria. Pp. 39–74 in *Thermophiles: General, Molecular and Applied Microbiology,* T. D. Brock, ed. John Wiley, New York.
12. **Blöchl, E., R. Rachel, S. Burggraf, D. Hafenbradl, H. W. Jannasch, and K. O. Stetter. 1997.** *Pyrolobus fumarii,* gen and sp. nov., represents a novel group of archaea, extending the upper temperature limit for life to 113°C. *Extremophiles* **1:** 14–21.
13. **Reysenbach, A. -L., G. S. Wickham, and N. R. Pace. 1994.** Phylogenetic analysis of the hyperthermophilic pink filament community in Octopus Spring, Yellowstone National Park. *Appl. Environ. Microbiol.* **60:** 2113–2119.
14. **Barns, S. M., R. E. Fundyga, M. W. Jeffries, and N. R. Pace. 1994.** Remarkable archaeal diversity detected in a Yellowstone National Park hot spring environment. *Proc. Natl. Acad. Sci. USA* **91:** 1609–1613.
15. **Barns, S. M., C. F. Delwiche, J. D. Palmer, and N. R. Pace. 1996.** Perspectives on archaeal diversity, thermophily and monophyly from environmental rRNA sequences. *Proc. Natl. Acad. Sci. USA* **93:** 9188–9193.
16. **Reysenbach, A. -L., M. A. Ehringer, K. Hershberger, R. Favre, M. Cermola, A. Palsdottir, G. Eggertsson, and N. R. Pace. 1995.** Analysis of microbial hot spring communities from Yellowstone National Park and Iceland by 16S rRNA sequence analysis [abstract]. In *Biodiversity, Ecology and Evolution of Thermophiles in Yellowstone National Park: Overviews and Issues.* Yellowstone National Park, Wyoming.
17. **Kirshtein, J., E. Corre, D. Prieur, G. Geesey, and A. -L. Reysenbach. 1997.** Microbial diversity associated with *in-situ* growth chambers deployed on deep-sea hydrothermal vents: analogues for subsurface microbial diversity? [Abstract]. Washington, DC. American Geophysical Union Subsurface Biosphere Workshop.
18. **Reysenbach, A. -L., M. A. Ehringer, K. Hershberger, and N. R. Pace. 1996.** Another member of the "Korarchaeota" revealed through molecular phylogenetic analysis of a thermal spring in Yellowstone National Park [abstract]. In *Thermophiles '96.* University of Georgia, Athens, Georgia.
19. **Hugenholz, P., C. Pitulle, K. L. Hershberger, and N. R. Pace. 1998.** Novel division level bacterial diversity in a Yellowstone hot spring. *J. Bacteriol.* **180:** 366–376.
20. **Reysenbach, A. -L., J. Graber, J. Kirshtein, and M. Speck. 1999.** The diversity of the deeply branching aquificales: from Yellowstone to the Azores to the deep sea. In *Biodiversity, Ecology and Evolution of Thermophiles in Yellowstone National Park.* A.-L. Reysenbach, M. Voytek, and R. Mancinelli, eds. Plenum, New York.
21. **Huber, C. and G. Wachtershauser. 1997.** Activated acetic acid by carbon fixation on (Fe,Ni)S under primordial conditions. *Science* **276:** 245–247.
22. **Beukes, N., and C. Klein. 1992.** Models of iron-formation deposition. Pp. 147–151 in *The Proterozoic Biosphere,* J. W. Schopf and C. Klein, eds. Cambridge University Press, Cambridge.
23. **Hartman, A. 1983.** The evolution of photosynthesis and microbial mats: a speculation on the banded iron formations. Pp. 441–454 in *Microbial Mats: Stromatolites,* Y. Cohen, R. W. Castenholz, and H. O. Halvorsen, eds. Alan R. Liss, New York.
24. **Braterman, P. S., A. G. Cairns-Smith, and R. W. Sloper. 1983.** Photo-oxidation of Fe^{2+}—significance for banded iron formations. *Nature* **303:** 163–164.
25. **Ehrenreich, A., and F. Widdel. 1994.** Anaerobic oxidation of fer-

rous iron by purple bacteria, a new type of phototrophic metabolism. *Appl. Environ. Microbiol.* **60:** 4517–4526.

26. **Widdel, F., S. Scnell, S. Hersing, A. Ehrenreich, B. Assmus, and B. Schink. 1993.** Ferrous iron oxidation by anoxygenic phototrophic bacteria. *Nature* **362:** 834–836.
27. **Kump, L. 1983.** Bacteria forge a new link. *Nature* **362:** 790–791.
28. **Nealson, K. H., and C. R. Myers. 1990.** Iron reduction by bacteria: a potential role in the genesis of banded iron formations. *Am. J. Sci.* **290A:** 35–45.
29. **Lovley, D. R. 1991.** Dissimilatory Fe (III) and Mn (IV) reduction. *Microbial. Rev.* **55:** 259–287.
30. **Hafenbadl, D., M. Keller, R. Dirmeier, R. Rachel, P. Robnagel, S. Burggraf, H. Huber, and K. O. Stetter. 1997.** *Ferroglobus placidus* gen. nov., sp. nov., a novel hyperthermophilic archaeum that oxidizes Fe^{2+} at neutral pH under anoxic conditions. *Arch. Microbiol.* **166:** 308–314.
31. **Walsh, M. M., and D. R. Lowe. 1985.** Filamentous microfossils from the 3,500-Myr-old Onverwacht Group, Barberton Mountain Land, South Africa. *Nature* **314:** 530–532.
32. **Schopf, J. W., and B. M. Packer. 1987.** Early Archaean (3.3 billion to 3.5 billion-year-old) microfossils from Warrawoona Group, Western Australia. *Science* **237:** 70–73.

Discussion

MARGULIS: Have you identified any live flagellated magnetotactic bacteria in any of these samples?

REYSENBACH: No.

MARGULIS: Are you sure that the mineral is magnetite?

REYSENBACH: That's my suspicion. I still can't say this with certainty since the analysis does not give a realistic oxygen signal.

MARGULIS: Have you identified any of the iron minerals in the microorganisms?

REYSENBACH: We can't say definitely.

PALMER: Since you mentioned my name in combination with the Korarchaeota, I think I must give a disclaimer that while my name appeared on the paper (1) that first proposed erection of a new kingdom, Korarchaeota, I fought tooth and nail with my collaborator, Norm Pace, to not erect it. I thought it was premature because the position of that clade Korarchaeota depends highly on the method of phylogenetic analysis on in-group/out-group inclusion, and so on. If you look at the paper by DeLong *et al.* (pp. 363–366) in these proceedings you will see a tree in which the Korarchaeota sequences do not go below the Crenarchaeota/euryarchaeota split, but above it.

REYSENBACH: I agree with your assessment that assigning the Korearchaeota as a separate kingdom is premature. Recall that I showed two similar trees, one in which the Eukarya (*Giardia*) were used as the out group, and one in which the Bacteria (*Aquifex*) were used as the outgroup. In the former, the Korearchaeota do branch independently of the Euryarchaeota and Crenarchaeota; and in the latter, the Korearchaeota branch within the Crenarchaeota.

PALMER: I think it is highly premature when all you have is a ribosomal RNA sequence, one whose position is clearly very volatile in phylogenetic analysis, to erect a new kingdom on that one highly volatile, poorly placed property. I think it is, therefore, incumbent on people in this field who are going to push for this as a new group, to go out and provide other evidence, to get other gene sequences to substantiate or refute the idea that this is a fundamentally new group of archaebacterial life.

SCHOPF: I find this all very interesting, and I think the question that you are asking is a good one. Certainly this association of hyperthermophilic microorganisms with very deep divergences is telling us something about what was going on. I'm puzzled as to exactly what it is telling us, but it seems to me that one might very well wish to find direct evidence for a hot thermophilic environment associated with very ancient fossils. Unfortunately, the oldest fossils that are known, from South Africa and from western Australia, are not thermophiles. They are not living in a thermophilic environment; they are living in shallow-water, storm-swept environments with pebbles and other normal environmental indicators that show they are not associated with hot springs or volcanic pools. However, these are only 3.5 or 3.3 billion years in age. There must have been substantial evolution prior to that time, so maybe if we get lucky, we can geologically find places where we might find fossils of the sort that you are looking for.

REYSENBACH: I don't think we are going to see a wonderful fossil like the ones you showed. I think the trick is to start looking for minerals that may have been produced by some of these organisms. I find it interesting that all of the organisms that I spoke about, especially the black filamentous organisms, grow between 60° and 85°C, optimally below 80°C, and that is the range for thermophily, not hyperthermophily. Even though this is just a "thermophilic kind of question"—are hyperthermophiles or thermophiles really the original ancestors?

GUERRERO: The hypothesis of the thermophilic origin of life is well known, but consider the following problem. To maintain a thermophilic environment, for example, in deep-sea vents, you need a huge mass of water at 40°C and a chemical gradient, because water is very unstable. This is a good environment in which to find organisms. One can consider the electron acceptor iron-converted magnetite, which may be the origin of the magnetic substance you found, but you also need an electron donor. The deep crust might harbor a very high concentration of hydrogen, and it is probable that organic matter and biologically important compounds like phosphate and ammonia are also present. The fact that the microorganisms are potentially chemoautotrophic is irrelevant since they are completely heterotrophic in the real world. My question is whether or not you checked the heterotrophic or chemoautotrophic nature of these microbes?

REYSENBACH: Yes, we're looking at all the possibilities. We were able to show that chemoautotrophy was occurring in this environment, and we will be examining the potential of heterotrophy in the next field season. However, in some of our enrichments we did add yeast extract, which would enable them to be heterotrophic. We do not know how important or dominant heterotrophs are in these systems.

Literature Cited

1. **Barns, S. M., C. F. Delwiche, J. D. Palmer, and N. R. Pace. 1996.** Perspectives on archaeal diversity, thermophily and monophyly from environmental rRNA sequences. *Proc. Natl. Acad. Sci. USA* **93:** 9188–9193.

Reference: *Biol. Bull.* **196:** 373–377. (June 1999)

The Last Universal Common Ancestor (LUCA), Simple or Complex?

PATRICK FORTERRE[1] AND HERVÉ PHILIPPE[2]

[1] *Institut de Génétique et Microbiologie, Bat 409; and* [2] *Laboratoire de Biologie cellulaire, Bat 444, Université Paris XI 91405 Orsay cedex, France*

The concept of Archaea (formerly Archaebacteria), introduced by Carl Woese at the end of the seventies, raised the hope that studying this third form of life on earth would help to reconstitute the Last Universal Common Ancestor (LUCA) to all living organisms. In the years that followed, a consensus emerged within the community of archaeobiologists about early cellular evolution and the nature of LUCA. In the new paradigm, Archaea are the sister group of Eukarya (formerly eukaryotes), and LUCA was a simple prokaryote with features between those of Archaea and Bacteria (1, 2). In this scenario, the complex and specific molecular traits of the Eukarya, such as nuclear pores, mRNA splicing, or an elaborated cytoskeleton, are late inventions in the eukaryal lineage.

This paradigm is usually justified by the rooting of the universal tree of life in the bacterial branch and the finding of eukaryal features in Archaea at the molecular level. In our opinion however, it is also based on the prejudice that "pro"karyotes predated "eu"karyotes in the course of early cellular evolution. Prokaryotes of course predate "modern" eukaryotes in the history of life since all present-day eukaryotes have probably descended from an ancestor that had already engulfed the bacterial endosymbiont which gave birth to mitochondria, (*e.g.*, 3). We think, however, that the relationships between present-day prokaryotes and the ancestral eukaryotic lineage (those which existed before the endosymbiotic event) are far from being definitely settled.

We have previously challenged several of the ideas behind the current paradigm. For example, we have shown that cladistic analysis (*sensu* Hennig) of the elongation factor protein data set does not support the rooting of the tree of life in the bacterial branch (4). In fact, many protein sequence data sets are saturated by mutations, suggesting that classical methods of molecular phylogeny are very poor at resolving ancient divergences (5). (See Fig. 1 for the case of Ile tRNA synthetases from the three domains of life.) In particular, this saturation will always lead to an early emergence of the fast-evolving lineages, whatever their true position, and this artifactual result can be statistically robust.

The rapid accumulation of new information about the molecular biology of Archaea, as well as the recent availability of several completely sequenced archaeal and bacterial genomes, has renewed the interest of the scientific community in the problem of LUCA (1, 6). These new data have usually been interpreted in terms of the above paradigm implying a "simple" LUCA. It has been proposed, in particular, that LUCA had a primitive replication apparatus (2) and even an RNA genome (7).

In this communication, we use this new genomic information differently: *i.e.*, to systematically reconsider all data supporting the bacterial rooting of the tree of life. Our results show that all the phylogenies that have been used to root the universal tree of life in the bacterial branch are unreliable. Beside the general problem of saturation, most of them are "confused"; that is, one or several domains are paraphyletic or polyphyletic in trees inferred from these data sets (8). As an example, Figure 2 shows a simplified version of the Val/Ile-t-RNA synthetase tree. These paralo-

---

This paper was originally presented at a workshop titled *Evolution: A Molecular Point of View*. The workshop, which was held at the Marine Biological Laboratory, Woods Hole, Massachusetts, from 24–26 October 1997, was sponsored by the Center for Advanced Studies in the Space Life Sciences at MBL and funded by the National Aeronautics and Space Administration under Cooperative Agreement NCC 2-896.

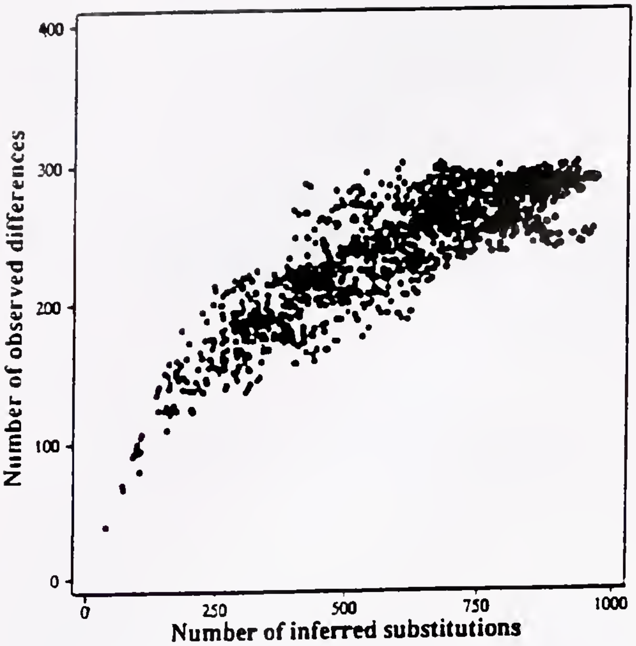

Figure 1. Saturation analysis of the Ile tRNA synthetases. The method of Philippe *et al.* (14) was applied to the set of sequences used in Figure 2. The number of substitutions between two species is estimated as the sum of the lengths of the branches linking these two species in the most parsimonious tree. Each point in the diagram corresponds to a couple of species, for which the abscissa is the number of inferred substitutions, and the ordinate is the number of observed differences. Near the origin, the curve is linear, indicating that the Ile tRNA synthetases are not mutationally saturated at small evolutionary distances (within methanogens, gram-positive, Fungi), but they are highly saturated at large evolutionary distances (between the three domains but also within each domain). For a couple of species, one can observe only 250 differences, but during the course of evolution, at least 1000 substitutions have occurred.

gous proteins have been previously used to root the tree of life, and previous analysis confirmed the bacterial rooting (9). After the addition of new sequences, the Archaea and Bacteria were both revealed as polyphyletic, raising doubts about any rooting result. The high level of saturation detected in Figure 1 could explain some, if not all, of these surprising results.

In the case of the elongation factor tree, we have shown that the positions that support the bacterial rooting in classical phylogenies are the most variable ones, *i.e.*, the least reliable (10). We conclude from our analyses that the classical methods of molecular phylogeny cannot solve the problem of rooting the tree of life. We favor the cladistic analysis (*sensu* Hennig) of slowly evolving positions (SEP), or indels, as the basis from which to infer phylogenies (11). However, the application of this method to the current data set clearly indicates that such characters are rare and, because of a high level of homoplasy, cannot easily be interpreted.

The difficulty of recovering the phylogenetic relationships between the three domains is not surprising when one considers the many problems encountered by molecular phylogenetic analysis when dealing with more recent divergence. For example, completely different topologies have been obtained recently for many groups of protists when different genes were used to construct eukaryotic phylogenetic trees (5). Organisms appeared, either in the crown of the eukaryotic tree when the reporter gene was a slowly evolving one, or as an early branching lineage when the gene was a fast-evolving one. This was due to the saturation of the data set used and to the long branch of the outgroup (Archaea or Bacteria).

A spectacular example of the problems that occur in the eukaryotic tree is the misplacement of microsporidia. Microsporidia are most likely fungi, as indicated by α and β tubulin, Hsp70, and RNA polymerase trees, as well as by several phenotypic characters (12). However, they are early branching in rRNA, elongation factors, and tRNA synthetase trees! This again emphasizes that elongation factors and tRNA synthetase are not good phylogenetic markers and cannot be used to root the tree of life.

Finally, even if the rooting problem is solved, the information gained will be insufficient to reveal the nature of LUCA. Indeed, all rooting is compatible with opposite

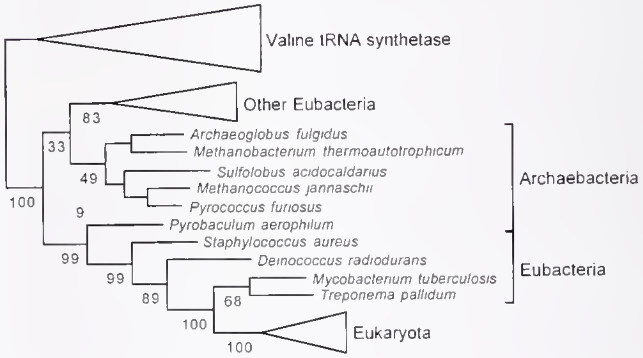

Figure 2. Phylogeny of Ile tRNA synthetases rooted on 20 Val tRNA synthetases. The tree was reconstructed by maximum parsimony (PAUP 3.1). The Archaea and Bacteria are both polyphyletic. Four bacterial sequences, far from the other Bacteria, are sister-groups of the Eukarya, with strong statistical support (bootstrap value of 100%). *Pyrobaculum*, a crenarchaeote, is the sister-group of the previous assemblage, also with strong statistical support (bootstrap value of 99%). This species is strikingly far from the other Archaea, especially from another crenarchaeote, *Sulfolobus*. Another surprising result is the sister-group of the other Archaea and the other Bacteria, but the statistical support is very low (33%). This reanalysis of the Ile tRNA synthetases, quite different from the first one (8), shows the importance of good species sampling: more species allow a better test of the monophyly of the domains and a better phylogenetic reconstruction.

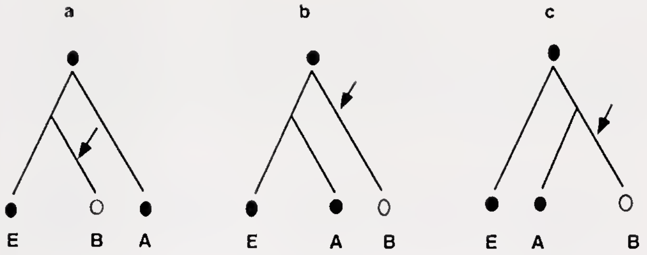

Figure 3. The three possible rootings of the universal tree of life connecting Archaea (A), Bacteria (B), and Eukarya (A) are equally parsimonious if characters shared only by Archaea and Eukarya (black circles) are primitive.

hypotheses about the presence or absence, in LUCA, of characters present in only two domains (*e.g.*, see the characters common to Eukarya and Archaea in Fig. 3). Thus the main problem is how to polarize such characters: that is, how to determine whether they are primitive (already present in LUCA) or derived, testifying for the sisterhood of these two domains.

The outcome of this problem is important indeed to our understanding of LUCA. For example, if characters present in both Archaea and Eukarya are primitive, LUCA might have been a complex organism, even harboring some features now present only in Eukaryotes (13). In this alternative scenario, present-day prokaryotes would be superficially and secondarily "simple," having being extensively streamlined in relation with their prokaryotic way of life. As a matter of fact, the extensive loss of genes is now well documented by comparative analyses of several completely sequenced bacterial genomes.

How the polarization problem will finally be solved is not clear at present. A possibility may be to reconstitute the pre-LUCA history of molecular mechanisms such as transcription, replication, or translation. However, we still lack a detailed description of these phenomena in the three domains and cannot therefore make safe assumptions about their nature in LUCA, let alone before LUCA. More descriptive molecular work, and not only on sequences, is then required to advance further in that direction.

Literature Cited

1. **Olsen, G. J., and C. R. Woese. 1997.** Archaeal genomics: an overview. *Cell* **89:** 991–994.
2. **Edgell, D. R., and W. F. Doolittle. 1997.** Archaea and the origin(s) of DNA replication proteins. *Bioessays* **19:** 1–4.
3. **Germot, A., H. Philippe, and H. Le Guyader. 1997.** Evidence for loss of mitochondria in Microsporidia from a mitochondrial-type HSP70 in *Nosema locustae. Mol. Biochem. Parasitol.* **87:** 159–168.
4. **Forterre, P., N. Benachenou, F. Confalonieri, M. Duguet, C. Elie, and B. Labedan. 1993.** The nature of the last universal ancestor and the root of the tree of life, still open questions. *Biosystems* **28:** 15–32.
5. **Philippe, H., and A. Adoutte. 1998.** Pp. 25–56 in *Evolutionary Relationships among Protozoa*, G. H. Coombs, K. Vickerman, M. A. Sleigh, and A. Warren, eds., Systematics Assoc. Spec. Vol. Ser., Kluwer Academic, Dordrecht, The Netherlands.
6. **Forterre, P. 1997.** What can we learn from archaeal sequences? *Current Opin. Genet. Dev.* **7:** 764–770.
7. **Mushegian, A. R., and E. V. Koonin. 1996.** A minimal gene set for cellular life derived by comparison of complete bacterial genomes. *Proc. Natl. Acad. Sci. USA* **93:** 10268–10273.
8. **Philippe, H., and Forterre, P. 1999.** The rooting of the universal tree of life is not reliable. *J. Mol. Evol.* (in press).
9. **Brown, J. R., and W. F. Doolittle. 1995.** Root of the universal tree of life based on ancient aminoacyl-tRNA synthetase gene duplications. *Proc. Natl. Acad. Sci. USA* **92:** 2441–2445.
10. **Lopez, P., P. Forterre, and H. Philippe. 1999.** The root of the tree of life in the light of the covarion model. *J. Mol. Evol.* (in press).
11. **Forterre, P. 1997.** Protein versus rRNA: rooting the universal tree of life? *ASM (Am. Soc. Microbiol.) News* **63:** 89–95.
12. **Embley, T. M., and R. P. Hirt. 1998.** Early branching eukaryotes? *Current Opin. Genet. Dev.* **8:** 624–629.
13. **Forterre, P., and H. Phillipe. 1999.** Where is the root of the universal tree? *Bioessays* (in press).
14. **Philippe, H., U. Sörhannus, A. Baroin, R. Perasso, F. Gasse, and A. Adoutte. 1994.** Comparison of molecular and paleontological data in diatoms suggest a major gap in fossil record. *J. Evol. Biol.* **7:** 247–265.

Discussion

OLSEN: In interpreting your trees, you said that the Hsp70 tree is correct and groups together microsporidia and fungi. But in examining the synthetase tree, you claim that there is a problem with this tree because the microsporidia are deeply branching. How do you choose which one is the good tree to place microsporidia; why do you think the Hsp70 tree is good and not the rRNA or the elongation factor trees?

FORTERRE: We make this choice because the conclusion that microsporidia should be grouped with fungi is supported not only by several molecular phylogenies but also by independent morphological arguments at the molecular level: for example, the presence of chitin in their cell wall, or an insertion common to fungi and microsporidia in the gene encoding elongation factor EF1α (1). This last point is especially interesting since, when you construct a traditional phylogenetic tree of elongation factor EF1α using all the sites, microsporidia are at the base of the tree. This indicates that a single good character, in that case an insertion, can give the right answer, whereas you get an artifactual answer when you use many bad characters such as rapidly evolving positions, or characters that make no sense because they cannot be polarized. In the case of the Hsp70 tree, we think that the position of microsporidiae is correctly inferred because the outgroup used, a Hsp70 protein sequence from α proteobacteria, is closely related to the microsporidial protein which is of mitochondrial origin (2). It is very important to use closely related outgroup sequences, in order to avoid long branch attraction, especially when using fast-evolving sequences such as those of microsporidia.

PALMER: The elongation factor of microsporidia has an insert that is actually a synapomorphy, not just with fungi, but animals plus fungi. The elongation factor sequences as a whole are evolving so quickly that when you use a eubacterial outgroup, the microsporidia actually drop below the archaebacterial eukaryotic sequence. Ribosomal RNA and elongation factors evolve at extremely high rates, which I think distorts indeed our view of microsporidial placement when we use these molecules. What are your hopes in trying to root the tree of life, or have you lost hope?

FORTERRE: I don't think it is possible to root the tree using the traditional approach of molecular phylogeny with the data sets which have been used up to now. I really don't know if it will be possible to find sequence data sets with sufficient remaining information to solve this question.

SCHOPF: You and a number of others would move microsporidia within the fungi. As I recall, the branch of the microsporidial lineage in the rRNA tree is quite long. It's even the longest of all branches in the eukaryotic tree, and presumably microsporidia are fast evolving. Yet the fungi that have also been sequenced with 18 sRNA correspond to a slowly evolving lineage. It is rather remarkable that you have a lineage based on genes or proteins that evolve slowly, but then you propose to move microsporidia in because they evolve very quickly. Doesn't that suggest a degree of inconsistency—some sort of a problem about inferred evolutionary rates?

FORTERRE: It is now clear that different genes in a given lineage can evolve at very different rates. Microsporidia are parasites with streamlined ribosomes, which can explain why their rRNA evolves more rapidly than those of other fungi. There are several problems with evolutionary rates. One is that rate varies tremendously from one site to another, making all phylogenetic reconstruction methods hazardous. If you have a sequence that evolves rapidly, it means you have many more sites that can and do vary, yet these same sites will be rapidly saturated by multiple substitutions. Under conditions of saturation, branches derived from rapidly evolving genes will be attracted by each other (3), producing a systematic bias in the interpretation of the data.

SCHOPF: If you can take a really fast-evolving lineage and put it into a really slowly evolving lineage and say that's perfectly fine, does it follow that the generalizations that we've all been using about fast-evolving and slowly evolving lineages simply are meaningless concepts?

R. DOOLITTLE: Bill (Schopf) is talking about rRNA. In our paper (4), it is the fungal proteins that are, in fact, changing faster than the animal and plant proteins. It is not a slowly evolving lineage for the fungi when it comes to proteins.

HASEGAWA: How many amino acid sites did you use in calculating the saturation curve of tRNA synthetase?

FORTERRE: We used about 400 sites in the tree that I presented, but we get the same result with a data set reduced to 250 sites.

HASEGAWA: I am concerned that you may be using too many sites.

FORTERRE: We started from the original alignment used by Brown and Doolittle (5) (kindly provided by Jim Brown) and removed the sequences of Leu-tRNA synthetases to get more positions that could be aligned without any ambiguities.

FELSENSTEIN: I was confused by your diagram; it shows an explosion, or star, tree with different length lineages, which on further analysis, become a resolved tree. I'm not aware of any methods, except ones that assume a clock, that would do that. Which methods were you assuming would be used to get you from the one tree to the other?

FORTERRE: This was done by Hervé Phillipe using computer simulation. Distance methods, parsimony, and maximum likelihood all produce an artifactual resolved tree. The slowly evolving genes were always found in the crown, and the fast-evolving genes were pushed away from the crown. As expected, however, ML was the method less sensitive to this artifact.

FELSENSTEIN: That's not what I would expect likelihood or distance matrix methods to do, so I am a bit surprised. I just want to express a queasy feeling about the result using these methods.

IBBA: Which part of the synthetase did you use? It is clear that the amino acid binding site and the nucleotide binding site change very slowly, whereas the tRNA binding sites change very fast and are very variable.

FORTERRE: We have used all positions that are clearly homologous, and include the two regions you mention. I have carried out a site-by-site analysis for the amino acid tRNA synthetase and was struck by the fact that about half of the sites are highly variable, and about half of the sites could be considered more-or-less slowly evolving; even in that case, I found about ten sites in the tRNA synthetase that could be polarized (6). However, these positions, which are *a priori* the best ones, give contradictory answers. The conclusion is clear: tRNA synthetases cannot be used to root the tree of life.

Literature Cited

1. **Kamaishi, T., T. Hashimoto, Y. Nakamura, F. Nakamura, S. Murata, N. Okada, K.-I. Okamoto, M. Shimizu, and M. Hasegawa. 1996.** Protein phylogeny of translation elongation factor EF-1a suggests microsporidians are extremely ancient eukaryotes. *J. Mol. Evol.* **42:** 257–263.
2. **Germot, A., H. Philippe, and H. Le Guyader. 1997.** Evidence for loss of mitochondria in Microsporidia from a mitochondrial- type HSP70 in *Nosema locustae. Mol. Biochem. Parasitol.* **87:** 159–168.
3. **Philippe, H., and A. Adoutte. 1998.** Pp. 25–56 in *Evolutionary Relationships Among Protozoa,* G. H. Coombs, K. Vickerman, M. A. Sleigh, and A. Warren, eds. Systematics Assoc. Special Vol. Ser., Kluwer Academic, Dordrecht, The Netherlands.
4. **Doolittle, R. F., D.-F. Feng, S. Tsang, G. Cho, and E. Little. 1996.** Determining divergence times of the major kingdoms of living organisms with a protein clock. *Science* **271:** 470–476.
5. **Brown, J. R., and W. F. Doolittle. 1995.** Root of the universal tree of life based on ancient animoacyl-tRNA synthetase gene duplications. *Proc. Natl. Acad. Sci. USA* **92:** 2441–2445.
6. **Forterre, P. 1997.** Protein versus rRNA: rooting the universal tree of life? *ASM (Am. Soc. Microbiol.) News* **63:** 89–95.

Reference: *Biol. Bull.* **196:** 378–380. (June 1999)

Rethinking the Origin of Eukaryotes

W. FORD DOOLITTLE

Canadian Institute for Advanced Research and Department of Biochemistry, Dalhousie University, Halifax, Nova Scotia, Canada

The field of early cellular evolution is currently in serious confusion. We have more and better data than we dared dream of a decade ago, and many of us have ventured to give strong answers to deep evolutionary questions. But now these answers often seem mutually incompatible, and no comprehensive scenario for early cell evolution can account for all the data that are available. Since many of the speakers before and after me have, or will have, addressed the conundra represented by individual sets of data, and since all recognize that there is a problem, I will try to present this problem from a comprehensive historical perspective.

Science is supposed to work through cycles of hypothesis formulation, casting and then testing predictions, and finally hypothesis confirmation, rejection, or reformulation. Sometimes we, and even more often our public, forget this. We and they sometimes see times of turmoil (such as that in which early cell evolution now seems to be) as evidence of the failure of the scientific enterprise—that the experts were wrong once again. In fact, turmoil and confusion show us that science is working as it should. Some of our hypotheses should fail or need drastic reformulation, and we should rejoice in the opportunity to invent new ways of thinking about patterns in the data.

The prokaryote/eukaryote dichotomy was promoted by Stanier and van Niel (1), Margulis (2), and others as the best way to partition the living world phenetically—and likely also as a gap bridged only once in cellular evolution, through the invention of a new cell ultrastructure driven by the advantage of predation. Margulis' refurbished version of the endosymbiont hypothesis emphasized the dual genetic inheritance of most eukaryotes, but fudged the issue of whether endosymbiosis was the *sine qua non* of the eukaryotic condition (3).

The endosymbiont hypothesis was the deep evolutionary scenario on which molecular phylogeny, and in particular rRNA-based molecular phylogeny, cut its first teeth. What the rRNA and protein analyses of the 1970s and 1980s actually proved was that mitochondria (plastids) are of alpha-proteobacterial (cyanobacterial) ancestry, while at least part of the nuclear-cytoplasmic component of eukaryotes is not. None of the cellular processes or biochemical selective advantages normally invoked in elaborations of the endosymbiont hypothesis were examined by these analyses, nor have they been since.

Ribosomal RNA phylogenies show that the deepest divisions in the eukaryotic tree (that is, the divisions leading to the eukaryotes that have been separated from us for the longest time) were those producing three of the four protist groups nominated by Cavalier-Smith as primitively amitochondriate (4). Such archezoa—which by their very existence bolstered faith in this part of the endosymbiont theory—should permit further tests of ideas about the endosymbiotic host. Similarly, rRNA showed us that there were two kinds of prokaryotes, radically different from each other, with one of these (the Archaea) perhaps more like what we might expect for the prokaryotic ancestor of the host. Rooting the tree with proteins of translation (primarily) have confirmed this Archaeal/Eukaryal affinity, and now we know that the cellular components considered by molecular biologists both fundamental and difficult to exchange—the molecular machineries of replication, transcription, and translation—are remarkably and specifically similar within the Archaeal/Eukaryal clade (5). Woese has argued, with justification, that the prokaryote/eukaryote dichotomy is misleading: if we are to have a dichotomy we should separate Bacteria from Archaea/Eukarya.

But the center has not altogether held: several observa-

This paper was originally presented at a workshop titled *Evolution: A Molecular Point of View*. The workshop, which was held at the Marine Biological Laboratory, Woods Hole, Massachusetts, from 24–26 October 1997, was sponsored by the Center for Advanced Studies in the Space Life Sciences at MBL and funded by the National Aeronautics and Space Administration under Cooperative Agreement NCC 2-896.

tions suggest that we should look to a period of abandonment or radical reformulation of broad hypothesis; look to it as a sign of the health of our science. I will discuss these observations in some detail.

First, one of the three archezoal lineages (the microsporidia) seems about to desert its deep position in the tree and (on the basis of several protein data sets) set up camp within the fungi (6). We are really not so sure as we thought we were about which groups are deep.

Second, all archezoal lineages (parabasalans and metamonads) have lost their innocence, mitochondrially (7, 8, 9, 10, 11, 12). All contain in their nuclear genomes alpha-proteobacterial genes whose products function in the mitochondria of mitochondriate eukaryotes. Either these protists had mitochondria, or they had a serious early involvement with alpha-proteobacterial symbionts (or alpha-proteobacterial food). The reduced mitochondrial genomes of animals and fungi (and even the larger ones of plants) are not the only possible end products of symbiosis; mitochondrial functions are not the only functions added (or substituted) by the influx of alpha-proteobacterial genes; and respiration may not have been the only, or most important, advantage accrued by the ancient hosts.

Third, endosymbiosis may no longer be the best way to accommodate all the data, and we must remind ourselves again that all that the molecular phylogenetic exercises of the 1970s and 1980s actually proved was that mitochondria (plastids) are of alpha-proteobacterial (cyanobacterial) ancestry, while at least part of the nuclear-cytoplasmic component of eukaryotes is not. As other papers in these proceedings will show, the alpha-proteobacterial inheritance of the eukaryotic nuclear genomic lineage is substantial and getting more substantial. Why don't we imagine that the host was an alpha-proteobacterium and the symbiont an archaeon, whose lasting contributions were the machineries of replication, transcription, and translation? Only, I think, because we see these functions as too fundamental to be replaced.

Fourth (for now), there is a problem with timing. Russell Doolittle's new dating scheme (pp. 356–358, these proceedings) has the divergence of cyanobacteria from the rest of the Bacteria as occurring much more recently than William Schopf's cyanobacterial fossils (pp. 351–355, these proceedings). In fact, no dating that accepts the standard tree and presumes a terrestrial origin for life can easily accommodate 3.5 billion-year-old cyanobacteria, and yet there they are (13).

So these are interesting times. New hypotheses (14) are required if we are not to abandon data which we have good reason to believe. Science is working!

Literature Cited

1. **Stanier, R. Y., and C. B. van Niel. 1962.** The concept of a bacterium. *Arch. Microbiol.* **42:** 17–35.
2. **Margulis, L. 1970.** P. 349 in *Origin of Eukaryotic Cells.* Yale University Press.
3. **Margulis, L. 1996.** Archael-eubacterial mergers in the origin of Eukarya: phylogenetic classification of life. *Proc. Natl. Acad. Sci. USA* **93:** 1071–1076.
4. **Cavalier-Smith, T. 1987.** The origin of cells: a symbiosis between genes, catalysts and membranes. *Cold Spring Harbor Symposium in Quantitative Biology* **52:** 805–824.
5. **Brown, J. R., and W. F. Doolittle. 1995.** Root of the universal tree of life based on ancient aminoacyl-tRNA synthetase gene duplications. *Proc. Natl. Acad. Sci. USA* **92:** 2441–2445.
6. **Keeling, P. J., and W. F. Doolittle. 1996.** Alpha-tubulin from early-diverging eukaryotic lineages and evolution of the tubulin family. *Mol. Biol. Evol.* **13:** 1297–1305.
7. **Roger, A. J., C. G. Clark, and W. F. Doolittle. 1996.** A possible mitochondrial gene in the early branching of amitochondriate protist *Trichomonas vaginalis. Proc. Natl. Acad. Sci. USA* **93:** 14618–14622.
8. **Horner, D., R. P. Hirt, S. Kilvington, D. Lloyd, and T. M. Embley. 1996.** Molecular data suggest an early acquisition of the mitochondrion endosymbiont. *Proc. R. Soc. London B* **263:** 1053–1059.
9. **Bui, E. T. N., P. J. Bradley, and P. J. Johnson. 1996.** A common evolutionary origin for mitochondria and hydrogenosomes. *Proc. Natl. Acad. Sci. USA* **93:** 9651–9656.
10. **Germot, A., H. Philippe, and H. Le Guyader. 1996.** Presence of a mitochondrial-type HSP70 in *Trichomonas* suggests a very early mitochondrial endosymbiosis in eukaryotes. *Proc. Natl. Acad. Sci. USA* **93:** 14614–14617.
11. **Germot, A., H. Philippe, and H. Le Guyader. 1997.** Loss of mitochondria in microsporidia: evidence from a mitochondrial-type HSP-70 in *Nosema locustae. Mol. Biochem. Parasitol.* **87:** 159–168.
12. **Roger, A. J., S. G. Svärd, J. Tovar, C. G. Clark, M. W. Smith, F. D. Gillin, and M. L. Sogin. 1998.** A mitochondrial-like chaperonin 60 gene in *Giardia lamblia*: evidence that diplomonads once harbored an endosymbiont related to the progenitor of mitochondria. *Proc. Natl. Acad. Sci. USA* **95:** 229–234.
13. **Doolittle, W. F. 1997.** Fun with geneaology. *Proc. Natl. Acad. Sci. USA* **94:** 12751–12753.
14. **Martin, W. F., and M. Müller. 1998.** The hydrogen hypothesis for the first eukaryote. *Nature* **392:** 37041.

Discussion

DESMARAIS: Shouldn't the cytoskeleton be an additional line of evidence, along with transcription, translation, and replication, as being difficult to replace and therefore supporting the ancestral eukaryote lineage?

F. DOOLITTLE: Yes, the cytoskeleton would be difficult to replace. It is not present in either Archaea or Bacteria. Whichever organism turns up with that cytoskeleton has a high probability of being the host.

REDFIELD: I want to point out that there is extensive evidence in bacteria for ongoing accumulation of genes (1). Somewhere between 15% and 30% of the *E. coli* genome is getting replaced about every 100 million years, depending on whose models you believe. If things are going on at that rate, it is surprising that we see any consistency in genomes.

F. DOOLITTLE: That is one of the things that's not given much thought in terms of lateral gene transfers. Suppose that I'm a bacterium and I want to get a new activity to do something. I've got my old activity, and one or two amino acid changes may not make it very different. However, if I can move to some other genus, I might pick up something that is ten amino acids different and has substantially different properties. It would be advantageous to acquire that change rather than to develop my own change.

REDFIELD: I will present a different perspective in my paper.

R. DOOLITTLE: I'm surprised that no one has yet brought up the matter of selfish operons. A paper that bears so heavily on what you just mentioned—exchanging large units among bacteria (2)—appeared last year.

ROGER: There are two kinds of evidence that I think are inconsistent with the Raff and Mahler model (3). One concerns vacuolar ATPases which, like informational molecules, reveal an affinity between Archaebacteria and eukaryotes (4), and these proteins function in the eukaryotic endomembrane system. The second is the signal recognition particle which, in Archaebacteria, appears to be much more similar to the eukaryotic particle than to the eubacterial version. The signal recognition particle is also functionally linked to the endomembrane system in eukaryotes. Therefore, there are at least two integral components of the endomembrane system of eukaryotes that have archaebacterial affinities. This suggests that the "host" organism possessing the endomembrane system that is required to engulf the endosymbiont was probably most closely related to present-day Archaebacteria, and that the alpha-proteobacterium was the endosymbiont that eventually became the mitochondrion—not the other way around.

F. DOOLITTLE: I think you've described the correct approach in trying to get new support for the endosymbiont hypothesis. I agree with you.

CAVALIER-SMITH: I also agree with Andrew (Roger). However, there are also the structural details that you rather dismissed. One of those details is that the alpha-proteobacteria have two membranes round them, whereas archaebacteria and eukaryotes do not. That is another really important structural similarity between the latter two groups. There are a number of additional molecular details shared by those groups; for example, the N-linked glycoproteins. It is not a very good idea to think that an alpha-proteobacterium was directly converted into the first eukaryote.

Literature Cited

1. **Lawrence, J. G., and H. Ochman. 1997.** Amelioration of bacterial genomes: rates of change and exchange. *J. Mol. Evol.* **44:** 383–397.
2. **Lawrence, J. G., and J. R. Roth. 1996.** Selfish operons: horizontal transfer may drive the evolution of gene clusters. *Genetics* **143:** 1843–1860.
3. **Mahler, H. R., and R. A. Raff. 1975.** The evolutionary origin of the mitochondrion: a non-symbiotic model. *Int. Rev. Cytol.* **43:** 2–124.
4. **Gogarten, J. P., H. Kibak, P. Dittrich, L. Taiz, E. J. Bowman, B. J. Bowman, M. F. Manolson, R. J. Poote, T. Date, and T. Oshima. 1989.** Evolution of the vacuolar H+-ATPase: implications for the origin of eukaryotes. *Proc. Natl. Acad. Sci. USA* **86:** 6661–6665.

Reference: *Biol. Bull.* **196:** 381–384. (June 1999)

Free-Living Flagellates From Anoxic Habitats and the Assembly of the Eukaryotic Cell

DAVID J. PATTERSON, ALASTAIR G. B. SIMPSON, AND NIMALIKA WEERAKOON

School of Biological Sciences, University of Sydney, NSW 2006, Australia

Comparative studies of protists conducted from the 1970s to 1990s led to models of their evolutionary relationships and, in turn, to models of the sequence in which eukaryotic cells were assembled (1, 2). In part, this was a result of ultrastructural studies of cell organization which had revealed that many familiar clusters of protists were polyphyletic. Such studies provided evolutionary biologists with a fairly robust catalog of about 70 types of eukaryotes (2, 3). Spurred on by ideas that early eukaryotes were created by symbiotic associations of previously independent organisms, investigators explored the relationships among many of these groups by a combination of ultrastructural and molecular comparisons; the latter were mostly based on the small subunit ribosomal RNA (4). An important feature of the emerging tree was that a number of lineages had arisen from early, pre-mitochondrial stages in eukaryote evolution and have survived to the present. These purportedly primitively amitochondriate protists included the microsporidia, pelobionts, diplomonads, retortamonads, oxymonads, entamoebae, trichomonads, and other parabasalids. Some or all of these taxa, in various combinations, have been referred to as the "Archezoa." This group has proven to be compositionally unstable, and it is paraphyletic. Nonetheless, the identification of this group assisted in the emergence of models of how eukaryotic cells might have developed. The models involved the autogenous emergence of the endoplasmic reticulum, nuclei, and dictyosomes and the autogenous or xenogenous evolution of flagella and microtubular and non-microtubular cytoskeletal structures, before the symbiotic acquisition of mitochondria and plastids. One strength of this model, with intermediate stages of eukaryote evolution being represented by extant "relict" organisms, is its testability through further phylogenetic analysis.

Over the last few years, further molecular studies seem to have refuted elements of this hypothesis. There is evidence that many archezoan groups are secondarily amitochondriate (4–8) although the diplomonads and parabasalids have clung more resolutely to the base of the eukaryotic tree than other taxa. The deep branching status of the pelobionts also remains in dispute (9–11). Largely because of the lack of appropriate investigations, there is no evidence that retortamonads or oxymonads have had a mitochondriate ancestry.

The case for primitively amitochondriate status remains unresolved for a number of taxa. If most or all of the groups assigned to the Archezoa are secondarily amitochondriate, then it significantly reduces our ability to present detailed and testable models of the sequence of innovations that led to the eukaryotic cell. We have addressed the possibility that there may be more primitively amitochondriate taxa that have not yet been described. We have used anoxic culture conditions to isolate amitochondriate (and mitochondriate) flagellates from low-oxygen freshwater, brackish, and marine habitats (12). We have been able to record previously unknown types of free-living protists from these habitats. Several of the organisms in question are described below and illustrated (Figs. 1, 2).

Mastigamoeba schizophrenia (Figs. 1.1, 2.1) is a pelobiont. In addition to lacking mitochondria, dictyosomes, and non-microtubular cytoskeletal structures, this species has some ultrastructural peculiarities including paired nuclei and basal bodies that lack the triplets of microtubules which characterize basal bodies in almost all other cells (10). These idiosyncrasies have been interpreted as evidence of a primitive status. However, other closely related species have now been examined and have more conventional arrangements of both organelles. This leaves open the alter-

---

This paper was originally presented at a workshop titled *Evolution: A Molecular Point of View*. The workshop, which was held at the Marine Biological Laboratory, Woods Hole, Massachusetts, from 24–26 October 1997, was sponsored by the Center for Advanced Studies in the Space Life Sciences at MBL and funded by the National Aeronautics and Space Administration under Cooperative Agreement NCC 2-896.

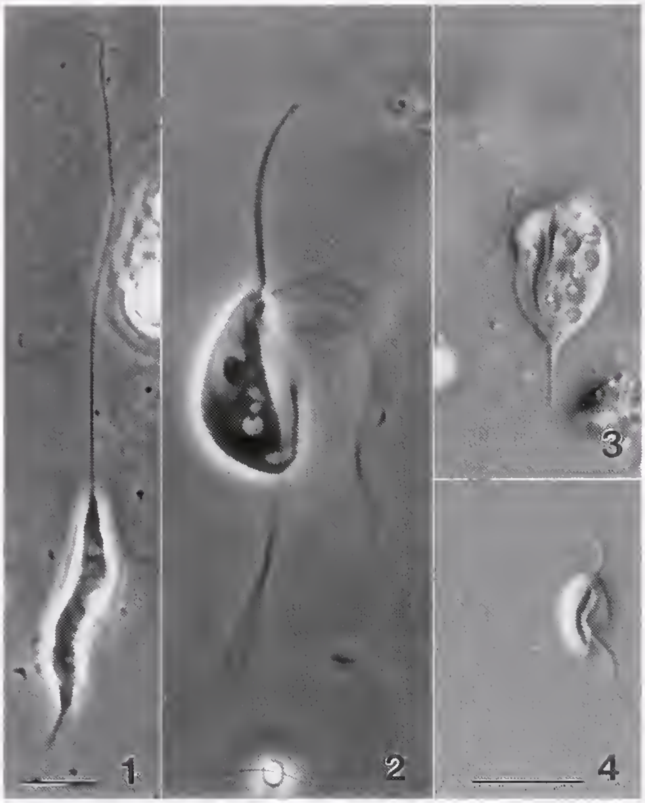

Figure 1. Light micrographs of living cells of selected free-living amitochondriate protists. (1) *Mastigamoeba schizophrenia* (phase contrast). (2) *Trimastix marina* (phase contrast). (3) *Chilomastix cuspidata* (differential interference contrast). (4) *Carpediemonas membranifera* (differential interference contrast). Scale bar for panel 1 represents 10 μm. Scale bar for panels 2–4 (in 4) represents 10 μm.

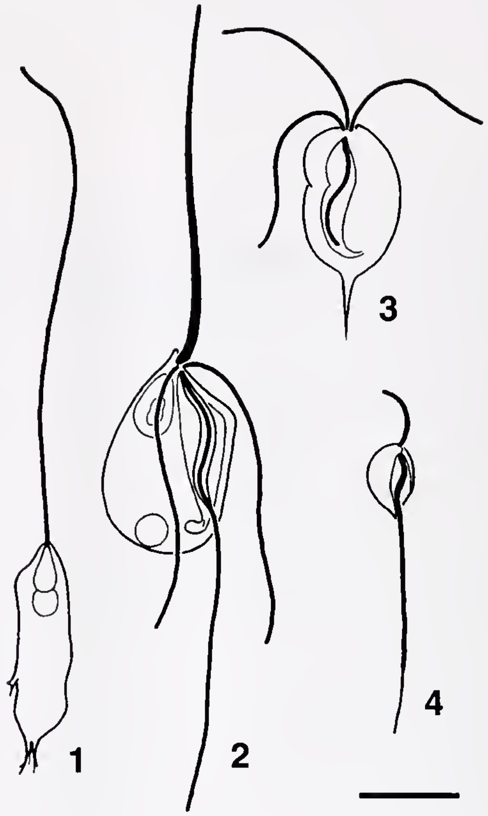

Figure 2. Line drawings of free-living amitochondriate protists. (1) *Mastigamoeba schizophrenia*. (2) *Trimastix marina*. (3) *Chilomastix cuspidata*. (4) *Carpediemonas membranifera*. Scale bar represents 10 μm for all panels.

native conclusion that the idiosyncrasies are derived within the pelobionts, unless the pelobionts are paraphyletic and basal.

The first ultrastructural survey (13) of a free-living retortamonad (*Chilomastix cuspidata*; Figs. 1.2, 2.2) isolated during these studies confirms the similarity with parasitic species and that the retortamonads are a monophyletic group. The group lacks mitochondria and is relevant to issues of early eukaryote evolution.

Trimastix was first described over a hundred years ago, but has been recorded only occasionally since that time. Recent ultrastructural observations of the type species, *T. marina* (Simpson, unpubl. obs.; Figs. 1.3, 2.3) and of *T. convexa* (14) have shown this group to be amitochondriate. This genus should be added to the group of potentially primitively amitochondriate taxa. The organization of *Trimastix* differs from that of all well-circumscribed groups but shares features with the retortamonads, jakobids (15), and *Carpediemonas* (see below).

Carpediemonas membranifera (Figs. 1.4, 2.4) is a small, recently described flagellate that lacks classical mitochondria (Simpson, unpubl. obs.). It has a ventral groove supported by a retortamonad-like system of flagellar roots, and a retortamonad-like arrangement of flagellar vanes, but is not assignable to the retortamonads. *Carpediemonas* and *Trimastix* also share several similarities with the mitochondriate jakobids (15).

The jakobids are a group of several genera of flagellates with two flagella inserting at the head of a ventral groove. They have mitochondria, but the mitochondrial genome of one species, *Reclinomonas americana*, is very unusual and argued to be primitive (16). These new studies lend support to the hypothesis that jakobids are evolutionarily linked with retortamonads, and that there remain a number of additional taxa that will contribute to understanding the evolution in this area. In attempting to understand evolutionary relationships among amitochondriate taxa, mitochondriate taxa should not, *a priori*, be excluded from study.

We are also attempting a broad survey approach to exploring whether the potentially amitochondriate taxa have more limited (or unusual) arrays of structural proteins than "complete" eukaryotes. Using immunocytochemical techniques such as indirect immunofluorescence microscopy and western blotting, we have sought to identify and localize actin, tubulin, and centrin (a member of the EF family of calcium-binding proteins) in *Chilomastix, Trimastix, Carpediemonas*, a pelobiont, and a trichomonad (Weerakoon, unpubl. obs.). All organisms studied have provided positive results with the antibody probes used in the immunofluorescence experiment, with the exception of a negative result for centrin in *Trimastix*.

The small number of primitively amitochondriate taxa will continue to hamper progress in understanding how eukaryotic cells were assembled. Our studies suggest that although there may not be a rich diversity of amitochondriate taxa, the exploration for previously unknown flagellates should be continued. Only with the isolation of more of these taxa can we fully realize the potential to reveal early events in eukaryotic evolution.

Acknowledgments

We thank the Australian Research Council and the Australian Biological Resources Study for financial support.

Literature Cited

1. **Cavalier-Smith, T. 1991.** Cell diversification in heterotrophic flagellates. Pp. 113–131 in *The Biology of Free-Living Heterotrophic Flagellates*, D. J. Patterson and J. Larsen, eds. Clarendon Press, Oxford.
2. **Patterson, D. J. 1994.** Protozoa, evolution and systematics. Pp. 1–14 in *Progress in Protozoology, Proceedings of the IX International Congress of Protozoology*, Fischer Verlag, Stuttgart.
3. **Patterson, D. J. 1999.** The diversity of Eukaryotes. *Am. Nat.* (in press).
4. **Sogin, M. L. 1991.** Early evolution and the origin of eukaryotes. *Curr. Opin. Genet. Dev.* **1:** 457–463.
5. **Roger, A. J., C. G. Clark, and W. F. Doolittle. 1996.** A possible mitochondrial gene in the early-branching amitochondriate protist *Trichomonas vaginalis*. *Proc. Natl. Acad. Sci. USA* **93:** 14618–14622.
6. **Keeling, P. J. 1998.** A kingdom's progress: Archezoa and the origin of eukaryotes. *Bioessays* **20:** 87–95.
7. **Hashimoto, T., L. B. Sanchez, T. Shirakura, M. Muller, and M. Hasegawa. 1998.** Secondary absence of mitochondria in *Giardia lamblia* and *Trichomonas vaginalis* revealed by valyl-trna synthetase phylogeny. *Proc. Natl. Acad. Sci. USA* **95:** 6860–6865.
8. **Roger, A. J., S. G. Svard, J. Tovar, C. G. Clark, M. W. Smith, F. D. Gillin, and M. L. Sogin. 1998.** A mitochondrial-like chaperonin 60 gene in *Giardia lamblia*: evidence that diplomonads once harbored an endosymbiont related to the progenitor of mitochondria. *Proc. Natl. Acad. Sci. USA* **95:** 229–234.
9. **Hinkle, G., D. D. Leipe, T. A. Nerad, and M. L. Sogin. 1994.** The unusually long small subunit ribosomal RNA of *Phreatamoeba balamuthi*. *Nucleic Acids Res.* **22:** 465–469.
10. **Simpson, A. G. B., C. Bernard, T. Fenchel, and D. J. Patterson. 1997.** The organisation of *Mastigamoeba schizophrenia* n. sp.: more evidence of ultrastructural idiosyncrasy and simplicity of pelobiont protists. *Eur. J. Protistol.* **33:** 87–98.
11. **Stiller, J. W., E. C. S. Duffield, and B. D. Hall. 1998.** Amitochondriate amoebae and the evolution of DNA-dependent RNA polymerase II. *Proc. Natl. Acad. Sci. USA* **95:** 11769–11774.
12. **Bernard, C., A. G. B. Simpson, and D. J. Patterson. 1999.** Some free-living flagellates (Protista) from anoxic habitats. *Ophelia* (in press).
13. **Bernard, C., A. G. B. Simpson, and D. J. Patterson. 1997.** An ultrastructural study of a free-living retortamonad, *Chilomastix cuspidata* (Larsen & Patterson, 1990) n. comb. (Retortamonadida, Protista). *Eur. J. Protistol.* **33:** 254–265.
14. **Brugerolle, G., and D. J. Patterson. 1997.** Ultrastructure of *Trimastix convexa* Hollande, an amitochondriate anaerobic flagellate with a previously undescribed organization. *Eur. J. Protistol.* **33:** 121–130.
15. **O'Kelly, C. J. 1993.** The jakobid flagellates: structural features of *Jakoba, Reclinomonas* and *Histiona* and implications for the early diversification of eukaryotes. *J. Eukaryot. Microbiol.* **40:** 627–636.
16. **Lang, B. F., G. Burger, C. J. O'Kelly, R. Cedergren, B. G. Golding, C. Lemieux, D. Sankoff, M. Turmel, and M. W. Gray. 1997.** *Reclinomonas americana* mitochondrial DNA: eubacterial genome in miniature. *Nature* **387:** 493–497.

Discussion

MARGULIS: What's the relation between thiobios that you describe and sulfuretum?

PATTERSON: The thiobios refers to that community which occurs in sediments below the aerated layer. It is distinguished by the black color of the metal sulfides. The thiobios was defined by Fenchel and Riedl (1). The sulfuretum is a habitat dominated by sulfur-metabolizing bacteria and is therefore largely the same thing.

MARGULIS: What about Foissner's Gondwanaland organism (2), *Hemimastix*? Where does it fit into your scheme?

PATTERSON: It has mitochondria and it is probably way up the tree.

MARGULIS: Does *Hemimastix* have any relatives?

PATTERSON: There are two related genera, together making up a group called the spironemids. The genera are *Hemimastix, Stereonema*, and *Spironema*, and as far as I understand, the group has got a worldwide distribution (2). They are all mitochondriate and probably don't bear on the early evolution of eukaryotes.

REDFIELD: Did you say that we should care about *Jakoba* partly because it has mitochondria, and then say that we shouldn't care about all of these other things because they had mitochondria and therefore weren't interesting?

PATTERSON: No, I didn't say that. The significance of *Jakoba* is that on morphological criteria it clusters with some of the potentially primitively amitochondriate taxa, such as retortamonads. This makes it unusual among the mitochondriate taxa. There clearly has been diversification going on in organisms without mitochondria, and the jakobids occupy a territory or one of the territories that should be targeted to understand where mitochondria were acquired.

REDFIELD: Do we know that *Hemimastix* couldn't possibly be interesting?

PATTERSON: *Hemimastix* currently has no relevance to the early evolution of eukaryotic cells because there is no evidence to group it with amitochondriate organisms.

GUERRERO: I think the difference between sulfureta and thiobios is clear. In a sulfuretum, the complete cycling of sulfur occurs and the aerobic consumption by chemolithotrophs is included. Have you observed any methanogenic bacterial symbionts? In other protists, methanogenic bacterial symbionts used for feeding have been observed.

PATTERSON: I stand corrected about sulfuretum, thank you. Only one of the species (*Postgaardi mariagerensis*) that we have looked at has got associated bacteria, and they are external to the body. In looking at flagellates from all kinds of habitats, a very high proportion carry endosymbiotic bacteria of some form.

PALMER: Am I correct that you are looking for eukaryotes, literally under the microscope?

PATTERSON: Yes.

PALMER: What are your criteria for identifying, or distinguishing, eukaryotes from non-eukaryotes? Could you be missing interesting things that are simple, small, and reduced? There are some eukaryotes that are very tiny and perhaps others that may be missed entirely that could be early arisers.

PATTERSON: The answer to the second part of your question is, of course, we could be missing something. There is no suggestion that our results represent a comprehensive survey. We have carried out direct ultrastructure examination of the sediments as well, and find a number of rather unusual things.

CAVALIER-SMITH: Mitch Sogin presented data at another conference in which he had a retortamonad as a sister group to diplomonads on a ribosomal RNA tree, and unless I am mistaken, that would be molecular evidence for two of the three Metamonad groups actually belonging together.

PATTERSON: I do not recollect the details of that tree. I have problems with a number of the taxa that are being included in sequence trees. We are not supplied with any evidence of why that name has been assigned to that organism, and therefore the identity of the sequence is not verified and possibly not verifiable. I am disquieted about the proliferation of information on organisms without confirmed identities.

CAVALIER-SMITH: You are saying that you don't actually know what that particular organism is.

PATTERSON: I have no idea of what the organism was. All I know is that one was given a name, *Retortamonas*, but I don't know that it is a *Retortamonas*.

UNIDENTIFIED: Have you caught any of these in division? What does the nucleus look like?

PATTERSON: Some of the pelobionts have rather unusual-looking nuclei, but we have not conducted a systematic survey. As far as we can see there are conventional nuclear pores in all species we have looked at. Some of the organisms lack separation of the two layers of the nuclear envelope. In some cases, nucleoli look unusual—at least, in one there is some kind of inclusion that we haven't been able to characterize. There is some sense that there is a bit more variation in nuclear appearance, but this has not been studied in any systematic fashion.

ROGER: I wanted to know what you really don't like about the taxon Archezoa. Is it that it is paraphyletic, or is it that the composition changes, or is it both? I use it because it is a useful term to describe the concept of pre-mitochondrial eukaryotes. We need a name for that group of organisms, even if they do not form a clade.

PATTERSON: Unfortunately there is an alternative name that is defined by evolutionary events. It is one that Mitch Sogin and I came up with but are a bit embarrassed about using—it is the name Hypochondria. This is defined phylogenetically as the eukaryotes excepting those derived after the origin of mitochondria. The problem with Archezoa is that it is a hybrid concept. It has a phylogenetic component and a compositional component. These components do not overlap perfectly, so that the different meanings of the term generate confusion and uncertainty. The composition of the group has been particularly unstable. When someone refers to Archezoa, I do not actually know which organisms they are talking about. Therefore, I guess that my primary concern is with the compositional instability. I think it would be better to refer to them as those eukaryotes that came before the appearance of mitochondria.

LEADBETTER: What is the evidence that these entities that you are calling mitochondria are really mitochondria? Have you done any functional studies on them, or is this simply electron microscopic evidence?

PATTERSON: My evidence is the ultrastructural appearance—two membranes with cristae.

LEADBETTER: So in terms of the function of these so-called mitochondria, could they be using something other than molecular oxygen as a terminal electron acceptor?

PATTERSON: I presume that is a possibility.

Literature Cited

1. **Fenchel, T., and R. J. Riedl. 1970.** The sulphide system: a new biotic community underneath the oxidized layer of marine sand bottoms. *Mar. Biol.* **7:** 255–268.
2. **Foissner, I., and W. Foissner. 1993.** Revision of the family Spironemidae Doflein (Protista, Hemimastigophora), with description of two new species, *Sprionema terricola* n. sp. and *Stereonema geiseri* n.g., n. sp. *J. Eukaryot. Microbiol.* **40:** 422–438.

Reference: *Biol. Bull.* **196:** 385–388. (June 1999)

The Effect of Secondary Loss on Our Views of Eukaryotic Evolution

C. GRAHAM CLARK

Department of Infectious and Tropical Diseases, London School of Hygiene and Tropical Medicine, London, England

Traditionally, phylogenetic relationships among eukaryotes have been inferred using morphological information. In prokaryotes, morphology is not very useful for this purpose and other approaches have been preferred. The morphological bias among those of us who study eukaryotes has led us into a number of traps. Even with the advent of molecular sequence data, we have failed to break some of our bad habits in interpreting phylogenetic trees. The common false assumption, in all its guises, can be boiled down to one phrase—simple equals primitive. The fundamental flaw that has been ignored time and time again is that simple can also mean derived. Misinterpreting the absence of a character as a sign of an organism's primitive nature often results in a false view of eukaryotic evolution.

Secondary loss is a pervasive characteristic of eukaryotic evolution. Parasites appear to be particularly susceptible to secondary simplification or loss of structure. This can be illustrated from our studies of the evolution of eukaryotic organelles.

A popular choice as paradigm for the ancestral eukaryote, especially among those who worked with the organism, was for many years *Entamoeba histolytica*, the agent of amoebic dysentery. This organism lacks many typical eukaryotic features—mitochondria, Golgi apparatus, flagella, rough endoplasmic reticulum—and has other unusual characteristics that could be interpreted as primitive. However, when ribosomal RNA-based phylogenetic trees that included *Entamoeba* species became available, the branch leading to these organisms was not basal to other eukaryotes, as had been expected, but instead arose relatively recently (1). Rather than accept that the unusual features of *Entamoeba* might be derived rather than primitive, some authors took the stance that the placement of *Entamoeba* on the ribosomal RNA tree must be wrong (2, 3).

It is quite clear that, although *Entamoeba* lacks a morphological Golgi apparatus and rough endoplasmic reticulum, it does have their functional equivalent. Proteins transported to the surface of the cell are processed as in more typical eukaryotes—signal peptides are cleaved, proteins are glycosylated, etc. Indeed, genes encoding some of the proteins known to be involved in those processes have recently been identified in *E. histolytica.* Evidence for the secondary loss of mitochondria has been more elusive. However, two genes coding for proteins with a mitochondrial location in other eukaryotes have been cloned and encode what appear to be signal peptides at the amino terminus of proteins, implying that a subcellular compartment still exists (4, 5). Extensive phylogenetic analyses of the gene encoding chaperonin 60 confirm the mitochondrial affinities of the *E. histolytica* gene (4, 5). Very recently, the location of the chaperonin 60 protein in the *E. histolytica* cell has been investigated, and it is indeed found in a small, subcellular compartment (6, 7). The putative signal peptide has also been shown to be required for the protein to reach this location (7), which appears to be a highly reduced mitochondrion.

Ribosomal RNA-based phylogenetic trees have consistently placed three other amitochondrial protistan lineages at the base, although their branching order is unresolved. These are the diplomonads, the trichomonads, and the microsporidia, all groups that consist largely of parasitic species (8). Together with a few free-living organisms, these constitute the Archezoa, a group of eukaryotes thought to be descended from ancestors that branched from the eukaryotic

---

This paper was originally presented at a workshop titled *Evolution: A Molecular Point of View*. The workshop, which was held at the Marine Biological Laboratory, Woods Hole, Massachusetts, from 24–26 October 1997, was sponsored by the Center for Advanced Studies in the Space Life Sciences at MBL and funded by the National Aeronautics and Space Administration under Cooperative Agreement NCC 2-896.

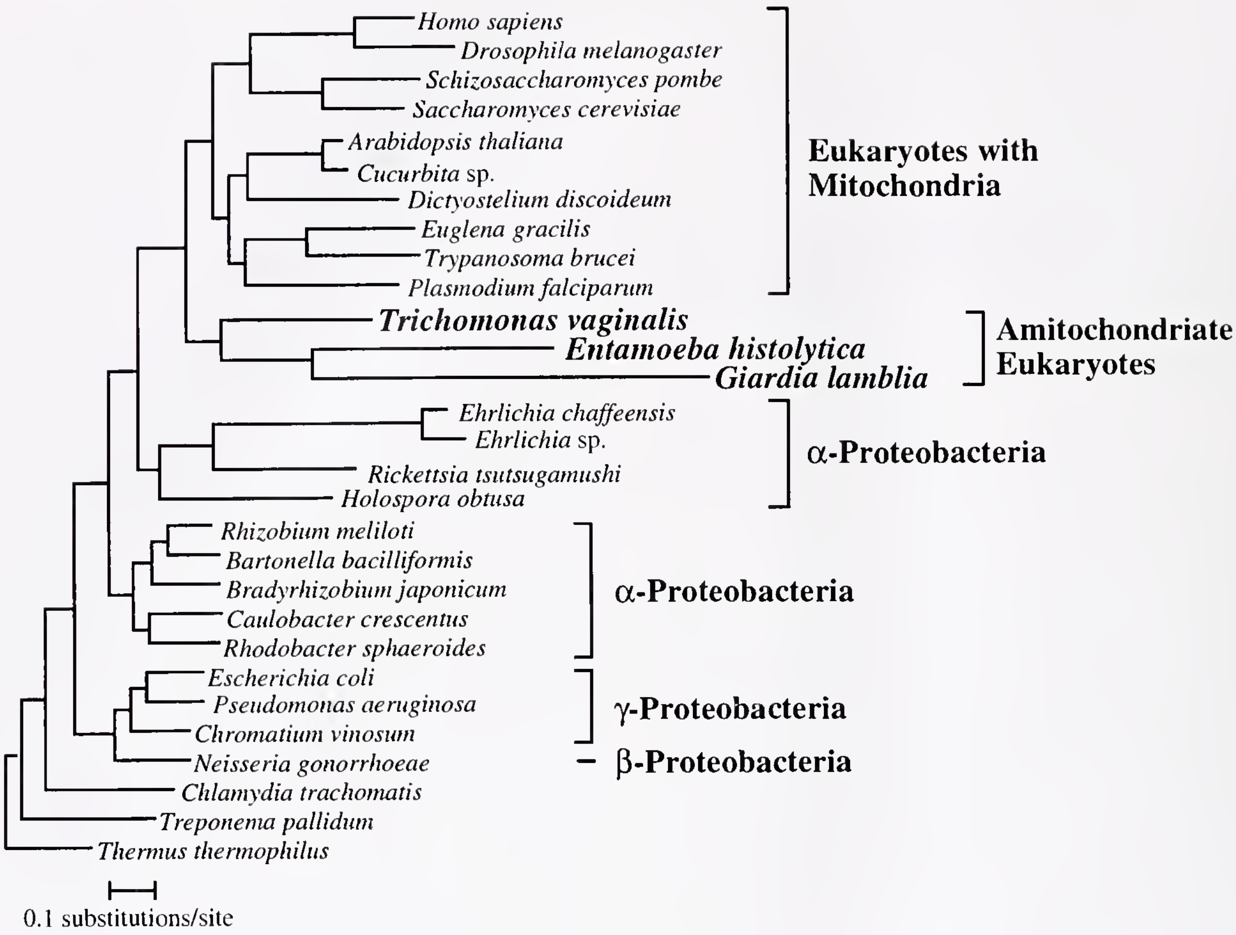
Homo sapiens
Drosophila melanogaster
Schizosaccharomyces pombe
Saccharomyces cerevisiae
Arabidopsis thaliana
Cucurbita sp.
Dictyostelium discoideum
Euglena gracilis
Trypanosoma brucei
Plasmodium falciparum
Eukaryotes with Mitochondria
Trichomonas vaginalis
Entamoeba histolytica
Giardia lamblia
Amitochondriate Eukaryotes
Ehrlichia chaffeensis
Ehrlichia sp.
Rickettsia tsutsugamushi
Holospora obtusa
α-Proteobacteria
Rhizobium meliloti
Bartonella bacilliformis
Bradyrhizobium japonicum
Caulobacter crescentus
Rhodobacter sphaeroides
α-Proteobacteria
Escherichia coli
Pseudomonas aeruginosa
Chromatium vinosum
γ-Proteobacteria
Neisseria gonorrhoeae
β-Proteobacteria
Chlamydia trachomatis
Treponema pallidum
Thermus thermophilus
0.1 substitutions/site

Figure 1. Protein Maximum Likelihood relationships among the eukaryotic chaperonins cpn60 and their bacterial GroEL homologs (modified from fig. 4 of ref. 5).

tree prior to the acquisition of the mitochondrial symbiont (9). (*Entamoeba* had also been included in this group before the ribosomal RNA sequence data became available.) The rationale for the Archezoa was

no mitochondria + early branch = primitive.

However, the experience with *Entamoeba* has shown that the lack of morphological mitochondria does not exclude the presence of mitochondrially derived genes, and even mitochondrially derived compartments. Recent data for species belonging to these three archezoan groups indicate that each contains chaperonin genes of mitochondrial origin (5, 10–15; Fig. 1). In the case of the trichomonads the proteins have been localized to the hydrogenosome (10), an energy-generating organelle that already had been suspected by some of having mitochondrial origins. The location of the chaperonin proteins in the other groups is as yet unknown. Although other scenarios might describe how these organisms acquired the chaperonin genes, descent from a mitochondrion-bearing ancestor remains the simplest explanation. The discovery of genes of mitochondrial origin in these lineages does not exclude the possibility that they represent the earliest branching eukaryotic lineages. Only the interpretation of their ancestor has changed.

The Archezoa as a taxon is largely defunct. We now have no strong candidates for extant, primitively amitochondriate eukaryotes, although a few organisms remain to be studied. Why have we not found any primitively amitochondriate eukaryotes? There are several possibilities.

1. They no longer exist. Extant life may have out-competed these early forms and led to their extinction.
2. We have not looked in the right place. The study of eukaryotes has been highly biased towards those that can be cultured, and especially towards parasitic forms among the amitochondriate organisms. We should be employing environmental PCR to detect the existence of earlier branching eukaryotes that cannot be cultured *in vitro*, as this method has been used successfully for Bacteria and Archaea.
3. Perhaps primitively amitochondriate eukaryotes never

> existed in the first place. Is it possible that the symbiosis that gave rise to the mitochondrion was also the impetus for the development of the nuclear membrane, the defining characteristic of the eukaryote?

Certain anaerobic ciliates, flagellates, and rumen fungi have also apparently lost mitochondria and have often gained hydrogenosomes. Loss, or apparent loss, of organelles is not limited to mitochondria. Apicomplexa are now known to have a drastically reduced plastid which was not identified until very recently, and until a few years ago its presence was not even suspected (16). There are many examples of other structures being lost secondarily. For example, amoeboid protists, which were initially thought to be primitive, are now known to be derived from cytoskeleton-bearing ancestors (17).

All of these conclusions about secondary loss depend on the tree being used having a topology that reflects the true pattern of evolution; but in many cases, specific relatives can be identified that have not undergone secondary loss. One surprising example of such a case is provided by *Blastocystis hominis.* This organism is a very common human intestinal parasite. In appearance it is a spherical cell, consisting of a large central vacuole surrounded by a thin layer of cytoplasm, and lacking cilia or flagella. Historically it has been described as either a yeast, a sporozoan, or an amoeba; but more recently it had languished among those frustrating organisms labeled *incertae cedis.* Much to everyone's surprise, *Blastocystis* was shown, by small subunit ribosomal RNA gene sequencing, to be a stramenopile or heterokont, and its closest relative is *Proteromonas,* a flagellate (18). *Blastocystis* has secondarily lost essentially all of the morphological characteristics that define an organism as a heterokont.

Secondary loss of organelles and other cell features has led us into false conclusions, both about recent lineages and about those at the base of the eukaryotic tree. I believe that we must be very careful before we interpret a character, or the absence of a character, as being a primitive feature, even when the organism is on an early branch. Perhaps we will be led into fewer traps in the future.

Literature Cited

1. **Sogin, M. L. 1991.** Early evolution and the origin of eukaryotes. *Curr. Opin. Genet. Dev.* **1:** 457–463.
2. **Meza, I. 1992.** *Entamoeba histolytica*: phylogenetic considerations. A review. *Arch. Med. Res.* **23:** 1–5.
3. **Bakker-Grunwald, T., and C. Wöstmann. 1993.** *Entamoeba histolytica* as a model for the primitive eukaryotic cell. *Parasitol. Today* **9:** 27–31.
4. **Clark, C. G., and A. J. Roger. 1995.** Direct evidence for secondary loss of mitochondria in *Entamoeba histolytica. Proc. Natl. Acad. Sci. USA* **92:** 6518–6521.
5. **Roger, A. J., S. G. Svärd, J. Tovar, C. G. Clark, M. W. Smith, F. D. Gillin, and M. L. Sogin. 1998.** A mitochondrial-like chaperonin 60 gene in *Giardia lamblia*: Evidence that diplomonads once harbored an endosymbiont related to the progenitor of mitochondria. *Proc. Natl. Acad. Sci. USA* **95:** 229–234.
6. **Mai, Z., S. Ghosh, M. Frisardi, B. Rosenthal, R. Rogers, and J. Samuelson. 1999.** Hsp60 is targeted to a cryptic mitochondrion-derived organelle ("Crypton") in the microaerophilic protozoan parasite *Entamoeba histolytica. Mol. Cell. Biol.* **19:** 2198–2205.
7. **Tovar, J., A. Fischer, and C. G. Clark. 1999.** The mitosome, a novel organelle related to mitochondria in the amitochondriate parasite *Entamoeba histolytica. Mol. Microbiol.* (In press).
8. **Leipe, D. D., J. H. Gunderson, T. A. Nerad, and M. L. Sogin. 1993.** Small subunit ribosomal RNA of *Hexamita inflata* and the quest for the first branch in the eukaryotic tree. *Mol. Biochem. Parasitol.* **59:** 41–48.
9. **Cavalier-Smith, T. 1987.** Eukaryotes with no mitochondria. *Nature* **326:** 332–333.
10. **Bui, E. T., P. J. Bradley, and P. J. Johnson. 1996.** A common evolutionary origin for mitochondria and hydrogenosomes. *Proc. Natl. Acad. Sci. USA* **93:** 9651–9656.
11. **Germot, A., H. Philippe, and H. Le Guyader. 1996.** Presence of a mitochondrial-type 70-kDa heat shock protein in *Trichomonas vaginalis* suggests a very early mitochondrial endosymbiosis in eukaryotes. *Proc. Natl. Acad. Sci. USA* **93:** 14614–14617.
12. **Horner, D. S., R. P. Hirt, S. Kilvington, D. Lloyd, and T. M. Embley. 1996.** Molecular data suggest an early acquisition of the mitochondrion endosymbiont. *Proc. R. Soc. Lond. B. Biol. Sci.* **263:** 1053–1059.
13. **Roger, A. J., C. G. Clark, and W. F. Doolittle. 1996.** A possible mitochondrial gene in the early-branching amitochondriate protist *Trichomonas vaginalis. Proc. Natl. Acad. Sci. USA* **93:** 14618–14622.
14. **Germot, A., H. Philippe, and H. Le Guyader. 1997.** Evidence for loss of mitochondria in Microsporidia from a mitochondrial-type HSP70 in *Nosema locustae. Mol. Biochem. Parasitol.* **87:** 159–168.
15. **Hirt, R. P., B. Healy, C. R. Vossbrinck, E. U. Canning, and T. M. Embley. 1997.** A mitochondrial Hsp70 orthologue in *Vairimorpha necatrix*: molecular evidence that microsporidia once contained mitochondria. *Curr. Biol.* **7:** 995–998.
16. **Kohler, S., C. F. Delwiche, P. W. Denny, L. G. Tilney, P. Webster, R. J. Wilson, J. D. Palmer, and D. S. Roos. 1997.** A plastid of probable green algal origin in Apicomplexan parasites. *Science* **275:** 1485–1489.
17. **Silberman, J. D., C. G. Clark, and M. L. Sogin. 1996.** *Dientamoeba fragilis* shares a recent common evolutionary history with the trichomonads. *Mol. Biochem. Parasitol.* **76:** 311–314.
18. **Silberman, J. D., M. L. Sogin, D. D. Leipe, and C. G. Clark. 1996.** Human parasite finds taxonomic home. *Nature* **380:** 398.

Discussion

FORTERRE: In your introduction, you mentioned the case of *Mycoplasma*, which has lost the cell wall. I find it strange that people have difficulty in accepting that the same thing occurred at the molecular level. For example, that bacteria have lost the archaeal transcription factors.

CLARK: I agree. There are lots of similarities between *Mycoplasma* and Microsporidia in terms of their lifestyle, genome reduction, and all sorts of other features. There are many parallels.

OLSEN: In both of these situations, it doesn't detract from the issue that the eukaryote, or any other organism, becomes simplified. Unless we want to invoke a miracle of special creation, organisms came from simpler progenitors. We are pushing the derivation point back in time. How did we get to the more complicated organisms? What you're pointing out in both cases is that we should think carefully about how to choose our examples of simple organisms.

CLARK: I agree; you must be careful not to jump to conclusions.

MARGULIS: Does *Blastocystis* have mitochondria, sexual recombination, chromosomes, a karyotype, and a mitotic spindle?

CLARK: Some of these properties have not been studied.

MARGULIS: Can this organism be cultivated?

CLARK: Yes, and in axenic culture too. It does have mitochondria, at least morphological mitochondria, but it does not appear to have cytochromes. It does have chromosomes; or at least pulse-field gel electrophoresis generates bands of megabase size that are probably equivalent to chromosomes. I don't believe they are visible under normal staining conditions. I'm not sure about the spindle, but recently there have been some good reviews on the organism that would give you additional information (1).

PALMER: You mentioned the scattered distribution of amoeba-like organisms on ribosomal RNA trees. However, almost all of the few sampled amoeba-like organisms except for *Entamoeba* clearly come together on actin trees. *Physarum*, *Dictyostelium*, and several others come together as a very, very tight-knit group. This suggests to me that there may be relatively few transitions to that state.

CLARK: Yes, you are correct. As I indicated, interpretation is all dependent upon the topology of the tree being examined. Amoeba-like organisms are scattered all over the place (on the ribosomal tree). However, that is not the case with the actin tree. It may be that actin is a special case, or it may be that ribosomal RNA is a special case. We don't really know which is correct. You are right, if they do cluster in the actin tree, as they do, then perhaps secondary loss leading to amoeba-like locomotion is not a common occurrence. It is, however, a common occurrence based on the ribosomal tree topology.

Literature Cited

1. **Stenzel, D. J., and P. F. L. Boreham. 1996.** *Blastocystis hominis* revisited. *Clin. Microbiol. Rev.* **9:** 563–584.

Reference: *Biol. Bull.* **196:** 389–392. (June 1999)

Phylogenetic Position of Amitochondriate Protists in the Evolution of Eukaryotes

MASAMI HASEGAWA AND TETSUO HASHIMOTO

The Institute of Statistical Mathematics, 4-6-7 Minami-Azabu, Minato-ku, Tokyo 106-8569 Japan

Mitochondria are very likely to have descended from eubacteria by endosymbiosis. Therefore, phylogenetic placement of amitochondriate protists is important in understanding the origin and early evolution of eukaryotes. That is, if some of the amitochondriate protists turn out to represent deep branchings in the eukaryotic tree, they are very likely to be living relics of the earliest phase of eukaryotic evolution—before the endosymbiotic origin of proto-mitochondria. We have investigated the phylogenetic relationship among protists, including amitochondrial ones, by analyzing amino acid sequences of translation elongation factors (EF-1alpha and EF-2) and isoleucyl- and valyl-tRNA synthetases (ileRS and valRS).

Until now, both of the EF phylogenies (EF-1alpha tree is shown in Fig. 1) clearly and consistently suggested (a) that three amitochondriate protists, *Glugea plecoglossi* (microsporidian), *Giardia lamblia* (diplomonad), and *Trichomonas tenax* (trichomonad), represent an early-branching eukaryotic group; and that among them, the divergence of *Glugea* seems to be the earliest (1–5); and (b) that another amitochondrial protist, *Entamoeba histolytica,* is likely to have diverged after the divergences of some mitochondrion-containing protists, but is not likely to have diverged later than euglenoids, as suggested by the SrRNA tree (6). Among the crown groups, animals and fungi form a clade that excludes plants as an outgroup (7).

Although the EF phylogenies suggest that, among eukaryotes, the branching of microsporidians was earliest, the HSP70 (heat-shock protein 70) phylogeny suggests that microsporidians are closely related to fungi, which diverged from animals at a later stage of eukaryotic evolution (8, 9). Thus there is a discrepancy among the data available, and more data and more careful analyses are therefore needed to finally determine the phylogenetic place of microsporidians. Since the edge lengths leading to microsporidians are very long relative to other lineages in the EF phylogenies, more sophisticated analyses might be needed to take account of the unusual mode of evolution. Molecular phylogenetics is still in its infancy with respect to explaining, or circumventing, abnormal modes of sequence evolution (10), and a methodological development of data analyses is really required.

There are thus some uncertainties about microsporidia, but the EF phylogenies might seem to be consistent with the proposal, made by Cavalier-Smith (11, 12) before any molecular data became available, that diplomonads (including *Giardia*), parabasalids (including *Trichomonas*), and microsporidia could be primitively amitochondriate, and that a taxon Archezoa could be created for these protists.

However, the early branching does not necessarily mean that these lineages lack mitochondria primitively. There still remains the possibility that they lost their mitochondria secondarily, during the course of evolution. To unravel this problem, several investigators have searched in amitochondriate species for genes that could have been part of the ancestral mitochondrion but were subsequently transferred to the nuclear genome. And such genes have been recently detected in several amitochondriate organisms. The most compelling data in this respect are heat shock proteins or molecular chaperones that play a key role in mitochondrial biogenesis. Genes for such proteins are found in the nuclear genomes of amitochondriate organisms, such as microsporidia (8, 13), parabasalids (14–17), and entamoebids (18). These results strongly argue that these organisms did not have amitochondriate ancestors. Among the early-branch-

This paper was originally presented at a workshop titled *Evolution: A Molecular Point of View.* The workshop, which was held at the Marine Biological Laboratory, Woods Hole, Massachusetts, from 24–26 October 1997, was sponsored by the Center for Advanced Studies in the Space Life Sciences at MBL and funded by the National Aeronautics and Space Administration under Cooperative Agreement NCC 2-896.

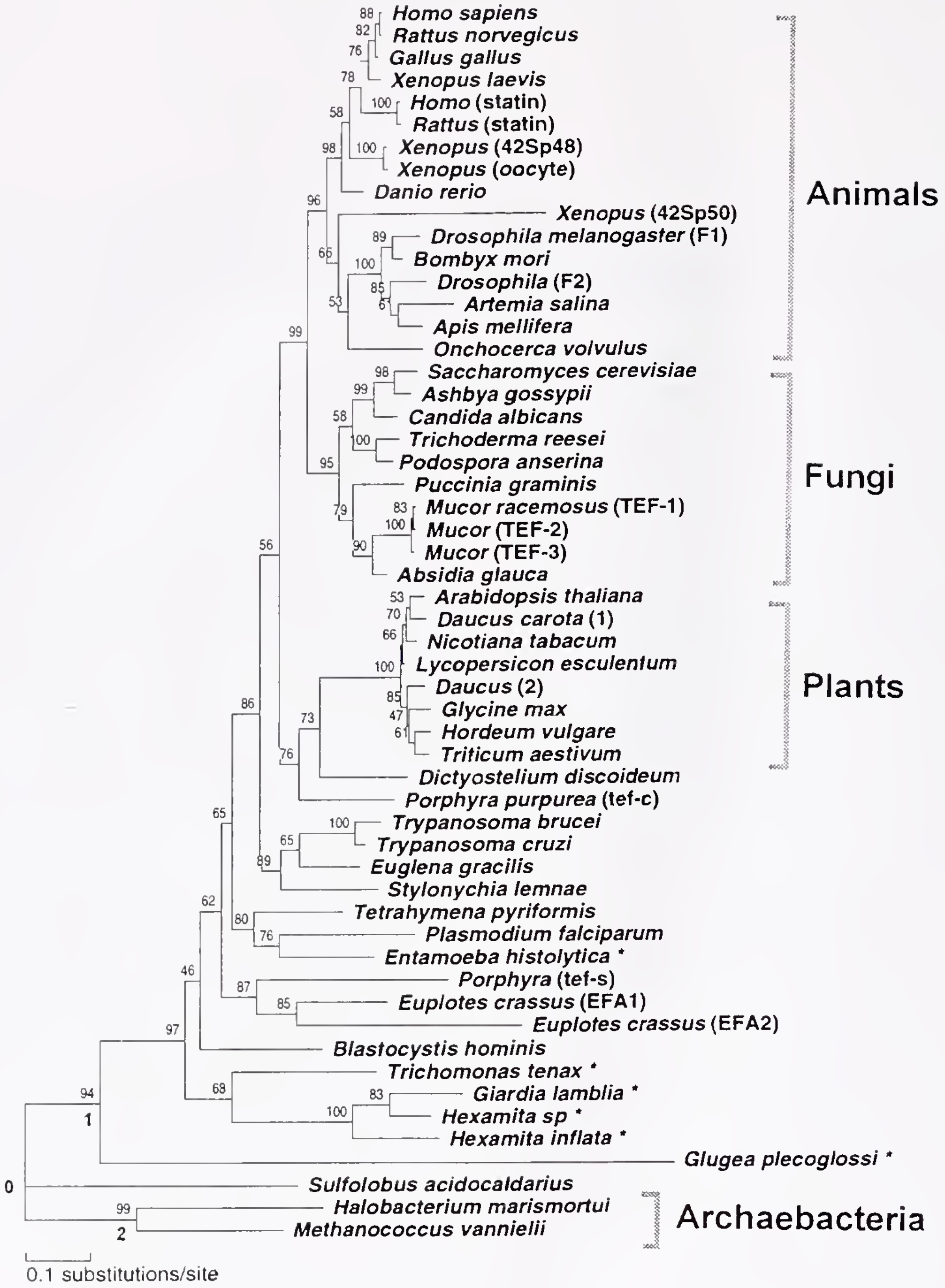
Homo sapiens
Rattus norvegicus
Gallus gallus
Xenopus laevis
Homo (statin)
Rattus (statin)
Xenopus (42Sp48)
Xenopus (oocyte)
Danio rerio
Xenopus (42Sp50)
Drosophila melanogaster (F1)
Bombyx mori
Drosophila (F2)
Artemia salina
Apis mellifera
Onchocerca volvulus
Animals
Saccharomyces cerevisiae
Ashbya gossypii
Candida albicans
Trichoderma reesei
Podospora anserina
Puccinia graminis
Mucor racemosus (TEF-1)
Mucor (TEF-2)
Mucor (TEF-3)
Absidia glauca
Fungi
Arabidopsis thaliana
Daucus carota (1)
Nicotiana tabacum
Lycopersicon esculentum
Daucus (2)
Glycine max
Hordeum vulgare
Triticum aestivum
Plants
Dictyostelium discoideum
Porphyra purpurea (tef-c)
Trypanosoma brucei
Trypanosoma cruzi
Euglena gracilis
Stylonychia lemnae
Tetrahymena pyriformis
Plasmodium falciparum
Entamoeba histolytica *
Porphyra (tef-s)
Euplotes crassus (EFA1)
Euplotes crassus (EFA2)
Blastocystis hominis
Trichomonas tenax *
Giardia lamblia *
Hexamita sp *
Hexamita inflata *
Glugea plecoglossi *
Sulfolobus acidocaldarius
Halobacterium marismortui
Methanococcus vannielii
Archaebacteria
0
1
2
0.1 substitutions/site

Figure 1. Eukaryotic tree of EF-1alpha with archaebacteria as an outgroup (22). The tree was estimated by the ProtML (protein maximum likelihood program; 23) with the Jones-Taylor-Thornton model. The horizontal length of each edge is proportional to the estimated number of amino acid substitutions. For each internal edge, a local bootstrap probability (LBP; in %) estimated by the RELL (resampling of estimated log-likelihood) method with 10,000 replications is shown. * Denotes a mitochondrion-lacking protozoan species.

ing amitochondriate protists, diplomonads remained as possible candidates for being primitively amitochondriate.

To test this possibility, we examined valyl-tRNA synthetase (ValRS) (19). Only a single gene for ValRS is present in the nuclear genomes of fungi and animals, and the product of this gene is thought to be functional, not only in the cytosol, but also in mitochondria. A ValRS phylogeny rooted with isoleucyl-tRNA synthetases (IleRS) showed that eukaryotic ValRS sequences form a monophyletic clade that is close to gram-negative bacteria, suggesting that the gene coding for this protein has been transferred from the ancestral mitochondrion (20). Brown and Doolittle sequenced a partial ValRS gene from *Trichomonas*, and showed that the gene of this amitochondriate eukaryote belongs to the same clade as the gene of mitochondriate eukaryotes. This suggests that, in its evolutionary past, *Trichomonas* once harbored mitochondria.

We sequenced the complete gene encoding ValRS from *Trichomonas vaginalis* and *Giardia lamblia* (19). The evidence obtained shows that not only *T. vaginalis*, but also *G. lamblia*, carries the relics of a past mitochondrial clade (21). The data mentioned above support the notion that the critical endosymbiotic event occurred before the divergence of the extant lineages of eukaryotes and make it unlikely that we will discover living relics of a putative premitochondrial state in eukaryotic evolution; that is, Archezoa.

Literature Cited

1. **Hashimoto, T., Y. Nakamura, F. Nakamura, T. Shirakura, J. Adachi, N. Goto, K. Okamoto, and M. Hasegawa. 1994.** Protein phylogeny gives a robust estimation for early divergences of eukaryotes: phylogenetic place of a mitochondria-lacking protozoan, *Giardia lamblia*. *Mol. Biol. Evol.* **11:** 65–71.
2. **Hashimoto, T., and M. Hasegawa. 1996.** Origin and early evolution of eukaryotes inferred from the amino acid sequences of translation elongation factors 1alpha/Tu and 2/G. *Adv. Biophys.* **32:** 73–120.
3. **Kamaishi, T., T. Hashimoto, Y. Nakamura, F. Nakamura, S. Murata, N. Okada, K. Okamoto, M. Shimizu, and M. Hasegawa. 1996.** Protein phylogeny of EF-1alpha suggests microsporidians are extremely ancient eukaryotes. *J. Mol. Evol.* **42:** 257–263.
4. **Kamaishi, T., T. Hashimoto, Y. Nakamura, Y. Masuda, F. Nakamura, K. Okamoto, M. Shimizu, and M. Hasegawa. 1996.** Complete nucleotide sequences of the genes encoding translation elongation factors 1alpha and 2 from a microsporidian parasite, *Glugea plecoglossi*: implications for the deepest branching of eukaryotes. *J. Biochem.* **120:** 1095–1103.
5. **Yamamoto, A., T. Hashimoto, E. Asaga, M. Hasegawa, and N. Goto. 1997.** Phylogenetic position of mitochondrion-lacking protozoan, *Trichomonas tenax*, based on amino acid sequences of elongation factors 1alpha and 2. *J. Mol. Evol.* **44:** 98–105.
6. **Nakamura, Y., T. Hashimoto, T. Kamaishi, J. Adachi, F. Nakamura, K. Okamoto, and M. Hasegawa. 1996.** Phylogenetic place of kinetoplastid protozoa inferred from protein phylogenies of elongation factors 1alpha and 2. *J. Biochem.* **119:** 70–79.
7. **Hasegawa, M., T. Hashimoto, J. Adachi, N. Iwabe, and T. Miyata. 1993.** Early branchings in the evolution of eukaryotes: Ancient divergence of Entamoeba that lacks mitochondria revealed by protein sequence data. *J. Mol. Evol.* **36:** 380–388.
8. **Germot, A., H. Philippe, and H. Le Guyader. 1997.** Evidence for loss of mitochondria in Microsporidia from a mitochondrial-type HSP70 in *Nosema locustae*. *Mol. Biochem. Parasitol.* **87:** 159–168.
9. **Keeling, P. J., and G. I. McFadden. 1998.** Origins of microsporidia. *Trends Microbiol.* **6:** 19–23.
10. **Cao, Y. 1998.** *Molecular Phylogeny and Evolution of Vertebrates.* Ph.D. dissertation, Tokyo Institute of Technology, Tokyo.
11. **Cavalier-Smith, T. 1983.** Endosymbiotic origin of the mitochondrial envelope. Pp. 265–279 in *Endocytobiology II, Intracellular Space as Oligogenetic Ecosystem.* Proceedings Second International Colloquium on Endocytobiology, H. E. A. Schenk and W. Schwemmler, eds. Walter de Gruyter, Berlin.
12. **Cavalier-Smith, T. 1983.** A 6-kingdom classification and a unified phylogeny. Pp. 1027–1034 in *Endocytobiology II, Intracellular Space as Oligogenetic Ecosystem.* Proceedings Second International Colloquium on Endocytobiology, H. E. A. Schenk and W. Schwemmler, eds. Walter de Gruyter, Berlin.
13. **Hirt, R. P., B. Healy, C. R. Vossbrinck, E. U. Canning, and T. M. Embley. 1997.** A mitochondrial Hsp70 orthologue in *Vairimorpha necatrix*: molecular evidence that microsporidia once contained mitochondria. *Curr. Biol.* **7:** 995–998.
14. **Bui, E. T. N., P. J. Bradley, and P. J. Johnson. 1996.** A common evolutionary origin for mitochondria and hydrogenosomes. *Proc. Natl. Acad. Sci. USA* **93:** 9651–9656.
15. **Germot, A., H. Philippe, and H. L. Guyader. 1996.** Presence of a mitochondrial-type 70-kDa heat shock protein in *Trichomonas vaginalis* suggests a very early mitochondrial endosymbiosis in eukaryotes. *Proc. Natl. Acad. Sci. USA* **93:** 14614–14617.
16. **Horner, D. S., R. P. Hirt, S. Kilvington, D. Lloyd, and T. M. Embley. 1996.** Molecular data suggest an early acquisition of the mitochondrion endosymbiont. *Proc. R. Soc. Lond.* **B263:** 1053–1059.
17. **Roger, A. J., C. J. Clark, and W. F. Doolittle. 1996.** A possible mitochondrial gene in the early-branching amitochondriate protist *Trichomonas vaginalis*. *Proc. Natl. Acad. Sci. USA* **93:** 14618–14622.
18. **Clark, C. G., and A. J. Roger. 1995.** Direct evidence for secondary loss of mitochondria in *Entamoeba histolytica*. *Proc. Natl. Acod. Sci. USA* **92:** 6518–6521.
19. **Hashimoto, T., L. Sanchez, T. Shirakura, M. Müller, and M. Hasegawa. 1998.** Secondary absence of mitochondria in *Giardia lamblia* and *Trichomonas vaginalis* revealed by tRNA synthetase phylogeny. *Proc. Natl. Acad. Sci. USA* **95:** 6860–6865.
20. **Brown, J. R., and W. F. Doolittle. 1995.** Root of the universal tree of life based on ancient aminoacyl-tRNA synthetase gene duplications. *Proc. Natl. Acad. Sci. USA* **92:** 2441–2445.
21. **Roger, A. J., S. G. Svärd, J. Tovar, C. G. Clark, M. W. Smith, F. D. Gillin, and M. L. Sogin. 1998.** A mitochondrial-like chaperonin 60 gene in *Giardia lamblia*: evidence that diplomonads once harbored an endosymbiont related to the progenitor of mitochondria. *Proc. Natl. Acad. Sci. USA* **95:** 229–234.
22. **Hashimoto, T., Y. Nakamura, T. Kamaishi, F. Nakamura, J. Adachi, K. Okamoto, and M. Hasegawa. 1995.** Phylogenetic place of a mitochondrion-lacking protozoan, *Giardia lamblia*, inferred from amino acid sequences of elongation factor 2. *Mol. Biol. Evol.* **12:** 782–793.
23. **Adachi, J., and M. Hasegawa. 1996.** MOLPHY Version 2.3: Programs for Molecular Phylogenetics Based on Maximum Likelihood. *Computer Science Monographs* **28:** 1–150. Institute of Statistical Mathematics, Tokyo.

Discussion

RUSSELL DOOLITTLE: Regarding the *Staphylococcus* isoleucine sequence, I notice that one tree from Patrick Forterre and you (Masami Hasegawa) (1) was completely different from one Ford (Doolittle) and Jim (Brown) did (2); and that we did independently as well. Something is really strange, quite apart from moving the root of the valine enzyme up into the fungi. In response to an earlier question about the regions being compared, ours use the entire sequence and put the *Staph.* where they belong. Can you comment on that?

FORTERRE: There are two *Staphylococcus aureus* sequences in the databases. Each of them belongs to a different group of bacterial synthetases.

RUSSELL DOOLITTLE: There is the answer.

CAVALIER-SMITH: If you had both the lamprey and the shark, what happens to your tree?

HASEGAWA: We get a very strange tree due to the lamprey.

FELSENSTEIN: Do you have any feeling about whether the absence of a rate correction on sites might have some effect on your trees?

HASEGAWA: In many cases there is no difference in estimating tree topology, but I'm not sure whether this is generally true. In some cases, including rate heterogeneity, changes in the topology were reported by David Penny's group (3).

ROGER: We find that *Giardia* chaperonin 60 clusters with the *Entamoeba* sequence with 100% bootstrap support using PROTML (protein maximum likelihood), and that's just not a reasonable grouping. When you look at it, there are two model violations. First, the amino acid frequencies in *Entamoeba* and *Giardia* differ significantly from the overall frequencies in the data set; and second, rate variation among sites is extreme for the entire data set. If both of these violations are taken into account—by introducing a gamma model, and switching to using nucleotides instead of the amino acids (hoping that that would get rid of some of the bias)—then the relationship between *Entamoeba* and *Giardia* totally disappears, when maximum likelihood is used (4). This is a case where different modes of evolution mislead the phylogenetic methods into grouping problematic sequences as specific relatives when they are not.

RUSSELL DOOLITTLE: Andrew (Roger), why do these organisms retain their chaperonins now that their mitochondria are gone?

ROGER: They might have relic organelles.

Literature Cited

1. **Hashimoto, T., L. Sanchez, T. Shirakura, M. Müller, and M. Hasegawa. 1998.** Secondary absence of mitochondria in *Giardia lamblia* and *Trichomonas vaginalis* revealed by valyl-tRNA synthetase phylogeny. *Proc. Natl. Acad. Sci. USA* **95:** 6860–6865.
2. **Brown, J. R., and W. F. Doolittle. 1995.** Root of the universal tree of life based on ancient aminoacyl-tRNA synthetase gene duplications. *Proc. Natl. Acad. Sci. USA* **92:** 2441–2445.
3. **Lockhart, P. J., A. W. D. Larkum, M. A. Steel, P. J. Waddell, and D. Penny. 1996.** Evolution of chlorophyll and bacteriochlorophyll: the problem of invariant sites in sequence analysis. *Proc. Natl. Acad. Sci. USA* **93:** 1930–1934.
4. **Roger, A. J., S. G. Svärd, J. Tovar, C. G. Clark, M. W. Smith, F. D. Gillin, and M. L. Sogin. 1998.** A mitochondrial-like chaperonin 60 gene in *Giardia lamblia:* evidence that diplomonads once harbored an endosymbiont related to the progenitor of mitochondria. *Proc. Natl. Acad. Sci. USA* **95:** 229–234.

Reference: *Biol. Bull.* **196:** 393–396. (June 1999)

Zooflagellate Phylogeny and the Systematics of Protozoa

T. CAVALIER-SMITH

Department of Botany, University of British Columbia, Vancouver, British Columbia, V6T 1Z4 Canada

In the six kingdom system of life, the kingdom Protozoa occupies a pivotal position between the ancestral kingdom Bacteria and the four derived eukaryotic kingdoms, Animalia, Plantae, Fungi, and Chromista (1). The diversification of the protozoans is fundamentally important for understanding both the early evolution of eukaryotes as a whole and the origins of these higher kingdoms. Recent advances in molecular phylogeny have led to many changes from the earlier protozoan system (2). Archezoa are now treated, not as a separate kingdom (2, 3), but as a subkingdom of the Protozoa, comprising only the two zooflagellate protozoan phyla, Metamonada and Parabasalia (1), which have no mitochondria and are microaerophilic or anaerobic. Parabasalia are clearly secondarily amitochondrial, since their hydrogenosomes probably evolved from mitochondria by the loss of cytochromes and DNA; protein phylogeny ((4); Hasegawa, pers. comm.) suggests that metamonads are also secondarily amitochondrial.

The kingdom Protozoa is currently divided into 13 phyla, of which eight contain zooflagellates (Table I; fuller details of this revised classification are in refs. 1, 5). Microsporidia have been removed from Protozoa and transferred instead to the Fungi; several protein phylogenies suggest that their deep divergence on rRNA trees is a gross artifact of an idiosyncratically high rate of rRNA evolution.

The first eukaryotes were probably zooflagellates similar to the enteromonad or the retortamonad metamonads. The basic backbone of the protozoan phylogenetic tree consists of zooflagellates (phagotrophic flagellates with no plastids) or amoeboflagellates. All other Protozoa, such as rhizopods, sporozoans, and ciliates, are derived from them, as are all eukaryotic algae (by the symbiogenetic origin of chloroplasts, or their lateral transfer by secondary symbiogeneses, as in the origin of chromists and chlorarachnean algae) and the four higher eukaryotic kingdoms. Some zooflagellates, notably in the Chromista and Dinoflagellata, have arisen secondarily by independent losses of plastids. Multiple losses of cilia, mitochondria (or their conversion to hydrogenosomes), and peroxisomes have also been important in eukaryote evolution. Spliceosomal introns are currently known only in the more advanced subkingdom Neozoa.

The earliest diverging aerobic phyla on rRNA trees are the Percolozoa and Euglenozoa, both of which have discoid mitochondrial cristae and are therefore grouped as infrakingdom Discicristata. The order of their divergence is still uncertain, but is important in relation to the origin of the *trans*-splicing that characterizes nuclear genes in Euglenozoa, and stands in contrast with the *cis*-splicing of Percolozoa and the nine higher protozoan phyla. Of these higher phyla, only two consist almost exclusively of flagellates: Dinozoa, which has a mix of zooflagellates and phytoflagellates; and the purely heterotrophic and largely zooflagellate Neomonada (3). Two other phyla with many amoebae (Amoebozoa, typically with lobose pseudopods; and Cercozoa (1, 5) with usually filose or reticulose pseudopods) also include some zooflagellates. The infraphyla Mycetozoa and Archamoebae, grouped together as subphylum Conosa within the Amoebozoa, usually diverge on rRNA trees below the megakaryote radiation (*i.e.*, the explosive radiation in which animals, fungi, plants, and chromists diverged). But most protein trees place Mycetozoa close to the opisthokonta (animals, fungi, and Choanozoa). Several protein trees suggest that the Discicristata may also be placed too low on rRNA trees and may have been part of, rather than occurring prior to, the megakaryote radiation.

The parasitic or predatory zooflagellates *Perkinsus* and

This paper was originally presented at a workshop titled *Evolution: A Molecular Point of View*. The workshop, which was held at the Marine Biological Laboratory, Woods Hole, Massachusetts, from 24–26 October 1997, was sponsored by the Center for Advanced Studies in the Space Life Sciences at MBL and funded by the National Aeronautics and Space Administration under Cooperative Agreement NCC 2-896.

Table I

Revised classification of the Kingdom Protozoa

- Subkingdom 1. Archezoa*
    - Phylum 1. Metamonada
        - Subphylum 1. Eopharyngia (*e.g., Giardia, Trepomonas, Chilomastix, Retortamonas*)
        - Subphylum 2. Axostylaria (*e.g., Oxymonas, Pyrsonympha*)
    - Phylum 2. Parabasalia (*e.g., Trichomonas, Trichonympha*)
- Subkingdom 2. Neozoa*
    - Infrakingdom 1. Discicristata
        - Phylum 1. Percolozoa
            - Subphylum 1. Tetramitia (*e.g., Percolomonas, Lyromonas, Naegleria, Tetramitus*)
            - Subphylum 2. Pseudociliata (*Stephanopogon*)
        - Phylum 2. Euglenozoa
            - Subphylum 1. Plicostoma (*e.g., Diplonema, Euglena, Petalomonas, Peranema*)
            - Subphylum 2. Saccostoma (*e.g., Bodo, Rhynchomonas, Trypanosoma, Leishmania, Postgaardi*)
    - Infrakingdom 2. Alveolata Cavalier-Smith 1991
        - Superphylum 1. Miozoa Cavalier-Smith 1987
            - Phylum 1. Dinozoa*
                - Subphylum 1. Protalveolata* (*e.g., Colponema, Ellobiopsis, Colpodella, Perkinsus*)
                - Subphylum 2. Dinoflagellata (*e.g., Noctiluca, Crypthecodinium, Amphidinium*)
            - Phylum 2. Sporozoa (syn. Apicomplexa Levine 1970)
                - Subphylum 1. Gregarinia (*e.g., Monocystis*)
                - Subphylum 2. Coccidiomorpha (*e.g., Eimeria, Sarcocystis, Paramyxa, Plasmodium, Babesia, Haplosporidium, Minchinia*)
                - Subphylum 3. Manubrispora (*Metchnikovella, Amphiacantha, Amphiamblys*)
        - Superphylum 2. Heterokaryota
            - Phylum Ciliophora
                - Subphylum 1. Tubulicorticata (*e.g., Loxodes, Stylonychia, Colpoda*)
                - Subphylum 2. Epiplasmata (*e.g., Tetrahymena, Paramecium, Vorticella*)
                - Subphylum 3. Filocorticata (*e.g., Spathidium*)
    - Infrakingdom 3. Sarcomastigota
        - Phylum 1. Foraminifera
            - Subphylum 1. Monothalamia (*e.g., Allogromia*)
            - Subphylum 2. Polythalamia (*e.g., Ammonia, Globigerina*)
        - Phylum 2. Cercozoa (Cavalier-Smith 1998a; called Rhizopoda in Cavalier-Smith 1997)
            - Subphylum 1. Phytomyxa (*e.g., Plasmodiophora*)
            - Subphylum 2. Reticulofilosa (*e.g., Chlorarachnion, Biomyxa, Gymnophrys*)
            - Subphylum 3. Monadofilosa (*e.g., Cercomonas, Bodomorpha, Heteromita, Thaumatomonas, Allas, Metromonas, Euglypha, Paulinella, Spongomonas, Rhipidodendron*)
        - Phylum 3. Amoebozoa
            - Subphylum 1. Lobosa (*e.g., Amoeba, Acanthamoeba, Arcella, Difflugia, Multicilia*)
            - Subphylum 2. Conosa [infraphyla Archamoebae (*e.g., Pelomyxa, Mastigamoeba, Phreatamoeba, Entamoeba*) and Mycetozoa (*e.g., Protostelium, Physarum, Dictyostelium*)]
        - Phylum 4. Neomonada*
            - Subphylum 1. Apusozoa* (*e.g., Apusomonas, Ancyromonas, Ebria, Jakoba, Histiona, Reclinomonas*)
            - Subphylum 2. Isomita (*e.g., Phalansterium, Kathablepharis, Nephromyces*)
            - Subphylum 3. Choanozoa* (*e.g., Monosiga, Diaphanoeca, Corallochytrium, Dermocystidium, Ichthyophonus, Ministeria, Nuclearia*)
    - Infrakingdom 4. Actinopoda
        - Phylum 1. Heliozoa (*e.g., Actinophrys, Acanthocystis*)
        - Phylum 2. Radiozoa
            - Subphylum 1. Spasmaria (*e.g., Acanthometra, Sticholonche*)
            - Subphylum 2. Radiolaria (*e.g., Thalassicolla, Aulacantha*)

* Probably paraphyletic.

Colpodella are now placed in the subphylum Protalveolata of the Dinozoa, and not with the Sporozoa. The Sporozoa are once again restricted to nonflagellate endoparasites, so the name Apicomplexa is abandoned. Metchnikovellids, because of their sporozoan-like cortical alveoli, are transferred from Microsporidia to Sporozoa, as the subphylum Manubrispora; they are probably yet another example of the secondary loss of mitochondria and peroxisomes.

The recently created Neomonada comprise three subphyla: Choanozoa (choanoflagellates, *Corallochytrium*, and the parasitic ichthyosporeans, all with predominantly flat cristae); Apusozoa (*Apusomonas* and its biciliate anisokont relatives, such as *Ancyromonas*); and Isomita (isokont usually biciliate zooflagellates). Apusozoa and Isomita include many of the tubulicristate zooflagellates that were formerly included in the Opalozoa. The latter taxon has been discontinued, because the Opalinata were transferred to the Heterokonta within the kingdom Chromista, and the sarcomonad flagellates (6) and numerous others (*e.g.*, *Spongomonas*) were removed to the Cercozoa. In addition to the sarcomonads, the new phylum Cercozoa includes many filose amoebae, chlorarachnean algae, the reticulose *Gymnophrys*, *Plasmodiophora*, and a variety of zooflagellates (*e.g.*, *Bodomorpha*, *Allas*) not previously classified. Cercozoa are a major novel clade within the megakaryote radiation and, due to their phyletic distinctiveness, might hold many surprises for cell and molecular biologists if they were seriously studied. Cercozoans, though severely neglected organisms, are very diverse and are of major ecological importance in soils, as well as in marine and freshwater habitats.

I have discussed here some of the recent molecular and ultrastructural evidence that supports the substantial changes to the high-level classification of the kingdom Protozoa and the phylogenetic ideas that underlie them. Ongoing molecular and ultrastructural studies will probably necessitate still further redistribution of taxa among the 13 phyla of the present protozoan system and their 26 subphyla. Despite the phylogenetic distinctiveness of the two groups, the phenetic boundary between the Neomonada and Cercozoa is particularly unclear, as are the affinities of the various heliozoans. Though future studies may also require the transfer of a few minor taxa from the Protozoa to the kingdom Chromista, the circumscription of the kingdom Protozoa as a whole will probably be more stable in the future than in the recent past. However, the branching order of the eight non-alveolate neozoan phyla relative to each other and to the alveolates, plants, and chromists is very uncertain and will be difficult to establish. The ancestral relationship between the neomonad subphylum Choanozoa and the animals and fungi, however, appears to be relatively solid.

Literature Cited

1. **Cavalier-Smith, T. 1998a.** A revised six-kingdom system of life. *Biol. Rev.* **73:** 203–266.
2. **Cavalier-Smith, T. 1993.** Kingdom Protozoa and its 18 phyla. *Microbiol. Rev.* **57:** 953–994.
3. **Cavalier-Smith, T. 1997.** Amoeboflagellates and mitochondrial cristae in eukaryote evolution: megasystematics of the new protozoan subkingdoms Eozoa and Neozoa. *Arch. Protistenkd.* **147:** 237–258.
4. **Roger, A. J., S. G. Svärd, F. D. Gillin, and M. L. Sogin. 1998.** Protists without mitochondria: an update on the status of the Archezoa hypothesis. *J. Eukaryot. Microbiol.* **45:** 5A.
5. **Cavalier-Smith, T. 1998b.** Neomonada and the origin of animals and fungi. Pp. 375–407 in *Evolutionary Relationships Among Protozoa*, G. H. Coombs, K. Vickerman, M. A. Sleigh, and A. Warren, eds. Chapman & Hall, London.
6. **Cavalier-Smith, T., and E. E. Chao. 1997.** Sarcomonad ribosomal RNA sequences, rhizopod phylogeny, and the origin of euglyphid amoebae. *Arch. Protistenkd.* **147:** 227–236.

Discussion

PALMER: When do you think eukaryotes arose?

CAVALIER-SMITH: I would think between about 600 and 1600 million years ago.

PALMER: On what evidence do you base this?

CAVALIER-SMITH: The fossil record. I don't think there is any other source of evidence. About 1600 million years ago there was a huge increase in cell size. Perhaps that change marked the origin of eukaryotes from bacteria. But between that event and the beginning of the Cambrian, about 550 million years ago, there's not a single group of fossils that can be positively identified with any extant eukaryote group. The protist fossil record is consistent with that of animals and plants in suggesting that there was a Cambrian explosion. Basically I equate that with the big diversification of what I am calling Neozoa plus the four higher kingdoms. I think that was about six hundred million years ago. If there really were some earlier groups, they could go back in the period between 600 million years and 1600 million years ago. There are large fossils that cannot be equated with any modern group; they might have been early eukaryotes, but we just don't really know what they were.

GUERRERO: Gonzalo Vidal put the origin at 1600–800 million years ago.

CAVALIER-SMITH: That is based on that large cell size argument. Some of those early fossils have an increased complexity that might have had something to do with the endomembrane system and secretion of complicated surface structures. I tend to favor an origin for eukaryotes that is earlier than 600 million years ago, but exactly when I wouldn't really know. Probably my more serious guess would be between 1000 and the date that you gave.

ELLINGTON: How do you choose which characteristics to study? Why is it that the number of membranes that a bacterium has is much more important that the entire chemical composition of that membrane?

Cavalier-Smith: Whether the number is more important or less is debatable. That is one reason why, at one time, I did accept Archaebacteria as a separate kingdom rather than just as an infrakingdom. There is not a hard and fast answer to your question. The number is important because it is very conservative in evolution. If something is very conservative and correlates with other characters, then one attributes great importance to it; so that character correlates with, for instance, the molecular trees on the whole. Each of the major clades on the ribosomal RNA tree has either one membrane or two. Therefore, that number hasn't changed within a clade; it changes very rarely.

Another problem is how the number of membranes changes. What mutational mechanism might lead to such a change? I've put forward a mechanism that would reduce the number from two to one: that is, producing more peptidoglycan between the membranes and throwing off the outer one. However, no one, as far as I know, has suggested a biophysical mechanism that would create a second membrane on the outside of the initial one, while meeting the need to target proteins and lipids. Concerted evolution of many components is necessary to create two membranes rather than one.

Jahnke: Regarding the timing of the origin of eukaryotes, there is some very excellent evidence in the organic molecular record for steranes in the 1500 to 1600 million year range.

Cavalier-Smith: That is definitely a reason for favoring the 1500. In most of my published work, that is the date that I have used, partly for that reason and partly for the increase in cell size. But we cannot be sure whether that event coincided with the origin of the eukaryotes, and that's why I have left this broad window of uncertainty.

Reference: *Biol. Bull.* **196:** 397–399. (June 1999)

Evolutionary History of Plastids

SUSAN E. DOUGLAS

Canadian Institute for Advanced Research, Program in Evolutionary Biology, and Institute for Marine Biosciences, National Research Council, Halifax, Nova Scotia, Canada

A major biological event contributing to the biodiversity of present-day organisms was the enslavement of a photosynthetic eubacterium by a primitive eukaryote and its entrapment as an integral part of the cell: the plastid. Since the first acquisition by eukaryotes of photosynthetic capability by primary endosymbiosis, two major lineages (red and green) appear to have arisen. Subsequently, an amazing variety of secondary endosymbioses took place, resulting in a complex assemblage of organisms containing photosynthetic organelles surrounded by multiple membranes. This assemblage includes the extant cryptomonads, chlorarachniophytes, chromophytes, haptophytes, euglenoids, and dinoflagellates. Superimposed upon this scenario were the activities of eukaryotes that were acquiring plastids by tertiary endosymbiosis from the green algal, cryptomonad, chromophyte, and haptophyte lineages (1), and others that were apparently losing the capacity to photosynthesize, while retaining vestigial plastids (*e.g.*, the extant apicomplexans, parasitic plants, colorless cryptomonads, and euglenoids).

Attempts to delineate the events leading to the multicolored array of extant photosynthetic eukaryotes started over one hundred years ago and were initially based on microscopic investigations (2). More recently, biochemical, molecular, and phylogenetic techniques have been employed to dissect the evolutionary history of plastids and their hosts. With the accumulation of molecular data, including the complete plastid sequences from several representative lineages (3) and sequences from nuclear (or nucleus-derived) compartments (4), a clearer picture of some of the events leading to extant photosynthetic eukaryotes is emerging.

The cryptomonad alga *Guillardia theta* provides a good model organism for tracing the ancestry of plastid-bearing eukaryotes. It is an example of a cell-within-a-cell, being composed of a flagellate host cell, complete with mitochondria and nucleus, surrounding a plastid lying within a reduced cytoplasmic compartment that contains a vestigial nucleus (or nucleomorph). Molecular data from the plastid, nucleomorph, and nucleus (5) are giving clues to the nature of the partners that make up this organism, as well as fascinating insights into the genome reduction that occurred during endosymbiosis.

Plastid genome

The plastid genome of *Guillardia theta* (121,524 bp) has been completely sequenced and bears striking resemblance to the 191,028 bp plastid genome of the rhodophyte *Porphyra purpurea* (6). Although much smaller, the cryptomonad plastid genome contains extensive synteny groups that are clearly recognizable and provide excellent evidence for the red algal ancestry of the cryptomonad plastid (Fig. 1). Furthermore, a comparison of the *Guillardia* plastid genome with the 35 kb plastid-like genome of the apicomplexan *Plasmodium falciparum* shows an almost identical gene order, with only a fraction of the cryptomonad genes present in the apicomplexan. This indicates that the reduced 35 kb circle perhaps had its origins as a cryptomonad plastid genome, which is not unlikely given the propensity for other members of this group (dinoflagellates) to take up cryptomonads as endosymbionts.

The cryptomonad genome contains a short (4.9 kb) inverted repeat containing the rRNA cistrons, 30 tRNA genes, 44 genes encoding proteins for photosynthesis, 44 ribosomal protein genes (26 large subunit and 18 small subunit), 5 genes for biosynthetic function, 19 genes involved in gene expression (including 3 hypothetical chloroplast reading frames or ycfs), 25 additional ycfs, and 9 open reading frames (ORFs) larger than 50 amino acids. Intergenic spac-

---

This paper was originally presented at a workshop titled *Evolution: A Molecular Point of View*. The workshop, which was held at the Marine Biological Laboratory, Woods Hole, Massachusetts, from 24–26 October 1997, was sponsored by the Center for Advanced Studies in the Space Life Sciences at MBL and funded by the National Aeronautics and Space Administration under Cooperative Agreement NCC 2-896.

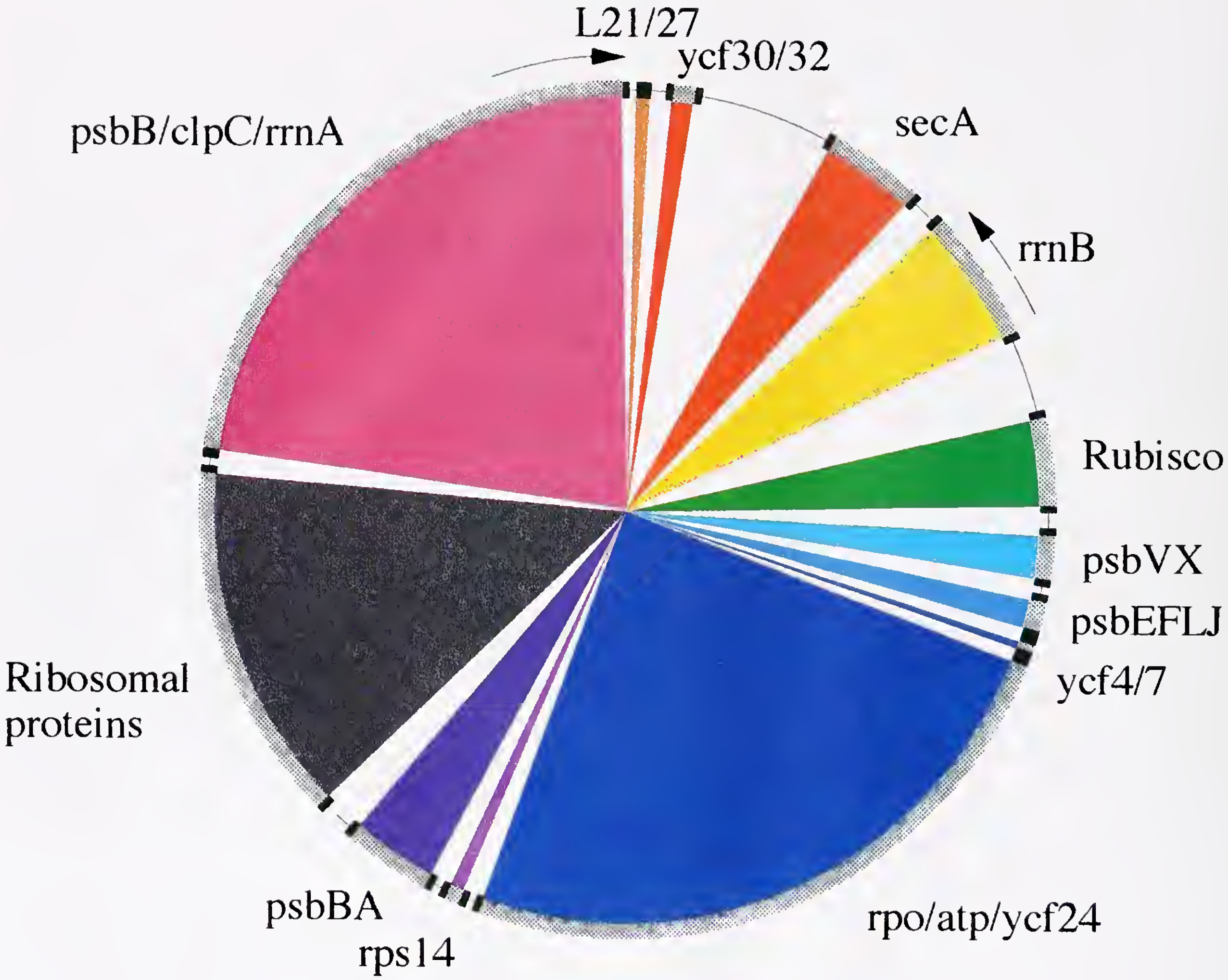

Figure 1. Synteny groups present on the *Guillardia theta* plastid genome. Colored wedges correspond to segments of the cryptomonad plastid genome where the gene order is colinear with that of the rhodophyte. *Porphyra purpurea*. The two rRNA cistrons are represented by arrows.

ers are very short, no introns have been detected, and several genes overlap, all resulting in a very compact genome. In addition, large clusters of genes (such as the ribosomal protein genes) are organized into single transcriptional units, again resulting in an economically organized genome (7).

Comparisons of plastid gene order and gene sequences support a monophyletic, primary origin of plastids and a subsequent divergence into red and green lineages. Particularly significant are gene clusters that are present in plastid genomes from several lineages, but absent in cyanobacteria (such as the atpA/rpo cluster and the psbBTNH cluster). These clusters most probably evolved post-endosymbiosis, or (less likely) were the product of extreme convergent evolution. Additional evidence for monophyly comes from phylogenetic trees constructed from several genes (such as SSU rRNA, atpB, and tufA).

Nucleomorph genome

One of the first steps in the evolution of a plastid from an endosymbiotic cyanobacteria was the massive loss of redundant genes and/or transfer to the host nucleus of the approximately 900 genes essential for photosynthesis. Since the nucleomorph genome of cryptomonads represents the vestigial nucleus of the host, it was suspected to contain these transferred genes. At an average of 1 kb/gene, this would require a genome of at least 900 kb to encode just the genes for photosynthesis. However, with such a small haploid genome size (520 kb), this scenario seemed less likely. Furthermore, hybridization analysis has shown that all three chromosomes contain repeats of the rRNA cistron (consisting of 18S-5.8S-28S-5S rRNA genes) and several downstream ORFs, each of which occupy about 12 kb. Most of the genes identified in the genome sequencing project are concerned with self-replication and gene expression, rather than with plastid biochemistry. Thus far, ftsZ (which is involved in cell division and may interact with the plastid-encoded ftsH) and a subunit of clpC are probable candidates for plastid-targeted proteins. With the acquisition of more gene sequences from the nucleomorph, it will be possible to determine more precisely the exact role of the nucleomorph in this complex cell.

Phylogenetic analyses performed with nucleomorph genes are thus far confined to the SSU rRNA and hsp70 gene. SSU rRNA phylogenies ally the nucleomorph with red algae (8), and the limited hsp70 data set places cryptomonads between green plants and trypanosomes with a weak bootstrap value (9). Additional evidence for a close relationship between the cryptomonad plastid and red algae is the paucity of introns in the genomes of both organisms.

Nuclear genome

Since the nucleomorph does not seem to encode an abundance of components that function in plastid biochemistry, the nucleus probably does. Although several nuclear genes have been identified and partially sequenced, the only identified gene presumed to code for a plastid component is cpeA, the alpha subunit of phycoerythrin. Analysis of nuclear genes encoding plastid proteins will help to clarify whether these genes were transferred from the nucleomorph during endosymbiosis or originated from a primary endosymbiont present in a photosynthetic host cell that was subsequently lost after acquisition of a eukaryotic endosymbiont, as hypothesized by Hauber *et al.* (10).

This is NRC publication number NRCC 42291.

Literature Cited

1. **Schnepf, E. 1993.** From prey *via* endosymbiont to plastid: comparative studies in dinoflagellates. Pp. 53–72 in *Origins of Plastids*, R. A. Lewin, ed. Chapman & Hall, New York.
2. **Schimper, A. F. W. 1883.** Über die Entwicklung der Chlorophyllkorner und Farbkorner (1 Teil). *Bot. Zeit.* **41:** 105–114.
3. **Reith, M. E. 1995.** Molecular biology of rhodophyte and chromophyte plastids. *Annu. Rev. Plant Physiol. Plant Mol. Biol.* **46:** 459–575.
4. **Palmer, J. D., and C. F. Delwiche. 1996.** Second-hand chloroplasts and the case of the disappearing nucleus. *Proc. Nat. Acad. Sci. USA* **93:** 7432–7435.
5. **McFadden, G. I., P. R. Gilson, S. E. Douglas, T. Cavalier-Smith, C. J. B. Hofmann, and U.-G. Maier. 1997.** Bonsai genomics: sequencing the smallest eukaryotic genomes. *Trends Genet.* **13:** 46–49.
6. **Reith, M. E., and J. Munholland. 1995.** Complete nucleotide sequence of *Porphyra purpurea* chloroplast genome. *Plant Mol. Biol. Rep.* **13:** 333–335.
7. **Wang, S.-L., X.-Q Liu, and S. E. Douglas. 1997.** The large ribosomal protein gene cluster of a cryptomonad plastid: gene organization, sequence and evolutionary implications. *Biochem. Mol. Biol. Int.* **41:** 1035–1044.
8. **Douglas, S. E., C. A. Murphy, D. F. Spencer, and M. W. Gray. 1991.** Cryptomonad algae are evolutionary chimaera of two phylogenetically distinct unicellular eukaryotes. *Nature* **350:** 148–151.
9. **Rensing, S. A., and U.-G. Maier. 1994.** Phylogenetic analysis of the stress-70 protein family. *J. Mol. Evol.* **39:** 80–86.
10. **Hauber, M. M., S. B. Muller, V. Speth, and U.-G. Maier. 1994.** How to evolve a complex plastid?—A hypothesis. *Bot. Acta* **107:** 383–386.

Discussion

MARGULIS: Are there any nucleosomes in the nucleomorph? Can you tell us about the nucleomorph genes in general with regard to their organization of DNA and histones? What do you mean by chromosomes?

DOUGLAS: We haven't looked at these organisms under the electron microscope. In the plastids there is a histone-like protein that has been identified. We haven't found any histone.

CAVALIER-SMITH: Why do you postulate two separate uptakes of red algae into chromophytes and cryptomonads rather than a single uptake into the ancestor of all three chromist groups?

DOUGLAS: The reason is that the host cells appear to be fairly different both in trees and ultrastructure.

ROTHSCHILD: In your presentation, did you intend to have the origin of the Cryptos coming out before the rest of the Chromista?

DOUGLAS: There was no timing involved there.

ROTHSCHILD: Would you like to hazard a guess on when that symbiosis arose? How long does it take to get through the nucleomorphisms?

DOUGLAS: One possible explanation of why the nucleomorph is there and why it's been lost in some lineages is that the secondary host also harbored an endosymbiont. Genes could have been transferred to lesser or greater degrees from that endosymbiont to that host. If all the genes that were sufficient for running a plastid were transferred, in the secondary endosymbiosis, the nucleomorph could have been lost. If an insufficient number of genes had been transferred to that nucleus of the second host, then it would still need to retain a nucleomorph.

Reference: *Biol. Bull.* **196:** 400–403. (June 1999)

A Genomics Approach to Mitochondrial Evolution

MICHAEL W. GRAY[1], GERTRAUD BURGER[2], ROBERT CEDERGREN[2],
G. BRIAN GOLDING[3], CLAUDE LEMIEUX[4], DAVID SANKOFF[5], MONIQUE TURMEL[4],
AND B. FRANZ LANG[2]

Program in Evolutionary Biology, Canadian Institute for Advanced Research, [1]Department of Biochemistry, Dalhousie University, Halifax, Nova Scotia, Canada; [2]Département de biochimie et [5]Centre de recherches mathématiques, Université de Montréal, Montréal, Québec, Canada; [3]Department of Biology, McMaster University, Hamilton, Ontario, Canada; and [4]Département de biochimie, Université Laval, Québec, Québec, Canada

The pathways of mitochondrial DNA (mtDNA) evolution are obscured by the extraordinary diversity in size, gene content, gene arrangement, and mode of expression of characterized mitochondrial genomes (1–3). For this reason, a comparison of mtDNAs in animals (4), plants (5), and fungi (6, 7) leads to few conclusions about the evolutionary pressures and mechanisms by which the mitochondrial genome has become so different in these multicellular eukaryotic lineages, or about the form and gene content of the mtDNA ancestor (proto-mitochondrial genome). Not only do the mitochondrial genomes in multicellular eukaryotes, especially animals and fungi, appear to be highly derived, but these lineages represent relatively recently evolved, terminal branches in the eukaryotic phylogenetic tree. Hence, the multicellular eukaryotes are likely to give us a highly biased picture of the mitochondrial genome and its evolution. To provide a phylogenetically more representative sampling of mitochondrial genome structure, it is necessary to examine mtDNA in a diversity of protists (primarily unicellular eukaryotes), a vast assemblage that comprises most of the evolutionary diversity of the eukaryotic lineage (8). Among the questions that a comprehensive and systematic comparative study of protist mtDNAs will better address are the following: Did the mitochondrial genome arise only once (monophyletic origin) or more than once (polyphyletic origin)? How was (were) the ancestral proto-mitochondrial genome (or genomes) organized, and what genes did it (they) contain? What are the pathways and mechanisms of mtDNA evolution that account for the current observed structural variation?

A program to sequence protist mitochondrial DNAs

In 1992, the Organelle Genome Megasequencing Program (OGMP) was initiated as a consortium of seven investigators from four eastern Canadian universities, having as one of its goals the complete sequencing of mitochondrial genomes from a wide range of protists. The experimental arm of the OGMP is a centralized sequencing facility (Sequencing Unit) located at the University of Montreal. The Unit comprises a Molecular Biology Division, within which sequences are determined and analyzed, and an Informatics Division, which develops informatics tools to aid in all aspects of sequence determination and analysis. To date, the OGMP has determined and analyzed 11 complete protist mtDNA sequences, with 3 additional mtDNA sequencing projects nearing completion. The accumulating data (representing >750,000 bp of finished sequence so far) are providing new insights into the questions raised above.

Gene content and genome organization in protist mitochondrial DNAs

To date, detailed descriptions of three protist mtDNAs sequenced by the OGMP have been published, representing a chlorophyte alga, *Prototheca wickerhamii* (9, 10); an amoeboid protozoon, *Acanthamoeba castellanii* (11); and a jakobid flagellate, *Reclinomonas americana* (12). For the other protist mtDNA sequencing projects, individual de-

---

This paper was originally presented at a workshop titled *Evolution: A Molecular Point of View*. The workshop, which was held at the Marine Biological Laboratory, Woods Hole, Massachusetts, from 24–26 October 1997, was sponsored by the Center for Advanced Studies in the Space Life Sciences at MBL and funded by the National Aeronautics and Space Administration under Cooperative Agreement NCC 2-896.

scriptions summarizing salient features of gene content, organization, and expression are available through the OGMP website (see below). Sequence data generated for protist mtDNAs by the OGMP and other groups have been compiled and reviewed in detail elsewhere (13). Among the findings and conclusions to emerge from this work are the following:

1. By and large, protist mtDNAs are A + T-rich genomes (usually >70%) with a median size of around 40 kbp. Typically, they are compactly organized, gene-rich, circular-mapping genomes with few, or no, large noncoding regions. Intergenic spacers usually account for less than 10% of the mtDNA, with coding regions often overlapping.
2. In general, protist mtDNAs encode substantially more genes than do animal and fungal mtDNAs. Additional genes that are widely found in protist mtDNAs include ones specifying extra subunits of respiratory complexes I (*nad*) and V (*atp*) and both large subunit and small subunit ribosomal proteins (*rpl* and *rps*, respectively). Animal and fungal mtDNAs completely, or almost completely (14), lack genes for ribosomal proteins. Animal mitochondrial genomes, in particular, appear to be exquisitely condensed versions of a much larger, protist-like progenitor.
3. In overall gene content, protist mtDNAs more closely resemble the much larger mitochondrial genomes of land plants. Genes shared between plant and protist mtDNAs include not only those that are absent from animal and fungal mtDNAs (noted above), but occasionally also genes encoding subunits of complex II (*sdh;* ref. 15) and 5S rRNA (*rrn5;* ref. 16). In spite of their larger size, plant mtDNAs do not encode substantially more genes than protist mtDNAs (13). In marked contrast to their animal counterparts, land plant mtDNAs appear to have expanded considerably in size, mostly through the acquisition of large amounts of noncoding spacer DNA.
4. Typically, the ribosomal and transfer RNAs encoded by protist mtDNAs are strikingly eubacteria-like in their secondary structures, lacking the anomalous features found in their fungal and particularly animal mitochondrial counterparts. Although a few protist mitochondrial genomes encode a minimal set of tRNA species that is sufficient to recognize all codons found in protein-coding genes, most do not (13). In these cases, the import of nucleus-encoded, cytosolic tRNAs into the mitochondria is assumed to make up the deficit.
5. At least half of the protist mtDNAs examined appear to use the standard genetic code, as does the plant mitochondrial genome. In the remaining protist mtDNAs, the codon UGA is used to specify tryptophan rather than termination. Phylogenetic considerations strongly indicate that this codon change has occurred independently in several branches of the eukaryotic tree during mitochondrial genome evolution.
6. Introns, either group I or group II, are conspicuously rare in protist mitochondrial genomes. Several protist mtDNAs lack introns entirely. Where introns are present, the evidence suggests that a number of them have been acquired by means of horizontal transfer events, rather than being inherited vertically from the proto-mitochondrial genome.
7. Aspects of protist mitochondrial gene content, primary and secondary structure, gene organization, and gene expression also serve to emphasize the underlying eubacterial character of the mitochondrial genome, reinforcing the theory that mitochondria originated in evolution from eubacteria-like symbionts. Mitochondrion-specific patterns of gene organization strongly support a single (monophyletic) origin of the mitochondrial genome.
8. Although some of the protist mtDNAs initially examined (*e.g.*, those of the green alga *Chlamydomonas reinhardtii* and the apicomplexan *Plasmodium falciparum*, the human malaria parasite) proved to have a very unusual—indeed bizarre—structure, subsequent work by the OGMP and other groups has indicated that these mtDNAs are likely to be highly derived. In fact, the most ancestral (least derived) mitochondrial genomes are to be found among the protists, particularly in free-living species whose mtDNA has not undergone the dramatic re-tailoring suffered by its counterpart in many parasites.
9. The most ancestral mitochondrial genome so far described, that of *Reclinomonas americana* (12), resembles nothing so much as a miniaturized eubacterial genome. In addition to encoding 5S and RNase P RNAs that are eubacteria-like in primary and secondary structure, *R. americana* mtDNA contains a set of genes never before found in mtDNA. Among the most intriguing are genes (*rpoA-D*) encoding a eubacteria-like ($\alpha_2\beta\beta'\sigma$) RNA polymerase. This finding raises intriguing questions about the evolution of the mitochondrial transcription system (17, 18), because a single-subunit, nucleus-encoded, bacteriophage T3/T7-like enzyme functions as the mitochondrial RNA polymerase in other eukaryotes (see, *e.g.*, ref. 19).

Future prospects and on-line access to the OGMP

Sequencing of protist mtDNAs is continuing in the OGMP, with the current emphasis on identification of further examples of ancestral mitochondrial genomes from organisms branching deep within the eukaryotic lineage. The new insights obtained will undoubtedly influence our ideas about the origin of the eukaryotic cell, and the crucial role that the acquisition of mitochondria has played in this process.

Information about the OGMP and about individual mtDNA sequencing projects and informatics tools may be obtained by consulting World Wide Web sites for the following organizations (URLs given below): the OGMP, the allied Protist Image Database (PID), the Organelle Genome Database (GOBASE) (20), and the Fungal Mitochondrial Genome Project (FMGP).

OGMP	http://megasun.bch.umontreal.ca/ogmp
PID	http://megasun.bch.umontreal.ca/protists
GOBASE	http://megasun.bch.umontreal.ca/gobase/
FMGP	http://megasun.bch.umontreal.ca/People/lang/FMGP/

Acknowledgments

Work described in this paper was supported by a Special Project grant (SP-34) from the Medical Research Council of Canada, a grant from the Canadian Genome Analysis and Technology Program (GO-12323), and by generous donations of equipment from Sun Microsystems Inc. and LI-COR Inc. Salary and interaction support from the Canadian Institute for Advanced Research (Program in Evolutionary Biology) are also gratefully acknowledged.

Literature Cited

1. **Gray, M. W. 1989.** Origin and evolution of mitochondrial DNA. *Annu. Rev. Cell Biol.* **5:** 25–50.
2. **Gray, M. W. 1992.** The endosymbiont hypothesis revisited. *Int. Rev. Cytol.* **141:** 233–357.
3. **Gillham, N. W. 1994.** *Organelle Genes and Genomes,* Oxford University Press, New York.
4. **Wolstenholme, D. R. 1992.** Animal mitochondrial DNA: structure and evolution. *Int. Rev. Cytol.* **141:** 173–216.
5. **Hanson, M. R., and O. Folkerts. 1992.** Structure and function of the higher plant mitochondrial genome. *Int. Rev. Cytol.* **141:** 129–172.
6. **Clark-Walker, G. D. 1992.** Evolution of mitochondrial genomes in fungi. *Int. Rev. Cytol.* **141:** 89–127.
7. **Paquin, B., M.-J. Laforest, L. Forget, I. Roewer, Z. Wang, J. Longcore, and B. F. Lang. 1997.** The fungal mitochondrial genome project: evolution of fungal mitochondrial genomes and their gene expression. *Curr. Genet.* **31:** 380–395.
8. **Patterson, D. J., and M. L. Sogin. 1992.** Eukaryote origins and protistan diversity. Pp. 13–46 in *The Origin and Evolution of the Cell.* H. Hartman and K. Matsuno, eds. World Scientific, Singapore.
9. **Wolff, G., G. Burger, B. F. Lang, and U. Kück. 1993.** Mitochondrial genes in the colourless alga *Prototheca wickerhamii* resemble plant genes in their exons but fungal genes in their introns. *Nucleic Acids Res.* **21:** 719–726.
10. **Wolff, G., I. Plante, B. F. Lang, U. Kück, and G. Burger. 1994.** Complete sequence of the mitochondrial DNA of the chlorophyte alga *Prototheca wickerhamii.* Gene content and genome organization. *J. Mol. Biol.* **237:** 75–86.
11. **Burger, G., I. Plante, K. M. Lonergan, and M. W. Gray. 1995.** The mitochondrial DNA of the amoeboid protozoon, *Acanthamoeba castellanii*: complete sequence, gene content and genome organization. *J. Mol. Biol.* **245:** 522–537.
12. **Lang, B. F., G. Burger, C. J. O'Kelly, R. Cedergren, G. B. Golding, C. Lemieux, D. Sankoff, M. Turmel, and M. W. Gray. 1997.** An ancestral mitochondrial DNA resembling a eubacterial genome in miniature. *Nature* **387:** 493–497.
13. **Gray, M. W., B. F. Lang, R. Cedergren, G. B. Golding, C. Lemieux, D. Sankoff, M. Turmel, N. Brossard, E. Delage, T. G. Littlejohn, I. Plante, P. Rioux, D. Saint-Louis, Y. Zhu, and G. Burger. 1998.** Genome structure and gene content in protist mitochondrial DNAs. *Nucleic Acids Res.* **26:** 865–878.
14. **Paquin, B., and B. F. Lang. 1996.** The mitochondrial DNA of *Allomyces macrogynus:* the complete genomic sequence from an ancestral fungus. *J. Mol. Biol.* **255:** 688–701.
15. **Burger, G., B. F. Lang, M. Reith, and M. W. Gray. 1996.** Genes encoding the same three subunits of respiratory complex II are present in the mitochondrial DNA of two phylogenetically distant eukaryotes. *Proc. Natl. Acad. Sci. USA* **93:** 2328–2332.
16. **Lang, B. F., L. J. Goff, and M. W. Gray. 1996.** A 5 S rRNA gene is present in the mitochondrial genome of the protist *Reclinomonas americana* but is absent from red algal mitochondrial DNA. *J. Mol. Biol.* **261:** 607–613.
17. **Cermakian, N., T. M. Ikeda, P. Miramontes, B. F. Lang, M. W. Gray, and R. Cedergren. 1997.** On the evolution of the single-subunit RNA polymerases. *J. Mol. Evol.* **45:** 671–681.
18. **Gray, M. W., and B. F. Lang. 1998.** Transcription in chloroplasts and mitochondria: a tale of two polymerases. *Trends Microbiol.* **6:** 1–3.
19. **Cermakian, N., T. M. Ikeda, R. Cedergren, and M. W. Gray. 1996.** Sequences homologous to yeast mitochondrial and bacteriophage T3 and T7 RNA polymerases are widespread throughout the eukaryotic lineage. *Nucleic Acids Res.* **24:** 648–654.
20. **Korab-Laskowska, M., P. Rioux, N. Brossard, T. G. Littlejohn, M. W. Gray, B. F. Lang, and G. Burger. 1998.** The Organelle Genome Database Project (GOBASE). *Nucleic Acids Res.* **26:** 138–144.

Discussion

MARGULIS: Can we argue that you have nearly a *Paracoccus* or other gram negative bacterial genome here, and therefore *Reclinomonas* acquired the oxygen-respiring symbiont very recently?

GRAY: In other mitochondrial genomes, the genes are a subset of the ones in *Reclinomonas* mitochondrial DNA. Exactly the same set of small subunit ribosomal protein genes is present in *Reclinomonas* mitochondrial DNA as in the mitochondrial genome of the liverwort *Marchantia polymorpha.* In all other mitochondrial DNAs, the ribosomal protein genes are a subset of the *Reclinomonas* ones.

MARGULIS: Is there no possibility of molecular convergence?

GRAY: I would say that the number of characters that we are starting to accumulate makes it very difficult to see how independent reduction of much larger genomes could converge on these multiple specific patterns, which include not only gene content but also specific losses of ribosomal protein genes within a large operon. It depends on your viewpoint. How easy or difficult is it to converge on this kind of pattern? I think it is probably difficult if you assume that various gene losses are independent events—that all of those genes didn't move at the same time. Even if they did, the same set would have had to have been selected for retention each time.

MARGULIS: Is it a question of relentless selection?

GRAY: This is looking at it with the idea that there is probably no good reason why those particular genes were lost.

CAVALIER-SMITH: The *Reclinomonas* ribosomal RNA sequence isn't deep, unlike the *Naegleria* one, but the depth of the *Naegleria* one on the ribosomal RNA tree is not supported by any currently available protein data. It could well be that at least all of the mitochondria-containing eukaryotes are simply a star phylogeny. If we look at it in that way, and also realize that the divergence of the plastid-containing groups is part of that star-like phylogeny, then we could say that possibly the serial endosymbiosis theory is wrong, and that there was, instead, a simultaneous symbiotic origin of mitochondria chloroplasts and, as I have argued, peroxisomes.

GRAY: The issue is, if *Reclinomonas* and the jakobids are deep, where is the crown radiation relative to the origin of the eukaryotes? Are these two points really far apart in time, or are they relatively close together? It could well be that all of these symbiotic events happened, if not simultaneously, then very close together in time.

KATZ: It is hard to evaluate the trees without any knowledge of the alignment and phylogenetic algorithms that you are using. What algorithms were you using for the trees that were uniting the *Reclinomonas* with the land plants? Were those relationships robust if you tried other phylogenetic methods?

GRAY: The tree was generated from a sequence alignment based on secondary structure, so that conserved regions were selected from complete ribosomal RNA sequences. The data set comprises about 290 eubacterial or organellar sequences, so what I showed was simply the alpha-proteobacterial branch of a much larger assemblage. The tree is a neighbor-joining one, and this particular example wasn't bootstrapped. I don't place any great significance on a mitochondrial small subunit ribosomal RNA tree because we've had this artifact (plants separate from other eukaryotes) for many years now. Because the tree represents the first time that we have found an organism (*i.e., Reclinomonas*) that goes together with land plants, I offer it simply as an illustration of what I think is happening here.

LANDWEBER: Do maximum likelihood and parsimony give you the same result?

GRAY: We haven't applied these methods to this particular data set.

JEFF PALMER: I'd like to respond to something Tom (Cavalier-Smith) said about possible simultaneous origin of chloroplasts and mitochondria. If that were the case, then a number of eukaryotes would have lost their chloroplasts entirely, which is reasonable; but it becomes less and less likely when we look at fully sequenced genomes such as those of yeast and *C. elegans.* If chloroplast loss had occurred in these organisms, and there had been substantial transfer of chloroplast-derived genes to the nucleus in the common ancestor of these groups, you should find nuclear genes of chloroplast origin in yeast and *C. elegans,* and there don't seem to be any.

CAVALIER-SMITH: In my presentation, I had chloroplasts originating a bit after the primary divergence of plants from the ancestor of animals and fungi, but I still wonder whether we can really be sure about what things might be retained after chloroplast loss.

Reference: *Biol. Bull.* **196:** 404–407. (June 1999)

The Problem of the Evolution of Sex

ROSEMARY J. REDFIELD

Department of Zoology, University of British Columbia, Vancouver, British Columbia, Canada

The unsolved problem of the evolution of sexual reproduction has been almost exclusively in the domain of population genetics. This suggests that new approaches may be fruitful; here I develop a molecular and phylogenetic framework.

The problem

Sexual reproduction is the cyclic alternation of (i) the fusion of haploid cells (often called *gametes*) to produce a diploid (the *zygote*), and (ii) the regeneration of haploid cells from a diploid cell by meiosis. Its best-known consequence is the random reassortment of chromosomes from one generation to the next. Sexual reproduction is so fundamental to our own reproduction, and so common among the organisms we normally see, that we often take it for granted, yet we do not know why it exists.

Old-fashioned textbooks explained sex as being good for the long-term evolution of the species; pointing out that offspring that differ from their parents might sometimes be better adapted, especially if the environment has changed. But sexual reproduction is difficult and expensive, and most biologists now believe that any advantage to the species would be too unpredictable, too weak, and too distant in the future to compensate for the immediate problems that sexual reproduction causes for individuals (1, 2, 3).

A number of population geneticists have sought alternative explanations for the evolution of sex, but no consensus has emerged. It is possible to contrive situations (both in mathematical models and in laboratory experiments) in which sexual reproduction has immediate benefits, but it is far from established that these benefits account for either the origin or maintenance of sex (4, 5). Thus sexual reproduction poses a serious paradox for biologists—its ubiquity implies that it must have major and reliable benefits, but these remain mysterious.

A phylogenetic framework

Population genetic analysis has concentrated on the best-known sexual organisms, the plants and animals. At the same time, geneticists and molecular biologists have carried out a detailed investigation into the mechanisms of meiosis and of mating, primarily in fungi. However, we now need to extend both kinds of analysis to organisms with deeper evolutionary significance.

Bacteria. No process comparable to meiotic sex is known in Bacteria; all genetic exchange occurs by three *parasexual processes* that are unidirectional, fragmentary, and infrequent. In considering the evolution of these processes it is important to distinguish their two components: gene transfer (movement of chromosomal DNA segments from one cell to another) and physical recombination (the breaking and joining of DNA strands that incorporates transferred segments into the recipient chromosome). Studies of the mechanisms show these components to be quite independent of each other, and to exist for reasons unrelated to any benefits of genetic exchange.

Gene transfer: Segments of bacterial chromosomes can be transferred to other bacteria by three naturally occurring mechanisms: plasmid conjugation, phage transduction, and transformation. However, the first two of these mechanisms have well-established functions unrelated to sex—the contagious transfer of plasmids and of phage genomes, respectively. The genes specifying the transfer process are located on the plasmid or phage genome that is usually transferred, suggesting that contagious transfer is their primary function. In contrast, no genes specify the steps that cause transfer of chromosomal segments (formation of F and integrated [Hfr] plasmids, and the packaging of chromosomal DNA in phage capsids), and these appear to be unselected side effects of

This paper was originally presented at a workshop titled *Evolution: A Molecular Point of View*. The workshop, which was held at the Marine Biological Laboratory, Woods Hole, Massachusetts, from 24–26 October 1997, was sponsored by the Center for Advanced Studies in the Space Life Sciences at MBL and funded by the National Aeronautics and Space Administration under Cooperative Agreement NCC 2-896.

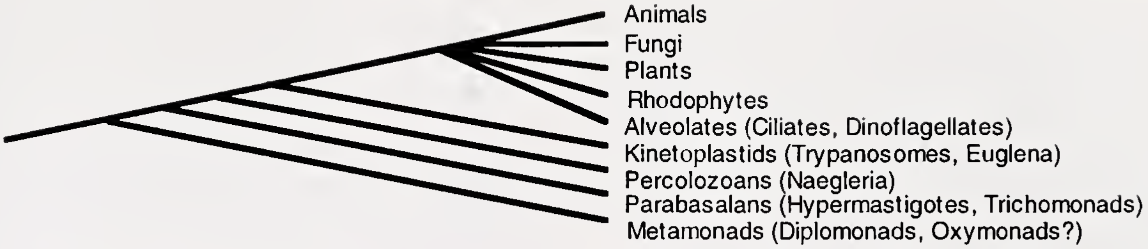
Animals
Fungi
Plants
Rhodophytes
Alveolates (Ciliates, Dinoflagellates)
Kinetoplastids (Trypanosomes, Euglena)
Percolozoans (Naegleria)
Parabasalans (Hypermastigotes, Trichomonads)
Metamonads (Diplomonads, Oxymonads?)

Figure 1. A very simplified eukaryote phylogeny, showing only the major groups relevant to this discussion.

their contagious-transfer functions. The third gene transfer process, DNA uptake by naturally competent bacteria, has no infectious-transfer component, and has been thought to exist for genetic exchange or possibly for DNA repair (6). However, our analysis of the regulation of competence suggests that DNA is taken up primarily as a nutrient. DNA damage does not induce competence in *Haemophilus influenzae* or *Bacillus subtilis,* contrary to predictions of the DNA-repair hypothesis (7). Furthermore, induction of competence in *H. influenzae* is controlled by adenylate cyclase and a fructose-specific phosphotransferase system, which together provide signals connecting shortages of preferred catabolites to induction of operons allowing use of alternative energy resources (8). Theoretical work also shows that competence is unlikely to provide significant recombination benefits, for two reasons. First, the available DNA will carry an excess of deleterious mutations, and second, it may carry alleles that preclude competence, especially if the competence cell has recently arisen in a population of noncompetent cells (9, 10).

Physical recombination: Although the many "*rec*" genes were identified in *Escherichia coli* because they are required for efficient recombination, analysis of their mechanisms and regulation shows that they evolved not for recombination with incoming DNA but for their roles in DNA replication and repair. For example, an excellent discussion of the primary function of RecA in DNA repair is given by Cox (11), and the importance of the RecBCD complex in DNA maintenance is revealed by the poor viability of cells lacking it (12).

It is important here to distinguish between evolutionary causes and evolutionary consequences. Although the parasexual processes of bacteria do not appear to have been selected for their ability to cause genetic exchange, they have undoubtedly had very significant consequences for long-term bacterial evolution (13).

Archaea. Plasmids, transposons, and phages are widespread in Archaea, as are the DNA repair and replication enzymes required for physical recombination of DNA, so presumably accidental exchange of chromosomal genes is not uncommon (14, 15). A novel process involving what appears to be exchange of plasmids by partial cell fusion has been observed in *Halobacterium volcanii* (16), and exchange of genetic markers has also been reported in *Sulfolobus acidocaldarius* (17).

Eukarya. Most members of the crown taxa are capable of sexual reproduction, as are at least some members of most early branches of the simplified tree in Figure 1. However, the branching order is far from finalized, and the evidence for or against sexual reproduction in these taxa is itself very sketchy. In what are probably the deepest branches, sex has been reported only for the essentially nonculturable Hypermastigote and Oxymonad members of the wood-digesting hindgut communities of termites and cockroaches, where it has been inferred from microscopic observation of cell and nuclear fusion and meiosis-like cell divisions (18, 19). In *Naegleria,* the population structure of environmental isolates is indicative of frequent genetic exchange, but sexuality has not been observed in culture (20).

Even within the crown taxa, sexual reproduction appears to have undergone very different evolutionary histories in different lineages. This is not surprising, because cycles of cell fusion and chromosome segregation provide very strong selective advantages to molecular parasites, such as transposable elements and meiotic drive genes, which have clearly modified the sexual process to further their own interests.

At present, everything we know about the mechanism and regulation of sexual reproduction was learned from the groups most closely related to us (animals, plants, and some fungi). Now the best payoff, in terms of insight into both evolutionary history and evolutionary causation, is likely to come from investigation into the sex lives of our most distant eukaryotic relatives.

Literature Cited

1. **Maynard Smith, J. 1978.** *The Evolution of Sex.* Cambridge University Press, Cambridge.
2. **Bell, G. 1982.** *The Masterpiece of Nature.* University of California Press, Berkeley.
3. **Michod, R. E., and B. R. Levin, eds. 1988.** *The Evolution of Sex.* Sinauer, Sunderland, MA.
4. **Hamilton, W. D., R. Axelrod, and R. Tanese. 1990.** Sex as an adaptation to resist parasites. *Proc. Natl. Acad. Sci. USA* **87:** 3566–3573.
5. **Kondrashov, A. 1994.** Sex and deleterious mutation. *Nature* **369:** 99–100.

6. **Michod, R. E., M. Wojciechowski, and M. Hoelzer. 1988.** DNA repair and the evolution of transformation in the bacterium *Bacillus subtilis. Genetics* **118:** 31–39.
7. **Redfield, R. J. 1993.** Evolution of natural transformation: testing the DNA repair hypothesis in *Bacillus subtilis* and *Haemophilus influenzae. Genetics* **133:** 755–761.
8. **Macfadyen, L. P., I. R. Dorocicz, J. Reizer, M. H. J. Saier, and R. J. Redfield. 1996.** Regulation of competence development and sugar utilization in *Haemophilus influenzae* Rd by a phosphoenopyruvate: fructose phosphotransferase system. *Mol. Microbiol.* **21:** 941–952.
9. **Redfield, R. J. 1988.** Evolution of bacterial transformation: is sex with dead cells ever better than no sex at all? *Genetics* **119:** 213–221.
10. **Redfield, R., M. Schrag, and A. Dean. 1997.** The evolution of bacterial transformation: sex with poor relations. *Genetics* **146:** 27–38.
11. **Cox, M. M. 1993.** Relating biochemistry to biology: how the recombinational repair function of RecA protein is manifested in its molecular properties. *Bioessays* **15:** 617–623.
12. **Myers, R. S., and F. W. Stahl. 1994.** Chi and the RecBCD enzyme of *Escherichia coli. Annu. Rev. Genet.* **28:** 49–70.
13. **Lawrence, J. C., and H. Ochman. 1997.** Amelioration of bacterial genomes: rates of change and exchange. *J. Mol. Evol.* **44:** 383–397.
14. **Schleper, C., I. Holz, D. Janekovic, J. Murphy, and W. Zillig. 1995.** A multicopy plasmid of the extremely thermophilic archaeon *Sulfolobus* effects its transfer to recipients by mating. *J. Bacteriol.* **177:** 4417–4426.
15. **Sandler, S. J., L. H. Satin, H. S. Samra, and A. J. Clark. 1996.** *recA*-like genes from three archaean species with putative protein products similar to Rad51 and Dmel proteins of the yeast *Saccharomyces cerevisiae. Nucleic Acids Res.* **24:** 2125–2132.
16. **Rosenshine, I., R. Tchelet, and M. Mevarech. 1989.** The mechanism of DNA transfer in the mating system of an archaebacterium. *Science* **245:** 1387–1389.
17. **Grogan, D. W. 1996.** Exchange of genetic markers at extremely high temperatures in the archaeon *Sulfolobus acidocaldarius. J. Bacteriol.* **178:** 3207–3211.
18. **Cleveland, L. R. 1950.** Hormone-induced sexual cycle of flagellates. II Gametogenesis, fertilization, and meiosis in *Oxymonas. J. Morphol.* **86:** 185–214.
19. **Cleveland, L. R. 1965.** Fertilization in *Trichonympha* from termites. *Arch. Protistenkd.* **108:** 1–5.
20. **Pernin, P., A. Ataya, and M. L. Cariou. 1992.** Genetic structure of natural populations of the free-living amoeba, *Naegleria lovaniensis.* Evidence for sexual reproduction. *Hereditary* **68:** 173–181.

Discussion

GUERRERO: A fourth kind of sex, not very well known, specific for actinomycetes (actinobacteria) is cytoplasmic fusion. Transformation occurs by means of a normal DNA transfer mechanism in bacteria which does not distinguish species. Transformation, not sex, is used to incorporate many external genes not only from their "own" species but any other. This is one reason that the concentration of external DNA, normal in both water and in soil, may be much higher outside than the concentration of DNA inside cells.

REDFIELD: There can be a surprisingly large amount of DNA outside of cells. However, I think it is extremely unlikely that the concentration would be higher than the concentration within the cell, with the possible exception being in the lungs of cystic fibrosis patients.

GUERRERO: It has been shown in natural habitats by Fuhrman in seawater and in soil by a group in Lyon, France. Is the sexy protein you made the same as competence factor made by Alexander Tomas?

REDFIELD: No, this is *Haemophilus influenza,* which has nothing to do with the competence factor. In response to your comments, I think you are wrong about the DNA concentrations. Although there is substantial DNA outside the cells, it's certainly not enough that the DNA is going to move down a concentration gradient into cells.

UNIDENTIFIED: I was waiting for you to say something positive about transformation. I thought you were hinting at the idea that even though sex is not particularly useful most of the time, in times of great stress, such as when everybody is dying around you—and perhaps they have accumulated some good mutations—that's the time to bring them in.

REDFIELD: All of the evidence of the regulation says that is not the case.

UNIDENTIFIED: What's that evidence?

REDFIELD: That it is regulated by nutritional signals.

UNIDENTIFIED: Lots of survival is regulated by nutrition, like sporulation. It's probably a mistake to sporulate if things are good around you.

REDFIELD: I'll just go back to my bottom-line statement: the idea that genetic exchange is good because it generates variation is very strongly entrenched in spite of the lack of evidence.

MARGULIS: I completely agree with you. In fact, I think that, as you showed for prokaryotes, direct selection never maintained or originated sex in eukaryotes either. Concerning *Bacillus,* do you have any insight into why competence has been seen to be light sensitive? Do we know what surface proteins are involved in competence?

REDFIELD: Yes, we know a lot about the proteins that are involved in competence in *Bacillus.* What has happened is that the simple regulatory system that responds to nutritional signals and causes cells to express DNA uptake systems has been linked to a complex regulatory network that is involved in secreting what are called *surfactant antibiotics.* These surfactants are releasing nutrients from the soil that *Bacillus* lives in; they may also kill other cells, and simultaneously there is a very weak link into this tight little regulatory network. When the surfactant is being excreted, competence is also turned on to take up any DNA that happens to be released.

SCHULTES: Although genetic algorithms are computer models, they are like binary DNA sequences that undergo point mutations or recombination in the computer. Because computer implementations of recombination can be studied under controlled circumstances, one can define conditions under which recombination (indeed, which recombination *rates*) will optimize your ability to solve certain problems.

REDFIELD: I am not saying that mutation and recombination have not produced evolutionary benefits. The benefits are absolutely clear from bacterial genomes, if nothing else, and from the fact that so much of the genetic variation that we have arose by mutation. All of the adaptive variation also arose by mutation. That does not mean that mutations, and the processes that cause mutations, exist because they produce beneficial mutations. The beneficial mutations are an unselected side effect. The benefits of these mutations have not fed back on the system that created them to cause it to create more. The system is under constant pressure to keep mutations down, but the cost of preventing mutations is so great that we get plenty of raw material for evolution without trying.

Reference: *Biol. Bull.* **196:** 408–410. (June 1999)

Evolution of Head Development

HANS BODE[1], DANIEL MARTINEZ[1,3], M. ANDREW SHENK[1], KERRY SMITH[1],
ROBERT STEELE[2], AND ULRICH TECHNAU[1]

[1]*Department of Developmental and Cell Biology, and* [2]*Department of Biological Chemistry, University of California, Irvine, California 92697; and* [3]*Department of Biology, Pomona College, Claremont, California 91711*

Accumulating evidence indicates that genes regulating developmental processes are, to a large extent, common among the metazoans despite the great variety of body plans among them. A prominent example are the *Hox* genes which specify body regions along the anterior-posterior axis. Of interest are questions concerning the evolution of these genes. When did a particular gene first appear in metazoan evolution, and to what extent has its function been conserved? These questions can be addressed by examining members of the Cnidaria, as this phylum arose very early in metazoan evolution. Further, examining these issues in hydra is of particular value because the processes governing the development of this animal are well understood at the tissue and cell level, and certainly much better understood than for any other cnidarian.

One approach is to examine the genes that govern the development of a particular region or structure of the animal. An interesting region would be the head. Although the head of a hydra does not resemble that of a vertebrate or an insect very closely, there are some common basic features. In hydra, as in other animals, the head is at the anterior end of the animal. The mouth, or opening to the gastric cavity, is in the hypostome, the apical part of the head (Fig. 1B, C). Although a hydra has no brain, the highest concentration of neurons is in the head. Further, though hydra does not have sense organs as do other animals, the cells controlling photoreception and phototaxis are in the head.

A number of genes have been isolated that encode transcription factors expressed in the developing head of both vertebrates and arthropods (1). Mutational analyses reveal that many of them play a critical role in head development. These include members of the *otx, emx, dlx, Hox* classes of homeobox genes, as well as homologs of the *fork head/HNF-3* class of winged helix genes. If the developmental mechanisms underlying head formation are related in hydra and the triploblastic organisms, one might expect to find some of these genes expressed in the developing hydra head. Commonly one would examine developing embryos. In hydra the tissue dynamics of the adult body are such that the patterning processes are constantly active to maintain the form of the adult animal. In addition, hydra reproduces asexually by budding. Hence, instead of examining hydra embryos, the patterns of expression were examined in the adult and during budding.

Some typical head genes have been isolated from hydra. Homologs of two *Hox* genes have been characterized. *Cnox-3,* whose closest relative is the *Drosophila labial* gene, and *Cnox-2,* the hydra homolog of the *Deformed* gene (2), are expressed in the same axial order as in arthropods and vertebrates (*e.g.,* 3). *Cnox-3* is strongly expressed in the ectoderm of the tentacle zone, which is the lower part of the head of hydra, and in the upper end of the body column (Fig. 1E). Since tissue of the upper body column and tentacle zone is continually displaced onto the tentacles, the gene could have a role in committing body column ectodermal cells to the formation of battery cells, the differentiated cell type of the ectoderm in the tentacles (Shenk *et al.,* unpubl. results). *Cnox-2* (Fig. 1A) is expressed in both tissue layers of the body column and foot, but not the head (4, 5). In a variety of experimental circumstances, when a part of the body column is converted into head tissue, *Cnox-2* expression always vanishes, suggesting that this gene could act as a repressor of head formation. An evolutionary parallel

---

This paper was originally presented at a workshop titled *Evolution: A Molecular Point of View*. The workshop, which was held at the Marine Biological Laboratory, Woods Hole, Massachusetts, from 24–26 October 1997, was sponsored by the Center for Advanced Studies in the Space Life Sciences at MBL and funded by the National Aeronautics and Space Administration under Cooperative Agreement NCC 2-896.

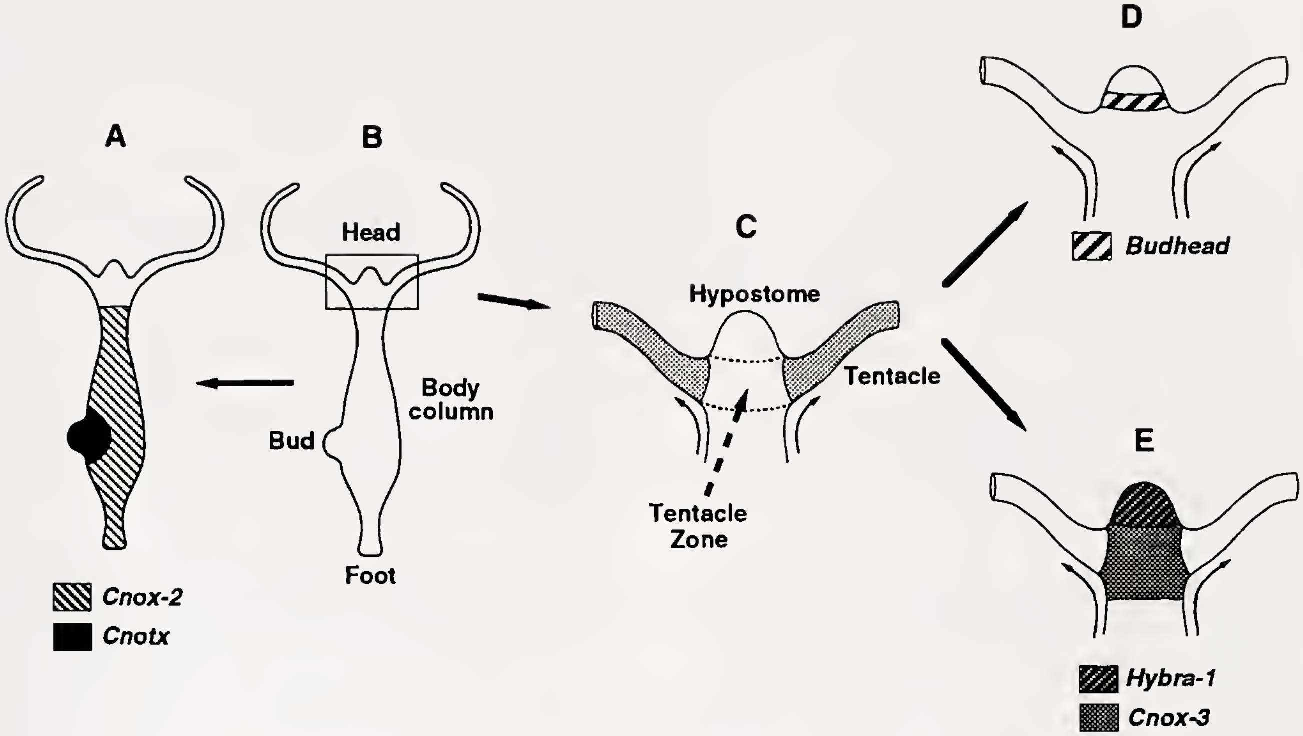

Figure 1. Expression patterns of several genes in hydra. The general form of the animal (B) and the parts of the head (C). Expression patterns of (A) *Cnox-2* and *Cnotx;* (D) *budhead;* and (E) *Hybra-1* and *Cnox-3.*

exists with its homolog, *Deformed,* in that this gene has recently been shown to act as both a negative and a positive regulator of head formation in *Drosophila* (6).

Two other homeobox genes known to play a role in head development in both arthropods and vertebrates have been characterized. *Cn-ems,* an *emx* homolog, has been isolated from *Hydractinia,* a close marine relative of hydra, and shown to be expressed in the endoderm of the hypostome (7). *Cnotx,* the hydra homolog of members of the *otx* family, is not expressed in the adult head, but has a role in head formation during budding, hydra's form of asexual reproduction (Fig. 1A). As soon as bud formation is initiated, *Cnotx* is strongly expressed in most of the tissue that will form the bud (8). As this tissue is also committed to the formation of a head, the initial steps of bud formation and head formation may be part of the same process, with *Cnotx* playing a role in the process. Here too, one of the pair of genes, *Cn-ems,* has a direct role, while the other, *Cnotx,* has a less clearly defined role in head formation.

Finally, two other genes provide an interesting example of how a developmental mechanism might be conserved. Homologs of the *fork head/HNF-3β* class of genes play a central role in organizing the development of the rostral part of vertebrate heads, as well as the notochord (*e.g.,* 1). *Budhead,* a hydra member of this class, is expressed in the lower half of the hypostome (Fig. 1D; 9). Further, this region has organizer activity in hydra, as defined by transplantation experiments (10). *Brachyury* expression and function is associated with the organization of the developing trunk of vertebrate embryos (11), and is expressed at the posterior gut of a developing fly embryo (12). In sharp contrast, the hydra homolog of this gene, *Hybra-1,* is expressed in the hypostome (Fig. 1E; 13). The interesting parallel is that, in several organisms, the *fork head/HNF-3β* gene and the *Brachyury* gene are expressed in the same location at a similar time in development, suggesting that both participate in a particular developmental mechanism. Since the co-expression of the two genes is in the head of a hydra, the developing notochord of a vertebrate, and the hindgut of an arthropod, the mechanism involving the two genes could have arisen early in metazoan evolution and been used subsequently in the development of different structures.

Thus, there are some parallels in the expression pattern of genes known to regulate head formation in triploblastic animals and their homologs in hydra. This would suggest that elements of the developmental mechanisms underlying head formation arose early in evolution and have been conserved in terms of the region where the gene functions. In other cases, developmental mechanisms arising early may have been used for head formation in hydra and later co-opted for other functions in more complex organisms.

Acknowledgments

This work was supported by grants to H.B. from NIH (PO1-HD27173) and NSF (IBN-9723660).

Literature Cited

1. **Bally-Cuif, L., and E. Boncinelli. 1997.** Transcription factors and head formation in vertebrates. *BioEssays* **19:** 127–135.
2. **Schummer, M., I. Scheurlen, C. Schaller, and B. Galliot. 1992.** HOM/HOX homeobox genes are present in hydra (*Chlorohydra viridissima*) and are differentially expressed during regeneration. *EMBO J.* **11:** 1815–1823.
3. **DeRobertis, E. M. 1994.** The homeobox in cell differentiation and evolution. Pp. 11–24 in *Guidebook to the Homeobox Genes*. D. Duboule, ed. Oxford University Press, New York.
4. **Shenk, M. A., H. R. Bode, and R. E. Steele. 1993.** Expression of *Cnox-2*, a HOM/HOX homeobox gene in hydra, is correlated with axial pattern formation. *Development* **117:** 657–667.
5. **Shenk, M. A., L. Gee, R. E. Steele, and H. R. Bode. 1993.** Expression of *Cnox-2*, a HOM/HOX gene, is suppressed during head formation in hydra. *Dev. Biol.* **160:** 108–118.
6. **Pinsonneault, J., B. Florence, H. Vaessin, and W. McGinnis. 1997.** A model for extradenticle function as a switch that changes HOX proteins from repressors to activators. *Embo J.* **16:** 2032–42.
7. **Mokady, O., M. H. Dick, D. Lackschweitz, B. Schierwater, and L. W. Buss. 1998.** Over one-half billion years of head conservation? Expression of an ems class gene in *Hydractinia symbiolongicarpus* (Cnidaria: Hydrozoa). *Proc. Natl. Acad. Sci. USA* **95:** 3673–8.
8. **Smith, K. M., L. Lydia, I. Blitz, and H. R. Bode.** *CnOtx*, a member of the Otx gene family, has a role in cell movement and anterior specification in hydra. *Dev. Biol.* (in press).
9. **Martinez, D. E., M. Jamrich, M. L. Dirksen, P. M. Bode, R. E. Steele, and H. R. Bode. 1997.** *Budhead*, a fork head/HNF-3 homologue, is expressed during axis formation and head specification in hydra. *Dev. Biol.* **192:** 523-536.
10. **MacWilliams, H. K. 1983.** Hydra transplantation phenomena and the mechanism of hydra head regeneration. I. Properties of the head activation. *Dev. Biol.* **96:** 239–257.
11. **Cunliffe, V., and J. C. Smith. 1992.** Ectopic mesoderm formation in *Xenopus* embryos caused by widespread expression of a *Brachyury* homologue. *Nature* **358:** 427–30.
12. **Kispert, A., B. G. Herrmann, M. Leptin, and R. Reuter. 1994.** Homologs of the mouse *Brachyury* gene are involved in the specification of posterior terminal structures in *Drosophila*, *Tribolium*, and *Locusta*. *Genes Dev.* **8:** 2137–50.
13. **Technau, U., and H. R. Bode. 1999.** *HyBra1*, a *Brachyury* homologue, acts during head formation in *Hydra*. *Development* **126:** 999–1010.

Discussion

UNIDENTIFIED: Have any of these genes been found in sponges?

BODE: There are a few reports of homeobox genes in sponges (1, 2). Kurosawa's group in Japan has described three homeobox-containing genes, *prox1*, *prox2*, and *prox3*, which are most closely related to the *NK-3* and *OM(1D)* genes of *Drosophila* and the *msh* gene respectively. They have also recently reported finding two genes that are homologous to members of the POU class of homeobox genes.

CAVALIER-SMITH: Hydroids are fairly simplified Cnidaria. Is anyone looking in anthozoan polyps for the distribution of the genes that you have described?

BODE: Homologs for *Hox* genes have been found in anthozoans and in other hydrozoans (3–5). There is little information about the expression patterns of these genes except for the expression of *Cnox-2* and *Cn-ems* in *Hydractinia* (6; P. Cartwright and L. Buss, pers. comm.). The *Cnox-2* pattern is similar to that observed in hydra (P. Cartwright and L. Buss, pers. comm.). I'm not aware that homologs for *Brachyury* and the *fork head/HNF-3b* homologs have been identified in other cnidarians.

Literature Cited

1. **Seimiya, M., H. Ishiguro, K. Miura, Y. Watanabe, and Y. Kurosawa. 1994.** Homeobox-containing genes in the most primitive metazoa, the sponges. *Eur. J. Biochem.* **221:** 219–25.
2. **Seimiya, M., Y. Watanabe, and Y. Kurosawa. 1997.** Identification of POU-class homeobox genes in freshwater sponge and the specific expression of these genes during differentiation. *Eur. J. Biochem.* **243:** 27–31.
3. **Schierwater, B., M. T. Murtha, M. H. Dick, F. H. Ruddle, and L. W. Buss. 1991.** Homeoboxes in Cnidarians. *J. Exp. Zool.* **260:** 413–416.
4. **Murtha, M. T., J. F. Leckman, and F. H. Ruddle. 1991.** Detection of homeobox genes in development and evolution. *Proc. Natl. Acad. Sci. USA* **88:** 10711–10715.
5. **Kuhn, K., B. Streit, and B. Schierwater. 1996.** Homeobox genes in the Cnidarian *Eleutheria dichotoma*: evolutionary implications for the origin of the *Antennapedia*-class (HOM/Hox) genes. *Mol. Phylogenet. Evol.* **6:** 30–38.
6. **Mokady, O., M. H. Dick, D. Lackschweitz, B. Schierwater, and L. W. Buss. 1998.** Over one-half billion years of head conservation? Expression of an ems class gene in *Hydractinia symbiolongicarpus* (Cnidaria: Hydrozoa). *Proc. Natl. Acad. Sci. USA* **95:** 3673–8.

Reference: *Biol. Bull.* **196:** 411–412. (June 1999)

Patterns of Mitochondrial DNA Strand Asymmetry Correlate With Phylogeny

SCOTT MOHR[1], JIM FREEMAN[2], TOM PLASTERER[2], AND TEMPLE SMITH[2]

[1]*Department of Chemistry and* [2]*BioMolecular Engineering Research Center, Boston University College of Engineering, 36 Cummington Street, Boston, Massachusetts 02215*

In the current era of megabase DNA sequencing, there is a need for analytical methods that extend beyond the level of single genes or gene clusters and allow us to characterize genome features more globally. Following up on the observations of Lobry (1, 2) concerning "GC skew" [relative enhancement of G in one strand over a given DNA segment: (G − C)/(G + C)], we have begun to examine "purine excess" in long DNA sequences. This function—defined as the sum of all purines minus the sum of all pyrimidines encountered in a sequence up to the given position—displays the overall strand asymmetry. In bacterial genomes, the minima and maxima of the purine excess curves correlate closely with, respectively, the origins and termini of replication (3). We have now calculated the purine-excess curves for 52 complete mitochondrial DNA sequences available from GenBank. They cover the entire range of eukaryotes, from yeast to human, and display intriguing patterns that correlate with phylogenetic relationships. The curves for closely related organisms (*e.g.*, sets of primates, pinnipeds, marsupials, fish, insects, or sea urchins) virtually superpose, whereas curves from more distant heterogeneous groups (*e.g.*, crustaceans plus insects) have recognizable similarities, but also clear differences of detail. Characteristically, the larger "ancestral" mtDNAs from single-celled organisms have "choppier" curves (see Fig. 1) with many sharp peaks and troughs, whereas the curves become smoother as one advances to the vertebrates with their "derived" mtDNAs of about 15 kb. Over the range from *Latimeria* to *Homo*—including 29 species—the purine excess curves quickly converge to forms closely resembling that of the chimpanzee (result shown in Fig. 1).

Possible explanations for the origins of these patterns involve asymmetrical features of DNA replication and transcription (3, 4), as well as the possible influence of horizontal gene transfer (5). In the case of bacterial genomes, we have computed a function ("coding-strand excess") that indicates whether a given nucleotide is part of a coding sequence, is complementary to a coding sequence, or neither (3). For nine complete bacterial genomes plus bacteriophage λ (data presented at http://bmerc-www.bu.edu/genomeplot/), this function correlates strongly with the purine excess; that is, coding sequences tend to become progressively purine-rich. When the coding sequence occurs in the presented strand, the purine-excess curve normally goes up; whereas if it occurs in the complementary strand, the purine-excess curves mostly have negative slopes. In cases where the identification of open reading frames (ORFs) has not been made or may be dubious, the purine-excess function may help to delineate the most probable ORF positions and orientations (J.H. Graber *et al.*, unpubl. data).

Using this principle we can interpret the features of two of the mitochondrial genomes shown in Figure 1. For *Saccharomyces cerevisiae*, for example, the pronounced upswing in the purine-excess curve, beginning at about position 31,000, corresponds to the major ORF cluster of the genome (*COX1* plus associated intronic ORFs). The same gene in *Prototheca wickerhamii* is oriented in the other direction (transcribed from right to left—off the complementary strand) starting at position 9413—which corresponds to a sharp minimum in the purine excess curve. The general upward trend of the curve beyond position 28,000 in this genome correlates with the tendency for rightward transcription of the genes on this half of the chromosome, most notably the rRNA gene which falls between positions 48,900 and 52,700. The remaining four mitochondrial ge-

---

This paper was submitted in conjunction with a workshop titled *Evolution: A Molecular Point of View*. The workshop, which was held at the Marine Biological Laboratory, Woods Hole, Massachusetts, from 24–26 October 1997, was sponsored by the Center for Advanced Studies in the Space Life Sciences at MBL and funded by the National Aeronautics and Space Administration under Cooperative Agreement NCC 2-896.

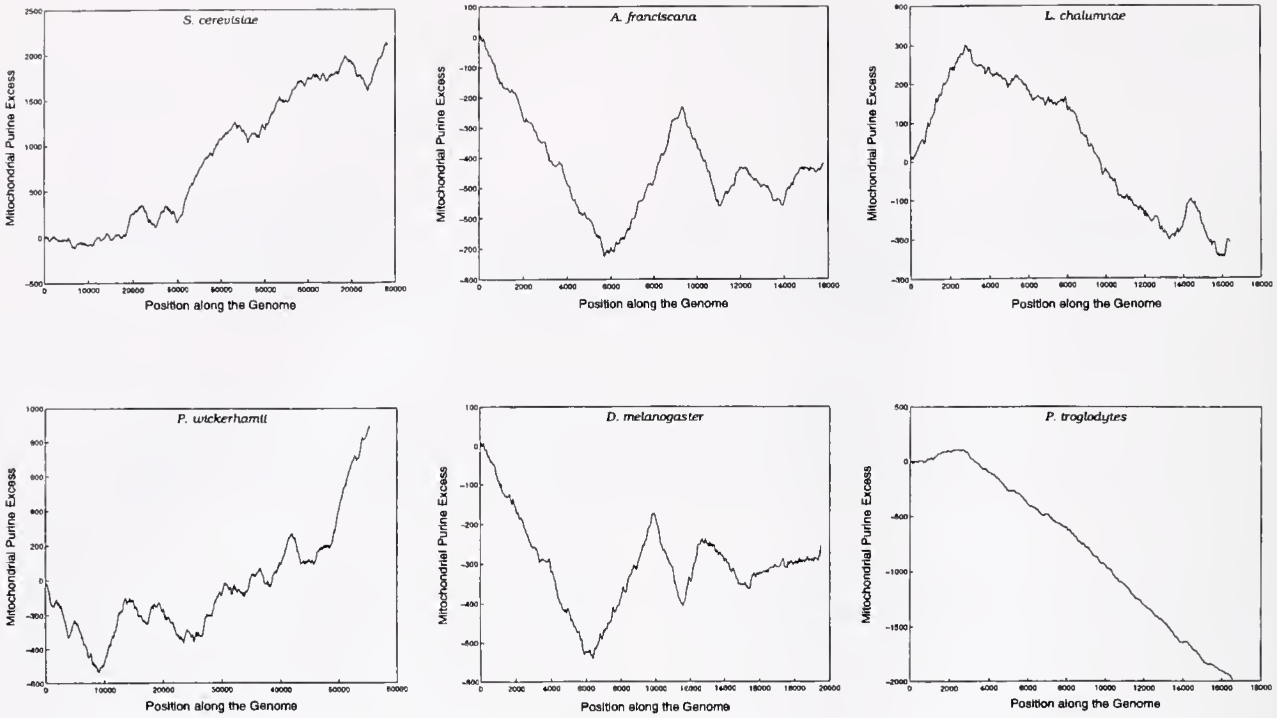

Figure 1. "Purine-excess" curves for selected mitochondrial DNAs. In order from left to right—TOP: *Saccharomyces cerevisiae* (baker's yeast), *Artemia franciscana* (brine shrimp), *Latimeria chalumnae* (coelacanth); BOTTOM: *Prototheca wickerhamii* (chlorophyte alga), *Drosophila melanogaster* (fruitfly), *Pan troglodytes* (chimpanzee). The ordinate is the purine excess calculated for the presented (displayed) strand, as retrieved from GenBank. Position numbering follows the deposited sequence where in most cases position 1 was arbitrarily chosen within the D-loop region. Since the molecules are circular, the starting points for the curves have no special significance, though they tend to fall close to the H (heavy) strand origin of replication.

nomes depicted in Figure 1 represent clear anomalies, however. In these cases (and many others not shown), the majority of the ORFs display *decreasing* purine excess in the transcribed direction. Considering that these are highly "derived" mitochondrial genomes with only a few remaining genes from the ancestral set (6), their anomalous behavior can be readily explained. The proteins they encode are specialized components of the inner mitochondrial membrane and hence are composed mostly of hydrophobic amino acids whose codons are pyrimidine-rich. For the highly derived genomes (beyond *Latimeria*), all but one of the ORFs are situated on the displayed strand (transcribed from left to right) *and* show the negative purine excess corresponding to hydrophobic proteins. The short initial segment of each of these genomes (*cf.* curve for chimpanzee mtDNA in Fig. 1) has a positive purine excess; this segment encodes ribosomal RNA—a gene product not translated, and thus unaffected by the relationship between the properties of the amino acid side-chains and the compositions of the codons.

Further analysis along these lines has the potential to cast light on the evolution and stabilization of mitochondrial genomes. It is well accepted that mtDNA has undergone many rearrangements—as well as truncations—over the eons since the original endosymbiosis event (7), and thus the blocks of genes, which are oriented with their transcription direction right-to-left, have probably been reshuffled so as to "streamline" the genome into the form seen in higher vertebrates. Exactly why this arrangement had a selective advantage remains to be determined.

Literature Cited

1. **Lobry, J. R. 1996.** Asymmetric substitution patterns in the two DNA strands of bacteria. *Mol. Biol. Evol.* **13:** 660–665.
2. **Lobry, J. R. 1996.** Origin of replication of *Mycoplasma genitalium*. *Science* **272:** 745–746.
3. **Freeman, J. M., T. N. Plasterer, T. F. Smith, and S. C. Mohr. 1998.** Patterns of genome organization in bacteria. *Science* **279:** 1827 [Extended information available at www.sciencemag.org/cgi/content/full/279/5358/1827a.]
4. **Francino, M. P., and H. Ochman. 1997.** Strand asymmetries in DNA evolution. *Trends Genet.* **13:** 240–245.
5. **Lawrence, J. G., and H. Ochman. 1997.** Amelioration of bacterial genomes: rates of change and exchange. *J. Mol. Evol.* **44:** 383–397.
6. **Gray, M. W., B. F. Lang, R. Cedergren, G. B. Golding, C. Lemieux, D. Sankoff, M. Turmel, N. Brossard, E. Delage, T. G. Littlejohn, I. Plante, P. Rioux, D. Saint-Louis, Y. Zhu, and G. Burger. 1998.** Genome structure and gene content in protist mitochondrial DNAs. *Nucleic Acids Res.* **26:** 865–878.
7. **Gillham, N. W. 1994.** *Organellar Genes and Genomes*, Oxford University Press, New York.

Reference: *Biol. Bull.* **196:** 413–414. (June 1999)

The Molecular Tangled Bank: Not Seeing the Phylogenies for the Trees

LYNN MARGULIS[1], MICHAEL DOLAN[2], AND RICARDO GUERRERO[3]

[1] *Department of Geosciences, University of Massachusetts, Amherst, Massachusetts 01003-5820;*
[2] *Organismic and Evolutionary Biology Graduate Program, University of Massachusetts, Amherst, Massachusetts 01003-5810; and* [3] *Department of Microbiology, University of Barcelona, Av. Diagonal, 645, Barcelona, Spain 08028*

About 40 years ago, in a gesture of civic enlightenment, the United States Congress passed legislation that converted the National Advisory Committee for Aeronautics (NACA; in existence since 1915) to NASA (National Aeronautics and Space Administration). The Space Act, no doubt in partial response to the launching of the first near-Earth satellite, Sputnik, by the Soviet Union, established NASA in 1958. This legislation is arguably the most well-written and enlightened government document to be created since the 18th century Jeffersonian Declaration of Independence.

Many of the stated goals of the 1958 Space Act were meant to generate new knowledge about the universe at large, but the statement that has most directly concerned molecular evolution is the following (1, p. 4):

> A major goal of the National Aeronautics and Space Administration is to understand the origin and evolution of life as a phenomenon in the solar system [or wherever in the universe it may reside].

Three objectives are seen as fundamental to planetary biology and chemical evolution (1, p. 5):

(1) Understanding the origin and evolution of life;
(2) understanding the cycles that sustain life—the interactions between the physical, chemical and biological phenomena on the surface of the planet Earth; and
(3) understanding the effects of life, both past and present, on the planet.

Clearly the stated goals of planetary biology and chemical evolution of the National Academy's Space Science Board are congruent with the evolutionary ones of the NASA-sponsored Center for Advanced Studies in the Space Life Sciences at the Marine Biological Laboratory. Only one specific goal was stated: the Center was meant to provide a forum "for scientists to think and discuss" about *Evolution: A Molecular Point of View.*

This meeting at the MBL examined and explored in a new way evidence for ancestral relationships among the multitudinous extant organisms on Earth. By examining the sequences of amino acids in proteins, and the sequences of nucleotides that constitute nucleic acids, the community of scholars attempts to reconstruct from extremely recent data the history of the lineages of major forms of extant life. Macromolecular sequencing techniques, high-speed computing, international telephone lines that confer access to, and connect, biochemical databases have unified the study of evolution as never before in the history of life science.

The advantages of molecular evolution in reconstructing the evolutionary history of life are indisputable. Macromolecular sequences of proteins or nucleic acids taken from living organisms provide a large quantity of detailed data hitherto unavailable. High-speed computers permit alignment and assessment of vastly more data than ever before in unique ways not possible until recently.

However, here we recognize some problems and goals.

Macromolecules are always extracted from single individuals or a number of like individuals that were living in the same place at the same time (a population) and are taken to represent the taxon in question (*e.g., Spongomonas* as Cercozoa, Cavalier-Smith, pp. 393–396, these proceedings). Clearly, there will be individual examples of named organ-

This paper was submitted in conjunction with a workshop titled *Evolution: A Molecular Point of View.* The workshop, which was held at the Marine Biological Laboratory, Woods Hole, Massachusetts, from 24–26 October 1997, was sponsored by the Center for Advanced Studies in the Space Life Sciences at MBL and funded by the National Aeronautics and Space Administration under Cooperative Agreement NCC 2-896.

isms that, in fact, are not proper representatives of the taxa placed on the branches of phylogenetic drawings.

Since just after the publication of *Origins of Species* by Charles Darwin, 19th century naturalists, especially Ernst Haeckel, recognized that drawings with branches (dubbed "phylogenetic trees") can represent in two dimensions our concepts of the evolutionary history of life. In the era immediately prior to the molecular biological revolution, a lengthy review of evolutionary relationships among the smaller eukaryotes was published by R. Klein (University of Vermont) and A. Cronquist (director of the Bronx Botanical Garden in New York) (2). In an era where all organisms were either animals or plants, Klein and Cronquist were oriented to the living world as botanists: and they called the unruly set of beings that they analyzed "Thallophytes" ("lower plants" including "plant-like protozoa"). The problem of partial phylogeny was well analyzed by these authors: branching diagrams for relations between the parts of organisms (partial phylogenies) can be depicted independent of any full phylogeny that attempts to show the evolutionary history of the entire population or species of organism in question. The points they made are still useful. Partial phylogenies, even when they are fully valid for the characteristics (genes, pigments, organs, etc.) in question, are not, nor should they ever claim to be, full phylogenies. All molecular phylogenies are partial. Investigators in the new science of molecular evolution often contend that phylogenies based on ribosomal RNA are superior (or inferior) to those derived from protein sequences. Single protein sequences are less effective than more than one in positioning organisms on phylogenetic diagrams. Yet even multiple protein phylogenies fall short of descriptions of the evolutionary history of a species since all organisms, except a few bacteria, have thousands of proteins that are required at all times for self-maintaining metabolism. This implies that, to date, all published phylogenetic diagrams based solely on data from nucleic acid sequences, protein sequences, or a combination of both are seriously deficient.

Because they failed to incorporate ideas of plastid and mitochondrial origins by symbiogenesis, Klein and Cronquist published many incongruent phylogenetic diagrams. Similar inconsistent and even mutually exclusive molecular phylogenies have been published and reviewed at this meeting. In part, the problems stem from differing alignments and computing methods. But probably far more relevant to both the molecular and taxonomic contentiousness is the problem of unstated or inexplicit assumptions about the organisms, their names, and the extent to which the phylogenies are partial.

The major egregious unstated hypothesis is that the amount of sequence divergence in the extant organisms studied directly reflects their evolutionary divergence from common ancestors. In fact, macromolecular sequence might easily be a more sensitive function of precise nuclease cleavage—highly selected genetic recombination leading to rearrangement of protein domains and consistent selective environmental constraints. Consider the case of all eukaryotes, from the time that they evolved through symbiosis (3), the rates of evolution of their component symbionts (bionts) have differed from the rates of the entire integrated organism (holobiont). Differences in the extent of genetic integration and the elimination of redundancy in multiple symbionts (*e.g.*, like the seven genomic components that constitute *Mesodinium rubrum* (as reviewed by G. Sellers, Univ. of Maryland, unpubl. data), or the five biotic components of *Mixotricha paradoxa*) exacerbate the problem.

We have mentioned here but a few of the oversights that have led to overinterpretation of molecular phylogenies as reflective of past history. We feel that no substitute exists for knowing the live organism in question, its life history and habitat. Natural history, life cycle details, morphology including ultrastructure, the history of environmental change as documented by the rock record, and good sense are all crucial elements in reconstructing the ancient lineages of life on Earth.

Perusing this set of papers makes clear that both the problems and prospects are enormous: no doubt molecular insights will be crucial in resolving the genealogies of our remote ancestors.

The value of this first meeting must be emphasized. Our colleagues raise awareness of the relation between the goals of NASA and the construction of molecular phylogenies, state problems of extrapolation and overinterpretation from limited data, and point out the immense range of microbes and their descendants worthy of study. Future scientific gatherings under this aegis, we hope, will make explicit, through open discussion, some of the unstated assumptions and will promote better-evaluated molecular data. The amazing revelation of macromolecular sequences will then be integrated into other ways of learning about the evolutionary past history of life and its environment on planet Earth.

Literature Cited

1. Space Science Board, Planetary Biology and Chemical Evolution, 1980, National Academy of Sciences, *National Academy of Sciences Press*, Washington DC.
2. **Klein, R., and A. Cronquist. 1967.** A consideration of the evolutionary and taxonomic significance of some biochemical, micromorphological and physiological characteristics in the Thallophytes. *Q. Rev. Biol.* **42:** 105–296.
3. **Margulis, L. 1996.** Archael-eubacterial merges in the origin of Eukarya: phylogenetic classification of life. *Proc. Natl. Acad. Sci. USA* **93:** 1071–1076.

Reference: *Biol. Bull.* **196:** 415–416. (June 1999)

Concluding Remarks

MITCHELL L. SOGIN

Josephine Bay Paul Center, Marine Biological Laboratory, 7 MBL Street, Woods Hole, Massachusetts 02543-1015

Christian Schwabe wrote many papers after Carl Woese described the Archaebacteria, and the last common ancestor, the progenote. Schwabe was frustrated because one could not really, in a convincing way, devise consistent phylogenetic trees based on shared derived biochemical characters. He contrived the following solution to this problem; the mechanism, although a bit far-fetched, is as follows. In the beginning there was a progenote, and the progenote was made up of a series of coding sequences (exons) that were interrupted by introns, but everything was scrambled and out of order. Out of the progenote came 10 billion or more different lineages that grew as microorganisms and multiplied. These organisms rearranged the orientation of their exons until, in the fullness of time, they got it right; and a horse, for instance, would suddenly appear—thus explaining punctuated equilibrium in the fossil record.

This was a form of molecular creationism, but Schwabe had at least presented a mechanism. I think that if we start throwing rocks at trees, we have to start thinking about why molecular trees from different genes are different. Why and under what conditions do they fail us?

To address this question, we have to step back and ask, Can we even build a gene tree? If we could find every homologous gene in every organism represented in an evolutionary tree, can we reconstruct the evolutionary history of that gene in the form of a phylogeny? Some of us would say, No; others would say, There are limitations. If we can build gene trees, are there any genes that are better than others? That's a question that we all pose when we attempt to reconstruct evolutionary history. If life involves as much free exchange of genetic information as I think it does, then there is more lateral gene flow than we understand, at least in the eukaryotic world. Are there genes that mark—and thus allow us to trace—the genetic core of a eukaryote from the time it diverged from prokaryotes?

One of the other major problems we face is the incongruence of the molecular and fossil record. How does one deal with cyanobacterial lineages that show up 3.5 billion years ago in the fossil record and yet diverge late in molecular trees?

I hope that readers from outside the field of molecular evolution will not have the impression that things are totally hopeless, and that we are in a complete state of chaos. Recent advances now enable us to obtain data that go beyond the single gene data sets provided by ribosomal RNA genes. We are starting to get reasonable numbers of different genes, but not yet sufficient taxonomic representation, for many other genes from many other kinds of organisms.

One of our roles at this meeting is to advise NASA as to the means and costs of harnessing the power of molecular ecology and molecular evolution directed towards understanding the origins of life and the evolutionary history of organisms on this planet.

This paper was originally presented at a workshop titled *Evolution: A Molecular Point of View*. The workshop, which was held at the Marine Biological Laboratory, Woods Hole, Massachusetts, from 24–26 October 1997, was sponsored by the Center for Advanced Studies in the Space Life Sciences at MBL and funded by the National Aeronautics and Space Administration under Cooperative Agreement NCC 2-896.

Discussion

GUERRERO: I agree with what you have said, but you seem to have omitted reference to the environment. Presentations at this meeting have only considered intrinsic consequences of genome evolution, including mutation and the fidelity of replication. However, the environment is essential for at least two reasons. First, an appropriate environment is necessary for evolution. The environment selects. What you have described could happen on any planet, but we know extant life on Earth needs biogeochemical cycles. Organisms differ physiologically. Unless one organism uses the excretory products of another, the biologically crucial elements will be exhausted in 1, 2, or 3 hundred million years. Cycling of the elements C, N, S, P, etc., is essential to life. This is an important concept and leads to the realization that we need an "origins of ecosystems hypothesis," as well as an "origins of life hypothesis." An understanding of the environment is essential if we are ever to understand evolution and the persistence of life.

SOGIN: Would you argue that it would be a useful endeavor to study evolution of environments, or even to model evolution of environments?

GUERRERO: Yes. A model that includes the interaction between the environments and the organisms is especially needed.

KUNKEL: Can we attract non-microbiologists into these studies and promote a universal interest in evolutionary biology?

SOGIN: It would be nice to see meetings on the evolution of complex systems, the evolution of the environment, life in extreme environments, and other topics in that general area—not just development.

CHANG: There are really three foundations, or pillars, that can support a truly evolutionary approach to understanding the history of life on the planet. Understanding requires the integration of environmental history with a phylogenic organismal history, and with an appreciation for the physiology of organisms in the environment—all three placed within an ecological context.

Most of what we have heard at this meeting has been devoid of an ecological context. Ecologists appreciate how organisms interact with other organisms and their common environment. Life is a planetary phenomenon, and NASA is interested in how, through their interplay, organisms and environments have affected each other through time.

Reference: *Biol. Bull.* **196:** 417–420. (June 1999)

Participants

DAVID BARTEL
Whitehead Institute for Biomedical Research
9 Cambridge Center
Cambridge, Massachusetts 02142
dbartel@wi.mit.edu

HANS BODE
Department of Developmental and Cell Biology
University of California
Irvine, California 92697-2300
hrbode@uci.edu

JAY BRANDES
Carnegie Geophysical Laboratory
5251 Broad Branch Road
Washington, DC 20015-1305
brandes@gl.ciw.edu

TOM CAVALIER-SMITH
Department of Botany
University of British Columbia
#3529-6270 University Boulevard
Vancouver, British Columbia
V6T 1Z4 Canada
tom@tcs.botany.ubc.ca

SHERWOOD CHANG
NASA Ames Research Center
Mail Stop 239-4
Exobiology Branch
Moffett Field, California 94035-1000

C. GRAHAM CLARK
Department of Infectious and Tropical Diseases
London School of Hygiene & Tropical Medicine
Keppel Street
London, WC1E 7HT
United Kingdom
g.clark@lshtm.ac.uk

KENNETH W. CULLINGS
Conservation Genetics Lab
Department of Biology
San Francisco State University
Pleasant Hill, California 94523
cullings@sfsu.edu

MICHAEL CUMMINGS
Marine Biological Laboratory
7 MBL Street
Woods Hole, Massachusetts 02543-1015
mike@bluefish.mbl.edu

ALAN CURNOW
Department of Molecular Biophysics and Biochemistry
Yale University
P.O. Box 208114, 266 Whitney Avenue
New Haven, Connecticut 06520-8114

HEATHER DEIDERICK
Department of Biology
Indiana University
Bloomington, Indiana 47405

EDWARD DELONG
Monteray Bay Aquarium Research Institute
P.O. Box 628, 7700 Sandholdt Road
Moss Landing, California 95039-0628
delong@mbari.org

DAVID DES MARAIS
NASA/Ames Research Center, MS 239-4
Moffett Field, California 94035-1000
ddesmarais@mail.arc.nasa.gov

MICHAEL DOLAN
Biology Department
University of Massachusetts at Amherst
Morrill Science Center
Amherst, Massachusetts 01003

RUSSELL F. DOOLITTLE
Center for Molecular Genetics, M-034
Department of Chemistry
University of California at San Diego
La Jolla, California 92093-0634
rdoolittle@ucsd.edu

W. FORD DOOLITTLE
Department of Biochemistry
Dalhousie University
Halifax, Nova Scotia
B3H 4H7 CANADA
ford@is.dal.ca

Susan Douglas
Institute for Marine Biosciences
National Research Council
1411 Oxford Street
Halifax, Nova Scotia
B3H 3Z1 Canada
susan.douglas@nrc.ca

Andrew Ellington
Department of Chemistry and Biochemistry
Institute for Cellular and Molecular Biology
University of Texas at Austin
26th and Speedway
Austin, Texas 78712
andy.ellington@mail.utexas.edu

Goezen Ertem
Department of Chemistry
Rensselaer Polytechnic Institute
Troy, New York 12180-3590
ertemg@rpi.edu

Naomi Fast
Department of Biochemistry
Dalhousie University
Halifax, Nova Scotia
B3H 4H7 Canada
nfast@is2.dal.ca

Joseph Felsenstein
Department of Genetics, Sk-50
University of Washington
Box 357360
Seattle, Washington 98195
joe@genetics.washington.edu

Da Fei Feng
Center for Molecular Genetics
University of California, San Diego
9500 Gilmah Drive
La Jolla, California 92093-0634
df@juno.ucsd.edu

James Ferris
Department of Chemistry
Rensselaer Polytechnic Institute
Troy, New York 12180-3590
ferrij@rpi.edu

Patrick Forterre
Institut de Génétique et Microbiologie
URA CNRS 2225, Bat 409
Université Paris-Sud
91405 Orsay Cedex
France
forterre@igmors.u-psud.fr

Peter Gogarten
Department of Molecular and Cell Biology
University of Connecticut
75 N. Eagleville Road U44
Storrs, Connecticut 06269-0001
gogarten@uconnvm.uconn.edu

Catherine Golden
Information Dynamics, Inc.
300 D Street, SW
Suite 801
Washington, DC 20024
catherine.golden@hq.nasa.gov

Michael Gray
Department of Biochemistry
Dalhousie University
Halifax, Nova Scotia
B3H 4H7 Canada
mwgray@is.dal.ca

Ricardo Guerrero
Department of Microbiology
University of Barcelona
Av. Diagonel, 645
08028 Barcelona
Spain
guerrero@bcn.servicom.es

Leslyn Hanakahi
Department of Molecular Biophysics and Biochemistry
Yale University
266 Whitney Avenue
New Haven, Connecticut 06520-8114
lhanakah@biomed.med.yale.edu

Masami Hasegawa
The Institute of Statistical Mathematics
4-6-7 Minami-Azabu, Minato-ku
Tokyo 106-8569
Japan
hasegawa@ism.ac.jp

Robert Hazen
Carnegie Geophysical Laboratory
5251 Broad Branch Road
Washington, DC 20015-1305

Elena Hilario
Department of Molecular and Cell Biology
University of Connecticut
75 N. Eagleville Road U44
Storrs, Connecticut 06269-0001

Christopher House
Department of Earth and Space Sciences
University of California, Los Angeles
Geology Building
Los Angeles, California 90095
chouse@ess.ucla.edu

Michael Ibba
Department of Molecular Biophysics and Biochemistry
Yale University
P.O. Box 208114
266 Whitney Avenue
New Haven, Connecticut 06520-8114

Kenichiro Ishida
Department of Botany
University of British Columbia
#3529-6270 University Boulevard
Vancouver, British Columbia
V6T 1Z4 Canada

Linda Jahnke
NASA Ames Research Center
Exobiology Branch, MS 239-4
Moffett Field, California 94035
ljahnke@mail.arc.nasa.gov

Ken James
Department of Chemistry
Indiana University
Bloomington, Indiana 47405
kdjames@ophelia.ucs.indiana.edu

Alex Jeffries
Institute for Marine Biosciences
National Research Council
1411 Oxford Street
Halifax, Nova Scotia
B3H 3Z1 Canada
alex.jeffries@nrc.ca

Laura A. Katz
Department of Ecology and Evolutionary Biology
Princeton University
Guyot Hall, Washington Road
Princeton, New Jersey 08544

Peter Kuhlman
Department of Biology
Indiana University
Bloomington, Indiana 47405

Shiuhyang Kuo
Department of Biochemistry and Molecular Biology
University of Florida
Box 100245
Gainesville, Florida 32610

Laura Landweber
Department of Ecology and Evolution
Princeton University
323/328 Guyot Hall
Princeton, New Jersey 08544-1003
lfl@princeton.edu

Nancy Maizels
Department of Molecular Biophysics and Biochemistry
Yale University
266 Whitney Avenue
New Haven, Connecticut 06520
nancy.maizels@yale.edu

Lynn Margulis
Geosciences Department
University of Massachusetts at Amherst
Morrill Science Center
Amherst, Massachusetts 01003

John Norman
Department of Biochemistry
Dalhousie University
Halifax, Nova Scotia
B3H 4H7 Canada

Lorraine Olendzensky
Department of Molecular and Cell Biology
University of Connecticut
75 N. Eagleville Road U44
Storrs, Connecticut 06269-0001

Gary Olsen
Department of Microbiology
University of Illinois
131 Burrill Hall
407 S. Goodwin Avenue
Urbana, Illinois 61801
gary@origin.life.uiuc.edu

Jeffrey Palmer
Biology Department
Indiana University
138 Jordan Hall
Bloomington, Indiana 47405
jpalmer@bio.indiana.edu

David J. Patterson
School of Biological Sciences A08
University of Sydney
Sydney, NSW 2006
Australia
djp@bio.usyd.edu.au

ROSEMARY REDFIELD
Department of Zoology
University of British Columbia
6270 University Boulevard
Vancouver, British Columbia
V6T 1Z4 Canada
redfield@unixg.ubc.ca

CLAUDIA REICH
Department of Microbiology
University of Illinois
B103 C&LSL, 601 South Goodwin Avenue
Urbana, Illinois 61801
claudia@phylo.life.uiuc.edu

ANNA-LOUISE REYSENBACH
Dept of Environmental Biology
Portland State University
P.O. Box 751
Portland, Oregon 97207-0751
reysenbach@pdx.edu

DREW RONNEBERG
Department of Chemistry
Princeton University
Guyot Hall, Washington Rd.
Princeton, New Jersey 08544-1003

LYNN ROTHSCHILD
NASA/Ames Research Center, MS 239-12
Moffett Field, California 94035-1000
lrothschild@mail.arc.nasa.gov

J. WILLIAM SCHOPF
Center for the Study of Evolution
University of California, Los Angeles
Geology Building, 405 Hilgard Avenue
Los Angeles, California 90095-1567
schopf@ess.ucla.edu

ERIK SCHULTES
Whitehead Institute for Biomedical Research
9 Cambridge Center
Cambridge, Massachusetts 02142

TOM SCOTT
Life and Biomedical Sciences and Applications Division
300 E Street SW, Code UL
NASA Headquarters
Washington, DC 20546
tscott@gm.olmsa.hq.nasa.gov

PAUL SHARP
Institute of Genetics, University of Nottingham
Queens Medical Centre
Nottingham NG7 2UH
United Kingdom
paul@evol.nott.ac.uk

PEI-YONG SHI
Department of Molecular Biophysics and Biochemistry
Yale University
P.O. Box 208114, 266 Whitney Avenue
New Haven, Connecticut 06520-8114

MITCHELL L. SOGIN
Marine Biological Laboratory
7 MBL Street
Woods Hole, Massachusetts 02543-1015
sogin@evol5.mbl.edu

DIETER SÖLL
Department of Molecular Biophysics and Biochemistry
Yale University
Box 208114, 266 Whitney Avenue
New Haven, Connecticut 06520-8114
soll@trna.chem.yale.edu

ULRICH TECHNAU
Department of Developmental and Cell Biology
University of California
Irvine, California 92697-2300

PETER UNRAU
Whitehead Inst. for Biomedical Research
9 Cambridge Center
Cambridge, Massachusetts 02142

COSTANTINO VETRIANI
CTAG
Institute for Marine & Coastal Sciences
Cook College, Rutgers University
New Brunswick, New Jersey 08903

CHARLES E. WADE
NASA Ames Research Center, MS 239-11
Moffett Field, California 94035-1000

ALAN WEINER
Department of Molecular Biophysics and Biochemistry
Yale University
New Haven, Connecticut 06520
weiner@biomed.med.yale.edu

MARK WELCH
Dept. of Molecular, Cellular & Developmental Biology
University of Colorado, Campus Box 347
Boulder, Colorado 80309-0347
welch@stripe.colorado.edu

MICHAEL YARUS
Dept. of Molecular, Cellular & Developmental Biology
University of Colorado, Campus Box 347
Boulder, Colorado 80309-0347
Michael.Yarus@Colorado.EDU

INDEX

A

A genomics approach to mitochondrial evolution, 400
Abyssal, 18
Acidification of the phagosome in *Crassotrea virginica* hemocytes following engulfment of zymosan, 26
Actinula larva, 45
Adhesion, 34
AFLP (amplified fragment length polymorphism), 80
AIDS, 338
Akiyama, Toshio, see Tatsuya Unuma, 199
Alberstadt, Philip, see Craig Steele, 295
Allometry, 281
Allozymes, 265
Aminoacyl synthetase, 327
Aminoacyl-tRNA synthetase, 335
Aminoacylation, 327
Annelid larva, 187
Anthozoa, 18
Anticancer natural products, 273
Anticodon, 331
Application of genomics for understanding the evolution of hyperthermophilic and nonthermophilic Crenarchaeota, 363
Aptamer, 315
Archaea, 331, 363, 367, 373
Archaeal aminoacyl-tRNA synthesis: unique determinants of a universal genetic code?, 335
Archezoa, 378, 393
Ascidian, 63, 94
Asteroids, 308

B

Bacteria, 367
Bailes, Elizabeth, see Paul M. Sharp, 338
Barry, James P., see J. Timothy Pennington, 245
Bartel, David P., Creation and evolution of new ribozymes, 322
Barton, Anise, see A. Richard Palmer, 281
Bathyal, 18
Bathymodiolus puteoserpentis, 265
Beaven, Amy E., and Kennedy T. Paynter, Acidification of the phagosome in *Crassotrea virginica* hemocytes following engulfment of zymosan, 26
Behavior, 1, 105, 163
  feeding, 295
Behavioral physiology of four crab species in low salinity, 163
Biggers, William J., and Hans Laufer, Settlement and metamorphosis of *Capitella* larvae induced by juvenile hormone-active compounds is mediated by protein kinase C and ion channels, 187
Bingham, Brian L., and Nathalie Reyns, Ultraviolet radiation and distribution of the solitary ascidian *Corella inflata* (Huntsman), 94
Biogeography, 122
Biomechanics, 281
Bode, Hans, Daniel Martinez, M. Andrew Shenk, Kerry Smith, Robert Steele, and Ulrich Technau, Evolution of head development, 408
Bono, J., see M. Ibba, 335
Bootstrap, 345
Brachiopod, 245
Brachyura, 281
Brain, 127
Bryostatin, 273
Bryozoa, 205, 273
Buettner, Garry R., see David W. Tapley, 52
Bugula neritina, 273
Buoyancy, 18
Burger, Gertraud, see Michael W. Gray, 400
Buss, Leo W., see Steve Dudgeon, 1

C

Ca^{++}, 187
Caenogastropod, 57
Calcium-dependence of settlement and nematocyst discharge in actinulae of the hydroid *Tubularia mesembryanthemum*, 45
Callinectes sapidus, 163
Cancer magister, 163
Capitella larva, 187
Carbonic anhydrase, 257
Carcinus maenas, 163
Caribbean, 80
Catalysis, 320
Catalytic RNA, 322
Cavalier-Smith, T., Zooflagellate phylogeny and the systematics of protozoa, 393
CCA-adding enzyme, 331
Cedergren, Robert, see Michael W. Gray, 400
Cellular computing, 324
Cellular evolution, 378
Cellulose, 113
Cereozoa, 393
Chang, Sherwood, Planetary environments and the origin of life, 308
Chaperonins, 385
Chemiluminescence, 52
Childress, James J., see Shana K. Goffredi, 257
Cho, Glen, see Russell F. Doolittle, 356
Clark, C. Graham, The effect of secondary loss on our views of eukaryotic evolution, 385
Claw, 281
Cnidaria, 1, 70
Coalescent, 343
Coalescents, phylogenies, and likelihoods, 343
Cofactor, 320
Colonial integration, 1
Colony, 1
Comets, 308
Comparative analysis of neurogenesis in the central olfactory pathway of adult decapod crustaceans by *in vivo* BrdU-labeling, 127
Comparative study of temporal resolution in the visual systems of mesopelagic crustaceans, 137
Coral reef, 80
Cosmopolitan species, 216
Coughlin, David J., and Lawrence C. Rome, Muscle activity in steady swimming scup, *Stenotomus chrysops*, varies with fiber type and body position, 145
Crab, 163, 281
Crayfish, 295
Creation and evolution of new ribozymes, 322
Cromarty, S. I., J. Mello, and G. Kass-Simon, Time in residence affects escape and agonistic behavior in adult male American lobsters, 105
Cross-species transmission, 338
Crustacea, 18, 105, 127, 281
  vision, 137
Cryptic species, 273

- Cummings, Michael P., Sarah P. Otto, and John Wakeley, Genes and other samples of DNA sequence data for phylogenetic inference, 345
- Curnow, A. W., see M. Ibba, 335
- Cuspidarid, 18
- Cuticle, 113, 281
- Cuticle strength and the size-dependence of safety factors in *Cancer* crab claws, 281
- Cyanobacteria, 351
- Cytochrome C oxidase subunit I, 273

D

- Davidson, Seana K., and Margo G. Haygood, Identification of sibling species of the bryozoan *Bugula neritina* that produce different anticancer bryostatins and harbor distinct strains of the bacterial symbiont "*Candidatus* Endobugula sertula," 273
- Decapod, 18
- Deep divisions in the tree of life—what does the fossil record reveal?, 351
- Deep sea, 18, 137
- DeLong, Edward F., Christa Schleper, Robert Feldman, and Ronald V. Swanson, Application of genomics for understanding the evolution of hyperthermophilic and nonthermophilic Crenarchaeota, 363
- Desaulniers, Nicole T., see Shana K. Goffredi, 257
- Determining divergence times with protein clocks, 356
- Development, 127, 245, 229
- Development, temperature tolerance, and settlement preference of embryos and larvae of the articulate brachiopod *Laqueus californianus*, 245
- Developmental basis of phenotypic variation in egg production in a colonial ascidian: primary oocyte production versus oocyte development, 63
- Differences in the composition of adhesive and nonadhesive mucus from the limpet *Lottia limatula*, 34
- Digestion, 1
- *Dinococcus*, 359
- Diplomonad, 389
- Divergence time, 356
- DNA, 345
  - computing, 324
  - strand symmetry, 411
- Doble, Karen E., see Hamid R. Khan, 153
- Dolan, Michael, see Lynn Margulis, 413
- Doolittle, Russell F., Da-Fei Feng, and Glen Cho, Determining divergence times with protein clocks, 356
- Doolittle, W. Ford, Rethinking the origin of eukaryotes, 378
- Douglas, Susan E., Evolutionary history of plastids, 397
- Dudgeon, Steve, Andreas Wagner, J. Rimas Vaišnys, and Leo W. Buss, Dynamics of gastrovascular circulation in the hydrozoan *Podocoryne carnea*: the one-polyp case, 1
- Dynamics of gastrovascular circulation in the hydrozoan *Podocoryne carnea*: the one-polyp case, 1

E

- Effect of steroids on gonadal growth and gametogenesis in the juvenile Red Sea urchin *Pseudocentrotus depressus*, 199
- Egg production, 63
- Elasmobranch, 18
- Electromyogram, 145
- Electron diffraction, 113
- Ellington, Andrew D., Molecular origins and the null hypothesis: motifs from our Maker? 315
- Embryo, 245
- EMG (electromyogram), 145
- Endosymbiont hypothesis, 400
- Endosymbiosis, 378
- Entamoeba, 385
- EPR spin trapping, 52
- Escape, 105
- Estrone, 199
- Ethoxyzolamide, 257
- Eukaryote, 378, 385, 397
  - early evolution of, 389
- Evolution, 229, 307, 308, 311, 315, 320, 322, 324, 327, 331, 335, 338, 343, 345, 351, 356, 359, 363, 367, 373, 378, 381, 385, 389, 393, 397, 400, 404, 408, 411, 413, 415
  - of head development, 408
  - of life, 367
- Evolution: a molecular point of view, 303
- Evolutionary history of plastids, 397
- Extreme environment, 363

F

- Feeding, 205
  - behavior, 295
- Feldman, Robert, see Edward F. DeLong, 363
- Felsenstein, Joseph, Coalescents, phylogenies, and likelihoods, 343
- Feng, Da-Fei, see Russell F. Doolittle, 356
- Ferris, James P., Prebiotic synthesis on minerals: bridging the prebiotic and RNA worlds, 311
- Fish, swimming, 145
- Flagellates, 381
- Flicker fusion frequency, 137
- Flow, 205
- Food search, 295
- Forterre, Patrick, and Hervé Philippe, The Last Universal Common Ancestor (LUCA): simple or complex?, 373
- Fossils, 351
- Frank, Tamara M., Comparative study of temporal resolution in the visual systems of mesopelagic crustaceans, 137
- Free radicals, 52
- Free radicals and chemiluminescence as products of the spontaneous oxidation of sulfide in seawater, and their biological implications, 52
- Free-living flagellates from anoxic habitats and the assembly of the eukaryotic cell, 381
- Freeman, Jim, see Scott Mohr, 411
- Froggett, Stephan J., and Esther M. Leise, Metamorphosis in the marine snail *Ilyanassa obsoleta*, yes or NO? 57
- Functional morphology, 281
- Fusetani, Nobuhiro, see Satoru Kawaii, 45

G

- Gametogenesis, 199
- Gao, Feng, see Paul M. Sharp, 338
- Gastropoda, 57, 153, 229
- Gastrovascular transport, 1
- Genes and other samples of DNA sequence data for phylogenetic inference, 345
- Genetic and morphometric characterization of mussels (Bivalvia: Mytilidae) from Mid-Atlantic hydrothermal vents, 265
- Genetic code, 335
- Genetic exchange, 404
- Genetic relationships (RAPD-PCR) between geographically separated populations of the "cosmopolitan" interstitial polychaete *Hesionides gohari* (Hesionidae) and the evolutionary origin of the freshwater species *Hesionides riegerorum*, 216
- Genome, 327
  - evolution, 324, 400, 411
  - plastid, 397
  - structure, 400
- Genomic tag, 327, 331
- Girguis, Peter R., see Shana K. Goffredi, 257
- Gluing, 34
- Goffredi, Shana K., Peter R. Girguis, James J. Childress, and Nicole T. Desaulniers, Physiological functioning of carbonic anhydrase in the hydrothermal vent tubeworm *Riftia pachyptila*, 257
- Gogarten, J. Peter, Ryan D. Murphey, and Lorraine Olendzenski, Horizontal gene transfer: pitfalls and promises, 359
- Golding, Brian, see Michael W. Gray, 400
- Gonad index, 199

Gray, Michael W., Gertraud Burger, Robert Cedergren, G. Brian Golding, Claude Lemieux, David Sankoff, Monique Turmel, and Franz Lang, A genomics approach to mitochondrial evolution, 400
Greenberg, Michael J., see Hamid R. Khan, 153
Growth, 205
Guadagnoli, J. A., see I. J. McGaw, 163
Guerrero, Ricardo, see Lynn Margulis, 413

H

Hahn, Beatrice H., see Paul M. Sharp, 338
Harzsch, Steffan, see Manfred Schmidt, 127
Hasegawa, Masami, and Tetsuo Hashimoto, Phylogenetic position of amitochondriate protists in the evolution of eukaryotes, 389
Hashimoto, Tetsuo, see Masami Hasegawa, 389
Haygood, Margo G., see Seana K. Davidson, 273
Head development, 408
Hemocyte, 26
Henley, Catherine, obituary, 227
High contents of trimethylamine oxide correlating with depth in deep-sea teleost fishes, skates, and decapod crustaceans, 18
Hilbish, Thomas J., see Diarmaid Ó Foighil, 122
Hirose, Euichi, Satoshi Kimura, Takao Itoh, and Jun Nishikawa, Tunic morphology and cellulosic components of pyrosomas, doliolids, and salps (Thaliacea, Urochordata), 113
HIV (human immunodeficiency virus), 338
Horizontal gene transfer, 359
Horizontal gene transfer: pitfalls and promises, 359
Huang, Faqing, Zhili Yang, and Mike Yarus, Self-capping RNA catalysts derived from selection-amplification, 320
Hydra, 408
Hydrothermal systems, 308
Hydrothermal vent, 52, 257
Hydrozoa, 1
Hypotrichous ciliates, 324

I

Ibba, M., A. W. Curnow, J. Bono, P. A. Rosa, C. R. Woese, and D. Soll, Archaeal aminoacyl-tRNA synthesis: unique determinants of a universal genetic code?, 335
Identification of sibling species of the bryozoan *Bugula neritina* that produce different anticancer bryostatins and harbor distinct strains of the bacterial symbiont "*Candidatus* Endobugula sertula," 273
Image analysis, 1
Impacts, 308
In vitro selection, 315
Inorganic carbon, 257
Interface, 308
Intertidal zone, 153
Intracapsular feeding by embryos of the gastropod genus *Littorina*, 229
Invertebrate distribution, 94
Ion channel, 187
Itoh, Takao, see Euichi Hirose, 113

J

JH activity, 187
Juvenile hormone (JH), 187

K

K^+, 187
Kass-Simon, G., see S. I. Cromarty, 105
Kawaii, Satoru, Keiji Yamashita, Mitsuyo Nakai, Miyuki Takahashi, and Nobuhiro Fusetani, Calcium-dependence of settlement and nematocyst discharge in actinulae of the hydroid *Tubularia mesembryanthemum*, 45
Kelly, Robert H., and Paul H. Yancey, High contents of trimethylamine oxide correlating with depth in deep-sea teleost fishes, skates, and decapod crustaceans, 18
Kersanach, Ralf, see Jose V. Lopez, 80
Keys to Marine Invertebrates of the Woods Hole Region, Announcement, 121
Khan, Hamid R., David A. Price, Karen E. Doble, Michael J. Greenberg, and A. S. M. Saleuddin, Osmoregulation and FMRFamide-related peptides in the salt marsh snail *Melampus bidentatus* (Say) (Mollusca: Pulmonata), 153
Kimura, Satoshi, see Euichi Hirose, 113
Kirshtein, J., see A. L. Reysenbach, 367
Knowlton, Nancy, see Jose V. Lopez, 80
Krupp, David A., see Jodi A. Schwarz, 70

L

Landweber, Laura F., The evolution of cellular computing, 324
Lang, Franz, see Michael W. Gray, 400
Larva, 57, 94, 177, 229, 245
  actinula, 45
  annelid, 187
  development, 70
  settlement, 187
  veliger, 57
Late larval development and onset of symbiosis in the scleractinian coral *Fungia scutaria*, 70
Laufer, Hans, see William J. Biggers, 187
Leise, Esther M., see Stephan J. Froggett, 57
Lemieux, Claude, see Michael W. Gray, 400
Libinia emarginata, 163
Likelihood, 338
Limpet, 34
Littorina, 229
Lopez, Jose V., Ralf Kersanach, Stephen A. Rehner, and Nancy Knowlton, Molecular determination of species boundaries in corals: genetic analysis of the *Montastraea annularis* complex using amplified fragment length polymorphisms and a microsatellite marker, 80
Lough Hyne (=Ine), 205
Lutz, Richard A., see Paula A. Y. Maas, 265

M

Maas, Paula A. Y., Gregory D. O'Mullan, Richard A. Lutz, and Robert C. Vrijenhoek, Genetic and morphometric characterization of mussels (Bivalvia: Mytilidae) from Mid-Atlantic hydrothermal vents, 265
Maizels, Nancy, Alan M. Weiner, Dongxian Yue, and Pei-Yong Shi, New evidence for the genomic tag hypothesis: archael CCA-adding enzymes and tDNA substrates, 331
Maizels, Nancy, see Alan M. Weiner, 327
Manahan, Donal T., see Jay Vavra, 177
Margulis, Lynn, Michael Dolan, and Ricardo Guerrero, The molecular tangled bank: not seeing the phylogenies for the trees, 413
Marshall, Bruce A., see Diarmaid Ó Foighil, 122
Martinez, Daniel, see Hans Bode, 408
Mathewson, Candice, see Craig Steele, 295
Maximum likelihood, 345
McGaw, I. J., C. L. Reiber, and J. A. Guadagnoli, Behavioral physiology of four crab species in low salinity, 163
McLaughlin, E., see A. L. Reysenbach, 367
Meiofauna, 216
Melampus, 153
Mello, J., see S. I. Cromarty, 105
Metabolism, 177
Metamorphosis, 57, 187
Metamorphosis in the marine snail *Ilyanassa obsoleta*, yes or NO?, 57
Microbial evolution, 413
Microsatellite, 80
Microsporidian, 389
Miniaturization, 205
Mitochondria, 400
Mitochondrial DNA, 400, 411
Mitochondrial genome, 345, 400

Mitochondriate protist, 389

Mohr, Scott, Jim Freeman, Tom Plasterer, and Temple Smith, Patterns of mitochondrial DNA strand asymmetry correlate with phylogeny, 411

Molecular clock, 338

Molecular constraints on a high-temperature evolution of early life, 367

Molecular determination of species boundaries in corals: genetic analysis of the *Montastraea annularis* complex using amplified fragment length polymorphisms and a microsatellite marker, 80

Molecular evolution, 315, 338

Molecular fossil, 327

Molecular origins and the null hypothesis: motifs from our Maker?, 315

Molecular phylogeny, 373, 413

Molecular taxonomy, 216

Mollusc, 57

Montastraea, 80

Moran, A. L., Intracapsular feeding by embryos of the gastropod genus *Littorina*, 229

Morphology, 205

Mortality, 94

mtDNA, 122, 265

Mucus, 34

Murphey, Ryan D., see J. Peter Gogarten, 359

Muscle activity in steady swimming scup, *Stenotomus chrysops*, varies with fiber type and body position, 145

Muscle physiology, 145

N

NADH dehydrogenase subunit 4, 265

Nakai, Mitsuyo, see Satoru Kawaii, 45

NASA, Evolution: a molecular point of view, 303

National Aeronautics and Space Administration (NASA), 303

Natural products, marine, 273

Neighbor joining, 345

Nematocyst discharge, 45

Neomonada, 393

Neurogenesis, 127

Neuropeptides, 153

New evidence for the genomic tag hypothesis: archael CCA-adding enzymes and tDNA substrates, 331

Nishikawa, Jun, see Euichi Hirose, 113

Nitric oxide, 57

Nuclear genome, 397

Nucleomorph, 397

Nutrition, 229

O

Ó Foighil, Diarmaid, Bruce A. Marshall, Thomas J. Hilbish, and Mario A. Pino, Trans-Pacific range extension by rafting is inferred for the flat oyster *Ostrea chilensis*, 122

O'Mullan, Gregory D., see Paula A. Y. Maas, 265

Okamura, Beth, and Julian C. Partridge, Suspension feeding adaptations to extreme flow environments in a marine bryozoan, 205

Olendzenski, Lorraine, see J. Peter Gogarten, 359

Olfaction, 127

Oral administration, 199

Organelle origins, 413

Organic matter, 308

Organization of chemically activated food search behavior in *Procambarus clarkii* Girard and *Orconectes rusticus* Girard crayfishes, 295

Origin of life, 311

Origins and evolution of AIDS viruses, 338

Osmolytes, 18

Osmoregulation, 153

Osmoregulation and FMRFamide-related peptides in the salt marsh snail *Melampus bidentatus* (Say) (Mollusca: Pulmonata), 153

Otto, Sarah P., see Michael P. Cummings, 345

Oxidative stress, 52

Oyster, 26, 122

P

Palmer, A. Richard, Graeme M. Taylor, and Anise Barton, Cuticle strength and the size-dependence of safety factors in *Cancer* crab claws, 281

Parsimony, 345

Partial phylogeny inadequacies, 413

Partridge, Julian C., see Beth Okamura, 205

Patterns of mitochondrial DNA strand asymmetry correlate with phylogeny, 411

Patterson, David J., Alastair G. B. Simpson, and Nimalika Weerkaoon, Free-living flagellates from anoxic habitats and the assembly of the eukaryotic cell, 381

Paynter, Kennedy T., see Amy E. Beaven, 26

Pelagic tunicate, 113

Pennington, J. Timothy, Mario N. Tamburri, and James P. Barry, Development, temperature tolerance, and settlement preference of embryos and larvae of the articulate brachiopod *Laqueus californianus*, 245

pH, 26
  regulation, 257

Phagosome, 26

Philippe, Hervé, see Patrick Forterre, 373

Photoreception, 137

Phylogenetic position of amitochondriate protists in the evolution of eukaryotes, 389

Phylogenetics, 345

Phylogeny, 343

Physiological functioning of carbonic anhydrase in the hydrothermal vent tubeworm *Riftia pachyptila*, 257

Physiology, 1, 163

Pino, Mario A., see Diarmaid Ó Foighil, 122

Planetary environments and the origin of life, 308

Planula larva, 70

Plasterer, Tom, see Scott Mohr, 411

Plastid, 397

Plastid genome, 397

Poly(A)polymerase, 331

Polychaete, 187, 216

Polyp, 1

Prebiotic evolution, 308

Prebiotic synthesis on minerals: bridging the prebiotic and RNA worlds, 311

Precambrian, 351

Price, David A., see Hamid R. Khan, 153

Primates, 338

Prolyl tRNA synthase, 359

Prosobranchia, 229

Protein, 177, 327

Protein clock, 356

Protein kinase C, 187

Protein metabolism in lecithotrophic larvae (Gastropoda: *Haliotis rufescens*), 177

Protist, 400

Protozoa, 381, 393

Purine excess, 411

Q

Quick, Tonya J., see Andrew M. Smith, 34

R

16S rRNA, 367

Recombination, 338, 404

Recruitment, 94

Redfield, Rosemary J., The problem of the evolution of sex, 404

Rehner, Stephen A., see Jose V. Lopez, 80

Reiber, C. L., see I. J. McGaw, 163

Replication, 327

Residence, 105

Rethinking the origin of eukaryotes, 378

Retrovirus, 338
Reyns, Nathalie, see Brian L. Bingham, 94
Reysenbach, A.-L., S. Seitzinger, J. Kirshtein, and E. McLaughlin, Molecular constraints on a high-temperature evolution of early life, 367
Ribozyme, 320
Riftia pachyptila, 257
RNA, 311, 320
  replication, 322
  splicing, 322
  world, 311, 315, 322, 327, 331
Robertson, David L., see Paul M. Sharp, 338
Rome, Lawrence C., see David J. Coughlin, 145
Rosa, P. A., see M. Ibba, 335

S

Saleuddin, A. S. M., see Hamid R. Khan, 153
Salinity, 163
Sankoff, David, see Michael W. Gray, 400
Scaling, 281
Schleper, Christa, see Edward F. DeLong, 363
Schmidt, Hartmut, and Wilfried Westheide, Genetic relationships (RAPD-PCR) between geographically separated populations of the "cosmopolitan" interstitial polychaete *Hesionides gohari* (Hesionidae) and the evolutionary origin of the freshwater species *Hesionides riegerorum*, 216
Schmidt, Manfred, and Steffan Harzsch, Comparative analysis of neurogenesis in the central olfactory pathway of adult decapod crustaceans by *in vivo* BrdU-labeling, 127
Schopf, J. William, Deep divisions in the tree of life—what does the fossil record reveal?, 351
Schwarz, Jodi A., David A. Krupp, and Virginia M. Weis, Late larval development and onset of symbiosis in the scleractinian coral *Fungia scutaria*, 70
Scrambled genes, 324
Sea urchin, 199
Seitzinger, S., see A. L. Reysenbach, 367
Selection, 320
SELEX, 315
Self-capping RNA catalysts derived from selection-amplification, 320
Settlement, 245
Settlement and metamorphosis of *Capitella* larvae induced by juvenile hormone-active compounds is mediated by protein kinase C and ion channels, 187
Sexual reproduction, 404
Sharp, Paul M., Elizabeth Bailes, David L. Robertson, Feng Gao, and Beatrice H. Hahn, Origins and evolution of AIDS viruses, 338
Shenk, M. Andrew, see Hans Bode, 408
Shi, Pei-Yong, see Nancy Maizels, 331
Shick, J. Malcolm, see David W. Tapley, 52
Sibling species, 80, 273
Signal
  processing, 1
  transduction, 187
Simpson, Alastair G. B., see David J. Patterson, 381
SIV (simian immunodeficiency virus), 338
Skate, 18
Skinner, Carol, see Craig Steele, 295
Smith, Andrew M., Tonya J. Quick, and Rachel L. St. Peter, Differences in the composition of adhesive and nonadhesive mucus from the limpet *Lottia limatula*, 34
Smith, Kerry, see Hans Bode, 408
Smith, Temple, see Scott Mohr, 411
Sogin, Mitchell L., 307, 415
Söll, D., see M. Ibba, 335
Species, non-indigenous, 273
Squid, 18
St. Peter, Rachel L., see Andrew M. Smith, 34
Steel, Robert, see Hans Bode, 408
Steele, Catherine, see Craig Steele, 295
Steele, Craig, Carol Skinner, Catherine Steele, Philip Alberstadt, and Candice Mathewson, Organization of chemically activated food search behavior in *Procambarus clarkii* Girard and *Orconectes rusticus* Girard crayfishes, 295
Steroid, 199
Stewart-Savage, J., Bradley J. Wagstaff, and Philip O. Yund, Developmental basis of phenotypic variation in egg production in a colonial ascidian: primary oocyte production versus oocyte development, 63
Sulfide oxidation, 52
Suspension feeding adaptations to extreme flow environments in a marine bryozoan, 205
Swanson, Ronald V., see Edward F. DeLong, 363
Symbiogenesis, 413
Symbiosis, 70, 257, 273
Systematics, 393

T

Tailflip, 105
Takahashi, Miyuki, see Satoru Kawaii, 45
Tamburri, Mario N., see J. Timothy Pennington, 245
Tapley, David W., Garry R. Buettner, and J. Malcolm Shick, Free radicals and chemiluminescence as products of the spontaneous oxidation of sulfide in seawater, and their biological implications, 52
Taylor, Graeme M., see A. Richard Palmer, 281
tDNA, 331
Technau, Ulrich, see Hans Bode, 408
Teleost, 18
Temperature, 245
Temporal resolution, 137
The effect of secondary loss on our views of eukaryotic evolution, 385
The evolution of cellular computing, 324
The genomic tag hypothesis: modern viruses as molecular fossils of ancient strategies for genomic replication, and clues regarding the origin of protein synthesis, 327
The Last Universal Common Ancestor (LUCA): simple or complex?, 373
The molecular tangled bank: not seeing the phylogenies for the trees, 413
The problem of the evolution of sex, 404
Thermophiles, 367
Time in residence affects escape and agonistic behavior in adult male American lobsters, 105
Trans-Pacific range extension by rafting is inferred for the flat oyster *Ostrea chilensis*, 122
Transformation, 404
Translation, 327, 331, 335
Tree of life, 351, 356
Trichomonad, 389
Trimethylamine oxide, 18
tRNA, 327, 331, 335
tRNA-like structure, 327
Tubeworm, 257
Tubularia mesembryanthemum
Tunic cell, 113
Tunic morphology and cellulosic components of pyrosomas, doliolids, and salps (Thaliacea, Urochordata), 113
Turmel, Monique, see Michael W. Gray, 400

U

Ultraviolet radiation and distribution of the solitary ascidian *Corella inflata* (Huntsman), 94
Unancestor, 373
Universal tree of life, 373
Unuma, Tatsuya, Takeshi Yamamoto, and Toshio Akiyama, Effect of steroids on gonadal growth and gametogenesis in the juvenile Red Sea urchin *Pseudocentrotus depressus*, 199
UV radiation, 94

V

V-ATPase, 359
Vaišnys, J. Rimas, see Steve Dudgeon, 1

Vavra, Jay, and Donal T. Manahan, Protein metabolism in lecithotrophic larvae (Gastropoda: *Haliotis rufescens*), 177

Veliger, 57

Videomicroscopy, 1

Virus, 327, 338

Vrijenhoek, Robert C., see Paula A. Y. Maas, 265

W

Wagner, Andreas, see Steve Dudgeon, 1

Wagstaff, Bradley J., see J. Stewart-Savage, 63

Wakeley, John, see Michael P. Cummings, 345

Weerkaoon, Nimalika, see David J. Patterson, 381

Weiner, Alan M., and Nancy Maizels, The genomic tag hypothesis: modern viruses as molecular fossils of ancient strategies for genomic replication, and clues regarding the origin of protein synthesis, 327

Weiner, Alan M., see Nancy Maizels, 331

Weis, Virginia M., see Jodi A. Schwarz, 70

Westheide, Wilfried, see Hartmut Schmidt, 216

Woese, C. R., see M. Ibba, 335

Y

Yamamoto, Takeshi, see Tatsuya Unuma, 199

Yamashita, Keiji, see Satoru Kawaii, 45

Yancey, Paul H., see Robert H. Kelly, 18

Yang, Zhili, see Faqing Huang, 320

Yarus, Mike, see Faqing Huang, 320

Yue, Dongzian, see Nancy Maizels, 331

Yund, Philip O., see J. Stewart-Savage, 63

Z

Zooflagellate, 393

Zooflagellate phylogeny and the systematics of protozoa, 393

Zooxanthellae, 70

MBL/WHOI LIBRARY
WH 1B34 P